Steffen Heegaard
Hans Grossniklaus
Editors

Eye Pathology

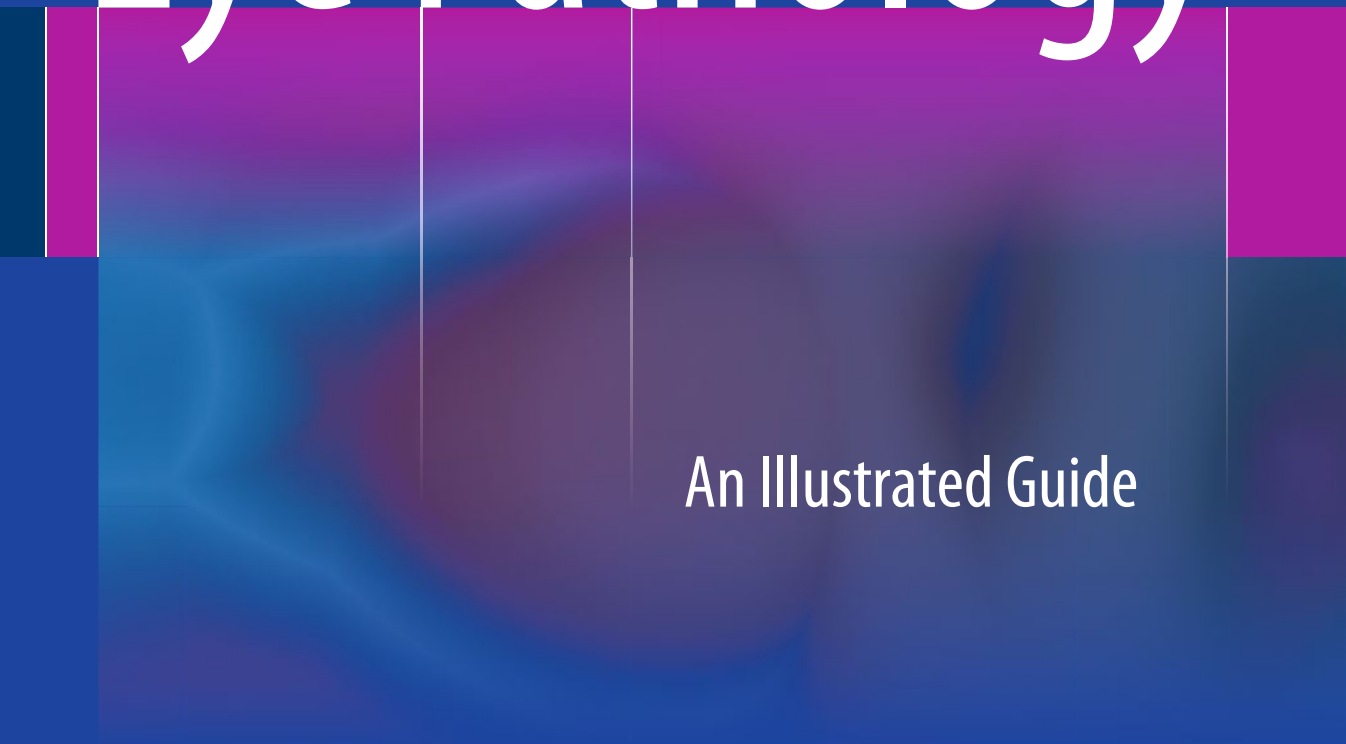

An Illustrated Guide

Springer

Eye Pathology

Steffen Heegaard • Hans Grossniklaus
Editors

Eye Pathology

An Illustrated Guide

Springer

Editors
Steffen Heegaard
Eye Pathology Section
Department of Ophthalmology
Glostrup Hospital
University of Copenhagen
Copenhagen
Denmark

Hans Grossniklaus
L.F. Montgomery Laboratory
Emory Eye Center
Atlanta, GA
USA

ISBN 978-3-662-43381-2 ISBN 978-3-662-43382-9 (eBook)
DOI 10.1007/978-3-662-43382-9
Springer Heidelberg New York Dordrecht London

Library of Congress Control Number: 2014951717

Contents

Contributors

Claudia Auw-Haedrich Histology Lab, Eye Center, University Freiburg, Freiburg, Germany

Emilio Balestrazzi Institute of Ophthalmology, Catholic University, Rome, Italy

Nikolaos E. Bechrakis, MD, FEBO Department of Ophthalmology, Innsbruck Medical University, Innsbruck, Austria

Maria Antonietta Blasi Institute of Ophthalmology, Catholic University, Rome, Italy

J. Douglas Cameron, MD, MBA Department of Ophthalmology and Visual Neuroscience and Laboratory Medicine and Pathology, University of Minnesota School of Medicine, Minneapolis, MN, USA

Sarah E. Coupland, MBBS, PhD, FRCPath Molecular and Clinical Cancer Medicine, Royal Liverpool and Broadgreen University Hospital NHS Trust, University of Liverpool, Liverpool, UK

Thomas J. Cummings, MD Department of Pathology, Duke University Medical Center, Durham, NC, USA

Lynn E. Harman, MD Section of Ophthalmology, Department of Ophthalmology, James A. Haley, VA Hospital, Morsani College of Medicine, University of South Florida, Tampa, FL, USA

Susan Kennedy The Royal Victoria Eye and Ear Hospital, Dublin, Republic of Ireland

Tero Kivelä, MD, FEBO Ophthalmic Pathology Laboratory, Department of Ophthalmology, Helsinki University Central Hospital, Helsinki, Finland

Philip J. Luthert, BSc, MBBS, FRCP, FRCPath, FRCOphth Department of Ophthalmology, UCL University College London, London, UK

Curtis E. Margo, MD, MPH Department Ophthalmology, and Pathology and Cell Biology, Morsani College of Medicine, University of South Florida, Tampa, FL, USA

Elisabeth M. Messmer, MD, FEBO Department of Ophthalmology, Ludwig-Maximilians-University, Munich, Germany

Peter Meyer Division of Histology Lab, Augenspital Basel, Basel, Switzerland

Cornelia M. Mooy, MD, PhD Laboratory for Pathology, Dordrecht, The Netherlands

Alexander Moulin, MD, MER, FEBO Department of Ophthalmology, Eye Pathology Laboratory, Jules-Gonin Eye Hospital, University of Lausanne, Lausanne, Switzerland

Irene Pecorella, MD, PhD Department of Experimental Medicine, University of Rome "Sapienza", Rome, Italy

Jan Ulrik Prause Eye Pathology Institute, Copenhagen, Denmark

Dejan M. Rašić Departments of Ophthalmology and Pathology, University of Belgrade School of Medicine, Belgrade, Serbia

Fiona Roberts Department of Pathology, Southern General Hospital, Glasgow, Scotland, UK

Beata Rymgayłło-Jankowska, MD, PhD Department of Diagnostics and Microsurgery of Glaucoma, Medical University of Lublin, Lublin, Poland

Diva Salomão Department of Pathology and Laboratory Medicine, Mayo Clinic, Rochester, MN, USA

Maria Antonia Saornil Instituto de Oftalmologia Aplicada, Facultad de Medicina, Valladolid, Spain

Stefan Seregard St. Eriks Eye Hospital, Karolinska Institutet, Stockholm, Sweden

Jeannette Tóth 2nd Department of Pathology, Faculty of General Medicine, Semmelweis University, Hungary

Paul van der Valk, MD, PhD Department of Pathology, Vrije Universiteit Medical Center, Amsterdam, MB, The Netherlands

Rita Van Ginderdeuren Department of Ophthalmology and Pathology, UZ Leuven, Leuven, Belgium

Robert M. Verdijk, MD, PhD Department of Ophthalmic Pathology, Erasmus University Medical Center, Rotterdam, The Netherlands

David J. Wilson, MD Casey Eye Institute, Oregon Health and Science University, Portland, OR, USA

The Eye

1

Jan Ulrik Prause and Maria Antonia Saornil

1.1 General Description

1.1.1 A Few Words of Introduction

The general pathologist may receive an eye for histopathological analysis for various reasons. Despite that the number of autopsies is steadily dropping all over the world, the eyes are still obtained for study due to severe acute trauma. The eye may also be suspected of harbouring the primary tumour that caused the death of the patient and may show important specific signs of systemic inflammatory or infectious general disease. Specific signs of disease or trauma may be obtained from a forensic point of view like in "battered child syndrome" or with the purpose of identifying the age of the patient [1]. The eye may be analysed because the patient at autopsy has donated organs. When the corneas are sent to the cornea bank, the remaining parts of the eyes should be examined to exclude any disease that could be transmitted.

J.U. Prause, MD, DMSc, DHC, FEBO (✉)
Eye Pathology Institute, University of Copenhagen,
Frederik V's Vej 11, Copenhagen,
DK 2100 Denmark
e-mail: jup@sund.ku.dk

M.A. Saornil, MD, PhD
Instituto de Oftalmologia Aplicada,
Facultad de Medicina, Ramon y Cajal 7,
Valladolid 47005, Spain
e-mail: saornil@ono.com

The eyes may also be sent to analysis directly from the ophthalmic departments because of specific eye diseases leading to enucleation or exenteration although these reasons have dropped drastically in number during the last many years [2]. A limited number of eyes are also removed despite being normal, because of massive, malignant tumours of the eyelids and orbit that cannot be surgically treated without causing permanent exposure of the globe. Despite this, the eyes are still to be examined when removed also to ensure tissue for the future. Most cases described in this chapter, their morphological characteristics and the related epidemiological data are based upon the database at the Eye Pathology Institute, University of Copenhagen (ØPI-KU). The database is national and has existed since 1910.

1.1.2 Orienting, Transillumination, Cutting and Embedding

The enucleated eye is inspected using a stereo microscope. Dimensions of the globe (length × width × height) and length of the optic nerve stump are obtained with a ruler. Note any ruptures of the sclera and cornea. Mostly, scleral ruptures pass along a rectus muscle insertion into the sclera. The cornea may be cloudy, preventing inspection of the anterior chamber. Extrabulbar extensions of intraocular tumours should be noted. Most are found at the emissaries (Fig. 1.1). The cranial end of the cut optic nerve is inspected for tumour infiltration.

S. Heegaard, H. Grossniklaus (eds.), *Eye Pathology: An Illustrated Guide*,
DOI 10.1007/978-3-662-43382-9_1,

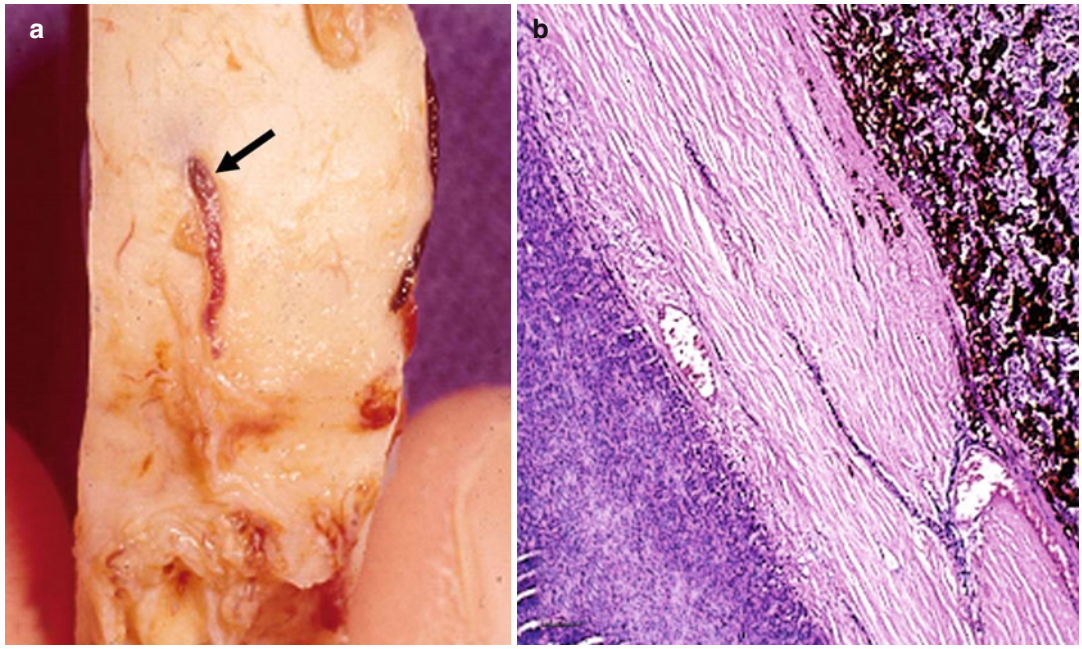

Fig. 1.1 Examination of the eyeball. (**a**) Note the extra-scleral extension of a malignant choroidal melanoma along the vessels (*arrow*). (**b**) Histological survey of a similar area

Internal tumours are looked for by transillumination. This is best performed with a fibre optic source in dimmed light (Fig. 1.2). Draw the outlines of the shadow with a tissue pencil upon the sclera to facilitate correct cutting of the globe.

The globe is by standard cut into three: two calottes and a central ring. Use disposable blades; those used for cleaning glass windows for sticky paper are excellent (Fig. 1.3). If no intraocular tumours are suspected, the globe is divided by horizontal cuts. The two cuts are placed with a distance of app. 8 mm to create a ring that includes the cornea, the sclera, the anterior chamber, the optic nerve, the fovea, and the lens.

Embedding in paraffin follows routine protocols; however, since the specimen is a ring with a stiff outer wall (the sclera) and a thin friable inner wallpaper (the choroid and the retina), only supported by a collapsed vitreous body (age or the fixative), most types of paraffin tend not to prevent artificial detachment of the retina during processing and cutting. Admixture of 7 % ordinary bee wax to the paraffin is a good solution to this problem.

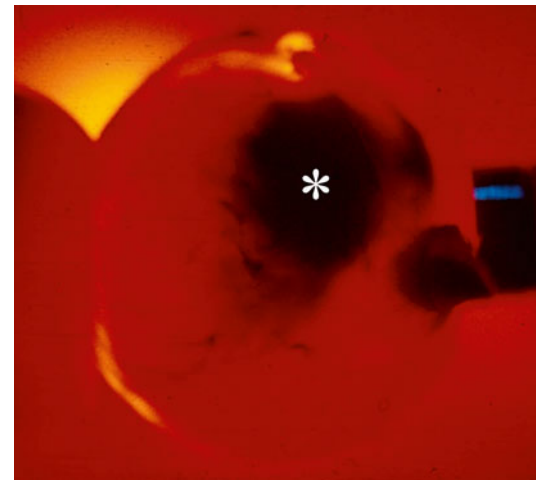

Fig. 1.2 Diascleral illumination of an eye with a malignant choroidal melanoma. The localisation and size of the tumour is determined from its shadow (*asterisk*)

Photographic documentation is performed in a photomicroscope equipped with focal light sources. Submersing of the central ring in water is recommendable to prevent multiple reflexes.

Fig. 1.3 Tools for sectioning of the eyeball

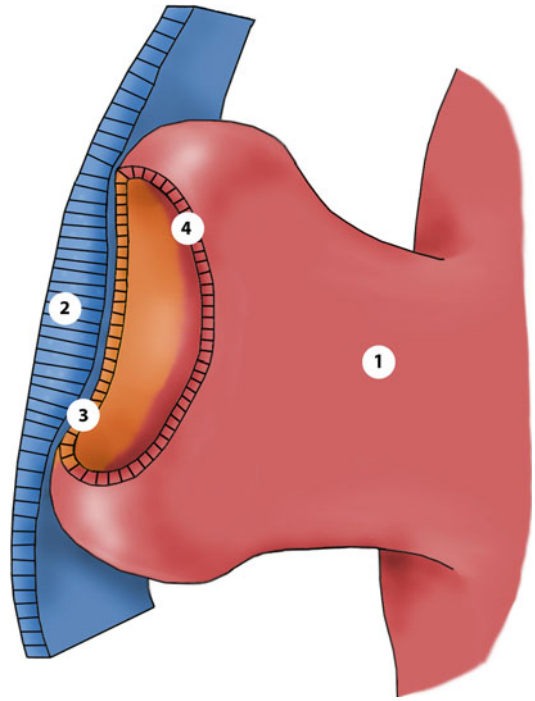

Fig. 1.4 Drawing of the optic vesicle. The vesicles evaginate from the anterior neural tube during the second foetal week. *1* optic vesicle, *2* lens placode, *3* future anterior iris epithelium + non-pigmented ciliary epithelium + neuroretina, *4* future anterior iris epithelium + outer ciliary epithelium + retinal pigment epithelium

1.1.3 The Ordinary Sequence in Which to Describe the Eye in Histopathology

By tradition, a sectioned eye is described in a specific sequence: cornea, limbal tissue, sclera, anterior chamber, iris, ciliary body, choroid, retina, optic nerve, optic disc, vitreous body and lens.

1.2 Embryology, Anatomy and Development

1.2.1 Embryology

The embryology of the eye has been splendidly described in classic textbooks [3] and in a series of more recent papers [4–7]. The embryonic development of the eye can be observed 3 weeks after conception when the optic sulci appear in the neural folds. The genesis of the eye is characterised, on the molecular level, by the expression of "eye-field transcription factors", regulating the development of the eye structures from the neuroectoderm, the surface ectoderm and the mesenchyme. When the neural tube closes, optic sulci deepen and become optic vesicles, arising as hemispherical extensions on the lateral sides of the forebrain vesicle and in continuity with the neural tube that is composed of neuroectodermal cells. At the end of the fourth week, the optic vesicles approach the surface ectoderm, inducing the formation of the lens placodes which invaginate, creating the two lens vesicles. Concurrently, the growth of the cells of the optic vesicle leads to infolding of the anterior part of the vesicle into the posterior part, forming the optic cup (Fig. 1.4).

During the second month the inner layer of the optic cup differentiates into the posterior iris epithelium, the inner ciliary epithelium and the neurosensory retina. The outer layer develops into

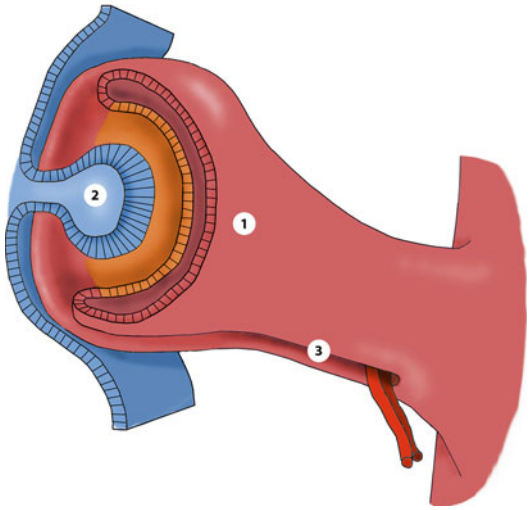

Fig. 1.5 At 4 weeks the optic cup is created by invagination of optic vesicle. Evagination of lens placode forms the lens vesicle. *1* outer layer of optic cup, *2* lens vesicle, *3* hyaloid artery enters through the open embryonic fissure

the anterior iris epithelium and the iris muscles, the outer ciliary epithelium and the retinal pigment epithelium (RPE). The cup is incomplete inferiorly. This cleft is called the embryonic fissure, and it extends from near the lens to the optic stalk and allows vessels of the hyaloid system to get into the eye (Fig. 1.5). Subsequently, the two edges of the fissure fuse.

Differentiation of the *neurosensory retina* begins with three to four rows of cells with high mitotic activity. The inner third is called inner marginal zone and differentiates into the nerve fibre layer. Neural and glial cells keep evolving simultaneously and develop into the inner and outer neuroblastic layers. They are separated by the transient nerve fibre layer of Chievitz, which around 10–12 weeks becomes the inner plexiform layer, except in the macule where it remains until birth. By the end of the third month, the four major horizontal layers of the retina are developed. Between the third and fifth month, the ganglion cells are the first to differentiate and axons enter the optic stalk, inducing the formation of the optic nerve. Photoreceptors arise from the outermost layer of neuroblastic cells, and the differentiation of cones starts in the future foveal area. The differentiation of cone outer segments begins at the fifth month, and the rod outer segments develop during the seventh month when also bipolar cells develop. The development of the retina originates from the posterior area, and prearrangement of foveal organisation starts early because it is the central point from where cells extend peripherally. The foveal pit is recognisable by the seventh month due to the thinning of the inner nuclear layer. By the eighth month, the ganglion cell layers have decreased to two layers, and the inner nuclear layer is reduced to three rows of cells or less because of a lateral displacement of the remaining layers. At birth, the fovea still contains the transient layer of Chievitz, and its maturation to form the foveola begins at 4 months after birth; the remodelling continues until 4 years of age.

Retinal pigment epithelium develops from the outer layer of the optic cup, and at week 6 melanogenesis begins. The RPE are the first cells in the body to produce melanin. The RPE cells turn into cuboidal and cylindrical cells by the fourth month, and RPE is supposed to be functional at this time.

A *primary vitreous* is established during the second month, when mesenchymal cells and the hyaloid system vessels enter the embryonic fissure. Subsequently, as the secondary vitreous develops and is composed of collagen fibrils and hyalocytes, the primary vitreous and its hyaloid system regress, leaving a remnant postnatal channel: the Cloquet's canal. The condensation of collagen fibrils around the lens equator and the outer vitreous constitutes the final tertiary vitreous (Fig. 1.6).

The optic nerve develops from the optic stalk, the connection between the forebrain and the optic vesicle. By the seventh week, the optic disc comprises the hyaloid artery surrounded by axons derived from the ganglion cells. The number of axons rises rapidly reaching the adult level around the 34th week. At birth 75 % of the growth of the optic nerve and disc has developed and 95 % is reached before 1 year of age.

The lens arises from the lens placode (surface ectoderm) under the induction from the underlying optic vesicle. Pax6 acts in this phase as the master control gene, and genes encoding cytoskeletal proteins, structural proteins and membrane proteins

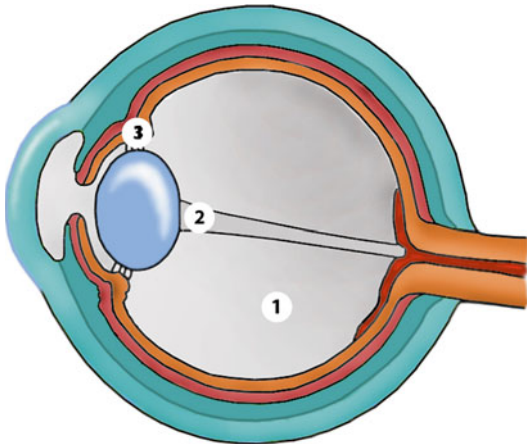

Fig. 1.6 At 9 weeks most structures of the future mature eye can be identified. *1* secondary vitreous, *2* canal of Cloquet, *3* tertiary vitreous

become activated (Fig. 1.5). Invagination of the lens placode leads to the formation of a lens vesicle, and the basal lamina of the epithelial cells makes up the lens capsule. The posterior row of cells stops to divide but elongate to reach the anterior part of the cells. Thereby the primary lens fibres and the embryonic nucleus are formed by the end of the second month. Pre-equatorial cells preserve the mitotic activity and produce the secondary lens fibres that are joined centrally in the shape of a Y anteriorly and as an inverted Y posteriorly. The cells in the anterior part of vesicle remain cuboidal and continue to divide through life. The zonules form from the tertiary vitreous and reach the lens by the fifth month.

The *cornea* develops from the surface ectoderm, when the lens vesicle move into the optic cup, and neural crest-derived cells from the periocular mesenchyme migrate in front of it and into the later cornea. Ectodermal cells form the epithelium. The neural crest-derived mesenchymal cells (mesectodermal cells) become keratocytes that produce collagen fibrils and matrix, thus creating the corneal stroma. The mesectodermal cells also form the corneal endothelium, which becomes a single layer of cells by the third month. The endothelial basement membrane produces the foetal Descemet's membrane.

The *sclera* derives also from the mesectodermal cells around the optic cup; posteriorly these cells migrate into the nerve fibres in the optic nerve to form the cribriform layer.

The *choroid* arises very early in the development from mesectodermal cells around the optic cup. They differentiate into the choroidal stroma, which initially is composed of a framework of collagen fibrils and fibroblasts. Melanocytes appear by the sixth month. A palisade of vessels form externally to the RPE, and the choriocapillaris begins to differentiate. They develop communications with the precursors of ciliary arteries by the second month. In the third month, an outer layer of large vessels (Haller's layer) develops, and along the fourth month, the anterior ciliary and long posterior ciliary arteries form the major arterial circle of the iris. The third layer of medium-sized vessels (Sattler's layer) develops at sixth month.

Ciliary body and iris development commences at the second month with the indentation of the outer pigmented layer of neuroectoderm (future pigmented ciliary epithelium) by small capillaries in the inner vascular mesenchyme. The vascular young branch, covered by a double layer of epithelial cells, enlarges and forms primitive radial folds around the lens, being the basis of the ciliary processes. The ciliary muscle differentiates between the fourth and fifth month from mesenchymal cells between the primitive ciliary epithelium and the anterior sclera. Iris development is related to the formation of a tunica vasculosa lentis. During the third month, there is an expansion of neuroepithelial cells at the cup anterior margin to the primitive ciliary body, growing centripetally between the primitive cornea and the lens surface, incorporating vessels from the pupillary membrane, lying on the anterior surface of the lens. The vascular mesenchyme forms the future iris stroma. Pigmentation of the posterior epithelial layer, which is a continuation of the non-pigmented layer of the ciliary body and neurosensory retina, is completed by the end of the seventh month. Sphincter muscle differentiation from the anterior layer of epithelium starts at 3 months, but complete development finishes at the 8th month. Dilator muscle appears at sixth month as basal extensions of the anterior pigmented iris epithelium, and differentiation continues after birth as well as the full development and pigmentation of stroma.

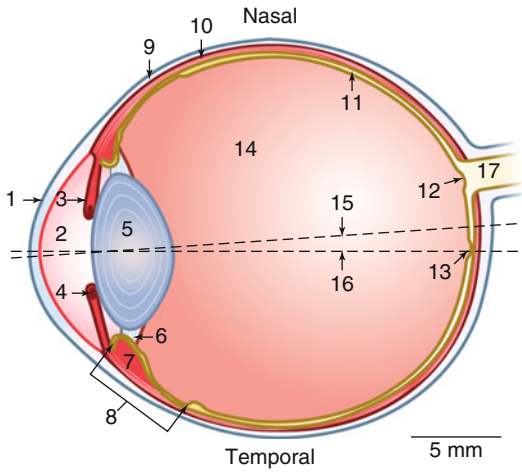

Fig. 1.7 Dimensions and details of a human eye. *1* cornea, *2* anterior chamber, *3* iris, *4* pupillary sphincter muscle, *5* lens, *6* zonules, *7* m. ciliaris, *8* ciliary body, *9* sclera, *10* choroid, *11* retina, *12* optic disc, *13* foveola, *14* vitreous body, *15–16* visual axis, *17* optic nerve

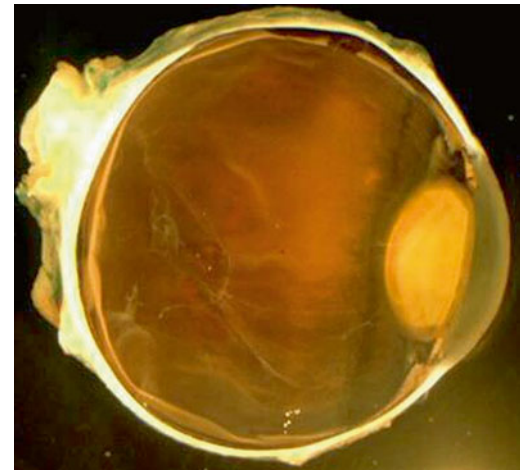

Fig. 1.8 Horizontal section of a human eye

1.2.2 Anatomy

The eye is a specialised organ in the transformation of light energy in the retina into neural potentials transmitted through the optic tract to the brain, where the information is processed as vision. Splendid surveys of the anatomy may be consulted [8, 9]. The eyeball or globe is an almost spherical structure with an anterior-posterior diameter in the adult of about 23–25 mm and 24 mm in transverse diameter. The eye is composed of three concentric layers: the external or fibrous (cornea and sclera), the middle or uvea (iris, ciliary body and choroid) and the inner or neural layer (retina and optic nerve). It contains also three compartments (anterior chamber, posterior chamber and vitreous cavity), and these chambers are filled with aqueous humour and the posterior cavity with the vitreous gel (Figs. 1.7 and 1.8).

1.2.3 External Layer

The external layer of the eyeball consists of the transparent cornea anteriorly (1/6) and the opaque sclera posteriorly (5/6). The transitional zone between the two is the corneal limbus. The external layer is composed of connective tissue with refractive (cornea) and protective functions.

The cornea is a transparent, nearly spherical structure, located in the centre of the anterior pole of the globe and continuous with the sclera at the limbus. In the adult, it measures 12 mm in the horizontal meridian and 11 mm in the vertical, being almost 1 mm thick in the periphery and 0.5 mm centrally. Corneal transparency is due to several characteristics: regularity of the epithelium, avascularity, regular arrangement of stromal components and relative dehydration. Its optical function is important being a positive lens of 43 diopters, i.e. the main refractive element of the eye. The exposed surface of the cornea is covered by the tear film, which is essential for normal corneal function. It lubricates and produces a smooth optical surface and provides nutrients and other components necessary for the maintenance of the ocular surface. The cornea is composed of five layers (Fig. 1.9).

The corneal epithelium is a stratified squamous non-keratinised epithelium of five or six layers attached to the underlying basement membrane by hemidesmosomes. It has a basal layer of columnar cells, then two or three layers of polygonal “wing cells”, and an outermost superficial layer of cells that are flattened and thin. New cells are derived from mitotic activity in the basal-peripheral cell layer. The new cells float towards the centre and displace older cells

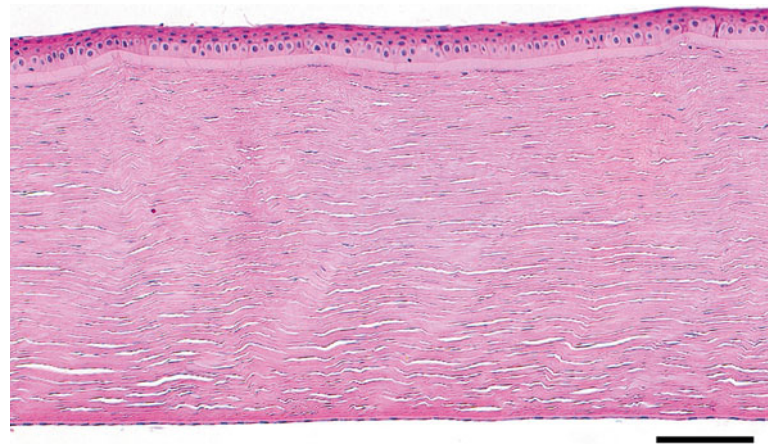

Fig. 1.9 The normal cornea is composed of five layers, i.e. the epithelium, Bowman's layer, the stroma, Descemet's membrane and the endothelium. H&E stain, bar = 100 µm

superficially and centripetally. Non-epithelial cells may appear as wandering histiocytes, macrophages, lymphocytes and antigen-presenting Langerhans cells.

The Bowman's membrane or layer is considered a modified region of the stroma and consists of a uniform acellular zone below the epithelial basement membrane, tightly bound to the corneal stroma. It is composed of small collagen fibres and has pores for the terminal branches of corneal nerves, which continue into the basal layers of the epithelial cells. Bowman's membrane is not regenerated after injury.

The stroma constitutes 90 % of the corneal thickness and is a dense connective tissue of extraordinary regularity and consists of collagenous lamellas oriented parallel to the corneal surface, with modified flattened fibroblast containing crystallines, termed keratocytes. The transparency of the cornea is highly dependent on the arrangement of the collagen fibrils, which is regulated by glycosaminoglycans and proteoglycans. The stroma is avascular but sensory nerve fibres are present in the anterior layers to reach the epithelium.

Descemet's membrane is the basal lamina of the corneal endothelium, and its thickness increases with age. It is composed of the anterior zone band, developed before birth, and the posterior non-banded zone formed by corneal endothelium. The non-banded zone grows through the entire life of the person.

A separate structure *the Dua layer* has recently been suggested to exist [10]. The layer is ascribed to the cleavage site when performing Descemet's membrane pealing. It is an acellular structure found beyond the last row of keratocytes, measuring 10 µm in thickness, and is composed of five to eight lamellas of predominantly type I collagen bundles arranged in transverse, longitudinal and oblique directions. Its recognition has not yet been confirmed by other authors and it cannot be identified by ordinary histology.

The corneal endothelium is a monolayer of hexagonal cells derived from the neural crest; they contain large nucleus and abundant mitochondria. The main function of the endothelium is to maintain corneal dehydration and transparency. The cells have a low regenerative capacity and decrease in number with age. Lost cells are replaced by spreading of the adjacent cells. Endothelial dysfunction leads to oedema of the stroma and loss of transparency.

The sclera, in contrast to the cornea, is opaque and has an anterior opening for the cornea and a posterior for the optic nerve, crossed by lamina cribrosa. It consists of bundles of collagen, fibroblasts and ground substance. It is essentially avascular except anteriorly where it is covered by episclera and is crossed by numerous emissary channels through which pass arteries, veins or nerves. The four rectus muscles insert anteriorly around the limbus forming the spiral of Tillaux. The medial rectus muscle inserts closer

to the limbus (5.5 mm) and the superior muscle the farthest (7.7 mm). The equator of the eyeball is approximately 16 mm behind the limbus (Fig. 1.10). Posteriorly, the insertions of oblique muscles in the temporal halves and the vortex veins in the four quadrants are found. The short posterior ciliary arteries and nerves enter around the optic nerve. Two long ciliary nerves and arteries enter at the horizontal meridian on each side of the optic nerve and advance through the suprachoroidal space to the ciliary body. The optic channel is crossed by a fenestrated plate, the lamina cribrosa, where the axons from the ganglion cells meet to exit the eye forming the optic nerve.

Fig. 1.10 An enucleated eye seen from behind. Note the emissaries as bluish structures

The limbus is the transitional zone between the transparent cornea and the opaque sclera, relevant due to the relation with the anterior chamber angle. At this location, the corneal epithelium is continued into the conjunctival epithelium, increasing the number of cell layers and with the appearance of a sub-conjunctival tissue containing vessels and progenitor stem cells, responsible for the turnover of corneal epithelial cells. Bowman's membrane ends, and the transparent corneal stroma continues with the opaque sclera, drawing a concavity called external scleral sulcus. Deep in the limbus, the Descemet's membrane ends in the Schwalbe's line where the anterior chamber angle begins (Fig. 1.11).

The anterior chamber angle is situated at the confluence of the cornea, sclera and iris and is limited anteriorly by Schwalbe's line and posteriorly by the scleral spur (Fig. 1.11). The inner sclera forms the internal scleral sulcus containing the trabecular meshwork and the Schlemm's canal, the main structures in the drainage of the

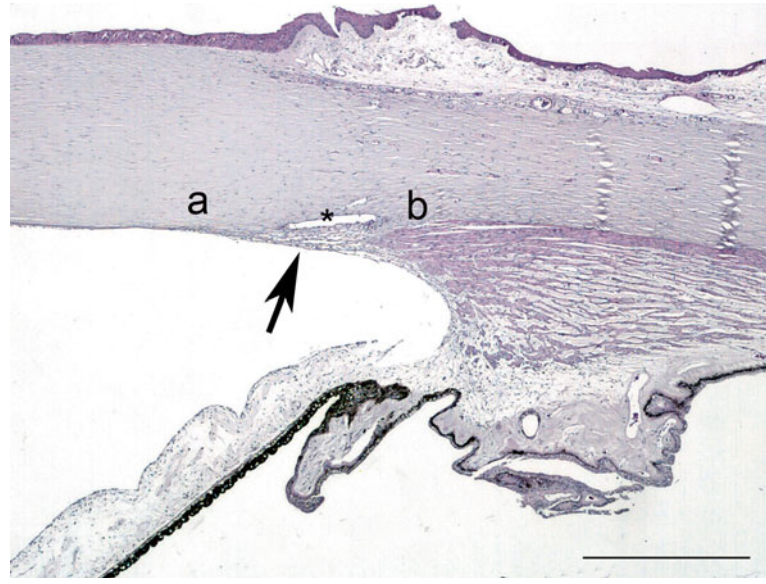

Fig. 1.11 The limbal area and the chamber angel. The trabecular meshwork (*arrow*) is located between the Schwalbe's line (*a*) and the scleral spur (*b*) and makes up the internal wall of the Schlemm's canal (*asterisk*). H&E stain, bar = 200 μm

aqueous humour. The longitudinal ciliary muscle fibre inserts in the scleral spur and myofibroblast-like cells are found circumferentially.

1.2.4 Middle Layer

The uveal tract is the middle vascular pigmented layer of the eye which consists of the choroid, ciliary body and iris. These constituents are continuous and have an opening anteriorly, the pupil, and posteriorly they surround the optic nerve channel. The uvea is responsible for the nutrition of most intraocular components, but the passage of nutrients into the eye is controlled by vascular barriers. In the iris, the capillary endothelium is non-fenestrated; in the ciliary body, the blood-aqueous barrier; and in the retina, the outer blood-retina barrier. The uvea is attached firmly to the sclera in three locations only: at the scleral spur, at the exits of the vortex veins and at the optic nerve.

The iris is the anterior part of the uvea and has a central hole, the pupil. The iris stroma adapts to its variable size being loose and mobile, presenting folds during mydriasis and being relatively smooth in miosis. It is the border between the anterior and the posterior chambers. The iris is composed of the anterior surface, the mesectodermal stroma and the two posterior, pigmented epithelia (Fig. 1.12). The anterior surface is an accumulation of stromal components, avascular and without continuous cell coverage, characteristically irregular with ridges and folds. The stroma is composed of connective tissue and pigmented and non-pigmented melanocytes whose density of pigmentation is responsible for the iris colour. The stroma near the pupil contains the sphincter muscle, a circular band of smooth muscle fibres around the pupillary margin (Fig. 1.13). Blood vessels follow a radial course from the major arterial circle towards the pupil forming the minor vascular circle of the iris, usually incomplete. The anterior epithelial layer emits non-pigmented cytoplasmic extensions with myofibrils constituting the iris dilator muscle. The posterior iris pigment epithelium is heavily pigmented. The two iris epithelia continue uninterruptedly with the ciliary epithelia.

The ciliary body has a triangular shape with the base in the iris and the vertex to the choroid. Its main functions are aqueous humour formation and lens accommodation. It is consists of a pars plicata and a pars plana (Fig. 1.14). The pars

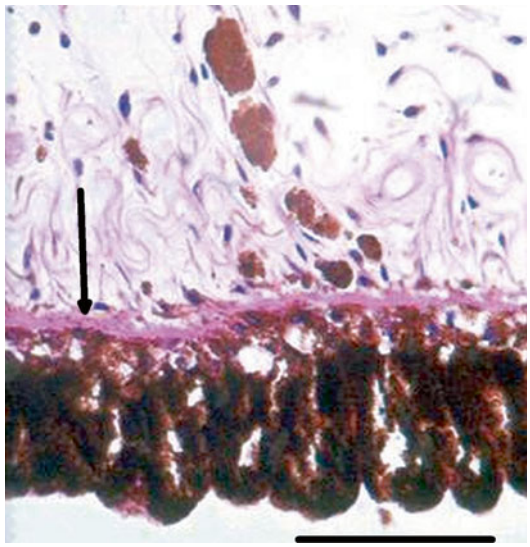

Fig. 1.12 The two pigmented epithelial layers of the iris. *Arrow* at dilatator muscle within the anterior epithelial layer. H&E stain, bar = 50 µm

Fig. 1.13 Pupillary margin. Note the sphincter muscle in the stroma near the pupil. H&E stain, bar = 100 µm

plicata is composed of approximately 70 radial folds, the ciliary processes, consisting of a vascular connective axis covered by a double epithelial layer (pigmented and non-pigmented) which continues uninterruptedly with the epithelium of the iris and the pars plana (Fig. 1.15).

The epithelial cells are joined by tight junctions forming a barrier to the passage of blood products to the posterior chamber, thus constituting the blood-aqueous barrier. In the depth of the pars plicata is the ciliary muscle with three layers: the outer-longitudinal, the middle-radial and the inner-circular muscles functioning as one unit. The zonules of the lens are attached to the ciliary processes. Contraction of the ciliary muscle relaxes the tensile force of the zonules, allowing accommodation of the lens for near vision. The pars plana consists of a thin layer of connective tissue covered by two separate epithelial cell layers, continuous with those of the pars plicata. The inner non-pigmented epithelium is pseudostratified and is strongly linked to the vitreous. The point where the non-pigmented inner layer becomes a multilayer marks the beginning of the neurosensory retina and is known as the ora serrata, with a characteristic anatomical and clinical morphology recognisable at clinical examinations (Fig. 1.15).

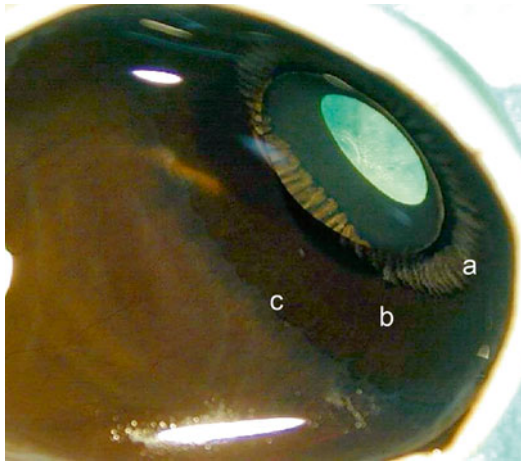

Fig. 1.14 View of ciliary body from behind. Pars plicata (*a*) has a folded structure, pars plana is flat (*b*) and ora serrata (*c*) is the border towards the retina

The choroid is the posterior portion of the uvea, and its main function is to nourish the outer portion of the retina and to keep the temperature of the retina within normal metabolic range – the photosensory mechanisms and the degradation of photons within the retina create immense heat. The choroid is composed of vessels, connective tissue and melanocytes. Perfusion comes from the long and short ciliary arteries and from retrograde branches from the perforating anterior ciliary arteries in the periphery. It consists of three

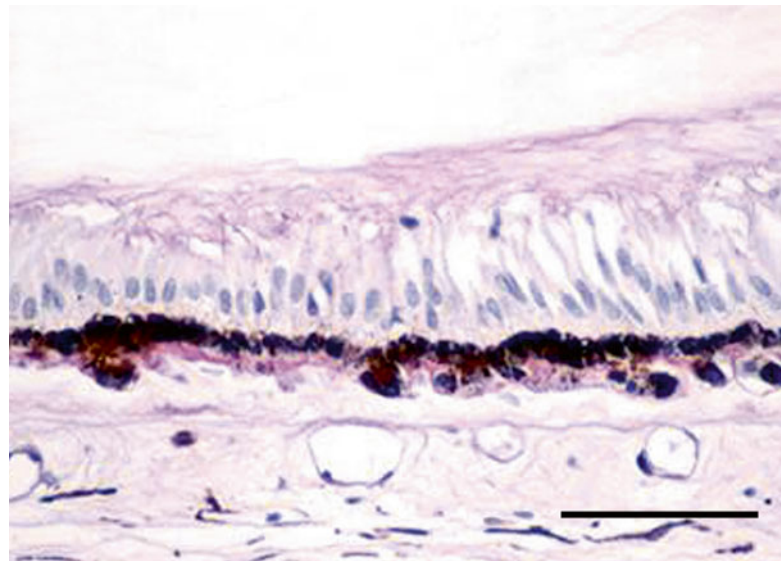

Fig. 1.15 Ora serrata. The non-pigmented ciliary epithelium transform to elongated cells that more posteriorly continues into the neuroretina. H&E, bar = 100 µm

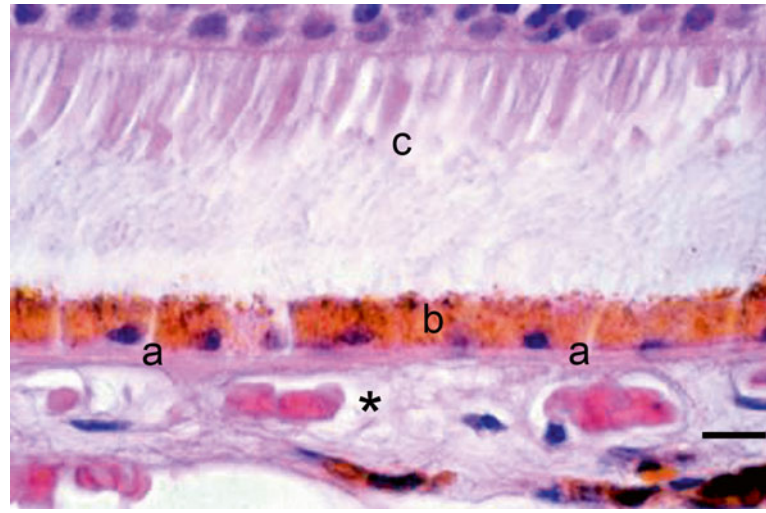

Fig. 1.16 Choriocapillaris (*asterisk*) is situated outside the Bruch's membrane (*a*), the retinal pigment epithelium (*b*) and the photoreceptor outer segments (*c*). H&E, bar = 10 μm

layers: externally large vessels, at the middle small vessels and at the innermost the choriocapillaris, with its tightly packed capillaries containing multiple fenestrations facing the retina. Bruch's membrane is a membrane resulting from the fusion of the basement membranes of the retinal pigment epithelium and the choriocapillaris. It is highly permeable to small molecules, but the tight junctions between the RPE cells prevent the free passage of substances into the retina, i.e. the outer blood-retina barrier (Fig. 1.16).

1.2.5 Inner Layer

The retina is the innermost layer of the eye. It is the focus for the eye's optical system and contains photoreceptors and neural elements in which photons are transformed to visual neural impulses that are transmitted to the brain. Branches from the central retinal artery vessels enter through the optic nerve and divide in nasal, temporal, superior and inferior branches. The blood vessels are similar to the cerebral blood vessels, composed of non-fenestrated endothelial cells with tight junctions, constituting the inner blood-retina barrier.

The retina is composed of the outer RPE and the inner neurosensory retina with nine different layers (Figs. 1.17 and 1.18).

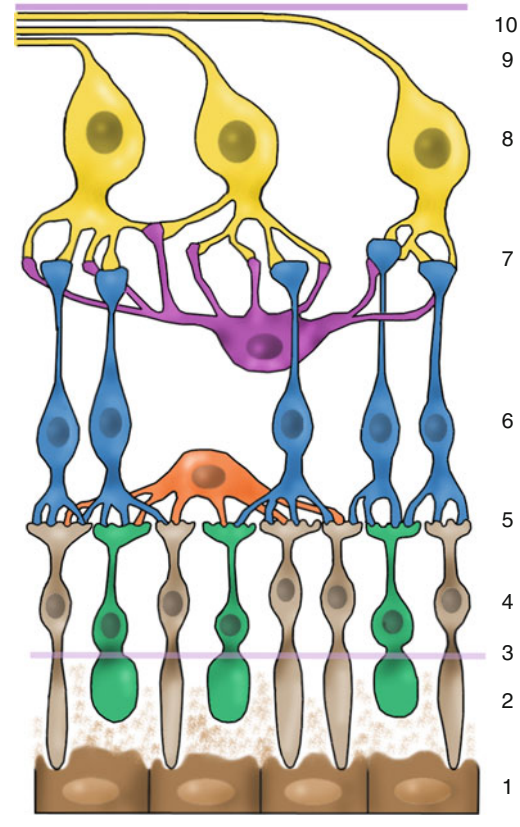

Fig. 1.17 Drawing of retina with major structures. *1* retinal pigment epithelium, *2* photoreceptor outer segments, *3* external limiting membrane, *4* outer nuclear layer, *5* outer plexiform layer, *6* inner nuclear layer, *7* inner plexiform layer, *8* ganglion cell layer, *9* nerve fibre layer, *10* internal limiting membrane

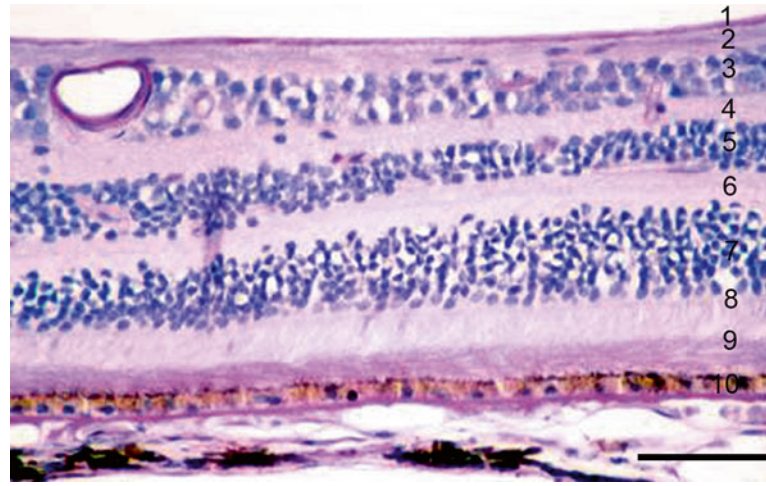

Fig. 1.18 The retinal layers. *1* internal limiting membrane, *2* nerve fibre layer, *3* ganglion cell layer, *4* inner plexiform layer, *5* inner nuclear layer, *6* outer plexiform layer. *7* outer nuclear layer, *8* outer limiting membrane, *9* photoreceptor outer segments. *10* retinal pigment epithelium. H&E, bar = 100 µm

RPE is a regular monolayer of highly pigmented cells continuous with the pigmented epithelium of the ciliary body. Its basal cytoplasmic membranes and its basement membrane form the inner layer of Bruch's membrane. The apical surface of the RPE cells has processes that surround the photoreceptor outer segments. The main functions include the outer blood-retina barrier (active transport of nutrients to the outer retinal layers), vitamin A metabolism, absorption of stray light and maintenance of the outer segments of the photoreceptors.

The neurosensory retina consists of neuronal and glial cells. The photoreceptors are highly specialised cells – rods and cones. Their outer segments are in contact with the apical processes of the RPE surrounded by a mucopolysaccharide matrix. The inner segment contains the synaptic body to establish the connection with dendrites from bipolar cells and horizontal cells. Axons from bipolar cells synapse with ganglion and amacrine cells. The axons from ganglion cells become parallel to the inner surface of the retina to form the nerve fibre layer and to merge to constitute the optic nerve. Temporal fibres follow a curved path around the macula, and fibres from the fovea travel straight to the optic nerve. Glial cells are mainly Müller cells that extend from the external to the internal limiting membrane and together with astrocytes and microglia provide support and nutrition to the retina.

The central retina – the posterior pole or the macula – lies between the temporal vascular arcades; outside this area is the peripheral retina. In the centre of the macula is an area 1.5 mm in diameter – the fovea – responsible for higher visual acuity and colour vision. At the centre of the fovea is a central depression, the foveola, approximately 0.35 mm in diameter. In this area, there is only the photoreceptor layer composed exclusively of cones and responsible for the highest visual acuity. In the macular area the retina is thicker; the RPE cells are taller and contain more and larger melanosomes. In the neuroretina of this region, the cones are still the dominant photoreceptor type, and the ganglion cell layer has several rows of cells (Fig. 1.19). In the periphery the retina is still thinner and dominated by rods (Fig. 1.20).

1.2.6 Optic Nerve

The ganglion cell axons meet at the back of the eyeball, preserving the retinotopic organisation in the optic nerve head formed by four layers.

The superficial nerve fibre layer, composed of the non-myelinated ganglion cell axons with spots of myelinated fibres resulting from migration of oligodendrocytes through the lamina cribrosa.

The pre-laminar region in which the ganglion cell axons are organised into bundles supported by astrocytic glial cells that pass through the lamina cribrosa.

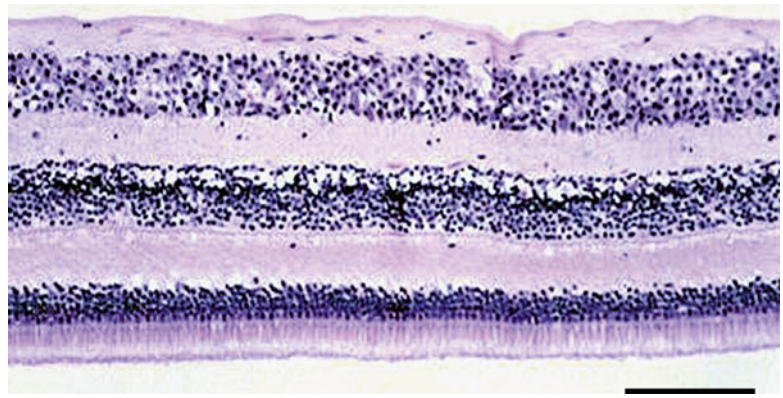

Fig. 1.19 Retina at the macular area. Note the thick ganglion cell layer. H&E, bar = 100 μm

Fig. 1.20 Retina at the equator has less ganglion cells than at the macula. H&E, bar = 100 μm

The laminar portion or lamina cribrosa consists of sheets of connective tissue with type I and III collagen, elastin, laminin and fibronectin, which comprise about ten fenestrated connective plates integrated with the sclera, and with pores traversed by the axon bundles (Fig. 1.21).

The retro-laminar portion, where nerve fibres become myelinated, is surrounded by meningeal sheaths constituting the optic nerve. This portion continues to the apex of the orbit forming the orbital part of the optic nerve (Fig. 1.21).

1.2.7 Lens

The lens is a biconvex structure located behind the posterior chamber and the pupil. Its main function is refractive. Reduced tension of the zonules, controlled by the ciliary muscle, changes the radius of curvature of the lens, creating the accommodation required for near vision. The lens lacks innervation, is avascular and depends on the aqueous and vitreous humour for nutrition. To understand the structure of the lens, it is necessary to remember its embryologic origin from an invagination of surface ectoderm. The lens capsule is the basement membrane of the lens epithelium. It is thicker in the front (as it is produced throughout life by the anterior epithelium) than in the back (only produced during the embryonic period where the posterior epithelium still exists as an epithelium). The anterior epithelium is a low prismatic monolayer located under the anterior capsule. It grows radially, and at the lens equator, the cells divide and migrate into the lens vesicle. The cells elongate, sending processes anteriorly and posteriorly, and mature to be lens fibres, forming the adult lens cortex. Mitotic activity is highest in

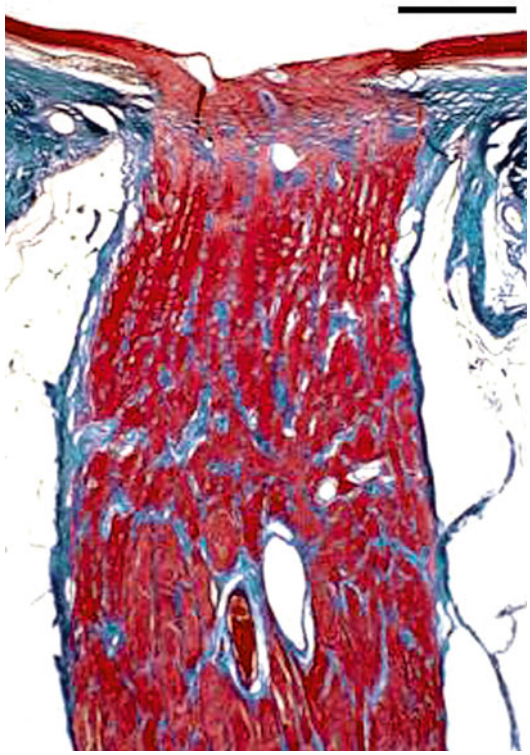

Fig. 1.21 Longitudinal section of the optic nerve. Masson trichrome stain, bar = 100 μm

the pre- and equatorial lens epithelium known as the germinative zone. The lens sutures are formed by the interdigitations of the anterior and posterior tips of the fibres. When new lens fibres are formed, the older are pushed deeper into the cortex. The old lens fibres do not contain nuclei. In the final transformation, the fibres fuse forming the adult lens nucleus.

1.2.8 Vitreous Body

The vitreous cavity occupies four fifth of the posterior eyeball having a volume close to 4 ml. The cavity contains the vitreous body, which has a gel-like structure. It contains 99 % water together with collagen fibres in which hyaluronic acid molecules are bound. Although the vitreous body is mainly acellular, a few cells – hyalocytes – appear mainly in the cortex. The main function of the vitreous body is the metabolic maintenance of intraocular structures like lens, ciliary body and retina. The vitreous body consists of the cortical and the central vitreous. The cortical vitreous contains more densely packed collagen fibrils that at the peripheral border form the hyaloid membrane. The hyaloid membrane is attached to the retina and pars plana by condensation of collagen fibrils. The binding is tight at the peripheral retina, along the margins of the optic disc and around the fovea and retinal vessels. The central vitreous is traversed by a central canal, the hyaloid or Cloquet's canal, representing the remnants of the hyaloid artery in the foetal eye.

1.3 Development

1.3.1 The Eyeball

The globe as such evolves throughout life, and the physiological changes can be observed as growth and ageing. The anterior-posterior diameter of the eye is approximately 16 mm at birth, reaching around 23 mm by 3 years of age and adult size before puberty. Details of the ocular development are presented in resent publications [8, 11].

In the cornea the Descemet's membrane increases its thickness through life. In elderly people, peripheral excrescences known as Hassall-Henle warts develop at the posterior aspect of the Descemet's membrane. Central excrescences (cornea guttata) may also appear with increasing age (Fig. 1.22). The number of endothelial cells decreases with age. There are approximately 4,000 cells/mm^2 at birth, 2,500 in middle age and 2,000 in old age. Consequently, with age, the hexagonal arrangement typical of young corneas is replaced by a fewer cells with heterogeneous size and shape. These cells have a low regenerative capacity and decrease in number with age, and lost cells are replaced by spreading of the adjacent cells.

The population of endothelial cells of *the trabecular meshwork* also decreases over time, and together with the deposition of extracellular materials in the trabeculum, the resistance to aqueous humour outflow increases and the intraocular pressure increases.

In the lens, the continuous process of proliferation and differentiation of epithelial cells from the

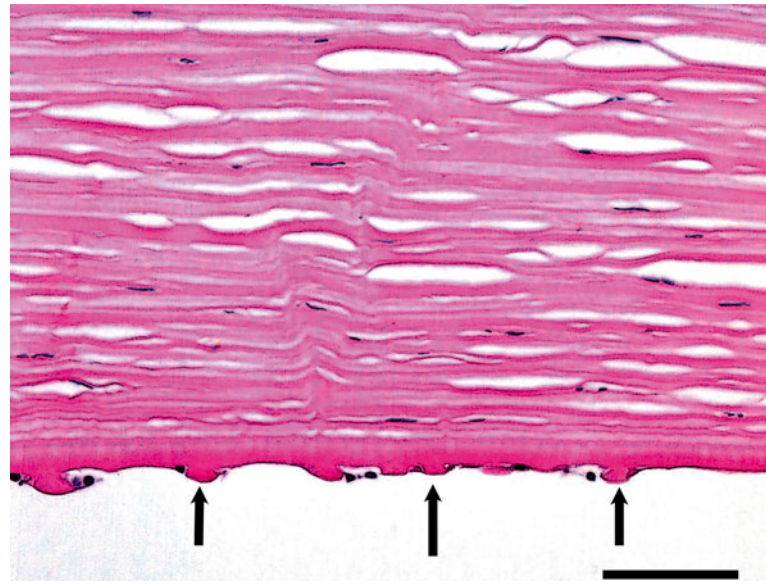

Fig. 1.22 Inner aspect of the cornea in a person with Fuch's endothelial dystrophy. *Arrows* at guttate excrescences on Descemet's membrane. H&E, bar = 75 µm

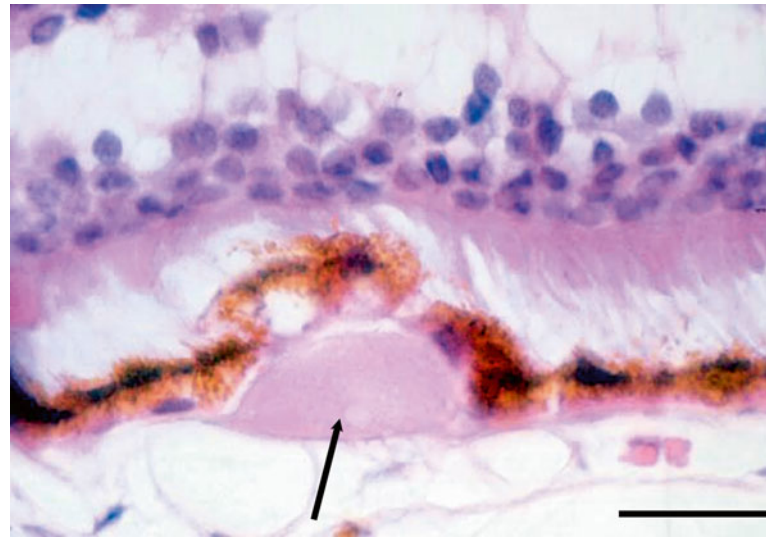

Fig. 1.23 Drusen (*arrow*) between the retinal pigment epithelium and Bruch's membrane. H&E, bar = 50 µm

equator and in ward continues throughout life. The lens nucleus increases the size and transparency gradually decreases. The anterior epithelium may disappear focally or may undergo fibrous metaplasia (anterior subcapsular opacities) or may migrate to the posterior subcapsular area.

Microcysts may appear in the peripheral *retina* immediately behind the ora serrata due to degenerative occlusive disease in the peripheral arterioles producing ischaemia: peripheral microcystoid degeneration. Cyst may join to form a retinoschisis in the outer plexiform layer or a large cyst. RPE display pleomorphism and a decrease in number. With time, the material from the degradation of outer segment discs gradually accumulates within the RPE as lipofuscin. A further, aberrant excretion of the material takes place in the form of basal laminar deposits and other substances at the retinal side of the Bruch's membrane forming drusen (Fig. 1.23).

1.4 Congenital Abnormalities

1.4.1 Anophthalmia

Definition
Anophthalmia means, in ophthalmic pathology, a complete lack of any ocular structures in the orbit.

Synonyms
Anophthalmos, anopia

Epidemiology
Extremely rare. In our files at ØPI-DK, there are none.

Aetiology
Complete lack of development of the ophthalmic vesicle in the fourth embryonic week results in a complete lack of an eyeball or any bulbar structures in a small orbit that contains orbital fat, vessels, peripheral nerves, rectus muscles (from the mesoderm not induced by the ophthalmic vesicle) and tear gland.

Clinical Features
The patient presents with rather normal eyelids and conjunctiva in a small orbit. No ocular structures can be detected by palpation and imaging including ultrasound, and no movements of an eye can be discerned. Mostly, when an eye cannot be detected clinically, anophthalmia is diagnosed. However, the histology of orbital tissue from such cases most often demonstrates rudimentary eye structures, i.e. a case of microphthalmia.

Genetics
A number of genetic disturbances are known to be involved in anophthalmia; however, these are also bound to the presence of microphthalmia, and since most of these studies are not based on a very careful analysis of the content of the orbit harbouring the anophthalmic eye, the known gene defects are termed to cause anophthalmia/microphthalmia. A recent review presents an up-to-date survey [12]. Some defects are also described under microphthalmia below.

1.4.2 Congenital Cystic Eye

Definition
Cystic structure lined by connective tissue, pigmented cells and glial strands

Epidemiology
Very rare

Aetiology
At the 7.5 mm stage of the embryo, the optic vesicle invaginates to form the optic cup. If this process is disturbed at this stage, the result is a disorganised cystic structure. The content of the cyst is glial structures, and the wall contains scleral lamellas, muscle and fibrovascular tissue.

1.4.3 Microphthalmia

Definition
The presence of a rudimentary eye in the orbit

Epidemiology
Very rare, 1–3/10,000 live births [13]. At the ØPI-KU, we have four cases; however, the two are associated with cysts (see below), one with cryptophthalmia and one with a PNET tumour of the optic nerve of that eye [14].

Aetiology
Causative chromosomal aberrations are found in approximately 30 % of cases, and the number of cases with known causative gene defects is increasing [15–18].

Clinical Features
The spectrum of clinical manifestations is wide from bilateral microphthalmia with severe cranial and systemic defects like in patients with SOX2 mutations [15, 16] to unilateral microphthalmia with limited systemic defects [12].

Histopathology
Histologically, the findings are very varied from small strands of neuroepithelium and lens anlage to small eyes with anterior segment dysgenesis,

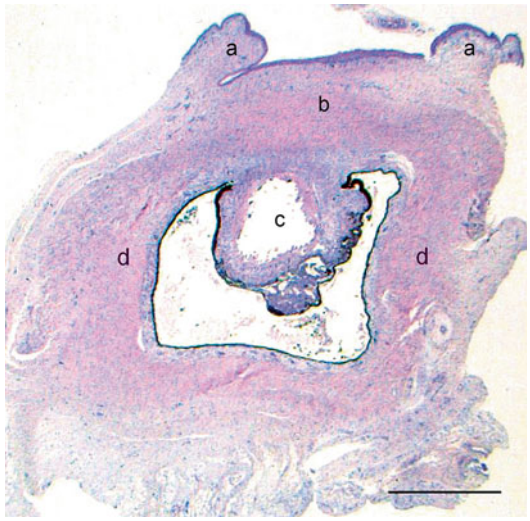

Fig. 1.24 Foetal microphthalmic eye. Eyelids are present (*a*). The anterior chamber is not formed and the cornea (*b*) rests against the cataractous lens (*c*). The sclera is formed (*d*). H&E, bar = 400 μm

iris coloboma, cataract retinal dysplasia and optic disc hypoplasia (Fig. 1.24) [18].

Genetics

A large series of genetic deviations and distinctive syndromes has been described with anophthalmia/microphthalmia and associated systemic findings – SOX2, OTX2, STRA6, BCOR, HCCS, BMP4 and SMOC1 [12, 19, 20]. But also a number of other chromosomal defects are found together with anophthalmia/microphthalmia like GDF6, VSX2, RAX, SHH, SIX6 and PAX6 [12, 19, 20].

1.4.4 Nanophthalmia

Definition

A small but otherwise normally composed eye

Synonyms

Nanophthalmos, dwarf eye

Epidemiology

Rare

Aetiology

Not known

Clinical Features

The eye appears with generally reduced ocular dimensions. Especially the anterior segment and chamber angles are involved [21]. The most important consequence of nanophthalmia is the thickened sclera which together with the changes in the anterior segment makes the eyes more prone to surgical complication like retinal detachment, choroidal effusion and glaucoma [21, 22].

Histopathology

The most striking feature is the thickened sclera in which the scleral lamellas seem wavier and are separated by an increased amount of glycosaminoglycan.

1.4.5 Cryptophthalmia

Definition

Cryptophthalmia indicates that the eye is hidden behind what looks like a normal facial skin, i.e. eyelid structures cannot be identified. Behind the skin, an eyeball may be palpated, movements may be seen and rarely the child reacts upon light through the skin in front of the orbit. The skin covering the eye consists of facial skin and of corneal tissue, indicating that the eye is not normally developed, and it is not possible to separate the skin over the eyeball from the cornea without entering the anterior chamber. This condition is very rare and is mostly combined with a microphthalmic eye [23].

1.4.6 Synophthalmia and Cyclopia

Definition

Appearance of a single eye structure in the midline of the face

Epidemiology

Very rare. At ØPI-KU we have two cases on file.

Fig. 1.25 Foetus with synophthalmus. Note the proboscis (*asterisk*) above the fused two eyes

Aetiology

Defective development of the frontal lobe of the face is associated with a defective separation of the two ocular anlage leading to fusion of the eyes.

Clinical Features

The face of the newborn is characteristic: the nose and the frontal part of the upper lip are replaced by a tubular structure – proboscis – over the single eye that is situated in the midline of the face (Fig. 1.25). The four eyelids surround the eye and may appear rather well developed. There is only one incomplete orbit and severe skull base defects behind it.

Fig. 1.26 Synophthalmic eye of a foetus (Fig. 1.25). Two corneas are present separated by limbal tissue covering the fused ciliary bodies

Macroscopy

In most cases, the single eye is a synophthalmic eye, and the cornea is therefore seen as a double structure (Fig. 1.26). The globe may have normal dimensions and have extraocular muscles. The optic nerve is mostly single and dysplastic.

Histopathology

The eye is very rarely a true single eye – cyclopia – but is an incomplete fusion of the two ocular anlage. Characteristically the fusion is less complete; the more anterior in the eye (Fig. 1.27). The two corneas are separated by a thin line of connective tissue. The iris and ciliary body are well developed in the peripheral parts, but rudimentary behind the corneal separation. The anterior chamber has two rooms and the lens is doubled. The sclera and choroid appear as one structure, the retina has a thin septum in the midline. The retina is thin and may contain dysplastic rosettes (Fig. 1.28). Most often there is only one optic disc and one dysplastic optic nerve.

Prognosis and Predictive Factors

Synophthalmia and true cyclopia are followed by other severe cerebral and cranial defects, and the conditions are not compatible with life.

Fig. 1.27 Anterior part of synophthalmic eye demonstrating two lenses behind the corneas. H&E, bar = 250 μm

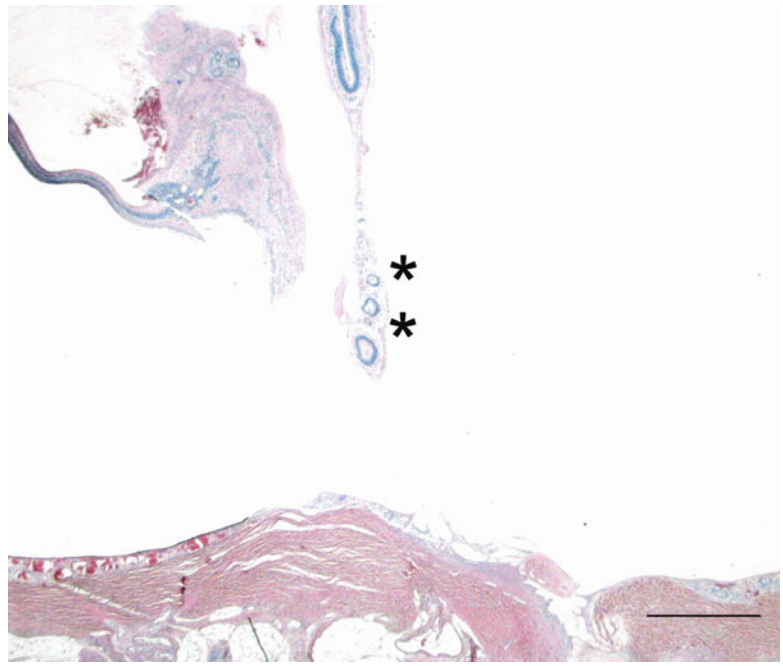

Fig. 1.28 Posterior part of synophthalmic eye with retinas. The retinal septum between the two parts is gliotic and contains malformation rosettes (*asterisks*). H&E, bar = 250 μm

1.4.7 Coloboma of Iris, Choroid, Retina and Optic Nerve

Definition

Defect in the involved tissue due to incomplete fusion of the fissure of the optic vesicle. In this chapter, the various colobomas, involving only parts of the globe, are briefly described because they are dealt with in details in their relevant chapters.

Aetiology

When the optic vesicle folds, forming the optic cup, creating the inner and outer layers of neuroepithelia in the eye, the folding is eccentric giving rise to a fissure below nasally involving also the anterior parts of the optic disc, the foetal fissure. Along the fissure the two neuroepithelial layers fuse. Defects in fusing of the foetal fissure result in coloboma formation. In the fissure, the inner layer

of the vesicle creates an everted cystic fold. In some cases of coloboma formation, this tissue is entrapped in the coloboma, giving rise to a glial scar and cyst formation.

1.4.7.1 Iris Coloboma

The coloboma involves all iris structures. The shape of the defect is like a rounded V pointing downwards and a little nasally. The pigment pupillary rim is missing in the coloboma and the sphincter function may be defective.

Histology

At the edges of the coloboma the iris structures are rounded, but no scarring is observed.

1.4.7.2 Retino-Uveal Coloboma

The lack of retinal tissue and RPE in the area of the coloboma induces a lack of normal formation of uveal tissue in the coloboma region. Therefore, the defect appears as a white lesion at ophthalmoscopy and at sectioning of the eye. The sclera is not missing in the coloboma area.

Histology

At the centre of the coloboma, the naked sclera is observed. Near the rim of the coloboma glial strands of the inner retina are found they represent the everted non-fused parts of the foetal fissure. Where normal retina appears outside the coloboma, it is followed by normal RPE and choroid.

1.4.7.3 Optic Disc Coloboma

Typically, the coloboma is located downwards in the disc extending through the lamina cribrosa to the optic nerve. The colobomatous defect may be partly filled with glial tissue.

Histology

At the rim of the coloboma, towards the retina, a complete lack of nerve fibres is observed, and the adjacent retina is dysplastic with rosettes; the RPE is missing. Inside the coloboma the normal disc structures are replaced by randomly arranged glial strands.

1.4.8 Microphthalmia with Cyst

Definition

In rare cases, the coloboma mainly involves the outer layer of the optic vesicle – the RPE to be – and the consequence is the formation of a microphthalmic eye with a defect of the sclera and/or optic nerve downwards and posterior through which a cyst from the inner layers of optic vesicle is formed.

Synonyms

Microphthalmic eye with cyst, cystic microphthalmic eye

Epidemiology

Very rare. At the ØPI-KU, we have collected four cases through 100 years; and less than 150 cases have been described in the literature, and only one third of them were bilateral [24].

Clinical Features

The cyst may be very small and the eye only slightly disturbed if the coloboma is limited. With larger coloboma the cyst involves all ocular layers and the optic vesicle, and the eye is clearly microphthalmic clinically. Microphthalmia with cyst is most often monolateral; however, bilateral cases have been documented [24, 25]. Typically the child present at birth with closed eyelids. The inferior eyelid appears expanded and blue (Fig. 1.29). Clinically an orbital bleeding or a tumour is suspected. Examination in general anaesthesia reveals the microphthalmic eye under the orbital roof (Fig. 1.30), and imaging demonstrates the small eye in connection with a cyst (Fig. 1.31).

Histopathology

The eye appears microphthalmic; however, changes are dependent of the localisation of the defect in the fissure from where the cyst develops. If the defect is posterior, involving only the most posterior part of the retina and extending down into the optic nerve, the intraocular structures may be rather normal. If the defect is anterior, the

Fig. 1.29 Newborn child with bilateral microphthalmic eyes with cysts. The inferior eyelids are expanded by the cysts giving the clinical impression of orbital haemorrhages

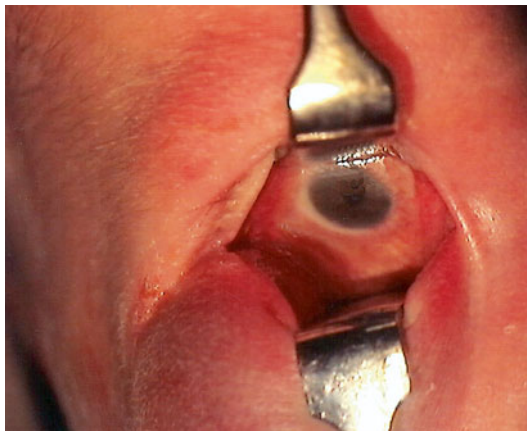

Fig. 1.30 Preoperative view of the right orbit. The microphthalmic eye is pushed up under the orbital roof

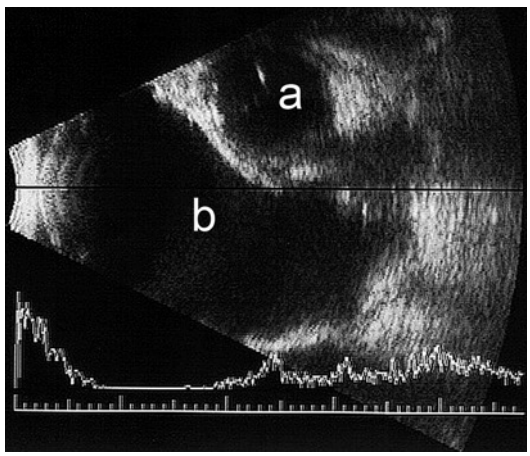

Fig. 1.31 Ultrasound scans of an orbit with a microphthalmic eye with cyst. The small eye (*a*) is seen above the large cyst (*b*)

intraocular structures are severely disturbed and the eye is without any visual capacity. The cyst itself is composed of gliotic retinal tissue covered with a thin layer of connective tissue – a thin sclera layer (Fig. 1.32). The glial tissue does not contain RPE cells but may have ganglion cells.

Differential Diagnosis

Other types of microphthalmia

Genetics

Extraocular malformations have been found more frequently with bilateral than with monolateral cases [26].

Prognosis and Predictive Factors

Microphthalmic eyes with cysts are mostly removed early because the cyst tends to grow and cause problems. However, in a few cases, surgery has successfully been performed removing the cyst and closing the defect towards the eye/optic nerve. In one such bilateral case, one of the eyes has even obtained a visual acuity of 0.1 [25].

1.4.9 Anterior Cleavage Syndrome

Definition

Defective formation of the anterior chamber

Aetiology

The surface ectoderm covering the optic cup is the future corneal epithelium. Neural crest cells migrate to fill the space between the surface ectoderm and the optic cup. This tissue gives rise to all tissues around the future anterior chamber. Defective separation leads to the various aspects of the anterior cleavage syndrome which are described in the cornea chapter (see also pages 85 and 206).

1.4.10 Buphthalmia

Definition

Large cloudy cornea present at birth in a glaucomatous eye

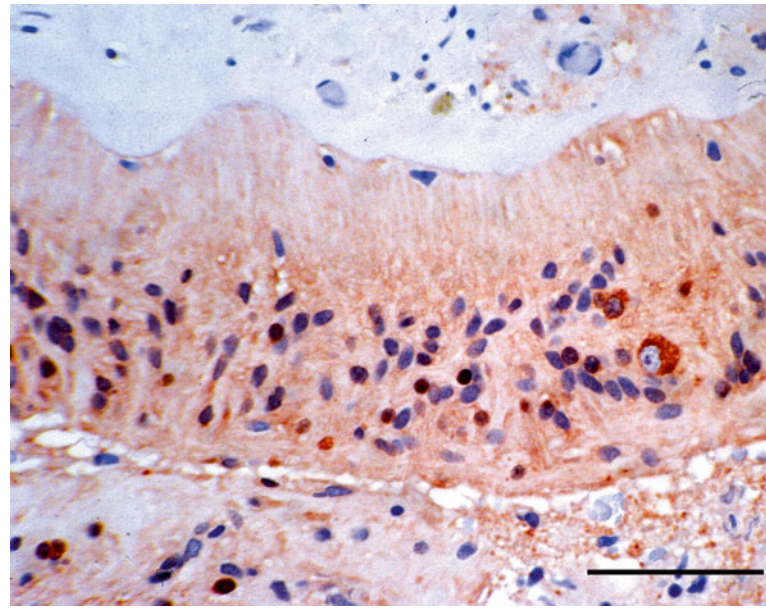

Fig. 1.32 Cyst wall from microphthalmic eye with cyst. In some areas the glial wall contains ganglion cells. S-100 stain, Bar = 100 µm

Epidemiology

Rare. Approximately half of the cases of congenital and early childhood glaucoma are hereditary, non-syndrome-linked primary open-angle glaucoma due to malformations in the drainage system.

Aetiology

During the formation of the anterior chamber disturbances in the formation of the chamber angle may lead to partial closing the angle, dys- or aplasia of Schlemm's canal, malpositioning of the scleral spur and defective trabeculum [27]. The result of these changes may be an increased intraocular pressure due to insufficient drainage of the aqueous humour during the intrauterine period. Since the foetal cornea, in contrast to the adult cornea, can distend in response to pressure, the result is a large cornea (as in oxen) that is cloudy due to oedema.

Macroscopy

The eye is often larger in all dimensions than according to age. The cornea has diameters >12 mm. The corneal stroma is opaque.

Histopathology

The main findings are as follows: The corneal epithelium is irregular and Bowman's layers may be partly missing, often due to a calcifying bandular keratopathy (Fig. 1.33). The stroma is oedematous. There may be ruptures in Descemet's membrane and partial loss of the endothelium. The trabecular meshwork is hypoplastic, Schlemm's canal is partially missing and retro displaced, the iris stroma may attach anteriorly to the trabeculum and the iris and ciliary body are atrophic. In the posterior part of the eye, classic changes related to glaucoma may be found like retinal atrophy and cupping of the optic disc (see also page 206).

1.4.11 Chromosomal Abnormities Involving the Eyeball

An immense number of chromosomal abnormities involve the eyeball. Classically trisomy 13-15, 16-18 and 21 and defect 5 are presented [28]. To the general pathologist this is of little importance since they are all rare and the defects are often known when the eyes are to be investigated in specialised pathology laboratories.

1.5 Inflammation

Ocular inflammation may involve one or more of the tissues of the eyeball. Only inflammation involving all intraocular structures or the complete eyeball is described in this chapter. The gen-

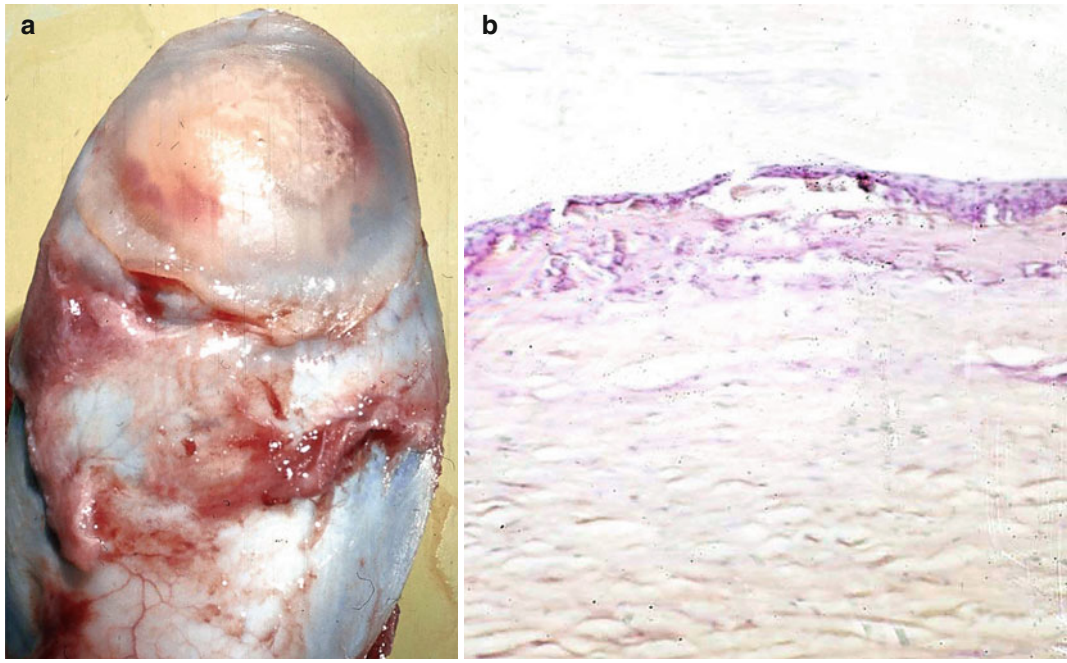

Fig. 1.33 (**a**) Buphthalmic eye with a large opaque cornea. (**b**) Histologically a bandular keratopathy with epithelial and subepithelial calcification is demonstrated. H&E, bar = 50 µm

eral pathologist may receive such eyes removed because they are blind, hypotonic, atrophic and painful or because they are chronically inflammatory and refractory to treatment [29]. Both conditions are often the final unsuccessful stage after repeated surgeries performed because of severe trauma, recurrent retinal detachments, repeated antiglaucoma surgeries, failed cataract extractions or after intravitreal, therapeutic injections [30].

1.5.1 Panophthalmia and Endophthalmia

Definition

Panophthalmia is an inflammatory process involving all tissues of the eyeball including the sclera and episclera. Endophthalmia is used to describe a similar process in which the sclera and episclera are not involved.

Epidemiology

Modern ocular surgery is very rarely complicated by infection or inflammation; however, since the number of surgeries has increased drastically during many years because of the technical improvements achieved, the eyes are still to be enucleated [30].

Aetiology

The eye contains avascular structures like the cornea, lens and vitreous. It also harbours immune privileged sites where the normal inflammatory response is different from the rest of the body, and the eye contains large fluid-filled compartments. These factors provide an ideal environment for growth of microorganisms. In addition they cause a reduced entrance of systemic antimicrobial drugs to the eye.

An eye sent to pathological analysis because of panophthalmia or endophthalmia most often has a known preceding cause [30]. Rare but frightening causes of bacterial endophthalmitis are iatrogenic. Cataract surgery is performed with high quality; however, if technical defects appear, the result may be an outbreak of bacterial endophthalmitis [31]. Likewise, the vast number of intraocular injections with anti-VEGF performed to reduce neovascular membrane formations in wet AMD has in

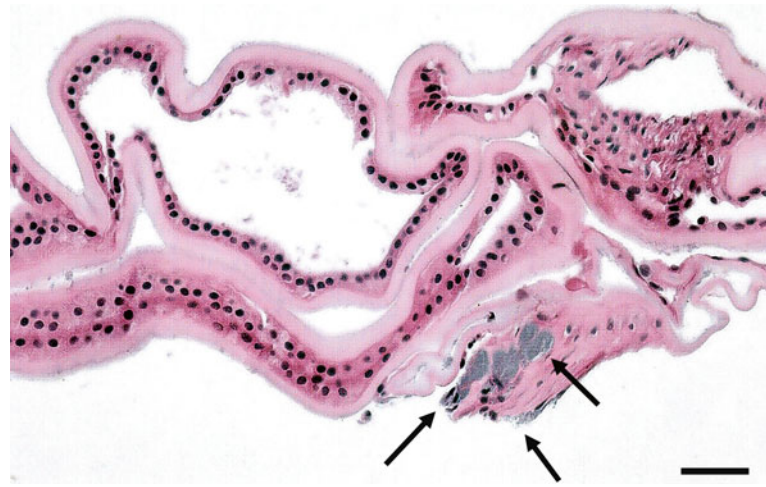

Fig. 1.34 Lens capsule with colonies of Gram-positive cocci (*arrows*). H&E, bar = 50 µm

rare instances given rise to streptococcal endophthalmitis [32]. Haematogenous infection may be from endocarditis or due to injection of contaminated drugs in addicts. Immune suppression increases the risk of especially metastatic endophthalmitis [33, 34].

1.5.2 Bacterial Pyogenic Endophthalmitis

Clinical Features

The symptoms at presentation are ocular discomfort, inflammatory signs (painful red eye, anterior chamber flare, hypopyon and vitritis) and loss of vision. The diagnosis in early stages is essential. Vitreous or anterior tap for microbiological identification and immediate administration of adequate intraocular and/or systemic antibiotic agents are mandatory.

Postoperative and traumatic cases mostly contain staphylococci; however, in bleb-related cases streptococci prevail [30, 35, 36]. Gram-negative microorganisms are also reported and the list of rare bacteria increases still. A separate chronic endophthalmitis is caused by the capture of microorganisms like *Staphylococcus epidermidis* in the capsular bag around inserted artificial lenses – capsular endophthalmitis [34].

Macroscopy

Most eyeballs present with creamy white exudates involving most intraocular structures.

Histopathology

All structures of the eye are involved. Characteristic is the hypopyon – the accumulation of serous exudates, debris, dead and viable granulocytes and mononuclear cells in the anterior chamber and also in the posterior chamber. The iris stroma is filled up by lymphocytes and plasma cells often to a degree that involves disorganisation of the stroma and the iris epithelia. The anterior surface of the iris may demonstrate neovascularisation. The ciliary body is packed with the same type of inflammatory cells, and the epithelia are covered by exudative inflammatory membranes that may encircle the lens and close the pupil. The choroid may also be involved especially in metastatic infections. The vitreous often contains abscesses. This is the best site to disclose the involved bacteria besides the lens capsule (Fig. 1.34). In addition, beware of the pigment granules that may look like microorganisms. Pigment granules are larger than cocci and are brown also in Gram stains.

In late enucleations, vasculitis with haemorrhagic infarction and necrosis are found in the retina. Choroidal detachment due to hypotonia and a non-granulomatous lymphocytic infiltrate is also a characteristic late feature (see also page 269).

1.5.3 Fungal Infection

Definition

Bulbar infection caused by fungi

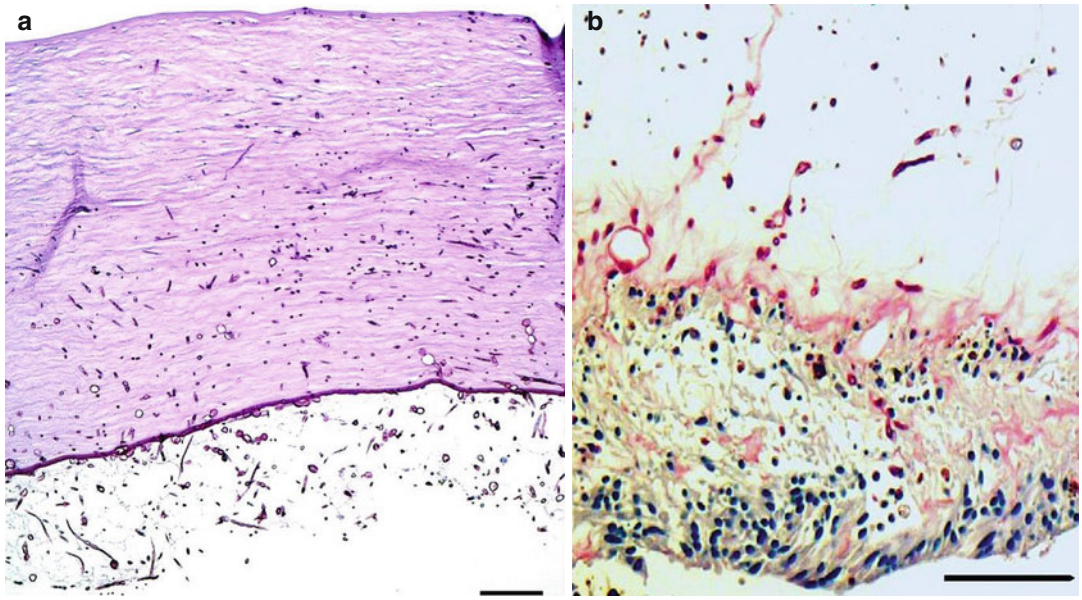

Fig. 1.35 Fungal endophthalmitis (*Fusarium*). (**a**) Cornea, note that the maximum of infection is at Descemet's membrane. P.A.S. stain, bar = 100 µm. (**b**) Retina with infection along the internal limiting membrane. P.A.S. stain, bar = 50 µm

Epidemiology

The most frequent fungal infections in the human eyes are due to *Candida* species; however, *Aspergillus* and *Fusarium* species are frequent in warmer climates. A series of other fungi are in addition important in endemic areas.

Clinical Features

Often the entrance to the eye is known form history like penetrating foreign bodies or severe keratitis. In immune-compromised patients also haematogenous spread to the eye is found. At surgery, performing vitreous tap or vitrectomy, it is important to secure material for culture, direct microscopy and molecular techniques [37, 38].

Macroscopy

There are no specific macroscopic morphological differences to bacterial infection.

Histopathology

The microscopic features are varied. Small vitreal fungal balls with limited inflammatory reaction may be found in *Candida*. Some species like *Fusarium* invade all basement membranes (Fig. 1.35) [39], and *Aspergillus* proliferates along the RPE. All fungi raise a marked lymphocytic and macrophagic reaction when the blood-aqueous barrier is broken and the immune privilege of the internal eye is lost.

1.5.4 Viral Infection

Aetiology

A long series of virus are able to infect the ocular tissues; however, in most cases, only specific tissues of the internal eye are involved like the herpes simplex virus and cytomegalovirus infections involved in the retinal necrosis syndrome (Fig. 1.36).

Histopathology

The histopathological findings of the various viral infections are presented under the relevant organ chapters.

1.5.5 Granulomatous Inflammation

Granulomatous pan- and endophthalmitis are rarely leading to loss of the involved eye, and even when the inflammation involves the entire eye, it is

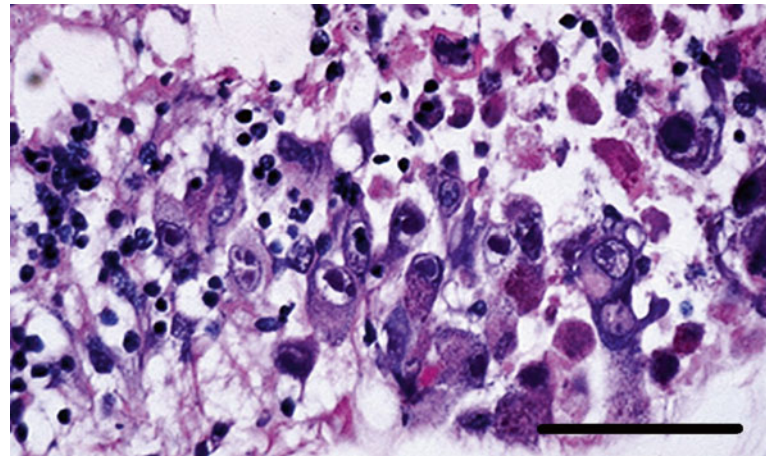

Fig. 1.36 Acute retinal necrosis due to CMV infection in an HIV-positive person. Giemsa stain, bar = 60 µm

always dominated by the specific site of the granulomatous reaction. The granulomatous inflammations can be divided into those that are specific like with tuberculosis, leprosy, sarcoidosis, syphilis and rheumatoid disease or related to protozoal diseases. The non-specific are those most often clinically termed idiopathic, but the group includes also diseases like heterochromic iridocyclitis, Vogt-Koyanagi-Harada syndrome and Behcet's syndrome. All granulomatous inflammatory manifestations have their maximum in a few of the intraocular structures. Consequently they are described in the chapters of these structures.

1.6 Injuries

Injuries causing loss of an eye account for one fourth of the eyes removed [40, 41]. Trauma may be mechanical or due to chemicals, radiation, toxins, etc. When dealing with ocular trauma, the most severe are those caused by mechanical trauma, mostly due to violent activities, traffic or war; however, the general pathologist may also receive eye due to more bizarre types of trauma like "shaken" baby syndrome and auto-enucleation performed by persons with severe psychotic illnesses like schizophrenia [42]. With the increased tendency to celebrate any occasion with the use of fireworks, firework-induced ophthalmic trauma has risen to approximately 20 % of injuries caused by fireworks [43].

Mechanical eye trauma can be divided into sharp and blunt lesions, and sharp lesions with or without foreign bodies, and this division, although of importance when evaluating the danger of later development of sympathetic ophthalmitis, has lost some of its importance since most traumatised eyes are today initially exposed to surgery and many are saved despite open globe injury and no light perception [44, 45]. For the general pathologist, it may be of most importance to divide the traumatised eyes received into those received in direct connection to the first surgical attempt to repair, i.e. the "irreparable eyes" [46], those removed in the short term after attempted repair, those that after a long time have developed phthisis (painful blind eyes) and those removed in fear of sympathetic ophthalmitis.

1.6.1 Irreparable Eye: Large Penetrating/Perforating Wounds of the Eyeball Walls

Definition

An eye, in which a blunt injury has caused a rupture of the corneo-scleral wall of the eye or in which a sharp injury has caused a similar lesion. In sharp injuries a distinction is made between penetrating injuries, i.e. those with an entrance wound but without an exit wound. A perforation is an injury with both an entrance and an exit wound.

Epidemiology

Complete data on eyeball trauma are not available on a world scale, and most injuries do not lead to the loss of an eye. An open globe eye injury still carries the worst prognosis [44, 45].

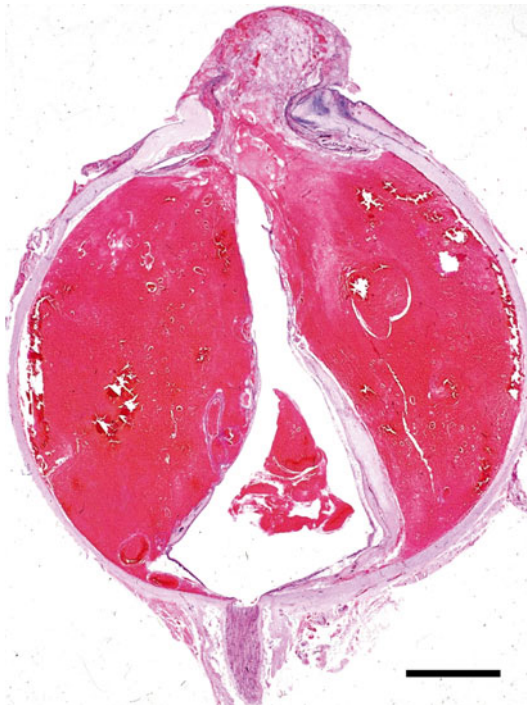

Fig. 1.37 Eye with expulsion haemorrhage and prolapsed intraocular structures through a penetrating corneal ulcer. H&E, bar = 1 mm

Aetiology

A blunt trauma results in an immediate dramatic increase in the intraocular pressure leading to rupture of the eye wall at its weakest point, i.e. posterior to the insertion of one of the rectus muscles. Sharp dilacerations are located according to where the causative weapon hits the globe – often involving the corneal limbus.

Clinical Features

The eye is often filled with blood preventing any inspection of internal structures. The eye is completely hypotonic and there is no light perception. The lens may be found near the bulbar rupture, and prolapse of uvea, vitreous body or retina is a characteristic feature.

Macroscopy

The collapsed eye is measured. The rupture is identified and prolapse of tissue is noted to support the clinical observations and the decision to enucleate (Fig. 1.37). The cutting of the globe is performed to ensure most of the rupture is in the central ring. Sometimes it is useful to make separate sections perpendicular to the plane of the rupture.

Histopathology

Often the ciliary body and iris root are separated from the sclera by the traumatic forces – irido-cyclo-dialysis. The bulbar cavity is filled with blood and within this the remaining choroid and retina are found. The degree of inflammation depends on the time to enucleation since the traumatic episode. After longer periods with intraocular bleeding and increased pressure, blood breakdown products accumulate and are visualised by a positive Prussian blue reaction (haemosiderosis bulbi) (Fig. 1.38). From the anterior chamber the blood products may enter the cornea and stain it brown red (haemochromatosis corneae) (Fig. 1.39). The stain is blood products accumulated in eosinophilic granules between the corneal lamellas at the site of necrotic keratocytes. The haemochromatotic cornea does not stain positive with Prussian blue.

1.6.2 Battered Child Syndrome

Definition

A form of abusive head trauma characterised by the application of repeated acceleration-deceleration forces with or without evidence of blunt head impact [47].

Synonyms

Shaken baby syndrome, abusive head trauma

Epidemiology

Rare but probably underreported

Aetiology

Repeated acceleration-deceleration forces to the eye induce massive traction between the retina-choroid layer and the vitreous body which leads to bleeding and oedema. Forces are strongest at the areas of adhesion like the fovea, ora serrata and optic disc.

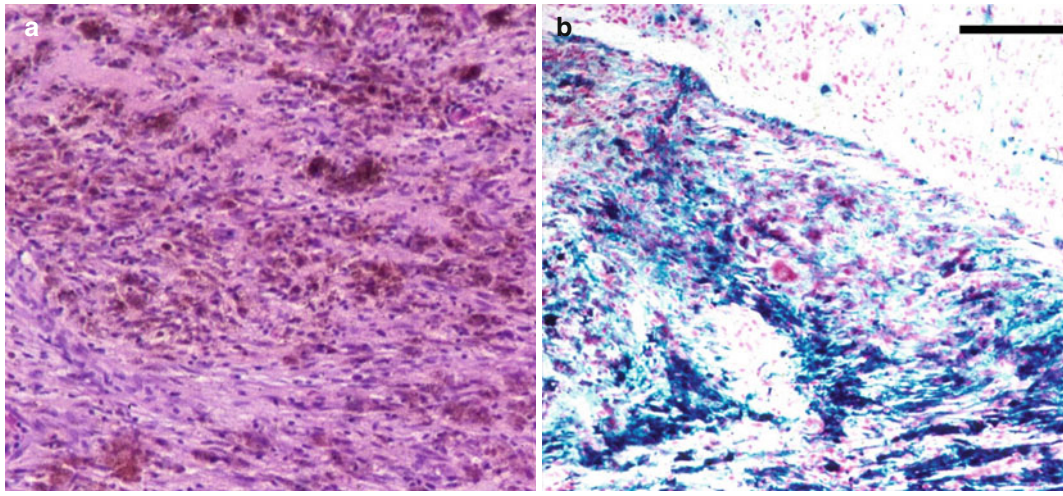

Fig. 1.38 Intraocular scarring with haemosiderosis (**a**, H&E). The blood pigments are demonstrated by a positive Prussian blue reaction (**b**, bar = 100 µm)

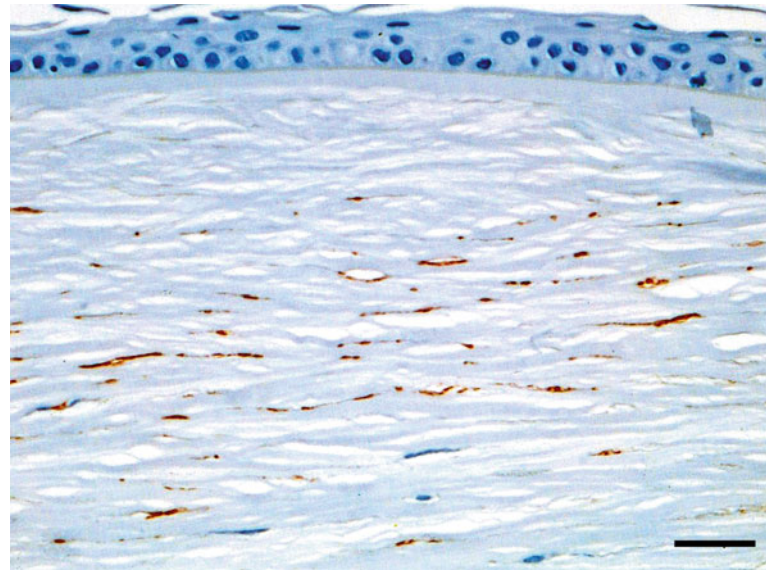

Fig. 1.39 Haemochromatosis corneae. Note that the staining from the erythrocytes is found in the intralamellar spaces where the keratocytes reside. H&E, bar = 40 µm

Localisation

Eyes, but often the small children also have signs of head injury, broken extremities and subcutaneous haemorrhages

Clinical Features

At ophthalmoscopy numerous retinal haemorrhages are seen. Two third of victims have too many haemorrhages to be counted [47]. Macular retinoschisis with blood accumulated between the internal limiting membrane of the retina and the nerve fibre layer is characteristic.

Macroscopy

If the eye is achieved within days after the last assault, the retinal bleedings can be seen and should be documented. Optic disc oedema may also be found as a result of increased intracranial pressure due to bleedings. Rarely intraorbital and episcleral haemorrhages can be observed.

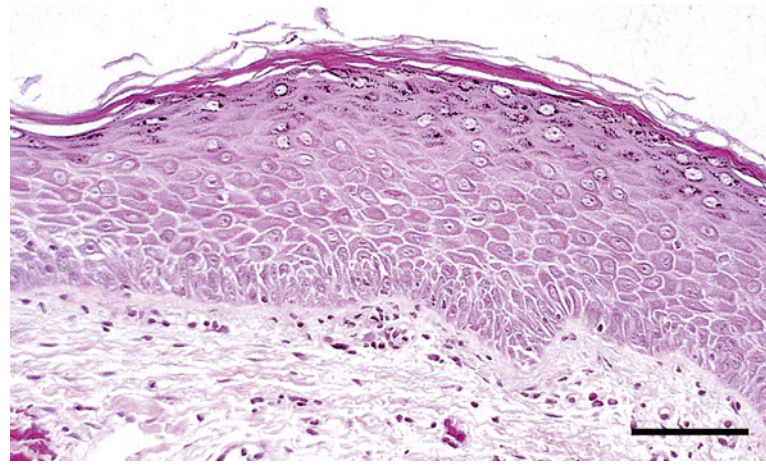

Fig. 1.40 Keratinised conjunctival epithelium in a person with severe dry eye condition. H&E, bar = 50 µm

Histopathology

The hallmark is the multiple retinal haemorrhages of the inner retina – bilaterally. Also preretinal, intra-choroidal and intrascleral haemorrhages – at the site of the circle of Zinn-Haller – are found [48]. The traction around the macula presents as a ring of retinal folds and haemorrhagic schisis.

Differential Diagnosis

The combination of findings presented together with other systemic indications of abuse is pathognomonic [47].

1.6.3 Irradiation Damage

Irradiation of the eye region for therapeutic reasons, i.e. external beam radiation for malignancies in the orbit and plaque radiation or proton beam radiation for malignant intraocular tumours, may be complicated with such side effects that the result is the enucleation/exenteration of the eye. The major terminal results of irradiation is a severely dry eye with recurrent corneal ulcers, severe chronic uveitis and scleral necrosis, retinal degeneration with traction detachment and complicated cataract. The end result is a blind painful, phthisic eye.

Histopathology

The most important findings are those described under phthisis bulbi. In addition, a severe squamous, keratinising metaplasia of the corneal and conjunctival epithelium is seen (Fig. 1.40).

1.6.4 Sympathetic Ophthalmia

Definition

Bilateral granulomatous uveitis. The one eye is the one that has suffered a sharp trauma and in which the autoimmune inflammation is generated. This eye may be termed the sympathigenic or exciting eye. The other eye, the one reacting upon the inflammation in "sympathy", is termed the sympathising eye [49, 50].

Epidemiology

Most cases of sympathetic ophthalmia accompany penetrating/perforating injuries of the eye and orbit in which the uveal tissue, especially the ciliary body, is traumatised and prolapsing through the sclera [49]. The disease has been recognised since ancient times. Sympathetic ophthalmia is reported to occur in <0.5 % of perforating injuries and in less than 0.01 % following intraocular surgery [50, 51] and may also rarely appear after exenteration and enucleation [52].

Aetiology

The aetiology is not completely described. An autoimmune predominantly T-cell driven reaction towards uveal antigens is at present the best suggestion [49, 50].

Clinical Features

Various latent periods after the injury to the eye, 5 days to 66 years and 90 % within the first year, the injured eye presents with disturbed

accommodation, photophobia and epiphora. At slit-lamp examination, a low-grade uveitis with mutton-fat or small white corneal precipitates is found. At ophthalmoscopy white spots in the RPE layer may be found representing the clinical manifestation of sub-RPE granulomas – Dalen-Fuchs nodules.

Macroscopy

The choroid is thickened, the retina may be detached and the ciliary body and lens are surrounded by inflammatory membranes.

Histopathology

There is no morphological difference between the two eyes. The main findings are those of a granulomatous pan-uveitis. Granulomas, predominantly containing histiocytes, mature lymphocytes and sometimes giant cells, dominate the thickened choroids. In some areas eosinophils may be found. Granulomas are characteristically also found between Bruch's membrane and the RPE – termed Dalen-Fuchs nodules. The retina is oedematous and has a lymfocytic perivasculitis. There is a vitritis increasing towards cyclic membranes encircling also the lens that may show signs of phacoanaphylaxis, a not uncommon complication. The T lymphocytes dominate and are initially CD4+, but later in the disease, CD8+ cytotoxic cells dominate.

Differential Diagnosis

Other granulomatous diseases like Vogt-Koyanagi-Harada syndrome and sarcoidosis should be ruled out; however, these have systemic manifestations and are rarely appearing after perforating injury.

Genetics

There is a link to HLA antigen profiles. Patients with HLA-A11, DRB1*04, DQA1*03 and DQB1*04 seem to be at risk.

Prognosis

Early enucleation of a severely injured eye – <2 weeks after the trauma – may prevent the development of sympathetic ophthalmia. If the disease has developed, systemic treatment with high doses steroids supplemented with cyclosporine A or cytostatics can in nearly all cases control the disease and prevent enucleation.

1.6.5 Phacoanaphylactic Endophthalmitis

Definition

A chronic endophthalmitis induced by an autoimmune inflammatory response to lens protein that occurs under special conditions and involved abrogation of tolerance to lens protein [53].

Synonyms

Lens-induced endophthalmitis, phacogenic endophthalmitis, lens-induced uveitis

Epidemiology

It is a rare disease, however, often underdiagnosed clinically [53, 54]. The disease may develop 4–5 weeks after disruption of the lens capsule but may be delayed for more than 50 years [54, 55].

Aetiology

Rupture of the lens capsule introduces lens proteins to the immune system. Despite the special immunological deviations of the eye, which may have been disturbed by the injury, the proteins seem to evoke an autoimmune response [53].

Clinical Features

The eye presents like any other endophthalmitis weeks after the injury or surgery. The inflammation may be mild with only a slight reaction in the anterior chamber and vitreous, or it may be dramatic with hypopyon, cataract, ciliary injection and low visual acuity. An anterior or posterior tap may be taken and may show granulomatous reaction or elevated autoantibodies against lens-specific proteins [54, 55].

Histopathology

The inflammatory reaction may be discrete and located to the lens material inside the rupture of the capsule and in the anterior chamber. More often inflammatory changes involve all intraocular structures. The focus of reaction

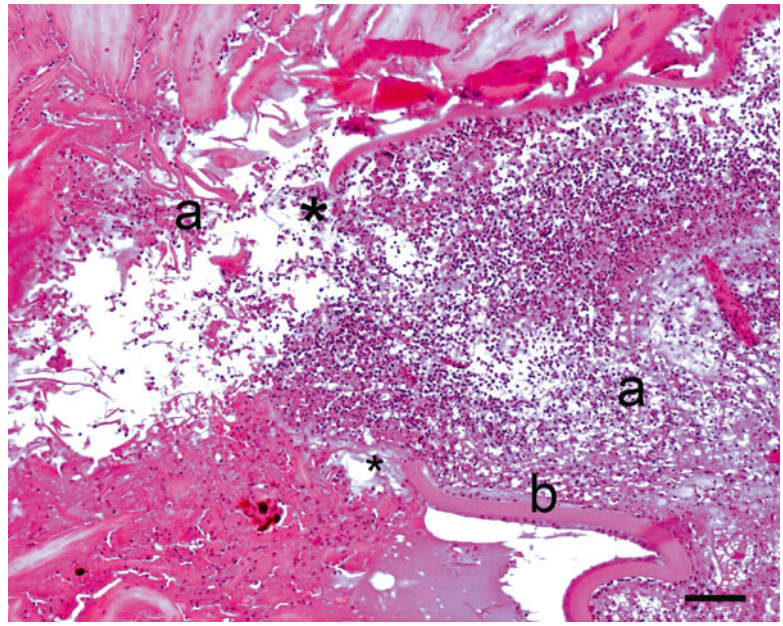

Fig. 1.41 Phacoanaphylactic endophthalmitis. The inflammation is most active at the site of the ruptured lens capsule (*asterisks*). Neutrophile granulocytes accumulate around cataractous lens fibres (*a*). Lens epithelial cells (*b*) are still present. P.A.S. bar = 50 µm

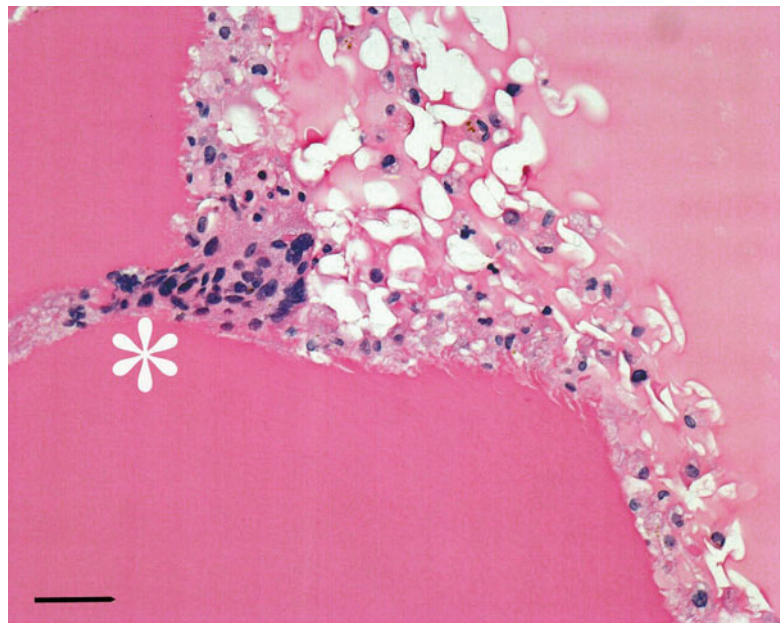

Fig. 1.42 High power of phacoanaphylactic endophthalmitis. The giant cells accumulate along the exposed lens fibres (*asterisk*). H&E, bar = 30 µm

is in the lens spreading from the ruptured lens capsule. A zonal, granulomatous inflammation is seen around lens material. In the more central areas of the lens, neutrophile granulocytes with adjacent layer of mononuclear cells, epitheloids and giant cells dominate (Figs. 1.41 and 1.42). Outside the lens capsule, the inflammatory reaction induces the formation of inflammatory, fibrovascular membranes.

The uvea including the choroid is in most cases (76 %) involved and presents a non-granulomatous mononuclear cell reaction [53]. The retina is involved in more than half of cases predominantly being detached and with a perivasculitis (see also page 183).

1.7 Degenerations

The end result of severe bulbar injury, chronic intraocular inflammation, repeated surgeries and radiation therapy is a blind, atrophic, hypotonic eye. Such an eye may be enucleated to relieve pain, because of suspicion of intraocular tumour or for cosmetic reasons. Two separate terms are used clinically to describe such eyes based on the degree of intraocular disorganisation: atrophia bulbi and phthisis bulbi. In histopathology the difference is not recognised and such eye is termed phthisic.

1.7.1 Phthisis

Definition

An eye in which internal structures are severely disorganised and the globe is reduced in size due to shrinkage.

Clinical Features

The eye is blind and is smaller than the normal eye. At inspection the eye may look like a box "bulbus quadratus". The shape is induced by the drag of the four rectus muscles upon the hypotonic soft eye. The cornea is often opaque.

Macroscopy

Small box-shaped eye, hard at palpation, the cornea is opaque (Fig. 1.43). At sectioning, the eye may be hard due to bone formation and fibrosis of the internal structures (Fig. 1.44).

Histopathology

The corneal epithelium is often thin with subepithelial calcification and destruction of Bowman's layers (bandular keratopathy); metaplasia, proliferation and exudation from the chronic, inflammatory iris and ciliary epithelia lead to the formation of irido-cyclic membranes; the choroid has a chronic lymphoid inflammation; and RPE proliferates and has islands of calcification and bone formation. The retina is detached and gliotic, and the optic nerve is atrophic with loss of nerve fibres. The lens, when present, is cataractous and may even contain bone formation.

Fig. 1.43 Bulbus quadratus – the terminal state of phthisis

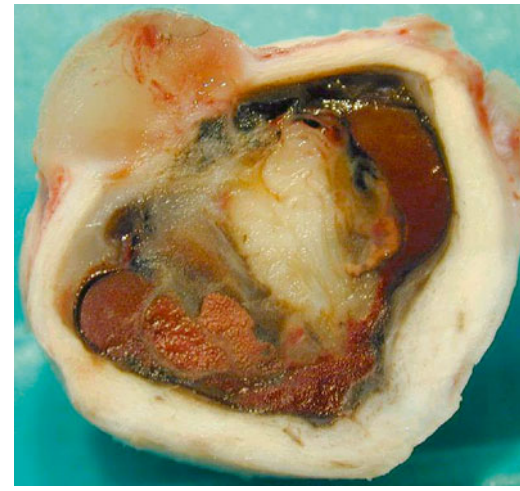

Fig. 1.44 Sectioned phthisic eye. The sclera is thick and the eye is filled with gliotic masses and bleeding

1.7.2 Diabetes

All layers and tissues of the eye may be involved in the diabetic disease (Table 1.1). When the eye is enucleated due to diabetes, it is mostly in painful phthisis due to repeated retinal reattachment surgeries sometimes with the use of silicon oil. At histology the eye has most of the features described under phthisis; however, the vacuolated

Table 1.1 Main histopathological changes of the eye due to diabetes

Bulbar structure	Pathological condition	Diabetic cause
Cornea	Bullous epitheliopathy	Neovascular glaucoma
	Neuroparalytic ulcer	Neuropathy
Sclera	Episcleritis/scleritis	Autoimmune component
Iris and chamber angle	Neovascular membranes on anterior iris surface and trabeculum	Retinal ischaemia and dysmetabolism
	Ectropion uveae	Shrinkage of neovascular membranes
	Vacuolated iris pigment epithelia	Storage of glycogen
Choroid	Increased atheromatosis	Diabetic vasculopathy
	Peripheral neovascular membranes to subretinal space	Ischaemia
	Chronic inflammation	
Optic nerve	Neovascular membranes on disc	Ischaemia, dysmetabolism
	Atrophy	Neuropathy
Retina	All stages of retinopathy	Ischaemia and dysmetabolism
Vitreous body	Asteroid hyalosis	Vascular leak
	Neovascular membranes and traction	Ischaemia
Lens	Cataract	Dysmetabolism

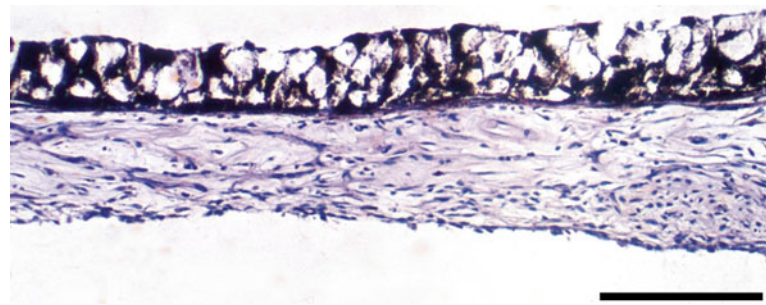

Fig. 1.45 Iris from a person with severe diabetes. The pigment epithelia have empty spaces due to storage of glycogen that is washed out during the histological preparation. H&E, bar = 50 µm

iris pigment epithelia (Fig. 1.45) and the marked hyalinisation of the ciliary processes are very characteristic. The detailed histopathological findings are given in the relevant chapters.

1.8 Neoplasms

No tumours involve the entire eyeball; however, most of the ocular structures may, with the infiltrative growth of the malignant cells, be involved. The various primary and secondary tumours of the eye are described in the relevant chapters. Enucleation or exenteration of the globe may be necessary due to extensive growth of orbital and/or eyelid tumours. The treatment of such lesions can necessitate surgical removal of large parts of the eyelids and orbital tissues leaving the eyeball unprotected from permanent exposure. The eye is therefore removed.

1.9 Artificial Eyes, Orbital Implants and Dry Socket

The loss of an eye has severe consequences. Besides the loss of the visual function of the eye, the patient also has lost an important part of their face and their facial expression; the patient may suffer from the eye amputation syndrome [40]. Patients that lose eyes are either enucleated, i.e. the entire eyeball is removed, or exenterated/eviscerated, i.e. the cornea and all intra sclera tissues are removed. After enucleation of the eye-

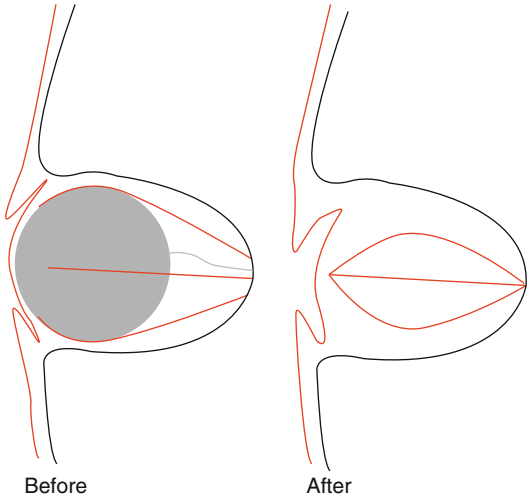

Fig. 1.46 Drawing of an enucleation. At removal of the eye, the extraocular muscles are sutured together and covered with conjunctiva

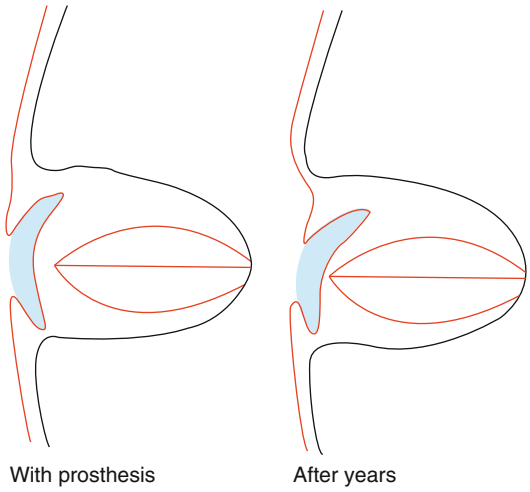

Fig. 1.47 An artificial eye – prosthesis – rests upon the fused extraocular muscles. After several years the orbital fat atrophies and the prosthesis slides down within the orbit creating a shallow inferior fornix

ball, the muscles are sutured together and covered with conjunctiva, creating a conjunctival pocket in which the mucosa-covered muscles protrude as a small hill that moves simultaneously with the other eye and on which an artificial eye may rest, kept in place by the eyelids (Figs. 1.46 and 1.47). Today, the loss of volume is compensated with an orbital implant to which the extraocular muscles are sutured. In cases of exenteration/evisceration, the empty sclera may be filled with the implant before the conjunctiva is closed. Despite this, most patients with a lost eye experience shrinkage of the orbit and conjunctival fornices with chronic irritation, recurrent infections and displacement of their prosthesis.

From eye-amputated patients, the general pathologist may receive artificial eyes, orbital implants and biopsies from patients suffering from dry socket syndrome. Below is an overview of what may be found at histopathology.

1.9.1 Artificial Eye

Definition

Prosthesis is placed in the conjunctival pocket resting upon the orbital content that is covered by conjunctival tissue (Fig. 1.47). The prosthesis may be of glass or acrylic resin. The front of the prosthesis is painted with layers of glass/acryl creating the impression of a clear cornea behind which are seen an iris and a black pupil.

Synonyms

Eye prosthesis, glass eye

Epidemiology

In most countries, the removal of eyes is drastically dropping because of the better treatment of ocular trauma, diseases and tumours [2]. At the ØPI-KU the annual number of received eyes and exenteration material is at present 130. The mean age of the patients is approximately 55 years. These patients may live a further 25 years giving a rough estimate of 3,000 persons having artificial eyes in Denmark with a population of 5.5 mio. A glass eye is changed every second year, while acrylic eyes may be used for 5 years before being changed. Only a very minor fraction of these prostheses ends up for pathology.

Aetiology

Prostheses for pathological examination are mostly examined because of severe secretion from the conjunctival fornices. This is mostly caused by defects in the surface of the prosthesis or due to or exposure of an orbital implant.

Clinical Features

The artificial eye appears often smaller than the other eye. The orbital content is atrophic leading to downward displacement of the prosthesis (Fig. 1.47), reduced mobility and hollowness under the eyebrow. The artificial eye is easily removed by pulling down the inferior eyelid and then pushing it out; a small suction cup can be used.

Histopathology

The surface of an artificial eye is slowly broken down by the organic acids liberated from the bacteria of the biofilm covering the artificial eye, a process resembling caries attaching on the teeth. Scrapings from the film may demonstrate microorganisms and debris.

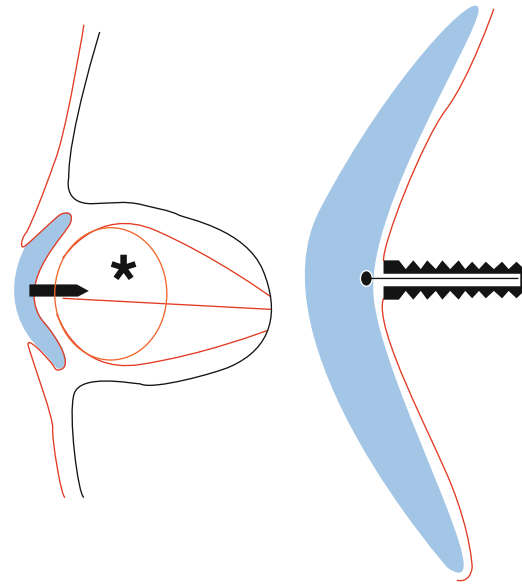

Fig. 1.48 Drawing of prosthesis with peg in an orbit with an implant (*asterisk*). In higher magnification it is shown how the peg is attached to the prosthesis via a titanic screw inserted into the implant

1.9.2 Orbital Implants

Definition

A structure of artificial material or autologous tissue implanted in the orbit to increase the volume behind the conjunctival pocket.

Clinical Features

Grafts consisting of autologous skin dermis are often sutured into the muscle cone primarily or secondary to enucleation. Muscle tissue with adjacent vascular supply may be used in cases of severe tissue loss. Mostly artificial material is used. Non-porous implants are not integrated into the orbital tissues, and they are with time covered by a pseudo-capsule. Porous implants may consist of hydroxyapatite [56, 57] or of other types of porous material [58–61]. Porous implants are integrated with time, i.e. connective tissue and vessels invade the porous structures.

The extraocular muscles are sutured to the surface of the implant or left attached to the sclera, in which the implant is placed; make the implant move parallel with the other eye. Thereby, the artificial eye achieves an important cosmetic improvement. To increase the mobility of the artificial eye, a cobbling peg may be inserted through the conjunctiva and into the implant (Fig. 1.48) [60]. The other end of the peg is connected to the posterior surface of the artificial eye (Fig. 1.49).

Orbital implants may be exposed with time leaving a conjunctival defect through which tear fluid and microorganisms invade the implant. Exposure is the most frequent reason for removal of an implant. Implants with pegs are more prone to exposure than those without [60, 62, 63].

Histopathology

The non-porous implants are not processed for histopathology. The porous types may be fixed in formalin and embedded in paraffin. Those of hydroxyapatite must be decalcified like bony tissues before embedding and sectioning. In such specimens the porous structure of the implant is seen as a connective tissue meshwork with large empty spaces – the dissolved hydroxyapatite trabeculae (Fig. 1.50). In older implants some bone formation may be observed (Fig. 1.51). When the implant is obtained because of exposure, bacterial growth may be detected in more than 50 % [59].

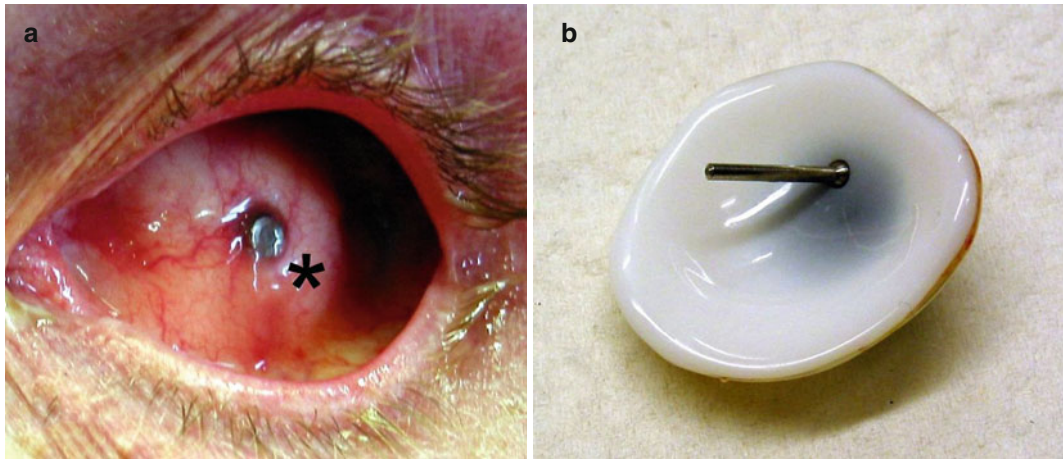

Fig. 1.49 (**a**) Photo of an integrated orbital implant in which a trans-conjunctival screw (*asterisk*) has been fitted to fit with the peg of the prosthesis (**b**)

Fig. 1.50 Orbital hydroxyapatite implant. The implant has been dissolved in acids leaving the vascular connective trabeculae. H&E, bar = 100 μm

Ingrowths of conjunctival epithelium between the pseudo-capsule enwrapping the implant and the implant itself are another frequent presentation. All implants removed because of exposure have a mild to marked, non-granulomatous inflammatory reaction.

1.9.3 Dry Socket

Definition

The term is used to describe the shrunken, dry condition of the conjunctival and orbital tissues of an atrophic, secondary anophthalmic orbit.

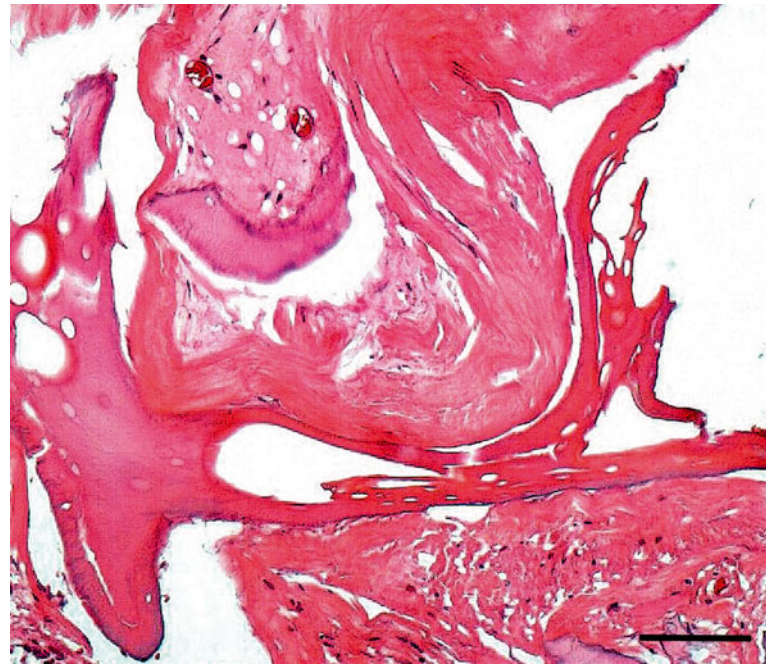

Fig. 1.51 Bone formation in a long-lasting, integrated, orbital, hydroxyapatite implant. H&E, bar = 100 µm

The tissue from this condition may be sent for pathological examination. Since such biopsies mostly are obtained from the chronically inflamed and atrophic conjunctiva, the histological findings are described in Chap. 2, the conjunctiva.

References

1. Lynnerup N, Kjeldsen H, Zweihoff R, Heegaard S, Jacobsen C, Heinemeier J. Ascertaining year of birth/age at death in forensic cases: a review of conventional methods and methods. Forensic Sci Int. 2010;201:74–8.
2. Hansen AB, Petersen C, Heegaard S, Prause JU. Review of 1028 bulbar eviscerations and enucleations. Changes in aetiology and frequency over a 20-year period. Acta Ophthalmol Scand. 1999;77:331–5.
3. Mann I. Developmental abnormalities of the eye. 2nd ed. London: BMA; 1957. p. 1–419.
4. American Academy of Ophthalmology. Chapter 5. Ocular development. In: Fundamentals and principles of ophthalmology. San Francisco: AAO; 2007–2008. p. 123–58.
5. Forrester J, Dick A, McMenamin P, Lee W. The eye. Basic sciences in practice. Chapter 2, embryology and early development of the eye and adnexa. London: W B Saunders; 1996. p. 87–116.
6. Graw J. Eye development. Curr Top Dev Biol. 2010;90:343–86.
7. Shaham O, Menuchin Y, Farhy C, Ashery-Padan R. Pax6: a multilevel-regulator of ocular development. Prog Retin Eye Res. 2012;31:351–76.
8. American Academy of Ophthalmology. Chapter 2. The eye. In: Fundamentals and principles of ophthalmology. San Francisco: AAO; 2007–2008. p. 43–89.
9. Forrester J, Dick A, McMenamin P, Lee W. The eye. Basic sciences in practice. Chapter 1, anatomy of the eye. London: W B Saunders; 1996. p. 1–86.
10. Dua HS, Faraj LA, Said DG, Gray T, Lowe J. Human corneal anatomy redefined: a novel pre-descemet's layer (Dua's layer). Ophthalmology. 2013. doi:10.1016/j.ophtha.2013.01.018. pii: S0161-6420(13)00020-1.
11. Pruett RC. Aging changes. In: Albert DM, Jakobiec F, editors. Principles and practice of ophthalmology. Basic sciences. Philadelphia: WB Saunders; 1994. p. 683–748.
12. Slavotinek AM. Eye development genes and known syndromes. Mol Genet Metabol. 2011;104:448–56.

13. Morrison D, Fitzpatrick D, Hanson I, Williamson K, van Heyningen V, Fleck B, Jones I, Chalmers J, Campbell H. National study of microphthalmia, anophthalmia, and coloboma (MAC) in Scotland: investigation of genetic aetiology. J Med Genet. 2002;39:16–22.
14. Alyahya GA, Heegaard S, Fledelius HC, Rechnitzer C, Prause JU. Primitive neuroectodermal tumour of the orbit in a 5-year-old girl with microphthalmia. Graefe's Arch Clin Exp Ophthalmol. 2000;238:801–6.
15. Clementi M, Tenconi R, Bianchi F, Botto L, Calabro A, Calzolari E, Cianciulli D, Mammi I, Mastroiacovo P, Meli P, Spagnolo A, Turolla L, Volpato S. Congenital eye malformations: a descriptive epidemiologic study in about one million newborns in Italy. Birth Defects Orig Artic Ser. 1996;30:413–24.
16. Warburg M, Jensen H, Prause JU, Bolund S, Skovby F, Miranda MJ. Anophthalmia-microphthalmia-oblique clefting syndrome: confirmation of the Fryns anophthalmia syndrome. Am J Med Genet. 1997;73:36–40.
17. Verma AS, FitzPatrick DR. Anophthalmia and microphthalmia. Orphanet J Rare Dis. 2007;26:47. doi:10.1186/1750-1172-2-47.
18. Bakrania P, Robinson DO, Bunyan DJ, Salt A, Martin A, Crolla JA, Wyatt A, Fielder A, Ainsworth J, Moore A, Read S, Uddin J, Laws D, Pascuel-Salcedo D, Ayuso C, Allen L, Collin JR, Ragge NK. SOX2 anophthalmia syndrome: 12 new cases demonstrating broader phenotype and high frequency of large gene deletions. Br J Ophthalmol. 2007;91:1471–6.
19. Chassainga N, Ragge N, Kariminejade A, Buffet A, Ghaderi-Sohie S, Martinovic J, Calvasa P. Mutation analysis of the STRA6 gene in isolated and non-isolated anophthalmia/microphthalmia. Clin Genet. 2013;83:244–50.
20. Yahyavi M, Abouzeid H, Gawdat G, de Preux A-S, Xiao T, Bardakjian T, Schneider A, Choi A, Jorgenson E, Baier H, El Sada M, Schorderet DF, Slavotinek AM. ALDH1A3 loss of function causes bilateral anophthalmia/microphthalmia and hypoplasia of the optic nerve and optic chiasm. Hum Mol Genet. 2013;22:1–9. doi:10.1093/hmg/ddt179.
21. Kara N, Baz O, Altinkaynak H, Altan C, Demirok A. Assessment of the anterior chamber angle in patients with nanophthalmos: an anterior segment optical coherence tomography study. Curr Eye Res. 2013;38:563–8.
22. Steijns D, Bijlsma WR, Van der Lelij A. Cataract surgery in patients with nanophthalmos. Ophthalmology. 2013;120:266–70.
23. Ehlers N. Cryptophthalmos with orbito-palpebral cyst and microphthalmos. Acta Ophthalmol. 1966;44: 84–94.
24. Porges Y, et al. Hereditary microphthalmia with colobomatous cyst. Am J Ophthalmol. 1992;114:30–4.
25. Andersen ST, Fledelius HC, Heegaard S, Prause JU. Bilateral microphthalmia with cyst. Acta Ophthalmol Scand. 2004;82:490–1.
26. Foxman S, Cameron JD. The clinical implications of bilateral microphthalmia with cyst. Am J Ophthalmol. 1984;97:632–8.
27. Perry LP, Jakobiec FA, Zakka FR, Walton DS. Newborn primary congenital glaucoma: histopathologic features of the anterior chamber filtration angle. J AAPOS. 2012;16:565–8.
28. Petry P, Polli JB, Mattos VF, Rosa RCM, Zen PRG, Graziadio C, Paskulin GA, Rosa RFM. Clinical features and prognosis of a sample of patients with trisomy 13 (Patau syndrome) from Brazil. Am J Med Genet. 2013;161A:1278–83.
29. Rasmussen MLR, Prause JU, Johnson M, Kamper-Jørgensen F, Toft PB. Review of 345 eye amputations carried out in the period 1996–2003, at Rigshospitalet, Denmark. Acta Ophthalmol. 2010; 88:218–21.
30. Fan JC, Niederer RL, von Lany H, Polkinghorne PJ. Infectious endophthalmitis: clinical features, management and visual outcomes. Clin Exp Ophthalmol. 2008;36:631–6.
31. Guerra RLL, Freitas BP, Parcero CMFM, Júnior OOM, Marback RL. An outbreak of forty five cases of pseudomonas aeruginosa acute endophthalmitis after phacoemulsification. Arq Bras Oftalmol. 2012;75:344–7.
32. Goldberg RA, Flynn Jr HR, Isom RF, Miller D, Gomzalez S. An outbreak of streptococcus endophthalmitis after intravitreal injection of bevacizumab. Am J Ophthalmol. 2012;153:204–8.
33. Margo CE, Mames RN, Guy JR. Endogenous klebsiella endophthalmitis. Report of two cases and review of the literature. Ophthalmology. 1994;95:1298–301.
34. Durand ML. Endophthalmitis. Clin Microbiol Infect. 2013;19:227–34.
35. Leng T, Miller D, Flynn HW, Jacobs DJ, Gedde SJ. Delayed-onset bleb-associated endophthalmitis(1996–2008) causative organisms and visual acuity outcomes. Retina. 2011;31:344–52.
36. Jacobs DJ, Leng T, Flynn Jr HW, Shi W, Miller D, Gedde SJ. Delayed-onset bleb-associated endophthalmitis: presentation and outcome by culture result. Clin Ophthalmol. 2011;5:739–44.
37. Sugita S, Kamoi K, Ogawa M, Watanabe K, Shimizu N, Mochizuki M. Detection of Candida and Aspergillus species DNA using broad-range real-time PCR for fungal endophthalmitis. Graefes Arch Clin Exp Ophthalmol. 2012;250:391–8.
38. Chang PHY, Chodosh J. Diagnostic and therapeutic considerations in fungal keratitis. Int Ophthalmol Clin. 2011;51:33–42.
39. Jørgensen JS, Prause JU, Kiilgaard JF. Bilateral endogenous Fusarium solani endophthalmitis in a liver transplanted patient. J Med Case Re 2014;8(1):101. doi: 10.1186/1752-1947-8-101.
40. Rasmussen MLR. The eye amputated. Consequences of eye amputation with emphasis on clinical aspects, phantom eye syndrome and quality of life. Acta Ophthalmol. 2010;88(thesis 2):1–25.
41. Ibanga A, Asana U, Nkanga D, Duke R, Etim B, Oworu O. Indications for eye removal in southern Nigeria. Int Ophthalmol. 2013;33:355–60.
42. Large MM, Nielssen OB. Self-enucleation: forget Freud and Oedipus, it's all about untreated psychosis. Br J Ophthalmol. 2012;96:1056–7.

43. Wisse RPL, Bijlsma WR, Stilma JS. Ocular firework trauma: a systematic review on incidence, severity, outcome and prevention. Br J Ophthalmol. 2010;94: 1586–91.
44. Agrawal R, Wei HS, Teoh S. Predictive factors for final outcome of severely traumatized eyes with no light perception. BMC Ophthalmol. 2012;12:16.
45. Knyazer B, Bilenko N, Levy N, Lifshitz T, Belfair N, Klemperer I, Yagev R. Open globe eye injury characteristics and prognostic factors in Southern Israel: a retrospective epidemiologic review of 10-years-experience. Isr Med Assoc J. 2013;15:158–62.
46. Lee WR. Ophthalmic pathology. 2nd ed. London: Springer; 2002. p. 1–475.
47. Levin AV. Retinal hemorrhage in abusive head trauma. Pediatrics. 2010;126:961–70.
48. Rohrbach M, Benz D, Friedrichs W, Thiel H-J, Wehner H-D. Ocular pathology of the battered-child syndrome. Klin Monatsbl Augenheilkd. 1997;210: 133–8.
49. Chaithanya N, Devireddy SK, Kumar KRV, Gali RS, Aneja V. Sympathetic ophthalmia: a review of literature. Oral Surg Oral Med Oral Pathol Oral Radiol. 2012;113:172–6.
50. Chu XK, Chan C-C. Sympathetic ophthalmia: to the twenty-first century and beyond. J Ophthal Inflamm Infect. 2013;3:49.
51. Ozbek Z, Arikan G, Yaman A, Oner H, Bajin MS, Saatci AO. Sympathetic ophthalmia following vitreoretinal surgery. Int Ophthalmol. 2010;30:221–7.
52. Tseng VL, Matoso A, Hofmann RJ. Sympathetic ophthalmia following enucleation. Graefes Arch Clin Exp Ophthalmol. 2013;251:393–4.
53. Marak GE. Phacoanaphylactic endophthalmitis. Surv Ophthalmol. 1992;36:325–39.
54. Thach AB, Marak GE, McLean IW, Green WR. Phacoanaphylactic endophthalmitis: a clinicopathological review. Int Ophthalmol. 1991;15:271–9.
55. Tanito M, Kaidzu S, Katsube T, Nonoyama S, Takai Y, Ohira A. Diagnostic western blot for lens-specific proteins in aqueous fluid after traumatic lens-induced uveitis. Jpn J Ophthalmol. 2009;53:436–9.
56. Jordan DR, Brownstein S, Faraji H. Clinicopathological analysis of 15 explanted hydroxyapatite implants. Ophthal Plast Reconstr Surg. 2004;20:285–90.
57. Yoon JS, Lew H, Kim SJ, Lee SY. Exposure rate of hydroxyapatite orbital implants: a 15-year experience of 802 cases. Ophthalmology. 2008;115: 566–72.
58. Blaydon SM, Shepler TR, Neuhaus RW, White WL, Shore JW. The porous polyethylene (Medpor) spherical orbital implant. A retrospective study of 136 cases. Ophthal Plast Reconst Surg. 2003;19: 364–71.
59. Chuo JY, Dolman PJ MD, Ng TL, Buffam FV MD, White VA. Clinical and histopathologic review of 18 explanted porous polyethylene orbital implants. Ophthalmology. 2009;116:349–54.
60. Karslıoğlu S, Buttanrı IB, KorhanFazıl K, Serin D, Akbaba M. Long-term outcomes of pegged and unpegged bioceramic orbital implants. Ophthal Plast Reconstr Surg. 2012;28:264–7.
61. Shevchenko L, Boss J, Shah CT, Droste PJ, Hassan AS. Alphasphere as a successful ocular implant in primary enucleation and secondary orbital implant exchange. Orbit. 2013;32:161–5.
62. Jordan DR. Hydroxyapatite implants. Ophthalmology. 2008;115:2320–1.
63. Oestreicher JH. Hydroxyapatite orbital implants. Ophthalmology. 2008;115:2096.

Conjunctiva

2

Stefan Seregard, Maria Antonietta Blasi,
and Emilio Balestrazzi

2.1 General Description

The conjunctiva is a thin and moist mucous membrane. It covers the anterior part of the eye, save for the cornea, reaches peripherally into the upper and lower fornices, and then reflects to outline the inner surface of the eyelids. This sac remains incomplete at the bottom as the conjunctival epithelium transitions into the corneal epithelium, leaving the cornea devoid of conjunctival tissue unless pathology supervenes. At the top of the conjunctival sac, the interpalpebral fissure opens into the sac and the anterior ocular surface. The conjunctiva serves many purposes including some of great importance to ocular function. First, it secretes mucous material onto the ocular surface and contributes to the tear film. Second, it provides an anatomical and cellular barrier to foreign particles and bacteria.

2.2 Embryology, Anatomy, and Development

The conjunctiva derives from the ectoderm and can be distinguished as a surface lining distinct from the skin and cornea around the 10th gestational week, corresponding to the 40–45 mm stage. The specialized goblet cells, interspersed in the bulbar conjunctival epithelium, are frequent around the 12th gestational week (60–70 mm stage) [1], but may appear earlier in the fornix (Fig. 2.1).

Although the conjunctiva is a continuous membrane which only gradually changes its appearance, it is for practical purposes divided in three distinct zones: the bulbar, forniceal, and palpebral (tarsal) conjunctiva. The bulbar conjunctiva extends from the limbal region at the corneoscleral junction where it merges with the cornea. The loose connective tissue stroma of the conjunctiva is separated from the episclera by Tenon's capsule composed of dense collagenous tissue. The conjunctival stroma is lined by stratified squamous, nonkeratinized epithelium. Further away from the limbus, goblet cells start to appear as individual cells lodged in the epithelium. Closer to the fornix, stromal inflammatory cells and lymphoid follicles become much more abundant. At the upper and lower fornix, the conjunctiva displays small folds to increase ocular mobility. The epithelium is markedly thinner than in the bulbar conjunctiva. The accessory lacrimal glands of Krause and Wolfring typically drain into the fornix. The conjunctival stroma is much reduced in thickness as the conjunctiva reflects onto the surface of the upper and lower eyelid. The number of goblet cells is reduced as the conjunctiva extends away from the fornix. The conjunctival epithelium is here markedly thin, featuring flattened cells at the mucocutaneous

S. Seregard (✉)
St Eriks Eye Hospital, Karolinska Institutet,
Polhemsgatan 50, SE 11282 Stockholm, Sweden
e-mail: stefan.seregard@sankterik.se

M.A. Blasi • E. Balestrazzi
Institute of Ophthalmology, Catholic University,
Rome, Italy

S. Heegaard, H. Grossniklaus (eds.), *Eye Pathology: An Illustrated Guide*,
DOI 10.1007/978-3-662-43382-9_2, © Springer-Verlag Berlin Heidelberg 2015

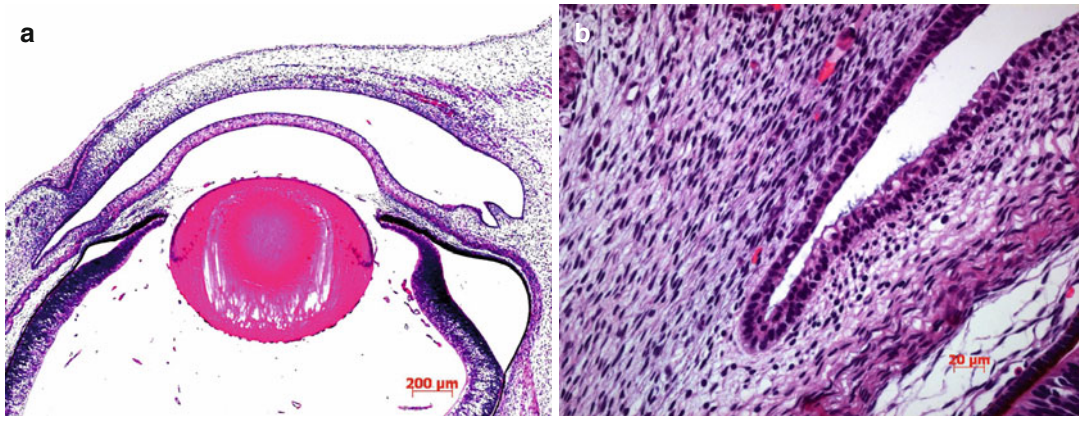

Fig. 2.1 Microphotograph of the eye (anterior segment) of a human fetus at the 42 mm stage (approximately 10th gestational week). (**a**) The conjunctival sac with its fornices is evident. Note that the eyelids remain fused, and they do not separate to form the interpalpebral fissure until after the 20th gestational week. HE stain. (**b**) Detail showing the conjunctival fornix lined by multilayered cuboidal epithelium. A few cells show intracytoplasmic vacuolization suggesting early formation of goblet cells. HE stain

junction at the eyelid margin. The epithelial thickness increases markedly as the conjunctiva extends into the bulbar surface. The bulbar stroma contains abundant small blood vessels and lymphatics. At the limbus, there is a specialized, delicate network of small interconnecting perilimbal blood vessels. The connective tissue stroma of the bulbar and forniceal conjunctiva is only very loosely connected to the eye and episclera as this allows for unhindered ocular movement. Conversely, the palpebral conjunctiva is firmly fixed to the tarsal plate of the eyelids.

Nasally, the conjunctival sac contains the semilunar fold, a remnant of the nictitating membrane seen in animals. Further nasally, the semilunar fold (the shape resembling a half-moon) connects to the caruncle which represents a transition zone to the skin. As such, the caruncle often contains sebaceous glands, typical of the skin, but not seen in the conjunctiva proper. Rarely, the caruncle may contain apocrine glands. Occasionally, supernumerary caruncles may be present [2].

2.3 Congenital Abnormalities

Cryptophthalmos (from the Greek *kryptos* meaning hidden and *ophthalmos* meaning eye) is a unilateral or more often bilateral congenital anomaly characterized by abnormal eyelids and eye covered by intact skin. Typically, the conjunctival sac is absent and the eye(s) is microphthalmic. Cryptophthalmos may be part of Fraser's syndrome, an entity defined by genital malformation and occasional malformation of the nose, ears, larynx, and renal system [3]. Fraser's syndrome is an autosomal recessive disease linked to the FRAS1 and FREM2 genes and mapped to chromosome 4q21 [4]. Recently, mutation of the GRIP1 gene has also been associated with Fraser's syndrome [5]. The incidence has been estimated to 0.043 in 10,000 live births [6].

Coloboma of the lid typically involves the palpebral conjunctiva as part of the defect. This congenital malformation may occur in association with an epibulbar choristoma and is sometimes a feature of the Goldenhar and Treacher Collins syndromes [7].

Hereditary hemorrhagic telangiectasia (Rendu–Osler–Weber disease) is characterized by systemic telangiectasia that may appear in the (often palpebral) conjunctiva and give rise to recurrent hemorrhages [1]. The *Sturge–Weber syndrome* (so-called nevus flammeus or angiomatosis associated with the trigeminal nerve branches) may have an ocular component characterized by diffuse choroidal hemangioma (essentially a hamartomatous malformation of the choroid) and episcleral and conjunctival vascular malformation. Importantly, children with Sturge–Weber syndrome may develop glaucoma

and a number of other ocular complications [8]. *Lymphangiectasia and lymphangioma* are congenital vascular lymphatic malformations that may be cystic and circumscribed or more extensive and part of an orbital lymphatic malformation. These lesions may appear in any part of the conjunctiva, but are most common on the bulbar conjunctiva away from the limbus [9]. Typically, the cyst-like spaces are filled with clear fluid, but may sometimes, in association with trauma or without any apparent cause, be filled with blood and appear as *hemorrhagic lymphangiectasia.*

Choristomas contain ordinary cells not normally present on the site often as a result from a developmental abnormality. Conjunctival choristomas include the *limbal dermoid* often associated with Goldenhar's syndrome. The limbal dermoid consists of hair shafts and sebaceous gland-like structures, believed to be displaced as a result of anomalous lid development. It typically occurs as a tan or pale dome-shaped structure at the inferior or temporal limbus [1]. *Lipodermoids* (alternatively termed dermolipoma) tend to present in the temporal periphery of the conjunctiva. These lesions are choristomas containing abundant fat (in contrast to limbal dermoids) and may fuse imperceptibly with the orbital fat. If excised they may present a surgical challenge because of the lack of a distinct cleavage plane. The rare *epicorneal lipodermoid* occurs centrally on the cornea and, in contrast to the limbal dermoid, appears not be associated with Goldenhar's syndrome [10]. *Complex choristomas* typically consist of several cellular components, e.g., cartilage, bone (*osseous choristoma*), or lacrimal gland tissue (*ectopic lacrimal glands*) [11].

2.4 Inflammation

Acute conjunctivitis is usually bilateral and features vascular dilation, stromal edema, and abundant polymorphonuclear leukocytes. Inflammation may sometimes be extensive and cause the lining conjunctival epithelium to be ulcerated. Rarely, the acute inflammation induces stromal necrosis. Typically, acute conjunctivitis is caused by any of a large number of viral agents. *Epidemic keratoconjunctivitis* is associated with adenovirus infection and is an aggressive, highly contagious subtype including some distinctive clinical characteristics. This variant may be associated with tarsal membrane formation [12]. Disease usually resolves without sequelae, but corneal scarring may develop.

Chronic conjunctivitis has nonspecific characteristics like a mild to moderately increased number of stromal lymphocytes and stromal edema. Long-standing disease may generate additional findings. These include stromal fibrosis, depletion of goblet cells, and epithelial infoldings that may generate inclusion cysts that sometimes include small calcifications [1]. Papillae of the tarsal conjunctiva may also be present. This is a nonspecific finding that may, however, also be present in vernal conjunctivitis and giant papillary conjunctivitis [1]. Follicles are composed of accumulation of lymphoid tissue sometimes with a germinal center. They appear as small nodules, approximately 1 mm in diameter, and typically present in the fornix. The causes of chronic conjunctivitis include a host of infectious agents (Fig. 2.2), local irritants, chemical compounds, topical medications, foreign bodies, and even neoplasms [1]. Some agents cause a distinct appearance like the bilateral epithelial hyperplasia with follicles and papilla and in particular extensive whitish scarring seen in the upper tarsal conjunctiva after long-standing *Chlamydia trachomatis* infection. Over eight million people are estimated to have trachomatous trichiasis as a result of scarring leading to entropion, and trachoma of the eye remains the leading infectious blinding disease worldwide [13, 14].

Granulomatous conjunctivitis is uncommon and often unilateral. Pertinent histopathological features include chronic inflammation associated with caseating or non-caseating granulomas. Granulomatous conjunctivitis may arise in combination with systemic disease including Wegener's granulomatosis and sarcoidosis [1, 15]. Occasionally, foreign bodies such as the hair shafts of caterpillars and infectious disease like onchocerciasis, blastomycosis, and tuberculosis may initiate granulomatous conjunctivitis [16–18]. Also, topical therapy including the use of preservatives has been associated with cicatrizing granulomatous conjunctivitis [19]. Secondary involvement of the tarsal conjunctiva may follow meibomian

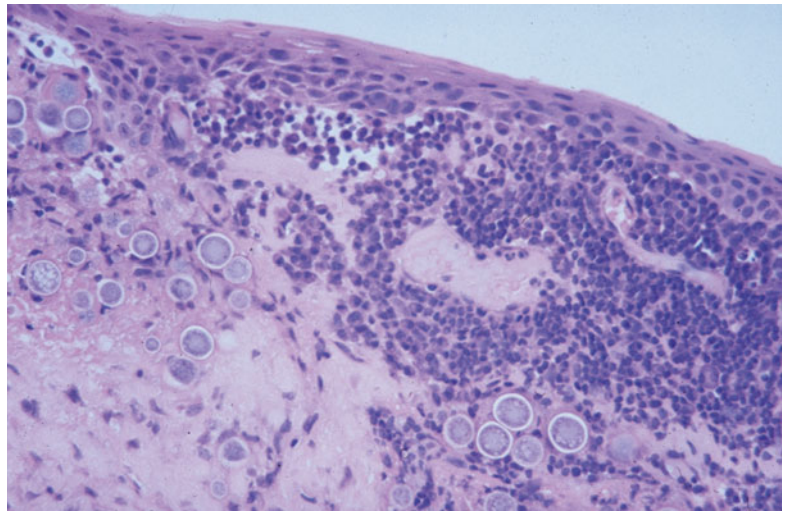

Fig. 2.2 Conjunctival coccidiomycosis. Numerous spherules about 60–80 µm in diameter and inflammatory cells are abundant in the conjunctival stroma. HE stain

gland inflammation with or without the presence of a chalazion [20]. Rarely, cat-scratch disease may cause conjunctival involvement as a feature of the oculoglandular syndrome of Parinaud [1].

Allergic conjunctivitis is very common in the Western world (reportedly occurring in up to 15–20 % of the population) [21]. It typically presents as seasonal or perennial conjunctivitis in children and adolescents associated with itching. *Vernal keratoconjunctivitis* is a subtype, more common in the tropics than temperate climates, and presents in a limbal and palpebral form that may coexist. The limbal form is characterized by the so-called Tranta's dots, but may also include giant papillae of the tarsal conjunctiva. Disease typically resolves by age 20 years. *Atopic keratoconjunctivitis* is another variant, often associated with atopic dermatitis. Histopathologically, the entity may feature giant papillae, but more commonly include conjunctival scarring. The conjunctiva is also prone to contact allergy caused by any of a range of low molecular weight substances. This reaction to a local irritant is cell mediated in contrast to the allergic variants listed above which are all IgE mediated [22].

Giant papillary conjunctivitis is caused by irritants and no longer believed to be an allergic reaction. These irritants include contact lenses, limbal sutures, ocular prostheses, and limbal dermoids [23, 24]. The histopathological features include the typical giant papillae of the upper tarsal conjunctiva (Fig. 2.3) and the presence of mast cells, basophils, and eosinophils. There is, however, no increase of IgE in the tear film as in true allergic conjunctivitis [22].

Hypersensitivity (phlyctenular) conjunctivitis is caused by proteins released by bacteria. In the Western world, this reaction to the eyelids and tarsal conjunctiva is often caused by hypersensitivity to staphylococcal infection. In a tropical setting, however, there is a significant association with coexisting tuberculosis [25]. Clinically, this entity is characterized by 2–3 mm whitish nodules composed of subepithelial acute and chronic inflammatory cells. These may cause an epithelial ulceration that eventually resolves by scarring [1].

Conjunctivitis may be associated with systemic disease, often dermatological disorders, like *atopic keratoconjunctivitis* (see above under allergic conjunctivitis), acne rosacea, mucous membrane pemphigoid, erythema multiforme (Stevens–Johnson syndrome), and epidermolysis bullosa [1]. *Acne rosacea* is a prevalent skin disease of middle-aged adults which frequently (58–72 %) is associated with manifestation in the eyelids and ocular surface [26]. The etiology and pathogenesis remain largely unknown. Skin involvement includes erythema, telangiectasia, papules, pustules, and phymatous changes in the cheeks, nose, chin, and central forehead. Changes may, however, be

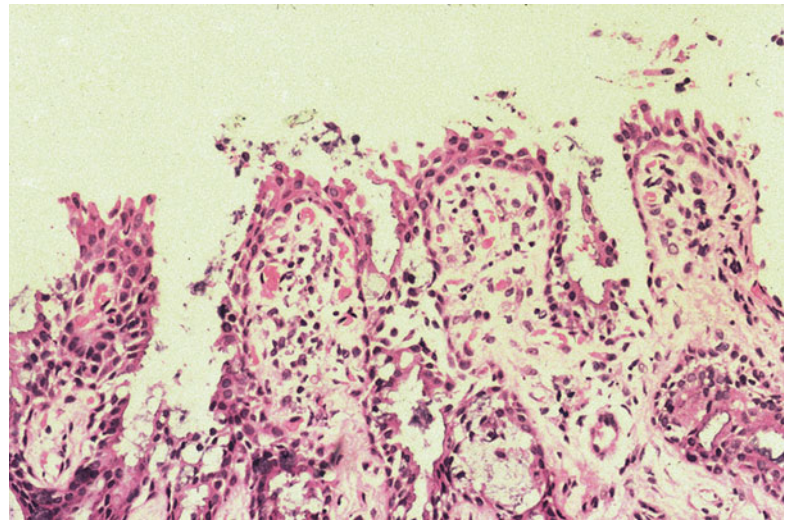

Fig. 2.3 Microphotograph of upper tarsal conjunctiva featuring giant papillae conjunctivitis with multiple infoldings. The stroma contains an increased number of chronic inflammatory cells and dilated blood vessels. HE stain

subtle, and acne rosacea may remain undiagnosed for prolonged periods of time. In some 20 % of patients, symptoms of ocular rosacea may precede skin symptoms [27]. Clinical signs suggestive of ocular rosacea include conjunctival and eyelid telangiectasia, eyelid and periocular edema, anterior blepharitis, and meibomian gland dysfunction [26]. Histopathologically, there is chronic conjunctivitis sometimes with the formation of papillae [27]. Disease intensity is variable, but keratitis and cicatrizing conjunctivitis may ensue [28]. *Ocular pemphigoid* (cicatricial pemphigoid) is a bilateral, albeit asymmetrical, autoimmune disease of the middle-aged and elderly. Diagnosis is made by immunofluorescent studies on conjunctival biopsies demonstrating basement membrane linear deposits of IgG, IgA, IgM, and complement 3 (C3) [29]. Sensitivity with this technique has been reported to range from 20 to 67 %, and a rebiopsy and/or additional techniques may be considered when a negative result is obtained in clinically suspicious disease. Standard histopathology is rarely conclusive often showing nonspecific features like subepithelial inflammation with lymphocytes, neutrophils, and histiocytes and reduced number of goblet cells. Occasional necrosis is accompanied by extensive stromal scarring. The characteristic subepithelial bullae are often not present or sometimes confused with the intraepithelial blisters occurring in pemphigoid. Ocular pemphigoid often runs an aggressive course and is a potentially blinding disease. A comprehensive review is available elsewhere [29].

Erythema multiforme (*toxic epidermal necrolysis*) and *Stevens–Johnson syndrome* are two of a group of acute blistering mucocutaneous disorders which often affects the conjunctiva [1]. Initiating events are usually drugs like allopurinol, anticonvulsants, and nonsteroidal anti-inflammatory drugs. Possibly, toxic epidermal necrolysis and the Stevens–Johnson syndrome are at two ends of a spectrum of disease. The average reported mortality for Stevens–Johnson syndrome is 1–5 % and 20–25 % for toxic epidermal necrolysis [30]. Disease may be preceded by fever, arthralgia, and malaise [1]. Clinically, the mucocutaneous lesions that follow are bilateral, multiple forms of vesicles and bullae combined with epidermal erosion (scalding). Histopathological examination of a skin biopsy reveals full-thickness epidermal necrolysis due to extensive keratinocyte apoptosis [30]. Scarring of the conjunctiva after healing may be extensive [1].

Epidermolysis bullosa is a rare, blistering mucocutaneous disease of autoimmune origin which may cause cicatrizing conjunctivitis. This entity is actually a heterogeneous group of disorders inherited in a dominant or recessive pattern. Epidermolysis bullosa disorders are caused by mutations of the structural proteins in the epidermis or dermoepidermal

Fig. 2.4 Ligneous conjunctivitis. (**a**) The patient has characteristic pseudomembranes and tumorlike subtarsal thickening of the upper eyelid. (**b**) Fibrin is deposited in the conjunctival stroma. The deposit is lined by a partially detached pseudomembrane consisting of cellular debris and numerous polymorphonuclear leukocytes. Edematous granulation tissue appears beneath the fibrinous deposit. HE stain

junction [31]. Currently, more than 1,500 different mutations in 17 different genes have been identified [32]. Diagnosis is made by a skin biopsy followed by immunofluorescence antigen mapping [31]. Transmission electron microscopy can detect the exact epidermal level of blistering and hence help to categorize disease into one of four groups now including more than 30 different subtypes. Signs of skin disease are often present shortly after birth and may be associated with involvement of the conjunctiva and other mucous membranes. Conjunctival vesicles, symblepharon, and chronic blepharoconjunctivitis as well as corneal involvement are hallmarks of ocular disease [1]. Intravenous immunoglobulin therapy may reverse the clinical course and improve ocular disease [33]. Disorders of the epidermolysis bullosa group are also candidates for protein replacement and gene therapy trials [34].

Ligneous conjunctivitis is a misnomer as the inflammation is secondary to extensive fibrin deposits, typically presenting in the upper tarsal conjunctiva. The surface epithelium is markedly thinned and atrophic or simply eroded. The surface is then covered by pseudomembranes largely consisting of cellular debris, fibrin, and polymorphonuclear leukocytes (Fig. 2.4). Ligneous conjunctivitis is caused by any of a range of mutations of the plasminogen gene. This causes functional plasminogen deficiency ultimately resulting in reduced fibrin clearance. Ligneous conjunctivitis may be associated with similar disease in, e.g., the mucous membranes of the airways and female genital tract [35].

2.5 Injuries

Thermal injuries may be caused by foreign bodies, exposure to cooled or heated air, flames, or fluids. Sometimes damage is iatrogenic, e.g.,

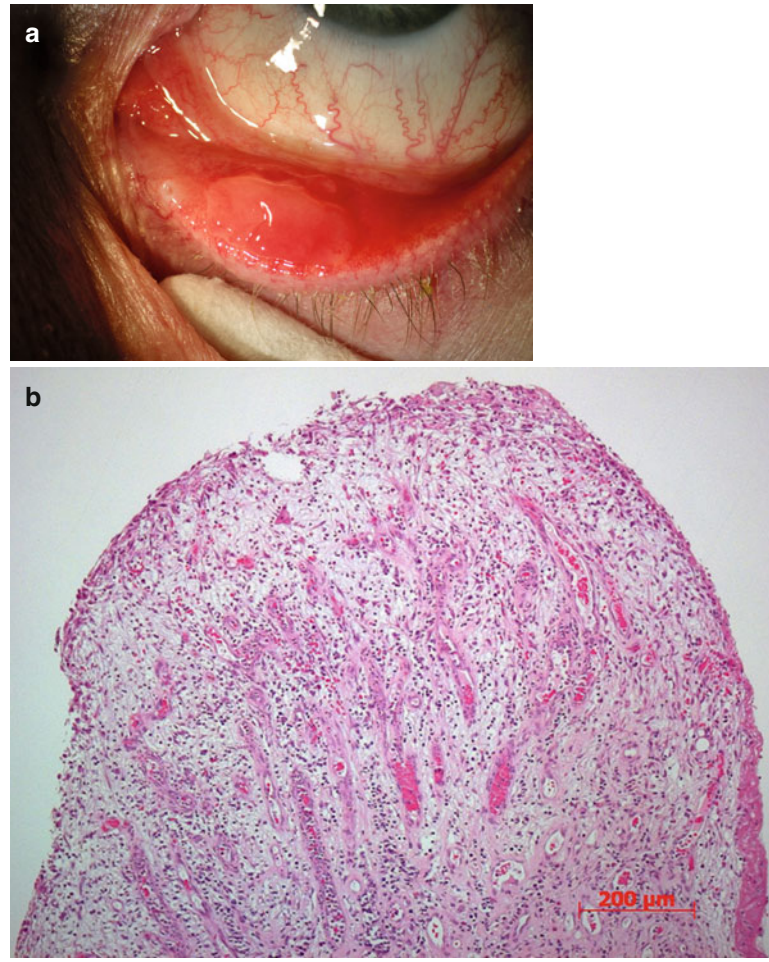

Fig. 2.5 Pyogenic granuloma. (**a**) Clinically, it arises from the tarsal conjunctiva close to the eyelid margin and lower eyelid punctum. (**b**) Histopathological examination shows dilated blood vessels, stromal edema, and numerous inflammatory cells. The epithelium is largely eroded

after the use of the triple freeze–thaw technique during removal of conjunctival tumors. The thermal response includes an initial phase of tissue destruction, an interval reactive phase, and a period of tissue repair [1]. Minor thermal injuries are typically limited to the conjunctival epithelium. Migration of peripheral epithelial cells then heals the ulceration with no scarring. Deeper injuries involve the stromal connective tissue and may cause a coagulation necrosis. The healing process will be prolonged and may result in significant scarring [1]. The extent of *chemical injuries* depends on exposure time and the ability to penetrate the conjunctival epithelium. Histopathologically, chemical injuries to the conjunctiva mimic the three phases listed above. Alkali burns are particularly feared, and late-phase excessive scarring may result in symblepharon and trichiasis secondary to entropion formation. Techniques to repair the ocular surface after both thermal and chemical injuries have much improved in recent years and include limbal stem cell grafting and amniotic membrane transplantation [36].

Aberrant wound healing may result in a *vascularized, hypertrophic scar* that mimics the appearance of a pterygium, but usually lack the stromal elastosis seen in pterygia. This scar may encroach on the corneal surface like a pterygium. Excessive wound healing may also cause a so-called pyogenic granuloma. This rapidly growing, protruding lesion is histologically defined by vascularized, edematous granulation tissue with abundant inflammatory cells (Fig. 2.5). The lining epithelium can be eroded, and pyogenic granuloma may bleed

intermittently. Usually, an underlying lesion like a chalazion or a history of trauma, e.g., previous surgery, can be identified. An inclusion cyst is not an infrequent finding in the conjunctiva following trauma or surgery (Figs. 2.6 and 2.7). These cysts derive from

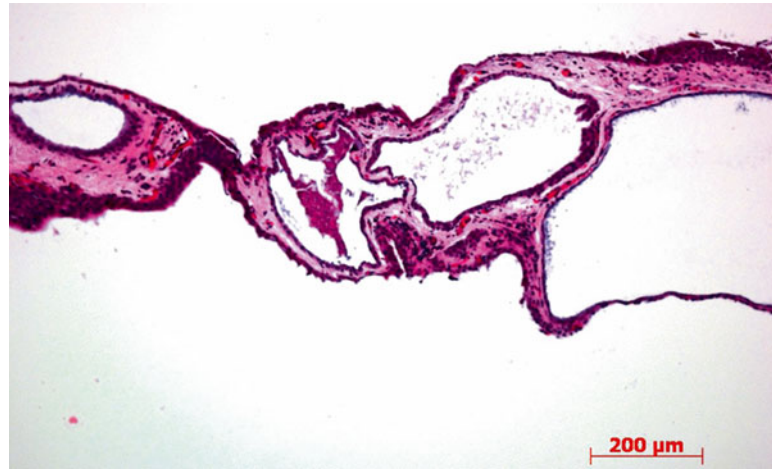

Fig. 2.6 Low-power microphotograph showing several conjunctival inclusion cysts after long-standing chronic conjunctivitis. HE stain

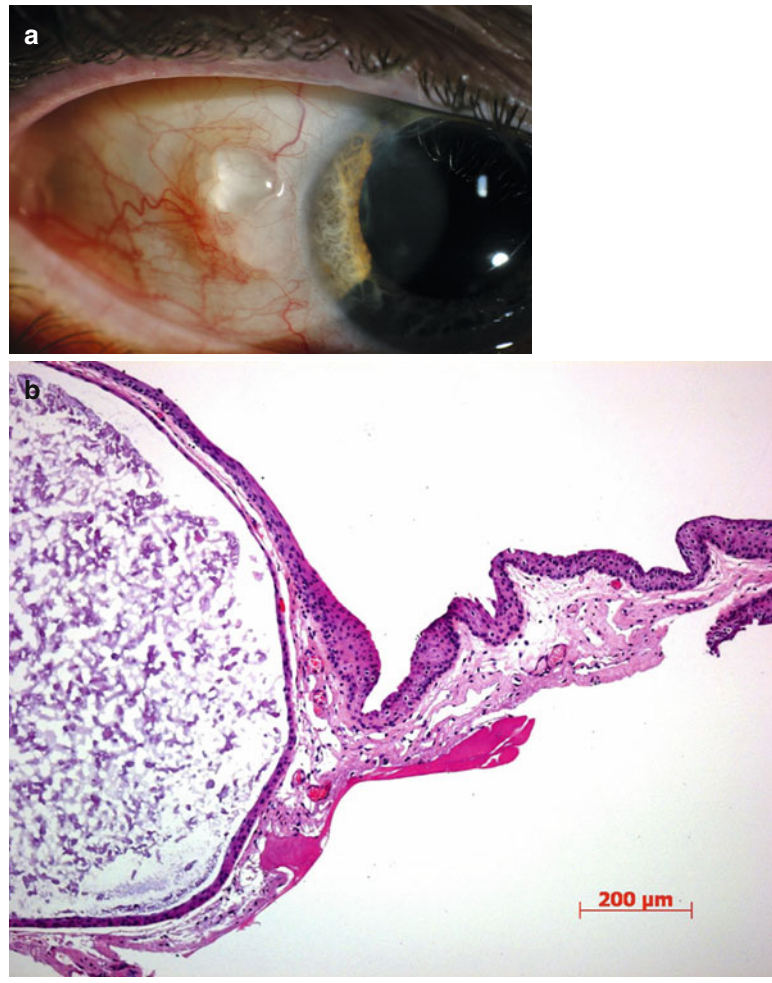

Fig. 2.7 Large conjunctival inclusion cyst. (**a**) Clinically, it is translucent and appears only to contain clear fluid. (**b**) Histopathological examination reveals the content to include desquamated cells and debris. HE stain

epithelial cells being displaced into the stroma and then proliferating into stromal cysts. Inclusion cysts may reach a significant size. Usually translucent, they may contain cellular debris and chronic inflammatory cells. *Retained foreign bodies* may be embedded in the conjunctival stroma and then elicit a mild foreign body reaction with the presence of giant cells of the foreign body type (see below under granulomatous conjunctivitis). Rarely, pigment may dissolve and cause conjunctival pigmentation that may simulate a melanocytic neoplasia (see below under Sect. 2.7.5).

2.6 Degenerations

Conjunctival xerosis (drying of the conjunctiva) may be congenital (very rare) or acquired and then usually associated with vitamin A deficiency or Sjögren's syndrome (keratoconjunctivitis sicca). Moreover, conjunctival xerosis may present following ectropion, proptosis, lacrimal gland dysfunction, and post-radiotherapy. Significant xerosis leads to metaplasia of the conjunctival epithelium with epidermalization including rete ridge formation and loss of goblet cells. The stroma displays abundant chronic inflammatory cells, blood vessel dilation, and vascular congestion [1]. Vitamin A deficiency remains a significant public health problem and globally causes a million instances of premature deaths and blindness every year [37]. *Sjögren's syndrome* is still the preferred term used for the drying of the cornea and conjunctiva initially associated with polymyalgia rheumatica, but later with other connective tissue disorders like rheumatoid arthritis, scleroderma, and systemic lupus erythematosus [1]. The xerosis in Sjögren's syndrome may affect mucosa at nonocular sites like the nasal, oral, and genital mucosa. Sjögren's syndrome is presumably an autoimmune disorder.

The *pingueculum* is a circumscribed nodular yellowish lesion appearing nasally or temporally or both at the perilimbal conjunctiva in the interpalpebral fissure. The histopathological features include significant stromal collagen degradation (sometimes termed elastoid degeneration although there is no clear evidence that collagen has been replaced by elastin fibers), stromal hypervascularization, and edema. The *pterygium* appears as a flat scar-like tissue extending onto the corneal surface from the nasal conjunctiva and is usually clinically distinct from the pinguecula. The histopathological appearance is, however, quite similar to the pinguecula, apart from vascularization being more common and prominent in a pterygium. Both lesions are more prevalent in the elderly and in a tropical setting. For this reason and because of the histopathological appearance, both lesions are regarded as actinic, presumably caused by excessive exposure to ultraviolet radiation. When a pterygium extends onto the cornea, it may need to be surgically removed. Traditionally, this has been associated with frequent recurrence, but recent techniques using no sutures or intraoperative topical mitomycin have reduced this [38, 39].

Conjunctival amyloidosis is relatively uncommon and most often occurs as primary localized amyloidosis without systemic involvement [40]. Rarely, conjunctival amyloid deposits may be the first sign of systemic amyloidosis [41]. Typically, amyloid deposits are circumscribed, yellowish-pink, subepithelial mass-like lesions. Clinical features may also include blepharoptosis and recurrent subepithelial conjunctival hemorrhage. Biopsy will reveal subepithelial amyloid deposits that show apple green birefringence under polarized light and stain positive with the Congo stain (Fig. 2.8). Conjunctival amyloid deposits may show intrinsic vascularization [40]. Amyloidosis is caused by deposits of a group of abnormally folded proteins. In localized amyloidosis, deposits occur at the site of protein synthesis, and in systemic disease, deposits occur distant to the site of protein secretion. The reason for the protein misfolding that generates insolvable cross β-sheet structures is unknown, but may involve a combination and/or environmental factors [42]. Amyloidosis may be secondary to renal disease, inflammatory bowel disease, and malignancies, notably myeloma.

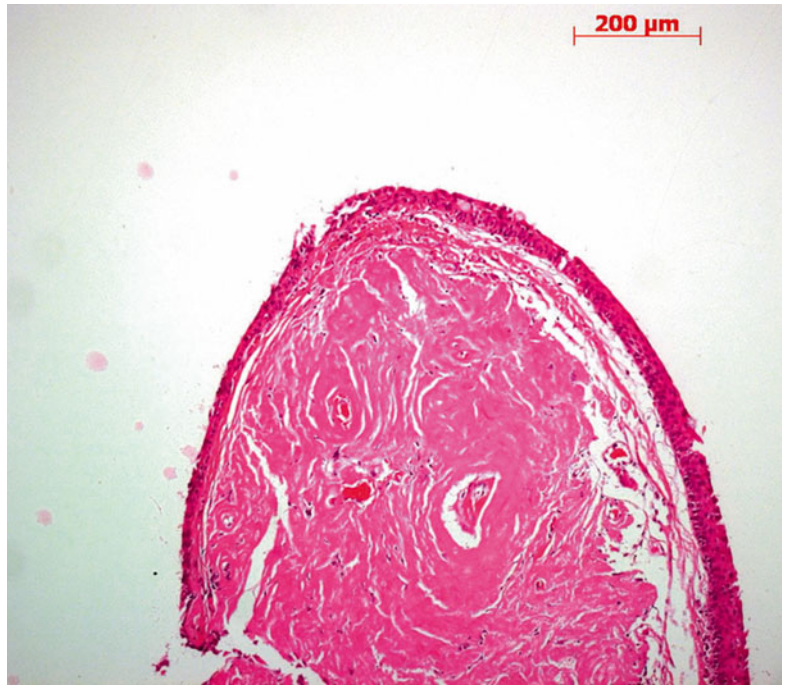

Fig. 2.8 Conjunctival amyloidosis. Abundant eosinophilic material is deposited in the conjunctival stroma. This stains positive with the Congo stain for amyloid and show birefringence in polarized light. HE stain

2.7 Neoplasia

2.7.1 Squamous Epithelial Lesions

2.7.1.1 Conjunctival Papillomas

Epidemiology

Papillomas are among the most frequent benign epithelial lesions arising within the conjunctiva of children or young adults.

Localization and Clinical Features

Preferred locations are the lid margin, interpalpebral conjunctiva, and caruncle. Most commonly they have an exophytic, sessile, or pedunculated appearance, with an irregular surface that sometimes may be cauliflower-like. When located at the limbus, they tend to remain flat.

Etiology

Various strains of human papillomavirus (HPV) have been identified in conjunctival papilloma. HPV types 6 and 11 are the most common types associated with conjunctival papilloma, and the HPV types 16 and 18 have also been found. p53 mutations in limbal epithelial cells, probably caused by ultraviolet irradiation, may be an early event in the development of some limbal tumors, including those associated with HPV.

Histopathology

Papillomas are composed of multiple fronds or fingerlike projections of conjunctival acanthotic epithelium that enclose cores of vascularized connective tissue (Fig. 2.9). Most lesions behave in a benign fashion and have little tendency to undergo malignant transformation; however, dysplastic changes can occur. Papillomas may have a mixed, or rarely an inverted, growth pattern.

The *inverted conjunctival papilloma* is a rare variant which typically has the propensity to invaginate into the underlying stroma instead of growing in the exophytic manner. Invasive lobules of benign epithelial cells are visible into the underlying connective tissue (Fig. 2.10). The presence of mucus-secreting cells is responsible for the term *mucoepidermoid papilloma*. Surgical excision with cryotherapy to the base and surrounding epithelium remains the most effective treatment [43–45].

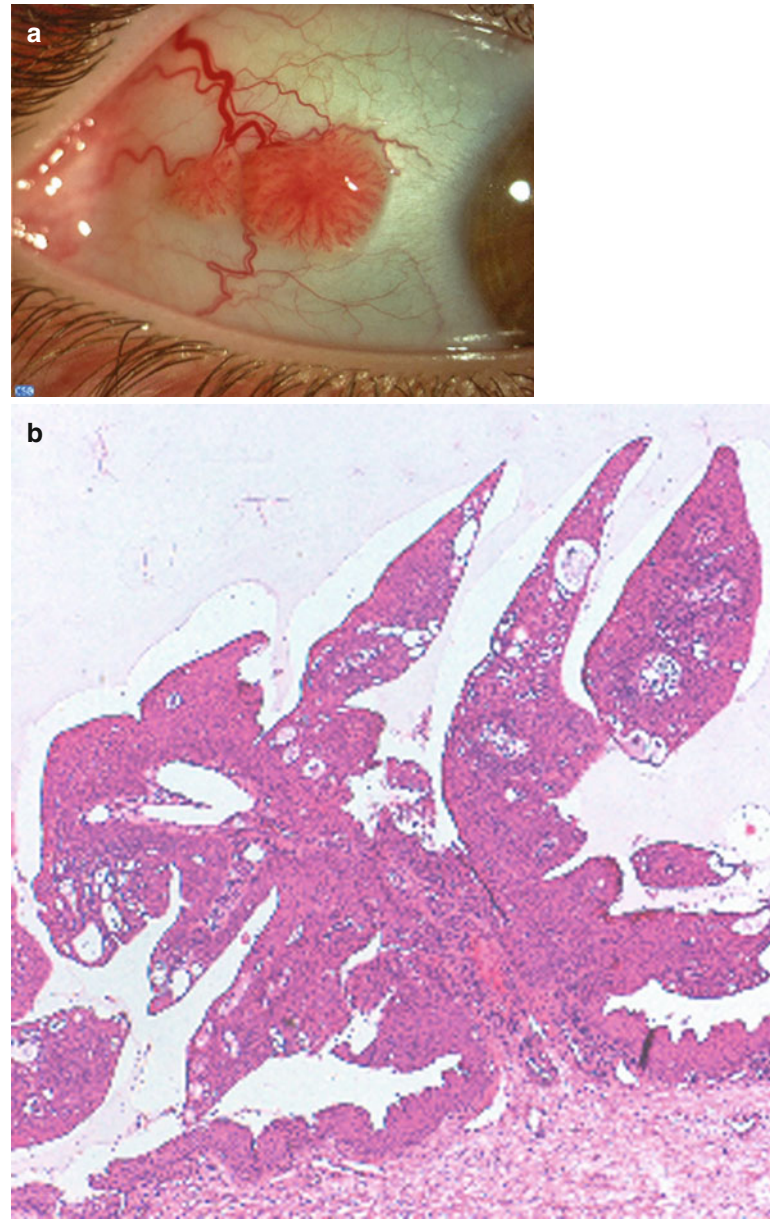

Fig. 2.9 Typical conjunctival papilloma. (**a**) Clinical appearance of an exophytic, sessile papilloma of the bulbar conjunctiva. (**b**) Histopathological features are those of fingerlike processes with a fibrovascular core covered by hyperplastic, nonkeratinized conjunctival epithelium. HE stain

Keratoacanthoma may be a specific variant of pseudoepitheliomatous hyperplasia, perhaps caused by a virus or more likely a low-grade type of squamous cell carcinoma.

Localization and Clinical Features

This rare, benign, solitary lesion presents as a white nodular mass, usually at the limbus, surrounded by dilated blood vessels and characterized by rapid enlargement.

Histopathology

The tumor forms central crater, with well-formed collarette, keratin filled, surrounded by invasive acanthotic epithelium exhibiting minimal cytologic atypia. The stroma may demonstrate elastotic degeneration and inflammatory infiltrate. Sometimes, the degree of atypia and invasive acanthosis may be more marked, causing difficulty in differential diagnosis from well-differentiated squamous cell carcinoma. Complete excision is recommended [1, 44, 46].

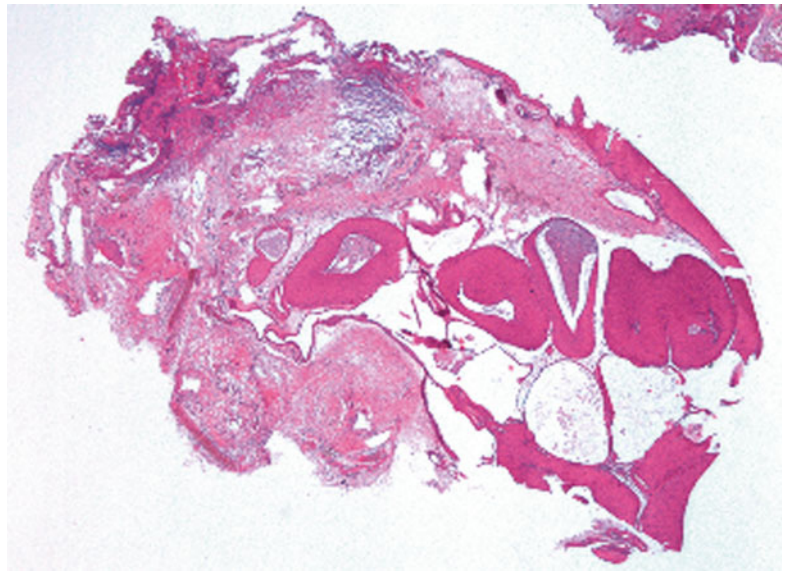

Fig. 2.10 Low-power histopathological features of an inverted papilloma. Lobules of epithelial cells have grown within the conjunctival stroma

Hereditary benign intraepithelial dyskeratosis (HBID) is a rare autosomal dominant disorder affecting family members of the Native American Haliwa–Saponi tribe.

Localization and Clinical Features

The condition is characterized by bilateral elevated white to grayish epithelial plaques on the exposed perilimbal conjunctiva, associated with dilated episcleral vessels, sometimes with encroachment of the cornea. The conjunctival leukoplakic lesions are readily moveable over the underlying tissue. The epibulbar blood vessels are commonly hyperemic and have given rise to the common colloquial term for HBID: *red eye disease.* The disorder can also affect the buccal mucosa. HBID has an apparent seasonal variation, becoming worse in the spring and summer and subsiding in the cooler weather of autumn.

Histopathology

The histologic features of surgically excised lesions of HBID include hyperplastic stratified squamous epithelium with an overlying multilayered parakeratotic mantle containing rounded cells with dense eosinophilic cytoplasm and pyknotic nuclei. A lymphoplasmacytic infiltrate within the subepithelial stroma beneath the affected epithelium is typical.

Genetics

A duplication in chromosome 4q35 is associated with HBID.

Prognosis

The condition is always benign, but it invariably recurs following surgical excision [47, 48].

Keratotic plaque. Leukoplakic lesions with no potential for malignant transformation may develop in the bulbar or limbal conjunctiva. Histologically, these lesions lack the dyskeratotic features of actinic keratosis, and the epithelial thickening is characterized mainly by acanthosis and parakeratosis or orthokeratosis [1].

Actinic keratoses are focal leukoplakic lesions, located near the limbus in the interpalpebral area. The lesions develop slowly and often occur within the epithelium overlying a preexisting pinguecula or pterygium. Microscopically there are irregular focal acanthosis of the epithelium by atypical epidermoid cells and a surface plaque of parakeratosis. The actinic elastosis in the substantia propria is considered as one of the characteristic features of this precancerous condition related to prolonged exposure of the conjunctiva to ultraviolet light (Fig. 2.11) [43].

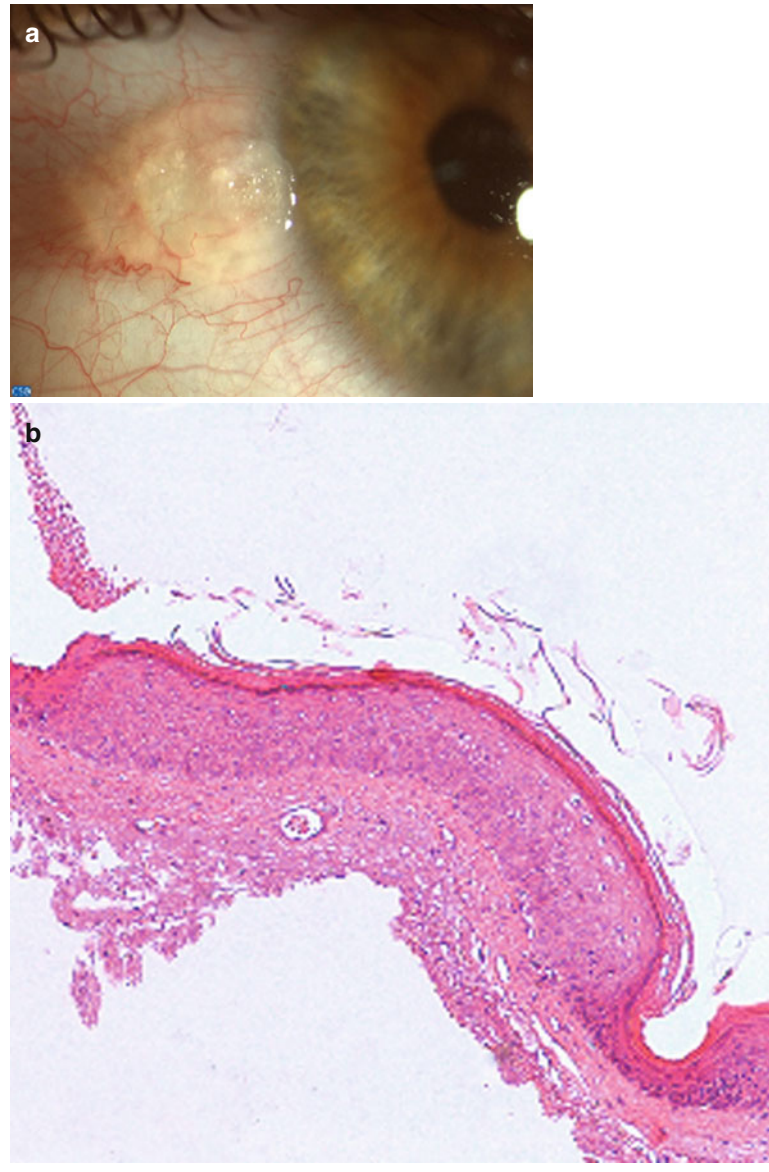

Fig. 2.11 Actinic keratosis. (**a**) Appearance of a limbal, vascularized, pearly lesion. (**b**) The conjunctival epithelium is thickened and shows acanthosis, parakeratosis, and mild dysplasia. Actinic elastosis is seen in the substantia propria

2.7.1.2 Ocular Surface Squamous Neoplasia (OSSN)

Definition

OSSN represents a spectrum of disease ranging from mild dysplasia to invasive squamous cell carcinoma (SCC).

Epidemiology

The incidence of conjunctival squamous cell carcinoma varies geographically, declining with greater distances from the equator, with Uganda having 1.2 cases per 100,000 persons per year, compared to the USA with an incidence of 0.03 per 100,000 persons per year.

Etiology

Traditionally, OSSN has been associated with the risk factors of male gender, old age, and ultraviolet light exposure and regarded as a relatively low-grade malignancy with uncommon intraocular invasion and metastasis. In the last decades,

the increased knowledge about the oncogenic influence of viruses, particularly HPV types 16 and 18 and human immunodeficiency virus (HIV), has led to the investigation of immunosuppression in the oncogenesis of conjunctival squamous cell carcinoma. More recently, HIV positivity was confirmed to be a highly significant risk factor for the development of SCC. In areas where HIV is endemic, SCC has become increasingly common and is presenting in much younger patients than before, with a dramatic shift toward female predominance.

Localization and Clinical Features

Mild dysplasia, intraepithelial neoplasia, and invasive squamous cell carcinoma are difficult to distinguish on clinical appearances alone. The lesions are described as being slightly elevated, variably shaped, relatively sharply demarcated from the surrounding normal tissues, accompanied by feeding blood vessels and colored from pearly gray to reddish gray depending on the vascularity of the tumor. They most commonly straddle the nasal or temporal limbus between the palpebral fissures [49, 50].

Conjunctival intraepithelial neoplasia (CIN) identifies the precancerous form of OSSN. It typically involves the limbus; is slightly elevated, with well-defined margins; and may be papilliform, leukoplakic, or gelatinous with characteristic tufts of blood vessels. Corneal involvement may be evident as contiguous areas of grayish epithelial thickening. Often the corneal neoplasia has a characteristic fimbriated margin with isolated clusters of gray spots (Fig. 2.12). Most lesions are unilateral.

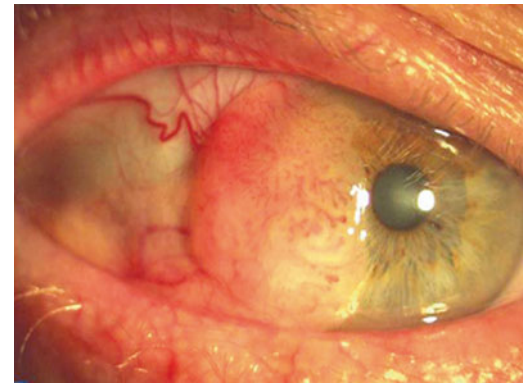

Fig. 2.12 Conjunctival intraepithelial neoplasia. There is a fleshy mass with characteristic tufts of blood vessels, located at the limbus and invading the cornea

Histopathology

Microscopic examination reveals the abrupt transition between the normal uninvolved epithelium and the epithelial neoplasia. Histologically, CIN connotes a partial-thickness to full-thickness intraepithelial neoplasia. Both lesions, however, are restrained by an intact basement membrane without invasion of the underlying substantia propria. The involved epithelium is thickened. The lesion may show mild, moderate, or severe dysplasia. The neoplastic cells characterized by hyperchromatic atypical nuclei and scant cytoplasm may be confined to the basal third of the epithelium (mild dysplasia), or the whole epithelium may be replaced by atypical, pleomorphic cells, with loss of cell polarity and mitotic figures (carcinoma in situ) (Fig. 2.13). Most CINs do not progress to invasive squamous carcinoma.

Prognosis

Despite its low virulence, CIN is difficult to cure. Recurrence rate may be as high as 50 % if the lesion is incompletely excised, and actually, positive pathologic margins are the strongest predictors of clinical recurrence. Mitomycin C, 5-fluorouracil, and interferon alpha 2b are used as the first treatment modality or as adjuvant therapy for incompletely excised or recurrent lesions [1, 43, 44].

Squamous cell carcinoma may arise de novo or from a preexisting CIN. Lesion can be papillary in configuration with many blood vessels and forms an exophytic mass, leukoplakic with a whitened keratinized plaque, or gelatinous and fleshy. The tumor, located within the interpalpebral fissure, often extends onto the cornea but is not strongly adherent.

Histopathology

In addition to the epithelial changes of CIN, there is invasion by the malignant squamous epithelial cells through the epithelial basement membrane deep into the subepithelial

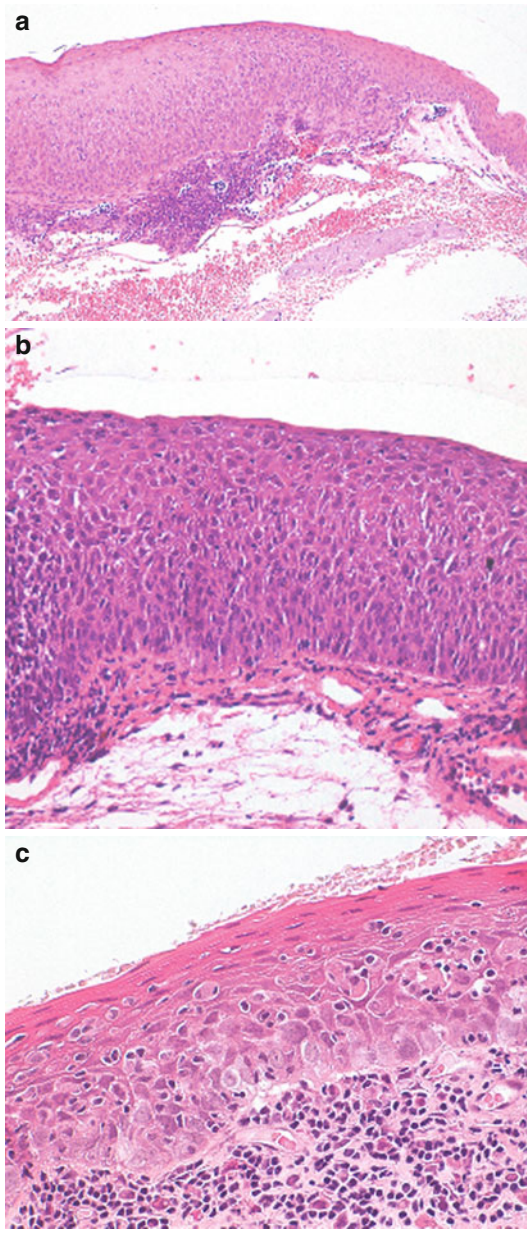

Fig. 2.13 Histopathological characteristics in conjunctival intraepithelial neoplasia (*CIN*). (**a**) Moderate dysplasia in CIN. The epithelium is thickened and largely replaced by atypical cells with hyperchromic and pleomorphic nuclei and scanty cytoplasm. Mitotic figures are restricted to the basal two-thirds of the epithelium. A slight surface differentiation is present and the basal membrane is intact. (**b**) Carcinoma in situ. The thickened epithelium has been completely replaced by spindle-shaped cells with severe nuclear and cytoplasmic atypia, loss of polarity, numerous mitoses, and absence of surface differentiation. Basement membrane is intact. (**c**) Carcinoma in situ with pagetoid features

tissue or even into adjacent structures. These lesions are usually well-differentiated carcinomas (Fig. 2.14). The substantia propria exhibits inflammatory cell infiltrate and contains atypical epithelial cells greatly variable in size and configuration, and depending on the degree of differentiation, the tumor may show hyperplastic and hyperchromatic cells, keratinized cells, concentric collections of keratinized cells (keratin pearls), loss of cellular cohesiveness, and atypical mitotic figures (Fig. 2.15). Conjunctival squamous cell carcinoma intensely expresses immunoreactivity for the tyrosine kinase EGF receptor. CIN and CSCC are associated with preferential expression of p63 in the immature dysplastic epithelial cells.

Spindle cell carcinoma is a rare variant of squamous cell carcinoma that may behave in a rather aggressive fashion. It is characterized by pleomorphic spindle cells with variably shaped nuclei, in comparison to the uniformity of the more common spindle cell, and frequent mitotic figures. Positive staining with cytokeratin, epithelial membrane antigen markers, and p63 is helpful in differentiating the variant from other spindle cell tumors such as amelanotic melanoma, malignant schwannoma, fibrosarcoma, leiomyosarcoma, and malignant fibrous histiocytoma (Fig. 2.16) [51].

Mucoepidermoid carcinoma contains cuboidal mucus-secreting cells with intracytoplasmic droplets, intermixed with epidermoid cells. Cells are arranged in nests and cords with secreted pools of mucin in the extracellular spaces. Mucinous secretion is detectable with the aid of special stains such as mucicarmine, alcian blue, and periodic acid–Schiff. A third type of cell, called intermediate or basal cell, may also be found. These tumors are uncommon in the conjunctiva and usually arise in elderly individuals in the seventh decade of life. They appear to be aggressive locally and tend to recur rapidly after excision [52, 53].

Basal cell carcinoma may rarely occur in the actinically exposed conjunctiva. Histologic examination discloses invasive epithelial lobules with a palisading outer border and peripheral cleft [1, 43, 54, 55].

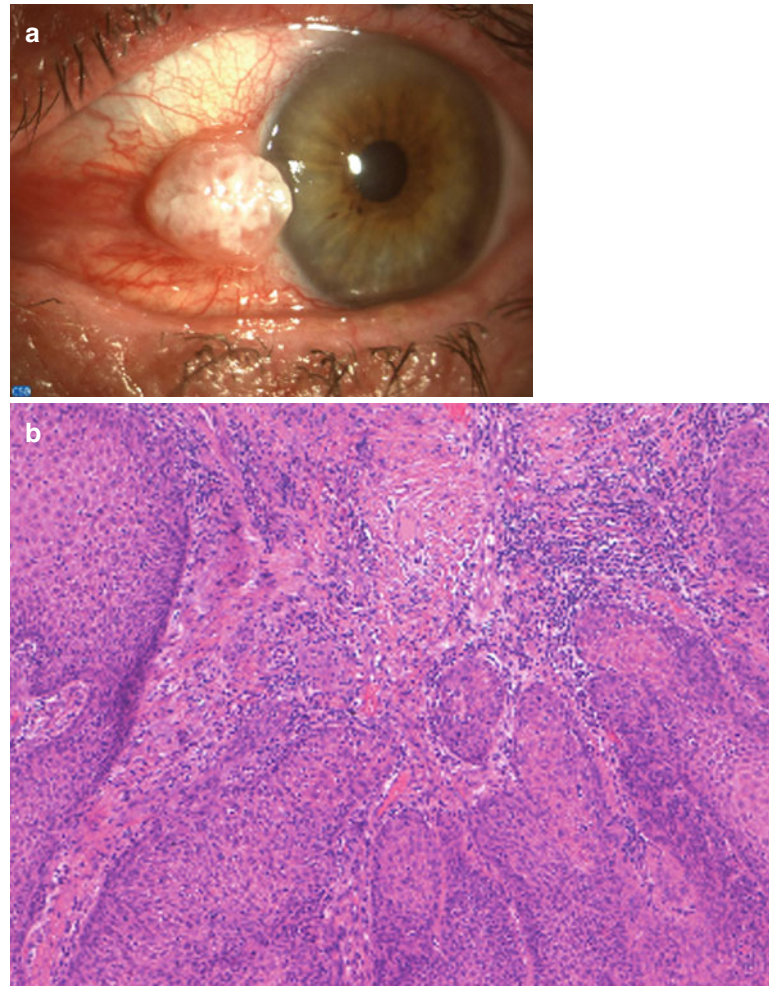

Fig. 2.14 Squamous cell carcinoma. (**a**) An exophytic, leukoplakic mass is present at the limbus. (**b**) Light microscopical examination reveals a well-differentiated carcinoma. The conjunctival stroma is infiltrated by nests of neoplastic squamous cells with large eosinophilic cytoplasm, intercellular bridges, and keratin pearls

Prognosis

Carcinoma of the ocular surface is generally regarded as low-grade malignancy. However, intraocular invasion has been reported in 11 %; corneal and/or scleral invasion was found in 30 %, and orbital invasion was noted in 15 % of patients (Fig. 2.17) [56]. Complete resection is the predominant treatment modality for OSSN, and the ocular surface is frequently reconstructed with amniotic membrane. Cryotherapy and/or topical chemotherapy (mitomycin C, 5-fluorouracil, interferon alpha-2b) may be considered as adjunctive therapies. Orbital exenteration may be required for extensive tumor involvement of orbital soft tissues. Clinical and pathologic staging is recommended, according to American Joint Committee on Cancer, using the TNM classification [57]. Histologic grade includes five categories: GX, grade cannot be assessed; G1, well differentiated; G2, moderately differentiated; G3, poorly differentiated; and G4, undifferentiated.

2.7.2 Adnexal Tumors

Sebaceous gland hyperplasia is a benign condition involving the sebaceous glands of the caruncle and usually manifests in middle-aged or older adults. The caruncle exhibits a yellow-white appearance with dilated sebaceous gland ducts visible at biomicroscopy. Histologic examination reveals enlarged gland lobules, composed of mature cells

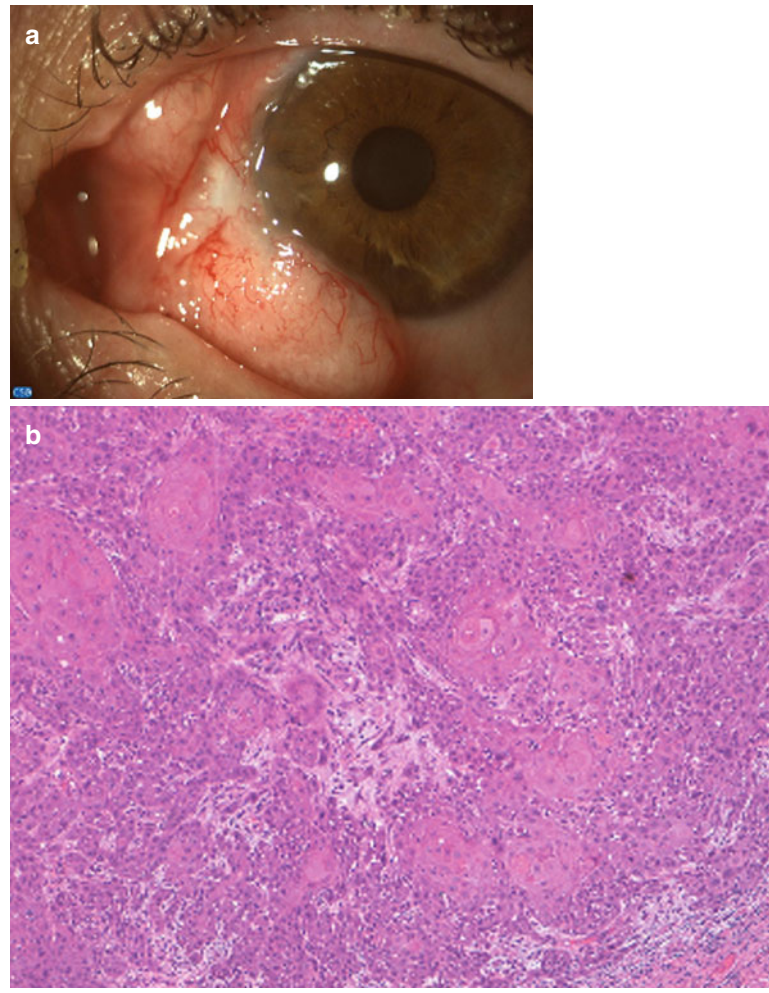

Fig. 2.15 Squamous cell carcinoma with superficial invasion. (**a**) There is a large, bilobate, vascularized mass of the bulbar conjunctiva. (**b**) Histopathologically, the basal membrane is interrupted. The epithelial cells display keratinization. At the edge of the infiltrating lobules, the cells have a more atypical appearance

with foamy cytoplasm grouped around a central dilated duct. A few inflammatory cells may be observed in the surrounding stroma [1, 58].

Oncocytoma (eosinophilic cystadenoma, oxyphilic cell adenoma, apocrine cystadenoma) is a rare tumor found most commonly in the caruncle, though it may also occur in the eyelid, lacrimal gland, and sac, especially in elderly women. It appears as a slow-growing raised pink-colored mass sometimes with a lobulated, fleshy, or cystic appearance.

Histopathology

Microscopically, oncocytoma is composed of benign epithelial cells with abundant eosinophilic granular cytoplasm, which is found on ultrastructural examination to be composed of altered mitochondria. Oncocytomas show a variable pattern, and the cells can arrange themselves in flat planes, strings, or nests and can form cystic or glandular structures (Fig. 2.18). Mitoses, pleomorphism, and necrosis are typically absent. The oncocytic cell transformation is not specific and takes place in other glands and mucous of the body and can represent a change of aging. Immunohistochemistry supports a glandular origin for oncocytoma. Surgical excision can be curative.

Prognosis

No malignant transformation of the tumor was found in the caruncular localization [59].

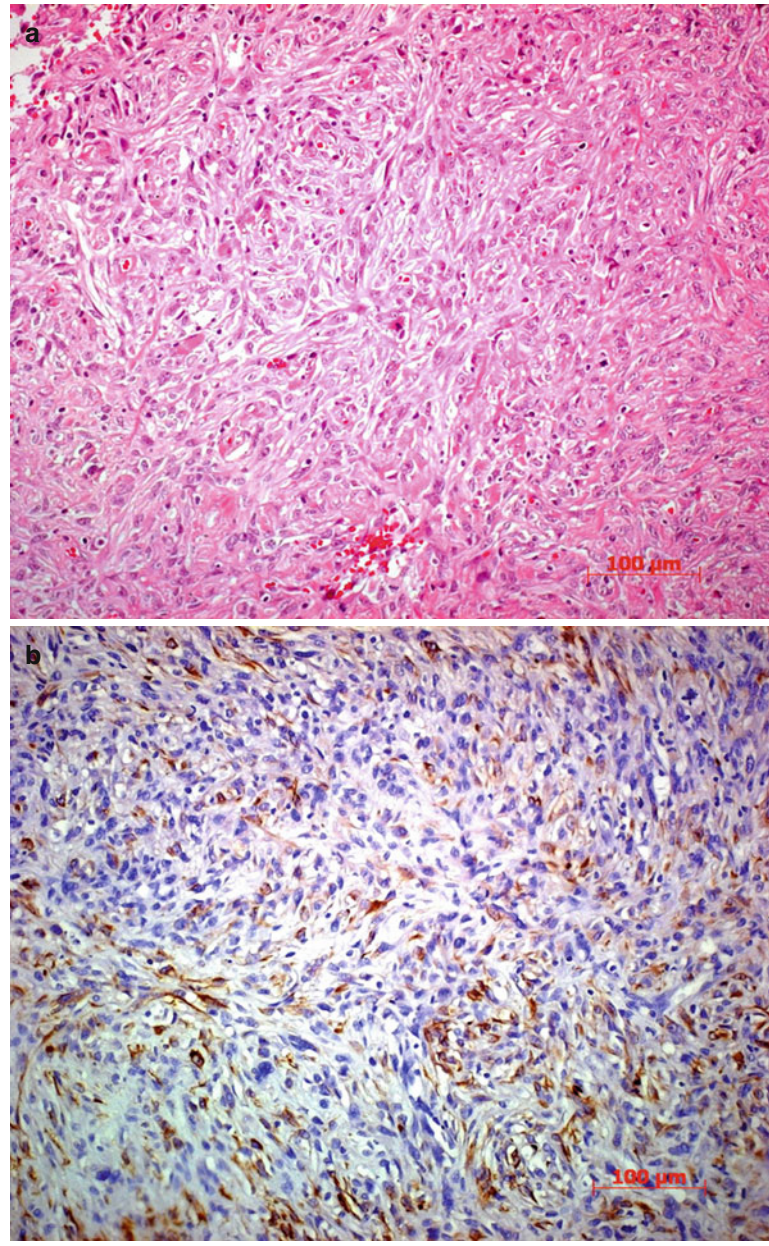

Fig. 2.16 Spindle cell carcinoma. (**a**) Histopathologically, the tumor cells grow in the conjunctival stroma beneath an intact epithelium. HE stain. (**b**) Immunohistochemical stain for cytokeratins 10, 17, and 18 is positive in most of the spindle tumor cells. The spindle cell type is more prominent in this microphotograph

2.7.3 Stromal Tumors

The conjunctival tissues may give rise to the entire spectrum of benign and malignant fibrous, xanthomatous, histiocytic, mesenchymal, vascular, and neural tumors. Many of these lesions arise very rarely from the conjunctiva, and often they are part of more extensive lesions affecting the eyelids or orbit or both [1].

Juvenile xanthogranuloma (JXG) belongs to the non-Langerhans cell histiocytoses and is a self-limited disorder of infants and young children characterized by cutaneous granulomatous disease. Ocular lesions occur in JXG in approximately 0.4–10 % of patients and may affect the iris, ciliary body, choroid, optic nerve, eyelids, and orbit [60]. Solitary JXG affecting the corneoscleral limbus is a rare form of ocular involvement.

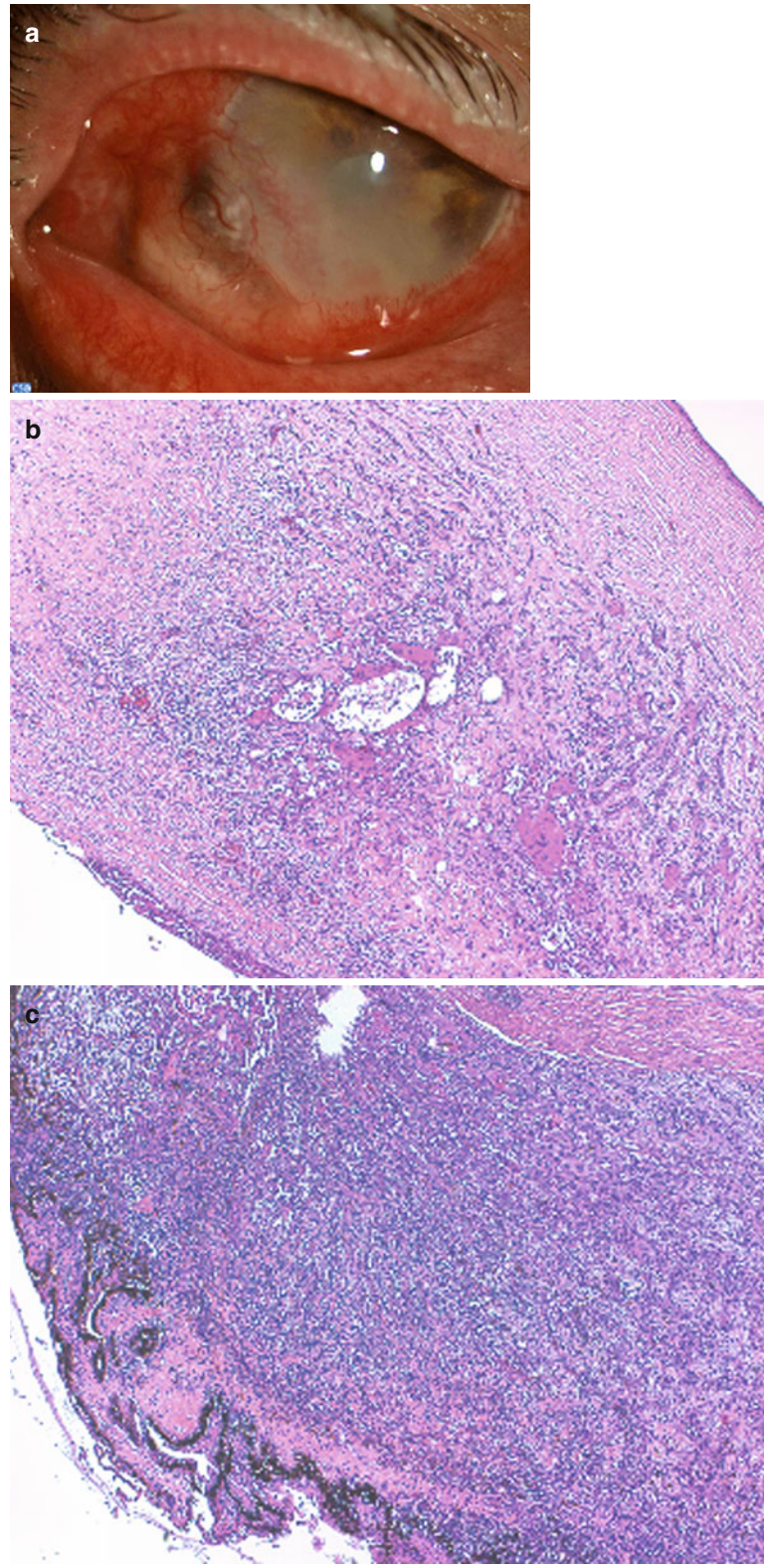

Fig. 2.17 Squamous cell carcinoma with intraocular invasion. (**a**) Neoplastic vascularized tissue infiltrates the cornea and the globe through the angle. (**b**) The corneal stroma is diffusely invaded by squamous cells. (**c**) Tumor cells are spreading into the ciliary body

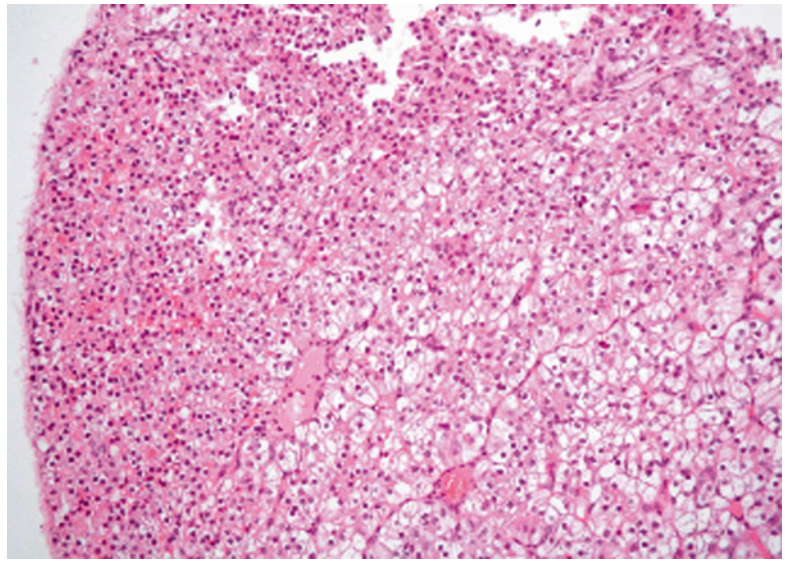

Fig. 2.18 Histopathological appearance of conjunctival oncocytoma. Solid clusters of tightly packed oncocytes are separated by thin strands of fibrovascular stroma. Neoplastic cells display large, eosinophilic, and finely granular cytoplasm. Nuclei are large and round with coarse chromatin and small nucleoli. Clear cell change is prominent in many tumor cells

Limbal lesions appear as raised yellow-orange mass and are commonly unilateral. The differential diagnosis includes epibulbar dermoid.

Histopathology

These lesions display the typical findings of JXG, a solid infiltrate, made up of foamy mononuclear cells, showing a xanthomatous morphology. In some areas, a spindle cell morphology with storiform growth pattern could be demonstrated. Scattered multinucleated giant cells with a Touton-like morphology, in association with sparse lymphocytes, small numbers of eosinophils, and some polymorphonuclear leukocytes, are observed. The tumor cells stain positive for CD68, but are negative for protein S-100, CD1a, and CD207 (Langerin) [61].

Fibrous histiocytomas (FHs) are mesenchymal tumors composed of cells with fibroblastic to histiocytic differentiation. They can be classified as benign or malignant. FH is found most commonly in the orbit and rarely presents as conjunctival tumor.

Histopathology

FH shows a characteristic, diphasic pattern with mainly storiform areas composed of fibrous spindle cells along with scattered areas showing single or grouped foamy histiocytes. Malignant FH shows a mixture of storiform and pleomorphic features and may be difficult to differentiate from other pleomorphic soft tissue tumors. Immunohistochemistry, although not specific, is essential for the diagnosis. FH displays variable positive immunoreactivity for markers of histiocytic (CD 68), myofibroblastic (smooth muscle actin), and even dendritic cell differentiation (factor XIIIa). The most appropriate management of FH is complete surgical excision [62, 63].

Fibroma. Ocular fibroma is extremely rare and seldom diagnosed. It has been described as indolent growths originating from the medial orbit, periorbita, episcleral plane, tarsus, and eyelids.

Histopathology

Fibroma is circumscribed but not encapsulated, and there is a hypocellular proliferation, without a zonal pattern, and there is no inflammation. Highly collagenized eosinophilic matrix, widely separating scant elongated and compressed fibroblasts, is the dominant feature. The collagen may assume a keloid-like configuration. Total excision is the recommended therapy, since fibroma may recur if incompletely excised [64].

Myxoma, derived from primitive mesenchymal cell, is a benign soft tissue tumor. Conjunctival myxoma is extremely rare.

Clinical Features

The typical presentation is a painless, circumscribed, rubbery, translucent/solid, yellow-pink mass or cyst in middle-aged patients. The lesion can be mistaken for amelanotic nevus, amelanotic melanoma, squamous cell carcinoma, lipoma, and cyst. Myxomas can occur as localized disease or as a component of the Carney complex, Mazabraud syndrome, and McCune–Albright syndrome. Carney complex includes myxomas (especially cardiac but also eyelid), spotty mucocutaneous (including conjunctiva), and endocrine overactivity (especially Cushing's syndrome). The Carney complex gene 1 has been identified as the regulatory subunit 1A of protein kinase A (PRKAR1A) located at 17q22–24.

Histopathology

Conjunctival myxoma has characteristic histopathological features. It consists of scattered, relatively small numbers of stellate- and spindle-shaped cells embedded in a mucinous matrix with delicate reticulin fibers, sparse vascular structures, and mature collagen fibers. Some of the tumor cells have clear, intranuclear inclusions and intracytoplasmic vacuoles. The presence of mast cell scattered throughout the myxoid stroma is an additional feature in conjunctival myxomas. Immunohistochemical studies show myxoma cells immunoreactive for vimentin and smooth muscle actin but negative for S-100 protein, desmin, and myoglobulin. The management is complete surgical resection [65, 66].

Rhabdomyosarcoma (RMS) is a malignant soft tissue tumor showing evidence of striated muscle differentiation. The conjunctiva may infrequently be the site of origin. Tumors originating in the conjunctiva show a propensity to arise in the superior or superonasal areas of fornix as a mass protruding into the palpebral aperture. The botryoid type of embryonal RMS involves mucous membranes, commonly the vagina and the bladder, rarely the conjunctiva.

Histopathology

It shows a condensation of neoplastic cells, called the *cambium layer*, beneath the epithelium. Embryonal RMS shows hypercellular areas of small to round spindle cells separated by hypocellular myxoid areas. This tumor is composed of primitive mesenchymal cells in various stages of myogenesis. Stellate cells with lightly amphophilic cytoplasm and central nuclei represent the most primitive end of this spectrum. Bright eosinophilia, cytoplasmic cross-striations, and multinucleation indicate terminal differentiation. Immunohistochemistry shows positivity for vimentin, myosin, myoglobin, muscle specific actin, desmin, myogenin, and Myo-D1. Cytogenetic studies of embryonal RMS have found complex structural and numerical chromosomal changes. The botryoid and spindle cell subtypes of embryonal RMS have a favorable prognosis. The treatment for botryoid rhabdomyosarcoma is basically surgical with the combined use of adjuvant polychemotherapy [64, 67].

Infantile capillary hemangioma generally appears shortly after birth and shows progressive growth for up to 2 years and then slowly regresses.

Localization and Clinical Features

The lesion appeared as a circumscribed or diffuse pink-red lesion anywhere in the conjunctiva, as well as an isolated lesion or in association with an eyelid or orbital capillary hemangioma.

Histopathology

Conjunctival capillary hemangioma is composed of lobules of proliferating endothelial cells separated by thin fibrous septae. In the early stage the lesion shows proliferating capillaries with little intervening stroma. Later on, the capillaries become dilated and filled with red blood cells, and fibrosis is found between the vessels. Most lesions were managed by observation only, and systemic corticosteroids were reserved for lesions that had contiguous eyelid or orbital involvement that threatened amblyopia.

Cavernous hemangioma can appear at any age as a red or blue multiloculated lesion in the conjunctival stroma and ranges from a small, subtle, circumscribed lesion to a large lesion that is readily apparent and may be similar clinically to lymphangioma. Cavernous hemangioma is usually solitary, but conjunctival vascular changes can occur in association with other vascular

syndromes, such as Sturge–Weber syndrome, blue rubber bleb nevus syndrome, and diffuse neonatal hemangiomatosis.

Histopathology

Microscopically, conjunctival cavernous hemangioma is identical to orbital cavernous hemangioma. It is well encapsulated by fibrous tissue and shows large, regularly shaped vascular channels lined by endothelial cells and surrounded by smooth muscle cells. The stroma consists of thick fibrous tissue that may contain bundles of smooth muscle and myxoid foci. Conjunctival cavernous hemangioma can be managed by periodic observation or local resection [9, 64].

Kaposi's sarcoma (KS). Conjunctival sarcoma is rare and is encountered mostly in patients with AIDS, in some cases as the initial manifestation.

Clinical Features

The clinical pathognomonic presentation is of a reddish or bluish, painless, vascular conjunctival lesion that may be diffuse or nodular.

Histopathology

Kaposi's sarcoma is a malignant tumor composed of spindle-shaped cells with elongated oval nuclei, well-formed capillary channels, and vascular slits containing erythrocytes, but without an endothelial lining (Fig. 2.19). The lesion can be mistaken for subconjunctival hemorrhage, pyogenic granuloma, and inflammatory lesion. New herpesvirus-like DNA sequences (KSHV) have been found in classic, endemic, and AIDS-associated KS. KSHV is a reliable marker (by polymerase chain reaction) to distinguish KS, particularly at the early stage, from other vascular lesions. Conjunctival Kaposi's sarcoma has been shown to respond to chemotherapy and low-dose radiotherapy. Interferon-2a has also been used. Surgical excision combined with cryotherapy is an appropriate management for smaller lesions [9, 44].

*Neurofibroma i*s a benign tumor that originates from peripheral nerves. The conjunctiva represents a rather unusual location for a neurofibroma that can be an isolated finding or rarely associated to neurofibromatosis. Isolated neurofibroma is a well-delimited, nonencapsulated mass composed of spindle-shaped cells with wavy nuclei. The axonal component, absent in schwannoma, can be demonstrated with neurofilament immunostaining. Similar to schwannoma, the tumor cells show positive immunostaining for S-100 protein [68].

Schwannoma or neurilemmoma is a benign tumor of Schwann cell origin that arises from a peripheral nerve forming an encapsulated mass. Schwannomas of ophthalmic interest more frequently involve the orbit, are rare, and can be associated to neurofibromatosis type 2. Some cases of conjunctival schwannoma are reported.

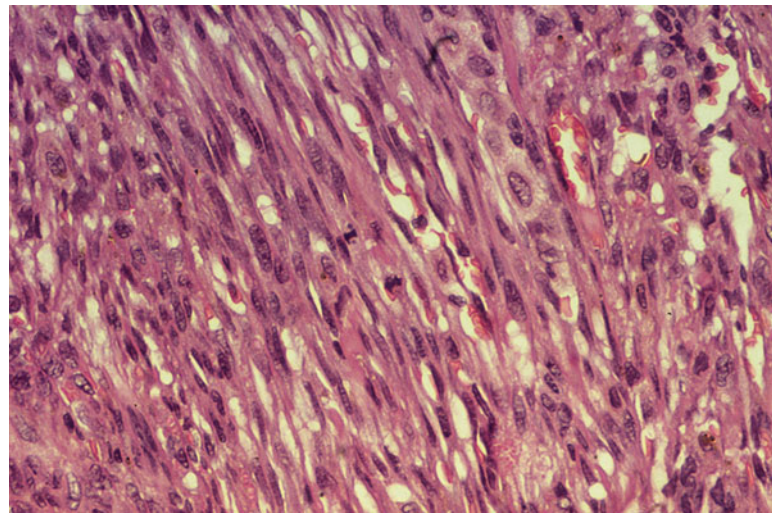

Fig. 2.19 Microphotograph of conjunctival Kaposi sarcoma. Spindle-shaped tumor cells are compressing slit-like spaces containing blood vessels and extravasated erythrocytes. HE stain

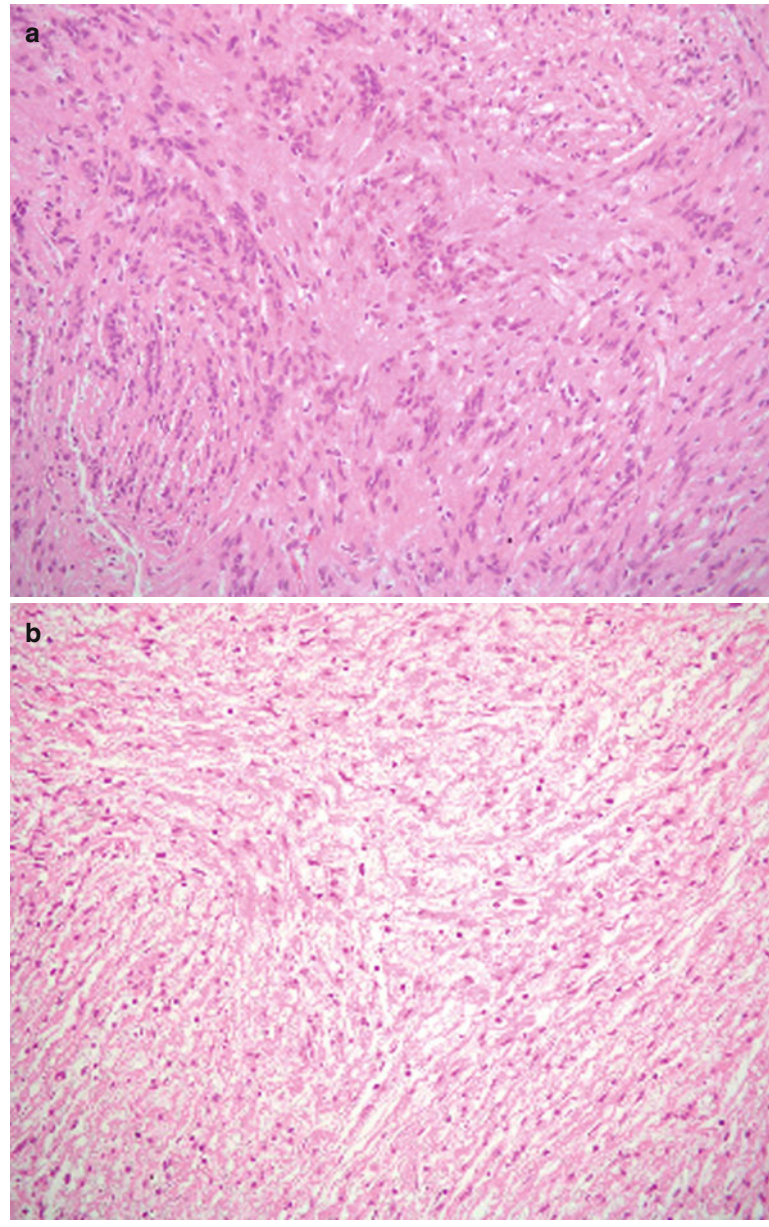

Fig.2.20 Microphotographs of conjunctival schwannoma. (**a**) Antoni A pattern, palisading of nuclei forming solid cellular areas. Verocay bodies (nuclear palisading and highly oriented, cytoplasmic processes) may be observed. (**b**) Antoni B pattern, areas of loose, stellate cells suspended in a mucinous matrix

Clinical Features

The lesion appears as an amelanotic, translucent, round, well-circumscribed, subconjunctival nodule.

Histopathology

It reveals a tumor composed of spindle. Two growth patterns have been described. The Antoni A area shows sheets of palisading spindle cells with spindle-shaped nuclei forming Verocay bodies and an Antoni B pattern of haphazardly arranged elongated cells in a myxoid stroma (Fig. 2.20). Immunohistochemistry shows positivity for S-100 protein [64, 69].

2.7.4 Lymphoid Tumors

Lymphoproliferative lesions in the conjunctiva encompass a wide spectrum of disorders, ranging from benign reactive lymphoid

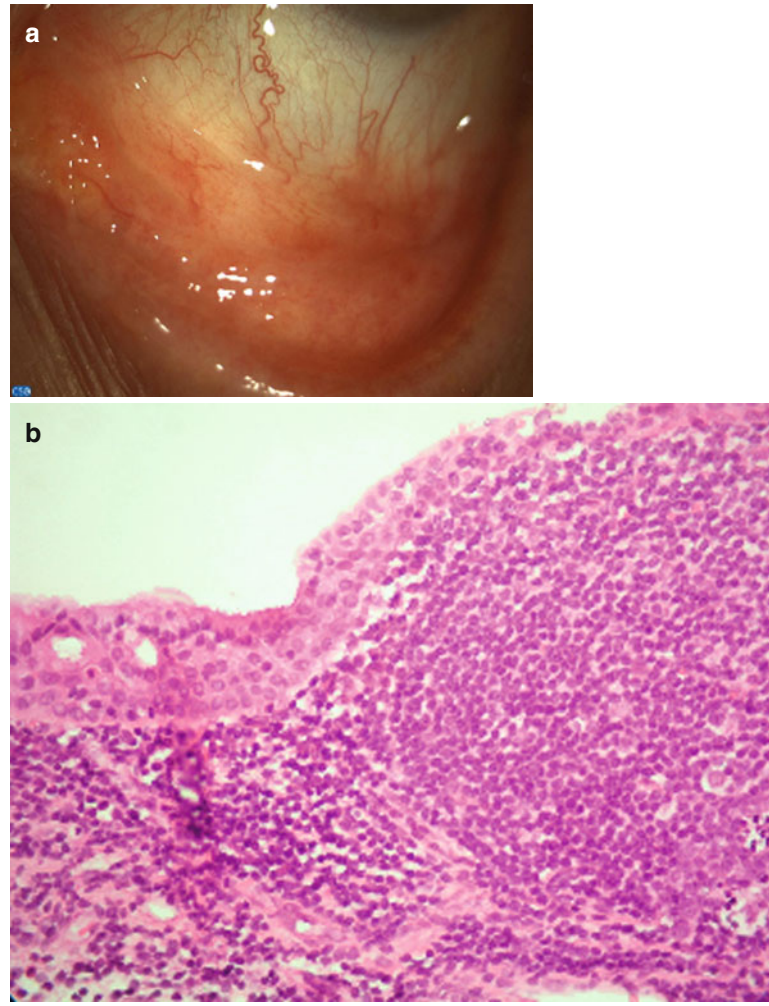

Fig. 2.21 Reactive lymphoid hyperplasia. (**a**) Mild thickening of the inferior fornix with small nodularities on the left. (**b**) Lymphoid infiltrate with germinal center is located within the subepithelial stroma

hyperplasia, that is, a nonspecific inflammation, to malignant lymphoma. Conjunctival lymphoid tumors typically present as a salmon-colored patch or infiltrate in the fornix or on the epibulbar surface. They usually are asymptomatic at presentation, with only negligible reports of a progressively enlarging mass, irritation, or ptosis. The tumors are usually unilateral, but may be bilateral, or may represent an extension from an orbital lymphoma [70].

Reactive lymphoid hyperplasia is a benign lesion occurring in patients over 40 years of age. It presents as minimally elevated salmon-colored tumor with a pebbly appearance.

Histopathology

Lymphoid hyperplasia is a polymorphous infiltrate composed of mature well-differentiated lymphocytes, often admixed with plasma cells, which contains benign reactive lymphoid follicles or germinal centers (Fig. 2.21). The reactive follicles are composed of large, pale, mitotically active immunoblasts and harbor tingible body macrophages that contain basophilic bodies of apoptotic nuclear debris. Immunohistochemical stains disclose CD20-positive B lymphocytes in the follicular centers and the surrounding mantle zone. Antiapoptotic Bcl-2 protein normally is absent in the reactive follicles. CD3-positive T

cells predominate in the interfollicular zone between the germinal centers [43].

2.7.4.1 Lymphoma

Epidemiology

Extranodal marginal zone lymphoma (EMZL) of mucosa-associated lymphoid tissue (MALT) is the most common subtype of conjunctival lymphoma, accounting for up to 80 % of cases of primary lymphoma. MALT lymphomas usually arise around the sixth decade of life, with female predominance. Often patients have a history of autoimmune disease or chronic inflammatory disorders. The majority of patients present with localized disease (AJCC, T1 stage) [57]. Disseminated disease can develop in approximately one-third of the patients.

Localization and Clinical Features

It is characterized by painless salmon-pink patches in the fornix or bulbar conjunctiva and has an indolent clinical course.

Histopathology

MALT lymphomas are characterized by an expansion of a heterogeneous cell population, consisting of centrocyte-like, monocytoid, and plasmacytoid cells, with occasional blasts in the marginal zone surrounding reactive follicles. Pathognomonic histopathological features include follicular colonization and lymphoepithelial lesions through invasion of neighboring epithelial structures by nests of MALT lymphoma cells. "Dutcher bodies," intranuclear pseudoinclusions of periodic acid–Schiff-positive eosinophilic cytoplasm, have been observed in low-grade lymphoid malignancies, especially in those with plasmacytoid differentiation. Immunophenotypically, MALT lymphomas have a characteristic profile, which allows their differentiation from benign lymphoproliferative disorders and other small B-cell lymphomas (Fig. 2.22). They are characterized by dense, CD20+, CD10−, CD23−, BCL-6− B-cell lymphocytic infiltrates, with few interspersed CD3+ T lymphocytes. They are almost always (95 %) negative for CD5. Immunoglobulin heavy- and light-chain gene rearrangements allow for detection of a clonal B-cell population [71].

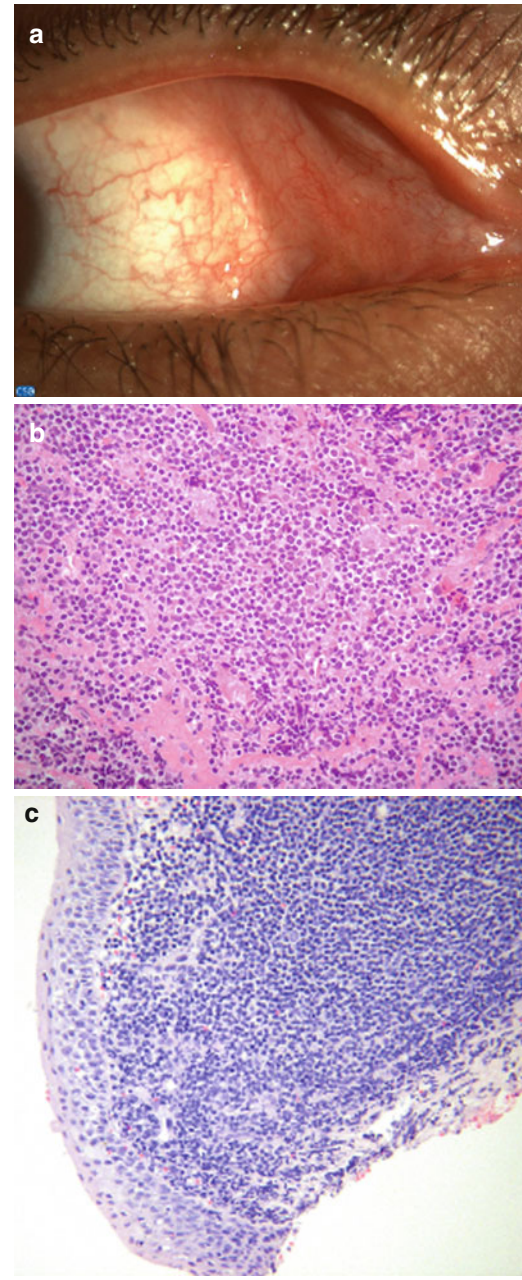

Fig. 2.22 Mucosa-associated lymphoid tissue (MALT) lymphoma. (**a**) Salmon-colored mass involving the superior fornix and the lacrimal gland. (**b**, **c**) Diffuse proliferation of atypical lymphocytes. (**d**) Immunohistochemistry reveals strong positivity for CD20

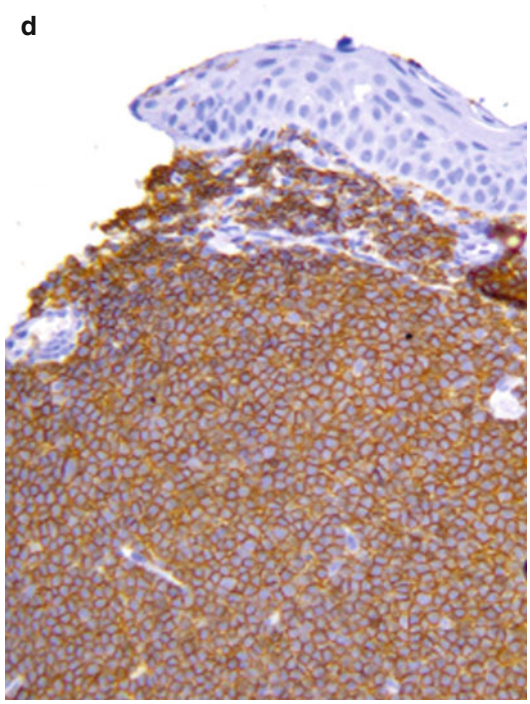

Fig. 2.22 (continued)

Genetics

Several genetic aberrations have been implicated in the development and progression of MALT lymphoma. The most common such translocation, observed in 15–40 % of patients, is t(11;18)(q21;q21) [72].

Prognosis

The prognosis of conjunctival MALT lymphoma is good, with reported 5-year disease-free survival and overall survival rates being 65 and 83 %, respectively. Local radiotherapy long has been the preferred treatment method; however, other options have been reported, including surgical resection, systemic or local chemotherapy with topical mitomycin C, and systemic antibiotic therapy. Recently, the trend has moved toward immune modulator therapy, such as with interferon-α and monoclonal anti-CD20 antibody [73]. Although the majority of lymphomas are primary neoplasms, 10–32 % are secondary tumors in patients with disseminated lymphoma, and more than 95 % are of B-cell origin (Fig. 2.23).

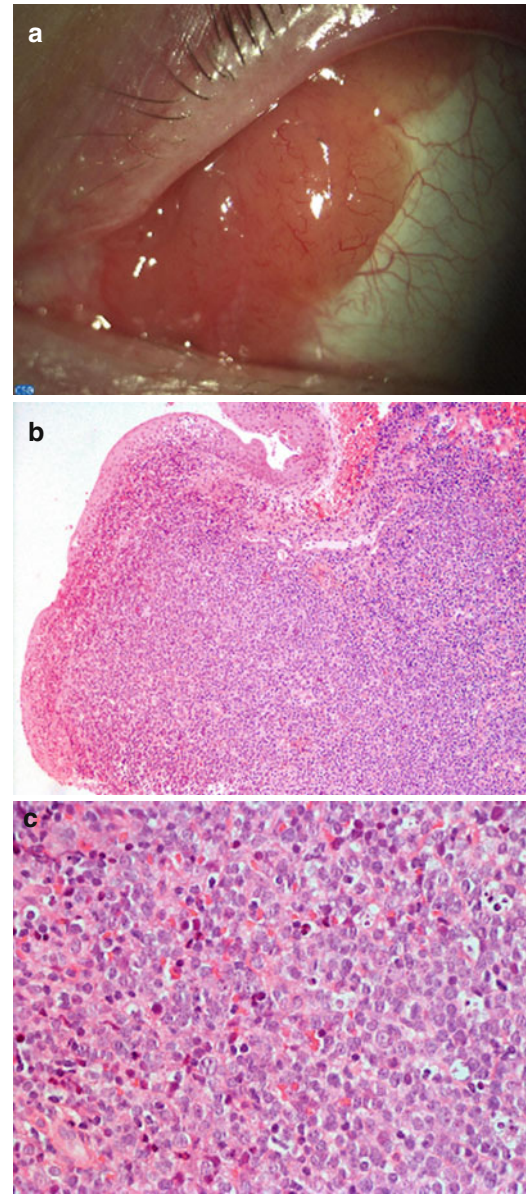

Fig. 2.23 Conjunctival presentation of disseminated lymphoma. (**a**) Salmon-colored mass, with smooth surface, extending from plica semilunaris to superior fornix. (**b**) Localized erosion of the epithelium, subepithelial neoplastic infiltration. (**c**) High-power magnification shows medium–large-sized lymphocytes

2.7.4.2 Metastases

Conjunctival metastases are exceedingly rare. Breast and lung carcinoma and cutaneous melanoma account for the majority of conjunctival metastases (Fig. 2.24). The conjunctiva may be the

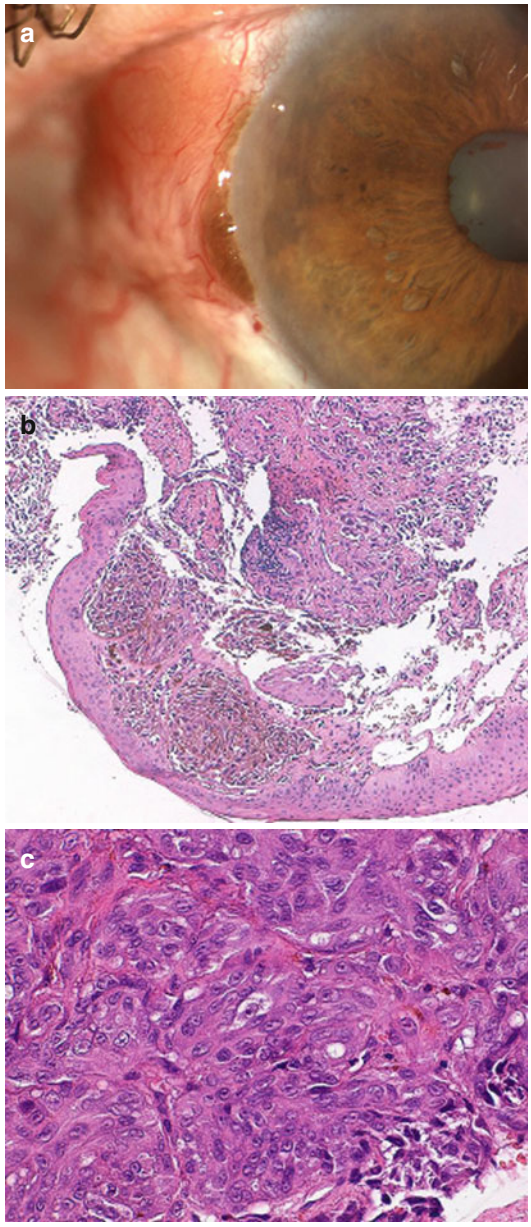

Fig. 2.24 Conjunctival metastasis from cutaneous melanoma (**a**) An intensively vascularized nodule at the limbus is contiguous with a pigmented fusiform thickening of the iris root. (**b**) Tumor cells are spreading to the conjunctival epithelium. (**c**) A few large, pleomorphic cells, with vesicular nuclei and prominent nucleoli, can be identified as epithelioid melanoma cells

only ocular site, or the iris and posterior uvea may be involved. Most metastases are solitary lesions with dilated overlying conjunctival vessels and not

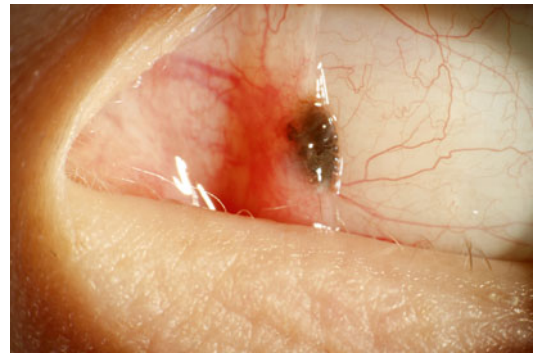

Fig. 2.25 Clinical photograph of conjunctival nevus at the plica semilunaris

Fig. 2.26 Clinical photograph of juxtalimbal conjunctival nevus

adherent to the underlying sclera. Conjunctival metastases are usually a sign of advanced malignant disease with poor prognosis [74].

2.7.5 Melanocytic Tumors

The common benign nevus of the conjunctiva typically presents as an acquired lesion in the bulbar conjunctiva often at the 3 and 9 o'clock positions of the limbus (Fig. 2.25) [75]. Almost a third of lesions arise in the semilunar fold (Fig. 2.26) or caruncle, but nevi of the tarsal or forniceal conjunctiva are very rare [76]. Akin to cutaneous nevi, most conjunctival nevi present in children or adolescents and may lack apparent pigmentation (Fig. 2.27). The melanocytic cells cluster to form nests at the junction zone of the epithelium and appear initially as junction

Fig. 2.27 Clinical photograph of patient with unpigmented conjunctival nevus. A few round clear spaces correspond to small inclusion cysts

nevi. Later, these melanocytic nests tend to drop down into the stroma transforming into a compound nevus. Eventually, the junctional component is completely lost, and a pure intrastromal nevus remains (Fig. 2.28). Later, these lesions may or may not undergo complete involution or remain as a regressed lesion. Conjunctival nevi often cause epithelial downgrowth as nevus cells descend into the stroma. This can be confusing, but should not suggest malignant transformation. Frequently, epithelial downgrowth generates clear cysts that may be clinically evident (Fig. 2.29). Consistent with the stromal component evolving over time, junction nevi are characteristically

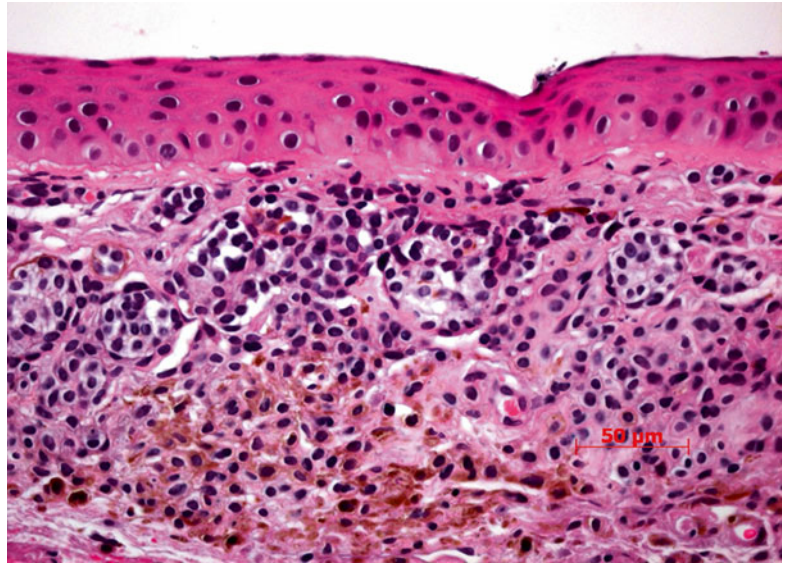

Fig. 2.28 Microphotograph of intrastromal conjunctival nevus. Nesting of nevus cells is evident in the superficial part. HE stain

Fig. 2.29 Microphotograph showing conjunctival nevus (*right*) associated with inclusion cysts (*left*). HE stain

found in younger individuals than either compound or intrastromal (subepithelial) lesions [76]. Importantly, many conjunctival nevi are clinically unpigmented at the time of presentation, and although most eventually become clinically pigmented, a third of these lesions remain unpigmented and may be confused with a range of non-melanocytic entities. Clinically, the typical conjunctival nevus is freely mobile upon the ocular surface, and only very rarely may a conjunctival nevus arise from the tarsal conjunctiva. Because case series usually are based on histopathological examination of excised lesion and many lesions are not surgically removed, the true incidence of conjunctival nevi remains unknown. The risk for malignant transformation of a typical nevus is quite small as conjunctival nevi are frequent and conjunctival melanoma is rare.

The *Spitz nevus* is rarely reported in the conjunctiva. It contains abundant spindle cells growing perpendicular to the surface, and these lesions may occasionally include an epithelioid component [77]. Spitz nevi may be clinically unpigmented and typically occur as juxtalimbal lesions in children or adolescents [78]. Although the Spitz nevus is benign, differentiation from conjunctival melanoma may be exceedingly difficult. An ever rarer benign variant is the pigmented spindle cell *nevus of Reed* [79]. The so-called blue nevus is named after its bluish clinical appearance in the skin caused by the Tyndall effect. The blue nevus of the conjunctiva, however, tends to have a dark brown or even black appearance. Histopathologically, the *blue nevus* is characterized by stromal spindle cells with a typical wavy configuration and may present in the conjunctiva as a solitary or multifocal lesion [80, 81]. The *cellular blue nevus* of the conjunctiva is a rare subtype that, akin to the skin variant, may transform into melanoma [80]. Although, *dysplastic nevi* are characterized by cellular or structural atypia, criteria for diagnosis have not always been consistent. Dysplastic nevi are very rarely described in the conjunctiva and are quite possibly underreported. Cutaneous dysplastic nevi may occur as a feature of the dysplastic nevus syndrome (familial atypical mole–melanoma syndrome), but this is likely a much less frequent finding in the conjunctiva [82]. The *pigmented epitheloid melanocytoma* has recently been reported as low-grade melanocytic tumor infrequently occurring in the palpebral conjunctiva [83]. A summary of details of rare variants of benign melanocytic lesions is available elsewhere [75, 84].

Like in the skin, a *freckle* (ephelis) may appear in sun-exposed conjunctiva as a small pigmented spot on the bulbar conjunctiva. This corresponds to a melanocytic hyperplasia of the basal epithelium that is histopathologically indistinguishable from the *ethnic (racial) melanosis* occurring in individuals with heavily pigmented skin. Clinically, however, this complexion-associated melanosis is symmetrical and most marked at the juxtalimbal region and then tends to fade in the conjunctiva away from the limbus. The lentigo simplex of the skin is characterized by melanocytic hyperplasia extending along the elongated rete of the epithelium. When marked atypia is present, these lesions are referred to as lentigo maligna (melanoma in situ). The rete is, however, not present in the conjunctival epithelium, and there is no perfect conjunctival counterpart of the lentigo. Arguably, the primary acquired melanosis of the conjunctiva is closely mimicking the lentigo of the skin. The terminology for lesions often referred to as primary acquired melanosis is contentious and is outlined below. Akin to conjunctival nevi, primary acquired melanosis may lack clinically detectable pigmentation (discussed below). Importantly, pigment may also spread from the melanocytes of the epithelium to adjacent keratinocytes particularly in heavily pigmented individuals. This may give rise to lesions, like the pigmented squamous cell carcinoma, easily confused with melanoma. Secondary pigmentation of the conjunctiva may appear after topical, or rarely systemic, medication; foreign bodies; and in entities like the Peutz–Jeghers syndrome [85]. Pigmented episcleral deposits may also occur after brachytherapy of intraocular tumors [86]. Typically, this pigment is lodged in macrophages, and as it is deep to the conjunctiva, it does not move with the conjunctiva. Clinically, it is important not to confuse this with extrascleral recurrence of an irradiated uveal melanoma. *Ocular melanocytosis* (termed *oculodermal melanocytosis* when a periocular

dermal component is included) is a congenital hyperproliferation of uveal melanocytes that often spread to the episclera. Clinically, this entity may be confused with a conjunctival pigmentation, but the episcleral dark grayish, smudgy, and feathery appearance is distinct. Oculo(dermal) melanocytosis has been estimated to be associated with a 0.25 % lifetime risk to develop uveal melanoma, but there is no apparent risk to develop conjunctival melanoma [87].

Primary acquired melanosis (PAM) is an entity that is not congenital and not secondary to any other condition. This purely descriptive terminology was introduced in the mid-1980s to avoid terms like precancerous melanosis believed by some to prompt overly aggressive treatment. Confusingly, this entity has been known by a number of names during the past decades, and the history how terminology evolved is intriguing [88]. This entity is actually a melanocytosis (proliferation of melanocytes) of the conjunctival epithelium, and in this aspect the word "melanosis" is a misnomer. Proliferation of melanocytes without apparent atypia initially occurs along the basal epithelium in a single row, and this is often referred to as PAM without atypia (Fig. 2.30). Other PAM-like lesions show cytological atypia with melanocytes invading the more superficial epithelial layers (structural atypia). This is then termed PAM with atypia (Fig. 2.31). Although PAM with atypia represents a continuum of lesions ranging from those with minimal cytological atypia and no structural atypia to lesions with full-thickness epithelial invasion, only the average risk of transformation to melanoma has been calculated [89]. Lesions without atypia are not believed to be associated with melanoma, but the frequency of PAM without atypia later transforming to PAM with atypia is unknown. Malignant transformation of PAM with atypia has been reported to occur in up to half of lesions [89]. The concept of PAM has been challenged by those who regard this as melanoma in situ [90, 91]. Currently, it is suggested that the term PAM with atypia be replaced by conjunctival melanocytic intraepithelial neoplasia (C-MIN) and the more aggressive of these lesions be labeled melanoma in situ [92]. Conceivably, a scoring system based on the cytological and structural atypia could be used for a more objective assessment, although such a system needs to be externally validated [92]. Clinically, PAM is a flat and variably brown unilateral lesion presenting in the middle-aged or elderly (Fig. 2.32) [88]. The clinical course of PAM is variable with typical "waxing and waning" over time [93]. Rarely, PAM may appear unpigmented and is then referred to as PAM "sine pigmento" [94]. Importantly, PAM without atypia may be difficult or impossible to distinguish clinically from PAM without atypia. Growth onto the cornea and extensive, multifocal conjunctival spread is suggestive of more aggressive growth (Fig. 2.33). A marked thickening may herald stromal invasion and hence transformation to invasive melanoma.

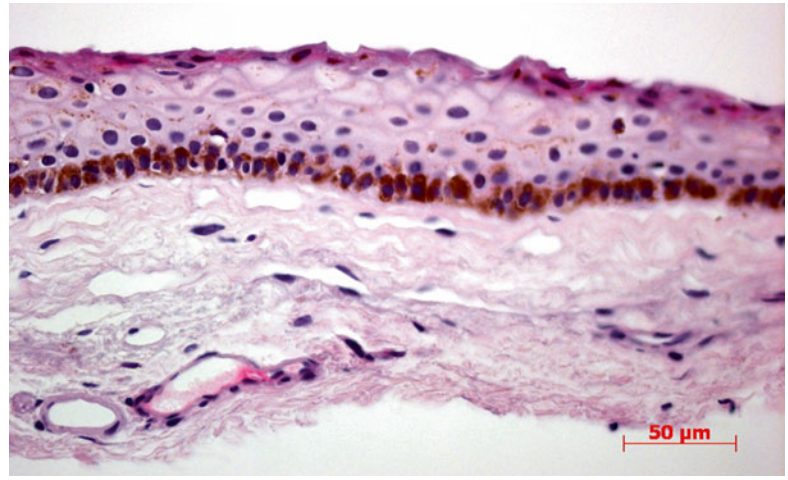

Fig. 2.30 Microphotograph of conjunctiva with basilar melanocytic hyperplasia of the epithelium or primary acquired melanosis (PAM). Melanocytes without apparent cytological atypia remain confined to the basal epithelium. Note pigment dispersion and uptake by squamous epithelial cells in the upper epithelial layers. HE stain

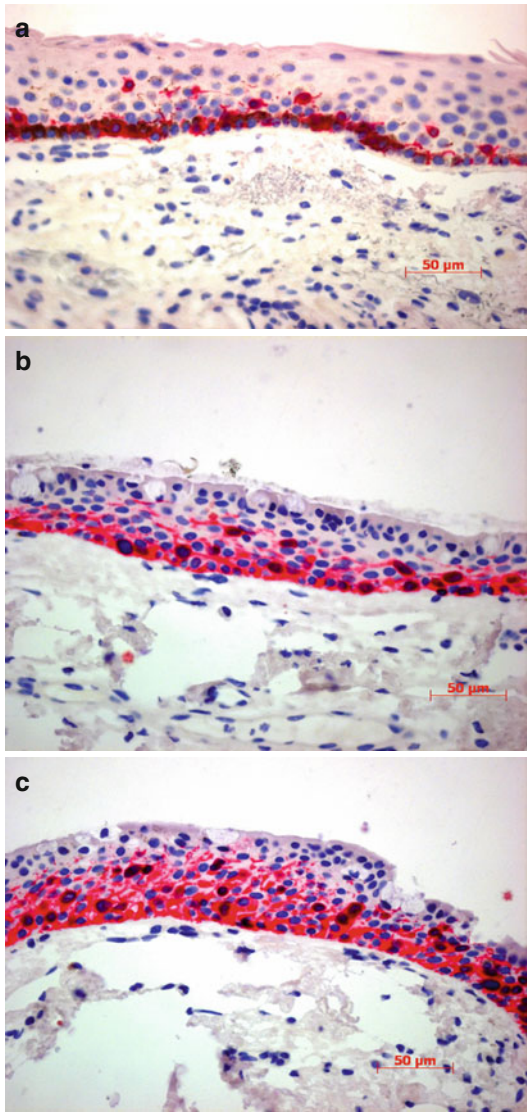

Fig. 2.31 Microphotographs with (**a**) primary acquired melanosis (PAM) with minimal atypia. A few melanocytes (*red*) without apparent cytological atypia appear as single cells in the mid and upper epithelial layers away from the junction zone. (**b**) PAM with moderate atypia. Atypical melanocytes (*red*) infiltrate about half or less of the epithelial thickness. (**c**) PAM with severe atypia. Atypical melanocytes (*red*) infiltrate more than half of the epithelial thickness. Melan-A stain

2.7.5.1 Conjunctival Melanoma

Definition

This invasive malignant melanocytic tumor may arise anywhere in the conjunctival sac.

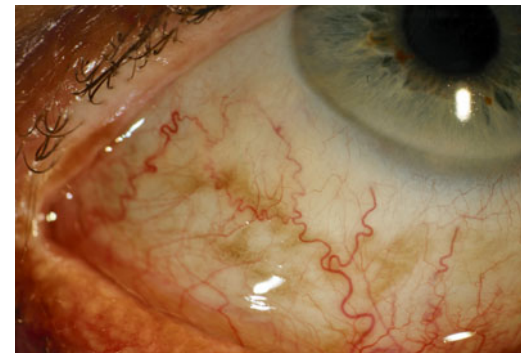

Fig. 2.32 Clinical photograph of primary acquired melanosis (PAM) with atypia. This subtle lesion is clinically indistinguishable from PAM without atypia

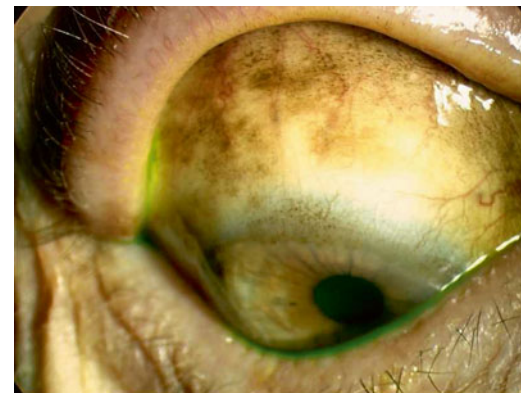

Fig. 2.33 Clinical photograph of widespread, extensive PAM with atypia

Epidemiology

Conjunctival melanoma is rare with an estimated annual age-adjusted incidence of about 1.5 cases per million in people more than 65 years of age [95]. In younger people, incidence is markedly lower, and conjunctival melanoma is extremely rare in children and adolescents [95].

Etiology

There are several reports indicating that, akin to cutaneous melanoma but in contrast to uveal melanoma, the incidence of conjunctival melanoma is rising [95–97]. Interestingly, this increase appears to take place predominantly in conjunctiva exposed to ultraviolet radiation (UVR). This largely corresponds to bulbar conjunctiva at the 3 and 9 o'clock positions (Fig. 2.34) [95]. Lesions like PAM with atypia and conjunctival melanoma both have been

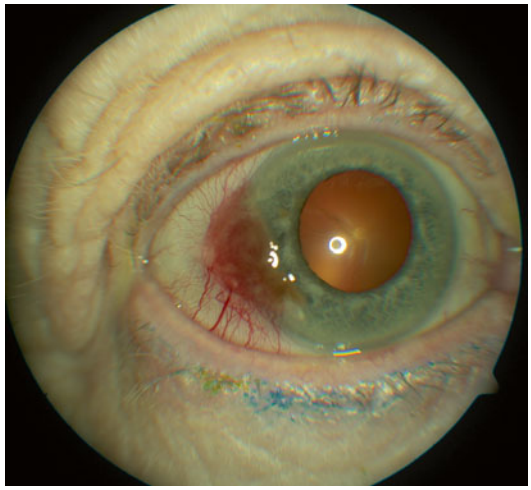

Fig. 2.34 Clinical photograph of a patient with juxtalimbal conjunctival melanoma. The lesion is lightly pigmented and features several dilated feeder vessels. Gross examination photograph of orbital exenteration specimen with recurrent conjunctival melanoma arising from the upper fornix adjacent to part of the lacrimal gland. HE stain

reported in patients with xeroderma pigmentosum and UVR-associated tumors [98, 99]. Combined with reported mutation findings in the BRAF gene (see below), this suggests a role for UVR in uveal melanoma pathogenesis [100].

Localization

Although conjunctival melanoma may arise from any part of the conjunctival sac, most tumors present in the bulbar, juxtalimbal area [88].

Clinical Features

Most conjunctival melanomas present as pigmented nodular growths, but a small proportion of tumors are clinically unpigmented [88]. Large tumors may occasionally harbor in any of the fornices and evade clinical detection for some time (Fig. 2.35).

Histopathology

The individual cells that make up a conjunctival melanoma may show quite different features and can include small polyhedral cells, spindle cells, epitheloid cells, balloon cells, or a combination of these [1]. The melanocytic lineage is usually easily detectable using a panel of monoclonal antibodies that may include S-100, HMB-45, MART-1, and Melan-A. Although immunoreactivity for HMB-45 is typically extensive in a melanoma, some staining in the superficial junction zone of a nevus may occur [101]. The separation of a melanoma from a benign nevus rather rests on a combination of features including cellular atypia, pagetoid invasion of the epithelium, and lack of maturation toward the base of the lesion [1]. Extensive staining for HMB-45 is suggestive, but not pathognomonic of melanoma [101]. A comprehensive review of the ultrastructural features of conjunctival melanoma is available elsewhere [102].

Differential Diagnosis

Unpigmented lesions may clinically be confused with, e.g., squamous cell carcinoma, papilloma, and pyogenic granuloma. Pigmented tumors are much more likely to be diagnosed correctly by the clinician, but can rarely be confused with, e.g., extraocular extension of a uveal melanoma or an epithelial inclusion cyst containing debris and hemorrhage [88, 103].

Histogenesis

Histopathological data suggest that conjunctival melanoma often occurs in the setting of PAM with atypia and that nevi only are present in one of five (or fewer) conjunctival melanomas (Fig. 2.36). Some conjunctival melanomas probably arise de novo without a precursor lesion [104].

Genetics

Mutations in BRAF, possibly induced by UVR, are seen in conjunctival melanoma, but not in uveal melanoma [105, 106]. Mutations of BRAF are also apparent in conjunctival and cutaneous nevi, but not in PAM with atypia [107]. Also, there is a discrepancy of GNAQ mutations in conjunctival melanoma compared to uveal melanoma [108]. Collectively, this suggests that the molecular mechanisms operating in conjunctival melanoma are different from those of uveal mela-

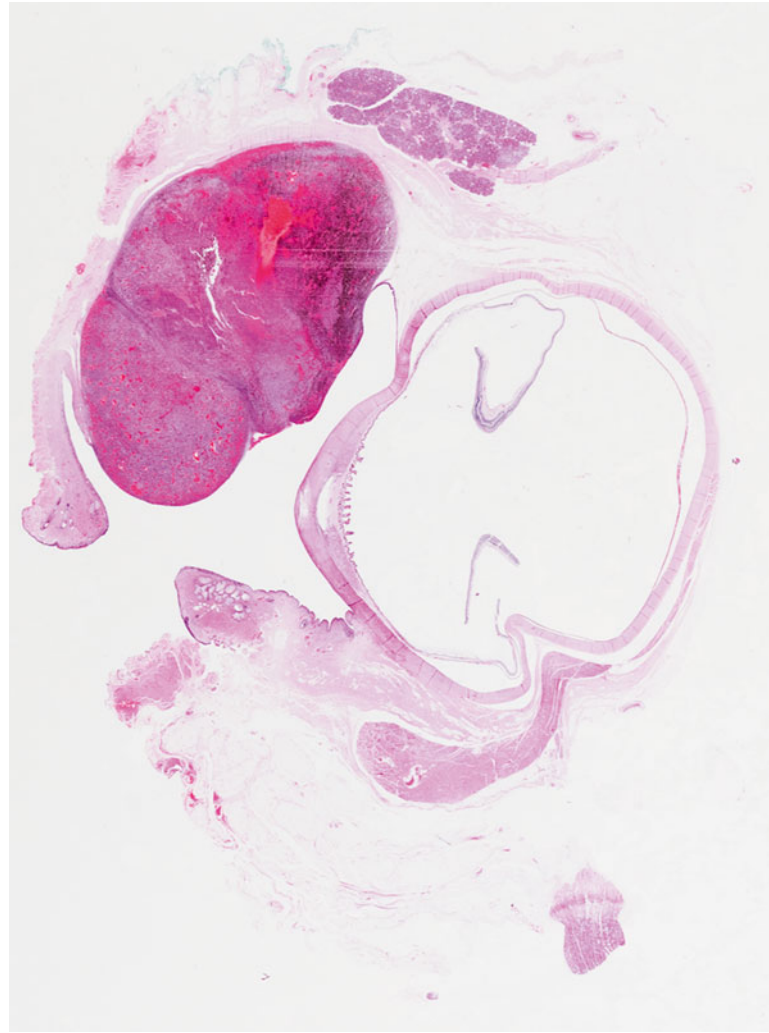

Fig. 2.35 Gross examination photograph of orbital exenteration specimen with recurrent conjunctival melanoma arising from the upper fornix adjacent to part of the lacrimal gland. HE stain

noma. It also suggests that conjunctival melanoma may be UVR inducible. Management is primarily surgical, but adjuvant brachytherapy may be considered [88]. Exenteration of the orbit is not believed to improve prognosis but is used to control local disease [109].

Prognosis

Unlike its uveal counterpart, conjunctival melanoma tends to spread to the regional lymphatic nodes and the parotid gland. The 10-year survival rate following conjunctival melanoma is approximately 70 %, but metastatic disease may be curable if confined to the regional nodes which then are cleared with a radical neck dissection [104, 110]. Thick, multifocal tumors and tumors in the caruncular region away from the limbus tend to carry a poorer prognosis [104, 110, 111]. Also, a conjunctival melanoma with many cycling tumor cells is more likely to metastasize [104, 112].

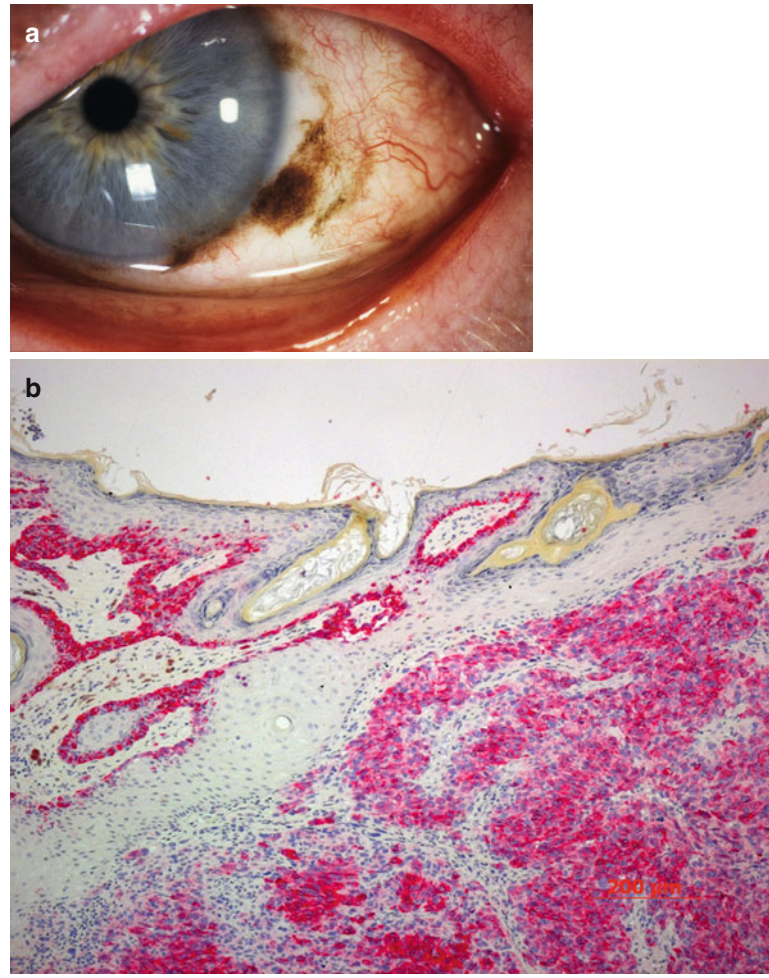

Fig. 2.36 Conjunctival melanoma. (**a**) Clinical photograph of recurrent melanoma (*dark brown* nodule) with extensive primary acquired melanosis (PAM). (**b**) Abundant melanocytes (*red*) are present as solid tumor growth (*right*) and as atypical melanocytic hyperplasia largely confined to the basilar epithelium but in some parts invading the more superficial layers (*left*). Melan-A stain

References

1. Spencer WH. Conjunctiva. In: Spencer WH, editor. Ophthalmic pathology an atlas and textbook, vol. 1. 4th ed. Philadelphia: W.B. Saunders; 1996.
2. Jakobiec FA, Lam H, Bhat P, Pineda R. Non-syndromic supernumerary caruncles causing ocular irritation after cataract surgery: a critical review of caruncular dysgeneses. Am J Ophthalmol. 2010;149(3):398–404 e1–2.
3. Fraser GR. The pool of harmful genes in human populations. Acta Genet Med Gemellol (Roma). 1962;11:284–7.
4. McGregor L, Makela V, Darling SM, et al. Fraser syndrome and mouse blebbed phenotype caused by mutations in FRAS1/Fras1 encoding a putative extracellular matrix protein. Nat Genet. 2003;34(2):203–8.
5. Vogel MJ, van Zon P, Brueton L, et al. Mutations in GRIP1 cause Fraser syndrome. J Med Genet. 2012;49(5):303–6.
6. Narang M, Kumar M, Shah D. Fraser-cryptophthalmos syndrome with colonic atresia. Indian J Pediatr. 2008;75(2):189–91.
7. Grover AK, Chaudhuri Z, Malik S, et al. Congenital eyelid colobomas in 51 patients. J Pediatr Ophthalmol Strabismus. 2009;46(3):151–9.
8. Sullivan TJ, Clarke MP, Morin JD. The ocular manifestations of the Sturge-Weber syndrome. J Pediatr Ophthalmol Strabismus. 1992;29(6):349–56.
9. Shields JA, Mashayekhi A, Kligman BE, et al. Vascular tumors of the conjunctiva in 140 cases. Ophthalmology. 2011;118(9):1747–53.
10. Jakobiec FA, Pineda R, Rivera R, et al. Epicorneal polypoidal lipodermoid: lack of association of central corneal lesions with goldenhar syndrome

verified with a review of the literature. Surv Ophthalmol. 2010;55(1):78–84.
11. Pokorny KS, Hyman BM, Jakobiec FA, et al. Epibulbar choristomas containing lacrimal tissue. Clinical distinction from dermoids and histologic evidence of an origin from the palpebral lobe. Ophthalmology. 1987;94(10):1249–57.
12. Chintakuntlawar AV, Chodosh J. Cellular and tissue architecture of conjunctival membranes in epidemic keratoconjunctivitis. Ocul Immunol Inflamm. 2010;18(5):341–5.
13. Rajak SN, Collin JR, Burton MJ. Trachomatous trichiasis and its management in endemic countries. Surv Ophthalmol. 2012;57(2):105–35.
14. Hu VH, Holland MJ, Burton MJ. Trachoma: protective and pathogenic ocular immune responses to Chlamydia trachomatis. PLoS Negl Trop Dis. 2013;7(2):e2020.
15. Clark GC, Moloney G, Sutton G. Ophthalmic presentation of Wegener's granulomatosis on a background of polymyalgia rheumatica. Clin Experiment Ophthalmol. 2010;38(1):65–7.
16. Slack JW, Hyndiuk RA, Harris GJ, Simons KB. Blastomycosis of the eyelid and conjunctiva. Ophthal Plast Reconstr Surg. 1992;8(2):143–9.
17. Saenchez MD, Orita VM, Nolan TJ. Pathology in practice. Focally extensive granulomatous and eosinophilic conjunctivitis with numerous intralesional nematodes, consistent with Onchocerca spp. J Am Vet Med Assoc. 2012;240(4):385–7.
18. Rose JS, Arthur A, Raju R, Thomas M. Primary conjunctival tuberculosis in a 14 year old girl. Indian J Tuberc. 2011;58(1):32–4.
19. Kahana A, Marcet MM, Albert DM, Thliveris AT. Drug-induced cicatrising granulomatous conjunctivitis. Br J Ophthalmol. 2007;91(5):691–2.
20. Suzuki T. Meibomitis-related keratoconjunctivitis: implications and clinical significance of meibomian gland inflammation. Cornea. 2012;31 Suppl 1:S41–4.
21. Wong AH, Barg SS, Leung AK. Seasonal and perennial allergic conjunctivitis. Recent Pat Inflamm Allergy Drug Discov. 2009;3(2):118–27.
22. Friedlaender MH. Ocular allergy. Curr Opin Allergy Clin Immunol. 2011;11(5):477–82.
23. Srinivasan BD, Jakobiec FA, Iwamoto T, DeVoe AG. Giant papillary conjunctivitis with ocular prostheses. Arch Ophthalmol. 1979;97(5):892–5.
24. Korb DR, Allansmith MR, Greiner JV, et al. Biomicroscopy of papillae associated with hard contact lens wearing. Ophthalmology. 1981;88(11):1132–6.
25. Rohatgi J, Dhaliwal U. Phlyctenular eye disease: a reappraisal. Jpn J Ophthalmol. 2000;44(2):146–50.
26. Vieira AC, Hofling-Lima AL, Mannis MJ. Ocular rosacea–a review. Arq Bras Oftalmol. 2012;75(5):363–9.
27. Ghanem VC, Mehra N, Wong S, Mannis MJ. The prevalence of ocular signs in acne rosacea: comparing patients from ophthalmology and dermatology clinics. Cornea. 2003;22(3):230–3.
28. Akpek EK, Merchant A, Pinar V, Foster CS. Ocular rosacea: patient characteristics and follow-up. Ophthalmology. 1997;104(11):1863–7.
29. Kirzhner M, Jakobiec FA. Ocular cicatricial pemphigoid: a review of clinical features, immunopathology, differential diagnosis, and current management. Semin Ophthalmol. 2011;26(4–5):270–7.
30. Harr T, French LE. Stevens-Johnson syndrome and toxic epidermal necrolysis. Chem Immunol Allergy. 2012;97:149–66.
31. Rao R, Mellerio J, Bhogal BS, Groves R. Immunofluorescence antigen mapping for hereditary epidermolysis bullosa. Indian J Dermatol Venereol Leprol. 2012;78(6):692–7.
32. Has C, Kiritsi D. Molecular therapies for epidermolysis bullosa. G Ital Dermatol Venereol. 2013;148(1):65–72.
33. Letko E, Bhol K, Anzaar F, et al. Chronic cicatrizing conjunctivitis in a patient with epidermolysis bullosa acquisita. Arch Ophthalmol. 2006;124(11):1615–8.
34. Hunefeld C, Mezger M, Kern JS, et al. One goal, different strategies–molecular and cellular approaches for the treatment of inherited skin fragility disorders. Exp Dermatol. 2013;22(3):162–7.
35. Schuster V, Seregard S. Ligneous conjunctivitis. Surv Ophthalmol. 2003;48(4):369–88.
36. Fish R, Davidson RS. Management of ocular thermal and chemical injuries, including amniotic membrane therapy. Curr Opin Ophthalmol. 2010;21(4):317–21.
37. Sommer A, Vyas KS. A global clinical view on vitamin A and carotenoids. Am J Clin Nutr. 2012;96(5):1204S–6.
38. Koranyi G, Artzen D, Seregard S, Kopp ED. Intraoperative mitomycin C versus autologous conjunctival autograft in surgery of primary pterygium with four-year follow-up. Acta Ophthalmol. 2012;90(3):266–70.
39. Koranyi G, Seregard S, Kopp ED. Cut and paste: a no suture, small incision approach to pterygium surgery. Br J Ophthalmol. 2004;88(7):911–4.
40. Demirci H, Shields CL, Eagle Jr RC, Shields JA. Conjunctival amyloidosis: report of six cases and review of the literature. Surv Ophthalmol. 2006;51(4):419–33.
41. Shields JA, Eagle RC, Shields CL, et al. Systemic amyloidosis presenting as a mass of the conjunctival semilunar fold. Am J Ophthalmol. 2000;130(4):523–5.
42. Blancas-Mejia LM, Ramirez-Alvarado M. Systemic amyloidoses. Annu Rev Biochem. 2013;82:745–74.
43. Eagle RC. Conjunctiva. In: Eye pathology an atlas and text. 2nd ed. Philadelphia: Lippincott; 2011.
44. Yanoff M, Sassani JW. Conjunctiva. In: Ocular pathology. Edinburgh: Mosby Elsevier; 2009.
45. Sjo NC, von Buchwald C, Cassonnet P, et al. Human papillomavirus in normal conjunctival tissue and in conjunctival papilloma: types and frequencies in a large series. Br J Ophthalmol. 2007;91(8):1014–5.
46. Hughes EH, Intzedy L, Dick AD, Tole DM. Keratoacanthoma of the conjunctiva. Eye (Lond). 2003;17(6):781–2.

47. Cummings TJ, Dodd LG, Eedes CR, Klintworth GK. Hereditary benign intraepithelial dyskeratosis: an evaluation of diagnostic cytology. Arch Pathol Lab Med. 2008;132(8):1325–8.
48. Allingham RR, Seo B, Rampersaud E, et al. A duplication in chromosome 4q35 is associated with hereditary benign intraepithelial dyskeratosis. Am J Hum Genet. 2001;68(2):491–4.
49. Karcioglu ZA, Wagoner MD. Demographics, etiology, and behavior of conjunctival squamous cell carcinoma in the 21st century. Ophthalmology. 2009;116(11):2045–6.
50. Waddell K, Kwehangana J, Johnston WT, et al. A case-control study of ocular surface squamous neoplasia (OSSN) in Uganda. Int J Cancer. 2010;127(2):427–32.
51. Seregard S, Kock E. Squamous spindle cell carcinoma of the conjunctiva. Fatal outcome of a plerygium-like lesion. Acta Ophthalmol Scand. 1995;73(5):464–6.
52. Hwang IP, Jordan DR, Brownstein S, et al. Mucoepidermoid carcinoma of the conjunctiva: a series of three cases. Ophthalmology. 2000;107(4):801–5.
53. Robinson JW, Brownstein S, Jordan DR, Hodge WG. Conjunctival mucoepidermoid carcinoma in a patient with ocular cicatricial pemphigoid and a review of the literature. Surv Ophthalmol. 2006;51(5):513–9.
54. Lee CS, Yang WI, Shin KJ, Lee SC. Rapid growth of choroidal melanoma during pregnancy. Acta Ophthalmol. 2011;89(3):e290–1.
55. Say EA, Shields CL, Bianciotto C, et al. Oncocytic lesions (oncocytoma) of the ocular adnexa: report of 15 cases and review of literature. Ophthal Plast Reconstr Surg. 2012;28(1):14–21.
56. McKelvie PA, Daniell M, McNab A, et al. Squamous cell carcinoma of the conjunctiva: a series of 26 cases. Br J Ophthalmol. 2002;86(2):168–73.
57. AJCC. Cancer staging manual. 7th ed. New York: Springer; 2010.
58. Crossman G, Mowatt L, Jaggon J. Sebaceous gland hyperplasia of the caruncle: an uncommon diagnosis. Graefes Arch Clin Exp Ophthalmol. 2013;251:2259–60.
59. Bielory BP, Lari HB, Mirani N, et al. Conjunctival squamous cell carcinoma harboring Leishmania amastigotes in a human immunodeficiency virus-positive patient. Arch Ophthalmol. 2011;129(9):1230–1.
60. Longmuir S, Dumitrescu A, Kwon Y, et al. Juvenile xanthogranulomatosis with bilateral and multifocal ocular lesions of the iris, cornealscleral limbus, and choroid. J AAPOS. 2011;15(6):598–600.
61. Chaudhry IA, Al-Jishi Z, Shamsi FA, Riley F. Juvenile xanthogranuloma of the corneoscleral limbus: case report and review of the literature. Surv Ophthalmol. 2004;49(6):608–14.
62. Balestrazzi E, Ventura T, Delle Noci N, et al. Malignant conjunctival epibulbar fibrous histiocytoma with orbital invasion. Eur J Ophthalmol. 1991;1(1):23–7.
63. Shukla D, Kim R. Giant nodular posterior scleritis simulating choroidal melanoma. Indian J Ophthalmol. 2006;54(2):120–2.
64. Salomao D, Roden AC. Orbital pathology. In: Albert DM, Jakobiec FA, editors. Principles and practice of ophthalmology. 3rd ed. Philadelphia: Saunders Elsevier; 2008.
65. Vezzosi D, Vignaux O, Dupin N, Bertherat J. Carney complex: clinical and genetic 2010 update. Ann Endocrinol (Paris). 2010;71(6):486–93.
66. Demirci H, Shields CL, Eagle Jr RC, Shields JA. Report of a conjunctival myxoma case and review of the literature. Arch Ophthalmol. 2006;124(5):735–8.
67. Mendez Mdel C, Muinos Y, Blanco G, et al. Embryonal rhabdomyosarcoma of the caruncle in a 4 year-old boy: case report. Arq Bras Oftalmol. 2012;75(3):207–9.
68. Freedman KA, Tran RM. Neurofibroma involving the caruncle. Arch Ophthalmol. 2004;122(2):294–5.
69. Demirci H, Shields CL, Bianciotto CG, Shields JA. Topical imiquimod for periocular lentigo maligna. Ophthalmology. 2010;117(12):2424–9.
70. Sehu KW, Lee WR. Conjunctiva. In: Ophthalmic pathology an illustrated guide for clinicians. Victoria: Blackwell; 2005.
71. Stefanovic A, Lossos IS. Extranodal marginal zone lymphoma of the ocular adnexa. Blood. 2009;114(3):501–10.
72. Schiby G, Polak-Charcon S, Mardoukh C, et al. Orbital marginal zone lymphomas: an immunohistochemical, polymerase chain reaction, and fluorescence in situ hybridization study. Hum Pathol. 2007;38(3):435–42.
73. Blasi MA, Tiberti AC, Valente P, et al. Intralesional interferon-alpha for conjunctival mucosa-associated lymphoid tissue lymphoma: long-term results. Ophthalmology. 2012;119(3):494–500.
74. Kiratli H, Shields CL, Shields JA, DePotter P. Metastatic tumours to the conjunctiva: report of 10 cases. Br J Ophthalmol. 1996;80(1):5–8.
75. Folberg R, Jakobiec FA, Bernardino VB, Iwamoto T. Benign conjunctival melanocytic lesions. Clinicopathologic features. Ophthalmology. 1989;96(4):436–61.
76. Gerner N, Norregaard JC, Jensen OA, Prause JU. Conjunctival naevi in Denmark 1960–1980. A 21-year follow-up study. Acta Ophthalmol Scand. 1996;74(4):334–7.
77. Vervaet N, Van Ginderdeuren R, Van Den Oord JJ, Foets B. A rare conjunctival Spitz nevus: a case report and literature review. Bull Soc Belge Ophtalmol. 2007;303:63–7.
78. Kantelip B, Boccard R, Nores JM, Bacin F. A case of conjunctival Spitz nevus: review of literature and comparison with cutaneous locations. Ann Ophthalmol. 1989;21(5):176–9.
79. Seregard S. Pigmented spindle cell naevus of reed presenting in the conjunctiva. Acta Ophthalmol Scand. 2000;78(1):104–6.

80. Demirci H, Shields CL, Shields JA, Eagle Jr RC. Malignant melanoma arising from unusual conjunctival blue nevus. Arch Ophthalmol. 2000;118(11):1581–4.
81. Berman EL, Shields CL, Sagoo MS, et al. Multifocal blue nevus of the conjunctiva. Surv Ophthalmol. 2008;53(1):41–9.
82. Seregard S, af Trampe E, Mansson-Brahme E, et al. Prevalence of primary acquired melanosis and nevi of the conjunctiva and uvea in the dysplastic nevus syndrome. A case-control study. Ophthalmology. 1995;102(10):1524–9.
83. Bissig A, Moulin A, Spahn B, et al. Conjunctival pigmented epithelioid melanocytoma: a clinicopathological case report. Arch Ophthalmol. 2012;130(11): 1478–9.
84. Jakobiec FA, Zuckerman BD, Berlin AJ, et al. Unusual melanocytic nevi of the conjunctiva. Am J Ophthalmol. 1985;100(1):100–13.
85. Meyerson MA, Cohen PR, Hymes SR. Lingual hyperpigmentation associated with minocycline therapy. Oral Surg Oral Med Oral Pathol Oral Radiol Endod. 1995;79(2):180–4.
86. Toivonen P, Kivela T. Pigmented episcleral deposits after brachytherapy of uveal melanoma. Ophthalmology. 2006;113(5):865–73.
87. Singh AD, De Potter P, Fijal BA, et al. Lifetime prevalence of uveal melanoma in white patients with oculo(dermal) melanocytosis. Ophthalmology. 1998; 105(1):195–8.
88. Seregard S. Conjunctival melanoma. Surv Ophthalmol. 1998;42(4):321–50.
89. Folberg R, McLean IW, Zimmerman LE. Primary acquired melanosis of the conjunctiva. Hum Pathol. 1985;16(2):129–35.
90. Ackerman AB, Sood R, Koenig M. Primary acquired melanosis of the conjunctiva is melanoma in situ. Mod Pathol. 1991;4(2):253–63.
91. Folberg R, Jakobiec FA, McLean IW, Zimmerman LE. Is primary acquired melanosis of the conjunctiva equivalent to melanoma in situ? Mod Pathol. 1992;5(1):2–5; discussion 6–8.
92. Damato B, Coupland SE. Conjunctival melanoma and melanosis: a reappraisal of terminology, classification and staging. Clin Experiment Ophthalmol. 2008; 36(8):786–95.
93. Jakobiec FA, Folberg R, Iwamoto T. Clinicopathologic characteristics of premalignant and malignant melanocytic lesions of the conjunctiva. Ophthalmology. 1989;96(2):147–66.
94. Paridaens AD, McCartney AC, Hungerford JL. Multifocal amelanotic conjunctival melanoma and acquired melanosis sine pigmento. Br J Ophthalmol. 1992;76(3):163–5.
95. Triay E, Bergman L, Nilsson B, et al. Time trends in the incidence of conjunctival melanoma in Sweden. Br J Ophthalmol. 2009;93(11):1524–8.
96. Yu GP, Hu DN, McCormick S, Finger PT. Conjunctival melanoma: is it increasing in the United States? Am J Ophthalmol. 2003;135(6): 800–6.
97. Tuomaala S, Eskelin S, Tarkkanen A, Kivela T. Population-based assessment of clinical characteristics predicting outcome of conjunctival melanoma in whites. Invest Ophthalmol Vis Sci. 2002; 43(11):3399–408.
98. Aoyagi M, Morishima N, Yoshino Y, et al. Conjunctival malignant melanoma with xeroderma pigmentosum. Ophthalmologica. 1993;206(3):162–7.
99. Paridaens AD, McCartney AC, Hungerford JL. Premalignant melanosis of the conjunctiva and the cornea in xeroderma pigmentosum. Br J Ophthalmol. 1992;76(2):120–2.
100. Seregard S, Triay E. New aspects on the pathogenesis of conjunctival melanoma. In: Reinhard T, editor. Essentials in ophthalmology. Berlin: Springer; 2007.
101. Jakobiec FA, Bhat P, Colby KA. Immunohistochemical studies of conjunctival nevi and melanomas. Arch Ophthalmol. 2010;128(2): 174–83.
102. Jakobiec FA. The ultrastructure of conjunctival melanocytic tumors. Trans Am Ophthalmol Soc. 1984;82:599–752.
103. Jeanniton C, Finger PT, Leung E, et al. Infected epithelial inclusion cyst simulating conjunctival melanoma. Ophthal Plast Reconstr Surg. 2013;29: e131–4.
104. Seregard S, Kock E. Conjunctival malignant melanoma in Sweden 1969–91. Acta Ophthalmol (Copenh). 1992;70(3):289–96.
105. Gear H, Williams H, Kemp EG, Roberts F. BRAF mutations in conjunctival melanoma. Invest Ophthalmol Vis Sci. 2004;45(8):2484–8.
106. Spendlove HE, Damato BE, Humphreys J, et al. BRAF mutations are detectable in conjunctival but not uveal melanomas. Melanoma Res. 2004;14(6): 449–52.
107. Goldenberg-Cohen N, Cohen Y, Rosenbaum E, et al. T1799A BRAF mutations in conjunctival melanocytic lesions. Invest Ophthalmol Vis Sci. 2005;46(9): 3027–30.
108. Dratviman-Storobinsky O, Cohen Y, Frenkel S, et al. Lack of oncogenic GNAQ mutations in melanocytic lesions of the conjunctiva as compared to uveal melanoma. Invest Ophthalmol Vis Sci. 2010;51(12):6180–2.
109. Paridaens AD, McCartney AC, Minassian DC, Hungerford JL. Orbital exenteration in 95 cases of primary conjunctival malignant melanoma. Br J Ophthalmol. 1994;78(7):520–8.
110. Paridaens AD, Minassian DC, McCartney AC, Hungerford JL. Prognostic factors in primary malignant melanoma of the conjunctiva: a clinicopathological study of 256 cases. Br J Ophthalmol. 1994;78(4):252–9.
111. Tuomaala S, Toivonen P, Al-Jamal R, Kivela T. Prognostic significance of histopathology of primary conjunctival melanoma in Caucasians. Curr Eye Res. 2007;32(11):939–52.
112. Seregard S. Cell proliferation as a prognostic indicator in conjunctival malignant melanoma. Am J Ophthalmol. 1993;116(1):93–7.

Cornea

3

Tero Kivelä, Elisabeth M. Messmer,
and Beata Rymgayłło-Jankowska

3.1 General Description

The cornea provides a clear entrance for light for processing by the visual pathway through the central nervous system. It is a transparent, avascular tissue that measures 11–12 mm horizontally and 10–11 mm vertically. The average radius of curvature of the anterior surface of the cornea (central cornea) is 7.8 mm (range, 6.7–9.4 mm) and that of its posterior surface is 6.9 mm (range, 5.2–8.2 mm).

The 43.25 dioptres of refractive power of the cornea contribute 74 % of the total 58.60 dioptre power of the average human eye. It separates the air, with a refractive index of 1.00, from the aqueous humour, with refractive index of 1.33, also shared by the tear fluid. The cornea is a major source of astigmatism in the optical system.

T. Kivelä, MD, FEBO (✉)
Ophthalmic Pathology Laboratory, Department of Ophthalmology, Helsinki University Central Hospital, Haartmaninkatu 4 C, PL 220, FI-00029 HUS Helsinki, Finland
e-mail: tero.kivela@helsinki.fi

E.M. Messmer, MD, FEBO
Department of Ophthalmology, Ludwig-Maximilians-University, Mathildenstrasse 8, D-80336 Munich, Germany
e-mail: elisabeth.messmer@med.uni-muenchen.de

B. Rymgayłło-Jankowska, MD, PhD
Tadeusz Krwawicz Chair of Ophthalmology, and Eye Hospital, Medical University of Lublin, ul. Chmielna 1, 20-079 Lublin, Poland
e-mail: brjankowska@gmail.com

Microscopically, the cornea consists of five layers: the epithelium, Bowman's layer, the stroma, Descemet's membrane, and the endothelium (Fig. 3.1). Besides the five layers, several cell populations are resident within or around the cornea. These include stromal and epithelial antigen-presenting cells (APCs: dendritic cells and macrophages), epithelial stem cells, limbal blood vessels, and corneal nerves.

The cornea is both avascular and devoid of lymphatic drainage. It is supplied with glucose by diffusion from the aqueous humour. The central part of the cornea receives oxygen indirectly from the air via oxygen dissolved in the tear film, whereas the peripheral part receives oxygen by diffusion from the anterior ciliary circulation. Direct exposure of tears to the atmosphere is essential for oxygenation of the cornea. Aqueous humour provides the cornea with amino acids, ascorbic acid (vitamin C), and other vitamins, and also lactic acid. All these nutrients together with glucose are required for the normal metabolism of the cornea.

The cornea is one of the highly sensitive tissues of the human body. Density of nerve ending in the cornea is about 300 times that of the skin. The sensitivity of the cornea is 100 times that of the conjunctiva. An area of 0.01 mm^2 of the cornea may contain as many as 100 nerve endings.

The cornea is thinnest at its centre, measuring about 550 µm, and thicker at the periphery, measuring about 700 µm. Because of tissue shrinkage, measurements taken from histological sections will be somewhat different.

S. Heegaard, H. Grossniklaus (eds.), *Eye Pathology: An Illustrated Guide*,
DOI 10.1007/978-3-662-43382-9_3, © Springer-Verlag Berlin Heidelberg 2015

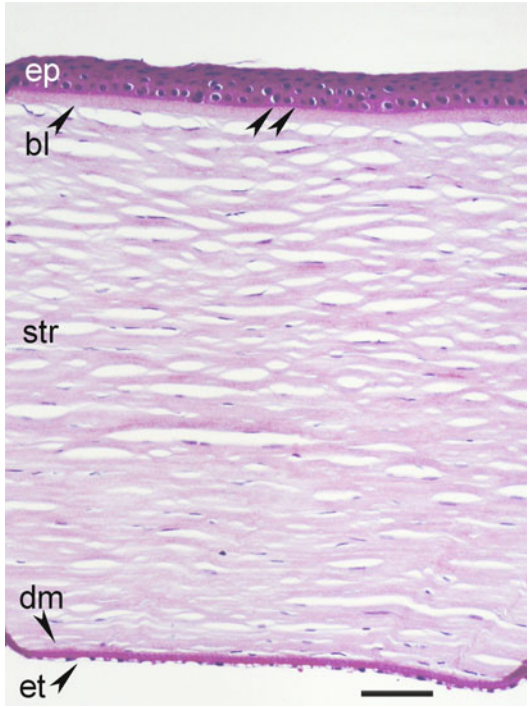

Fig. 3.1 Normal cornea. Layers of the cornea include epithelium (*ep*), Bowman's layer (*bl*), stroma (*str*), Descemet's membrane (*dm*), and endothelium (*et*). The basement membrane (*bm*) of the corneal epithelium is a thin layer between the epithelium and Bowman's layer, whereas the basement of the endothelium – the Descemet's membrane – is thick and thickens with advancing age. Haematoxylin-eosin, bar = 50 µm

3.2 Embryology, Anatomy, and Development

3.2.1 Embryology and Development

Soon after the lens vesicle has separated from the surface ectoderm (about fifth gestational week), the latter differentiates into a two-layered epithelium. By the end of week 6, junctional complexes appear between cells. During the next 1–2 weeks, the epithelium stratifies and becomes three to four cell layers thick, and the lens completes its formation and detaches from the surface ectoderm. Almost immediately after the separation of the lens, waves of neural crest cells migrate into the space between the lens and epithelium. These cells become the corneal endothelium and the stromal keratocytes [1]. The endothelium forms as a double layer of cuboidal cells. During week 8, they start to produce a basement membrane – Descemet's membrane.

During month 3, fibroblasts and collagen fibrils appear. The fibroblasts start to synthesise a glycosaminoglycan-rich ground substance. Keratan sulphate production becomes apparent. Bowman's layer is first identified during month 4; it develops as an extension of filaments from the basal lamina of the epithelium. It is also approximately this time that tight junctions form between the apices of the endothelial cells. Further development results in growth of the cornea and in dehydration of its stroma to form a transparent structure [2, 3].

3.2.2 Anatomy

The cornea consists of five layers: the epithelium, Bowman's layer, the stroma, Descemet's membrane, and the endothelium.

3.2.2.1 Epithelium

The corneal epithelium is composed of non-keratinised, stratified squamous epithelial cells. The thickness of the corneal epithelium is approximately 50 µm and makes up about 10 % of the total thickness of the cornea. It is constant over the entire corneal surface.

The epithelium consists of five to six layers of three different types of epithelial cells: two to three layers of superficial cells, two to three layers of wing cells, and a monolayer of columnar basal cells that adhere to the basement membrane overlying Bowman's layer (Fig. 3.2).

Only the basal cells of the corneal epithelium proliferate. The daughter cells differentiate into wing cells and subsequently into superficial cells, gradually migrating to the corneal surface. This differentiation process requires 7–14 days, after which the superficial cells are desquamated into the tear film.

The epithelium and the tear film contribute to the maintenance of an optically smooth corneal surface. Another important physiological function of the corneal epithelium is to provide a barrier to external insults. The junctional complexes between adjacent epithelial cells prevent passage

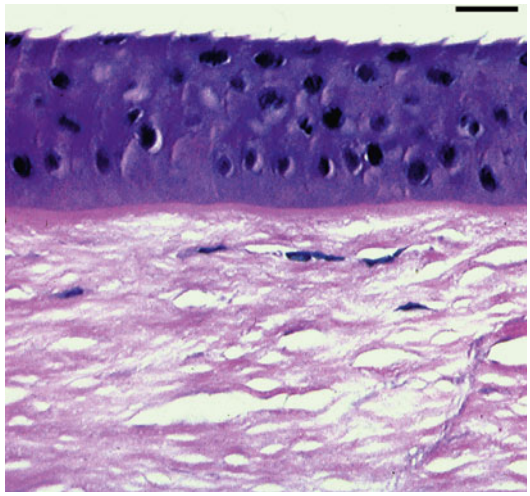

Fig. 3.2 Normal corneal epithelium. Haematoxylin-eosin, bar = 25 μm

of chemical substances into the deeper layers of the cornea. Defects or loss of corneal epithelial cells result in penetration of fluid into the stroma, causing stromal edema [2, 4].

Cell-to-matrix and cell-to-cell communication are important for maintenance of the normal stratified structure and physiological functions of the corneal epithelium. Tight junctions are present mostly between cells of the superficial cell layer and, together with interdigitations, they provide an extremely effective barrier to prevent the penetration of fluid (tears). Zonulae adhaerentes and desmosomes are present in all layers of the corneal epithelium. However, gap junctions which allow the passage of small molecules between cells are found only in the wing cell and basal cell layers of the epithelium.

Components of the cytoskeleton, including actin filaments, microtubules, and intermediate filaments, contribute to the shape of all cells. Intermediate filaments are composed of specific types of acidic (type I) and basic (type II) cytokeratin molecules. The cytokeratin pair 3 and 12 (64 kDa keratin) is typically expressed in the epithelium of the cornea [2, 5].

Cellular components of the epithelium participate in corneal immunity. Dendritic cells of the epithelium, i.e. Langerhans cells, express human lymphocyte antigen (HLA) class II molecules and act by presenting antigens to T-cells. Langerhans cells are abundant in the peripheral corneal epithelium; the central corneal epithelium and stroma contain numerous dendritic cells, but the latter are HLA class II negative [6, 7].

3.2.2.2 Superficial Cell Layer

The superficial cell layer is two to three cells thick. The cells are flat and polygonal with a diameter of 40–60 μm and a thickness of 2–6 μm with horizontal nuclei. Their surface is covered with microvilli that form microplicae [8].

Two different types of superficial corneal epithelial cells are found by scanning electron microscopy: large dark cells and small light cells. The former are mature and have many microvilli, whereas the latter have fewer microvilli and are thought to be less mature.

Superficial cells are well differentiated; they do not proliferate, have a low metabolic activity, and contain fewer organelles and less RNA than the other types of corneal epithelial cells. The glycocalyx present at the anterior surface of the superficial epithelial cells interacts with the mucinous layer of the tear film and helps to maintain the normal trilayered structure of the tear film.

The superficial cells of the corneal epithelium are joined by desmosomes and tight junctions that prevent the inflow of substances through the intercellular space. Interruption of the continuity of the corneal epithelium allows fluid to penetrate into the corneal stroma [2–4].

3.2.2.3 Wing Cell Layer

The wing cell layer constitutes the middle zone cells that are polyhedral with convex anterior surfaces and concave posterior surfaces (the characteristic wing-like shape) [2–4]. Their nuclei are oval to round. Multiple desmosomes attach the cells to their neighbours. The lateral borders of the cells show many interdigitations. The presence of numerous gap junctions permits free intercellular communication in this zone.

3.2.2.4 Basal Cell Layer

The deepest zone, basal cells are tall columnar cells that form a single layer resting on a basement

membrane [2–4]. Of all corneal epithelial cells, only the basal cells show mitotic activity. Basal cells are the source of wing cells and superficial cells. Basal cells contain more intracellular organelles, free ribosomes, rough endoplasmic reticulum, mitochondria, centrioles, microfilaments, microtubules, and glycogen granules than do wing or superficial cells. Their lateral borders interdigitate with one another and are attached by desmosomes, gap junctions, and zonulae adhaerentes. Hemidesmosomes attach the basal cells to the basement membrane. Hemidesmosomes are joined with anchoring fibrils, composed of type VII collagen, that pass through the basement membrane and Bowman's layer. After multiple branchings in the stroma, they form anchoring plaques together with type I collagen, a main component of the stroma. The anchoring fibrils are crucial for providing the adhesion of basal cells to the basement membrane and stroma.

3.2.2.5 Basement Membrane

Corneal basal epithelial cells secrete the components essential for basement membrane formation. Type IV collagen and laminin, which are both produced by basal cells, are the main components of the epithelial basement membrane. Transmission electron microscopy shows that the basement membrane (40–60 nm thick) is composed of two layers: a pale layer (lamina lucida) located just posterior to the cell membrane of the basal cells and an electron-dense layer (lamina densa). The corneal epithelial basement membrane contains type IV (α5) and VII, laminin-1, laminin-5, fibronectin, heparan sulphate proteoglycans, and fibrin.

The presence of basement membrane between the basal cell layer and the stroma assures the polarity of epithelial cells. The basement membrane also provides a matrix on which epithelial cells can migrate, and it is important for maintenance of the stratified, well-organised corneal epithelium [2–4].

3.2.2.6 Bowman's Layer

Bowman's layer lies directly beneath the basement membrane of the corneal epithelium, between the corneal epithelium and the corneal stroma proper. It measures 8–12 μm in thickness. It is an acellular structure consisting of randomly arranged collagen fibres and proteoglycans. The collagen fibres of Bowman's layer are primarily type I and III collagen and measure 20–30 nm in diameter. These fibres are finer and more randomly arranged than those in the corneal stroma proper. Bowman's layer is considered to be the anterior border of the corneal stroma. It does not regenerate after injury [2, 4].

3.2.2.7 Stroma

The stroma forms the largest portion, more than 90 % of corneal thickness. It consists of extracellular matrix, keratocytes (corneal fibroblasts), and nerve fibres. The cellular components form only 2–3 % of the total volume of the stroma [9]; the remaining space is occupied mostly by the extracellular matrix components: collagen and glycosaminoglycans. Collagen makes up more than 70 % of the dry weight of the cornea. The stroma is composed mainly of type I collagen, with smaller amounts of types III, V, and VI [10]. Stromal collagen fibres are identical in diameter (22.5–35 nm) and the distances between them are also identical (41.4 nm) [9]. The direction of the collagen fibres in any given lamella is the same, but they run at right angles to those of adjacent lamellae. Such a regular distribution of collagen fibres and lamellae is the main determinant of corneal transparency. Recently, the existence of a distinct pre-Descemet's layer was proposed [11].

Various glycosaminoglycans can be found between the collagen fibres of the corneal stroma. Keratan sulphate constitutes about 65 % of the total glycosaminoglycan content and is the most abundant glycosaminoglycan in the cornea. The other glycosaminoglycans are chondroitin sulphate and dermatan sulphate.

Glycosaminoglycans bind to core proteins to form proteoglycans, which are thought to modulate collagen fibrillogenesis. Lumican, keratocan, and mimecan (osteoglycan) are present in the corneal stroma as keratan sulphate proteoglycans and decorin as a chondroitin sulphate or dermatan sulphate proteoglycan. These core proteins first accumulate as low-sulphate glycoproteins in the embryonic stroma and subsequently bind glycosaminoglycans to form proteoglycans in the adult cornea.

Keratocytes form the main cellular component of the corneal stroma and are thought to turn over about every 2–3 years. Keratocytes have a spindle shape and they are scattered between the lamellae of the stroma. These cells extend long processes that are connected with processes of neighbouring cells by gap junctions [4].

Keratocytes are similar to fibroblasts and have an extensive intracellular cytoskeleton, including prominent actin filaments [5]. This allows the cells to contract and may be responsible for the maintenance of corneal shape and for the packed structure of collagen in the stroma [4].

Some cellular components of the corneal stroma play an important role in corneal immunity. Recent studies have revealed that the corneal stroma is endowed with significant numbers of resident inflammatory and antigen-presenting cells. This includes bone marrow-derived dendritic cells and macrophages. These dendritic cells present in the stroma do not express HLA class II molecules [6, 7].

3.2.2.8 Descemet's Membrane

Descemet's membrane is the basement membrane of the corneal endothelium and lies on the posterior surface of the stroma. It gradually increases in thickness from birth (3 μm) to adulthood (8–10 μm). Histological analysis shows Descemet's membrane to be stratified into a thin (0.3 μm) non-banded layer adjacent to the stroma, an anterior banded zone (2–4 μm), and a posterior amorphous, non-banded zone (less than 4 μm) that represents up to two-thirds of the thickness of the membrane and is deposited over time [4]. Descemet's membrane is composed mainly of type IV collagen fibrils arranged in a hexagonal pattern. It contains also laminin and fibronectin.

Descemet's membrane adheres tightly to the posterior surface of the corneal stroma and reflects any change in the shape of the latter. If the corneal stroma swells, Descemet's folds can be observed clinically. Descemet's membrane as such does not regenerate, but if endothelial cells migrate over the bare stroma after a Descemet's tear, new membrane will be deposited, and once it covers the injured area, stromal edema decreases [2, 4, 7].

3.2.2.9 Endothelium

The corneal endothelium consists of a single layer of flattened, uniformly 5 μm thick and 20 μm wide, polygonal (mostly hexagonal) cells, arranged into a mosaic pattern. Endothelial cells contain a large nucleus, numerous mitochondria, a prominent endoplasmic reticulum, free ribosomes, and a Golgi apparatus, which indicates that the cells are metabolically active and secretory. The anterior surface of endothelial cells is flat and adheres to Descemet's membrane. The posterior surface forms microvilli and marginal folds that protrude into the anterior chamber, thus maximising the surface area exposed to aqueous humour. The endothelial cells contain various junctional complexes: zonulae occludentes, maculae occludentes, and maculae adhaerentes, but not desmosomes. Gap junctions allow the transfer of small molecules and electrolytes between the endothelial cells.

Endothelial cells play a major role in controlling the normal hydration of the cornea, both by a permeable barrier function, limiting access of water from the aqueous humour to the corneal stroma, and by an active transport mechanism. Essential to this energy-determined process is the role of Na/K-ATPase and carbonic anhydrase. Bicarbonate ions produced by the action of carbonic anhydrase are translocated across the cell membrane, allowing water to passively follow. Loss or damage of endothelial cells results in increased absorption of water by the corneal stroma [2, 4].

Corneal endothelial cells do not proliferate in humans (unlike in rabbits). Thus, in the normal healthy cornea, the endothelial cell density decreases with age [12]. Between the ages of 20 and 80 years, the reduction in cell density averages 0.6 % per year, with concomitant increases in polymegethism (variation in size) and pleomorphism (variation in shape).

3.2.2.10 Blood Supply and Lymphatic Drainage

Under normal conditions the cornea does not contain any blood vessels. It is also devoid of lymphatic drainage.

Anterior ciliary arteries, branches of the ophthalmic artery, form a vascular arcade in the limbal region and contribute to corneal metabolism

and wound repair by providing nourishment. Absence of blood vessels from cornea is one of the factors contributing to its transparency [2, 4].

3.2.2.11 Nerve Supply

The cornea is one of the highly sensitive tissues of the human body. It is primarily innervated through one of three ophthalmic branches of the trigeminal nerve. The ophthalmic division of the trigeminal nerve has three parts: the frontal nerve, the lacrimal nerve, and the nasociliary nerve. The nasociliary nerve provides sensory innervation to the cornea, mainly through the long ciliary nerves. The long ciliary nerves enter the eye around the optic nerve, then run anteriorly in the suprachoroidal space. A short distance from the limbus, they pierce the sclera, divide, connect with each other and conjunctival nerves, and form the pericorneal (annular) plexus of nerves.

Approximately 60–80 myelinated branches enter the corneal stroma. Further division occurs, and the fibres lose their myelin sheaths. Next they unite to form the stromal plexus located in the mid-stroma. Subsequently, nerve fibres pass anteriorly and form the subepithelial plexus. Fine terminal branches pierce Bowman's layer and pass between the epithelial cells to form the intraepithelial plexus. Specialised nerve endings are absent. The axons are bare and devoid of a Schwann cell sheath [2, 13].

3.2.2.12 Limbal Stem Cells

Corneal epithelial cells renew rapidly and repeatedly in order to maintain a stratified squamous epithelium. The maintenance of the corneal epithelial cells is accomplished by a defined population of unipotent stem cells located in the basal epithelium of the corneoscleral limbus within so called "palisades of Vogt". The limbus (corneoscleral junction) is a specific and unique area, which is highly innervated, vascularised, and protected from potential damage from ultraviolet light by the presence of melanin pigmentation [7, 14]. Limbal stem cells are supported by a unique stromal microenvironment called the "stem cell niche", which consists of certain extracellular matrix components, cell membrane-associated molecules, and cytokines [15].

Limbal stem cells are the precursors for all other cells of the corneal epithelium and have a self-maintaining population. In vivo, they show slow cycling, but in vitro they demonstrate a high potential to proliferate [8, 14]. Stem cells in the limbus divide to produce a daughter stem cell and a transient amplifying cell. The transient amplifying cells migrate within the cornea to reside in the basal layer of corneal epithelium. Further cellular divisions of the transient amplifying cells produce post-mitotic cells that lie in the suprabasal layers. Progressive differentiation of post-mitotic cells produce terminally differentiated cells, which lie in the superficial corneal epithelial layers. These terminally differentiated cells are non-keratinised, stratified, squamous corneal epithelial cells. These cells are continually sloughed off the corneal surface and replaced by maturing, underlying cell layers [7, 14]. A number of molecular markers have been used to characterise limbal stem cells: ABCG2, p63, and cytokeratins 14/5 and 19 [5, 7].

3.3 Congenital Abnormalities

3.3.1 Abnormalities of Corneal Size

3.3.1.1 Microcornea

By definition, a cornea with a diameter less than 11 mm is designated microcornea.

3.3.1.2 Megalocornea

By definition, a cornea with a diameter more than 13 mm is designated megalocornea.

3.3.2 Abnormalities of Corneal Shape

3.3.2.1 Cornea Plana

Definition

Cornea plana, literally flat cornea, is an inherited bilateral abnormality characterised by a reduced corneal curvature.

Epidemiology

A very rare congenital anomaly.

Etiology and Genetics

Autosomal dominant type (CNA1; OMIM %121400) arises from an unknown gene on chromosome 12 [16] and autosomal recessive type

(CNA2; OMIM %217300) from mutations in *KERA*, encoding keratocan, also located on chromosome 12 and encoding keratocan, a proteoglycan [17].

Clinical Findings

Most eyes are hyperopic, in CNA2 severely so (>10 D), and have an indistinct corneal limbus with peripheral scleralisation [18, 19]. The axial length of the eye is normal [20]. CNA2 can be associated with malformations of the iris, iridocorneal adhesions, and stromal opacities [21, 22].

Histopathology

Histopathological findings of uncomplicated cornea plana have not been reported [23]. By clinical confocal microscopy, a thin epithelium and stroma, absence of Bowman's layer, diminished subbasal nerve fibre bundles, and abnormal stromal extracellular matrix were found in CNA2 [22].

Prognosis

CNA1 is mild but CNA2 is severe. Nonprogressive, but carries a risk for glaucoma and, rarely, corneal decompensation.

3.3.2.2 Sclerocornea

Sclerocornea is a poorly defined congenital condition in which the cornea is replaced by whitish tissue resembling sclera in texture and curvature [24]. It is not a single entity and can be associated with a number of different defined and undefined anomalies of the eye and other organs. It was recently proposed that this diagnosis should no longer be used as a primary diagnosis [25].

3.3.3 Abnormalities of the Anterior Segment of the Eye with Corneal Involvement

3.3.3.1 Axenfeld-Rieger Syndrome

Definition

Axenfeld-Rieger syndrome is an inherited disorder of the morphogenesis of the peripheral cornea, the iris, and the chamber angle often associated with glaucoma.

Epidemiology

A rare congenital anomaly.

Etiology and Genetics

The syndrome results from autosomal dominant mutations in *PITX2* (RIEG1, OMIM #180500) encoding paired-like homeodomain transcription factor 2, an unknown gene on chromosome 13 (RIEG2; OMIM %601499) or *FOXC1* (RIEG3; OMIM #602482) encoding forkhead box C1, a transcription factor [26, 27], which controls corneal vascularisation in mice [28]. Axenfeld-Rieger syndrome may result from a late developmental arrest of neural crest-derived anterior ocular structures.

Clinical Characteristics

A combination of an anteriorly displaced Schwalbe's line (posterior embryotoxon) and iris bands attached to the peripheral cornea (Axenfeld's anomaly), associated glaucoma from a defective trabecular meshwork (Axenfeld's syndrome), associated iris and pupillary abnormalities (Rieger's anomaly), and associated hypoplasia of the maxilla and dental anomalies including anodontia, oligodontia, microdontia, or peglike incisors (Rieger's syndrome) is variably present [29, 30]. Cardiac, craniofacial, and pituitary abnormalities also may be present [27, 31].

Histopathology

A prominent, anteriorly displaced Schwalbe's line and iris processes that bridge the chamber angle and insert onto the embryotoxon are present [29, 30]. The eye may also show abnormalities of the iris including stromal hypoplasia and slitlike, multiple, and false pupils.

Prognosis

Nonprogressive, but expressivity varies, and often complicated with chronic glaucoma.

3.3.3.2 Peters' Anomaly

Definition

Peters' anomaly is a developmental defect of the cornea, the iris, and the lens and may be associated with additional ocular anomalies.

Synonyms

An alternative name of kerato-irido-lenticular dysgenesis has been proposed [25].

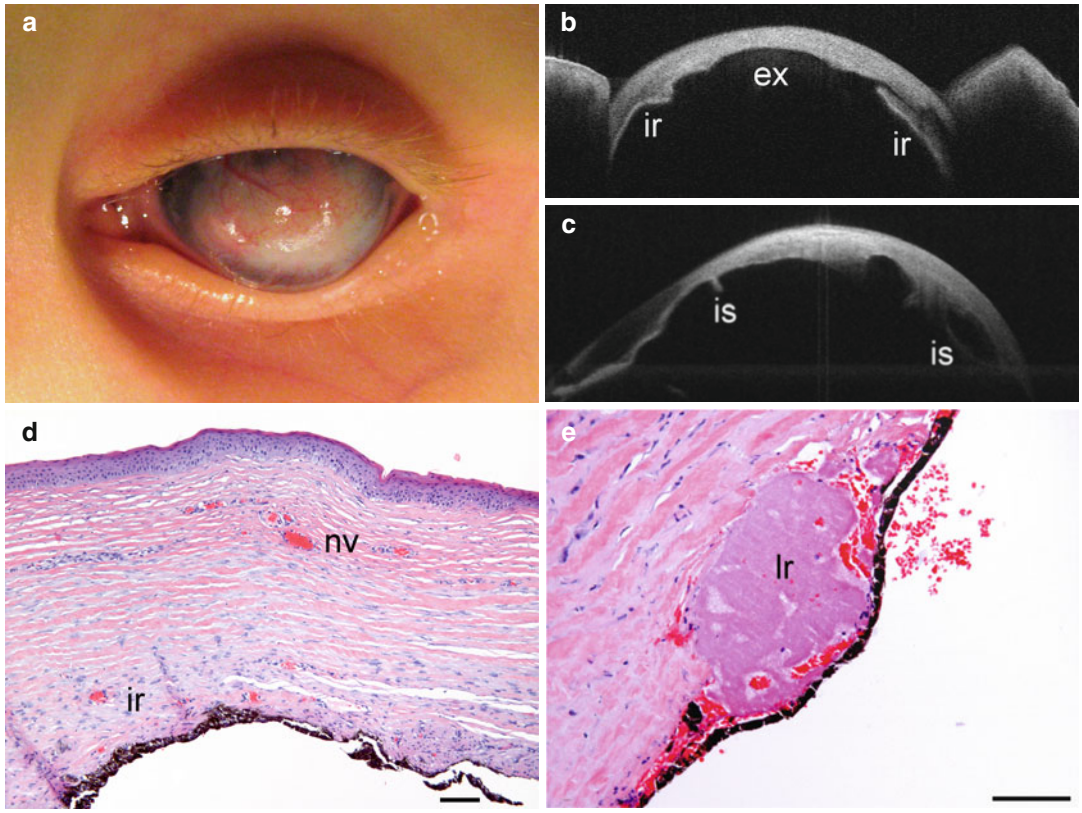

Fig. 3.3 Peters' anomaly. Congenitally opaque, vascularised cornea that prevents evaluation of iris structures (**a**). Anterior segment optical coherence tomography reveals a concave posterior corneal excavation (*ex*), a partly adherent iris (*ir*) (**b**), and iris strands (*is*) that attach to the cornea (**c**). Corneal epithelium is keratinised from exposure, Bowman's layer is absent, the loosely arranged stroma has neovascular vessels (*nv*), and the iris (*ir*) adheres to the corneal stroma without an intervening Descemet's membrane (**d**). A lens remnant (*lr*) is incarcerated within the posterior corneal stroma and under a rudimentary iris epithelium; note haphazard corneal stromal lamellae with abundant extracellular material (**e**). Haematoxylin-eosin (**d**, **e**), bars = 100 μm

Epidemiology

A rare congenital anomaly.

Etiology and Genetics

Peters' anomaly (OMIM #604229) results from either mutated paired box 6 (*PAX6*), paired-like homeodomain transcription factor 2 (*PITX2*), cytochrome P450, subfamily I, polypeptide 1 (*CYP1B1*), forkhead box C1 (*FOXC1*) or forkhead box E3 (*FOXE3*) gene [25], or fetal alcohol syndrome. Peters-plus syndrome (OMIM #261540) adds distinctive facies, cleft lip and palate, short hands and feet, and other anomalies and results from mutated beta-1,3-galactosyltransferase-like (*B3GALTL*) gene [32]. Inheritance is autosomal recessive, but rare dominant transmission is also reported.

Clinical Features

In type 1, a centrally located, avascular corneal opacity involves the posterior stroma, Descemet's membrane, and endothelium and is associated with iridocorneal adhesions [24, 33–35] that are best resolved with anterior segment optical coherence tomography [36]. In type 2, the lens has failed to separate and is adherent to or incarcerated within the cornea, which is vascularised (Fig. 3.3a–c).

Histopathology

A concave defect of the posterior layers of the cornea is present and the stroma borders directly to the anterior chamber within this area without Descemet's membrane or endothelium and shows irregular collagen lamellae with plump fibroblasts (Fig. 3.3d, e) [37–40]. The anterior central stroma is

cloudy and swollen. Bowman's layer ranges from abnormally thick to absent. Iridocorneal adhesions often are found at the rim of the corneal defect.

Prognosis

In type 1, corneal transplantation may partially restore vision, but in type 2 prognosis is uncertain because of associated anomalies and glaucoma [41, 42].

3.3.3.3 Posterior Keratoconus

A congenital corneal abnormality resembling the stromal defect of Peters' anomaly but with an intact Descemet's membrane, endothelium, and lens is known as posterior keratoconus [43, 44].

3.3.3.4 Congenital Anterior Staphyloma

Definition

Congenital anterior staphyloma is a developmental defect of the anterior ocular segment characterised by a cloudy, bulging, vascularised, staphylomatous cornea.

Synonyms

Congenital corneal staphyloma.

Epidemiology

A very rare congenital anomaly.

Etiology

An early developmental arrest of neural crest-derived anterior ocular structures is presumed. No underlying gene has been identified.

Clinical Features

The anterior segment abnormalities include a central corneal opacity, a sclerocornea, a hypoplastic iris that adheres to the cornea, a hypoplastic ciliary body, and a rudimentary or absent lens (Fig. 3.4a, b) [45–52]. The posterior segment is normal but the fellow eye is usually microphthalmic. Extraocular anomalies are rarely associated with this condition.

Histopathology

The cornea ranges from thin to thick, depending on stretching of the staphyloma [45–52]. The corneal epithelium is hyperkeratotic and the stroma swollen with variable degrees of inflammation from exposure. Bowman's layer and Descemet's membrane are typically absent (Fig. 3.4c, d). The stroma has irregular lamellae and plump fibroblasts. The neuroepithelial layers of the iris adhere to the cornea with little or no intervening iris stroma.

Prognosis

Corneal transplantation may enhance cosmesis and partially restore vision, but long-term prognosis is guarded.

3.3.3.5 Congenital Keratectasia

Congenital keratectasia may resemble congenital anterior staphyloma but differs from it by the presence of normal corneal layers and absence of adherent iris. It is postulated to be secondary to intrauterine keratitis or nutritional deficiency.

3.4 Inflammation

3.4.1 General Considerations

Corneal inflammation is a non-specific result of tissue damage. Direct injury from foreign bodies and chemical or thermal burns can elicit inflammation. The two most common etiologies, however, are microbial infections and various immunologic conditions [53]. Macrophages that process antigens and polymorphonuclear leucocytes with destructive proteolytic enzymes are relevant factors that initiate the inflammatory response. Antigens lead to an immune response, and B- and T-lymphocytes are responsible for subsequent antibody and cytotoxic reactions, respectively. Leucocytes migrate toward the site of the initiating inflammatory stimulus, following interlamellar pathways of the corneal stroma, and produce irregularities in the alignment of its lamellae [54].

Stromal swelling typically accompanies inflammation and leads to an increase in corneal thickness from accumulation of fluid within and between the stromal lamellae, swelling of keratocytes, and influx of

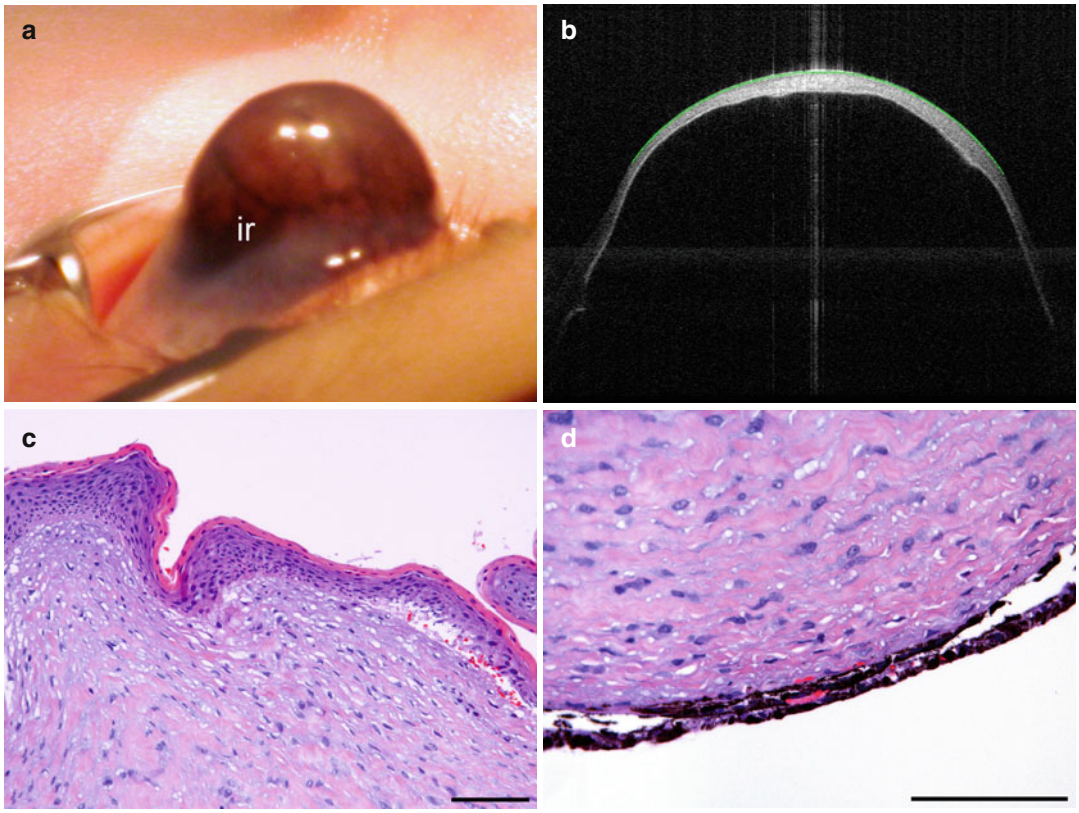

Fig. 3.4 Congenital anterior staphyloma. Grossly bulging cornea with attached stretched iris (*ir*) on its posterior surface in a newborn baby (**a**). Anterior segment optical coherence tomography reveals extreme thinning of the cornea with swelling in its centre (**b**). Corneal epithelium is keratinised from exposure, Bowman's layer is absent, and corneal stroma is replaced by haphazardly arranged fibroblasts and thin, wavy collagen strands (**c**). Descemet's membrane and iris stroma are absent, and the primitive iris epithelium adheres to the cornea; note inconspicuous corneal lamellae with abundant intervening fibroblasts (**d**). Haematoxylin-eosin (**c**, **d**), bars = 100 µm

inflammatory cells. Histopathologically, artifactual separation of lamellae should not be mistaken for stromal edema; true swelling actually tends to decrease such separation. The swollen stroma is less eosinophilic and less birefringent under polarised light. The source of the fluid varies: tears in superficial lesions, leaking limbal vasculature in anterior and mid-stromal lesions, and aqueous humour in posterior lesions [54].

The initial vascular reaction to corneal inflammation is perilimbal injection, which may extend around the entire limbus. The limbal vasculature contains anastomotic connections between the superficial vessels, derived from the conjunctival circulation, and the deep vessels, derived from the anterior ciliary-episcleral circulation connected to the iris vasculature. Therefore, reflex dilatation of iris vessels, iritis, and hypopyon formation in the anterior chamber can accompany keratitis.

The combination of swelling, cellular infiltration, and lamellar distortion interferes with light transmission, and, hence, with transparency of the cornea [54].

3.4.1.1 Corneal Ulceration and Sequelae

Corneal stromal ulceration is of great clinical significance as it is frequent, and difficult to treat, and leads to considerable ocular morbidity and sight-threatening sequelae. Relevant cellular events and interactions include a preceding

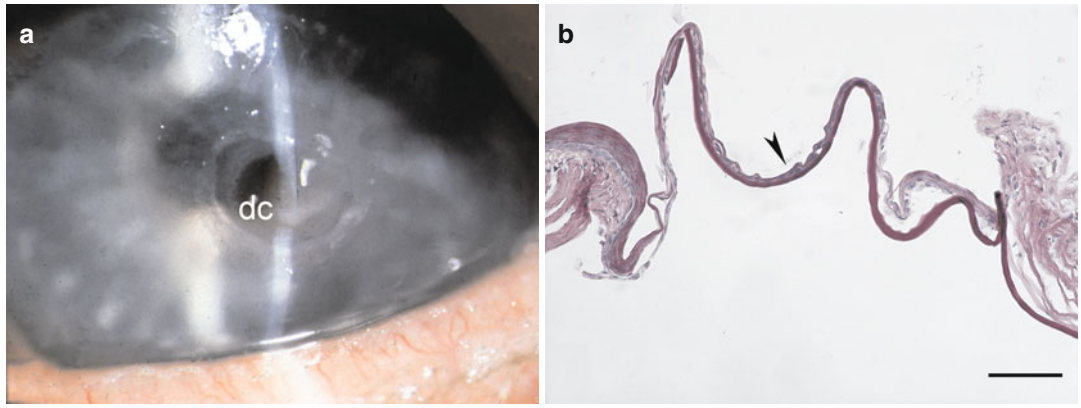

Fig. 3.5 Descemetocele. Sterile descemetocele (*dc*) in a patient with rheumatoid arthritis (**a**). Histopathology of descemetocele with remnants of epithelium (*arrowhead*), nearly complete loss of stroma, and bulging of Descemet's membrane that is devoid of endothelial cells (**b**). Periodic acid-Schiff, bar = 100 µm

epithelial defect, inflammatory cell migration, release of collagenases and other hydrolases by injured corneal epithelium, keratocytes and polymorphonuclear leucocytes, activation of latent collagenases, tissue necrosis, and failure of normal wound healing processes [55].

Scar Formation (Macula and Leucoma)

Healing of a corneal wound begins when epithelial cells migrate into the ulceration from its margins. Limbal vessels and reactive stromal fibroblasts grow beneath the newly formed epithelium; macrophages assist in removing cell debris. A connective tissue scar, known as a macula or a leucoma depending on its extent, begins to form, which interferes with transparency. On microscopic examination, clinically visible scars may not be evident at all or will only correspond to minor irregularities in stromal fibre arrangement. Routine haematoxylin-eosin stain shows keratocytes with large, darkly staining nuclei and a more eosinophilic cytoplasm than those among older corneal fibres. Bowman's layer in deeper scars is often replaced by connective tissue [56].

Keratectasia

A keratectasia, an ectatic corneal scar, is defined as bulging of a thinned, scarred cornea. It differs from a staphyloma in that uveal tissue does not line the scar.

Descemetocele

Sloughing of the inflamed, sometimes infected, corneal stroma may lead to severe thinning of the stromal layers. Descemet's membrane, on the other hand, is quite resistant to inflammation and necrosis and will often remain intact after loss of most of the stroma (Fig. 3.5a). A herniation of this extremely elastic membrane through a corneal ulcer is known as a descemetocele that may be covered by fibrinous exudate, a few posterior stromal lamellae, and corneal epithelium (Fig. 3.5b). It may rupture as a result of intense stretching, enzymatic digestion, or sudden increase in intraocular pressure [56].

Adherent Leucoma

After penetrating corneal injury or spontaneous perforation of an ulcer, an adherent leucoma can form. It typically consists of a dense corneal scar with adherent intraocular tissue such as iris, lens material, vitreous, or even retina.

3.4.1.2 Corneal Neovascularisation

The cornea is one of the few tissues which actively maintain an avascular state, i.e. the absence of blood and lymphatic vessels (corneal [lymph] angiogenic privilege). Neovascularisation of the cornea can follow numerous inflammatory diseases of the anterior segment including trachoma, luetic and viral interstitial keratitis, microbial

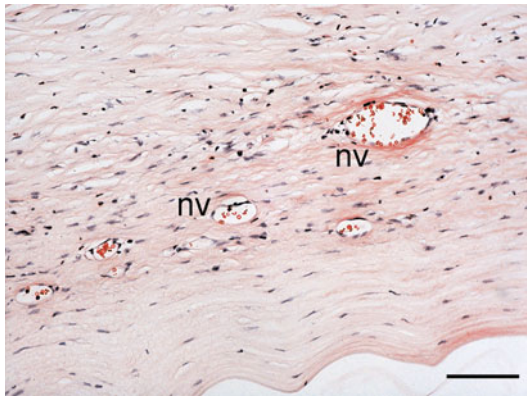

Fig. 3.6 Corneal neovascularisation. Scar formation with deep stromal neovascular vessels (*nv*). Haematoxylin-eosin, bar = 100 µm

keratitis, and the immune reaction elicited by corneal transplantation. Diapedesis of leucocytes into the stroma with extravasation of fibrin and other serum proteins is followed by vascular endothelial migration and proliferation from the limbus adjacent to the site of inflammation. Subepithelial vascular growth (superficial neovascularisation) is typically present with superficial lesions. In deep neovascularisation, buds of endothelial cells emerge from limbal capillaries, extend between stromal lamellae, and become canalised thereafter (Fig. 3.6) [56]. The extent of neovascularisation depends on the severity and extent of the inflammatory focus and its duration. As the inflammation subsides, the vascular channels regress and are seen clinically as non-perfused "ghost vessels".

Ingrowth of blood and lymphatic vessels into the cornea not only reduces corneal transparency and thereby visual acuity, but also significantly increases the rate of graft rejection if corneal transplantation becomes necessary [57].

3.4.1.3 Corneal Lymphangiogenesis

The normal cornea is not only avascular but also devoid lymphatic vessels, thus allowing for its unique immune privileged status. It can, however, acquire lymphatic vessels secondary to a variety of corneal diseases and surgical manipulations. Whereas corneal hemangiogenesis is obvious both clinically and histologically, detection of associated corneal lymphangiogenesis has long been hampered by virtual invisibility of lymphatic vessels and lack of specific markers. This has changed with the recent discovery of lymphatic endothelial markers: vascular endothelial growth factor receptor 3, lymphatic endothelium-specific hyaluronan receptor-1 (LYVE-1), Prox 1, and podoplanin. Corneal inflammation and wound healing are now known to be typically associated with lymphangiogenesis by vascular endothelial growth factor (VEGF-C/-D/VEGFR-3)-mediated mechanisms [57–59].

3.4.2 Ocular Surface Disease

Ocular surface disease is a common clinical entity but will only rarely be seen by the ophthalmic pathologist.

3.4.2.1 Dry Eye Syndrome

Definition

The Dry Eye WorkShop has defined dry eye syndrome as a multifactorial disease of the tears and ocular surface that results in symptoms of discomfort, visual disturbance, and tear film instability with potential damage to the ocular surface [60]. This syndrome is accompanied by increased osmolarity of the tear film and inflammation of the ocular surface (Fig. 3.7a). It is typically associated with older age, female gender, and certain systemic diseases such as Sjögren's syndrome.

Histopathology

In dry eye syndrome, the conjunctiva is affected before the cornea. It shows loss of goblet cells, conjunctival stromal edema, loss of epithelial cell surface microplicae, increased epithelial cell desquamation, and progressive squamous metaplasia [61, 62]. The cornea is more resistant to ocular surface disease. In severe cases, however, ribbon-like threads of desiccated corneal epithelial cells with associated mucus may pile up on the epithelial surface (Fig. 3.7b) [63]. In severe dry eye syndrome, sterile corneal melting, ulceration, and spontaneous perforation can occur (Fig. 3.5).

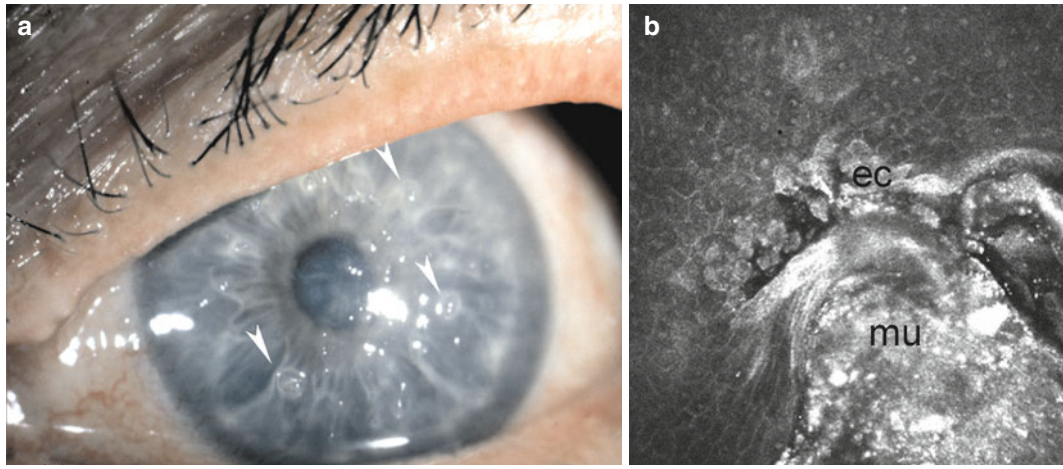

Fig. 3.7 Dry eye syndrome. Filiform keratitis demonstrating threads of desiccated corneal epithelial cells with associated mucus (*arrowheads*) in a severe dry eye syndrome (**a**). The epithelial cells (*ec*) and mucus (*mu*) as imaged by in vivo confocal microscopy (**b**)

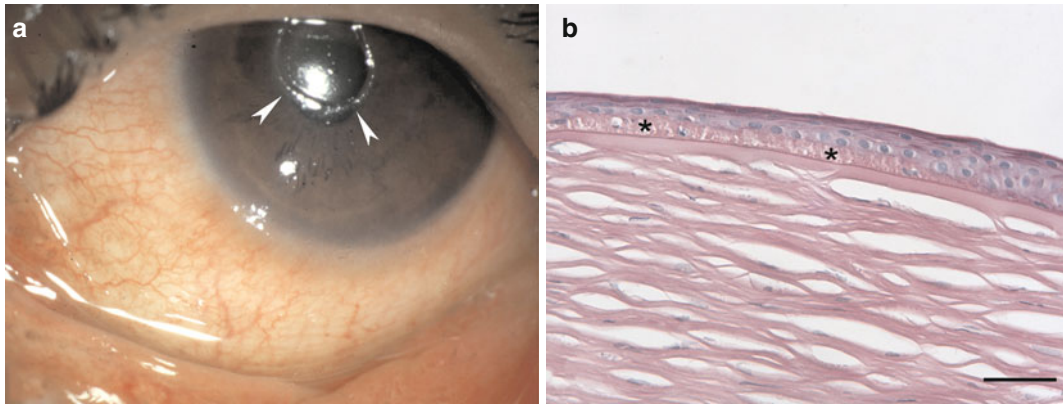

Fig. 3.8 Atopic keratoconjunctivitis. Corneal ulceration (*arrowheads*) in a patient with atopic keratoconjunctivitis (**a**). Linear deposition of subepithelial eosinophil granular substance in a corneal button (*asterisks*). The material was identified as major basic protein and eosinophil granule protein by immunofluorescence (**b**). Haematoxylin-eosin, bar = 50 µm

3.4.3 Immunologic Disease

3.4.3.1 Atopic/Vernal Keratoconjunctivitis

Definition

Corneal pathology caused by severe ocular allergy in patients with atopy.

Epidemiology

In a retrospective study of 45 patients with atopic keratoconjunctivitis, 34 patients had keratopathy and 21 had persistent corneal epithelial defects causing severe visual impairment (Fig. 3.8a) [64].

Histopathology

Toxic granule proteins of eosinophils such as major basic protein (MBP) and eosinophil cationic protein (ECP) inhibit epithelial cell migration and protein synthesis. These factors are typically involved in corneal ulceration in atopy. A linear subepithelial deposition of eosinophil granular substance can be detected in corneal buttons

removed at transplantation in patients with atopic keratoconjunctivitis, associated with infiltration of eosinophils into the corneal stroma (Fig. 3.8b). Immunofluorescence staining is helpful in identifying this material as MBP and ECP [65].

Prognosis

Penetrating keratoplasty may be required in these cases, but a high rate of complications and graft rejections may occur [66].

3.4.3.2 Peripheral Ulcerative Keratitis

Staphylococcus-Associated Blepharokeratoconjunctivitis

Definition

Marginal keratitis, leading to corneal ulceration, is frequently observed in association with staphylococcus-associated blepharokeratoconjunctivitis. It is thought to be a hypersensitivity reaction to staphylococcal antigen.

Histopathology

Microscopic examination shows necrosis of the involved cornea and infiltration by neutrophils. Healing occurs by fibroblastic proliferation and may be associated with neovascularisation from the limbus [56].

Peripheral Ulcerative Keratitis Associated with Collagen Vascular Disease

Definition

Corneal inflammation and ulceration associated with acquired connective tissue and vasculitic disorders, including rheumatoid arthritis, psoriatic arthritis, systemic lupus erythematosus, polyarteritis nodosa, Wegener's granulomatosis, and relapsing polychondritis. Ocular inflammation may portend catastrophic extraocular vasculitis.

Etiology

Pathophysiologic factors involved include immune complex deposition in the limbal area with activation of the complement cascade, release of inflammatory mediators, and attraction of neutrophils with resultant tissue destruction and corneal stromal melting [67].

Histopathology

Necrotising occlusive vasculitis is observed within the peripheral cornea and perilimbal lesions in patients with Wegener's granulomatosis and polyarteritis nodosa [68, 69]. On microscopic examination, necrosis of the corneal epithelium and peripheral stroma is present with ulceration and acute inflammatory cell infiltrate. Granulomatous inflammation may be observed. The adjacent sclera is generally involved. A thinned vascularised stromal scar typically remains after healing.

Mooren's Ulcer

Definition

Mooren's ulcer is an idiopathic peripheral ulcerative keratitis, occurring without any identifiable systemic disorder.

Etiology

The exact pathophysiology remains uncertain, but the evidence suggests that it is an autoimmune process combining cell-mediated immunity against corneal antigens with humoral components.

Clinical Features

Mooren's ulcer begins as a painful, yellow-grey infiltrate adjacent to the limbus and spreads circumferentially and centrally. Characteristically, it has an overhanging edge centrally. The sclera is not involved. After healing, the damaged cornea peripheral to the active, advancing front remains thinned, scarred, and vascularised leaving the patient with poor vision (Fig. 3.9a).

Histopathology

On histology, lymphocytes, plasma cells, neutrophils, mast cells, and eosinophils are present in the area of ulceration. High levels of proteases and collagenases have been detected with destruction of the collagen matrix. Reactive keratocytes and disorganisation of collagen lamellae are present in midstroma (Fig. 3.9b).

Descemet's membrane and endothelium are spared [70, 71].

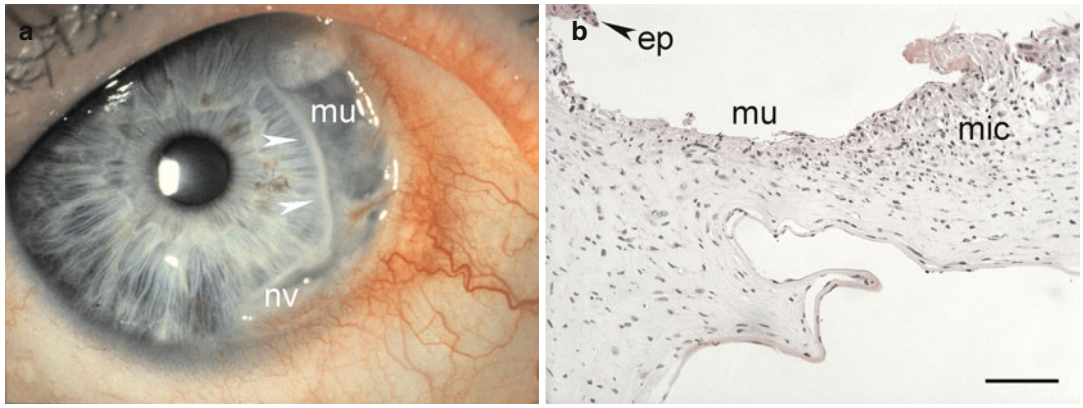

Fig. 3.9 Mooren's ulcer. A typical Mooren's ulcer (*mu*) with an overhanging central edge (*arrowheads*) and neovascular vessels (*nv*) from the limbal conjunctiva (**a**). Loss of epithelium (*ep*) within the ulcer (*mu*) and mixed inflammatory cells (*mic*) within the stroma (**b**). Haematoxylin-eosin, bar = 100 µm

3.4.3.3 Interstitial Keratitis

Syphilitic Stromal Keratitis

Definition

Syphilitic interstitial stromal keratitis results from congenital luetic infection. It is a rare disorder in developed countries. The course of the disease suggests an immune reaction toward *Treponema pallidum*.

Histopathology

Only a few histological studies of active disease are available. The entire cornea is edematous, inflamed, and necrotic with lymphocyte infiltration and early neovascularisation in the middle and deep stroma [56]. Necrosis of Descemet's membrane and corneal endothelium may occur. Healing leaves a vascularised scar often with non-perfused "ghost vessels". In chronic interstitial keratitis, the regenerating endothelium can produce focal or diffuse multilaminar thickening of Descemet's membrane. These retrocorneal scrolls contain type I, III, IV, VI, and VII collagens as well as proteoglycans and are lined with attenuated corneal endothelium.

Cogan's Syndrome

Definition

Cogan's syndrome is a non-syphilitic interstitial keratitis typically associated with vestibuloauditory symptoms in young adults. An immune reaction against a common antigen of the cornea and inner ear is suggested.

Clinical Features

The mostly bilateral disease starts with diffuse or sectoral subepithelial infiltrates and progresses to classic interstitial keratitis. Episcleritis, scleritis, and uveitis can be associated with it. The end stage is a vascularised, scarred cornea with irregular astigmatism. Life-threatening aortic insufficiency and serious systemic necrotising vasculitis can complicate the course.

3.4.4 Infection

An intact corneal epithelium and a healthy tear film serve as an effective barrier to most bacterial, viral, mycotic, and parasitic infections. Interruption of this barrier, e.g. by contact lens wear, injury, or rupture of epithelial bullae, allows entrance and spread of microorganisms. Sequelae from microbial keratitis are a leading cause of corneal blindness word wide.

3.4.4.1 Bacterial Keratitis

Etiology

Bacterial keratitis can result from infection by virtually any virulent pyogenic organism

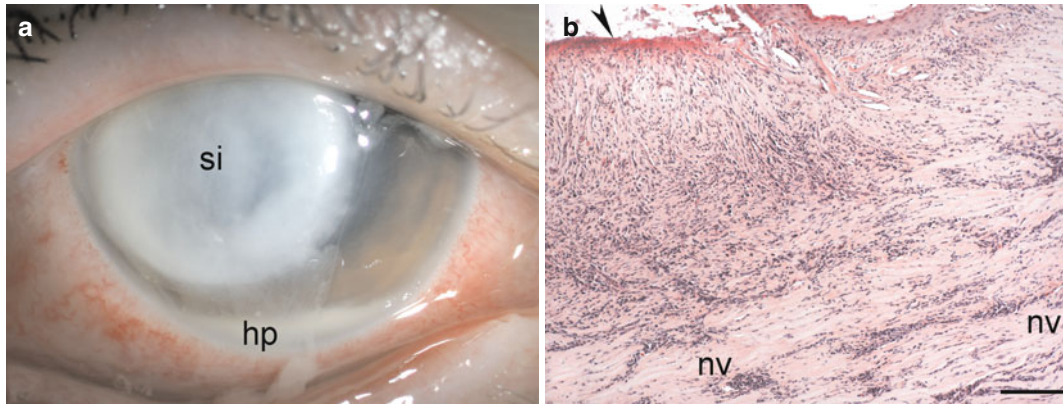

Fig. 3.10 Bacterial keratitis. Severe bacterial keratitis caused by *Pseudomonas aeruginosa* with a large whitish corneal stromal infiltrate (*si*) and hypopyon (*hp*) at the bottom of the anterior chamber (**a**). Histopathology of a corneal button after bacterial keratitis demonstrates loss of epithelium (*arrowhead*), massive invasion by chronic inflammatory cells, and neovascular vessels (*nv*) within the corneal stroma (**b**). Haematoxylin-eosin, bar = 100 µm

(Fig. 3.10a), but the most frequent microbial species encountered in developed countries are *Staphylococcus*, *Pseudomonas*, other Gram-negative species, *Streptococcus*, and *Corynebacterium* [72, 73]. Primary tuberculous keratitis by *Mycobacterium tuberculosis* is now extremely rare. Non-tuberculous *Mycobacteria*, including *Mycobacterium fortuitum*, *M. chelonae*, *M. gordonae*, and *M. avium-intracellulare*, are all capable of causing an indolent, intractable keratitis. They are observed with increasing incidence after foreign-body injury or following office surgical procedures such as laser in situ keratomileusis (LASIK) [74]. *Mycobacterium leprae* is the causative agent of leprous keratitis.

Histopathology

On histology, bacterial keratitis can be divided into distinct stages of progressive infiltration, active ulceration, regression, and healing (Fig. 3.10b). After adherence and entry of the organism, bacterial and neutrophil enzymes facilitate progressive bacterial invasion into the cornea. Tissue necrosis with subsequent sloughing of the epithelium and stroma takes place. Progressive keratolysis, descemetocele formation, and spontaneous perforation may follow. Gram stain will confirm microbial invasion. Giemsa stain is most frequently used to determine the type of infection present. Special stains include carbolfuchsin or Ziehl-Neelsen acid-fast stain for identification of suspected *Mycobacterium*, *Actinomyces,* or *Nocardia*. Mycobacteria may invade along peripheral corneal nerves and cause a non-necrotising, granulomatous inflammation with histiocytes and giant cells containing large numbers of acid-fast-staining lepra bacilli [75, 76].

3.4.4.2 Viral Keratitis

Adenoviral Keratoconjunctivitis Including Epidemic Keratoconjunctivitis

Definition

Adenovirus serotypes 8 and 19 are primarily responsible for epidemic keratoconjunctivitis (EKC).

Clinical Features

A flu-like illness may be associated. Following an acute follicular conjunctivitis, epithelial keratitis will develop in 80 % of patients, associated with marked discomfort, photophobia, epiphora, and blepharospasm. The keratitis evolves through four stages: stage 1, a diffuse, fine superficial epithelial punctate keratitis caused by live virus; stage 2, coalescence of the lesions to focal punctate, slightly raised whitish epithelial ones that last for approximately 10 days; stage 3, combined epithelial and subepithelial lesions by week 2 when all replicating virus has been removed by the host immune response; and stage 4, subepithelial nummular

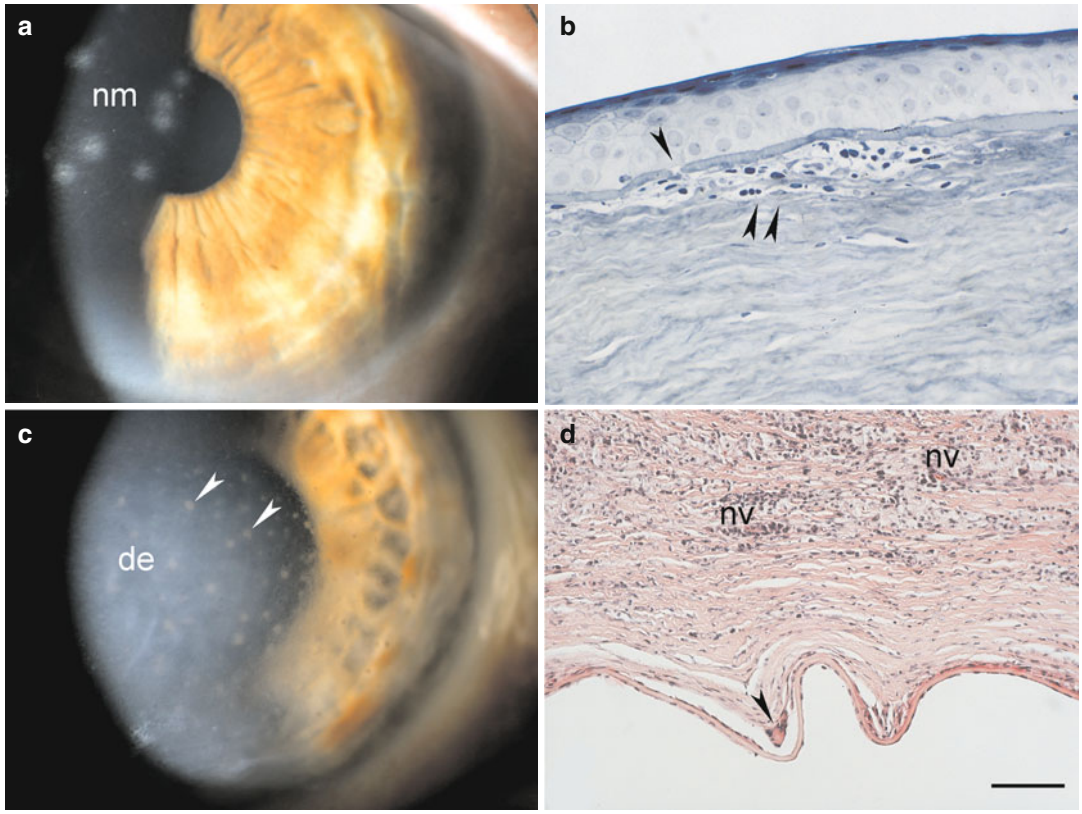

Fig. 3.11 Viral keratitis. Subepithelial stromal infiltrates (nummuli; *nm*) after epidemic keratoconjunctivitis (**a**). Specimen of a patient with nummuli 2 years after epidemic keratoconjunctivitis. Breaks in Bowman's layer (*arrowhead*) with subepithelial accumulations of lymphocytes, histiocytes, and fibroblasts (*double arrowhead*) are present (**b**). An eye with *Herpes simplex* keratitis shows viral endotheliitis with endothelial precipitates (*arrowheads*) and disciform edema (*de*) of the corneal stroma (**c**). Stromal infiltration with granulomatous reaction to Descemet's membrane (*arrowhead*), neovascular vessels (*nv*), and chronic inflammatory cells (**d**). Alcian blue, bar = 50 µm (**b**), and haematoxylin-eosin, bar = 100 µm (**d**)

opacities [77, 78]. The subepithelial nebulae may persist for several months, causing glare and diminished vision before gradually resolving (Fig. 3.11a).

Histopathology

Histopathological studies of adenoviral keratoconjunctivitis are rare. Adenovirus-like particles have been demonstrated within corneal epithelial cells of a patient with EKC caused by adenovirus serotype 8 [77]. Replica imprints of corneal epithelium in acute EKC show diffuse mild epithelial edema with scattered swollen and deformed cells that may be fused to small syncytial formations with pseudopodia-like processes. Intranuclear vacuolar inclusions and dense bodies with replicating virus are observed [79]. A corneal specimen taken from a patient who underwent lamellar keratoplasty for permanent visual loss due to EKC 2 years earlier revealed lymphocytes, histiocytes, and fibroblasts in the deep epithelial layers and anterior stroma. Breaks in Bowman's layer were present (Fig. 3.11b) [80]. Virus could not be recovered by culture or visualised by electron microscopy, lending support to the theory that nummular infiltrates result from host immune and inflammatory responses to residual viral antigen.

Herpes Simplex Viral Keratitis

Definition

Herpes simplex virus (HSV), the most ubiquitous communicable infectious virus in humans,

causes a vast variety of chronically recurring ocular disease.

Epidemiology

Herpes simplex virus keratitis is the leading infectious cause of corneal blindness in developed countries [81].

Clinical Features

Primary ocular involvement may present as an acute follicular keratoconjunctivitis with unspecific keratitis and associated vesicular periocular skin involvement. Recurrent corneal herpes may manifest in the epithelium as infectious epithelial keratitis (dendritic keratitis, geographic ulcers) or as a trophic (metaherpetic) keratopathy. Stromal disease may be divided into categories according to the currently accepted pathogenetic mechanisms: viral interstitial keratitis, immune rings, and limbal vasculitis (antigen-antibody-complement-mediated immune disease) and disciform edema/endotheliitis (delayed hypersensitivity immune disease; Fig. 3.11c).

Histopathology

Histologically, the dendrites correspond to epithelial cell loss. In the vicinity of the dendrite, rounded epithelial cells and variably sized syncytia containing nuclei with bizarre shapes are present. Pseudopodia-like processes containing viral DNA and some RNA extend from the syncytia into the surrounding epithelial cells, which on coming into contact with these processes become rounded and liquefied, and give rise to another syncytium. The infected epithelial cells show intranuclear and cytoplasmic inclusion bodies and polykaryocyte formation [82]. Epithelial giant cells may be present adjacent to the sites of epithelial cell loss.

In stromal disease, edema, migration of inflammatory cells from the limbus, and subsequent necrosis occur. Whereas neutrophils and macrophages are the predominant cell types in early stages, T-lymphocytes dominate later on. Animal experiments show that HSV-1-induced corneal tissue destruction is mainly mediated by mononuclear cells and neutrophils and that these cells are probably attracted into the cornea by cytokines secreted by activated CD4+, Vβ8+ T-cells [83]. Blood vessels invade the stroma only in case of necrosis. Healing is slow and involves deposition of irregular collagen bundles. Residual inflammation can be observed histopathologically long after the acute infection. Inflammation was present in the majority of corneal buttons removed at penetrating keratoplasty after HSV disease, despite being clinically inactive for more than 6 months prior to surgery. A large amount of HSV genome was detected in 86 % of quiescent corneas with a history of herpetic keratitis. However, HSV DNA in low quantities was also present in 11 % of control corneas and was also detected in corneal buttons of clinically unsuspected cases [84, 85].

Histopathological inflammation is associated with an increased rate of graft rejection after corneal transplantation [86]. A granulomatous reaction to Descemet's membrane (Fig. 3.11d), in the posterior stroma, and the in anterior chamber was present in 39 % of specimens analysed in one study [87].

Varicella Zoster Virus Keratitis

Definition

Varicella zoster virus (VZV) may involve any structure of the anterior segment of the eye.

Epidemiology

Whereas chickenpox is the primary disease, herpes zoster ophthalmicus (HZO) is a recurrent infection caused by the VZV. Of every 1,000 people surviving to the age of 85 years, 500 will have one attack of dermatomal herpes zoster, and 10 will have had two attacks. Age and impaired immunity greatly enhance the risk for development of herpes zoster [88, 89]. HZO is second only to thoracic zoster in frequency [90].

Clinical Features

In chickenpox, the cornea may develop infectious superficial punctate keratitis or branching, dendritic ulcers without terminal knobs. These lesions are positive for VZV DNA [91]. Disciform keratitis similar to that caused by herpes simplex virus may develop.

Two-thirds of HZO patients have corneal involvement. Punctate keratitis or pseudodendrites,

anterior stromal infiltrates, sclerokeratitis, keratouveitis-endotheliitis, peripheral ulcerative keratitis, delayed mucous plaques, disciform keratitis, neurotrophic keratitis, and exposure keratitis can occur [92]. VZV can typically be isolated from dendritic epithelial lesions and ulcerations [91, 93]. However, VZV DNA shedding is highly variable, age-dependent, and probably related to the host's immune status [94]. Immune keratitis similar in appearance to HSV stromal disciform edema/endotheliitis may occur. If there is an associated interstitial keratitis, there is an increased chance of deep neovascularisation with lipid deposition and fibrovascular scarring. Assays for VZV DNA have been positive in some cases [87, 95–97]. Sixty percent of HZO patients develop moderate to complete corneal anaesthesia secondary to destructive VZV ganglionitis and to aqueous tear deficiency [92, 98]. Neurotrophic keratopathy may progress to ulceration and perforation.

Histopathology

Histopathological reports of acute and chronic HZO reveal normal corneas or corneal inflammation with macrophages at the level of the endothelium associated with non-granulomatous inflammation, consisting mainly of lymphocytes and plasma cells, in the uveal tissue [96, 99, 100]. Chronic HZO keratitis may present with a giant cell reaction at the level of Descemet's membrane [87]. VZV DNA may be detected in human corneas at least 8 years after the acute event [96, 100]. Viral DNA was mainly found in mononuclear cells with eosinophilic intracytoplasmic inclusions within vascular stromal scars, in keratocytes, and in epithelial cells [96].

3.4.4.3 Fungal Keratitis

Definition

Fungal keratitis is one of the most challenging types of microbial keratitis to diagnose and treat.

Epidemiology

The incidence of fungal keratitis in temperate climates is low compared to bacterial infection, but tends to be more commonly seen in rural areas and warm climates.

Etiology

Candida, *Aspergillus*, and *Fusarium* species are the most frequently isolated fungi in fungal keratitis. Fungi gain access into the corneal stroma through an epithelial defect caused by injury, contact lens wear, an otherwise compromised surface, or following surgery.

Clinical Features

Clinically, the following features are suggestive of fungal infection: stromal infiltrate with feathery edges, grey and elevated infiltrates, satellite lesions, presumed immune rings, and endothelial plaques (Fig. 3.12a). Corneal scrapings are typically performed to culture fungi from the cornea, but due to the location of the pathogen deep in the stroma, a corneal biopsy submitted to microbiological and histopathological analysis will often yield better results. Fungi typically cause inflammation and necrosis with penetration deep to the corneal stroma and may perforate through an intact Descemet's membrane. Organisms that have penetrated into the anterior chamber, iris, or lens, or have infiltrated the sclera, are extremely difficult to control. Keratoplasty is sometimes necessary in acute disease when medical treatment fails, and infection may progress to deep ulceration and spontaneous perforation [101].

Histopathology

Intact organisms are rarely observed within active necrosis, but they can be found in the surrounding stroma, even in culture-negative specimens. Gram stain identifies yeast, and Giemsa stain is useful in detecting fungal elements. However, if fluorescein microscopy is available, acridine orange and calcofluor white are the stains of choice. Fungal hyphae oriented perpendicular to corneal lamellae and penetration of an intact Descemet's membrane are suggestive of progressive pathogenicity (Fig. 3.12b) [101, 102].

3.4.4.4 Parasitic Keratitis

Acanthamoeba

Definition

Acanthamoeba are small, free-living ubiquitous protozoa that exist in two life forms, an active

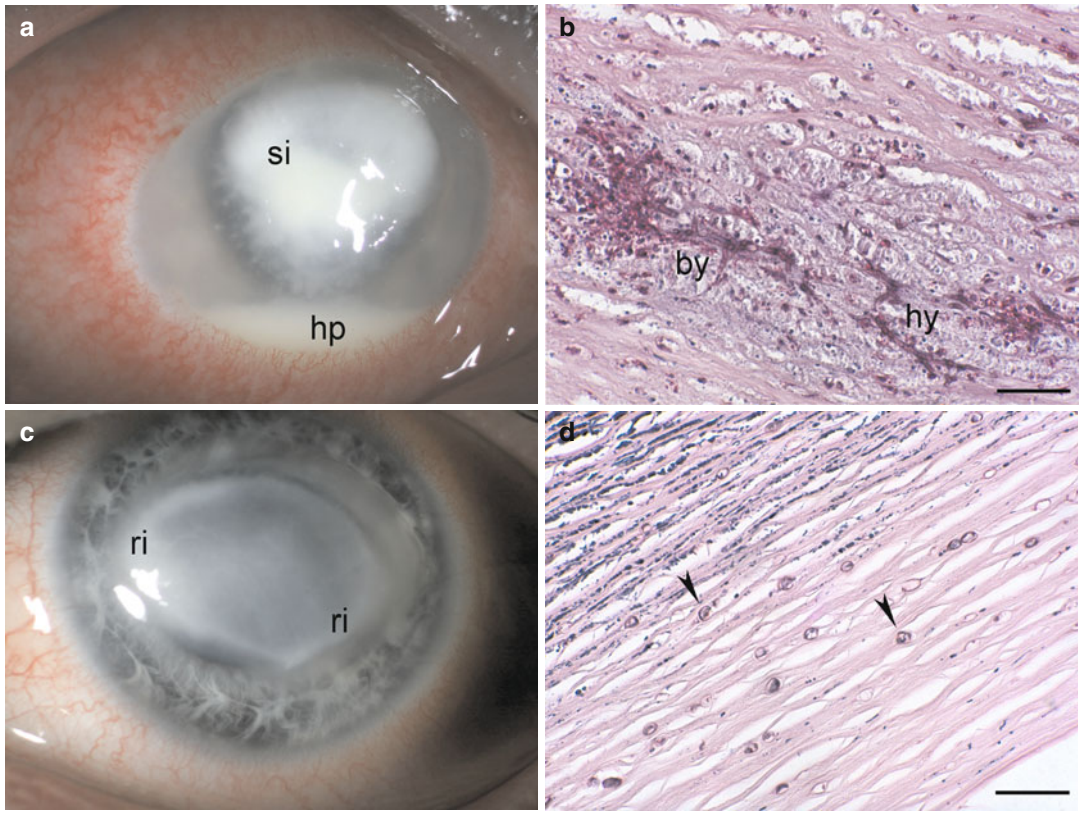

Fig. 3.12 Fungal and parasitic keratitis. Keratitis from *Aspergillus* species. Deep stromal infiltrate (*si*) with feathery edges and a hypopyon (*hp*) at the bottom of the anterior chamber (**a**). Fungal keratitis caused by *Candida* species. Necrotising stromal inflammation with infiltration by chronic inflammatory cells, branching hyphae (*hy*), pseudohyphae, and budding yeasts (*by*) are visible (**b**). *Acanthamoeba* keratitis with a typical ring infiltrate (*ri*) in a contact lens wearer (**c**). Chronic inflammation and multiple *Acanthamoeba* cysts (*arrowheads*) within the stroma (**d**). Periodic acid-Schiff, bars = 50 µm

trophozoite and a dormant cyst. Encystment is the major factor accounting for the severity of *Acanthamoeba* infections. The first published reports of *Acanthamoeba* keratitis appeared in the 1970s; it remains unclear whether earlier cases had gone undiagnosed [103]. In a retrospective study of host corneal tissue after therapeutic keratoplasty from 1955 to 1970, no case of *Acanthamoeba* was identified, suggesting that this may be a new infectious entity [104].

Epidemiology

The estimated annual incidence is 0.14 per 100,000 [105]. Contact lens wear is a recognised risk factor, but cases in non-contact lens wearers are also reported [105].

Clinical Features

Clinically, severe pain is a typical feature. *Acanthamoeba* keratitis can present as a superficial epithelial disease – often confused with HSV keratitis – anterior stromal infiltrates, disciform keratitis, keratoneuritis, and ring infiltrate. Anterior chamber reaction is rare (Fig. 3.12c).

Histopathology

Acanthamoeba cysts can remain in corneal tissue for an extended period of time following keratitis (in one study up to 31 months even following anti-amoebic treatment) and they may cause persistent corneal and scleral inflammation in the absence of active amoebic infection [106]. Gram, Giemsa, and haematoxylin-eosin stains

do not stain *Acanthamoeba*, making detection of this organism difficult. Histopathological studies have demonstrated both trophozoites and cysts (Fig. 3.12d) using methenamine-silver, periodic acid-Schiff, Masson's trichrome, and iron-haematoxylin-eosin stains [107, 108]. In addition, trophozoite and cyst forms in paraffin-embedded corneal tissue sections can be rapidly and differentially stained with calcofluor white. Under the fluorescence microscope, the trophozoites are bright red-orange and cyst cell walls fluoresce bright apple-green with red-orange cytoplasm. Retrospective identification is possible by destaining haematoxylin-eosin-stained sections. Digesting corneal tissue with trypsin or collagenase and hyaluronidase solutions helps to more readily identify trophozoites [107–109].

Histopathological findings in corneal specimens with intractable *Acanthamoeba* keratitis include epithelial denudation and variable degrees of necrosis, inflammation, and cysts or trophozoites of *Acanthamoeba* within the stroma. No neovascular vessels were found in the stroma despite long-standing corneal inflammation [110]. A granulomatous reaction with many multinucleated giant cells, some with engulfed cysts of *Acanthamoeba*, can be present in the posterior corneal stroma and anterior chamber along Descemet's membrane [111].

Corneal Microsporidiosis

Definition

Microsporidia are ubiquitous, obligate intracellular spore-forming protozoan parasites.

Etiology

Microsporidia infections of the cornea typically involve immunocompromised hosts or follow injury, but have been reported in healthy contact lens wearers [112, 113]. Ocular disease is typically transmitted by direct inoculation.

Clinical Features

Most patients present with a punctate epithelial keratoconjunctivitis with small foci of anterior stromal infiltrations [114]. Hyphaema and necrotising keratitis have been reported.

Histopathology

Diagnosis requires demonstration of oval *Microsporidia* spores in specimens obtained by superficial corneal scraping or corneal and conjunctival biopsy. Spores stain Gram-positive and may show a periodic acid-Schiff positive body at one end of an oval spore. Staining is variable with routine methods such as Giemsa, Gomori silver, or Ziehl-Neelsen acid-fast staining. Calcofluor white and modified trichrome stains are preferred. Electron microscopy readily reveals the characteristic coiled tubules within the spore coat of *Microsporidia* [113, 115].

3.5 Injuries and Surgery

3.5.1 Chemical and Thermal Injury

3.5.1.1 Chemical Injury

Definition

Chemical injury to the ocular surface can be acidic, alkaline, or toxic.

Histogenesis

In alkali injury, hydroxyl ions rapidly advance through ocular tissues causing saponification of cellular membranes with massive cell death and extensive hydrolysis of the corneal extracellular matrix. Acidic compounds precipitate proteins within the ocular surface epithelium, thus acting as a partial barrier to further penetration. However, strong acids can overcome these precipitated proteins and progress through tissue much as alkali. Toxic agents include a wide variety of chemicals that are destructive to biological tissue, but are not particularly acidic or alkaline.

Epidemiology

Industrial accidents are far more common than domestic accidents despite mandatory preventative measures, especially in developing countries.

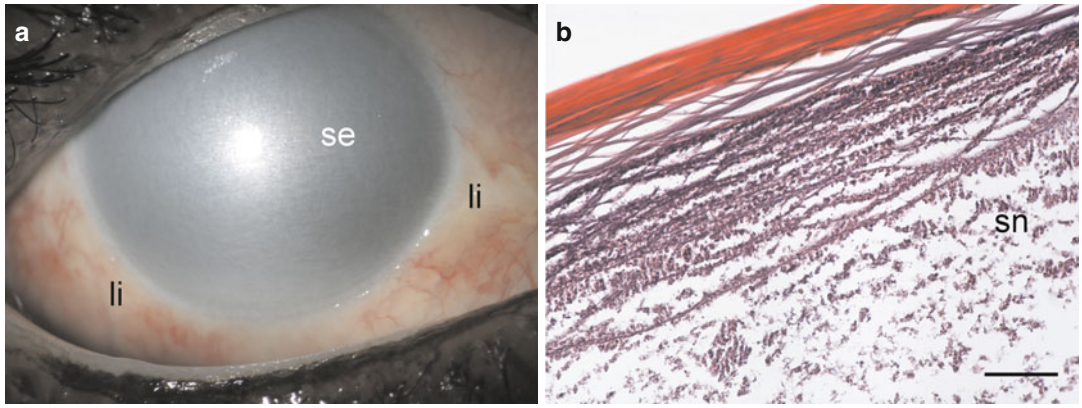

Fig. 3.13 Chemical injury. Severe alkali burn with limbal ischemia (*li*), complete loss of corneal epithelium, and severe stromal edema (*se*) of the cornea (**a**). Histopathology 12 weeks after severe alkali burn. Loss of epithelium, stromal inflammation, and stromal necrosis (*sn*) that is nearly complete (**b**). Haematoxylin-eosin, bar = 100 µm

The majority of chemical trauma affects males and is mild [116].

Clinical Features

Depending on the strength of the chemical, epithelial defects, corneal stromal opacity with melting and secondary infection, and perilimbal ischemia, necrosis or both with subsequent limbal stem cell insufficiency can occur (Fig. 3.13a). Penetration of the chemical into the anterior chamber may result in secondary glaucoma through prostaglandin release or scarring of the outflow channels, hypotony through necrosis of the ciliary body, mydriasis, cataract, and even phthisis bulbi.

Typically, a severe fibrinous inflammatory reaction develops in the anterior segment of the eye that is not necessarily time limited. Externally, the inflammation can lead to major conjunctival scarring with symblepharon formation.

Histopathology

Concentrated alkali strips the cornea of vital cells and glycosaminoglycans, leaving behind acellular, denatured collagen framework (Fig. 3.13b). Inflammatory mediators are released that are chemotactic to neutrophils [117], which release leukotrienes and cause further tissue damage through a respiratory burst. Interleukin (IL-1 alpha and IL-6) levels are markedly elevated in the regenerating corneal epithelium during the early stages of an alkali burn and may play an important role in associated corneal damage and repair [118]. Collagenase production by the epithelium, leucocytes, and fibroblasts results in corneal ulceration [119]. Fibroblasts that invade the cornea after severe alkali burn to promote healing are immature. Ascorbate deficiency following chemical injury further restricts the stromal repair process.

Prognosis

Factors influencing final outcome are (1) corneal and conjunctival surface injury, repair, and differentiation, (2) corneal stromal matrix injury, repair and ulceration, and (3) corneal inflammation [120]. Therapy depends on prompt irrigation and removal of the chemical, promoting re-epithelialisation, preventing corneal ulceration, and controlling inflammation. Even without limbal ischemia, secretion of new basement membrane and epithelial readhesion may be delayed [121]. Early surgeries may include removal of necrotic tissue, amniotic membrane transplantation, and tenoplasty. In complete limbal stem cell insufficiency, limbal autograft or allograft transplantation or limbokeratoplasty is performed later [120].

3.5.1.2 Thermal Injury

Definition

Thermal injury usually is less severe than chemical assaults to the cornea, possibly because the

contact with the heat is generally of lesser duration.

Clinical Features

Thermal injury will coagulate corneal epithelium, which becomes opaque and may slough off. The stroma beneath usually remains clear in the acute phase.

A special instance is thermal damage to the corneoscleral wound during phacoemulsification ("phakoburn") that may result in difficulty with wound closure and lead to wound leakage, damage to the adjacent corneal stroma and endothelium, fistula formation, and high degrees of postoperative astigmatism [122].

Histopathology

The primary effect of thermal energy on the corneal stromal layer is on the collagen matrix. A reversible contraction, seen clinically as corneal striae, is followed by irreversible collagen damage, including lysis of the interhelix covalent bonds and triple helix destruction of the collagen fibrils [122].

3.5.1.3 Gas Injuries

Exposure to tear gas or other gaseous irritants may cause epithelial defects, which heal without sequelae. High concentrations of gaseous substances may cause corneal necrosis.

Etiology

Sulphur mustard gas injuries, mostly suffered during chemical warfare, have been studied extensively. Sulphur mustard is a vesicant agent with severe irritating effects on many tissues.

Clinical Features

Ocular involvement is seen in 75–90 % of individuals exposed to sulphur mustard. Most cases resolve uneventfully; however, a minority of exposed patients will have either a persistent smouldering inflammation (chronic form) or late-onset corneal lesions appearing many years after a variable "silent" period (delayed form) [123]. Corneal signs after mustard gas injury include corneal scars or opacities, limbal stem cell insufficiency, epithelial defects and irregularities, corneal neovascularisation, and secondary degenerative changes, including lipid and amyloid deposition [124].

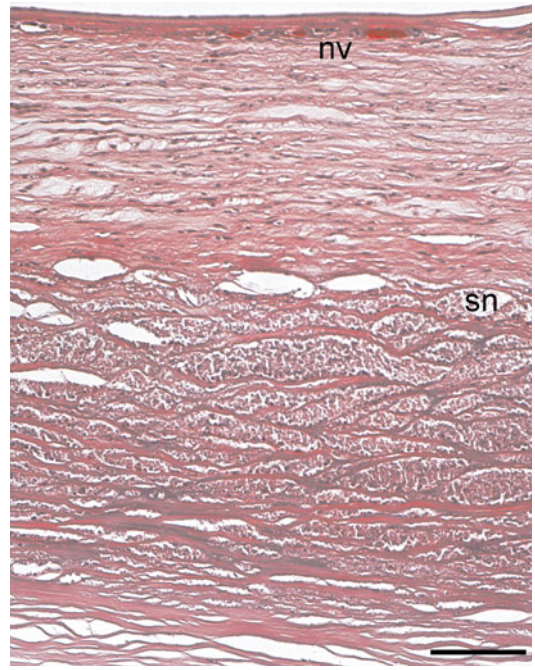

Fig. 3.14 Mustard gas injury. Absence of corneal epithelium, thickened epithelial basement membrane, destroyed Bowman's layer, fibrovascular pannus, superficial neovascular vessels (*nv*), and massive stromal necrosis (*sn*) 13 years after exposure to sulphur mustard (Courtesy of Dr. Miriam Richter, Charité-Campus Benjamin Franklin). Haematoxylin-eosin, bar = 100 µm

Histopathology

Excised corneal buttons after keratoplasty for sulphur mustard injury (Fig. 3.14) disclose absence or irregular epithelium, thickened epithelial basement membrane, destroyed Bowman's layer, fibrovascular pannus, stromal necrosis with chronic inflammation, stromal scarring with keratocyte loss, amyloid deposition, and neovascularisation [124–126].

3.5.2 Physical Injury

Physical injury to the cornea can have potentially devastating effects on the integrity of the globe and on vision. Blunt trauma including corneal

abrasion and corneal foreign body must be discriminated from sharp injuries, i.e. penetrating or perforating corneal injury.

3.5.2.1 Blunt Trauma

Corneal Abrasion Including Recurrent Erosion Syndrome

Definition

Traumatic partial or complete loss of the corneal epithelium is one of the most common ocular injuries.

Etiology

Tangential impact from foreign bodies, including fingernail, paper, plants, or brushes, is the most common cause of corneal abrasion. Recurrent erosion syndrome usually follows a scraping caused by organic material, such as paper or fingernail.

Histogenesis

Full-thickness corneal epithelial defects rapidly heal from the periphery toward the centre via a combination of migration of polygonal cells and proliferation of newly formed basal cells. Keratocyte apoptosis beneath an epithelial debridement wound is thought to be an initiating event in wound healing [127].

Clinical Features

Although patients with traumatic corneal erosions are less likely to have recurrent disease than patients with basement membrane dystrophy, up to 46 % of patients may be symptomatic 4 years following injury [128]. Recurrent erosion syndrome is characterised by repeated episodes of sudden onset of pain usually at night or upon awakening, accompanied by redness, photophobia, and epiphora. These symptoms are related to corneal de-epithelialisation in an area in which the previously injured epithelium is weakly adherent [129].

Histopathology

When scraped loosened sheets of corneal epithelium from corneal epithelial wounds in patients with posttraumatic recurrent erosion syndrome are examined, a defect in collagen fibrils that anchor the epithelial basement membrane to Bowman's layer is detected. Hemidesmosomes do not seem to be impaired [130]. Recurrences were associated with upregulation of matrix metalloproteinase-2 and -9 in the tear fluid [131].

Prognosis

In the majority of cases, management of the acute episode by patching, cycloplegics and topical antibiotic ointment with prophylactic application of gels during daytime and ointment at night prevents further erosion. In a minority of patients these measures prove insufficient and they may need alternative treatment modalities including doxycycline and corticosteroids, therapeutic contact lens wear, anterior stromal puncture, superficial keratectomy, and, most effectively, excimer laser therapy (phototherapeutic keratectomy) [129, 132].

Severe Blunt Trauma

Severe corneal contusion insufficient to rupture the globe may result in a transient ring-shaped corneal edema [133] and rupture of Descemet's membrane.

Etiology

Obstetric forceps and vacuum extraction injuries are classic examples of severe blunt trauma with Descemet's rupture. Complete corneal rupture is uncommon following blunt trauma, unless predisposing factors such as keratoconus, pellucid marginal degeneration, Terrien's marginal degeneration, or prior corneal surgery are present [134, 135]. The rupture may occur at the point of application of the pressure but, more frequently, is of the countercoup type.

Histopathology

Histology of ring-shaped corneal edema after blunt trauma may demonstrate focal, deep stromal lamellar disruption and endothelial cell damage surrounding the injury site [136]. Especially in young individuals who have a thin Descemet's membrane, its rupture may lead to acute corneal

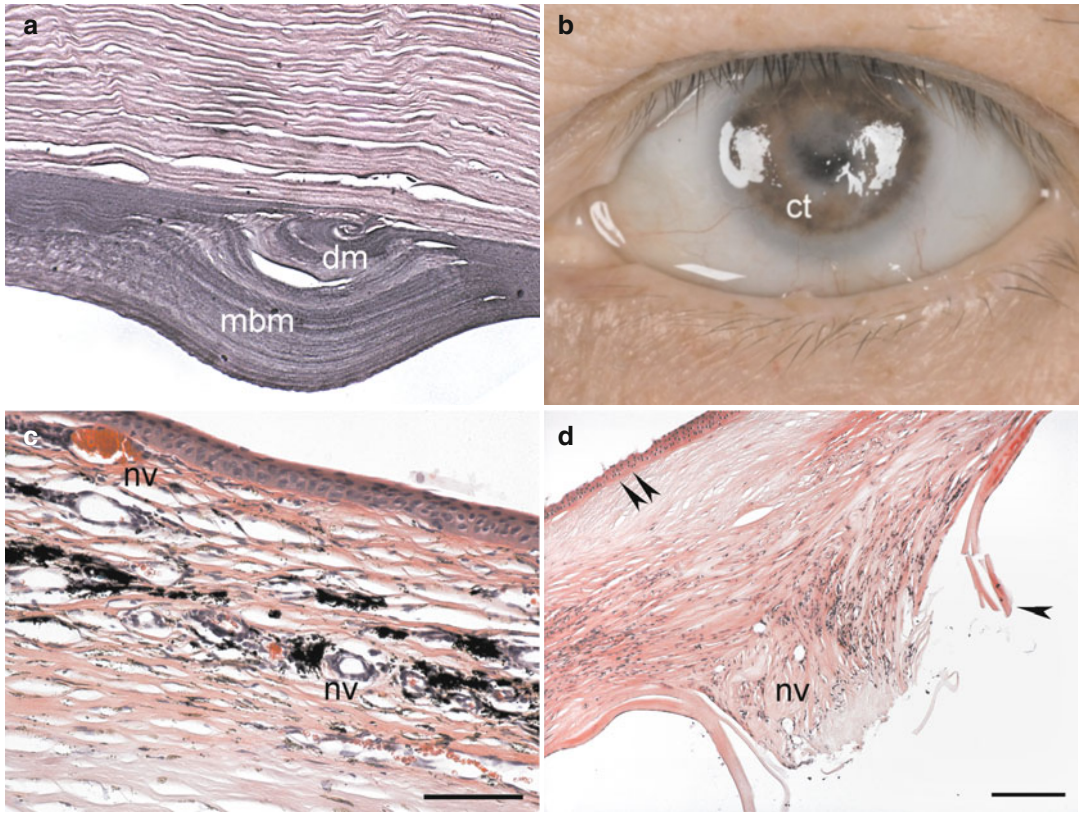

Fig. 3.15 Physical corneal injury. Blunt injury from obstetrical forceps delivery. Corneal specimen of 51-year-old patient with coiled Descemet's membrane (*dm*) within a thick deposit of multilaminar basement membrane (*mbm*) with only few attenuated endothelial cells (**a**; Courtesy of Dr. Irene Pecorella, University of Rome). Corneal tattooing (*ct*) of a leucoma from perforating ocular injury (**b**). Corneal tattooing in a specimen with scar and neovascular vessels (*nv*) within the corneal stroma as evidenced by clumps of brown-black granules within the anterior corneal stroma within the cytoplasm of keratocytes and in the extracellular matrix (**c**). Severe perforating corneal injury with loss of Bowman's layer (*double arrowhead*), irregular stroma, a break in Descemet's membrane (*arrowhead*) with complete endothelial cell loss, and neovascular vessels (*nv*) in a posterior scar (**d**). Periodic acid-Schiff, bar = 50 μm (**a**), haematoxylin-eosin, bar = 100 μm (**c**), and bar = 200 μm (**d**)

swelling and cellular infiltration. However, healthy endothelium is able to heal such ruptures by migrating over the area of retracted Descemet's membrane, usually over 3 months. Recurrences of the edema may occur even years later in the area of injured endothelium [137].

After obstetric forceps injury, histopathology shows (1) large tears of Descemet's membrane with a fragment of Descemet's membrane extending into the anterior chamber at one end of the tear and scroll formation at the other end, (2) scrolls of Descemet's membrane at each margin of the original break, (3) small breaks in Descemet's membrane and healing by fibrosis, and (4) a small break in Descemet's membrane with minimal fibrosis (Fig. 3.15a). Scanning electron microscopy reveals folds in Descemet's membrane and attenuation or absence of endothelium. Spindle- and stellate-shaped cells and pigment granules are present in the area of the tear in most cases [138]. In addition, epithelial-like metaplasia of endothelial cells in the area of rupture may be noted [139].

3.5.2.2 Sharp Injury

Lacerations, punctures, surgical incisions, and foreign bodies can produce penetrating and perforating injuries of the cornea.

Penetrating Wounds

Penetrating wounds that do not perforate the cornea are often caused by foreign bodies. Superficial wounds may heal by proliferation of epithelium dipping down into the defect. Healing of deeper wounds will additionally involve keratocytes recruited from adjacent stroma.

Corneal Tattooing

Definition

Corneal tattooing to reduce glare following traumatic loss of iris and tattooing of corneal leucoma for cosmetic purposes are typical examples of surgically induced penetrating corneal wounds (Fig. 3.15b) [140]. A plethora of techniques and instruments to apply the dye to the anterior corneal stroma exist. India ink, metallic colours, organic dyes, and uveal pigment from animal eyes are used.

Histopathology

Keratocytes can actively ingest and retain tattooing particles of non-metallic dyes within their cell membrane for very long periods of time. Histologically, clumps of brown to black granules are present mainly in the midstroma (Fig. 3.15c). By electron microscopy, numerous round and oval electron-dense particles are seen in the cytoplasm of keratocytes, arranged as clusters or patches. No granules are detected in the extracellular matrix [141].

Prognosis

Complications such as toxic reaction, iridocyclitis, persistent corneal epithelial defects, and corneal ulceration as well as granulomatous keratitis have been reported following corneal tattooing [142].

Perforating Corneal Wounds

Perforating corneal wounds that penetrate into the eye typically lead to corneal scar formation and endothelial cell loss, which correlates closely with wound length [143].

Lacerations

Lacerations are typically induced by sharp cutting objects. Whereas shelved (oblique) incisions tend to close spontaneously, vertical (perpendicular) lacerations open spontaneously and require suture repair. Typically, lacerations are associated with loss of the anterior chamber and incarceration or prolapse of the iris. Ciliary body and lens can also prolapse (Fig. 3.15d)

Puncture Wounds

Puncture wounds result from thorns or tiny sharp instruments. The wound itself is small and heals promptly. However, damage to the intraocular structures such as cataract after lens injury as well as endophthalmitis can complicate the course.

Surgical Wounds

Surgical wounds have a lot in common with corneal lacerations. They show clean, sharply incised edges. With the exception of keratoplasty, they are typically located at the corneoscleral limbus. Modern small-incision intraocular surgery and advanced suturing techniques have reduced the risk of surgical wound dehiscence.

Wound Healing After Corneal Perforating Injury

Histogenesis

Following perforating corneal injury, a fibrin plug forms at the posterior wound. Transforming growth factor beta-2 (TGFβ2) is released by the corneal epithelium into the stroma as soon as its basement membrane is destroyed [144]. Bowman's layer has no capacity to regenerate. Corneal stromal edema develops during the first hour after injury. Thereafter, fibroblast repair tissue originating from corneal stromal keratocytes and histiocytes fills and seals the wound.

Histopathology

Even after many months of healing, collagen remodelling in corneal scar tissue is not complete. Collagen interweaving, lack of a lamellar structure, and enlarged, disordered fibrils are visible by electron microscopy [145, 146]. Descemet's membrane curls after the initial injury, and endothelial cells from wound margins

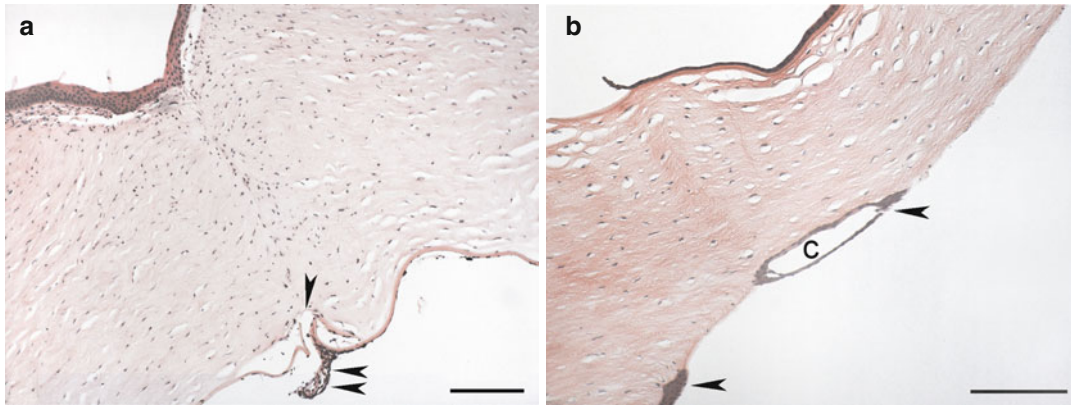

Fig. 3.16 Surgical corneal wounds. Penetrating corneal wound after perforating keratoplasty with deranged stromal lamellar structure, curling and duplication of Descemet's membrane (*arrowhead*), endothelial cell loss, and adhesion of iris stroma (adherent leucoma; *double arrowhead*) to the posterior edge of the wound (**a**). Epithelial ingrowth after lamellar keratoplasty. Multilayered corneal epithelium (*arrowheads*) with cyst (*c*) formation is present on the posterior surface of the graft corresponding to the lamellar interface (**b**). Haematoxylin-eosin, bar = 100 µm (**a**) and bar = 200 µm (**b**)

extend across the defect and lay down new basement membrane (Fig. 3.16a).

Epithelial downgrowth

Definition

Epithelium may show ingrowth into a corneal wound in the beginning of the healing response, but it is normally displaced to the surface level with time. However, incarcerated epithelial islands or cysts may remain within the stroma. If the wound leaks, the epithelium may even grow through a full-thickness corneal wound into the anterior chamber to line the endothelial surface, extending to the anterior chamber angle and iris surface (epithelialisation of the anterior chamber). Occasionally, the ingrowth may form a cyst.

Clinical Features

Clinically, epithelial ingrowth can cause glaucoma, fistula formation, retrocorneal membranes, uveitis, iris cysts, bullous keratopathy, and corneal graft failure. It can present decades after initial injury [147]. Although rare with modern surgical techniques, the incidence of epithelial ingrowth has increased again after introduction of lamellar corneal surgical techniques.

Histopathology

Analysis of 207 consecutive cases of epithelial ingrowth showed that it was cystic in 40 cases and diffuse in 167. Interestingly, it was not suspected prior to histopathological examination in 36 % of cases. It was mainly caused by penetrating injury, cataract surgery, and penetrating keratoplasty. Histologically a multilayered surface epithelium was present on intraocular surfaces such as the cornea, iris, chamber angle, ciliary body, and lens capsule (Fig. 3.16b) [148].

3.5.3 Postsurgical Pathology

3.5.3.1 Corneal Collagen Cross-Linking

Definition

Corneal collagen cross-linking using ultraviolet light (UVA) and the photosensitiser riboflavin was originally introduced to prevent progression of corneal ectasia in keratoconus [149]. Animal and human studies show a significant increase in corneal rigidity by approximately 70 % [150].

Histopathology

Analysis of human corneas following cross-linking demonstrates a significant increase in collagen fibre diameter in the anterior stroma.

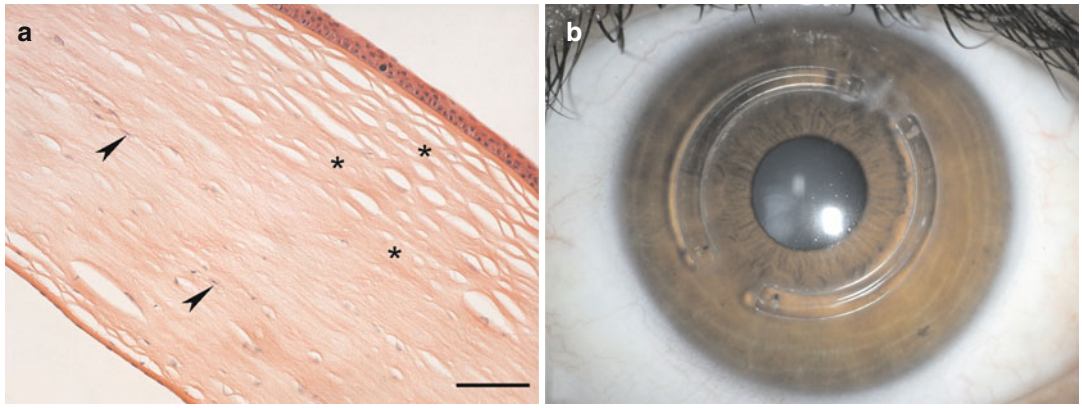

Fig. 3.17 Postsurgical corneal pathology. Histopathology of corneal collagen cross-linking for progressive keratoconus. Loss of keratocyes (*arrowheads*) from the anterior and middle layers (*asterisks*) of the corneal stroma (**a**). Intrastromal corneal ring segments implanted for progressive keratoconus (**b**). Haematoxylin-eosin, bar = 100 μm

Keratocyte proliferation was increased 6 months following cross-linking as evidenced by increased Ki-67 immunopositivity [151]. A considerable keratocyte loss in the anterior and midstroma of the central and peripheral cornea (Fig. 3.16) was present even 30 months postoperatively [152]. Keratocyte differentiation into myofibroblasts does not seem to play a crucial role in the postoperative flattening of the cornea [151, 152] (Fig. 3.17a).

3.5.3.2 Intrastromal Ring Implants

Definition

Intrastromal corneal ring segments are polymethyl methacrylate (PMMA) corneal implants for the correction of low to moderate myopia. They are also used for the treatment of corneal ectasia in keratoconus or after laser in situ keratomileusis (LASIK) to prevent or delay the need for a corneal transplant (Fig. 3.17b) [153].

Histopathology

In rabbit models, new collagen formation with lamellar organisation and increased keratocyte density are observed adjacent to the implant [154]. Weeks and months after implantation in humans, lamellar channel deposits consisting of intracellular lipids occur around the implants without alteration of optical performance [153]. Histopathology of a cornea following intrastromal ring segment implantation for corneal ectasia after LASIK showed peripheral focal thickened areas around the implant channel. Adjacent collagen lamellae were displaced. The stroma around the segment stained with periodic acid-Schiff stain. On electron microscopy, the stroma contained deposits of electron-dense granular material with interspersed empty spaces. Overlying the implants, a small area of epithelial hypoplasia was present [155].

Prognosis

Spontaneous extrusion of intrastromal ring segments has been reported. Rare complications necessitating removal of implants include keratitis, stromal necrosis, and corneal melting [156].

3.5.3.3 Radial Keratotomy (RK)

Definition

Incisional procedures to alter refraction by weakening corneal structure and by producing surface gaps to increase anterior corneal surface volume. Near full-thickness radial incisions known as radial keratotomy (RK) are used for correction of myopia (Fig. 3.18a). The greater accuracy and precision of photorefractive keratotomy (PRK) and laser in situ keratomileusis (LASIK) have diminished the role of RK in refractive surgery.

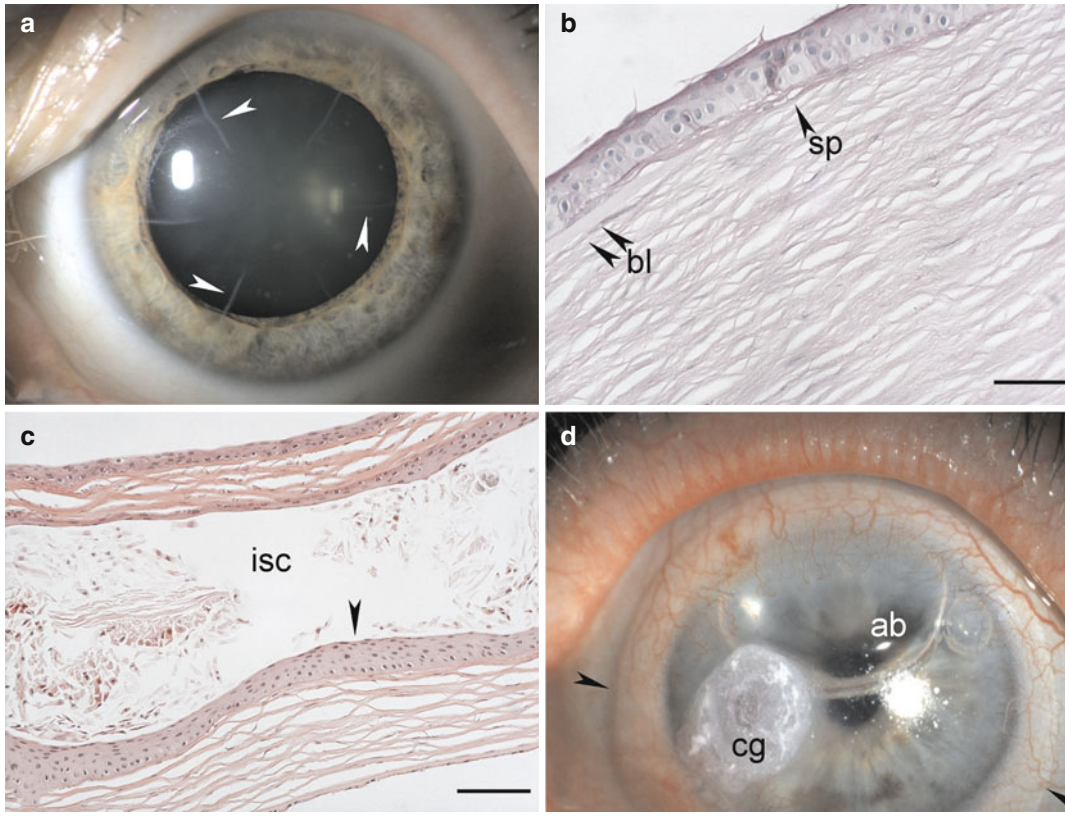

Fig. 3.18 Postsurgical corneal pathology. Radial keratotomy cuts (*arrowheads*) for progressive keratoconus (**a**). Histopathology after phototherapeutic keratectomy. Loss of Bowman's layer (*bl*) within the ablated area that shows a nonvascularised subepithelial pannus (*sp*) instead (**b**). Histopathology following complicated laser in situ keratomileusis (LASIK). Epithelial ingrowth (*arrowhead*) into the flap interface with intrastromal cyst (*isc*) formation (**c**). Tissue adhesive (*cg*; cyanoacrylate glue) with a contact lens (*between arrowheads*) and an intraocular air bubble (*ab*) to seal a descemetocele (**d**). Periodic acid-Schiff, bar = 50 µm (**b**), and haematoxylin-eosin, bar = 100 µm (**c**)

Histopathology

Animal studies have shown that healing of RK incisions by wound fibrosis is accomplished by transformation of adjacent keratocytes to myofibroblasts, eventually leading to stromal wound contraction [157]. In humans, many incisions retain epithelial plugs. Underneath these plugs, the epithelial-stromal interface is characterised by three adjacent zones: a duplicated basement membrane complex, a zone that resembles Bowman's layer, and a zone in which the collagenous fibres are oriented parallel to the plugs. Scar tissue orientation is transverse at the base of the plug and sagittal in deeper wound regions [158, 159].

Prognosis

Variability in wound healing responses and incomplete wound healing may be responsible for postoperative complications. The risk of corneal rupture at the incision sites after minor blunt trauma is increased after RK [160, 161].

3.5.3.4 Epikeratoplasty

Definition

Epikeratoplasty was originally performed for aphakia, keratoconus, and myopia. The procedure includes suturing a commercially cryolathed corneal-derived lenticule (epikeratophakos) with a specific dioptric power onto de-epithelialised

central cornea. Epikeratoplasty is rarely performed today.

Histopathology

Human corneas after epikeratoplasty show thickened epithelium, bends and fractures in Bowman's layer, interface epithelial ingrowth and cyst formation, absence of keratocytes and stromal abnormalities in the lenticule, and abnormal host keratocytes in the recipient lamellar bed [162–165]. The interfibrillar collagen distance of the lenticule was increased compared with that of the host cornea. The central thickness of the lenticule increased the total corneal thickness by 56 % [163].

3.5.3.5 Photoablative Refractive Surgery with Excimer Laser

Phototherapeutic and Photorefractive Keratectomy

Definition

The excimer laser, which uses ultraviolet radiation (193 nm), is applicable to both phototherapeutic (PTK) and photorefractive (PRK) keratectomy.

Histopathology

In both procedures, the corneal epithelial cells with their basement membrane, Bowman's layer and the anterior stroma are disrupted. Re-epithelialisation typically occurs within 24–48 h, followed by subepithelial synthesis of new collagen, reorganisation of the epithelium, production of type VII collagen (a major component of anchoring fibrils), proliferation of reactive keratocytes, and increase in clinically visible subepithelial haze that decreases within 6 months [166, 167]. Between 6 and 15 months, the epithelium is thicker than normal, Bowman's layer remains absent, and superficial stromal scarring with an increase in the number of keratocytes has developed in the area of ablation (Fig. 3.18b). Ultrastructural studies show that the epithelial basement membrane has focal discontinuities. The stroma underlying and surrounding the scar remains normal [168].

Laser In Situ Keratomileusis

Definition

In laser in situ keratomileusis (LASIK), a mechanical microtome or a femtosecond laser is used to create a hinged corneal flap that is 120–180 μm in thickness and has a diameter of 8–10 mm. The flap is lifted, and excimer laser ablation of the corneal stromal bed is performed. Finally, the flap is repositioned without sutures.

Clinical Features

LASIK provides advantages compared to photorefractive keratectomy (PRK) including no significant central corneal haze, faster visual recovery, less postoperative discomfort, and less myopic regression [169]. Unlike after incisional refractive surgery, eyes that have undergone LASIK do not have an increased risk for globe rupture compared to normal eyes [161]. Corneal ectasia is a devastating complication after LASIK and, less frequently, after PRK.

Histopathology

In animal studies, apoptosis of keratocytes occurs 1 day after LASIK in a zone approximately 50 μm anterior and posterior to the lamellar flap incision [170]. Proliferation, migration, and differentiation of keratocytes into myofibroblasts and inflammatory cell infiltration are observed during the following 3 months [171, 172].

Histopathology of human corneas obtained at autopsy 2 months to 6.5 years after uncomplicated LASIK showed focal epithelial hypertrophic modifications, focal undulations in Bowman's layer, and a variably thick lamellar stromal interface scar in all specimens with variable degrees of epithelial ingrowth at the peripheral wound. The flap wound margin, which was adjacent to the epithelium, healed by producing an approximately 8-μm-thick hypercellular fibrotic stromal scar, whereas the central and paracentral wound regions healed with a thinner hypocellular primitive stromal scar. The stroma contained eosinophilic deposits, periodic acid-Schiff-positive, electron-dense granular material

interspersed with randomly ordered collagen fibrils, increased spacing between collagen fibrils, and widely spaced banded collagen. Immunofluorescence microscopy identified increased type III collagen and myofibroblasts in the hypercellular fibrotic scar regions and decreased or absent amounts of all corneal stromal components other than type I collagen in the hypocellular primitive scar regions [173, 174].

Prognosis

Intrastromal epithelial ingrowth with or without cyst formation can occur after LASIK (Fig. 3.18c). Histopathological and ultrastructural findings in cases with corneal ectasia following refractive surgery include epithelial hypoplasia, breaks in Bowman's layer, stromal thinning in the ectatic region, and a thin residual stromal bed. Studies suggest that interfibre fracture with interlamellar and interfibrillar biomechanical slippage occurs as is also seen in keratoconus [175].

During the immediate postoperative period, flap displacement and both micro- and macrostriae may occur. Traumatic displacement of the LASIK flap has been reported as a late complication and can predispose to diffuse lamellar corneal inflammation [176, 177].

3.5.3.6 Tissue Adhesive

Definition

Tissue adhesives are used to strengthen or seal ulcerating and perforated corneas.

Clinical Features

Corneal gluing appears to decrease the number of inflammatory cells in the stroma surrounding ulcerations and perforations (Fig. 3.18d). Application of tissue adhesive to sterile ulcers prevents further stromal loss [178].

Histopathology

Effects of surgical adhesives in the rabbit cornea included neovascularisation and a noticeable inflammatory response surrounding cyanoacrylate adhesive [179].

3.5.3.7 Conjunctival Flap

Definition

Creation of a conjunctival flap for the treatment of chronic, non-healing corneal ulceration especially in eyes with poor visual potential was described by Gunderson in the late 1950s and has become a standard procedure [54]. A pedunculated flap of bulbar conjunctiva is mobilised and secured with sutures over the cornea.

Histopathology

The integrity of the globe is successfully maintained in most eyes, but retraction or dehiscence of the flap with re-exposure of the cornea, infection, progression of the inflammation beneath the flap, loss of the flap from epithelial ingrowth, and epithelial cyst formation have been described [180].

3.5.3.8 Amniotic Membrane Transplantation

Definition

Amniotic membrane transplantation is used increasingly to treat persisting epithelial defects, corneal ulcers, and alkali burns. Amniotic membrane is the innermost avascular layer of the placenta and consists of a monolayer of cuboidal epithelium, a basement membrane, and a stromal layer [181].

Clinical Features

Used as a graft, amniotic membrane is intended to provide a new basement membrane for corneal epithelial cells (Fig. 3.19a). Used as a biological shield, growth of new corneal epithelium is promoted by growth factors released beneath the amniotic membrane.

Histopathology

Histological evidence confirms that an amniotic membrane can be integrated into the corneal surface and can persist for months in one of four patterns: (1) intraepithelial, (2) subepithelial (Fig. 3.19b), (3) intrastromal with various grades of retraction, and (4) superficial (disintegrated)

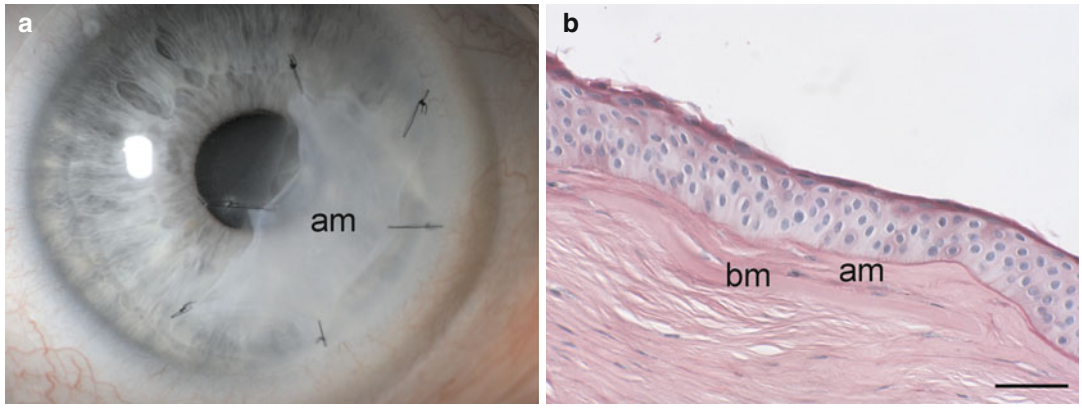

Fig. 3.19 Amniotic membrane transplantation. Amniotic membrane (*am*) graft for persistent corneal trophic ulcer (**a**). The amniotic membrane (*am*) graft is integrated into the cornea subepithelially. Note loss of Bowman's layer (*bl*) centrally and the subepithelial pannus that replaces it (**b**). Periodic acid-Schiff, bar = 50 μm

[182]. Firm adhesion between the amniotic membrane and corneal epithelial cells is established by newly formed basement membrane, interdigitating microvillous cell processes, and formation of desmosomes and gap junctions [182–184]. Transformed corneal stroma-derived cells migrate from the anterior stroma through breaks in Bowman's layer into the connective tissue of the amniotic membrane, integrating the membrane with corneal tissue and allowing healing of the corneal stroma [185].

3.5.3.9 Limbal Stem Cell Transplantation

Definition

Reconstruction of the ocular surface in patients with limbal stem cell insufficiency (LSCI) and subsequent conjunctivalisation of the corneal surface remains challenging. The objective of limbal stem cell transplantation is to restore the corneal surface with normal corneal epithelium.

Clinical Features

In unilateral total LSCI, a limbal autograft from the healthy eye is transplanted in order to prevent an immune rejection. In bilateral, total LSI a cadaver or a living limbal allograft from a relative is used for transplantation followed by systemic immunosuppression [186].

Histopathology

Rabbit corneas showed a decrease in corneal vascularisation after surgical removal of their limbal area and consecutive limbal transplantation and, even more importantly, a corneal phenotype of the transplant-derived regenerated epithelium [187]. Donor-derived epithelial cells were detected long term in the paracentral cornea of patients after limbal allograft transplantation [188].

3.5.3.10 Keratoplasty

Penetrating Keratoplasty

Definition

Penetrating keratoplasty (PK) refers to surgical removal of the central diseased cornea with replacement by full-thickness corneal donor tissue, usually cadaveric. It is performed for optical, tectonic, or therapeutic reasons.

Epidemiology

In clinical situations with a low risk of rejection, PK is one of the most successful transplantations, with a 10-year success rate, defined as corneal clarity, of up to 92 % without routine human leucocyte antigen (HLA) matching or systemic immunosuppression [189]. In high-risk situations such as when the cornea is vascularised, after previous grafting, or when using a large graft, success rates drop to 40–50 % [53, 190].

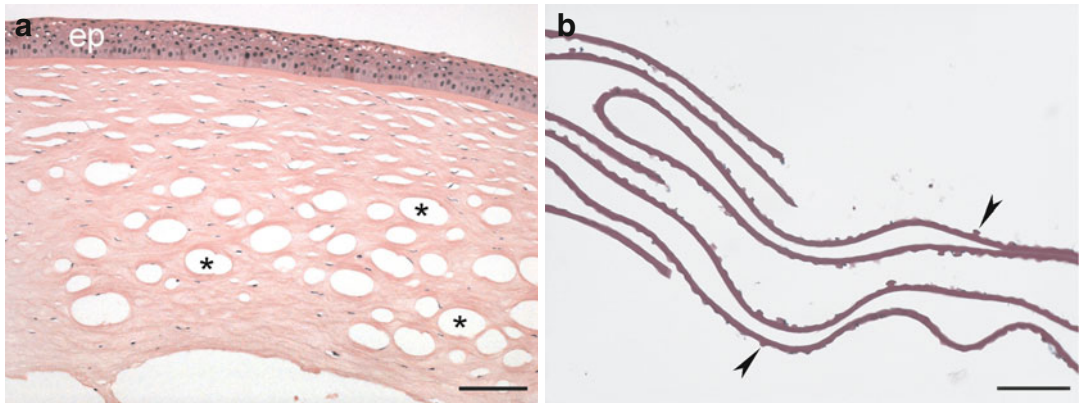

Fig. 3.20 Lamellar keratoplasty. Deep anterior lamellar dissection with intrastromal air injection. Note epithelial edema (*ep*) and massive intrastromal air emphysema (*asterisks*) related to the surgical procedure (**a**). Descemet's membrane with excrescences (*arrowheads*) and loss of endothelial cells compatible with Fuchs' endothelial dystrophy from posterior lamellar keratoplasty (**b**). Haematoxylin-eosin, bar = 100 µm (**a**), and periodic acid-Schiff, bar = 50 µm (**b**)

Histopathology

In experimental corneal graft rejection, any or all of three layers of the cornea can be involved. In epithelial rejection, congestion of limbal vessels is followed by the appearance of an elevated epithelial rejection line that migrates centrally. This type of rejection is benign. Stromal rejection can manifest as subepithelial infiltrates, which respond readily to topical steroids. Diffuse stromal rejection in combination with an endothelial rejection is observed in rabbit models, but is rare in humans [191].

Endothelial rejection with an endothelial rejection line composed of lymphoid cells, known as the Khodadoust line, will develop in approximately 20 % of KP patients [192]. Untreated, this rejection proceeds across the donor endothelium leaving damaged endothelium behind. Keratic precipitates composed of lymphoid cells and an anterior chamber reaction are typically present.

Lamellar Keratoplasty

Anterior Lamellar Keratoplasty

Definition

Anterior lamellar keratoplasty (ALK) is defined as the removal and replacement of deformed or diseased anterior corneal tissue while sparing the Descemet's membrane and endothelium. Midstromal dissection is associated with interface scarring. Therefore, deep anterior lamellar keratoplasty (DALK) with or without baring of Descemet's membrane is now preferred [193].

Clinical Features

Anterior lamellar keratoplasty is indicated for the treatment of corneas that have a healthy endothelium but have pathological changes anterior to Descemet's membrane such as anterior stromal scars or keratoconus. Various procedures have been designed to facilitate separation of the posterior stroma. Currently, the most popular is dissection by insufflated intrastromal air ("big bubble" technique).

Histopathology

Intrastromal air insufflation may complicate the histopathological workup of excised corneal tissue, which often floats in formalin (Fig. 3.20a). In one study, 58 % of corneal buttons were affected by air emphysema, 5 % by epithelial edema related to the hydrodelamination procedure that mimicked bullous keratopathy, and 1 % were lost specimens. Histopathological evidence of conus formation could not be detected in 7.4 % of DALK specimens as compared to 1.6 % of PK specimens of keratoconus [194].

Posterior Lamellar Keratoplasty

Definition

Posterior lamellar keratoplasty is the replacement of the corneal endothelium without corneal surface incisions or sutures in the management of corneal endothelial disorders. The most popular procedure is known as Descemet's stripping automated endothelial keratoplasty (DSAEK). The graft contains endothelium, Descemet's membrane, and a thin layer of donor corneal stroma. In Descemet's membrane endothelial keratoplasty (DMEK), only Descemet's membrane and endothelium are transplanted.

Clinical Features

Posterior lamellar keratoplasty is indicated for replacement of diseased or damaged endothelium such as in Fuchs' endothelial corneal dystrophy or pseudophakic bullous keratopathy. After unfolding and proper orientation of the posterior transplant, an anterior chamber air bubble is insufflated to support attachment of the graft.

Histopathology

Examination of failed grafts after DSAEK reveal attenuation of endothelial cells, fibrocellular tissue in the graft-host interface, retained Descemet's membrane, epithelial ingrowth, or a combination thereof. Decentred DSAEK grafts may have full-thickness corneal layers at one edge [195]. In addition, metaplasia of attenuated corneal endothelial cells with formation of an abnormal posterior collagenous layer may contribute to an impaired visual function despite complete graft adherence after DMEK [196]. Pathologists have to get used to seeing specimens with only Descemet's membrane and a variable number of endothelial cells. The diagnosis of endothelial disease must be established without analysing epithelial and stromal pathological features (Fig. 3.20b).

Prognosis

Early visual recovery and excellent postoperative functional results have been reported. The major complication is incomplete attachment of the graft in the early postoperative period, leading to repositioning with air bubbles. Inadvertent grafting of a partially full-thickness graft in DSAEK may lead to epithelial ingrowth between the graft and host cornea or into the anterior chamber. Causes of primary donor failure in DMEK include upside-down positioning of the graft and endothelial cell loss due to excessive surgical manipulation [197].

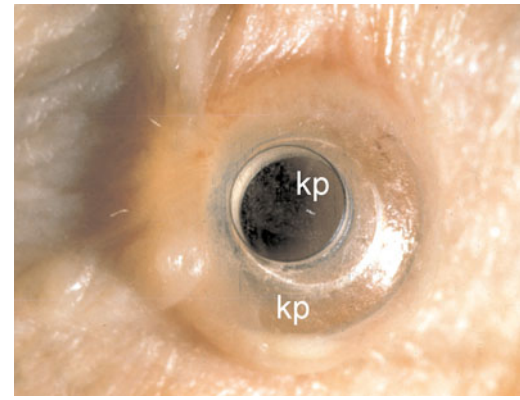

Fig. 3.21 Osteo-odonto keratoprosthesis. Keratoprosthesis (*kp*) in a patient with end-stage mucous pemphigoid. The base of the prosthesis is intrastromal

3.5.3.11 Keratoprosthesis

Definition

In patients with numerous failed keratoplasties or when keratoplasty otherwise has been deemed to be hopeless, keratoprosthesis surgery is performed (Fig. 3.21).

Clinical Features

Current approaches include an osteo-odonto-keratoprosthesis made of an osteodental lamina as a skirt for a polymethyl methacrylate (PMMA) cylinder, a hydrogel sheet with porous edges, and double-plated PMMA devices with holes for nutrition and hydration of a carrier corneal graft. Complications after keratoprosthesis surgery include surface complications, chronic inflammation, retroprosthesis membrane formation, glaucoma, endophthalmitis, and keratoprosthesis extrusion [198–200].

Histopathology

A transparent tissue layer consisting of non-keratinised squamous epithelium of corneal origin can cover the anterior surface of the keratoprosthesis representing bio-integration of the device [201].

Histopathology of failed keratoprostheses revealed invasion of the porous hydrogel keratoprosthesis by reactive fibroblasts and multinucleated foreign-body giant cells. In the area of dehiscence, thinning, and lysis of collagen fibres, infiltration by lymphocytes and plasma cells with a sheet of fibroinflammatory tissue, extending into the anterior chamber, was evident [200].

Retroprosthetic membranes occur in 25–65 % of patients with the double-plated PMMA keratoprosthesis. They represent stromal downgrowth from the host corneal stroma. These membranes grow through gaps in Descemet's membrane to reach behind the back plate and may adhere to the anterior iris surface [202]. In patients with inflammatory preoperative diagnoses, massive inflammatory cell infiltration, tissue necrosis with stromal melting adjacent to the transcorneal stem of the prosthesis and epithelial fistula formation may be observed [203].

In a case of failed osteo-odonto-keratoprosthesis, the osteodental laminae showed various degrees of transformation and resorption with associated inflammation and downgrowth of keratinising squamous epithelium [204].

Prognosis

Long-term success is good in noninflammatory situations; however, prognosis is guarded for patients with autoimmune disease such as pemphigoid, Stevens-Johnson syndrome, severe chemical burn, and uveitis [203]. When the alveolar-dental ligament is preserved in osteo-odonto-keratoprosthesis, long-term survival of the prosthesis has been reported [205, 206].

3.6 Degenerations and Dystrophies

3.6.1 Degenerations

3.6.1.1 Keratoconus and Keratoglobus

Definition

Keratoconus and keratoglobus refer to an idiopathic bilateral corneal ectasia which is conical or globular in shape, respectively.

Epidemiology

Keratoconus is the most common primary corneal degeneration with a prevalence of 1:500–1:2000 [207]. Keratoglobus is rare [208]. The diagnosis is usually made in early adulthood.

Etiology

The pathophysiology of keratoconus remains open. Both genetic and environmental factors, including rubbing of the eyes and autosomal dominant inheritance with incomplete penetrance, have been proposed and both may play a role [207, 209, 210]. Genetic mapping has identified candidate loci on chromosomes 1, 2, 3, 5, 8, 9, 13, 14, 15, 16, 20, and 21, suggesting genetic heterogeneity. Most cases are sporadic. Keratoconus is frequent in some syndromes including Down's syndrome, Marfan's syndrome, and Leber's congenital amaurosis. It is associated also with atopy and vernal keratoconjunctivitis.

Clinical Features

Keratoconus presents with regular myopic astigmatism, followed by irregular astigmatism and poor visual acuity once this cannot be adequately compensated with spectacles [211]. Progressive axial steepening and ectasia are associated with stromal thinning (Fig. 3.22a, b). Focal anterior stromal scarring at the apex of the cone, an iron line around the base of the cone (Fleischer's ring), and vertical stress lines in the stroma (Vogt's striae) are common. Descemet's membrane may eventually break leading to acute corneal swelling (hydrops).

Histopathology

The epithelium and stroma are abnormally thin at the apex of the cone (Fig. 3.2c, d) [207, 212, 213]. Descemet's membrane and endothelium are generally normal, but in more advanced cases the endothelial density may be reduced at the base of the cone, and the membrane demonstrates a break in acute hydrops (Fig. 3.22e). Later, the break is sealed by migrating endothelial cells and newly deposited basement membrane. Bowman's layer frequently has breaks that may be associated with anterior stromal scarring at the apex of the cone (Fig. 3.22f). In keratoglobus, corneal thinning is either uniform or

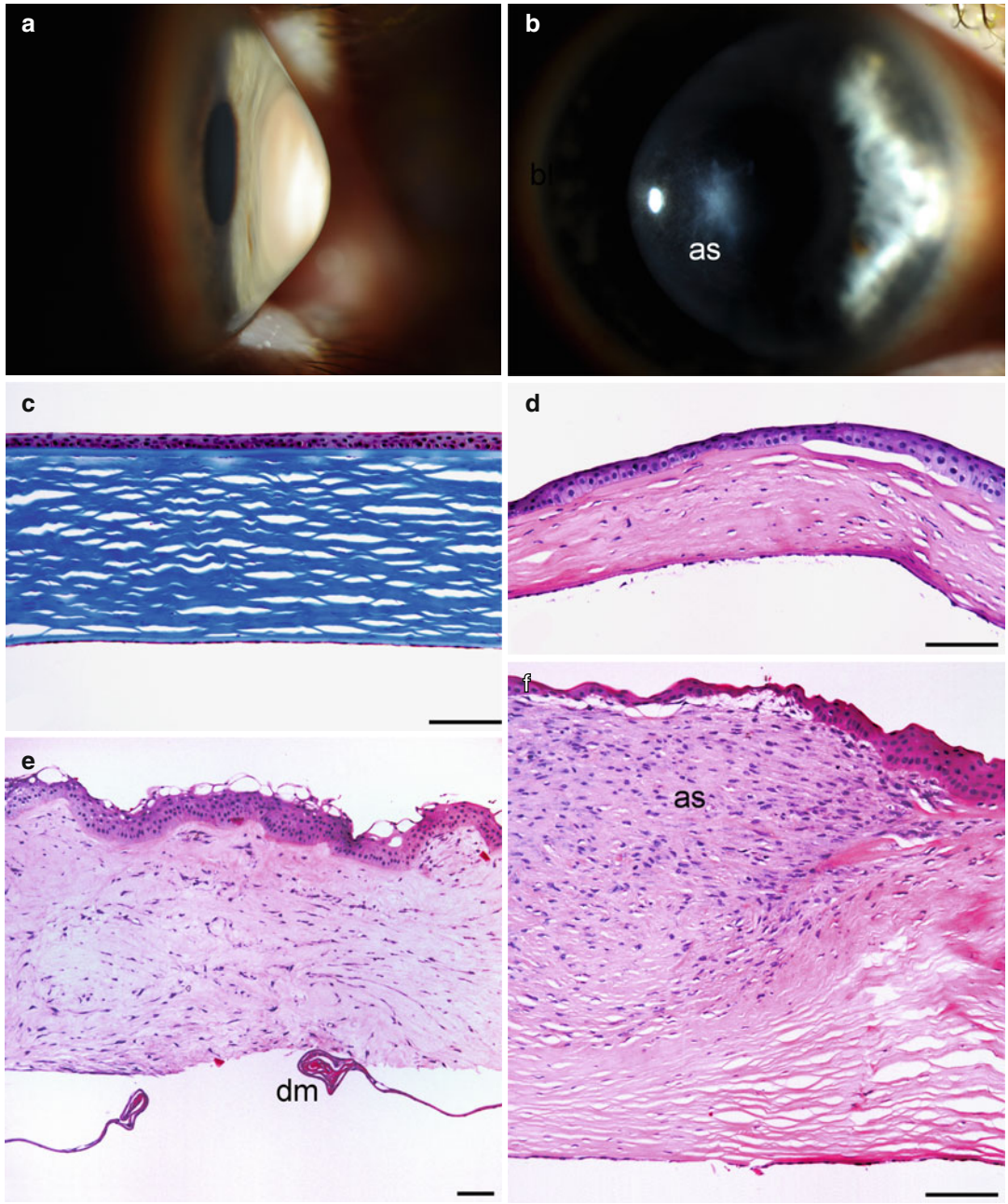

Fig. 3.22 Keratoconus. Conical ectasia of the cornea just below the optic axis (**a**). Greyish apical scar (*as*) from chronic stretching that has led to breaks in Bowman's layer and a subsequent reparative reaction (**b**). Moderate keratoconus: corneal epithelium and stroma are thinner than average (300 µm) but otherwise normal, and Bowman's layer is intact (**c**). Advanced keratoconus: Bowman's layer is destroyed at the apex of the cone, stroma is extremely thin (120 µm), and stromal lamellae are irregular from scarring (**d**). Complicated keratoconus: epithelial edema with stromal swelling (hydrops) and disorganisation after rupture of Descemet's membrane (*dm*); note curling of the ends of the ruptured membrane (**e**). Complicated keratoconus: exuberant hyperplastic apical scarring (*as*) after repeated rupturing of Bowman's layer at the apex of the cone (**f**). Masson's trichrome (**c**), haematoxylin-eosin (**d**–**f**), bars = 100 µm

circumferential, and Bowman's membrane tends to be absent [214].

Prognosis

Keratoconus is progressive but varies widely in severity. Mild cases stabilise by the age of 40 years without need for surgery. In more aggressive cases, corneal collagen cross-linking or intracorneal rings slow progression (see Sect. 3.5.3.1–3.5.3.2). Rapidly progressive cases benefit from anterior lamellar or penetrating keratoplasty, which has an excellent prognosis in keratoconus. Keratoglobus is more difficult to manage surgically.

3.6.1.2 Pellucid Marginal Degeneration

Definition

Pellucid marginal degeneration refers to a bilateral corneal ectasia located at the inferior periphery of the cornea, which is considered different from keratoconus and keratoglobus.

Synonyms

Keratotorus.

Epidemiology

A rare degeneration usually diagnosed at the age of 20–40 years.

Etiology

This degeneration is idiopathic.

Clinical Features

Pellucid marginal degeneration is asymptomatic except for progressive irregular astigmatism [215]. The thinning typically affects the inferior cornea from the 4 o'clock to the 8 o'clock meridian and is separated from the limbus by 1–2 mm of normal cornea. Corneal hydrops is very rare.

Histopathology

Light microscopic findings mimic those of keratoconus but are located in the corneal periphery and the thinning is more abrupt toward the central cornea [216]. Descemet's membrane is typically intact even when the ectasia is very advanced.

Prognosis

Pellucid marginal degeneration varies widely in severity. Keratoplasty is difficult because of the location of the thinning.

3.6.1.3 Bullous Keratopathy

Definition

Bullous keratopathy means corneal swelling that results from insufficiency of the corneal endothelial pump.

Epidemiology

This degeneration is common and affects, among others, 0.1 % of patients undergoing cataract surgery. It is mainly affects the elderly because of age-related loss of the endothelial cells and the need for intraocular surgery for cataract or glaucoma.

Etiology

This degeneration is a sequel of inflammation, certain corneal dystrophies, or mechanical injury, such as intraocular surgery, which has damaged the endothelial cells, a cell type that does not regenerate. The most common underlying factor is cataract surgery, and eyes with Fuchs' dystrophy are especially susceptible (see Sect. 3.6.2.4).

Clinical Features

Failing of the endothelial pump causes corneal stromal swelling, which is evident as a diffuse haze and, in advanced cases, as folds in Descemet's membrane with concomitantly reduced visual acuity (Fig. 3.23a, b). Epithelial edema is evident as microcysts and, in more advanced cases, as bullae between epithelial cells or epithelial cells and Bowman's layer. The bullae cause discomfort and lead over time to secondary epithelial basement membrane dystrophy.

Histopathology

This degeneration is best evaluated with periodic acid-Schiff and trichrome stains. The

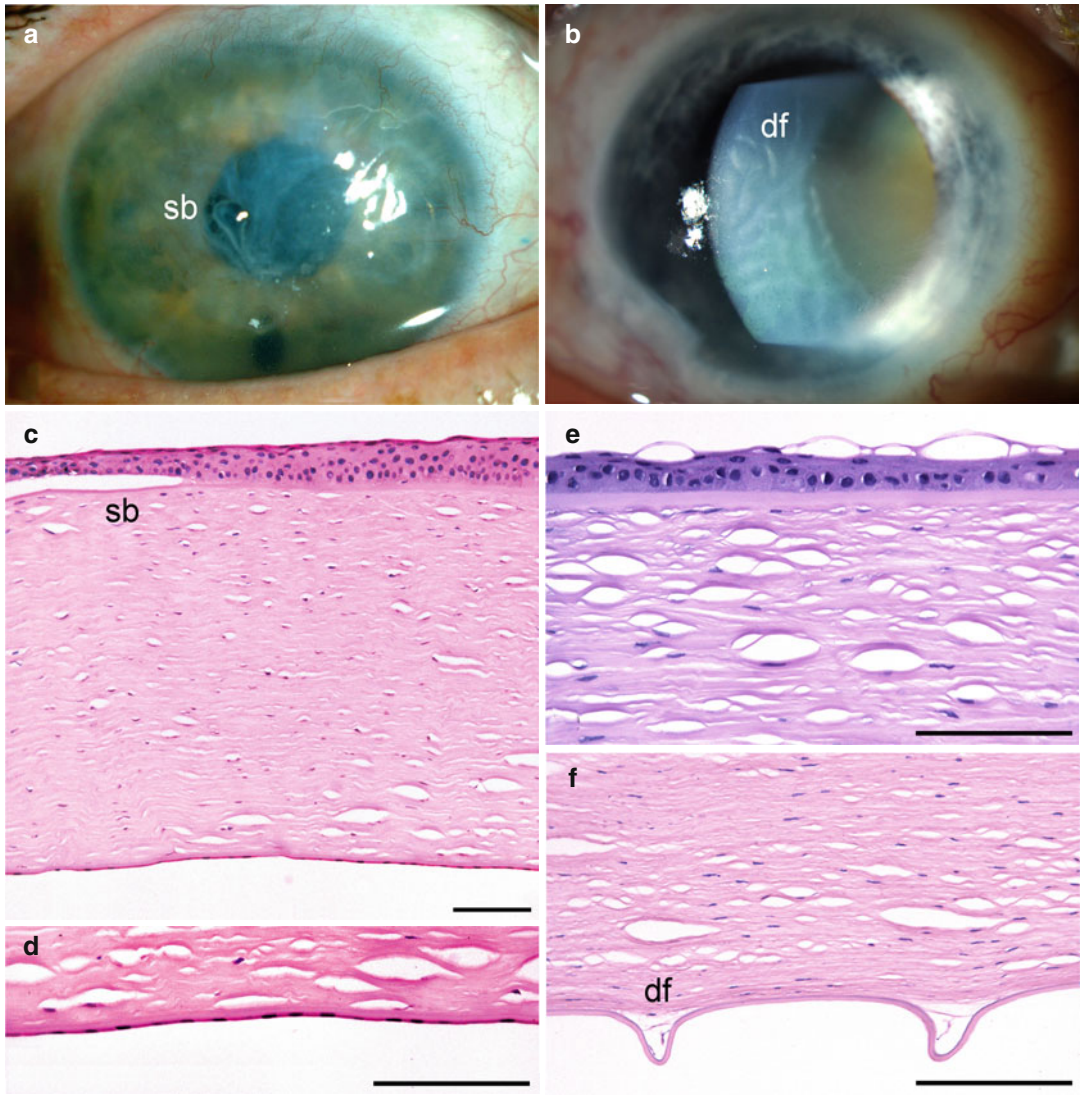

Fig. 3.23 Bullous keratopathy. Chronic swelling of the cornea with subepithelial bullae (*sb*) visible as dark blisters in a background of a greyish degenerative pannus; note irregular light reflex from an uneven epithelium (**a**). Folds in Descemet's membrane (*df*) visible in oblique illumination (**b**). Irregular corneal epithelium is partly separated from Bowman's layer by a subepithelial bulla (*sb*); the stroma is thick (700 µm) and devoid of usual artificial separation of lamellae because of swelling (**c**). Endothelial cell density is lower than average and the cells are flat from stretching to fill in gaps from lost endothelial cells (**d**). Epithelial thinning and superficial microbullae associated with chronic decompensation (**e**). Folds in Descemet's membrane (*df*); note almost complete absence of endothelial cells (**f**). Haematoxylin-eosin (**c**–**f**), bars = 100 µm

cornea is thicker than average and often has less artificial clefts between lamellae than normally (Fig. 3.23c–f). If epithelial edema is present, the basal cells appear pale and fluid may be present between epithelial cells or under the epithelium. Superficial cells may show blisters. In long-standing cases, a degenerative pannus (see Sect. 3.6.1.5) with or without superficial corneal neovascularisation may be present between the epithelium and Bowman's layer. Deposition of basement membrane material within the epithelium is also frequent evidence of previously ruptured bullae. Descemet's membrane is of normal thickness if the underlying factor is not endothelial dystrophy, but the endothelial cell density is low, often markedly so. The remaining

cells are flat and have spread out to fill in gaps left by damaged endothelial cells.

Prognosis

Bullous keratopathy will most often need posterior lamellar or penetrating keratoplasty, depending whether or not permanent damage has developed in the stroma.

3.6.1.4 Pterygium

Definition

Pterygium is a wedge-shaped reactive ingrowth of conjunctival tissue extending a variable distance over the cornea.

Epidemiology

Pterygium is most frequent in dry equatorial areas, increasing in prevalence from less than 1–25 % from high to low latitudes [217]. The incidence is highest among 20- to 40-year-old men.

Etiology

Long-standing exposure to ultraviolet light, dust, and wind predispose to pterygia [217, 218]. Limbal stem cell deficiency and altered angiogenesis or metalloproteinase activity may be mediators of pterygium growth [219–222].

Localisation

Pterygia are usually bilateral and located at the nasal limbus.

Clinical Features

A small pterygium is harmless and only a cosmetic blemish. Many stop growing and are aborted early, persisting as a thin, vascularised, semitransparent membrane [220, 221, 223]. Others continue to grow toward the visual axis, become thicker, and cause variable visual impairment and irritation (Fig. 3.24a). Linear iron deposition called Stocker's line and whitish patches called îlots de Fuchs may be seen at the advancing border of active pterygia.

Histopathology

Excised pterygia should be studied histopathologically because they can be confused or may coexist with conjunctival intraepithelial neoplasia and limbal squamous cell carcinoma [224–226]. The epithelium resembles conjunctival epithelium. Bowman's layer is absent and the pterygium typically is more vascular than normal conjunctiva with a variable infiltrate of mainly lymphocytes and especially plasma cells (Fig. 3.24b–d) [220, 222, 227]. Its collagen frequently has a bluish tint as a sign of actinic damage in haematoxylin-eosin-stained sections.

Prognosis

Pterygia often recur after surgical excision and can then become fleshy and faster growing [223]. Optimal treatment strategy is still debated.

3.6.1.5 Pannus

Definition

Pannus (plural: panni) refers to an ingrowth of fibrous or fibrovascular tissue between the epithelium of the cornea and Bowman's layer usually secondary to chronic irritation.

Epidemiology

Pannus is a common sequel especially to chronic corneal edema and thus is most frequent in the elderly [228]. It can also follow corneal injury.

Etiology

The fibroblasts either originate from the limbus or gain access to subepithelial space through breaks in Bowman's layer. The neovascular vessels originate from limbal conjunctiva, likely driven by growth factors.

Localisation

Panni generally originate near the limbus but may eventually extend across the cornea.

Clinical Features

Most panni are degenerative and visible as greyish thin subepithelial membranes, which are either avascular or show limbal neovascularisation (Fig. 3.25a). Infrequently, they may become exuberant and thick (Fig. 3.25c, e), either because of accumulation of collagen (keloidal pannus) or proliferation of myofibroblasts (hypertrophic pannus) [228].

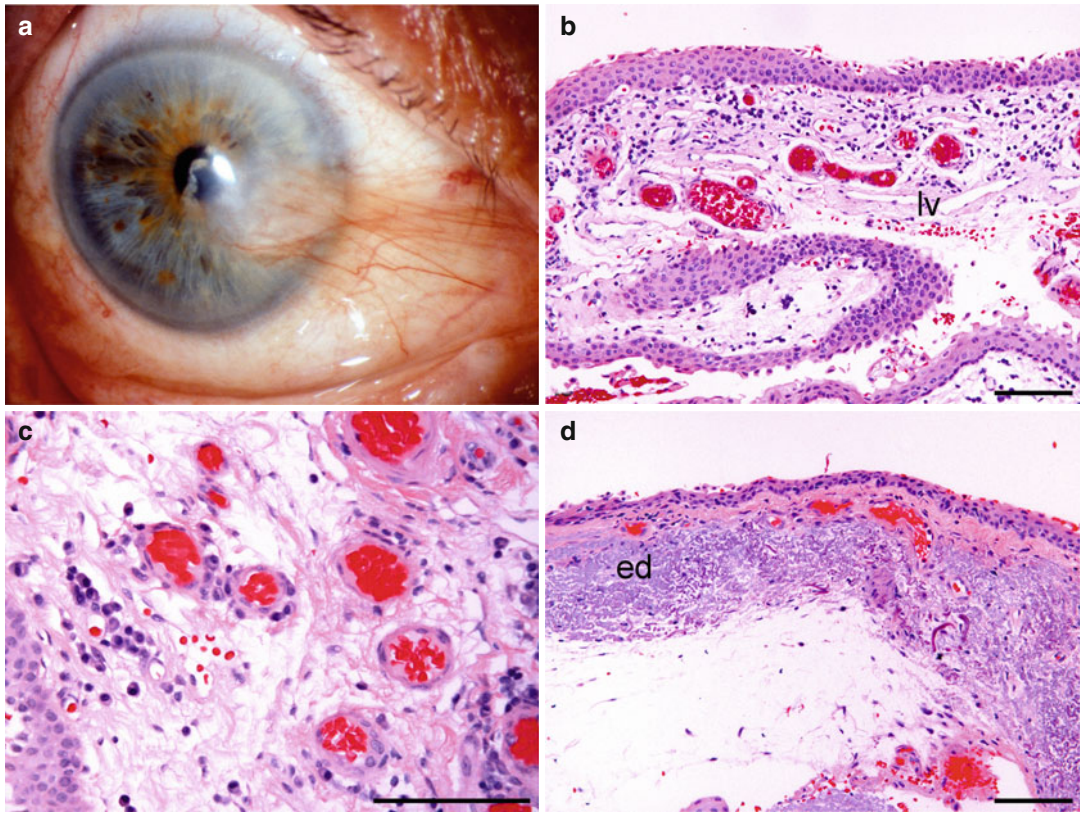

Fig. 3.24 Pterygium. Cornea is overgrown by vascularised tissue extending from the nasal bulbar conjunctiva; note whitish flecks at the advancing border (îlots de Fuchs) (**a**). An excised pterygium is characterised by a loose stroma with moderate numbers chronic inflammatory cells, lymphatic vessels (*lv*) and many capillaries (**b**). The inflammatory infiltrate consists mostly of plasma cells with some lymphocytes (**c**). Elastotic degeneration (*ed*) or actinic damage is revealed by basophilic rather than usual eosinophilic staining of stromal collagen (**d**). Haematoxylin-eosin (**b**–**d**), bars = 100 µm

Histopathology

The corneal epithelium often varies in thickness and may show secondary epithelial basement membrane dystrophy from the underlying disease. A degenerative pannus consists of collagenous extracellular material, thin fibroblasts, and an occasional leucocyte, and they can vary 10–500 µm in thickness (Fig. 3.25b). A keloidal pannus or corneal keloid is characterised by thick, wavy collagen lamellae resembling scleral architecture (Fig. 3.25d) [229–231] and a hyperplastic pannus by spindle-shaped, plump, activated myofibroblasts (Fig. 3.25f), which react with antibodies to alpha-smooth muscle actin and overlie a layer of neovascularisation [228].

Prognosis

Prognosis depends on the underlying disease. Panni can be surgically excised by peeling.

3.6.1.6 Peripheral Hypertrophic Subepithelial Degeneration

Definition

Peripheral hypertrophic subepithelial degeneration (PHSD) is a localised, perilimbal, subepithelial, generally bilateral ingrowth of fibrous scar tissue, resembling a keloidal corneal pannus.

Epidemiology

PHSD is a recently defined degeneration that might be fairly common [232–235]. About 90 % of patients are 35- to 65-year-old women.

Etiology

Chronic low-grade inflammation has been hypothesised [232, 233].

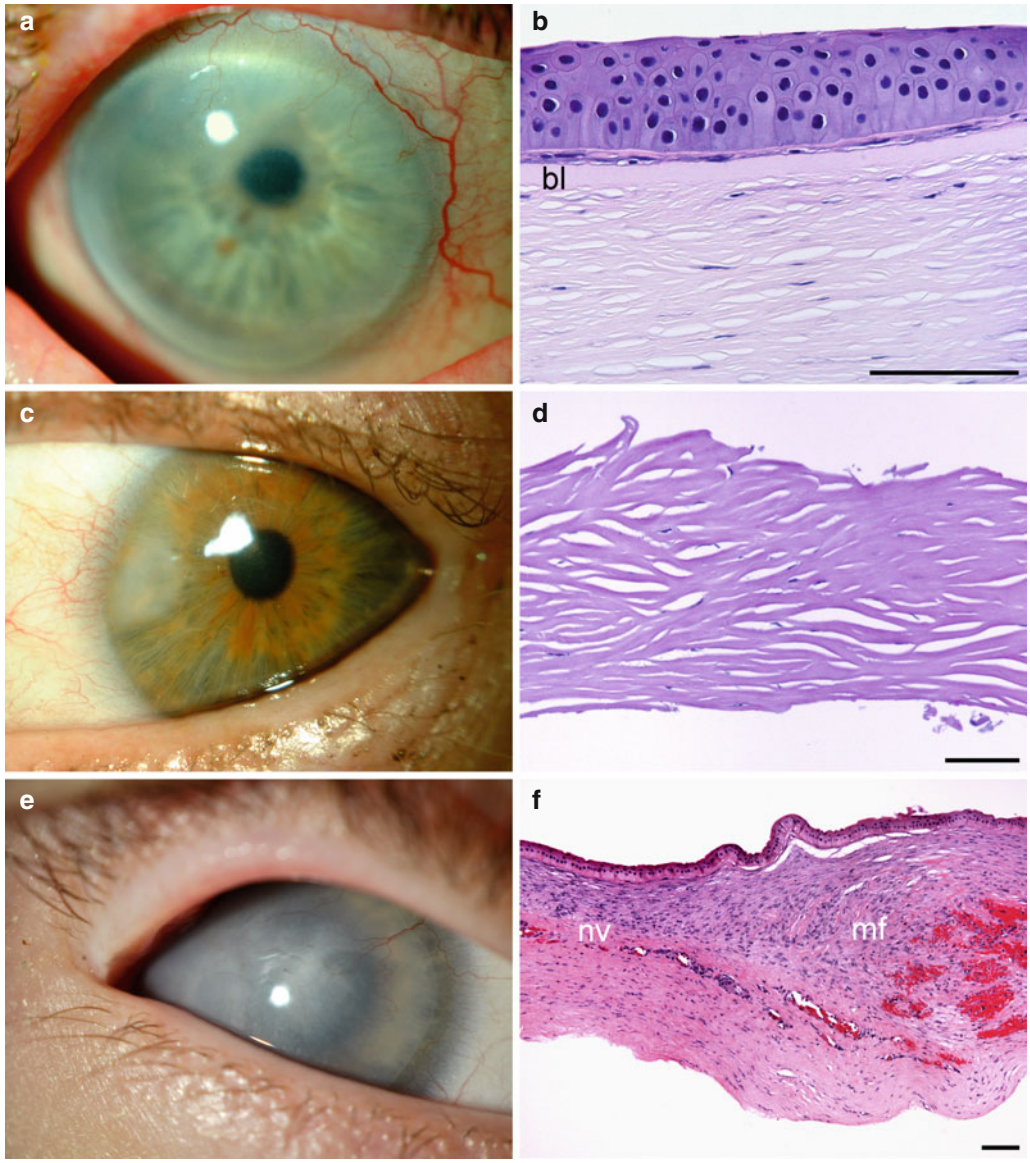

Fig. 3.25 Pannus. Three different types of corneal panni. Sparsely vascularised, thin, greyish degenerative pannus located superonasally (**a**). Flattened fibroblasts with sparse extracellular material are present between Bowman's layer (*bl*) and the corneal epithelium (**b**). Avascular, elevated, whitish keloidal pannus located nasally (**c**). Lamellar, wavy, collagenous scar tissue and flattened fibroblasts imitate scleral architecture (**d**). Vascularised, centrally located hyperplastic pannus (**e**). Superficial layer of myofibroblasts (*mf*) is separated by neovascular vessels (*nv*) from a deeper collagenous layer with fibroblasts (**f**). Haematoxylin-eosin (**b**, **d**, **f**), bars = 100 µm

Clinical Features

PHSD develops frequently in the upper nasal quadrant as a whitish perilimbal elevation associated with faint superficial limbal vascularisation (Fig. 3.26a, b) and is typically bilateral and symmetric [232–235]. The leading symptom is reduced vision from irregular astigmatism. Symptoms of ocular surface disease may be present.

Histopathology

The epithelium over the subepithelial fibrosis is thin to compensate for the thickening (Fig. 3.26c) [232–236]. The basement membrane often is discontinuous. Bowman's layer is typically absent from excised specimens but may have remained in the surgical bed. The collagenous, wavy, fibrotic tissue recapitulates the lamellar corneal architecture

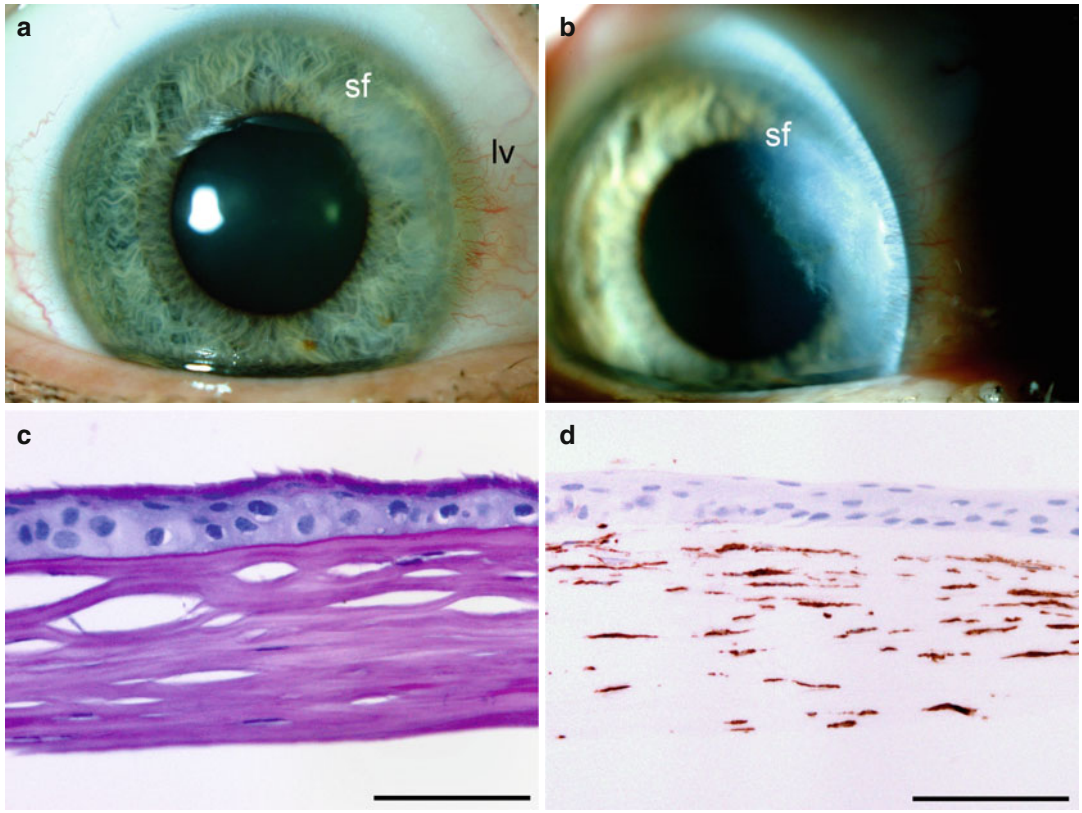

Fig. 3.26 Peripheral hypertrophic subepithelial degeneration. Greyish, elevated, subepithelial perilimbal fibrosis (*sf*) with adjacent inconspicuous limbal vessels (*lv*) located in a characteristic superotemporal position; a similar fibrosis was also present in the fellow eye (**a**). The subepithelial fibrosis (*sf*) is better visible with oblique illumination (**b**). Corneal epithelium is thin and Bowman's layer is absent over the excised fibrosis (**c**). Although the fibrotic tissue appears hypocellular, antibodies to vimentin reveal abundant flattened fibroblasts (**d**). Periodic acid-Schiff (**c**), immunoperoxidase (**d**), bars = 100 µm

with intervening quiescent cells that resemble keratocytes. The fibrosis appears hypocellular but antibodies to vimentin reveal numerous flattened fibroblast-like cells between the lamellae (Fig. 3.26d) [236]. Some react for alpha-smooth muscle actin and thus represent myofibroblasts [236]. Inflammatory infiltration is minimal.

Prognosis

Patients develop disturbing irregular astigmatism, which is relieved by lamellar keratectomy [233].

3.6.1.7 Salzmann's Nodular Degeneration

Definition

Salzmann's nodular degeneration is characterised by a unilateral or, more rarely, bilateral subepithelial, elevated whitish corneal nodules anterior to Bowman's layer.

Epidemiology

This infrequent degeneration affects women in about 75 % of the cases with a mean age of 60 years [237, 238].

Etiology

The pathogenesis is unknown, but chronic inflammation, Meibomian gland dysfunction, and contact lens wear have been suspected.

Clinical Features

The nodules are typically multiple, located paracentrally and occur in any meridian [236–238]. Depending on their number and location, they may be asymptomatic, cause foreign-body

sensation, or disturb vision by inducing astigmatism and hyperopia.

Histopathology

The nodules consist of collagenous tissue that resembles corneal stroma with wavy lamellae [239, 240]. The overlying epithelium is atrophic, but the basement membrane may be thick. Bowman's layer is variably present, disrupted, or destroyed. Oxytalan fibres can be detected within the lesion [234].

Prognosis

Visual disturbance is relieved by lamellar keratectomy.

3.6.1.8 Band Keratopathy

Definition

Band keratopathy refers to non-specific precipitation of calcium salts in the interpalpebral area of Bowman's layer, and sometimes in adjacent layers, forming a linear belt-like pattern.

Synonyms

Zonular keratopathy.

Epidemiology

This degeneration is fairly frequent and can occur in any age.

Etiology

Band keratopathy is a common sequel to chronic uveitis and to a plethora of other chronic eye diseases [241]. It may also accompany defects of calcium metabolism such as hypocalcaemia and hypophosphataemia, complicate certain corneal dystrophies such as posterior polymorphous dystrophy or, rarely, be an isolated inherited trait. The actual mechanism of calcium deposition is unknown.

Clinical Features

Band keratopathy is visible as a greyish white band with Swiss cheese-like holes corresponding to canals of corneal nerves (Fig. 3.27a) [241]. Initially, only the limbal parts are present. When fully developed, band keratopathy involves the entire interpalpebral area, running across the cornea almost from limbus to limbus.

Histopathology

This degeneration is best evaluated with von Kossa or other stains for calcium, but it is detectable in haematoxylin-eosin sections as basophilic granular deposits of calcium phosphate and calcium carbonate involving first the epithelial basement membrane, then Bowman's layer, and eventually even adjacent corneal stroma (Fig. 3.27b) [241, 242].

Prognosis

Band keratopathy is amenable to either chemical, surgical, or excimer laser debridement but it may recur.

3.6.1.9 Haematocornea

Definition

Haematocornea refers to corneal staining and opacification from anterior chamber haemorrhage in the presence of high intraocular pressure.

Etiology

When a haemorrhage does not rapidly clear from the anterior chamber and the intraocular pressure is elevated, degradation products of haemoglobin enter the cornea to deposit in its stroma [243, 244].

Clinical Features

The cornea is diffusely hazy and yellowish in colour (Fig. 3.27c).

Histopathology

Myriad small spherical to ovoid eosinophilic granules are present throughout the corneal stroma (Fig. 3.27d) [243, 244].

Prognosis

The deposits will slowly clear. Corneal transplantation may alternatively be performed.

3.6.1.10 Climatic Droplet Keratopathy

Definition

Climatic droplet keratopathy is an elastotic degeneration of the cornea.

Synonyms

Spheroidal degeneration.

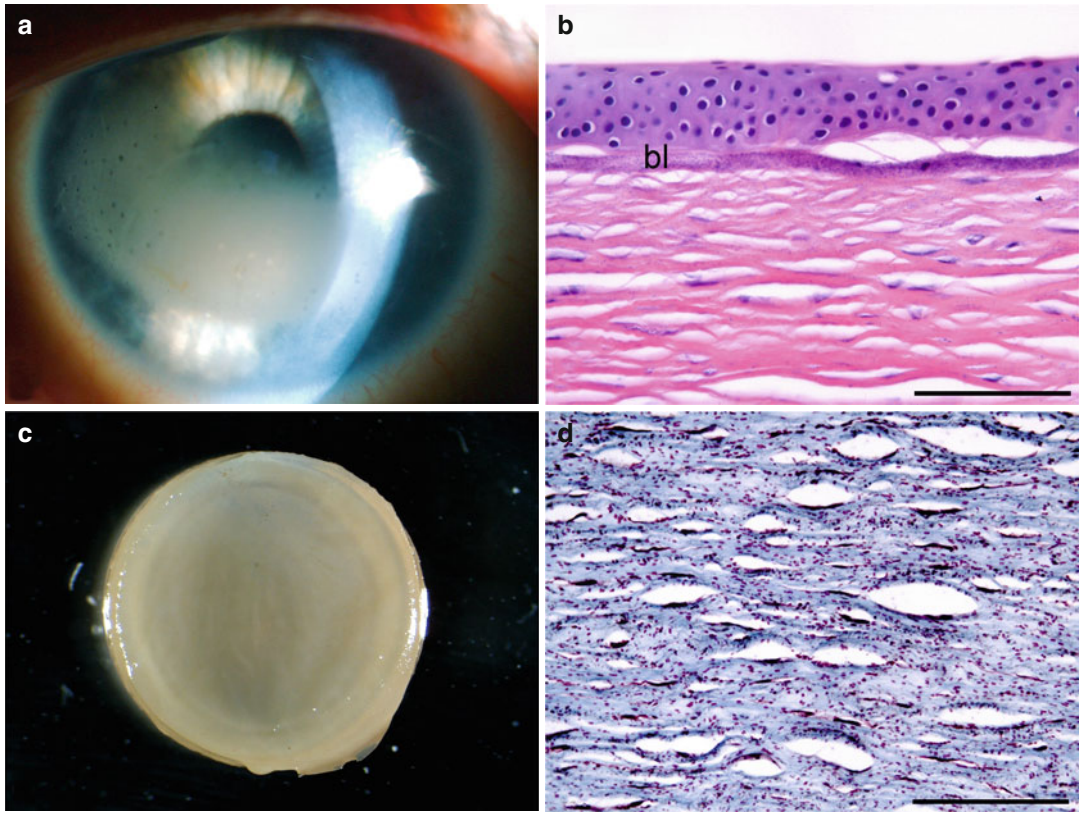

Fig. 3.27 Band keratopathy (**a**, **b**) and haematocornea (**c**, **d**). Greyish band of calcification extends across the superficial interpalpebral zone of the cornea; note small black holes in the calcification that correspond to canals of subepithelial nerves (**a**). Calcification of Bowman's layer (*bl*) is evident as myriad basophilic dots (**b**). Diffusely hazy, yellowish corneal button removed from a blood stained cornea (**c**). Myriad spherules of degraded haemoglobin are present at all levels of the stroma (**d**). Haematoxylin-eosin (**b**), Masson's trichrome (**d**), bars = 100 μm

Epidemiology

This generally rare degeneration affects predominantly males over 40 years old who work outdoors, especially in some geographic areas such as Argentina [245, 246].

Etiology

Environmental factors including strong winds, sunshine, low humidity, and ultraviolet exposure in both hot and cold climates are implicated in high prevalence areas. Proposals for histogenesis include altered advanced glycation end-product deposition or matrix metalloproteinase activity [247, 248].

Clinical Features

This degeneration is characterised by yellowish spherules of proteinaceous, hyaline material in the anterior stroma, resembling droplets of olive oil [245, 249–251].

Histopathology

This degeneration is best evaluated with van Gieson or other elastin stains. The amorphous hyaline deposits are amphophilic in haematoxylin-eosin sections and stain intensely for elastin [249, 252]. This staining persists when sections are pretreated with elastase.

Prognosis

Secondary scarring can lead to visual impairment when the keratopathy is long-standing.

3.6.2 Dystrophies

Corneal dystrophies as a group are typically inherited diseases limited to corneal tissue that are generally bilateral and more or less symmetric, slowly progressive, and without relationship to environmental or systemic factors or diseases

Table 3.1 Categories indicating the level of evidence supporting the existence of a given corneal dystrophy as defined by the International Committee for Classification of Corneal Dystrophies (IC3D) [253]

Category 1	A well-defined corneal dystrophy in which the gene has been mapped and identified and specific mutations are known
Category 2	A well-defined corneal dystrophy that has been mapped to one or more specific chromosomal loci, but the gene or genes remains to be identified
Category 3	A well-defined corneal dystrophy in which the disorder has not yet been mapped to a chromosomal locus
Category 4	A category reserved for a suspected new or previously documented corneal dystrophy, although the evidence for it being a distinct entity is not yet convincing

[253, 254]. Exceptions to these rules are sometimes present either as regards apparent heredity or laterality.

As hereditary diseases, corneal dystrophies as a rule are listed in the Online Mendelian Inheritance in Man (OMIM®) database, a continuously updated catalog of human genetic disorders [255]. In this database, each disease has a numeric unique identifier, which is preceded by the symbol # if the phenotype has a known molecular basis but it does not represent a unique locus and by the symbol % if the phenotype is associated with a locus for which the underlying molecular basis is not yet known.

Corneal dystrophies have recently been reclassified by the International Committee for Classification of Corneal Dystrophies (IC3D), affiliated with the Cornea Society [253]. In this classification, each dystrophy is assigned to one of four categories (C1–C4) which indicate the level of evidence supporting the existence of a given dystrophy (Table 3.1).

In the following descriptions, the OMIM number and the IC3D category are given for ease of reference for each corneal dystrophy. Only most recently used synonyms are given in addition to the preferred IC3D terminology.

3.6.2.1 Epithelial and Subepithelial Dystrophies

Epithelial Basement Membrane Dystrophy

Definition

Epithelial basement membrane dystrophy (EBMD; OMIM #121820, IC3D C1) refers to redundant deposition of basement membrane material within the corneal epithelium [256].

Synonyms

Map-dot-fingerprint dystrophy.

Epidemiology

EBMD is the most frequent corneal dystrophy and may affect at least 2 % of the population.

Etiology and Genetics

Autosomal dominant mutations in *TBFBI*, encoding transforming growth factor beta-induced protein (keratoepithelin), is reported in two families [257]. Most are secondary to chronic injury such as long-standing corneal edema in bullous keratopathy or Fuchs' endothelial dystrophy [258].

Clinical Features

EBMD is diagnosed in adult life. It is visible especially with retroillumination as irregular islands of thickened, grey, hazy epithelium (Fig. 3.28a–c) with circumscribed borders ("maps"); round, oval, or comma-shaped grey opacities ("dots"); and parallel curvilinear lines ("fingerprints") [253, 256, 259, 260]. In addition, blebs may be seen. These changes affect mostly central or paracentral cornea. Confocal microscopy and anterior segment optical coherence tomography produce images similar to those seen by light microscopy [261–263].

Histopathology

EBMD is best evaluated with periodic acid-Schiff and Masson's trichrome stains, which highlight basement material in purple and blue, respectively (Fig. 3.28d–f). Excessive material is present under and within the corneal epithelium as intraepithelial sheets ("maps"), pseudocysts containing debris ("dots"), and cordlike extensions ("fingerprints") [264]. Blebs correspond to deposition of basement membrane material beneath the epithelium without intraepithelial accumulation [265].

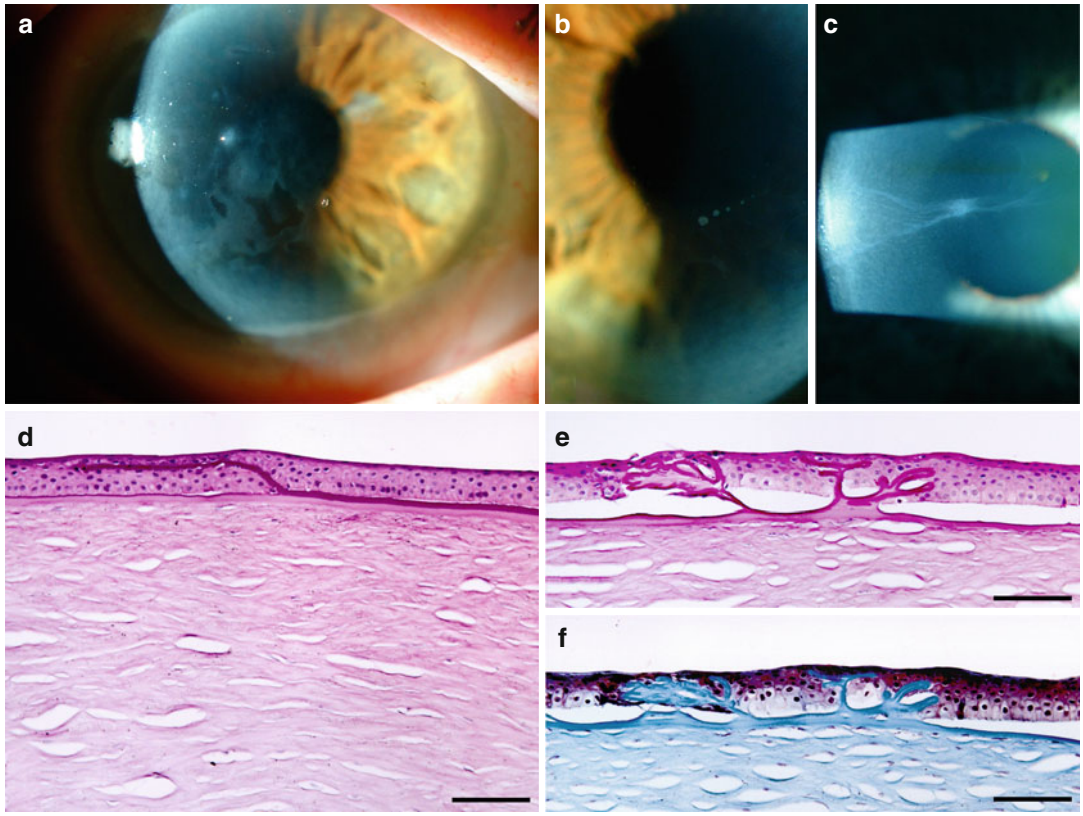

Fig. 3.28 Epithelial membrane dystrophy. Greyish map-like (**a**), dot-like (**b**), and wavy fingerprint-like patterns (**c**) of excessive basement membrane material are highlighted with oblique illumination. Periodic acid-Schiff stain colours purple abnormal intraepithelial basement membrane material that forms sheets (**d**) corresponding to map and folds (**e**) corresponding to fingerprint patterns. Masson's trichrome stain colours the same material blue (**f**), bars = 100 μm

Prognosis

Poor adhesion of the epithelium to abnormal basement membrane predisposes to recurrent painful corneal erosions. Irregular astigmatism may develop and change over time.

Epithelial Recurrent Erosion Dystrophy

Definition

Epithelial recurrent erosion dystrophy (ERED; OMIM %122400, IC3D C3) is characterised by painful recurrent corneal erosions that develop spontaneously or follow minimal ocular injury, inherited as an autosomal dominant trait [253].

Synonyms

Phenotypic variants are described under various names: Franceschetti [266, 267], Smolandiensis [268], and Helsinglandica [269, 270] dystrophies.

Epidemiology

Isolated families.

Etiology and Genetics

The responsible gene(s) remain unknown.

Clinical Features

ERED presents during the first decade of life. The cornea may show subepithelial haze or blebs under the slit lamp, especially with retroillumination

[267]. Between attacks the cornea appears normal. Later, subepithelial pannus develops. Confocal microscopy shows absence of Bowman's layer, irregular epithelium, and altered keratocytes in the anterior stroma [268, 270].

Histopathology

In the Franceschetti variant, damaged Bowman's layer and a fibrous pannus can eventually be found [267]. In the Smolandiensis variant, the epithelium is hyperplastic and Bowman's layer is absent [268].

Prognosis

The attacks become less severe and disappear toward middle age. Permanent subepithelial opacities or keloids may develop [268, 269].

Subepithelial Mucinous Corneal Dystrophy

Definition

Subepithelial mucinous corneal dystrophy (SMCD; OMIM 612867, IC3D C4) is characterised by painful attacks of recurrent corneal erosions and is most likely an autosomal dominant trait [253].

Epidemiology

Single family [271].

Etiology and Genetics

The responsible gene is unknown.

Clinical Features

SMCD begins during the first decade of life. Subepithelial opacities and haze eventually involve the entire cornea, especially its centre.

Histopathology

Subepithelial band of eosinophilic, periodic acid-Schiff and Alcian blue-positive, hyaluronidase-sensitive material is visible anterior to Bowman's layer [271]. It is labelled with antibodies to chondroitin-4-sulphate and dermatan sulphate.

Prognosis

Alleviates during adolescence but leads to progressive loss of vision.

Meesmann's Corneal Dystrophy

Definition

Meesmann's corneal dystrophy (MECD; OMIM #122100; IC3D C1) refers to recurrent corneal erosions due to abnormal corneal cytokeratins, a component of the cytoskeleton which maintains the structural integrity of cells [253]. It is inherited as an autosomal dominant trait.

Synonyms

A variant is known as Stocker-Holt dystrophy.

Epidemiology

Rare.

Etiology and Genetics

MECD results from mutations in either *KRT3* or *KRT12* that code cytokeratin 3 and 12, respectively [272]. The intermediate filaments of corneal epithelial cells are assembled from this pair. The *KRT12* variant (Stocker-Holt) is more severe [273].

Clinical Features

MECD begins in early childhood and is slowly progressive [274]. Patients are asymptomatic, complain of glare and light sensitivity, or have recurrent painful punctate corneal erosions. Multiple tiny epithelial vesicles are seen with the slit lamp and clinical confocal microscopy, which are most numerous in the interpalpebral area and may form whorls, wedges, lines, and other patterns [275–277]. In retroillumination, the vesicles appear isolated.

Histopathology

MECD is best evaluated with periodic acid-Schiff stain that shows a thick basement membrane, sometimes with epithelial basement membrane dystrophy-like extensions into the epithelium, and intraepithelial cysts filled with debris [276, 278, 279]. The epithelium may be thick and irregular. Intracellular fibrogranular "peculiar material" surrounded by tangles of filaments is visible by electron microscopy.

Prognosis

Favourable, some patients experience mild visual loss.

Lisch Epithelial Corneal Dystrophy

Definition

Lisch epithelial corneal dystrophy (LECD; OMIM %300778, IC3D C2) is characterised by painful attacks of recurrent erosions inherited as an X-linked dominant trait [253, 280].

Epidemiology

Isolated families.

Etiology and Genetics

The gene is unknown.

Clinical Features

LECD begins in childhood, is slowly progressive, and is initially asymptomatic [280]. Slit lamp shows various localised patterns of greyish cystic opacities such as whorls, lines, bands, flames, and clubs. Hyperreflective epithelial cytoplasm with hyporeflective nuclei are seen with confocal microscopy [281]. Blurred vision develops if the central cornea becomes involved. In retroillumination, the vesicles appear crowded.

Histopathology

Corneal epithelial cells contain diffuse cytoplasmic vacuoles that are optically empty or contain weakly osmiophilic, partly lamellar material as seen by electron microscopy [280, 282].

Prognosis

Favourable, some patients experience mild visual loss.

Gelatinous Drop-Like Corneal Dystrophy

Definition

Gelatinous drop-like corneal dystrophy (GDLD; OMIM #204870, IC3D C1) refers to a localised corneal amyloidosis inherited as an autosomal recessive trait [253, 283].

Epidemiology

Rare except in Japan [284].

Etiology and Genetics

Most cases result from mutations in *TACSTD2*, which codes tumour-associated calcium signal transducer 2 [285, 286]. It is postulated that the mutations compromise the epithelial barrier function, leading to tear fluid permeation into corneal tissue and deposition of lactoferrin as amyloid.

Clinical Features

GDLD begins in the first to second decade of life. Subepithelial amyloid deposits initially imitate band keratopathy or form mulberry-like nodules [283, 284, 287, 288]. They progress to stromal opacification or larger protruding kumquat-like nodules and cause redness, tearing, sensitivity to light, and marked visual loss. Superficial neovascularisation is frequent.

Histopathology

GDLD is best evaluated with Congo red stain that labels amyloid deposits beneath the epithelium and in the stroma, which distort both layers [287, 289, 290]. Immunohistochemically, the deposits react for lactoferrin [291].

Prognosis

Guarded, recurs after keratoplasty.

3.6.2.2 Dystrophies Affecting Predominantly the Region of Bowman's Layer

Although these dystrophies lead to secondary changes in the acellular Bowman's layer, the primary defect lies in the corneal epithelial cells and affects additionally the superficial stromal layers.

Reis-Bücklers' Corneal Dystrophy

Definition

Reis-Bücklers' corneal dystrophy (RBCD; OMIM #608470, IC3D C1) is a superficial, geographic dystrophy related to granular corneal

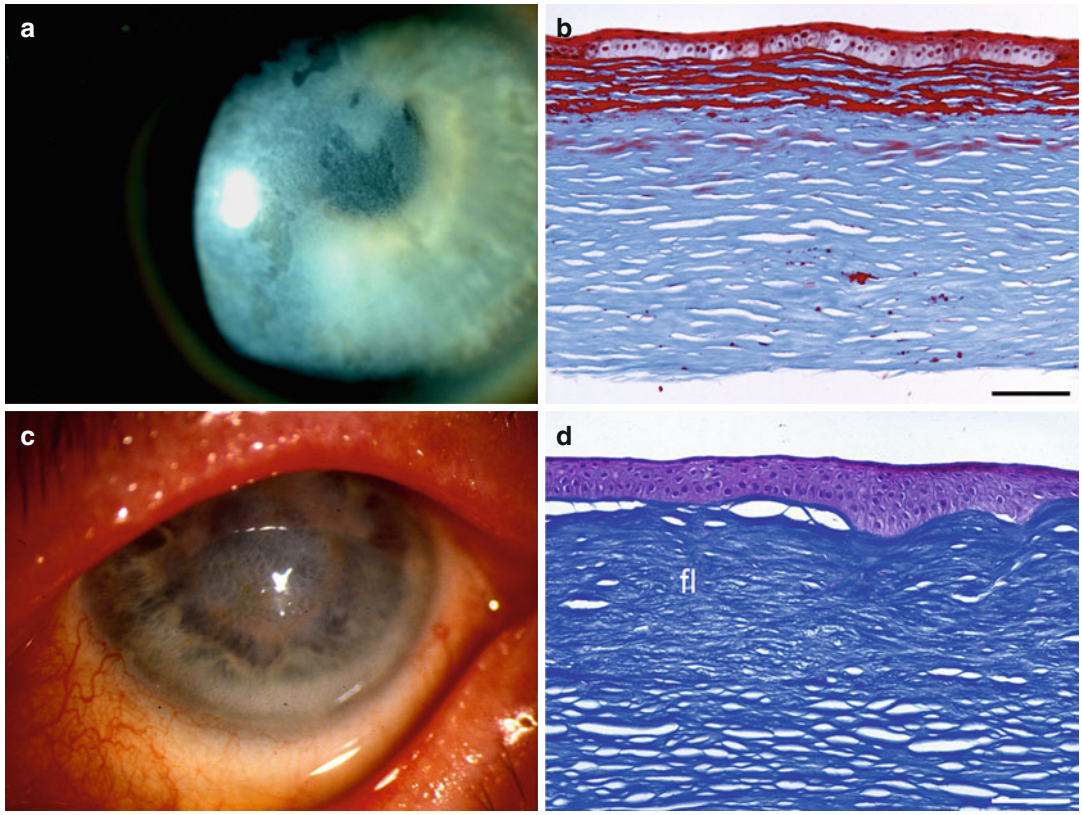

Fig. 3.29 Reis-Bücklers' (**a**, **b**) and Thiel-Behnke (**c**, **d**) corneal dystrophies. Geographic subepithelial stromal opacity from Arg124Leu *TGFBI* mutation (**a**). Keratohyalin deposits, which stain red with Masson's trichrome, replace the destroyed Bowman's layer and are additionally found especially between superficial stromal lamellae; specimen is from anterior lamellar keratoplasty and thus lacks Descemet's membrane and endothelium (**b**). Honeycomb-shaped central corneal opacity from Arg555Gln *TGFBI* mutation (**c**). Bowman's layer is destroyed and replaced by a thick, uneven fibrous layer (*fl*) that stains blue with Masson's trichrome and forms a sawtooth pattern under the epithelium (**d**), bars = 100 µm

dystrophy [253] and has often been confused with Thiel-Behnke dystrophy [292, 293].

Epidemiology

Rare.

Etiology and Genetics

A classic autosomal dominant *TGFBI* dystrophy associated with the Arg124Leu mutation [294, 295].

Clinical Features

The dystrophy begins in childhood with painful corneal erosions, superficial corneal opacification, and gradual visual loss [296]. Confluent irregular, coarse, geographic opacities replace Bowman's layer and also appear in the superficial stroma (Fig. 3.29a). They can be confused with those of Thiel-Behnke dystrophy and variant lattice corneal dystrophies. Confocal microscopy and optical coherence tomography shows highly reflective deposits in the basal epithelial and Bowman's layers [297].

Histopathology

RBCD is best evaluated with Masson's trichrome stain. Bowman's layer is replaced with sheetlike deposits of red keratohyalin granules that eventually also involve the superficial stroma (Fig. 3.29b) [292]. Electron microscopy demonstrates electron-dense, rod-shaped subepithelial

bodies identical to those of granular dystrophy, type 1 [292].

Prognosis

Leads to keratoplasty and can recur in the graft.

Thiel-Behnke Corneal Dystrophy

Definition

Thiel-Behnke corneal dystrophy (TBCD; OMIM #608470, IC3D C1) is characterised by replacement of Bowman's layer with fibrous tissue in a honeycomb pattern, which has often been confused with Reis-Bücklers' dystrophy [292, 293].

Epidemiology

Rare.

Etiology and Genetics

A classic autosomal dominant *TBFBI* dystrophy from the Arg555Gln mutation [295]. Alleged variant of dubious identity is mapped to 10q24 [298, 299].

Clinical Features

TBCD begins in the first decade of life with recurrent painful corneal erosions which may alleviate with time [293, 300]. Subepithelial reticular opacities develop which initially spare the corneal periphery (Fig. 3.29c). Gradual visual loss develops. The clinical appearance can be confused with those of Reis-Bücklers' and variant lattice corneal dystrophies. Confocal microscopy and optical coherence tomography parallel the histopathological sawtooth pattern and additionally show homogenous deposits in the basal epithelial layer and irregular material instead of Bowman's layer [297, 301].

Histopathology

TBCD is best evaluated with Masson's trichrome stain, which shows abnormal, wavy, sawtooth-like fibrous tissue that stains blue and replaces Bowman's layer (Fig. 3.29d) [292]. The epithelium varies in thickness and forms ridges and furrows over the subepithelial fibrous tissue. Electron microscopy displays curly collagen fibres, diameter of 9–15 nm.

Prognosis

Phototherapeutic keratectomy is effective and delays the need for keratoplasty.

Grayson-Wilbrandt Corneal Dystrophy

Grayson-Wilbrandt corneal dystrophy (GWCD; IC3D C4) has only been described in one family [302]. Bowman's layer showed diffuse mottling or diffuse greyish opacities, which extended to the epithelium and gave rise to recurrent erosions. Refractile bodies were seen in the stroma. Its status as a separate dystrophy is debated, but homogeneous eosin-staining material between Bowman's layer and the epithelium, which stained with Periodic acid-Schiff but not with Masson's trichrome or Alcian blue stain, does not fit other known dystrophies.

3.6.2.3 Dystrophies Affecting Primarily Corneal Stroma

Lattice Corneal Dystrophy, Classic and Variants

Definition

Lattice corneal dystrophy (LCD1; OMIM #122200, IC3D C1) refers to a group of autosomal dominant *TBFBI* dystrophies characterised by localised corneal amyloid deposition, typically in linear patterns. It must be differentiated from familial amyloidosis, Finnish (FAF; OMIM #105120, also known as Meretoja syndrome), an autosomal dominant systemic amyloidosis characterised by cranial neuropathy, bulbar signs, skin changes, and a corneal amyloidosis previously called lattice corneal dystrophy, type II [303–305]. This is a misnomer because it is not a true dystrophy but a manifestation of systemic disease [253].

Epidemiology

Infrequent, although in some countries the most common of the *TGFBI* dystrophies [306]. Meretoja syndrome, although found in many countries, is rare except in Finland [305].

Etiology and Genetics

Classic LCD (formerly known as type I) is caused by the Arg124Cys mutation [294]. Variants result from more than 30 less frequent mutations [253]. Before the era of genetics, an

attempt was made to classify these variants by phenotype, such as type III, IIIA, I/IIIA, and IV, but this approach has mostly been abandoned in favour of mutation analysis. In contrast, FAF arises from mutations in *GSN*, coding gelsolin, a plasma protein [307, 308].

Clinical Features

LCD is slowly progressive. Classic LCD starts during the first decade when asymptomatic linear deposits of amyloid appear, followed by discomfort, pain, corneal erosions, and gradual visual loss, necessitating corneal transplantation (Fig. 3.30a) [253]. Both subepithelial granular and stromal branching, refractile, linear deposits sparing the corneal periphery are seen with the slit lamp. Later the cornea may appear diffusely hazy. In variant lattice dystrophies and related phenotypes, the lines may be unusually thick or thin, or not visible at all; the phenotype may also mimic dystrophies affecting mainly Bowman's layer (Fig. 3.30b, c) [309–312]. In FAF, asymptomatic linear deposits of amyloid appear during the third or fourth decade, followed by discomfort, pain, corneal erosions, and gradual moderate visual loss. Both subepithelial

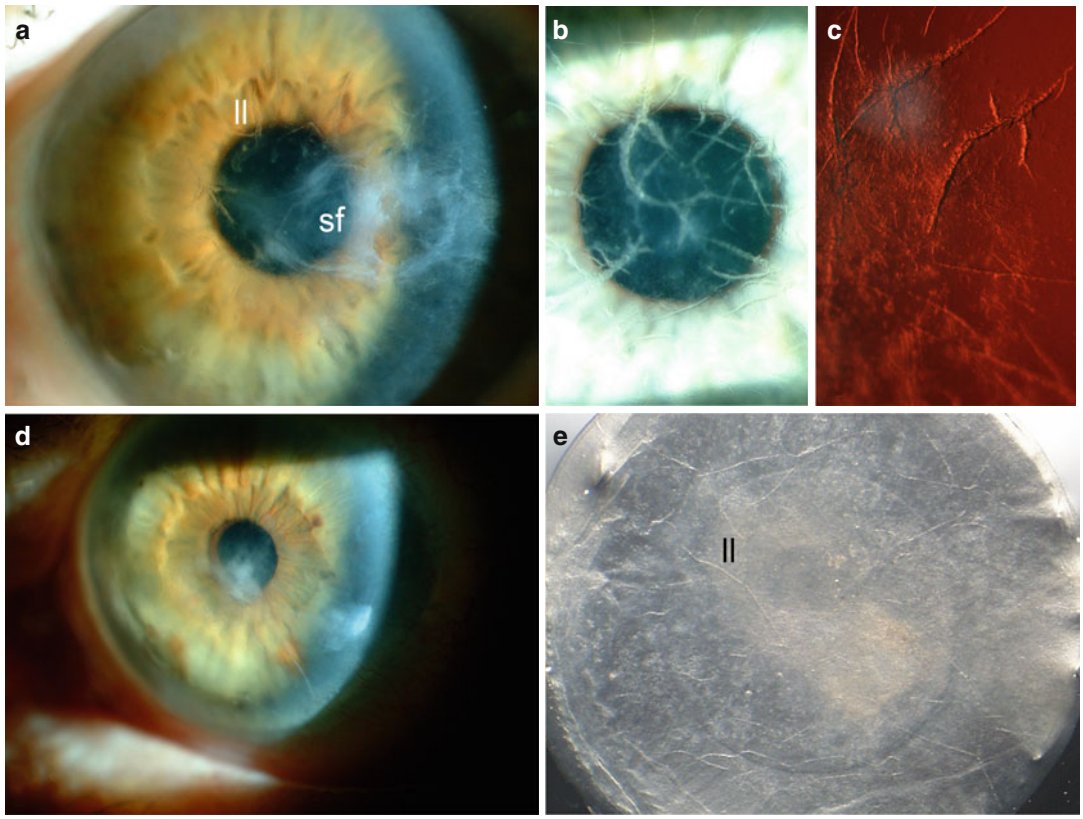

Fig. 3.30 Lattice dystrophy (**a**–**c**, **f**–**i**) as compared to corneal amyloidosis in Meretoja syndrome (**d**, **e**, **j**, **k**). Transparent lattice lines (*ll*) and secondary subepithelial fibrosis (*sf*) in classic corneal lattice dystrophy, Arg124Cys *TGFBI* mutation (**a**). Coarser lattice lines seen by direct (**b**) and retroillumination (**c**) in variant lattice dystrophy, His626Arg *TGFBI* mutation. In familial amyloidosis, Finnish type (Meretoja syndrome), delicate lattice lines may be obscured by subepithelial fibrosis (**d**) but are conspicuous macroscopically in the removed corneal button (**e**). Microscopically, a continuous layer of amyloid underlies and partially destroys Bowman's layer (*bl*) and deposits corresponding to lattice lines (*ll*) are visible in the stroma with Congo red (**f**). The deposits are birefringent and exhibit red-green dichroism under polarised light (**g**). In variant dystrophies, the subepithelial deposit at the level of Bowman's layer (*bl*) may be less conspicuous whereas lattice lines (*ll*) may be much larger (**h**, **i**). In Meretoja syndrome, Bowman's layer (*bl*) is eventually destroyed by amyloid deposits but lattice lines (*ll*) remain thin (**j**, **k**). Congo red under non-polarised (**f**, **h**, **j**) and polarised (**g**, **i**, **k**) light, bars = 100 μm

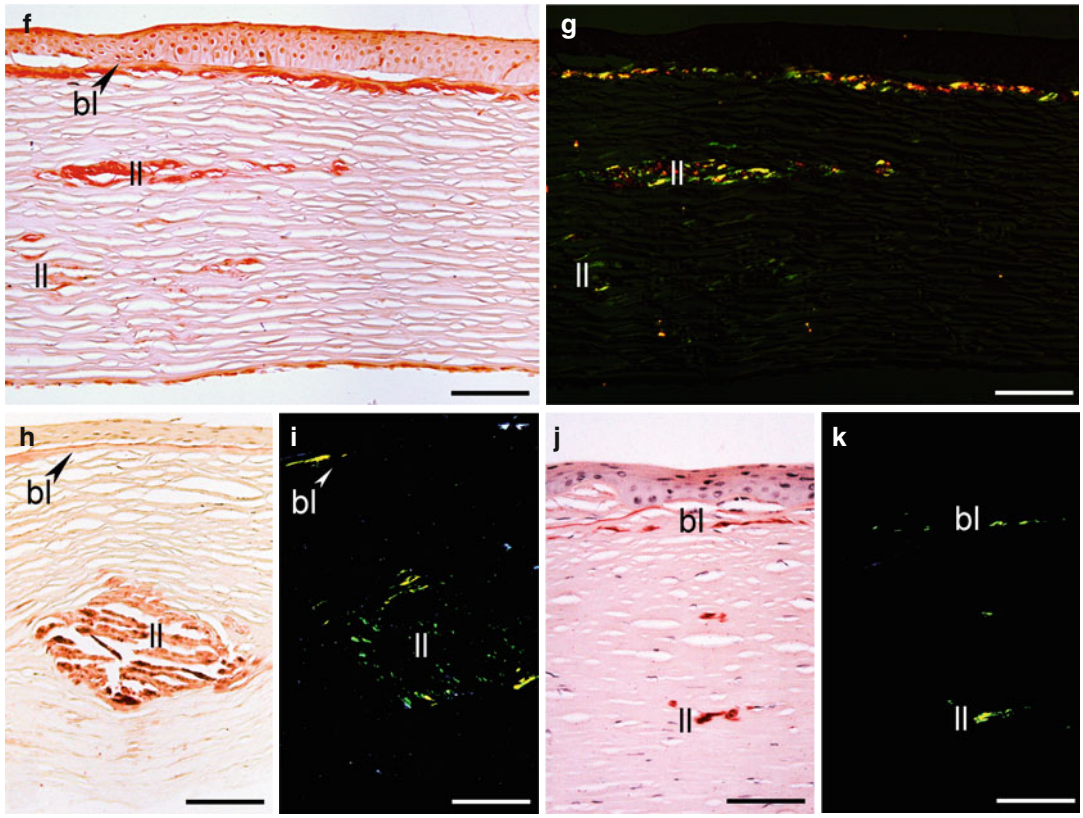

Fig. 3.30 (continued)

granular and stromal branching, refractile, linear deposits based in the corneal periphery are seen with the slit lamp (Fig. 3.30d, e) [313, 314]. In addition, progressive dermatochalasis, lagophthalmos, facial paresis, bulbar palsy, and laxity of the facial skin are typical later in life [303, 304].

Histopathology

LCD is best evaluated with Congo red staining, which highlights dichroic, birefringent amyloid deposits (Fig. 3.30f–i) [313, 315]. The epithelium and Bowman's layer are thin, irregular, and partially destroyed by a layer of amyloid, and intrastromal amyloid deposits distort the lamellar architecture. They stain red with haematoxylin-eosin, do not stain with periodic acid-Schiff, and show metachromasia with crystal violet. Occasionally, the deposits may partially stain red with Masson's trichrome even in face of the classic Arg124Cys mutation [316–318]. Electron microscopy shows fine, electron-dense, randomly aligned extracellular fibrils 8–10 nm in diameter. In FAF, similar amyloid deposits partially destroy Bowman's layer but intrastromal deposits are less conspicuous than in LCD (Fig. 3.30j, k) [313, 315]. Immunohistochemically, mutated gelsolin is deposited in the conjunctiva, sclera, ciliary body, choriocapillaris, perineurium of ciliary nerves, walls of ciliary vessels, and optic nerve [319]. Extraocularly, amyloid is deposited in arterial walls, peripheral nerves, and renal glomeruli [303].

Prognosis

Keratoplasty will often become necessary, and the dystrophy can recur in the graft and even behind the lamellar graft.

Granular Corneal Dystrophy, Type 1 and Variants

Definition

Granular corneal dystrophy (GCD; OMIM #121900, IC3D C1) refers to a group of classic autosomal dominant *TBFBI* dystrophies [253].

Epidemiology
Rare.

Etiology and Genetics
The classic type 1 (GCD1) is caused by the Arg555Trp mutation [294]. A number of phenotypic variants are known to result from this mutation [320, 321].

Clinical Features
This progressive dystrophy begins in early childhood. White to translucent keratohyalin deposits are accompanied by glare, recurrent corneal erosions, and gradual visual loss [322]. Slit lamp reveals in the anterior stroma well-defined, white, breadcrumb-like granules that are composed of small translucent dots that do not extend to the limbus (Fig. 3.31a). With time, they spread to the deeper stroma. Their number, size, and appearance vary widely between families.

Histopathology
GCD1 is best evaluated with Masson's trichrome stain, which colours bright red the granules that distort Bowman's membrane and stromal lamellae (Fig. 3.31b) [316]. Immunohistochemically, they react with antibodies to keratoepithelin (transforming growth factor beta-induced protein). The deposited material is rod-shaped by electron microscopy [323].

Prognosis
Lamellar or penetrating keratoplasty will become necessary, and the dystrophy can recur in the graft and behind a lamellar graft.

Granular Corneal Dystrophy, Type 2

Definition
Granular corneal dystrophy type 2 (GCD2; OMIM #607541, IC3D C1) is a classic autosomal dominant *TBFBI* dystrophy characterised by dual deposition of keratohyalin and amyloid [253, 324].

Synonyms
Avellino corneal dystrophy, according to an Italian region. It is, however, globally distributed.

Epidemiology
Rare, although in some countries the second most common *TGFBI* dystrophy [306].

Etiology and Genetics
GCD2 is caused by the Arg124His mutation [294].

Clinical Features
GCD2 begins in early childhood to adolescence with gradual visual loss and mild corneal erosions. Slit lamp reveals in the anterior stroma whitish keratohyalin deposits often in characteristic stellate and icicle shapes, which are made of small translucent dots and are less numerous than in GCD1 (Fig. 3.31c) [42, 324, 325]. Rings may appear after the granules erode. However, phenotypic variation is marked [326–328]. Refractile lattice lines located deeper than the keratoepithelin deposits are easily missed so that the ophthalmic pathologist may be the first one to make the correct diagnosis.

Histopathology
GCD2 is best evaluated by combining Masson's trichrome and Congo red stains. The former highlights bright red subepithelial and stromal keratohyalin and the latter dichroic, birefringent amyloid deposits (Fig. 3.31d–f) [316, 324, 325]. Anterior deposits typically are stained with both, whereas the deeper lattice lines only stain with Congo red. As a caveat, dual staining can sometimes occur in deposits of classic lattice dystrophy from the Arg124Cys mutation and in variant TGFBI dystrophies [316–318]. Electron microscopy shows rod-shaped and randomly aligned amyloid fibres [324].

Prognosis
Although phenotypic variation is large, penetrating keratoplasty may become necessary, and the dystrophy can recur in the graft. Lamellar corneal surgery may precipitate a rapid recurrence in the surgical interphase [329].

Macular Corneal Dystrophy

Definition
Macular corneal dystrophy (MCD; OMIM #217800, IC3D C1) is an autosomal recessive

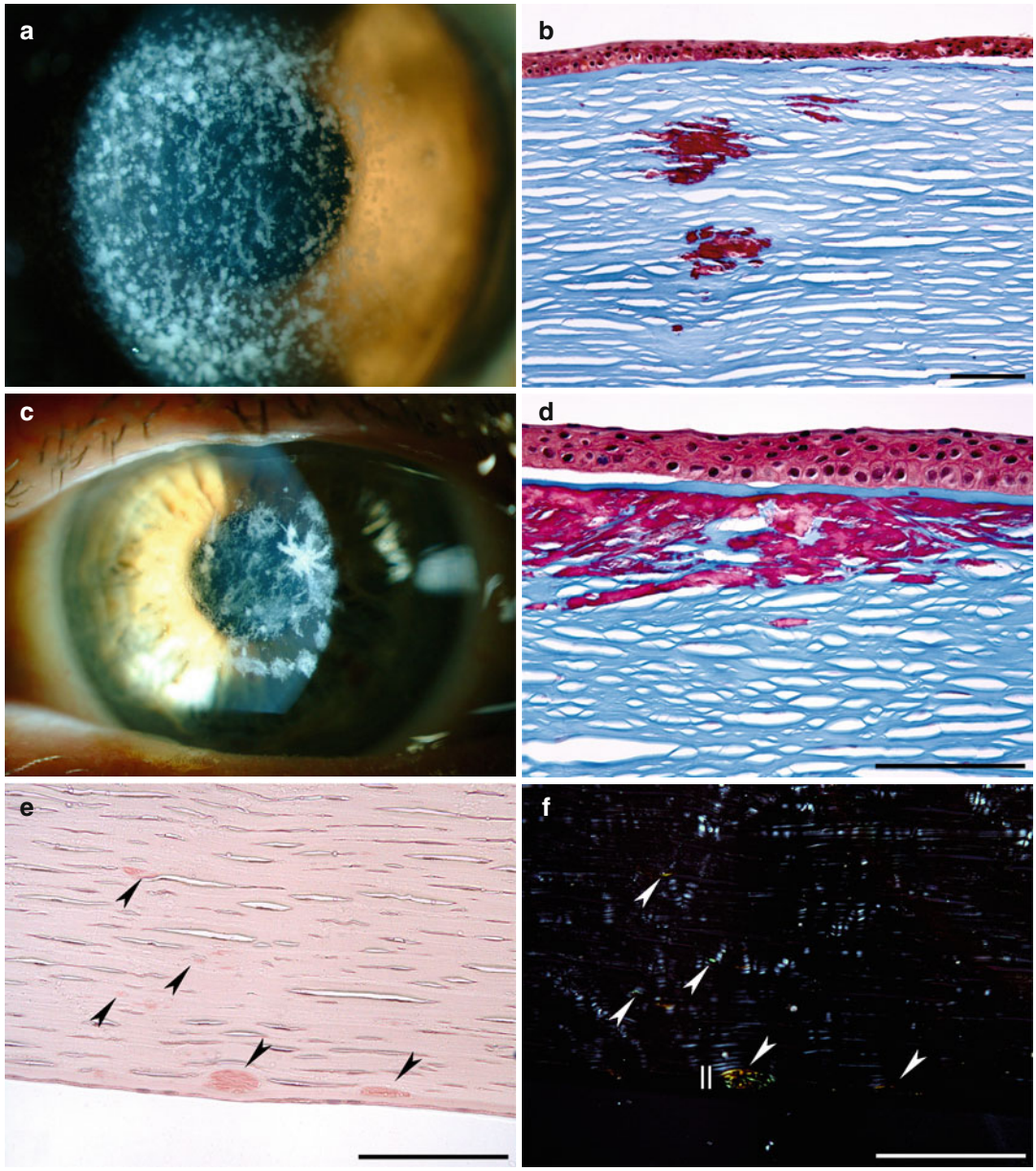

Fig. 3.31 Granular dystrophy, type 1 (**a**, **b**) and type 2 (**c**–**f**). Abundant bread crump-like whitish deposits at all levels of the corneal stroma, mutation unknown (**a**). Irregular epithelium with minor keratohyalin deposits, which stain red with Masson's trichrome, at the level of Bowman's layer and major deposits between stromal lamellae; specimen is from anterior lamellar keratoplasty and thus lacks Descemet's membrane and endothelial cells (**b**). Characteristic star- or snowflake-shaped and patch-like whitish keratohyalin deposits dominate over delicate, deeper, translucent lattice lines that are difficult to identify clinically, Arg124His *TGFBI* mutation (**c**). Microscopically, keratohyalin granules, which also stain partially with Congo red, are prominent in the superficial and midstroma (**d**), whereas small birefringent amyloid deposits (*arrowheads*) are found in the deep stroma (**e**, **f**). Congo red under non-polarised (**e**) and polarised (**f**) light, bars = 100 μm

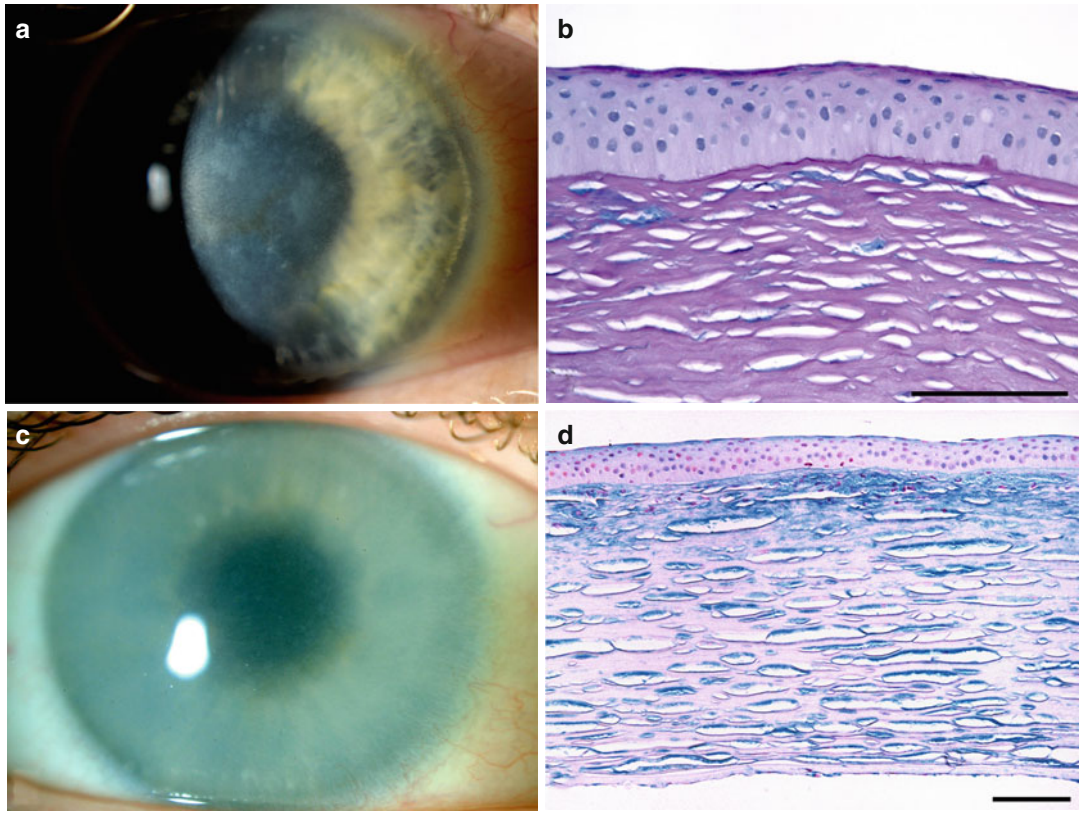

Fig. 3.32 Macular dystrophy (**a**, **b**) as compared with glycosaminoglycan deposition in systemic mucopolysaccharidosis (**c**, **d**). Multiple superficial, centrally located, irregular whitish stromal opacities with background stromal haze (**a**). Bowman's layer has degenerated and blue glycosaminoglycan deposits are seen between stromal lamellae (**b**). Diffuse stromal haze without focal opacities in Hurler-type systemic mucopolysaccharidosis I (MPS IH) (**c**). Bowman's layer is absent and extensive blue glycosaminoglycan deposits are seen throughout the stroma and at the level of the endothelium (**d**). Combined periodic acid-Schiff and Alcian blue (**b**), Alcian blue (**d**), bars = 100 μm

localised corneal mucopolysaccharidosis characterised by deposition of glycosaminoglycans [253, 330].

Epidemiology

Rare except in Iceland [331]; in some countries the rarest stromal dystrophy [306].

Etiology and Genetics

MCD is caused by one of several dozen different mutations in CHST6, coding carbohydrate sulfotransferase 6 [253, 332–334]. It must be differentiated from systemic mucopolysaccharidoses (MPS) with corneal involvement, including Hurler (MPS IH), Scheie (MPS IS), Morquio (MPS IV), Maroteaux-Lamy (MPS VI), and Sly (MPS VII) syndromes [335–337].

Clinical Features

MCD begins in childhood leading to sensitivity to light, occasional recurrent erosions, and severe visual loss by 10–30 years of age. Diffuse haze throughout the cornea is initially seen, followed by superficial, central, elevated, irregular whitish stromal opacities (Fig. 3.32a) [330, 331, 338, 339]. Eventually, Descemet's membrane develops wartlike excrescences and the cornea swells from endothelial decompensation. In systemic mucopolysaccharidoses, diffuse haze persists without localised opacities (Fig. 3.32c).

Histopathology

MCD is best evaluated with Alcian blue stain, which colours blue glycosaminoglycan deposits in stromal keratocytes, extracellularly between stromal lamellae, in endothelial cells, and in Descemet's membrane (Fig. 3.32b). The deposition is more extensive in systemic mucopolysaccharidoses (Fig. 3.32d) [340–344]. Bowman's layer ranges from normal to degenerated. Electron microscopy shows vacuoles and lamellar bodies in keratocytes and endothelial cells and extracellular fibrillogranular material. Antibodies to sulphated epitopes on keratan sulphate distinguish three immunophenotypes [253]. In type I, no reactivity is detected, in type IA keratocytes are immunopositive but extracellular material is not, and in type II, all deposits are immunopositive.

Prognosis

Penetrating keratoplasty will usually become necessary, earlier in systemic mucopolysaccharidoses.

Schnyder's Corneal Dystrophy

Definition

Schnyder's corneal dystrophy (SCD; OMIM #21800, IC3D C1) refers to autosomal dominant deposition of esterified and unesterified phospholipids and cholesterol in the cornea [253].

Synonyms

Previously SCD was designated "crystalline corneal dystrophy", which was misleading because only half of the patients develop intracorneal crystals and patients without them were incorrectly diagnosed with "central discoid corneal dystrophy", which was later shown to be synonymous with SCD [345, 346].

Epidemiology

Infrequent.

Etiology and Genetics

SCD is caused by mutations in *UBIAD1*, coding UbiA prenyltransferase domain-containing 1 [346, 347]. Patients may have hyperlipoproteinaemia type IIa, III, or IV [348, 349].

Clinical Features

SCD begins in childhood but diagnosis in delayed to the second or third decade [348–350]. Patients initially show central corneal haze. Between 25 and 40 years, arcus lipoides develops (Fig. 3.33a, b). After this, midperipheral haze appears, making the cornea entirely hazy. Crystals can emerge or dissolve at any time. Progressive visual loss and glare are typical.

Histopathology

SCD is best evaluated with Sudan Black, Oil Red O, or other lipid stains in fresh-frozen sections, which highlight intra- and extracellular deposits of lipid in basal epithelium, Bowman's layer, and stroma (Fig. 3.33c–e) [351]. Because solvents and resins dissolve lipids, the ophthalmologist should inform the pathologist in advance that lipid stains are requested. The lipid deposits are also visible by electron microscopy [351, 352].

Prognosis

Keratoplasty will usually become necessary.

Congenital Stromal Corneal Dystrophy

Definition

Congenital stromal corneal dystrophy (CSCD; OMIM #610048, IC3D C1) is an autosomal dominant congenital dystrophy causing moderate to severe visual loss [253].

Epidemiology

Rare.

Etiology and Genetics

CSCD is caused by mutations in *DEN*, coding decorin, a pericellular matrix proteoglycan [353, 354].

Clinical Features

CSCD is minimally progressive. The slit lamp shows diffuse corneal clouding and flake-like, whitish stromal opacities at all levels [355]. The cornea is thick.

Histopathology

Under the light microscope, basic corneal architecture is normal, although deposition of

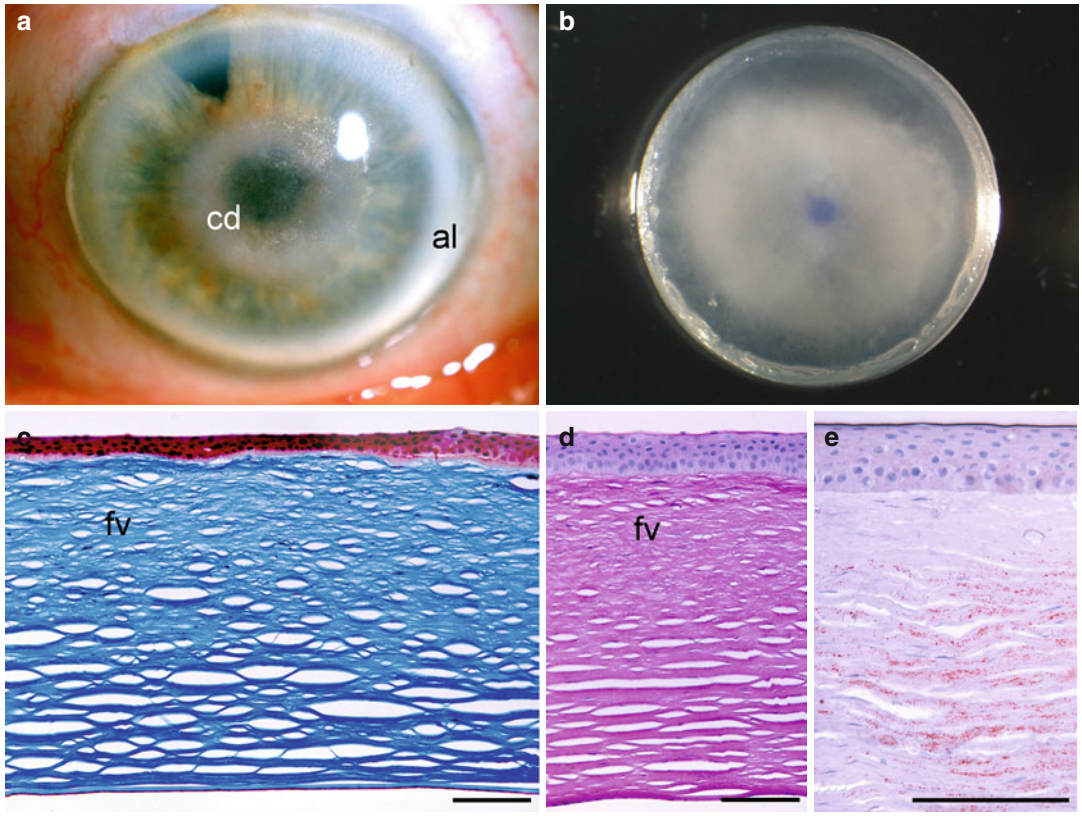

Fig. 3.33 Schnyder's corneal dystrophy. Central disc of deposited lipid (*cd*) with scattered crystals and a prominent peripheral arcus lipoides (*al*) but still clear midperipheral corneal stroma (**a**). Corneal button with a central disc of lipid without crystals from another patient (**b**). Irregular corneal epithelium, destroyed Bowman's layer, and foamy vacuolation of the superficial stroma without any visible deposits either with Masson's trichrome (**c**) or periodic acid-Schiff stains (**d**) in routinely processed tissue. Oil Red O staining of frozen tissue shows myriad tiny lipid droplets within the stroma (**e**), bars = 100 µm

amorphous material may be visible. CSCD is best evaluated by electron microscopy. Abnormal lamellae consisting of randomly arranged thin filaments in electron-lucent ground substance separate normal appearing lamellae [355]. The collagen fibril diameter is approximately half the diameter of normal corneal collagen fibrils.

Prognosis

Penetrating keratoplasty is necessary.

Fleck Corneal Dystrophy

Definition

Fleck corneal dystrophy (FCD; OMIM #121850, IC3D C1) refers to small, discoid or dandruff-like, translucent, sparsely scattered stromal opacities inherited as an autosomal dominant trait [253].

Epidemiology

Rare.

Etiology and Genetics

FCD is caused by mutations in *PIKFYVE*, coding phosphoinositide kinase, FYVE finger-containing, a phosphotransferase of the lipid kinase family, previously also known as *PIP5K3* from 1-phosphatidylinositol-3-phosphate 5-kinase, type III [356].

Clinical Features

FCD is congenital, asymptomatic, and nonprogressive [357–360].

Histopathology

Specimens are rare. FCD is best evaluated with Alcian blue and lipid stains such as Sudan Black and Oil Red O. Swollen, vacuolated keratocytes containing glycosaminoglycans and complex lipids are detected [360]. Electron microscopy shows membrane-based inclusions containing delicate granular material.

Prognosis

Remains typically asymptomatic.

Posterior Amorphous Corneal Dystrophy

Definition

Posterior amorphous corneal dystrophy (PACD; OMIM %612868, IC3D C1) is characterised by a thin, flat cornea, stromal opacification, and involvement of Descemet's membrane [253].

Epidemiology

Rare

Etiology

Deletion of *KER*, *LUM*, *DCN* and *EPYC* on chromosome 12, encoding keratocan, lumican, decorin and epiphycan, respectively [361]. PACD may represent a mesodermal dysgenesis rather than a true dystrophy [362].

Clinical Features

PACD is minimally progressive and causes mild to moderate visual loss [363–366]. It may be associated with iris abnormalities such as posterior embryotoxon, iris processes, pupillary membrane remnants, iridocorneal adhesions, corectopia, and pseudopolycoria.

Histopathology

The posterior stroma is irregular and Descemet's membrane is thin [365]. Electron microscopy shows abnormally oriented collagen fibres and keratocytes in the posterior stroma. A fibrillar layer resembling stromal collagen interrupts Descemet's membrane.

Prognosis

Vision remains adequate in most cases.

Central Cloudy Dystrophy of François

Central cloudy dystrophy of François (CCDF; OMIM #217600, IC3D C4) is clinically similar to posterior crocodile shagreen, a frequent, asymptomatic putative corneal degeneration, and is supposedly transmitted as an autosomal dominant trait [253, 367–369]. It is asymptomatic and nonprogressive. In both conditions, extracellular vacuoles, some of which had fibrillogranular material and electron-dense deposits, were detected by electron microscopy [368, 369].

Pre-Descemet Corneal Dystrophy

Definition

Pre-Descemet corneal dystrophy (PDCD; IC3D C4) refers to fine, grey asymptomatic opacities in the posterior stroma [253].

Etiology

PDCD is an ill-defined, sometimes familial condition without definite pattern of inheritance, and many cases likely represent age-related or secondary degenerative changes; similar findings can be associated with ichthyosis [370].

Clinical Features

Focal to diffuse, fine, grey opacities possibly corresponding to cholesterol sulphate in the posterior stroma anterior to Descemet's membrane are seen with the slit lamp [358, 371, 372].

Histopathology

Light and electron microscopic findings include enlarged keratocytes containing vacuoles and intracellular lipid-like inclusions [373], but have been inconsistent.

3.6.2.4 Descemet's Membrane and Endothelial Dystrophies

Fuchs' Endothelial Corneal Dystrophy

Definition

Fuchs' endothelial corneal dystrophy (FECD; OMIM #136800, IC3D C1/2/3) is characterised by general and focal thickening of Descemet's membrane, loss of endothelial cells, and subsequent stromal and epithelial corneal edema [253].

Epidemiology

About 5 % of patients older than 40 years of age have some drop-like excrescences on Descemet's membrane ("guttae") [374], and the lifetime risk of FCD may approach 0.1 %.

Etiology and Genetics

Most instances of FECD are nonhereditary, but a minority are inherited as a dominant trait and map to chromosomes 13, 15, and 18 [375, 376]. An early-onset variant arises from *COL8A2* mutations on chromosome 1 [377, 378], coding collagen type VIII alpha 2. Late-onset variants have been traced to *ZEB1* on chromosome 10 [379], encoding zinc-finger E box-binding homeobox 1; *AGBL1* on chromosome 15 [380], encoding ATP/GTP-binding protein-like 1; *LOXHD1* and *TCF4* on chromosome 18 [381], encoding lipoxygenase homology domains 1 and transcription factor 4, respectively; and *SLC4A11* on chromosome 20 [382], encoding solute carrier family 4, member 11, but none of these associations are confidently identified as causative [376].

Clinical Features

FCD presents in the fourth to fifth decade, but the early-onset variant causes episodic symptoms already in childhood [374]. Pain, tearing, and sensitivity to light from recurrent erosions are followed by progressive visual loss. The endothelial layer resembles beaten metal under the slit lamp and displays guttae (Fig. 3.34a, c). Stromal and intraepithelial edema with bullae eventually mimic bullous keratopathy (Fig. 3.34b). Subepithelial scarring and neovascular vessels are late findings.

Histopathology

Epithelial bullae, secondary basement membrane dystrophy, and subepithelial fibrous tissue (pannus) are frequent in advanced cases (Fig. 3.34d). All routine stains highlight diffuse thickening and lamination, focal hyaline excrescences (guttae, resembling age-related Hassall-Henle warts), or both, in Descemet's membrane (Fig. 3.34e, f) [383–385]. Endothelial cell density is diminished and the remaining cells have flattened and spread to fill in the gaps. Electron microscopy shows multiple layers of basement membrane material on the posterior aspect of Descemet's membrane, and degenerating endothelial cells [386, 387].

Prognosis

Many patients will progress so as to eventually need lamellar or penetrating keratoplasty.

Posterior Polymorphous Corneal Dystrophy

Definition

Posterior polymorphous corneal dystrophy (PPCD; OMIM #122000, #609140, and #609141, IC3D C1/2) refers to a spectrum of corneal disease that results from mesenchymal to epithelial transition of endothelial cells and varies widely in its clinical presentation, symptoms, extent, and laterality [253].

Etiology and Genetics

Most cases of PPCD are inherited as an autosomal dominant trait. The gene for PPCD1 on chromosome 20 is unknown [376], PPCD2 on chromosome 1 has been associated with – like early-onset Fuchs' corneal dystrophy – with mutations in *COL8A2*, coding collagen type VIII alpha 2 [388], but the evidence is not conclusive [376], and PPCD3 on chromosome 10 arises from mutated *ZEB1* [389, 390] coding zinc-finger E box-binding homeobox 1, a transcription factor. Sporadic cases unrelated to these genes are also known.

Clinical Features

PPCD is often asymmetric, presents in childhood, and is slowly progressive [234, 391–394]. Its severity varies from corneal clouding at birth through later corneal decompensation to no visual loss. By the slit lamp, nodular, vesicular, blister-like, pit-like, and railroad track-like lesions as well as a greyish haze are seen at the level of Descemet's membrane (Fig. 3.35a, b). Peripheral iridocorneal adhesions are seen in one quarter of patients and they may be associated with secondary glaucoma [395].

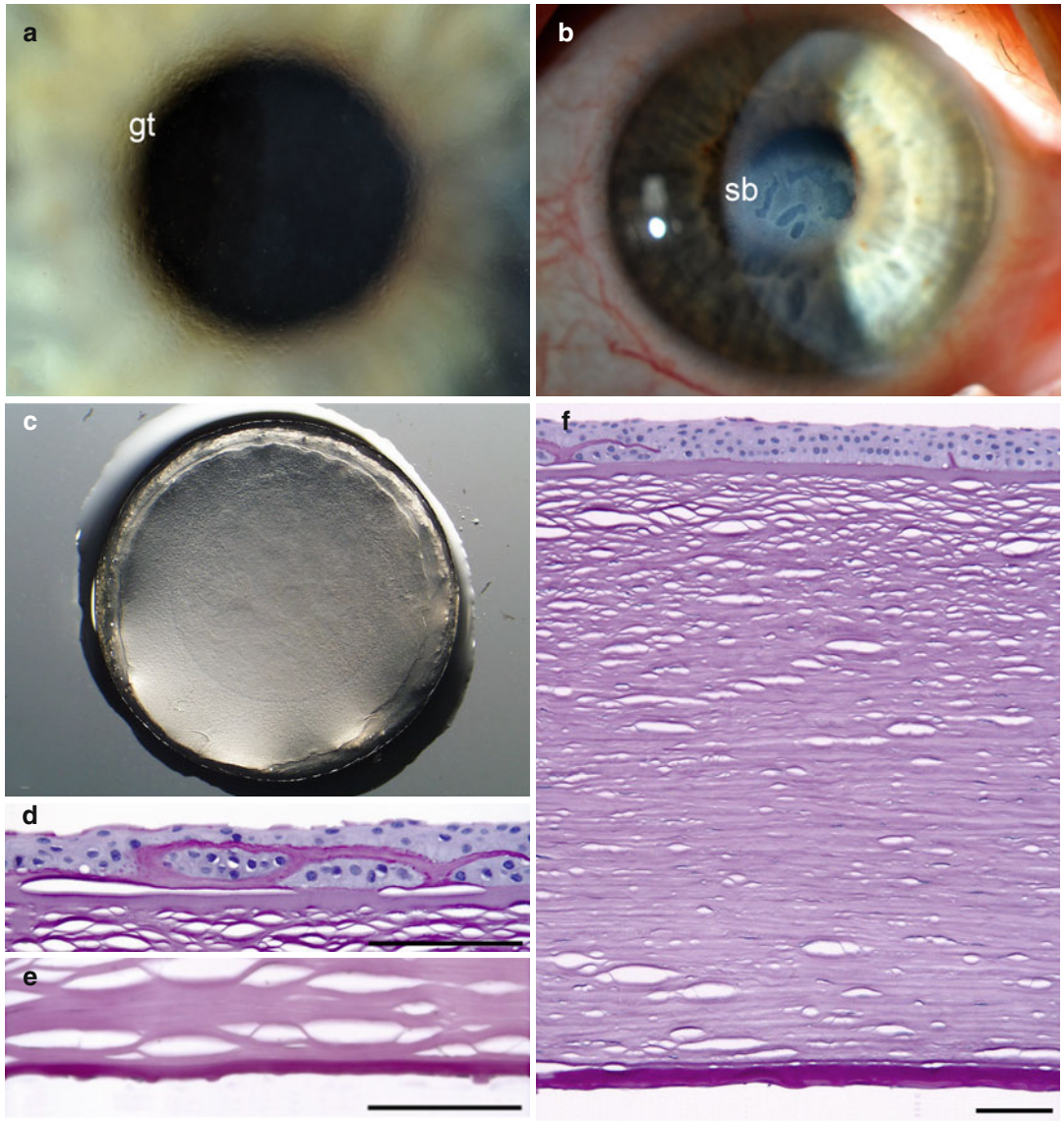

Fig. 3.34 Fuchs' endothelial dystrophy. The posterior cornea at the level of Descemet's membrane is scattered with small drop-like excrescences (guttae, *gt*), which is best appreciated against the pupillary margin (**a**). Secondary epithelial edema with subepithelial bullae (*sb*) and fibrosis (**b**). The guttae cover the entire posterior surface of the corneal button as seen macroscopically; the faint ring is a depression from the trephine used during keratoplasty (**c**). Microscopically, secondary intraepithelial deposition of basement membrane from ruptured bullae mimic epithelial basement membrane dystrophy (**d**). Descemet's membrane either has diffuse multiple guttae (**e**), is diffusely thickened and multilaminar (**f**), or both; note the thick stroma (1,100 µm) and minimal artificial separation of corneal lamellae, indicating marked corneal decompensation. Periodic acid-Schiff (**d**–**f**), bars = 100 µm

Histopathology

PPCD is best evaluated with periodic acid-Schiff and Masson's trichrome stains, which highlight abnormal layers of collagen in Descemet's membrane (Fig. 3.35c–f). In addition, the endothelial layer variably shows blebs, pits, and overlapping cells [393, 396]. By immunohistochemistry, the endothelial cells are labelled especially with antibodies to cytokeratin 7 and 19 like epithelial cells [397]. Electron microscopy reveals thinning or absence of the posterior, non-banded layer of Descemet's

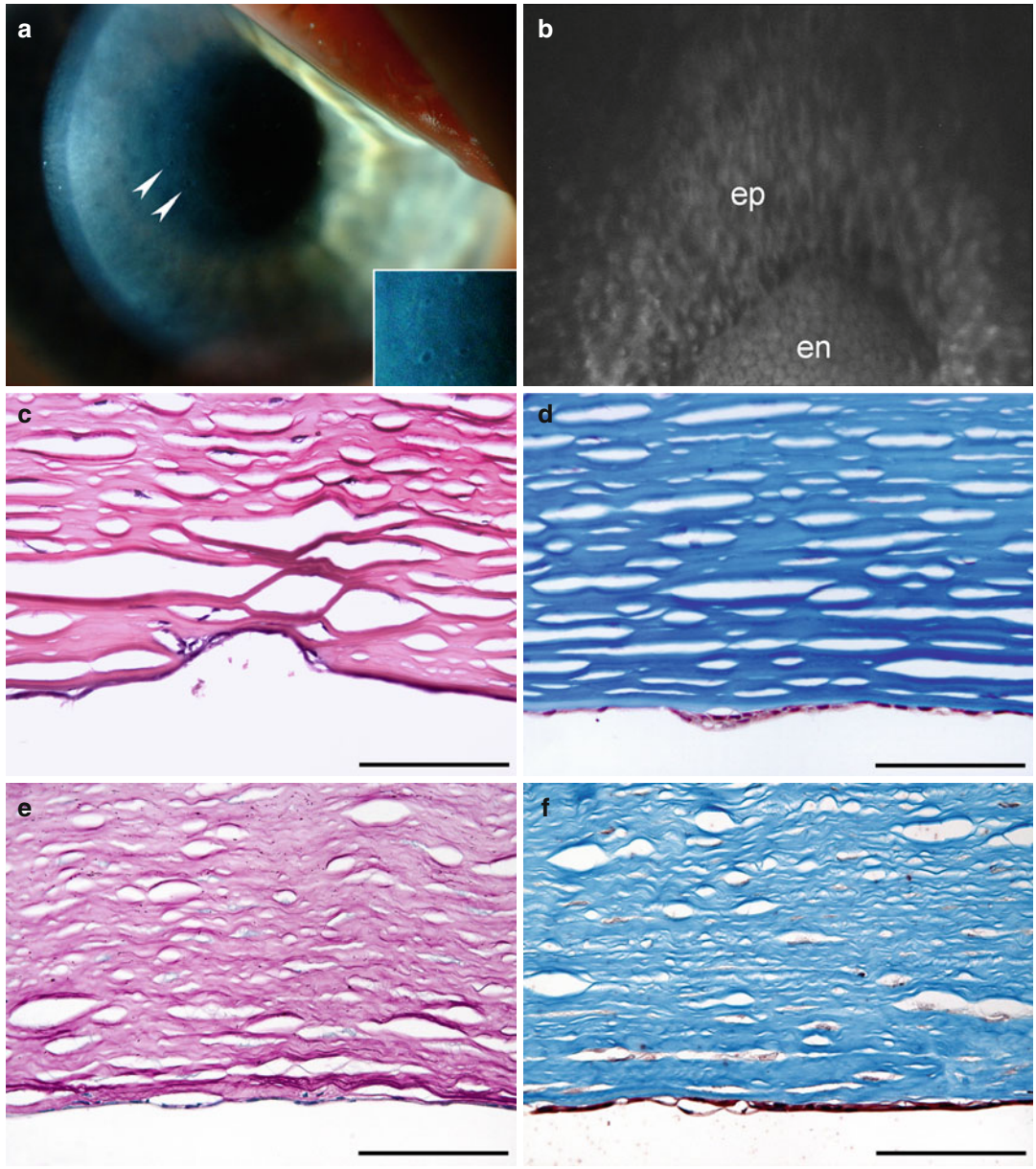

Fig. 3.35 Posterior polymorphous dystrophy. The posterior cornea shows several small pits, visible as darker dots (*arrowheads and inset*) and greyish patches at the level of Descemet's membrane (**a**). Clinical confocal microscopy shows patches of irregular endothelial cells that share characteristics of epithelial cells (*ep*) alternating with more normal endothelial-like (*en*) cells (**b**). Microscopically, the endothelium is replaced with flat epithelial-like cells which dip into posterior stromal defects (**c**), focally grow as more than one layer of cells (**d**), secrete redundant basement membrane material that is multilayered and does not stain strongly with periodic acid-Schiff (**e**) like normal Descemet's membrane does but stains blue with Masson's trichrome (**f**), form blisters (**e**, **f**), and occasionally give rise to elevated strands. Periodic acid-Schiff (**c**, **e**), Masson's trichrome (**d**, **f**), bars = 100 μm

membrane with an abnormal collagenous layer [393, 396, 398]. Microvilli and desmosomes are seen as epithelial cell-like features.

Prognosis

Variable, ranging from asymptomatic cases to need of paediatric keratoplasty. PPMD3 may

progress to corneal ectasia that can be confused with keratoconus [399].

Congenital Hereditary Endothelial Dystrophy

Definition

Congenital hereditary endothelial dystrophies (CHED1; OMIM %121700, IC3D C3, and CHED2; OMIM #217700, IC3D C1) are inherited traits characterised by extreme swelling of the cornea in early childhood [253].

Epidemiology

Rare.

Etiology

CHED1 is autosomal dominant, progressive, and linked to the same locus on chromosome 20 [400] than some cases of posterior polymorphous corneal dystrophy (PPCD1). Because of their overlapping features and rarity, it is unsure whether they are truly separate dystrophies [376]. CHED2 is autosomal recessive, is minimally progressive, and arises from mutations in *SLC4A1* on chromosome 17, coding solute carrier family 4, member 11 [401, 402].

Clinical Features

Both forms are asymmetric [395, 403–407]. CHED1 presents during the first years of life. Mild cases show an endothelium with a moon crater-like texture. Advanced cases result in clouding and extreme swelling of the cornea to up to three times its normal thickness. CHED2 is congenital. The cornea is cloudy, ranging from diffuse haze to a ground glass appearance. Light sensitivity and tearing are minimal, but nystagmus is frequent and the cornea is two to three times its normal thickness.

Histopathology

Both dystrophies are best evaluated with periodic acid-Schiff and Masson's trichrome stains. Findings in CHED1 mimic those of posterior polymorphous dystrophy. In CHED2, Descemet's membrane is diffusely thickened and laminated [403, 404, 406, 408]. The endothelium is atrophic. Electron microscopy shows vacuoles in the remaining endothelial cells [404, 406].

Prognosis

Guarded, paediatric keratoplasty is necessary. Patients with CHED2 may go on to develop sensorineural hearing loss (Harboyan syndrome) [409, 410].

X-Linked Endothelial Corneal Dystrophy

Definition

X-linked endothelial corneal dystrophy (XECD; OMIM %300779, IC3D C2) is characterised by congenital corneal clouding in males [253, 410].

Epidemiology

Rare.

Etiology and Genetics

The gene remains unknown [411].

Clinical Features

XECD is asymptomatic in heterozygotic female carriers. Males experience progressive visual blurring [411]. Slit lamp findings include cratered-like appearance of the endothelial cell layer in females to congenital diffuse haze or ground glass-like appearance in males.

Histopathology

XECD is best evaluated with periodic acid-Schiff stain. The epithelium and Bowman's layer are thin and discontinuous, and the anterior stromal lamellae are irregular [411]. Descemet's membrane is irregularly thickened and has small excavations. Endothelial cells may appear abnormal. Electron microscopy shows subepithelial accumulations of amorphous granular material, absence of the posterior non-banded zone of Descemet's membrane, and absence of desmosome-like junctions and tonofilament bundles from endothelial cells.

Prognosis

Paediatric keratoplasty is needed for severe affection.

3.7 Neoplasms

3.7.1 Primary Tumours

The cornea together with the lens are exceptional tissues in which primary tumours are thought not to develop.

3.7.2 Secondary Tumours

Conjunctival intraepithelial neoplasia (CIN) (see Chap. 2) typically arises at the limbus and often extends to the cornea.

Primary acquired melanosis of the conjunctiva with atypia, (see Chap. 2) alternatively called conjunctival melanocytic intraepithelial neoplasia (C-MIN), will typically extend to the corneal epithelium when the atypical melanocytes have reached the corneal limbus.

Conjunctival melanomas (see Chap. 2) can rarely either loose connection with the limbal conjunctiva and be carried to the cornea or arise from primary acquired melanosis with atypia that has spread to the cornea [412].

References

1. Zieske JD. Corneal development associated with eyelid opening. Int J Dev Biol. 2004;48:903–11.
2. Snell RS, Lemp MA. Clinical anatomy of the eye. 2nd ed. Malden: Blackwell Science; 1998.
3. Yanoff M, Duker JS. Ophthalmology. 2nd ed. St.Louis: Mosby; 2004.
4. Krachmer JH, Mannis M, Holland EJ. Cornea. 2nd ed. Philadelphia: Elsevier Mosby; 2005.
5. Kivelä T, Uusitalo M. Structure, development and function of cytoskeletal elements in non-neuronal cells of the human eye. Prog Retin Eye Res. 1998;17:385–428.
6. Hamrah P, Liu Y, Zhang Q, Dana MR. The corneal stroma is endowed with a significant number of resident dendritic cells. Invest Ophthalmol Vis Sci. 2003;44:581–9.
7. Naumann GOH, Holbach L, Kruse FE. Applied pathology for ophthalmic microsurgeons. Berlin: Springer; 2008.
8. Lavker RM, Tseng SC, Sun TT. Corneal epithelial stem cells at the limbus: looking at some old problems from a new angle. Exp Eye Res. 2004;78:433–46.
9. Giraud JP, Pouliquen Y, Offret G, Payrau P. Statistical morphometric studies in normal human and rabbit corneal stroma. Exp Eye Res. 1975;21:221–9.
10. Komai Y, Ushiki T. The three-dimensional organization of collagen fibrils in the human cornea and sclera. Invest Ophthalmol Vis Sci. 1991;32:2244–58.
11. Dua HS, Faraj LA, Said DG, Gray T, Lowe J. Human corneal anatomy redefined: a novel pre-Descemet's layer (Dua's layer). Ophthalmology. 2013;120:1778–85.
12. Laule A, Cable MK, Hoffman CE, Hanna C. Endothelial cell population changes of human cornea during life. Arch Ophthalmol. 1978;96:2031–5.
13. Müller LJ, Marfurt CF, Kruse F, Tervo TM. Corneal nerves: structure, contents and function. Exp Eye Res. 2003;76:521–42.
14. Schlötzer-Schrehardt U, Kruse FE. Identification and characterization of limbal stem cells. Exp Eye Res. 2005;81:247–64.
15. Grueterich M, Espana EM, Tseng SC. Ex vivo expansion of limbal epithelial stem cells: amniotic membrane serving as a stem cell niche. Surv Ophthalmol. 2003;48:631–46.
16. Aldave AJ, Sonmez B, Bourla N, Schultz G, Papp JC, Salem AK, Rayner SA, Yellore VS. Autosomal dominant cornea plana is not associated with pathogenic mutations in DCN, DSPG3, FOXC1, KERA, LUM, or PITX2. Ophthalmic Genet. 2007;28:57–67.
17. Pellegata NS, Dieguez-Lucena JL, Joensuu T, Lau S, Montgomery KT, Krahe R, Kivelä T, Kucherlapati R, Forsius H, de la Chapelle A. Mutations in KERA, encoding keratocan, cause cornea plana. Nat Genet. 2000;25:91–5.
18. Sigler-Villanueva A, Tahvanainen E, Lindh S, Dieguez-Lucena J, Forsius H. Autosomal dominant cornea plana: clinical findings in a Cuban family and a review of the literature. Ophthalmic Genet. 1997;18:55–62.
19. Forsius H, Damsten M, Eriksson AW, Fellman J, Lindh S, Tahvanainen E. Autosomal recessive cornea plana. A clinical and genetic study of 78 cases in Finland. Acta Ophthalmol Scand. 1998;76:196–203.
20. Al Hazimi A, Khan AO. Axial lengths in children with recessive cornea plana. Ophthal Genet. 2013; Epub ahead of print.
21. Eriksson AW, Lehmann W, Forsius J. Congenital cornea plana in Finland. Clin Genet. 1973;4:301–10.
22. Vesaluoma MH, Sankila EM, Gallar J, Müller LJ, Petroll WM, Moilanen JA, Forsius H, Tervo TM. Autosomal recessive cornea plana: in vivo corneal morphology and corneal sensitivity. Invest Ophthalmol Vis Sci. 2000;41:2120–6.
23. Ruprecht KW, Naumann G. Perforierende Keratoplastik und Histopathologie der Cornea plana. Klinische, histopathologische und elektronenmikroskopische Befunde bei 3 Patienten einer Familie sowie Literaturübersicht. Klin Monbl Augenheilkd. 1974;165:585–94.

24. Harissi-Dagher M, Colby K. Anterior segment dysgenesis: Peters anomaly and sclerocornea. Int Ophthalmol Clin. 2008;48:35–42.
25. Nischal KK. A new approach to the classification of neonatal corneal opacities. Curr Opin Ophthalmol. 2012;23:344–54.
26. Alward WL. Axenfeld-Rieger syndrome in the age of molecular genetics. Am J Ophthalmol. 2000;130: 107–15.
27. Chang TC, Summers CG, Schimmenti LA, Grajewski AL. Axenfeld-Rieger syndrome: new perspectives. Br J Ophthalmol. 2012;96:318–22.
28. Seo S, Singh HP, Lacal PM, Sasman A, Fatima A, Liu T, Schultz KM, Losordo DW, Lehmann OJ, Kume T. Forkhead box transcription factor FoxC1 preserves corneal transparency by regulating vascular growth. Proc Natl Acad Sci U S A. 2012;109: 2015–20.
29. Shields MB. Axenfeld-Rieger syndrome: a theory of mechanism and distinctions from the iridocorneal endothelial syndrome. Trans Am Ophthalmol Soc. 1983;81:736–84.
30. Shields MB, Buckley E, Klintworth GK, Thresher R. Axenfeld-Rieger syndrome. A spectrum of developmental disorders. Surv Ophthalmol. 1985;29:387–409.
31. Ozeki H, Shirai S, Ikeda K, Ogura Y. Anomalies associated with Axenfeld-Rieger syndrome. Graefes Arch Clin Exp Ophthalmol. 1999;237:730–4.
32. Lesnik Oberstein SA, Kriek M, White SJ, Kalf ME, Szuhai K, den Dunnen JT, Breuning MH, Hennekam RC. Peters Plus syndrome is caused by mutations in B3GALTL, a putative glycosyltransferase. Am J Hum Genet. 2006;79:562–6.
33. Heon E, Barsoum-Homsy M, Cevrette L, Jacob JL, Milot J, Polemeno R, Musarella MA. Peters' anomaly. The spectrum of associated ocular and systemic malformations. Ophthalmic Paediatr Genet. 1992;13:137–43.
34. Ozeki H, Shirai S, Nozaki M, Sakurai E, Mizuno S, Ashikari M, Matsunaga N, Ogura Y. Ocular and systemic features of Peters' anomaly. Graefes Arch Clin Exp Ophthalmol. 2000;238:833–9.
35. Bhandari R, Ferri S, Whittaker B, Liu M, Lazzaro DR. Peters anomaly: review of the literature. Cornea. 2011;30:939–44.
36. Majander AS, Lindahl PM, Vasara LK, Krootila K. Anterior segment optical coherence tomography in congenital corneal opacities. Ophthalmology. 2012;119:2450–7.
37. Kuper C, Kuwabara T, Stark WJ. The histopathology of Peters' anomaly. Am J Ophthalmol. 1975;80: 653–60.
38. Fogle JA, Green WR, Kenyon KR, Naquin S, Gadol J. Peripheral Peters' anomaly: a histopathologic case report. J Pediatr Ophthalmol Strabismus. 1978;15: 71–6.
39. Myles WM, Flanders ME, Chitayat D, Brownstein S. Peters' anomaly: a clinicopathologic study. J Pediatr Ophthalmol Strabismus. 1992;29:374–81.
40. Ohkawa K, Saika S, Hayashi Y, Tawara A, Ohnishi Y. Cornea with Peters' anomaly: perturbed differentiation of corneal cells and abnormal extracellular matrix in the corneal stroma. Jpn J Ophthalmol. 2003;47: 327–31.
41. Yang LL, Lambert SR, Lynn MJ, Stulting RD. Surgical management of glaucoma in infants and children with Peters' anomaly: long-term structural and functional outcome. Ophthalmology. 2004;111: 112–7.
42. Chang JW, Kim MK, Kim JH, Kim SJ, Wee WR, Yu YS. Long-term visual outcomes of penetrating keratoplasty for Peters anomaly. Graefes Arch Clin Exp Ophthalmol. 2013;251:953–8.
43. Rao SK, Padmanabhan P. Posterior keratoconus. An expanded classification scheme based on corneal topography. Ophthalmology. 1998;105:1206–12.
44. Varma DK, Brownstein S, Hodge WG, Faraji H. Generalized posterior keratoconus: clinical pathologic correlations. Can J Ophthalmol. 2008;43: 480–2.
45. Tanenbaum HL, Rosen DA. Congenital anterior staphyloma. Am J Ophthalmol. 1966;61:336–40.
46. Gupta DK, Mohan H, Sen DK. Congenital anterior staphyloma. J All India Ophthalmol Soc. 1969;17: 64–6.
47. Leff SR, Shields JA, Augsburger JJ, Sakowski Jr AD, Blair CJ. Congenital corneal staphyloma: clinical, radiological, and pathological correlation. Br J Ophthalmol. 1986;70:427–30.
48. Loeffler KU. Unilateral congenital corneal staphyloma with retinal neovascularization. A case report. Graefes Arch Clin Exp Ophthalmol. 1992;230:318–23.
49. Mikami T, Hayasaka S, Nagaki Y, Yanagisawa S, Futatani T, Takano Y. Congenital corneal staphyloma associated with aphakia. J Pediatr Ophthalmol Strabismus. 2004;41:180–2.
50. Kim MJ, Choung HK, Kim NJ, Khwarg SI. Congenital corneal staphyloma treated by evisceration and primary implant placement: 3 cases. Can J Ophthalmol. 2008;43:111–3.
51. Lunardelli P, Matayoshi S. Congenital anterior staphyloma. J Pediatr Ophthalmol Strab. 2009; Epub Jun 25. doi: 10.3928/01913913-20090616-09.
52. Verschooten R, Foets B, de Ravel T, van Ginderdeuren R, Lombaerts R, Casteels I. Clinical spectrum of congenital corneal staphyloma: a case report. Bull Soc Belge Ophtalmol. 2011;318:7–10.
53. Coster DJ. Treacher Collins Prize Essay, 1979. Inflammatory disease of the outer eye. Trans Ophthalmol Soc U K. 1979;99:463–80.
54. Gundersen T. Conjunctival flaps in the treatment of corneal disease with reference to a new technique of application. Arch Ophthalmol. 1958;60:880–8.
55. Kenyon KR. Inflammatory mechanisms in corneal ulceration. Trans Am Ophthalmol Soc. 1985;83: 610–63.
56. Spencer WH. Cornea. In: Ophthalmic pathology. An atlas and textbook. Philadelphia: WB Saunders; 1985.

57. Bock F, Maruyama K, Regenfuss B, Hos D, Steven P, Heindl LM, Cursiefen C. Novel anti(lymph)angiogenic treatment strategies for corneal and ocular surface diseases. Prog Retin Eye Res. 2013;34:89–124.
58. Cursiefen C, Chen L, Dana MR, Streilein JW. Corneal lymphangiogenesis: evidence, mechanisms, and implications for corneal transplant immunology. Cornea. 2003;22:273–81.
59. Patel SP, Dana R. Corneal lymphangiogenesis: implications in immunity. Semin Ophthalmol. 2009;24: 135–8.
60. The definition and classification of dry eye disease: report of the Definition and Classification Subcommittee of the International Dry Eye WorkShop (2007). Ocul Surf. 2007;5:75–92.
61. Abdel-Khalek LM, Williamson J, Lee WR. Morphological changes in the human conjunctival epithelium. II. In keratoconjunctivitis sicca. Br J Ophthalmol. 1978;62:800–6.
62. Tseng SC. Staging of conjunctival squamous metaplasia by impression cytology. Ophthalmology. 1985;92:728–33.
63. Fraunfelder FT, Wright P, Tripathi RC. Corneal mucus plaques. Am J Ophthalmol. 1977;83:191–7.
64. Foster CS, Calonge M. Atopic keratoconjunctivitis. Ophthalmology. 1990;97:992–1000.
65. Messmer EM, May CA, Stefani FH, Welge-Luessen U, Kampik A. Toxic eosinophil granule protein deposition in corneal ulcerations and scars associated with atopic keratoconjunctivitis. Am J Ophthalmol. 2002;134:816–21.
66. Ghoraishi M, Akova YA, Tugal-Tutkun I, Foster CS. Penetrating keratoplasty in atopic keratoconjunctivitis. Cornea. 1995;14:610–3.
67. Messmer EM, Foster CS. Vasculitic peripheral ulcerative keratitis. Surv Ophthalmol. 1999;43: 379–96.
68. Austin P, Green WR, Sallyer DC, Walsh FB, Kleinfelter HT. Peripheral corneal degeneration and occlusive vasculitis in Wegener's granulomatosis. Am J Ophthalmol. 1978;85:311–7.
69. Frayer WC. The histopathology of perilimbal ulceration in Wegener's granulomatosis. Arch Ophthalmol. 1960;64:58–64.
70. Brown SI. Mooren's ulcer. Histopathology and proteolytic enzymes of adjacent conjunctiva. Br J Ophthalmol. 1975;59:670–4.
71. Foster CS, Kenyon KR, Greiner J, Greineder DK, Friedland B, Allansmith MR. The immunopathology of Mooren's ulcer. Am J Ophthalmol. 1979;88:149–59.
72. Orlans HO, Hornby SJ, Bowler IC. In vitro antibiotic susceptibility patterns of bacterial keratitis isolates in Oxford, UK: a 10-year review. Eye. 2011;25:489–93.
73. Lichtinger A, Yeung SN, Kim P, Amiran MD, Iovieno A, Elbaz U, Ku JY, Wolff R, Rootman DS, Slomovic AR. Shifting trends in bacterial keratitis in Toronto: an 11-year review. Ophthalmology. 2012;119:1785–90.
74. Solomon R, Donnenfeld ED, Azar DT, Holland EJ, Palmon FR, Pflugfelder SC, Rubenstein JB. Infectious keratitis after laser in situ keratomileusis: results of an ASCRS survey. J Cataract Refract Surg. 2003;29: 2001–6.
75. Allen JH, Byers JL. The pathology of ocular leprosy. I. Cornea. Arch Ophthalmol. 1960;64:216–20.
76. Messmer EM, Raizman MB, Foster CS. Lepromatous uveitis diagnosed by iris biopsy. Graefes Arch Clin Exp Ophthalmol. 1998;236:717–9.
77. Dawson CR, Hanna L, Togni B. Adenovirus type 8 infections in the United States. IV. Observations on the pathogenesis of lesions in severe eye disease. Arch Ophthalmol. 1972;87:258–68.
78. Chodosh J, Miller D, Stroop WG, Pflugfelder SC. Adenovirus epithelial keratitis. Cornea. 1995;14: 167–74.
79. Maudgal PC. Cytopathology of adenovirus keratitis by replica technique. Br J Ophthalmol. 1990;74: 670–5.
80. Lund OE, Stefani FH. Corneal histology after epidemic keratoconjunctivitis. Arch Ophthalmol. 1978;96:2085–8.
81. Liesegang TJ, Melton III LJ, Daly PJ, Ilstrup DM. Epidemiology of ocular herpes simplex. Incidence in Rochester, Minn, 1950 through 1982. Arch Ophthalmol. 1989;107:1155–9.
82. Maudgal PC, Missotten L. Histopathology of human superficial herpes simplex keratitis. Br J Ophthalmol. 1978;62:46–52.
83. Heiligenhaus A, Foster CS. Histological and immunopathological analysis of T-cells mediating murine HSV-1 keratitis. Graefes Arch Clin Exp Ophthalmol. 1994;232:628–34.
84. Mietz H, Cassinotti P, Siegl G, Kirchhof B, Krieglstein GK. Detection of herpes simplex virus after penetrating keratoplasty by polymerase chain reaction: correlation of clinical and laboratory findings. Graefes Arch Clin Exp Ophthalmol. 1995;233:714–6.
85. Shimomura Y, Deai T, Fukuda M, Higaki S, Hooper LC, Hayashi K. Corneal buttons obtained from patients with HSK harbor high copy numbers of the HSV genome. Cornea. 2007;26:190–3.
86. Shtein RM, Garcia DD, Musch DC, Elner VM. Herpes simplex virus keratitis: histopathologic inflammation and corneal allograft rejection. Ophthalmology. 2009;116:1301–5.
87. Green WR, Zimmerman LE. Granulomatous reaction to Descemet's membrane. Am J Ophthalmol (Suppl). 1967;64:555–8.
88. Dolin R, Reichman RC, Mazur MH, Whitley RJ. NIH conference. Herpes zoster-varicella infections in immunosuppressed patients. Ann Intern Med. 1978;89:375–88.
89. Miller AE. Selective decline in cellular immune response to varicella-zoster in the elderly. Neurology. 1980;30:582–7.
90. Mahalingam R, Wellish M, Wolf W, Dueland AN, Cohrs R, Vafai A, Gilden D. Latent varicella-zoster viral DNA in human trigeminal and thoracic ganglia. N Engl J Med. 1990;323:627–31.

91. Pavan-Langston D, Yamamoto S, Dunkel EC. Delayed herpes zoster pseudodendrites. Polymerase chain reaction detection of viral DNA and a role for antiviral therapy. Arch Ophthalmol. 1995;113: 1381–5.
92. Liesegang TJ. Corneal complications from herpes zoster ophthalmicus. Ophthalmology. 1985;92: 316–24.
93. Pavan-Langston D, McCulley JP. Herpes zoster dendritic keratitis. Arch Ophthalmol. 1973;89:25–9.
94. Zaal MJ, Volker-Dieben HJ, Wienesen M, D'Amaro J, Kijlstra A. Longitudinal analysis of varicella-zoster virus DNA on the ocular surface associated with herpes zoster ophthalmicus. Am J Ophthalmol. 2001;131:25–9.
95. Yu DD, Lemp MA, Mathers WD, Espy M, White T. Detection of varicella-zoster virus DNA in disciform keratitis using polymerase chain reaction. Arch Ophthalmol. 1993;111:167–8.
96. Wenkel H, Rummelt C, Rummelt V, Jahn G, Fleckenstein B, Naumann GO. Detection of varicella zoster virus DNA and viral antigen in human cornea after herpes zoster ophthalmicus. Cornea. 1993;12:131–7.
97. Wenkel H, Rummelt V, Fleckenstein B, Naumann GO. Detection of varicella zoster virus DNA and viral antigen in human eyes after herpes zoster ophthalmicus. Ophthalmology. 1998;105:1323–30.
98. Heigle TJ, Pflugfelder SC. Aqueous tear production in patients with neurotrophic keratitis. Cornea. 1996;15:135–8.
99. Naumann G, Gass JD, Font RL. Histopathology of herpes zoster ophthalmicus. Am J Ophthalmol. 1968;65:533–41.
100. Hedges III TR, Albert DM. The progression of the ocular abnormalities of herpes zoster. Histopathologic observations of nine cases. Ophthalmology. 1982;89: 165–77.
101. Forster RK, Rebell G. Therapeutic surgery in failures of medical treatment for fungal keratitis. Br J Ophthalmol. 1975;59:366–71.
102. Naumann G, Green WR, Zimmerman LE. Mycotic infections: a histopathologic study of 73 cases. Am J Ophthalmol. 1967;64:668–82.
103. Lund OE, Stefani FH, Dechant W. Amoebic keratitis: a clinicopathological case report. Br J Ophthalmol. 1978;62:373–5.
104. Kelly LD. Reevaluation of host corneal tissue 1955 to 1970: Calcofluor white staining for occult acanthamoebic infection. Ann Ophthalmol. 1992;24: 345–6.
105. Radford CF, Lehmann OJ, Dart JK. Acanthamoeba keratitis: multicentre survey in England 1992-6. National Acanthamoeba Keratitis Study Group. Br J Ophthalmol. 1998;82:1387–92.
106. Yang YF, Matheson M, Dart JK, Cree IA. Persistence of acanthamoeba antigen following acanthamoeba keratitis. Br J Ophthalmol. 2001;85:277–80.
107. Marines HM, Osato MS, Font RL. The value of calcofluor white in the diagnosis of mycotic and Acanthamoeba infections of the eye and ocular adnexa. Ophthalmology. 1987;94:23–6.
108. Silvany RE, Luckenbach MW, Moore MB. The rapid detection of Acanthamoeba in paraffin-embedded sections of corneal tissue with calcofluor white. Arch Ophthalmol. 1987;105:1366–7.
109. Wilhelmus KR, Osato MS, Font RL, Robinson NM, Jones DB. Rapid diagnosis of Acanthamoeba keratitis using calcofluor white. Arch Ophthalmol. 1986;104:1309–12.
110. Kremer I, Cohen EJ, Eagle Jr RC, Udell I, Laibson PR. Histopathologic evaluation of stromal inflammation in Acanthamoeba keratitis. CLAO J. 1994;20:45–8.
111. Mietz H, Font RL. Acanthamoeba keratitis with granulomatous reaction involving the stroma and anterior chamber. Arch Ophthalmol. 1997;115: 259–63.
112. Lowder CY, Meisler DM, McMahon JT, Longworth DL, Rutherford I. Microsporidia infection of the cornea in a man seropositive for human immunodeficiency virus. Am J Ophthalmol. 1990;109:242–4.
113. Theng J, Chan C, Ling ML, Tan D. Microsporidial keratoconjunctivitis in a healthy contact lens wearer without human immunodeficiency virus infection. Ophthalmology. 2001;108:976–8.
114. Lowder CY, McMahon JT, Meisler DM, Dodds EM, Calabrese LH, Didier ES, Cali A. Microsporidial keratoconjunctivitis caused by Septata intestinalis in a patient with acquired immunodeficiency syndrome. Am J Ophthalmol. 1996;121:715–7.
115. Rossi P, Urbani C, Donelli G, Pozio E. Resolution of microsporidial sinusitis and keratoconjunctivitis by itraconazole treatment. Am J Ophthalmol. 1999;127:210–2.
116. Kuckelkorn R, Luft I, Kottek AA, Schrage NF, Makropoulos W, Reim M. Veratzungen und Verbrennungen im Einzugsbereich der RWTH Aachen. Analyse der Unfalle über 1 Jahr mit Hilfe einer neuen automatischen Befunddokumentation. Klin Monatsbl Augenheilk. 1993;203:34–42.
117. Pfister RR, Haddox JL, Sommers CI, Lam KW. Identification and synthesis of chemotactic tripeptides from alkali-degraded whole cornea. A study of N-acetyl-proline-glycine-proline and N-methyl-proline-glycine-proline. Invest Ophthalmol Vis Sci. 1995;36:1306–16.
118. Sotozono C, He J, Matsumoto Y, Kita M, Imanishi J, Kinoshita S. Cytokine expression in the alkali-burned cornea. Curr Eye Res. 1997;16:670–6.
119. Brown SI, Weller CA, Akiya S. Pathogenesis of ulcers of the alkali-burned cornea. Arch Ophthalmol. 1970;83:205–8.
120. Wagoner MD. Chemical injuries of the eye: current concepts in pathophysiology and therapy. Surv Ophthalmol. 1997;41:275–313.
121. Hirst LW, Fogle JA, Kenyon KR, Stark WJ. Corneal epithelial regeneration and adhesion following acid burns in the rhesus monkey. Invest Ophthalmol Vis Sci. 1982;23:764–73.

122. Sippel KC, Pineda Jr R. Phacoemulsification and thermal wound injury. Semin Ophthalmol. 2002;17:102–9.
123. Baradaran-Rafii A, Eslani M, Tseng SC. Sulfur mustard-induced ocular surface disorders. Ocul Surf. 2011;9:163–78.
124. Javadi MA, Yazdani S, Sajjadi H, Jadidi K, Karimian F, Einollahi B, Ja'farinasab MR, Zare M. Chronic and delayed-onset mustard gas keratitis: report of 48 patients and review of literature. Ophthalmology. 2005;112:617–25.
125. Richter MN, Wachtlin J, Bechrakis NE, Hoffmann F. Keratoplasty after mustard gas injury: clinical outcome and histology. Cornea. 2006;25:467–9.
126. Kanavi MR, Javadi A, Javadi MA. Chronic and delayed mustard gas keratopathy: a histopathologic and immunohistochemical study. Eur J Ophthalmol. 2010;20:839–43.
127. Wilson SE, He YG, Weng J, Li Q, McDowall AW, Vital M, Chwang EL. Epithelial injury induces keratocyte apoptosis: hypothesized role for the interleukin-1 system in the modulation of corneal tissue organization and wound healing. Exp Eye Res. 1996;62:325–7.
128. Heyworth P, Morlet N, Rayner S, Hykin P, Dart J. Natural history of recurrent erosion syndrome - a 4 year review of 117 patients. Br J Ophthalmol. 1982;1998:26–8.
129. Das S, Seitz B. Recurrent corneal erosion syndrome. Surv Ophthalmol. 2008;53:3–15.
130. Chen YT, Huang CW, Huang FC, Tseng SY, Tseng SH. The cleavage plane of corneal epithelial adhesion complex in traumatic recurrent corneal erosion. Mol Vis. 2006;12:196–204.
131. Sakimoto T, Sawa M. Metalloproteinases in corneal diseases: degradation and processing. Cornea (Suppl). 2012;31:S50–6.
132. Dursun D, Kim MC, Solomon A, Pflugfelder SC. Treatment of recalcitrant recurrent corneal erosions with inhibitors of matrix metalloproteinase-9, doxycycline and corticosteroids. Am J Ophthalmol. 2001;132:8–13.
133. Slingsby JG, Forstot SL. Effect of blunt trauma on the corneal endothelium. Arch Ophthalmol. 1981;99:1041–3.
134. Rohrbach JM, Weidle EG, Steuhl KP, Meilinger S, Pleyer U. Traumatic wound dehiscence after penetrating keratoplasty. Acta Ophthalmol Scand. 1996;74:501–5.
135. Foroutan AR, Gheibi GH, Joshaghani M, Ahadian A, Foroutan P. Traumatic wound dehiscence and lens extrusion after penetrating keratoplasty. Cornea. 2009;28:1097–9.
136. Wittpenn Jr JR, Hirst LW, Green WR. Histopathologic study of traumatic corneal endothelial rings. Md State Med J. 1982;31:43–5.
137. Spencer WH, Ferguson Jr WJ, Shaffer RN, Fine M. Late degenerative changes in the cornea following breaks in Descemet's membrane. Trans Am Acad Ophthalmol Otolaryngol. 1966;70:973–83.
138. Honig MA, Barraquer J, Perry HD, Riquelme JL, Green WR. Forceps and vacuum injuries to the cornea: histopathologic features of twelve cases and review of the literature. Cornea. 1996;15:463–72.
139. Tetsumoto K, Kubota T, Rummelt V, Holbach LM, Naumann GO. Epithelial transformation of the corneal endothelium in forceps birth-injury-associated keratopathy. Cornea. 1993;12:65–71.
140. Reed JW. Corneal tattooing to reduce glare in cases of traumatic iris loss. Cornea. 1994;13:401–5.
141. Sekundo W, Seifert P, Seitz B, Loeffler KU. Long-term ultrastructural changes in human corneas after tattooing with non-metallic substances. Br J Ophthalmol. 1999;83:219–24.
142. Sharma A, Gupta P, Dogra MR, Hidayat AA, Gupta A. Granulomatous keratitis following corneal tattooing. Indian J Ophthalmol. 2003;51:265–7.
143. Kletzky DL, Parver LM, Mathers WD. Correlation of full-thickness corneal wound length with endothelial cell loss. Ophthalmic Surg. 1992;23:342–6.
144. Stramer BM, Zieske JD, Jung JC, Austin JS, Fini ME. Molecular mechanisms controlling the fibrotic repair phenotype in cornea: implications for surgical outcomes. Invest Ophthalmol Vis Sci. 2003;44:4237–46.
145. Connon CJ, Meek KM. The structure and swelling of corneal scar tissue in penetrating full-thickness wounds. Cornea. 2004;23:165–71.
146. McCally RL, Freund DE, Zorn A, Bonney-Ray J, Grebe R, de la Cruz Z, Green WR. Light-scattering and ultrastructure of healed penetrating corneal wounds. Invest Ophthalmol Vis Sci. 2007;48:157–65.
147. Rosentreter A, Schild AM, Wedemeyer I, Dietlein TS. Epithelimplantationszysten – 48 Jahre nach Bulbuspenetration. Ophthalmologe. 2010;107:753–6.
148. Küchle M, Green WR. Epithelial ingrowth: a study of 207 histopathologically proven cases. Ger J Ophthalmol. 1996;5:211–23.
149. Wollensak G, Spoerl E, Seiler T. Riboflavin/ultraviolet-A-induced collagen crosslinking for the treatment of keratoconus. Am J Ophthalmol. 2003;135:620–7.
150. Wollensak G, Spoerl E, Seiler T. Stress-strain measurements of human and porcine corneas after riboflavin-ultraviolet-A-induced cross-linking. J Cataract Refract Surg. 2003;29:1780–5.
151. Mencucci R, Marini M, Paladini I, Sarchielli E, Sgambati E, Menchini U, Vannelli GB. Effects of riboflavin/UVA corneal cross-linking on keratocytes and collagen fibres in human cornea. Clin Exp Ophthalmol. 2010;38:49–56.
152. Messmer EM, Meyer P, Herwig MC, Loeffler KU, Schirra F, Seitz B, Thiel M, Reinhard T, Kampik A, Auw-Haedrich C. Morphological and immunohistochemical changes after corneal cross-linking. Cornea. 2013;32:111–7.
153. Ruckhofer J, Twa MD, Schanzlin DJ. Clinical characteristics of lamellar channel deposits after implantation of Intacs. J Cataract Refract Surg. 2000;26:1473–9.

154. Twa MD, Ruckhofer J, Kash RL, Costello M, Schanzlin DJ. Histologic evaluation of corneal stroma in rabbits after intrastromal corneal ring implantation. Cornea. 2003;22:146–52.
155. Spirn MJ, Dawson DG, Rubinfeld RS, Burris C, Talamo J, Edelhauser HF, Grossniklaus HE. Histopathological analysis of post-laser-assisted in situ keratomileusis corneal ectasia with intrastromal corneal ring segments. Arch Ophthalmol. 2005;123: 1604–7.
156. Bourges JL, Trong TT, Ellies P, Briat B, Renard G. Intrastromal corneal ring segments and corneal anterior stromal necrosis. J Cataract Refract Surg. 2003;29:1228–30.
157. Garana RM, Petroll WM, Chen WT, Herman IM, Barry P, Andrews P, Cavanagh HD, Jester JV. Radial keratotomy. II. Role of the myofibroblast in corneal wound contraction. Invest Ophthalmol Vis Sci. 1992;33:3271–82.
158. Jester JV, Villasenor RA, Schanzlin DJ, Cavanagh HD. Variations in corneal wound healing after radial keratotomy: possible insights into mechanisms of clinical complications and refractive effects. Cornea. 1992;11:191–9.
159. Melles GR, Binder PS, Moore MN, Anderson JA. Epithelial-stromal interactions in human keratotomy wound healing. Arch Ophthalmol. 1995;113: 1124–30.
160. Vinger PF, Mieler WF, Oestreicher JH, Easterbrook M. Ruptured globes following radial and hexagonal keratotomy surgery. Arch Ophthalmol. 1996;114: 129–34.
161. Peacock LW, Slade SG, Martiz J, Chuang A, Yee RW. Ocular integrity after refractive procedures. Ophthalmology. 1997;104:1079–83.
162. Binder PS, Beal Jr JP, Zavala EY. The histopathology of a case of keratophakia. Arch Ophthalmol. 1982;100:101–5.
163. Binder PS, Baumgartner SD, Fogle JA. Histopathology of a case of epikeratophakia (aphakic epikeratoplasty). Arch Ophthalmol. 1985;103: 1357–63.
164. Wang RG, Hjortdal JO, Ehlers N, Krogh E. Histopathological findings in failed human epikeratophakia lenticules. Acta Ophthalmol. 1994;72: 363–8.
165. Zamir E, Solomon A. Interface corneal epithelial cyst following epikeratoplasty. Arch Ophthalmol. 2003;121:1510.
166. SundarRaj N, Geiss III MJ, Fantes F, Hanna K, Anderson SC, Thompson KP, Thoft RA, Waring III GO. Healing of excimer laser ablated monkey corneas. An immunohistochemical evaluation. Arch Ophthalmol. 1990;108:1604–10.
167. Kahle G, Daqun X, Seiler T, Schroter-Kermani C, Wollensak J. Wundheilung der Kornea von Neuweltaffen nach flachiger Keratektomie: Er:YAG-Excimerlaser. Fortschrit Ophthalmol. 1991;88: 380–5.
168. Wu WC, Stark WJ, Green WR. Corneal wound healing after 193-nm excimer laser keratectomy. Arch Ophthalmol. 1991;109:1426–32.
169. Farah SG, Azar DT, Gurdal C, Wong J. Laser in situ keratomileusis: literature review of a developing technique. J Cataract Refract Surg. 1998;24: 989–1006.
170. Helena MC, Baerveldt F, Kim WJ, Wilson SE. Keratocyte apoptosis after corneal surgery. Invest Ophthalmol Vis Sci. 1998;39:276–83.
171. Mohan RR, Hutcheon AE, Choi R, Hong J, Lee J, Mohan RR, Ambrosio Jr R, Zieske JD, Wilson SE. Apoptosis, necrosis, proliferation, and myofibroblast generation in the stroma following LASIK and PRK. Exp Eye Res. 2003;76:71–87.
172. Alio JL, Javaloy J. Corneal inflammation following corneal photoablative refractive surgery with excimer laser. Surv Ophthalmol. 2013;58:11–25.
173. Dawson DG, Kramer TR, Grossniklaus HE, Waring III GO, Edelhauser HF. Histologic, ultrastructural, and immunofluorescent evaluation of human laser-assisted in situ keratomileusis corneal wounds. Arch Ophthalmol. 2005;123:741–56.
174. Kramer TR, Chuckpaiwong V, Dawson DG, L'Hernault N, Grossniklaus HE, Edelhauser HF. Pathologic findings in postmortem corneas after successful laser in situ keratomileusis. Cornea. 2005;24:92–102.
175. Dawson DG, Randleman JB, Grossniklaus HE, O'Brien TP, Dubovy SR, Schmack I, Stulting RD, Edelhauser HF. Corneal ectasia after excimer laser keratorefractive surgery: histopathology, ultrastructure, and pathophysiology. Ophthalmology. 2008;115:2181–91.
176. Geggel HS, Coday MP. Late-onset traumatic laser in situ keratomileusis (LASIK) flap dehiscence. Am J Ophthalmol. 2001;131:505–6.
177. Aldave AJ, Hollander DA, Abbott RL. Late-onset traumatic flap dislocation and diffuse lamellar inflammation after laser in situ keratomileusis. Cornea. 2002;21:604–7.
178. Fogle JA, Kenyon KR, Foster CS. Tissue adhesive arrests stromal melting in the human cornea. Am J Ophthalmol. 1980;89:795–802.
179. Robin JB, Lee CF, Riley JM. Preliminary evaluation of two experimental surgical adhesives in the rabbit cornea. Refract Corneal Surg. 1989;5:302–6.
180. Lim LS, How AC, Ang LP, Tan DT. Gundersen flaps in the management of ocular surface disease in an Asian population. Cornea. 2009;28:747–51.
181. von Versen-Höynck F, Syring C, Bachmann S, Möller DE. The influence of different preservation and sterilisation steps on the histological properties of amnion allografts–light and scanning electron microscopic studies. Cell Tissue Bank. 2004;5: 45–56.
182. Resch MD, Schlötzer-Schrehardt U, Hofmann-Rummelt C, Sauer R, Kruse FE, Beckmann MW, Seitz B. Integration patterns of cryopreserved

amniotic membranes into the human cornea. Ophthalmology. 2006;113:1927–35.
183. Stoiber J, Muss WH, Pohla-Gubo G, Ruckhofer J, Grabner G. Histopathology of human corneas after amniotic membrane and limbal stem cell transplantation for severe chemical burn. Cornea. 2002;21:482–9.
184. Seitz B, Resch MD, Schlötzer-Schrehardt U, Hofmann-Rummelt C, Sauer R, Kruse FE. Histopathology and ultrastructure of human corneas after amniotic membrane transplantation. Arch Ophthalmol. 2006;124:1487–90.
185. Said DG, Nubile M, Alomar T, Hopkinson A, Gray T, Lowe J, Dua HS. Histologic features of transplanted amniotic membrane: implications for corneal wound healing. Ophthalmology. 2009;116:1287–95.
186. Kenyon KR, Tseng SC. Limbal autograft transplantation for ocular surface disorders. Ophthalmology. 1989;96:709–22.
187. Tsai RJ, Sun TT, Tseng SC. Comparison of limbal and conjunctival autograft transplantation in corneal surface reconstruction in rabbits. Ophthalmology. 1990;97:446–55.
188. Shimazaki J, Kaido M, Shinozaki N, Shimmura S, Munkhbat B, Hagihara M, Tsuji K, Tsubota K. Evidence of long-term survival of donor-derived cells after limbal allograft transplantation. Invest Ophthalmol Vis Sci. 1999;40:1664–8.
189. Thompson Jr RW, Price MO, Bowers PJ, Price Jr FW. Long-term graft survival after penetrating keratoplasty. Ophthalmology. 2003;110:1396–402.
190. Waldock A, Cook SD. Corneal transplantation: how successful are we? Br J Ophthalmol. 2000;84:813–5.
191. Khodadoust AA, Silverstein AM. The survival and rejection of epithelium in experimental corneal transplants. Invest Ophthalmol. 1969;8:169–79.
192. Boisjoly HM, Bernard PM, Dube I, Laughrea PA, Bazin R, Bernier J. Effect of factors unrelated to tissue matching on corneal transplant endothelial rejection. Am J Ophthalmol. 1989;107:647–54.
193. Arenas E, Esquenazi S, Anwar M, Terry M. Lamellar corneal transplantation. Surv Ophthalmol. 2012;57:510–29.
194. Ting DS, Ramaesh K, Srinivasan S, Sau CY, Mantry S, Roberts F. Deep anterior lamellar keratoplasty: challenges in histopathological examination. Br J Ophthalmol. 2012;96:1510–2.
195. Suh LH, Dawson DG, Mutapcic L, Rosenfeld SI, Culbertson WW, Yoo SH, O'Brien TP, Dubovy SR. Histopathologic examination of failed grafts in Descemet's stripping with automated endothelial keratoplasty. Ophthalmology. 2009;116:603–8.
196. Heindl LM, Schlötzer-Schrehardt U, Cursiefen C, Bachmann BO, Hofmann-Rummelt C, Kruse FE. Myofibroblast metaplasia after Descemet membrane endothelial keratoplasty. Am J Ophthalmol. 2011;151:1019–23.
197. Ham L, van der Wees J, Melles GR. Causes of primary donor failure in Descemet membrane endothelial keratoplasty. Am J Ophthalmol. 2008;145:639–44.
198. Netland PA, Terada H, Dohlman CH. Glaucoma associated with keratoprosthesis. Ophthalmology. 1998;105:751–7.
199. Nouri M, Terada H, Alfonso EC, Foster CS, Durand ML, Dohlman CH. Endophthalmitis after keratoprosthesis: incidence, bacterial causes, and risk factors. Arch Ophthalmol. 2001;119:484–9.
200. Chalam KV, Chokshi A, Agarwal S, Edward DP. Complications of AlphaCor keratoprosthesis: a clinicopathologic report. Cornea. 2007;26:1258–60.
201. Kiang L, Rosenblatt MI, Sartaj R, Fernandez AG, Kiss S, Radcliffe NM, D'Amico DJ, Sippel KC. Surface epithelialization of the type I Boston keratoprosthesis front plate: immunohistochemical and high-definition optical coherence tomography characterization. Graefes Arch Clin Exp Ophthalmol. 2012;250:1195–9.
202. Stacy RC, Jakobiec FA, Michaud NA, Dohlman CH, Colby KA. Characterization of retrokeratoprosthetic membranes in the Boston type 1 keratoprosthesis. Arch Ophthalmol. 2011;129:310–6.
203. Dudenhoefer EJ, Nouri M, Gipson IK, Baratz KH, Tisdale AS, Dryja TP, Abad JC, Dohlman CH. Histopathology of explanted collar button keratoprostheses: a clinicopathologic correlation. Cornea. 2003;22:424–8.
204. Stoiber J, Csáky D, Schedle A, Ruckhofer J, Grabner G. Histopathologic findings in explanted osteo-odontokeratoprosthesis. Cornea. 2002;21:400–4.
205. Caiazza S, Falcinelli G, Pintucci S. Exceptional case of bone resorption in an osteo-odonto-keratoprosthesis. A scanning electron microscopy and X-ray microanalysis study. Cornea. 1990;9:23–7.
206. Ricci R, Pecorella I, Ciardi A, Della Rocca C, Di Tondo U, Marchi V. Strampelli's osteo-odonto-keratoprosthesis. Clinical and histological long-term features of three prostheses. Br J Ophthalmol. 1992;76:232–4.
207. Gokhale NS. Epidemiology of keratoconus. Indian J Ophthalmol. 2013;61:382–3.
208. Wallang BS, Das S. Keratoglobus. Eye. 2013;27:1004–12.
209. Wheeler J, Hauser MA, Afshari NA, Allingham RR, Liu Y. The genetics of keratoconus: a review. Reprod Syst Sex Disord. 2012;(Suppl 6):001, doi: 10.4172/2161-038X.S6-001.
210. Davidson AE, Hayes S, Hardcastle AJ, Tuft SJ. The pathogenesis of keratoconus. Eye. 2014;28:189–95.
211. Romero-Jimenez M, Santodomingo-Rubido J, Wolffsohn JS. Keratoconus: a review. Cont Lens Anterior Eye. 2010;33:157–66.
212. Fernandes BF, Logan P, Zajdenweber ME, Santos LN, Cheema DP, Burnier Jr MN. Histopathological study of 49 cases of keratoconus. Pathology. 2008;40:623–6.

213. Sykakis E, Carley F, Irion L, Denton J, Hillarby MC. An in depth analysis of histopathological characteristics found in keratoconus. Pathology. 2012;44: 234–9.
214. Meghpara B, Nakamura H, Vemuganti GK, Murthy SI, Sugar J, Yue BY, Edward DP. Histopathologic and immunohistochemical studies of keratoglobus. Arch Ophthalmol. 2009;127:1029–35.
215. Jinabhai A, Radhakrishnan H, O'Donnell C. Pellucid corneal marginal degeneration: a review. Cont Lens Anterior Eye. 2011;34:56–63.
216. Akhtar S, Kirat O, Alkatan H, Shu X, Almubrad T. Ultrastructural features of corneas with pellucid marginal degeneration. Microsc Res Tech. 2013;76:404–11.
217. Liu L, Wu J, Geng J, Yuan Z, Huang D. Geographical prevalence and risk factors for pterygium: a systematic review and meta-analysis. BMJ Open. 2013;3:e003787.
218. Taylor HR. Risk factors for pterygium. Ophthalmology. 2013;120:441.
219. Perra MT, Maxia C, Zucca I, Piras F, Sirigu P. Immunohistochemical study of human pterygium. Histol Histopathol. 2002;17:139–49.
220. Reid TW, Dushku N. What a study of pterygia teaches us about the cornea? Molecular mechanisms of formation. Eye Contact Lens. 2010;36:290–5.
221. Chui J, Coroneo MT, Tat LT, Crouch R, Wakefield D, Di Girolamo N. Ophthalmic pterygium: a stem cell disorder with premalignant features. Am J Pathol. 2011;178:817–27.
222. Livezeanu C, Craitoiu MM, Manescu R, Mocanu C, Craitoiu S. Angiogenesis in the pathogenesis of pterygium. Rom J Morphol Embryol. 2011;52:837–44.
223. Eze BI, Maduka-okafor FC, Okoye OI, Chuka-okosa CM. Pterygium: a review of clinical features and surgical treatment. Niger J Med. 2011;20:7–14.
224. Hirst LW, Axelsen RA, Schwab I. Pterygium and associated ocular surface squamous neoplasia. Arch Ophthalmol. 2009;127:31–2.
225. Artornsombudh P, Sanpavat A, Tinnungwattana U, Tongkhomsai V, Sansopha L, Tulvatana W. Prevalence and clinicopathologic findings of conjunctival epithelial neoplasia in pterygia. Ophthalmology. 2013;120:1337–40.
226. Oellers P, Karp CL, Sheth A, Kao AA, Abdelaziz A, Matthews JL, Dubovy SR, Galor A. Prevalence, treatment, and outcomes of coexistent ocular surface squamous neoplasia and pterygium. Ophthalmology. 2013;120:445–50.
227. Vojniković B, Njirić S, Zamolo G, Toth I, Apanjol J, Coklo M. Histopathology of the pterygium in population on Croatian Island Rab. Coll Antropol. 2007;31 Suppl 1:39–41.
228. Jakobiec FA, Stacy RC, Mendoza PR, Chodosh J. Hyperplastic corneal pannus: an immunohistochemical analysis and review. Surv Ophthalmol. 2014;59:448–53.
229. Bourcier T, Baudrimont M, Boutboul S, Thomas F, Borderie V, Laroche L. Corneal keloid: clinical, ultrasonographic, and ultrastructural characteristics. J Cataract Refract Surg. 2004;30:921–4.
230. Chawla B, Agarwal A, Kashyap S, Tandon R. Diagnosis and management of corneal keloid. Clin Experiment Ophthalmol. 2007;35:855–7.
231. Vanathi M, Panda A, Kai S, Sen S. Corneal keloid. Ocul Surf. 2008;6:186–98.
232. Maust HA, Raber IM. Peripheral hypertrophic subepithelial corneal degeneration. Eye Contact Lens. 2003;29:266–9.
233. Jeng BH, Millstein ME. Reduction of hyperopia and astigmatism after superficial keratectomy of peripheral hypertrophic subepithelial corneal degeneration. Eye Contact Lens. 2006;32:153–6.
234. Gore DM, Iovieno A, Connell BJ, Alexander R, Meligonis G, Dart JK. Peripheral hypertrophic subepithelial corneal degeneration: nomenclature, phenotypes, and long-term outcomes. Ophthalmology. 2013;120:892–8.
235. Järventausta PJ, Holopainen JM, Zalentein WN, Paakkanen R, Wennerström A, Seppänen M, Lokki ML, Tervo TM. Peripheral hypertrophic subepithelial corneal degeneration: characterization, treatment and association with human leucocyte antigen genes. Acta Ophthalmol. 2014;92: 71–6.
236. Järventausta PJ, Tervo TM, Kivelä T, Holopainen JM. Peripheral hypertrophic subepithelial corneal degeneration-clinical and histopathological features. Acta Ophthalmol. 2014.
237. Graue-Hernandez EO, Mannis MJ, Eliasieh K, Greasby TA, Beckett LA, Bradley JC, Schwab IR. Salzmann nodular degeneration. Cornea. 2010;29:283–9.
238. Hamada S, Darrad K, McDonnell PJ. Salzmann's nodular corneal degeneration (SNCD): clinical findings, risk factors, prognosis and the role of previous contact lens wear. Cont Lens Anterior Eye. 2011;34:173–8.
239. Meltendorf C, Buhren J, Bug R, Ohrloff C, Kohnen T. Correlation between clinical in vivo confocal microscopic and ex vivo histopathologic findings of Salzmann nodular degeneration. Cornea. 2006;25:734–8.
240. Stone DU, Astley RA, Shaver RP, Chodosh J. Histopathology of Salzmann nodular corneal degeneration. Cornea. 2008;27:148–51.
241. Jhanji V, Rapuano CJ, Vajpayee RB. Corneal calcific band keratopathy. Curr Opin Ophthalmol. 2011;22: 283–9.
242. O'Connor GR. Calcific band keratopathy. Trans Am Ophthalmol Soc. 1972;70:58–81.
243. Hunold AC, Dithmar S. Hämatokornea. Klin Monbl Augenheilkd. 2007;224:736–7.
244. Graf B, Calvet MA, D'esperey-Fougères R-E, hamard H, Dhermy P, Pouliquen Y. Les siderosomes dans l'hematocornee. Arch Ophtalmol Rev Gen Ophtalmol. 1974;34:477–88.
245. Urrets-Zavalia JA, Knoll EG, Maccio JP, Urrets-Zavalia EA, Saad JA, Serra HM. Climatic droplet keratopathy in the Argentine Patagonia. Am J Ophthalmol. 2006;141:744–6.

246. Schurr TG, Dulik MC, Cafaro TA, Suarez MF, Urrets-Zavalia JA, Serra HM. Genetic background and climatic droplet keratopathy incidence in a mapuche population from Argentina. PLoS One. 2013;8:e74593.
247. Kaji Y, Nagai R, Amano S, Takazawa Y, Fukayama M, Oshika T. Advanced glycation end product deposits in climatic droplet keratopathy. Br J Ophthalmol. 2007;91:85–8.
248. Holopainen JM, Serra HM, Sanchez MC, Sorsa T, Zalentein WN, Barcelona PF, Moilanen JA, Tervahartiala T, Tervo TM, Cafaro TA, Virtanen I, Urrets-Zavalia EA, Bhattacharya SK, Urrets-Zavalia JA. Altered expression of matrix metalloproteinases and their tissue inhibitors as possible contributors to corneal droplet formation in climatic droplet keratopathy. Acta Ophthalmol. 2011;89:569–74.
249. Gray RH, Johnson GJ, Freedman A. Climatic droplet keratopathy. Surv Ophthalmol. 1992;36:241–53.
250. Urrets-Zavalia JA, Croxatto JO, Holopainen JM, Cafaro TA, Esposito F, Neira W, Serra HM. In vivo confocal microscopy study of climatic droplet keratopathy. Eye. 2012;26:1021–3.
251. Bhikoo R, Niederer RL, Hart R, Sherwin T, McGhee CN. In vivo confocal microscopy of climatic droplet keratopathy. Clin Exp Optom. 2013;96:430–2.
252. Johnson GJ, Overall M. Histology of spheroidal degeneration of the cornea in Labrador. Br J Ophthalmol. 1978;62:53–61.
253. Weiss JS, Møller HU, Lisch W, Kinoshita S, Aldave AJ, Belin MW, Kivelä T, Busin M, Munier FL, Seitz B, Sutphin J, Bredrup C, Mannis MJ, Rapuano CJ, Van Rij G, Kim EK, Klintworth GK. The IC3D classification of the corneal dystrophies. Cornea. 2008;27 Suppl 2:S1–83.
254. Aldave AJ. The genetics of the corneal dystrophies. Dev Ophthalmol. 2011;48:51–66.
255. Online Mendelian Inheritance in Man, OMIM®. 2014. McKusick-Nathans Institute of Genetic Medicine, Johns Hopkins University, Baltimore, MD. 15 Dec 2013. http://omim.org/.
256. Wood TO, Griffith ME. Corneal epithelial basement membrane dystrophy. Trans Am Ophthalmol Soc. 1987;85:281–92.
257. Boutboul S, Black GC, Moore JE, Sinton J, Menasche M, Munier FL, Laroche L, Abitbol M, Schorderet DF. A subset of patients with epithelial basement membrane corneal dystrophy have mutations in TGFBI/BIGH3. Hum Mutat. 2006;27:553–7.
258. Ehlers N, Møller HU. Dot-map-fingerprint dystrophy – Cogan's microcystic dystrophy – normal reactions of the corneal epithelium? Acta Ophthalmol Suppl. 1987;182:62–6.
259. Cogan DG, Donaldson DD, Kuwabara T, Marshall D. Microcystic dystrophy of the corneal epithelium. Trans Am Ophthalmol Soc. 1964;62:213–25.
260. Laibson PR. Recurrent corneal erosions and epithelial basement membrane dystrophy. Eye Contact Lens. 2010;36:315–7.
261. Rosenberg ME, Tervo TM, Petroll WM, Vesaluoma MH. In vivo confocal microscopy of patients with corneal recurrent erosion syndrome or epithelial basement membrane dystrophy. Ophthalmology. 2000;107:565–73.
262. Labbe A, Nicola RD, Dupas B, Auclin F, Baudouin C. Epithelial basement membrane dystrophy: evaluation with the HRT II Rostock Cornea Module. Ophthalmology. 2006;113:1301–8.
263. Bozkurt B, Irkec M. In vivo laser confocal microscopic findings in patients with epithelial basement membrane dystrophy. Eur J Ophthalmol. 2009;19:348–54.
264. Cogan DG, Kuwabara T, Donaldson DD, Collins E. Microcystic dystrophy of the cornea. A partial explanation for its pathogenesis. Arch Ophthalmol. 1974;92:470–4.
265. Dark AJ. Bleb dystrophy of the cornea: histochemistry and ultrastructure. Br J Ophthalmol. 1977;61:65–9.
266. Bron AJ, Burgess SE. Inherited recurrent corneal erosion. Trans Ophthalmol Soc U K. 1981;101(Pt 2):239–43.
267. Lisch W, Bron AJ, Munier FL, Schorderet DF, Tiab L, Lange C, Saikia P, Reinhard T, Weiss JS, Gundlach E, Pleyer U, Lisch C, Auw-Haedrich C. Franceschetti hereditary recurrent corneal erosion. Am J Ophthalmol. 2012;153:1073–81.
268. Hammar B, Lagali N, Ek S, Seregard S, Dellby A, Fagerholm P. Dystrophia Smolandiensis: a novel morphological picture of recurrent corneal erosions. Acta Ophthalmol. 2010;88:394–400.
269. Hammar B, Björck E, Lind H, Lagerstedt K, Dellby A, Fagerholm P. Dystrophia Helsinglandica: a new type of hereditary corneal recurrent erosions with late subepithelial fibrosis. Acta Ophthalmol. 2009;87:659–65.
270. Neira W, Hammar B, Holopainen JM, Tuisku I, Dellby A, Tervo T, Fagerholm P. Dystrophia Helsinglandica – corneal morphology, topography and sensitivity in a hereditary corneal disease with recurrent erosive episodes. Acta Ophthalmol. 2010;88:401–6.
271. Feder RS, Jay M, Yue BY, Stock EL, O'Grady RB, Roth SI. Subepithelial mucinous corneal dystrophy. Clinical and pathological correlations. Arch Ophthalmol. 1993;111:1106–14.
272. Irvine AD, Corden LD, Swensson O, Swensson B, Moore JE, Frazer DG, Smith FJ, Knowlton RG, Christophers E, Rochels R, Uitto J, McLean WH. Mutations in cornea-specific keratin K3 or K12 genes cause Meesmann's corneal dystrophy. Nat Genet. 1997;16:184–7.
273. Sullivan LS, Baylin EB, Font R, Daiger SP, Pepose JS, Clinch TE, Nakamura H, Zhao XC, Yee RW. A novel mutation of the Keratin 12 gene responsible for a severe phenotype of Meesmann's corneal dystrophy. Mol Vis. 2007;13:975–80.
274. Ehlers N, Hjortdal J, Nielsen K, Thiel HJ, Orntoft T. Phenotypic variability in Meesmann's dystrophy: clinical review of the literature and presentation of a family genetically identical to the original family. Acta Ophthalmol. 2008;86:40–4.

275. Patel DV, Grupcheva CN, McGhee CN. Imaging the microstructural abnormalities of Meesmann corneal dystrophy by in vivo confocal microscopy. Cornea. 2005;24:669–73.
276. Javadi MA, Rezaei-Kanavi M, Javadi A, Naghshgar N. Meesmann corneal dystrophy; a clinicopathologic, ultrastructural and confocal scan report. J Ophthalmic Vis Res. 2010;5:122–6.
277. Ogasawara M, Matsumoto Y, Hayashi T, Ohno K, Yamada H, Kawakita T, Dogru M, Shimazaki J, Tsubota K, Tsuneoka H. KRT12 Mutations and in vivo confocal microscopy in two Japanese families with Meesmann corneal dystrophy. Am J Ophthalmol. 2014;157:93–102.
278. Fine BS, Yanoff M, Pitts E, Slaughter FD. Meesmann's epithelial dystrophy of the cornea. Am J Ophthalmol. 1977;83:633–42.
279. Tremblay M, Dube I. Meesmann's corneal dystrophy: ultrastructural features. Can J Ophthalmol. 1982;17:24–8.
280. Lisch W, Steuhl KP, Lisch C, Weidle EG, Emmig CT, Cohen KL, Perry HD. A new, band-shaped and whorled microcystic dystrophy of the corneal epithelium. Am J Ophthalmol. 1992;114:35–44.
281. Kurbanyan K, Sejpal KD, Aldave AJ, Deng SX. In vivo confocal microscopic findings in Lisch corneal dystrophy. Cornea. 2012;31:437–41.
282. Alvarez-Fischer M, de Toledo JA, Barraquer RI. Lisch corneal dystrophy. Cornea. 2005;24:494–5.
283. Kawasaki S, Kinoshita S. Clinical and basic aspects of gelatinous drop-like corneal dystrophy. Dev Ophthalmol. 2011;48:97–115.
284. Ide T, Nishida K, Maeda N, Tsujikawa M, Yamamoto S, Watanabe H, Tano Y. A spectrum of clinical manifestations of gelatinous drop-like corneal dystrophy in Japan. Am J Ophthalmol. 2004;137:1081–4.
285. Tsujikawa M, Kurahashi H, Tanaka T, Nishida K, Shimomura Y, Tano Y, Nakamura Y. Identification of the gene responsible for gelatinous drop-like corneal dystrophy. Nat Genet. 1999;21:420–3.
286. Ren Z, Lin PY, Klintworth GK, Iwata F, Munier FL, Schorderet DF, El ML, Theendakara V, Basti S, Reddy M, Hejtmancik JF. Allelic and locus heterogeneity in autosomal recessive gelatinous drop-like corneal dystrophy. Hum Genet. 2002;110:568–77.
287. Uhlig CE, Groppe M, Busse H, Saeger W. Morphological and histopathological changes in gelatinous drop-like corneal dystrophy during a 15-year follow-up. Acta Ophthalmol. 2010;88:e273–4.
288. Magalhaes OA, Rymer S, Marinho DR, Kwitko S, Cardoso IH, Kliemann L. Optical coherence tomography image in gelatinous drop-like corneal dystrophy: case report. Arq Bras Oftalmol. 2012;75:356–7.
289. Quantock AJ, Nishida K, Kinoshita S. Histopathology of recurrent gelatinous drop-like corneal dystrophy. Cornea. 1998;17:215–21.
290. Akiya S, Furukawa H, Sakamoto H, Takahashi H, Sakka Y. Histopathologic and immunohistochemical findings in gelatinous drop-like corneal dystrophy. Ophthalmic Res. 1990;22:371–6.
291. Klintworth GK, Valnickova Z, Kielar RA, Baratz KH, Campbell RJ, Enghild JJ. Familial subepithelial corneal amyloidosis – a lactoferrin-related amyloidosis. Invest Ophthalmol Vis Sci. 1997;38:2756–63.
292. Küchle M, Green WR, Völcker HE, Barraquer J. Reevaluation of corneal dystrophies of Bowman's layer and the anterior stroma (Reis-Bücklers and Thiel-Behnke types): a light and electron microscopic study of eight corneas and a review of the literature. Cornea. 1995;14:333–54.
293. Weidle EG. Die wabenformige Hornhautdystrophie (Thiel-Behnke). Neubewertung und Abgrenzung gegenüber der Reis-Bücklers'schen Hornhautdystrophie. Klin Monbl Augenheilkd. 1999;214:125–35.
294. Munier FL, Korvatska E, Djemai A, le Paslier D, Zografos L, Pescia G, Schorderet DF. Kerato-epithelin mutations in four 5q31-linked corneal dystrophies. Nat Genet. 1997;15:247–51.
295. Okada M, Yamamoto S, Tsujikawa M, Watanabe H, Inoue Y, Maeda N, Shimomura Y, Nishida K, Quantock AJ, Kinoshita S, Tano Y. Two distinct kerato-epithelin mutations in Reis-Bücklers corneal dystrophy. Am J Ophthalmol. 1998;126:535–42.
296. Bücklers M. Über eine weitere familiäre Hornhautdystrophie (Reis). Klin Monbl Augenheilkd. 1949;114:386–97.
297. Kobayashi A, Sugiyama K. In vivo laser confocal microscopy findings for Bowman's layer dystrophies (Thiel-Behnke and Reis-Bücklers corneal dystrophies). Ophthalmology. 2007;114:69–75.
298. Nakamura H, Li FT, Foltermann MO, Macsai M, Ma X, Zhao XC, Flaherty K, Yee RW. Individual phenotypic variances in a family with Thiel-Behnke corneal dystrophy. Cornea. 2012;31:1217–22.
299. Lisch W, Kivelä T. Individual phenotypic variances in a family with Thiel-Behnke corneal dystrophy. Cornea. 2013;32:e192–3.
300. Thiel HJ, Behnke H. Eine bisher unbekannte subepitheliale hereditäre Hornhautdystrophie. Klin Monbl Augenheilkd. 1967;150:862–74.
301. Chen YJ, Chen JT, Lu DW, Tai MC. In vivo corneal confocal microscopic findings and gene analysis of three patients with Thiel-Behnke corneal dystrophy. Br J Ophthalmol. 2010;94:262–4.
302. Grayson M, Wilbrandt H. Dystrophy of the anterior limiting membrane of the cornea. (Reis-Bückler type). Am J Ophthalmol. 1966;61:345–9.
303. Meretoja J. Familial systemic paramyloidosis with lattice dystrophy of the cornea, progressive cranial neuropathy, skin changes and various internal symptoms. A previously unrecognized heritable syndrome. Ann Clin Res. 1969;1:314–24.
304. Pihlamaa T, Rautio J, Kiuru-Enari S, Suominen S. Gelsolin amyloidosis as a cause of early aging and progressive bilateral facial paralysis. Plast Reconstr Surg. 2011;127:2342–51.

305. Kiuru-Enari S, Haltia M. Hereditary gelsolin amyloidosis. Handb Clin Neurol. 2013;115:659–81.
306. Abreu EB, Novaes GA, Fernandes BF, Odashiro PR, Odashiro AN, Parizotto IO, Burnier Jr MN. Corneal stromal dystrophies: a clinical pathologic study. Arq Bras Oftalmol. 2012;75:390–3.
307. Maury CP, Kere J, Tolvanen R, de la Chapelle A. Finnish hereditary amyloidosis is caused by a single nucleotide substitution in the gelsolin gene. FEBS Lett. 1990;276:75–7.
308. Levy E, Haltia M, Fernandez-Madrid I, Koivunen O, Ghiso J, Prelli F, Frangione B. Mutation in gelsolin gene in Finnish hereditary amyloidosis. J Exp Med. 1990;172:1865–7.
309. Gruenauer-Kloevekorn C, Clausen I, Weidle E, Wolter-Roessler M, Tost F, Völcker HE, Schulze DP, Heinritz W, Reinhard T, Froster U, Duncker G, Schorderet D, Auw-Haedrich C. TGFBI (BIGH3) gene mutations in German families: two novel mutations associated with unique clinical and histopathological findings. Br J Ophthalmol. 2009;93:932–7.
310. Hirano K, Hotta Y, Nakamura M, Fujiki K, Kanai A, Yamamoto N. Late-onset form of lattice corneal dystrophy caused by Leu527Arg mutation of the TGFBI gene. Cornea. 2001;20:525–9.
311. Takács L, Losonczy G, Matesz K, Balogh I, Sohajda Z, Tóth K, Fazakas F, Vereb G, Berta A. TGFBI (BIGH3) gene mutations in Hungary – report of the novel F547S mutation associated with polymorphic corneal amyloidosis. Mol Vis. 2007;13:1976–83.
312. Liskova P, Klintworth GK, Bowling BL, Filipec M, Jirsova K, Tuft SJ, Bhattacharya SS, Hardcastle AJ, Ebenezer ND. Phenotype associated with the H626P mutation and other changes in the TGFBI gene in Czech families. Ophthalmic Res. 2008;40:105–8.
313. Meretoja J. Comparative histopathological and clinical findings in eyes with lattice corneal dystrophy of two different types. Ophthalmologica. 1972;165:15–37.
314. Rosenberg ME, Tervo TM, Gallar J, Acosta MC, Müller LJ, Moilanen JA, Tarkkanen AH, Vesaluoma MH. Corneal morphology and sensitivity in lattice dystrophy type II (familial amyloidosis, Finnish type). Invest Ophthalmol Vis Sci. 2001;42:634–41.
315. Kivelä T, Tarkkanen A, McLean I, Ghiso J, Frangione B, Haltia M. Immunohistochemical analysis of lattice corneal dystrophies types I and II. Br J Ophthalmol. 1993;77:799–804.
316. Folberg R, Stone EM, Sheffield VC, Mathers WD. The relationship between granular, lattice type 1, and Avellino corneal dystrophies. A histopathologic study. Arch Ophthalmol. 1994;112:1080–5.
317. Patel DA, Chang SH, Harocopos GJ, Vora SC, Thang DH, Huang AJ. Granular and lattice deposits in corneal dystrophy caused by R124C mutation of TGFBIp. Cornea. 2010;29:1215–22.
318. Edelstein SL, Huang AJ, Harocopos GJ, Waltman SR. Genotype of lattice corneal dystrophy (R124C mutation in TGFBI) in a patient presenting with features of Avellino corneal dystrophy. Cornea. 2010;29:698–700.
319. Kivelä T, Tarkkanen A, Frangione B, Ghiso J, Haltia M. Ocular amyloid deposition in familial amyloidosis, Finnish: an analysis of native and variant gelsolin in Meretoja's syndrome. Invest Ophthalmol Vis Sci. 1994;35:3759–69.
320. Zhao SJ, Zhu YN, Shentu XC, Miao Q. Chinese family with atypical granular corneal dystrophy type I caused by the typical R555W mutation in TGFBI. Int J Ophthalmol. 2013;6:458–62.
321. Zhu Y, Shentu X, Wang W. The TGFBI R555W mutation induces a new granular corneal dystrophy type I phenotype. Mol Vis. 2011;17:225–30.
322. Møller HU. Granular corneal dystrophy Groenouw type I. 115 Danish patients. An epidemiological and genetic population study. Acta Ophthalmol (Copenh). 1990;68:297–303.
323. Leopardi S, Cucinotta A, Chetri A, Appolloni R, Balacco-Gabrieli C. Histochemistry and electron-microscopic observation in two cases of granular dystrophy of the cornea. Ophthalmologica. 1991;203:164–7.
324. Folberg R, Alfonso E, Croxatto JO, Driezen NG, Panjwani N, Laibson PR, Boruchoff SA, Baum J, Malbran ES, Fernandez-Meijide R. Clinically atypical granular corneal dystrophy with pathologic features of lattice-like amyloid deposits. A study of these families. Ophthalmology. 1988;95:46–51.
325. Kim SW, Hong S, Kim T, Kim KS, Kim TI, Chung WS, Kim EK. Characteristic features of granular deposit formation in granular corneal dystrophy type 2. Cornea. 2011;30:848–54.
326. Rosenwasser GO, Sucheski BM, Rosa N, Pastena B, Sebastiani A, Sassani JW, Perry HD. Phenotypic variation in combined granular-lattice (Avellino) corneal dystrophy. Arch Ophthalmol. 1993;111:1546–52.
327. Han KE, Choi SI, Chung WS, Jung SH, Katsanis N, Kim TI, Kim EK. Extremely varied phenotypes in granular corneal dystrophy type 2 heterozygotes. Mol Vis. 2012;18:1755–62.
328. Abazi Z, Magarasevic L, Grubisa I, Risovic D. Individual phenotypic variances in a family with Avellino corneal dystrophy. BMC Ophthalmol. 2013;13:30.
329. Aldave AJ, Sonmez B, Forstot SL, Rayner SA, Yellore VS, Glasgow BJ. A clinical and histopathologic examination of accelerated TGFBIp deposition after LASIK in combined granular-lattice corneal dystrophy. Am J Ophthalmol. 2007;143:416–9.
330. Klintworth GK, VOGEL FS. Macular corneal dystrophy. An inherited acid mucopolysaccharide storage disease of the corneal fibroblast. Am J Pathol. 1964;45:565–86.
331. Jonasson F, Oshima E, Thonar EJ, Smith CF, Johannsson JH, Klintworth GK. Macular corneal dystrophy in Iceland. A clinical, genealogic, and immunohistochemical study of 28 patients. Ophthalmology. 1996;103:1111–7.

332. Akama TO, Nishida K, Nakayama J, Watanabe H, Ozaki K, Nakamura T, Dota A, Kawasaki S, Inoue Y, Maeda N, Yamamoto S, Fujiwara T, Thonar EJ, Shimomura Y, Kinoshita S, Tanigami A, Fukuda MN. Macular corneal dystrophy type I and type II are caused by distinct mutations in a new sulphotransferase gene. Nat Genet. 2000;26:237–41.
333. Liu NP, Smith CF, Bowling BL, Jonasson F, Klintworth GK. Macular corneal dystrophy types I and II are caused by distinct mutations in the CHST6 gene in Iceland. Mol Vis. 2006;12:1148–52.
334. Klintworth GK, Smith CF, Bowling BL. CHST6 mutations in North American subjects with macular corneal dystrophy: a comprehensive molecular genetic review. Mol Vis. 2006;12:159–76.
335. Kenyon KR. Ocular manifestations and pathology of systemic mucopolysaccharidoses. Birth Defects Orig Artic Ser. 1976;12:133–53.
336. Ashworth JL, Biswas S, Wraith E, Lloyd IC. Mucopolysaccharidoses and the eye. Surv Ophthalmol. 2006;51:1–17.
337. Ganesh A, Bruwer Z, Al-Thihli K. An update on ocular involvement in mucopolysaccharidoses. Curr Opin Ophthalmol. 2013;24:379–88.
338. Klintworth GK. Macular corneal dystrophy-a localized disorder of mucopolysaccharides metabolism? Prog Clin Biol Res. 1982;82:69–101.
339. Ahmed TY, Turnbull AM, Attridge NF, Biswas S, Lloyd IC, Au L, Ashworth JL. Anterior segment OCT imaging in mucopolysaccharidoses type I, II, and VI. Eye. 2014;28(3):327–36.
340. Goldberg MF, Duke JR. Ocular histopathology in Hunter's syndrome. Systemic mucopolysaccharidosis type II. Arch Ophthalmol. 1967;77:503–12.
341. Rosen DA, Haust MD, Yamashita T, Bryans AM. Keratoplasty and electron microscopy of the cornea in systemic mucopolysaccharidosis (Hurler's disease). Can J Ophthalmol. 1968;3:218–30.
342. Zabel RW, MacDonald IM, Mintsioulis G, Addison DJ. Scheie's syndrome. An ultrastructural analysis of the cornea. Ophthalmology. 1989;96:1631–8.
343. Iwamoto M, Nawa Y, Maumenee IH, Young-Ramsaran J, Matalon R, Green WR. Ocular histopathology and ultrastructure of Morquio syndrome (systemic mucopolysaccharidosis IV A). Graefes Arch Clin Exp Ophthalmol. 1990;228:342–9.
344. Rummelt V, Meyer HJ, Naumann GO. Light and electron microscopy of the cornea in systemic mucopolysaccharidosis type I-S (Scheie's syndrome). Cornea. 1992;11:86–92.
345. Weiss JS. Schnyder crystalline dystrophy sine crystals. Recommendation for a revision of nomenclature. Ophthalmology. 1996;103:465–73.
346. Weiss JS, Wiaux C, Yellore V, Raber I, Eagle R, Mequio M, Aldave A. Newly reported p.Asp240Asn mutation in UBIAD1 suggests central discoid corneal dystrophy is a variant of Schnyder corneal dystrophy. Cornea. 2010;29:777–80.
347. Weiss JS, Kruth HS, Kuivaniemi H, Tromp G, White PS, Winters RS, Lisch W, Henn W, Denninger E, Krause M, Wasson P, Ebenezer N, Mahurkar S, Nickerson ML. Mutations in the UBIAD1 gene on chromosome short arm 1, region 36, cause Schnyder crystalline corneal dystrophy. Invest Ophthalmol Vis Sci. 2007;48:5007–12.
348. Weiss JS. Schnyder corneal dystrophy. Curr Opin Ophthalmol. 2009;20:292–8.
349. Weiss JS, Khemichian AJ. Differential diagnosis of Schnyder corneal dystrophy. Dev Ophthalmol. 2011;48:67–96.
350. Weiss JS. Visual morbidity in thirty-four families with Schnyder crystalline corneal dystrophy. Trans Am Ophthalmol Soc. 2007;105:616–48.
351. Garner A, Tripathi RC. Hereditary crystalline stromal dystrophy of Schnyder. II. Histopathology and ultrastructure. Br J Ophthalmol. 1972;56:400–8.
352. Freddo TF, Polack FM, Leibowitz HM. Ultrastructural changes in the posterior layers of the cornea in Schnyder's crystalline dystrophy. Cornea. 1989;8:170–7.
353. Bredrup C, Knappskog PM, Majewski J, Rodahl E, Boman H. Congenital stromal dystrophy of the cornea caused by a mutation in the decorin gene. Invest Ophthalmol Vis Sci. 2005;46:420–6.
354. Rodahl E, van Ginderdeuren R, Knappskog PM, Bredrup C, Boman H. A second decorin frame shift mutation in a family with congenital stromal corneal dystrophy. Am J Ophthalmol. 2006;142:520–1.
355. Witschel H, Fine BS, Grutzner P, McTigue JW. Congenital hereditary stromal dystrophy of the cornea. Arch Ophthalmol. 1978;96:1043–51.
356. Li S, Tiab L, Jiao X, Munier FL, Zografos L, Frueh BE, Sergeev Y, Smith J, Rubin B, Meallet MA, Forster RK, Hejtmancik JF, Schorderet DF. Mutations in PIP5K3 are associated with François-Neetens mouchetée fleck corneal dystrophy. Am J Hum Genet. 2005;77:54–63.
357. Patten JT, Hyndiuk RA, Donaldson DD, Herman SJ, Ostler HB. Fleck (mouchetée) dystrophy of the cornea. Ann Ophthalmol. 1976;8:25–32.
358. Holopainen JM, Moilanen JA, Tervo TM. In vivo confocal microscopy of Fleck dystrophy and pre-Descemet's membrane corneal dystrophy. Cornea. 2003;22:160–3.
359. Can E, Kan E, Akgun HI. Clinical features and in-vivo confocal microscopic imaging of fleck corneal dystrophy. Semin Ophthalmol. 2013;28:239–41.
360. Purcell Jr JJ, Krachmer JH, Weingeist TA. Fleck corneal dystrophy. Arch Ophthalmol. 1977;95:440–4.
361. Kim MJ, Frausto RF, Rosenwasser GO, Bui T, Le DJ, Stone EM, Aldave AJ. Posterior amorphous corneal dystrophy is associated with a deletion of small leucine-rich proteoglycans on chromosome 12. PLoS One. 2014;9:e95037.
362. Grimm BB, Waring GOI, Grimm SB. Posterior amorphous corneal dysgenesis. Am J Ophthalmol. 1995;120:448–55.
363. Carpel EF, Sigelman RJ, Doughman DJ. Posterior amorphous corneal dystrophy. Am J Ophthalmol. 1977;83:629–32.

364. Dunn SP, Krachmer JH, Ching SS. New findings in posterior amorphous corneal dystrophy. Arch Ophthalmol. 1984;102:236–9.
365. Johnson AT, Folberg R, Vrabec MP, Florakis GJ, Stone EM, Krachmer JH. The pathology of posterior amorphous corneal dystrophy. Ophthalmology. 1990;97:104–9.
366. Roth SI, Mittelman D, Stock EL. Posterior amorphous corneal dystrophy. An ultrastructural study of a variant with histopathological features of an endothelial dystrophy. Cornea. 1992;11:165–72.
367. Strachan IM. Cloudy central corneal dystrophy of François. Five cases in the same family. Br J Ophthalmol. 1969;53:192–4.
368. Karp CL, Scott IU, Green WR, Chang TS, Culbertson WW. Central cloudy corneal dystrophy of François. A clinicopathologic study. Arch Ophthalmol. 1997;115:1058–62.
369. Belliveau MJ, Brownstein S, Agapitos P, Font RL. Ultrastructural features of posterior crocodile shagreen of the cornea. Surv Ophthalmol. 2009;54:569–75.
370. Chen PL, Tang KP, Liang JB. Pre-Descemet's corneal dystrophy associated with ichthyosis. Zhonghua Yi Xue Za Zhi. 2002;65:407–9.
371. Ye YF, Yao YF, Zhou P, Pan F. In vivo confocal microscopy of pre-Descemet's membrane corneal dystrophy. Clin Experiment Ophthalmol. 2006;34:614–6.
372. Kontadakis GA, Kymionis GD, Kankariya VP, Papadiamantis AG, Pallikaris AI. Corneal confocal microscopy findings in sporadic cases of pre-Descemet corneal dystrophy. Eye Contact Lens. 2014;40:e8–12.
373. Curran RE, Kenyon KR, Green WR. Pre-Descemet's membrane corneal dystrophy. Am J Ophthalmol. 1974;77:711–6.
374. Eghrari AO, Gottsch JD. Fuchs' corneal dystrophy. Expert Rev Ophthalmol. 2010;5:147–59.
375. Hamill CE, Schmedt T, Jurkunas U. Fuchs endothelial cornea dystrophy: a review of the genetics behind disease development. Semin Ophthalmol. 2013;28:281–6.
376. Aldave AJ, Han J, Frausto RF. Genetics of the corneal endothelial dystrophies: an evidence-based review. Clin Genet. 2013;84:109–19.
377. Gottsch JD, Sundin OH, Liu SH, Jun AS, Broman KW, Stark WJ, Vito EC, Narang AK, Thompson JM, Magovern M. Inheritance of a novel COL8A2 mutation defines a distinct early-onset subtype of Fuchs corneal dystrophy. Invest Ophthalmol Vis Sci. 2005;46:1934–9.
378. Liskova P, Prescott Q, Bhattacharya SS, Tuft SJ. British family with early-onset Fuchs' endothelial corneal dystrophy associated with p.L450W mutation in the COL8A2 gene. Br J Ophthalmol. 2007;91:1717–8.
379. Riazuddin SA, Zaghloul NA, Al-Saif A, Davey L, Diplas BH, Meadows DN, Eghrari AO, Minear MA, Li YJ, Klintworth GK, Afshari N, Gregory SG, Gottsch JD, Katsanis N. Missense mutations in TCF8 cause late-onset Fuchs corneal dystrophy and interact with FCD4 on chromosome 9p. Am J Hum Genet. 2010;86:45–53.
380. Riazuddin SA, Vasanth S, Katsanis N, Gottsch JD. Mutations in AGBL1 cause dominant late-onset Fuchs corneal dystrophy and alter protein-protein interaction with TCF4. Am J Hum Genet. 2013;93:758–64.
381. Riazuddin SA, Parker DS, McGlumphy EJ, Oh EC, Iliff BW, Schmedt T, Jurkunas U, Schleif R, Katsanis N, Gottsch JD. Mutations in LOXHD1, a recessive-deafness locus, cause dominant late-onset Fuchs corneal dystrophy. Am J Hum Genet. 2012;90:533–9.
382. Vithana EN, Morgan PE, Ramprasad V, Tan DT, Yong VH, Venkataraman D, Venkatraman A, Yam GH, Nagasamy S, Law RW, Rajagopal R, Pang CP, Kumaramanickevel G, Casey JR, Aung T. SLC4A11 mutations in Fuchs endothelial corneal dystrophy. Hum Mol Genet. 2008;17:656–66.
383. Klien B. Fuchs' epithelial dystrophy of the cornea; a clinical and histopathologic study. Am J Ophthalmol. 1958;46:297–304.
384. Eagle Jr RC, Laibson PR, Arentsen JJ. Epithelial abnormalities in chronic corneal edema: a histopathological study. Trans Am Ophthalmol Soc. 1989;87:107–19.
385. Waring GOI, Rodrigues MM, Laibson PR. Corneal dystrophies. II. Endothelial dystrophies. Surv Ophthalmol. 1978;23:147–68.
386. Bergmanson JP, Sheldon TM, Goosey JD. Fuchs' endothelial dystrophy: a fresh look at an aging disease. Ophthalmic Physiol Opt. 1999;19:210–22.
387. Yuen HK, Rassier CE, Jardeleza MS, Green WR, De La Cruz Z, Stark WJ, Gottsch JD. A morphologic study of Fuchs dystrophy and bullous keratopathy. Cornea. 2005;24:319–27.
388. Biswas S, Munier FL, Yardley J, Hart-Holden N, Perveen R, Cousin P, Sutphin JE, Noble B, Batterbury M, Kielty C, Hackett A, Bonshek R, Ridgway A, McLeod D, Sheffield VC, Stone EM, Schorderet DF, Black GC. Missense mutations in COL8A2, the gene encoding the alpha2 chain of type VIII collagen, cause two forms of corneal endothelial dystrophy. Hum Mol Genet. 2001;10:2415–23.
389. Krafchak CM, Pawar H, Moroi SE, Sugar A, Lichter PR, Mackey DA, Mian S, Nairus T, Elner V, Schteingart MT, Downs CA, Kijek TG, Johnson JM, Trager EH, Rozsa FW, Mandal MN, Epstein MP, Vollrath D, Ayyagari R, Boehnke M, Richards JE. Mutations in TCF8 cause posterior polymorphous corneal dystrophy and ectopic expression of COL4A3 by corneal endothelial cells. Am J Hum Genet. 2005;77:694–708.
390. Yellore VS, Rayner SA, Nguyen CK, Gangalum RK, Jing Z, Bhat SP, Aldave AJ. Analysis of the role of ZEB1 in the pathogenesis of posterior polymorphous corneal dystrophy. Invest Ophthalmol Vis Sci. 2012;53:273–8.

391. Strachan IM, Maclean H. Posterior polymorphous dystrophy of the cornea. Br J Ophthalmol. 1968;52:270–2.
392. Cullen AP, Hawkins RS, Medina AA. Clinical observation of posterior polymorphous dystrophy. Am J Optom Physiol Opt. 1976;53:244–8.
393. Threlkeld AB, Green WR, Quigley HA, De La Cruz Z, Stark WJ. A clinicopathologic study of posterior polymorphous dystrophy: implications for pathogenetic mechanism of the associated glaucoma. Trans Am Ophthalmol Soc. 1994;92:133–65.
394. Grupcheva CN, Chew GS, Edwards M, Craig JP, McGhee CN. Imaging posterior polymorphous corneal dystrophy by in vivo confocal microscopy. Clin Experiment Ophthalmol. 2001;29:256–9.
395. Mullaney PB, Risco JM, Teichmann K, Millar L. Congenital hereditary endothelial dystrophy associated with glaucoma. Ophthalmology. 1995;102:186–92.
396. Johnson BL, Brown SI. Posterior polymorphous dystrophy: a light and electron microscopic study. Br J Ophthalmol. 1978;62:89–96.
397. Jirsova K, Merjava S, Martincova R, Gwilliam R, Ebenezer ND, Liskova P, Filipec M. Immunohistochemical characterization of cytokeratins in the abnormal corneal endothelium of posterior polymorphous corneal dystrophy patients. Exp Eye Res. 2007;84:680–6.
398. Hanna C, Fraunfelder FT, McNair JR. An ultrastructure study of posterior polymorphous dystrophy of the cornea. Ann Ophthalmol. 1977;9:1371–8.
399. Aldave AJ, Ann LB, Frausto RF, Nguyen CK, Yu F, Raber IM. Classification of posterior polymorphous corneal dystrophy as a corneal ectatic disorder following confirmation of associated significant corneal steepening. JAMA Ophthalmol. 2013;131:1583–90.
400. Toma NM, Ebenezer ND, Inglehearn CF, Plant C, Ficker LA, Bhattacharya SS. Linkage of congenital hereditary endothelial dystrophy to chromosome 20. Hum Mol Genet. 1995;4:2395–8.
401. Vithana EN, Morgan P, Sundaresan P, Ebenezer ND, Tan DT, Mohamed MD, Anand S, Khine KO, Venkataraman D, Yong VH, Salto-Tellez M, Venkatraman A, Guo K, Hemadevi B, Srinivasan M, Prajna V, Khine M, Casey JR, Inglehearn CF, Aung T. Mutations in sodium-borate cotransporter SLC4A11 cause recessive congenital hereditary endothelial dystrophy (CHED2). Nat Genet. 2006;38:755–7.
402. Sultana A, Garg P, Ramamurthy B, Vemuganti GK, Kannabiran C. Mutational spectrum of the SLC4A11 gene in autosomal recessive congenital hereditary endothelial dystrophy. Mol Vis. 2007;13:1327–32.
403. Pearce WG, Tripathi RC, Morgan G. Congenital endothelial corneal dystrophy. Clinical, pathological, and genetic study. Br J Ophthalmol. 1969;53:577–91.
404. Kenyon KR, Antine B. The pathogenesis of congenital hereditary endothelial dystrophy of the cornea. Am J Ophthalmol. 1971;72:787–95.
405. Judisch GF, Maumenee IH. Clinical differentiation of recessive congenital hereditary endothelial dystrophy and dominant hereditary endothelial dystrophy. Am J Ophthalmol. 1978;85:606–12.
406. Kirkness CM, McCartney A, Rice NS, Garner A, Steele AD. Congenital hereditary corneal oedema of Maumenee: its clinical features, management, and pathology. Br J Ophthalmol. 1987;71:130–44.
407. Ehlers N, Modis L, Møller-Pedersen T. A morphological and functional study of congenital hereditary endothelial dystrophy. Acta Ophthalmol Scand. 1998;76:314–8.
408. Sekundo W, Marshall GE, Lee WR, Kirkness CM. Immuno-electron labelling of matrix components in congenital hereditary endothelial dystrophy. Graefes Arch Clin Exp Ophthalmol. 1994;232:337–46.
409. Desir J, Abramowicz M. Congenital hereditary endothelial dystrophy with progressive sensorineural deafness (Harboyan syndrome). Orphanet J Rare Dis. 2008;3:28.
410. Siddiqui S, Zenteno JC, Rice A, Chacon-Camacho O, Naylor SG, Rivera-de la Parra D, Spokes DM, James N, Toomes C, Inglehearn CF, Ali M. Congenital hereditary endothelial dystrophy caused by SLC4A11 mutations progresses to Harboyan syndrome. Cornea. 2014;33:247–51.
411. Schmid E, Lisch W, Philipp W, Lechner S, Göttinger W, Schlötzer-Schrehardt U, Müller T, Utermann G, Janecke AR. A new, X-linked endothelial corneal dystrophy. Am J Ophthalmol. 2006;141:478–87.
412. Tuomaala S, Aine E, Saari KM, Kivelä T. Corneally displaced malignant conjunctival melanomas. Ophthalmology. 2002;109:914–9.

The Sclera

4

Fiona Roberts

4.1 General Description

The sclera is the main outer coating of the eye. It is roughly spherical in shape and consists almost entirely of collagen. It is relatively avascular and contains scanty sclerocytes.

It provides a tough protective coating for the intraocular structures from injury and mechanical displacement. It also helps to maintain intraocular pressure and resists deformation of the globe due to contraction of the extraocular muscles.

The sclera is covered by loose connective tissue on the outside, the episclera. The episclera is continuous with the loose tissue of Tenon's capsule, while its deeper layers are more compact merging with the sclera proper.

4.2 Embryology, Anatomy and Development

The sclera is composed of compact interlacing bundles of collagen with some elastic tissue and a small quantity of ground substance (chondroitin sulphate, dermatan sulphate and hyaluronic acid). The predominant collagen type is type I with a moderate amount of type III collagen [1]. The elastic fibres are intimately associated with the collagen and are predominantly found adjacent to the choroid. The collagen bundles are mostly parallel to the surface but cross in all directions, branch and fuse. This pattern makes blunt dissection of the sclera difficult. The sclerocytes (fibroblasts) are scattered between the collagen bundles as flattened cells with small nuclei and long branching processes. Melanocytes and pigmented macrophages are present in the deeper scleral lamellae derived from the choroid.

The sclera is relatively avascular but obtains branches from the anterior ciliary arteries in the region of Schlemm's canal, and posteriorly the short ciliary arteries supply branches to the disc and peripapillary sclera. The episclera plexus sends fine branches to the sclera. The close apposition of the choroid also provides the sclera with nourishment.

The sclera is considered to derive predominantly from the neural crest except a small temporal region which develops from the mesoderm [2]. The differentiation of neural crest cells into the sclera (and choroid) occurs around week 6 of development starting anteriorly and progressing posteriorly reaching the posterior pole by week 12 [3, 4]. The differentiation is induced by the retinal pigment epithelium [5]. The developing lens is required for normal growth and development. By the 4th month, circularly orientated fibres form the sclera spur, and by the 5th month scleral fibres around the optic nerve form the lamina cribrosa.

In infants, the sclera is relatively thin which allows the pigmented cells of the choroid to show through and give it a bluish colour. The

F. Roberts, BSc, MBChB, MD, FRCPath
Department of Pathology, Southern General Hospital, Govan Road, Glasgow G51 4TF, Scotland, UK
e-mail: fiona.roberts@ggc.scot.nhs.uk

S. Heegaard, H. Grossniklaus (eds.), *Eye Pathology: An Illustrated Guide*,
DOI 10.1007/978-3-662-43382-9_4, © Springer-Verlag Berlin Heidelberg 2015

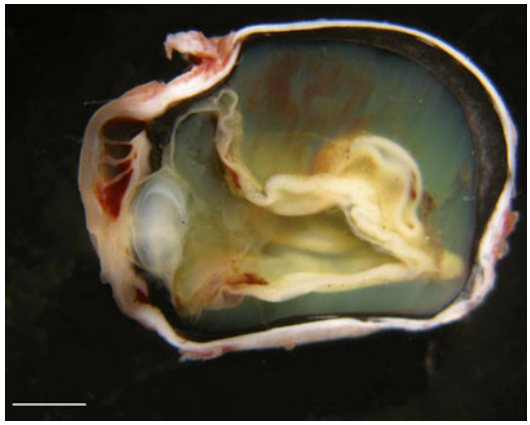

Fig. 4.1 A buphthalmic eye in a case of neurofibromatosis typeie type 1. The sclera is very distensible in the infant eye, and the eye becomes uniformly enlarged due to increased pressure with thinning of the sclera. In addition there has been corneal trauma with a fibrous ingrowth, cataract formation and retinal detachment (scale bar 1 cm)

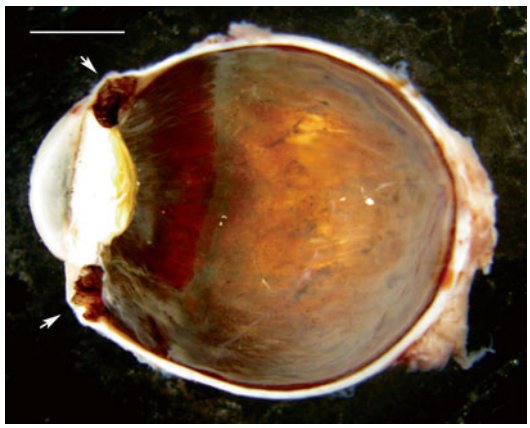

Fig. 4.2 Anterior staphyloma. In a case of long-standing childhood glaucoma, the globe is enlarged, and there is marked thinning of the sclera anteriorly (*arrows*). The lens also contains a cataract (scale bar 1 cm)

tissue is also distensible such that stretching may occur in congenital glaucoma resulting in a buphthalmic eye (Fig. 4.1). The sclera gradually becomes thicker, whiter and less distensible and more opaque during childhood and adolescence.

In adults, the sclera is poorly distensible, and ectasias (local protrusion of thinned sclera) or staphylomas (scleral thinning with uveal show) may occur after trauma or inflammation (Fig. 4.2).

4.3 Congenital Abnormalities

4.3.1 Synophthalmia and Cyclopia

Definition

This is the partial (synophthalmia) or total (cyclopia) union of the elements of the two eyes in the midline region of the forehead to form a single structure.

Epidemiology

The true incidence of cyclopia and synophthalmia in humans is unknown, but it has been estimated at around 1 in 40,000 births.

Aetiology

These anomalies may be familial, can occur in twins and are seen in consanguineous marriages. Chromosomal abnormalities have been found in 36 % of cases with trisomy 13 being the most common anomaly [6]. Deletion of chromosome 18p also occurs [7].

Clinical Features and Pathology

Abnormal formation of the mesoderm between the optic vesicles leads to partial (synophthalmia) or complete (cyclopia) of the eyes. This usually occurs in association with malformation of the anterior neural plate. In synophthalmia there will be two corneas, two lenses and parts of the iris, ciliary body and retina (Fig. 4.3) [8]. There may be a fused medial sclera, or the midline sclera and uveal tissue may be absent [9] (see also page 17).

4.3.2 Microphthalmos and Nanophthalmos

Definition

Microphthalmos is a condition in which the eye is smaller than normal and may be associated with other developmental defects. Nanophthalmos is used when the eye is microphthalmic but otherwise normal.

Epidemiology

Microphthalmos and nanophthalmos have been reported to occur in up to 30 per 100,000 of the population. Microphthalmia occurs in up to 11 % of blind children.

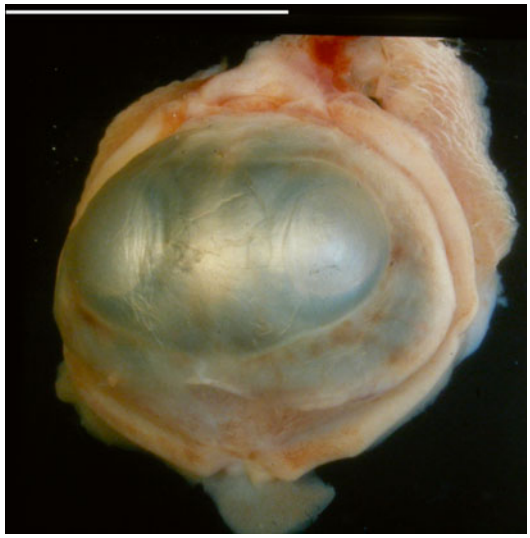

Fig. 4.3 A synophthalmic eye with two corneas and an enlarged scleral envelope (scale bar 1 cm)

Aetiology

Microphthalmia is associated with chromosomal abnormalities and single-gene disorders. Many genes have been implicated. It has also been associated with foetal alcohol syndrome and various maternal infections including rubella and cytomegalovirus.

Clinical Features and Pathology

In both microphthalmos and nanophthalmos, the sclera is abnormally thick. As previously mentioned, additional developmental defects including retinal dysplasia may be present in microphthalmos. In nanophthalmos the eye appears normal in structure, but the morphology of the sclera is abnormal. The collagen is unusually thickened, and the bundles are irregularly interlacing [10]. Biochemical studies have shown a loss of chondroitin sulphate proteoglycan compared with controls [11] (see also page 16).

4.3.3 Osteogenesis Imperfecta

Definition

Osteogenesis imperfecta is a congenital bone disorder.

Synonyms

This condition is also known as brittle bone disease or Lobstein syndrome.

Epidemiology

The estimated incidence of osteogenesis imperfecta is 1 in 20,000 births.

Aetiology

The osteogenesis imperfecta group of genetic disorders predominantly affects the bones, and sufferers are prone to bones that break easily following mild trauma. There are at least 8 recognised forms of varying severity [12, 13]. Osteogenesis imperfecta is most commonly caused by mutation in genes encoding the alpha-1 and alpha-2 chains of type 1 collagen or proteins involved in posttranslational modification of type 1 collagen. The most common mutation is autosomally dominantly inherited and due to a null allele in the *COL1A1* gene [13].

Clinical Features and Macroscopy

The mildest form (type I) is characterised by a blue-grey tint to the sclera [14]. Scleral abnormalities occur to a lesser extent in other forms of the disease. The sclera is thin and translucent allowing the underlying uvea to become partially visible.

Histopathology

The sclera may appear thinner than normal on histology due to a reduced thickness in the collagen fibres [15, 16].

4.3.4 Ochronosis

Definition

This is a syndrome caused by the accumulation of homogentisic acid in the connective tissues which is usually associated with underlying alkaptonuria.

Epidemiology

Alkaptonuria occurs in 1:100,000 to 1:250,000 live births in most European countries. The incidence is very high in Slovakia, 1:19,000.

Aetiology

This is an autosomal recessive condition due to homogentisic acid oxidase deficiency due to mutations on chromosome 3q21-q23. This enzyme deficiency affects tyrosine metabolism

resulting in accumulation of homogentisic acid in collagenous structures [17].

Clinical Features and Macroscopy

Progressive pigmentation of the sclera, along with the skin, auricular cartilage and large joints, may occur in alkaptonuria.

Histopathology

On histology there is deposition of brown pigment in the scleral tissues [18, 19].

4.3.5 Systemic Mucopolysaccharidosis (MPS)

Definition

The systemic mucopolysaccharidoses are a group of metabolic disorders caused by the absence of malfunction of lysosomal enzymes required to break down glycosaminoglycans.

Synonyms

Hurler syndrome, Hurler-Scheie syndrome, Scheie syndrome, Hunter syndrome, Sanfilippo syndrome, Morquio syndrome, Maroteaux-Lamy syndrome, Sly syndrome, Natowicz syndrome

Epidemiology

The incidence varies for the many different types and subtypes. Some subtypes are lethal; others are compatible with longer-term survival. The incidence varies from around 1:250,000 for Hunter syndrome to 1 in 75,000 for Morquio syndrome.

Aetiology

The mucopolysaccharidoses are autosomally recessive disorders due to mutation in different lysosomal enzymes.

Clinical Features and Pathology

The sclera may be thickened due to deposition of glycosaminoglycans [20, 21]. This has been reported in both Hunter syndrome (MPS type II) [21, 22] and Maroteaux-Lamy syndrome (MPS type VI) [23]. Bilateral uveal effusions have been reported in a patient with Hunter syndrome. This was presumed to be secondary to scleral thickening and reduced number of vortex veins [24]. It is possible that the thickening of sclera also contributes to optic nerve swelling.

4.3.6 Ocular Melanosis and Oculodermal Melanocytosis

Definition

This is a congenital disorder resulting in pigmentation of the ocular structures (ocular melanosis) and surrounding skin (oculodermal melanocytosis).

Synonyms

Naevus of Ota

Epidemiology

Ocular melanosis occurs in around 4 per 1,000 Caucasians. Oculodermal melanocytosis occurs in around 3 per 1,000 Caucasians. The incidence is much higher in the Chinese population.

Aetiology

The aetiology is unknown.

Clinical Features and Pathology

In congenital oculodermal melanocytosis, there is slate-grey pigmentation of the sclera (Fig. 4.4). This is due to collections of heavily pigmented melanocytes in the uveal tract, but pigmented dendritic melanocytes are also identified within the sclera [25].

Prognosis and Predictive Factors

There is an increased risk of uveal melanoma in these patients.

4.4 Inflammation

4.4.1 Episcleritis

Definition

Inflammation occurring in the episclera, a thin layer of tissue covering the sclera.

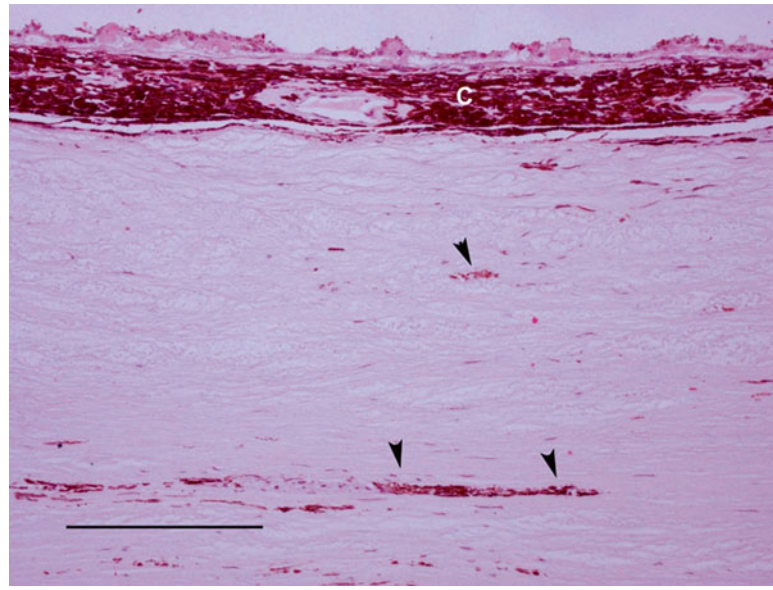

Fig. 4.4 An enucleation specimen from a patient with oculodermal melanocytosis. There is hyperpigmentation of the choroid (*c*) with patchier pigmentation of the sclera (*arrowheads*) (scale bar 100 μm)

Epidemiology

It affects all age groups but most commonly occurs in middle-aged women. As initially stated, the majority of cases are isolated, but between 26 and 32 % of cases may be associated with systemic disease or be the herald of a systemic disease [26].

Aetiology

Diseases associated with episcleritis show crossover with those associated with scleritis (see later) and include vasculitides, connective tissue disease, inflammatory bowel disease and relapsing polychondritis.

Clinical Features and Macroscopy

Isolated inflammation of the episclera is usually benign and self-limiting and may be diffuse, sectoral or nodular.

Diffuse and Sectoral

Either diffuse or sectoral redness of the eye may occur sometimes associated with pain and tearing.

Nodular

This presents as small, usually single, episcleral nodules with overlying dilated conjunctival vessels. These are more commonly associated with underlying diseases, particularly rheumatoid arthritis.

Histopathology

Since it is benign and self-limiting, biopsy of episcleritis is uncommon. Diffuse and sectoral episcleritis will show vascular dilatation and congestion with a perivascular lymphocytic infiltrate and variable stromal oedema.

Histology of nodular episcleritis reveals a non-granulomatous, non-specific inflammatory process. The presence of necrobiotic granulomas or a vasculitis should alert the pathologist to the possibility of underlying disease such as rheumatoid arthritis or Wegener's granulomatosis.

Prognosis and Predictive factors

As previously stated, this is usually a benign and self-limiting condition, and ocular complications resulting from episcleritis are less frequent than that with scleritis.

4.4.2 Scleritis

Definition

Inflammation occurring in the sclera.

Epidemiology

Scleritis is not a particularly common disease. It tends to be more common in women and is most common in the fourth to sixth decades of life.

Aetiology

Inflammatory disease of the sclera may be primary and confined to the eye or seen in association with systemic disease. The incidence of systemic disease is reported to be between 39 and 50 % [27–29]. Scleritis may involve the anterior or posterior sclera, and concurrent and depending on the cause, sequential involvement of both the anterior and posterior sclera may occur [27]. Scleritis is most commonly associated with rheumatoid disease, but there is a broad differential diagnosis [27, 28].

Autoimmune Disease

Rheumatoid Arthritis – 17–33 % of patients with scleritis have rheumatoid arthritis. By contrast only 0.2–6.3 % of patients with rheumatoid arthritis have scleritis [30]. Scleritis may be associated with peripheral ulcerative keratitis. Rheumatoid factor is positive in 60–80 % of these patients.

Wegener's Granulomatosis – Ocular involvement occurs in around 50 % of patients with Wegener's granulomatosis [31]. Orbital involvement is more common, but scleritis occurs in around 7–10 % of patients particularly in association with peripheral ulcerative keratitis [31]. Serum c-ANCA is raised in the majority of patients.

Relapsing Polychondritis – Ocular symptoms occur in up to 65 % of patients with relapsing polychondritis at some point during the course of the disease [32]. Episcleritis and scleritis are the most common ocular manifestations occurring in approximately 47 % of patients.

Systemic Lupus Erythematosus – Ocular manifestations are relatively common in systemic lupus erythematosus. Scleritis may occur and be isolated or in association with episcleritis [33]. Antinuclear antibodies may be positive, and anti-double-stranded DNA is present in 30–50 % of patients.

Polyarteritis Nodosa – Ophthalmic manifestations are less common in polyarteritis nodosa than in Wegener's granulomatosis occurring in around 10 % of patients [34]. Episcleritis is more common but severe progressive scleritis may occur, and scleritis may occur in association with ulcerative keratitis [35].

Behçet's's Disease – Scleritis has rarely been described in association with Behçet's disease [36, 37].

Infectious Scleritis

Infectious scleritis is uncommon particularly in the absence of associated keratitis. Infectious scleritis may be caused by virus, bacteria, fungi or parasites.

Herpes zoster is the most common cause of infectious scleritis as part of herpes zoster ophthalmicus [38]. *Pseudomonas aeruginosa* is the most common postsurgical bacterial infection along with staphylococcal species [39]. Fungal scleritis is common in certain parts of the world usually due to *Aspergillus* [40, 41]. *Acanthamoeba* scleritis is usually a secondary consequence of keratitis [42, 43]. *Toxoplasma* scleritis occurs secondary to the retinochoroiditis [44, 45].

Surgically Induced Scleral Necrosis

Surgically induced necrotising scleritis (SINS) is a local autoimmune reaction known to develop near previous surgical wounds for cataract pterygium, glaucoma, strabismus and retinal detachment [46]. It appears to occur more commonly following postsurgical infection [47]. Usually the scleritis is localised, but surgically induced diffuse scleritis (SIDS) is also recognised [48].

Risedronate-Associated Scleritis

Bisphosphonate drugs are used for the prevention of osteoporosis but may cause ocular inflammation including conjunctivitis and uveitis. Scleritis in association with risedronate therapy has also been described [49].

Irradiation-Induced Scleritis

This is rare because the sclera is radioresistant and scleral necrosis is a rare complication of radiotherapy for uveal melanoma. It has been described in association with plaque brachytherapy [50] and very occasionally following proton beam therapy usually in association with an underlying inflammatory or systemic disease [51].

Clinical Features, Macroscopy and Histopathology

Scleritis is usually classified into anterior scleritis or posterior scleritis (occurring posterior to the

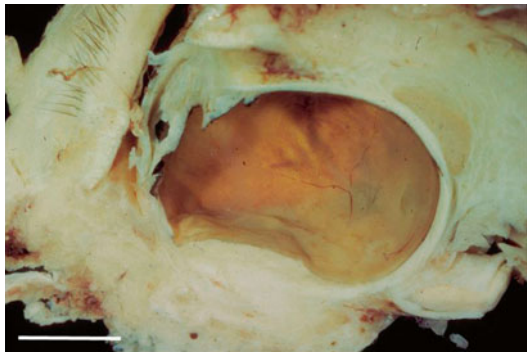

Fig. 4.5 An exenteration specimen showing a nodular posterior scleritis forming a mass lesion with exudative retinal detachment mistaken for melanoma (scale bar 1 cm)

equator of the eye). The onset of scleritis is often gradual, the main symptom being severe pain which may be exacerbated by eye movement and is often worse at night. Patients with anterior scleritis may develop a visible area of redness and tenderness. Posterior scleritis may be asymptomatic although pain and visual disturbance are common. The inflammation in the sclera may result in exudative retinal and choroidal detachment, chorioretinal inflammation and disc swelling. This can occasionally be mistaken clinically for an intraocular tumour (Fig. 4.5) [52, 53]. Severe swelling of the sclera and retro-ocular tissues can produce proptosis.

Anterior Scleritis

Anterior scleritis (scleritis occurring anterior to the equator) is more common than posterior scleritis because of the more abundant anterior vascular supply. There are three clinical subtypes of anterior scleritis, diffuse, nodular and necrotising, and most patients' disease remains in that subtype throughout the course of their disease.

Diffuse Anterior Scleritis

Diffuse anterior scleritis is characterised by severe pain often in the distribution of the trigeminal nerve with redness and swelling of a sector of sclera and episclera. The condition is bilateral in about 50 % of cases. Specimens are rarely submitted to the histology laboratory.

Nodular Anterior Scleritis

Nodular anterior scleritis is characterised by well-defined nodules in the sclera which are not mobile and may be multiple. The overlying episclera and conjunctiva may be inflamed and congested but are separate from these nodules.

Necrotising Anterior Scleritis

Necrotising anterior scleritis may occur with or without inflammation.

With inflammation: When it occurs with inflammation, it is severely painful and destructive and is bilateral in about 50 % of cases. There is an area of severe scleral oedema and congestion, and the overlying episclera may be avascular. The process usually starts in one area and may then spread circumferentially around the globe to involve the whole of the anterior segment.

Without inflammation: Unlike necrotising anterior scleritis with inflammation, this process is rarely painful. There is a grey or yellow patch on the anterior sclera which represents an area of necrosis. This may eventually slough from the underlying sclera, leaving the choroid covered by only a thin layer of conjunctiva as in scleromalacia perforans (Fig. 4.6).

Posterior Scleritis

Posterior scleritis may occur in association with anterior scleritis or may be isolated. Posterior scleritis is usually unilateral. In addition to pain there may be secondary inflammation in the choroid with exudative retinal detachment and optic disc swelling. Diffuse and nodular forms are also recognised.

Diffuse Posterior Scleritis

In diffuse posterior scleritis, a large area of scleral collagen is thickened by the inflammatory process, the so-called brawny scleritis (Fig. 4.7). There may be large areas of necrotic scleral collagen surrounded by granulomatous inflammation (Fig. 4.8). Alternatively, there may be diffuse granulomatous or non-granulomatous inflammation without areas of necrosis. As this is often a chronic process, there may be associated reactive fibrosis, and the sclera becomes massively thickened. As the process burns out, there may be scleral thinning resulting in staphyloma formation.

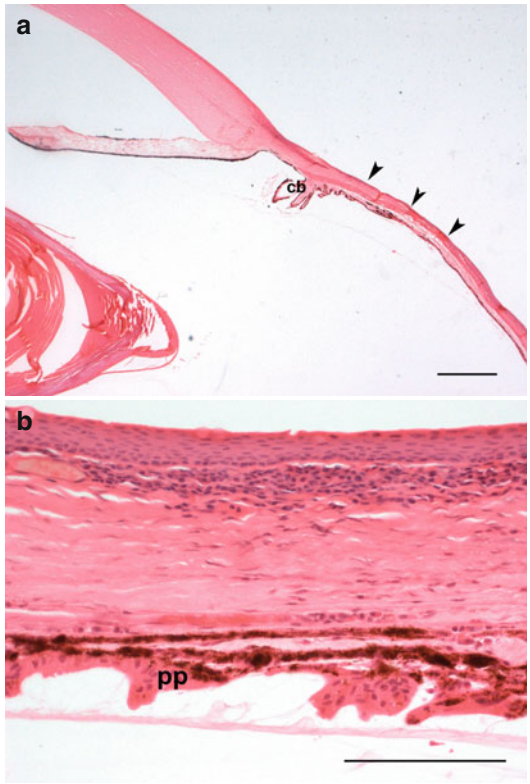

Fig. 4.6 (**a**) In scleromalacia perforans, there is marked thinning of the anterior sclera (*arrowheads*). The ciliary body (*cb*) is stretched (scale bar 100 μm). (**b**) A higher-power view of scleromalacia perforans. The pars plicata (PP) of the ciliary body is stretched. Inflammation is minimal (scale bar 100 μm)

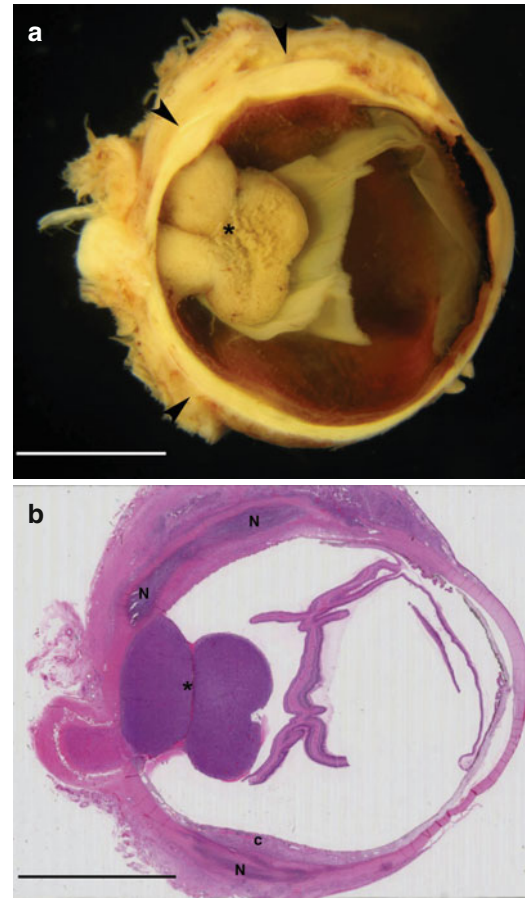

Fig. 4.7 (**a**) This eye with malignant melanoma (*) developed a diffuse posterior scleritis. The posterior sclera is irregularly thickened (scale bar 1 cm). (**b**) Histology of this eye shows large areas of scleral necrosis (*N*) not related to the melanoma (*). The choroid (*c*) is secondarily involved by inflammation (scale bar 1,000 μm)

Nodular Posterior Scleritis

In nodular posterior scleritis, the inflammatory process forms a localised mass around an area of collagen necrosis. In nodular scleritis there is usually a discrete zone of necrotic scleral collagen surrounded by granulomatous inflammation.

In any form of scleritis, the presence of vasculitis in association with scleritis is in keeping with a systemic immune-mediated condition such as Wegener's granulomatosis or rheumatoid disease (Fig. 4.9). The presence of microabscesses in areas of scleral collagen necrosis should prompt a search for infectious organisms (Fig. 4.10).

Prognosis and Predictive Factors

The aim of treatment is to control inflammation and maintain vision. It is also important to treat patients as the associated systemic disease has an increased mortality in patients with scleritis [54]. Loss of vision is much more common in patients with posterior scleritis due to secondary macular changes or optic atrophy [27].

Masquerade Scleritis

Very rarely malignancies can masquerade as scleritis. Ocular inflammation can be the initial manifestation of choroidal melanomas or metastatic carcinoma [55–57]. Scleritis can present a diagnostic challenge especially since it may be the sole initial manifestation of an occult systemic problem. Treatment-resistant scleritis should raise the suspicion of an infectious or malignant masquerade.

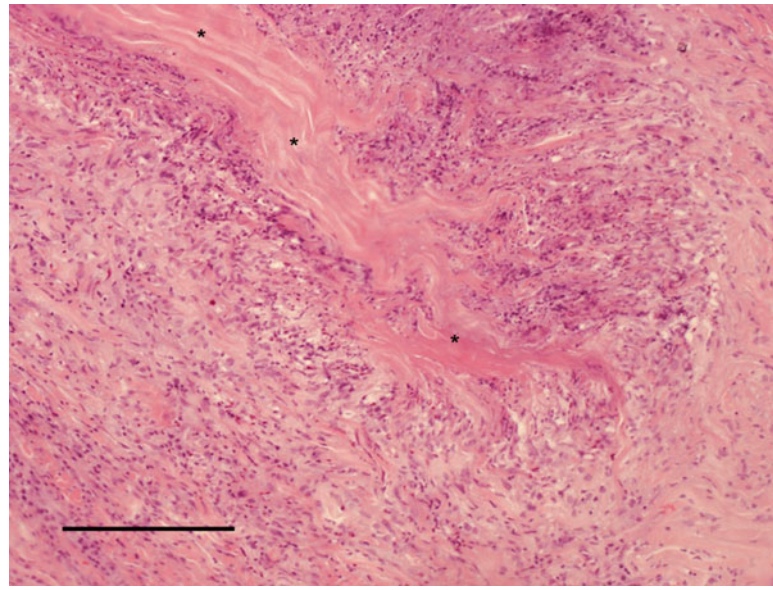

Fig. 4.8 Posterior scleritis showing a zone of necrobiotic collagen (*) surrounded by a palisaded granulomatous reaction (scale bar 100 μm)

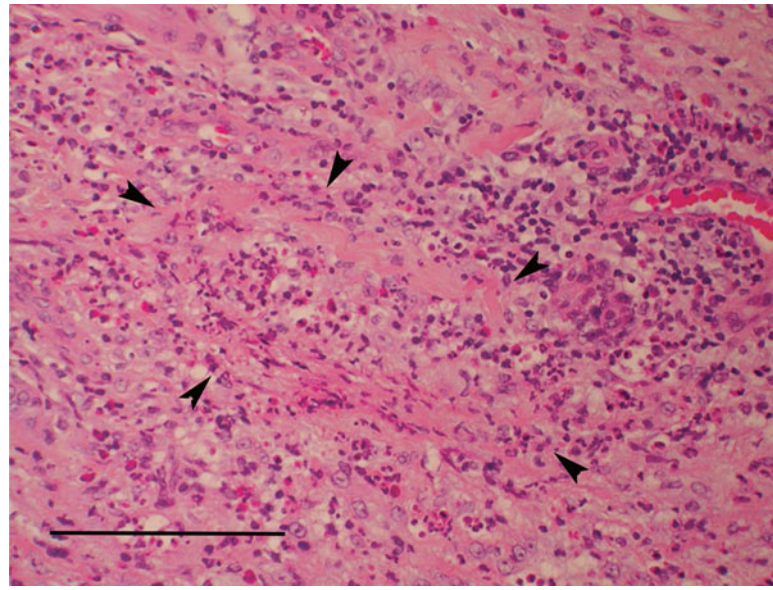

Fig. 4.9 Small blood vessels (*arrowheads*) with inflammatory infiltration of the wall and occlusion of the lumen in Wegener's granulomatosis (scale bar 100 μm)

IgG4-Related-Disease-Associated Scleritis

IgG4-related disease is a fibrosing and inflammatory disease process that may affect many organs [58]. It is characterised by the presence of prominent IgG4-positive plasma cells within the affected tissues with fibrosis and occasionally thrombophlebitis [58]. It was first recognised in association with autoimmune pancreatitis but is now known to affect multiple sites including the orbit and lacrimal gland [58]. The condition has also rarely been described in the sclera. In one case, this formed a localised mass simulating a tumour [59]. In a second case, this was a diffuse scleritis in association with pachymeningitis [60].

Sarcoidosis

Sarcoidosis may rarely involve the sclera where histology will show non-necrotising granulomas with minimal associated inflammation [61–63].

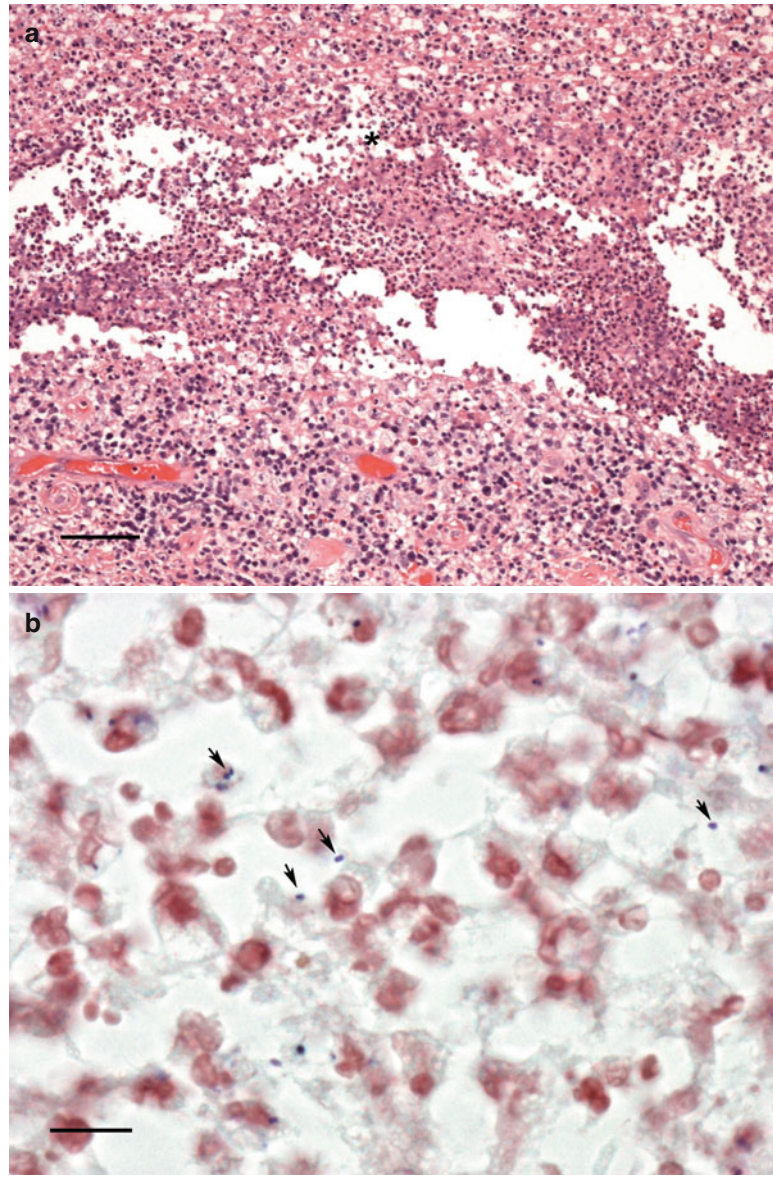

Fig. 4.10 (**a**) In infectious scleritis there may be microabscesses (*) surrounded by granulation tissue or histiocytes (scale bar 100 μm). (**b**) In this case gram-positive diplococci (*arrows*) were identified within the abscesses (scale bar 10 μm)

4.5 Injuries

Scleral wounds occur commonly in the context of serious eye trauma (Fig. 4.11). A wound may be a direct effect of penetrating or blunt trauma or may occur secondarily from tissue necrosis as a result of posttraumatic inflammation or infection. Scleral and corneoscleral wounds should be repaired where possible, and healing occurs by scarring.

4.6 Degenerations

4.6.1 Melanoma-Associated Spongiform Scleropathy (MASS)

Melanoma-associated spongiform scleropathy describes areas of disintegration in the scleral collagen in the sclera overlying a choroidal or ciliary body melanoma [63]. On histopathological

examination the fibres have a feathery appearance in longitudinal section and a dot morphology in cross section (Fig. 4.12) [63]. It is found in about a third of eyes enucleated for melanoma. It is more common in older patients and is found exclusively in areas of direct contact between the tumour and the sclera. There is collagen degradation in the sclera associated with excess deposition of glycosaminoglycans which accumulate water further loosening the degraded collagen bundles [64]. Matrix metalloproteinase 2 appears to play a role in the development of MASS [65].

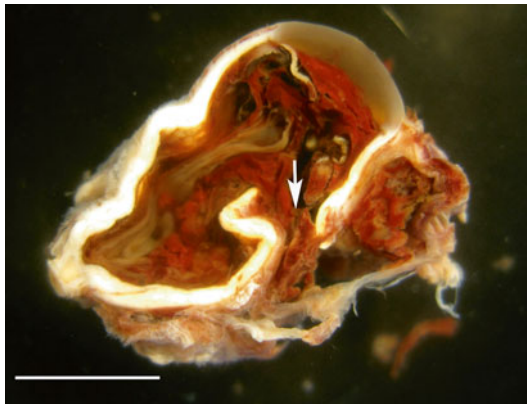

Fig. 4.11 An eye removed for irretrievable posttraumatic disorganisation due to a large scleral wound (*arrow*). There is iridocyclodialysis on the same side of the wound. The lens has been lost. The retina is detached and there is subretinal haemorrhage (scale bar 1 cm)

4.6.2 Myopia

In the myopic eye there is scleral thinning and localised ectasia in the posterior sclera (Fig. 4.13) [66]. This is due to atrophy of the collagen fibres (both fibre number and dimension). These changes are considered a consequence rather than a cause of myopia. Accompanying changes include choroidal atrophy and elongation with fibrosis of the choriocapillaris and breaks in Bruch's membrane.

4.6.3 Scleropachynsis

Scleropachynsis is a bilateral localised thickening of the posterior temporal sclera due to accumulation of glycosaminoglycans between the scleral collagen bundles. This accumulation may cause choroidal compression and maculopathy [67].

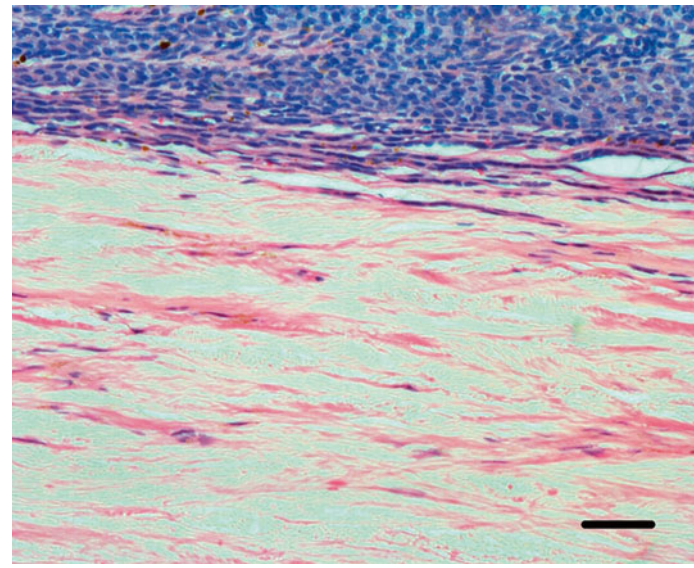

Fig. 4.12 Melanoma-associated spongiform scleropathy showing a feathery appearance to the scleral collagen. The choroidal melanoma is shown at the top of the picture (scale bar 100 μm) (Courtesy of Steffan Heegaard, Copenhagen, Denmark)

Fig. 4.13 In advanced myopia there is ectasia and thinning of the posterior sclera with atrophy of the peripapillary choroid and retina (scale bar 1 cm)

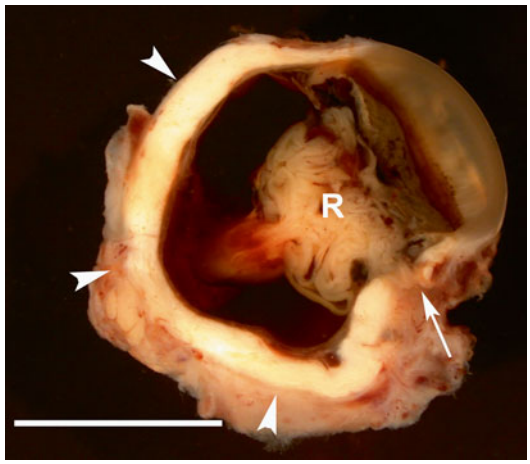

Fig. 4.14 A posttraumatic phthisical eye with a thickened, folded sclera (*arrowheads*). There is a healed scleral wound (*arrow*), and the retina (*R*) is detached and fibrotic (scale bar 1 cm)

4.6.4 Phthisis Bulbi

Marked scleral thickening occurs in association with atrophy and disorganisation of intraocular structures (Fig. 4.14) (see also page 32).

4.6.5 Amyloidosis

Amyloid deposits in the sclera are rare. This may occur as a localised or in association with systemic amyloidosis [68]. Amyloid deposits occur in the elderly and occasionally following scleral inflammation [69]. Amyloid characteristically stains red with Congo or Sirius red stains with apple-green birefringence on polarisation.

4.6.6 Calcium Deposition

4.6.6.1 Senile Scleral Plaques

These occur in those over 60 years of age usually as bilateral, symmetrical patches in the interpalpebral region anterior to the insertion of the horizontal recti muscles. On histology these are areas of calcification within scleral collagen with the adjacent scleral fibres showing a corkscrew morphology (Fig. 4.15) [70]. Actinic damage may play a role as there is frequently elastosis in the overlying conjunctiva.

4.6.6.2 Other Causes of Calcium Deposition

Calcium deposition may occur in the sclera in association with other causes of hypercalcaemia

Fig. 4.15 A calcified scleral plaque. The section has torn during cutting (*arrowheads*) (scale bar 100 μm)

including hypervitaminosis D, sarcoidosis and hyperparathyroidism.

4.6.7 Age-Related Degeneration

With advancing age the sclera becomes yellowish due to deposition of lipids, usually cholesterol esters and sphingomyelin, which become trapped between collagen fibres [71].

4.7 Neoplasms

Tumours of the sclera and episclera are very rare. The majority are secondary to spread from an intraocular malignancy along intrascleral vascular and neural channel or from a malignancy of the overlying conjunctiva.

4.7.1 Primary

4.7.1.1 Episcleral Osseous Choristoma

These uncommon tumours occur in the upper temporal quadrant behind the limbus. On histology they are composed of cancellous bone surrounded by connective tissue (Fig. 4.16) [72, 73].

4.7.1.2 Nodular Fasciitis

Episcleral nodular fasciitis may present as an uncomfortable enlarging nodule at the limbus or overlying the sclera adjacent to the insertion of a rectus muscle [74]. The history is usually short [75]. The lesions vary in size from 5 to 15 mm. On histology they are composed of fibroblastic tissue with a "tissue-culture" quality (Fig. 4.17). There may be focal haemorrhage. Older lesions may be more fibrosed. Immunohistochemical staining is usually positive for smooth muscle actin, but desmin is negative excluding a smooth muscle tumour. The prognosis is excellent and excision is curative.

4.7.1.3 Haemangioma

Episcleral capillary haemangiomas occur early in life and may initially grow rapidly but regress by 5 years although a small portion may persist. These can be isolated or a manifestation of encephalofacial angiomatosis (Sturge-Weber syndrome) [76, 77]. Cavernous haemangiomas may be a manifestation of orbital lesions. The histology is similar to other sites with either small interconnecting capillary channels or large dilated cavernous channels along with secondary changes including inflammation and thrombosis. Conservative management is usually satisfactory, and biopsy is uncommon.

4.7.1.4 Nerve Sheath Tumours

Neurofibromas may occur in the episclera and can involve intrascleral nerves in neurofibromatosis type 1 [78]. Plexiform neurofibromas may infiltrate the sclera [79]. The histology of the abnormal nerves is identical to other body sites with nerves expanded by variable numbers of Schwann cells and fibroblasts (Fig. 4.18). They should be distinguished from intrascleral nerve loops which represent an anastomosis of the long ciliary nerve that turns to enter the sclera before turning back again to continue to the ciliary body (Fig. 4.19).

Schwannomas have also rarely been described in the sclera [80, 81]. Again the appearances are identical to their counterparts in other tissues.

4.7.2 Secondary

The sclera and episclera may be involved by direct spread of intraocular uveal melanoma or less commonly retinoblastoma. Spread of squamous cell carcinoma of the conjunctiva into the episclera and anterior sclera may also occur. Secondary tumours or metastases from elsewhere are rare but include metastatic breast carcinoma, cutaneous melanoma and lymphoma.

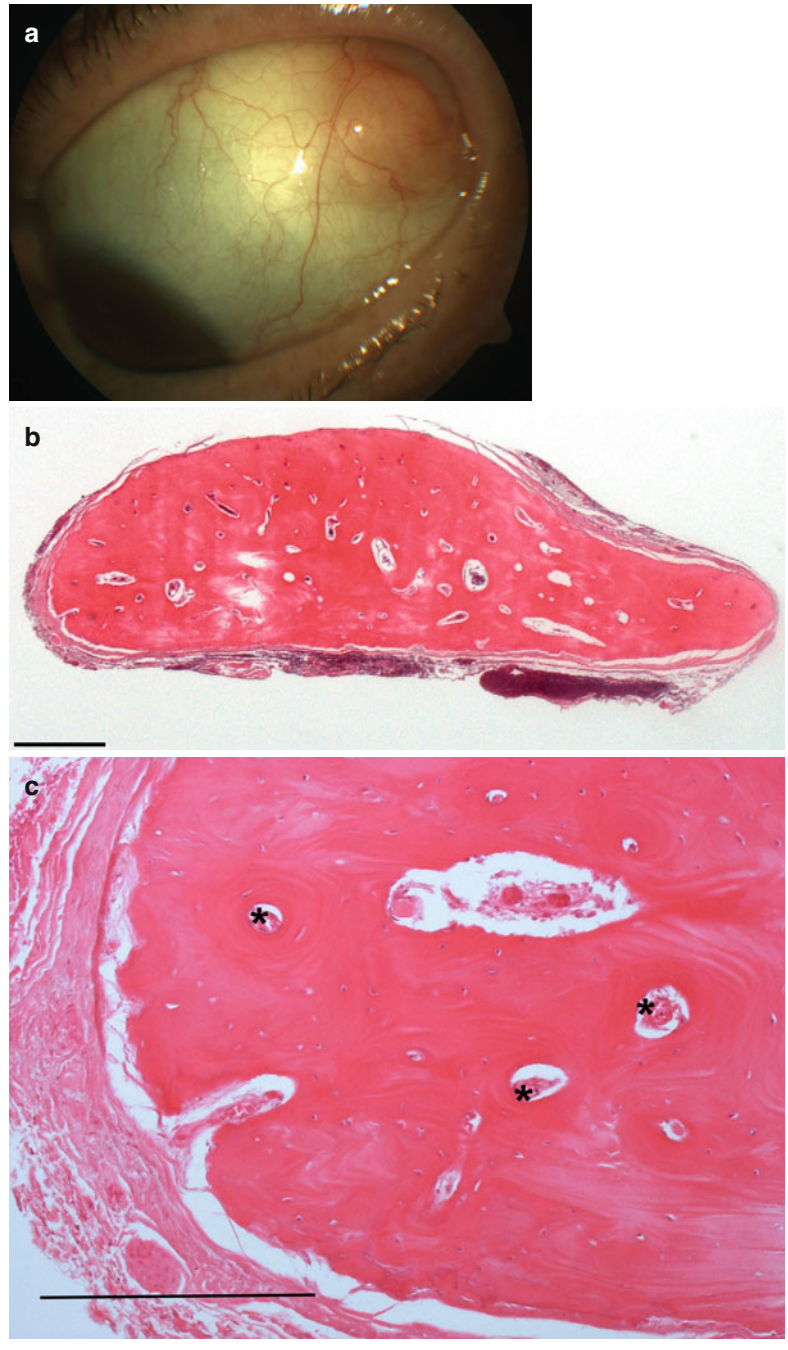

Fig. 4.16 (**a**) Clinical appearance of an episcleral osseous choristoma. (**b**) The episcleral osseous choristoma consists of a well-defined nodule of cancellous bone surrounded by connective tissue (scale bar 100 µm) (**c**) On higher-power Haversian systems (*) can be seen in this bony nodule (scale bar 100 µm) (Courtesy of Karin Loeffler, Bonn, Germany)

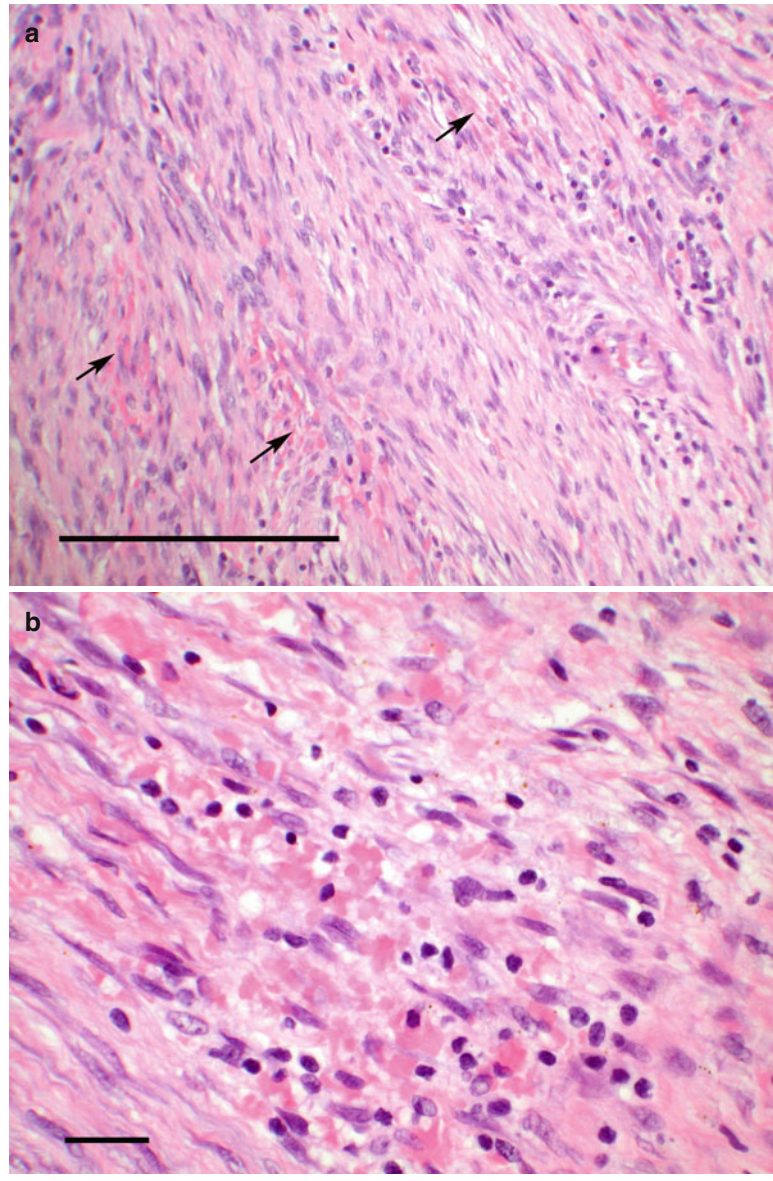

Fig. 4.17 (**a**) Nodular fasciitis is a proliferation of fibroblastic cells with scattered inflammatory cells and areas of haemorrhage (*arrows*) (scale bar 100 μm) (**b**) The oedematous stroma with inflammatory cells and localised haemorrhage can be appreciated on higher power (scale bar 100 μm)

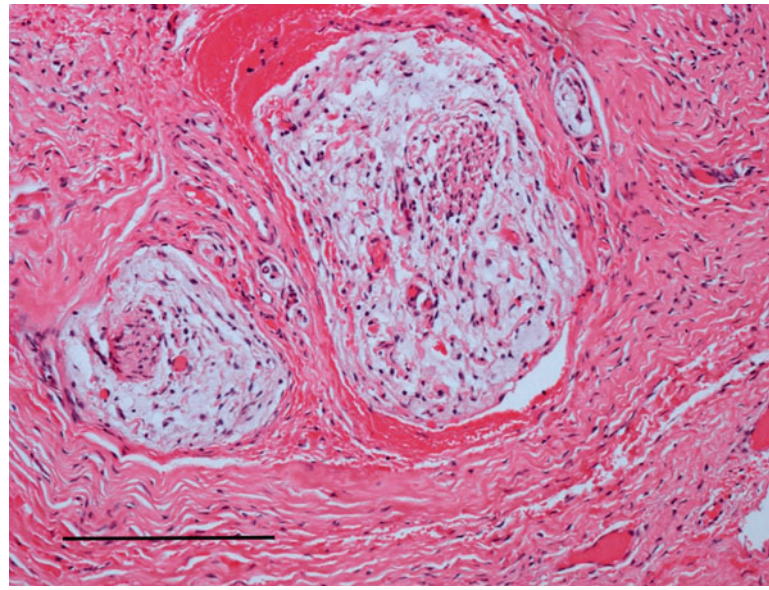

Fig. 4.18 Abnormal episcleral nerves in a case of neurofibromatosis. The nerves are expanded by a myxoid stroma (scale bar 100 μm)

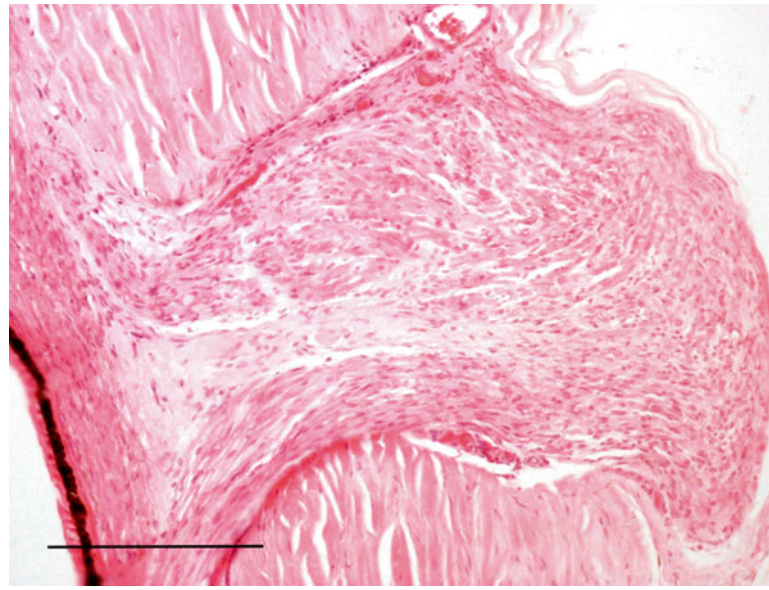

Fig. 4.19 An incidental intrascleral nerve loop in an enucleated eye. These usually occur overlying the pars plana (scale bar 100 μm)

References

1. Bron AJ, Tripathi R, Tripathi BJ. The cornea and sclera. In: Wolff's Anatomy of the eye and orbit. 8th ed. London: Chapman and Hall; 1997. p. 233–78.
2. Johnston MC, Noden DM, Hazelton RD, et al. Origins of avian ocular and periocular tissues. Exp Eye Res. 1979;29:27.
3. Sellheyer K, Spitznas M. Development of the human sclera: a morphological study. Graefes Arch Clin Exp Ophthalmol. 1988;226:89.
4. Brusilovsky AI, Shapovalova EY. Morphological criteria of the human early embryonal histogenesis: development of the ocular auxiliary apparatus. Arkh Anat Gistol Embriol. 1991;100:34.
5. Ozanics F, Rayborn M, Sagun D. Some aspects of corneal and scleral differentiation of the primate. Exp Eye Res. 1976;22:305.
6. Chan A, Lakshiminrusimha S, Heffner R, Gonzalez-Fernandez F. Histogenesis of retinal dysplasia in trisomy 13. Diagn Pathol. 2007;18:2–48.
7. Howard RO. Chromosomal abnormalities associated with cyclopia and synophthalmia. Trans Am Ophthalmol Soc. 1977;75:505–38.

8. Yamada S, Uwabe C, Fujii S, Shiota K. Phenotypic variability in human embryonic holoprosencephaly in the Kyoto collection. Birth Defects Res A Clin Mol Teratol. 2004;70:495–508.
9. Torzczynski E, Jacobiec FA, Johnston MC, Font RL, Madewell JA. Synophthalmia and cyclopia: a histopathologic, radiographic, and organogenetic analysis. Doc Ophthalmol. 1977;44:311–78.
10. Shiono T, Shoji A, Mutoh T, Tamai M. Abnormal sclerocytes in nanophthalmos. Graefes Arch Clin Exp Ophthalmol. 1992;230:348–51.
11. Fukuchi T, Sawada H, Seki M, Oyama T, Cho H, Abe H. Changes of scleral sulfated proteoglycans in three cases of nanophthalmos. Jpn J Ophthalmol. 2009; 53:171–5.
12. Byers PH, Krakow D, Nunes ME, Pepin M. Genetic evaluation of suspected osteogenesis imperfecta (OI). Genet Med. 2006;8:383–8.
13. Pagon RA, Adam MP, Ardinger HH et al. (eds). Seattle (WA): University of Washington, Seattle; 1993–2014
14. Byers PH, Pyott SM. Recessively inherited forms of osteogenesis imperfecta. Annu Rev Genet. 2012;46: 475–97.
15. Eichholtz W, Müller D. Electron microscopy findings on the cornea and sclera in osteogenesis imperfecta. Klin Monbl Augenheilkd. 1972;161:646–53.
16. Chan CC, Green WR, De la Cruz ZC, Hillis A. Ocular findings in osteogenesis imperfecta congenita. Arch Ophthalmol. 1982;100:1459–63.
17. Felbor U, Mutsch Y, Grehn F, Muller C, Kress W. Ocular ochronosis in alkaptonuria patients carrying mutations in the homogentisate 1,2-dioxygenase gene. Br J Ophthalmol. 1999;83:680–3.
18. Stumer J, Lang GK, Munzer M. Ochronosis oculi. Pathologie. 1988;9:295–301.
19. Gaines JJ. The pathology of alkaptonuric ochronosis. Hum Pathol. 1989;20:40–6.
20. Ashworth JL, Biswas S, Wraith E, Lloyd IC. Mucopolysaccharidoses and the eye. Surv Ophthalmol. 2006;51:1–17.
21. McDonnell JM, Green WR, Maumenee IH. Ocular histopathology of systemic mucopolysaccharidosis, type II-A (Hunter syndrome, severe). Ophthalmology. 1985;92:1772–9.
22. Topping TM, Kenyon KR, Goldberg MF, Maumenee AE. Ultrastructural ocular pathology of Hunters syndrome. Systemic mucopolysaccharidosis type II. Arch Ophthalmol. 1971;86:164–77.
23. Kenyon KR, Topping TM, Green WR, Maumenee AE. Ocular pathology of the Maroteaux-Lamy syndrome [systemic mucopolysaccharidosis type VI]: histologic and ultrastructural report of two cases. Am J Ophthalmol. 1972;73:718–41.
24. Vine AK. Uveal effusion in Hunter's syndrome. Evidence that abnormal sclera is responsible for the uveal effusion syndrome. Retina. 1986;6:57–60.
25. Liesegang TJ. Pigmented conjunctival and scleral lesions. Mayo Clin Proc. 1994;69:151–61.
26. Alpek EK, Uy HS, Christen W, Gurdal C, Foster CS. Severity of episcleritis and systemic disease association. Ophthalmology. 1999;106:729–31.
27. Okhravi N, Odufuwa B, McCluskey P, Lightman S. Scleritis. Surv Ophthalmol. 2005;50:351–63.
28. Riono WP, Hidayat AA, Rao NA. Scleritis. A clinicopathologic study of 55 cases. Ophthalmology. 1999; 106:1328–33.
29. Jabs DA, Mudun A, Dunn JP, Marsh MJ. Episcleritis and scleritis: clinical features and treatment results. Ophthalmology. 2000;130:469–76.
30. de la Maza S, Foster CS, Jabbur NS. Scleritis associated with rheumatoid arthritis and with other systemic immune-mediated diseases. Ophthalmology. 1994; 101:1281–6.
31. Tarabishy AN, Schulte M, Papaliodis GN, Hoffman GS. Wegener's granulomatosis: clinical manifestations, differential diagnosis and management of ocular and systemic disease. Surv Ophthalmol. 2010;55: 429–44.
32. Yoo JH, Chodosh J, Dana R. Relapsing polychondritis: systemic and ocular manifestations, differential diagnosis, management and prognosis. Semin Ophthalmol. 2011;26:261–9.
33. Sivraj RR, Durrani OM, Denniston AK, Murray PI, Gordon C. Ocular manifestations of systemic lupus erythematosus. Rheumatology. 2007;46:1757–62.
34. Rothschild PR, Pagnoux C, Seror R, Brezin AP, Delair E, Guillevin L. Ophthalmologic manifestations of systemic necrotizing vasculitides at diagnosis: a retrospective study of 1286 patients and review of the literature. Semin Arthritis Rheum. 2013;42:507–14.
35. Narag RB, Samuels AJ, Orlin SE, Brent LH. Polyarteritis nodosa complicated by severe progressive scleritis. J Rheumatol. 1999;26:1213–4.
36. Khairallah M, Accorinti M, Muccioli C, Kahloun R, Kempen JH. Epidemiology of Behcet disease. Ocul Immunol Inflamm. 2012;20:324–35.
37. Dursun D, Akova Y, Yucel E. Myositis and scleritis associated with Behcet's disease: an atypical presentation. Ocul Immunol Inflamm. 2004;12:329–32.
38. Gungor IU, Ariturk N, Beden U, Darka O. Necrotizing scleritis due to varicella zoster infection: a case report. Ocul Immunol Inflamm. 2006;14:317–9.
39. Rich RM, Smiddy WE, Davis JL. Infectious scleritis after retinal surgery. Am J Ophthalmol. 2008;145: 696–9.
40. Fincher T, Fulcher SF. Diagnostic and therapeutic challenge of Aspergillus flavus scleritis. Cornea. 2007;26:618–20.
41. Garg P. Fungal, mycobacterial, and nocardia infections and the eye: an update. Eye. 2012;26:245–51.
42. Ebrahimi KB, Green WR, Grebe R, Jun AS. Acanthamoeba sclerokeratitis. Graefes Arch Clin Exp Ophthalmol. 2009;247:283–6.
43. Chatterjee S, Agrawal D, Vemuganti GK. Granulomatous inflammation in Acanthamoeba sclerokeratitis. Ind J Ophthalmol. 2013;61:300–2.
44. Schuman JS, Weinberg RS, Ferry AP, Guerry RK. Toxoplasmic scleritis. Ophthalmology. 1988;95: 1399–403.
45. Kamath YS, Rathinam SR, Kawali A. Ocular toxoplasmosis associated with scleritis. Ind J Ophthalmol. 2013;61:295–7.

46. O'Donoghue E, Lightman S, Tuft S, Watson P. Surgically induced necrotising sclerokeratitis (SINS)- precipitating factors and response to treatment. Br J Ophthalmol. 1992;76:17–21.
47. Doshi RR, Harocopos GJ, Schwab IR, Cunningham Jr ET. The spectrum of postoperative scleral necrosis. Surv Ophthalmol. 2013;58:620–33.
48. Scott JA, Clearkin LG. Surgically induced diffuse scleritis following cataract surgery. Eye. 1994;8: 292–7.
49. Hemmati I, Wade J, Kelsall J. Risedronate-associated scleritis: a case report and review of the literature. Clin Rheumatol. 2012;31:1403–5.
50. Radin PP, Lumbroso-Le R, Levy-Gabriel C, Dendalale R, Sastre X, Desjardins L. Scleral necrosis after radiation therapy for uveal melanomas: report of 23 cases. Graefes Arch Clin Exp Ophthalmol. 2008;246:1731–6.
51. Passarin O, Zografos L, Schalenbourg A, Moulin A, Guex-Crosier Y. Scleritis after proton therapy in uveal melanoma. Klin Monatsbl Augenheilkd. 2012;229: 395–8.
52. Demirici H, Shields CL, Honavar SG, Shields JA, Bardenstein DS. Long-term follow-up of giant nodular posterior scleritis simulating choroidal melanoma. Arch Ophthalmol. 2000;118:1290–2.
53. Shukla D, Kim R. Giant nodular posterior scleritis simulating choroidal melanoma. Ind J Ophthalmol. 2006;54:120–2.
54. Foster CS, Forstot SL, Wilson LA. Mortality rate in rheumatoid arthritis patients developing necrotizing scleritis or peripheral ulcerative keratitis. Effects of systemic immunosuppression. Ophthalmology. 1984; 91:1253–63.
55. Fraser Jr DJ, Font RL. Ocular inflammation and hemorrhage as initial manifestations of uveal malignant melanoma: incidence and prognosis. Arch Ophthalmol. 1979;97:1482–6.
56. Kafkala C, Daoud YJ, Paredes I, Foster CS. Masquerade scleritis. Ocul Immunol Inflamm. 2005;13:479–82.
57. Yap EY, Robertson DM, Buettner H. Scleritis as an initial manifestation of choroidal malignant melanoma. Ophthalmology. 1992;99:1693–7.
58. Cheuk W, Chan JKC. IgG4-related sclerosing disease. A critical appraisal of an evolving clinicopathologic entity. Adv Anat Pathol. 2010;17:303–32.
59. Ohno K, Sato Y, Ohshima K, Takata K, Ando M, Al-Kader LA, Iwaki N, Takeuchi M, Orita Y, Yoshino T. IgG4-related disease involving the sclera. Mod Rheumatol. 2014;24:195–8.
60. Kim EC, Lee SJ, Hwang HS, Kim J, Kim MS. Bilateral diffuse scleritis as a first manifestation of immunoglobulin G4-related sclerosing pachymeningitis. Can J Ophthalmol. 2013;48:e31–3.
61. Helligenhaus A, Michel D, Koch JM. Nodular scleritis in patient with sarcoidosis. Br J Ophthalmol. 2003;87:507–8.
62. Jabs DA, Johns CJ. Ocular involvement in chronic sarcoidosis. Am J Ophthalmol. 1986;102:297–301.
63. Alyahya GA, Heegaard S, Prause JU. Characterization of melanoma associated spongiform scleropathy. Acta Ophthalmol Scand. 2002;80:322–6.
64. Alyahya GA, Ribel-Madsen SM, Heegaard S, Prause JU, Trier K. Melanoma-associated spongiform scleropathy: biochemical changes and possible relation to tumour extension. Acta Ophthalmol Scand. 2003;81:625–9.
65. Alyahya GA, Kolko M, Prause JU, Nielsen BS, Wang J, Heegaard S. Matrix metalloproteinase-2 is expressed in melanoma-associated spongiform scleropathy. Ophthalmol Vis Sci. 2008;49:2806–11.
66. Summers Rada JA, Shelton S, Norton TT. The sclera in myopia. Exp Eye Res. 2006;82:185–200.
67. Conn H, Green WR, de la Cruz ZC, Hillis A. Scleropachynsis maculopathy. Arch Ophthalmol. 1982;100:793–9.
68. Varga J, Wohlgethan JR. The clinical and biochemical spectrum of hereditary amyloidosis. Semin Arthritis Rheum. 1988;18:14–28.
69. Liew SC, McCluskey PJ, Parker G, Taylor RE. Bilateral uveal effusion associated with scleral thickening due to amyloidosis. Arch Ophthalmol. 2000;118:1293–5.
70. Scroggs MW, Klintworth GK. Senile scleral plaques: a histopathologic study using energy-dispersive x-ray microanalysis. Hum Pathol. 1991;22:557–62.
71. Broekhuyse RM. The lipid composition of aging sclera and cornea. Ophthalmologica. 1975;171:82.
72. Shields CL, Quershi A, Eagle Jr RC, Lally SE, Shields JA. Epibulbar osseous choristoma in 8 patients. Cornea. 2012;31:756–60.
73. Tsai AS, Lee KY, Al Jajeh I, Sittampalam K, Fong KS. Epibulbar osseous choristoma: a report of two cases. Orbit. 2008;27:231–3.
74. Font R, Zimmerman LE. Nodular fasciitis of the eye and adnexa. A report of ten cases. Arch Ophthalmol. 1966;75:475.
75. Holds JB, Mamalis N, Anderson RL. Nodular fasciitis presenting as a rapidly enlarging episcleral mass in a 3-year-old. J Pediatr Ophthalmol Strabismus. 1990;27:157–60.
76. Berk DR. Episcleral haemangioma as an isolated finding. Eur J Ophthalmol. 2010;20:807.
77. Celebi S, Alagoz G, Aykan U. Ocular findings in Sturge-Weber syndrome. Eur J Ophthalmol. 2000; 10:239–43.
78. Kumar BV, Rennie IG, Mudhar HS. A case of episcleral cellular neurofibroma. Int Ophthalmol. 2005;26:239–41.
79. Then SY, De Sousa JL, Chandrasekharn L, Francis I, Malhotra R. Scleral infiltration in orbitotemporal plexiform neurofibromatosis. Clin Experiment Ophthalmol. 2007;35:773–5.
80. Quintana M, Lee WR. Intrascleral schwannoma. Ophthalmologica. 1976;173:64–9.
81. Hosseini H, Eghtedari M, Roozitalab M, Ashraf M, Shahrzad S. Intrasclera schwannoma. BMJ Case Rep. 2011;3:2011.

The Crystalline Lens

5

J. Douglas Cameron and Dejan M. Rašić

5.1 General Description

The crystalline lens is the second most powerful refracting structure of the eye. The cornea has the major refractive power. The lens is the optical element that allows voluntary variation of focusing from distance to near. At birth the lens is nearly totally transparent and is malleable (Fig. 5.1a, b). The lens doubles in volume between birth and age 70 years because of continuous addition of new lens fibers to the peripheral layers [1, 2]. Unlike the skin, the older layers cannot be desquamated to the exterior but accumulate in the central portion of the lens. At approximately age 40 years, the lens loses pliability and optical correction is necessary to focus at near (bifocals). At approximately age 70 years, the lens becomes progressively more opaque. When the loss of transparency affects activities of daily living, the lens is termed a cataract (Fig. 5.2a, b).

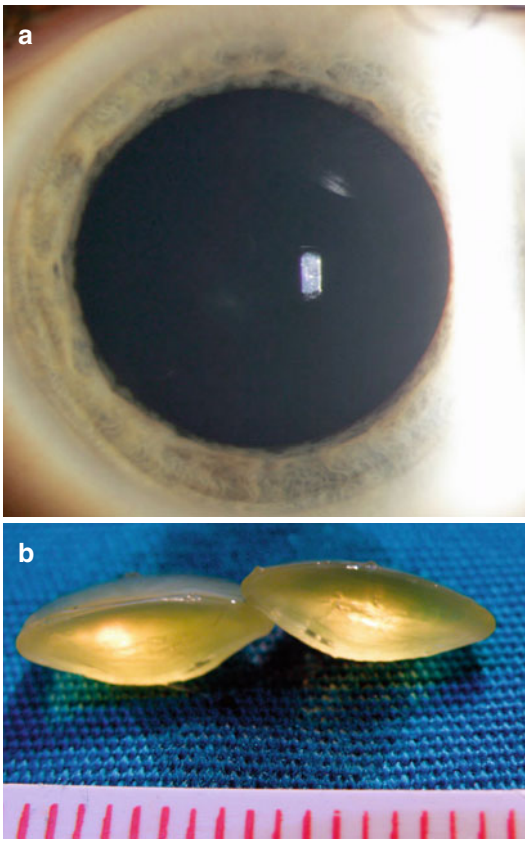

Fig. 5.1 The normal lens (**a**) examined by a slit lamp (biomicroscopy). No incident light is reflected by the lens tissue, as would be the case with a lenticular opacity (cataract). This shows the gross cross-sectional features of a lens (**b**) from a 50-year-old man without a significant clinical cataract. The lens contour is ovoid rather than spherical as found in more elderly individuals. The lens doubles in volume between birth and age 70 years

J.D. Cameron, MD, MBA (✉)
Departments of Ophthalmology and Visual Neuroscience and Laboratory Medicine and Pathology, University of Minnesota School of Medicine, 420 Delaware Ave. SW, MMC-493, Minneapolis, MN, USA
e-mail: camer001@umn.edu

D.M. Rašić
Departments of Ophthalmology and Pathology, University of Belgrade School of Medicine, Belgrade, Serbia

S. Heegaard, H. Grossniklaus (eds.), *Eye Pathology: An Illustrated Guide*,
DOI 10.1007/978-3-662-43382-9_5, © Springer-Verlag Berlin Heidelberg 2015

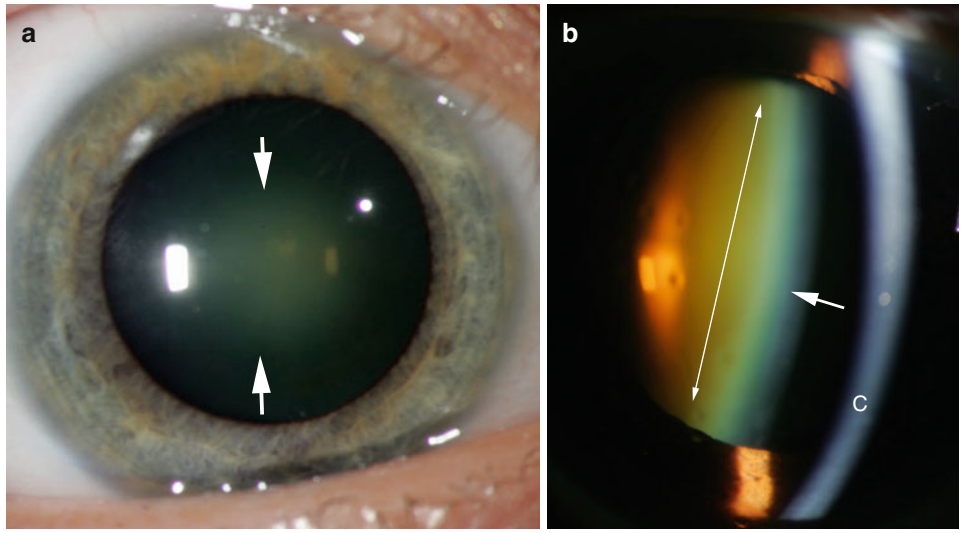

Fig. 5.2 A nuclear sclerotic cataract (**a**) as seen by direct illumination. The central portion of the lens (nuclear) has become opaque and is reflecting light (*arrows*). This degree of opacification may be associated with decreased visual acuity. A nuclear sclerotic cataract (**b**) as seen by slit beam illumination. The nuclear area of the lens (*double arrows*) has become brown-orange because of the deposition of adrenochrome pigment. The anterior lens capsule is indicated by the *single arrow*. The cornea is at the level indicated by *C*. The area between is the fluid-filled anterior chamber. The aqueous normally does not reflect light and the space is "optically empty"

A primary cataract is a lens opacity developing as an expected event in aging. Age-related cataracts many have variable clinical and histopathologic features such as nuclear sclerosis, cortical opacities, or posterior subcapsular opacities. A secondary cataract is a lens opacity developing as part of a systemic disease process or an external event. Examples include developmental (persistent fetal vasculature, or persistent hyperplastic primary vitreous), trauma (posterior subcapsular cataract), endocrine (galactosemic cataract), toxic (siderotic cataract), and neoplasia (zonal cataract from mechanical compression of a ciliary body melanoma). There are no absolute differentiating histopathologic features among the various groups; however, certain patterns many be suggestive of a possible cause. For example, posterior subcapsular cataracts are associated with the use of steroids, severe diabetes mellitus, and intraocular or idiopathic inflammation.

Generally, surgical removal of either a primary or secondary cataract restores functional vision. The opaque natural lens is replaced with an intraocular lens (IOL) made of biocompatible synthetic material (e.g., polymethylmethacrylate [PMMA], acrylic, or silicone) (Fig. 5.3). The lens is placed within the native lens capsule in the posterior chamber of the eye (Fig. 5.4).

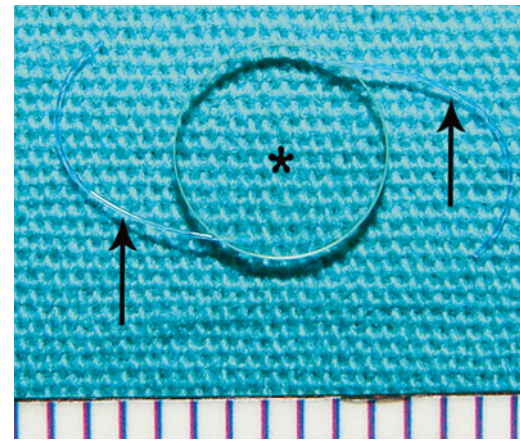

Fig. 5.3 At the time of surgery the cataractous lens is replaced by a synthetic intraocular lens (*IOL*). Generally only the lens cortex is removed. The lens capsule is left in place and is used as a repository for the replacement lens. There are many different styles; however one of the most commonly used lens is this three-piece, posterior chamber intraocular lens. The central optic (*) focuses light on the retina to form an image. The lens is supported by two lens loops (*arrows*) within the lens capsule

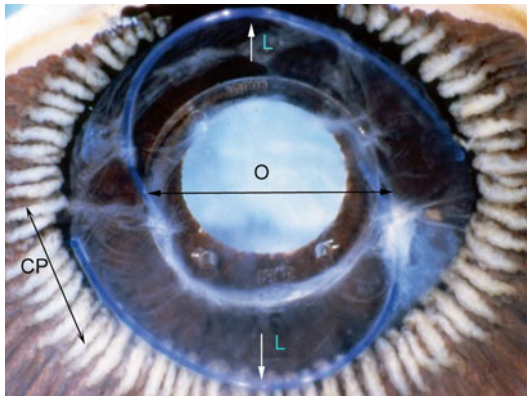

Fig. 5.4 Posterior view of an intraocular lens in situ. Ciliary processes (*CP double arrow*) are present in the peripheral posterior chamber. The intraocular lens optic (*O double arrow*) is roughly centered over the pupil. The tips of the arrows mark the insertion of the lens loops (*L single arrow*) into the lens optic. The lens loops are within the lens capsule, which is translucent except in an opaque region at the loop which has undergone focal fibrous metaplasia of equatorial lens epithelium

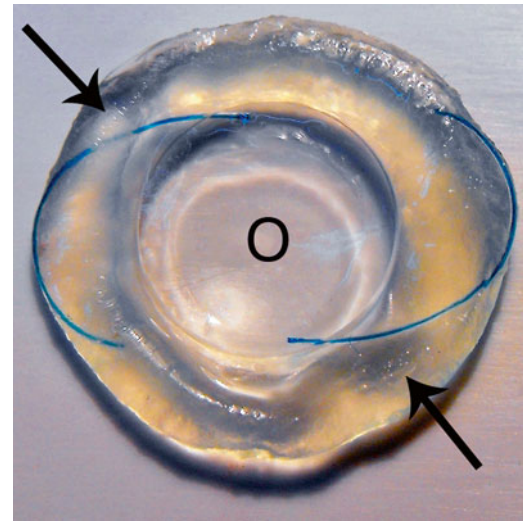

Fig. 5.5 This illustration demonstrates the desired position of an intraocular lens within the lens capsule. The optic (*O*) is placed in the visual axis. The intraocular lens loops (*arrows*) are encased in the residual cortex. The IOL is entirely within the lens capsule. This specimen is from an eye removed as part of an exenteration procedure in a case of adenoid cystic carcinoma of the lacrimal gland. The eye was not directly affected by the malignancy

The current procedure for removal of a cataract is to use a double-lumen cannula with an ultrasound tip to fragment the lens cortical fibers while leaving the surface capsule intact. Irrigation fluid is introduced through the outer cannula lumen, and fragmented tissue is aspirated though the central lumen of the cannula. The IOL is positioned permanently within the original lens capsule. The fragmented lens tissue is usually of no diagnostic value and is not submitted for histopathologic evaluation.

The pathologist may encounter specimens containing lens material in cases of enucleation (removal of the entire eye), evisceration (removal of the cornea and intraocular contents), and exenteration (removal of all of orbital tissue including the globe). In many cases, evaluation of alteration of the lens position and character is helpful in determining mechanisms of end-stage glaucoma, a common final pathway leading to enucleation of the eye. Lens tissue may be an important finding in extruded intraocular contents from a ruptured globe, a vitreous aspirate, or surgical removal of a nonfunctioning IOL (Fig. 5.5). Malignant transformation of crystalline lens material has not been observed [3].

5.2 Embryology, Anatomy, and Development

The crystalline lens is formed from the surface ectoderm at the 28th day of gestation at a point of physical contact with elements of neuroectoderm that have extended laterally from the anterior neural groove. The surface ectodermal cells elongate and penetrate internally to form a sphere of cells (the lens vesicle), which detaches from the surface. With the support of surrounding neural crest tissue, the lens matures by elongating the cells of the posterior hemisphere, which come to occupy the central lumen of the sphere to form a solid cellular structure. As the posterior cells elongate to form the primary lens fibers, most of the cell organelles and the entire lens nucleus involute creating an "anucleate" cell with homogeneous cytoplasm. These cell structure characteristics remain throughout life and contribute to the ability of lens tissue to efficiently transmit light [4].

The anterior hemisphere cells remain and function in proliferation of new lens fibers from stem cells near the lens equator and are essential

Fig. 5.6 In the developed lens, epithelial cells are only present on the anterior hemisphere. The posterior hemisphere is tightly adherent to the anterior vitreous face. New lens fibers are produced at the lens equator in the region of zonular insertions (*) where cell nuclei separate from the lens capsule. These lens stem cells form a curvilinear arrangement, the lens "bow" indicated by the *double headed arrow*. *COR* indicates position of the cornea. *CB* indicates the position of the ciliary body

Fig. 5.7 The developing eye at an early stage of embryogenesis. The posterior lens epithelial cells have migrated anteriorly as primary lens fibers (*P*) to obliterate the cavity of lens vesicle. At this point nutrition to the lens is supplied by the anterior tunica vasculosa lentis (*arrows*) and the posterior tunica vasculosa lentis (*)

for maintaining diffusion gradients for glucose and other molecules necessary to sustain lens fibers (Fig. 5.6). Initially, development of the lens is maintained by diffusion from surrounding tissues. As the structure enlarges, there is a transient vascular supply with contributions from the primitive iris vasculature and the posterior hyaloid artery system. Near the time of birth, this transient vascular system, the tunica vasculosa lentis, involutes by apoptosis, as the primary fibrovascular vitreous is replaced by acellular secondary vitreous (Figs. 5.7 and 5.8). Tight adhesions form between the lens capsule and the anterior vitreous in focal areas. Nutrition supplied by the temporary vascular system is replaced by a transudate of plasma (aqueous fluid which contains no red blood cells) produced by the nonpigmented epithelium of the ciliary processes. At this point of development, the fundamental organizational anatomy of the crystalline lens is complete and changes very little throughout life.

The crystalline lens is located in the anterior segment of the eye bordered anteriorly by the cornea, laterally by the trabecular meshwork and the ciliary body, and posteriorly by the anterior

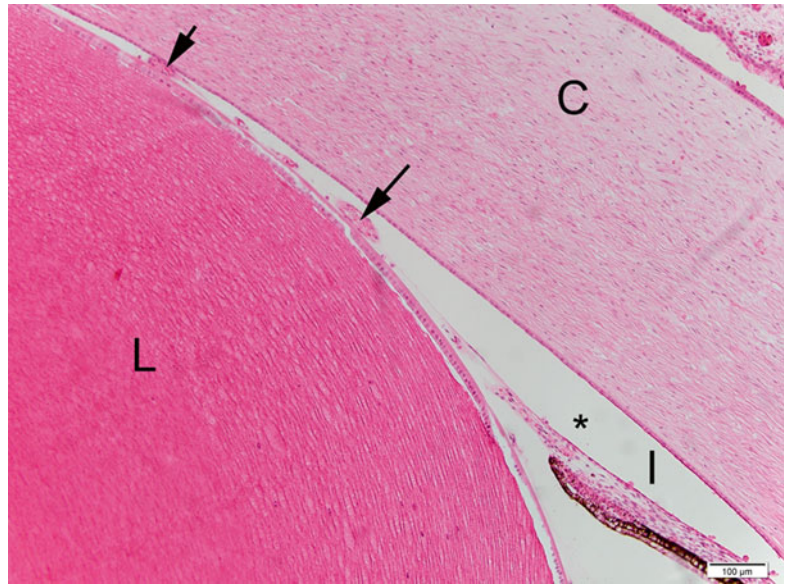

Fig. 5.8 Early in the development of the eye, the nutritional support of the lens (*L*) is provided by a network of vessels (tunica vasculosa lentis) (*arrows*) until aqueous is produced by the ciliary body. The tunica vessels of the anterior hemisphere originate from the vascular system of the iris (*I*) via channels from the minor arterial circle of the ciliary body (*). The position of the cornea is indicated by (*C*)

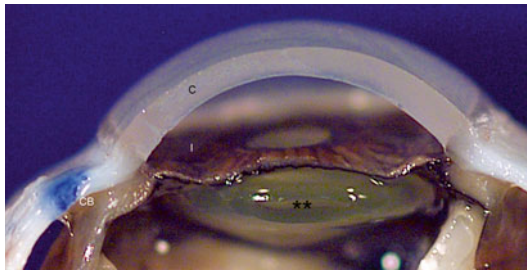

Fig. 5.9 The lens (**) is located in the posterior chamber behind the iris diaphragm (*i*) and within the ring of the ciliary body (*CB*). The cornea (*C*) is the most powerful optical element of the eye. There is no cataract in this case

vitreous face (Fig. 5.9). The anterior segment is divided into anterior and posterior chambers by the iris diaphragm. The pupil of the iris diaphragm allows aqueous fluid formed by the ciliary processes in the posterior chamber to circulate to the anterior chamber and exit the eye through the trabecular meshwork. The pupil also has optical functions in adjusting the quantity and quality of light entering the eye. The crystalline lens measures, in the adult, approximately 9–9.5×9–9.5 in diameter and ×3.5–4.5 from the anterior to the posterior surface. The lens is suspended in the posterior chamber by delicate, acellular elastic fibers, the zonules, which originate at the vitreous base and portions of the ciliary processes. The zonules insert directly to the lens capsule anteriorly and posteriorly near the equator but do not involve the central visual axis of the lens (Fig. 5.10a, b) [3].

The lens capsule, one of the thickest basement membranes of the body, is composed of type IV collagen, laminin, and heparin sulfate. This semipermeable membrane is thickest in the region of zonular insertion laterally and is thinnest at central anterior surface and the central posterior surface to maximize transmission of light. The anterior capsule thickens throughout life by the addition of basement membrane secreted by the anterior hemispheral epithelial cells. There are no similar cells on the posterior surface of the lens; therefore the posterior lens capsule remains thin throughout life (Fig. 5.11a, b) [5].

The overall configuration of the lens is that of a biconvex oval that becomes more spherical with advancing age. The structure is completely cellular with essentially no extracellular space. There is no innervation. There is no direct vascular supply indicating that the metabolic demands of the lens are met completely by diffusion across the lens capsule from surrounding aqueous. Interruption of aqueous flow will cause degeneration of the lens as is observed in conditions such as acute narrow angle glaucoma.

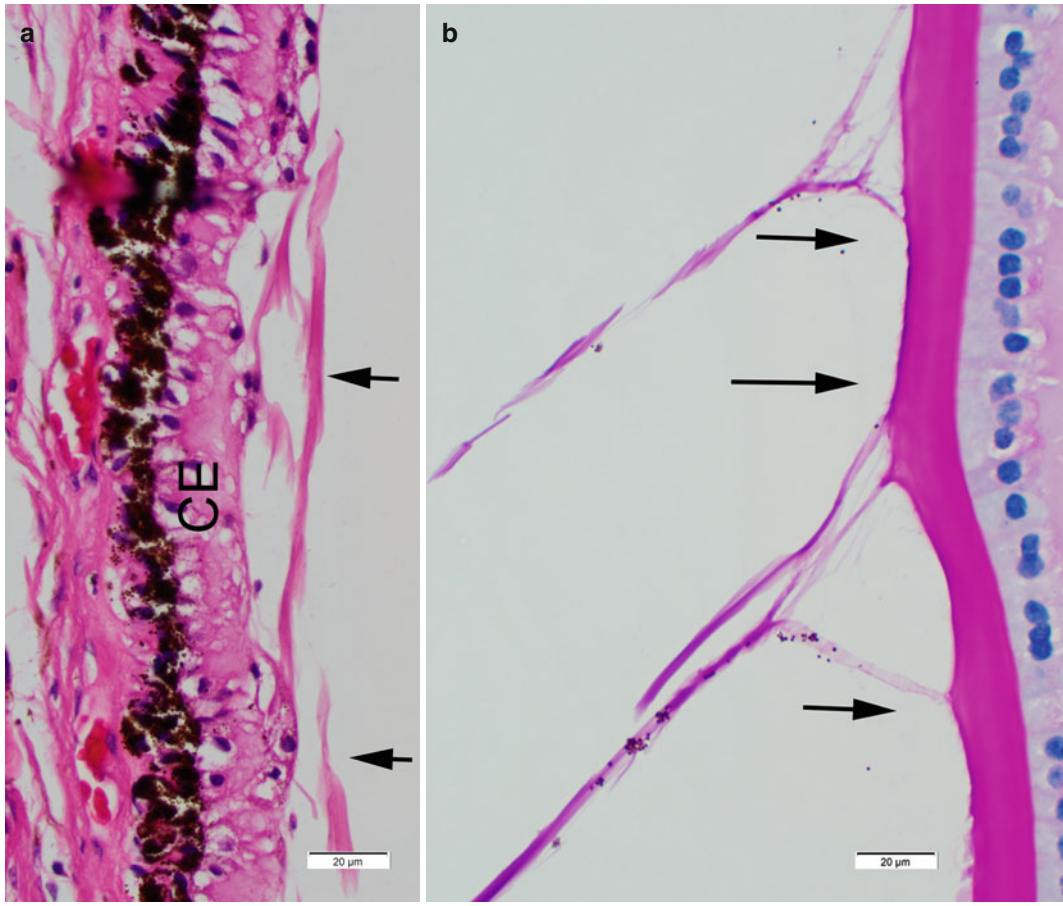

Fig. 5.10 The zonules suspend the lens in the posterior chamber. These acellular fibers (*arrows*) arise from the nonpigmented epithelium of the pars plana (*CE*) just anterior to the vitreous base (**a**) and pass through the fluid-filled posterior chamber. The zonular fibers insert onto the surface of the lens capsule (**b**) in the region of the lens equator. In addition, the zonules along with the muscles of the pars plicata participate in changing the lens contours in accommodation

The original intraocular lens was developed during World War II when surgeons caring for injured Spitfire pilots noted that intraocular foreign body fragments from the cockpit canopy material were well tolerated and appeared to be biostable. The material, Perspex or polymethyl methacrylate (PMMA), was used to fabricate a replacement lens of roughly the same dimensions as the native crystalline lens. The type of surgery commonly used during that time, extracapsular cataract extraction, allowed the lens to be placed in the posterior chamber without additional support. The lens, however, was quite heavy and tended to dislocate into the anterior chamber or into the vitreous. Despite these problems, many of the IOLs were retained and provided serviceable vision for decades. Over the last 50 years, the design of IOLs and the method of placement have improved considerably. A folded IOL is now injected through a large-bore cannula via a small (2.6 mm clear corneal incision) to spontaneously uncurl and position within the posterior chamber and within the lens capsule. Dislocation from the posterior chamber is currently an infrequent occurrence. Visual recovery from cataract surgery now generally restores vision to the full potential of the person's retina. Coexisting macular degeneration is one of the major limiting factors to full vision rehabilitation [6].

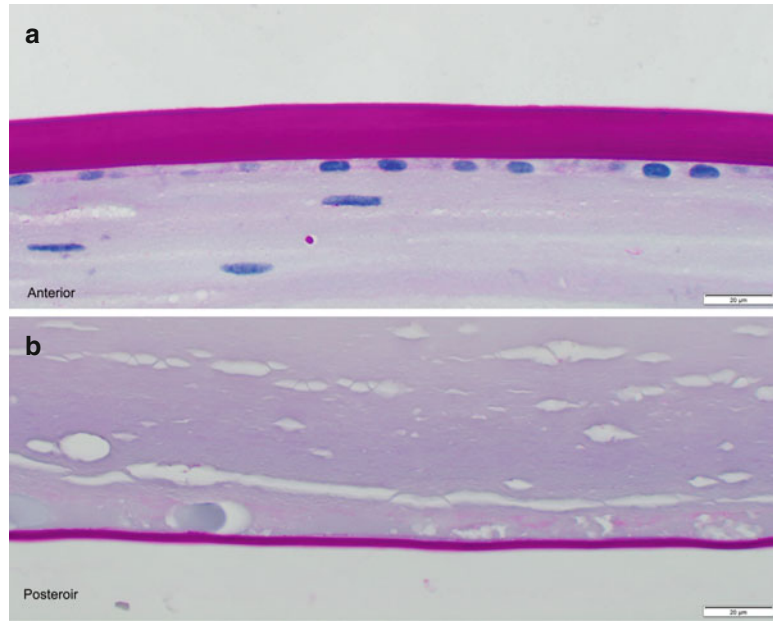

Fig. 5.11 The lens capsule of the anterior hemisphere (anterior) is associated with active lens epithelial cells, which add to the capsular thickness throughout life. The lens capsule of the posterior hemisphere is not associated with active lens epithelial cell and remains thin throughout life

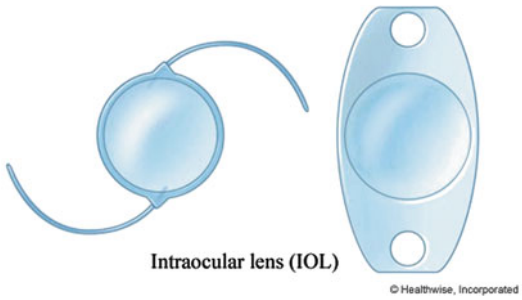

Fig. 5.12 There are two general designs of intraocular lenses used commonly: the three-piece intraocular lens (two loops and a central optic) and a one-piece plate lens. Both of these types of lenses are placed in the lens capsule in the posterior chamber. Another type of lens may infrequently be placed in the anterior chamber

Intraocular lenses are generally one of two basic designs (Fig. 5.12). The first is a lens constructed of three pieces: a central optic fabricated to the optical power needed to correct the cataract patient's anticipated residual refractive error and two loops swedged into the optic to expand and support the optic within the lens capsule. The second category of design is a plate configuration that is a single flat piece of synthetic material with the optical power located in the center of the lens and the maximal dimensions of the lens calculated to optimally stabilize the device within the lens capsule. There are literally hundreds of other designs some with special applications such as implanting the lens anterior to the iris diaphragm in the anterior chamber [6].

Except for silicone and Supramid, most of the intraocular lens materials are soluble in the organic solvents used for the preparation of paraffin-embedded material. Generally, the presence of an intraocular lens in sectioned tissue depends on recognizing the void in tissue (shadow) left by the intraocular lens material (Fig. 5.13). Generally, there is no tissue reaction to the material itself; however fibrous tissue may form in the immediate environment of the IOL (Fig. 5.14). Occasionally, there may be an inflammatory reaction to the materials of the lens loops (Fig. 5.15).

Histopathologic features of congenital lens abnormalities are similar to those resulting from degeneration or injury. Congenital variations of the lens consist of failure of formation of transparent tissue, alteration of contours and refractive index affecting optical power, and abnormal positioning of the lens due to dysfunction of zonular support. Most of these features are readily apparent by clinical examination but are subtle or obscure by histopathologic examination (Fig. 5.16a, b) [7].

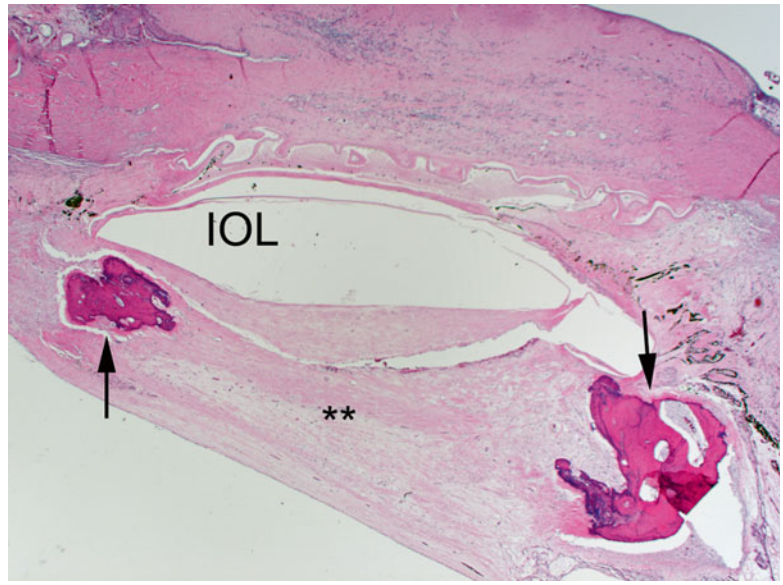

Fig. 5.13 A biconvex intraocular lens optic (*IOL*) was present in the posterior chamber; however the material was solubilized by the organic solvents used in tissue processing. Fibrous tissue has formed in the posterior capsule and in the space behind the lens (**) resulting in a cyclitic membrane. Osseous metaplasia (*arrows*) has formed in the abnormal fibrous tissue

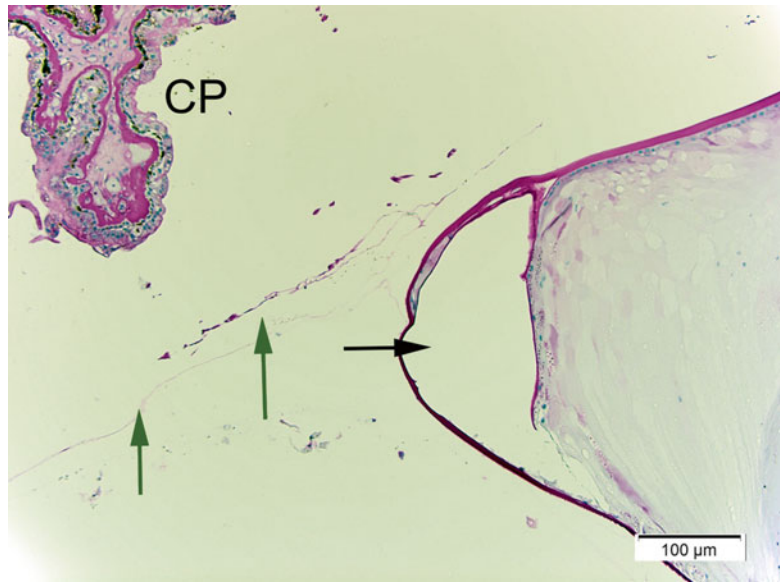

Fig. 5.14 An intraocular lens has been placed in a lens capsule with a moderate amount of lens cortex remaining. The lens loop material has dissolved but the negative image of its cross section is apparent (*black arrow*). Lens zonules (*Green arrows*) and the tips of ciliary processes (*CP*) are evident

Congenital absence of the crystalline lens in an otherwise normally developed globe has not been observed. The most likely reason is that the lens is one of two fundamental differentiating tissues necessary for eye development. In some cases the lens may have formed but then has degenerated. Malformation of lens fibers leading to focal opacification of the lens during gestation is a relatively common event and is usually dependent on toxic changes or microbial infection of the lens environment. If the event is brief and minimal, the opacity may be seen clinically but may not progress of cause loss of ocular function.

One of the clearest examples of histopathologic verification of a congenital lens abnormality is a phakomatous choristoma (Zimmerman tumor) [8]. This lesion consists of an asymptomatic area of palpable induration of the subcutaneous tissue the lower eyelid, usually nasally, and most often identified in early childhood. The indurated tissue

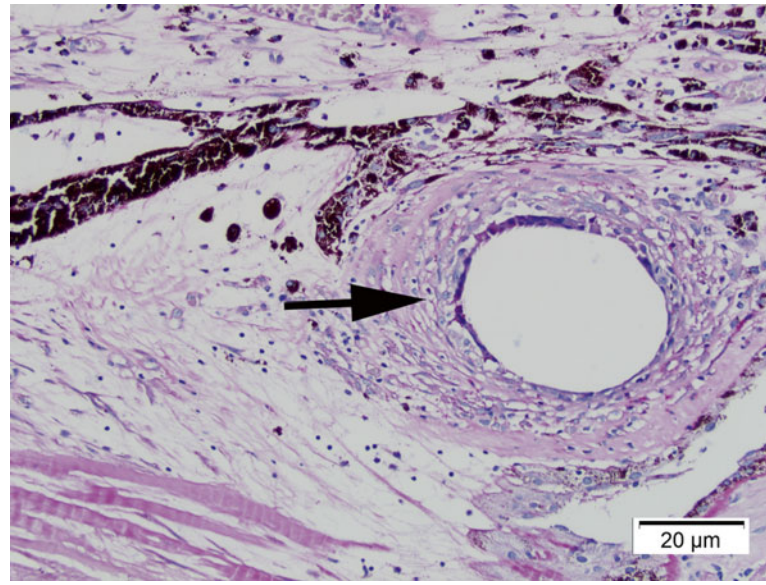

Fig. 5.15 An intraocular lens loop (*arrow*) has been placed in the posterior chamber posterior to the iris but outside of the lens capsule. The loop material has stimulated an inflammatory response either because of the loop material itself or because of some antigen on the surface of the material

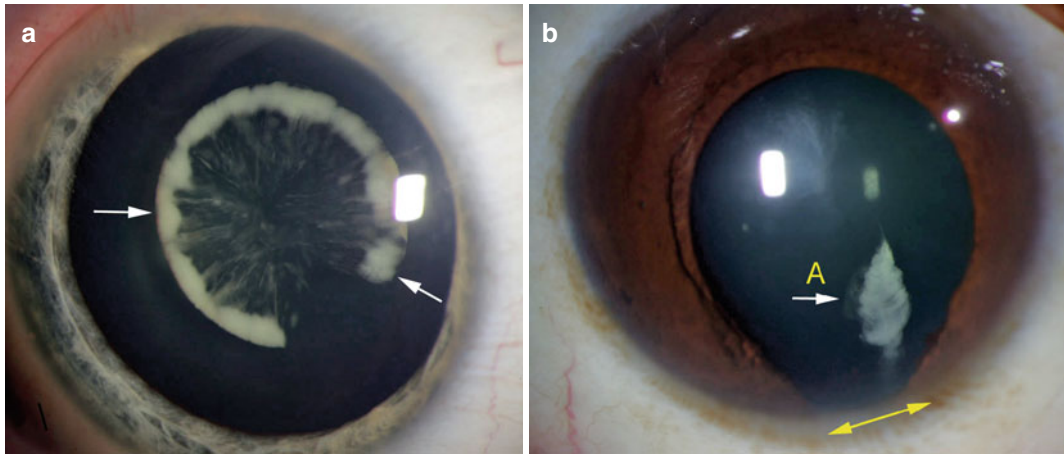

Fig. 5.16 Two cases of congenital cataract (lens opacity present at birth). The opacity in **a** is at level of the nucleus. The opacity surrounds the margin of the nucleus leaving the periphery relatively clear. The opacity in (**b**) is in the superficial cortex (*A*) and is associated with a defect (coloboma) of the iris (*double arrow*.) Estimating the vision in cases of congenital cataract is difficult; the vision in (**a**) was 20/30, while the vision in (**b**) was 20/80

evolves from an ectopic rest of primitive lens material characterized by a prominent PAS-positive membrane surrounding large epithelial cells that are similar in appearance to the cells of a posterior subcapsular cataract (Fig. 5.17). The entity is treated with total surgical excision and does not recur.

The most dramatic congenital abnormality of the eye is cyclopia or synophthalmos. This condition results from the failure of development the diencephalon that is most often associated with fetal death. In the autopsy specimens the eye tissue in synophthalmos generally preserves the anterior segments, while there is apparent "fusion" of the posterior segment characterized by major posterior tissue abnormalities. The crystalline lenses may appear to be remarkably normal (Fig. 5.18). Similarly, the lens of a cyclopean eye may have few abnormal features [9].

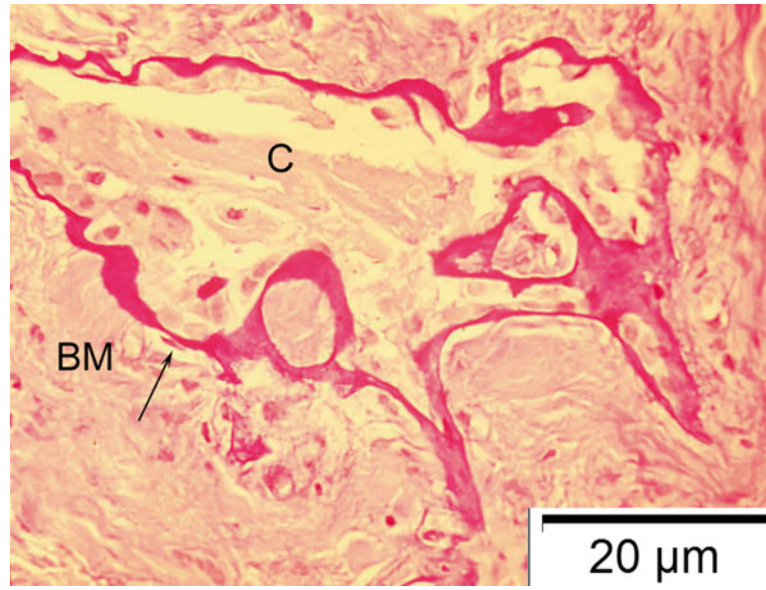

Fig. 5.17 Phakomatous choristoma (Zimmerman tumor) is an ectopic lens tissue in the lower eyelid presenting as an indurated tumor of childhood. It is composed of lens cortical cells (*C*) surrounded by irregular basement membrane (*BM*) forming a lens capsule

Fig. 5.18 Synophthalmos is a developmental abnormality of the development of the eye early in embryogenesis. There is a fault in the development of the intervening brain making the posterior segment appear to be "fused." The anterior segment including the lens may be remarkably normal (Courtesy of Alan Prioa, MD, Eastern Ophthalmic Pathology Conference, Duke University, Durham, North Carolina, 2007)

Alteration of the shape of the lens because of abnormalities of the lens capsule can seriously disrupt the refractive function of the lens. One example is lenticonus associated with Alport's syndrome. Alport's syndrome is a rare genetically determined disorder generally with an x-linked pattern of inheritance that causes a defect in type IV collagen, a major component of basement membrane including the glomerulus of the kidney and the lens capsule [10]. The weakened capsule allows an increase in the radius of curvature of either the anterior or posterior lens surfaces (Fig. 5.19) causing a marked decrease in visual function. The alteration of curvature is clearly evident by biomicroscopy. The lens may contain a congenital or an acquired cataract. By light microscopy the lens capsular thickness is reduced by two-thirds and appears more fibrillar than the normal lens capsule. By electron microscopy large numbers of partial

Fig. 5.19 A developmental abnormality of type IV collagen formation in the lens capsule has caused a thinning of the lens capsule. The thinning has caused an increase in the radius of curvature of the posterior surface of the lens significantly altering the optical qualities of the lens

capsular dissidences are present throughout the lens capsule that contains cellular debris [11].

A pyramidal cataract is a feature of failure of separation of the lens vesicle from the surface ectoderm. The cataract clinically appears as a well-demarcated and densely opaque pyramid projecting from the central anterior surface of the lens into the anterior chamber. The opacity is composed of a region of fibrous metaplasia of the anterior lens epithelium. The cataract is generally not progressive and may have a minimal effect on visual function [12].

5.3 Inflammation

Crystalline lens material does not excite an intraocular inflammatory response unless the cortical material is exposed to the immune system. If an entire crystalline lens is dislocated with the crystalline lens capsule intact, the lens will not induce an inflammatory response even though the position of the lens, particularly in the pupillary space, may induce secondary glaucoma (e.g., pupillary block glaucoma). If, however, the crystalline lens cortex is displaced from the protection of the lens capsule, the cortical material will induce a severe granulomatous inflammatory reaction (Fig. 5.20). In the setting of

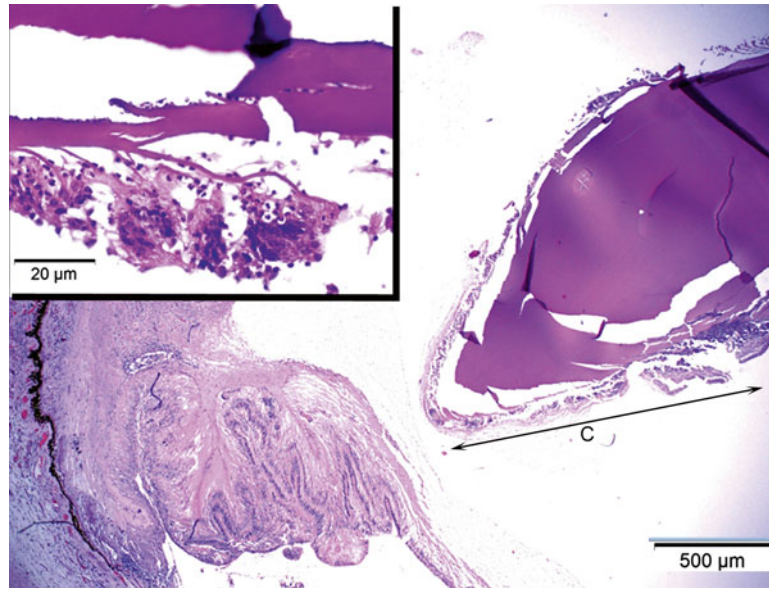

Fig. 5.20 Lens cortex not covered by an intact lens cortex will induce granulomatous inflammation and potentially cause extensive destruction of intraocular tissue. There is an extensive inflammatory reaction on the surface of the lens nucleus (*C*, *double arrows*). The inflammatory reaction is characterized by epithelioid histiocytes (*insert*)

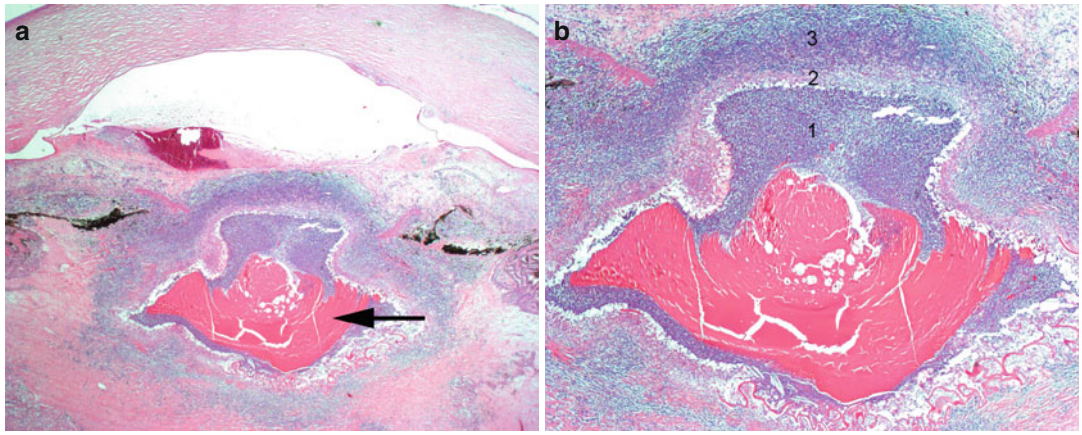

Fig. 5.21 (**a**) The lens capsule has become disassociated from the cortex (*arrow*) stimulating a massive inflammatory reaction. The reaction is in the posterior chamber and has completely destroyed the anterior uveal tract. (**b**) The inflammatory reaction is zonal: (*1*) a concentration of acute inflammatory cells in contact with lens cortical protein, (*2*) a region of accumulation of epithelioid histiocytes, and (*3*) a peripheral accumulation of lymphocytes and plasma cells

trauma, the condition is called lens-induced uveitis or phacoanaphylactic endophthalmitis. If the lens cortex is dislocated during cataract extraction, the condition is called a "dropped nucleus."

Phacoanaphylactic (phacoantigenic) endophthalmitis is an intraocular inflammation following disruption of the lens capsule in the setting of either accidental trauma or intraocular surgery [13–15]. Despite the implications of the name, the process is neither anaphylactic nor toxic. The inflammatory reaction is directed toward lens proteins, crystallins. Crystallins are found not only in the lens but also in the retina and skeletal muscle. The inflammatory reaction depends more on altered tolerance to lens protein than as an immune reaction to previously sequestered antigens [16, 17]. The histopathologic pattern of inflammation is zonal: a zone of polymorphonuclear leukocytes (PMN) directly adjacent to exposed lens protein, surrounded by a layer of epithelioid histiocytes, with a peripheral region of a lymphoplasmacytic infiltrate. The inflammation in the eye is generally limited to the anterior segment and vitreous (Fig. 5.21a, b). Only a mild reactive inflammatory infiltrate is usually present in other posterior segment structures [18]. This type of inflammatory reaction has the potential to completely destroy the internal contents of the eye. Treatment is usually directed to surgically removing the retained lens cortical remnants.

Inflammation in the anterior chamber (anterior uveitis, iridocyclitis) may result in either an anterior subcapsular cataract (fibrous metaplasia of the crystalline lens epithelium) or posterior subcapsular cataract (posterior migration of nucleated lens bow cells) (Fig. 5.22a, b). An anterior subcapsular cataract is located at the geographic center of the anterior surface of the lens. Lens epithelial cells rendered necrotic by the toxic effects of inflammation stimulate remaining viable epithelial cells to respond by fibrous metaplasia forming a subcapsular collagenous plaque. The remaining epithelial cells may form a posterior monolayer that secretes a new basement membrane on its basal surface. Contraction of myofibroblastic cells of the collagenous plaque results in wrinkling of the anterior contour of the lens capsule. The process is irreversible and may cause considerable loss of visual function. Aqueous status may occur if fibrinous adhesions form in the region of iris-lens contact (posterior synechiae) leading to additional epithelial cell damage because of depletion of nutrients. Treatment is limited to cataract extraction after inflammation is controlled or eliminated.

A posterior subcapsular cataract is found not only in the setting of inflammation but also with the use of therapeutic cortical steroids, diabetes mellitus, and trauma and without apparent cause.

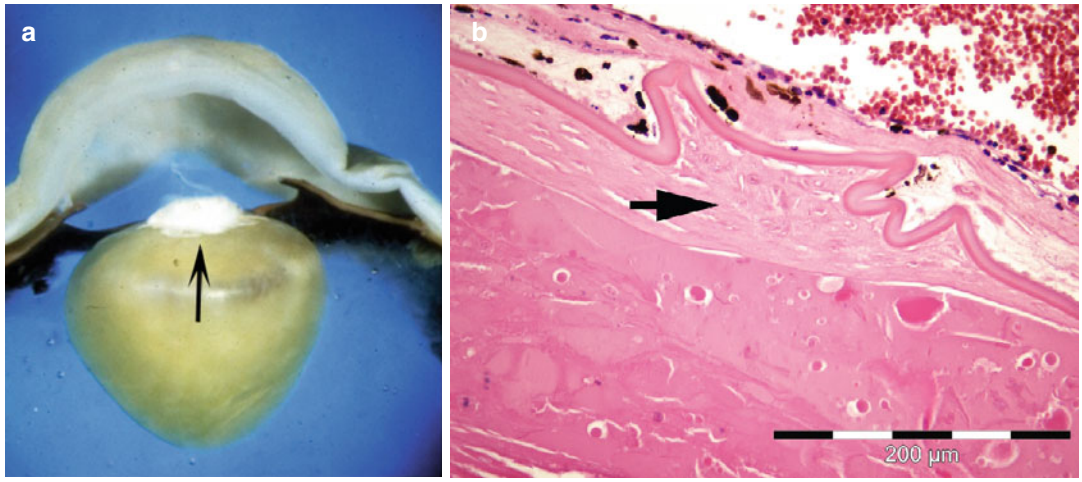

Fig. 5.22 Anterior chamber inflammation has caused a well-demarcated, elevated, totally opaque opacity of the anterior lens (**a**). In this case of necrotic malignant melanoma (**b**), fibrous metaplasia (*arrow*) of the anterior subcapsular lens epithelium has occurred. The epithelium has been replaced by collagenous tissue inside the lens capsule. Fibrous tissue has also been induced on the external surface of the capsule by anterior uveitis

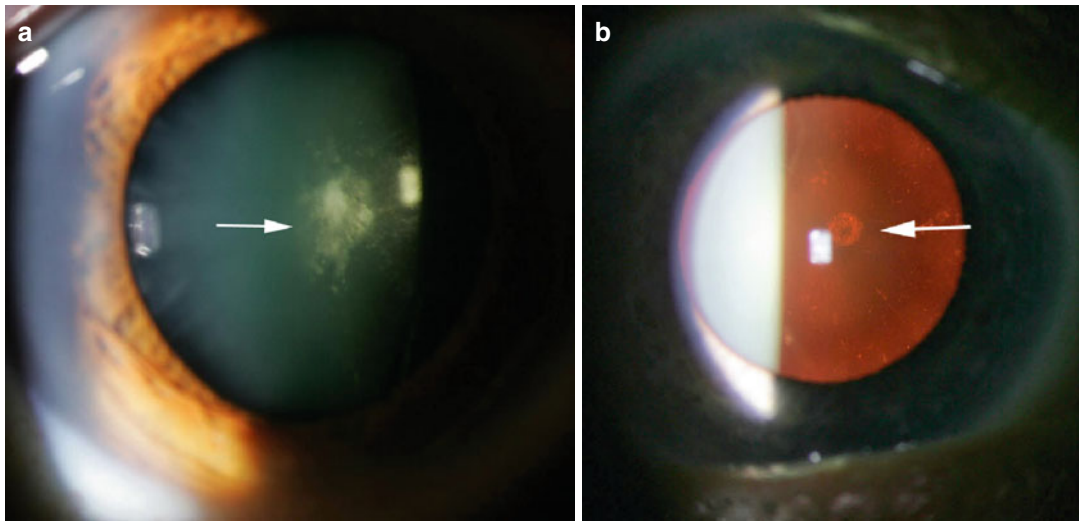

Fig. 5.23 Two cases of posterior subcapsular cataract are illustrated. This type of cataract presents as a "ground glass" opacity just anterior to the posterior capsule. The view (**a**) is by direct illumination and (**b**) by slit lamp biomicroscopy. Cataracts in this location tend to interfere with vision early in the natural history of cataract because of their location at the visual axis

The opacity may be very subtle consisting of granular opacities in the visual axis of the lens on the internal surface of the lens capsule (Fig. 5.23a, b). Epithelial cells migrating to the anterior hemisphere replace normally aging epithelial cells. If a toxic stimulus is concentrated in the posterior cortex, the lens epithelial cells may migrate posteriorly in the subcapsular space of the posterior hemisphere. In this circumstance, the lens cells do not lose their nucleus or cell organelles. The migrating cells do not form normal delicate strap cells but assume a pleomorphic globular configuration and congregate at the posterior pole of the lens (Fig. 5.24). Individual cells do

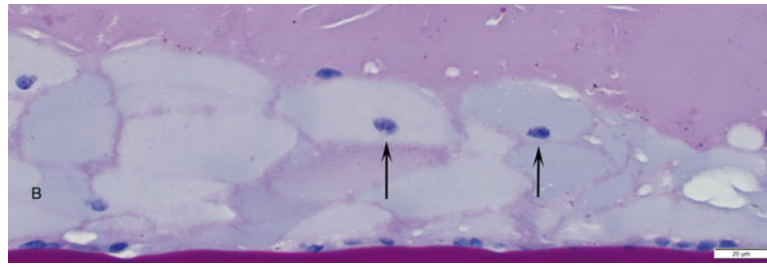

Fig. 5.24 Lens epithelial cells (*arrows*) have migrated from the lens equator along the posterior capsular internal surface to the posterior axial region of the lens. The cells have retained their nuclei but have formed irregular globular cells (*Wedl cells or bladder cells*) instead of the uniform lens fibers normally found in this region

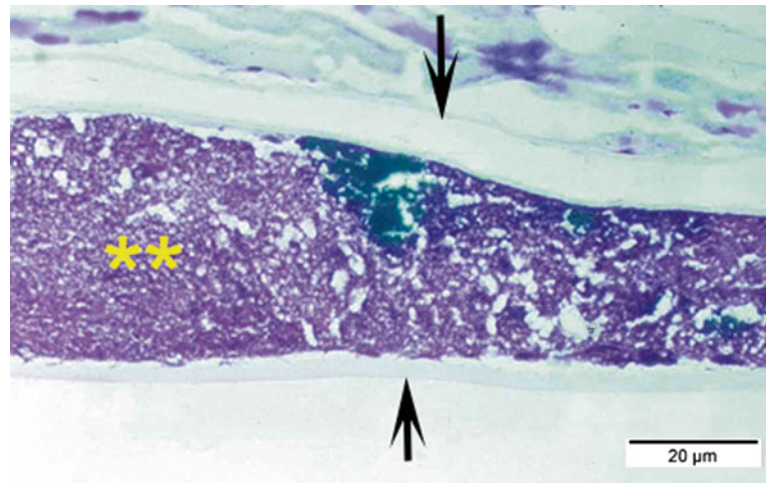

Fig. 5.25 *P. acnes* organisms (**) mechanically introduced during the time of surgical extraction of the lens cortex have proliferated within residual lens capsule (*arrows*). The organisms (**) are protected from phagocytosis by the lens capsule

not transmit light but reflect light giving the appearance of ground glass when viewed by biomicroscopy. This type of cataract is unpredictable; it may progress over months or may remain stable for decades. The process is irreversible and is treated by standard cataract extraction at a time when there is control of the original stimulating condition.

The most common type of microbial infection of the lens is acquired during cataract surgery when surface flora becomes established within the lens capsule and proliferates. The disrupted edges of the lens capsule fuse forming a pocket of basement membrane that protects the organism from innate inflammation. The organism is often *S. epidermidis* or *P. acnes*, both low-virulence bacteria (Fig. 5.25). Low-virulence endophthalmitis is recognized clinically several days to weeks following cataract surgery as a low-grade anterior uveitis associated with progressive opacification of lens capsular remnants. The inflammation may lead to secondary glaucoma or cystoid macular edema. Treatment consists of intraocular antibiotics or surgical removal of infected lens capsular and cortical remnants. Organisms within the lens remnants are clearly identified by Gram or Brown-Hopps stains.

Of historical and possible future significance is infection of the developing crystalline lens by rubella virus. In the early 1960s in the United States and Europe, there was an epidemic of gestational rubella infections resulting in a large number of children with congenital cataracts, congenital glaucoma, congenital deafness, cardiac defects, and mental retardation [19]. The infection of the lens by live virus is recognized clinically as a densely opaque, "pearl-like" nuclear opacity with a relatively uninvolved

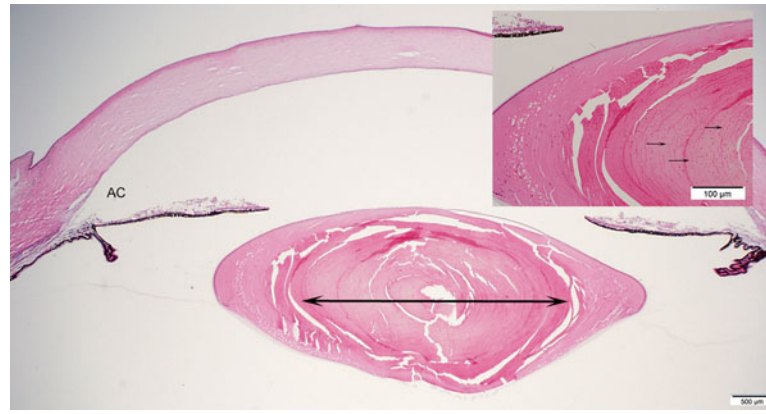

Fig. 5.26 The eye of this child was infected with the rubella virus during gestation. At birth a dense, well-demarcated nuclear opacity was present (*double arrow*). Lens nuclear cells retained their cellular nuclei indicating an arrest in normal development of anucleate lens fibers. The nucleated cells are infected with the rubella virus. In addition, the anterior chamber angle structures (*AC*) and iris are abnormal

peripheral cortex (Fig. 5.26). At the time of the epidemic, only primitive methods of cataract extraction were available. The common procedure was to lacerate the anterior capsule with a needle and intentionally disrupt the opaque cortex. The native cortical material could not be aspirated until several days later when due to the action of released proteases the material became less viscous. What was not recognized at the time was that the disrupted cortical cells exposed to the aqueous contained live virus, which was released and infected vulnerable intraocular tissue causing viral endophthalmitis. Many eyes were lost because of this complication. In intact lenses the infection was identified by retention of nucleated cells in the center of the embryonic nucleus. These nucleated cells provided the necessary environment for the obligate intracellular parasitic virus to proliferate [20]. It is now known that the rubella virus can remain viable under these conditions for many years. Current cataract extraction methods nearly completely remove the infected tissue at the time of cataract surgery, which considerably reduces the risk of subsequent viral endophthalmitis (see also page 30).

5.4 Trauma

The crystalline lens has delicate biochemical mechanisms and anatomic structures all of which are easily damaged by trauma. The final common outcome of trauma to the crystalline lens is the formation of a cataract. The specific type of injury may cause characteristic patterns of damage that allow identification of the cause (Fig. 5.27).

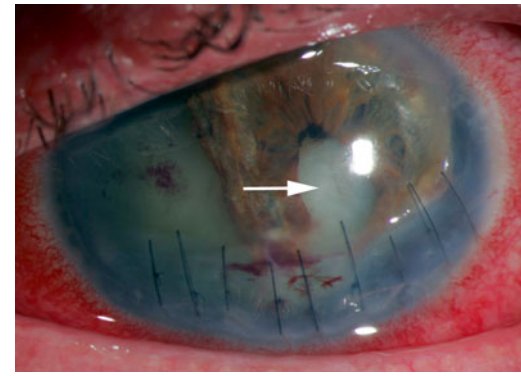

Fig. 5.27 A linear laceration of the inferior cornea has been repaired with sutures. The iris architecture is severely disrupted. Cataractous lens remnants (*arrow*) are present behind the remaining iris tissue

Iron ions in high concentration either from a retained metal foreign body (siderosis) or from degenerating blood (hemosiderosis) are toxic to the metabolism of the lens epithelial cells. Iron oxide is Prussian blue-positive material that may accumulate in anterior subcapsular tissue. This "rust" is clearly visible by biomicroscopy.

Accidental contact with high concentrations of alkali agents (sodium hydroxide, anhydrous ammonia) may diffuse through the cornea and across the anterior chamber to cause generalized necrosis of the lens epithelial and strap cells to cause formation of a cataract. Contact with other high-energy forms including lightning and

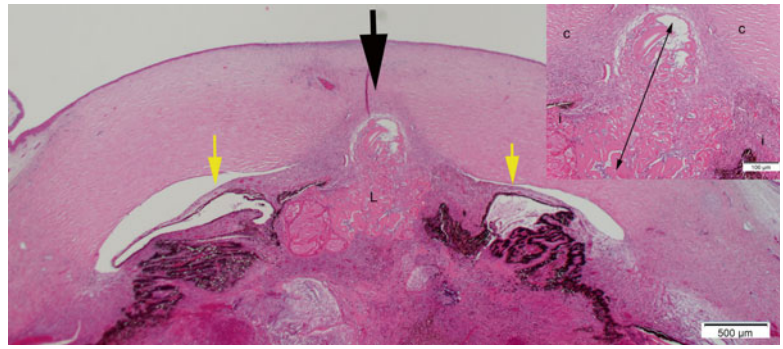

Fig. 5.28 A well-healed perforating injury of the central cornea (*arrow*) contains partially extruded remnants of the lens. Only lens capsule remains (*insert*). The anterior chamber (*yellow arrows*) remains formed

therapeutic radiation (200–500 cGy) may also opacify the crystalline lens.

Blunt injury to the eye may cause regional necrosis of lens epithelium and fibers (petaloid/rosette opacity). Occasionally pigment from the iris pigment epithelium is displaced during trauma to the anterior surface of the lens capsule (Vossius ring). The lens zonules are acellular extracellular matrix fibers that may rupture resulting in dislocation of the lens. Luxation is the total displacement from the normal anatomic site, while subluxation is the partial dislocation.

Perforating wounds of the sclera or cornea may be associated with significant loss of intraocular contents including the lens (Fig. 5.28).

Because the lens cortex is relatively dehydrated and the lens fiber cells are so highly organized, any mechanical disruption of the lens capsule will result in near instantaneous swelling and thus opacification of the lens fibers. Extremely small rents in the lens capsular barrier may, on occasion, spontaneously repair; however, that sequence of events leading to useful vision is unusual. Currently, surgical methods for removing a severely damaged lens are efficient and thorough even at the time of initial repair of a traumatic ocular wound. The problem arises in cases with less severe injury, and more potential for resorting vision, where hemorrhage obscures the surgical field and tissues are difficult to identify by macroscopic characteristics. For example, deoxygenated blood and uveal tract appear very similar when displaced to the ocular surface. Avulsed vitreous and retina are both transparent. The surgical repair strategy can

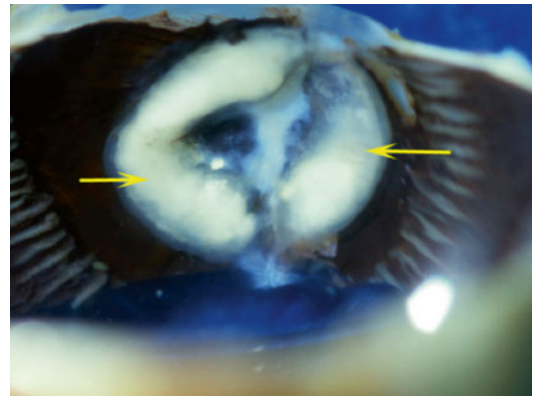

Fig. 5.29 The central lens cortex has been lost during an episode of trauma. The retained peripheral cortex has become densely opaque. The disrupted anterior capsule has become adherent to the remaining central posterior capsule preventing granulomatous inflammation of the remaining cortical tissue

be clarified by microscopic evaluation of any material extruded from an ocular wound. Frozen section evaluation may be indicated, but certainly permanent sections on all extruded tissue are obviously in the patient's best interest. The information, particularly when portions of retina are identified, will aid in deciding whether vitrectomy/lensectomy or enucleation is the next indicated procedure.

In the time of less technical sophistication in tissue repair, significant amounts of lens could not be removed surgically and remained within the inflamed eye, and crystalline lens remnants remained in the field of injury. A Soemmering ring cataract is the retention of a large amount of tissue, usually cortex at the lens equator (Fig. 5.29). The anterior and posterior capsules may fuse by fibrous

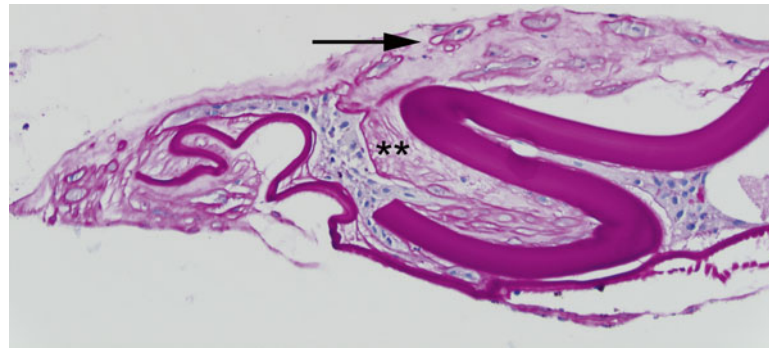

Fig. 5.30 The thick anterior capsule has become opposed to the thinner posterior capsule. The breach has been sealed by fibrous metaplasia of remaining viable lens epithelial cells (**). This case was further complicated by iris neovascularization. The neovascular channels (*arrow*) cover the anterior surface of the central Soemmering ring cataract

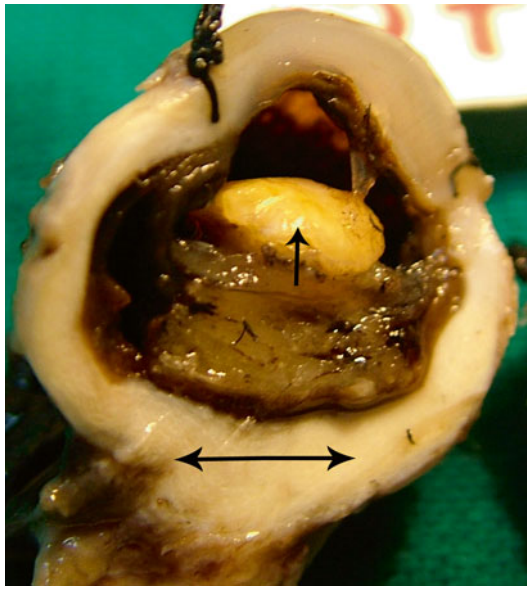

Fig. 5.31 The eye has degenerated and become shrunken (phthisical). The lens (*single arrow*) has become calcified by intrinsic dystrophic calcification. The sclera (*double arrow*) has thickened

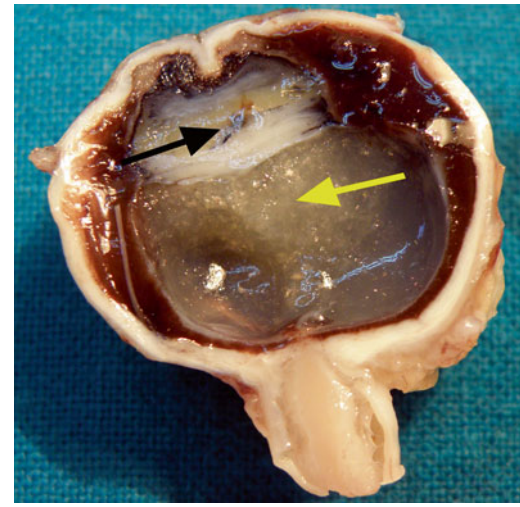

Fig. 5.32 The lens has degenerated to the point where it is barely recognizable (*black arrow*). Cholesterol (*yellow arrow*) has precipitated in the posterior segment from vitreous hemorrhage

metaplasia (Fig. 5.30). Elschnig's pearls on the other hand are small amounts of lens material that remains as small, smooth translucent, or opaque bodies at the site of injury.

Trauma may cause total degeneration of the eye (phthisis bulbi). With loss of intraocular pressure, the globe shrinks in size and assumes a squared-off appearance due to external compression by the rectus muscles. The cornea and sclera may appear thickened. The lens may calcify. Generally, no other normal intraocular structures can be identified (Fig. 5.31). In other cases the lens may completely disintegrate. Cholesterol crystals are a sign of lipid degeneration often from hemorrhage (Fig. 5.32).

5.4.1 Degeneration

A cataract is a lens that has become sufficiently biochemically and anatomically altered to the point that the tissue no longer efficiently transmits light to the retina but increasingly reflects light. The opaque material of the lens nucleus is partially formed by pigments, which differentially block certain wavelengths of light, particularly in the blue region of visible electromagnetic spectrum. The lens also changes anatomically with the

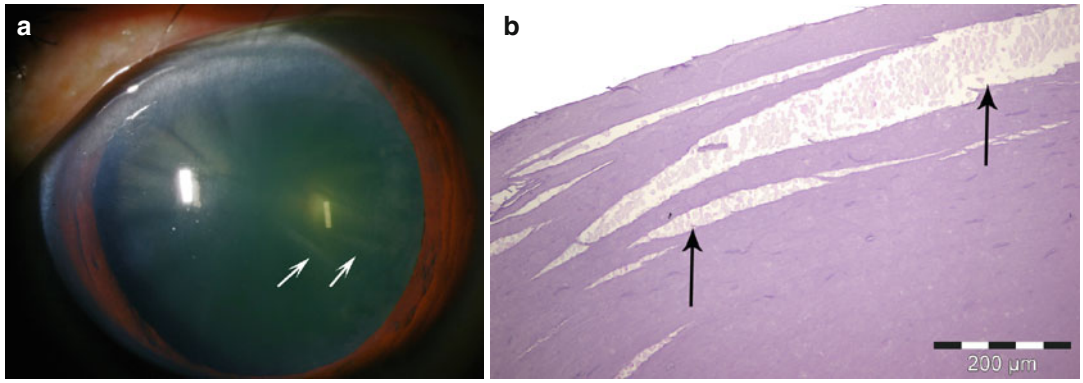

Fig. 5.33 One of the earliest signs of clinically significant cataract occurs at the lens cortex as translucent to opaque curvilinear opacities perpendicular to the periphery of the lens (**a**). The opacities are caused by circumscribed areas of lens fiber degeneration (**b**)

result of nearly doubling volume from birth to age 70 years. This opaque lens can be replaced with a synthetic lens in order to restore transmission of light to the retina. At this time intraocular lens technology is just beginning to address restoration of accommodation (i.e., surgical treatment for presbyopia). The most common types of age-related (degenerative) cataracts are cortical, nuclear, and posterior subcapsular [18, 21].

5.4.1.1 Cortical Cataract

A cortical cataract is a regional opacification of the superficial, peripheral lens cortex usually presenting during middle age (Fig. 5.33a, b). This type of opacity is thought to be due a disorder of oxidative metabolism. The opacity is initially translucent and limited to an apparent single bundle of fibers or a partially demarcated opacity in the peripheral regions of the crystalline lens.

The light microscopic appearance is of regional clefts containing low-viscosity eosinophilic material (disassociated lens protein) and cell fragments (Morgagnian globules). The changes are similar to processing artifacts commonly seen in the lens, which tend to be more angular than the naturally occurring change. There is generally no reaction by adjacent lens epithelial cells. Focal areas of dystrophic calcification may be present. Ultrastructural features include linear breaks of the lens fibers perpendicular to the long axis of the fiber and splitting of suture lines.

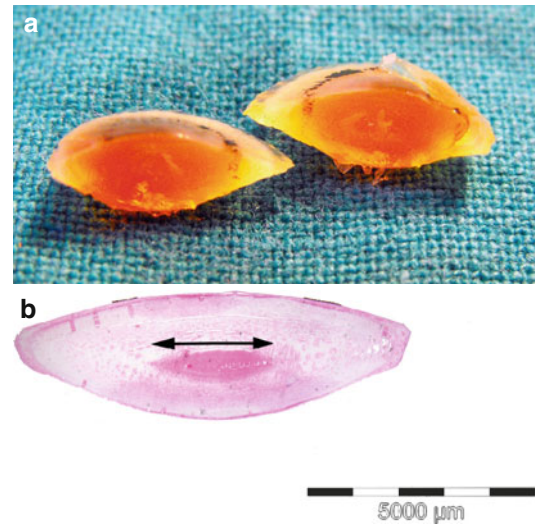

Fig. 5.34 With aging a nuclear opacity develops. The central nuclear area becomes orange (**a**) due to the accumulation of adrenochrome pigments. In addition the nuclear region becomes progressively more opaque (**b**) due to compression of spent cortical fibers (*double arrow*). These changes in the lens cause loss of color perception, particularly at the blue end of the spectrum, and vision loss due to opacification and alterations of the optical characteristics of the lens

5.4.1.2 Nuclear Cataract (Nuclear Sclerosis)

A nuclear sclerotic cataract presents as a region of opacification in the geographic center of the crystalline lens (Fig. 5.34). This is the most common type of cataract. The opacity can be identified in early middle age but generally does not

significantly interfere with visual function until the sixth or seventh decade.

Light microscopic characteristics include a loss of lamellar character of the lens fibers centrally with some variable preservation of the lens fiber pattern peripherally. The central area of the lens is homogeneous and may contain multiple artifactual cracks. A considerable amount of adrenochrome pigment may accumulate in the nuclear region making the cataract appear black (cataracta nigra) (Fig. 5.35). The ultrastructural characteristics of this process are those of nonspecific degeneration.

Degeneration of a nuclear cataract is progressive. As the lens enlarges (intumescent lens), it may impinge upon the iris diaphragm limiting the exit of aqueous into the anterior chamber (pupillary obstruction glaucoma, narrow angle glaucoma) (Fig. 5.36a, b). The cortical lens fibers undergo proteolysis forming globules of protein of irregular size and shape. This process in its early stages is characterized by a sharp demarcation from adjacent, normal appearing lens fibers (Fig. 5.37a, b). The lens cortex ultimately liquefies, and protein diffuses across an intact lens capsule into the surrounding aqueous (hypermature cataract) (Fig.5.38a, b). The nucleus is resistant to the proteolysis that affects the peripheral cortex and remains suspended in a location within the lens capsule determined by gravity (Morgagnian cataract) (Fig. 5.39 LM hypermature lens). The liberated lens protein is phagocytized by macrophages in the anterior chamber. The macrophages or toxic products of protein degeneration can cause dysfunction of the trabecular meshwork and increased intraocular pressure (phacolytic glaucoma).

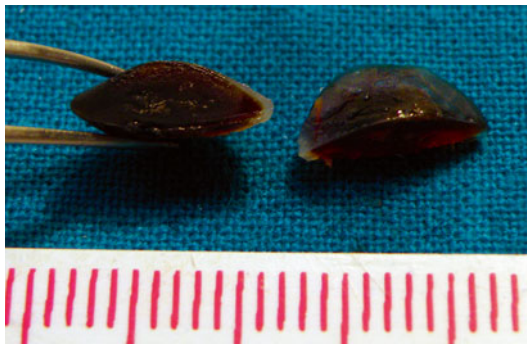

Fig 5.35 With progressive accumulation of pigment in the lens nucleus, the lens becomes *black* (cataracta nigra)

One of the clinically most important types of cataract is the exfoliative cataract [22–24]. The fundamental abnormality in this case is a defect in basement membrane production. Particulate material accumulates on the surface of the lens capsule, which appears as fragments of dandruff (Fig. 5.40). This type of cataract is found more commonly in Scandinavia and Saudi Arabia, but

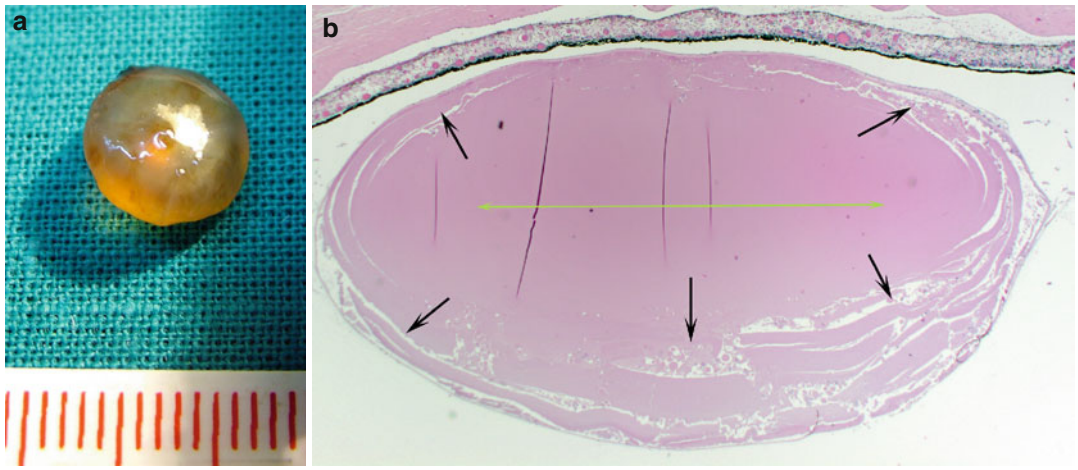

Fig. 5.36 Two cases of nuclear sclerosis. As the cataractogenesis progresses, the lens becomes more spherical (**a**), which may displace the iris diaphragm anteriorly. The lens cortical fibers (**b**) begin to fragment and form large globules (*black arrows*). This process does not occur in the hardened nuclear region (*double yellow arrow*)

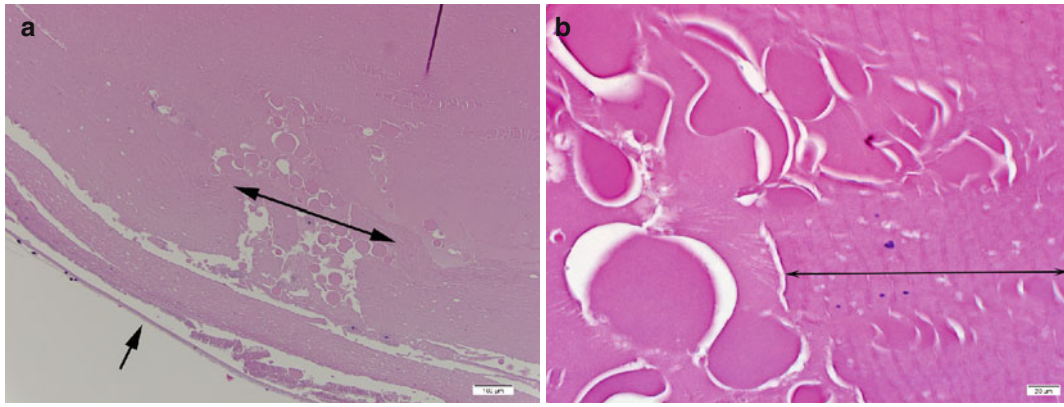

Fig. 5.37 In this case (**a**), the cortex adjacent to the posterior capsule (*single arrow*) is intact. More centrally the lens fibers have fragmented into globules (Morgagnian globules) of protein of irregular size and shape. Because these elements are no longer homogeneous, they will reflect light (appear *opaque*) rather than transmit light. In the second case (**b**), the demarcation between the tissue undergoing degeneration and normal appearing fibers (*double arrow*) is often well defined. Clinically, these areas of degeneration may appear as translucent "waterclefts" or opaque "spokes" in the lens cortex

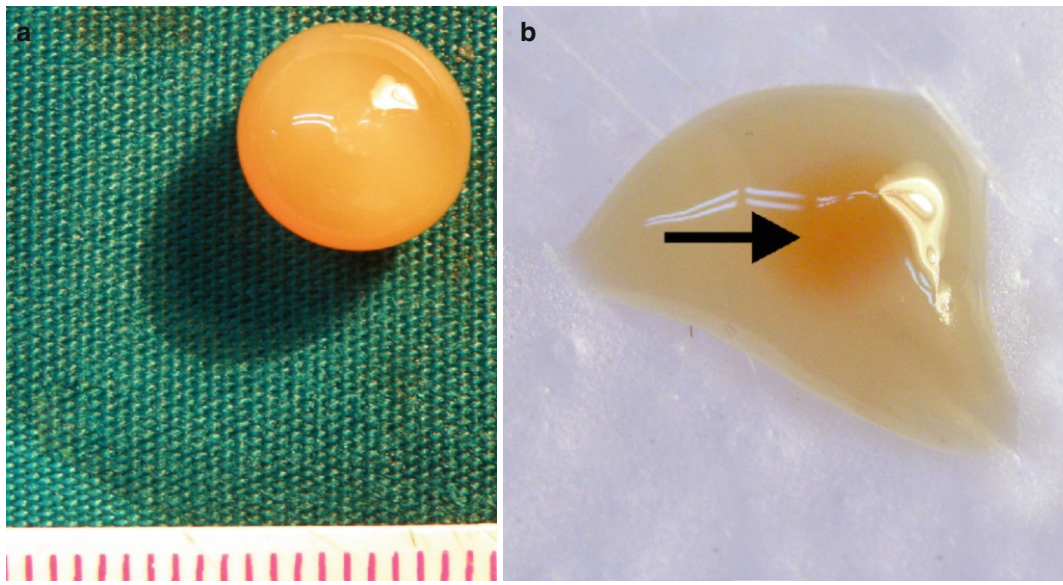

Fig. 5.38 Lens cortical degeneration has progressed to total liquefaction of the lens cortex resulting in a spherical shape (**a**). With loss of cortical fluid, the lens assumes a partially shrunken shape (**b**). The nucleus, which is not affected by the liquefaction process, is visible as a poorly defined orange spheroid surrounded by lens capsule (*arrow*)

is present in all ethnic groups. Exfoliative glaucoma may be more unpredictable and more aggressive than the more common chronic open angle glaucoma. Exfoliative material has been found in many tissues throughout the body.

In this condition, the iris cannot dilate fully because of degeneration of the iris musculature making cataract extraction difficult. In addition the lens zonules are defective and support of the lens is weak. These factors combine to increase the risk of lens dislocation at the time of cataract extraction.

By light microscopy the material can be readily identified on the surface of the lens

capsule and zonules as irregular eosinophilic "iron filings." The posterior contour of the iris pigment epithelium in cross sections of the eye has a serrated appearance reflecting the biochemical dysfunction of the iris musculature.

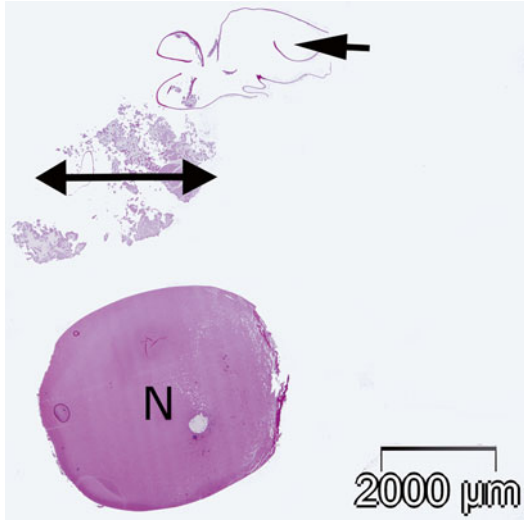

Fig. 5.39 With tissue processing the elements of the cataractous lens have disassembled. The sclerotic lens nucleus (*N*) maintains its integrity and shape. The residual protein debris of the degenerated lens cortex (*double arrow*) remains as an amorphous, slightly granular mass. The lens capsule (*single arrow*) is not affected by the degenerative process

5.4.1.3 Posterior Subcapsular Cataract

A posterior subcapsular cataract presents as a region of opacification just anterior to the posterior lens capsule (Fig. 5.24). This is the most infrequently encountered type of degenerative cataracts and is indistinguishable clinically and histopathologically from trauma-induced, diabetes-induced, and corticosteroid-induced posterior subcapsular opacities. The opacity may present in early middle age. The rate of progression is unpredictable over a range of months to decades. Treatment is the standard cataract extraction with intraocular lens implantation.

The light microscopic characteristics are distinctive, composed of a layer of large bizarrely shaped cells with vesicular cytoplasm and small nuclei, accumulating in a region internal to and parallel with the posterior lens capsule (Wedl cells or bladder cells) [25]. Characteristic organelles of fibroblasts are found in the more mature cells although extracellular matrix production is rarely seen. Once formed the plaque of abnormal cells generally remains stable.

5.5 Tissue Processing and Artifacts

The crystalline lens is easily dislocated during gross sectioning. This is best avoided by opening the globe from posterior to anterior from a point

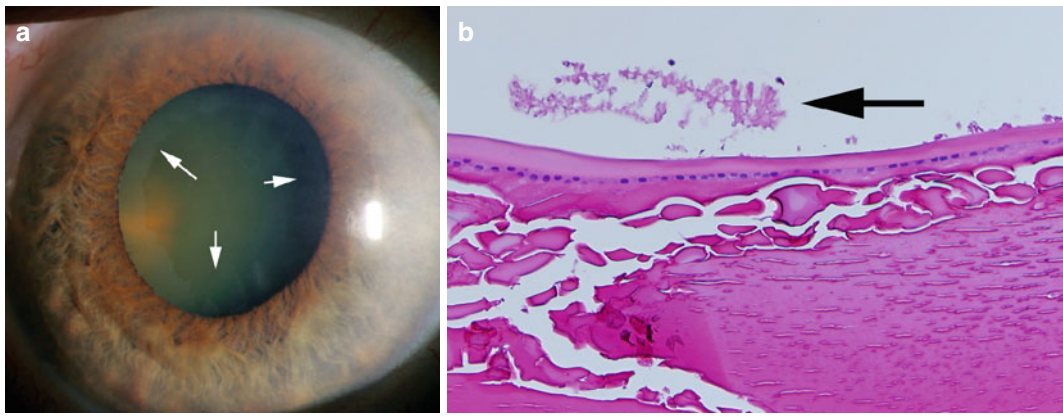

Fig. 5.40 Biomicroscopy of an exfoliative cataract (**a**). The arrows indicate the presence of pathologic protein accumulation on the anterior surface of the lens. The material on the central portion of the lens has been swept away by contraction and dilation of the iris. A faint nuclear sclerotic cataract is also present. Light microscopy of exfoliative material (**b**). The material appears as linear accumulations of protein (*arrow*) perpendicular to the lens capsule from which the protein originated

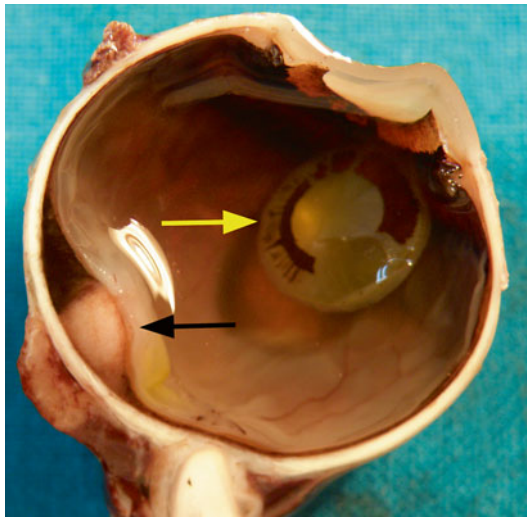

Fig. 5.41 The lens (*yellow arrow*) has been dislocated during gross sectioning. Pigment from the iris pigment epithelium (*white arrow*) has been transferred from the iris to the anterior lens capsule. A serous detachment of the retina (*black arrow*) has developed in the region of a uveal melanoma

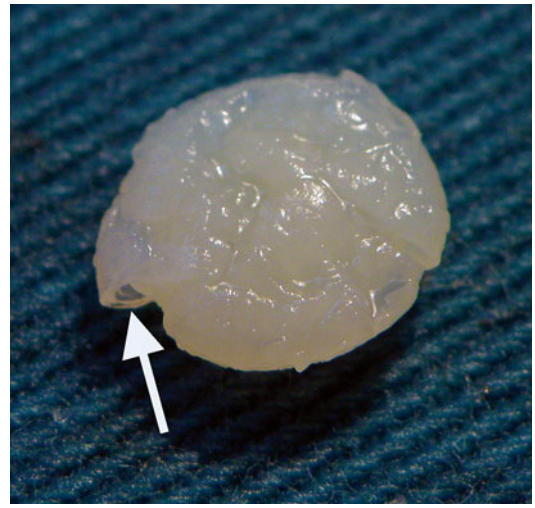

Fig. 5.42 The lens cortex has degenerated to total opacity. The lens capsule was separated from the cortex during gross tissue preparation. A small portion of lens capsule remains intact (*arrow*)

2 mm lateral to the optic nerve on the scleral surface to exit the globe 2 mm inside the limbus. This maneuver allows the lens to be supported by the iris diaphragm and cornea instead of dislocating the lens into the vitreous cavity as often occurs during anterior to posterior cutting (Fig. 5.41). If the lens is totally dislocated during gross sectioning, it can be repositioned during the time of final paraffin embedding.

A formalin-fixed lens is translucent. Truly cataractous lenses are at least focally opaque and may be darkly opaque. Advanced cataracts may be dark orange or even black due to accumulation of phenochrome pigment in the lens during degeneration. The degenerated lens is composed of frail tissue, and the capsule may become separated from the cortex during tissue preparation (Fig. 5.42). Dystrophic calcification of the lens may make sectioning difficult and decalcification necessary.

Only in the case of the lens of an infant is lens structure physically preserved during sectioning with a microtome. The nuclear lens tissue is brittle and fragmentation during microscopic sectioning is the rule. The lens capsule is often intact, but parallel cracking, dislocation, and loss of cortical tissue are common. Areas of focal calcification only increase the number and extent of artifact formation. Periodic acid/Schiff stain highlights features of the lens capsule and is routinely used in histopathologic. Many of the features of certain types of cataract formation, e.g., anterior subcapsular cataract and posterior subcapsular cataract, are the result of fibrous metaplasia or posterior migration of the lens epithelial cells and are generally affected less by tissue processing and sectioning. Lens tissue is frequently lost during perforating trauma to the eye. The lens tissue may be reduced to small sections of PAS-positive membrane encased in fibrous reactive tissue. In many cases differentiating residual lens capsule from residual Descemet's membrane may be difficult.

With the exception of silicone and some Supramid and metal loops, the intraocular lens material totally dissolves in the organic solvents used to process tissue for paraffin infiltration. Some of the original designs for iris-supported intraocular lenses were supported by metal loops (platinum) attached to the iris diaphragm at the pupil. This metal can seriously damage microtome knife cutting edges. Either the material needs to be identified and removed prior to sectioning or disposable blades should be used.

The position of intraocular lenses or any other implantable device is generally recognized by the negative image of the material within fibrous reactive tissue. The most common site with the presence of IOL loop material is within the native lens capsule or in the region of fibrous reaction anterior to the vitreous base. The IOL generally remains within the posterior chamber but may be dislocated to any site in the anterior or posterior segments. Foreign body granulomatous reaction may be found associated with suture material or retained cortex, but the material of the IOL does not excite an inflammatory response.

Acknowledgment The work of J. Douglas Cameron, MD, MBA, is supported in part by an unrestricted grant from Research to Prevent Blindness to the Department of Ophthalmology and Visual Sciences of the University of Minnesota.

References

1. Duncan G, Wormstone IM, Davies PD. The aging human lens: structure, growth, and physiological behaviour. Br J Ophthalmol. 1997;81:818–23.
2. Al-Ghoul KJ, Nordgren RK, Kusak AJ, Freel CD, Costello J, Kusak JR. Structural evidence of human nuclear fiber compaction as a function of ageing and cataractogenesis. Exp Eye Res. 2001;72:199–214.
3. Cameron JD, Streeten BW. Pathology of the crystalline lens. In: Albert DM, Miller N, editors. Principles and practice of ophthalmology. 3rd ed. New York: Elsevier; 2008. p. 3653.
4. Guernsey DL, Robitaille JM, Cameron JD, Heathcote JG. Embryological development of the eye. In: Klintworth GK, Garner A, editors. Gardner and Klintworth's pathobiology of ocular disease. New York: Informa Healthcare; 2008. p. 1091.
5. Fine BS, Yanoff M. The lens. Ocular histology: a text and atlas. 2nd ed. Hagerstown: Harper & Row; 1979. p. 149–59.
6. Apple DJ, Escobar-Gomez M, Zaugg B, Kleinmann G, Borkenstein AF. Modern cataract surgery: unfinished business and unanswered questions. Surv Ophthalmol. 2011;56:S3–53.
7. Amaya L, Taylor D, Russell-Effitt I, Nischal KK, Lengyel D. The morphology and natural history of childhood cataracts. Surv Ophthalmol. 2003;48(2):124–44.
8. Zimmerman LE. Phakomatous choristoma of the eyelid. A tumor of lenticular anlage. Am J Ophthalmol. 1971;71:169–77.
9. Lowe RJ. Synophthalmos: report of a case. Surv Ophthalmol. 1967;12:145–51.
10. Savige J, Colville D. Opinion: ocular features aid the diagnosis of Alport syndrome. Nat Rev Nephrol. 2009;5(6):356–60. Epub 2009/05/29.
11. Streeten BW, Robinson MR, Wallace R, Jones DB. Lens capsule abnormalities in Alport's syndrome. Arch Ophthalmol. 1987;105(12):1693–7. Epub 1987/12/01.
12. Cunningham A, Harris H, Gnanaraj L. Anterior pyramidal congenital cataract. J Pediatr Ophthalmol Strabismus. 2011;48:192.
13. Verhoeff F, Lemoine A. Endophthalmitis phacoanaphylactica. Am J Ophthalmol. 1922;5:737–45.
14. Henkind P, editor. Phacoanaphylactic endophthalmitis. Verhoeff Society meeting; Washington, DC; Apr 1983.
15. Eagle RJ. The Lens. In: Spencer W, editor. Ophthalmic pathology: an atlas and textbook. Philadelphia: WB Saunders; 1996. p. 372–437.
16. Tsai JH, Rao NA. Intraocular manifestations of immune disorders. In: Klintworth GK, Garner A, editors. Garner and Klintworth's pathobiology of ocular disease. New York: Informa Healthcare; 2008. p. 76–8.
17. Marak GJ, Lim L, Rao NA. Abrogation of tolerance to lens protein. II. Allogenic effect. Ophthalmic Res. 1982;14:176–81.
18. Eagle RJ. The lens. Eye pathology an atlas and text. 2nd ed. Philadelphia: Wolters Kluwer/Lippincott Williams & Wilkins; 2011. p. 107–19.
19. Yanoff M, Schaffer DB, Scheie HG. Rubella ocular syndrome. Clinical significance of viral and pathologic studies. Trans Am Acad Ophthalmol Otolaryngol. 1968;72:896–902.
20. Zimmerman LE. Histopathologic basis for ocular manifestations of congenital rubella syndrome. The Eighth Hamlin Wilder Memorial Lecture. Am J Ophthalmol. 1968;65:837–62.
21. Costello MJ, Kuzak JR. The types, morphology, and causes of cataracts. In: Klintworth GK, Garner A, editors. Garner and Klintworth's pathobiology of ocular disease. 3rd ed. New York: Informa Healthcare; 2008. p. 469–94.
22. Asano N, Schlotzer-Schrehard U, Naumann G. A histopathologic study of iris changes in pseudoexfoliation syndrome. Arch Ophthalmol. 1995;110:1279.
23. Schlotzer-Schrehardt U, Naumann G. Ocular and systemic pseudoexfoliation syndrome. Am J Ophthalmol. 2006;141:921–37.
24. Schlotzer-Schrehard U, Streeten B. Pseudoexfoliation syndrome. In: Klintworth GK, Garner A, editors. Garner and Klintworth's pathobiology of ocular disease. New York: Informa Healthcare; 2008. p. 505–36.
25. Streeten B, Eshaghian J. Human posterior subcapsular cataract: a gross and flat preparation study. Arch Ophthalmol. 1978;96:1653–8.

Glaucoma

6

Claudia Auw-Haedrich, Peter Meyer,
and Rita Van Ginderdeuren

6.1 General Description

Glaucoma is characterised by a pathological excavation of the optic nerve head (Figs. 6.1 and 6.2) and is thought to be caused by a too high intraocular pressure of the eye. The glaucomatous excavation causes visual field defects, classically beginning at the Bjerrum area within the central 30° (Fig. 6.3). The detection of early-stage glaucoma is not seldom missed by the ophthalmologist, since early visual field damage is not noticed by the patients in the daily life due to central compensation mechanisms. Not every glaucoma is associated with elevated intraocular eye pressure. Most people have an eye pressure of 15–20 mmHg. There are patients with such normal or low eye pressure, who nevertheless develop glaucomatous excavation of the optic nerve head. Here, alteration of the blood circulation, e.g. caused by low blood pressure at night or insufficient oxygen supply due to stenosis of the A. carotis interna, is present causing the reduced resistance of the optic nerve tissue against the "normal" intraocular pressure. The aqueous humour is produced by the non-pigmented epithelium of the ciliary body (Fig. 6.4) at a rate of 2–6 µm [1, 2]. Its flow exiting the eye is passing the posterior eye chamber, the slit between the pupil and lens, the trabecular meshwork and Schlemm's canal towards the episcleral veins at the eye's surface (Fig. 6.5). Any pathological process leading to structural changes of the area of the anterior chamber angle can cause decreased outflow of the aqueous humour with increase of intraocular pressure. This can happen with the angle structures being "open", that means that the problem lies in the trabecular meshwork as the tightest area to pass either with degenerative changes of the trabecular meshwork itself ("primary open-angle glaucoma") or with the trabecular meshwork being steroid-induced altered or clogged by various particles like pseudoexfoliation material, pigment, blood and macrophages ("secondary open-angle glaucoma"). The treatment of open-angle glaucoma consists of reduction of aqueous humour production and/or increasing aqueous humour outflow, which can be achieved by various eye drops (beta blocker, carboanhydrase inhibitor, prostaglandin analogue, etc.) or by various surgical methods either decreasing the outflow resistance (trabeculectomy, glaucoma implant insertion) or decreasing the aqueous humour production (cyclodestructive methods).

The other forms of glaucoma show impaired outflow of the aqueous humour due

C. Auw-Haedrich (✉)
Histology Lab, Eye Center, University Freiburg,
Killianstr. 5, 79106 Freiburg, Germany
e-mail: claudia.auw-haedrich@uniklinik-freiburg.de

P. Meyer
Division of Histology Lab, Augenspital Basel,
Mittlere Strasse 91, 4056 Basel, Switzerland
e-mail: pemeyer@uhbs.ch

R. Van Ginderdeuren
Department of Ophthalmology and Pathology, UZ
Leuven, Kapucijnenvoer 33, 3000 Leuven, Belgium
e-mail: rita.vanginderdeuren@uzleuven.be

S. Heegaard, H. Grossniklaus (eds.), *Eye Pathology: An Illustrated Guide*,
DOI 10.1007/978-3-662-43382-9_6,

Fig. 6.1 (**a**) Intense glaucomatous excavation of the optic nerve head, in comparison to small physiological central excavation (**b**) (Courtesy of Christian Richter, University Eye Hospital Freiburg)

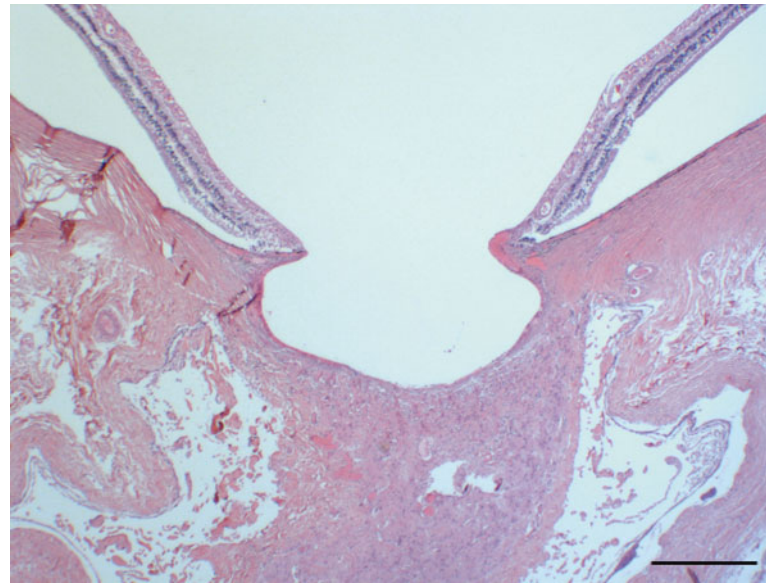

Fig. 6.2 Optic nerve head excavation in progressive pseudoexfoliation glaucoma (same eye as Fig. 6.10). Bar = 0.3 mm

to angle-closure, pretrabecular or posttrabecular problems. Angle closure tends to occur in short eyes (under 21 mm axial length), especially in mydriasis with pupil dilation followed by a dramatic decrease of the aqueous humour outflow with acute increase of intraocular pressure reaching 70 mmHg or more (Fig. 6.6, "primary angle-closure glaucoma").

This situation can be imitated in normal-sized eyes by thickening of the lens or a process of the ciliary body pressing upon the anterior chamber angle from behind, like a ciliary neoplasm, e.g. malignant melanoma. The treatment of the acute angle-closure glaucoma consists in systemic carboanhydrase inhibition leading to immediate reduction of the aqueous humour production and for the long term a surgical iridectomy in primary closed-angle glaucoma where the pupillary block is bypassed and the aqueous humour directly flows from the posterior into the anterior chamber through the artificial opening in the iris basis (Fig. 6.7).

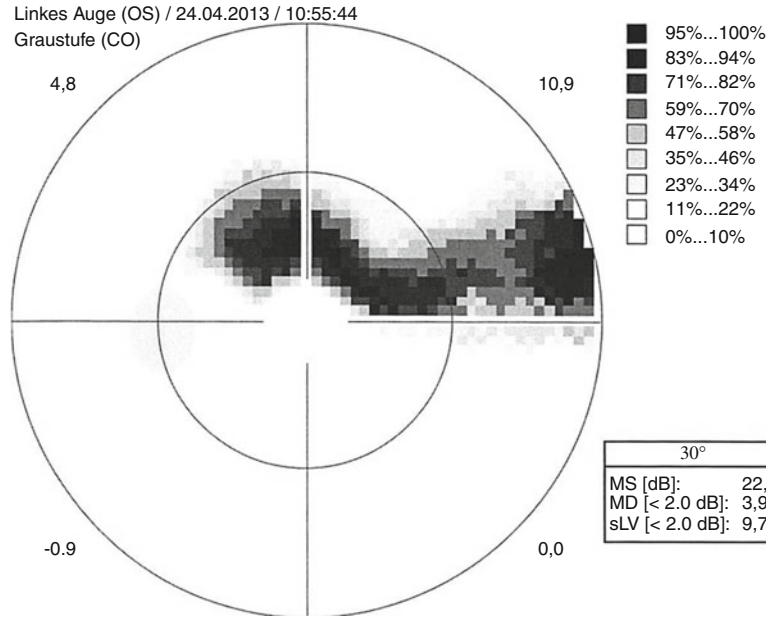

Fig. 6.3 Bjerrum scotoma, a sickle-shaped scotoma with extension to the blind spot which can be located superiorly, here in automated 30° perimetry of a left eye (Courtesy of Milena Stech, University Eye Hospital Freiburg)

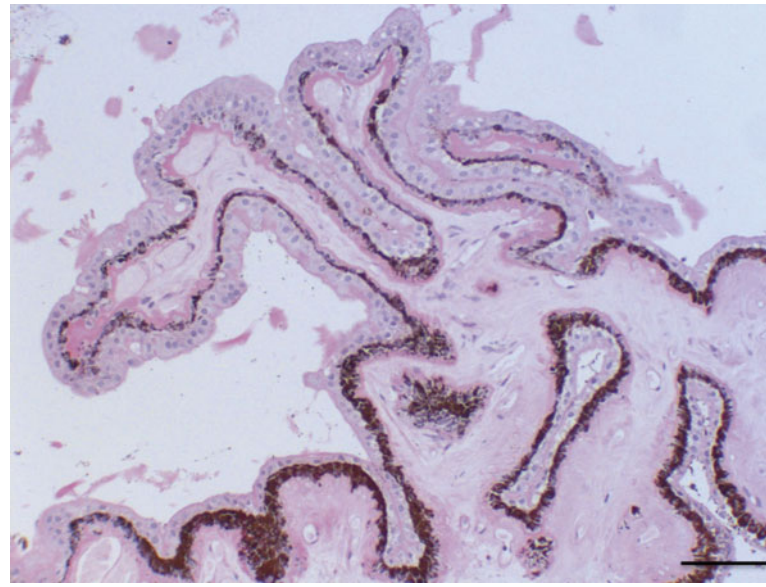

Fig. 6.4 Ciliary body with slight fibrosis and normal pigmented and unpigmented epithelium (PAS, bar = 50 µm)

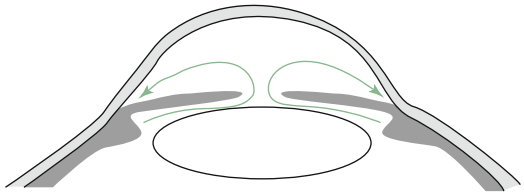

Fig. 6.5 Scheme of the aqueous humour flow from the ciliary body towards the trabecular meshwork passing the slit between the lens and pupil (Courtesy of Dr. Günther Schlunck, University Eye Hospital Freiburg)

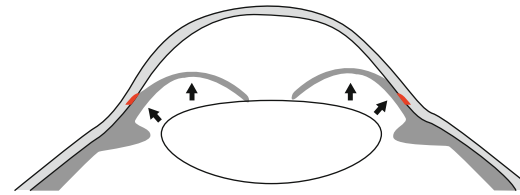

Fig. 6.6 Scheme of a pupillary block with blockage of the aqueous humour flow between the lens and iris and forward bulging of the iris obstructing the anterior chamber angle (*red*)

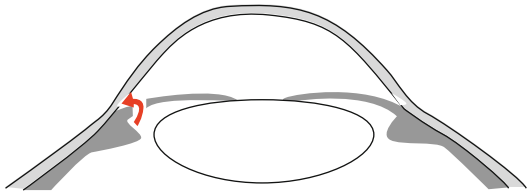

Fig. 6.7 Flow of the aqueous humour in pupillary block after performed iridectomy (Courtesy of Dr. Günther Schlunck, University Eye Hospital Freiburg)

Pretrabecular blockage of the aqueous flow occurs in developmental glaucomas and in eyes with ingrowth of various tissue types as fibro (vascular) tissues or epithelial cells. Posttrabecular blockage of the aqueous flow occurs in processes, which impair the flow of the episcleral veins as it happens in patients with nevus flammeus of the face or in sinus cavernosus thrombosis. This chapter contains only processes confined to the eye. While the different morphological changes of the anterior segment leading to increased intraocular pressure are described in the following sections of the chapter according to their specific underlying pathogenesis, the morphological changes of the posterior segment are quite uniform in the different glaucoma types and will be addressed here.

Progression of glaucoma-related optic nerve damage is judged by the morphological changes of the optic nerve head (ONH). The ONH shows a pathological excavation (Figs. 6.1 and 6.2), which enlarges in the case of progression. Histologically, the morphological changes of the glaucomatous excavated ONH consist of nerve fibre atrophy, alterations of the lamina cribrosa and glial cell activation. The lamina cribrosa is typically bowed posteriorly with loss of nerve fibres, neural connective tissue and vessels. Within years, the lamina cribrosa becomes attenuated and the edge below the scleral ring bulged due to a remodelling process: increased intraocular pressure and ischemia activate glial cells, i.e. astrocytes and Müller cells, which induce degenerative changes in the extracellular matrix, upregulation of matrix metalloproteinases, proteolytic enzymes, cytokines and tenascin [3, 4]. The progression of glaucomatous excavation is thus considered not only as the result of mechanical impact of elevated intraocular pressure but a complex bioactive process. As a secondary change, atrophy of the retinal ganglion cell layer occurs (Fig. 6.8).

6.2 Anatomy and Embryology

6.2.1 Anatomy

Most important anatomical landmarks involved in glaucoma are the ciliary body as producer of the aqueous humour, the anterior chamber angle (posterior cornea, trabecular meshwork and iris root) as drainage place and the optic nerve with the ganglion cell layer in the retina as structural endpoint of glaucoma damage. Episcleral veins drain the humour of Schlemm's canal via intrascleral channels out of the eye into the conjunctival veins.

The trabecular meshwork is a three-dimensional sieve-like structure in a triangle in the angle between the iris root and the posterior side of the cornea (Fig. 6.9a–c).

It is built of a core of collagen fibres with elastin and covered by a thin layer of endothelium cells. The mechanism of filtration of fluid must be kept in balance to keep the pressure in the eye at very constant levels; therefore, there is no direct communication: the fluid leaves the anterior chamber through the trabecular meshwork by giant vacuoles (Fig. 6.10).

The meshwork may be divided into three anatomical portions: (a) uveal meshwork, (b) corneoscleral meshwork and (c) juxtacanalicular tissue which is also referred to as the cribriform layer.

The uveal meshwork: this inner most portion is adjacent to the aqueous humour in the anterior chamber and is arranged in bands or ropelike trabeculae that extend from the iris root and ciliary body to the peripheral cornea. The arrangement of the trabecular bands creates irregular openings that vary in size from 25 to 75 μ [5]. The corneoscleral meshwork: this portion extends from

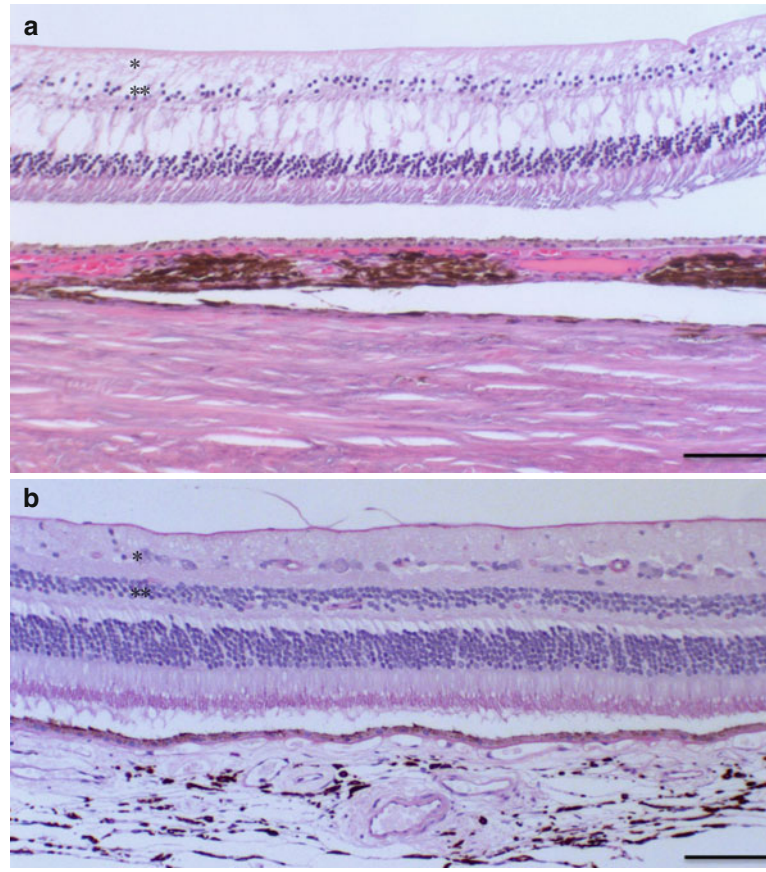

Fig. 6.8 Atrophy of the retinal ganglion cell layer (*) and the outer nuclear layer (**) in secondary glaucoma following contusion and panretinal laser treatment with clumping of choroidal melanocytes (**a**, *above*), in comparison to the normal eye (**b**, *below*), HE, bar = 100 µm

the scleral spur to the anterior wall of the scleral sulcus and consists of sheets of trabeculae that are perforated by elliptical openings. These holes become progressively smaller as the trabecular sheets approach Schlemm's canal with a diameter range of 5–50 µm [5]. The trabecular bands or sheets are composed of four concentric layers. First, an inner connective tissue core of typical collagen fibres types I and II and elastin [6, 7], basement membrane and continuous covering endothelium forms. The outermost portion of the meshwork adjacent to Schlemm's canal consists of a layer of connective tissue lined on either side by endothelium; the outer endothelial layer comprises the inner wall of Schlemm's canal, in between is a central connective tissue layer with variable thickness and not fenestrated with several layers of parallel spindle-shaped cells loosely arranged in a connective tissue ground substance [8].

Schlemm's canal is a circular channel in the sclera and lined by a single endothelial layer. The anterior-posterior length is between 250 and 300 µ; the final flow of aqueous to this canal is by transition through giant vacuoles in the lining endothelium. Many of the cells of the inner wall contain giant vacuoles [9, 10]. These vacuoles seem to be transcellular micro channels by which aqueous humour can pass into Schlemm's canal. From the outer wall of Schlemm's canal, 25–35 channels emerge, which are connected to the vascular system of the limbal region.

The optic nerve head (or optic disc, or papilla) is formed by 1.1–1.2 million axons of retinal ganglion cells and glial cells, which behave as astrocytes or supporting cells. In the optic nerve head, these axons are bundled as regularly aligned and spaced columns [11]. Only outside the eye the glial cells form myelin and behave as oligodendrocytes. Between these fibres are

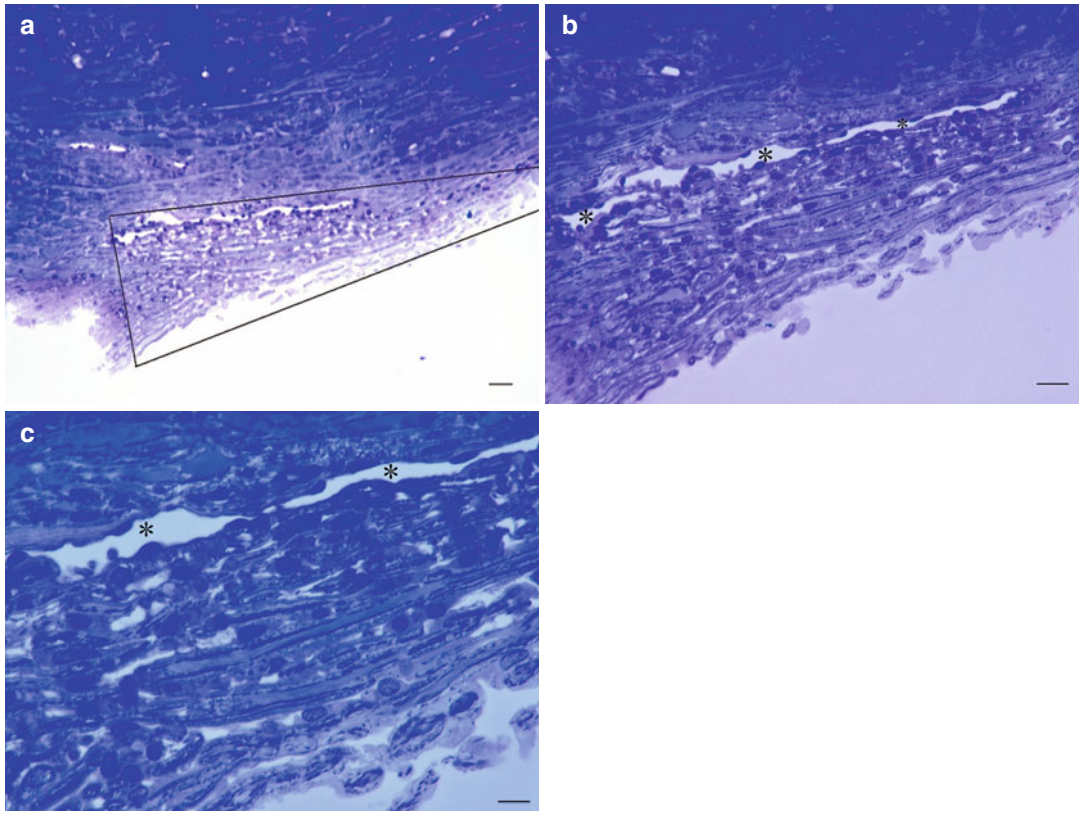

Fig. 6.9 Normal trabecular meshwork and Schlemm's canal (*) from donor eye of a 52-year-old patient, toluidine blue staining. (**a**) Overview of the sieve-like, triangular structure. Trabecular meshwork is between the lines of the triangle. (**b**, **c**) Further magnification of (a). Bars = 100 µm, 50 µm and 25 µm, resp

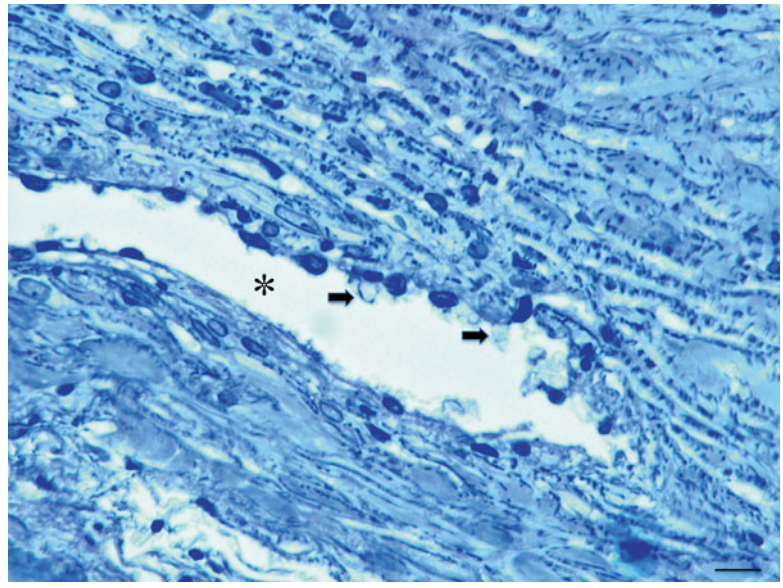

Fig. 6.10 Trabeculectomy specimen of a 79-year-old glaucoma patient. Trabecular meshwork and Schlemm's canal (*) with giant vacuoles (*arrows*), toluidine blue staining, bar = 25 µm

the connective tissue components with vascular supply. At the optic nerve head, all the axons of the retinal nerve fibre layer come together and become so raised towards the vitreal surface that they create the nipple-lie elevation that gave rise to the designation of "papilla". The optic nerve head is about 1 mm in length and is often described in three parts [11]: the lamina retinalis, the lamina choroidalis and the lamina scleralis; other terms used to describe the regional histology of the optic disc are based on the position of the lamina cribrosa of the sclera; these terms are prelaminar, laminar and retrolaminar. The lamina cribrosa is the vascular connective tissue that penetrates the lamina scleralis of the optic nerve head. The lamina scleralis or the posterior scleral foramen is a truncated cone having an anterior diameter of 2.0 mm or less and a posterior diameter of 3.5 mm. The sclera is perforated by approximately 300 canals that are extensions of the connective tissue of the inner one-third of the sclera, the lamina cribrosa. The other two-thirds of the sclera do not contribute to the lamina cribrosa but blend into the dural attachments of the optic nerve.

The increase of the physiological cup of the optic nerve head is the most accessible sign of POAG damage and is the result of neuronal atrophy and connective tissue changes with concave bending of the lamina cribrosa. Clinically, optic nerve damage is recognised by enlarging and deepening of the optic cup accompanied by thinning of the neural rim.

Cupping of the optic disc may occur as a part of normal embryologic development or as a part of a pathological process. The size of the optic cup is highly variable and depends on the size of the scleral canal. Cupping results from a mismatch of the size of the scleral canal with the number of axons passing through the optic nerve head. In glaucoma, cupping occurs when there is a decreased amount of neural tissue entering the scleral canal. Studies of the lamina cribrosa in glaucoma patients have shown collapse and rotation of the plates of the lamina cribrosa which would distort axon paths, interrupt axonal transport and predispose to cell death probably by apoptosis [5, 12].

6.2.2 Embryology

The eye is formed in the very early stages of development within the third and fourth week of foetal life, and if the formation of the anterior chamber is not perfect, there are repercussions on the cornea, lens, iris, trabecular meshwork and outflow [13, 14]. This means that in most developmental problems, all these structures can be more or less involved. The known genes in these diseases specify the problem, but the individual expression of the syndrome can even in dominant cases be very different in members of the same family.

In the development of the eye, mostly cells derived from the neuroectoderm play a role [15]. In the third gestational week, small bulbs sprout on both sides out of the wall of the diencephalon in what later becomes the forebrain region. With increasing growth, the bulb-like optic vesicles invaginate to form the two optic cups. The interior layer of the optic cup will become the retina and the exterior layer will develop into the pigment epithelium. The proximal region of the optic cup will form the optic stalk and develop later in the optic nerve.

In response to inductive signals, the overlying surface ectoderm which covers the region of the optic cup forms a vesicle as well just opposite of the optic cup and separates later from the superficial ectoderm. This then provides the basis for future lens development. In this stage, the Pax6 gene is mostly involved [16]. From the same ectoderm will form the corneal and conjunctival epithelium and at a later embryonic stage, the eyelids. All the other ocular structures are developed from cranial neural crest cells and cranial paraxial mesoderm-derived cells.

During the third gestational month, the lens is situated directly behind the cornea, the iris has only partially developed and the anterior chamber will gradually deepen during the weeks and months that follow. This leads to an increased distance between the lens and cornea. The ciliary body begins to form; the next step is the growth and maturation of the iris and the anterior chamber. The insertion of the iris and ciliary body migrates posteriorly, which is a necessary step

for TM development. At 7 months gestation, the TM is separated from the anterior chamber by the layer of neural crest cells and little aqueous can drain. Retraction of these cells allows exposure of the TM and therefore drainage of aqueous (Fig. 6.11a–d) [17].

If this process of differentiation is defective or incomplete, the newborn's trabecular meshwork cannot properly drain the aqueous humour, thus resulting in an increase of intraocular pressure (IOP). In all cases of aberrant lens development, the normal formation of the anterior chamber is also disturbed and developmental glaucoma is often found in neonatal cataract syndromes [18].

The development of the optic nerve starts with the out sprouting growth of the axons of the ganglion cells of the retina; these nerve fibres find their way through the optic disc and form the optic nerve and the optic chiasm and end in the brain in the lateral geniculate bodies. Much more nerve fibres are formed during this process, but only a small part find his connection to the brain; the other part disappears

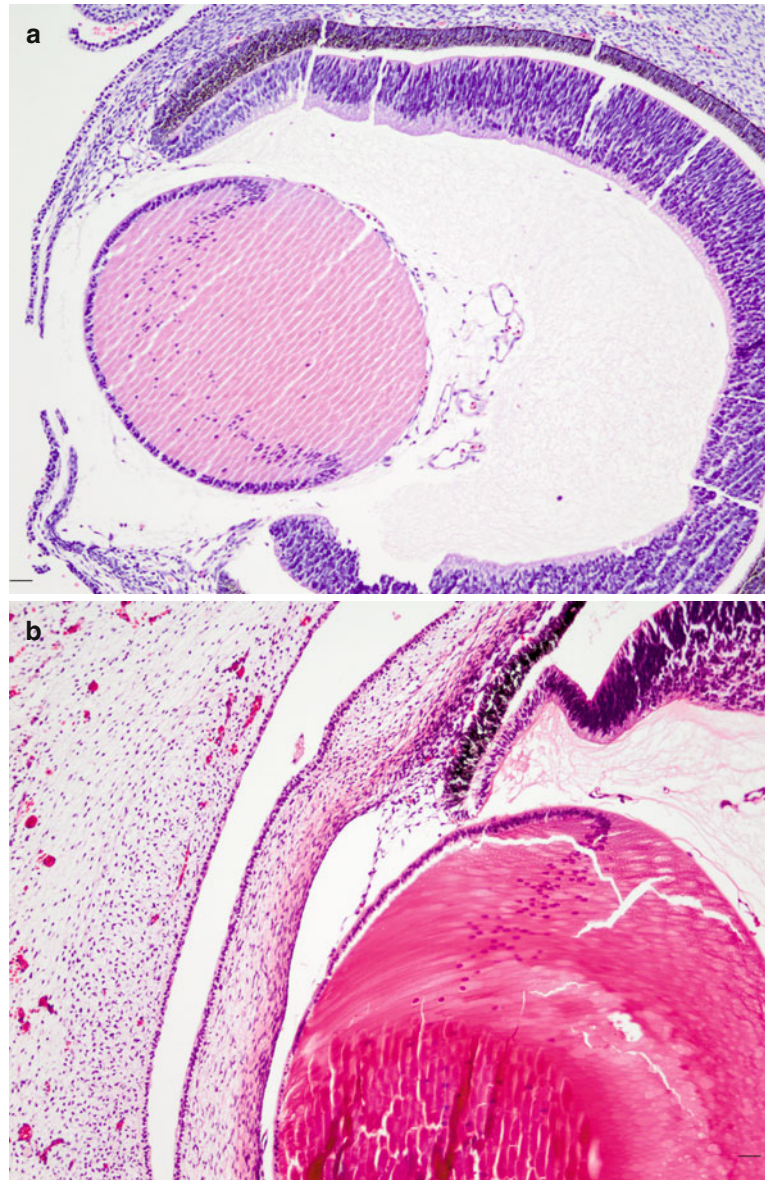

Fig. 6.11 (**a**) A 7-week-old foetus (HE, bar = 50 µm); (**b**) 12-week-old; (**c**) 18-week-old; (**d**) 23-week-old (HE, bars = 20 µm). Major steps in the development of the eye, HE staining. At 7 and 12 weeks' gestational age, the iris is not yet separated from the pigmented layer. At 18 weeks, a rudimentary iris starts to sprout out. At 23 weeks, the anterior chamber angle is open with an immature iris and trabecular meshwork (Courtesy of Dr Rob Verdyck)

Fig. 6.11 (continued)

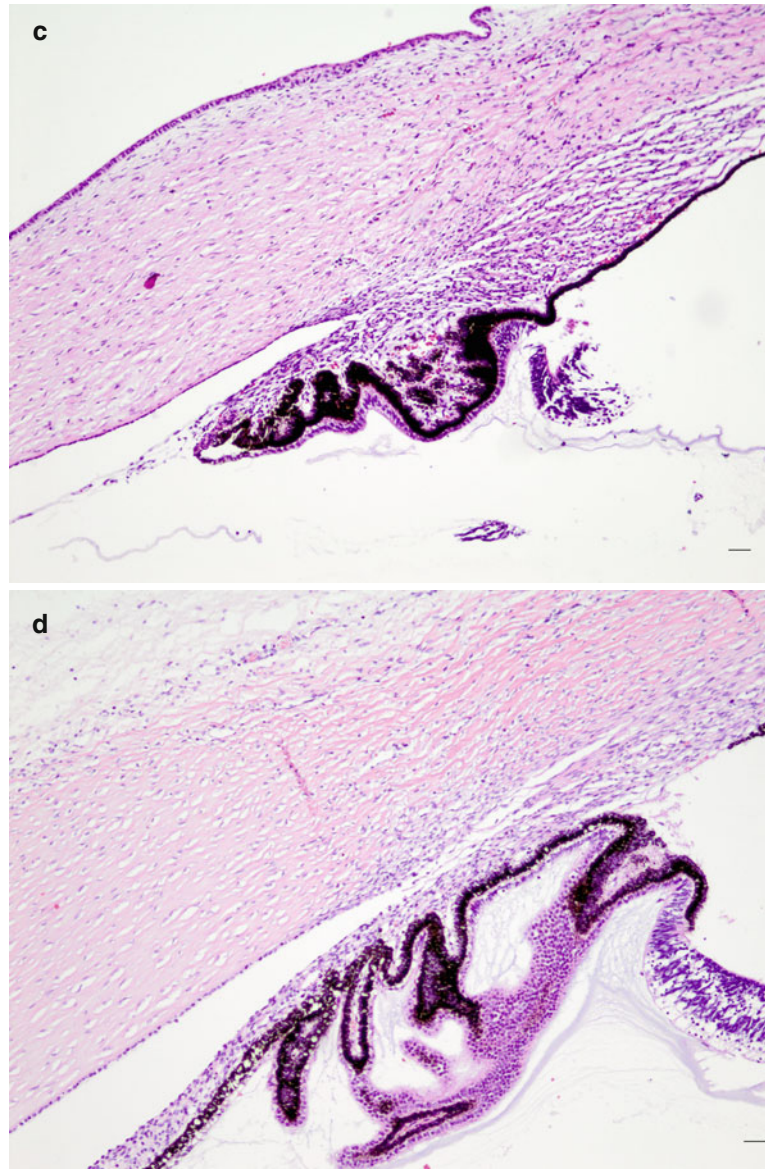

in a self-controlling way. Only later they are populated by septa of vascular connective tissue to form the blood supply and the structural support to pass through the scleral openings.

6.3 Developmental Glaucoma

The most common reason for an IOP increase is reduced outflow capacity usually located at the anterior chamber angle and the trabecular meshwork. Although the chance of developing an elevated IOP significantly rises as one ages, an increase in the IOP can occur at any age. Congenital glaucoma affects babies who are born with high IOP or develop an increase shortly after birth. An elevated IOP during childhood is defined as infantile glaucoma.

The term ocular anterior segment dysgeneses (anterior segment dysgeneses-neural crest, anterior segment cleavage syndrome) is a newer name for a genetically heterogeneous group of

developmental disorders with malformations of the structures of the anterior segment that share some common features and a high prevalence of associated glaucoma [16, 19, 20]. Glaucoma can also be part of a syndrome with other ocular and non-ocular malformations, called developmental glaucoma with associated anomalies. In all these cases, there is a malformation of parts of the anterior chamber structures with malfunction of the trabecular meshwork. The most common genetic causes of anterior segment dysgeneses have been identified as mutations affecting the function of the PITX2 and FOXC1 transcription factors [21].

The most prevalent conditions associated with glaucoma, although all very rare, are primary congenital glaucoma, Axenfeld and Rieger anomaly, Peters anomaly and aniridia. Classification was formerly based on clinical grounds, but since more genes are detected, other categories will be formed [21].

Although medical management of developmental glaucoma is often a temporising measure, early surgical intervention is the definitive treatment. The choices of techniques are directed by the stepladder classification: in simple cases of congenital glaucoma, first, a goniotomy is performed then a trabeculotomy; if this treatment is not sufficiently lowering the pressure, a trabeculectomy is executed, followed by eventually a second trabeculectomy. It this is not successful, a glaucoma drainage device is implanted. If all these techniques are failing, then as last hope, cyclodestructive procedures are necessary [22].

6.3.1 Primary Congenital Glaucoma

Congenital glaucoma is a rare form of glaucoma. 1/10,000 newborns are affected. Both eyes are usually involved but to varying degrees; boys are affected slightly more frequently than girls. A hereditary factor is occasionally present and is mostly autosomal recessive; it is rare except in consanguineous marriages. The most prevalent gene involved is CYP1B1 [23]. The IOP elevation is caused by the failure of the anterior chamber angle and the trabecular meshwork to develop appropriately during intrauterine development. The trabecular meshwork has not yet fully developed and is still partially covered by a non-perforated immature structure of collagen fibres [24]. As consequence, the eyeball enlarges due to distensible sclera of a baby and especially the cornea expands (megalocornea). The Descemet membrane of the cornea is less elastic, and stretching may result in small tears that cause a central opacification (Fig. 6.12) (see also page 21). These opacifications form lines, called Haab's stria, and are visible for the rest of life. Histologically, they are visible as longitudinal scrolls of the PAS-positive Descemet membrane at the posterior side of the cornea (Fig. 6.12c, d), with an increased diameter of the cornea. There is an anterior displacement of the iris insertion and ciliary body [25, 26].

6.3.2 Axenfeld and Rieger Anomaly (AXRA)

In AXRA, tissue strands of variable thickness are bridging the anterior chamber from the peripheral iris to a prominent anteriorly displaced Schwalbe's line (white line on the posterior aspect of the cornea); there is thinning of the iris with eventual hole formation in the iris [19]. The disorder in which this Schwalbe's line is markedly anteriorly displaced and thickened is called "posterior embryotoxon" [27, 28]. It may be an isolated finding without glaucoma or seen in the presence of other ocular anomalies, in particular AXRA syndrome [29].

The iris may be inserted into the trabecular meshwork with incomplete development of the TM and Schlemm's canal [25]. AXRA has an autosomal dominant inheritance, and 50 % of those with AXRA develop glaucoma; the rise in IOP is most likely to occur in childhood [19, 21, 30].

6.3.3 Peters Anomaly

This anomaly is caused by focal absence of corneal endothelium, Descemet membrane and posterior corneal stroma. Usually, this occurs in the

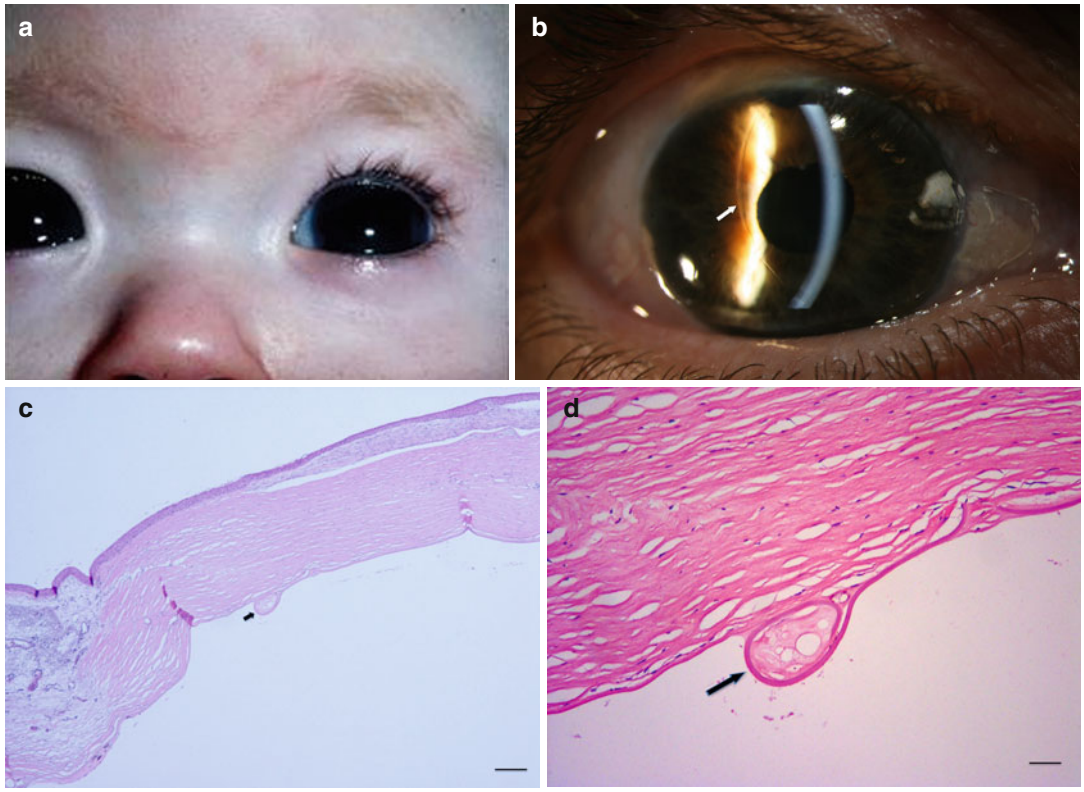

Fig. 6.12 (**a**) Congenital glaucoma baby with bilateral enlarged cornea (Courtesy of Ingele Casteels, Department of Ophthalmology, Leuven). (**b**) Clinical picture of Haab's striae in a 63-year-old adult (*arrow*), bilateral Haab's striae, diagnosed as baby with congenital glaucoma. *Vertical bended line* at the posterior side of the cornea, visible in retrograde illumination; signs of anterior synechiae between the cornea and iris at 5 o' clock. (**c**, **d**) Cornea with image of Haab's striae as Descemet scroll, after evisceration of blind eye with congenital glaucoma (*arrow*), HE staining. Bars = 100 and 50 μm, resp

central cornea, leading to a central corneal opacity. Iris synechiae extend from the iris collarette to this defect. There are adhesions between the lens and the cornea with corneal opacity. Glaucoma occurs in about 50 % of cases [31]. In more severe cases, the lens, iris and cornea are not separated from each other without an open anterior chamber and forward bulging of the cornea can occur (also known as anterior staphyloma).

This causes glaucoma in 90 % of cases, which is difficult to manage and often refractory to medications. Treatment must be performed in very young age because of the risk of glaucoma damage and amblyopia. The structural defects have their origin in a genetic defect, different genes are responsible; recessive as well as dominant familial cases and sporadic patients are known. The most prevalent gene defects are located in the Pax6, C-Maf and Fox genes [19–21]. In sporadic cases, some environmental influences are present as in foetal alcoholic syndrome. The formation of the anterior segment occurs in the first trimester of pregnancy and babies are born with this congenital defect. There is a broad spectrum of clinical findings, also in the same family with the same gene defect and also a large variation between the right and left eye. Peters anomaly may also be associated with other ocular or systemic abnormalities (trisomy 13–15, Norrie disease). Most cases are bilateral and asymmetric (Fig. 6.13).

6.3.4 Aniridia

In aniridia, the iris is only rudimentary developed [32]. The spectrum of this disease varies from a

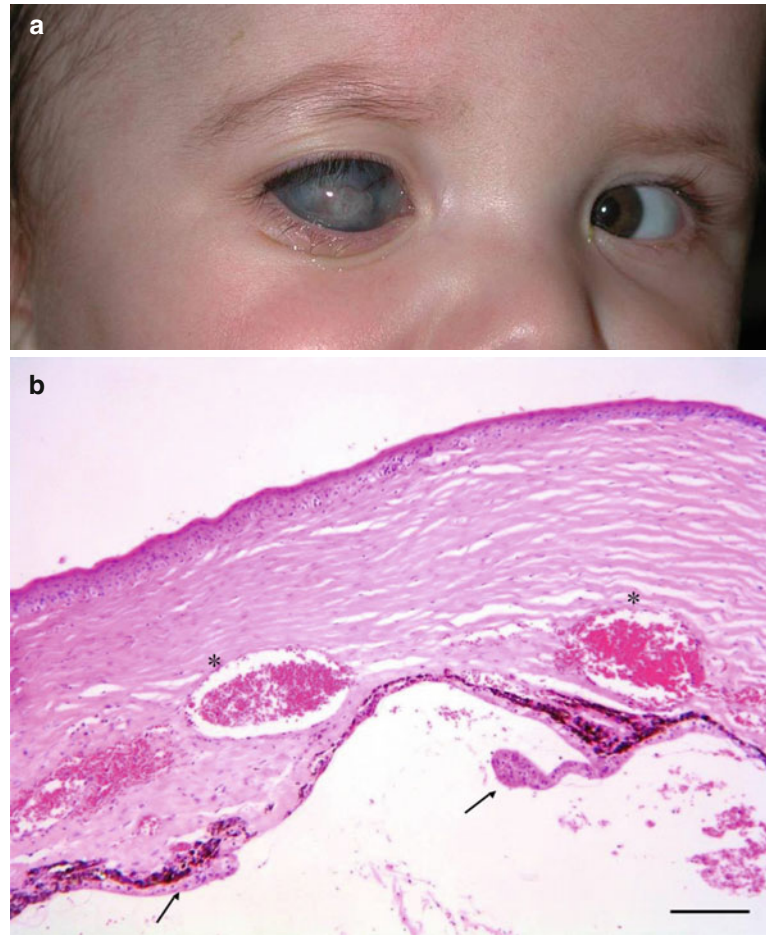

Fig. 6.13 (**a**) Child with severe form of unilateral Peters anomaly with enlarged and hazy vascularised cornea. (**b**) Histopathology of cornea after evisceration of eye with Peters anomaly. Irregular corneal stroma with abnormal vascularisation (*asterisks*); iris and ciliary body remnants on the posterior side of the cornea (*arrows*). H&E staining. Bar = 100 µm

nearly normal thin iris to very small iris tufts at the normal place of the iris root. The gene Pax6 had a wide expression in the developing eye and Pax6 mutations account for most cases of aniridia; the majority of Pax6 mutations are nonsense, splicing, insertions and deletions [16, 18]. The TM changes are variable, which also accounts for a variable glaucoma disease. During embryogenesis, there is a disruption of the trabecular meshwork development and adhesion between the iris periphery and cornea in the juvenile eyes. In a few cases of children examined by Margo, the trabecular meshwork and Schlemm's canal were not seen. The anterior border of the iris extended anteriorly to the Descemet membrane, the internal sulcus being filled with iris tissue. Later in adult life, there is a complete closure of the iridocorneal angle by a slow and continuous process of contraction; this causes then the IOP rise and degenerative changes in optic nerve axons and to glaucoma [33].

6.4 Primary Open-Angle Glaucoma (POAG)

POAG is the most prevalent form of glaucoma with an incidence of 5–10 % in elderly people [34–36]. The incidence is greater in families, and the presence of genetic factors plays a role in the pathogenesis of POAG; 14 linkage loci have been identified and are designated as GLC1A through GLC1N [37] with myocilin, optineurin genes [38]. Gradual changes in the outflow capacities causes changes in eye pressure and slowly destructive effects on the optic nerve and retinal ganglion cells. In the normal-aging eye, the trabecular beams thicken as a result of thickening

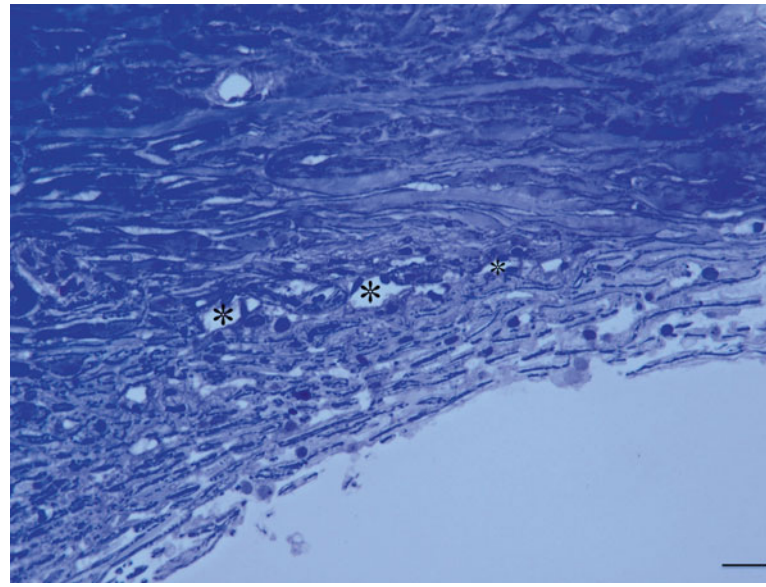

Fig. 6.14 Trabeculectomy specimen of a 79-year-old glaucoma patient. Trabecular meshwork is partially collapsed and contains less cells than normal. Schlemm's canal (*) is partially closed with partial loss of endothelial cells. Toluidine blue staining, bar = 50 µm

of the subendothelial basement membranes and changes of the extracellular matrix in the central core. There is also a continuous loss of cells within the corneoscleral and uveal part of the trabecular meshwork [39, 40] (Fig. 6.14).

In the cribriform layer, the main change is the development of extracellular material appearing as plaques by long-spacing collagen accumulation. The deposition of plaque material continuously increases with age. These changes cause an increase in outflow resistance. Morphological changes of the outflow pathway in POAG are marked by an extreme exaggerated aging process. The trabecular meshwork endothelium cells diminish in number and the meshwork becomes thicker with diminished capacities of filtrating the aqueous humour [41–43]. The loss of cells causes a fusion of denuded beams and contributes to collapses of the intertrabecular spaces especially in the uveal meshwork. A significant increase of plaque-like material deposited within the cribriform layer and in the wall of Schlemm's canal is noted compared to age-matched controls [44, 45]. Also, there is a reduction in the dimensions of Schlemm's canal (Fig. 6.14) [46]. POAG is more prevalent and more severe in black people [47, 48], with more advanced histological changes in the TM and Schlemm's canal [43, 49].

Optic nerve cupping is typical as described in section anatomy: there is a gradual decrease in nerve tissue fibres at the optic nerve head, with diminishing retinal ganglion cells.

6.5 Primary Angle-Closure Glaucoma (PACG)

6.5.1 Acute Primary Angle-Closure Glaucoma

The predisposing cause of PACG is the anatomy of the eye: a smaller eye with smaller axial length, typical an hyperopic eye, combined with a thicker lens due to aging. The lens and the iris touch each other and the normal flow through this slit is hampered. In these predisposing cases, a dilation of the pupil by darkness, stress or medication causes a thick plicated iris, in a small angle with blockage of the humour flow. If the pressure gradient between anterior and posterior chamber increases, the root of the iris is mechanically pushed against the cornea and trabecular meshwork, hindering the flow entering the TM. The secondary oedema of the iris and forward pushing of the iris raise the pressure very high to more than 60 mmHg in a very short time. This very high eye pressure pushes fluid in the corneal

layers exceeding the pumping capacity of the corneal endothelial cells provoking corneal oedema resulting in hazy vision. Extension of the sclera causes extreme pain. The IOP can become higher than the arterial tension and interferes arterial blood entering the eye with ischemia as consequence. Only acute intervention with making a hole in the iris (iridectomy) and pressure lowering medication can stop the damage (Figs. 6.6 and 6.7). Consequences of the acute attack are sustained high IOP, uveal and optic nerve atrophy and cataract.

Light microscopy at the acute moment showed swelling of endothelial cells in the TM and separation of the cells obscuring trabecular beams and almost obliteration intertrabecular spaces; there is accumulation of pigment granules, red blood cells, macrophages, leucocytes and amorphous debris with widening and fusion of adjacent trabecular beams [50].

Light microscopy at a later stage shows fewer and narrower trabecular spaces and fusion of trabecular beams and loss of endothelial cells, with the remaining cells becoming polymorphic (Fig. 6.15a, b). In terminal cases, occlusion of Schlemm's canal is seen [51]. The optic nerve shows thinning by atrophy without the typical cupping.

6.5.2 Chronic Angle-Closure Glaucoma

This term refers to an eye with a high IOP and with an anterior chamber which is narrow and closed in places by synechiae of the iris and peripheral cornea; these can be caused by an acute attack of chronic angle-closure glaucoma with reopening of the angle or due to intraocular inflammations. The prevalence is higher in East Asian compared to European people [52]. In chronic primary angle-closure glaucoma, TM showed a gross alteration of the architecture and arrangement of the trabecular beams, with fewer, narrower and more irregular trabecular spaces [50]. There is obliteration of Schlemm's canal and fused beams denuded of endothelium cells with obliteration of endothelium cells [43].

Fan-shaped trabecular beams form peripheral anterior synechiae between the peripheral cornea and iris, together with endothelium cell loss [53].

6.6 Secondary Open-Angle Glaucoma

The secondary open-angle glaucoma with trabecular resistance to the aqueous outflow can be caused either by clogging of the trabecular meshwork by various particle types or by ultrastructural changes of the trabecular meshwork itself.

6.6.1 Pretrabecular

6.6.1.1 Neovascularisation Glaucoma

Neovascular glaucoma, a special form of secondary angle closure (pretrabecular), is caused by synechial angle closure by contraction of fibrovascular tissue. The aqueous outflow is impaired and results in elevation of IOP.

In the early stage, fibrovascular membrane may form on the anterior surface of the iris (neovascularisation of the iris (NVI) Fig. 6.16a–d). At this stage, the IOP is normal and the neovascularisation may regress. In the later state, the fibrovascular membrane grows over the trabecular meshwork and leads gradually to circumferential synechial angle closure; thus, in this stage, it should be classified as secondary angle-closure glaucoma (see below) [54]. The corneal endothelium may then be stimulated to proliferate and migrate over the false angle. A contraction of the membrane on the iris surface causes an anterior bowling of sphincter and iris pigment epithelium (ectropium uveae, Fig. 6.16d) and can lead to an irregular dilatation of the pupil [55].

Neovascularisation occurs when larger segments of the retina lack adequate perfusion. It has been postulated that the ischemic retina produces angiogenic factors, especially VEGF that enters the anterior chamber triggering the growth of new blood vessels on the retina and on the iris surface as well. This is a dreaded

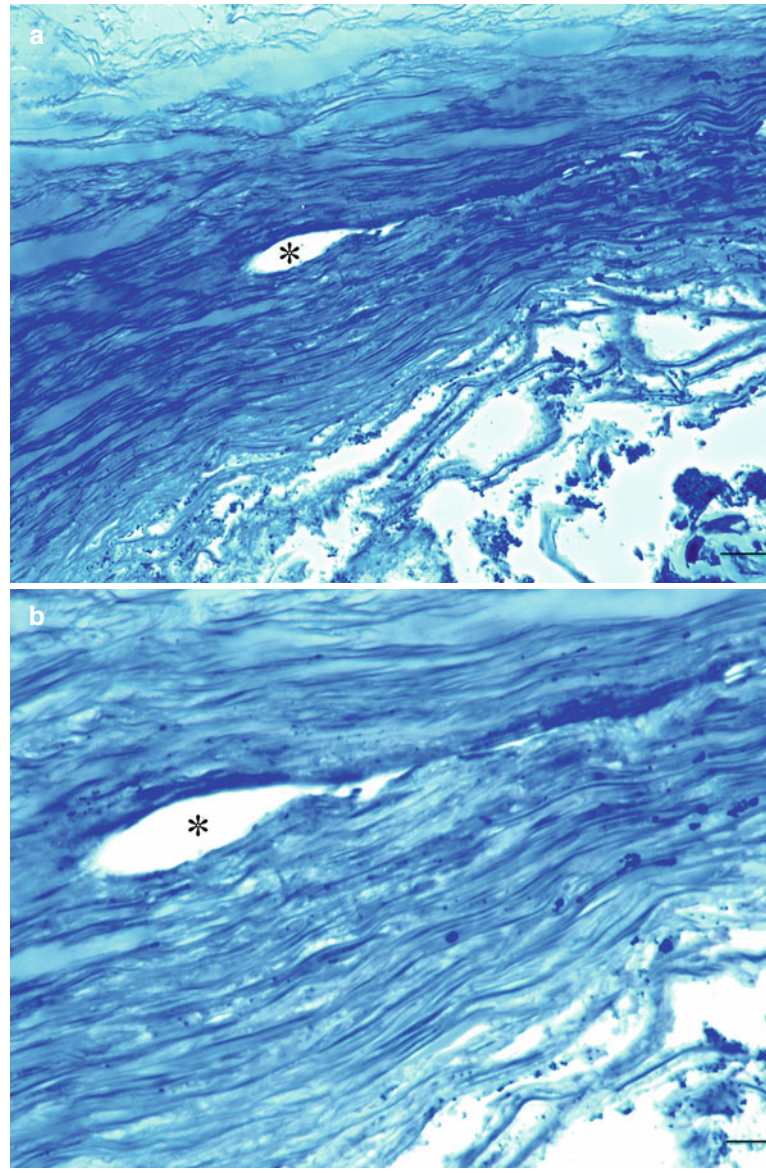

Fig. 6.15 (**a**, **b**) Trabeculectomy specimen of end-stage closed-angle glaucoma patient. Trabecular meshwork is totally collapsed without cells. Schlemm's canal (*) is partially closed with loss of all endothelial cells. Toluidine blue staining. Bars = 50 and 25 µm, resp

complication of ischemic central retinal vein occlusion, proliferative diabetic retinopathy, chronic intraocular inflammation and intraocular tumours.

Management during the late state of neovascular glaucoma is very difficult. To prevent this complication or progression of early-detected NVI, an adequate treatment of the underlying cause of posterior segment hypoxia (panretinal photocoagulation) is mandatory [56].

6.6.1.2 Endothelial Layer

Iridocorneal Endothelial Syndrome

Iridocorneal endothelial syndrome (ICE) includes progressive essential iris atrophy, Cogan-Reese syndrome or iris nevus syndrome, Chandler's syndrome and mixed forms [55]. This very rare disease typically occurs unilateral in middle-aged women. The aetiology is still unknown, but an abnormal individual reaction to a virus infection of the herpes genus (herpes simplex, Epstein-Barr) has been proposed [57, 58]. Different names

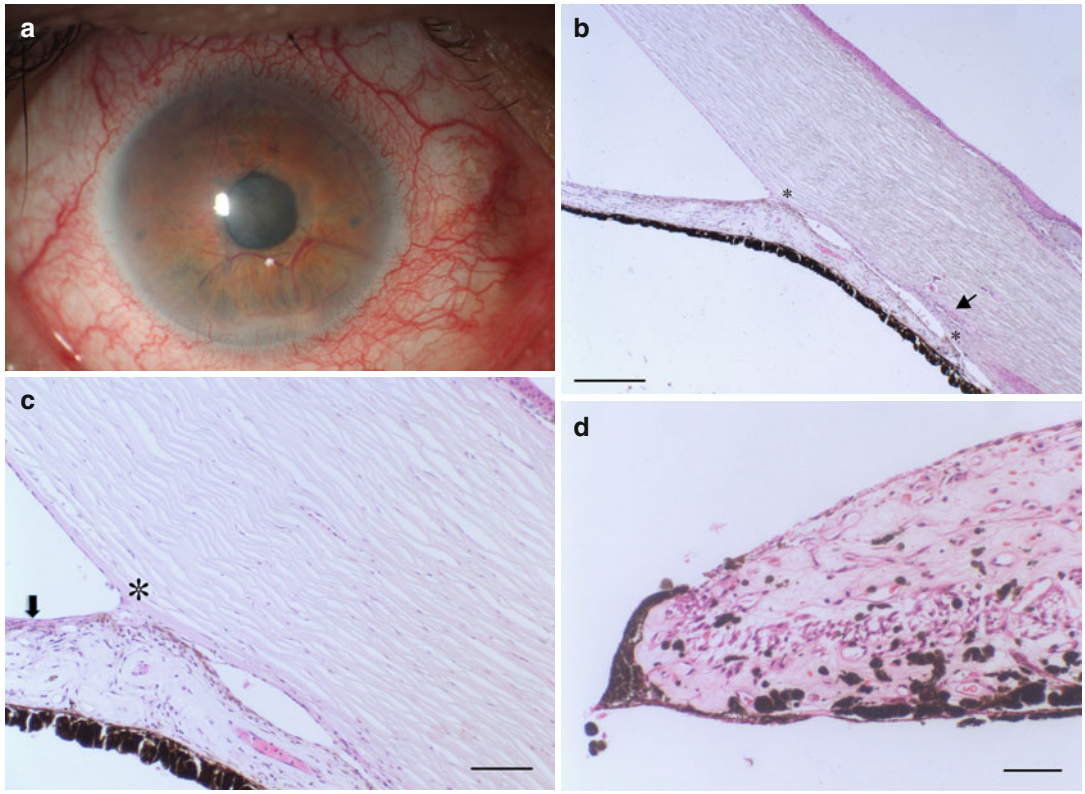

Fig. 6.16 (**a**) NVI with intense neovascularisation at the iris and lens surface. (**b**) Anterior synechiae (*asterisks*) forming in NVI, Schlemm's canal is narrowed (*arrow*), HE, bar = 100 µm. (**c**) Fibrovascular membrane at the anterior surface of the iris containing tiny neovascularisation vessels (*arrow*), anterior synechia (*asterisk*) HE, bar = 50 µm. (**d**) Ectropion uveae with anterior displacement of the pigment epithelium due to traction of fibrovascular membrane at the iris surface, HE. Bar = 50 µm

are given for a wide spectrum of the same disease with different clinical characteristics and common underlying pathogenic mechanism.

Migration of an abnormal corneal endothelial cell layer across the anterior chamber angle and at the anterior surface of the iris is responsible for corneal oedema, secondary glaucoma, noduli and atrophy of the iris and pupillary distortion (Fig. 6.17a). The contraction of the migrated membrane-like ICE tissue produces holes in the iris, usually unilateral. In young patients, glaucoma and oedema of the cornea are the main therapeutic problems.

Histopathology shows a monolayer of endothelial-like cells with Descemet-like membrane which covers the anterior chamber angle and the anterior border of the iris. This membrane is contracting and causing closure of the angle; on the iris surface, it causes holes in the iris stroma [59–61]. The diseased endothelial layer gets epithelial characteristics with cellular proliferation [62]. Progress over time is going through any degree of change from normal iris through marked corectopia and hole formation.

6.6.2 Trabecular

6.6.2.1 Degenerative

Two degenerative disorders causing trabecular problems are the pseudoexfoliatio lentis and the pigmentary glaucoma.

Pseudoexfoliation Glaucoma

The name pseudoexfoliatio derives from the fact that the dandruff-like material deposited on the

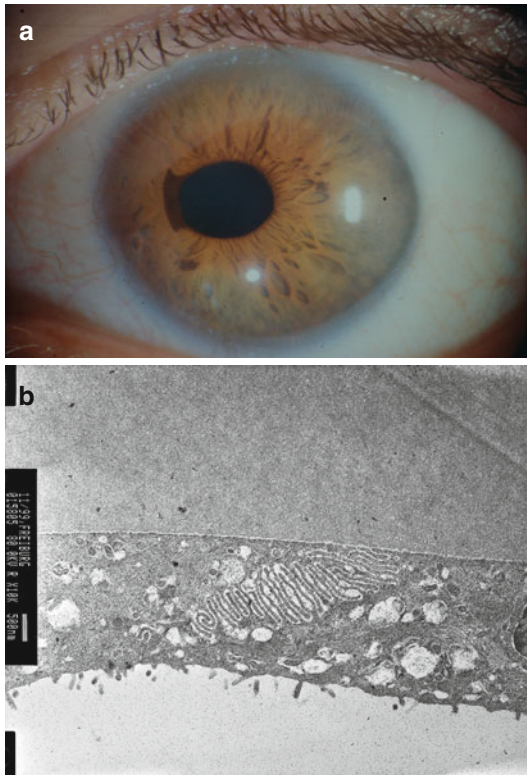

Fig. 6.17 (**a**) Corectopia of the pupil in iridocorneal syndrome, peripheral corneal opacification due to oedema. (**b**) Microvilli of corneal endothelial cells (*epithelialisation*) in iridocorneal syndrome of a 45-year-old patient

lens reminded on heat-associated genuine exfoliation of the anterior aspect of the lens (Fig. 6.18). The cause is not known; there are hints that the disease is inherited (see below). The pseudoexfoliation material is composed by various glycoproteins forming a fibrillary protein coated by amorphous material and is also found elsewhere in the body like the skin, lungs, heart, liver, kidney and the cerebral meninges. Intraocularly, it seems to be produced by endothelial cells of the trabecular meshwork, lens epithelium, ciliary body epithelium or iris cells. The pseudoexfoliation material clogs the trabecular meshwork and is phagocytosed by the trabecular meshwork endothelial cells and thus causes increase of the outflow resistance (Fig. 6.19). Pseudoexfoliation is associated with vascular abnormalities of the iris with deposition of the material within the iris vessels and increased pigment loss causing pupillary ruff atrophy and additional clogging of the

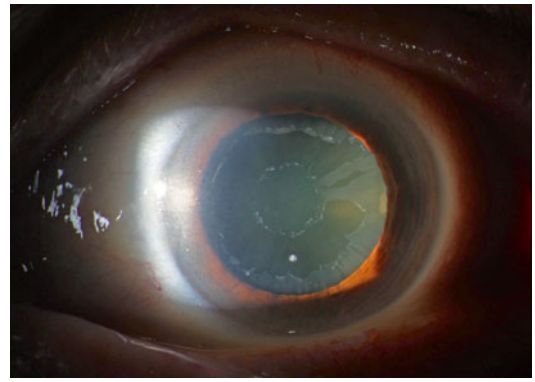

Fig. 6.18 Intense pseudoexfoliation at the anterior aspect of the lens with a free zone between the centre and periphery due to pupillary movement (Courtesy of Dr. Jan Lübke, University Eye Hospital Freiburg)

trabecular meshwork by the pigment particles. Mydriasis can cause extensive pigment liberation from the histologically sawtooth-like configurated pigment epithelium at the posterior side of the iris (Fig. 6.19) causing hyperpigmentation of the trabecular meshwork and possibly also IOP elevation in many cases. Pseudoexfoliation is not confined to the trabecular meshwork but is also associated with changes of the cornea, ciliary body (Fig. 6.19) and lamina cribrosa. The cornea shows less epithelial and endothelial cells, less subbasal nerve plexus causing decreased corneal sensitivity and increased corneal morbidity, e.g. after cataract surgery [63]. It is known that eyes with pseudoexfoliatio lentis are more susceptible to glaucoma damage in case the intraocular pressure rises. The morphological correlate was shown by Schlötzer-Schrehardt et al. demonstrating a pseudoexfoliatio specific elastinopathy of the lamina cribrosa with decreased expression of LOXL1 protein and decreased amount of elastic fibres. It was also shown in vitro that the assembly of elastic fibres by the optic nerve head astrocytes was impaired by the inhibition of LOXL1 [64]. Single-nucleotide polymorphisms of the LOXL1 gene are known to increase the susceptibility for pseudoexfoliation [65]; hints towards association with other genes like clusterin, adenosine receptor A3, matrix metalloproteinases, glutathione transferase, contactin-associated protein-like 2 and tumour necrosis factor alpha gene [66] are found though not associated with the strong correlation

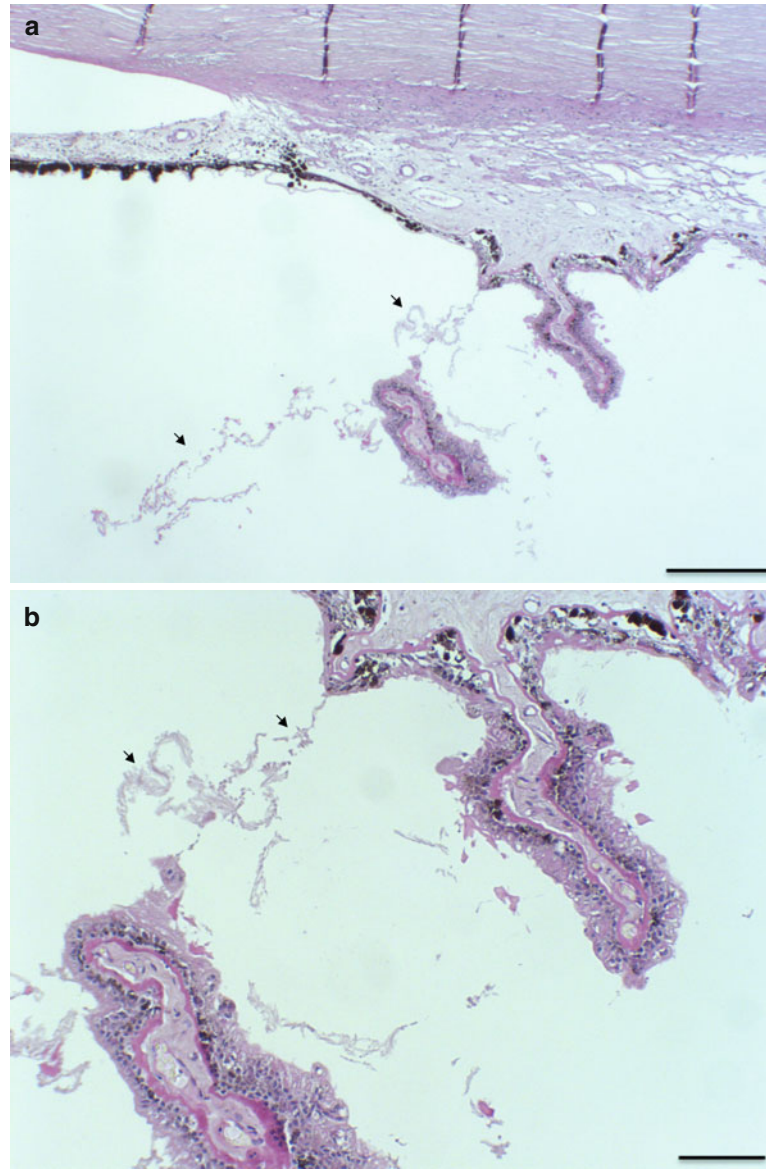

Fig. 6.19 (**a**) PEX material around the ciliary body processes (*arrows*). Sawtooth-like appearance of the rather loose pigment epithelium at the posterior aspect of the iris (PAS, bar = 300 µm). (**b**) PEX material around the ciliary body processes (*arrows*, PAS, bar = 100 µm)

shown by LOXL1. In contrast to POAG, the optic nerve in pseudoexfoliation glaucoma does not show increased connective tissue in the septa [67].

Pigmentary Glaucoma

PDS (pigment dispersion syndrome) is a syndrome where pigment is released from the posterior iris pigment epithelial cells due to anatomical variation (see below). It precedes pigmentary glaucoma and typically affects young myopes [68]. PDS affects women and men equally, but 78–93 % of PG patients are males [69]. There are hints that the disease is inherited (see below).

Pigmentary glaucoma is caused by pigment-related changes of the trabecular meshwork. The pigment originates from the pigmented iris epithelium, which is liberated due to abnormal iris configuration with the posterior iris rubbing at the lens zonulae, especially those forming bundles which are inserting into the anterior lens capsule causing radial iris defects (Fig. 6.20). The histological correlate of the iris transillumination defect is missing iris pigment epithelium (Fig. 6.21). The pigment epithelium membranes are disrupted with dispersion of their pigment granule content [70]. The liberated pigment is

found in the corneal endothelium and can be visualised clinically as a Krukenberg spindle (Figs. 6.22 and 6.23) and in the endothelial cells of the trabecular meshwork causing narrowing of the aqueous humour pathway with increased outflow resistance but also in the meshwork itself [2] (Fig. 6.24a, b). Murphy et al. and Gottanka et al. have shown a marked loss of trabecular meshwork cells [71, 72]. Presumably, this cell loss occurs after overload of TM (trabecular meshwork) cells with pigment granules. Denuded TM lamellae fuse and the TM collapses. In the subendothelial region of these collapsed TM areas, an increase in extracellular matrix presumably due to underperfusion was observed. At other places, Schlemm's canal was occluded and the cribriform region appeared disorganised [72]. The full circumference of the TM tends to be affected, although pigmentation is more prominent inferiorly, possibly owing to gravity [73] (Figs. 6.25 and 6.26) [72]. Occlusion of TM spaces by pigment granules or cells laden with pigment was not seen in eyes with pigmentary glaucoma [72]. Families suffering from pigmentary glaucoma with autosomal dominant mode of inheritance [74] but also autosomal recessive in four generations [75] are described. Several genetic loci are proposed to be related to pigment dispersion syndrome/pigmentary glaucoma like muscarinic acetylcholine receptor, myocilin and others [76].

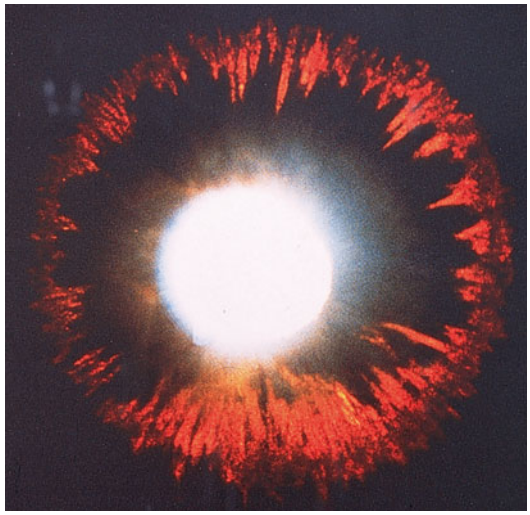

Fig. 6.20 Radial iris transillumination over the whole circumference in pigmentary glaucoma (From Flammer [54])

6.6.2.2 Other Trabecular Glaucoma Causes

Uveitis, e.g. Fuchs heterochromic cyclitis

Uveal inflammation, e.g. in heterochromia shown here, can cause pigment liberation originating from the iris pigment epithelium as in pigmentary glaucoma with increased pigmentation of the anterior chamber angle. Because of different pathogenesis, the iris transillumination usually has not a radial orientation, and heterochromia is seen clinically (Fig. 6.27). The pigment can be phagocytosed by macrophages (Fig. 6.28, arrows) which clog the trabecular meshwork. In

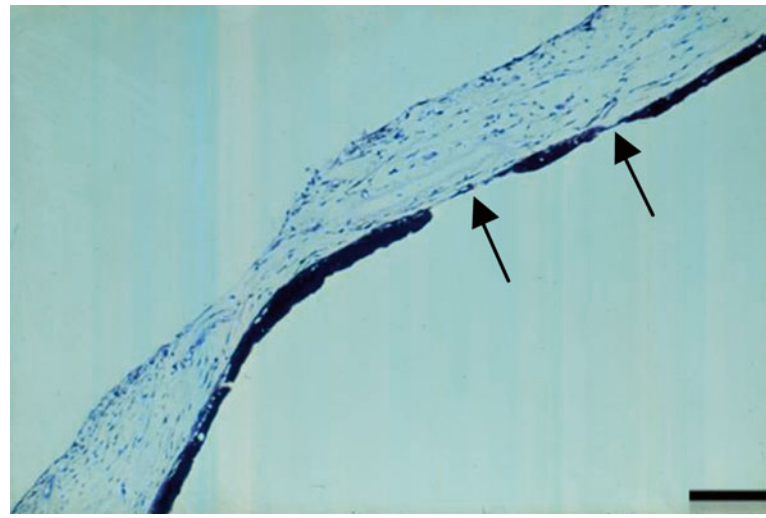

Fig. 6.21 Patchy atrophy of the iris pigment epithelium (*arrows*, HE, bar = 250 µm)

addition, Naumann et al. observed fine capillary bridges in the anterior chamber angle and propose a particular form of NVI in this uveitis type [2]. Our case illustrated here shows in contrast to his observation NVI of the non-angle area (Fig. 6.18, asterisk). Advanced cases, as usually those requiring enucleation, show fibrous changes of the trabecular meshwork which are considered pathognomonic for this condition [9, 77–79].

6.6.2.3 Blood

Blood cells can clog the trabecular meshwork causing intraocular pressure raise, e.g. following mechanical trauma of the anterior segment (contusio bulbi, Figs. 6.29 and 6.30a, b). Usually, the blood will be resorbed spontaneously; seldom, an anterior chamber irrigation becomes necessary. In long-standing cases, the erythrocytes degrade [80] and the Berlinerblau staining will be positive due to the hemosiderin content of macrophages and the haemolytic process causes haemolytic glaucoma (Fig. 6.31a, b).

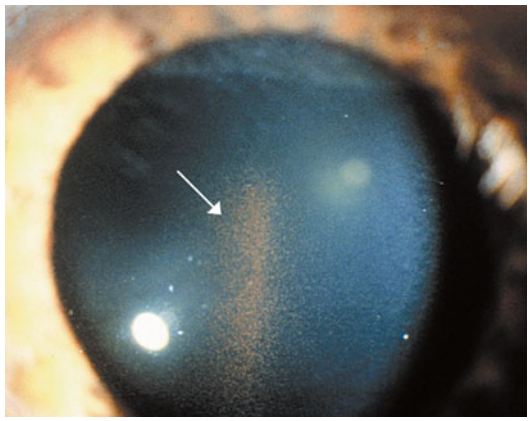

Fig. 6.22 Krukenberg spindle at the posterior aspect of the cornea in pigmentary glaucoma (*arrow*)

6.6.2.4 Lens Particle Glaucoma

In case of trauma- or surgery-induced lens fragmentation, lens particles can clog the trabecular meshwork (Fig. 6.32a, b) with intraocular pressure raise [81, 82]. Rarely, it might occur many years following cataract surgery [83, 84] or following intraocular lens dislocation in pseudoexfoliation syndrome with liberation of lens material clogging the trabecular meshwork [85].

6.6.2.5 Macrophages

Various conditions attract macrophages into the anterior chamber causing clogging of the trabecular meshwork. They tend to be located at the uveal meshwork because of their large size of 20 µm, while the space between the trabeculae measures about 10 µm [2].

Phacolytic Glaucoma

Free-floating lens material from mature cataract or injured lens induces a foreign body reaction with macrophages phagocytosing the lens particles. This results in PAS-positive cells, which are found around the lens (material) (Fig. 6.33a, arrows), in the anterior chamber angle (Fig. 6.33b). In our case, there was a history of vitrectomy and the lens containing macrophages were even found on the optic nerve head (Fig. 6.33c).

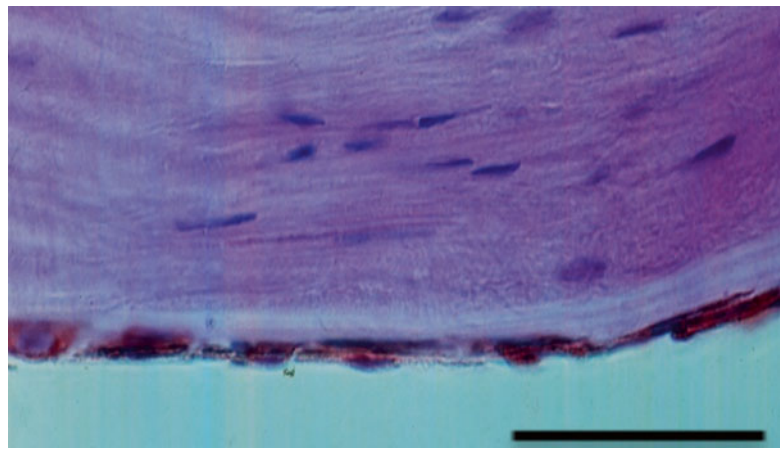

Fig. 6.23 Histological correlate of Krukenberg spindle is pigment deposition within the corneal endothelial cells (HE, bar = 50 µm)

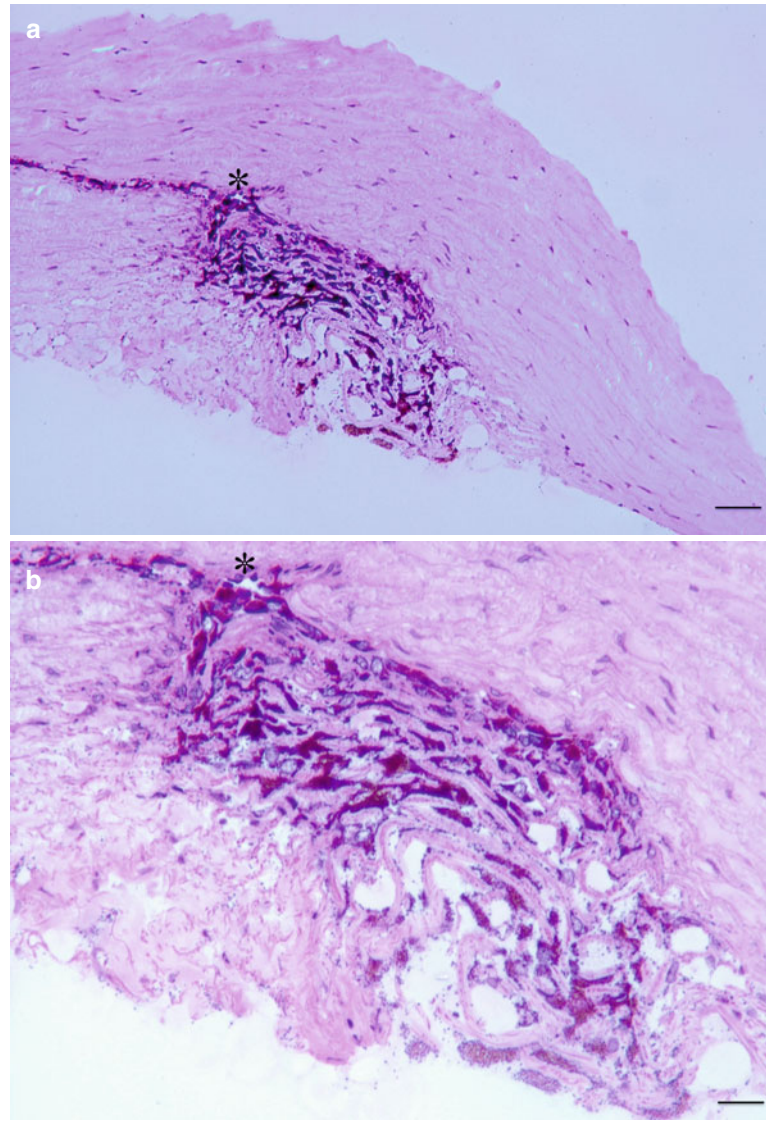

Fig. 6.24 (**a**, **b**) Trabeculectomy specimen of a pigmentary glaucoma patient. Trabecular meshwork is nearly totally collapsed and contains multiple pigmented clumps; the number of cells is diminished. Schlemm's canal (*) is partially closed and clogged with pigmented clumps. HE, bars = 100 and 50 µm, resp

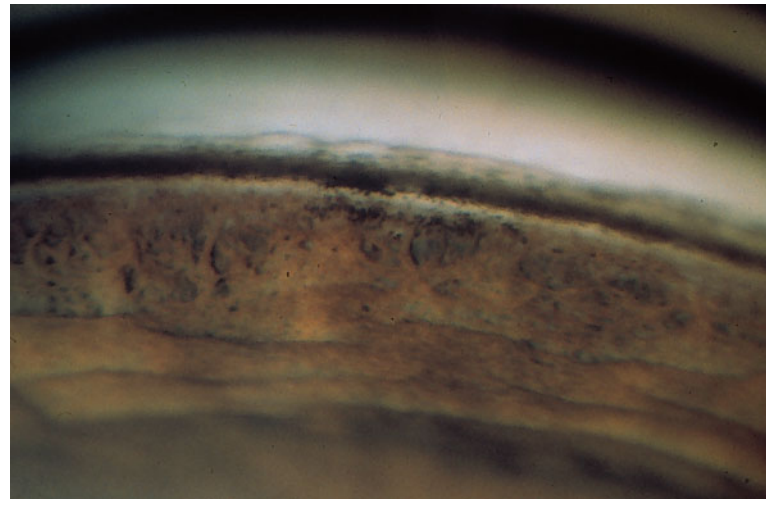

Fig. 6.25 Hyperpigmentation of the trabecular meshwork in pigmentary glaucoma

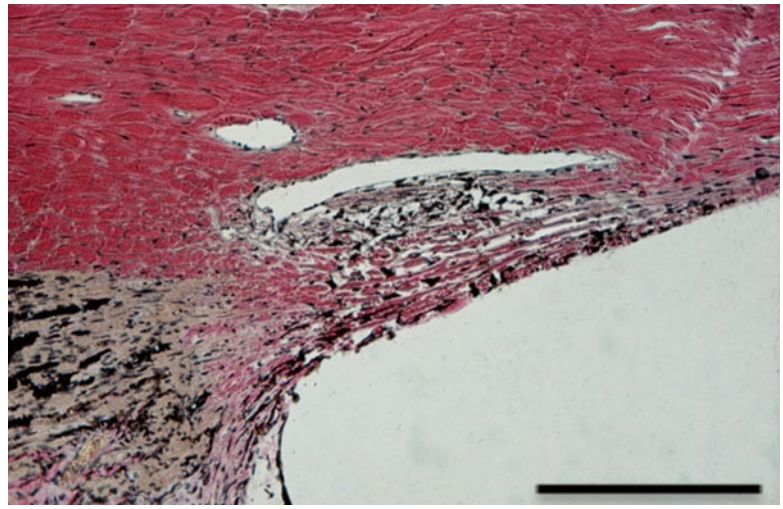

Fig. 6.26 Histological correlate of the trabecular meshwork hyperpigmentation is pigment deposition within the trabecular meshwork endothelial cells (Elastica van Gieson, bar = 200 µm)

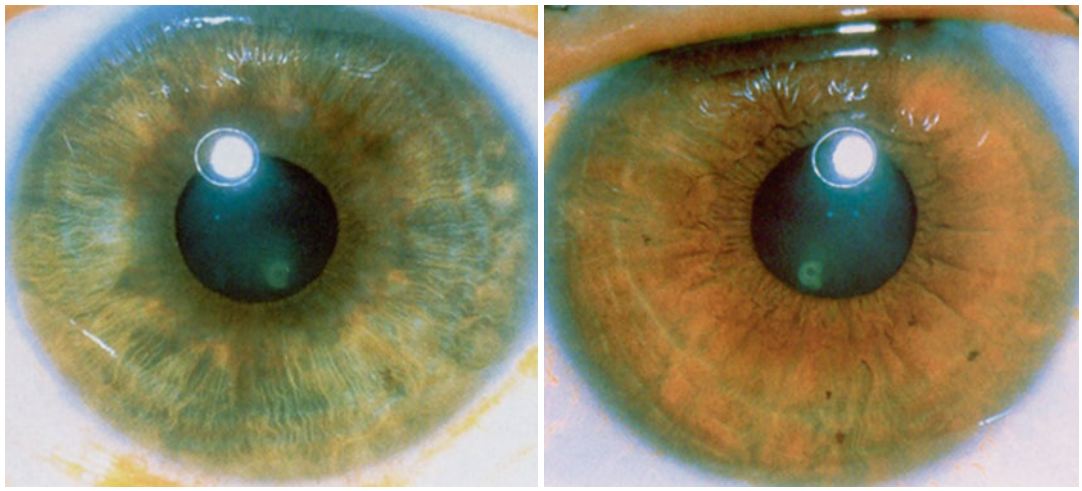

Fig. 6.27 Iris heterochromia with lighter iris of the right eye (*left*) in Fuchs heterochromic cyclitis

Neoplastic Cells

Necrotic intraocular tumours can resolve and disperse into the anterior chamber clogging the trabecular meshwork and causing raise of intraocular pressure with subsequent glaucoma. In most of the cases, these are malignant tumours like retinoblastoma (Fig. 6.34a, b) or choroidal melanoma. Another cause of IOP raise in intraocular tumours is the neovascularisation glaucoma as it often occurs in medulloepithelioma of the ciliary body. Benign tumour cells like melanocytes in nevus of Ota can cause clogging of the trabecular meshwork (Fig. 6.35). There are few cases described in the literature; pigmented nevus of Ota patients seem to be more prone to develop glaucoma [86].

6.6.3 Alterations of the Trabecular Meshwork

6.6.3.1 Steroid-Induced Glaucoma

One-third of the population develop IOP raise following topical steroid application, about 5–6 % develop severe IOP raise >31 mmHg or 15 mmHg above the baseline and two-thirds are nonresponders with an IOP raise of under 6 mmHg or none at all [87, 88]. Steroid-induced

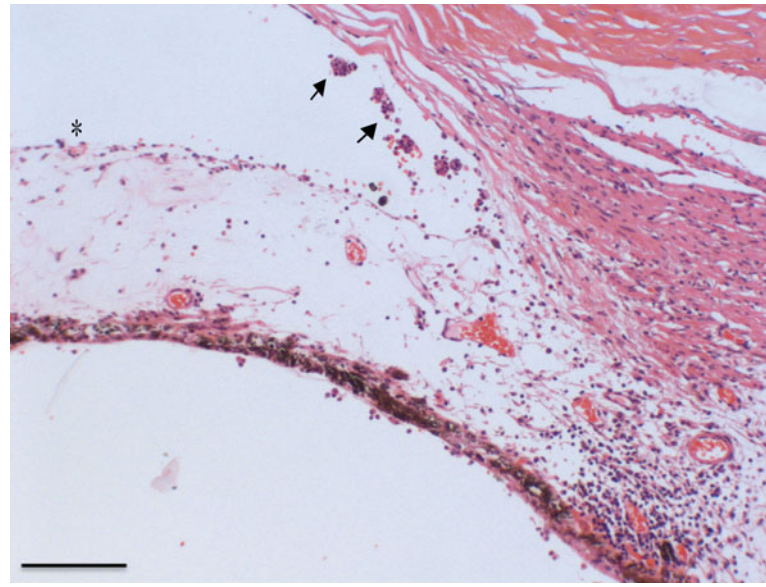

Fig. 6.28 Anterior chamber angle in Fuchs heterochromic cyclitis with pigment containing macrophages (*arrows*) clogging the trabecular meshwork and NVI (*asterisk*). Chronic inflammatory infiltrate adjacent to the ciliary body, HE, bar = 300 µm

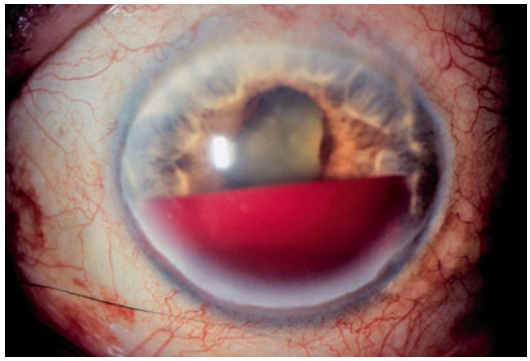

Fig. 6.29 Severe hyphaema in the anterior chamber due to blunt contusion

IOP raise occurs following steroid application as eyedrops, subconjunctival, intravitreal, periocular, but also after application to the skin [89, 90], intranasally and systemically [91]. The IOP raise occurs not prior to 5 days [92] and most often within 6–8 weeks following topical steroid application [93–96]. In most cases, it is reversible especially if the steroids have not been applied more than 12 months [97] within 2–4 weeks [98]. Risk factors are pre-existing POAG, age (old [93, 94] and children under 10 years [99]).

In steroid-induced glaucoma, there is – like in POAG – an increase in fine fibrillar material in the subendothelial region of SC. In contrast to the POAG eyes, these fibrils do not adhere to the sheath of the elastic fibres but are deposited underneath the inner wall endothelium. The main finding in steroid-induced glaucoma is an accumulation of basement membrane-like material staining for type IV collagen. These accumulations are found throughout all layers of the TM [45]. In addition elastin, laminin, fibronectin and glycosaminoglycans are found as a result of overproduction and reduced degradation due to inactivation of matrix metalloproteinases [100]. The phagocytotic activity of the trabecular meshwork cells is suppressed by dexamethasone with the consequence of debris accumulation within the trabecular meshwork and increase of outflow resistance [101]. In cell culture, dexamethasone leads to increase of the tight junction protein ZO-1, gap junction protein connexin 43 and cross-linking with tangling of the intracellular F-actin which was more pronounced in cells of POAG trabecular meshwork [102].

6.6.3.2 Trauma (Angle Recession)

Blunt trauma (contusio bulbi) can cause a tear of the anterior ciliary body with subsequent posterior displacement of the iris root leading to angle recession. Scar tissue and/or endothelial cells grow over/into the injured anterior chamber angle and cause IOP raise provided that the ciliary body still produces the normal amount of aqueous humour.

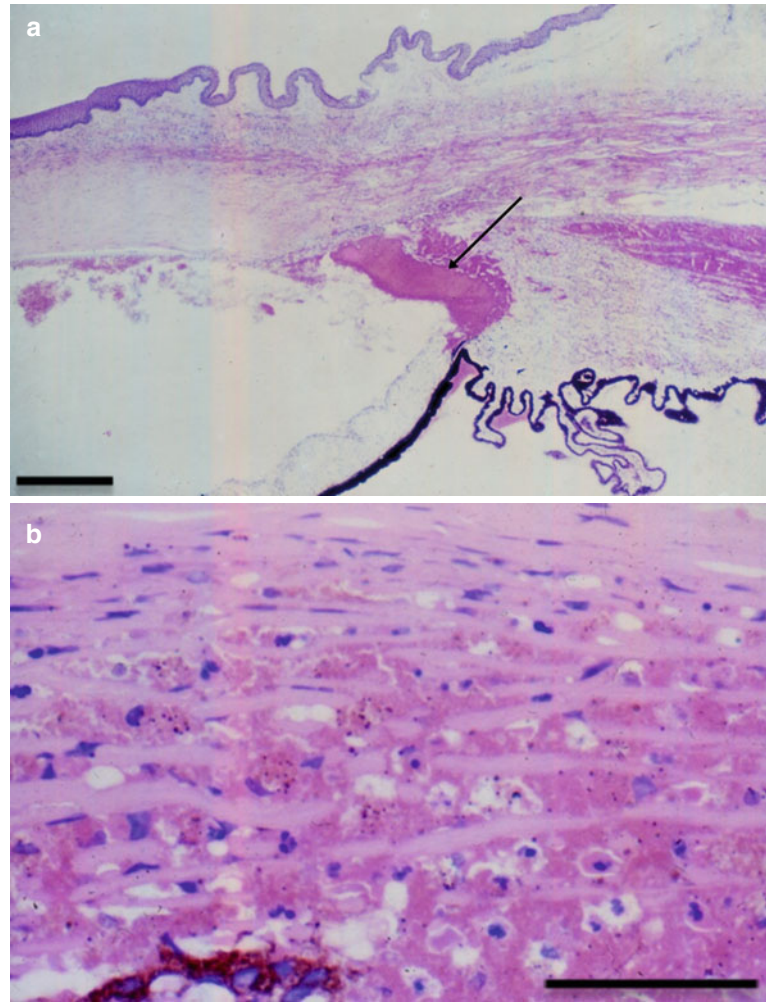

Fig. 6.30 (**a**) Blood mainly consisting of erythrocytes in the anterior chamber and angle clogging the trabecular meshwork (*arrow*, bar = 300 µm). (**b**) Erythrocytes in the trabecular meshwork not yet containing Berliner blue-positive hemosiderin (Berliner Blau staining, bar = 135 µm)

Wolff and Zimmerman [103] described in 1962 the early and late histopathological changes of angle recession in a series of eyes enucleated after ocular contusion. In early cases, they noted lacerations into the face of the ciliary body with damage to the ciliary muscle. Those lacerations that passed between the circular and longitudinal muscles of the ciliary body resulted in posterior displacement of the former along with the iris root and pars plicata. They also noted disruption of the trabecular meshwork. In late cases, they noted atrophy of the circular muscle fibres that had been separated from the longitudinal fibres and advanced degenerative changes of the trabecular meshwork consisting of atrophy, fibrosis and hyalinisation of the trabeculae and obliteration of the intertrabecular spaces and Schlemm's canal (Figs. 6.36 and 6.37a, b). In many cases, there was a newly formed hyaline membrane covering the inner surface of the trabeculae continuous with Descemet membrane and often extending into the recessed angle covering the longitudinal muscle [104].

6.7 Secondary Angle-Closure Glaucoma

There are two mechanisms of the secondary narrowing of the anterior chamber angle, namely, the pupillary and the ciliolenticular block [2]. In pupillary block, the flow of the aqueous humour between the lens and iris is blocked first and then the posterior chamber is overfilled and the anterior chamber angle is narrowing due to the

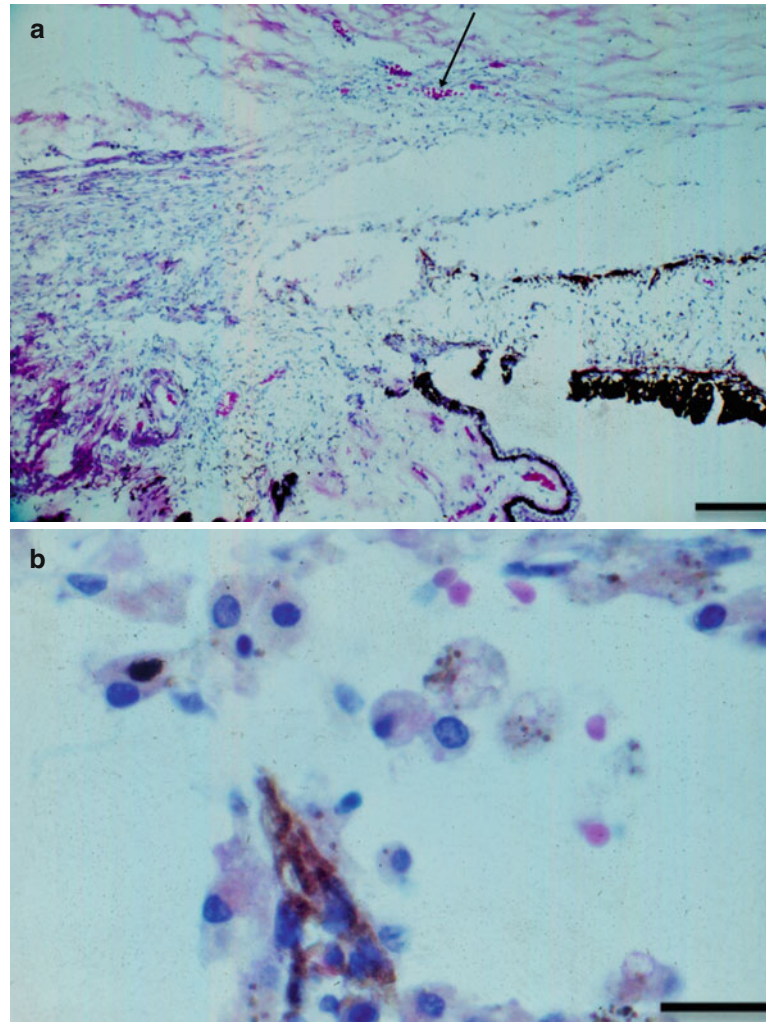

Fig. 6.31 (**a**) Macrophages in the anterior chamber in haemolytic glaucoma (*arrow*, bar = 100 µm). (**b**) Macrophages in the anterior chamber containing Berliner blue-positive hemosiderin in haemolytic glaucoma (Berliner Blau staining, bar = 50 µm)

forward bulging iris from behind (Fig. 6.38). This can happen in cases with intraocular inflammation with subsequent increased viscosity of the aqueous humour, iris thickening due to oedema and posterior synechiae, or in the eyes, which underwent anterior segment surgery or suffered from haemorrhage. Tumours located behind the iris (Figs. 6.39 and 6.40) might push the iris forward and cause a partial closure of the anterior chamber angle, and due to the vascular leakage with increased viscosity of the aqueous humour, a pupillary block might be induced in addition causing an acute increase of intraocular pressure. The ciliolenticular block occurs in eyes with a large lens where the contracted ciliary muscle "embraces" the lens not allowing the aqueous humour passing into the anterior chamber. In contrast to the pupillary block, not only the iris but the complete iris-lens diaphragm is pushed forward (Fig. 6.41).

A third kind of secondary angle-closure glaucoma is caused by neither a pupillary nor a ciliolenticular block but due to pretrabecular reasons like posttraumatic anterior synechiae impeding the outflow of the aqueous humour and giving rise of intraocular pressure (Fig. 6.42). Various types of secondary open-angle glaucomas might develop into this type of secondary angle-closure glaucoma if there is a progression of the underlying cause like neovascular membrane in neovascularisation glaucoma or endothelial overgrowth in ICE syndrome with narrowing of the anterior chamber angle due to adhesion and fibrosis between the iris and trabecular meshwork.

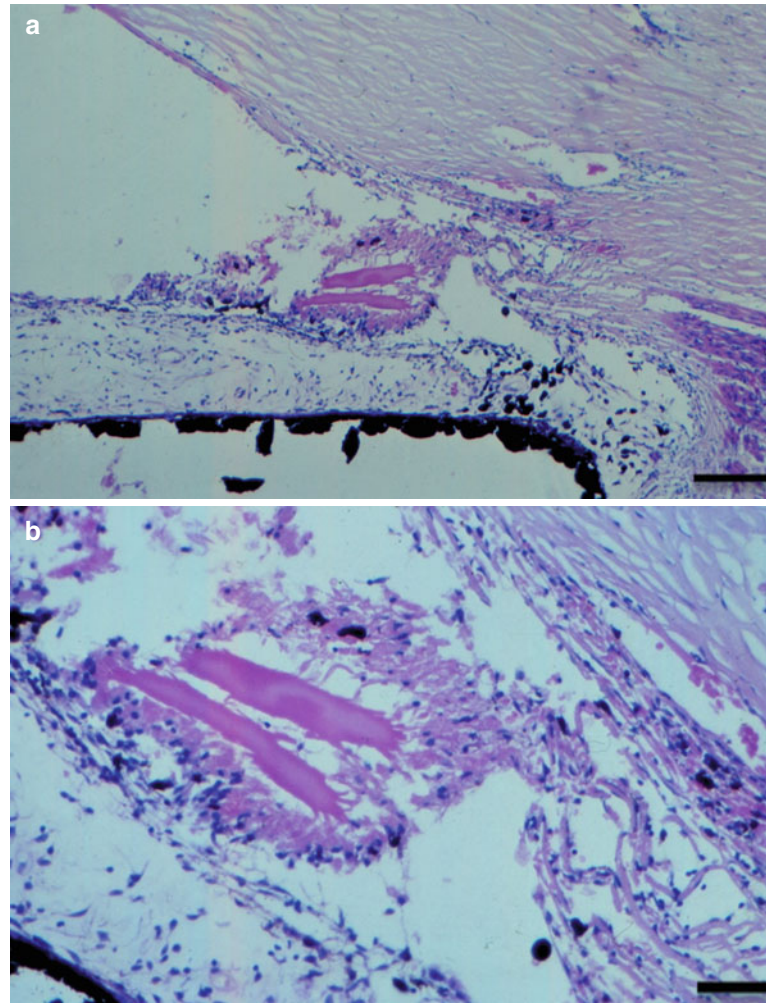

Fig. 6.32 (**a**) Lens particles in the anterior chamber angle clogging the trabecular meshwork (PAS, bar = 100 µm). (**b**) Lens particles in the anterior chamber angle clogging the trabecular meshwork (PAS, bar = 50 µm)

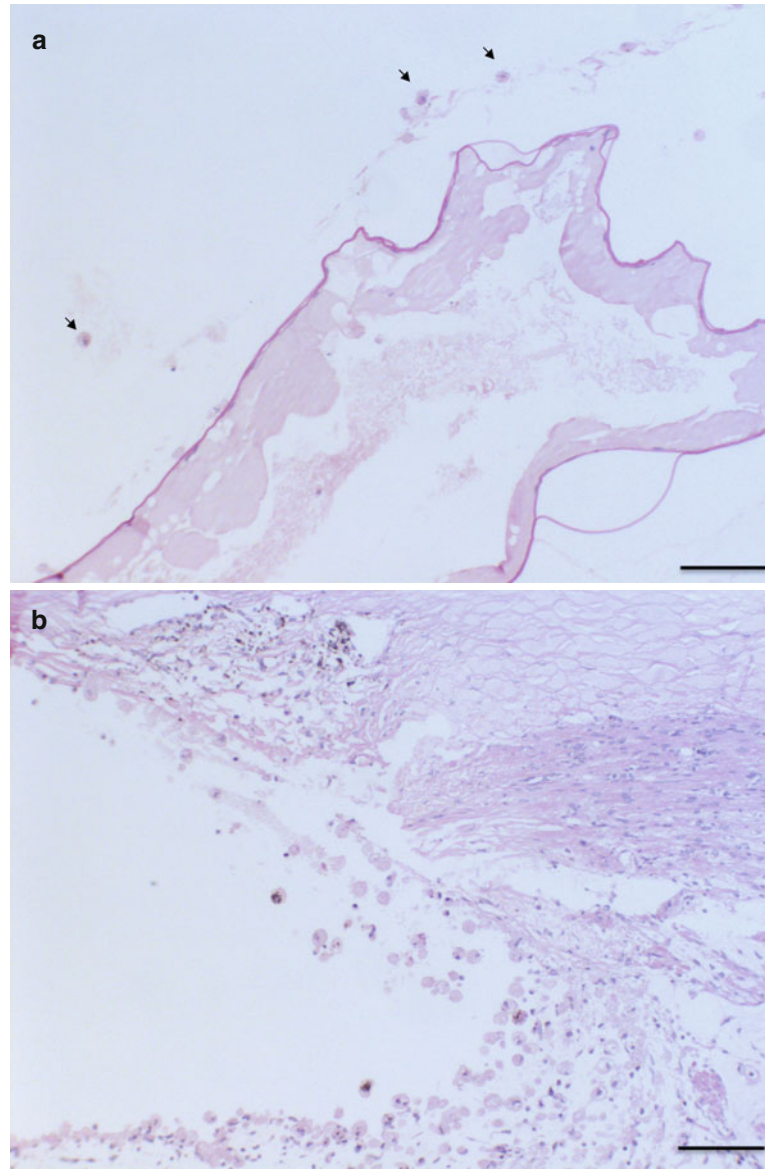

Fig. 6.33 (**a**) Dissolving cataractous lens surrounded by lens material containing macrophages in phacolytic glaucoma (*arrows*, PAS, bar = 100 µm). (**b**) Macrophages in the anterior chamber angle clogging the trabecular meshwork (*arrows*, PAS, bar = 100 µm). (**c**) Lens containing macrophages (*arrows*) were also found on the optic nerve head (HE, bar = 100 µm)

Fig. 6.33 (continued)

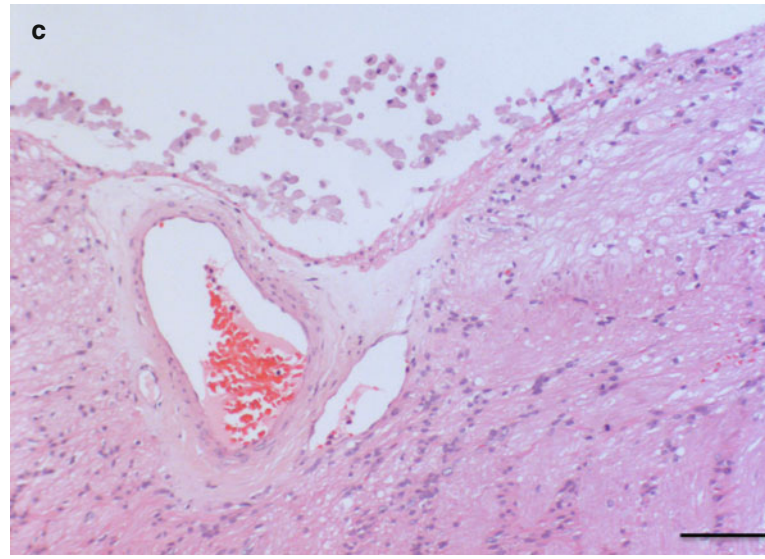

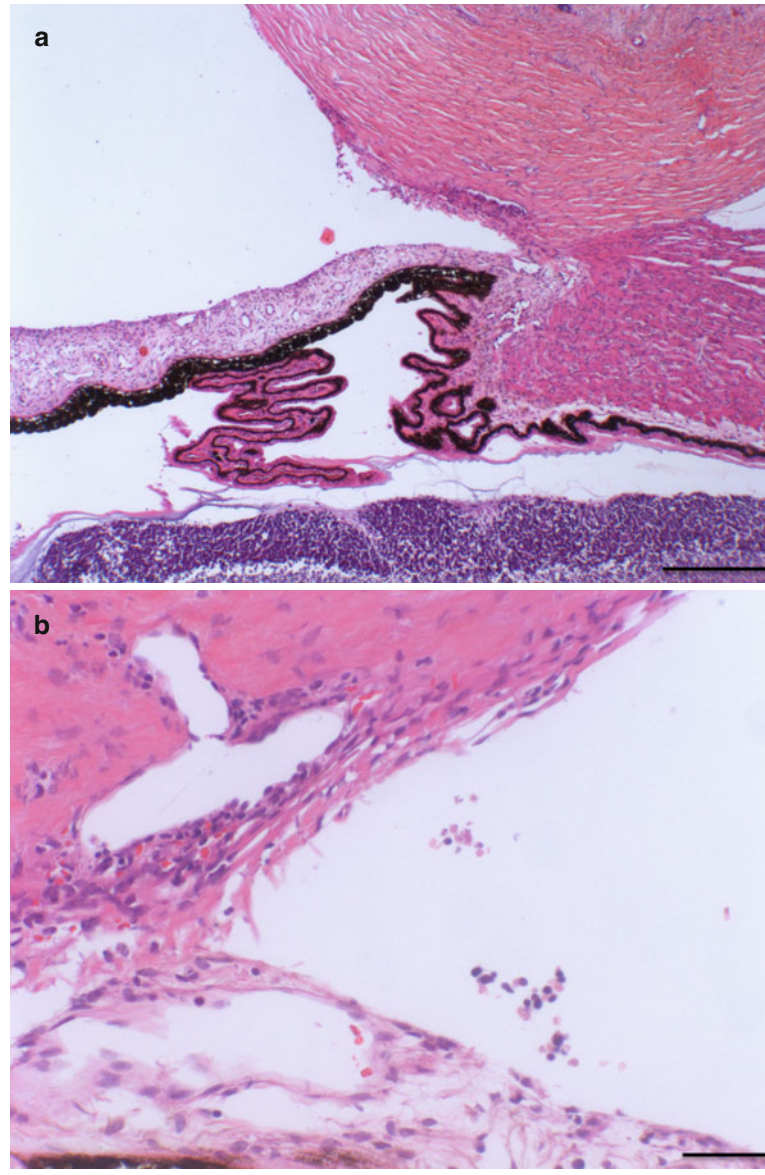

Fig. 6.34 (**a**) Retinoblastoma expanding towards the posterior chamber directly behind the ciliary body with tumour cells spreading to the anterior chamber angle (HE, bar = 300 µm). (**b**) Tumour cells of the retinoblastoma in the anterior chamber and trabecular meshwork (*arrows*, HE, bar = 100 µm)

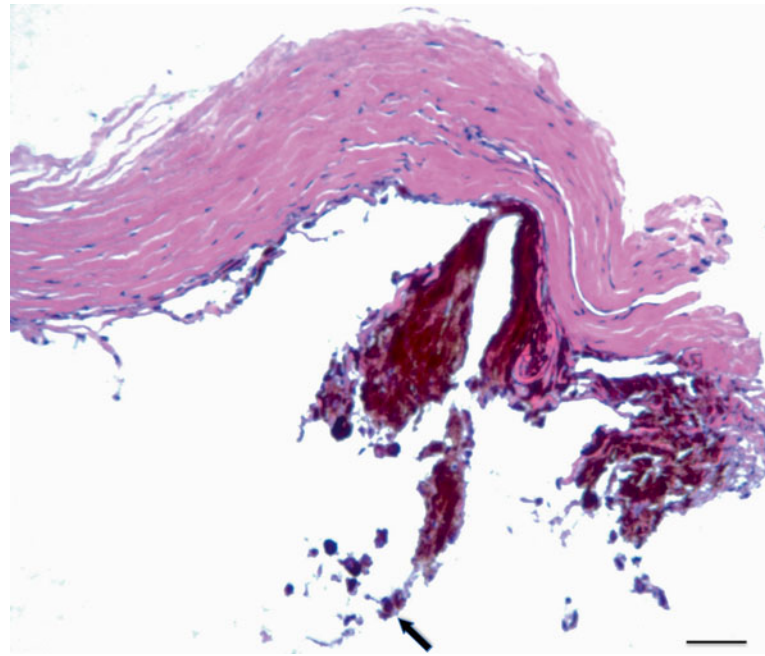

Fig. 6.35 Trabeculectomy specimen of pigmentary glaucoma patient with nevus of Ota, some of the infiltrating cells are melanoma cells (*arrow*). Later a full melanoma developed. Trabecular meshwork is nearly totally collapsed and contains multiple pigmented clumps. HE, bar = 100 µm

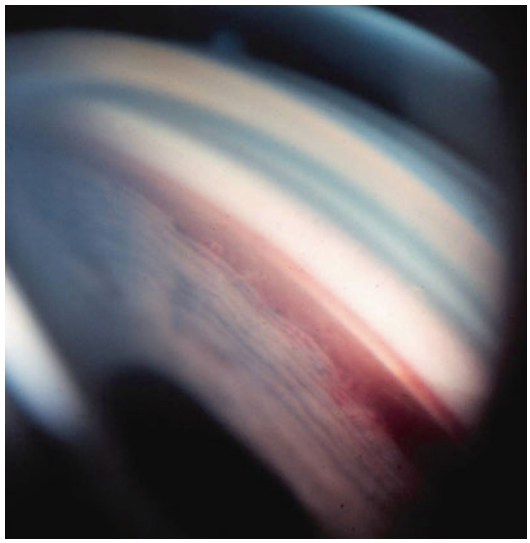

Fig. 6.36 Angle recession with a tear at the iris basis and exposed injured ciliary body

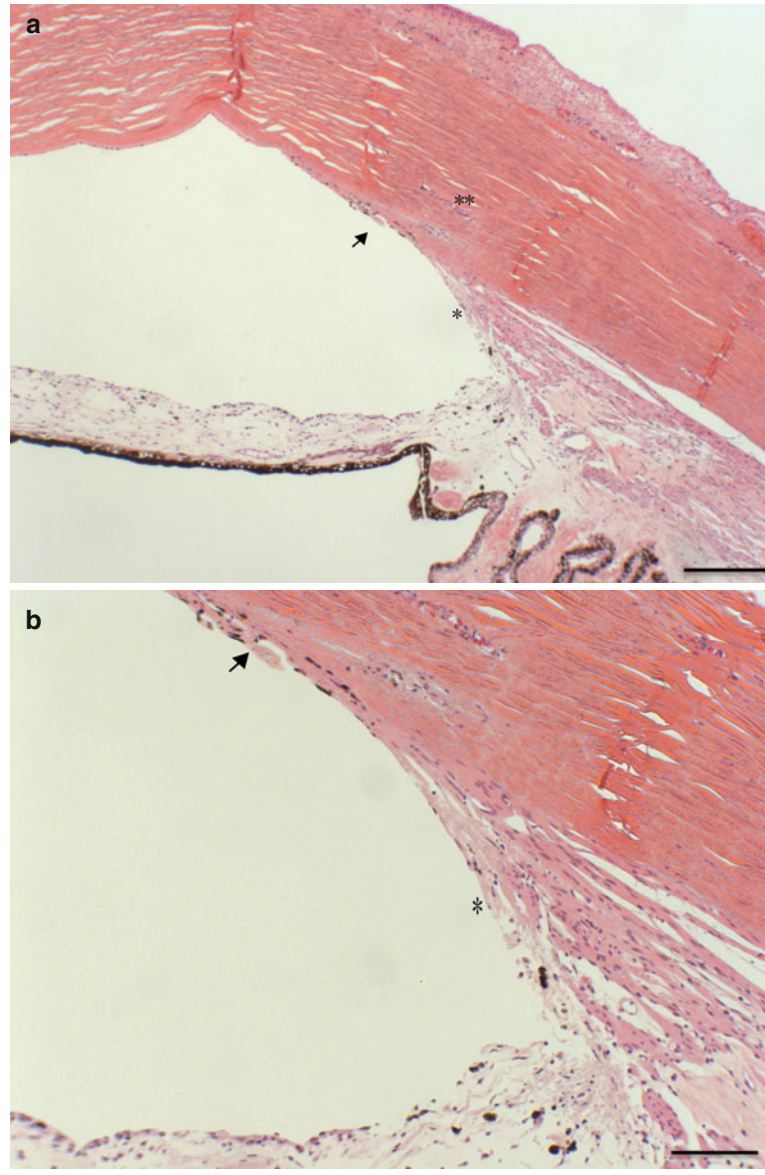

Fig. 6.37 (**a**) Histological aspect of angle recession glaucoma with fibrotic trabecular meshwork (*arrow*) and fibrotic membrane at the injured anterior part of the ciliary body (*). Obliterated Schlemm's canal (**) (HE, bar = 300 μm). (**b**) Histological aspect of angle recession glaucoma with fibrotic trabecular meshwork (*arrow*), fibrotic membrane at the injured anterior part of the ciliary body (*) HE, bar = 100 μm)

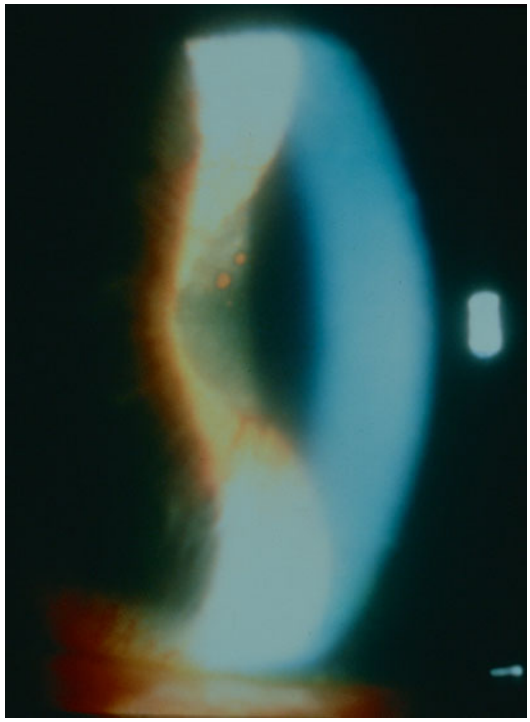

Fig. 6.38 Secondary pupillary block in an eye with normal length due to aqueous humour with increased viscosity due to inflammation and subsequent posterior synechiae

Fig. 6.39 Choroidal melanoma of the ciliary body causing partial angle closure (*arrow*). Mature cataract (*asterisk*)

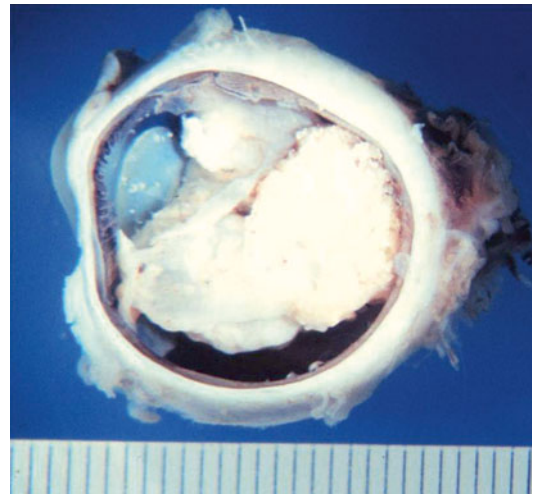

Fig. 6.40 Large retinoblastoma causing secondary angle-closure glaucoma (*arrows*). *Asterisk*: closed chamber angle

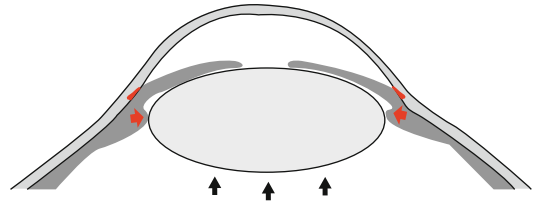

Fig. 6.41 Ciliolenticular block with adhesion between large lens and ciliary body, obstructing the anterior chamber angle (*red*) causing forward bulging of the whole iris-lens diaphragm in the late phase (Courtesy of Dr. Günther Schlunck, University Eye Hospital Freiburg)

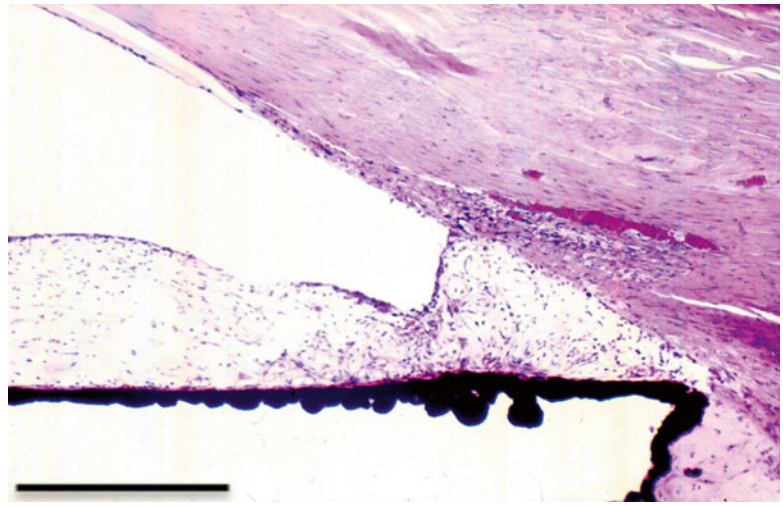

Fig. 6.42 Secondary angle-closure glaucoma with normal angle configuration but pretrabecular anterior synechiae impeding aqueous humour flow (haematoxylin-eosin, bar = 300 µm)

References

1. Moses RA. A graphic analysis of aqueous humor dynamics. Am J Ophthalmol. 1972;73(5):665–9.
2. Naumann GOH. Pathologie des Auges. 1. Aufl. Springer; Berlin Heidelberg. 1980.
3. Johnson EC, Jia L, Cepurna WO, Doser TA, Morrison JC. Global changes in optic nerve head gene expression after exposure to elevated intraocular pressure in a rat glaucoma model. Invest Ophthalmol Vis Sci. 2007;48(7):3161–77.
4. Pena JD, Varela HJ, Ricard CS, Hernandez MR. Enhanced tenascin expression associated with reactive astrocytes in human optic nerve heads with primary open angle glaucoma. Exp Eye Res. 1999;68(1):29–40.
5. Flocks M. The anatomy of the trabecular meshwork as seen in tangential section. AMA Arch Ophthalmol. 1956;56(5):708–18.
6. Murphy CG, Yun AJ, Newsome DA, Alvarado JA. Localization of extracellular proteins of the human trabecular meshwork by indirect immunofluorescence. Am J Ophthalmol. 1987;104(1):33–43.
7. Gong HY, Trinkaus-Randall V, Freddo TF. Ultrastructural immunocytochemical localization of elastin in normal human trabecular meshwork. Curr Eye Res. 1989;8(10):1071–82.
8. Fine BS, Yanoff M, Stone RA. A clinicopathologic study of four cases of primary open-angle glaucoma compared to normal eyes. Am J Ophthalmol. 1981;91(1):88–105.
9. Lee WR, Doyne L. The pathology of the outflow system in primary and secondary glaucoma. Eye (Lond). 1995;9(Pt 1):1–23.
10. Tripathi RC. Mechanism of the aqueous outflow across the trabecular wall of Schlemm's canal. Exp Eye Res. 1971;11(1):116–21.
11. Wirtschafter JD. Optic nerve axons and acquired alterations in the appearance of the optic disc. Trans Am Ophthalmol Soc. 1983;81:1034–91.
12. Quigley HA, Green WR. The histology of human glaucoma cupping and optic nerve damage: clinicopathologic correlation in 21 eyes. Ophthalmology. 1979;86(10):1803–30.
13. O'Rahilly R. The prenatal development of the human eye. Exp Eye Res. 1975;21(2):93–112.
14. Cook CS. Experimental models of anterior segment dysgenesis. Ophthalmic Paediatr Genet. 1989;10(1):33–46.
15. Tripathi BJ, Tripathi RC. Neural crest origin of human trabecular meshwork and its implications for the pathogenesis of glaucoma. Am J Ophthalmol. 1989;107(6):583–90.
16. Churchill A, Booth A. Genetics of aniridia and anterior segment dysgenesis. Br J Ophthalmol. 1996;80(7):669–73.
17. Kupfer C, Kaiser-Kupfer MI, Kuwabara T. Histopathology of abnormalities of the anterior chamber with glaucoma. Trans Am Ophthalmol Soc. 1986;84:71–84.
18. Gould DB, Smith RS, John SWM. Anterior segment development relevant to glaucoma. Int J Dev Biol. 2004;48(8–9):1015–29.
19. Idrees F, Vaideanu D, Fraser SG, Sowden JC, Khaw PT. A review of anterior segment dysgeneses. Surv Ophthalmol. 2006;51(3):213–31.
20. Reis LM, Semina EV. Genetics of anterior segment dysgenesis disorders. Curr Opin Ophthalmol. 2011;22(5):314–24.
21. Sowden JC. Molecular and developmental mechanisms of anterior segment dysgenesis. Eye (Lond). 2007;21(10):1310–8.
22. Ou Y, Caprioli J. Surgical management of pediatric glaucoma. Dev Ophthalmol. 2012;50:157–72.
23. Sarfarazi M, Stoilov I. Molecular genetics of primary congenital glaucoma. Eye (Lond). 2000;14(Pt 3B):422–8.

24. Barkan O. Pathogenesis of congenital glaucoma: gonioscopic and anatomic observation of the angle of the anterior chamber in the normal eye and in congenital glaucoma. Am J Ophthalmol. 1955;40(1):1–11.
25. Shields MB. A common pathway for developmental glaucomas. Trans Am Ophthalmol Soc. 1987;85:222–37.
26. Perry LP, Jakobiec FA, Zakka FR, Walton DS. Newborn primary congenital glaucoma: histopathologic features of the anterior chamber filtration angle. J AAPOS. 2012;16(6):565–8.
27. Burian HM, Braley AE, Allen L. External and gonioscopic visibility of the ring of Schwalbe and the trabecular zone; an interpretation of the posterior corneal embryotoxon and the so-called congenital hyaline membranes on the posterior corneal surface. Trans Am Ophthalmol Soc. 1955;1954(52):389–428.
28. Rennie CA, Chowdhury S, Khan J, Rajan F, Jordan K, Lamb RJ UA. The prevalence and associated features of posterior embryotoxon in the general ophthalmic clinic. Eye (Lond). 2005;19(4):396–9.
29. Sim KT, Karri B, Kaye SB. Posterior embryotoxon may not be a forme fruste of Axenfeld-Rieger's syndrome. J AAPOS. 2004;8(5):504–6.
30. Alward WL. Axenfeld-Rieger syndrome in the age of molecular genetics. Am J Ophthalmol. 2000;130(1):107–15.
31. Harissi-Dagher M, Colby K. Anterior segment dysgenesis: Peters anomaly and sclerocornea. Int Ophthalmol Clin. 2008;48(2):35–42.
32. Lee H, Khan R, O'Keefe M. Aniridia: current pathology and management. Acta Ophthalmol. 2008;86(7):708–15.
33. Margo CE. Congenital aniridia: a histopathologic study of the anterior segment in children. J Pediatr Ophthalmol Strabismus. 1983;20(5):192–8.
34. Leske MC, Connell AM, Schachat AP, Hyman L. The Barbados Eye Study. Prevalence of open angle glaucoma. Arch Ophthalmol. 1994;112(6):821–9.
35. Mitchell P, Smith W, Attebo K, Healey PR. Prevalence of open-angle glaucoma in Australia. The Blue Mountains Eye Study. Ophthalmology. 1996;103(10):1661–9.
36. Quigley HA, Broman AT. The number of people with glaucoma worldwide in 2010 and 2020. Br J Ophthalmol. 2006;90(3):262–7.
37. Allingham RR, Liu Y, Rhee DJ. The genetics of primary open-angle glaucoma: a review. Exp Eye Res. 2009;88(4):837–44.
38. Fan BJ, Wiggs JL. Glaucoma: genes, phenotypes, and new directions for therapy. J Clin Invest. 2010;120(9):3064–72.
39. Alvarado J, Murphy C, Polansky J, Juster R. Age-related changes in trabecular meshwork cellularity. Invest Ophthalmol Vis Sci. 1981;21(5):714–27.
40. Grierson I, Howes RC, Wang Q. Age-related changes in the canal of Schlemm. Exp Eye Res. 1984;39(4):505–12.
41. Alvarado J, Murphy C, Juster R. Trabecular meshwork cellularity in primary open-angle glaucoma and nonglaucomatous normals. Ophthalmology. 1984;91(6):564–79.
42. Rohen JW, Witmer R. Electron microscopic studies on the trabecular meshwork in glaucoma simplex. Albrecht Von Graefes Arch Klin Exp Ophthalmol. 1972;183(4):251–66.
43. Pary-Van Ginderdeuren P, Kaimbo Wa Kaimbo D, Goethals M, Missotten L. Differences in the trabecular meshwork between Belgian and Congolese patients with open-angle glaucoma. Bull Soc Belge Ophtalmol. 1997;267:183–90.
44. Rohen JW, Lütjen-Drecoll E, Flügel C, Meyer M, Grierson I. Ultrastructure of the trabecular meshwork in untreated cases of primary open-angle glaucoma (POAG). Exp Eye Res. 1993;56(6):683–92.
45. Tektas O-Y, Lütjen-Drecoll E. Structural changes of the trabecular meshwork in different kinds of glaucoma. Exp Eye Res. 2009;88(4):769–75.
46. Allingham RR, de Kater AW, Ethier CR. Schlemm's canal and primary open angle glaucoma: correlation between Schlemm's canal dimensions and outflow facility. Exp Eye Res. 1996;62(1):101–9.
47. Martin MJ, Sommer A, Gold EB, Diamond EL. Race and primary open-angle glaucoma. Am J Ophthalmol. 1985;99(4):383–7.
48. Wilson R, Richardson TM, Hertzmark E, Grant WM. Race as a risk factor for progressive glaucomatous damage. Ann Ophthalmol. 1985;17(10):653–9.
49. Leske MC, Wu S-Y, Hennis A, Honkanen R, Nemesure B. Risk factors for incident open-angle glaucoma: the Barbados Eye Studies. Ophthalmology. 2008;115(1):85–93.
50. Sihota R, Lakshmaiah NC, Walia KB, Sharma S, Pailoor J, Agarwal HC. The trabecular meshwork in acute and chronic angle closure glaucoma. Indian J Ophthalmol. 2001;49(4):255–9.
51. Hamanaka T, Kasahara K, Takemura T. Histopathology of the trabecular meshwork and Schlemm's canal in primary angle-closure glaucoma. Invest Ophthalmol Vis Sci. 2011;52(12):8849–61.
52. He M, Foster PJ, Johnson GJ, Khaw PT. Angle-closure glaucoma in East Asian and European people. Different diseases? Eye (Lond). 2006;20(1):3–12.
53. Sihota R, Goyal A, Kaur J, Gupta V, Nag TC. Scanning electron microscopy of the trabecular meshwork: understanding the pathogenesis of primary angle closure glaucoma. Indian J Ophthalmol. 2012;60(3):183–8.
54. Flammer J. Glaucoma: a guide for patients, an introduction for care-providers, a quick reference. 3., überarb. A. Hogrefe Verlag GmbH + Co., Bern; 2006.
55. Spencer WH. Ophthalmic pathology: an atlas and textbook. 4. Aufl. Saunders, Philadelphia; 1996.
56. Cashwell LF, Marks WP. Panretinal photocoagulation in the management of neovascular glaucoma. South Med J. 1988;81(11):1364–8.
57. Groh MJ, Seitz B, Schumacher S, Naumann GO. Detection of herpes simplex virus in aqueous humor in iridocorneal endothelial (ICE) syndrome. Cornea. 1999;18(3):359–60.

58. Alvarado JA, Underwood JL, Green WR, Wu S, Murphy CG, Hwang DG, et al. Detection of herpes simplex viral DNA in the iridocorneal endothelial syndrome. Arch Ophthalmol. 1994;112(12):1601–9.
59. Quigley HA, Forster RF. Histopathology of cornea and iris in Chandler's syndrome. Arch Ophthalmol. 1978;96(10):1878–82.
60. Eagle Jr RC, Font RL, Yanoff M, Fine BS. The iris naevus (Cogan-Reese) syndrome: light and electron microscopic observations. Br J Ophthalmol. 1980;64(6):446–52.
61. Levy SG, Kirkness CM, Moss J, Ficker L, McCartney AC. The histopathology of the iridocorneal-endothelial syndrome. Cornea. 1996;15(1):46–54.
62. Hirst LW, Bancroft J, Yamauchi K, Green WR. Immunohistochemical pathology of the corneal endothelium in iridocorneal endothelial syndrome. Invest Ophthalmol Vis Sci. 1995;36(5):820–7.
63. Zheng X, Shiraishi A, Okuma S, Mizoue S, Goto T, Kawasaki S, et al. n vivo confocal microscopic evidence of keratopathy in patients with pseudoexfoliation syndrome. Invest Ophthalmol Vis Sci. 2011;52(3):1755–61.
64. Schlötzer-Schrehardt U, Hammer CM, Krysta AW, Hofmann-Rummelt C, Pasutto F, Sasaki T, Kruse FE, Zenkel M. LOXL1 deficiency in the lamina cribrosa as candidate susceptibility factor for a pseudoexfoliation-specific risk of glaucoma. Ophthalmology. 2012;119(9):1832–43.
65. Schlötzer-Schrehardt U, Naumann GOH. Ocular and systemic pseudoexfoliation syndrome. Am J Ophthalmol. 2006;141(5):921–37.
66. Elhawy E, Kamthan G, Dong CQ, Danias J. Pseudoexfoliation syndrome, a systemic disorder with ocular manifestations. Hum Genomics. 2012;6:22.
67. Gottanka J, Kuhlmann A, Scholz M, Johnson DH, Lütjen-Drecoll E. Pathophysiologic changes in the optic nerves of eyes with primary open angle and pseudoexfoliation glaucoma. Invest Ophthalmol Vis Sci. 2005;46(11):4170–81.
68. Farrar SM, Shields MB. Current concepts in pigmentary glaucoma. Surv Ophthalmol. 1993;37(4):233–52.
69. Siddiqui Y, Ten Hulzen RD, Cameron JD, Hodge DO, Johnson DH. What is the risk of developing pigmentary glaucoma from pigment dispersion syndrome? Am J Ophthalmol. 2003;135(6):794–9.
70. Campbell DG. Pigmentary dispersion and glaucoma. A new theory. Arch Ophthalmol. 1979;97(9):1667–72.
71. Murphy CG, Johnson M, Alvarado JA. Juxtacanalicular tissue in pigmentary and primary open angle glaucoma. The hydrodynamic role of pigment and other constituents. Arch Ophthalmol. 1992;110(12):1779–85.
72. Gottanka J, Johnson DH, Grehn F, Lütjen-Drecoll E. Histologic findings in pigment dispersion syndrome and pigmentary glaucoma. J Glaucoma. 2006;15(2):142–51.
73. Kupfer C, Kuwabara T, Kaiser-Kupfer M. The histopathology of pigmentary dispersion syndrome with glaucoma. Am J Ophthalmol. 1975;80(5):857–62.
74. Mandelkorn RM, Hoffman ME, Olander KW, Zimmerman TJ, Harsha D. Inheritance and the pigmentary dispersion syndrome. Ophthalmic Paediatr Genet. 1985;6(1–2):325–31.
75. STANKOVIC I. A contribution to the knowledge of the heredity of pigment glaucoma. Klin Monbl Augenheilkd Augenarztl Fortbild. 1961;139:165–74.
76. Lascaratos G, Shah A, Garway-Heath DF. The genetics of pigment dispersion syndrome and pigmentary glaucoma. Surv Ophthalmol. 2013;58(2):164–75.
77. Regenbogen LS, Naveh-Floman N. Glaucoma in Fuchs' heterochromic cyclitis associated with congenital Horner's syndrome. Br J Ophthalmol. 1987;71(11):844–9.
78. Wilhelmus KR, Grierson I, Watson PG. Histopathologic and clinical associations of scleritis and glaucoma. Am J Ophthalmol. 1981;91(6):697–705.
79. Jones NP. Fuchs' heterochromic uveitis: an update. Surv Ophthalmol. 1993;37(4):253–72.
80. Campbell DG, Essigmann EM. Hemolytic ghost cell glaucoma. Further studies. Arch Ophthalmol. 1979;97(11):2141–6.
81. Ellant JP, Obstbaum SA. Lens-induced glaucoma. Doc Ophthalmol. 1992;81(3):317–38.
82. Epstein DL. Diagnosis and management of lens-induced glaucoma. Ophthalmology. 1982;89(3):227–30.
83. Barnhorst D, Meyers SM, Myers T. Lens-induced glaucoma 65 years after congenital cataract surgery. Am J Ophthalmol. 1994;118(6):807–8.
84. Kee C, Lee S. Lens particle glaucoma occurring 15 years after cataract surgery. Korean J Ophthalmol. 2001;15(2):137–9.
85. Lim MC, Doe EA, Vroman DT, Rosa Jr RH, Parrish 2nd RK. Late onset lens particle glaucoma as a consequence of spontaneous dislocation of an intraocular lens in pseudoexfoliation syndrome. Am J Ophthalmol. 2001;132(2):261–3.
86. Liu JC, Ball SF. Nevus of Ota with glaucoma: report of three cases. Ann Ophthalmol. 1991;23(8):286–9.
87. Armaly MF, Becker B. Intraocular pressure response to topical corticosteroids. Fed Proc. 1965;24(6):1274–8.
88. Becker B. Intraocular pressure response to topical corticosteroids. Invest Ophthalmol. 1965;4:198–205.
89. Cubey RB. Glaucoma following the application of corticosteroid to the skin of the eyelids. Br J Dermatol. 1976;95(2):207–8.
90. Zugerman C, Saunders D, Levit F. Glaucoma from topically applied steroids. Arch Dermatol. 1976;112(9):1326.
91. Urban Jr RC, Dreyer EB. Corticosteroid-induced glaucoma. Int Ophthalmol Clin. 1993;33(2):135–9.
92. Cibis G. 2008-2009 Basic and clinical science course, section 2: Fundamentals and principles of ophthalmology. Revised. American Academy of Ophthalmology; San Francisco, 2008.
93. Armaly MF. Effect of corticosteroids on intraocular pressure and fluid dynamics. I. The effect of dexamethasone in the normal eye. Arch Ophthalmol. 1963;70:482–91.

94. Armaly MF. Effect of corticosteroids on intraocular pressure and fluid dynamics. II. The effect of dexamethasone in the glaucomatous eye. Arch Ophthalmol. 1963;70:492–9.
95. BECKER B, MILLS DW. Corticosteroids and intraocular pressure. Arch Ophthalmol. 1963;70:500–7.
96. Carnahan MC, Goldstein DA. Ocular complications of topical, peri-ocular, and systemic corticosteroids. Curr Opin Ophthalmol. 2000;11(6):478–83.
97. Razeghinejad MR, Katz LJ. Steroid-induced iatrogenic glaucoma. Ophthalmic Res. 2012;47(2):66–80.
98. Tripathi RC, Parapuram SK, Tripathi BJ, Zhong Y, Chalam KV. Corticosteroids and glaucoma risk. Drugs Aging. 1999;15(6):439–50.
99. Lam DSC, Fan DSP, Ng JSK, Yu CBO, Wong CY, Cheung AYK. Ocular hypertensive and anti-inflammatory responses to different dosages of topical dexamethasone in children: a randomized trial. Clin Experiment Ophthalmol. 2005;33(3):252–8.
100. Tawara A, Tou N, Kubota T, Harada Y, Yokota K. Immunohistochemical evaluation of the extracellular matrix in trabecular meshwork in steroid-induced glaucoma. Graefes Arch Clin Exp Ophthalmol. 2008;246(7):1021–8.
101. Wordinger RJ, Clark AF. Effects of glucocorticoids on the trabecular meshwork: towards a better understanding of glaucoma. Prog Retin Eye Res. 1999;18(5):629–67.
102. Zhuo YH, He Y, Leung KW, Hou F, Li YQ, Chai F. Dexamethasone disrupts intercellular junction formation and cytoskeleton organization in human trabecular meshwork cells. Mol Vis. 2010;16:61–71.
103. Wolff SM, Zimmerman LE. Chronic secondary glaucoma. Associated with retrodisplacement of iris root and deepening of the anterior chamber angle secondary to contusion. Am J Ophthalmol. 1962;54:547–63.
104. Mooney D. Angle recession and secondary glaucoma. Br J Ophthalmol. 1973;57(8):608–12.

Optic Nerve

7

Thomas J. Cummings and Paul van der Valk

7.1 General Description

The optic nerves (cranial nerve II) are white matter tracts that join at the optic chiasm and which serve to connect the retina with the brain. Therefore, they are "central" nerves, not peripheral nerves. The optic nerves contain the axons from the retinal ganglion cells as they make their way to the brain. The axons pass through the pores of the lamina cribrosa and become myelinated, causing the nerve to double in diameter to approximately 3 mm at the outer surface of the sclera. The nerve head, within the globe, is completely unmyelinated, as are the intraocular segments of the retinal ganglion cell axons. After making a sharp turn and traversing the lamina cribrosa, the axons are organized in bundles that are separated from one another by vascular septa and "columns" of glial cells. The intraorbital segment of nerve is ensheathed by the arachnoid and dura; the subarachnoid space of the nerve is continuous with the intracranial subarachnoid space. The nerve is approximately 50 mm long, a little longer than the distance from the posterior end of the globe to the optic canal, hence the somewhat tortuous trajectory of the nerve within the orbit [1–3].

The histology of the normal optic nerve is readily recognizable in longitudinal section (Figs. 7.1 and 7.2) and in cross section (Figs. 7.3 and 7.4). The main components of the nerve are axons (Fig. 7.5) and glia, including oligodendrocytes (which produce myelin), astrocytes, and microglia (Fig. 7.6). The central artery and vein enter the nerve approximately 1 cm from the sclera and move towards the center of the nerve. The capillary blood supply is from the ophthalmic artery, either through the choroidal vessels or the subarachnoidal perineurial plexus [2, 3]. In cross section the compartmentalized appearance and protective meningeal coverings of the nerve are seen.

The optic nerve is subject to a wide range of physiological and mechanical pathologies. The normal clinical appearance of the optic nerve head (Fig. 7.7a) must be contrasted with the appearance of a swollen nerve head (Fig. 7.7b). Papilledema or swelling of the tissues of the optic nerve head may result from a variety of causes, including increased intracranial pressure, increased intraorbital pressure, systemic hypertension, and hypercapnia. Papilledema can often be diagnosed during ophthalmological examination, and a careful search for its etiology should ensue. Histological examination may disclose edema, hemorrhages, exudate, and axonal swelling. Prolonged swelling may result

T.J. Cummings, MD (✉)
Department of Pathology,
Duke University Medical Center,
3712, Durham, NC 27710, USA
e-mail: thomas.cummings@duke.edu

P. van der Valk, MD, PhD
Department of Pathology,
Vrije Universiteit Medical Center,
7507, 1007 MB Amsterdam, The Netherlands
e-mail: p.vandervalk@vumc.nl

S. Heegaard, H. Grossniklaus (eds.), *Eye Pathology: An Illustrated Guide*,
DOI 10.1007/978-3-662-43382-9_7,

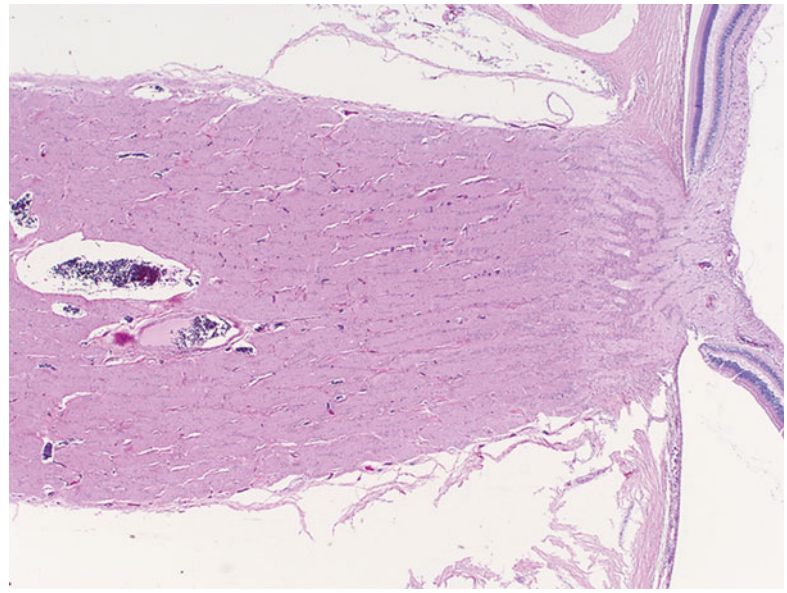

Fig. 7.1 Longitudinal section of optic nerve. The lamina cribrosa sieve-like partition is to the right of the image. The central retinal artery and vein are seen at the left of the image

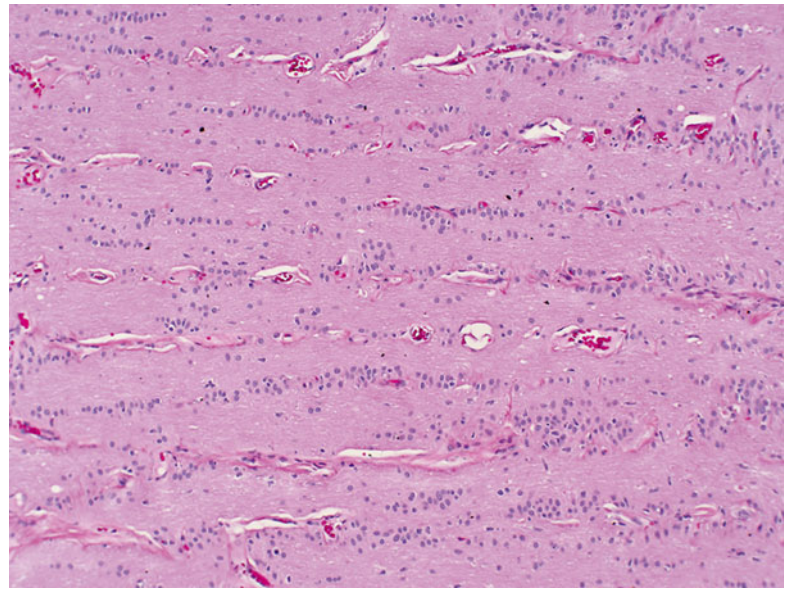

Fig. 7.2 Higher magnification of this figure shows the orderly columnar arrangement of optic nerve glia

in a secondary glial proliferation [1]. Optic nerve atrophy and cupping of the disk are well-recognized effects of increased ocular pressure (glaucoma) and the degenerative sequelae of retinal ganglion cell loss. The nerve is also affected by a range of metabolic, vascular, and nutritional anomalies, many of which will only be apparent if the nerve can be examined postmortem.

7.2 Embryology, Anatomy, and Development

The development of the eye is an incredibly complex sequence of events. Three primary bulges appear in the future brain region of the neural tube: the forebrain (prosencephalon), the midbrain (mesencephalon), and the hindbrain (rhombencephalon). A secondary bulge, the optic

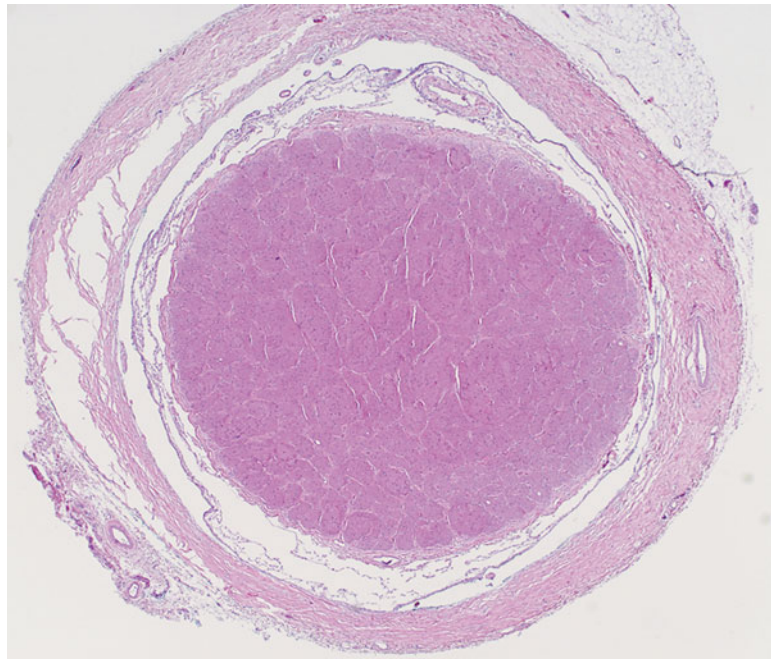

Fig. 7.3 Normal optic nerve in cross section surrounded by meninges

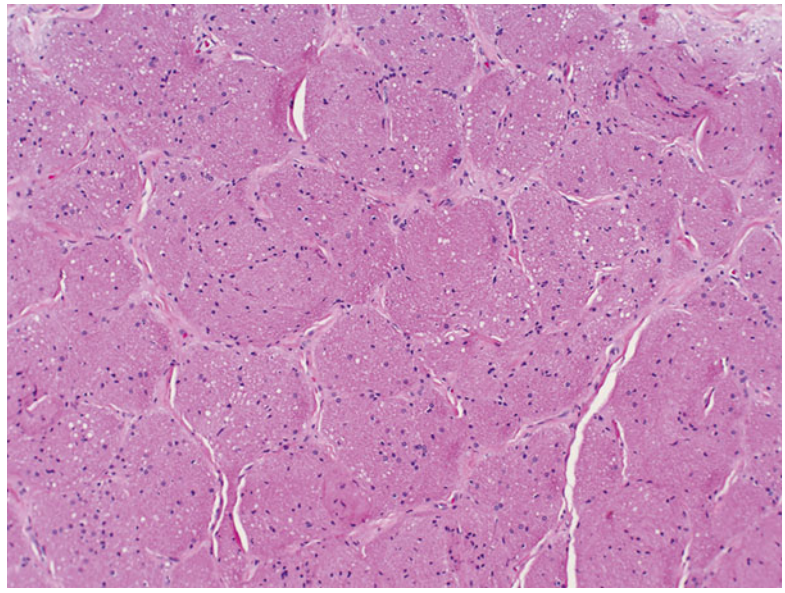

Fig. 7.4 Higher magnification of this figure shows the compartmentalized appearance of the nerve in cross section

vesicle, extends from each side of the forebrain and differentiates to form an optic cup, an optic stalk, and eventually an optic nerve and different components of the eye.

For the optic nerve, there are a few crucial processes, but since development is an orderly sequence, any disruptions, even in "distant" parts of the eye, may influence formation of apparently non-related parts or segments. The first important process is the formation of the optic cup itself and the thinning of the connection to the neural tube, i.e., the formation of the optic stalk, at

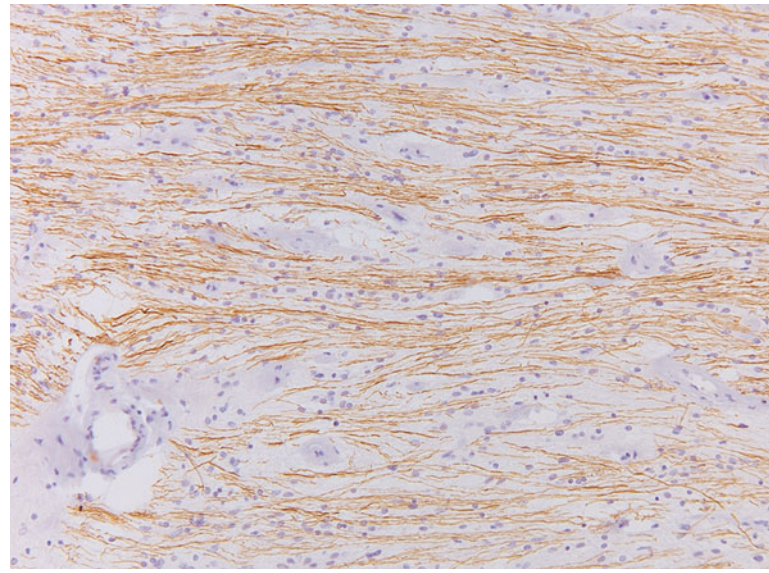

Fig. 7.5 Normal optic nerve. Neurofilament axonal immunohistochemical stain of a longitudinal section of the nerve

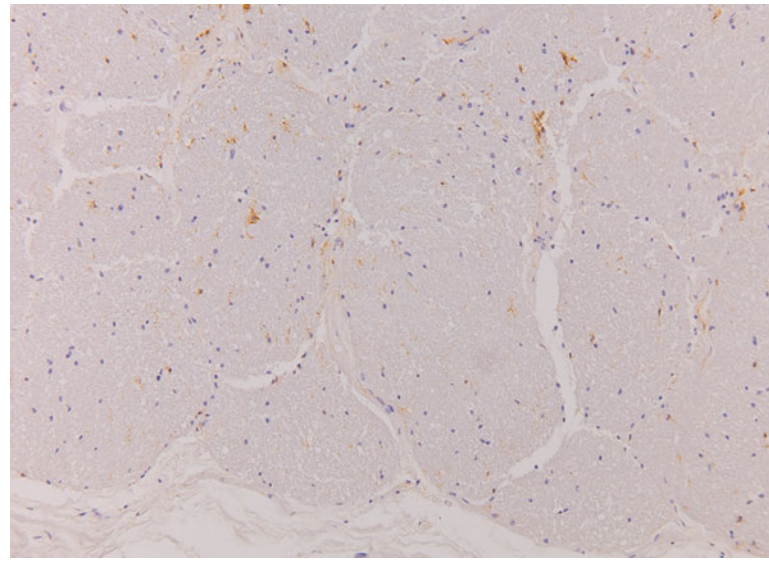

Fig. 7.6 Normal optic nerve. HLA-DR immunohistochemical stain demonstrating scattered microglial cells in the optic nerve. The relative light staining indicates the microglial cells are not activated

approximately 1 month of gestation. The neuroepithelium of the optic stalk will act as a supportive layer for the axons of the ganglion cells (developing in the retina) during the 2nd month, forming the optic nerve proper. The second important process is the formation of the embryonic or optic fissure; this will make place for the hyaloid vascular system that will vascularize the inner segments of the eye. The fissure will eventually envelop the hyaloid artery and will close. The closure of the fissure occurs in the 2nd month. From the 4th month the hyaloid vessel system starts to regress, but the more proximal parts will remain, forming the central retinal artery and vein, and later the vascularization of the retina. Myelination of the fibers of the optic nerve will start in the third trimester and will be completed only after birth.

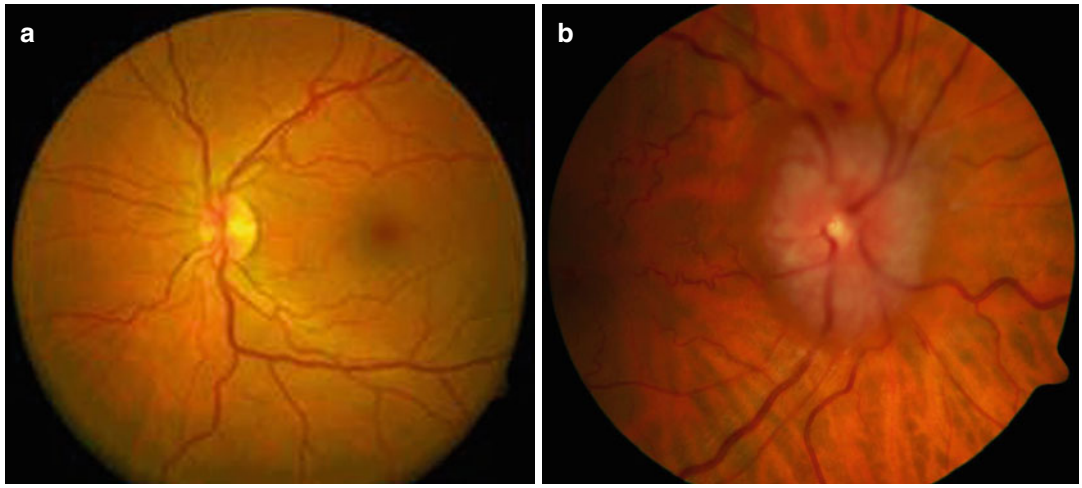

Fig. 7.7 (**a**) Clinical image of normal fundus. (**b**) Papilledema: clinical image of the fundus showing marked swelling of the optic nerve head

7.3 Congenital Abnormalities

Congenital or developmental disorders which affect the optic nerve are more likely to be recognized in postmortem examinations than in surgical specimens. Optic nerve aplasia and optic nerve hypoplasia likely are part of a spectrum of aberrant development and ocular embryogenesis. True optic nerve aplasia occurs when the optic nerve fails to develop, either because the retinal ganglion cells do not develop or they fail to form nerve fibers. In optic nerve hypoplasia, the nerve has fewer nerve fibers than normal, and there are a diminished number of retinal ganglion cells. Optic nerve aplasia and hypoplasia may either occur unilaterally or bilaterally. Some other developmental anomalies of the optic nerve include megalopapilla, tilted disks, optic nerve head pits, Aicardi syndrome, peripapillary staphyloma, myelinated nerve fibers, optic nerve drusen, and optic disk pigmentation [1]. In the morning glory syndrome, a funnel-shaped optic nerve disk is surrounded by chorioretinal pigmentation, and centrally the disk appears to contain Bergmeister's papilla representing persistence of the hyaloid system.

Colobomas of the optic disk occur when there is incomplete closure of the posterior portion of the fetal fissure. Colobomas can affect all parts of the globe, including the optic nerve, and they may be limited to the disk or may be associated with colobomas of the choroid, ciliary body, iris, retina, or sclera. A known association of coloboma is a microphthalmic eye with choristomatous malformation (microphthalmos with cyst).

Mitochondrial disease also can affect the optic nerve, the best example being Leber's hereditary optic atrophy [4]. The histology is characterized by loss of axons and myelin, sometimes with a variable degree of inflammation, with macrophages clearing myelin debris, and some T lymphocytes. In this, the pathology can show similarities with that of multiple sclerosis [5].

7.4 Inflammation and Ischemia

7.4.1 Optic Neuritis

Optic neuritis is an inflammation of the optic nerve that has a variety of causes, including infectious, ischemic, and (autoimmune) demyelinating. Most of these conditions represent

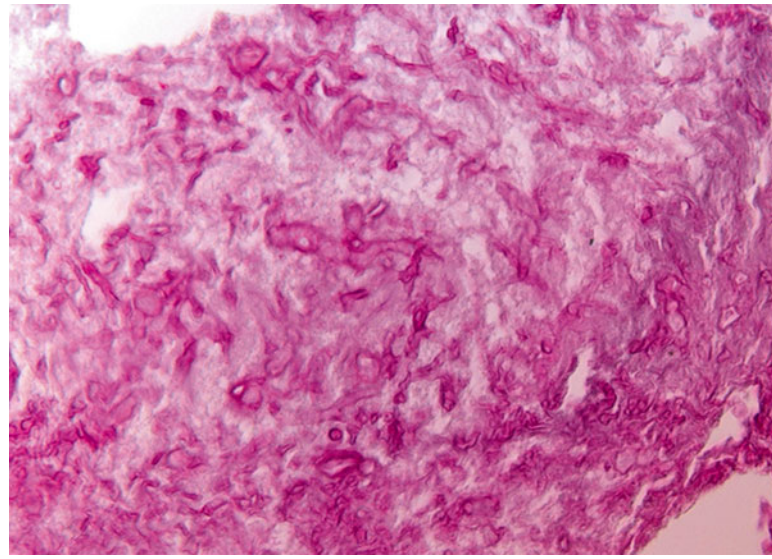

Fig. 7.8 Mucormycosis/zygomycosis. Periodic acid-Schiff (PAS)-stained orbital biopsy section in a patient with mucormycosis (the patient was diabetic). A large portion of the material was necrotic, due to vascular occlusion by the fungus. The characteristic broad and irregular hyphae can be seen, branching at right angles

secondary involvement of the optic nerve. Clinically, almost invariably, inflammation of the nerve causes severe visual impairment.

7.4.1.1 Infection

Almost all infections of the optic nerve are secondary to infections elsewhere, reflecting the well-protected position of the nerve. However, intraocular infections, such as corneal ulcerations, endophthalmitis, and chorioretinitis, can spread to involve the nerve. Likewise, infections in the orbit themselves not infrequently originating from the sinonasal compartment (zygomycosis) [6] or from the cranial vault (meningitis) can involve the optic nerve by direct spread. More rarely, more distant infections can result in secondary optic nerve inflammation, e.g., bacterial endocarditis, tuberculous infections, syphilis, and others. All of these have become rarities, especially in the developed countries. However, in patients with compromised immune systems, even in the developed countries, rhino-cerebro-orbital infections are seen with some frequency, and it is necessary to realize that immune dysfunctions can be obvious (transplantation, AIDS [acquired immune deficiency syndrome] patients, and chemotherapy treatment) but also can be less so obvious (diabetes mellitus) [7, 8] (Fig. 7.8).

Symptoms in individuals with inflammatory or infectious pathologies are variable degrees of visual impairment, and, of course, also the signs and symptoms of the underlying condition.

The pathology is highly inflammatory, with infiltration with many inflammatory cells, with the organism responsible determining the nature of the infiltrate. In some cases, it will be possible to demonstrate the offending organism with appropriate histochemical or immunohistochemical stains or molecular techniques (polymerase chain reaction). Fungal infections can show vaso-invasive properties that cause infarction and necrosis, contributing to optic nerve damage [9, 10]. This is the prime reason that in such cases surgical treatment is mandatory, as fungicidal antibiotics alone will not cure these patients.

7.4.1.2 Inflammation Secondary to Vascular Disease and Ischemia

The optic nerve can also be affected by ischemic changes secondary to vascular disorders including occlusion of the internal carotid artery, occlusion of the central retinal artery and vein, occlusion of the ophthalmic artery, carotid-cavernous sinus fistula, and vasculitis.

Vasculitis can be a local or systemic process, and this varied group of disorders can in princi-

ple affect any part of the body. Giant cell arteritis (also referred to as temporal arteritis) deserves mention as it not infrequently can lead to visual disturbances. It is a poorly understood condition in which there is chronic, often (partly) granulomatous mural inflammation of the somewhat larger arteries. The giant cells seem to focus on the internal elastic lamina, but they are not always found when an affected artery is biopsied (almost always the temporal artery) [11, 12] (Fig. 7.9). In such instances, the inflammation is usually composed of lymphocytes and plasma cells, and the designation giant cell arteritis is somewhat of a misnomer. When the inflammatory infiltrate consists of eosinophils, the possibility of Churg-Strauss syndrome should be considered, which may rarely involve the temporal artery. The pathology of the vasculitides, including the temporal artery, is known to be patchy and sometimes referred to as "skip lesions." It is therefore recommended to submit a segment of artery at least two centimeters in length. The vessel should be placed on end, serially sectioned, submitted entirely, and multiple step sections

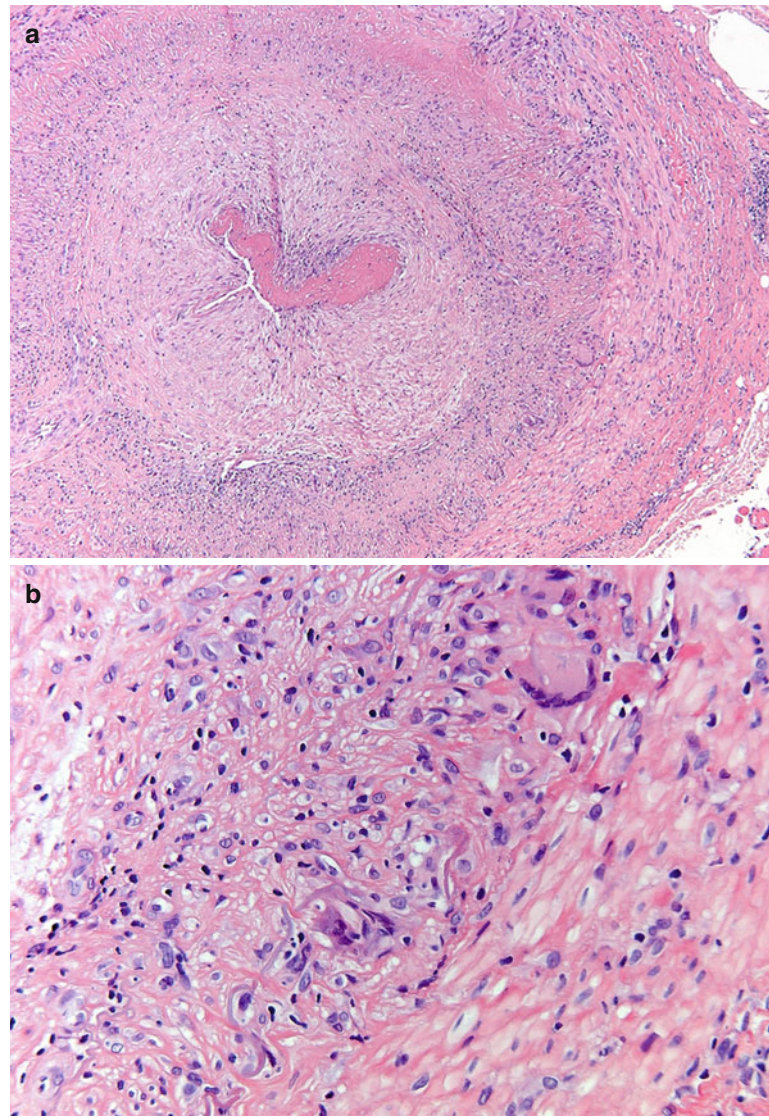

Fig. 7.9 Giant cell arteritis. (**a**) Temporal artery specimen showing transmural inflammation of the vessel wall (H&E). (**b**) A few multinucleated giant cells are identified and are centered on the internal elastic lamina (H&E). (**c**) Elastic stain showing fragmentation of the internal elastic lamina

Fig. 7.9 (continued)

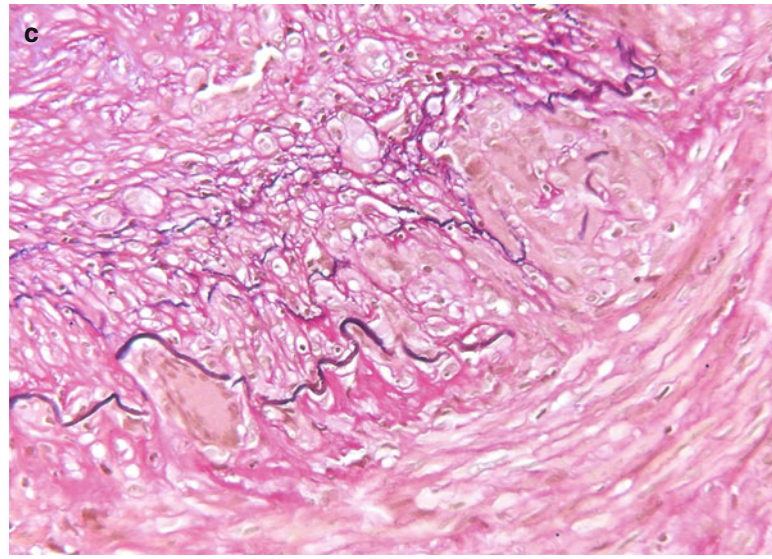

submitted through the paraffin block; this will give the best chance to see a focal area of inflammation. Sometimes the inflammatory component might be quenched by preoperative steroid therapy, and there will scarring of the vessel wall consistent with a "healing" arteritis. A Masson trichrome histochemical stain can be useful to highlight the scarring.

Ischemia is the hallmark of two, probably related, conditions, whose pathophysiology is unclear: non-arteritic anterior ischemic optic neuropathy and neuroretinitis. They both target the anterior portion of the nerve and cause abrupt loss of visual acuity and visual field defects. The former is seen in a somewhat older age group. The histology is relatively noninflammatory, with edema [13].

7.4.1.3 Inflammation Secondary to Demyelinating and/or Autoimmune Disease

The primary category here is retrobulbar or optic neuritis in multiple sclerosis (MS) [14]. Clinically, this is characterized by a rapidly progressive loss of vision, especially central vision, disturbances in color vision, and sometimes pain [15]. In a few weeks vision recovers. The widely held concept that MS is an autoimmune disease in which myelin is attacked by the immune system is increasingly challenged; possibly the demyelination in MS is secondary [to axonal damage, for instance] and the inflammation in its turn is secondary to the demyelination. Whatever the sequence of events is, lesions in MS show influx of macrophages and a varying number of lymphocytes that are predominantly found in the perivascular spaces (i.e., outside the central nervous system tissue proper). The macrophages phagocytose myelin debris, turning into foam cells and clearing the way for remyelination. As the myelin in the center of a lesion is cleared, the macrophages also disappear, first leaving a rim of foamy macrophages around a hypocellular center, and eventually they disappear altogether, leaving a burnt-out, demyelinated, and hypocellular plaque [16, 17] (Fig. 7.10a–c). Remyelination ensues, but subsequent new attacks of demyelination exhaust the brain tissue's regenerative capacity and eventually leave completely the above-described demyelinated, noninflammatory lesions or plaques. Most optic nerves from MS patients investigated involve postmortem material and will show these burnt-out, scar-like lesions. In rare instances a lesion will be found in which foamy macrophages can be found, with a little lymphocytic (perivascular) infiltrate. The lymphocytes are predominantly T lymphocytes. Invariably, there is astrogliosis, with hypertrophic astrocytes (i.e., astrocytes with abundant cytoplasm and cellular protrusions).

The number of axons is variable; sometimes damage can be demonstrated by loss of axons and by axonal swellings, indicative of damage. In other cases changes are hardly noticeable (Fig. 7.10d).

Neuromyelitis optica (NMO) or Devic's disease was once considered a potential variant of MS. However, NMO is now known to be caused by an autoimmune reaction to aquaporin 4, a water channel protein on astrocytes [18]. It is, therefore, a true autoimmune disease. Clinically, there is rapid loss of vision to complete blindness and paraplegia, caused by a destructive process in the spinal cord. The brain is typically not involved, although it may be involved in some cases. The characteristic abnormalities in the optic nerve are demyelination and the disappearance of astrocytes from the tissue. In the acute phase there are many inflammatory cells, including lymphocytes and foamy macrophages, but often also neutrophils.

A variety of drugs, metabolic diseases, and radiation therapy can also cause secondary inflammation of the optic nerve.

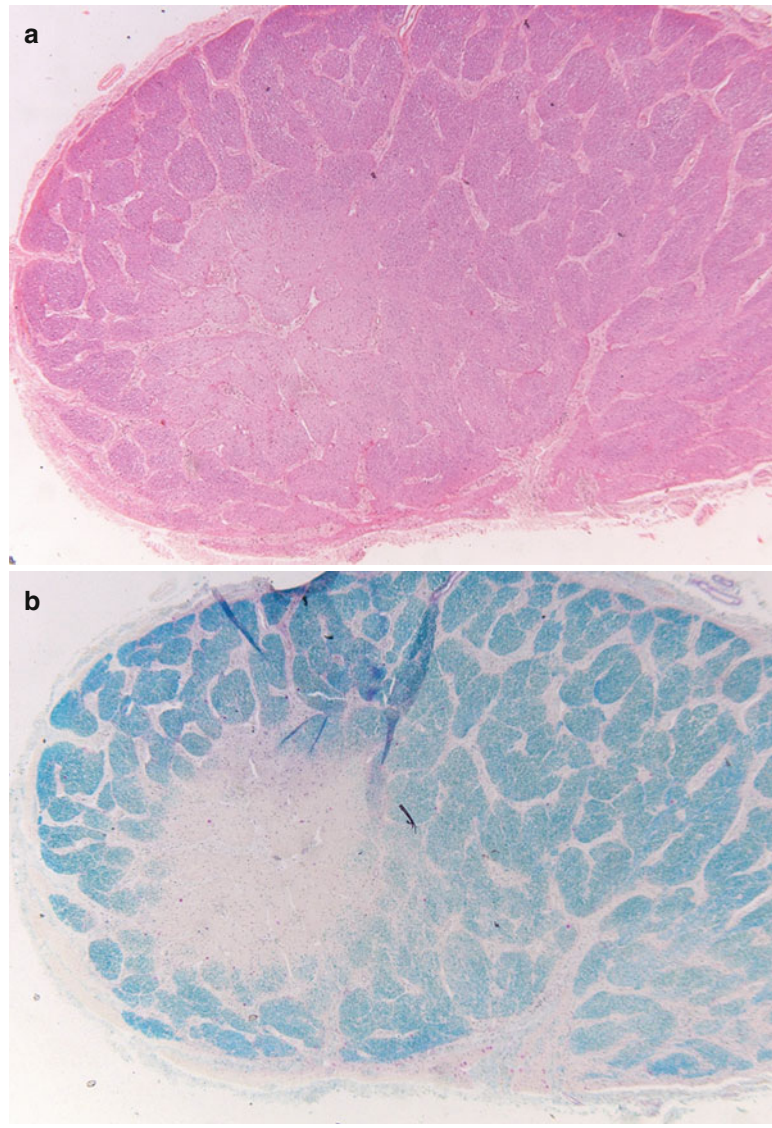

Fig. 7.10 Multiple sclerosis. (**a**) Optic nerve with a paracentral zone of pallor (H&E). (**b**) Luxol fast blue stain shows reduced myelin staining consistent with myelin loss in the nerve. (**c**) HLA-DR staining. The center of the lesion is less heavily infiltrated with microglial cells, whereas the rim shows increased numbers of activated microglia. (**d**) Neurofilament stain shows no clear difference areas in the number of axons between the demyelinated area and the myelinated area

Fig. 7.10 (continued)

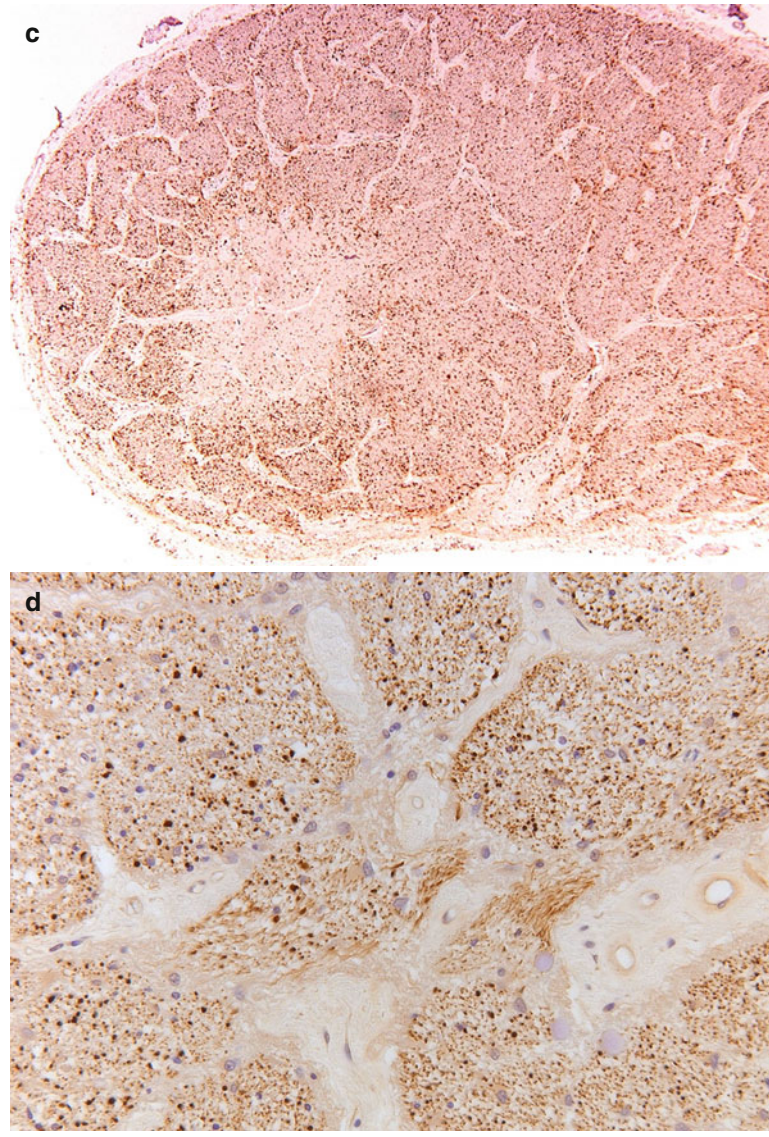

7.5 Injuries

External force or trauma to the optic nerve may result in mechanical injury including stretching, tearing, torsional stress, avulsion at the optic disk, avulsion at the optic canal, and chiasm. Penetrating injuries from foreign bodies or iatrogenic injections have been reported. Compression of the nerve may occur secondary to hemorrhage, inflammation, tumors such as meningiomas, and thickening of the extraocular muscles in cases of thyroid ophthalmopathy [1].

7.6 Degenerations

Degeneration of the optic nerve typically refers to optic atrophy, a clinical term describing optic pallor, avascularity, and cupping of the optic disk. Cavernous degeneration is a form of optic atrophy characterized by the formation of hyaluronic acid-filled cavernous spaces in the retrolaminar/anterior segment of the nerve. Hyaluronic acid is an acid mucopolysaccharide that is sensitive to hyaluronidase and is believed to be derived from the vitreous.

Schnabel's cavernous optic atrophy refers to the association of cavernous degeneration with glaucoma [1]. Alcian blue and colloidal iron stains can be useful in highlighting the mucopolysaccharide accumulations.

7.7 Optic Nerve Tumors

7.7.1 Introduction

Tumors of the optic nerve, optic chiasm, and optic nerve sheath comprise a narrow yet fascinating spectrum of lesions familiar to the ophthalmic pathologist and neuropathologist. These include optic nerve gliomas; meningiomas of the optic nerve sheath; melanocytomas and medulloepitheliomas of the optic nerve head; secondary tumors including metastases, retinoblastoma with nerve invasion, and retinoinvasive uveal melanoma; hemangiopericytoma and hemangioblastoma; and optic nerve choristoma. Finally, a few other rare reported tumors involving the nerve and its sheath will be mentioned.

A review of the early history of optic nerve gliomas can be found in the textbook of the late Sir W. Stewart Duke-Elder, with references about the earliest case reports dating back to the early nineteenth century [19]. The occurrence of an optic nerve glioma with von Recklinghausen neurofibromatosis was first noted by von Michel in 1873, and a significant association between these two entities was documented by Davis in 1940 [20]. In 1912, Hudson reviewed 182 optic nerve tumors, distinguished optic nerve gliomas from optic sheath meningiomas, and divided them into three classes: gliomatous (within the nerve), endotheliomatous, and fibromatous (associated with the nerve sheath) [21]. In 1922, Verhoeff noted that some tumors of the optic nerve were gliomas similar to those of the brain and had no relation to malignant retinal "gliomas" (retinoblastomas) [22]. Shortly thereafter, Martin and Cushing described seven gliomas involving the intracranial portion of the optic nerve and chiasm [23].

7.7.2 Optic Nerve Gliomas

Definition

Gliomas of the optic nerve are tumors derived from glial (astrocytic) cells within the optic nerve and chiasm. Optic nerve gliomas are traditionally thought of as pilocytic astrocytomas. However, low-grade (pilocytic astrocytoma, diffuse astrocytoma) and high-grade (glioblastoma) astrocytomas may involve the nerve, and therefore, an attempt to best grade and classify these tumors should be made. Correlation with clinical features, neuroimaging, and intraoperative findings is recommended in these cases.

Epidemiology

Optic nerve gliomas represent approximately 4 % of intracranial gliomas and 66 % of primary optic nerve tumors [24–27]. Approximately 90 % are diagnosed within the first two decades of life. The median age is 7 years and ranges from birth to the eighth decade. The female-to-male ratio is approximately 3:2, and both genders appear to be equally affected when the neoplasm involves the optic chiasm.

Etiology

Optic nerve gliomas derive from glial cells within the optic nerve. While the term "glioma" comprises astrocytic, oligodendroglial, and ependymal neoplasms, ependymal tumors have not been reported in the optic nerve, and only rare putative cases of oligodendroglioma are in the literature. Glioneuronal tumors (gangliglioma) are exceptionally rare in the optic nerve.

Clinical Features

Individuals with optic nerve gliomas may present clinically with a wide spectrum of ophthalmic abnormalities including visual impairment, optic atrophy, and proptosis [28–31]. Malignant gliomas of the anterior visual pathway are a clinical entity distinct from benign gliomas of childhood and they typically present with unilateral or bilateral visual loss and subsequent blindness [32]. The optic disk may initially appear normal but eventually evolves into papilledema or optic

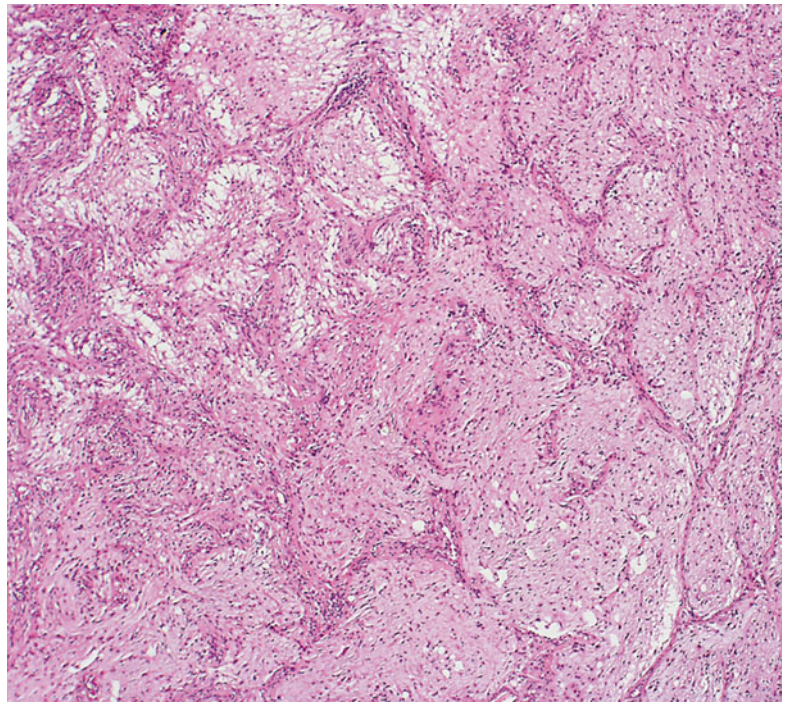

Fig. 7.11 Pilocytic astrocytoma of the optic nerve showing expansion of the septa (From Cummings [171], Figure 8.3, Page 158. With kind permission of Springer Science + Business Media)

atrophy. These aggressive tumors can spread via the optic radiations, leptomeninges, or cerebrospinal fluid both intracranially and to the spinal neuraxis [33, 34]. Rare glioblastomas of the optic nerve have been reported in childhood, either arising de novo [35], from malignant transformation of a pilocytic astrocytoma [36], or secondary to radiation therapy [37, 38].

Macroscopy

Optic nerve pilocytic astrocytomas often exhibit a smooth, fusiform, intradural enlargement of the nerve and acquire an hourglass shape when they spread through the optic foramen. They are white to tan in color and often contain abundant mucous imparting a soft gelatinous consistency. Small cystic spaces and foci of hemorrhage are sometimes seen [39, 40]. Extensive hemorrhage within a cyst resulting in rapid proptosis is rare [41]. Two architectural forms can be seen at the gross and microscopic level. One is a diffuse expansion of the optic nerve without extensive subarachnoid spread, and the other has a prominent infiltration of the subarachnoid space causing a rim of tumor around a mildly involved nerve [26, 42, 43]. The ability to invade the subarachnoid space and exhibit leptomeningeal dissemination and metastasis confirms that optic nerve pilocytic astrocytomas are true neoplasms rather than hamartomas [26, 42, 44].

Primary gliomas of the optic nerve head may also involve the adjacent retina [45]. Aside from gliomas that arise in the optic nerve, others may infiltrate the nerve after originating in the optic chiasm, floor of the third ventricle, thalamus, or hypothalamus. Sometimes it may be difficult, if not impossible, to determine the exact site of tumor origin among these sites radiographically, intraoperatively, or at postmortem examination [45, 46].

Histopathology

Pilocytic astrocytomas may expand the septa of the optic nerve (Fig. 7.11) or exhibit a biphasic growth pattern. Malignant astrocytomas also expand the septa and must be considered in the differential diagnosis (Fig. 7.12). Squash preparations will often highlight the delicate hairlike (pilo [L.] *hair*) processes and granular bodies or protein droplets (Fig. 7.13). Rosenthal fibers are

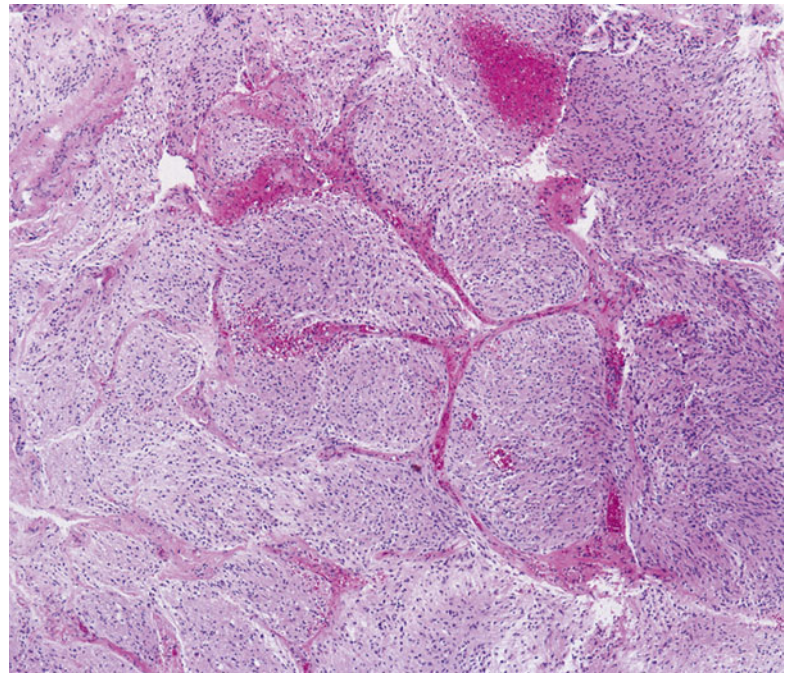

Fig. 7.12 Low-magnification view showing expansion of the optic nerve septa by glioblastoma (From Cummings [171], Figure 8.12, Page 163. With kind permission of Springer Science + Business Media)

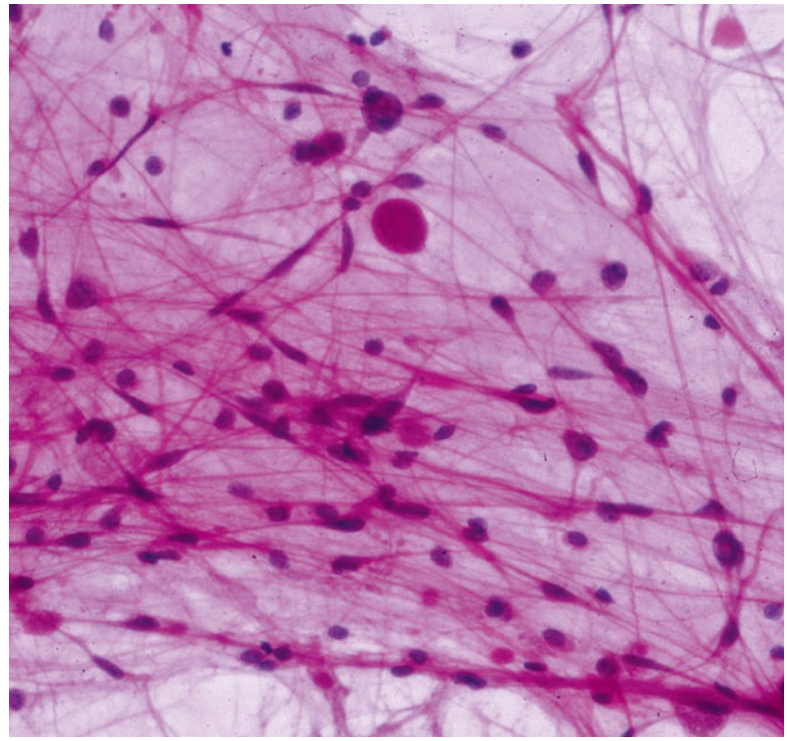

Fig. 7.13 Cytology squash preparation of an optic nerve pilocytic astrocytoma showing bipolar delicate hairlike processes and a round protein droplet. Hematoxylin and eosin staining is most useful in cytology preparations of brain tumors (From Cummings [171], Figure 8.4, Page 158. With kind permission of Springer Science + Business Media)

frequently seen in the compact areas (Fig. 7.14) and are diagnostically useful when present, although sometimes they are few in number (Fig. 7.15). Rosenthal fibers are a characteristic degenerative change found in pilocytic astrocytomas of all locations. They are not exclusively

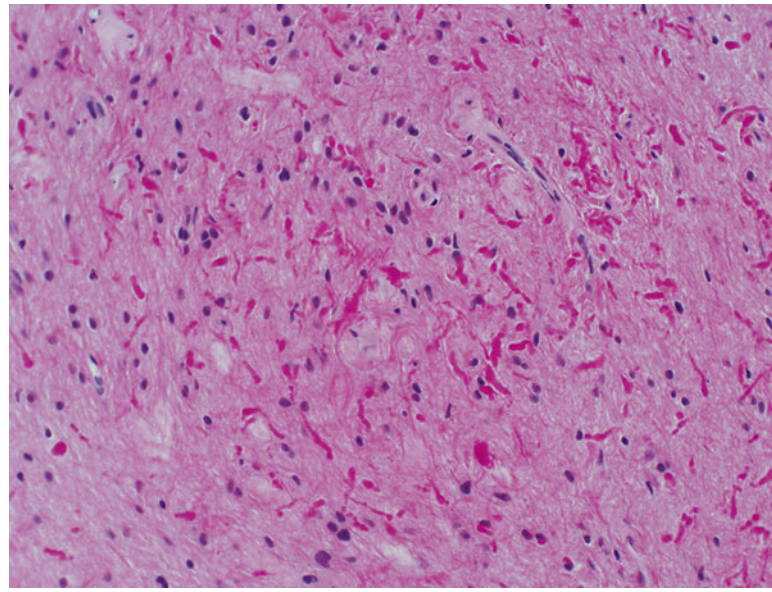

Fig. 7.14 Pilocytic astrocytoma of the optic nerve with numerous Rosenthal fibers. A case like this might be challenging to distinguish from reactive piloid gliosis (From Cummings [171], Figure 8.6, Page 159. With kind permission of Springer Science + Business Media)

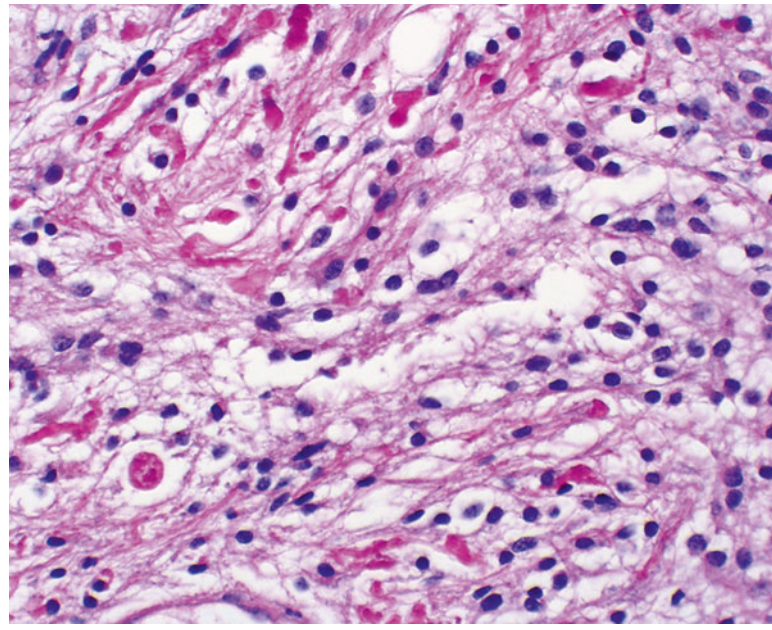

Fig. 7.15 Pilocytic astrocytoma of the optic nerve showing bright pink waxy Rosenthal fibers. A round eosinophilic granular body is seen towards the bottom left (From Cummings [171], Figure 8.5, Page 159. With kind permission of Springer Science + Business Media)

associated with pilocytic astrocytomas and may occasionally be found in other glial tumors including ganglioglioma and pleomorphic xanthoastrocytoma. They are also commonly found in association with chronic reactive gliosis, for example, in the regions adjacent to craniopharyngiomas, capillary hemangioblastomas, and syringomyelia cavities, within pineal cysts, and, in Alexander disease, a neurodegenerative disease of childhood characterized by absent myelination and numerous and often perivascular Rosenthal fibers. Rosenthal fibers are opaque, homogeneous, strongly eosinophilic, and corkscrew or beaded masses, and the vertebrate lens protein αβ-crystallin is a major component of them. In 1898, Rosenthal reviewed an

intramedullary spinal cord tumor associated with a gliotic syringomyelia and described the fibers which would eventually become eponymously linked to him [47, 48].

Most optic nerve gliomas are pilocytic astrocytomas that resemble equivalent tumors in other sites of the central nervous system, but these tumors can be a diagnostic challenge for the surgical pathologist because of histological heterogeneity among and within tumors. Verhoeff described three histological patterns of optic nerve pilocytic astrocytomas including the coarsely reticulated, coarsely fibrillated, and finely reticulated types [49]. These patterns are recognized as variants of pilocytic astrocytomas, and although transition types and combinations of patterns can be found in any given tumor, usually one pattern predominates. The coarsely reticulated pattern is characterized by the classic biphasic pattern of coarse bipolar astrocytic cells either tightly compacted around blood vessels or loosely woven around microcystic spaces containing abundant mucin. Tumors with this histological pattern are commonly associated with Rosenthal fibers, eosinophilic granular bodies, and protein droplets. Blood vessels vary in number and may be hyalinized. The coarsely fibrillar pattern (also known as the spindle-cell type), consists of coarse neuroglial fibrils and spindle neuroglia cells generally arranged in fairly definite bundles. This pattern appears to describe the so-called adult variant of pilocytic astrocytoma as described by Rubinstein [50]. The finely reticulated pattern resembles an expansion of the indigenous neuroglia of the optic nerve, in which small round or ovoid nuclei are embedded within a delicate reticulated syncytium of neuroglial fibers. This pattern can be confused histologically with a well-differentiated infiltrative fibrillary astrocytoma (WHO grade II).

Immunohistochemical staining for glial fibrillary acidic protein [GFAP] highlights the tumor cells and their processes in optic nerve gliomas confirming a glial origin. The Ki-67 (Mib-1) proliferation-related labeling index of pilocytic astrocytomas of the optic nerve and other sites of the central nervous system is often low, less than 1 % [51, 52]. Some reports of optic nerve pilocytic astrocytomas, however, have documented elevated Mib-1 indices [52–57], which appears to agree with the natural history of many of these neoplasms that increase in size and then stabilize, especially in individuals younger than 20 years of age.

Differential Diagnosis

Potential pitfalls in pilocytic astrocytoma include piloid gliosis which can mimic and be difficult to distinguish from pilocytic astrocytoma. Optic nerve gliosis may include arachnoid gliomatosis [42] and diffuse hyperplastic gliosis and may be seen in patients with and without neurofibromatosis type 1 (NF1) [27, 58]. Diffuse leptomeningeal glioma may rarely involve the optic nerve sheath [59]. Optic nerve gliomas can be associated with meningothelial hyperplasia, and the pathologist must be aware of a superficial biopsy of the meninges to avoid making an incorrect diagnosis of meningioma [60]. On a tiny biopsy, the histological distinction of pilocytic astrocytoma from a diffuse or fibrillary (WHO grade II) astrocytoma might not be possible. Recent molecular advances have shown optic nerve gliomas with pilocytic features to harbor *KIAA1549*:*BRAF* fusions typical of pilocytic astrocytomas in other locations, resulting in mitogen-activated protein kinase (MAPK) pathway activation and signaling. In contrast to diffuse or infiltrating astrocytomas, IDH1 and IDH2 mutations are absent in pilocytic astrocytomas [61].

Some pilocytic astrocytomas exhibit anaplastic features including an increased number of mitoses, vascular proliferation, and necrosis with pseudopalisading [62–65]. Beware of misdiagnosing malignant glioma (glioblastoma WHO grade IV) in these cases. Glioblastomas are malignant astrocytomas characterized histologically by cytological pleomorphism, mitoses, microvascular proliferation (Fig. 7.16), and necrosis with or without pseudopalisading (Fig. 7.17). Attention to the clinical setting and radiographic appearance is recommended in these case.

Pilomyxoid astrocytoma (WHO grade II) is closely related to pilocytic astrocytoma, but these tumors are more aggressive and usually involve

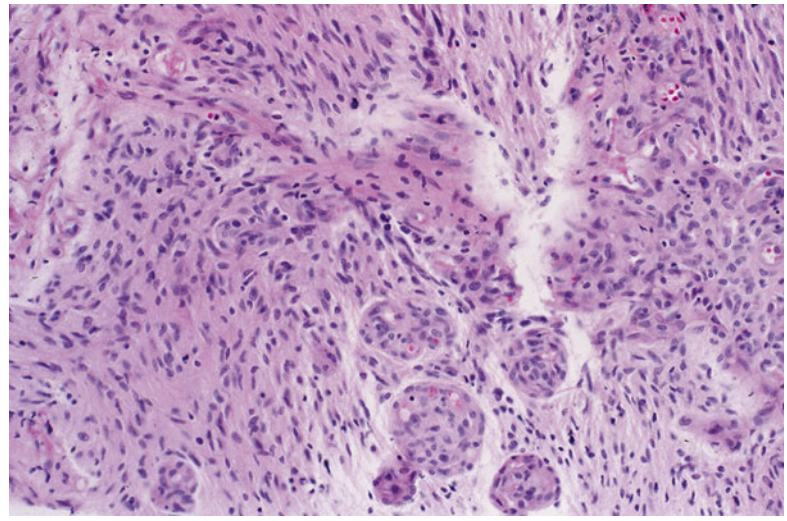

Fig. 7.16 Optic nerve glioblastoma showing microvascular proliferation (From Cummings [171], Figure 8.13, Page 164. With kind permission of Springer Science + Business Media)

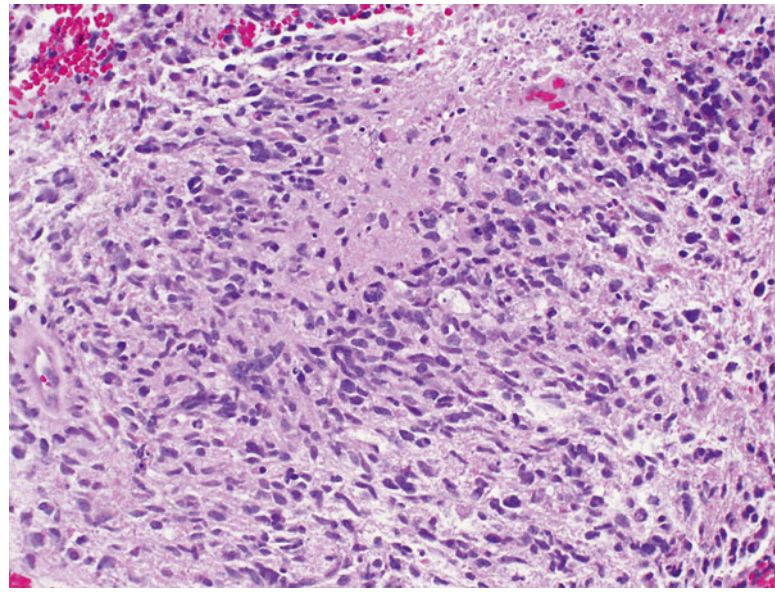

Fig. 7.17 Optic nerve glioblastoma showing pseudopalisading necrosis (From Cummings [171], Figure 8.14, Page 164. With kind permission of Springer Science + Business Media)

the hypothalamic/chiasmal region in young children. Rosenthal fibers and eosinophilic granular bodies are typically absent, and the tumor cells have perivascular orientations that resemble ependymal perivascular pseudorosettes (Fig. 7.18).

Although oligodendrocytes are part of the normal cellular composition of the optic nerve, oligodendroglial neoplasms rarely have been reported to involve the optic nerve and chiasm [26, 28, 66, 67]. Gliomatosis cerebri is a rare diffuse WHO grade III glioma characterized by an extensive infiltration of neoplastic cells that do not form a defined mass lesion but can involve the supratentorial, infratentorial, and intraspinal compartments [68]. The tumor cells diffusely invade the brain parenchyma and frequently migrate along myelinated white matter fiber tracts including the optic pathway. Gliomatosis cerebri uncommonly presents with ophthalmological signs and symptoms including visual loss, diplopia, nystagmus, and homonymous hemianopia [69]. Few reports of gliomatosis cerebri have

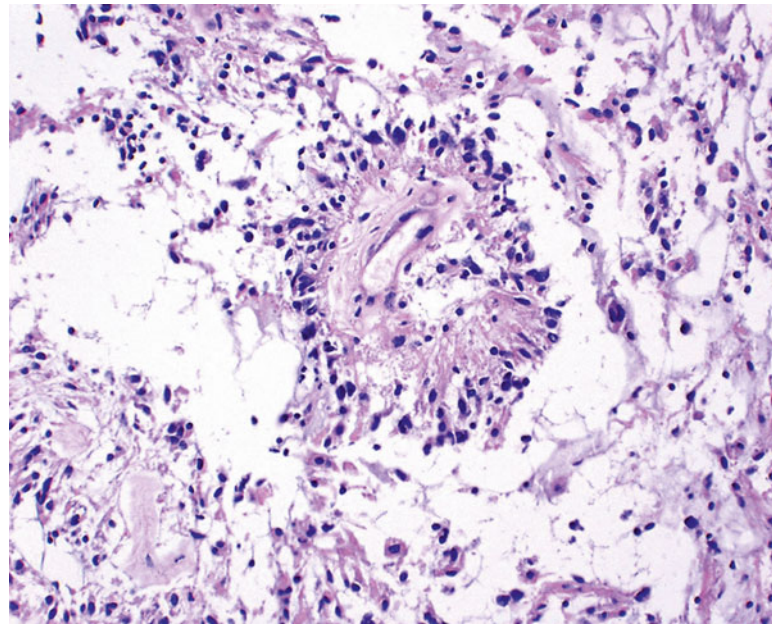

Fig. 7.18 Pilomyxoid astrocytoma characterized by perivascular tumor cell accumulations not to be mistaken for perivascular pseudorosettes of ependymoma (From Cummings [171], Figure 8.8, Page 161. With kind permission of Springer Science + Business Media)

documented involvement of the optic nerves and chiasm [70–73].

Genetics

NF1 has a well-recognized association with tumors of the central nervous system, especially gliomas of the optic pathways [26, 27, 39, 74–82]. About 70 % of optic pathway gliomas are associated with NF1 [39], and these tumors have a generally more favorable outcome than non-NF1-associated gliomas, as most tumors grow slowly or not at all [27, 39, 58, 74, 79, 83, 84]. Approximately 20 % of optic nerve tumors affect both nerves in patients with NF1 [25, 85], yet extensive bilateral involvement of the visual tracts is rare [86]. Nonetheless, tumor enlargement and progressive visual impairment occurs occasionally in children with NF1 [39, 77, 84, 87] Although exceptional, malignant change has been reported in optic nerve gliomas in patients with NF1 [66, 88] or with a family history of NF1 [89]. Pilocytic astrocytomas of the optic pathway may show deletions and allelic losses involving the *NF1* gene on the long arm of chromosome 17 and upregulation of NF1 gene transcripts, and it is thought that different mechanisms involving the *NF1* tumor suppressor gene may play an important primary genetic event in the promotion or initiation of NF1-associated pilocytic astrocytomas [90–96]. NF1-associated pilocytics typically lack the genetic changes associated with aggressive fibrillary astrocytomas [97]. Although p53 protein accumulations can be detected by immunohistochemistry, mutations of the *TP53* gene are rare [92, 98–101]. Molecular profiling using oligonucleotide microarray analysis has been able to demonstrate distinct gene expression patterns in pilocytic astrocytomas. Compared with glioblastomas, genes that encode cell motility were expressed at lower levels, while genes involved in suppressing migration were expressed at higher levels [102].

Prognosis and Predictive Factors

Pilocytic astrocytomas typically occur in children and young adults, and they are usually slow growing with a favorable prognosis. Despite incomplete surgical resection, some remain quiescent for extended periods of time and fail to recur, suggesting either arrest of tumor progression or deceleration in growth. Neuroimaging studies have documented spontaneous regression of large, clinically symptomatic optic pathway pilocytic astrocytomas [103–106]. Theories as to why these tumors spontaneously regress

Fig. 7.19 Optic nerve glioblastoma. Contrast-enhanced T_1-weighted axial magnetic resonance imaging (MRI) of the brain showing enhancement of the optic nerves and chiasm (From Cummings [171], Figure 8.9, Page 162. With kind permission of Springer Science + Business Media)

include individual tumor cell programmed death outpacing cellular proliferation, decreased vascular engorgement of the tumor, and resorption of the tumor-secreting mucosubstance [103, 107]. Some tumors, however, despite years of relative quiescence, retain the ability to grow and invade adjacent structures such as the optic chiasm and hypothalamus, resulting in considerable morbidity and mortality and a poorer prognosis than gliomas confined to a single optic nerve [24, 39, 46, 57, 74, 87, 108–112]. Others rarely exhibit malignant transformation and progression to anaplastic astrocytoma or glioblastoma [108]. Optic nerve glioblastomas typically occur in older adults, and patients present with unilateral or bilateral visual loss that often progresses to blindness. Glioblastomas are highly invasive and usually fatal within 1 year [31, 33]. Tumor may spread via the optic radiations to the occipital pole (Figs. 7.19 and 7.20).

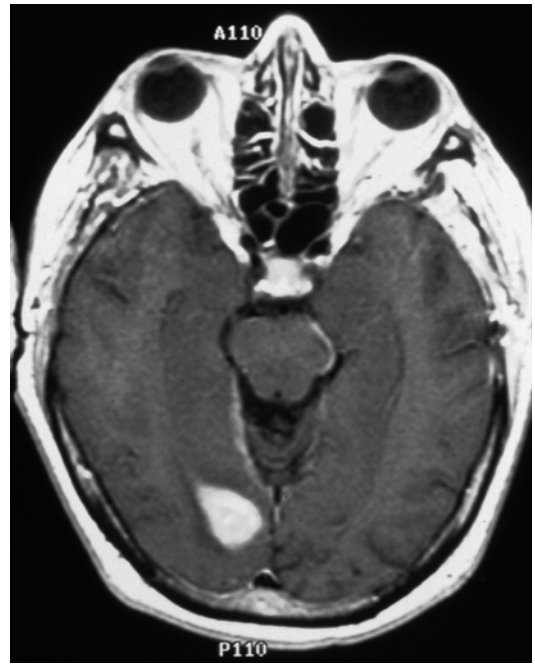

Fig. 7.20 Contrast-enhanced T_1-weighted axial MRI of the brain showing extension of glioblastoma along the optic radiations to the visual cortex in the occipital pole (From Cummings [171], Figure 8.10, Page 162. With kind permission of Springer Science + Business Media)

7.7.3 Optic Nerve Meningiomas

Definition

Meningiomas are tumors thought to arise from meningothelial cells in the arachnoid mater of the optic nerve leptomeninges.

Epidemiology

Similar to meningiomas elsewhere in the CNS, those arising in the optic nerve sheath and orbit occur more often in females than in males. Conceivably, the increased incidence in females may possibly be related to the known presence of progesterone and estrogen receptors in meningiomas [113]. Similar to intracranial and intraspinal meningiomas, the majority of primary orbital meningiomas present in the fifth decade of life. In the experience of some investigators [114], about one-fourth of the cases of primary orbital meningiomas become symptomatic before 10 years of age, in sharp contrast to intracranial

meningiomas, which are rarely apparent before the age of 20 [115]. However, this early age of onset has not confirmed in other studies [116].

Etiology and Localization

Meningiomas may arise anywhere along the optic nerve sheath (Fig. 7.4) (see also page 640), but the vast majority found within the orbit are direct extensions of intracranial meningiomas from along the wing of the sphenoid bone (sphenoidal ridge meningioma) [117, 118], the tuberculum sellae (suprasellar meningioma), or above and adjacent to the cribriform plate (olfactory groove meningioma) [119]. Sphenoorbital meningiomas (SOMs) involve the sphenoid wing, orbit, and cavernous sinus. They typically are associated with exuberant hyperostosis of the sphenoidal wing and direct involvement of the orbit (Fig. 7.21). The hyperostosis is due to direct tumor invasion of the bone [120]. SOMs represent up to 9 % of all intracranial meningiomas, and they are associated with a high rate of recurrence, up to 35–50 %. Clinically, patients with SOMs typically present with headaches, focal retroorbital pain, proptosis, visual field defects, and ocular paresis. Ectopic orbital meningiomas may reside outside the muscle cone without an attachment to the optic nerve [114, 121] or rarely external to the periosteal coverings of the orbital walls. Orbital meningiomas are seldom bilateral [122]. Other meningiomas of ophthalmological importance sometimes arise beneath the conjunctiva or caruncle [123], within the optic canal [124], paranasal sinuses, and the skin around the eye [125].

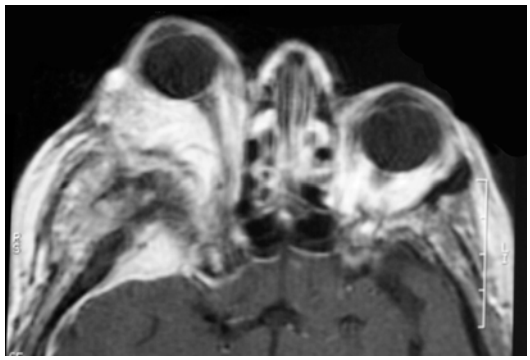

Fig. 7.21 Contrast-enhanced T_1-weighted axial MRI of a sphenoorbital meningioma showing marked enhancement and proptosis of the right orbit (From Cummings [171], Figure 8.20, Page 167. With kind permission of Springer Science + Business Media)

Clinical Features

Meningiomas typically spread within the optic nerve sheath causing compression of the optic nerve resulting in visual loss as the principal complaint (Fig. 7.22). Nerve compression may

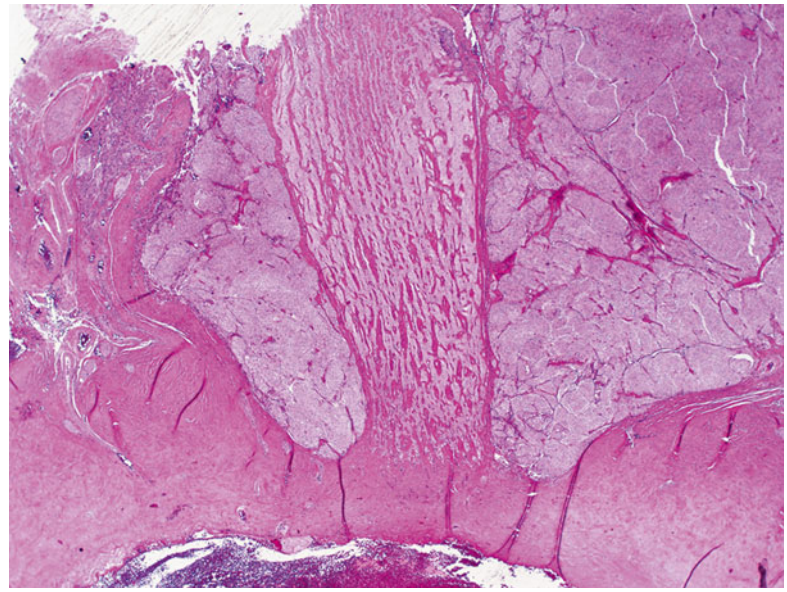

Fig. 7.22 Optic nerve surrounded by meningioma (From Cummings [171], Figure 8.15, Page 165. With kind permission of Springer Science + Business Media)

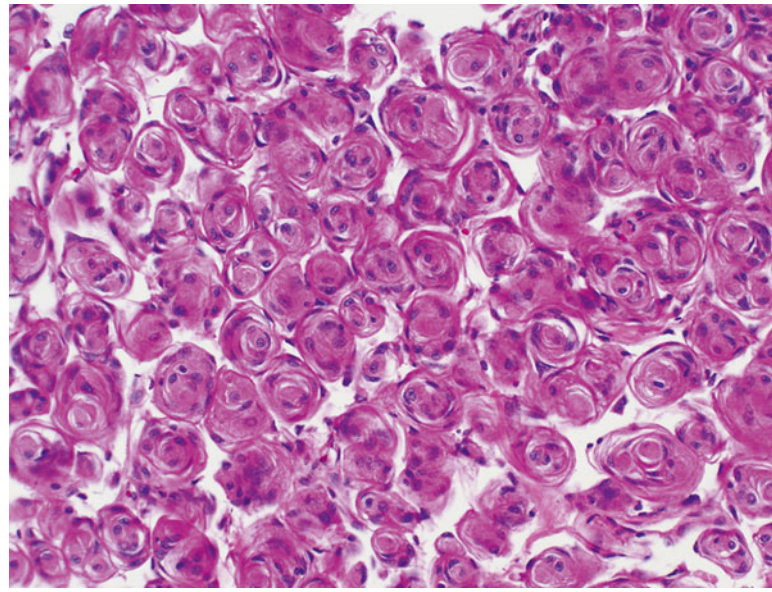

Fig. 7.23 Optic nerve meningioma with numerous whorl formations (From Cummings [171], Figure 8.16, Page 165. With kind permission of Springer Science + Business Media)

also be revealed by the emergence of prominent optociliary shunt vessels at the optic disk [126]. Meningioma rarely spreads anteriorly as far as the globe and may invade the choroid [127]. Metastasis is an exceedingly rare phenomenon but meningiomas can be locally infiltrative and subject to recurrence.

Macroscopy

Meningiomas tend to have a firm, fibrous appearance and may appear gritty if there are frequent psammoma bodies.

Histopathology

Meningiomas are one of the most heterogeneous neoplasms encountered by the surgical pathologist. Although 15 histological subtypes and three histological grades are recognized by the WHO's classification of tumors of the nervous system, many of these are unlikely to present within the orbit [128]. WHO grade I subtypes include meningothelial, fibroblastic, transitional, secretory, psammomatous, angiomatous, microcystic, lymphoplasmacyte-rich, and metaplastic. Most orbital meningiomas tend to be of the meningothelial subtype. Classical histological features include whorl formations (Fig. 7.23), psammoma bodies (Fig. 7.24), and intranuclear pseudoinclusions (Fig. 7.25). Secretory meningiomas may occur in the orbit and are characterized by pseudopsammoma bodies (Fig. 7.26) which are positive with a periodic acid-Schiff histochemical stain (Fig. 7.27) and a carcinoembryonic antigen (CEA) immunohistochemical stain (Fig. 7.28) [129]. Cytokeratin (Fig. 7.29) usually prefers to highlight the cells surrounding the pseudopsammoma bodies.

Approximately 8 % of orbital meningiomas are considered to be WHO grade II meningiomas [128]. They are associated with a greater likelihood of recurrence and/or aggressive behavior and include the atypical, clear cell, and chordoid histological subtypes. Grade II meningiomas are defined by the WHO as a meningioma with increased mitotic activity (four or more mitoses per ten high-power fields) or three or more of the following features: increased cellularity, small cells with high nucleus/cytoplasm ratio, prominent nucleoli, uninterrupted patternless or sheet-like growth, and foci of "spontaneous" or "geographic" necrosis. A meningioma with brain invasion is also considered a grade II tumor. Anaplastic (malignant) meningiomas (WHO grade III) very rarely involve the orbit and exhibit histological features of frank malignancy far in excess of the abnormalities present in a grade II meningioma including malignant cytology with an appearance similar to carcinoma, sarcoma, or

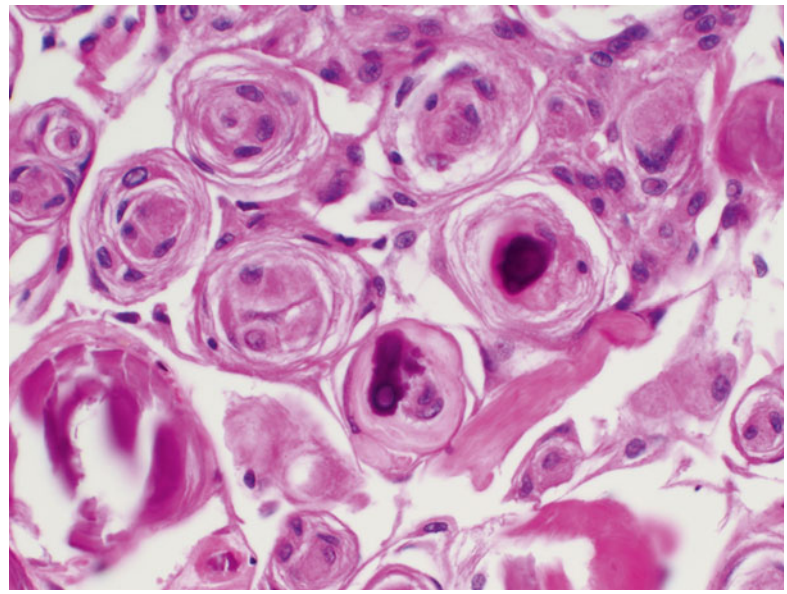

Fig. 7.24 Meningioma with a fractured psammoma body in the bottom left side of image. A few whorls in the center of the image show early central calcification; these will eventually develop into psammoma bodies (From Cummings [171], Figure 8.18, Page 166. With kind permission of Springer Science + Business Media)

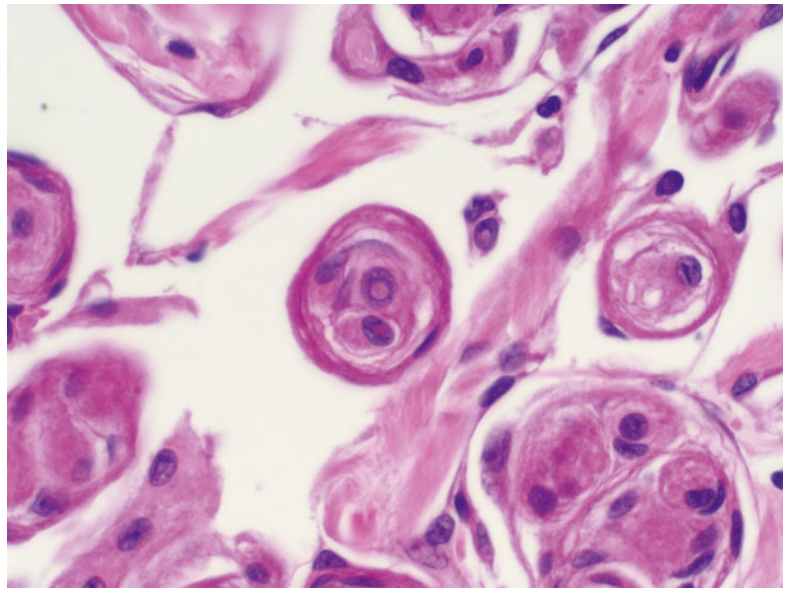

Fig. 7.25 Optic nerve meningioma with a whorl formation and a nuclear pseudoinclusion in the cell in the center of the image. The nuclear membrane surrounding the pseudoinclusion can be seen. Pseudoinclusions may either have a vacuolated clear/glycogenated appearance or have an eosinophilic appearance from artifactual cytoplasmic invagination into the nucleus. Electron microscopy of cytoplasmic invagination will confirm this to be a pseudoinclusion (e.g., unlike a true nuclear inclusion from a virus infection) by showing cytoplasmic organelles that appear to be within the nucleus (From Cummings [171], Figure 8.17, Page 166. With kind permission of Springer Science + Business Media)

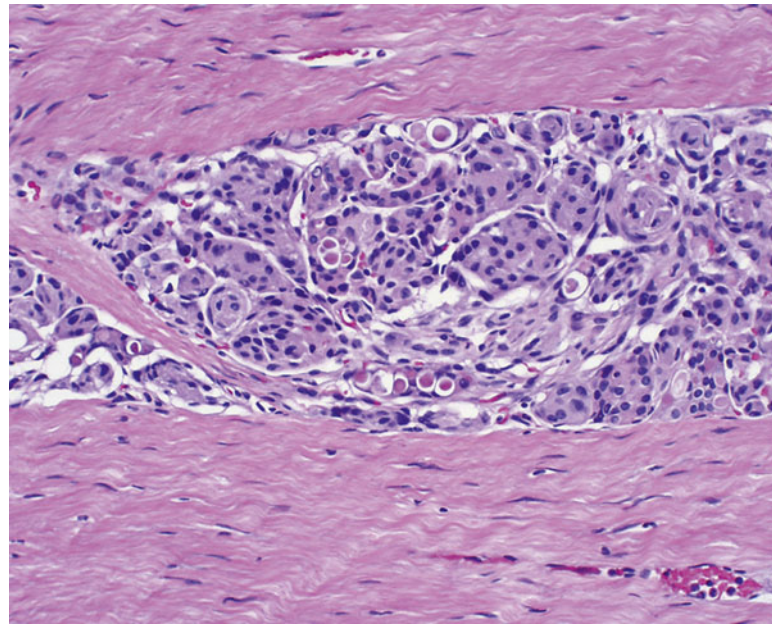

Fig. 7.26 Secretory variant of an orbital meningioma showing a whorled appearance and round pink pseudopsammoma bodies (From Cummings [171], Fig. 8.21, Page 168. With kind permission of Springer Science + Business Media)

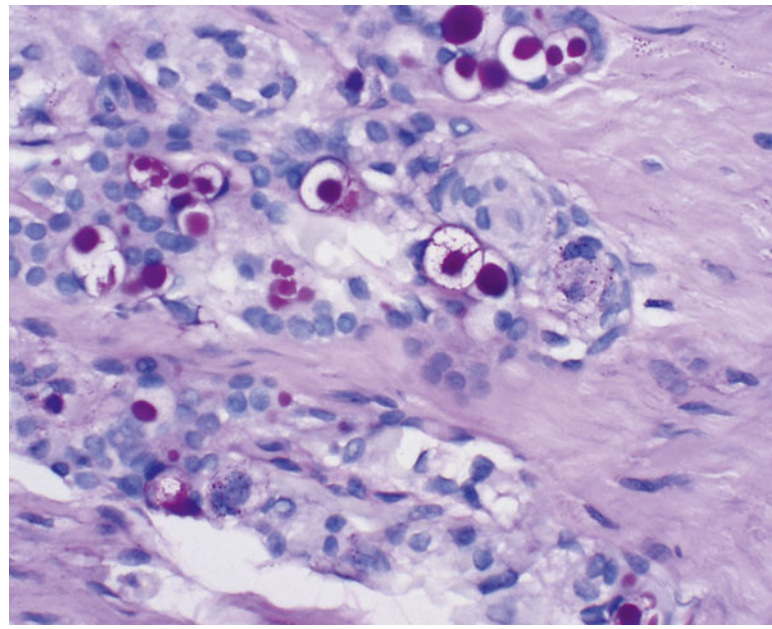

Fig. 7.27 Secretory variant of orbital meningioma. A PAS stain highlights the pseudopsammoma bodies in secretory meningioma (From Cummings [171], Fig. 8.22, Page 168. With kind permission of Springer Science + Business Media)

malignant melanoma, or a high mitotic index (20 or more mitoses per ten high-power fields).

Differential Diagnosis

Meningiomas are to be distinguished from optic nerve gliomas and from orbital tumors including the solitary fibrous tumor (SFT)/hemangiopericytoma (HPC) family of tumors. Immunohistochemistry can often distinguish these tumors. Meningiomas are typically immunopositive for EMA; gliomas are immunopositive for GFAP; and SFTs/HPCs are immunopositive for CD34. Electron microscopy studies are rarely needed to make the diagnosis,

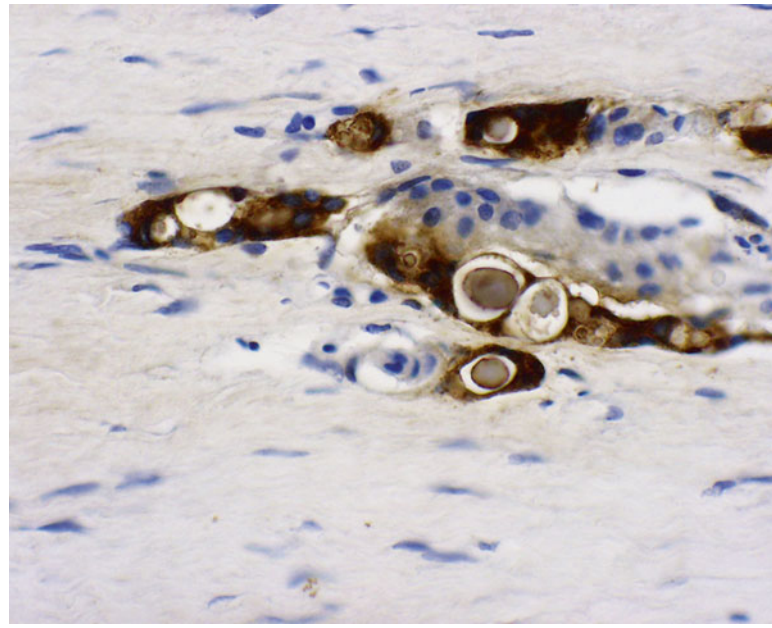

Fig. 7.28 Secretory variant of orbital meningioma. A carcinoembryonic antigen immunohistochemical stain highlights the pseudopsammoma bodies (From Cummings [171], Fig. 8.23, Page 169. With kind permission of Springer Science + Business Media)

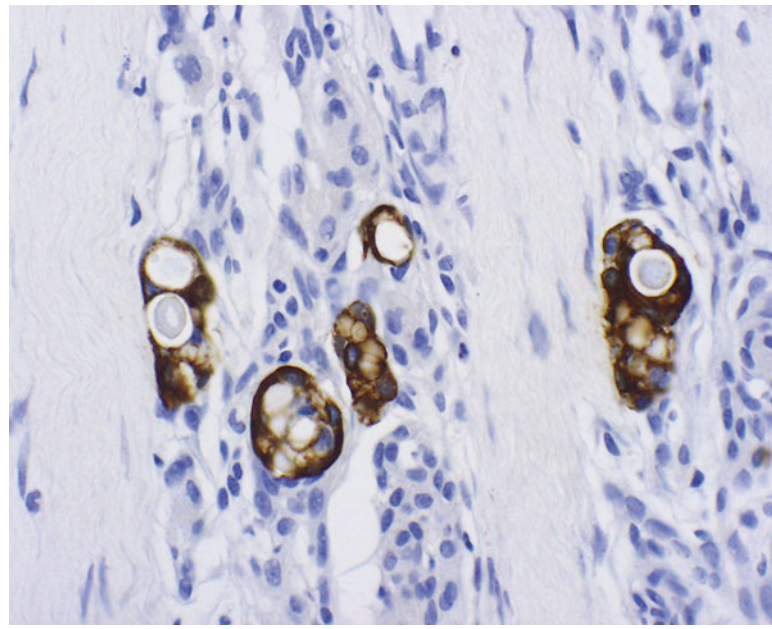

Fig. 7.29 Secretory variant of orbital meningioma. A cytokeratin immunohistochemical stain highlights the cells surrounding the pseudopsammoma bodies (From Cummings [171], Figure 8.24, Page 169. With kind permission of Springer Science + Business Media)

although meningiomas have characterized ultrastructural features including complex interdigitating cell processes between contiguous tumor cells and the presence of desmosomes and hemidesmosomes [130]. Meningeal hyperplasia may occur in cases of optic glioma and should be distinguished from meningioma [131].

Histogenesis

Meningiomas are thought to originate from meningothelial cells located in the arachnoid layer of the meninges. The meningothelial cells of the optic nerve sheath are the source of most primary orbital meningiomas, while other primary orbital meningiomas not connected to the

optic nerve probably arise from meningothelial cells in an ectopic location.

Genetics

Multiple meningiomas are a feature of neurofibromatosis type 2 (NF2), and in these individuals, they tend to occur earlier in life than sporadic meningiomas [114, 115, 132]. A tumor suppressor gene for meningioma has been identified on the long arm of chromosome 22 [22q12.3-qter], and this is at a locus different from the gene responsible for NF2 [133, 134]. Losses of chromosomes 1p, 6q, and 14q have been associated with atypical and anaplastic meningiomas [134, 135].

Prognostic and Predictive Factors

Prognosis depends primarily on size, location, and the histological classification of the meningiomas as WHO grade I, II, or III.

Ganglioglioma

Gangliogliomas are typically well-differentiated mixed glioneuronal neoplasms of the central nervous system that involve the temporal lobe in young adults. Rare examples of this tumor involving the optic nerve and chiasm have been reported, and they are histologically identical to similar tumors elsewhere in the central nervous system [136–145]. They contain a combination of neoplastic mature ganglion cells admixed with neoplastic glial cells that typically represents a pilocytic astrocytoma. Since the optic nerve is normally a pure white matter fiber tract that lacks ganglion cells, theories for the presence of ganglion cells in optic nerve gangliogliomas include ectopic neurons [139] and aberrant autonomic nerves and sympathetic ganglia [146]. Another theory suggests that gangliogliomas of the optic nerve and chiasm can derive from the undifferentiated neuroepithelium of the optic stalk lumen that conceivably can differentiate concurrently into both glial and ganglionic derivatives with neoplastic potential [138]. When a ganglioglioma involves the region of the optic chiasm and hypothalamus, the pathologist must determine if the neuronal component represents entrapped non-neoplastic hypothalamic neurons.

Melanocytoma (Magnocellular Nevus)

Melanocytomas are typically encountered in the optic nerve head, uveal tract, and conjunctiva. Optic nerve head melanocytomas may extend posterior to the lamina cribrosa. They are more likely to occur in deeply pigmented individuals. On gross examination, melanocytomas appear darkly pigmented or "jet-black." The tumor cells of melanocytoma are deeply pigmented. In order to evaluate the cytology of the cells, the slide must be "bleached" with the potassium permanganate technique. Microscopically, melanocytoma cells typically have a bland, monomorphic appearance with generally inconspicuous nucleoli. Although rare, some melanocytomas will undergo malignant transformation and have a malignant melanoma component.

Medulloepithelioma

Medulloepitheliomas are tumors that typically arise from the ciliary body and rarely from the optic nerve [147, 148]. They are believed to arise from embryonic neuroepithelium that lines the optic vesicle and cavities of the nerve [149]. In 1904 Verhoeff proposed the term "teratoneuroma" for a case which he described histologically and differentiated from retinoblastoma [150]. The alternative designation "diktyoma" (Greek: diktyon, a net) was suggested by Fuchs because of the netlike character of the neuroepithelial bands that extend into the adjacent cavities of the eye [151].

Medulloepitheliomas are characterized architecturally by convoluted cords and ribbons of multilayered undifferentiated neoplastic cells that enclose lumina of variable shape and size that mimic the primitive neural tube. The inner free surface is bounded by a limiting membrane, but at the opposite side the cells rest on a tenuous supporting stroma. There is often a characteristic neoplastic cyclitic membrane [152]. Teratoid medulloepitheliomas contain tissues not normally found during ocular development, including hyaline cartilage and skeletal muscle. Hyaline cartilage occurs most frequently and is found in up to 20 % of these tumors, and rarely the tumor may resemble a rhabdomyosarcoma [153]. Malignant

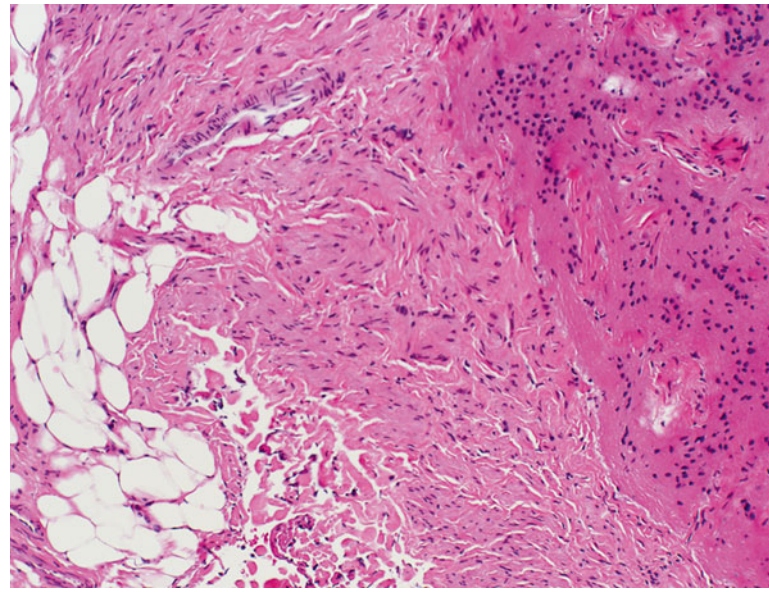

Fig. 7.30 Optic nerve choristoma. These rare lesions of the optic nerve are characterized by adipose tissue (*left*) and smooth muscle (*center*) among the glial tissue of the optic nerve (*right*) (From Cummings [171], Figure 8.25, Page 170. With kind permission of Springer Science + Business Media)

transformation of an optic nerve medulloepithelioma is a rare event [149, 154].

Hemangioblastoma

Hemangioblastomas rarely involve the optic nerve [155, 156]. They can be either sporadic or associated with von Hippel-Lindau disease. Histologically, they are identical to hemangioblastomas of the brain and spinal cord and are characterized by a capillary-rich network, foamy, lipid-rich "stromal" cells with nuclear cytological atypia (sometimes there is marked atypia, but this is not a negative prognostic feature), mast cells, and hemangiopericytomatous blood vessels.

Hemangiopericytoma

Hemangiopericytomas are orbital tumors which may arise from or secondarily involve the optic nerve sheath [157–160]. Histologically, they are characterized by vascular channels with a typical branching or "staghorn" appearance. Most tumors are densely cellular although some may exhibit foci of dense perivascular and intercellular collagen production. The clinical and pathological distinction of hemangiopericytoma from solitary fibrous tumor continues to evolve [161]. Intracranial meningeal-based hemangiopericytomas may exhibit a propensity for biologically aggressive behavior including metastasis, and similar concerns may be implicated for those of the optic nerve sheath.

Optic Nerve Choristoma

Optic nerve choristomas are rare lesions that may enter the clinical and radiological differential diagnosis of optic nerve glioma. Individuals often present with decreased visual acuity and progressive visual loss. Choristomas are defined as proliferations of normal, mature tissue at an abnormal location, and they are thought to be malformative and nonneoplastic. Histological findings in optic nerve choristoma include an admixture of benign adipose tissue and smooth muscle among the glial tissue of the optic nerve (Fig. 7.30, 7.31, and 7.32) [162, 163]

Secondary Tumors

The optic nerve may be involved secondarily by a variety of tumors [164]. When a globe is enucleated for retinoblastoma, it is imperative for the pathologist to document the surgical margin and the extent of involvement [if any] of the optic nerve by tumor. This may have prognostic and therapeutic implications. If tumor does infiltrate into the nerve, it can be categorized relative to the lamina cribrosa as prelaminar, intralaminar,

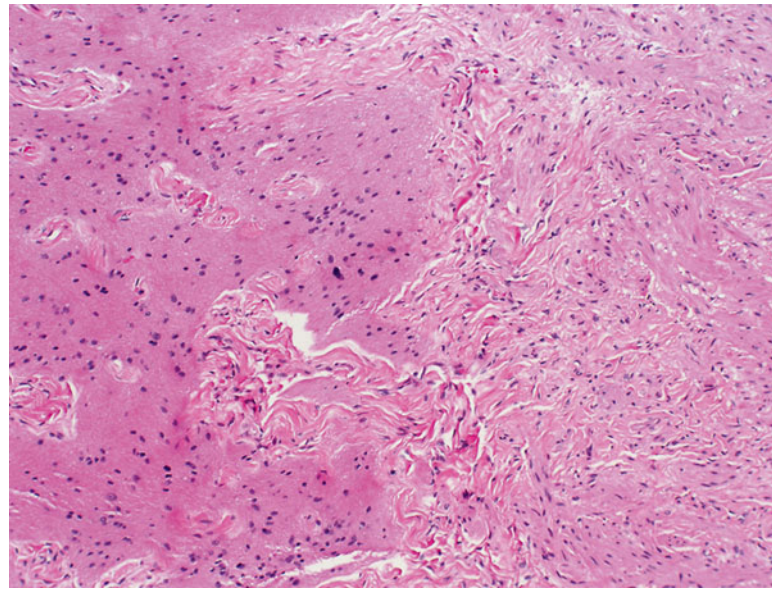

Fig. 7.31 Optic nerve choristoma showing optic nerve glial tissue (*left half of image*) and choristomatous smooth muscle (*right half of image*) (From Cummings [171], Figure 8.26, Page 171. With kind permission of Springer Science + Business Media)

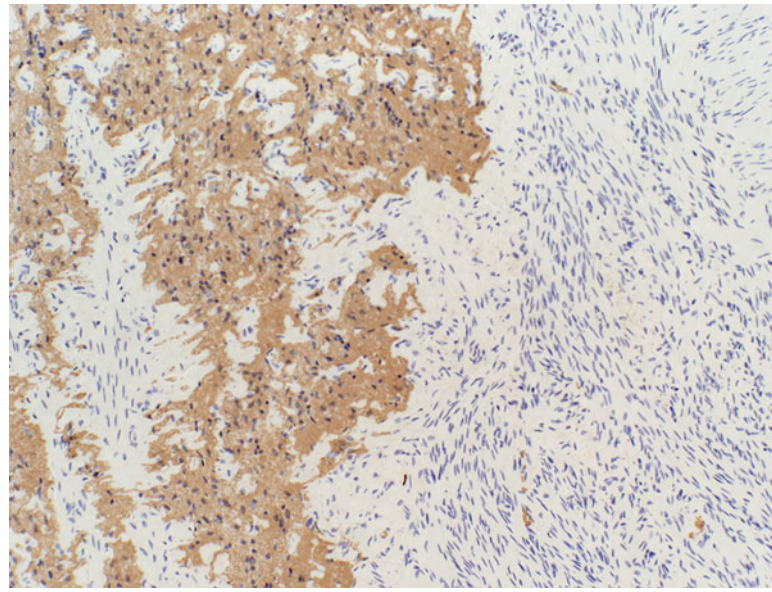

Fig. 7.32 Optic nerve choristoma. A GFAP immunohistochemical stain highlights the optic nerve glial tissue (*left half of image*). The smooth muscle component (*right half of image*) was immunopositive for smooth muscle actin (not shown) (From Cummings [171], Figure 8.27, Page 171. With kind permission of Springer Science + Business Media)

postlaminar, or at the surgical margin. The true margin can be demarcated with ink and submitted in a separate cassette.

The optic nerve may be secondarily involved by uveal melanoma [165, 166]. Peripapillary and diffuse melanomas may infiltrate the retina ("retinoinvasive" melanoma) and extend into the optic nerve. Primary malignant melanomas rarely arise from indigenous melanocytes of the optic nerve meninges (similar to primary brain and spinal cord melanocytic tumors). The optic nerve may be involved by metastatic tumors, including lung, breast, and stomach carcinomas, and by leukemia and lymphoma [167]. The optic nerve and chiasm are also vulnerable to compression or infiltration from gliomas, pituitary adenomas, craniopharyngiomas, and other intracranial tumors.

Other Rare Tumors

Other rare tumors reported to involve the optic nerve and chiasm include Langerhans cell histiocytosis [168], juvenile xanthogranuloma, and germ cell tumors [169]. An unusual salivary gland choristoma involving the optic nerve sheath has been reported [170].

References

1. Rao NA, Spencer WH. Optic nerve. In: Spencer WH, editor. Ophthalmic pathology. An atlas and textbook. Philadelphia: W.B. Saunders Company; 1996. p. 513–622.
2. Klintworth GK, Cummings TJ. The optic nerve. Chapter 13: Normal eye and ocular adnexa. In: Mills S, editor. Histology for pathologists. 4th ed. Philadelphia: Lippincott Williams & Wilkins; 2012.
3. Yanoff M, Fine BS. Normal anatomy in Chapter 13: Optic nerve. From: Ocular pathology, 5th ed. Philadelphia: Mosby; 2002.
4. Merz B. Eye disease linked to mitochondrial defect. JAMA. 1988;19:260–894.
5. La Russa A, Cittadella R, Andreoli V, Valentino P, Trecroci F, Caracciolo M, Gallo O, Gambardella A, Quattrone A. Leber's hereditary optic neuropathy associated with a multiple sclerosis-like picture in a man. Mult Scler. 2011;17:763–6.
6. Mohindra S, Mohindra S, Gupta R, Bakshi J, Gupta SK. Rhinocerebral mucormycosis: the disease spectrum in 27 patients. Mycoses. 2007;50:290–6.
7. Ibrahim AS, Spellberg B, Walsh TJ, Kontoyiannis DP. Pathogenesis of mucormycosis. Clin Infect Dis. 2012;54:S16–22.
8. Petrikkos G, Skiada A, Lortholary O, Roilides E, Walsh TJ, Kontoyiannis DP. Epidemiology and clinical manifestations of mucormycosis. Clin Infect Dis. 2012;54:S23–34.
9. Marthur S, Karimi A, Mafee MF. Acute optic nerve infarction demonstrated by diffusion-weighted imaging in a case of rhinocerebral mucormycosis. AJNR Am J Neuroradiol. 2007;28:489–90.
10. Alsuhaibani AH, Al-Thubaiti G, Al Badr FB. Optic nerve thickening and infarction as the first evidence of orbital involvement with mucormycosis. Middle East Afr J Ophthalmol. 2012;19:340–2.
11. McDonnell PJ. Ocular manifestations of temporal arteritis. Curr Opin Ophthalmol. 1990;1:158.
12. Schmidt D, Löffler KU. Temporal arteritis: comparison of histologic and clinical findings. Acta Ophthalmol. 1994;72:319–25.
13. Henkind P, Charles NC, Pearson J. Histopathology of ischemic optic neuropathy. Am J Ophthalmol. 1970;69:78–90.
14. Brass SD, Zivadinov R, Bakshi R. Acute demyelinating optic neuritis: a review. Front Biosci. 2008;13:2376–90.
15. Chan JW. Optic neuritis in multiple sclerosis. Ocul Immunol Inflamm. 2002;10:161–86.
16. van der Valk P, de Groot CJ. Staging of multiple sclerosis [MS] lesions: pathology of the time frame of MS. Neuropathol Appl Neurobiol. 2000;26:2–10.
17. van der Valk P, Amor S. Preactive lesions in multiple sclerosis. Curr Opin Neurol. 2009;22:207–13.
18. Ratelade J, Verkman AS. Neuromyelitis optica: aquaporin-4 based pathogenesis mechanisms and new therapies. Int J Biochem Cell Biol. 2012;44:1519–30.
19. Duke-Elder S. Tumours of the optic nerve and its sheaths. In: Duke-Elder S, editor. System of ophthalmology. St. Louis: The C.V. Mosby Company; 1976. p. 229–68.
20. Davis FA. Primary tumors of the optic nerve (a phenomenon of Recklinghausen's disease): a clinical and pathological study with a report of five cases and a review of the literature. Arch Ophthalmol. 1940;23:957–1022.
21. Hudson AC. Primary tumors of the optic nerve. R Lond Ophthalmol Hosp Rep. 1912;18:317–27.
22. Verhoeff FH. Primary intraneural tumors (gliomas) of the optic nerve. Arch Ophthalmol. 1922;51:120–40.
23. Martin P, Cushing H. Primary gliomas of the chiasm and optic nerves in their intracranial portion. Arch Ophthalmol. 1923;52:209–41.
24. Dutton JJ. Optic nerve gliomas and meningiomas. Neurol Clin. 1991;9(1):163–77.
25. Hollander MD, FitzPatrick M, O'Connor SG, Flanders AE, Tartaglino LM. Optic gliomas. Radiol Clin N Am. 1999;37(1):59–71.
26. Listernick R, Louis DN, Packer RJ, Gutmann DH. Optic pathway gliomas in children with neurofibromatosis 1: consensus statement from the NF1 optic pathway glioma task force. Ann Neurol. 1997;41(2):143–9.
27. Lynch TM, Gutmann DH. Neurofibromatosis 1. Neurol Clin. 2002;20(3):841–65.
28. Eggers H, Jakobiec FA, Jones IS. Tumors of the optic nerve. Doc Ophthalmol. 1976;41(1):43–128.
29. Dutton JJ. Gliomas of the anterior visual pathway. Surv Ophthalmol. 1994;38(5):427–52.
30. Khafaga Y, Hassounah M, Kandil A, Kanaan I, Allam A, El Husseiny G, et al. Optic gliomas: a retrospective analysis of 50 cases. Int J Radiat Oncol Biol Phys. 2003;56(3):807–12.
31. Nomura S, Suzuki R, Sugiyama S, Nogami K, Ito H. Optic glioma with characteristic bilateral optic atrophy in a 3-year-old girl. Pediatr Neurosurg. 1999;31(4):213–8.
32. Hoyt WF, Meshel LG, Lessell S, Schatz NJ, Suckling RD. Malignant optic glioma of adulthood. Brain. 1973;96(1):121–32.
33. Shapiro SK, Shapiro I, Wirtschafter JD, Mastri AR. Malignant optic glioma in an adult: initial CT abnormality limited to the posterior orbit, leptomeningeal seeding of the tumor. Minn Med. 1982;65(3):155–9.
34. Murphy M, Timms C, McKelvie P, Dowling A, Trost N. Malignant optic nerve glioma: metastases to the spinal neuraxis. Case illustration. J Neurosurg. 2003;98(1 Suppl):110.

35. Cirak B, Unal O, Arslan H, Cinal A. Chiasmatic glioblastoma of childhood. A case report. Acta Radiol. 2000;41(4):375–6.
36. Wilson WB, Feinsod M, Hoyt WF, Nielsen SL. Malignant evolution of childhood chiasmal pilocytic astrocytoma. Neurology. 1976;26(4):322–5.
37. Safneck JR, Napier LB, Halliday WC. Malignant astrocytoma of the optic nerve in a child. Can J Neurol Sci. 1992;19(4):498–503.
38. Dirks PB, Jay V, Becker LE, Drake JM, Humphreys RP, Hoffman HJ, et al. Development of anaplastic changes in low-grade astrocytomas of childhood. Neurosurgery. 1994;34(1):68–78.
39. Listernick R, Charrow J, Gutmann DH. Intracranial gliomas in neurofibromatosis type 1. Am J Med Genet. 1999;89(1):38–44.
40. Cummings TJ, Chu CT, Pollock SC, Klintworth GK. Optic nerve astrocytoma with angiogenesis and neovascular glaucoma. Ophthalmic Pract. 2000;18: 227–30.
41. Charles NC, Nelson L, Brookner AR, Lieberman N, Breinin GM. Pilocytic astrocytoma of the optic nerve with hemorrhage and extreme cystic degeneration. Am J Ophthalmol. 1981;92(5):691–5.
42. Stern J, Jakobiec FA, Housepian EM. The architecture of optic nerve gliomas with and without neurofibromatosis. Arch Ophthalmol. 1980;98(3):505–11.
43. Stern J, DiGiacinto GV, Housepian EM. Neurofibromatosis and optic glioma: clinical and morphological correlations. Neurosurgery. 1979;4(6):524–8.
44. Bruggers CS, Friedman HS, Phillips PC, Wiener MD, Hockenberger B, Oakes WJ, et al. Leptomeningeal dissemination of optic pathway gliomas in three children. Am J Ophthalmol. 1991;111(6):719–23.
45. Davis PC, Hoffman Jr JC, Weidenheim KM. Large hypothalamic and optic chiasm gliomas in infants: difficulties in distinction. AJNR Am J Neuroradiol. 1984;5(5):579–85.
46. McDonnell P, Miller NR. Chiasmatic and hypothalamic extension of optic nerve glioma. Arch Ophthalmol. 1983;101(9):1412–5.
47. Liber AF. The nature of Rosenthal fibers. J Nerv Ment Dis. 1937;85:286–304.
48. Rosenthal W. Über eine eigenthumliche, mit syringomyelie complicierte geschwulst des rückenmarks. Zieglers Beitr Path Anat Allg Path. 1898;23:110.
49. Verhoeff FH. Tumors of the optic nerve. Cytology and cellular pathology of the nervous system. New York: Hafner Publishing Company; 1965. p. 1029–39.
50. Rubinstein LJ. Atlas of tumor pathology: tumors of the central nervous system. 2nd ed. Washington, D.C: Armed Forces Institute of Pathology; 1972.
51. Machen SK, Prayson RA. Cyclin D1 and MIB-1 immunohistochemistry in pilocytic astrocytomas: a study of 48 cases. Hum Pathol. 1998;29(12):1511–6.
52. Burger PC, Shibata T, Kleihues P. The use of the monoclonal antibody Ki-67 in the identification of proliferating cells: application to surgical neuropathology. Am J Surg Pathol. 1986;10(9):611–7.
53. Dirven CM, Koudstaal J, Mooij JJ, Molenaar WM. The proliferative potential of the pilocytic astrocytoma: the relation between MIB-1 labeling and clinical and neuroradiological follow-up. J Neurooncol. 1998;37(1):9–16.
54. Louis DN, Edgerton S, Thor AD, Hedley-Whyte ET. Proliferating cell nuclear antigen and Ki-67 immunohistochemistry in brain tumors: a comparative study. Acta Neuropathol. 1991;81(6):675–9.
55. Matsumoto T, Fujii T, Yabe M, Oka K, Hoshi T, Sato K. MIB-1 and p53 immunocytochemistry for differentiating pilocytic astrocytomas and astrocytomas from anaplastic astrocytomas and glioblastomas in children and young adults. Histopathology. 1998;33(5): 446–52.
56. Takeuchi H, Kabuto M, Sato K, Kubota T. Chiasmal gliomas with spontaneous regression: proliferation and apoptosis. Childs Nerv Syst. 1997;13:229–33.
57. Cummings TJ, Provenzale JM, Hunter SB, Friedman AH, Klintworth GK, Bigner SH, et al. Gliomas of the optic nerve: histological, immunohistochemical (MIB-1 and p53), and MRI analysis. Acta Neuropathol. 2000;99(5):563–70.
58. Rush JA, Younge BR, Campbell RJ, MacCarty CS. Optic glioma. Long-term follow-up of 85 histopathologically verified cases. Ophthalmology. 1982;89(11): 1213–9.
59. Bernardini FP, Croxatto JO, Nozza P, Rossi A, Capris P. Primary diffuse leptomeningeal gliomatosis in children: a clinical pathologic correlation. Ophthal Plast Reconstr Surg. 2013;29(2):93–7.
60. Cooling RJ, Wright JE. Arachnoid hyperplasia in optic nerve glioma: confusion with orbital meningioma. Br J Ophthalmol. 1979;63(9):596–9.
61. Rodriguez FJ, Ligon AH, Horkayne-Szakaly I, Rushing EJ, Ligon KL, Vena N, et al. BRAF duplications and MAPK pathway activation are frequent in gliomas of the optic nerve proper. J Neuropathol Exp Neurol. 2012;71(9):789–94.
62. Burger PC, Scheithauer BW, Paulus W, Szymas J, Giannini C, Kleihues P. Pilocytic astrocytoma. In: Kleihues P, Cavenee WK, editors. World Health Organization. Pathology and genetics, tumours of the nervous system. Lyon: IARC Press; 2000. p. 45–51.
63. Burger PC, Scheithauer BW, Vogel FS. The brain – tumors. In: Burger PC, Scheithauer BW, Vogel FS, editors. Surgical pathology of the nervous system and its coverings. Philadelphia: Churchill Livingstone; 2002. p. 203–15.
64. Lach B, Al Shail E, Patay Z. Spontaneous anaplasia in pilocytic astrocytoma of cerebellum. Br J Neurosurg. 2003;17(3):250–2.
65. Tomlinson FH, Scheithauer BW, Hayostek CJ, Parisi JE, Meyer FB, Shaw EG, et al. The significance of atypia and histologic malignancy in pilocytic astrocytoma of the cerebellum: a clinicopathologic and flow cytometric study. J Child Neurol. 1994;9(3):301–10.
66. Rubinstein LJ. Pathological features of optic nerve and chiasmatic gliomas. Neurofibromatosis. 1988;1(3): 152–8.

67. Reese AB. Tumors of the eye. Hagerstown: Harper & Row; 1963. p. 134–5.
68. Cummings TJ, Hulette CM, Longee DC, Bottom KS, McLendon RE, Chu CT. Gliomatosis cerebri: cytologic and autopsy findings in a case involving the entire neuraxis. Clin Neuropathol. 1999;18(4):190–7.
69. Couch JR, Weiss SA. Gliomatosis cerebri. Report of four cases and review of the literature. Neurology. 1974;24(6):504–11.
70. Kawano N, Miyasaka Y, Yada K, Atari H, Sasaki K. Diffuse cerebrospinal gliomatosis. Case report. J Neurosurg. 1978;49(2):303–7.
71. Zaman K, Hardy DG. Diffuse cerebrospinal gliomatosis: clinical and radiological findings. Br J Neurosurg. 1988;2(3):415–8.
72. Felsberg GJ, Glass JP, Tien RD, McLendon R. Gliomatosis cerebri presenting with optic nerve involvement: MRI. Neuroradiology. 1996;38(8):774–7.
73. Traynis I, Singer S, Winterkorn J, Rosenblum M, Dinkin M. Infiltration of the optic chiasm, nerve, and disc by gliomatosis cerebri. J Neuroophthalmol. 2014; 34(1):44–6.
74. Alvord Jr EC, Lofton S. Gliomas of the optic nerve or chiasm. Outcome by patients' age, tumor site, and treatment. J Neurosurg. 1988;68(1):85–98.
75. Bianchi-Marzoli S, Brancato R. Tumors of the optic nerve and chiasm. Curr Opin Ophthalmol. 1994;5(6): 11–7.
76. Listernick R, Charrow J, Greenwald MJ, Esterly NB. Optic gliomas in children with neurofibromatosis type 1. J Pediatr. 1989;114(5):788–92.
77. Listernick R, Charrow J, Greenwald M, Mets M. Natural history of optic pathway tumors in children with neurofibromatosis type 1: a longitudinal study. J Pediatr. 1994;125(1):63–6.
78. Listernick R, Charrow J, Gutmann DH. Comments on neurofibromatosis 1 and optic pathway tumors. Am J Med Genet. 2001;102(1):105.
79. Gutmann DH, Rasmussen SA, Wolkenstein P, MacCollin MM, Guha A, Inskip PD, et al. Gliomas presenting after age 10 in individuals with neurofibromatosis type 1 (NF1). Neurology. 2002;59(5):759–61.
80. Farmer JP, Khan S, Khan A, Ortenberg J, Freeman C, O'Gorman AM, et al. Neurofibromatosis type 1 and the pediatric neurosurgeon: a 20-year institutional review. Pediatr Neurosurg. 2002;37(3):122–36.
81. Rosser T, Packer RJ. Intracranial neoplasms in children with neurofibromatosis 1. J Child Neurol. 2002;17(8):630–7.
82. Deliganis AV, Geyer JR, Berger MS. Prognostic significance of type 1 neurofibromatosis (von Recklinghausen disease) in childhood optic glioma. Neurosurgery. 1996;38(6):1114–8.
83. de Keizer RJ, Wolff-Rouendaal D, Bots GT, Thomeer RT, Brouwer OF, Vielvoye GJ. Optic glioma with intraocular tumor and seeding in a child with neurofibromatosis. Am J Ophthalmol. 1989;108(6):717–25.
84. Janss AJ, Grundy R, Cnaan A, Savino PJ, Packer RJ, Zackai EH, et al. Optic pathway and hypothalamic/chiasmatic gliomas in children younger than age 5 years with a 6-year follow-up. Cancer. 1995;75(4): 1051–9.
85. Ersahin Y, Yunten N. Bilateral optic nerve glioma. Pediatr Neurosurg. 1999;31(3):168.
86. Shah JR, Patkar DP, Pungavkar SA, Parmer H. Extensive gliomas of visual tract in a patient of neurofibromatosis-I. Indian J Pediatr. 2000;67(12):939–40.
87. Balcer LJ, Liu GT, Heller G, Bilaniuk L, Volpe NJ, Galetta SL, et al. Visual loss in children with neurofibromatosis type 1 and optic pathway gliomas: relation to tumor location by magnetic resonance imaging. Am J Ophthalmol. 2001;131(4):442–5.
88. Borit A, Richardson Jr EP. The biological and clinical behaviour of pilocytic astrocytomas of the optic pathways. Brain. 1982;105(Pt 1):161–87.
89. Rubinstein LJ. Tumeurs et hamartomes dans la neurofibromatose central. In: Michaux L, Feld M, editors. Les Phakomatoses Cérébrales. Paris: SPEI Editeurs; 1963. p. 427–51.
90. Wimmer K, Eckart M, Meyer-Puttlitz B, Fonatsch C, Pietsch T. Mutational and expression analysis of the NF1 gene argues against a role as tumor suppressor in sporadic pilocytic astrocytomas. J Neuropathol Exp Neurol. 2002;61(10):896–902.
91. Gutmann DH, Donahoe J, Brown T, James CD, Perry A. Loss of neurofibromatosis 1 (NF1) gene expression in NF1-associated pilocytic astrocytomas. Neuropathol Appl Neurobiol. 2000;26(4):361–7.
92. Lang FF, Miller DC, Pisharody S, Koslow M, Newcomb EW. High frequency of p53 protein accumulation without p53 gene mutation in human juvenile pilocytic, low grade and anaplastic astrocytomas. Oncogene. 1994;9(3):949–54.
93. Platten M, Giordano MJ, Dirven CM, Gutmann DH, Louis DN. Up-regulation of specific NF 1 gene transcripts in sporadic pilocytic astrocytomas. Am J Pathol. 1996;149(2):621–7.
94. Kluwe L, Hagel C, Tatagiba M, Thomas S, Stavrou D, Ostertag H, et al. Loss of NF1 alleles distinguish sporadic from NF1-associated pilocytic astrocytomas. J Neuropathol Exp Neurol. 2001;60(9):917–20.
95. von Deimling A, Louis DN, Menon AG, von Ammon K, Petersen I, Ellison D, et al. Deletions on the long arm of chromosome 17 in pilocytic astrocytoma. Acta Neuropathol. 1993;86(1):81–5.
96. Tada K, Kochi M, Saya H, Kuratsu J, Shiraishi S, Kamiryo T, et al. Preliminary observations on genetic alterations in pilocytic astrocytomas associated with neurofibromatosis 1. Neuro Oncol. 2003;5(4): 228–34.
97. Li J, Perry A, James CD, Gutmann DH. Cancer-related gene expression profiles in NF1-associated pilocytic astrocytomas. Neurology. 2001;56(7): 885–90.
98. Cheng Y, Pang JC, Ng HK, Ding M, Zhang SF, Zheng J, et al. Pilocytic astrocytomas do not show most of the genetic changes commonly seen in diffuse astrocytomas. Histopathology. 2000;37(5):437–44.

99. Patt S, Gries H, Giraldo M, Cervos-Navarro J, Martin H, Janisch W, et al. p53 gene mutations in human astrocytic brain tumors including pilocytic astrocytomas. Hum Pathol. 1996;27(6):586–9.
100. Ishii N, Sawamura Y, Tada M, Daub DM, Janzer RC, Meagher-Villemure M, et al. Absence of p53 gene mutations in a tumor panel representative of pilocytic astrocytoma diversity using a p53 functional assay. Int J Cancer. 1998;76(6):797–800.
101. Raffel C. Molecular biology of pediatric gliomas. J Neurooncol. 1996;28(2–3):121–8.
102. Rickman DS, Bobek MP, Misek DE, Kuick R, Blaivas M, Kurnit DM, et al. Distinctive molecular profiles of high-grade and low-grade gliomas based on oligonucleotide microarray analysis. Cancer Res. 2001;61(18):6885–91.
103. Parsa CF, Hoyt CS, Lesser RL, Weinstein JM, Strother CM, Muci-Mendoza R, et al. Spontaneous regression of optic gliomas: thirteen cases documented by serial neuroimaging. Arch Ophthalmol. 2001;119(4):516–29.
104. Rossi LN, Triulzi F, Parazzini C, Maninetti MM. Spontaneous improvement of optic pathway lesions in children with neurofibromatosis type 1. Neuropediatrics. 1999;30(4):205–9.
105. Schmandt SM, Packer RJ, Vezina LG, Jane J. Spontaneous regression of low-grade astrocytomas in childhood. Pediatr Neurosurg. 2000;32(3):132–6.
106. Yoshikawa G, Nagata K, Kawamoto S, Tsutsumi K. Remarkable regression of optic glioma in an infant. Case illustration. J Neurosurg. 2003;98(5):1134.
107. Liu GT, Lessell S. Spontaneous visual improvement in chiasmal gliomas. Am J Ophthalmol. 1992;114(2): 193–201.
108. Wong JY, Uhl V, Wara WM, Sheline GE. Optic gliomas. A reanalysis of the University of California, San Francisco experience. Cancer. 1987;60(8):1847–55.
109. McCullough DC, Epstein F. Optic pathway tumors. A review with proposals for clinical staging. Cancer. 1985;56(7 Suppl):1789–91.
110. Regueiro CA, Ruiz MV, Millan I, de la Torre A, Romero J, Aragon G. Prognostic factors and results of radiation therapy in optic pathway tumors. Tumori. 1996;82(4):353–9.
111. Aarabi B, Long DM, Miller NR. Enlarging optic chiasmal glioma with stable visual acuity. Surg Neurol. 1978;10(3):175–7.
112. Nishio S, Takeshita I, Fujiwara S, Fukui M. Opticohypothalamic glioma: an analysis of 16 cases. Childs Nerv Syst. 1993;9(6):334–8.
113. Wan WL, Geller JL, Feldon SE, Sadun AA. Visual loss caused by rapidly progressive intracranial meningiomas during pregnancy. Ophthalmology. 1990;97(1):18–21.
114. Karp LA, Zimmerman LE, Borit A, Spencer W. Primary intraorbital meningiomas. Arch Ophthalmol. 1974;91(1):24–8.
115. Merten DF, Gooding CA, Newton TH, Malamud N. Meningiomas of childhood and adolescence. J Pediatr. 1974;84(5):696–700.
116. Wright JE. Primary optic nerve meningiomas: clinical presentation and management. Trans Sect Ophthalmol Am Acad Ophthalmol Otolaryngol. 1977;83(4): 617–25.
117. Finn JE, Mount LA. Meningiomas of the tuberculum sellae and planum sphenoidale. A review of 83 cases. Arch Ophthalmol. 1974;92(1):23–7.
118. Radhakrishnan S, Lee MS. Optic nerve sheath meningiomas. Curr Treat Options Neurol. 2005;7(1):51–5.
119. Stern WE. Meningiomas in the cranio-orbital junction. J Neurosurg. 1973;38(4):428–37.
120. Pieper DR, Al Mefty O, Hanada Y, Buechner D. Hyperostosis associated with meningioma of the cranial base: secondary changes or tumor invasion. Neurosurgery. 1999;44(4):742–6.
121. Mandelcorn MS, Shea M. Primary orbital perioptic meningioma: a case report. Can J Ophthalmol. 1971; 6(4):293–7.
122. Sood GC, Malik SK, Gupta DK, Gupta AN. Bilateral meningiomas of the orbit. Am J Ophthalmol. 1966; 61(6):1533–5.
123. Macmichael IM, Cullen JF. Primary intraorbital meningioma. Br J Ophthalmol. 1969;53(3):169–73.
124. Kennerdell JS, Maroon JC. Intracanalicular meningioma with chronic optic disc edema. Ann Ophthalmol. 1975;7(4):507–12.
125. Lopez DA, Silvers DN, Helwig EB. Cutaneous meningiomas – a clinicopathologic study. Cancer. 1974;34(3):728–44.
126. Saeed P, Rootman J, Nugent RA, White VA, Mackenzie IR, Koornneef L. Optic nerve sheath meningiomas. Ophthalmology. 2003;110(10):2019–30.
127. Moore CE. Sphenoidal ridge meningioma with optic nerve metastasis. Br J Ophthalmol. 1968;52(8):636–9.
128. Jain D, Ebrahimi KB, Miller NR, Eberhart CG. Intraorbital meningiomas: a pathologic review using current World Health Organization criteria. Arch Pathol Lab Med. 2010;134(5):766–70.
129. Karikari IO, Syed NA, Cummings TJ. Secretory meningiomas of the orbit. Orbit. 2009;28(6):408–11.
130. Copeland DD, Bell SW, Shelburne JD. Hemidesmosome-like intercellular specializations in human meningiomas. Cancer. 1978;41(6):2242–9.
131. Perry A, Lusis EA, Gutmann DH. Meningothelial hyperplasia: a detailed clinicopathologic, immunohistochemical and genetic study of 11 cases. Brain Pathol. 2005;15(2):109–15.
132. Bosch MM, Boltshauser E, Harpes P, Landau K. Ophthalmologic findings and long-term course in patients with neurofibromatosis type 2. Am J Ophthalmol. 2006;141(6):1068–77.
133. Collins VP, Nordenskjold M, Dumanski JP. The molecular genetics of meningiomas. Brain Pathol. 1990;1(1):19–24.
134. Perry A, Gutmann DH, Reifenberger G. Molecular pathogenesis of meningiomas. J Neurooncol. 2004; 70(2):183–202.
135. Heimberger AB, Wiltshire RN, Bronec R, McLendon RE, Cummings TJ. Biphasic malignant meningioma: a comparative genomic

hybridization study. Clin Neuropathol. 2002; 21(6):258–64.
136. Liu GT, Galetta SL, Rorke LB, Bilaniuk LT, Vojta DD, Molloy PT, et al. Gangliogliomas involving the optic chiasm. Neurology. 1996;46(6):1669–73.
137. Sadun F, Hinton DR, Sadun AA. Rapid growth of an optic nerve ganglioglioma in a patient with neurofibromatosis 1. Ophthalmology. 1996;103(5):794–9.
138. Lu WY, Goldman M, Young B, Davis DG. Optic nerve ganglioglioma. Case report. J Neurosurg. 1993;78(6):979–82.
139. Chilton J, Caughron MR, Kepes JJ. Ganglioglioma of the optic chiasm: case report and review of the literature. Neurosurgery. 1990;26(6):1042–5.
140. Lowes M, Bojsen-Moller M, Vorre P, Hedegaard O. An evaluation of gliomas of the anterior visual pathways. A 10-year survey. Acta Neurochir. 1978; 43(3–4):201–6.
141. Cohen M. Primary intradural tumor of the orbital portion of the optic nerve. Arch Ophthalmol. 1919; 48:19–22.
142. Sugiyama K, Goishi J, Sogabe T, Uozumi T, Hotta T, Kiya K. Ganglioglioma of the optic pathway. A case report. Surg Neurol. 1992;37(1):22–5.
143. Gritzman MC, Snyckers FD, Proctor NS. Ganglioglioma of the optic nerve. A case report. S Afr Med J. 1983;63(22):863–5.
144. Bergin DJ, Johnson TE, Spencer WH, McCord CD. Ganglioglioma of the optic nerve. Am J Ophthalmol. 1988;105(2):146–9.
145. Rodriguez LA, Edwards MS, Levin VA. Management of hypothalamic gliomas in children: an analysis of 33 cases. Neurosurgery. 1990;26(2):242–6.
146. Cogan DG, Poppen JL, Hicks SP. Ganglioneuroma of chiasm and optic nerves. Arch Ophthalmol. 1961;43:481–2.
147. Green WR, Iliff WJ, Trotter RR. Malignant teratoid medulloepithelioma of the optic nerve. Arch Ophthalmol. 1974;91(6):451–4.
148. Vadmal M, Kahn E, Finger P, Teichberg S. Nonteratoid medulloepithelioma of the retina with electron microscopic and immunohistochemical characterization. Pediatr Pathol Lab Med. 1996; 16(4):663–72.
149. Lindegaard J, Heegaard S. Tumors of the optic nerve. Expert Rev Ophthalmol. 2009;4(2):197–206.
150. Verhoeff FH. A rare tumor arising from the pars ciliaris retinae (terato-neuroma), of a nature hitherto unrecognized, and its relation to the so-called glioma retinae. Trans Am Ophthalmol Soc. 1904;10(part 2): 351–77.
151. Fuchs E. Wucherungen and Geschwulste des Ciliarepithels. Graefes Arch Clin Exp Ophthalmol. 1908;68:534–87.
152. Shields JA, Eagle Jr RC, Shields CL, Potter PD. Congenital neoplasms of the nonpigmented ciliary epithelium (medulloepithelioma). Ophthalmology. 1996;103(12):1998–2006.
153. Zimmerman LE. Verhoeff's "terato-neuroma". A critical reappraisal in light of new observations and current concepts of embryonic tumors. Am J Ophthalmol. 1971;72(6):1039–57.
154. Lindegaard J, Heegaard S, Toft PB, Nysom K, Prause JU. Malignant transformation of a medulloepithelioma of the optic nerve. Orbit. 2010;29(3): 161–4.
155. Zywicke H, Palmer CA, Vaphiades MS, Riley KO. Optic nerve hemangioblastoma: a case report. Case Rep Pathol. 2012;2012:915408.
156. Barrett R, Meyer D, Boulos A, Eames F, Torres-Mora J. Optic nerve hemangioblastoma. Ophthalmology. 2008;115(11):2095.
157. Manjandavida FP, Honavar SG, Gowrishankar S, Mulay K, Reddy VA, Vemuganti GK. Optic nerve meningeal hemangiopericytoma: a clinicopathological case report. Surv Ophthalmol. 2013;58(4): 341–7.
158. Croxatto JO, Font RL. Hemangiopericytoma of the orbit: a clinicopathologic study of 30 cases. Hum Pathol. 1982;13(3):210–8.
159. Schwent BJ, Wojno TH, Grossniklaus HE. Hemangiopericytoma of the optic nerve sheath. Am J Ophthalmol. 2007;143(5):904–6.
160. Boniuk M, Messmer EP, Font RL. Hemangiopericytoma of the meninges of the optic nerve. A clinicopathologic report including electron microscopic observations. Ophthalmology. 1985;92(12): 1780–7.
161. Furusato E, Valenzuela IA, Fanburg-Smith JC, Auerbach A, Furusato B, Cameron JD, et al. Orbital solitary fibrous tumor: encompassing terminology for hemangiopericytoma, giant cell angiofibroma, and fibrous histiocytoma of the orbit: reappraisal of 41 cases. Hum Pathol. 2011;42(1):120–8.
162. Spencer A, Lee J, Prayson RA. Optic nerve choristoma. Ann Diagn Pathol. 2005;9(2):93–5.
163. Giannini C, Reynolds C, Leavitt JA, Schultz GA, Garrity JA, Ebersold MJ, et al. Choristoma of the optic nerve: case report. Neurosurgery. 2002;50(5): 1125–8.
164. Christmas NJ, Mead MD, Richardson EP, Albert DM. Secondary optic nerve tumors. Surv Ophthalmol. 1991;36(3):196–206.
165. Lindegaard J, Isager P, Prause JU, Heegaard S. Optic nerve invasion of uveal melanoma. APMIS. 2007;115(1):1–16.
166. Kivela T, Summanen P. Retinoinvasive malignant melanoma of the uvea. Br J Ophthalmol. 1997; 81(8):691–7.
167. Ferry AP, Font RL. Carcinoma metastatic to the eye and orbit. I. A clinicopathologic study of 227 cases. Arch Ophthalmol. 1974;92(4):276–86.
168. Hervey-Jumper SL, Ghori A, Ziewacz JE, McKeever PE, Chandler WF. Langerhans cell histiocytosis of the optic chiasm: case report. Neurosurgery. 2011; 68(2):E556–61.
169. DiLuna ML, Two AM, Levy GH, Patel T, Huttner AJ, Duncan CC, et al. Primary, non-exophytic, optic nerve germ cell tumors. J Neurooncol. 2009;95(3): 437–43.

170. Hintz EB, Yeaney GA, Buchberger GK, Vates GE. Intracranial salivary gland choristoma within optic nerve dural sheath: case report and review of the literature. World Neurosurg. 2014;81(5-6):842.e1–842.

171. Cummings TJ. Chapter 8: Optic nerve. In: Ophthalmic pathology: a concise guide. New York: Springer; 2013.

Pathology of the Vitreous

8

Curtis E. Margo and Lynn E. Harman

8.1 Introduction

The vitreous is a watery, loose connective tissue whose properties are appropriately suited to serve as optical medium, mechanical buffer, and interface to the neurosensory retina. The seemingly simple, water-rich composition of the vitreous belies its physiological complexity. At times referred to as vitreous humor or vitreous body, this clear medium is rarely the site of primary disease but is susceptible to a variety of injuries and degenerations that can adversely affect vision directly or through interactions with adjacent tissues.

8.2 Anatomy

The vitreous conforms in shape to the tissues that surround it. A physical gel, it behaves as a coherent mass but is neither solid nor liquid. The vitreous makes up approximately 80 % of the globe by volume, the largest single tissue of the eye. It fills the space between the lens and ciliary body anteriorly and the retina and optic nerve head posteriorly (Fig. 8.1).

The vitreous is 98 % water and contains a network of long, unbranched collagen fibrils (90 % type II collagen) that share chemical

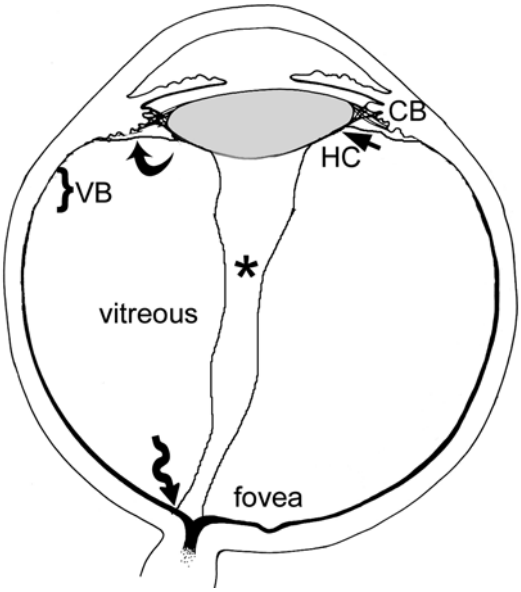

Fig. 8.1 Diagram shows normal ocular and vitreous landmarks. Cloquet's canal is located centrally (*), with the annular attachment of vitreous to the lens represented by the hyalocapsular ligament (*HC*). The vitreous base (*VB*) straddles the junction of ora serrata and pars plana; the ciliary body (*CB*) is just external and anterior to the face of anterior hyaloid (*arrow*). A firm attachment of vitreous surrounds the optic nerve head (*wavy arrow*)

C.E. Margo, MD, MPH (✉)
Departments of Ophthalmology, and Pathology and Cell Biology, Morsani College of Medicine, University of South Florida, 12901 Bruce D. Downs Blvd., MDC Box 21, Tampa, FL 33612, USA
e-mail: cmargo@heath.usf.edu

L.E. Harman, MD
Section of Ophthalmology, Department of Surgery, James A. Haley, VA Hospital, Morsani College of Medicine, University South Florida, 12901 Bruce B. Downs. Blvd., MDC Box 21, Tampa, FL 33612, USA
e-mail: lynn.harman@va.gov

S. Heegaard, H. Grossniklaus (eds.), *Eye Pathology: An Illustrated Guide*,
DOI 10.1007/978-3-662-43382-9_8,

similarities to the fibrils of articular cartilage [1]. Unlike opaque articular cartilage with its densely packed collagen, the fibrils of vitreous are widely separated. The optical transparency of vitreous is attributed to three factors: the thinness of the fibrils (8–16 nm), their wide separation, and random orientation. Given the near absence of cellular elements in the normal vitreous, light scatter is minimal, although some structural organization is perceptible with good quality slit lamp biomicroscopy.

A third critical constituent of vitreous is hyaluronic acid. As the major glycosaminoglycan of the vitreous, hyaluronic acid is a macromolecule whose flexible coiled configuration and anionic charges are ideally designed to interact with other molecules [2]. The most important interaction hyaluronic acid has is with collagen fibrils. It is through this interaction that collagen traps water and maintains proper spacing between neighboring fibrils.

Soluble proteins, low molecular weight organic and inorganic salts, and glycoproteins are also found in the vitreous [3]. Their concentrations usually mirror those in serum. The vitreous contains high levels of ascorbic acid and lactic acid. The concentration of the latter metabolite is highest in vitreous cortex presumably due to aerobic metabolism of glucose in the retina. After death, the osmolality of human vitreous is slightly greater than that of serum [4].

Notwithstanding its near optical transparency, the vitreous has a deceptively elusive architecture, best seen with magnification and special methods of illumination. Investigators attempting to characterize the gross assembly of the vitreous body have yet to arrive at any consensus [5]. Most descriptions appreciate concentric funnels each delineated as a diaphanous chamber whose apex converges on the optic disc. The most central of these funnels is Cloquet's canal, the vestigial remnants of the hyaloid vascular system. The vitreous cortex refers to the outer shell of vitreous approximately 100 μm in thickness. It corresponds anatomically to more densely packed collagen fibrils [6]. Immediately internal to the optic disc and macula, the vitreous lacks the same density of collagen fibrils found in other regions of the posterior cortex. The surface of the anterior hyaloid separates the vitreous from the posterior chamber.

The normal vitreous cortex contains cells known as hyalocytes, which by light and electron microscopy resemble macrophages. The density of hyalocytes in the cortex is low. Although they can function as phagocytic cells when appropriately stimulated, their role in normal vitreous development and homeostasis remains unclear.

The internal limiting membrane of the retina interfaces the vitreous. It is a composite structure made up of the basement membrane of Mueller cells and an inner portion of vitreous fibrils [5]. The vitreous contributions to the internal limiting membrane are anchoring fibrils, whose strength of attachment likely varies due to their density and lengths of insertion. The strongest attachments are found at the vitreous base (an approximately 3 mm zone that straddles the ora serrata), along major retinal vessels, and at the margins of the optic disc. Notable attachments are also present in the fovea and parafoveal areas. The vitreous also adheres to the posterior surface of the lens. This so-called hyaloideocapsular ligament represents an annular adhesion in the outer third of the lens capsule.

8.3 Embryology

Not long after conception, the crescent-shaped cavity between the posterior surface of the lens vesicle and inner wall of the optic cup fills with a primordial jelly known as the primary vitreous. This primitive mesenchyme is identifiable after the 3rd week of gestation; by 8 weeks, the development of primary vitreous is nearly complete. Other than minor modifications, it will remain sandwiched between lens and developing retina until completely replaced with tissue resembling adult vitreous in the last trimester.

Between the 5th and 6th weeks, the primary vitreous is invaded by vasoformative cells originating near the lens (capsula perilenticularis) and at the optic nerve head. These sprouting vessels grow towards each other to form the hyaloid vascular system, a transient vascular supply that begins to regress during the 7th month and fully involutes before birth.

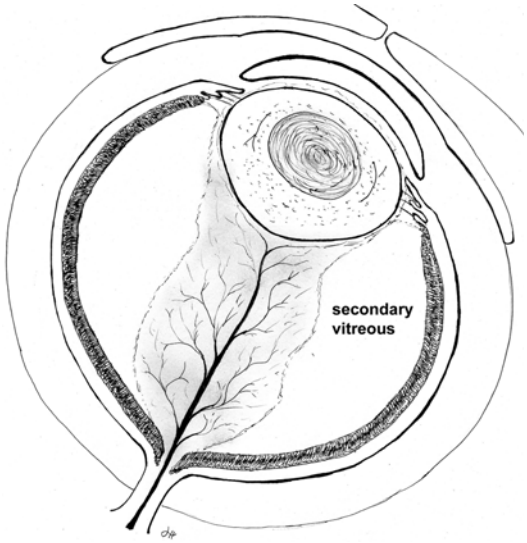

Fig. 8.2 The illustration shows the relation of the vascularized primary vitreous when it is surrounded by secondary vitreous at roughly the second month of gestation

The primary vitreous is replaced by the secondary vitreous, a process that starts at the inner surface of the retina and then progresses centrally (Fig. 8.2). As the secondary vitreous increases in mass, it compresses the vascularized primary vitreous, eventually leaving a thin layer of connective tissue surrounding the major hyaloid vessels. After the largest of these vessels regress, diaphanous sheets of connective tissue (known as Cloquet's canal) are all that remain of the embryonic hyaloid vascular system. The cell responsible for the coordinated synthesis of secondary vitreous is subject to debate.

According to the terminology just cited (originated by Ida Mann), the concept of vitreous development is biphasic. The tertiary vitreous, which refers to the suspensory ligament of the lens, is not the subject of this chapter.

8.4 Congenital Abnormalities

8.4.1 Persistent Hyperplastic Primary Vitreous

Failure of the primary vitreous to completely regress is the most common developmental anomaly of the vitreous, although in absolute terms it is a relatively rare condition. Historically, this congenital anomaly has been called persistent hyperplastic primary vitreous (PHPV), but some argue the term *persistent fetal vasculature* (PFV) is more appropriately descriptive [7]. Traditionally, PHPV was divided into anterior and posterior forms. Ninety percent of cases are unilateral, and most occur as sporadic anomalies. The genetic locus of a familial non-syndromic form of PHPV has been found on chromosome 10q11-q21 [8]. This inherited variety is transmitted as an autosomal recessive trait. Anterior PHPV presents clinically with leukocoria, as the white persistent primary vitreous is observed through a clear lens. Typically, the eye is small and has elongated ciliary processes visible around the lens when the pupil is dilated.

Histologically, anterior PHPV is characterized by a vascularized mass of loose connective tissue behind the lens (Fig. 8.3a, b). The persistent primary vitreous appears to drag ciliary processes inward. The contractile nature of this tissue is inferred by the wrinkling it causes in the posterior lens capsule (Fig. 8.3b). The posterior lens capsule may eventually tear under this stress, resulting in a granulomatous inflammatory reaction to exposed lens protein, a condition referred to as *phacoantigenic uveitis* (also incorrectly called *phacoanaphylactic uveitis* in the literature).

Posterior PHPV can be seen as an isolated malformation or associated with anterior PHPV. Failure of the hyaloid vascular system to regress behind the equator of the eye defines posterior PHPV. The posterior variant of PHPV can range from a small tuft of fibroglial tissue on the optic nerve (Bergmeister's papillae) to a patent hyaloid artery coursing to the lens. These stalks of vascular tissue can be associated with retinal folds. Small amounts of persistent primary vitreous can be associated with other developmental anomalies of the eye and should not be confused with classic sporadic PHPV [9].

8.4.2 Congenital Vitreous Cyst

Congenital vitreous cyst is a rare malformation usually detected in childhood but occasionally

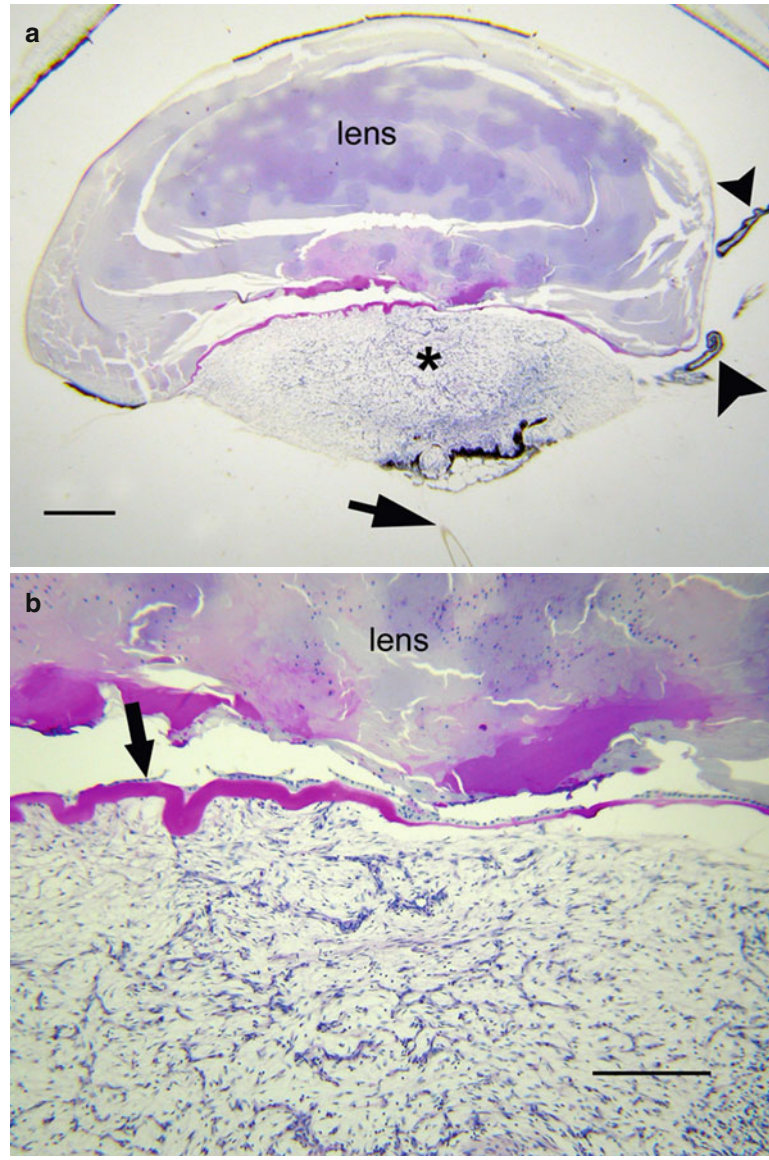

Fig. 8.3 (**a**) Persistent hyperplastic primary vitreous (*PHPV*) (*) seen with residual hyaloid artery (*arrow*) and elongated ciliary processes (*arrowheads*) (bar = 800 μ). (**b**) Higher magnification of **a** shows undulating posterior lens capsule (*arrow*) of widely varying thickness. The persistent primary vitreous is composed of bland, widely separated spindle cells (bar = 160 μ)

delayed until adulthood when the cyst causes symptoms [10–12]. The origin of vitreous cyst is speculative, with some observations supporting a choristomatous malformation related to failed regression of the hyaloid vascular system. Other evidence suggests these cysts arise from developmental defects of the retinal pigment or ciliary epithelia. Most vitreous cysts reported in the literature have been free-floating, but some are tethered to the optic nerve head. It is the latter group that implicates defective regression of the fetal hyaloid vascular system.

Clinically, vitreous cysts are nearly spherical and vary in color from gray to brown. On B-scan they appear as hypoechogenic masses. Their edges are hyperreflective. Those cysts studied histologically consist of a monolayer of cuboidal cells, either nonpigmented or partially pigmented with melanin. The cells are polarized with basement membrane on the internal surface [10]. The monolayer of cuboidal cells resembles retinal pigment or ciliary epithelia.

Congenital vitreous cysts need to be distinguished from acquired traumatic cysts, which

also occur free-floating. Their morphology, down to the ultrastructural level, can be identical to congenital vitreous cyst [13]. The critical differentiating features of this form of acquired cyst are documented absence prior to trauma and clear evidence of traumatic injury.

8.4.3 Congenital Vitreous Liquefaction

Congenital liquefaction, or syneresis of the vitreous, is a manifestation of several inherited disorders including Stickler syndrome types 1 and 2, Wagner syndrome type 1, Goldmann-Favre syndrome (enhanced S-cone syndrome), and snowflake vitreoretinal degeneration. Wagner syndrome has been associated with a mutation in the gene encoding for chondroitin sulfate, one of the minor proteoglycans of the vitreous [14]. Although early onset syneresis is a consistent feature of these vitreoretinal syndromes, histological examination of the vitreous has no routine role in clinical evaluation. Each of the above named syndromes has prominent retinal findings and, in the case of Stickler syndrome, characteristic systemic abnormalities as well [15].

8.5 Inflammation

Vitreous inflammation is virtually always a manifestation of disturbances originating outside the vitreous cavity, such as trauma, primary disorders of neighboring tissues (e.g., uveitis, scleritis, etc.), or systemic disease (e.g., sepsis, vasculitis, etc.). While the potential causes of vitreous inflammation are vast, the mechanisms of vitreous injury share common pathways. Regardless of underlying type of injury, plasma proteins and polymorphonuclear leukocytes (neutrophils) enter the vitreous, followed by macrophages. Enzymatic breakdown of the collagen latticework begins almost immediately. The result is destruction of glycosaminoglycans, collapse of the fibrillar cytoarchitecture, and liquefaction of the gel. Aggregates of insoluble proteins and clumps of inflammatory cells cause varying degrees of opacification. In terms of cellular infiltrate, vitritis traverses the spectrum of acute to chronic inflammation, including granulomatous. Since exclusion of infectious disease is a priority when confronted with vitritis, biopsy for culture and other ancillary studies play a key role in clinical evaluation.

8.5.1 Infectious Endophthalmitis

8.5.1.1 Purulent Endophthalmitis

Infectious endophthalmitis following surgery, accidental trauma, or sepsis is characterized by acute inflammation of the vitreous or, less commonly, a mixture of acute and granulomatous inflammation. How the infectious organism gained entrance to the eye (e.g., cornea, surgical wound, blood-borne, etc.) determines the general pattern of ocular inflammation. Regardless whether the trauma is surgical or accidental, the earliest and often the most intense inflammation is associated with the location of microbial contamination (Fig. 8.4). Unlike externally acquired infections, blood-borne pathogens most commonly seed the posterior segment of the eye, often in multiple locations (Fig. 8.5a, b). Even low-virulence microorganisms like *Staphylococcus epidermidis* can result in highly destructive infections inside the eye given the vulnerability of intraocular tissues and the lack of local defense mechanisms [16]. In end-stage endophthalmitis, inflammation may be so widespread that determining the anatomic starting point may no longer be possible. Tissue Gram stain, while critical for rapid identification of putative organisms, is relatively insensitive and nonspecific compared to culture or new molecular microbial technologies. Despite the limitation of tissue Gram stain, large colonies of bacteria can often be found in purulent endophthalmitis (Fig. 8.6). Since melanin granules approximate the size and shape of bacterial cocci, microscopic screening for microorganisms is tedious.

Essentially, any infectious organism or parasite can result in vitritis. Although fungi may not have as explosive a clinical onset as bacterial infection, most cause suppurative inflammation

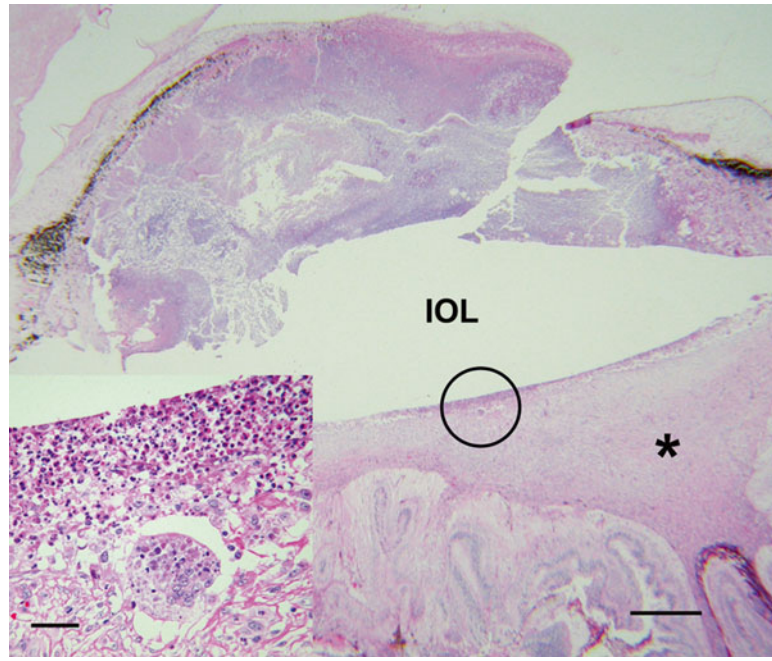

Fig. 8.4 Fungal endophthalmitis following cataract extraction shows purulent exudate anterior to the intraocular lens (*IOL*) implant. The vitreous (*) is organized and chronically inflamed. The retina is detached (bar = 800 μ). Inset shows the field within circle. There is suppurative inflammation immediately behind the IOL with necrosis, acute inflammation, and giant cells (bar = 20 μ)

within the eye, with a substantial minority inducing a mixed purulent-granulomatous pattern of inflammation. Special stains for fungus (periodic acid-Schiff or Gomori methenamine silver) are invaluable diagnostic aids (Fig. 8.5b).

8.5.1.2 Viral Endophthalmitis

Viral endophthalmitis is an elusive nosological entity, overlapping conceptually with viral uveitis, a term that implies the uveal tract as the target tissue, and viral retinitis, a relatively specific clinical condition. Since viruses require living cells to replicate, the hypocellular vitreous is an unlikely host tissue for viral infection. This is not to say that viral particles and viral DNA cannot be found in the vitreous because they are, but usually when the retina or retina-choroidal complex is the primary site of infection. This spillover phenomenon is usually accompanied by varying degrees of retinal inflammation. Spillover vitritis has been documented for retinitis due to herpes simplex type 1, herpes simplex type 2, varicella-zoster virus, cytomegalovirus (CMV), West Nile virus, and Rift Valley virus [17–20].

The clinical diagnosis of a spillover vitritis due to virus is often based on the funduscopic appearance of the retina. The clinical pattern described as acute retinal necrosis (ARN), for instance, may not be pathognomonic of a single virus, but it restricts the differential diagnosis to several principle viruses [17]. Systemic evaluation and ancillary studies enhance diagnostic certainty, often obviating the need of biopsy for culture or polymerase chain reaction (PCR). Studies of spillover vitritis have shown that PCR assays performed on aqueous humors have comparable sensitivity and specificity as samples harvested from vitreous [21].

Retinitis due to coxsackievirus, Epstein-Barr virus, rubeola virus (both congenital and acquired), and human immunodeficiency virus usually does not result in clinically significant vitreous inflammation [22].

Presumed herpetic vitritis, also referred to as herpetic uveitis, can occur in the absence of retinal inflammation [17]. These cases present as so-called idiopathic vitritis, though most patients have a history of past herpetic eye disease. The diagnosis is confirmed by harvesting vitreous for viral culture or PCR [17].

Is it possible that other viruses might be responsible for idiopathic vitritis (or uveitis)? One study examined vitreous samples from over 100 patients with retinitis or vitritis for DNA

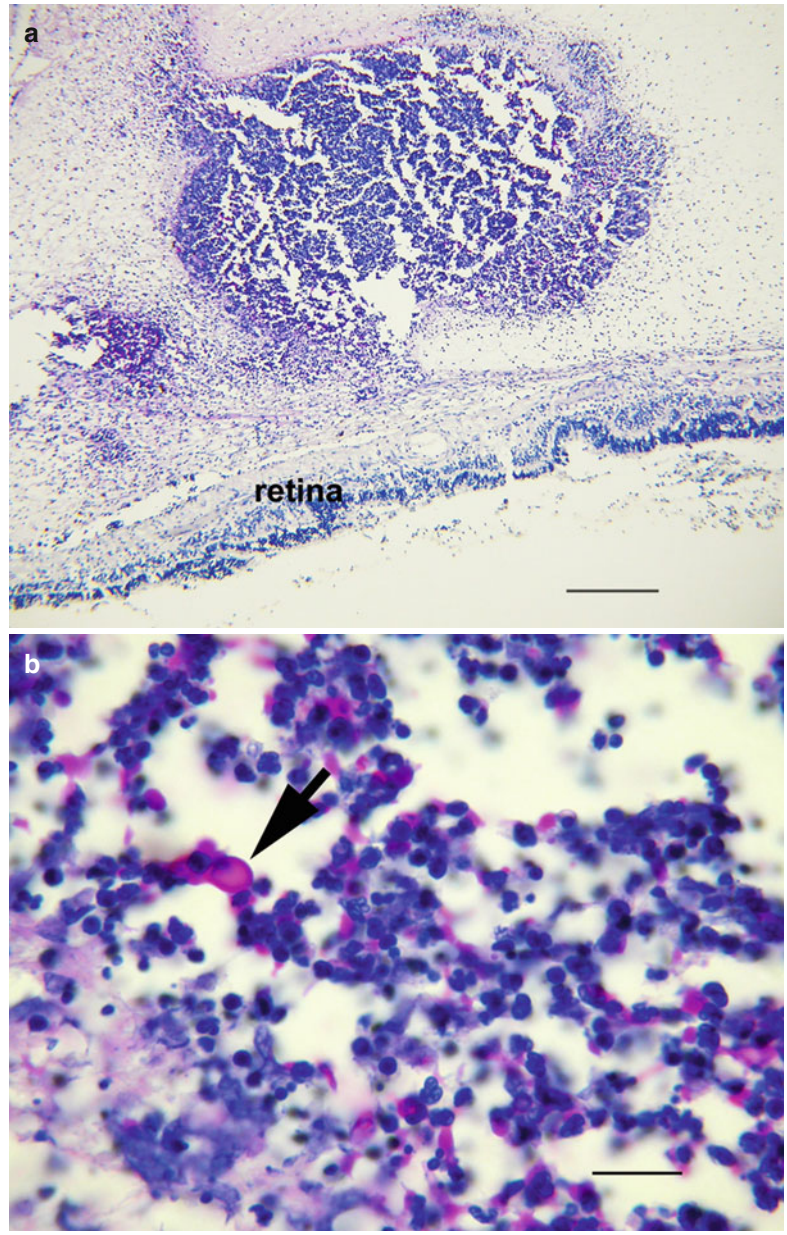

Fig. 8.5 (**a**) Endophthalmitis due to blood-borne infection with *Candida albicans*. A vitreous abscess is present immediately anterior to the retina (bar = 250 μ). (**b**) High magnification of **a** shows yeasts within the abscess (periodic acid-Schiff stain; bar = 35 μ)

from human herpesvirus 6A, 6B, and 7. Using PCR, they reported detectable viral DNA from less than 2 % of samples from patients with inflammation [23]. The search for putative viral pathogens is ongoing.

Histopathology: The histopathology of viral vitritis is documented haphazardly in the literature in studies dealing with idiopathic uveitis and posterior segment inflammation of unknown cause [18, 22, 24, 25]. Vitreous samples reveal nonspecific chronic inflammation. Unless an inadvertent piece of retina is mixed in the sample, cytopathic viral changes are usually not observed.

8.5.1.3 Low-Virulence Bacterial Endophthalmitis

Propionibacterium acnes endophthalmitis is a delayed-onset infection following cataract

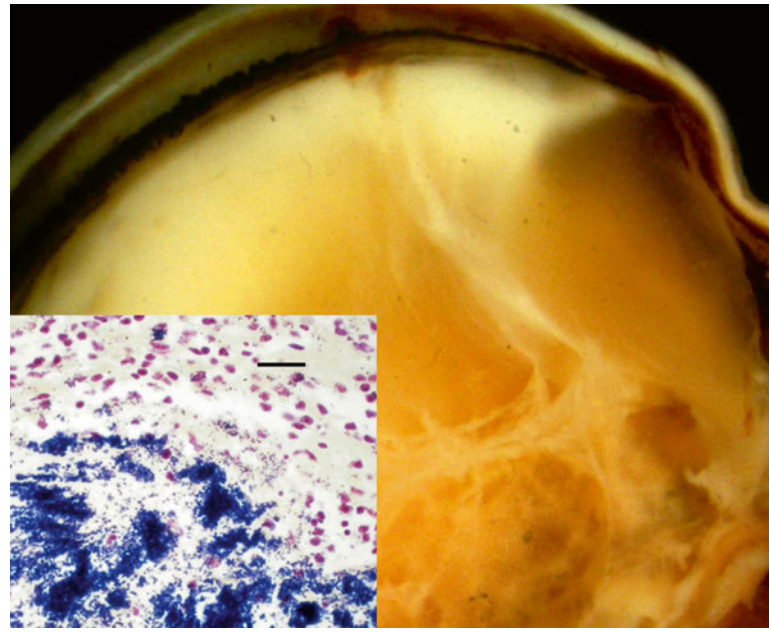

Fig. 8.6 Suppurative endophthalmitis due to a viridans streptococcus. The internal structures of the eye are effaced by purulent exudate. The vitreous has been transformed into loculated pus. *Inset* shows myriad bacteria with tissue Gram stain (Gram stain; bar = 30 μ)

surgery with implantation of a posterior chamber lens. Clinical manifestations begin several weeks or months after the procedure. Its pathogenesis and histological findings are distinctive enough to deserve separate discussion. A commensal microbe of skin and lid margin, *P. acnes* is a low-virulence Gram-positive coccus. The bacterium is introduced into the capsular bag at the time of surgery when the artificial lens is inserted into the eye. Bacteria dragged into the eye are wedged between lens capsule and lens implant, where they grow relatively unimpeded. A chronic low-grade uveitis weeks or months after cataract surgery is often the first sign of intraocular infection [26]. White plaques within the capsular bag, often near the equator, are seen in some cases. These plaques correlate with myriad bacteria sequestered between folds of lens capsule or between lens capsule and lens implant. Anterior chamber inflammation may demonstrate large or *mutton-fat* keratic precipitates. Neodymium-yttrium-aluminum-garnet (YAG) laser capsulotomy can release bacteria into anterior vitreous, provoking more intense inflammation. Vitrectomy and posterior capsulotomy are necessary when uveitis fails to respond antibiotic therapy.

Vitreous harvested at surgery yields *P. acnes*, although the organism may take weeks to grow in culture. Histologically, the Gram-positive organism is usually found next to lens capsule, often without significant contiguous inflammation (Fig. 8.7)

Similar clinical scenarios have been reported with other low-virulence organisms, such as *S. epidermidis*, *Corynebacterium*, *Achromobacter*, and several types of fungi (Fig. 8.8).

8.5.2 Whipple's Disease

Whipple's disease is a chronic infection of *Tropheryma whipplei*, a fastidious intracellular bacillus that cannot be routinely cultured [27]. The epidemiology of Whipple's disease is incompletely understood and had been considered for many years an intestinal dystrophy characterized by infiltration of the small bowel with PAS-positive macrophages. It is now known that those PAS-positive cells contain the causative organism and that the clinical spectrum of the disease is much wider than originally believed. The organism is known to involve the central nervous

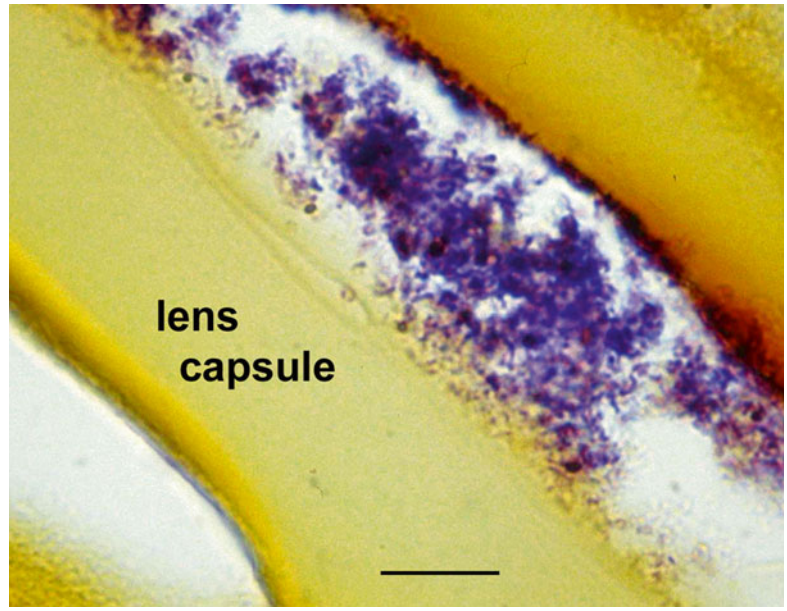

Fig. 8.7 Chronic vitritis after cataract surgery due to *P. acne* infection. Lens capsule was removed during therapeutic vitrectomy. Markedly degenerating, Gram-positive organisms are present without inflammation (tissue Gram stain; bar = 6 μ)

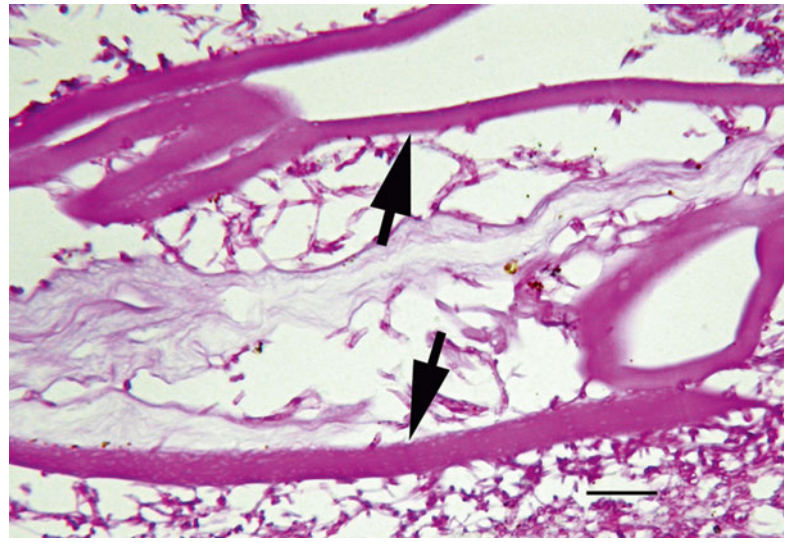

Fig. 8.8 Surgically removed lens capsule for low-grade uveitis following cataract surgery shows folded lens capsule (*arrows*). The hematoxylin-eosin stain reveals numerous fungal hyphae in the absence of inflammatory cells (bar = 15 μ)

system, joints, lymph nodes, and the eye, where it most commonly presents as vitritis (uveitis) [28]. The diagnosis of ocular Whipple's disease is elusive and might not even come to mind in the absence of malabsorption syndrome.

Vitreous biopsy of Whipple's disease shows atypical macrophages with partially vacuolated cytoplasm (Fig. 8.9). The cells may appear less "foamy" than those seen in the small bowel and can resemble macrophages infected with *M. avium-intracellulare*. Cells similar to Whipple's cells have been described in treated endophthalmitis from a coryneform bacterium (Fig. 8.10) [29]. Even though *Tropheryma whipplei* cannot be routinely cultured, vitreous fluid can be collected for polymerase chain reaction, which is highly sensitive and specific in identifying the organism [30].

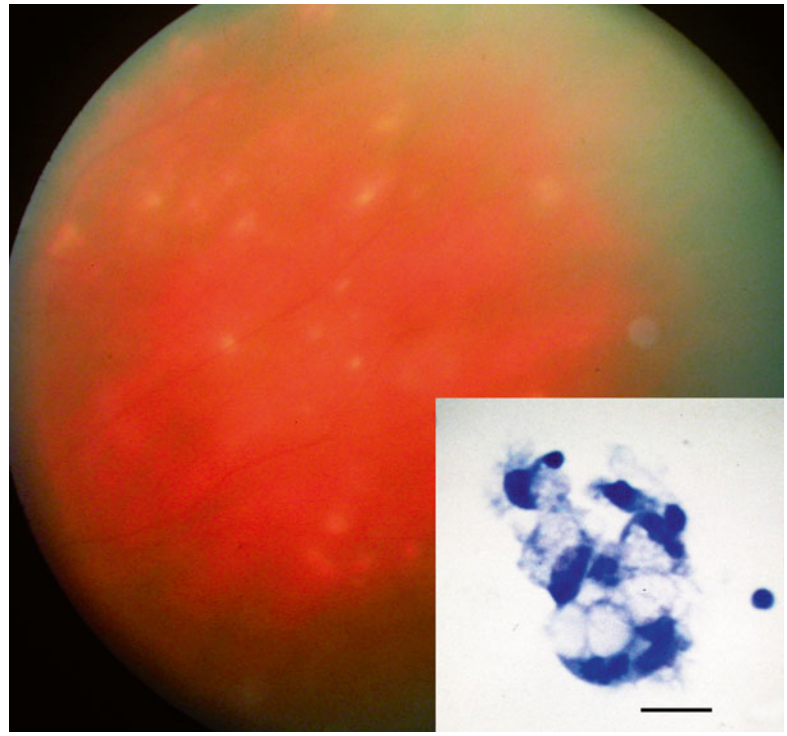

Fig. 8.9 Fundus photograph of 68-year-old woman with bilateral uveitis due to Whipple's disease. Small hypopigmented lesions of the retina are noted. *Inset* shows clump of macrophages with vacuolated cytoplasm from vitreous biopsy, which leads to confirmatory jejunal biopsy (bar = 20 μ) (Courtesy of Alan Friedman, MD. Presented at 1986 Eastern Ophthalmology Pathology Society Meeting)

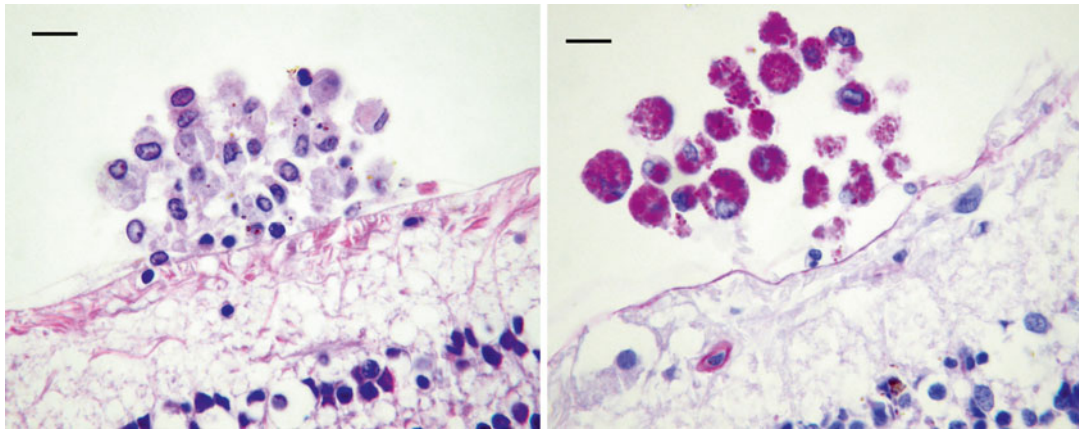

Fig. 8.10 Treated coryneform bacterium endophthalmitis shows a clump of macrophages with pale cytoplasm resting near the retina on left. With PAS (*on the right*) the cells are filled with bright magenta granules. The eye was obtained at autopsy (death unrelated to surgery). The macrophages are virtually indistinguishable from cells in Whipple's disease (bars = 20 μ)

8.5.3 Vitreous Inflammation from Parasites

8.5.3.1 Toxocara Endophthalmitis

Human infection with *Toxocara canis* is acquired through the ingestion of soil contaminated with encysted larva. This intestinal roundworm is a cosmopolitan parasite ubiquitous in the dog family, but its life cycle cannot be completed in humans. It is the second or third larval stage of the parasite that gives rise to the human disorder known as visceral larval migrans (VLM), a

disease seen primarily in children. The average age at diagnosis is 7 years, but in some regions the peak incidence is between 1 and 3 years. The majority of those infected present before the age of 16 [31]. Not all children infected with *T. canis* are symptomatic with VLM, which usually causes low-grade fever, coughing or wheezing, lassitude, and weight loss. Some children escape the systemic illness related to generalized migration of the larvae, only later to present with isolated end organ disease. Ocular infection is almost always due to a single larva. Though theoretically the larva could affect any portion of the eye, many appear to enter the globe at or near the optic disc before dying in the vitreous.

Clinical Features: Ocular toxocariasis usually presents as a single mass lesion either in or beneath the retina or in the vitreous, associated with inflammation [32]. Often a vitreoretinal membrane connecting the optic disc to the inflammatory mass can be seen ophthalmoscopically. This membrane represents the presumed larval path prior to death. More advanced cases are characterized by either heavy vitritis, which precludes direct visualization of the retina, or a white pupil reflex (leukocoria).

The cellular responses to dead and dying larvae are similar regardless of the tissue involved, but when *T. canis* dies within vitreous, the reaction can be exuberant, particularly in terms of fibroplasia (Fig. 8.11a).

Histopathology: The early cellular response is characterized by eosinophils and plasma cells. An eosinophilic abscess is a histological hallmark of the infection and marks the presumed location of larval death (Fig. 8.11b). Plasma proteins and degranulating eosinophils mixed with other acute inflammatory cells give the tissue a smudgy pink color with hematoxylin-eosin stain. This amorphous hyaline material is referred to as the Splendore-Hoeppli phenomenon and is associated with a variety of parasites and fungi (Fig. 8.12) [33]. Granulomatous inflammation is also a frequent finding, but is usually focal and can include multinucleated giant cells of the foreign body type (Fig. 8.13).

T. canis is about 400 μ in length and 15–20 μ in diameter. Fragments of the dead organism can be difficult to find in tissue section, and seldom has a completely intact larva been observed. The outer cuticle of the nematode encircles its digestive tract and rarely escapes partial destruction. Larvae dying in or near the vitreous will incite a profound inflammatory reaction. The chances of sampling an organism on vitreous biopsy are remote, but the inflammatory reaction often includes eosinophils and plasma cells. Neglected cases can proceed to retinal detachment followed by chronic inflammation and scarring. Exuberant fibroplasia resulting in replacement of the vitreous with dense collagen has been referred to as sclerosing endophthalmitis. Although fibrous replacement of the vitreous is not specific for toxocariasis, few other disorders, particularly in childhood, have been associated with this robust pattern of scarring. Even at a late stage of tissue repair, eosinophilic abscesses and portions of larva can be found (Fig. 8.14).

Laboratory studies play a role in the evaluation of children suspected of having ocular toxocariasis. Since ocular manifestations of *T. canis* typically are temporally removed from systemic dissemination of larva, eosinophilia is usually not present. The enzyme-linked immunosorbent assay (ELISA) for *T. Canis* has good diagnostic sensitivity, but some assays cross-react with other helminths. Strong presumptive evidence of ocular toxocariasis exists when ELISA titers from aqueous or vitreous fluids are higher than simultaneous serum samples [34].

8.5.4 Other Nematodes

Diffuse unilateral subacute neuroretinitis, or DUSN, is a generalized inflammatory disorder of the retina, choroid, and optic nerve. This unilateral inflammatory condition has been linked to infection with two related intestinal nematodes found in raccoons and squirrels. The putative worms are distinguished clinically by their size. The larger *Baylisascaris procyonis* measures about 2 mm, while the smaller *Ancylostoma caninum* is 0.4 mm [35, 36]. The clinical diagnosis depends on identifying the worm at the slit lamp. It is usually found beneath the neurosensory

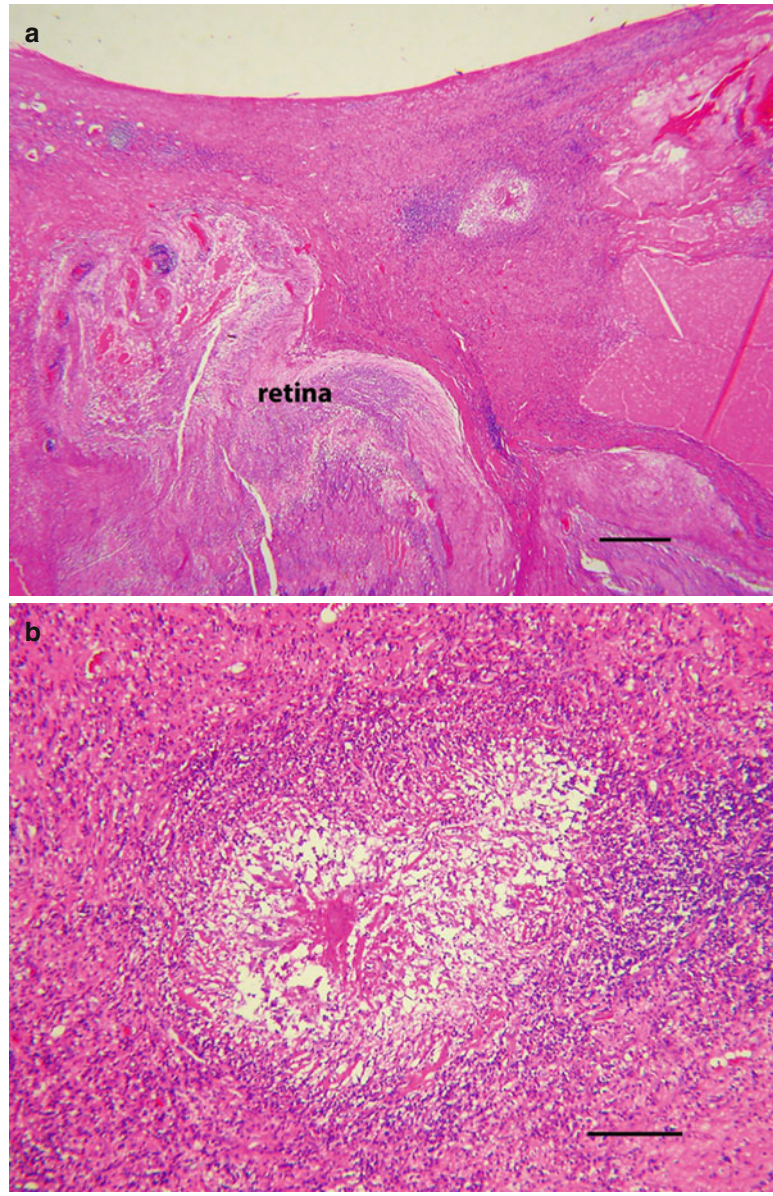

Fig. 8.11 (**a**) Toxocara endophthalmitis in a young boy. The retina is detached and the vitreous is replaced with inflamed fibrous tissue. Centrally within the densely collagenized vitreous is an area of necrosis (bar = 130 μ). (**b**) Higher magnification of **a** shows the area of necrosis and chronic inflammation, the presumed site of a degenerated nematode. The clinical diagnosis was supported by high ELISA titers for *T. canis* (bar = 35 μ)

retina. The heat of a laser can provoke the worm to move. On occasion, worms have been found in the vitreous, where they can be extracted surgically [36].

Live nematodes have been reported in the vitreous of persons infected with the larva stage of *Gnathostoma*, a parasite endemic in Southeast Asia and India [37]. Humans acquire the infection by eating raw or undercooked freshwater fish. Subcutaneous infection around the eye precedes ocular involvement. The larva gains access to the conjunctiva and the deeper tunics of the globe in route to the vitreous. The larva is accompanied by vitreous inflammation and, occasionally, hemorrhage.

Microfilariae capable of invading the vitreous include the larva stage of *Onchocerca volvulus*, the microfilaria of *Wuchereria bancrofti*, and the third stage larva of *Angiostrongylus cantonensis* [38]. Vitreous involvement with these particular nematodes occurs with signs of widespread ocular inflammation. Vitreous involvement with *Angiostrongylus cantonensis* is associated with eosinophilic meningitis [38, 39].

Fig. 8.12 Splendore-Hoeppli phenomenon in a case of clinically supported Toxocara endophthalmitis. The smudgy pink deposits (*) mark the assumed path of the dying larva (bar = 95 μ)

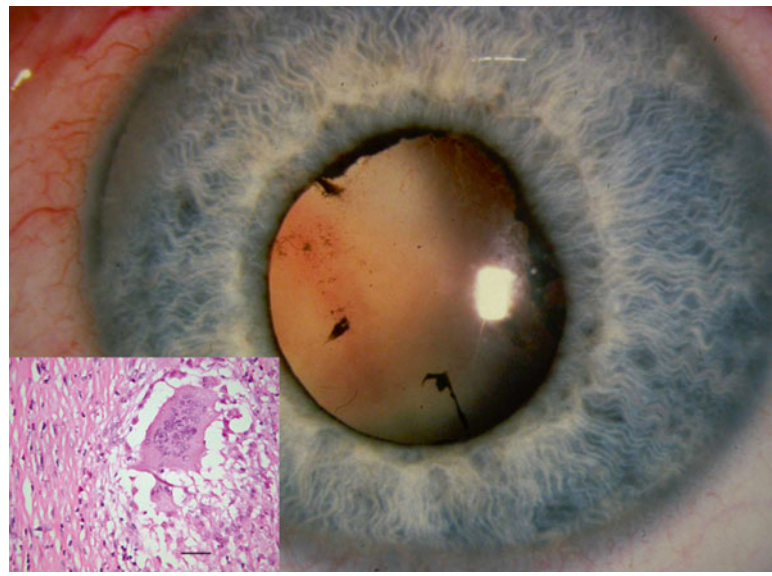

Fig. 8.13 Toxocara endophthalmitis in a child with leukocoria. Inset of the enucleated eye shows vitreous fibrosis with a single focus of granulomatous inflammation. Multinucleated giant cells were found at the presumed site of nematode death (bar = 20 μ)

8.5.5 Cestodes

Taenia solium, or pork tapeworm, gives rise to the human infection taeniasis or cysticercosis. The life cycle begins with the adult worm inhabiting the small intestine of humans and culminates with the larval stage and systemic dissemination. Cysticercosis occurs worldwide and is acquired by eating raw or undercooked pork. Usually, one adult worm lives in the small intestine of humans, but it can attain a length of 2–4 m. The human host must shed gravid proglottides before the pig (intermediate host) can complete the life cycle. After the pig ingest proglottides, eggs hatch inside the intestine and then disseminate through the blood and lymphatics, finally lodging in the muscle. Humans eating inadequately cooked pork that contains cysticerci (or auto-infect themselves with eggs or proglottides) are at

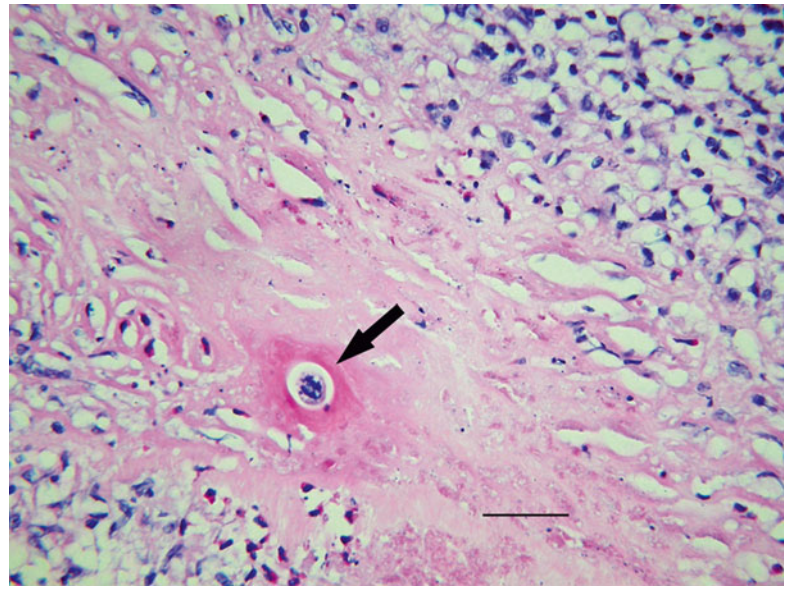

Fig. 8.14 Minute fragment of presumed helminth (*arrow*) embedded in dense fibrous tissue that replaced the vitreous (bar = 25 μ)

risk of developing the disseminated larval stage of the disease.

The larvae of *Taenia solium* most often invade the subcutaneous tissue, muscle, brain, and eye. Those that migrate to the eye have been reported in conjunctiva and beneath the retina [38]. Cysticerci can enter the vitreous where they develop into cysts, ranging upward to 8 mm in diameter. The white scolex, which moves when irritated by the light of the ophthalmoscope, is a key diagnostic finding. Cysts can be removed surgically and the diagnosis confirmed histologically [40]. Cysts are filled with turbid fluid. Microscopically, the cyst wall is composed of an outer cuticle and inner layer of smooth muscle (Fig. 8.15). The scolex contains a sucker and hooklets.

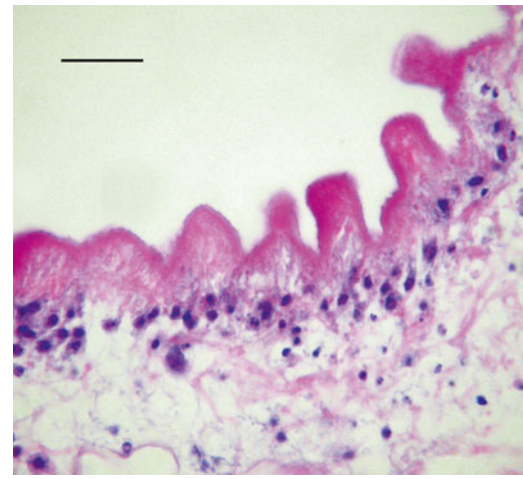

Fig. 8.15 Cysticercus removed from the eye surgically. The cyst wall is nodular. This region of the tegument lacks discernible smooth muscle; only degenerating nuclei are visible beneath the outer cuticle (bar = 25 μ)

8.5.6 Vitreous Ophthalmomyiasis

The larvae of parasite flies of humans belong to the order Diptera. Members of this order are also important vectors of bacterial, viral, and protozoan diseases. The larvae (commonly referred to as maggots) are capable of invading the eye, where they can be found in the vitreous (Fig. 8.16). Ophthalmomyiasis is the term given to maggots that burrow through ocular tissues. Most of these parasite flies belong to the genus *Cuterebra* [41].

8.6 Autoimmune Vitritis and Spillover

A variety of autoimmune diseases and uveitic syndromes are associated with vitritis. This heterogeneous group of disorders includes such entities as sympathetic ophthalmia, birdshot retinochoroidopathy, and Vogt-Koyanagi-Harada syndrome to name a few. Vitreous inflammation in these conditions is considered spillover from

the primary site of involvement. Clinical diagnoses usually depend on recognition of other key findings and ancillary laboratory studies. Vitreous biopsy is usually considered to have a role in this setting when clinical features are insufficient to exclude an infection or neoplastic vitritis.

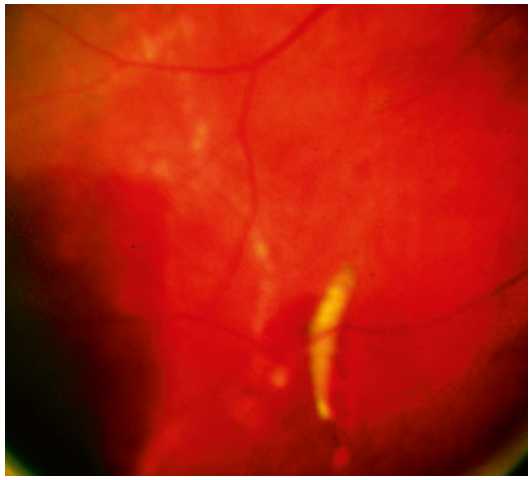

Fig. 8.16 Fundus photograph of ophthalmomyiasis and vitreous hemorrhage. A little maggot resides in the subretinal space contemplating a sojourn in vitreous

8.6.1 Phacoantigenic Uveitis

Phacoantigenic (phacoanaphylactic) uveitis is a morphologically distinct autoimmune disorder of the eye. Its pathogenesis is thought to represent an immunological and cellular reaction to normal lens protein following exposure of sequestered proteins by accidental or surgical trauma. Lens proteins are isolated from the immune system throughout life by a thick basement membrane (lens capsule), making them theoretically foreign antigens to the body's immune system. Vitritis is a consistent clinical manifestation of phacoantigenic uveitis, although other complications may dominate the clinical picture.

The inflammatory reaction directed against normal lens is usually intense, initially involving neutrophils and then lymphocytes and epithelioid histiocytes (Fig. 8.17). A mixture of both acute and chronic granulomatous inflammation is almost always seen histologically. Inflammatory cells intimately surround exposed lens, forming a mantle of neutrophils and epithelioid histiocytes. If the inciting lens protein is not removed, acute inflammatory cells are eventually replaced with

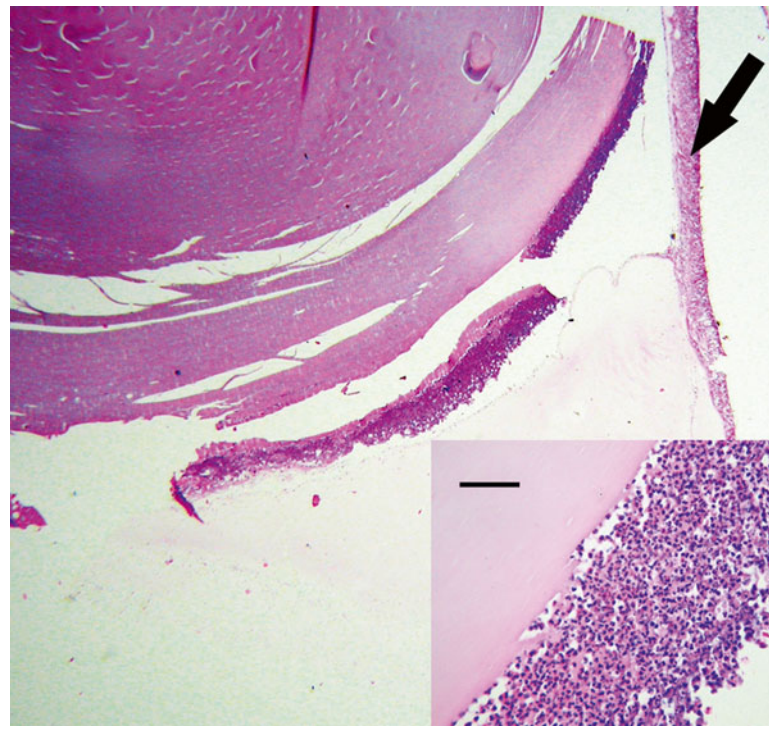

Fig. 8.17 Phacoantigenic endophthalmitis with dislocated lens in the vitreous. *Arrow* points to the retina. *Inset* shows higher magnification of the lens, which is covered posteriorly by a rim of acute inflammatory cells. There is no lens capsule (bar = 35 μ)

histiocytes and fibrous tissue. The pattern of chronic inflammation may become that of a palisading granuloma, with large histiocytes oriented perpendicular to residual lens. Neglected phacoantigenic uveitis causes considerable ocular morbidity. Not unexpectedly, phacoantigenic uveitis is associated with sympathetic uveitis, since both conditions are causally linked to trauma. Treatment involves surgical removal of the inciting lens material, plus adjuvant medical therapy to control inflammation (see also pages 30 and 183).

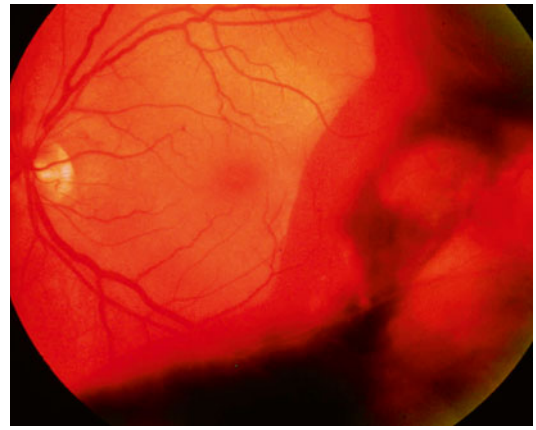

Fig. 8.18 Vitreous hemorrhage obscures visualization of the retina. Red blood cells or varying density allow partial to no view of retina

8.7 Hemorrhage

Since the presence of blood in the vitreous is abnormal, the determination of the underlying cause of bleeding is essential. From the pathologist's vantage point, the diagnostic problem is twofold: first, to accurately identify red blood cells (and, if possible, estimate the stage of catabolism) and, second, to determine the source of bleeding. The second objective may not be possible if working with a limited sample such as vitreous biopsy, but may be achievable when examining the eye in its entirety [42].

The precise location of blood in the vitreous space affects its clinical features and determines the rate of cellular catabolism. Hemorrhage within the gel differs from retrohyaloid hemorrhage because blood in the later space is located outside the vitreous proper (Fig. 8.18). Blood in the retrohyaloid space sits between the posterior hyaloid surface and internal limiting membrane and tends to thrombose and lyse more rapidly than blood when confined to vitreous [43].

Etiology: The causes of vitreous hemorrhage are vast, from trauma and diabetic retinopathy to macular degeneration and blood dyscrasia [42]. In clinical practice, the most common causes of vitreous hemorrhage are retinal neovascularization (most often due to diabetes and retinal vascular occlusive disease) and retinal tears involving overlying (bridging) vessels, usually associated with age-related vitreous syneresis. Similarly, an acute posterior vitreous detachment can also deroof a superficial retinal blood vessel resulting in vitreous hemorrhage. Identifying the source of vitreous hemorrhage, for which clinical algorithms exist, is beyond the scope of this chapter.

Blood that enters the vitreous degrades differently from blood in other extravascular sites, as the vitreous modulates the interaction of red blood cells with other cells and with enzymes. Red cells in the vitreous form a fibrin thrombus relatively quickly, but the cellular response of neutrophils and macrophages is delayed. Because of the lack of intrinsic vasculature and the inhibitory effects of vitreous on phagocytosis, the breakdown of red blood cells is prolonged in vitreous compared to other connective tissues [44, 45]. Erythrocytes release iron when hemolyzed, making it possible for unbound ions to induce free radical injury. The vitreous, unlike most other tissues, can have a substantial number of erythrocytes escape hemolytic destruction, giving rise to erythroclasts, or ghost cells.

Observations in experimental studies and in humans show that iron is present in macrophages within 2–4 days after intraocular hemorrhage [42, 46, 47]. Most of these iron-bearing cells are found in or near the uveal tract, but with time intracellular catabolism of erythrocytes becomes more widespread. Histological evidence of red blood cell catabolism ranges from free erythroclasts (Fig. 8.19a) and macrophages stuffed with degenerating erythrocytes (Fig. 8.19b) to extracellular clear spaces

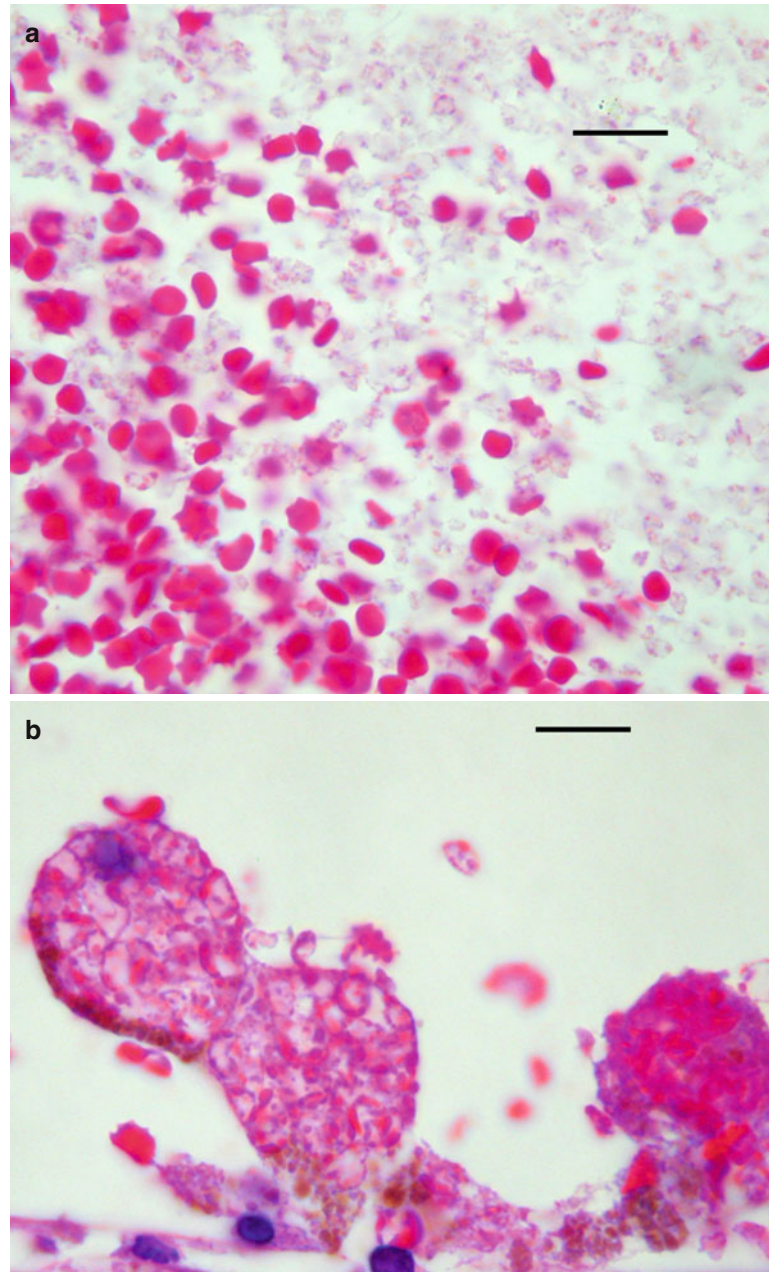

Fig. 8.19 (**a**) Vitreous hemorrhage shows both intact red blood cells to the left and erythroclasts to the right (bar = 20 μ). (**b**). Vitreous hemorrhage with macrophages filled with degenerating red blood cells (bar = 20 μ)

(cholesterol clefts) with foreign body granulomatous inflammation (Fig. 8.20).

Histopathology: Red blood cells that elude phagocytosis undergo slower, alternative forms of degradation. Hemoglobin from these cells is degraded through other pathways, but the walls of erythroclasts usually demonstrate deposits of denatured hemoglobin (i.e., Heinz bodies). Clinically, ghost cells residing in the vitreous appear as ochre-colored membranes. Histologically, the hollow carcasses of red blood cells are easily visible. With Giemsa stain, numerous Heinz bodies are seen stuck to the walls of these degenerating cells. Erythroclasts are relatively inflexible compared to normal erythrocytes. If ghost cells from a vitreous

hemorrhage find their way into the anterior chamber, they tend to become lodged in the trabecular meshwork, causing elevated intraocular pressure, or so-called ghost cell glaucoma.

Extracellular breakdown of vitreous blood can also lead to the liberation of free hemoglobin from the red cell membrane, where, for reasons not understood, the molecules aggregate into 10–20 μ spherules (Fig. 8.21). These free, unbound clumps of hemoglobin are referred to collectively as hemoglobin spherulosis. The recognition of this morphological curiosity can be confirmed by immunohistochemical stains for hemoglobin A [48].

The rate of clearance of vitreous blood is highly variable, ranging from months to 2 years, depending in part on the volume of initial hemorrhage and its location. Other than secondary syneresis, vitreous blood can also contribute to the formation and propagation of membranes.

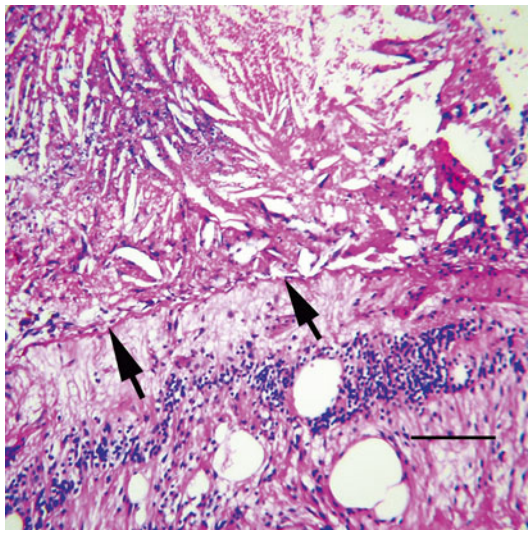

Fig. 8.20 Site of remote vitreous hemorrhage just anterior to internal limiting membrane (*arrows*) of retina shows numerous cholesterol clefts and chronic inflammation. Cystic edema is noted in the retina (bar = 60 μ)

8.8 Membranous Proliferations

The growth of membranes on the surface of the retina and in the vitreous cavity is a manifestation of a heterogeneous group of conditions. There is no universally accepted method of classifying vitreous membranes. One scheme based on anatomical and physiological criteria places membranes into three groups: (1) epiretinal membranes (ERM), (2) ocular ischemia-related retinal neovascular membranes, and (3) proliferative vitreoretinopathy (PVR). These membranes have overlapping characteristics morphologically and cytologically [49]. Unlike

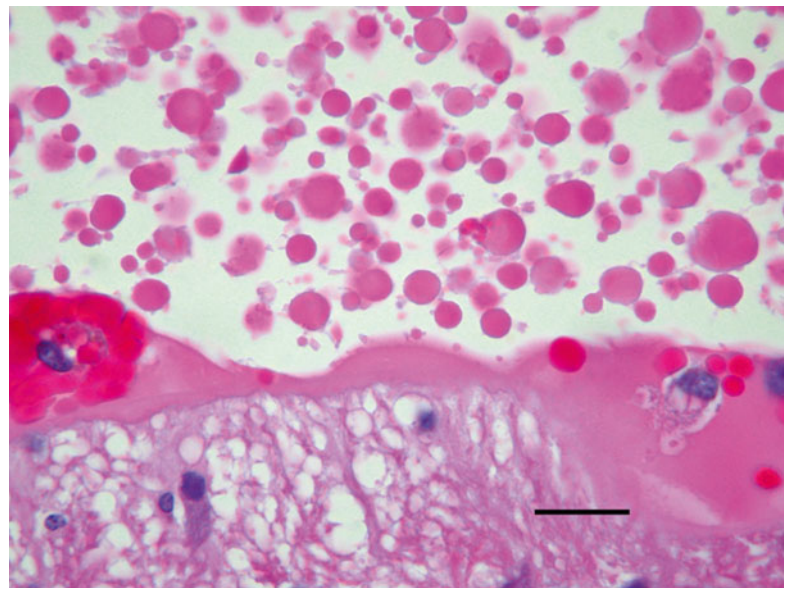

Fig. 8.21 Remote vitreous hemorrhage shows numerous globules of free hemoglobin, a process collectively referred to as hemoglobin spherulosis (bar = 20 μ)

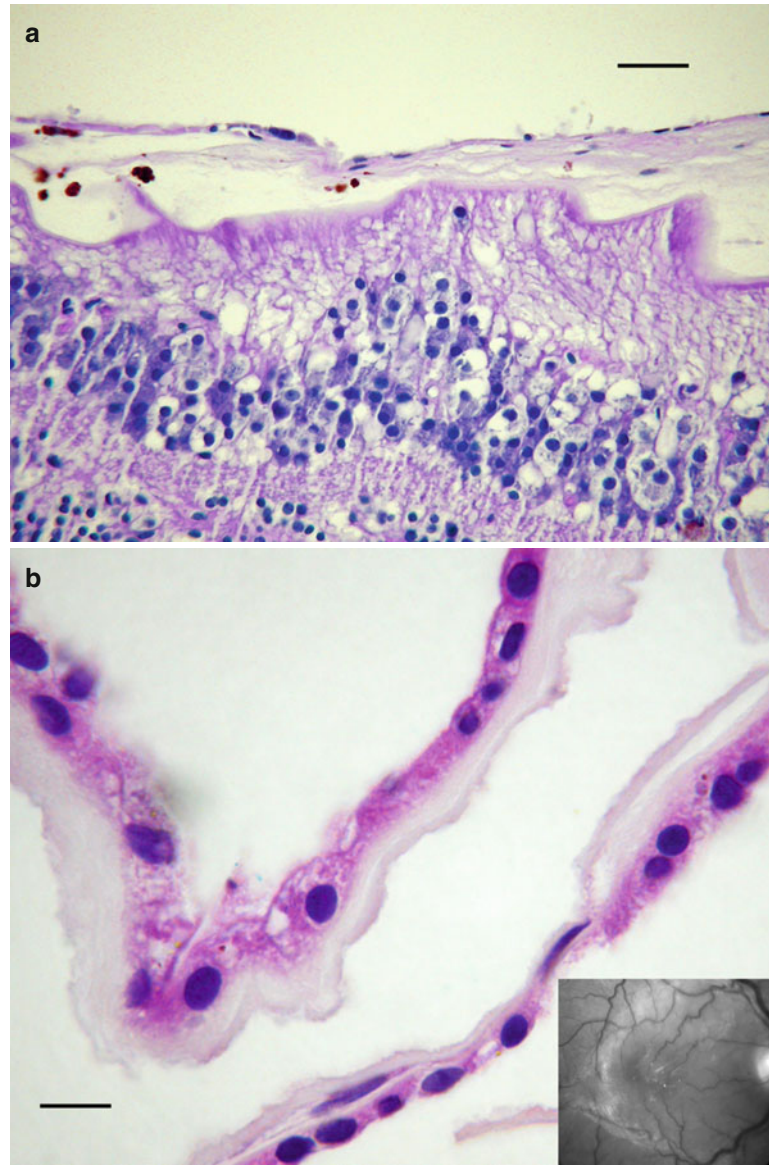

Fig. 8.22 (**a**) An avascular epiretinal membrane (*ERM*) composed of sparse spindle cells. This ERM developed after treatment of rhegmatogenous retinal detachment and vitreous hemorrhage. Pigmented cells contain hemosiderin (bar = 35 μ). (**b**) A surgically excised idiopathic epiretinal membrane consists of a monolayer of nonpigmented cuboidal cells and basement membrane (bar = 35 μ). The cell origin is presumed retinal pigment epithelium. *Inset* shows clinical appearance of this membrane in a red-free fundus photograph

PVR and retinal neovascularization, however, ERMs are avascular.

8.8.1 Epiretinal Membranes

Epiretinal membranes are found on the inner surface of the retina and are composed of mixtures of glial cells, transformed retinal pigment epithelium (RPE), fibrocytes, macrophages, and myofibroblasts. Epiretinal membranes are associated with several common conditions like macular holes and retinal tears, but most have no identifiable cause (Fig. 8.22a). By default, this latter group is called idiopathic ERM. It is assumed that microscopic breaks in the internal limiting membrane are a conduit for cells to reach the retinal surface. The prevalence of idiopathic ERM increases with age. The predominant cell type in epiretinal membranes is a fibrous astrocyte or metaplastic fibroblast, but on occasion can consist of cuboidal cells growing in a monolayer

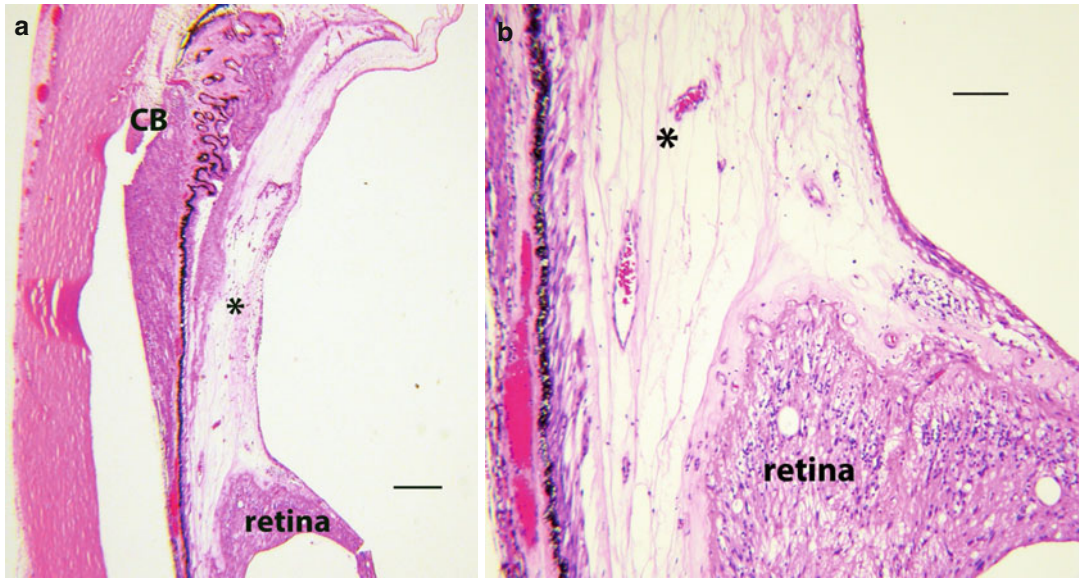

Fig. 8.23 (**a**) Anterior proliferative vitreoretinopathy. The membrane (*) has formed between the peripheral retina and ciliary body (*CB*) having used residual vitreous cortex after vitrectomy as a scaffold (bar = 470 μ). (**b**) Higher magnification of the anterior vitreous membrane shown in Fig. 8.20a. The membrane is mildly inflamed and contains relatively few vessels (bar = 40 μ)

(Fig. 8.22b). These cuboidal cells are a presumptively retinal pigment epithelium and may lack identifiable melanin. The pathology of ERMs is more thoroughly reviewed under disorders of the retina.

8.8.2 Proliferative Vitreoretinopathy

Proliferative vitreoretinopathy describes an exuberant cellular process characterized by the growth of membranes on surfaces of the retina and in the vitreous. The term proliferative vitreoretinopathy was introduced in 1983 by the Retina Society Terminology Committee to improve communication among clinicians and researchers, since earlier names like massive vitreous retraction and periretinal proliferation lead to confusion in the literature [50].

Ultrastructural studies have shown up to five types of cells in these membranes, but RPE cells and metaplastic fibroblasts are the foremost inhabitants. The membranes of PVR cover surfaces and efface the normal tissues they grow on. In the vitreous, membranes can become bulky and densely fibrotic. Their contractile properties distort underlying tissues and propagate retinal detachment. When the majority of PVR exists anterior to the equator and in cortical vitreous, it is referred to as anterior PVR (Fig. 8.23). Proliferative vitreoretinopathy needs to be distinguished from the so-called massive gliosis of the retina, another uncontrolled reparative phenomenon. Like PVR, massive gliosis can fill the vitreous cavity, but this exuberant form of reactive gliosis is essentially an intraretinal process that expands into the vitreous cavity as the gel collapses (Fig. 8.24a, b).

The term *cyclitic membrane* refers to an anatomical subset of PVR that uses the anterior hyaloid face as scaffolding. In this situation, fibrovascular tissue grows like a diaphragm from the ciliary body across the retrolenticular space (Fig. 8.25). Cyclitic membranes are usually associated with significant injury or inflammation and are common in phthisical eyes. The membranes themselves contribute to hypotony by exerting traction on ciliary processes thereby reducing aqueous production.

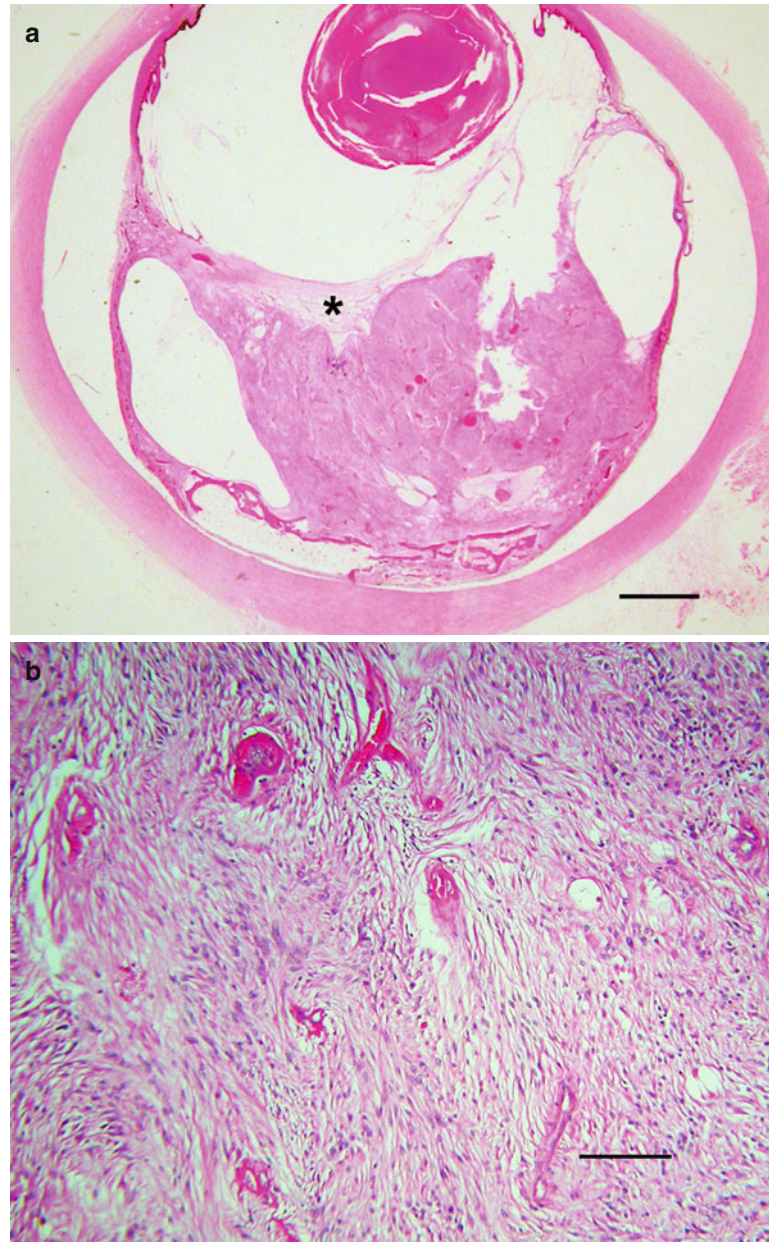

Fig. 8.24 (**a**) Reactive gliosis in a phthisical eye. The vitreous cavity in this eye has been compressed by voluminous glial tissue, a process referred to as massive gliosis. The remaining vitreous (*) can still be seen surrounded by reactive glial tissue (bar = 2.5 mm). (**b**) Higher magnification of the reactive glial tissue seen in Fig. 8.21a shows the typical interlacing fascicles of spindle-shaped astrocytes (bar = 70 μ)

8.8.3 Extraretinal Neovascular Membranes

Fibrovascular membranes due to ocular ischemia from conditions like diabetes mellitus or retinal vein occlusion represent a third category of vitreous membranes characterized by new vessel formation. The natural history of these retinal neovascular membranes tend to vary according to the underlying disease to which they are linked. Although referred to as *retinal*, these vasoactive tissues grow outside the retina and are thus extraretinal. The adjective *retinal* is thus misleading as the membranes exist in an extraretinal location. Despite morphological overlap with ERM and PVR, retinal neovascular membranes are considered nosologically distinct.

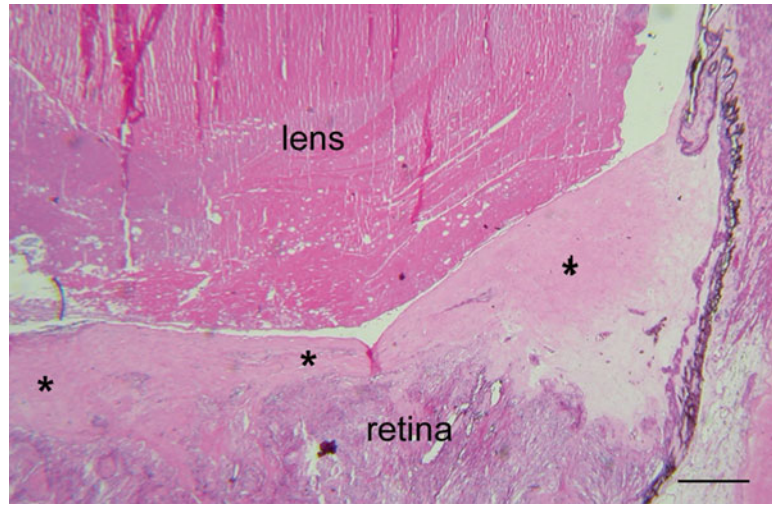

Fig. 8.25 Cyclitic membrane (*) is a subset of proliferative vitreoretinopathy that fills the space internal to the ciliary body. The membrane grows like a constricting diaphragm behind the plane of the lens and iris (bar = 0.5 mm)

The classic example of retinal neovascularization occurs with diabetes, where it is the defining feature of proliferative retinopathy. Neovascularization begins within the retina (referred to as intraretinal microangiopathy or IRMA) or within the optic nerve head. Once incipient vessels break through internal limiting membrane or the attenuated footplates of Mueller cells, the stage of retinopathy is classified as *proliferative* (Fig. 8.26a, b). The factors that promote angiogenesis are complex, but diabetic neovascularization probably originates from retinal venules. These new vessels lack pericytes and have fragile walls. After gaining access to the vitreous cortex, endothelial cells recruit fibroblasts for support. Fibroblasts increase their production of collagen, using hyaloid surfaces as scaffolds. The new blood vessels have fenestrated endothelium, but some junctional complexes develop as the vessels age. These neovascular membranes also have contractile properties. Regressed membranes, due to either treatment or spontaneous involution, leaves ghost vessels intertwined with fibrous tissue.

Complications of retinal neovascularization are common and involve hemorrhage into the vitreous and damage to the retina caused by traction. The consequences of vitreous hemorrhage have already been described. The neurosensory retinal tolerates traction poorly. If prolonged, traction results in a deterioration of vascular homeostasis and the accumulation of extracellular fluid. Macular edema, however, is a common response to retinal injury and occurs in nonproliferative diabetic retinopathy as well. If proliferative membranes continue to exert traction on the retina, they will detach the neurosensory retina from underlying RPE (Figs. 8.27 and 8.28). Similar changes are found with other ocular ischemic disorders, but diabetes is the single most prevalent cause of retinal (vitreous) neovascularization.

8.8.4 Retinopathy of Prematurity

Neovascular membranes of the vitreous are also a feature of retinopathy of prematurity (ROP). These membranes fall within the broad category of ischemia-related neovascular membranes, although causational factors and pathogenic mechanisms differ from the more prevalent acquired vascular diseases just discussed. Originally described in 1942, ROP (and originally called retrolental fibroplasia) is a disorder of premature, low birth weight infants (less than 1,500 g) [51]. Although the two-phase hypothesis of ROP development is based on animal models from the 1950s, the proposal remains robust, withstanding the test of time. Briefly, an initial

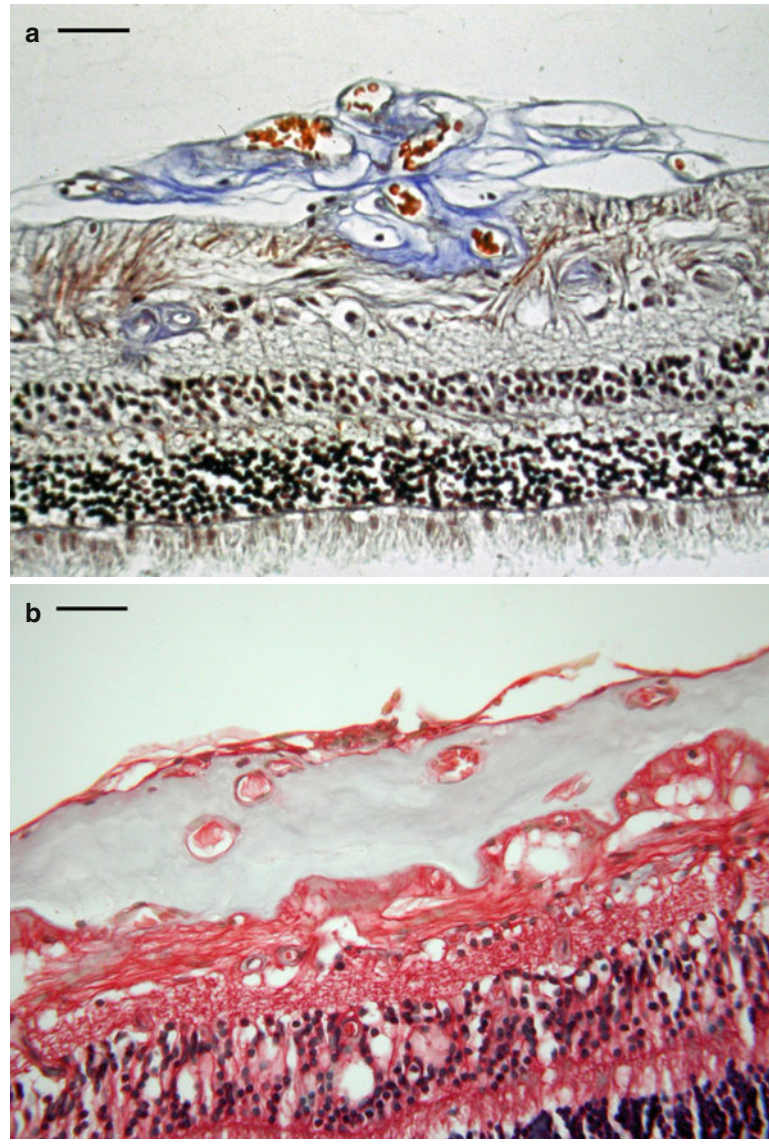

Fig. 8.26 (**a**) Early proliferative diabetic retinopathy. This neovascular membrane has broken through the internal limiting membrane of the retina. It consists mostly of vessels with little supporting connective tissue (Masson trichrome stain; bar = 50 μ). (**b**). An example of late proliferative diabetic retinopathy on the surface of the retina. This extraretinal membrane is fibrotic and contains a few small vessels with patent lumens (Masson trichrome stain bar = 80 μ)

vaso-obliterative phase of ROP is induced by high levels of oxygenation. This exposure results in vascular obliteration and delayed retinal vascular development. A vasoproliferative phase then follows when the infant is returned to ambient air. If severe enough (stage 3 or greater on the ROP severity scale) vitreous neovascularization occurs. Secondary tractional retinal detachment characterizes stages 4 and 5 on the ROP severity scale. Given the trend in improved survival of low birth weight infants, this bilateral vision-threatening disease will continue to be a major public health problem worldwide.

Essentially, all the complications of vitreous neovascularization seen in adults occur in infants and children with ROP, including vitreous hemorrhage, retinal detachment, and various patterns of secondary retinal injury, from edema and neural atrophy to reactive gliosis. Histologically, new vessels in ROP appear similar to vitreous neovascularization due to other causes (Fig. 8.29).

Fig. 8.27 Proliferative diabetic retinopathy shows a neovascular membrane (*NVM*) growing along the posterior hyaloid (*PH*). The membrane appears to exert traction on the underlying macula, where it separates from the internal limiting membrane (*ILM*). The retina shows cystic edema (bar = 80 μ)

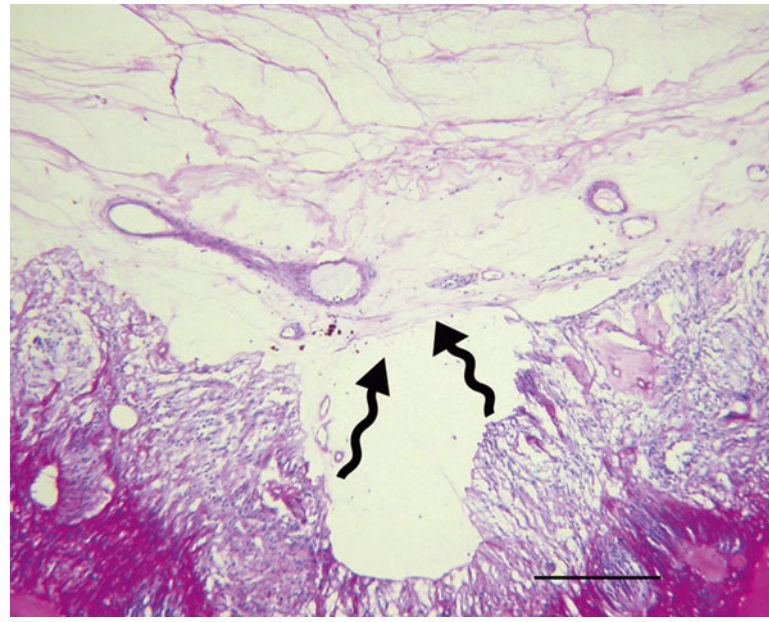

Fig. 8.28 Advanced proliferative diabetic retinopathy with tractional retinal detachment. The vitreous cortex is replete with new vessels. Fibrous tissue exerts an inward force on the retina (*wavy arrows*) pulling it away from underlying retinal pigment epithelium (periodic acid-Schiff; bar = 130 μ)

8.8.5 Familial Exudative Vitreoretinopathy

Familial exudative vitreoretinopathy (FEVR) shares several clinical similarities with ROP, but is not associated with low birth weight or high oxygenation levels. The pathogenesis of FEVR is poorly understood, but the disorder is inherited as an autosomal dominant trait with its principal locus (EVR1) on chromosome 11q13q23 [52].

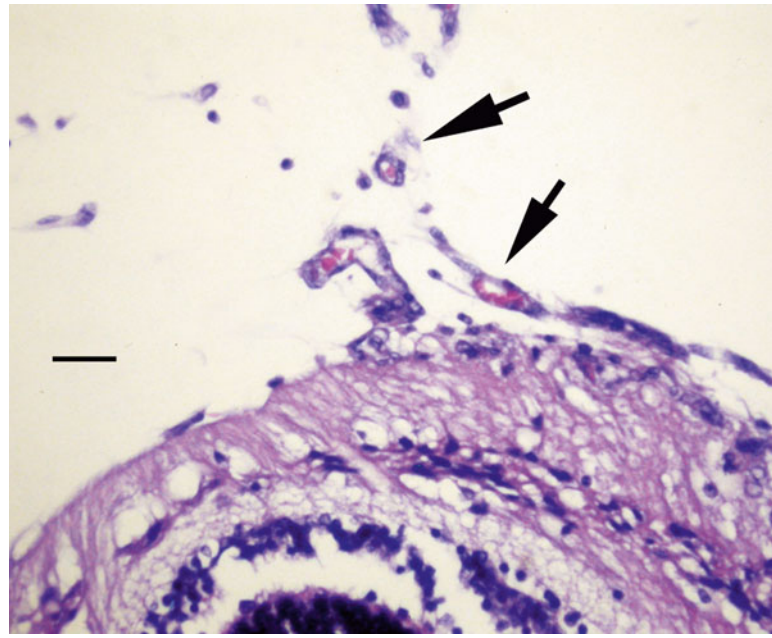

Fig. 8.29 Vitreous neovascular membrane in retinopathy of prematurity. These small-caliber vessels (*arrows*) are arising from the peripheral retina (bar = 20 μ)

Clinically FEVR is characterized by tractional dragging of macula, retinal folds, preretinal membrane formation, and exudative retinal detachment [53]. This clinical picture can be further complicated by secondary rhegmatogenous detachment of the retina [54]. Like ROP, there is incomplete vascularization of the peripheral retina. Although failure to vascularize peripheral retina is the unifying feature of FEVR, visual impairment is due to the secondary complications that follow retinal angiogenic arrest. Eyes with FEVR examined histologically usually have end-stage findings, with total retinal detachment and extensive retinal and subretinal exudation. The vitreous is effaced by fibrovascular membranes, and there is extensive atrophy and gliosis of neurosensory retina.

8.9 Vitreous Substitutes

Any discussion about vitreous membranes would be incomplete without mentioning the effects of vitreous substitutes on surrounding tissues. Advances in vitreoretinal surgery have led to the development and refinement of vitreous replacement fluids. These substitutes vary considerably in chemical and physical properties, ranging from air and balanced salt solutions to expansible gases and synthetic polymers [55]. Each substance interacts differently with human tissue, but for the most part these substances are relatively inert, at least in the short term (e.g., weeks to months). Finding a vitreous substitute within a blind, painful eye removed surgically has now become commonplace.

Silicone oil is one of the most widely used vitreous substitutes for complex retinal detachment surgery. A hydrophobic fluid with high surface tension, silicone oil has a chemical composition similar to silicone rubber but with less cross-linking. It serves as a mechanical tamponade, usually staying in the vitreous cavity from 6 to 30 months.

In the pathology laboratory, silicone oil is a clear liquid that flows freely from the cut surface of the globe. The material has a sticky-oily feel and does not mix with blood. Histologically, silicone oil induces a mild inflammatory reaction. Small oil droplets can be found in tissues it has come in contact with. Foreign body giant cells are occasionally seen. Vacuolated cytoplasm is particularly prominent in glial cells, macrophages, and retinal pigment epithelium (Fig. 8.30).

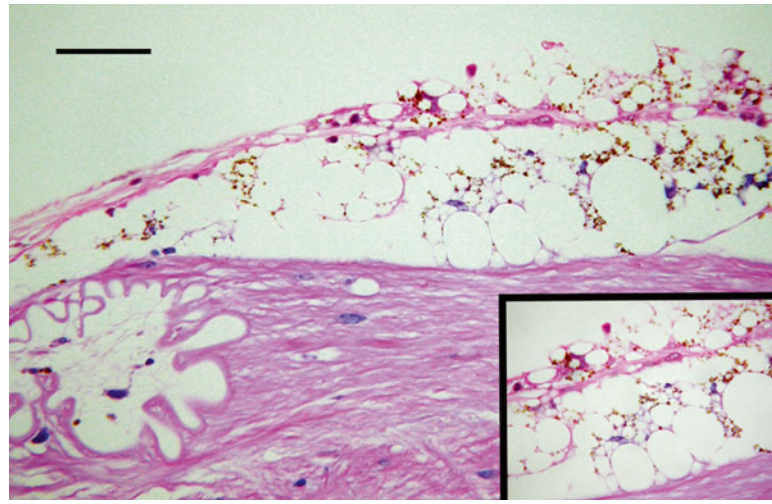

Fig. 8.30 Epiretinal membrane (*ERM*) in a silicone oil-filled eye. Cells making up the membrane contain numerous clear vacuoles of varying size admixed with melanin (bar = 20 μ). Inset shows key cells of the ERM in isolation

Cytoplasmic vacuoles vary considerably in size. A single large liquid silicone droplet can displace the nucleus to the periphery resulting in a signet ring appearance, while multiple minute droplets can result in foam cells.

8.10 Degenerations

8.10.1 Aging

Longitudinal changes in the composition and structure of vitreous have been deduced from cross-sectional studies. The hallmark of vitreous aging is syneresis, which has been documented in children as young as four years of age [56]. By the time the eye has reached its adult size, some may contain as much as 20 % collagen-free vitreous. Clinically detectable syneresis, however, does not typically occur until middle age, when an obvious increase in the ratio of liquid to gel is apparent with slit lamp biomicroscopy. Myopic eyes tend to experience accelerated age-related syneresis. This degenerative process continues through the ninth decade of life [57]. The molecular bases for the transformation of vitreous gel to liquid are incompletely understood. There is a transition zone between vitreous gel and vitreous liquid, but when studied ultrastructurally neither cellular remnants nor fragments of collagen are found [58]. Laboratory models of vitreous aging and syneresis have been hampered by the fact that almost any form of injury, no matter how trivial, results in liquefactive degeneration of the gel. The introduction of blood, inflammatory cells, or even a relatively inert foreign material into the vitreous induces regional syneresis, albeit to different degrees (Fig. 8.31). Inflammatory cells, with their host of enzymes, are particularly destructive.

Chronic photodegradation of vitreous is a presumptive cause of vitreous syneresis, but hard evidence is difficult to come by. Animal studies have shown that light breaks down hyaluronic acid over time and that free radical formation is a by-product that could potentiate further structural damage [59, 60].

The progressive degeneration of vitreous collagen leads to generalized loss of the structural integrity of the gel. As pockets of liquid vitreous collect and spacing of collagen fibrils becomes irregular and more compact, there is greater awareness of entropic images (i.e., visual perceptions produced by intrinsic structures of the eye), although it causes no permanent injury to the visual pathway. With time, syneresis will result in separation of the posterior vitreous cortex from its attachments to the retina.

Posterior vitreous detachment (PVD) has been broadly subdivided into acute and chronic, depending on clinical history. Acute PVD is characterized by sudden onset flashing lights and

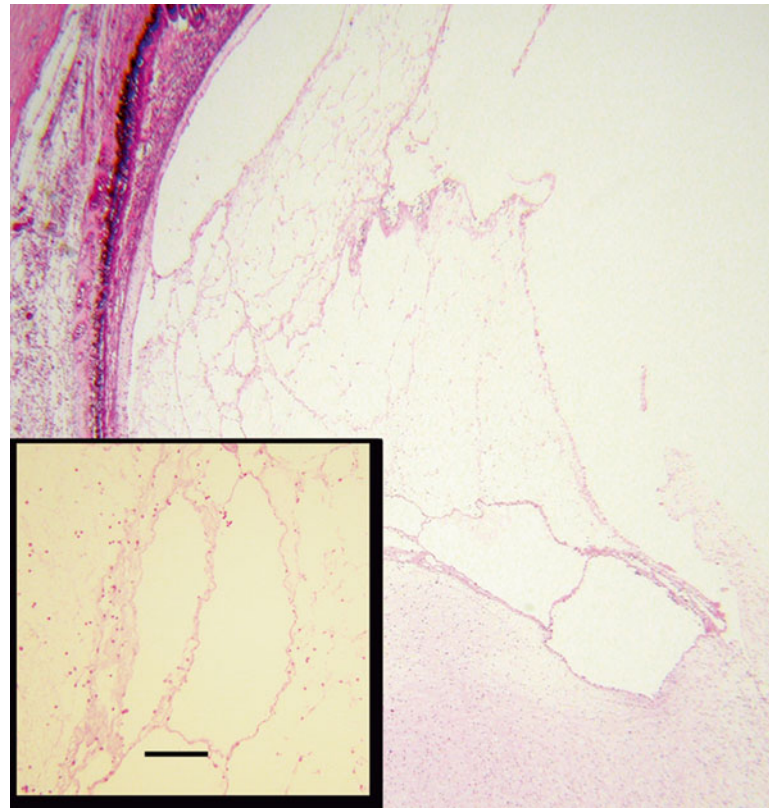

Fig. 8.31 Vitreous syneresis in a blind eye removed with uveitic glaucoma. Collagen fibrils are separated forming pockets of liquefied gel. *Inset* shows the degenerative process at higher magnification along with spillover inflammation and red blood cells (bar = 130 μ)

floaters (entopic images), symptoms attributed to traction on the neurosensory retina and the presence of condensed (collapsed) posterior cortical vitreous immediately anterior to the retina [61]. It is the shadows cast by the newly condensed gel that produce symptomatic floaters. Based on clinical and autopsy observations, most spontaneous PVDs do not result in symptomatic flashing lights and floaters. Given the nearly universal presence of PVDs in the elderly, many evolve without producing acute symptomatology. Posterior vitreous detachment is clinically important because of its association with retinal tear and detachment [62, 63].

The mechanical forces associated with collapse of the vitreous gel combined with vitreous adhesions to retina can result in a full-thickness tear of neurosensory retina. Any retinal vessel bridging a tear has the potential to bleed into the vitreous. Continued traction on the torn edges of the retina contributes to further detachment of the neurosensory retina from the underlying RPE. Although stepwise mechanisms of rhegmatogenous detachment are not fully understood, intraocular currents due to rotational inertia likely permit liquid vitreous to enter the subretinal space.

8.10.2 Miscellaneous Vitreoretinal Degenerations

The intimate relationship of retina and vitreous can confound judgment on where to place the primary pathogenic processes. The term *vitreoretinal degeneration* describes this etiological confusion. Lattice degeneration is the prime example where speculation dictates the assignment of culpability to either retina or vitreous.

Uncommon during the first decades of life, the circumferential lesions of peripheral lattice degeneration are characterized by the white hyalinized vessels responsible for the name. Lattice degeneration is found in about 6–9 % of

eyes, but is associated with nearly a third of all rhegmatogenous retinal detachments [64]. More common in myopic eyes, nearly half of patients have bilateral involvement. Usually oriented concentric to the ora serrata, the mean number of lesions per eye is roughly three. Individual lesions measure, on average, about 2 mm in length by 0.5 mm in width. Histologically, the retina is atrophic and the overlying vitreous is liquid. At the edge of the pocket of liquefied gel, the vitreous is condensed and adherent to the retina. The RPE beneath and adjacent to atrophic retina is also abnormal. The risk of rhegmatogenous detachment of the retina with lattice degeneration is likely attributable to the combination of neurosensory retinal atrophy and abnormal vitreous adhesions.

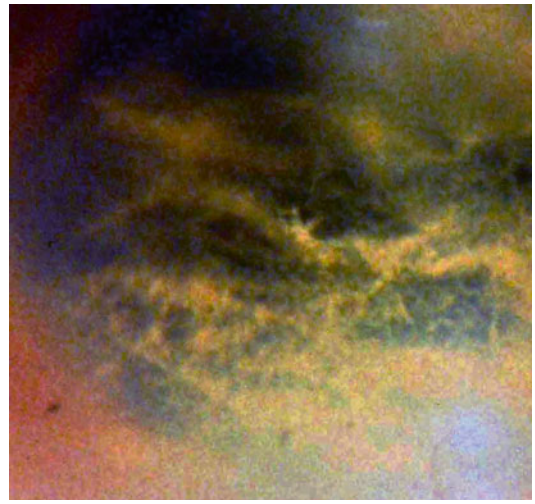

Fig. 8.32 Vitreous amyloid visualized through a cataract at the time of surgery. The delicate strands look like cotton candy (or glass wool) clinically

8.10.3 Amyloidosis

Amyloidosis describes a heterogeneous group of disorders characterized by the accumulation of an abnormal insoluble protein (amyloid). Many of the physical properties of amyloid are related to its beta-pleated sheet structure and secondary configuration, especially the propensity of adjacent polypeptide strands to align themselves in opposite directions. Besides resistance to enzymatic digestion, these entangled proteins give amyloid an affinity to certain dyes like Congo red and the optical properties of birefringence and dichroism. Birefringence means the protein rotates polarized light, while dichroism describes the preferential transmission of specific wavelengths along the axes of the molecule.

The classification of amyloidosis has undergone considerable modification and standardization as knowledge on the type of precursor protein of amyloid accumulates [65]. The precursor protein to vitreous amyloid is transthyretin, a normal component of plasma [66]. The protein is produced in the liver, choroid plexus of the brain, and RPE. An acidic protein found in the prealbumin fraction of serum on electrophoresis, transthyretin functions as a carrier molecule for retinol-binding protein and thyroxine.

Point mutation of the transthyretin gene gives rise to transthyretin amyloid. The disorder is inherited as an autosomal dominant trait with variable expression or occurs as a sporadic mutation. At least 100 different mutations have been identified, giving rise to a variety of clinical manifestations, most commonly polyneuropathy and autonomic dysfunction. Along with vitreous opacities, other tissues affected by transthyretin amyloid include the heart, central nervous system, and soft tissue of the wrist (carpal tunnel syndrome). Precisely why certain amino acid substitutions give rise to different phenotypic expressions is unclear, but vitreous opacities are seen in about 20 % of transthyretin mutations [67]. Those patients tend to present later in life with symptoms of floaters or decreased vision, which may be the initial manifestation of the disease. The prevalence of vitreous opacities with certain mutations is high, as exemplified by the Try114Cys substitution in which vitreous amyloid is found in nearly all affected individuals [68].

Vitreous amyloid clinically has been likened to "glass wool," the name for fiberglass insulation in the United Kingdom. American ophthalmologists find the vitreous deposits evocative of cotton candy (Fig. 8.32). When the opacities interfere with visual function, vitrectomy

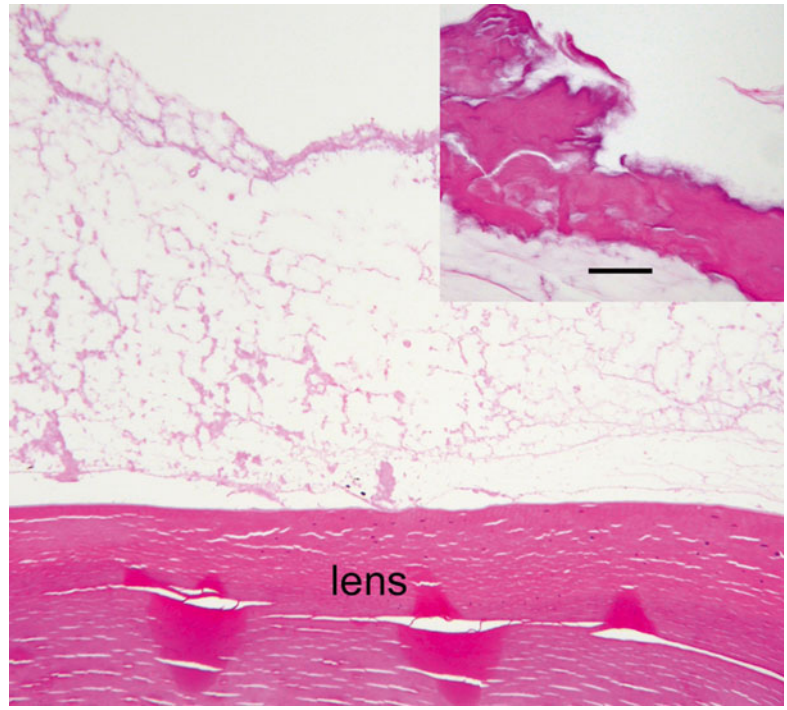

Fig. 8.33 Familial amyloidosis involving the vitreous. The amorphous eosinophilic material behind the lens was left after an earlier vitrectomy. *Inset* shows higher magnification of transthyretin amyloid (bar = 25 μ)

becomes a clinical option. Removal of the vitreous accomplishes two goals: it improves visual function and provides tissue for diagnostic studies.

Transthyretin amyloid has similar features of amyloid proteins elsewhere. By light microscopy, the amorphous material has a hyaline appearance. Although no stain is absolutely specific for amyloid, Congo red has enjoyed the status of gold standard but is not necessarily superior in terms of specificity or sensitivity to other stains [69]. Red polarization after toluidine blue, for instance, is a reliable alternative [70]. In context of a vitreous biopsy, however, the sparse amount of tissue may not permit the easy recognition of the classic features of amyloid under the microscope. Ultrastructurally, the deposits consist of interlacing fibrils between 80 and 100 Å in diameter, with a beaded periodicity of 75 Å.

Relatively few eyes from patients with the transthyretin mutation have been examined histologically (Fig. 8.33). Those that have been studied reveal the greatest concentration of amyloid in the cortical vitreous, usually associated with deposits in the inner retina, typically around larger vessels. Lesser degrees of extracellular amyloid can be found in iris, ciliary body, choroid, and choriocapillaris [66]. Nonfamilial amyloidosis can also result in the accumulation of intraocular amyloid, usually in the choroid and choriocapillaris [71]. Rarely, amyloid can be found in the choroid with secondary amyloidosis [72]. Amyloid in the neurosensory retina or vitreous, however, is the hallmark of a systemic disease, most often familial amyloidosis.

8.10.4 Asteroid Hyalosis

Asteroid hyalosis is spherical deposits found in the vitreous in about 1 % of persons over the age of 50 [73]. The condition is unilateral in about three-quarter of affected patients. Although some studies have reported statistical associations to common diseases like atherosclerosis and hypertension, no biologically plausible connection has been found between asteroid hyalosis and any systemic or local disorder [74, 75]. Clinically, the deposits are cream to buff colored and are adherent to vitreous fibrils. Their suspension in vitreous is reminiscent of a "string of pearls" (Fig. 8.34, inset).

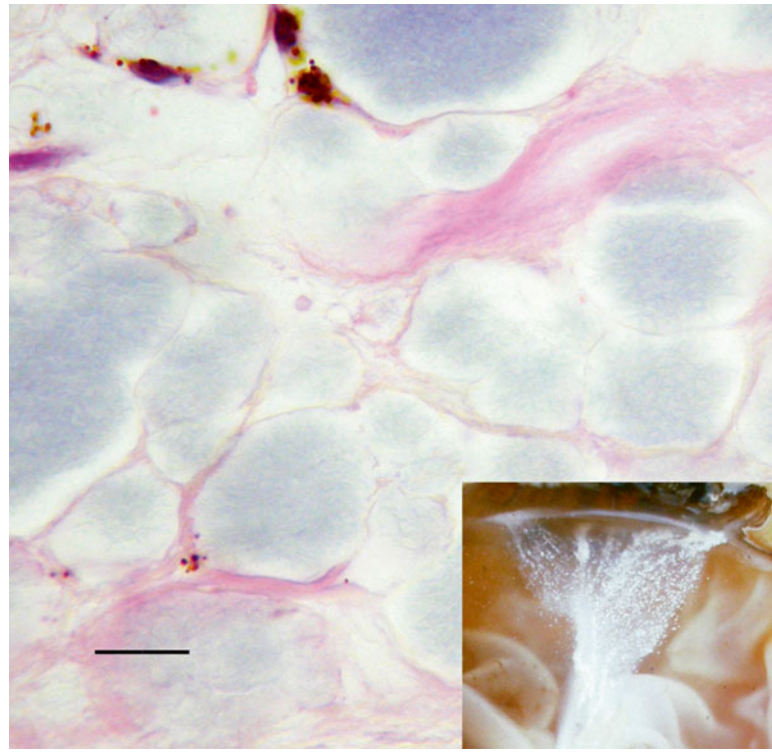

Fig. 8.34 Asteroid bodies in vitreous admixed with a few melanin-containing cells. The material has a gray color on hematoxylin-eosin stain (bar = 30 μ). *Inset* shows gross appearance of asteroid hyalosis within collapsed, funnel-shaped vitreous

Histologically, the spheres are 50–175 μm in diameter and stain blue-gray on routine hematoxylin-eosin (Fig. 8.34). They light up brilliantly under cross-polarized light (Fig. 8.35). Chemically the deposits contain calcium, phosphorus, and small amounts of sulfur [76, 77]. Ultrastructural studies show amorphous electron-dense material mixed with multilaminar membranes [78]. Despite numbering in the hundreds, these curious deposits cause few if any clinical symptoms. Although relatively inert, asteroid bodies occasionally illicit a foreign body giant cell reaction (Fig. 8.36). They also can be enveloped in a mildly inflamed but otherwise typical idiopathic epiretinal membrane.

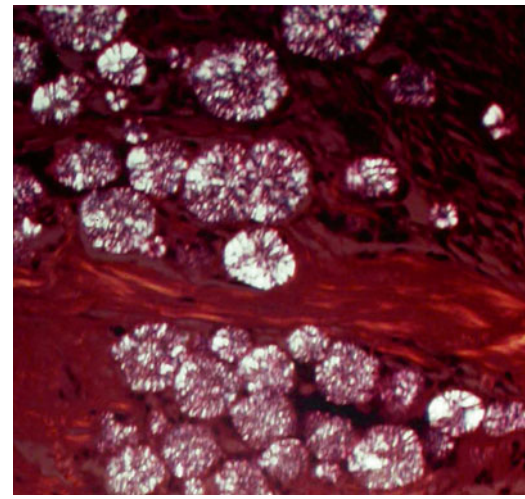

Fig. 8.35 Asteroid body under cross-polarized light displays characteristic birefringence

8.10.5 Synchysis Scintillans

Synchysis scintillans refers to the appearance of glistening crystals found in liquefied vitreous. Originally described clinically more than a century ago, these highly reflective crystals are dispersed with eye movement. Unlike asteroid bodies that are tethered to the vitreous, the crystals of synchysis scintillans are associated with advanced syneresis and settle in the dependent portion of the vitreous cavity. The crystals are cholesterol, usually derived from the breakdown of red blood cells [79]. By themselves, cholesterol crystals are not visible on

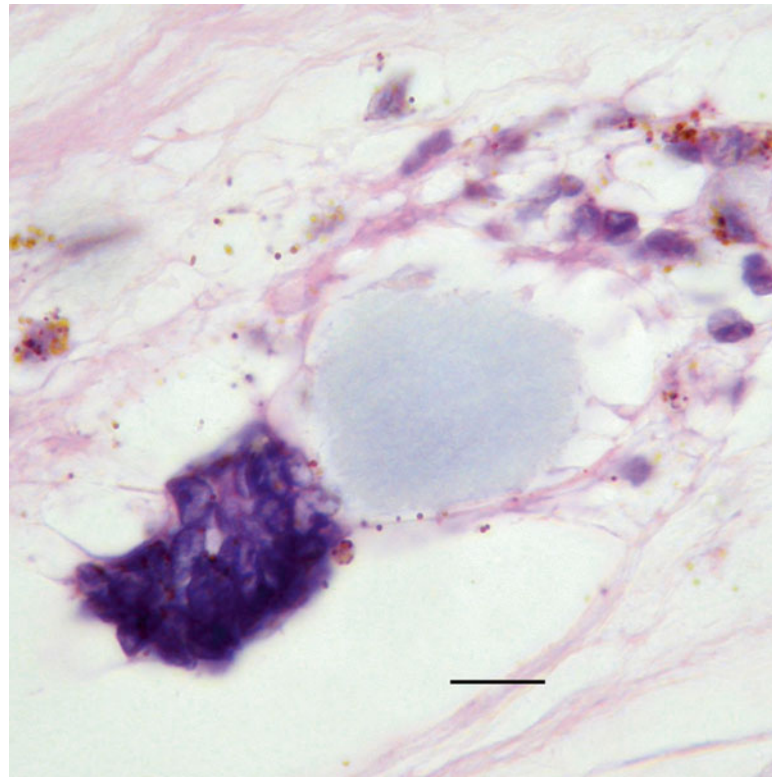

Fig. 8.36 Asteroid body next to a multinucleated foreign body giant cell (bar = 30 μ)

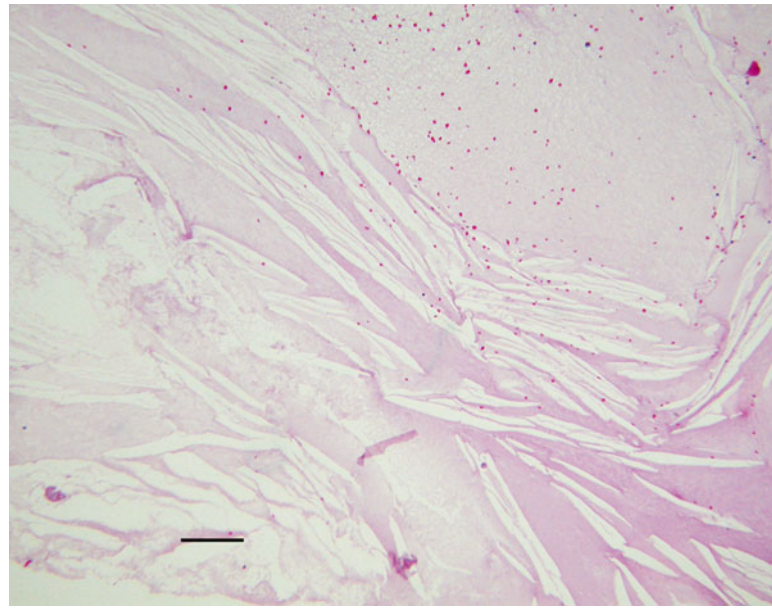

Fig. 8.37 Vitreous cholesterolosis consists of myriad clear spaces within degenerating vitreous. The dotlike red blood cells likely contaminated the vitreous during surgical enucleation (bar = 110 μ)

hematoxylin-eosin-stained sections, since lipid-soluble compounds are lost during routine processing. The crystals, however, do incite a foreign body giant cell reaction in soft tissue. This particular phenomenon is seen within organizing hemorrhages of the vitreous or in the subretinal space (Fig. 8.37). Myriad cholesterol crystals are often referred to clinically as cholesterolosis.

8.11 Neoplasms

8.11.1 Primary Intraocular Lymphoma

Primary intraocular lymphoma (PIOL) (see also page 428), or primary vitreoretinal lymphoma, is a subset of primary central nervous system (CNS) lymphoma and the most common malignancy affecting the vitreous [80]. Although other lymphomas can rarely arise within the eye in the absence of predecessor systemic lymphoma, none display the unique tropism for the retina and CNS as this particular neoplasm does. PIOL is usually a diffuse large B cell lymphoma, although rarely other lymphoma types have been reported, including T cell [81]. Up to a quarter of patients with primary CNS lymphoma will ultimately develop ocular involvement, and as many as 90 % of persons PIOL will go on to have primary CNS lymphoma [82].

Patients are typically elderly, with a peak incidence between 75 and 84 years [83]. The early, painless proliferation of neoplastic B cells in the retina and vitreous can clinically mimic posterior autoimmune uveitis. In such a clinical situation, failure to respond to anti-inflammatory therapy typically prompts further study through either vitreous biopsy or systemic evaluation that uncovers primary CNS lymphoma. For unknown reasons, cells in PIOL have a propensity to proliferative between Bruch's membrane and RPE, resulting in large, irregular plaques of tumors (RPE detachments). These mounds of tumor typically have a yellow color due to overlying atrophy or destruction of the RPE (Fig. 8.38). Diffuse involvement is less common and imparts a leopard-spot pattern of discoloration.

Histopathology

Histological examination of early PIOL reveals characteristic collections of lymphoma cells between Bruch's membrane and the RPE (Fig. 8.39). Most PIOLs consist of large atypical lymphocytes with irregularly shaped nucleus, prominent nucleoli, and little cytoplasm (Fig. 8.40a, b). Although invasion of retina with spread to the vitreous commonly occurs (Fig. 8.41a), occasionally vitreous involvement with PIOL exists in the absence of a detectable tumor mass elsewhere in the eye. Necrosis may be a prominent feature of PIOL that confounds the cytological diagnosis by reducing the number of intact cells (Fig. 8.41b).

Immunoprofile: Viable cells usually express B cell markers such as CD19, CD20, and CD22.

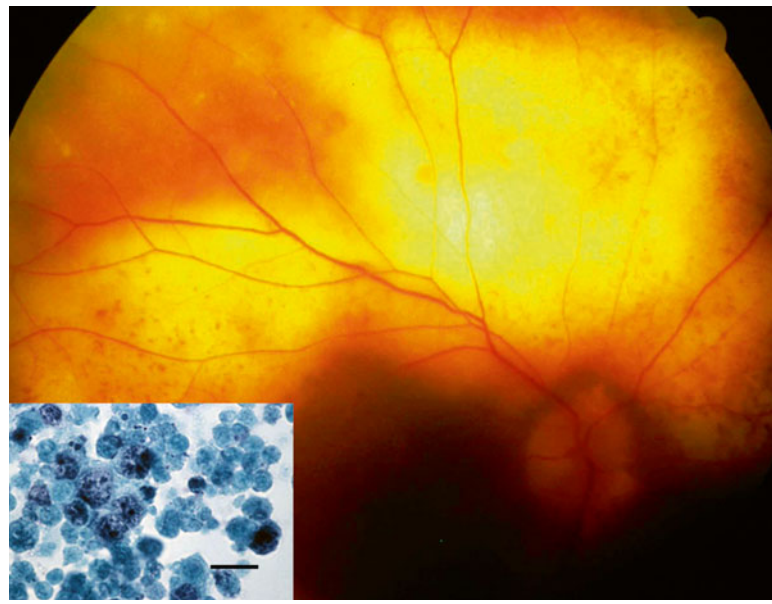

Fig. 8.38 Fundus photograph of primary intraocular lymphoma was taken after vitreous biopsy. Discrete yellow lesions are deep to the retina. *Inset* shows large malignant cells harvested at vitrectomy. There is considerable necrosis and many cells lack nuclear detail (bar = 25 μ)

Fig. 8.39 Primary intraocular lymphoma with large tumor cells beneath the retinal pigment epithelium and above Bruch's membrane (*arrows*). Tumor cells and necrosis are also found beneath the neurosensory retina (bar = 110 μ)

Tumors display κ or λ clonal restriction, but monoclonal light chains are not demonstrable in all cases despite sufficient sample [84]. Some investigators have reported BCL6 expression in PIOL, a proto-oncogene that is normally found in germinal center B cells [80]. The utility and prognostic significance of MUM1 expression, another oncogene associated with PIOL, remains to be determined [80].

Differential Diagnoses: Vitritis and Uveitis

The cytopathological distinction between benign and malignant cells lies at the heart of the differential diagnosis of PIOL and those conditions that mimic it, such as autoimmune uveitis or infectious vitritis. Under ideal circumstances the differences between neoplastic and reactive lymphocytes are straightforward based on relative and absolute sizes of nucleus and cytoplasm and the structural organization of nuclear chromatin.

The interpretation of PIOL through vitreous biopsy, however, is challenged by three variables: (1) the concentration of neoplastic cells in the vitreous, (2) the loss of cellular morphology after biopsy and with fixation, and (3) the intensity of reactive lymphocyte response to tumor (Fig. 8.42) [85–92]. At times, reactive CD3+ T cells are so prominent in the vitreous that they can outnumber neoplastic B cells. Harvesting subretinal cells via transretinal biopsy technique for cytological examination is an option when diagnostic cells cannot be found in vitreous and typical RPE detachments are present (Fig. 8.43) [87, 93]. Some surgeons prefer obtaining tissue through a more invasive chorioretinal biopsy [84].

Vitreous biopsy obtained with simple needle aspiration results in a limited sample. Given anecdotal experiences with false-negative vitreous biopsy, it is justified to perform a core vitrectomy to ensure a superior sample when PIOL is suspected [80, 84, 89]. Core vitrectomy, which employs a cutting instrument to minimized excessive stress on the gel and retinal traction, dilutes the biopsy with irrigating solution. Before the irrigating solution is employed, a small vitreous aspirate can be examined undiluted as a direct smear. The diluted specimen obtained with infusion fluid and a cutting instrument should be transported promptly in the original cassette for immediate processing. This sample requires concentration with cytocentrifugation or Millipore filter techniques. Commonly used stains after fixation include Giemsa, Diff-Quick, Papanicolaou, and hematoxylin-eosin. The supernatant fluid may also be used for cultures or other ancillary studies.

The selection of an optimal fixative is a matter of debate [85, 86, 88, 90–92]. Some like to work with fresh specimens, while others prefer placing

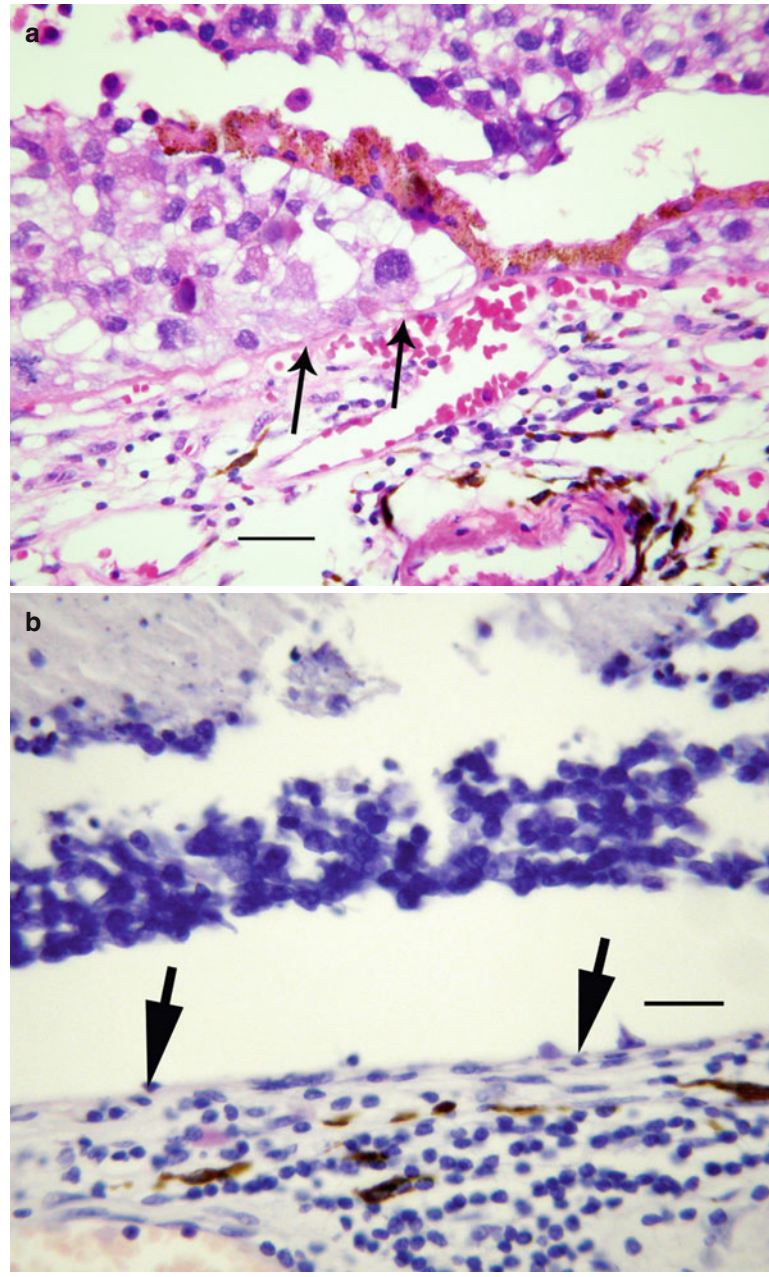

Fig. 8.40 (**a**) Higher magnification of Fig. 8.33 shows tumor cells between Bruch's membrane (*arrows*) and retinal pigment epithelium. Tumor cells are three to five times larger than reactive lymphocytes present in the choroid (bar = 45 μ). (**b**). Primary intraocular lymphoma is present between RPE and Bruch's membrane (*arrows*). Tumor cells in this case are more than twice the size of reactive lymphocytes in adjacent choroid (bar = 40 μ)

samples in fixative immediately after harvest. Vitreous biopsy along with surgical infusion fluid can be mixed with tissue-culture medium (e.g., Roswell Park Memorial Institute culture medium) or with 50 % ethyl alcohol (Fig. 8.42). Preliminary reports using HOPE fixation (HEPES-glutamic acid buffer-mediated Organic solvent Protection Effect) are promising [88]. Specimens fixed in formalin can be cytocentrifuged and cut as a cell block, at the risk of denaturing epitopes needed for successful immunohistochemistry [84, 85]. Given the variation of laboratory methods and preferences, surgeons should alert pathologists in advance of a planned biopsy. The practice of refrigerating specimens collected at inopportune times during the day or week should be discouraged because of the risk of losing cellular morphology.

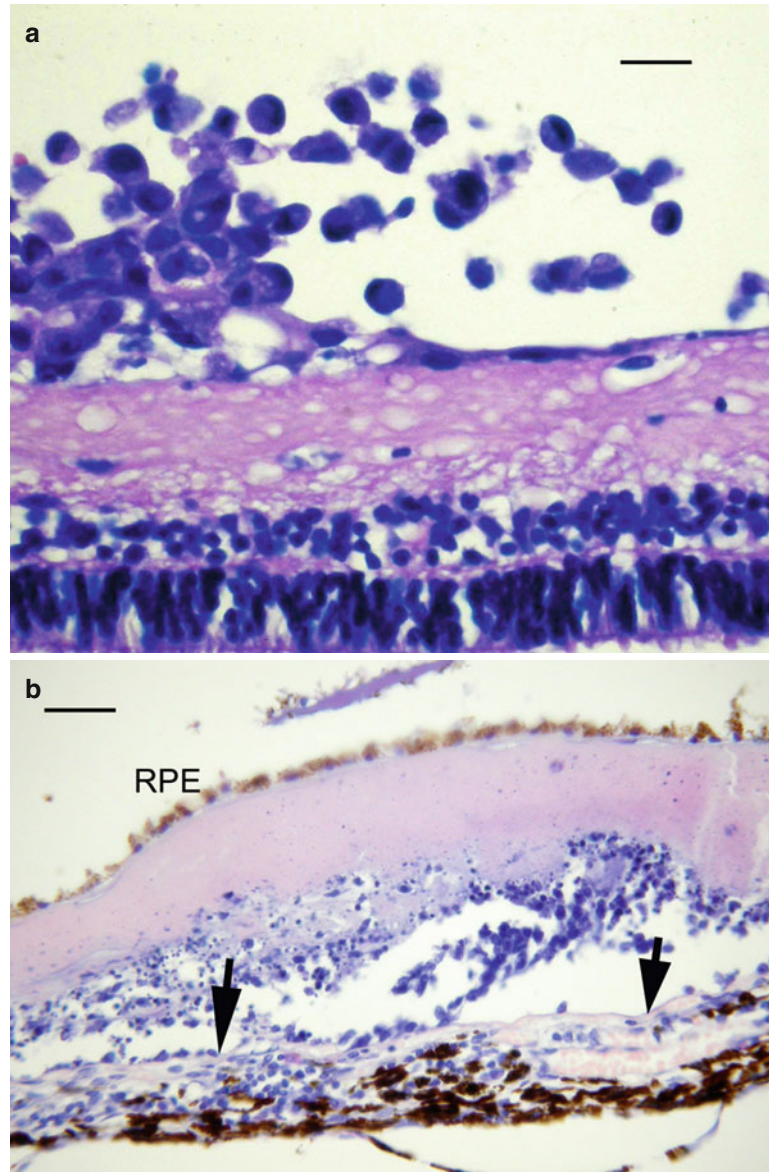

Fig. 8.41 (**a**) Primary intraocular lymphoma shows malignant cells resting on the surface of the retina. Vitreous involvement clinically obscured visualization of the retina (bar = 30 μ). (**b**) Primary intraocular lymphoma between the retinal pigment epithelium (*RPE*) and Bruch's membrane (*arrows*). Most of the material above the malignant lymphocytes is necrotic (bar = 60 μ)

Direct smears are useful diagnostic adjuvants, but require immediate fixation while wet to preserve cellular detail. Common fixatives for this purpose are 95 % ethyl alcohol and 100 % methanol. Spray fixatives are also commercially available.

Other ancillary test are helpful, particularly IgH gene rearrangement and T cell receptor gene rearrangement [94, 95]. Even when ample DNA is available for analysis, however, as many as 40 % of positive cytologies for lymphoma are not confirmed with a positive clonal gene rearrangement [92]. FR2, FR3, and/or CDR3 primers are recommended for demonstrating B cell monoclonality [95]. Flow cytometry can also be employed but requires a minimal threshold cellularity, which some PIOLs fall short of. The diagnostic utility of detecting elevated IL-10 levels of ocular fluids or finding IL-10 to IL-6 ratio of greater than 1 is questionable, since the sensitivity and specificity are relatively low. Aberrant levels of interleukins or abnormal ratios are not specific enough alone to establish the diagnosis of PIOL [90].

8.11.2 Vitreous Metastases

Most systemic metastases to the posterior segment of the eye involve choroid. Some metastases invade the retina and spill into the vitreous. Isolated metastasis to vitreous without a detectable choroidal lesion is exceptional but has been reported with several malignancies, including breast cancer and cutaneous melanoma [96, 97]. Diagnosis ultimately depends on vitreous biopsy with cytological examination. Immunohistochemical stains may be helpful in establishing the source of the tumor when cells lack cytological clues to their origin (Fig. 8.44).

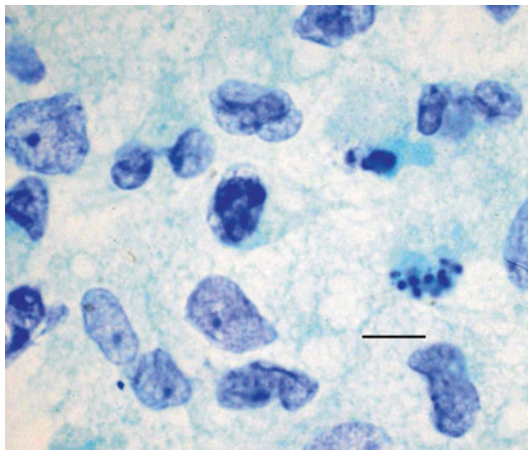

Fig. 8.42 Vitreous biopsy shows primary intraocular lymphoma. Cells have large irregular nuclei and little discernible cytoplasm (air-dried smear; Diff-Quick; bar = 30 μ)

8.11.3 Primary Ocular Malignancies with Vitreous Shedding

Both retinoblastoma and uveal melanoma have the potential to shed cells into the vitreous. This phenomenon occurs predictably with retinoblastoma, where the clinical finding of vitreous seeding relegates such eyes to Group 5, according to the classification system or Reese-Ellsworth. As retinoblastoma breaks through the internal limiting membrane, neoplastic cells are spewed into vitreous where they appear as gray to translucent clumps of tissue. Identifying vitreous involvement in eyes enucleated for the treatment of retinoblastoma presents little difficulty

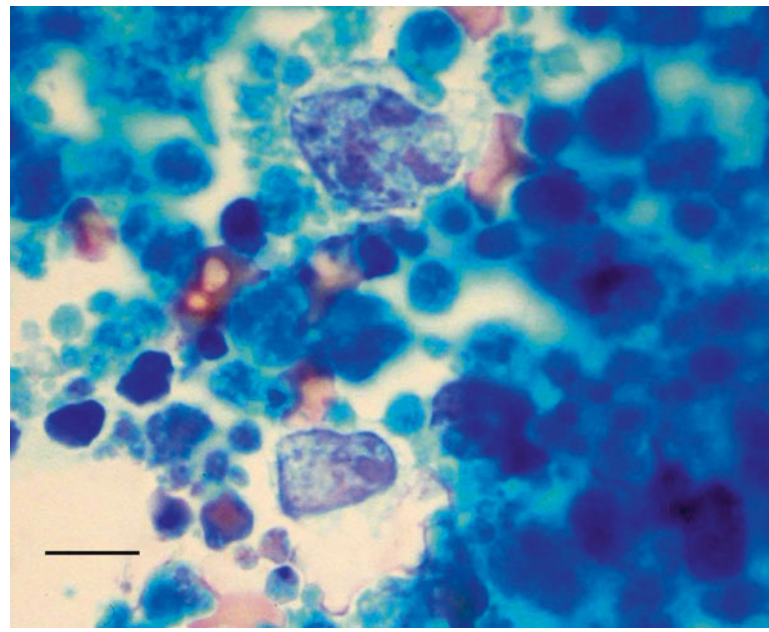

Fig. 8.43 A primary intraocular lymphoma with cells harvested from a subretinal (actually subretinal pigment epithelium) biopsy. Initial vitreous biopsy showed reactive lymphocytes only, but clinically the tumor had ophthalmoscopic features of primary intraocular lymphoma. The second biopsy beneath the retina reveals large cells with irregular nuclear shapes and clumped chromatic. There is extensive necrosis as well (Papanicolaou stain; bar 35 μ)

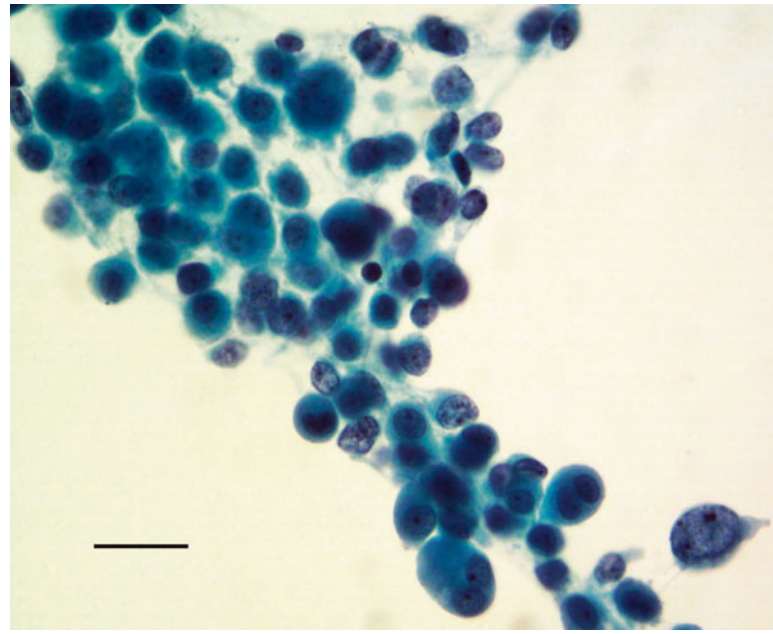

Fig. 8.44 Vitreous biopsy of metastatic cutaneous melanoma shows a cluster of malignant cells. Several cells are pigmented. The patient had widespread systemic metastasis but no discernible tumor mass within the eye (Papanicolaou, bar 45 μ)

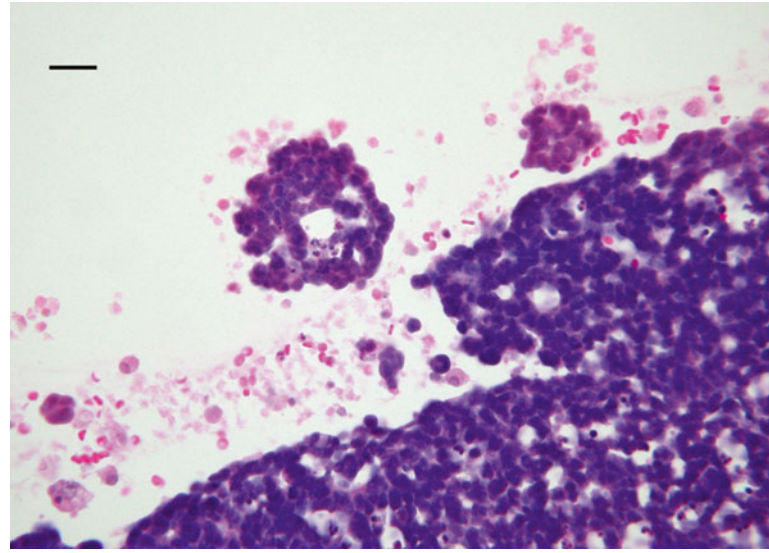

Fig. 8.45 Typical endophytic retinoblastoma is shown seeding the vitreous. Cells are shed from the surface of the tumor individually and in clumps (bar 40 μ)

(Fig. 8.45). Vitreous biopsy in children with unsuspected retinoblastoma often proves more challenging. In such situations, the harvested cells are undifferentiated and contain little cytoplasm; a few viable cells are frequently associated with sheets of necrotic debris (Fig. 8.46a). Tumor cells can grow into spheroidal aggregates having diameters of over 250 μm. Neuroepithelial rosettes, such as the Flexner-Wintersteiner rosette, provide evidence of retinoblastoma, but are rarely present (Fig. 8.46b). Immunohistochemical stains using neuroepithelial markers may help in cases of cellular ambiguity.

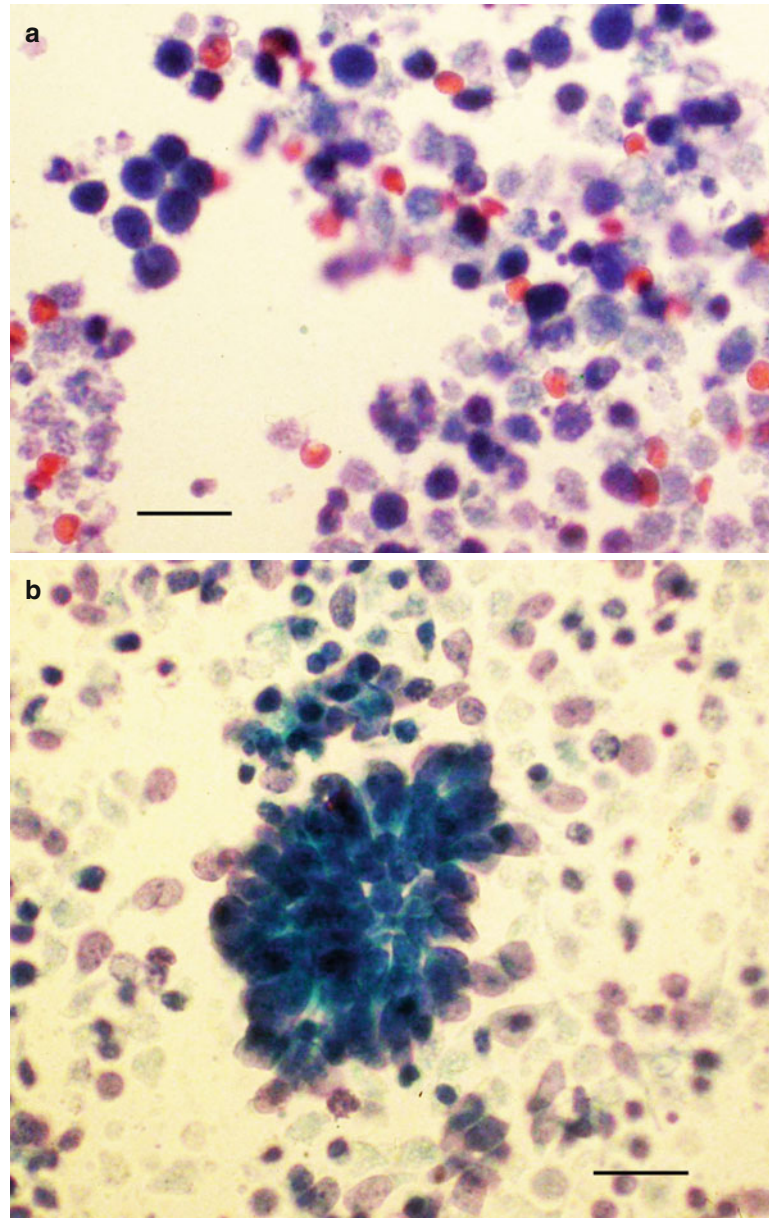

Fig. 8.46 (**a**) Vitreous biopsy in a case of unsuspected retinoblastoma shows mostly necrotic debris and naked nuclei suspicious for retinoblastoma. Further evaluation confirmed the diagnosis (Papanicolaou stain; bar =20 μ). (**b**) Cluster of undifferentiated tumor cells from vitreous biopsy of unsuspected retinoblastoma. The cohesive organization of cells suggests a neuroepithelial rosette (Papanicolaou stain; bar = 40 μ)

Clinically significant vitreous involvement from a primary uveal melanoma is distinctly uncommon. In such cases, neoplastic melanocytes floating in the vitreous that come to rest on the inner surface of internal limiting membrane have vaguely resembled retinitis pigmentosa (Fig. 8.47) [98]. Clinically, melanoma cells shed from a posterior uveal melanoma without a typical mushroom shape can be difficult to distinguish from cutaneous melanoma metastatic to the posterior segment. A primary melanoma of the skin needs to be excluded when a pigmented intraocular tumor presents with disproportionate involvement of the retina or vitreous.

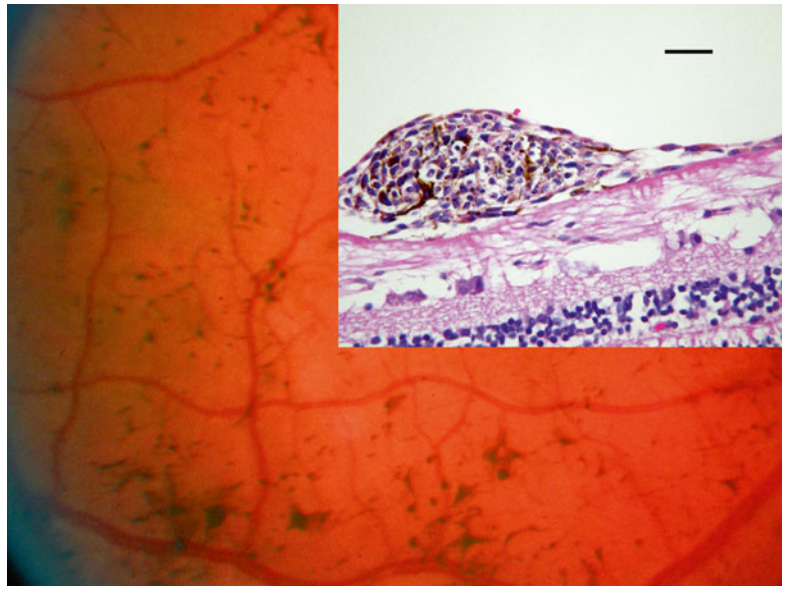

Fig. 8.47 Fundus photograph shows pigment deposits on surface of retina associated with a primary melanoma of the peripheral choroid that shed tumor cells into the vitreous. *Inset* from the enucleated eye reveals a mound of spindle melanoma cells resting on the surface of the retina (bar = 35 μ)

8.12 Summary

The hypocellular vitreous is rarely the site of primary disease processes. A variety of disorders affect the vitreous secondarily, most often with spillover inflammation from contiguous tissues. Familial amyloidosis and PIOL are two disorders that involve the vitreous primarily. Primary ocular lymphoma is usually a large B cell lymphoma. This high-grade lymphoma is known to clinically mimic autoimmune uveitis in older patients. The role of cytopathology in diagnosing vitreous disease has increased as the safety of harvesting tissue from inside the eye has improved.

Results of vitreous cytology can be generally divided into three broad categories: inflammation, neoplasm, and hemorrhage [99]. Although invaluable in establishing a diagnosis of PIOL in clinically undiagnosed vitritis, vitreous cytology can result in false-negative diagnoses in this setting. Cytological features of benign vitreous conditions often lack specificity, but the presence of eosinophils or granulomas helps narrow the differential diagnosis [100, 101]. Special stains for microorganisms may be rewarding, but they are relatively insensitive adjuncts for identifying pathogens. Knowledge of disease processes that affect the vitreous is crucial to maximizing strategies in diagnostic histopathology.

References

1. Moorhead LAC. Chapter 7: Vitreous. In: Anderson RE, editor. Biochemistry of the eye. San Francisco: American Academy of Ophthalmology; 1983. p. 145–63.
2. Snowden JM. The stabilization of in vivo assembled collagen fibrils by proteoglycans /glycosaminoglycans. Biochem Biophy Acta. 1982;703:21–5.
3. Sebag J. Chapter 9: The vitreous. In: Hart Jr HM, editor. Adler's physiology of the eye. 9th ed. St Louis: CV Mosby; 1992. p. 268–334.
4. Sturner WQ, Dowdey AB, Putnam RS, et al. Osmolality of other chemical determinations in postmortem human vitreous humor. J Forensic Sci. 1972;17(3):387–93.
5. Green WR. Chapter 117: Vitreoretinal juncture. In: Ryan SJ, editor. Retina, vol. 3. St Louis: CV Mosby Company; 1989. p. 13–69.
6. Theopold H, Faulborn J. Scanning electron microscopy of the vitreous body. Massive retraction after perforating injury. Albrecht Von Graefes Arch Klin Exp Ophthalmol. 1979;211(3):259–64.
7. Goldberg MF. Persistent fetal vasculature (PFV): an integrated interpretation of signs and symptoms associated with persistent hyperplastic primary vitreous (PHPV). LIV Edward Jackson Memorial Lecture. Am J Ophthalmol. 1997;124(5):587–626.
8. Khaliq S, Hameed A, Ismail M, et al. Locus for autosomal recessive nonsyndromic persistent hyperplastic primary vitreous. Invest Ophthalmol Vis Sci. 2001; 42(10):2225–8.
9. Shastry BS. Persistent hyperplastic primary vitreous: congenital malformation of the eye. Clin Experiment Ophthalmol. 2009;37(9):884–90.

10. Nork TM, Millecchia LL. Treatment and histopathology of a congenital vitreous cyst. Ophthalmology. 1998;105(5):825–30.
11. Aydin E, Demir HD, Tasliyurt T. Idiopathic pigmented free-floating posterior vitreous cyst. Int Ophthalmol. 2009;29(4):299–301.
12. Bayraktar Z, Kapran Z, Ozdogan S. Pigmented congenital vitreous cyst. Eur J Ophthalmol. 2004;14(2): 156–8.
13. Orellana J, O'Malley RE, McPherson AR, Font RL. Pigmented free-floating vitreous cysts in two young adults. Electron microscopic observations. Ophthalmology. 1985;92(2):297–302.
14. Brown DM, Graemiger RA, Hergersberg M, et al. Genetic linkage of Wagner disease and erosive vitreoretinopathy to chromosome 5q13-14. Arch Ophthalmol. 1995;113(5):671–5.
15. Graemiger RA, Niemeyer G, Schneeberger SA, et al. Wagner vitreoretinal degeneration. Follow-up of the original pedigree. Ophthalmology. 1995;102(12): 1830–9.
16. Margo CE. Chapter 9: Bacterial infections. In: Klintworth GK, Garner A, editors. Pathobiology of ocular disease. New York: Informa; 2008. p. 213–34.
17. Wensing B, de Groot-Mijnes JD, Rothova A. Necrotizing and nonnecrotizing variants of herpetic uveitis with posterior segment involvement. Arch Ophthalmol. 2001;129(4):403–8.
18. Mruthyunajaya P, Jumper JM, McCallum R, et al. Diagnostic yield of vitrectomy in eyes with suspected posterior segment infection or malignancy. Ophthalmology. 2002;109(6):1123–9.
19. Yoser SL, Foster DJ, Rao NA. Systemic viral infection and their retinal and choroidal manifestations. Surv Ophthalmol. 1993;7(5):312–52.
20. Ormerod LD, Larkin JA, Margo CE, et al. Rapidly progressive herpetic retinal necrosis: a blinding disease characteristic of advanced AIDS. Clin Inf Disease. 1998;26:34–45.
21. Tran TH, Rozenberg F, Cassoux N, et al. Polymerase chain reaction analysis of aqueous humour samples in necrotising retinitis. Br J Ophthalmol. 2003;87(1): 79–83.
22. Gass JDM. Stereoscopic atlas of macular disease, vol. 2. St Louis: CV Mosby; 1987. p. 455–550.
23. Cohen JI, Fahle G, Kemp MA, et al. Human herpesvirus 6-A, 6-B, and 7 in vitreous fluid samples. J Med Virol. 2010;82:996–9.
24. Garweg JG, Wanner D, Sarra GM, et al. The diagnostic yield of vitrectomy specimen analysis in chronic idiopathic endogenous uveitis. Eur J Ophthalmol. 2006;16(4):588–94.
25. Manku MP. Diagnostic vitreous biopsy in patients with uveitis: a useful investigation? Clin Experiment Ophthalmol. 2005;33(6):604–10.
26. Meisler DM, Palestine AG, Vastine DW, et al. Chronic Propionibacterium endophthalmitis after extracapsular cataract extraction and intraocular lens implantation. Am J Ophthalmol. 1986;102(6):733–9.
27. Raoult D, Birg ML, La Scola B, et al. Cultivation of the bacillus of Whipple's disease. N Engl J Med. 2000;342(9):620–5.
28. Touitou V, Fenollar F, Cassoux N, et al. Ocular Whipple's disease: therapeutic strategy and long-term follow-up. Ophthalmology. 2012;119(7):1465–9.
29. Margo CE, Pavan PR, Groden LR. Chronic vitritis with macrophagic inclusions. A sequela of treated endophthalmitis due to a coryneform bacterium. Ophthalmology. 1988;95(2):156–61.
30. Ramzan NN, Loftus Jr E, Burgart LJ, et al. Diagnosis and monitoring of Whipple disease by polymerase chain reaction. Ann Intern Med. 1997; 126(7):520–7.
31. Brown DH. Ocular *Toxocara canis*. II. Clinical review. J Pediatr Ophthalmol. 1970;7:182–91.
32. Shields JA. Ocular toxocariasis. A review. Surv Ophthalmol. 1984;28(5):361–81.
33. Neafie RC, Connor DH. Chapter 7: Visceral larva migrans. In: Bindford CH, Connor DH, editors. Pathology of tropical and extraordinary diseases, vol. 2. Washington, DC: Armed Forces Institute of Pathology; 1976. p. 433–7.
34. Nussenblatt RB, Whitcup SM, Palestine AG. Chapter 16. Uveitis: fundamentals and clinical practice. 2nd ed. St Louis: CV Mosby; 1996. p. 238–43.
35. Fox AS, Kazacos KR, Gould NS, et al. Fatal eosinophilic meningoencephalitis and visceral larva migrans caused by the raccoon ascarid *Baylisacaris procyonis*. N Engl J Med. 1985;312:1619–23.
36. Yannuzzi LA. The retinal atlas. Philadelphia: Saunders/Elsevier; 2010. p. 366–7.
37. Bhattacharjee H, Das D, Medhi J. Intravitreal gnathostomiasis and review of literature. Retina. 2007;27: 67–73.
38. Bindford CH, Connor DH, editors. Pathology of tropical and extraordinary diseases, vol. 2. Washington, DC: Armed Forces Institute of Pathology; 1976. p. 340–575.
39. Sinawat S, Sanguansak T, Angkawinijwong T, et al. Ocular angiostrongyliasis: clinical study of three cases. Eye. 2008;22:1226–8.
40. Zinn KM, Fuillory SL, Friedman AH. Removal of intravitreous cysticerci from the surface of the optic nerve head. Arch Ophthalmol. 1980;98:714–6.
41. Custis PH, Pakalnis VA, Klintworth GK, et al. Posterior internal ophthalmomyiasis: identification of a surgically removed *Cuterebra* larva by scanning electron microscopy. Ophthalmology. 1983;90: 1583–90.
42. Spraul CW, Grossniklaus HE. Vitreous hemorrhage. Surv Ophthalmol. 1997;42(1):3–39.
43. Bishop PN. Part A, Chapter 29: Disorders of the vitreous. In: Garner A, Klintworth GK, editors. Pathobiology of ocular disease. 3rd ed. New York: Informa; 2008. p. 591–612.
44. Forrester JV, Balazs EA. Effect of hyaluronic acid and vitreous on macrophage phagocytosis. Trans Ophthalmol Soc UK. 1977;97(4):554–7.

45. Forrester JV, Prentice CR, Williamson J, Forbes CD. Fibrinolytic activity of the vitreous body. Invest Ophthalmol. 1974;13(11):875–9.
46. Forrester JV, Grierson I, Lee WR. Comparative studies of erythrophagocytosis in the rabbit and human vitreous. Albrecht Von Graefes Arch Klin Exp Ophthalmol. 1978;208(1–3):143–58.
47. Forrester JV, Lee WR, Williamson J. The pathology of vitreous hemorrhage. II. Gross and histopathologic appearances. Arch Ophthalmol. 1978;96(4): 703–10.
48. Grossniklaus HE, Frank KE, Farhi DC, et al. Hemoglobin spherulosis in the vitreous cavity. Arch Ophthalmol. 1988;106(7):961–2.
49. Kampik A, Kenyon KR, Michels RG, et al. Epiretinal and vitreous membranes: comparative study of 56 cases. Arch Ophthalmol. 1981;99(8):1445–54.
50. The Retina Society Terminology Committee. The classification of retinal detachment with vitreoretinopathy. Ophthalmology. 1983;90(2):121–5.
51. Hartnett ME, Penn JS. Mechanism and management of retinopathy of prematurity. N Engl J Med. 2012; 367(26):2515–26.
52. Toomes C, Bottomley HM, Jackson RM, et al. Mutations in LRP5 underlie the common familial exudative vitreoretinopathy locus on chromosome 11q. Am J Hum Genet. 2004;74(4):721–30.
53. Ranchod TM, Ho LY, Drenser KA, et al. Clinical presentation of familial exudative vitreoretinopathy. Ophthalmology. 2011;118(10):2070–5.
54. Chen S-N, Hwang J-F, Lin C-J. Clinical characteristics and surgical management of familial exudative vitreoretinopathy-associated rhegmatogenous retinal detachment. Retina. 2012;32(2):220–5.
55. Kleinberg TT, Tzekov RT, Stein L, et al. Vitreous substitutes: a comprehensive review. Surv Ophthalmol. 2011;56(4):300–23.
56. Balazs EA, Denlinger JL. Aging changes in the vitreous. In: Dismukes N, Sekular R, editors. Aging and human visual function. New York: Alan R Liss; 1982. p. 45–57.
57. O'Malley P. The pattern of vitreous syneresis. A study of 800 autopsy eyes. In: Irvine AR, O'Malley C, editors. Advances in vitreous surgery. Springfield: Charles C. Thomas; 1976. p. 17–33.
58. Los LI, van der Worp RJ, et al. Age-related liquefaction of the human vitreous body. LM and TEM evaluation of the role of proteoglycans and collagen. Invest Ophthalmol Vis Sci. 2003;44(7):2826–33.
59. Lapcik Jr L, Omelka L, Kuběna K, et al. Photodegradation of hyaluronic acid and the vitreous body. Gen Physiol Biophys. 1990;9(4):419–29.
60. Ueno N, Sebag J, Hirokawa H, Chakrabarti B. Effects of visible-light irradiation on vitreous structure in the presence of a photosensitizer. Exp Eye Res. 1987; 44(6):863–70.
61. Margo CE, Harman LE. Posterior vitreous detachment. How to approach sudden-onset floaters and flashing lights. Postgrad Med. 2005;117(3):37–42.
62. Boldrey EE. Risk of retinal tears in patients with vitreous floaters. Am J Ophthalmol. 1983;96(6):783–7.
63. Byer NE. Natural history of posterior vitreous detachment with early management as the premier line of defense against retinal detachment. Ophthalmology. 1994;101(9):1513–4.
64. Straatsma BR, Zeegan PD, Foos RY, et al. Lattice degeneration of the retina. XXX Edward Jackson Memorial Lecture. Am J Ophthalmol. 1974;77(5):619–49.
65. Klintworth GK. Chapter 37: Amyloidoses. In: Klintworth GK, Garner A, editors. Pathobiology of ocular disease. New York: Informa; 2008. p. 835–55.
66. Sandgren O. Ocular amyloidosis, with special reference to the hereditary forms with vitreous involvement. Surv Ophthamol. 1995;40(3):173–96.
67. Ciulla TA, Tolentino F, Morrow JF, Dryja TP. Vitreous amyloidosis in familial amyloidotic polyneuropathy. Report of a case with Val30Met transthyretin mutation. Surv Ophthalmol. 1995;40(3):197–206.
68. Kono S, Manabe Y, Tanaka T, et al. A case of familial amyloid polyneuropathy due to Phe33Val TTR with vitreous involvement as the initial manifestation. Intern Med. 2010;49(12):1213–6.
69. Margo CE. Corneal amyloid. Selecting the right histochemical stain. Cornea. 1986;5:125–6.
70. Wolman M. Amyloid its nature and molecular structure, comparison of a new toluidine-blue polarized light methods with traditional procedure. Lab Invest. 1971;25(2):104–10.
71. Tso MOM, Bettman JW. Occlusion of choriocapillaris in primary nonfamilial amyloidosis. Arch Ophthalmol. 1971;86(3):281–6.
72. Rodrigues M, Zimmerman LE. Secondary amyloidosis in ocular leprosy. Arch Ophthalmol. 1971;85(3): 277–9.
73. Bergren RL, Brown GC, Duker JS. Prevalence and association of asteroid hyalosis with systemic diseases. Am J Ophthalmol. 1991;111(3):289–93.
74. Luxenberg M, Sime D. Relationship of asteroid hyalosis to diabetes mellitus and plasma lipid levels. Am J Ophthalmol. 1969;67(3):406–13.
75. Hatfield RE, Gastineau CF, Rucker CW. Asteroid bodies in the vitreous: relationship to diabetes and hypercholesterolemia. Mayo Clin Proc. 1962;37:513–4.
76. Rodman HJ, Johnson FB, Zimmerman LE. New histopathological and histochemical observations concerning asteroid hyalitis. Arch Ophthalmol. 1961; 66:552–63.
77. March W, Shoch D, O'Grady R. Composition of asteroid bodies. Invest Ophthalmol. 1974;13(9):701–5.
78. Streeten BW. Vitreous asteroid bodies: ultrastructural characteristics and composition. Arch Ophthalmol. 1982;100(6):969–75.
79. Wand M, Smith TR, Cogan DG. Cholesterolosis bulbi: the ocular abnormality known as synchysis scintillans. Am J Ophthalmol. 1975;80(2):177–83.
80. Chan C-C, Wallace DJ. Intraocular lymphoma. Update on diagnosis and management. Cancer Control. 2004;11:385–95.

81. Coupland SE, Anastassiou G, Bornfeld N, et al. Primary intraocular lymphoma of T-cell type: report of a case and review of the literature. Graefes Arch Clin Exp Ophthalmol. 2005;243(3):189–97.
82. Chan C-C, Rubenstein JL, Coupland SE, et al. Primary vitreoretinal lymphoma: a report from an international Primary Central Nervous System Lymphoma Collaborative Group symposium. The Oncologist. 2011;16(11):1589–99.
83. Coupland SE, Heimann H, Bechrakis NE. Primary intraocular lymphoma: a review of the clinical, histopathological and molecular biological features. Graefes Arch Clin Exp Ophthalmol. 2004;242(11): 901–13.
84. Faia LJ, Chan C-C. Primary intraocular lymphoma. Arch Pathol Lab Med. 2009;133:1228–32.
85. Gonzales JA, Chan C-C. Biopsy techniques and yields in diagnosing primary intraocular lymphomas. Int Ophthalmol. 2007;27(4):241–50.
86. Kinoshita Y, Takasu K, Adachi Y, et al. Retrospective cytological study of intraocular lymphoma using vitreous and intraocular perfusion fluid. Diagn Cytopathol. 2012;40(7):604–7.
87. Coupland SE, Bechrakis NE, Anastassiou G, et al. Evaluation of vitrectomy specimens and chorioretinal biopsies in the diagnosis of primary intraocular lymphoma in patients with masquerade syndrome. Graefes Arch Clin Exp Ophthalmol. 2003;24(10): 860–70.
88. Coupland SE, Perez-Canto A, Hummel M, et al. Assessment of HOPE fixation in vitrectomy specimens in patients with chronic bilateral uveitis (masquerade syndrome). Graefes Arch Clin Exp Ophthalmol. 2005;243(9):847–52.
89. Whitcup SM, de Smet MD, Rubin BI, et al. Primary intraocular lymphoma: clinical and histopathological diagnosis. Ophthalmology. 1993;100(9):1399–406.
90. Ikeda K, Tate G, Suzuki T, Mitsuya T. Comparison of immunocytochemical sensitivity between formalin-fixed and alcohol-fixed specimens reveals the diagnostic value of alcohol-fixed cytocentrifuged preparations in malignant effusions. Am J Clin Pathol. 2011;136(6):934–42.
91. Karma A, von Willebrand EO, Tommila PV, et al. Primary ocular lymphoma. Improving the diagnostic procedure. Ophthalmology. 2007;114(7):1372–7.
92. Levasseur SD, Wittenberg LA, White VA. Vitreoretinal lymphoma. A 20-year review of incidence, clinical and cytologic features, treatment, and outcome. JAMA Ophthalmol. 2013;131(1): 50–5.
93. Pavan PR, Oteiza E, Margo CE. Ocular lymphoma diagnosed by internal subretinal pigment epithelial biopsy. Arch Ophthalmol. 1995;113(10):1233–4.
94. Shen DF, Zhuang Z, LeHoang P, et al. Utility of microdissection and polymerase chain reaction for the detection of immunoglobulin gene rearrangement and translocation in primary intraocular lymphoma. Ophthalmology. 1998;105(9):1664–9.
95. Chan CC. Molecular pathology of primary intraocular lymphoma. Trans Am Ophthalmol Soc. 2003;101: 275–92.
96. Jaissle GB, Szurman P, Rohrbach JM, et al. A case of cutaneous melanoma metastatic to the vitreous cavity: possible pathomechanism and review of the literature. Graefes Arch Clin Exp Ophthalmol. 2007;245(5):733–40.
97. Soheilian M, Mirbabai F, Shahsavari M, et al. Metastatic cutaneous melanoma to the vitreous cavity masquerading as intermediate uveitis. Eur J Ophthalmol. 2002;12(4):324–7.
98. Pavan PR, Margo CE, Drucker M. Malignant melanoma of the choroid with vitreous seeding. Arch Ophthalmol. 1989;107(1):130.
99. Liu K, Klintworth GK, Dodd LG. Cytologic findings in vitreous fluids. Analysis of 74 specimens. Acta Cytol. 1999;43(2):201–6.
100. Wittenberg LA, Maberley DA, Ma PE, et al. Contribution of vitreous cytology to final clinical diagnosis fifteen-year review of vitreous cytology specimens from one institution. Ophthalmology. 2008;115(11):1944–50.
101. Zhai J, Harbour JW, Smith ME, Dávila RM. Correlation study of benign cytomorphology and final clinical diagnosis. Acta Cytol. 2008;52(2): 196–200.

Retina

9

Nikolaos E. Bechrakis, Philip J. Luthert,
and David J. Wilson

9.1 General Description

The retina lines the inside of the eyeball and extends from the optic disk to the ora serrata, where it merges with the pars plana of the ciliary body. The basic histological studies of the light microscopic structure of the retina have been carried out by Heinrich Müller (Würzburg, 1820–1864) and Santiago Felipe Ramón y Cajal (Madrid, 1852–1934) and are still valid today. The retinal thickness varies between 560 µm near the optic disk and the foveal margin and 102 µm at the ora serrata. It is the thinnest in the center of the fovea at 100 µm. The retina merges posteriorly with the optic nerve, and anteriorly the neuroretinal portion of the retina is continuous anterior to the ora serrata with the nonpigmented epithelium of the pars plana of the ciliary body.

N.E. Bechrakis, MD, FEBO (✉)
Department of Ophthalmology,
Innsbruck Medical University,
Anichstrasse 35, A-6020 Innsbruck, Austria
e-mail: nikolaos.bechrakis@i-med.ac.at

P.J. Luthert, BSc, MBBS, FRCP, FRCPath, FRCOphth
Department of Ophthalmology,
UCL University College London,
11-43 Bath Street, London EC1V 9EL, UK
e-mail: p.luthert@ucl.ac.uk

D.J. Wilson, MD
Casey Eye Institute, Oregon Health and Science
University, 3375 SW Terwilliger Blvd,
Portland, OR 97221, USA
e-mail: wilsonda@ohsu.edu

9.2 Embryology

The primary optic vesicles develop bilaterally at the apical end of the neural canal in the 3rd–4th week of gestation as protuberances of neuroectoderm. An invagination and detachment of the surface ectoderm form the lens vesicle. The secondary optic vesicle (optic cup) is formed between the 4th and 7th week of embryogenesis. The rim of the optic cup corresponds to the pupil. The nonpigmented epithelium of the ciliary body and the neurosensory retina develop from the inner leaf of the optic cup. The pigmented layers of the iris and ciliary body epithelium anteriorly and the retinal pigment epithelium (RPE) posteriorly develop from the outer leaf of the optic cup.

The formation of the primary optic vesicle is accompanied by the invagination of the hyaloid artery inferiorly into the developing optic cup. At the end of the 6–7th week after the hyaloid artery has penetrated into optic cup, it closes. Incomplete closure of the optic cup can result in typical colobomas, which can be isolated to the iris or ciliary body but also to the retina/choroid and/or in the optic disk or in various combinations, depending on the situation and the stage of their occurrence.

9.2.1 Anatomy of the Retina

For clinical purposes, the retina is divided topographically into a central region (within the vascular arcades), a mid peripheral zone (between

S. Heegaard, H. Grossniklaus (eds.), *Eye Pathology: An Illustrated Guide*,
DOI 10.1007/978-3-662-43382-9_9, © Springer-Verlag Berlin Heidelberg 2015

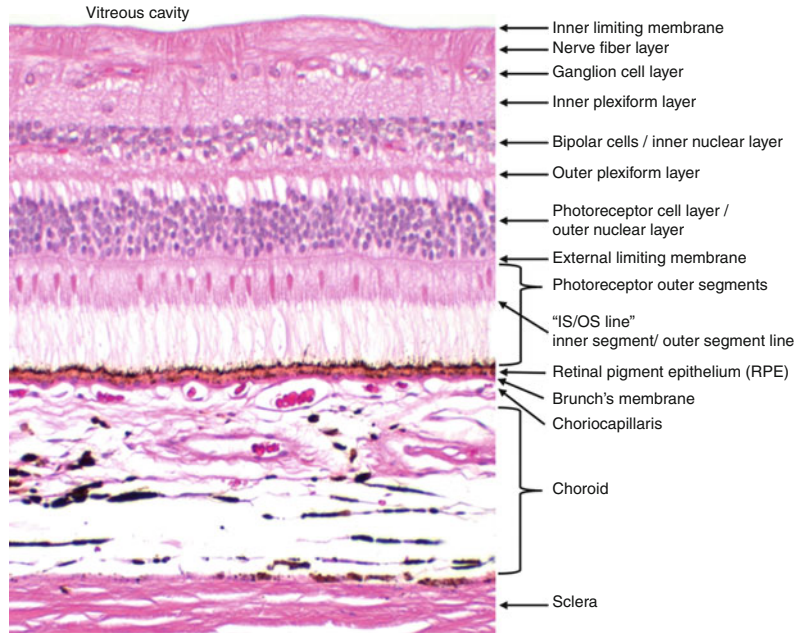

Fig. 9.1 Histological section of the retina, the retinal pigment epithelium, choroid, and sclera

vascular arcades and the equator), and the peripheral area or post-equatorial retina that ends anteriorly at the ora serrata. The posterior temporal retina contains the most important part of the retina clinically, namely, the macula.

The macula is located at the center of the posterior pole of the retina. It is an oval, yellowish area with a diameter of about 5 mm. It has a central pit, the fovea centralis, which has the highest density of retinal photoreceptors. The term "macula lutea" is derived from histopathological observations, where the yellowish, so-called macular pigment xanthophyll becomes visible through fixation and loss of blood circulation. Clinically, it is not apparent on regular ophthalmoscopy but can be assessed using fundus autofluorescence imaging or psychophysical techniques. The macular region has the highest density of cones, and more peripherally, their density is reduced in favor of the rods.

Quantitative data on the density and distribution of photoreceptors were first made by Østerberg [1] and more recently by Curcio et al. [2–4]. Throughout the retina, there are approximately 60–125 million rods, 3.2–6.5 million red and green cones, and 300,000–600,000 blue cones. The highest cone density is at the center of the fovea (approximately 175,000/mm^2), where there are only red and green cones. Overall, however, only 5 % of all cones are present in the fovea, so, for example, in a full-field electroretinogram, their isolated loss in the foveal region is not readily apparent. The density of cones decreases rapidly towards the retinal periphery. The rods have their highest density approximately 20° lateral to the fovea.

The optic disk (papilla) is approximately 3 mm nasal and slightly superiorly located in relation to the fovea. The papilla has a cuplike depression centrally. The nonmyelinated nerve fibers from the retinal ganglion cells travel within the nerve fiber layer of the retina and extend into the optic disk, where they concentrate into bundles surrounded by a connective tissue meshwork, the lamina cribrosa. The optic disk has a diameter of approximately 1.5 mm at the level of the lamina cribrosa. Beyond the lamina cribrosa, the nerve fibers are myelinated and form the optic nerve, which is about 5–6-mm thick in the postlaminar region, including its surrounding tissues the pia mater, arachnoid, and dura mater.

A cross section of the retina contains several well-defined layers (Fig. 9.1). The outer retina lies on the RPE, and the innermost layer abuts the

vitreous. The two outer layers consist of the inner and outer segments of the photoreceptor cells. The external limiting membrane is located at the level of transition between the outer inner photoreceptor segments and the thin fiber that connects the inner segment with the cell body. It is not a conventional membrane but a histologically defined zone of junctional complexes ("zonula adherens"), usually between the inner photoreceptor segments and the Müller cells, but also between adjacent Müller cells, and less frequently between the inner segments of photoreceptors themselves.

The Müller cell endings connect photoreceptors to each other but also interlock with the microvilli of the retinal pigment epithelium. The outer segments of the photoreceptor cells (rods and cones) are embedded into the RPE microvilli depending on the light adaptation. Photoreceptor outer segment renewal takes place by the shedding of the tips with subsequent phagocytosis by RPE cells where lysosomal degradation and, for some molecules, recycling to photoreceptors take place.

The outer nuclear layer consists of the nuclei of the rods and cones and is located just external to the outer plexiform layer. The nuclei of the cones are located closer to the external limiting membrane than the rod nuclei are. The outer two thirds of the outer plexiform layer consist of axons of the photoreceptor cells, while the inner third contains the synaptic connections between the photoreceptor axons and the axons of the bipolar, horizontal, and amacrine cells that comprise the inner nuclear layer. This cellular/synaptic complex is located approximately in the center of the retina and is an important physical barrier for exudates and defines the outermost extent of the deep retinal capillary plexus that lies approximately parallel to the vascular network in the nerve fiber layer.

Internal to the outer plexiform layer is inner nuclear layer, which consists of the cell bodies of bipolar, amacrine, horizontal, and Müller cells. This layer is richly perfused by retinal capillaries. The nuclei of the bipolar and Müller cells are located in the middle layers of the inner nuclear layer, whereas the nuclei of horizontal cells lie towards the outer plexiform layer and the amacrine cells towards the inner plexiform layer. The inner plexiform layer is composed of the axons of the bipolar and amacrine cells, the dendrites of the ganglion cells, and their interconnecting synapses. The ganglion cell layer is composed of multiple cell layers only in the macular area, whereas is composed of a cellular monolayer outside the macular area. The nerve fiber layer is composed of nonmyelinated axons of the ganglion cells. The inner limiting membrane (ILM) is a basement membrane in which the footplates of Müller cells are embedded. Its inner face is smooth, and the outer aspect is irregular and varies in thickness across the retina. It is thinnest near the optic disk and overlying the retinal vessels.

9.2.1.1 The Macula

The macula has a diameter of approximately 5 mm and is located within the temporal vascular arcades. It includes the perifovea, the parafovea, the fovea, the foveola, and the central umbo. Histologically, the macula differs from the peripheral retina by having a multilayered arrangement of ganglion cells, which is thickest at the fovea where there is the higher density of cones. The foveola forms the center of the fovea and macula and has a diameter of 0.35 mm. Due to the lateral displacement of the inner retina and the fact that the umbo and the foveola contain only cones and Müller cells, its thickness is only 130 μm.

The axons of the cones at the fovea are called Henle fibers and are displaced laterally in an oblique fashion so that they border directly to the vitreous cavity. This is associated with a lateral displacement of the second and third neurons. Macular pigment binds particularly strongly within the Henle fiber layer.

9.2.1.2 The Retinal Pigment Epithelium (RPE)

Immediately underneath the neurosensory retina, in close contact with the photoreceptor outer segments, lies a monolayer of approximately one million polarized pigmented retinal pigment epithelial cells (RPE). In contrast to the sensory retina, this layer has no photoreceptive neural functions but is essential for the function and

metabolic health of the photoreceptors. The RPE cells contain numerous melanin granules in the apical cytoplasm. They are cuboidal and hexagonal viewed en face and vary in size from 10 μm diameter at the macula to 60 μm in diameter in the periphery, where they are also flatter. RPE cells are largely postmitotic cells that decline in density throughout life, especially at the periphery. In humans there is no apparent RPE renewal by mitosis, although inflammation or trauma can cause a temporary reactive mitotic response. The RPE only extremely rarely becomes neoplastic, but often in pathological processes, it becomes metaplastic, forming, for instance, myoepithelial cells, fibrous scar tissue, or even bone. The apical region of the RPE cells is directed towards the photoreceptors, whereas the basal portion is attached to Bruch's membrane and separated from it only by its thin basement membrane. The cell nucleus and mitochondria are located in the base of the cell. At the retinal periphery close to the ora serrata, RPE cells often can be multinucleated. It has been proposed that in that region RPE stem cells are present. Abundant mitochondria within the RPE reflect the high metabolic capacity of the cell. RPE cells are bound together by tight junctions, which are located near the cell apex (Verhoeff's membrane). These junctions form the outer retinal blood–retinal barrier, whereas the inner retinal blood–retinal barrier is formed by the endothelium of the intraretinal blood vessels.

9.2.1.3 Bruch's Membrane

Bruch's membrane lies between the RPE and the choroid. Passing progressively towards the choroid from the RPE, Bruch's membrane is composed of the RPE basement membrane, an inner collagenous layer, an elastic layer, an outer collagenous layer, and the basement membrane of the endothelial cells of the choriocapillaris.

9.3 Congenital Anomalies

Definition

Congenital anomalies of the retina fall into two general categories, stable structural or developmental anomalies and progressive inherited retinal degenerations. These latter conditions are usually the result of single or multiple genetic mutations. A list of stable structural or developmental anomalies is shown in Table 9.1. By definition, the structural and developmental lesions are not progressive disease processes. However, secondary changes can occur due to degeneration associated with the congenital condition, e.g., retinal detachment due to persistent fetal vasculature or choroidal neovascularization associated with macular telangiectasia.

Table 9.1 Structural developmental anomalies

Vascular
Cavernous hemangioma of the retina
Macular telangiectasia
Coats' disease
Neuronal
Albinism
Color blindness
Combined hamartoma
Congenital hypertrophy of the RPE
Retinal dysplasia
Vitreous
Persistent fetal vasculature
Cyst

The inherited conditions are for the most part progressive disorders. The age at which a disease phenotype appears is variable. Despite the hundreds of individual gene defects, there are certain stereotypical tissue responses that characterize progressive retinal degeneration: (1) photoreceptor atrophy associated with RPE hyperplasia, (2) photoreceptor atrophy combined with RPE atrophy, and (3) production of abnormal extracellular matrix. A sampling of inherited retinal disorders is listed on the basis of these tissue responses and is provided in Table 9.2. These tissue responses will be illustrated in the histopathology section below.

Epidemiology

Structural or developmental anomalies of the retina are rare. Of these, abnormalities of the vasculature are by far the most common. The prevalence of persistence of the fetal vasculature is quite variable depending on how it is defined. Very mild persistence occurs in almost all infants

Table 9.2 Inherited retinal degenerations

Retinal atrophy and RPE hyperplasia
Retinitis pigmentosa
Neuronal ceroid lipofuscinosis
Stargardt disease (severe phenotype)
Retinal atrophy and RPE atrophy
Gyrate atrophy
Choroideremia
Cone dystrophy
Stargardt disease (moderate phenotype)
Abnormal extracellular matrix
Sorsby's fundus dystrophy
Best disease
Stargardt disease (mild phenotype)

with the last vestiges of the tunica vasculosa lentis regressing in the first few days after birth. However, more severe cases of persistent fetal vasculature are quite rare.

Inherited retinal degenerations are also uncommon. The prevalence of typical retinitis pigmentosa is approximately 1:5,000 worldwide. The incidence of Stargardt disease is 1:8,000 to 1:10,000. Retinitis pigmentosa and Stargardt disease are the most common of the progressive inherited retinal degenerations.

Clinical Features

The clinical features of the structural or developmental anomalies vary considerably based on what type and location of tissue are involved with the anomaly. As mentioned above, the most common of the congenital structural anomalies is persistent fetal vasculature [5]. During fetal development, there is a system of vessels that extends through the vitreous cavity and surrounds the lens. This vasculature system is called the hyaloid vasculature. With normal retinal development, these vessels regress. However, in some instances, there is persistence of these vessels. The clinical findings are quite variable based on the extent of the remaining vessels. In some instances, only a small dot-like cataract is present on the posterior surface of the lens, a so-called Mittendorf dot. However, in some cases there is persistence of the fetal vasculature on the optic nerve, and these persistent vessels can exert traction on the peripapillary retina (Fig. 9.2). Persistence of the fetal vasculature is also associated with cataract. In very severe cases, eyes with persistent fetal vasculature may be enucleated due to poor vision and concern that the changes in the eye are due to an intraocular malignancy (retinoblastoma).

Another relatively common vascular anomaly that is of significance to the eye pathologist is Coats' disease. In Coats' disease, there are telangiectatic vessels within and on the surface of the retina. These vessels are prone to leakage, and the leakage of fluid and serum lipid can accumulate in the retina causing a mass that can mimic retinoblastoma (Fig. 9.3). This accumulation of fluid and lipid can be progressive over time, causing growth of the lesion, further confusing the clinical distinction between Coats' disease and retinoblastoma. Eyes with Coats' disease sometimes are enucleated due to concern that the intraocular changes could be retinoblastoma.

There is a vast literature on the clinical features of the inherited retinal degenerations, and a complete summary is beyond the scope of this chapter. However, the clinical features of three of the diseases listed in Table 9.2 will suffice to provide correlative material for the histopathological section that follows. Retinitis pigmentosa is an inherited retinal degeneration characterized by initial difficulty in seeing at night (nyctalopia) and loss of peripheral vision. With progression, central vision may become affected as well. Retinitis pigmentosa is a heterogeneous disorder, with close to 200 individual causative mutations having been identified. It can be inherited as an X-linked recessive, autosomal recessive, or autosomal dominant trait. On examination, the fundus appearance is characterized by prominent RPE hyperplasia, with the pigmented cells giving a "bone spicule" appearance due to the predilection of the hyperplastic RPE cells to accumulate around retinal vessels (Fig. 9.4).

Gyrate atrophy is another inherited retinal degeneration, which is due to genetic defects affecting ornithine aminotransferase. Gyrate atrophy is an autosomal recessive disorder and is prototypical of the inherited retinal degenerations that are characterized by retinal atrophy as well as RPE atrophy (Fig. 9.5). In gyrate atrophy,

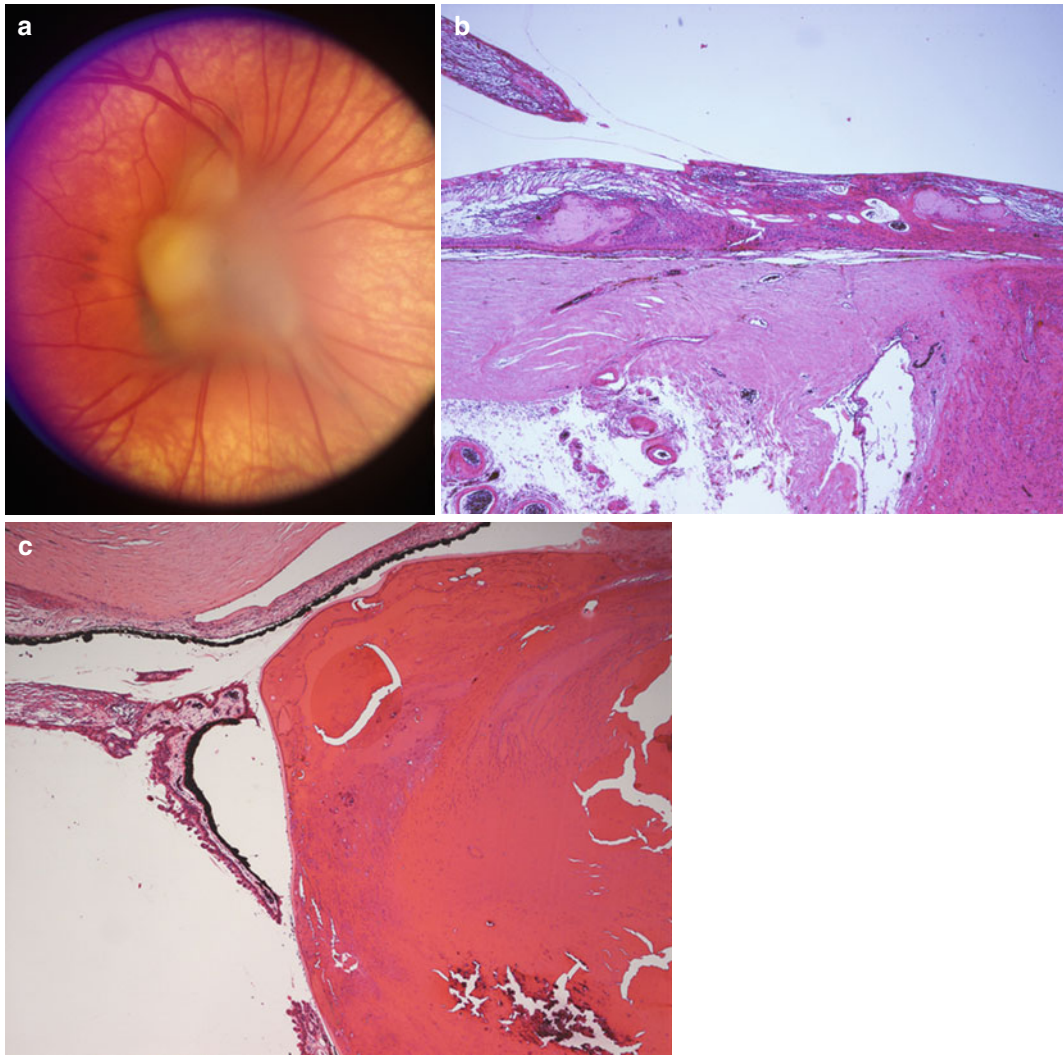

Fig. 9.2 Persistent fetal vasculature. (**a**) Clinical photograph showing gliosis and distortion of the retina surrounding the optic nerve. (**b**) Section through the nerve and peripapillary retina showing distortion of the retinal layers and gliosis. The persistent fetal vasculature is evident overlying the retina and is contiguous with the retinal tissue at other levels of section. (**c**) Anteriorly, the persistent fetal vasculature pulls the ciliary processes centripetally and is associated with cataractous changes in the lens

patients are symptomatic due to their loss of peripheral visual field.

Sorsby's macular dystrophy is an autosomal recessive trait characterized by extensive changes in the extracellular matrix due to an abnormality of a tissue inhibitor of metalloproteinase (TIMP-3). Patients with Sorsby's disease have prominent deposits of extracellular material beneath the retina. This material and associated damage to Bruch's membrane are associated with the growth of abnormal blood vessels beneath the retina – so-called choroidal neovascularization. The growth of blood vessels in this location leads to scarring with associated severe decrease in vision (Fig. 9.6).

In Stargardt disease, any of the three stereotypical tissue responses can occur. Some patients maintain relatively good vision and only manifest some subretinal deposits. Others have moderate disease that manifests as focal loss of

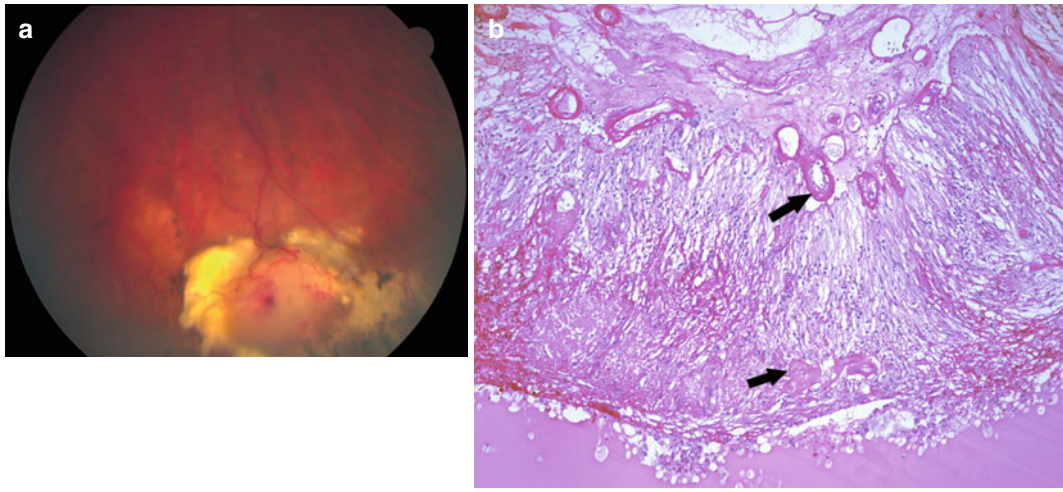

Fig. 9.3 Coats' disease. (**a**) Clinical photograph showing white to yellow lesion in the retinal periphery with prominent vasculature. (**b**) Section showing telangiectatic vessels (*arrows*) within the retina and on the retinal surface. The retina is detached. There are lipid-laden macrophages in the subretinal space

photoreceptors and atrophy of the underlying RPE. And the most severely affected patients have diffuse loss of photoreceptors associated with RPE hyperplasia and migration into the retina.

Histopathology

Of the structural and developmental anomalies, the conditions of greatest relevance to a general pathologist are persistent fetal vasculature and Coats' disease. The histopathology of persistent fetal vasculature is variable, but in the more extensive cases, there is persistence of hyaloid vessels arising from the optic nerve and extending anteriorly to the posterior lens and ciliary body. The tissue associated with the vessels can contain myofibroblasts, and traction on adjacent tissues can lead to traction detachment of the peripapillary retina posteriorly and central dragging of the ciliary processes in the anterior portion of the eye. Contact with the posterior lens capsule is associated with cataract formation (Fig. 9.2).

In Coats' disease, there are telangiectatic vessels in the retina. In enucleated eyes, there is generally a total exudative retinal detachment present. In the subretinal space, there are often macrophages that have "foamy" lipid-containing cytoplasm. Cholesterol clefts may be present in the subretinal space consistent with the prior presence of abundant cholesterol (Fig. 9.3).

Histopathological study of the eyes from patients with retinitis pigmentosa reveals there is marked loss of the photoreceptor layer [6]. This is most severe peripherally, but in advanced cases, there can be loss of photoreceptors in the fovea as well. The RPE becomes hyperplastic, and there is migration of pigment-laden RPE cells to a position surrounding the retinal vasculature (Fig. 9.4). In addition to the striking changes at the level of the photoreceptors and RPE, there are changes that occur in the inner retina. The normal inner retinal circuitry is not maintained, and there is sprouting of neurites and gliosis. Both of these latter changes may limit future therapeutic options as the inner retinal changes may compromise re-establishment of a functioning visual pathway.

In patients with gyrate atrophy [7], there is loss of the photoreceptor layer, but unlike retinitis pigmentosa, the RPE does not become hyperplastic. In fact, the RPE in the areas of photoreceptor degeneration is completely absent. Where the photoreceptors are preserved, they have a remarkably normal appearance (Fig. 9.5).

Sorsby's macular dystrophy [8] is characterized by prominent deposits of eosinophilic material beneath the RPE and the ciliary epithelium

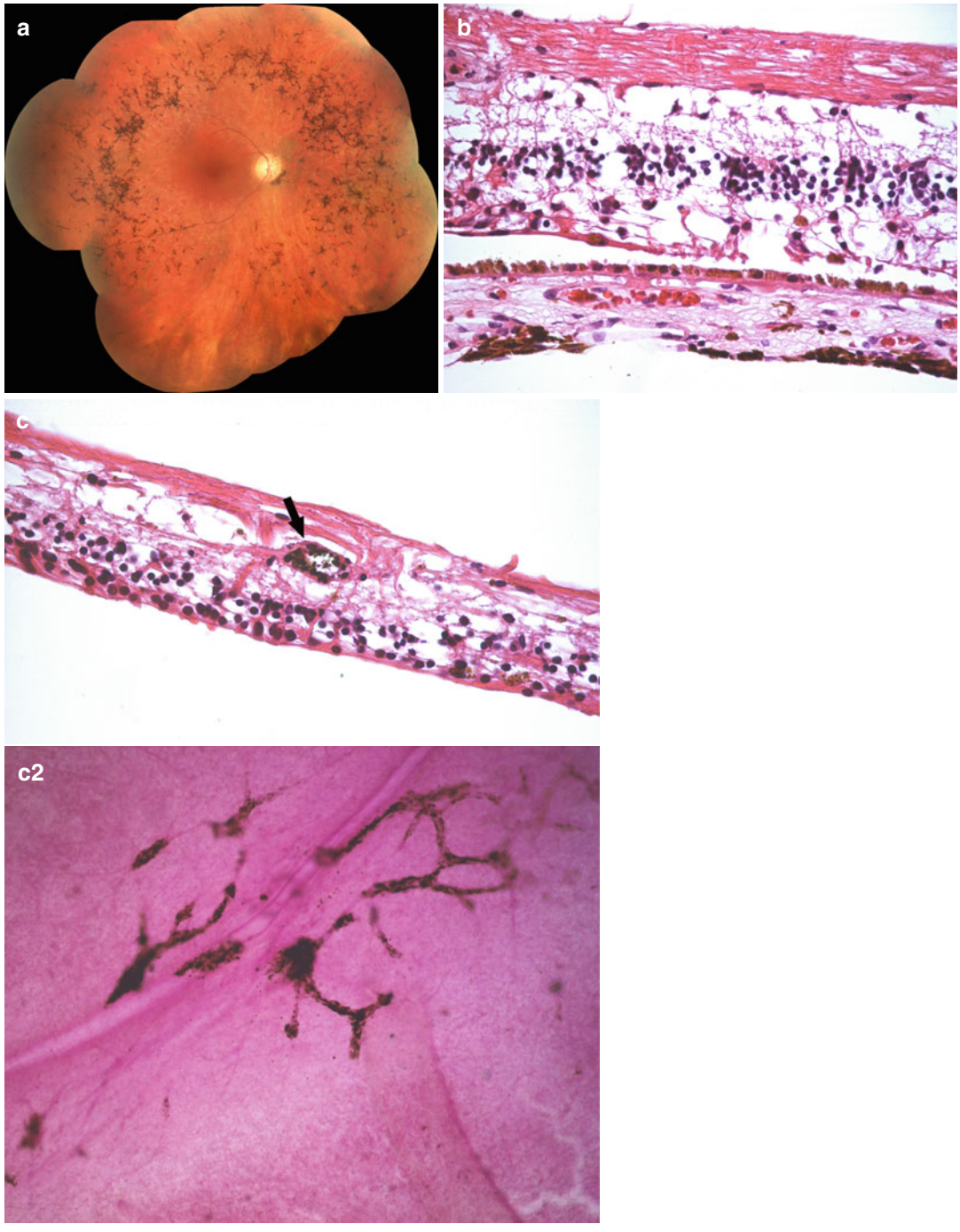

Fig. 9.4 Retinitis pigmentosa. (**a**) Clinical photograph showing marked RPE hyperplasia and atrophy in the peripheral retina. (**b**) Histopathology reveals there is marked loss of the photoreceptor layers. The inner retina has some alteration in the normal lamellar architecture consistent with some remodeling occurring due to the loss of photoreceptors. (**c**) The hyperplastic RPE has migrated into the retina and surrounds retinal vessels (*arrow*) as shown in the (**c2**) retinal whole mount and cross section

Fig. 9.5 Gyrate atrophy. (**a**) Clinical photograph showing abrupt transition from small area of relatively normal retina in macula and surrounding nerve to area of marked atrophy of the choroid, RPE, and retina. (**b**) Section in the transition zone showing complete loss of the RPE and anterior choroid with preservation of the inner retinal layers

(Fig. 9.6). These deposits are associated with the ingrowth of blood vessels from the underlying choroid. Leakage of fluid from this neovascularization results in hyperplasia of the RPE and atrophy of the overlying photoreceptors.

Prognosis and Predictive Factors

Congenital structural abnormalities are only progressive on the basis of secondary changes that occur as a result of the anomaly. For example, with Coats' disease, progressive leakage from the telangiectatic vessels can lead to retinal detachment. In addition, this leakage and secondary gliosis can lead to an intraocular mass that masquerades as retinoblastoma. Treatment of the abnormal blood vessels with laser or cryotherapy can prevent either retinal detachment or the development of a large mass. However, frequently the presence of the abnormal vessels is not known early enough to permit treatment.

The prognosis for the inherited retinal degeneration varies based on the disease. In general, diseases characterized by diffuse photoreceptor atrophy and RPE hyperplasia have a poor prognosis for vision. An intermediate prognosis is present for those diseases with regional photoreceptor atrophy associated with RPE atrophy. Those diseases with genetic abnormalities primarily affecting the extracellular space have a variable prognosis based on the secondary complications that may ensue. Mild Stargardt disease has a fairly good prognosis whereas Sorsby's macular dystrophy is associated with severe vision central vision loss.

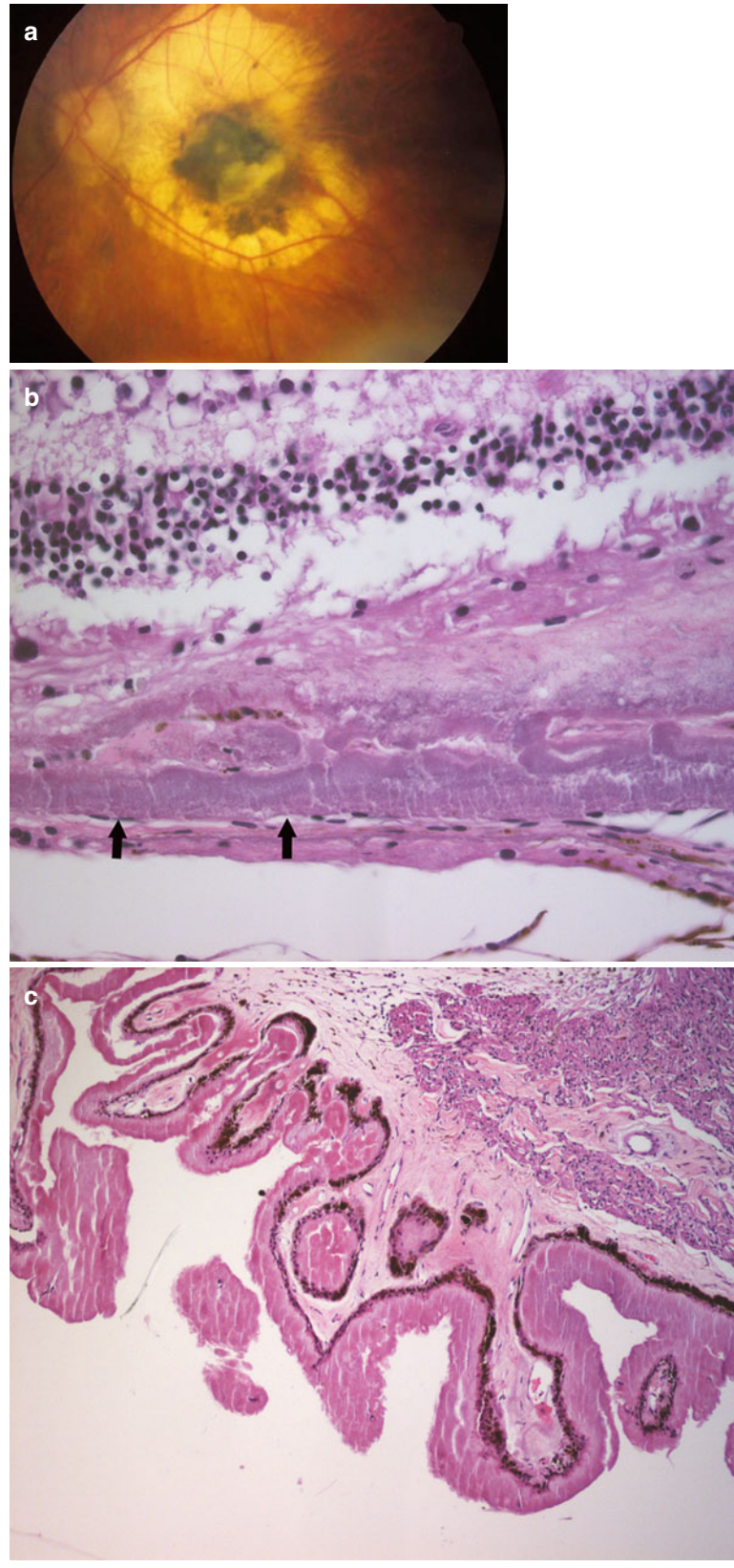

Fig. 9.6 Sorsby's macular dystrophy. (**a**) Clinical photograph showing the macular changes of subretinal exudate and RPE hyperplasia secondary to subretinal neovascularization associated with this condition. (**b**) Histological sections demonstrate a marked increase in extracellular matrix both in the area of Bruch's membrane. (**c**) Similar extracellular material associated with the nonpigmented epithelium of the ciliary body

9.4 Retinal Inflammatory Conditions

Definition

Diseases that have a predominant inflammatory etiology can be further classified into those that are due to an identifiable infectious agent (Table 9.3) and those that are noninfectious (Table 9.4). This classification is of benefit both from a clinical standpoint in which treatment will be markedly affected by identifying an infectious agent; but, also the pathology of infectious inflammatory conditions is quite distinct from the noninfectious inflammatory disorders.

Epidemiology

Infectious retinitis is relatively common. The most common cause for infectious retinitis is bacterial infection following cataract surgery. This type of infection occurs in 0.03–0.16 % of cases [9, 10].

Table 9.3 Infectious retinal inflammatory conditions

Viral
Cytomegalovirus
Herpes simplex
Herpes zoster
Bacterial
Exogenous
Postsurgical
Traumatic
Endogenous
Fungal
Exogenous
Postsurgical
Traumatic
Endogenous
Protozoal (toxoplasmosis, etc.)

Table 9.4 Noninfectious retinal inflammatory conditions

Autoimmune retinopathy
Cancer-associated retinopathy (CAR)
Melanoma-associated retinopathy (MAR)
Acute zonal occult outer retinopathy (AZOOR)
Multiple evanescent white dot syndrome (MEWDS)
Adamantiades–Behçet's disease
Eales' disease

Bacterial or fungal retinal infections also occur without prior surgery, so-called endogenous endophthalmitis. This latter type of infection occurs most commonly in patients with indwelling central lines but may also be the result of systemic immunosuppression as is seen in post organ transplant patients. Endogenous bacterial endophthalmitis comprises 2–8 % of bacterial endophthalmitis [11]. Viral retinal infections are most common in immunosuppressed patients, most typically HIV-infected patients with low CD4 counts. Viral retinal infections also occur as reactivation of herpes zoster. Finally, toxoplasmosis is a frequent cause of infectious retinitis. Toxoplasmosis can be an acquired infection or can be the result of reactivation of a congenitally acquired infection.

There are certain epidemiologic associations with noninfectious retinitis as well. Notably, autoimmune retinopathy occurs in association with systemic malignancy, and Adamantiades–Behçet's disease is associated with the HLA B51 haplotype.

Etiology

The etiology of the conditions resulting from infectious organisms is straightforward. The various infectious agents gain access to the eye either as the result of introduction during surgery (postsurgical endophthalmitis), as the result of injury, or due to hematogenous dissemination. In the case of toxoplasmic retinitis, the initial retinal infection may have occurred in utero due to transplacental infection with toxoplasmosis. Quiescent, postinfectious scars may harbor encysted toxoplasmic organisms which reactivate creating acute disease in children or adults.

The etiology of autoimmune retinopathy has been speculated to be similar to other paraneoplastic disorders: a remote malignancy elaborates an antigenic substance that is sufficiently similar to a retinal antigen that the resulting antibody and immunologic reaction results in damage to the retina. In the case of AZOOR and MEWDS, the autoimmune response is hypothesized to be triggered by a previous viral infection.

Clinical Features

Postsurgical infections present as intense acute inflammation in the aqueous and vitreous. The

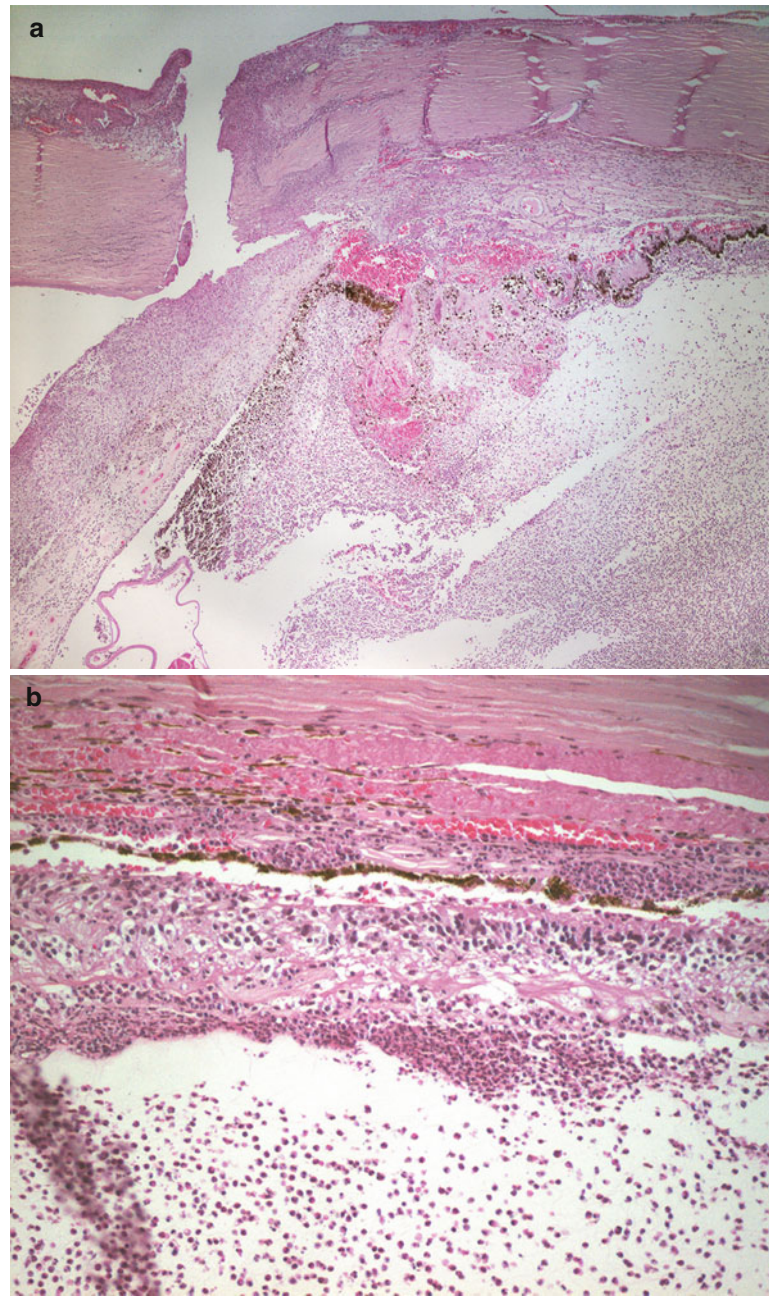

Fig. 9.7 Postoperative endophthalmitis. (**a**) The unhealed limbal wound is evident. There is marked acute inflammation in the anterior and posterior chambers. (**b**) There is marked acute inflammation involving the vitreous, with infiltration of the retina and choroid

presence of the intense neutrophil infiltrate obscures vision resulting in symptoms of decreased vision, photosensitivity, and pain. Most cases of postsurgical endophthalmitis will be diagnosed on the basis of culture of aqueous and vitreous fluid. Typically, intravitreal injections of antibiotics or antifungals will be administered immediately following acquisition of fluid for culture. Injections of this type are usually effective in eradicating the infection, but in some cases, the extent of retinal damage or secondary changes will result in enucleation of a painful globe. This is more likely to occur in cases of infections with more aggressive bacteria, such as pneumococcus or Gram-negative bacteria (Fig. 9.7). Posttraumatic infections, particularly

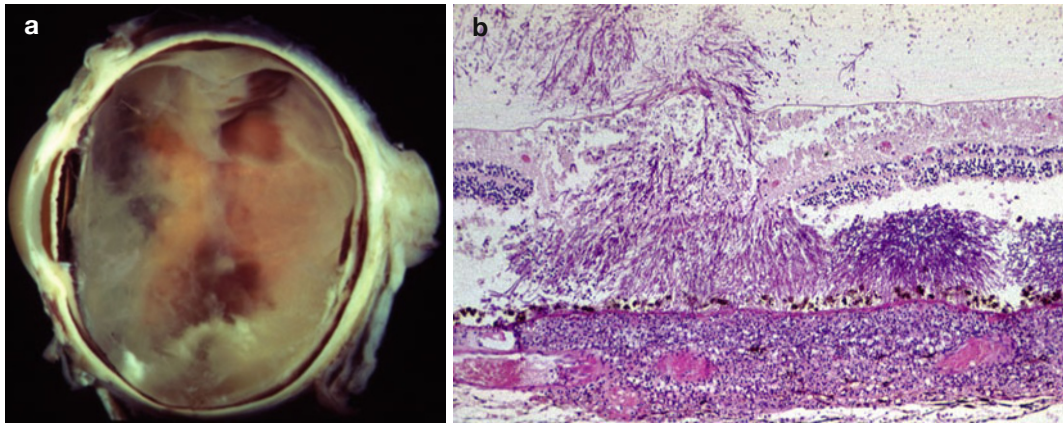

Fig. 9.8 Endogenous fungal aspergillus endophthalmitis. (**a**) Gross photograph showing intraretinal hemorrhages and retinal whitening in the areas of fungal infection. There is also overlying vitreous opacity. (**b**) There are fungal aspergillus hyphae throughout the retina and extending into the vitreous. There is a prominent inflammatory in filtrate in the choroid

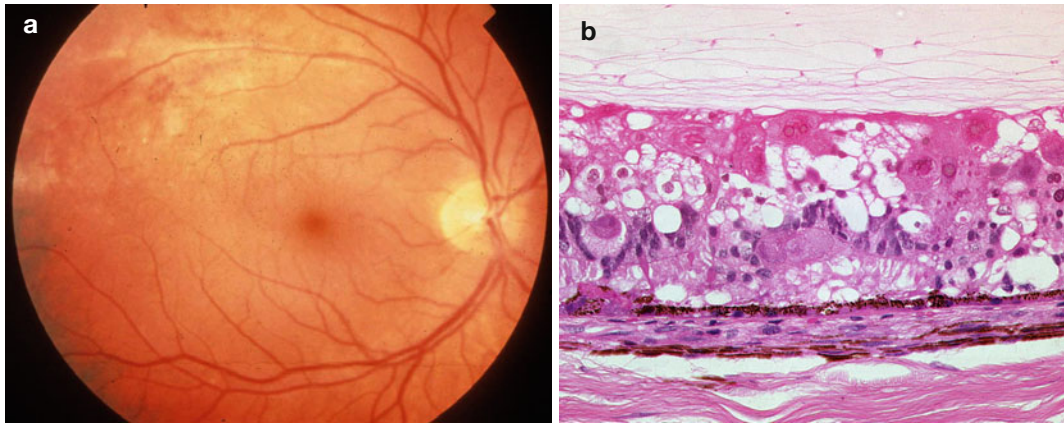

Fig. 9.9 CMV retinitis. (**a**) Clinical photograph. There is retinal whitening and intraretinal hemorrhage along the superior arcade. (**b**) Section through an area of CMV-retinitis reveal prominent cytomegalic cells with intranuclear and intracytoplasmic inclusions, as well as atrophy and necrosis in the inner and outer retinal layers

if *Bacteroides* is the infecting agent, are also likely to result in severe retinal injury that may lead to enucleation of the globe.

Endogenous endophthalmitis also presents as decreased vision due to inflammation-induced loss of clarity of the optical media or due to direct infection of the central retina. Examination discloses a white infiltrate in the retina with overlying inflammation (Fig. 9.8). The patient typically has an indwelling central line or is immunocompromised. CMV infection of the retina is a common finding in patients infected with HIV who have CD4 counts below 50 per ml. CMV retinitis has a distinctive clinical appearance with the retina having dense whitening associated with intraretinal hemorrhage (Fig. 9.9). Strikingly, there is generally very little vitreous inflammation associated with the retinal infection. This aids in distinguishing CMV infection from acute retinal necrosis (see below) and toxoplasmosis. As the infection destroys the retina, the retinal whitening disappears and is

replaced by markedly thinned retina with pigmentation due to RPE hyperplasia. The infection proceeds centripetally from its initial focus so that in more long-standing infections there are areas of thinned, variably pigmented retina surrounded by a border of whitened retina representing the location of the active infection.

Acute retinal necrosis (ARN) describes a clinical presentation of marked retinal whitening due to necrosis (Fig. 9.10). Typically the area of involvement begins peripherally and moves centrally, although the opposite pattern has been reported (this latter pattern is referred to as progressive outer retinal necrosis, PORN). In contrast to CMV retinitis, ARN occurs in immunocompetent patients and is associated with prominent intraocular inflammation. Acute retinal necrosis may be due to herpes zoster or herpes simplex.

Toxoplasmic retinitis also presents with decreased vision due to intraocular inflammation or due to direct involvement of the central retina with the infection (Fig. 9.11). The white retinal infiltrate is classically described as a "headlight" in the "fog" of vitreous inflammation. If the ocular media are sufficiently clear, it is possible to see that the area of active infection may be adjacent to an old scar. This latter feature is a strong indication that the infection is due to toxoplasmosis.

CMV, H. zoster, H. simplex, and toxoplasmosis may be diagnosed by PCR of vitreous or aqueous samples. In some cases in which the diagnosis is not established by PCR, retinal biopsy may be performed to try to confirm a diagnosis.

As indicated in Table 9.4, there are several noninfectious entities that may lead to retinal inflammation. There are several distinct clinical entities that are hypothesized to be a form of retinal autoimmunity: cancer-associated retinopathy (CAR), melanoma-associated retinopathy (MAR), acute zonal occult outer retinopathy (AZOOR), and multiple evanescent white dot syndrome (MEWDS).

The clinical manifestations of CAR are typically subacute onset and progressive loss of vision, nyctalopia, measurable visual field loss, and diminished electroretinogram. Some patients will also have floaters and photophobia. The vision loss may progress to very severe visual impairment. At the time of onset of visual symptoms, patients may or may not have a history of prior malignancy. CAR is most often associated with lung cancer but has also been described in patients with carcinoma of the colon, uterus, cervix, breast, and prostate. The clinical manifestations of MAR are nyctalopia, pigmentary changes in the retina and vitiligo. Patients with MAR have clinical and electrophysiologic findings similar to patients with congenital stationary night blindness. MAR patients are likely to have already been diagnosed with cutaneous melanoma prior to the onset of their visual symptoms.

AZOOR and MEWDS are clinically defined entities that occur more commonly in women. AZOOR is characterized by patients that present with the abrupt onset of a blind spot and photopsias. The fundus initially appears normal but with time an area of retinal atrophy and RPE hyperplasia develops. There is no sign of inflammation.

MEWDS patients often describe a flulike illness preceding their symptoms of decreased vision and photopsias. Examination discloses a granular appearance to the fovea and faint, transient white opacities at the level of the retinal pigment epithelium and deep retina.

Adamantiades–Behçet's disease is a systemic vasculitis that has prominent ophthalmologic features. In addition to the orogenital ulcers present in Adamantiades–Behçet's disease, there is prominent intraocular inflammation with occlusive retinal vasculitis.

Eales' disease is characterized by the presence of a peripheral perivasculitis involving retinal veins. Venous occlusions lead to non-perfusion and peripheral retinal neovascularization. Vitreous hemorrhages and traction retinal detachments may develop secondary to the neovascularization. The disease is typically bilateral, but there may be a considerable time interval before involvement of the second eye.

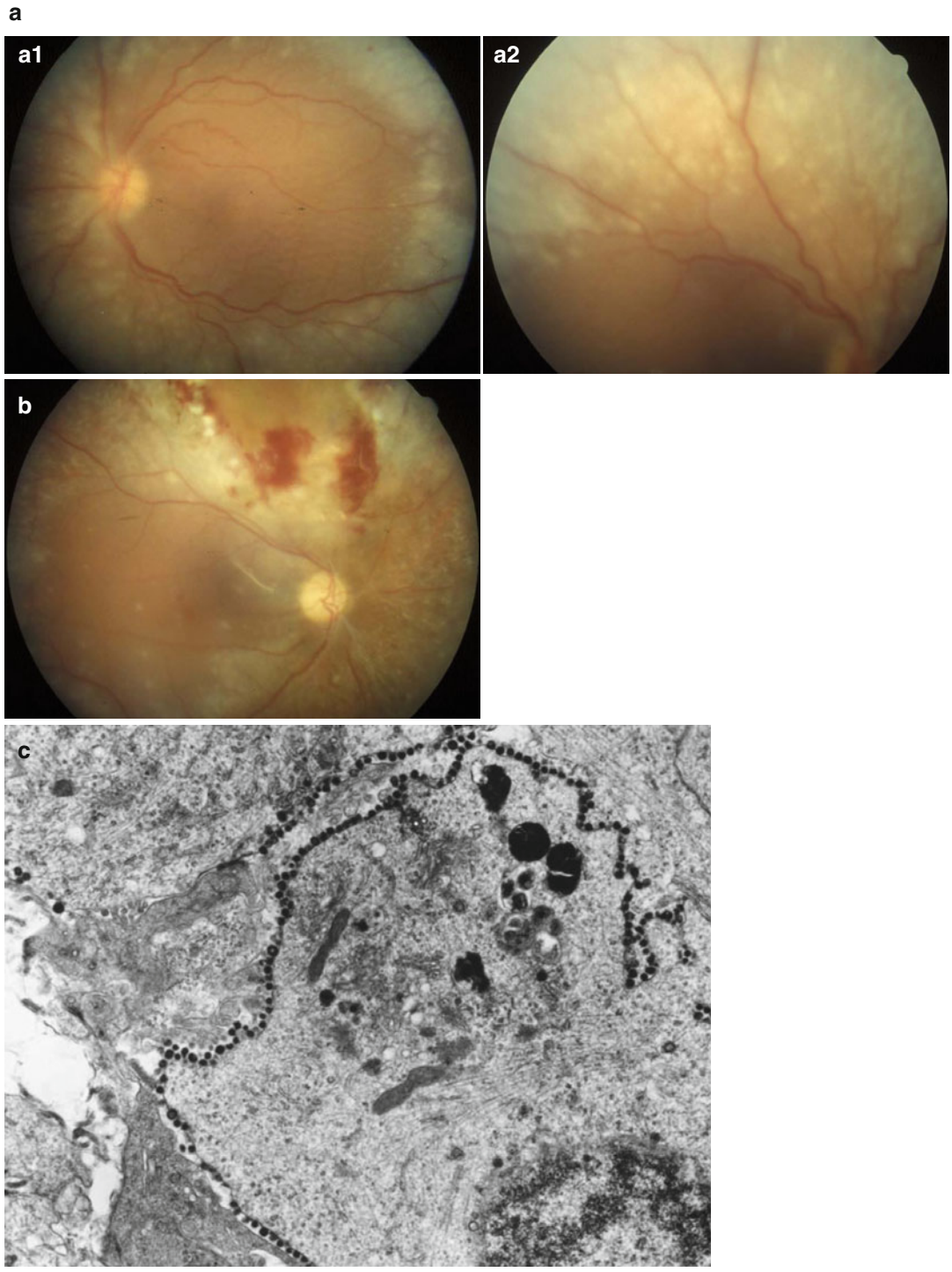

Fig. 9.10 Acute retinal necrosis. (**a**) Clinical photographs showing bilateral retinal whitening outside of the area of the retinal arcades. (**a1**) Left eye, (**a2**) right eye. (**b**) Clinical photograph showing retinal biopsy site, with mild retinal hemorrhage at the margin of the area of biopsy. (**c**) Electron microscopy of the biopsy shows numerous viral particles decorating the periphery of a retinal cell

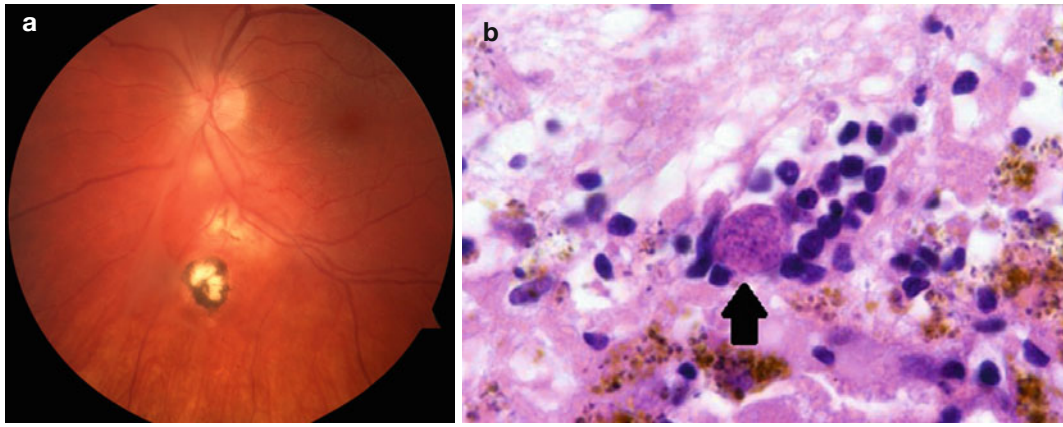

Fig. 9.11 Toxoplasmic retinochoroiditis. (**a**) Clinical photograph showing retinal scars at different stages of evolution. The most inferior lesion is an old pigmented scar. Superior to this there is a more recent area of retinal involvement, and inferior to the optic nerve there is an area of active retinitis. (**b**) Section through retina of a patient with toxoplasmosis. The retina is necrotic, and there are numerous encysted toxoplasmic organisms evident (*arrow*)

Histopathology

In acute bacterial infections (endophthalmitis) resulting from surgical procedures, there is a marked infiltrate of neutrophils in the choroid, retina, and vitreous. The bacteria causing the infection were generally introduced into the eye at the time of surgery, so there is typically no bacterial infiltrate in the eye wall. Most cases of endophthalmitis that come to the pathology laboratory will have been treated aggressively with intravitreal antibiotics, so it is uncommon to see bacterial organisms even in severe cases of endophthalmitis. Edema and hemorrhage in the retina are common in longer-standing infections.

With endogenous fungal endophthalmitis, fungus reaches the eye through the bloodstream, and infection generally begins in the choroid. However, extension of the infection to the retina and vitreous is typical. Both yeasts and hyphae may be evident within the area of infection. Lesions may have the histopathological features of an abscess with central necrosis surrounded by acute inflammation, with a perimeter of chronic and granulomatous inflammation.

Retinal infection with CMV leads to full-thickness destruction of the retina and with healing there is a thin fibroglial scar replacing the retina. In active infections, there are intranuclear and intracytoplasmic eosinophilic inclusions within large neurons (cytomegalic cells).

Similarly with acute retinal necrosis from either herpes simplex or herpes zoster, there is necrosis of the full thickness of the retina. Occasional intranuclear inclusions may be present. There is prominent retinal vasculitis and diffuse inflammation in the vitreous and uvea.

In toxoplasmic retinitis, the infection or reactivation of infection begins in the retina. There is necrosis of the retina with surrounding acute inflammation. The inflammatory response will extend into the vitreous and to the adjacent choroid. Cysts containing the *Toxoplasma* organism are often evident. Free organisms may also be seen.

The histopathology of CAR is strikingly different than that of the infectious retinal inflammatory conditions (Fig. 9.12). In CAR, there is no necrosis and cell death appears to be the result of apoptosis. There is marked and relatively selective loss of photoreceptor cells. These histopathological findings are consistent with retinal autoantibody-induced damage to the photoreceptor cells.

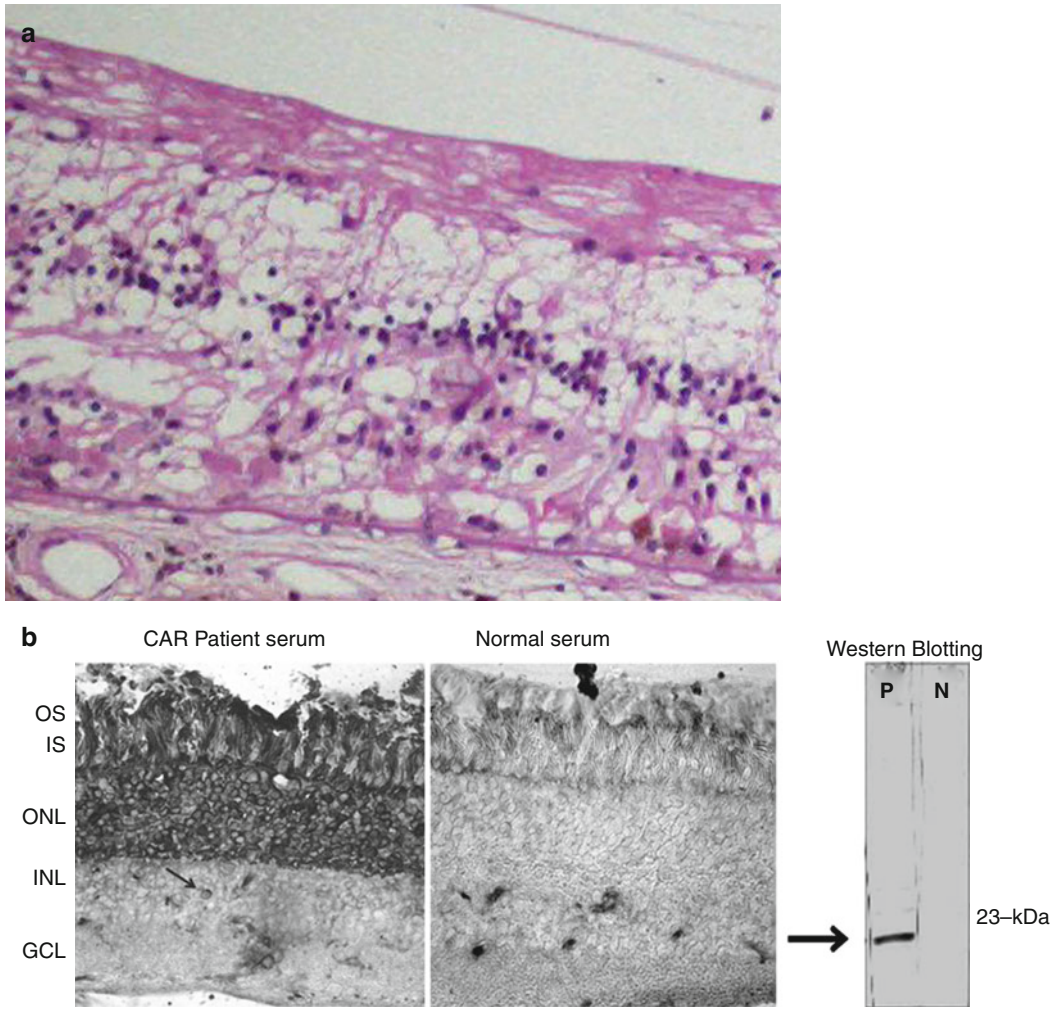

Fig. 9.12 Cancer-associated retinopathy. (**a**) There is complete loss of the photoreceptor layer and partial loss of the inner nuclear layer; notably there is no inflammation. The RPE is partially absent. In other areas the RPE is hyperplastic with some migration into the retina. (**b**) Immunohistochemistry and Western blot of serum from a patient with CAR. The Western blot shows there is an antibody in the patient's serum that reacts with a 23-kDa protein (recoverin). Immunoperoxidase staining of normal retina shows that when the patient's serum is used as a primary antibody (*left panel*), there is prominent labeling of the photoreceptor nuclei, inner and outer segments

In MAR, again, there is minimal to no inflammatory cell infiltrate. The cell loss in MAR is at the level of the inner nuclear layer and in particular appears to involve primarily ON bipolar cells [12]. There is also narrowing of the outer plexiform layer.

The histopathology of Behçet and Eales' disease is similar and is characterized by a vaso-occlusive vasculitis. Histological findings of retinal ischemia: cotton wool spots, retinal hemorrhage, and retinal thinning are generally present. Acute and chronic inflammation within the iris and ciliary body are also present.

Prognosis and Predictive Factors

The prognosis for bacterial endophthalmitis is based on the infecting organism and the time between onset of the infection and treatment.

As most bacterial endophthalmitis is postsurgical and is the result of *Staphylococcus* epidermidis, a relatively benign bacteria, the outcome in these patients is generally good. In the Endophthalmitis Vitrectomy Study, more than 50 % of patients achieved a visual acuity of 20/40 or better at 9 months following treatment. Seventy-five percent of patients achieved a vision of 20/100 or better [13].

The visual outcome for endogenous endophthalmitis is also variable, depending primarily on the organism causing infection, the immune status of the patient, and the location of the retinal involvement. Mild *Candida* endophthalmitis, diagnosed early and treated, has an excellent prognosis. Bacterial endogenous endophthalmitis [14] and *Aspergillus* endophthalmitis in an organ transplant patient have a poor prognosis for vision. In addition, endogenous *Aspergillus* endophthalmitis is almost certainly associated with disseminated *Aspergillus*, and the prognosis for patient survival is poor [15].

CMV retinitis is very amenable to treatment, either by improving the patient's immune status, use of systemic or intravitreal antiviral agents or both. HIV-infected patients that develop CMV retinitis are generally treated with systemic and/or intravitreal antiviral agents but can often be weaned from these if their CD4 counts respond to highly active antiretroviral therapy (HAART).

Of the patients with noninfectious retinal inflammatory conditions, patients with MEWDS have an excellent visual prognosis and generally recover normal vision with no treatment. AZOOR patients may show progression but usually achieve an inactive status over the course of 1 year. The involvement is sectoral, and central vision is usually spared.

Patients with ARN or PORN can also be treated with antiviral therapy. These patients' visual prognosis depends on the extent to which the central retina has been damaged from direct viral infection and whether they develop a secondary retinal detachment. Similarly, toxoplasmosis patients will generally maintain good vision as long as the central retina is not directly damaged by the initial or recurrent bouts of active infection.

Cancer-associated retinopathy has been treated with immunosuppression. There are anecdotal reports of stabilization and improvement in vision, but no large series are available to confirm a specific treatment or prognosis.

9.5 Retinal Injury

Definition

Retinal injury can be defined as any perturbation that disrupts the cellular constituents or extracellular matrix of the retina sufficiently to cause transient or permanent alterations in retinal function, physiology, or structure. Defined in this fashion, retinal injury is a broad term that can encompass changes in the retina that occur secondary to a variety of processes. Permanent changes in the cellular makeup of the retina occur secondary to apoptosis, necrosis or autophagy. Permanent changes might also occur due to changes that are largely in the extracellular matrix, e.g., following vitreous detachment. Apoptosis is a process of programmed cell death. Apoptosis can be elicited by several mechanisms of injury, including inherited retinal diseases or metabolic disease. Characteristically, it occurs in the absence of inflammation. Necrosis occurs more typically with mechanical trauma or infectious injury mechanisms. Autophagy is a process of degradation of dysfunctional cellular components. In extreme situations it may be viewed as another form of programmed cell death. There are, of course, types of injury that elicit both apoptosis and necrosis, for example, ischemic injury. As ischemic injury and retinal degeneration are covered as separate topics, this section will deal with retinal injury as a result of direct and indirect mechanical and thermal injury to the retina.

Epidemiology

Mechanical eye injury is very common. It is estimated that over two million eye injuries occur each year in the USA [16]. Predisposing factors for injury relate to occupation, age, and sporting activities. Males are much more likely to sustain eye trauma than females. A special form of eye trauma is nonaccidental trauma seen as a result of

child abuse. The constellation of mechanical eye injuries in this setting is generally referred to as "shaken baby syndrome" and occurs primarily in children under the age of 1.

A subcategory of mechanical eye trauma is surgical trauma. In the case of surgical trauma, injury to eye tissue is purposeful, in an effort to improve a disease state. Surgical trauma to the retina occurs as a result of laser treatment and with surgical incisions in the retina. Laser-induced injury to the retina is very common, while surgical incisions of the retina are less common. The pathology of both types of injury is relevant to the interpretation of tissue received in the pathology laboratory.

Clinical Features

Blunt trauma to the retina induces multiple types of retinal injury. Injury to the retina occurs as a result of direct trauma and from counter coup injury due to vitreous perturbations from deformation of the globe. Commotio retina (Fig. 9.13a) is a term that describes the clinical appearance of the retina with blunt injury. This retinal whitening is due to shearing of the photoreceptor outer segments [17]. With more severe trauma, the injury can be more extensive, and full-thickness necrosis of the retina may occur and is called "sclopetaria" (Fig. 9.13b, c). Blunt trauma may also result in retinal injury in the form or retinal tears, dialysis, or macular hole. Retinal and vitreous hemorrhage is a frequent accompaniment of this type of injury. Retinal detachment is a common sequela following retinal tear.

As mentioned above, a special form of blunt injury occurs with the nonaccidental trauma of "shaken baby syndrome." With this injury, there are numerous intraretinal hemorrhages, generally present in both the anterior and posterior retina. As the retinal injuries are typically accompanied by head trauma resulting in subarachnoid hemorrhage, there is often prominent optic nerve head edema present [18].

Penetrating or perforating injuries of the eye may result in lacerations or tears of the retina. Such injuries are often complicated by a later development of retinal detachment due to the cellular proliferation that occurs as part of the wound healing process [19].

Laser treatment to the retina induces thermal injury (Fig. 9.14). Laser treatment is done for three principal reasons: to create an adhesion between the retina and the underlying RPE and choroid, to indirectly induce regression of retinal vessels and retinal neovascularization, and to directly destroy a lesion.

Histopathology

Age-related degeneration of the vitreous or blunt trauma can result in vitreous traction on the retina sufficient to cause a retinal tear (Fig. 9.15). The retina contains very little collagenous extracellular matrix, so the structural integrity of the retina is principally derived from the retinal vasculature. The local tissue response to a retinal tear consists of loss of photoreceptor cells in the area of the tear and focal gliosis; but more importantly, a retinal tear predisposes to a retinal detachment. Retinal detachment results in marked changes within the retina and the underlying RPE. Changes begin almost immediately following detachment. Early changes include transition of the Müller cell from a cell that is supporting neuronal function to a cell forming glial scars on the anterior and posterior surface of the retina. Normally, the RPE cell is mitotically inactive, but following retinal detachment, RPE cells begin to "bud off" from the RPE monolayer and migrate into the subretinal and vitreous spaces. The photoreceptor outer segments degenerate. Approximately 3 days to one week following detachment apoptosis of the photoreceptor cells begins. With chronic detachment, the retina loses its lamellar architecture. The neuronal cell populations are absent, and the retina consists of primarily glial tissue. There can be membranes on the anterior and posterior surface of the retina, composed primarily of RPE cells and glial cells. The clinical term used to refer to these membranes is proliferative vitreoretinopathy. The constellation of retinal changes occurring with retinal detachment has been well characterized in experimental studies of retinal detachment and in human postmortem studies [20, 21].

Penetrating or perforating injuries of the retina have some similarities to retinal tears but are

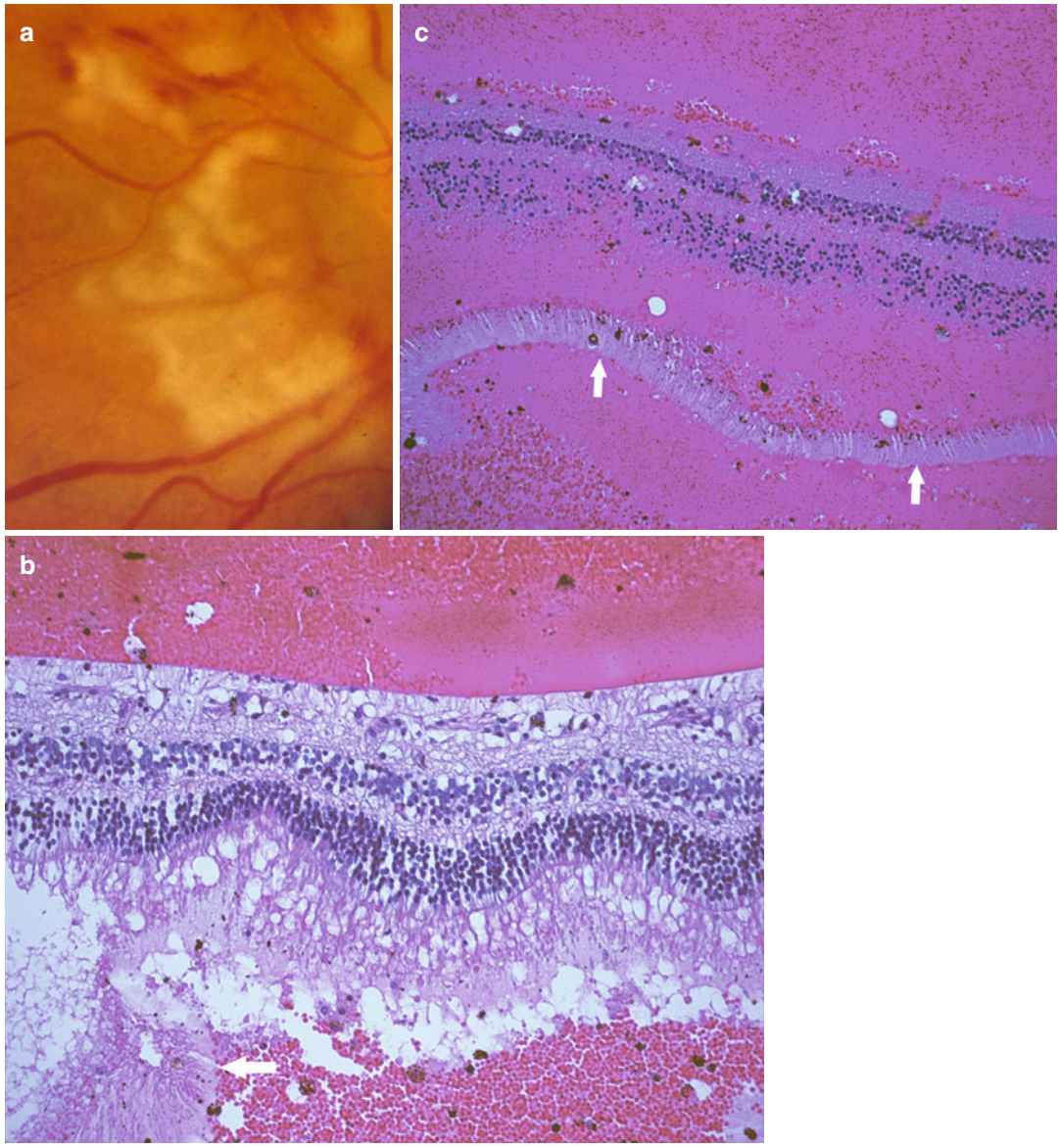

Fig. 9.13 (**a**) Clinical photograph showing severe blunt retinal injury resulting in full-thickness necrosis of the retina, so-called retinal sclopetaria. (**b**) Section of adjacent retina shows separation of the outer segments (*arrow*), but the remaining retina is relatively intact. (**c**) Histopathology of full-thickness retinal trauma. There is necrosis of the full thickness of the retina. The outer segments of the photoreceptors (*arrows*) are separated from the overlying retina. The retinal nuclei are hyperchromatic

much more likely to result in transection of the vessels within the retina. When the retina is lacerated, there is no capacity for healing of the defect. So, if no retinal detachment ensues, the margin of the retina heals by glial cell proliferation with the development of a chorioretinal adhesion (Fig. 9.16).

Thermal laser photocoagulation is a very common type of retinal injury. Most lasers used in treating retinal disease or during retinal surgery have a wavelength that leads to energy absorption by hemorrhage or melanin pigment (pigment within the RPE or choroid). The extent of the retinal damage will be determined by the power

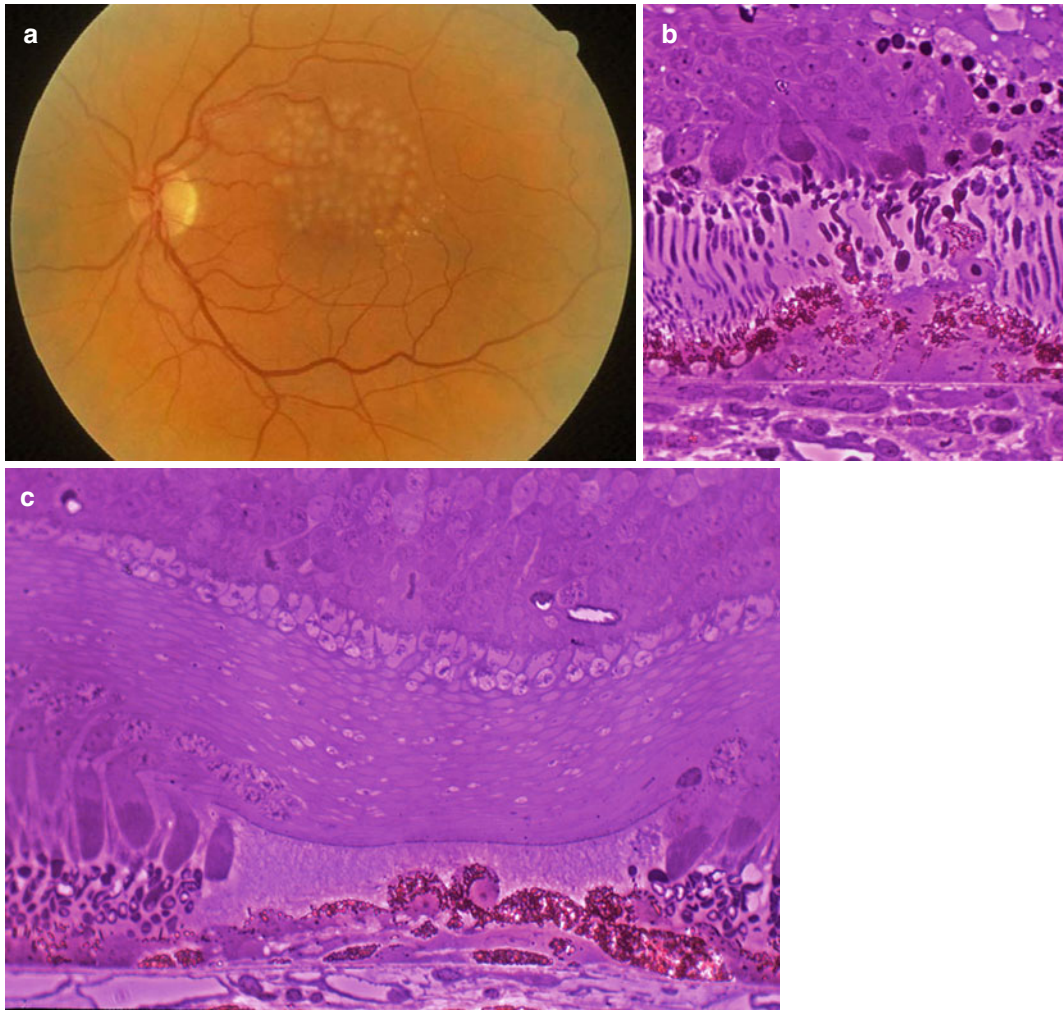

Fig. 9.14 (**a**) Clinical photograph of laser photocoagulation burns in the retina. (**b**) Acute laser burn showing necrosis of the photoreceptor layer and RPE cells of the retina. (**c**) Healed laser burn showing the focal defect in the photoreceptor layer that is filled primarily with extracellular matrix. The RPE cell monolayer has reformed, but there is some RPE hyperplasia in the area of the laser treatment

of the laser setting and the amount of hemorrhage and pigment in the path of the laser beam. With laser treatment, the type of injury is thermal necrosis. Typically, the power of the laser is adjusted to obtain necrosis of the outer retina and RPE while retaining an intact inner retina. Figure 9.14 illustrates the very focal RPE and outer retinal injury that occurs with laser photocoagulation. With healing, the RPE adjacent to the injury site divides and reforms the RPE monolayer. There is no healing of the photoreceptor layer, and the absence of cells in the photoreceptor layer is filled with extracellular matrix or glial cell processes. In addition to the loss in the retina and the RPE changes, there is loss of the choriocapillaris in the area of laser treatment. This does not appear to reform following photocoagulation.

Prognosis and Predictive Factors

A common clinical endpoint for many types of retinal injury is retinal detachment. For retinal detachment, the injury and wound healing factor that is most predictive of prognosis are the presence

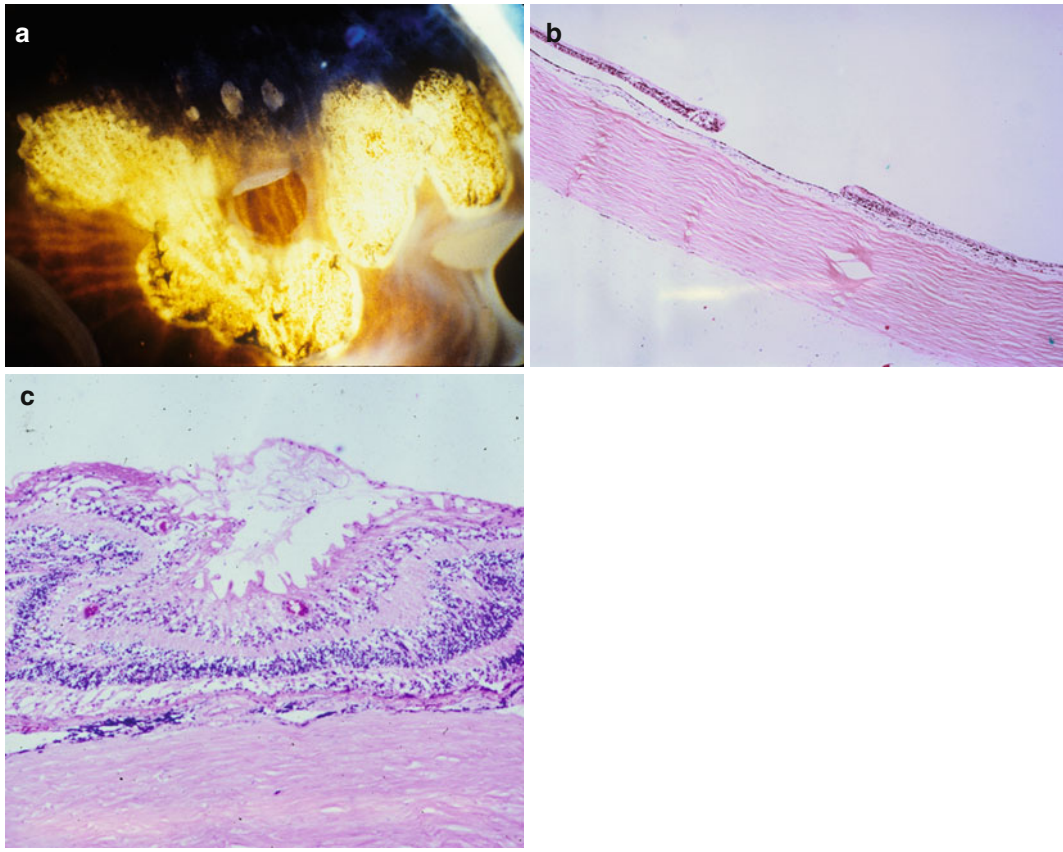

Fig. 9.15 (**a**) Gross photograph of a retinal tear, surrounded by cryotherapy scars. (**b**) Histopathology showing retinal defect corresponding to the tear. Note there is mild glial proliferation at the margin of the tear. (**c**) Proliferative vitreoretinopathy characterized by cellular proliferation on the surface of the retina. The surface of the retina is wrinkled due to the presence of a glial membrane on the vitreous surface of the retina. There is marked loss of the photoreceptor layer, and there is a thin glial membrane beneath the retina

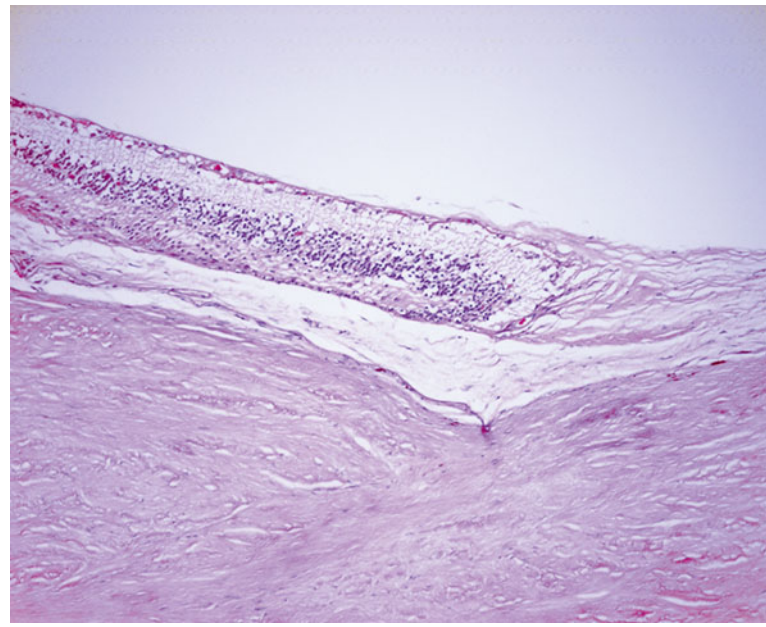

Fig. 9.16 Healed retinal laceration site. There is abrupt termination of the retina with the defect filled with fibrous tissue

or absence of proliferative vitreoretinopathy. If severe membranes are present on the anterior or posterior surface of the retina, it is much more likely that retinal detachment will be present and/or recur following surgical repair. In addition, glial cell membranes that extend over the posterior surface of the retina interfere with the re-establishment of photoreceptor–RPE contact that is essential for normal retinal function. Consequently, retinas with posterior membranes are unlikely to have as much visual acuity recovery even with successful retinal reattachment. Recovery of vision will also depend on the preservation of the photoreceptors. As noted above, photoreceptor apoptosis occurs 3–7 days following detachment, so prognosis will depend on the duration of the detachment as well as wound healing factors.

9.6 Retinal Degenerations

9.6.1 Age-Related Macular Degeneration

Definition

Age-related macular degeneration (AMD) is a degenerative condition affecting the retina, Bruch's membrane, and choroid. Early disease is characterized by focal and diffuse sub-RPE deposits, with or without pigment irregularity and later disease by associated choroidal neovascularization and/or atrophy of pigment epithelium and outer retina known as geographic atrophy.

Epidemiology

AMD is the most common cause of untreatable blindness in the elderly [22]. It is especially prevalent in industrial societies. It is becoming more apparent in Asia, but interestingly there appear to be subtle phenotypic differences in different populations. Particularly in Asians, there is, in addition, a variant of AMD known as polypoidal choroidal vasculopathy [23]. There appears to be relatively little AMD in Africa.

Etiology

Smoking is a well-established risk factor, and diet probably has a role to play with evidence to suggest a "healthy" diet is protective and a "Western" lipid-rich diet a risk. Sunlight exposure, perhaps surprisingly, has not been a consistent risk factor in epidemiological investigations of AMD. There are strong genetic risk factors with major influence from polymorphisms associated with complement factor H (CFH) and the ARMS2/HTRA1 locus on chromosome 10 [24]. The CFH findings, particularly when associated with the existence of other genetic risk factors in other genes linked to the control of complement activation, have moved the role of inflammation and the innate immune system center stage. Other inherited disorders, including Sorsby's fundus dystrophy, have focused attention on abnormalities of the extracellular matrix and its turnover. Further genes with high-risk polymorphisms and gene products with functions linked to lipid metabolism align with the potential importance of diet.

Clinical Features

In early AMD, patients may be asymptomatic or complain of poor night vision. Loss of rod photoreceptors is an early feature [25]. As choroidal neovascularization develops, there may be loss or distortion of central vision. Visual loss will be sudden if there is subretinal or intravitreal bleeding.

On fundoscopy, in early disease the main finding is of macular drusen (focal sub-RPE deposits). If very small and relatively few in number, these are considered part of normal aging and carry little risk of progression to visual loss. If larger or associated with pigmentary changes, the risks of eventual visual impairment increase. The classification of early AMD has recently been revised [26] and linked to risk of progression. Diffuse deposits cannot be seen clinically as there are no contrast-rich edges. Choroidal neovascular membranes can be associated with hemorrhage, edema, and/or scarring. Geographic atrophy can develop with a variety of patterns best seen with autofluorescence fundus imaging. Curiously the fovea is often spared until late in the evolution of geographic atrophy. What may be regarded as variants of AMD exist. In polypoidal choroidal vasculopathy, ectatic-looking vessels in the choroid, best visualized with

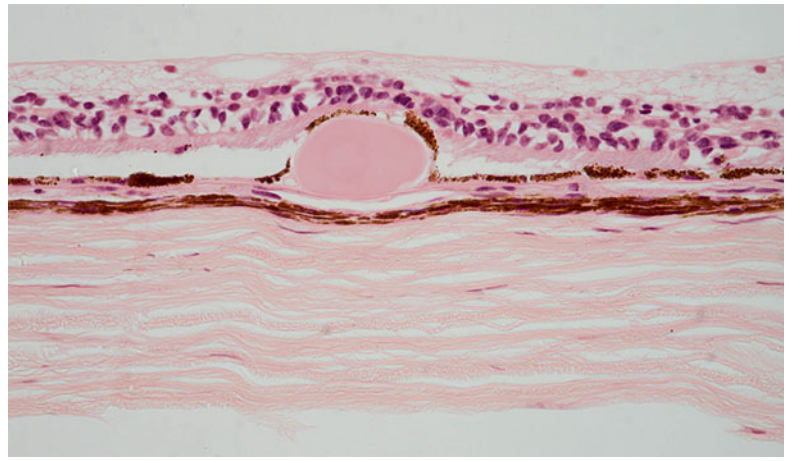

Fig. 9.17 Peripheral retina overlying a small, hard druse. The retinal pigment epithelium partially covers the druse. The choroid in this case is very thin

indocyanine green angiography, may leak or bleed with relatively massive subretinal hemorrhage. Reticular pseudodrusen are increasingly recognized as a clinical feature of AMD [27] associated with risk of progression to blinding disease and characterized by what appear to be ribbonlike deposits and lesions which, particularly on near-infrared imaging, look like small dark rings with a central dot.

Macroscopy

The macroscopic features are essentially those seen on fundoscopy although the clouding of the retina that occurs ex vivo makes the focal deposits harder to see.

Histopathology

The histopathology of AMD is complex, reflecting significant variation from case to case as well as evolution of changes with time. An additional consideration is how the pathology of AMD links to aging, so it is important to first describe what might be seen in the eye of an aged individual without AMD.

One common feature of aging and AMD is the presence of focal sub-RPE deposits, known as drusen. When these are relatively homogeneous with well-defined edges, they are known as hard drusen (Fig. 9.17), and a scattering of these, especially if small (<75 um) and extramacular, is a common finding in elderly eyes. Another common, indeed almost universal feature of the aging eye is thickening of Bruch's membrane [28, 29]. This thickening is within the inner collagenous zone through to the outer collagenous zone and does not, typically, include a significant degree of basal laminar deposit formation (see below). The other finding that is not apparent in routine sections but can be visualized clinically with fundus autofluorescence imaging or under fluorescence microscopy (the fluorescein filter set works well) is the accumulation of lipofuscin in the retinal pigment epithelium [28]. Finally, in normal aging, there is loss of endothelium from the choriocapillaris [29]. This may not be apparent as the relatively solid connective tissue around the vessels remains intact, but if an endothelial cell marker is used, many of these spaces appear empty (see below).

In early AMD there may be many hard drusen but also soft drusen (Fig. 9.18), which in contradistinction to hard drusen, often appear more heterogeneous, involve a greater extent of Bruch's membrane and are of particular significance with regard to AMD and risk of disease progression to geographic atrophy or choroidal neovascularization. Sometimes they appear more apparent clinically than histologically, and in this instance they are probably at least in part pigment epithelial detachments (Fig. 9.19), a further well-recognized clinical feature of AMD. Important in considering their relation to the diffuse deposits discussed below, hard and soft drusen form external to the RPE basement membrane. Reticular pseudodrusen are an important risk factor for advanced disease, but the histopathological correlate of these phenomena is controversial and discussed below.

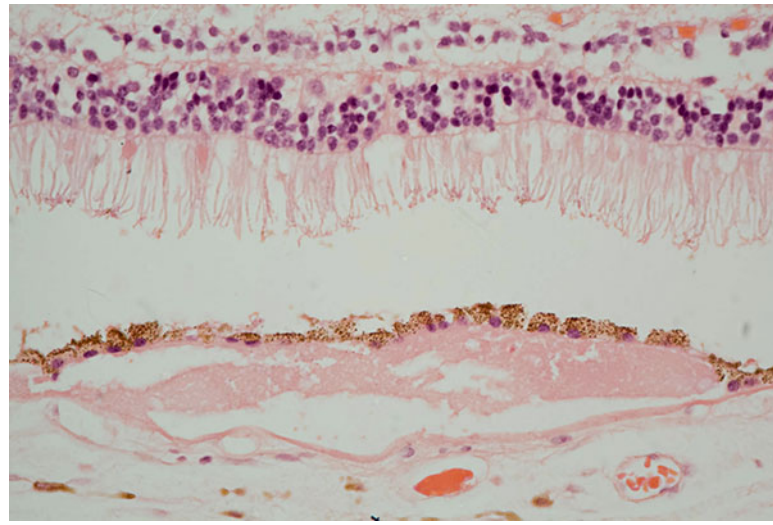

Fig. 9.18 There is neural retina at the top of the figure and reasonable numbers of rod outer segments remain. The neural retina is separated from RPE by an artifactual space. Beneath the RPE, there is amorphous eosinophilic material that would have probably appeared as a soft druse clinically

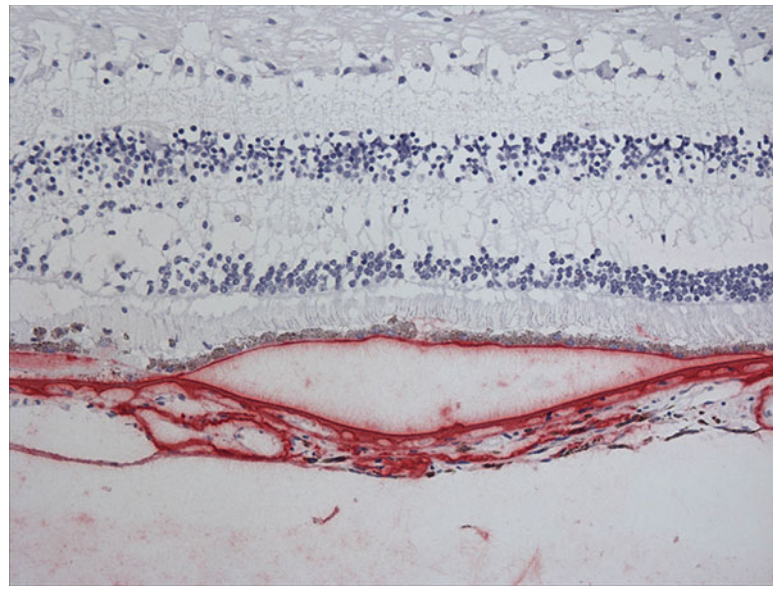

Fig. 9.19 Retina and choroid with immunostaining for vitronectin (*red*). Note that RPE is separated from Bruch's membrane. This represents a pigment epithelial detachment

The classification of diffuse deposits has been confusing in the past, but there is now reasonable consensus that the protein-rich material that accumulates between the RPE and the RPE basement membrane should be called basal laminar deposit (Fig. 9.20) and the often more lipid-rich material external to the RPE basement membrane but internal to or involving the inner collagenous layer of Bruch's membrane should be called basal linear deposit [30]. Basal laminar deposit often includes wide-spacing material (sometimes known as long-spacing collagen), which may also be seen at other levels within the Bruch's membrane complex. Sometimes within H + E-stained sections, basal laminar deposit has a striated appearance (Fig. 9.21) with the striations oriented perpendicular to Bruch's membrane. However, without electron microscopy, it is not possible to distinguish between basal linear deposit and basal laminar deposit. As discussed above, Bruch's membrane complex thickens with age, at least in part due to small amounts of basal laminar and basal linear deposit, but the total increase in diffuse deposits is much greater in

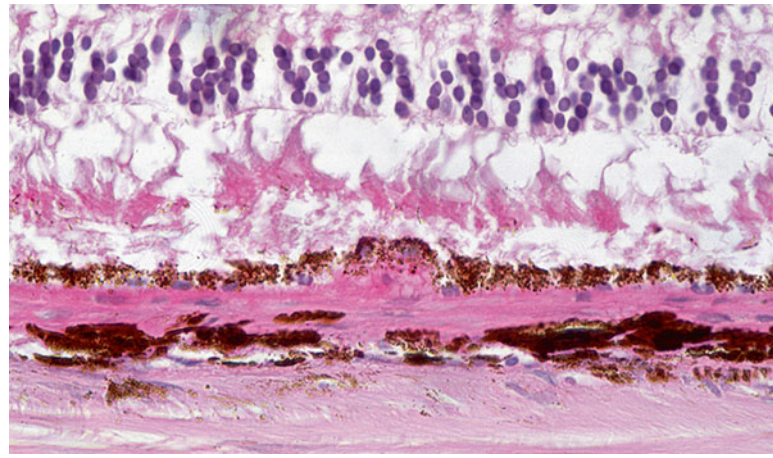

Fig. 9.20 Outer retina showing disorganization of photoreceptor outer segments. There is eosinophilic material beneath the RPE. It is not possible to distinguish on which side of the RPE basement membrane this is by light microscopy, but at least a component is likely to be internal to the basement membrane and hence basal laminar deposit

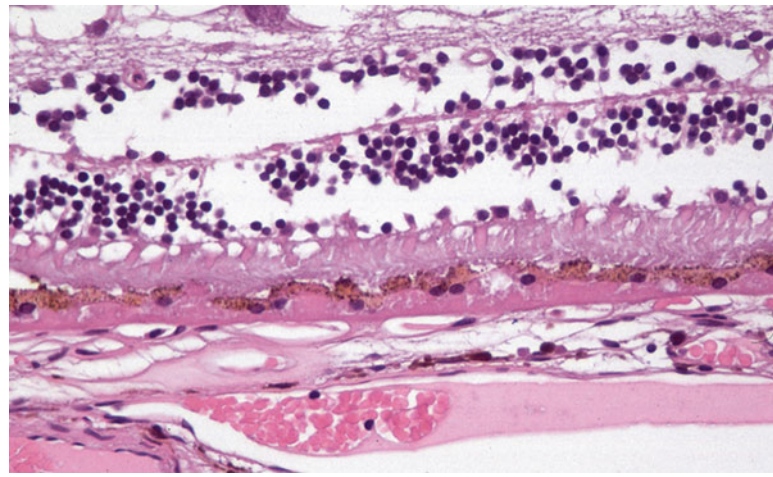

Fig. 9.21 There are poorly defined striations in the sub-RPE material. This is typical of basal lamina deposit although confirmation would require electron microscopy

AMD. As a rule of thumb, if the thickening is readily appreciated in an H+E staining section, it is likely to be significant. The biochemistry of drusen and diffuse deposits is complex and includes complement components, coagulation factors, vitronectin (Fig. 9.19) [31], and TIMP-3 (Fig. 9.22).

Clinically, another feature of early AMD with adverse prognostic significance is pigmentary abnormality. The histopathology of this has not been well characterized. Early rod loss, an important clinical manifestation of early disease, is hard to detect subjectively in sections. Similarly, even though degeneration of the choriocapillaris is quite possibly of significance in terms of pathogenesis, it is difficult to appreciate in routine sections. With immunohistochemistry for an endothelial cell marker, the "gaps" in the sub-Bruch's connective tissue become much more apparent (Fig. 9.23).

Choroidal neovascularization (CNV) in AMD is generally sited at the posterior pole although it is important to note that peripheral CNV can occur and is sometimes encountered as an incidental finding. The number of breaches in Bruch's membrane, which give the choroidal circulation access to the sub-RPE and subretinal spaces, is generally small [32], and no continuity between the choroid and the neovascular membrane is evident in most cases unless serial sections are examined. The neovascular membrane may, as described, be situated between the RPE and Bruch's membrane (Fig. 9.24), the classical location for AMD-associated CNV, or between the

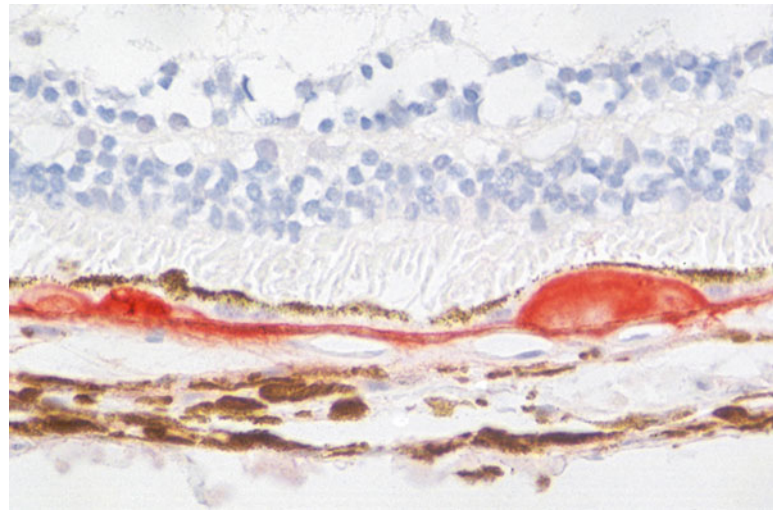

Fig. 9.22 Sub-RPE deposit with immunoreactivity for TIMP-3 (*red-brown*)

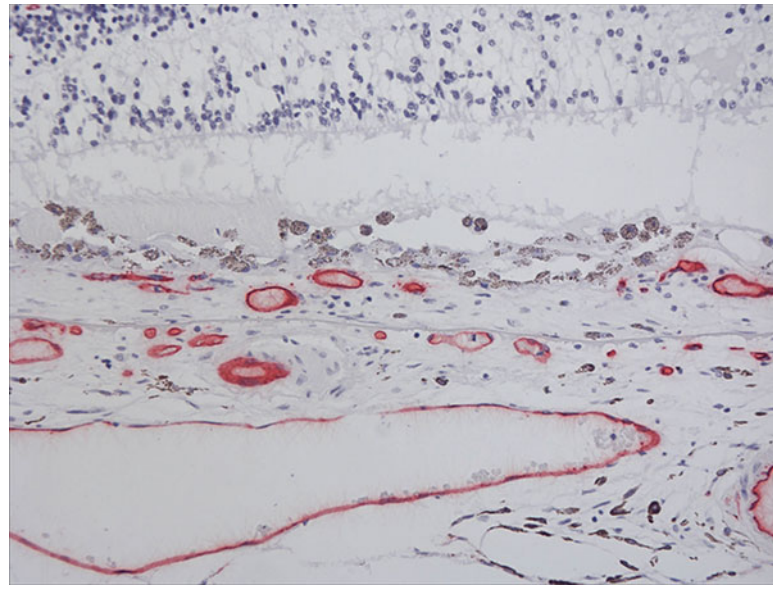

Fig. 9.23 Outer retina, choroidal neovascular membrane, and choroid from a case of age-related macular degeneration. Immunostaining for CD31 (*red*). Note vessels internal to Bruch's membrane in the neovascular membrane and gaps under Bruch's membrane where segments of choriocapillaris have been lost

neural retinal and RPE (Fig. 9.25) or indeed, both (Fig. 9.26). Sub-RPE membranes are sometimes referred to as type I membranes and subretinal membranes as type II. The surgical removal of sub-RPE membranes is generally not successful as the native RPE is removed as well, leaving the photoreceptors without any support leading to what is essentially geographic atrophy. The membranes often contain clumps of migrated RPE that may form apex-to-apex tubes and complexes, and the RPE will often depigment (Fig. 9.25). This can on occasion lead to histological misinterpretation as a retinal metastasis. The RPE may generate, within the membrane, material reminiscent of basal laminar deposit that can sometimes be extensive (Fig. 9.27). There is often a scattering of inflammatory cells (mainly lymphocytes and macrophages (Fig. 9.28) with rare mast cells), and a giant cell reaction to damaged Bruch's membrane or basal laminar material (Fig. 9.29) is occasionally seen.

If CNV membranes are excised surgically and submitted for examination (Fig. 9.30), it can be difficult to orient them accurately as the RPE can

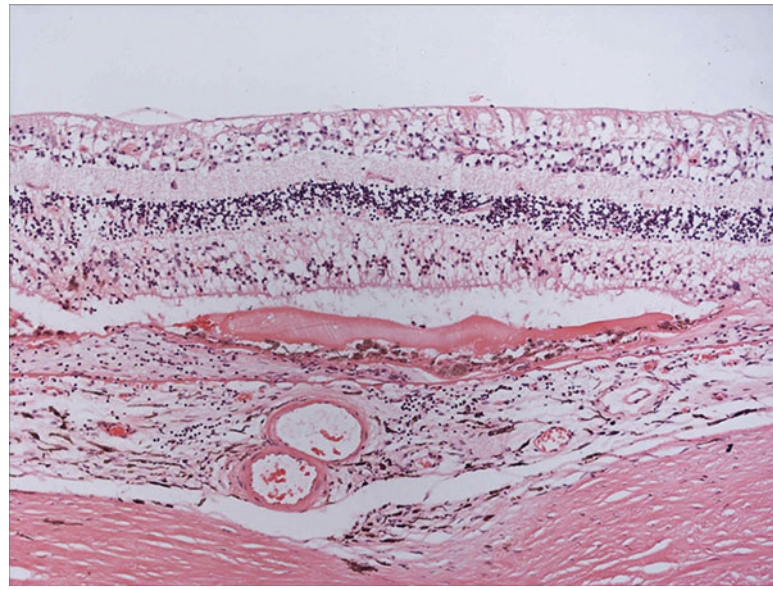

Fig. 9.24 Choroidal neovascular membrane between the RPE and Bruch's membrane. Note there is also some subretinal fluid

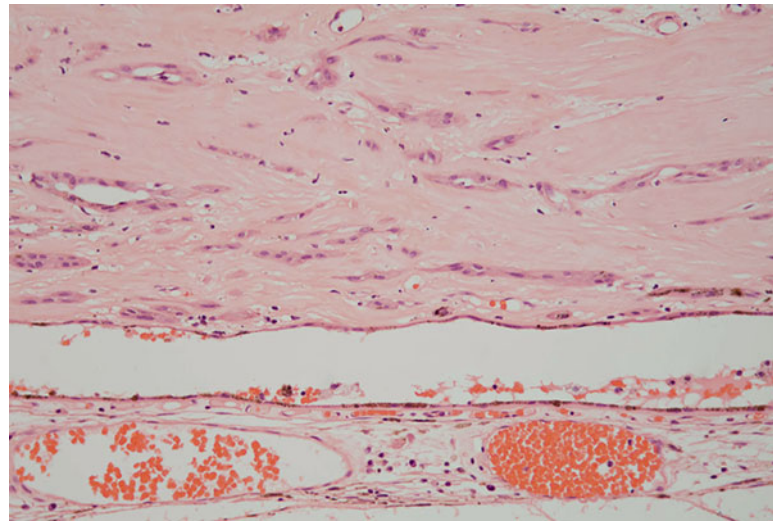

Fig. 9.25 Islands of largely depigmented RPE within a relatively hypocellular, densely fibrotic neovascular membrane. In this instance the membrane lies internal to host RPE which is atrophic and has migrated under the membrane

migrate over the undersurface of the membrane (Fig. 9.25). Indeed, drusen-like structures may form upside down if RPE migrates over the underside of the neural retinal (Fig. 9.31). If an opinion is to be given as to whether the membrane is subretinal or sub-RPE, it is helpful if either photoreceptor outer segments (or sometimes inter-photoreceptor "ghost" matrix (Fig. 9.24)) or Bruch's membrane is present on one side or the other. It is also important to remember that combined membranes are not uncommon and that this may not be apparent unless step or serial sections are taken through the entire membrane.

The retina over a membrane, which if fibrotic as is usually the case if they reach a histopathologist and is often known as a disciform scar, is predictably atrophic. Bruch's membrane is remarkably resilient and is usually identifiable even in a profoundly disorganized posterior pole. A PAS stain may help. The choriocapillaris is often atrophied under a scar, and, indeed, chorio-

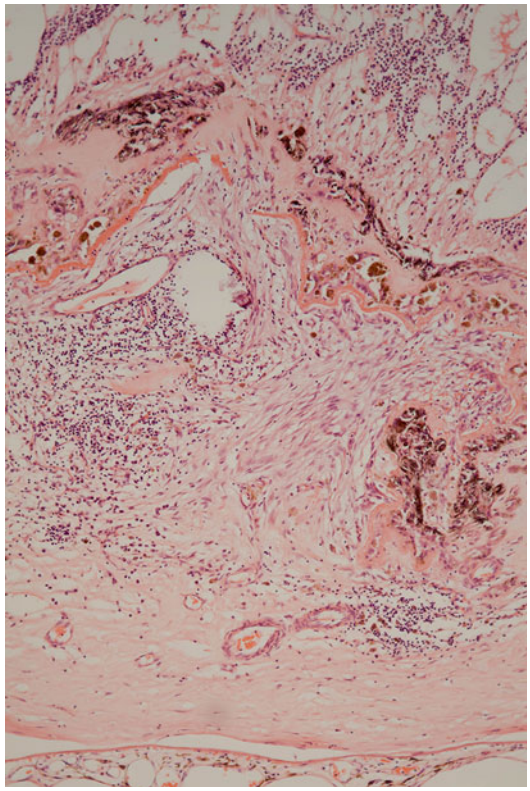

Fig. 9.26 A large subretinal neovascular complex with one component between disorganized neural retina at the top and an irregular remnant of basal laminar deposit and another, occupying most of the field, between the basal laminar deposit and RPE and Bruch's membrane and choroid at the bottom of the image

capillaris dropout may be an important early step in the pathogenesis of a scar and contribute to the hypoxic drive supporting new vessel formation.

In some instances, it is massive intraocular hemorrhage (Fig. 9.32) that precipitates enucleation, and the eye may be removed because it is not possible to ascertain whether or not there is a covert posterior pole neoplasm. Extensive organization of the hemorrhage can confound interpretation, but careful examination of multiple blocks and levels is usually sufficient. If there is major bleeding, particularly if the choroid is involved, the possibility of polypoidal choroidal vasculopathy should be considered. This condition, which is linked to but possibly separate from AMD, is more common in Asians although currently likely to be underdiagnosed in Western populations. The presence of large dilated polypoidal vessels in the choroid is the key to histopathological diagnosis.

Geographic atrophy is characterized by combined loss of RPE, photoreceptors, and choriocapillaris with in extreme cases downstream atrophy of inner retina (Fig. 9.33). There is a perhaps surprising variability in the concordance of the photoreceptor, RPE, and choriocapillaris degenerations, and it is certainly a challenge to identify which element degenerates first. It may be better to consider geographic atrophy a "system" disorder involving all the components of the retina–RPE–Bruch's–choroid complex. As with

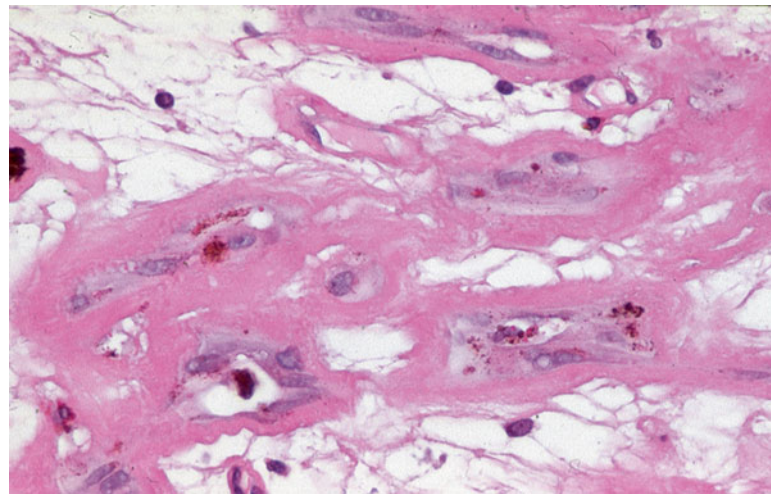

Fig. 9.27 Basal laminar deposit-like material being deposited by RPE that has migrated into a neovascular membrane

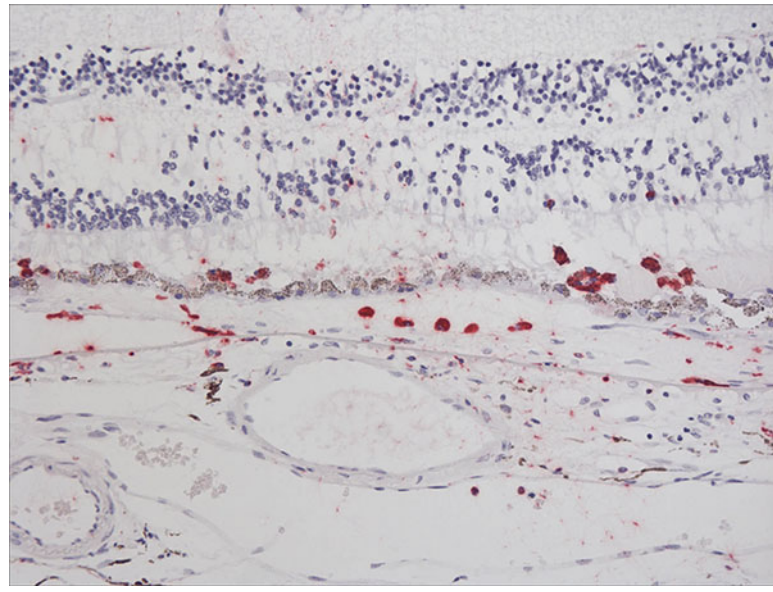

Fig. 9.28 Macrophages in association with a choroidal neovascular membrane (CD68 – *red*)

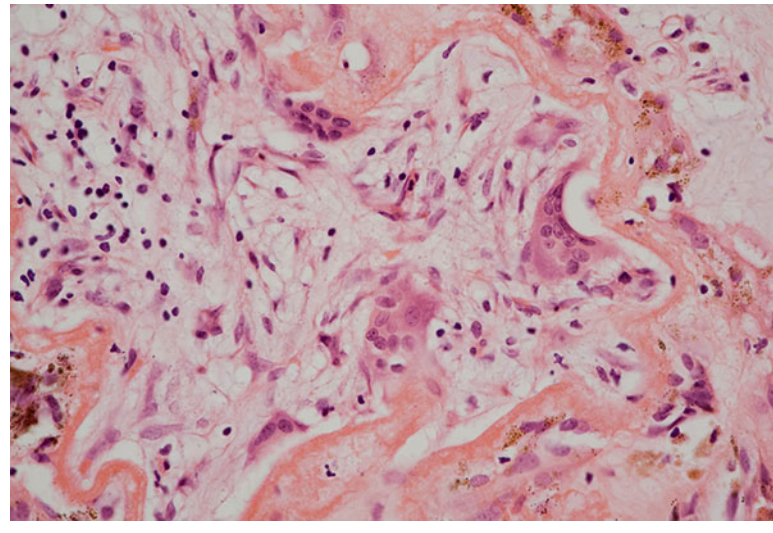

Fig. 9.29 Multinucleated giant cells associated with basal laminar deposit-like material in a choroidal neovascular membrane

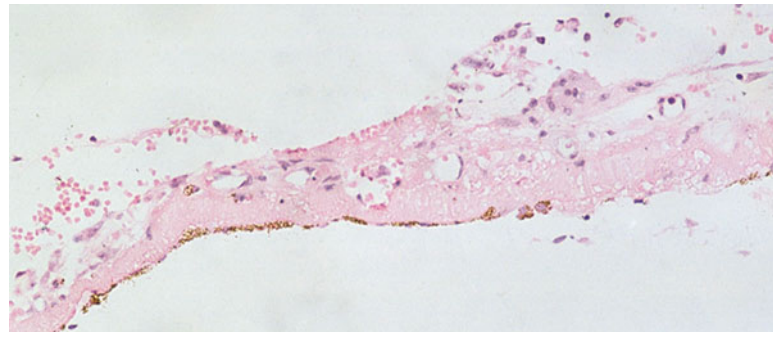

Fig. 9.30 An excised subretinal membrane with RPE that has possibly migrated, partially lining one aspect

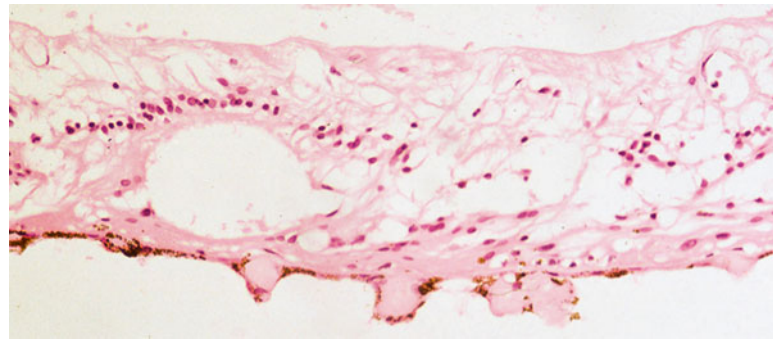

Fig. 9.31 Drusen-like structures on the underside of gliotic retina, the RPE having migrated across the subretinal space

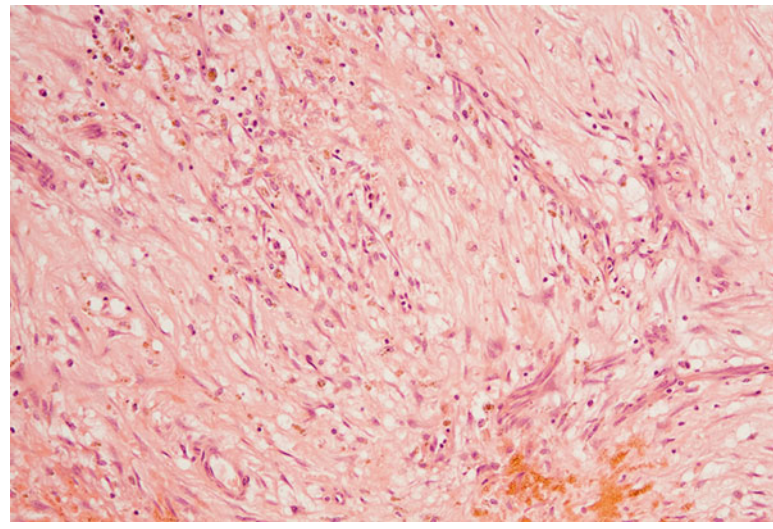

Fig. 9.32 Organized intraocular hemorrhage

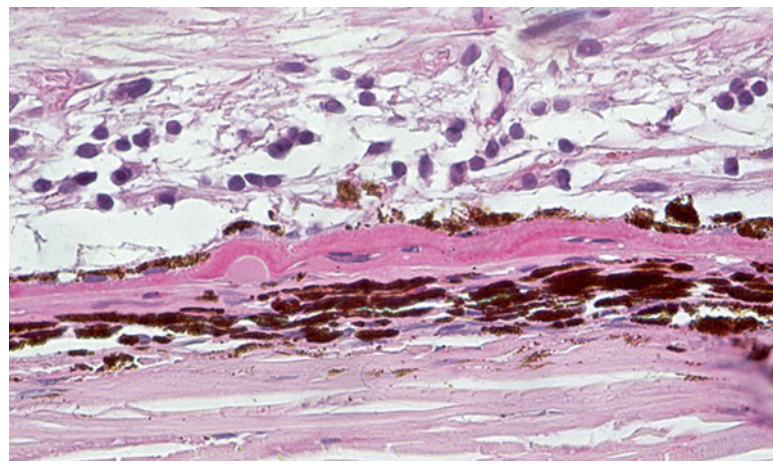

Fig. 9.33 Marked retinal atrophy (the nerve fiber layer is at the *top* of the figure although the inner limiting membrane is not included). There is patchy loss of RPE and a small druse as well as basal laminar/basal linear deposit that contribute to the separation of RPE from Bruch's membrane. The choroid is atrophic

other epithelia, the RPE strives to maintain integrity over the surface of Bruch's membrane in the face of even marked cell loss. There can be marked attenuation with loss of pigment including lipofuscin. It is therefore possible that RPE remains even when the autofluorescence signal on fundus imaging is lost.

The term reticular pseudodrusen relates to a clinical appearance at the posterior pole characterized by ribbonlike areas of alternating light and dark and scattered, small, ringlike lesions, often with a central spot. These are best seen using near-infrared reflectance imaging. It has been proposed that these correspond to subretinal drusen-like deposits that are seen on OCT imaging, but the interpretation of these images, which are computer reconstructions, is a little unclear and although subretinal debris has been seen histopathologically, definitive clinicopathological correlation is not yet available.

Special stains, including immunohistochemistry, are of limited value in the assessment of these cases. A periodic acid–Schiff stain can highlight some of the deposits and Bruch's membrane, and a vascular marker can make it easier to assess the loss of choriocapillaris (which is sometimes masked by the presence of "holes" in the choroidal stroma that remain after the endothelium has died). A pan cytokeratin can assist in identifying migrated, depigmented RPE. There is sometimes ambiguity of staining with CD68 as RPE cells, particularly in pathological states, can express this marker as well as macrophages.

Differential Diagnosis

One main differential diagnosis of early AMD is of "normal" aging. If there are scattered small hard drusen without CNV or GA in an elderly patient, the findings are best considered those of aging alone. Large macular soft drusen with or without extensive sub-RPE deposits are indicative of AMD.

The differential diagnosis of advanced AMD is most often an issue in younger patients. Here it is important to consider rare inherited disorders such as Sorsby's fundus dystrophy, Malattia leventinese, and late-onset retinal degeneration (L-ORD). These conditions lead to thick, extensive sub-RPE deposits and CNV. Sorsby's fundus dystrophy also leads to deposition of abnormal extracellular material over the epithelium of the pars plicata of the ciliary body, not something seen in AMD. A variety of other rare conditions can lead to diffuse deposit formation, but these are hardly ever an issue. There are very many causes of choroidal neovascularization, and before assuming that it is due to AMD, it is important to consider these. Pathological myopia leads to an enlarged eye, breaks in Bruch's membrane, and CNV. Almost any inflammatory process, infectious, or otherwise, at the back of the eye can result in CNV as can trauma, laser photocoagulation, radiation retinopathy and other degenerative changes in Bruch's membrane such as angioid streaks arising in pseudoxanthoma elasticum. What is a challenging issue is how to classify CNV in an elderly patient without obvious other histopathological or clinical features of AMD. This may be designated idiopathic, but this may turn out to be a genuine subtype of AMD as it becomes clearer what the pathogenesis of the condition truly is.

Genetics

The genetics of AMD is now understood in great detail, remarkably so for a complex age-related disorder. A significant component of the risk of developing disease rests with polymorphisms in the complement factor H (CFH) locus on chromosome 1 and with polymorphisms at the ARMS2/HTRA1 locus on chromosome 10. Other genes that contribute to risk in some individuals include other genes with a role in complement activation, other aspects of innate immunity or inflammation, genes associated with high-density lipoprotein metabolism, and several rare variants. Furthermore, copy number variation, epigenetic factors, and mitochondrial genetics may be important.

Prognosis and Predictive Factors

The main environmental risk factor for AMD is smoking, and there is evidence to suggest that a healthy diet is protective, particularly for those with a high-risk genotype, whereas elements of a "Western" diet associated with a poor cardiovascular risk also are adverse risk factors for AMD.

9.6.2 Retinal Detachment

Definition

Retinal detachment arises in a number of circumstances that all lead to separation of the neural retina from the retinal pigment epithelium (RPE). Rhegmatogenous retinal detachment arises when the retina is disrupted, relatively rarely as a result of trauma to the eye and more often due to the development of tractional forces between the retina and vitreous. Fluid from the vitreous cavity thereby gains access to the subretinal space, and RPE may access the outer retinal surface. In non-rhegmatogenous retinal detachment, the retina remains intact. A common cause of the latter is when exudate accumulates between the retina and RPE. For many pathologists, this is most often seen when examining eyes with choroidal melanomas. In central serous retinopathy, apparently spontaneous accumulation of subretinal fluid is seen, often in young patients. Tractional retinal detachment develops where preretinal membranes, with or without a vascular component, display typical contraction associated with a wound healing process.

Epidemiology

Relatively little is known of the epidemiology of retinal detachment although a recent meta-analysis gave an incidence of approximately 6–18 per 100,000 population [33].

Etiology

As discussed above, trauma is an important cause of retinal detachment and, whether associated with trauma or other processes at the vitreoretinal interface such as diabetic neovascularization, in many instances the retina is pulled away from the RPE by traction, essentially of contracting vitreous collagen on the inner limiting membrane of the retina. Retinal detachment may be preceded by vitreous detachment. Certain disorders of the peripheral retina such as lattice degeneration and holes and tears that form without obvious cause as well as macular hole (see below) all predispose to retinal detachment [34]. High myopia with enlargement of the eye is another risk factor. Accumulation of material under the retina is a further cause of detachment. Commonly, exudative detachment is seen adjacent to a choroidal melanoma because of the leakage of fluid from the tumor. A similar process operates over many choroidal neovascular membranes.

Clinical Features

Depending on the location and cause, patients may experience the sudden appearance of "floaters" or flashing lights. They may witness a "shadow" appearing across their vision.

Macroscopy

The outside of the eye should be examined for evidence of encircling bands, plombs, or other forms of surgical intervention. When the eye is opened, there is sometimes an outpouring of silicone oil that has been used surgically to keep the retina flat following a vitrectomy. The intraocular macroscopic findings may be dominated by other pathology, for instance, an underlying disciform scar, proliferative vitreoretinopathy, or choroidal tumor. In other instances, it may be difficult to distinguish a real detachment from an artifactual one, or a very careful examination of the peripheral retina for an area of lattice degeneration is required.

Histopathology

The retina often rapidly becomes edematous (Fig. 9.34), and with time, loss of outer segments gives way to outer retinal atrophy. Gliosis may be marked, and Müller cells may extend and/or migrate into the subretinal space (Fig. 9.35) preventing reattachment. Similarly, they can move onto the anterior retinal surface (Fig. 9.36), often passing through the inner limiting membrane just anterior to retinal vessels. Particularly if there is a retinal break, the preretinal proliferation may include migrating RPE cells which can then, with the glial cells, generate a complex membrane capable of contraction and exacerbating the clinical situation.

In long-standing retinal detachment, the retinal gliosis becomes very marked, and the normal laminar appearance of the retinal can be lost (Fig. 9.37). There may be some intraretinal mineralization, and RPE may migrate into the retina and as in other retinal degenerations such as retinitis pigmentosa (see above) aggregate around retinal blood vessels.

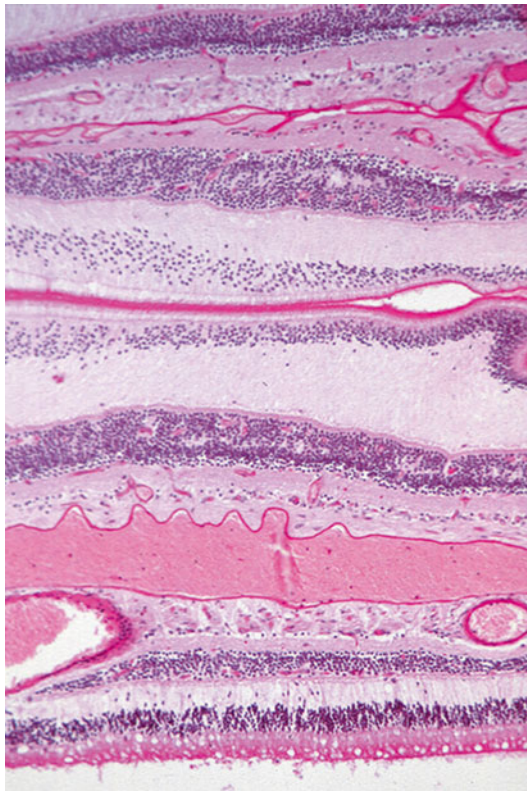

Fig. 9.34 Multiple layers of retina folded across each other in an eye removed shortly after traumatic retinal detachment. The outer plexiform layer especially (*middle* of the figure) is edematous (PAS)

If the detachment is large enough, it can lead to a so-called funnel-shaped detachment with retina gathered up behind the lens (Fig. 9.38), if present, and a tube of retina extends posteriorly to the optic nerve head.

The composition of the material in the subretinal space can vary depending on the cause of the detachment. Adjacent to a choroidal melanoma, there is usually rather homogeneous protein-rich fluid (Fig. 9.39). In Coats' disease there is typically an abundance of foamy macrophages and cholesterol clefts. The RPE may round up or migrate. In long-standing detachment, it is often the case that drusen-like sub-RPE deposits are present. These drusen-like structures are often arranged in clusters (Fig. 9.40).

There may be evidence of underlying causal pathology. For instance, there may be a healed scleral wound indicative of previous trauma or abnormal preretinal vessels indicative of proliferative diabetic retinopathy or retinopathy of prematurity.

There may also be evidence of therapeutic intervention ranging from subtle pars plana scars at the site of vitrectomy through to encircling bands (Figs. 9.41 and 9.42) and silicone oil. The latter can reside within the eye and cause relatively little damage, or it can provoke a widespread, macrophage-rich inflammatory cell

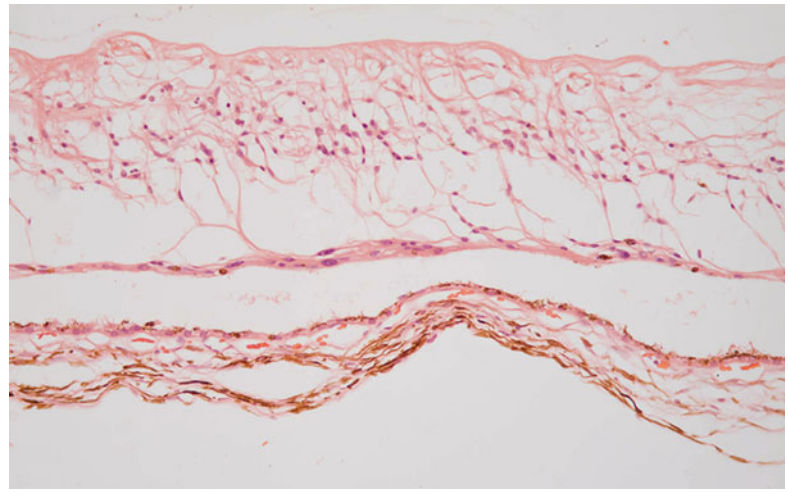

Fig. 9.35 Glial cells have migrated along the underside of the retina to form a scar. There is artifactual separation between this and the subjacent RPE

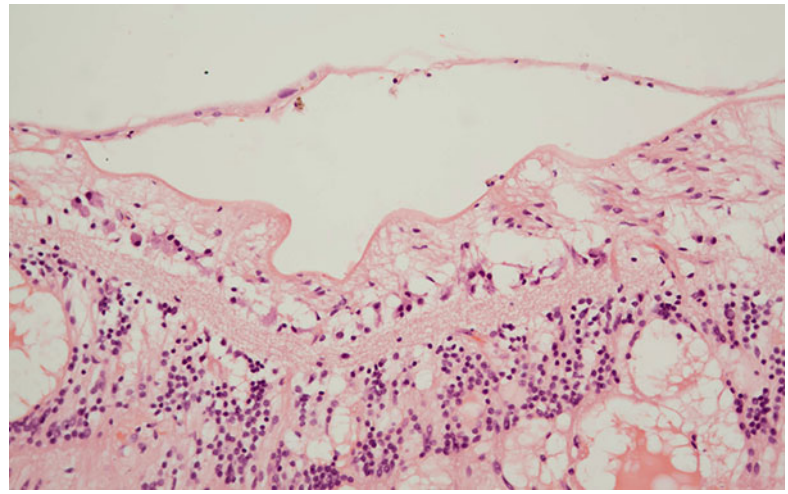

Fig. 9.36 A thin glial membrane is seen bridging two parts of the inner limiting membrane. Note the presence of edema with proteinaceous fluid in microcysts in the inner nuclear layer and outer plexiform layer

Fig. 9.37 Long-standing retinal detachment with disorganization and gliosis of the retina. Note the presence of an epiretinal membrane that is apparently causing retinal traction. The retina is, however, attached

infiltrate. Oil can extend as far posteriorly as the optic nerve head and anterior to the drainage apparatus (Figs. 9.43 and 9.44) may even exit anteriorly through trabeculectomy wounds into the subconjunctival space. It is sometimes difficult to distinguish intraretinal degenerative cystic change from spaces due to oil. A useful pointer to the latter is the presence of RPE granules, which impart a "dirty" quality to the vacuoles (Figs. 9.45 and 9.46). It is possible that the RPE granules are in part responsible for emulsifying the oil.

Differential Diagnosis

The retina often separates artifactually from the RPE following removal or during processing. This is easily distinguished from true detachment because there is no material visible in the subretinal space; usually the photoreceptor outer segments are present (unless there is some other disease), and the outer segment tips are lightly decorated with elongated pigment granules from the apical processes of the RPE (Fig. 9.47). Distinguishing between different causes of retinal detachment often requires clinicopathological correlation, and certainly, in end-stage eyes, it can be very difficult to ascertain what the primary pathology was.

Genetics

A variety of conditions with a genetic basis are associated with retinal detachment. These include

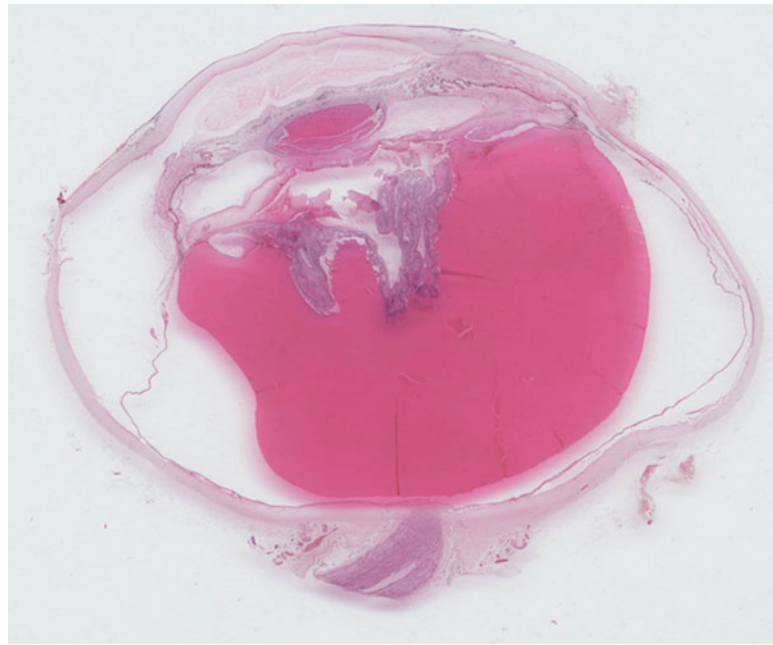

Fig. 9.38 A complete section of a globe with extensive retinal detachment, the subretinal space filled with proteinaceous fluid, and the retina itself gathered up behind the lens

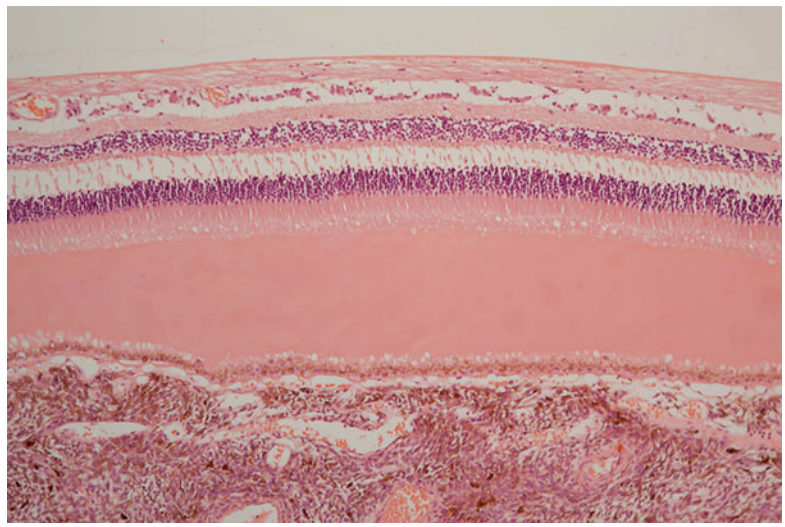

Fig. 9.39 Protein-rich exudate separating retina from RPE over a choroidal melanoma. The layer of fluid is relatively thin, and there remains preservation of some photoreceptors and their outer segments

Stickler's syndrome (*COL2A1*, *COL11A1*, *COL11A2*, *and COL9A1*), Coats' disease (in which there may be mutations in *norrin*), and familial exudative vitreoretinopathy (*frizzled-4*). For other conditions such as retinopathy of prematurity and lattice degeneration, there are genetic risk factors. A recent GWAS study has identified high-risk loci for rhegmatogenous detachment [35].

9.6.3 Myopia

Definition

Clinically, myopia is short-sightedness where the image forms only in a plane anterior to the photoreceptors. It may be classified into two broad categories. One, axial myopia, arises because the eye is abnormally long. The other, refractive myopia, arises because either the refractive index of the

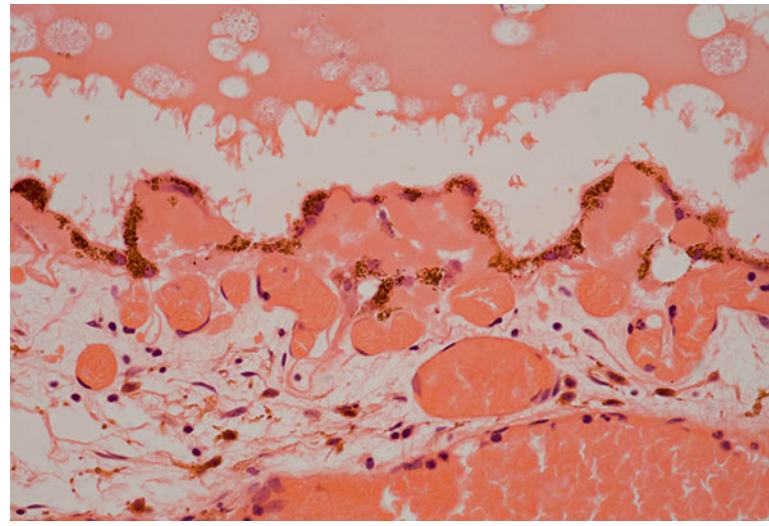

Fig. 9.40 Drusen-like deposits under the RPE in a case of long-standing retinal detachment

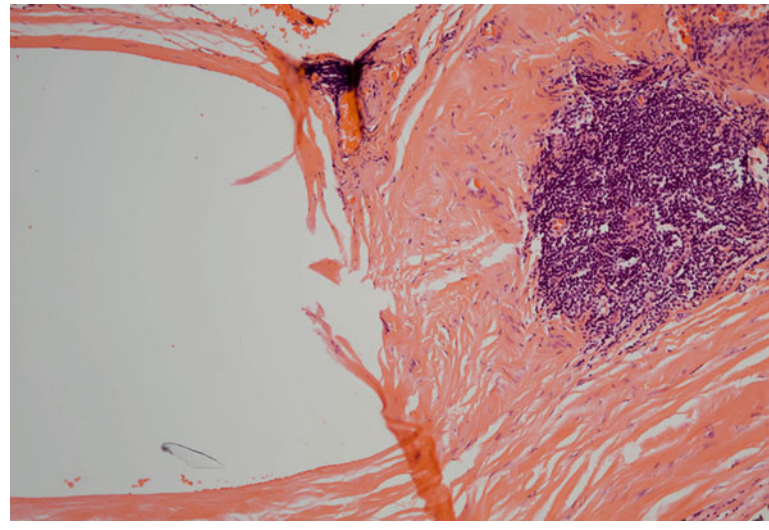

Fig. 9.41 The cavity on the left of the figure was occupied by an encircling band from a retinal detachment procedure. On the right, a focus of chronic inflammatory cell infiltrate is present in the scarred episcleral tissue

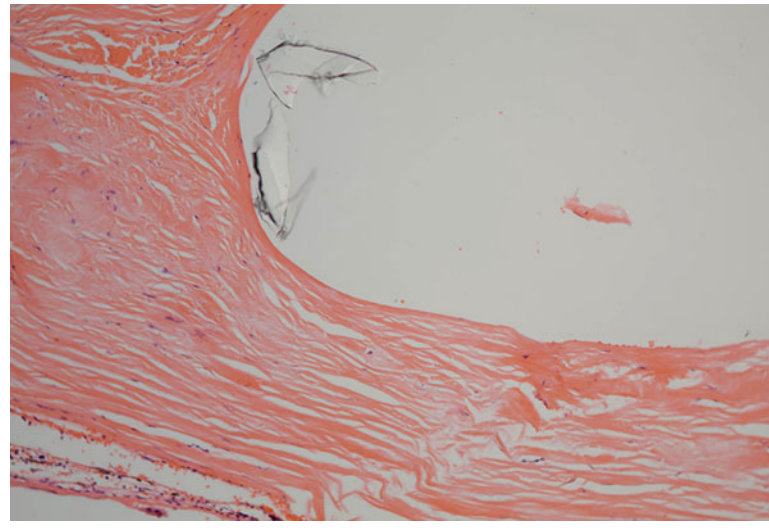

Fig. 9.42 An encircling band similar to Fig. 9.26 with some thinning of the sclera and some of the material from the band apparent in the space in the upper right portion of the figure

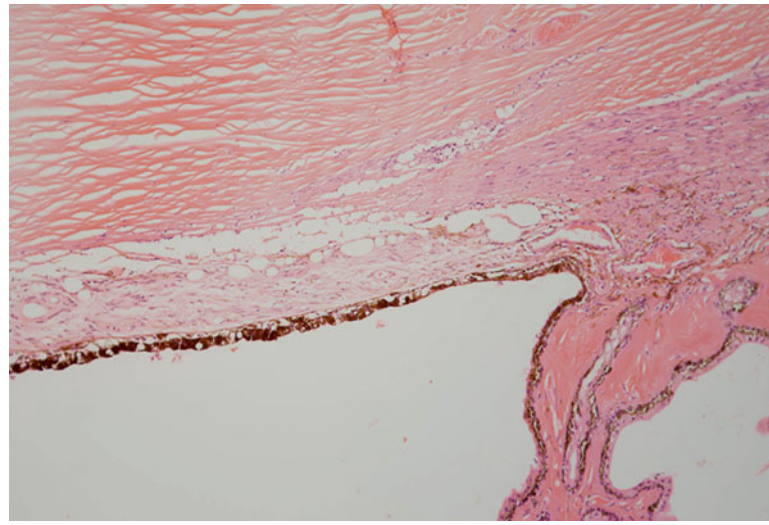

Fig. 9.43 An occluded anterior chamber and chamber angle due to low-grade inflammation associated with silicone oil droplets. Some oil is probably also present in the drainage system

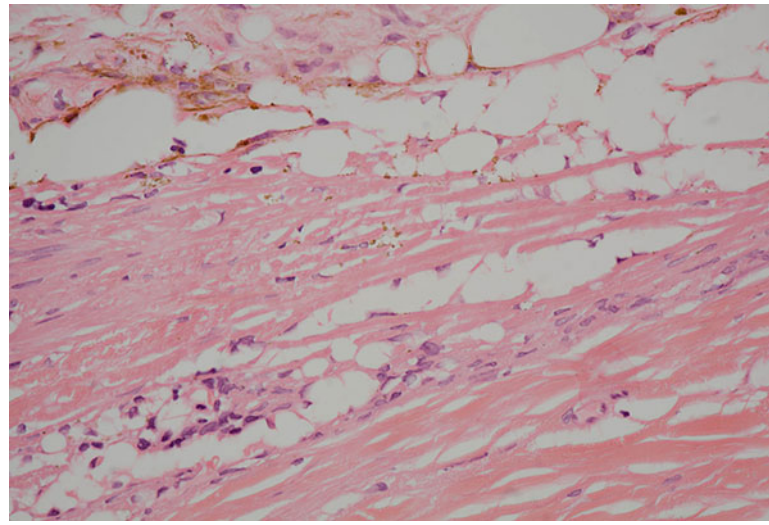

Fig. 9.44 High-power image of silicone oil, evident as round optically empty spaces, present in the anterior chamber angle (*top*), trabecular meshwork, and proximal drainage apparatus (*bottom left*)

optical media is altered or because of abnormalities of curvature of one or more optical surfaces in the eye, typically the cornea. This section will describe the changes in the eye in the former type. Significant pathology only tends to arise where there is so-called high myopia where the refractive abnormality is greater than 6.0 diopters. It is in this group that changes that a pathologist can identify tend to become apparent.

Synonyms

Myopia, short-sightedness, and near-sightedness are all the same. The terms pathological or degenerative myopia are sometimes used as a synonym for high myopia, but they are perhaps better reserved for instances where pathological changes beyond increased axial length are apparent.

Epidemiology

Myopia is very common, but pathological myopia probably develops in about 2 % of myopic patients overall. However, the prevalence appears to be much higher in Asian populations. In East Asia it affects 80–90 % of school leavers with 10–20 % of those completing secondary education suffering from high myopia [36].

Etiology

The etiology of myopia is complex and not fully understood. There is no doubt that genetics are important and there do appear to be important racial differences, but environmental factors appear to be of dominant significance. Urbanization with relative lack of time spent outdoors seems to be of major importance. It may be that lack of green cues is particular critical.

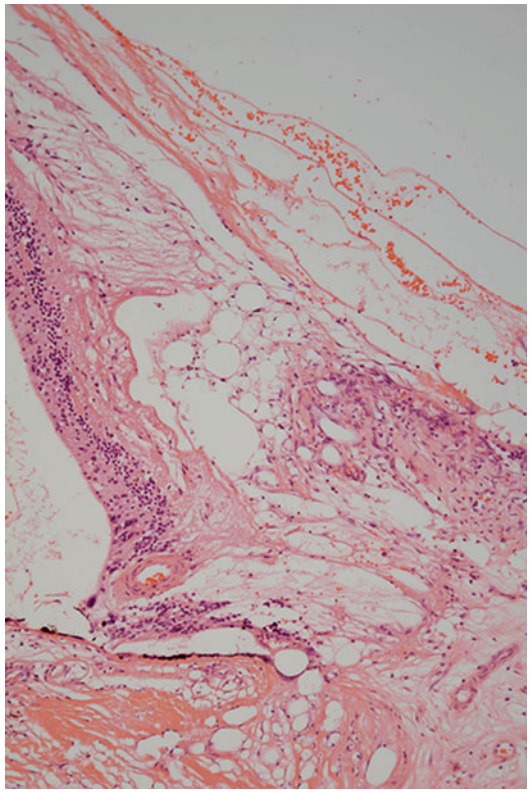

Fig. 9.45 Tractional retinal detachment close to the optic nerve head (*bottom right*) with numerous droplets of silicone oil

Clinical Features

The defining clinical feature is abnormal refraction, and increased axial length can be determined by ultrasound. Fundus examination may disclose posterior vitreous detachment, a crescent of apparent depigmentation adjacent to the optic nerve head, retinal detachment due to lattice degeneration or retinal holes, myopic degeneration with punched out areas of retinal, RPE and choroidal degeneration or lacquer cracks which represent breaks in Bruch's membrane. These breaks may give rise to choroidal neovascularization, and associated subretinal fibrosis with pigment migration is known as a Fuchs' spot.

Macroscopy

The normal eye has an axial length of 24–5 mm. If it is larger than this, the possibility of myopia should be considered. In severely myopic eyes, the axial length may increase to 29 mm or more. Generally the eye becomes elongated, so horizontal and vertical diameters are usually normal. The expansion of the sclera is often most marked

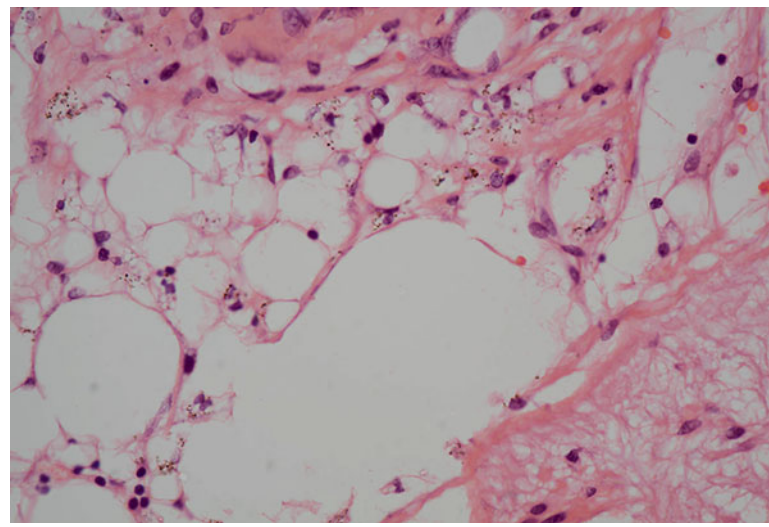

Fig. 9.46 High-power image of silicone oil droplets. Note how the admixture of RPE pigment granules gives a "dirty" appearance to the droplets. This can be helpful in distinguishing oil from microcystic degeneration in the retina

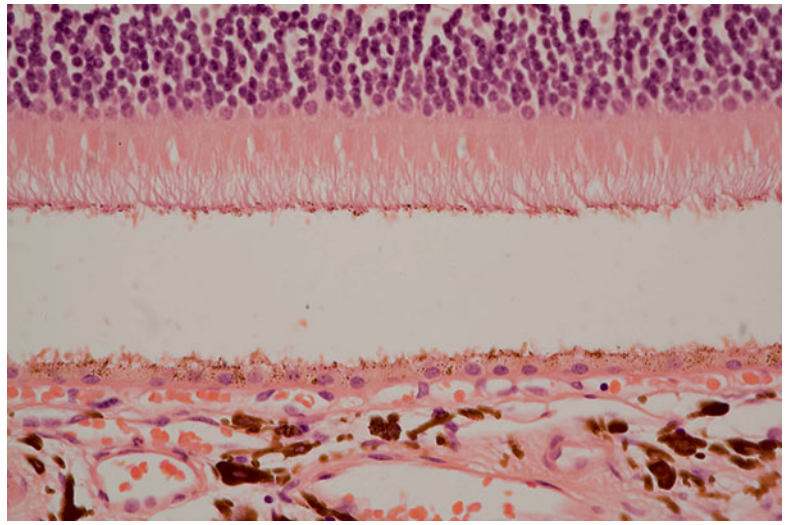

Fig. 9.47 Artifactual retinal detachment. Note the well-preserved outer segments and how they are decorated with RPE pigment from disrupted RPE apical microvilli

posteriorly, and there may be a distinct bulging of the sclera known as a staphyloma. The stretching leads to scleral thinning which may make the eye difficult to open. Irregular expansion of the eye is more likely to be associated with pathological myopic changes, but such irregularities can be harder to assess in the enucleated eye because of the loss of intraocular pressure. Intraocular examination may appear to be relatively normal or any of the clinical features listed above may be apparent. Peripheral cobblestone degeneration may be more common in myopia, but it is present in a significant proportion of eyes over 20 years of age without myopia.

Histopathology

The histopathological findings in a myopic eye are often complex and include the complications of myopia and any subsequent therapy. For instance, retinal detachment may then be complicated by proliferative vitreoretinopathy. The features to be focused on in this section are those arising primarily from the myopia itself.

The histopathology of myopia has been described thoroughly by Grossniklaus and Green [37]. A common feature, seen in over a third of their cases, is the temporal displacement of the optic nerve head. This leads to choroid overriding the nasal nerve head and a shift of choroid, retinal pigment epithelium, and neural retina away from the temporal margin of the optic nerve head. Where the sclera is stretched, there is thinning of the neural retina and choroid (Fig. 9.48a), and there may be secondary holes or schisis cavities in the retina that may predispose to retinal detachment (see above). Areas of atrophy may be quite striking with extreme thinning of the retina and choroid with loss of retinal pigment epithelium. Breaks in Bruch's membrane (lacquer cracks) may be found rarely, and choroidal neovascularization where present is more apparent.

Differential Diagnosis

Each of the components of the myopic eye has its own differential although in general once the different elements have been put together there is no great diagnostic challenge. The optic nerve head changes need to be distinguished from glaucomatous change. Although the peripapillary pallor seen clinically may be mistaken for peripapillary atrophy when viewed en face, it is seen to be displacement and not atrophy histologically. Any areas of atrophy and choroidal neovascularization must be distinguished from age-related macular degeneration and posterior staphylomas from other causes such as inflammation or buphthalmos.

Genetics

GWAS studies [38] have identified a significant number of genes related to extracellular matrix modeling, neural transmission, retinoic acid

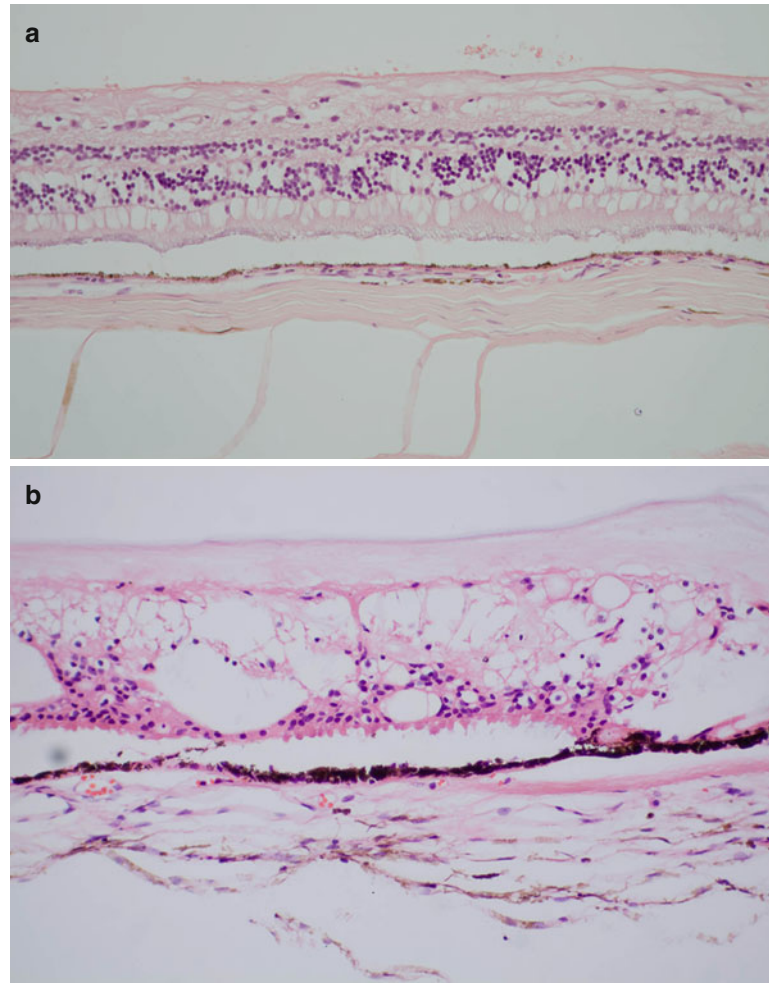

Fig. 9.48 (**a**) Thinning of retina and choroid in a myopic eye. (**b**) Peripheral microcystoid degeneration of the retina

metabolism, and eye development that explain a modest degree of the variation in expression of myopia. Further studies, particularly with exome sequencing, are likely to generate further insights, but it seems probable the detailed pathogenesis of myopia will be complex.

9.6.4 Retinal Holes, Tears, Schisis, and Related Degenerations

Definitions and Clinical Features

The retina is vulnerable to a wide range of acquired structural degenerations or defects, some of which may predispose to retinal detachment. Others are of no particular clinical importance.

Retinal holes may be incidental defects that may or may not be associated with other degenerative abnormalities of the retina or adjacent vitreous. They may be associated with rhegmatogenous retinal detachment. Another clinically important form of retinal hole is the macular hole, which forms centered on the fovea. Lattice retinal degeneration is usually found in the peripheral retina. The abnormal area of retina may contain foci of heaped up retinal pigment epithelium and pale hyalinized blood vessels.

Cobblestone or paving stone degeneration is commonly seen just behind the ora serrata and consists of irregular, small pale patches. Also common and just posterior to the ora serrata is peripheral microcystoid degeneration, which has a fine honeycomb appearance. This is generally

without consequence although it can lead to retinoschisis, splitting of the retina in a plane parallel to the inner limiting membrane, and retinal detachment.

Histopathology

The edges of retinal holes are generally rounded and can be distinguished from artifactual tears. Macular holes evolve through a series of stages and may be associated with a tiny operculum just anterior to the hole, and as with other structural retinal defects, there is often apparent vitreous traction. Vitrectomy, sometime with stripping of the inner limiting membrane, may cause the hole to close, supporting the notion that vitreous traction is important in pathogenesis. In peripheral microcystoid degeneration, small cysts appear first in the outer plexiform layer and then more anteriorly (Fig. 9.48b). In cobblestone degeneration, there is full-thickness atrophy of retina, retinal pigment epithelium and choroid.

9.7 Retinal Vascular Disease

Retinal vascular disease covers a wide range of inherited and acquired conditions, some of which have been included elsewhere. This section will focus on vascular changes associated with diabetes mellitus and hypertension as well as retinal artery and retinal vein occlusions.

9.7.1 Diabetic Retinopathy

Definition

Diabetic retinopathy can be considered in three phases. Late-stage proliferative diabetic retinopathy is characterized by the presence of newly formed blood vessels, typically anterior to the retina. Pre-proliferative or background retinopathy has no such vascular proliferation, but small hemorrhages, exudates, and cotton wool spots are evident. It is useful to also recognize an even earlier phase where no obvious clinical or histopathological abnormalities are present, yet it is clear that there are functional and probably very subtle structural changes. In this section the focus will be on pre-proliferative and proliferative diabetic retinopathy. A significant cause of visual impairment is the development of diabetic macular edema, and a predominantly ischemic form of the disease with progressive enlargement of the foveal avascular zone is also recognized.

Epidemiology

It is well established that diabetes, especially type II diabetes, is increasing in prevalence in industrial societies at an alarming rate over much of the world, and diabetic retinopathy is set to follow [39].

Etiology

Elevated blood sugar levels, other metabolic factors and, where present, coincident hypertension all contribute to the pathology seen in the eye.

Clinical Features

Patients with early disease are likely to be visually asymptomatic, and it is for this reason that screening programs for diabetic retinopathy can be so effective. With advancing disease, visual acuity can drop progressively, or if there is significant vitreous hemorrhage, it can drop precipitously.

Macroscopy

In an enucleated eye, it can be difficult to see focal pathology, but cotton wool spots and small retinal hemorrhages may be evident, but such eyes are very rarely received. More often, vitreous hemorrhage has provoked enucleation and this is readily identified or the eye has become phthisical and end stage where macroscopic examination confirms disorganized intraocular contents but generally offers little if any insight into the underlying pathology. Evisceration specimens are equally hard to access.

Histopathology

The histopathology of the diabetic eye is often complex, particular in advanced disease where there has been therapeutic intervention. Eyes with nonproliferative disease are rarely submitted for examination but may be received incidentally because of, for instance, an exenteration for

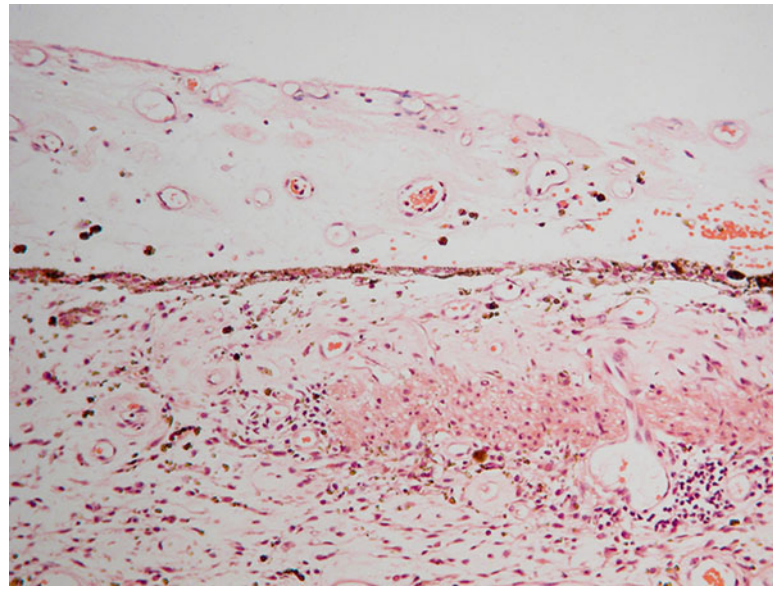

Fig. 9.49 Rubeosis iridis with a pronounced neovascular layer along the anterior surface of the iris (*top*). The iris stroma is somewhat edematous, and there is a patchy chronic inflammatory cell infiltrate

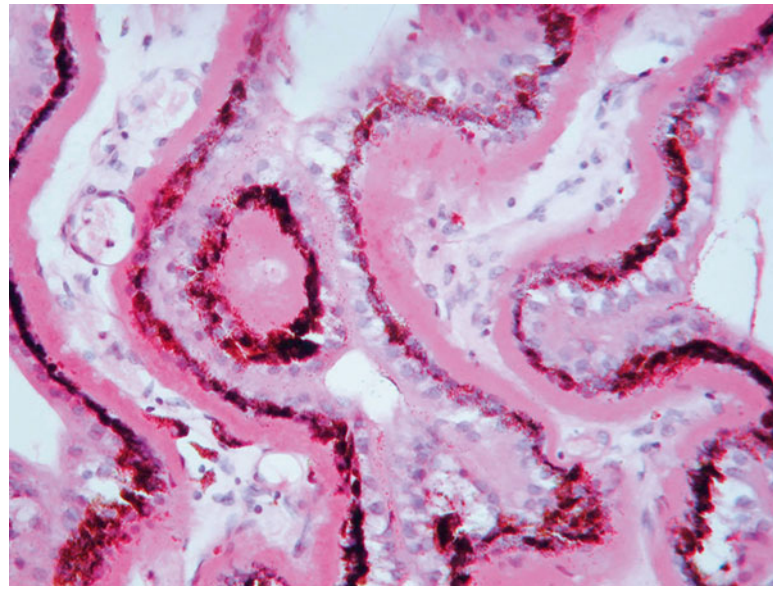

Fig. 9.50 Thickening of the basement membrane of the pigmented epithelium of the ciliary body in the eye of a diabetic patient (PAS)

anterior malignancy. Anterior changes can include rubeosis iridis (Fig. 9.49), lacy vacuolization of the iris pigment epithelium (due to glycogen accumulation), cataract, and thickening of the basement membrane of the ciliary epithelium (Fig. 9.50).

In very early disease, the retina may appear normal by conventional microscopy. If cotton wool spots or other focal pathology are identified macroscopically, they are more readily sampled for microscopic examination than if "random" levels are taken.

Cotton wool spots are essentially focal areas of ischemia in the nerve fiber layer. Axonal transport is impaired, and as a result, cytoplasmic organelles and other material accumulate at the site of hypoxia resulting in swelling of nerve fibers, which are known as "cytoid bodies" (Fig. 9.51). Cotton wool spots disappear after a few weeks leaving a barely discernible glial scar in the nerve

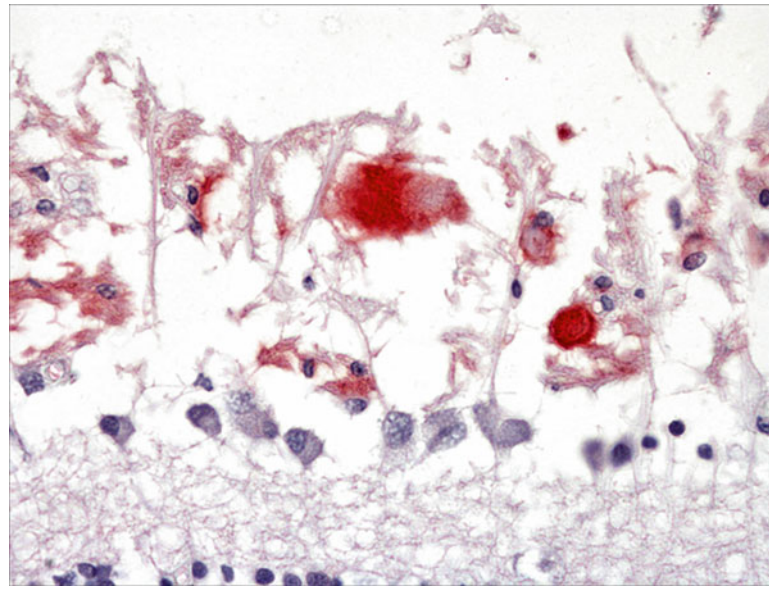

Fig. 9.51 The nerve fiber layer from a patient with SLE and extensive ischemic change within the retina. The swollen axons are demonstrated with immunohistochemistry for a mitochondrial protein, which highlights the so-called cytoid bodies. Note a row of ganglion cells and the inner plexiform layer at the inferior aspect of the image

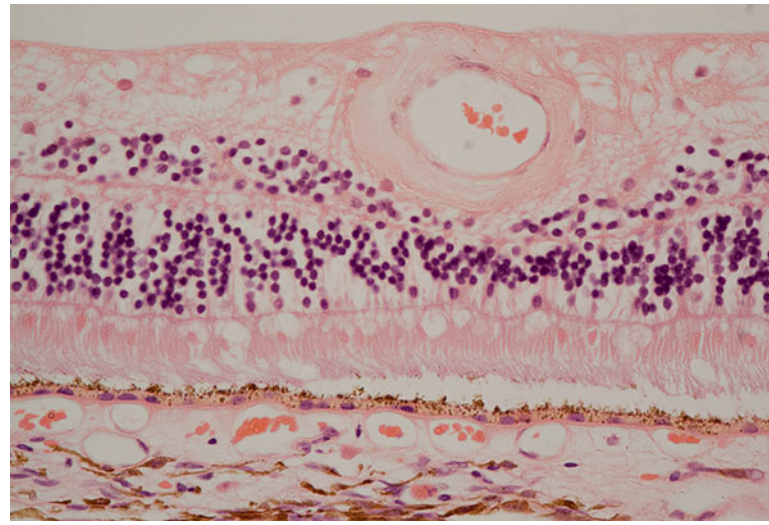

Fig. 9.52 Thickening of the wall of a retinal arteriole in a patient with diabetes mellitus

fiber layer. Intraretinal hemorrhages again are straightforward to diagnose when present.

It is often stated that thickening of microvascular basement membrane is an early and significant feature of diabetic retinopathy [40]. This is, however, surprisingly difficult to demonstrate in routine preparations, even with PAS staining although when present can be quite striking (Fig. 9.52). What is not infrequently seen is thickening of the vessel wall in a way that is similar if not identical to that seen in hypertension, and, of course, hypertensive disease is quite likely to coexist. Also difficult to demonstrate is the presence of pericyte degeneration, another early and probably significant change in diabetes. Interestingly, the retinal microvessels in health have an unusually high ratio of pericytes to endothelial cells, and this may be important in the local control of retinal blood flow.

What is almost impossible to appreciate without whole mounts combined with specific staining for vessels is the presence of microaneurysms and capillary dropout. Also difficult to visualize are intraretinal microvascular abnormalities (IRMAs) that, along with the other microvascular changes, may be seen very clearly with fluorescein angiography.

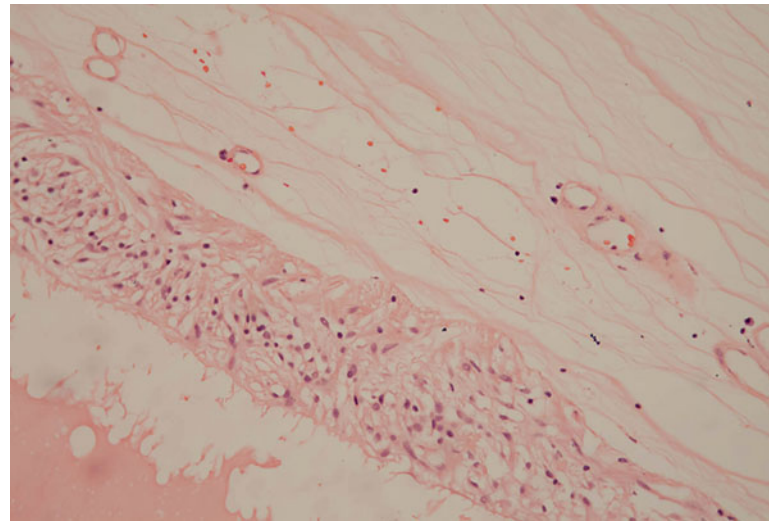

Fig. 9.53 Thin-walled poorly supported vessels anterior to thin, gliotic, detached retina in a patient with diabetes mellitus

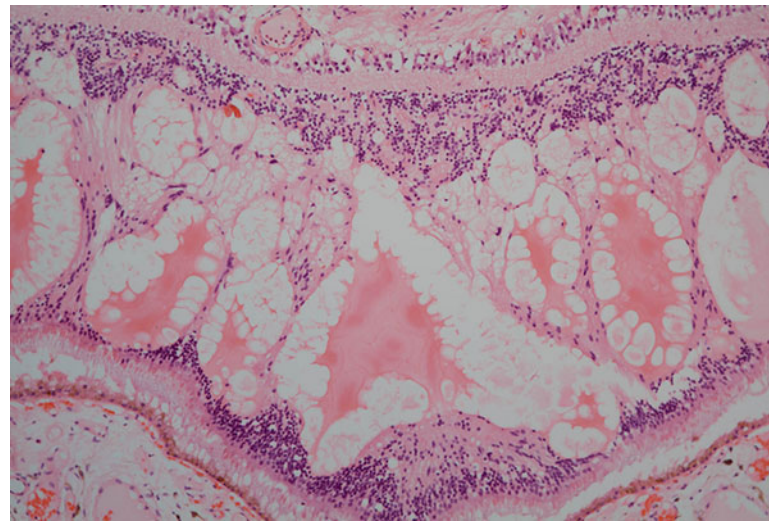

Fig. 9.54 Massive cystoid macular edema

Proliferative disease is readily appreciated with what are usually thin-walled, poorly supported vessels just anterior to the retina (Fig. 9.53) where in health there are no vessels and virtually no cells. These may be associated epiretinal membrane formation and not infrequently in cases that come to pathological examination there is associated fibrosis. The resulting fibrovascular bands contract and can cause retinal disturbance and ultimately tractional retinal detachment.

Diabetic macular edema is identified by the presence of large cystic spaces within the macular retina containing eosinophilic material (Fig. 9.54).

Often in eyes from diabetics coming to histopathology, there is evidence of therapeutic intervention. There may have been cataract extraction, and scattered photocoagulation burns are frequently identified (Fig. 9.55). These are usually multiple and consist of a focal atrophy of the retina with a residual glial scar that is adherent to the underlying Bruch's membrane. The RPE may be rounded up or absent. At low power, the adhesions often "spot weld" the otherwise artifactually detached retina to the RPE–Bruch's membrane complex. Other intervention may include treatment of complications such as retinal detachment.

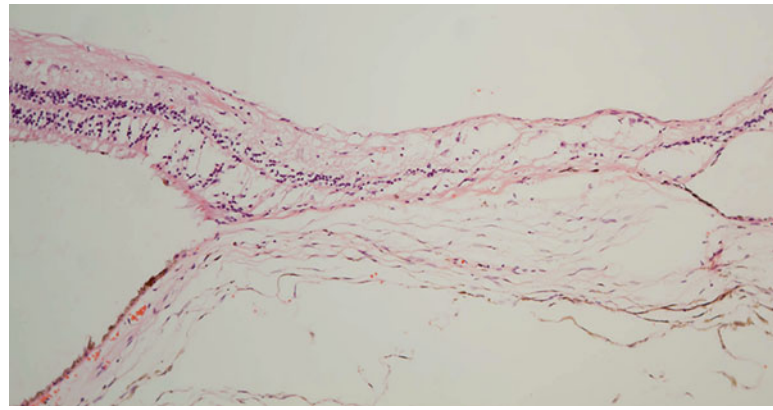

Fig. 9.55 A chorioretinal scar at the site of laser photocoagulation

Differential Diagnosis

Usually clinical information make the diagnosis clear. Hypertension may lead to similar inner retinal vascular changes, and macular edema is seen in a very wide range of inflammatory, vascular, tractional, and degenerative conditions as well as after a variety of surgical procedures. Interestingly, similar findings to nonproliferative diabetic retinopathy have been seen in the context of HIV infection. Preretinal vascularization is sometimes seen in the context of proliferative vitreoretinopathy (although this is classically an avascular preretinal proliferation.) Other important vascular retinopathies include sickle cell disease and retinal vein occlusion.

Genetics

Studies of the genetics of type II diabetes have revealed some genetic factors for the development of diabetic retinopathy, and several polymorphisms have been implicated in the inheritability of diabetes [41], but in general the contribution of genetic factors to the development of diabetic retinopathy per se is probably quite small.

9.7.2 Retinal Vascular Occlusions

Definition

Retinal vein occlusions are classified by site, central retinal vein occlusion (CRVO) versus branch retinal vein occlusion (BRVO) and by whether or not the occlusion is associated with ischemia as defined by area of capillary non-perfusion. Arterial occlusions may also affect different points within the vascular tree, namely, carotid or ophthalmic artery, central retinal artery, or branch retinal arteries.

Epidemiology

Retinal vein occlusions (RVOs) are relatively common and lead to significant visual impairment. The prevalence rate of CRVO in middle-aged and elderly is around 0.1–0.5 %. BRVO occurs significantly more frequently. Vein occlusion is the second most common cause of visual impairment due to retinal vascular disease after diabetic retinopathy. Younger patients with vein occlusion are more likely to have a systemic vasculitis or increased clotting tendency.

Etiology

The usual factors that increase risk of thrombosis operate in the context of central retinal vein occlusions. The patients are often elderly with hypertension, possibly diabetes and sometimes open angle glaucoma. The latter could reduce ocular perfusion pressure and hence retinal blood flow. The age group affected and risk factors such as hypertension, together with the apparent development during the night, are reminiscent of the context of stroke, and there are possibly important parallels in terms of pathogenesis with lower systemic blood pressure and impaired flow through an aged vascular bed likely to be of great significance. The retinal vein narrows as it passes through the lamina cribrosa, and this is likely to generate turbulence or local flow-mediated

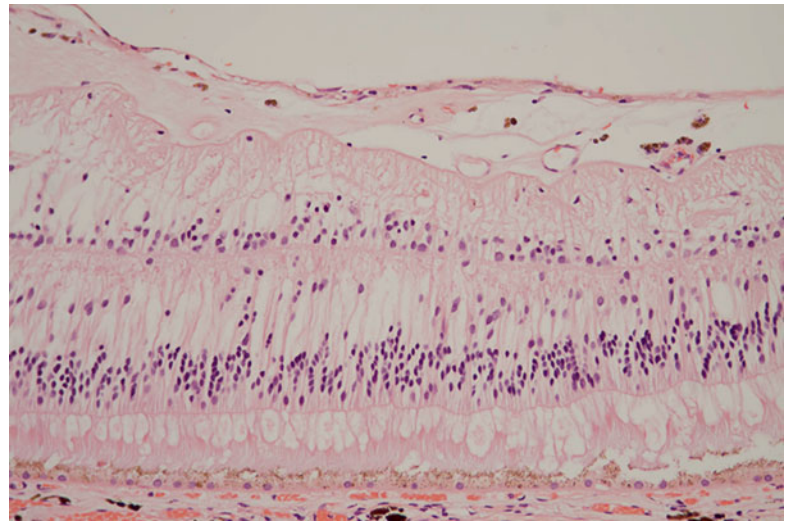

Fig. 9.56 Marked thinning of the inner nuclear layer and preretinal neovascularization in a patient with central retinal vein occlusion

endothelial cell damage. Branch vein occlusions often appear to arise where retinal arteries and veins cross, and again, local endothelial cell damage and turbulence may be important. Retinal arterial occlusions usually result from embolic disease although local thrombosis may occur. However, at the level routinely examined in the distal optic nerve and optic nerve head, atheroma is not normally apparent.

Clinical Features

The main symptom following vein occlusion is of impaired vision in one eye typically apparent on waking. The condition affects mainly the elderly. Fundoscopy discloses extensive retinal hemorrhages, engorged, tortuous retinal veins, and macular edema. Fluorescein angiography demonstrates vascular leakage and areas of nonperfusion. In some instances of CRVO, there may be some spontaneous recovery, but particularly in the ischemic form, sustained or progressive visual impairment is likely. Unless the angiogenic drive from the ischemic retina is not suppressed by laser photocoagulation development of intransigent, difficult to treat, rubeotic glaucoma is the likely outcome within a small number of months. It is this category of case that is most likely to be submitted for examination. BRVO is much less likely to progress to rubeotic glaucoma, presumably because there is insufficient extent of ischemic retina. Arterial occlusion usually leads to sudden onset of visual loss. The retina appears pale on fundoscopy, with the exception central macula where the choroidal circulation can be seen through the fovea (cherry red spot).

Macroscopy

The macroscopic features of RVO depend on the stage of the disease. There may be extensive retinal hemorrhages, or these may have cleared to leave sequelae of rubeotic glaucoma with cupped optic disk, pigmentary abnormalities, and areas of retinal opacity associated with preretinal membranes. Phthisis has often set in by the time of enucleation. Arterial occlusion leads to pallor of the retina.

Histopathology

Usually CRVO eyes are received at late stages of disease. There may be evidence of hemorrhage (generally old), but generally the most obvious features of a RVO are a gliotic retina with selective loss of cells from the inner nuclear layer (due the ischemia) (Fig. 9.56) and recanalized inner retinal vessels (Figs. 9.57 and 9.58). In longstanding disease, there is often rubeosis with angle closure and glaucomatous changes with ganglion cell loss in the retina and cupping of the optic nerve head. The only indication of hemorrhage in the past may be a little pigment associated with the retina (which must be distinguished

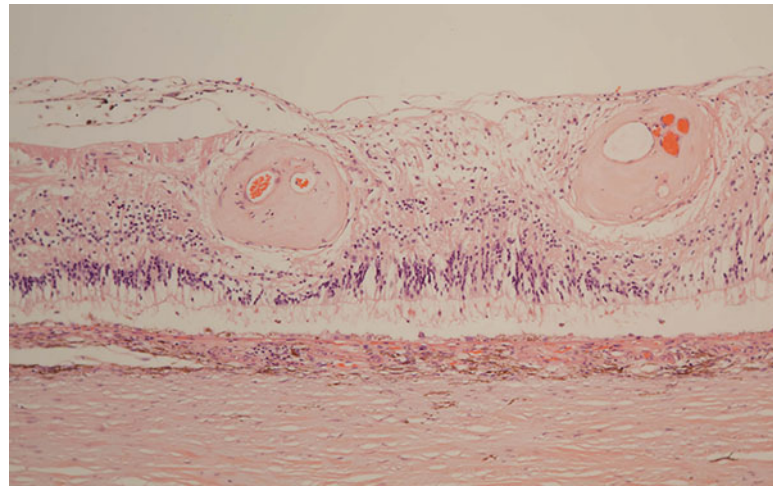

Fig. 9.57 Recanalization of retinal vessels in a patient with central retinal vein occlusion

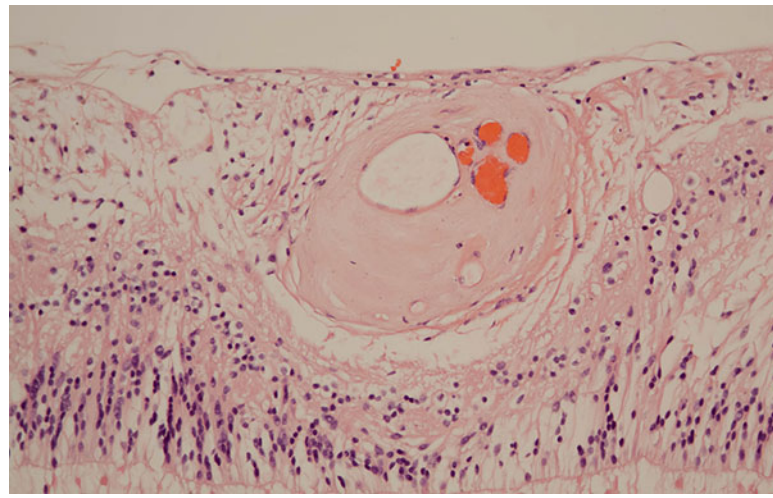

Fig. 9.58 Higher-power image of one of the vessels in Fig. 9.57

from migrated RPE) (Fig. 9.56) and, in Perl's stain (Fig. 9.59), diffuse as well as focal macrophage – associated with positivity. Depending on the level and severity of arterial occlusion, there is ischemic atrophy of variable extent of the inner retina. If there is choroidal ischemia as well, the outer retina may be affected also.

In routine examination of sections of the eye, it is rare to find evidence of occlusion at the central retinal vein or with BRVO at the retinal arteriovenous crossing where occlusion is believed to selectively occur. This reflects stage of disease; there is often clearance of the occlusion by the time eyes are enucleated and during sampling problems. The classical studies of central retinal vein occlusion have been carried out on extensive sets of serial sections. A final consideration is whether thrombosis, when identified, is the primary pathology or forms secondarily.

There is often atrophy of the optic nerve, secondary to glaucoma. There may be evidence of recanalization of the central retinal vein or the present of prominent preexisting or possibly new draining vessels in the optic nerve head/optic nerve.

As with other conditions, it is always important to look for pathological changes associated with therapy. Photocoagulation burns (Fig. 9.60) may be seen in vein occlusion cases as well as in diabetic retinopathy.

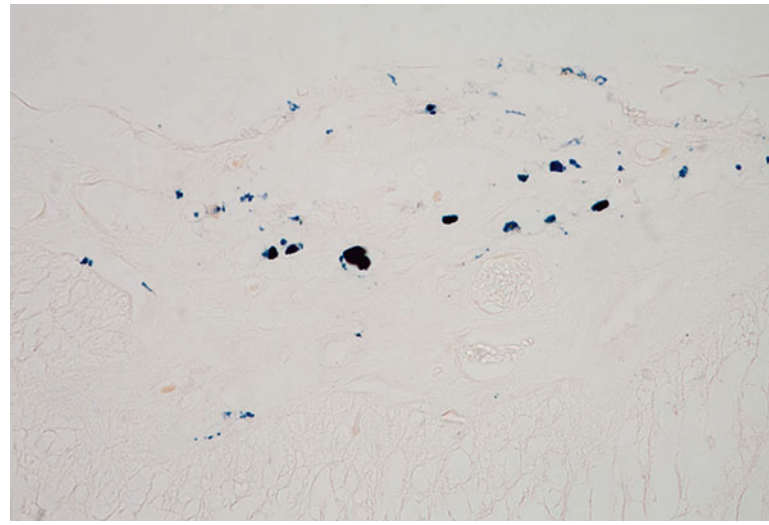

Fig. 9.59 Stainable iron (hemosiderin) in the anterior retina of a patient with central retinal vein occlusion

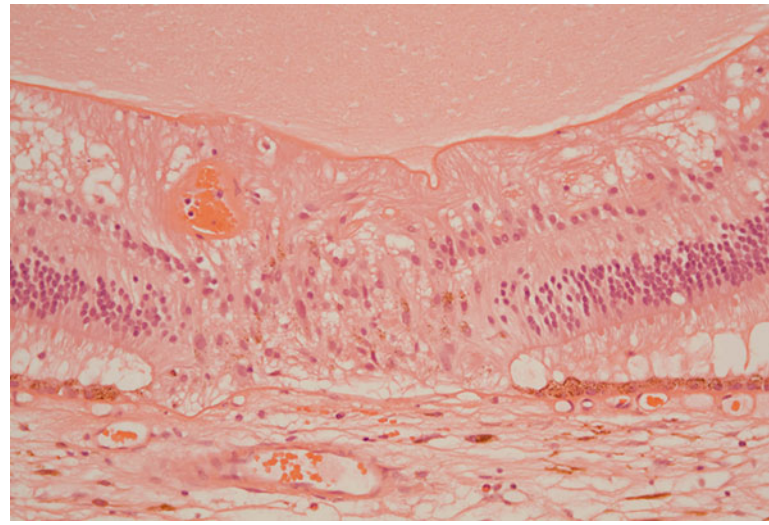

Fig. 9.60 A photocoagulation scar in a patient with central retinal vein occlusion. There is abnormal proteinaceous material anterior to the retina

Differential Diagnosis

If the clinical history is given, there is usually little room for doubt, but without it, the main consideration is whether or not the primary pathology is of diabetes or vein occlusion. Of course, the two pathologies may coexist.

9.7.2.1 Pathogenesis

The age group affected and risk factors such as hypertension, together with the apparent development during the night, are reminiscent of the context of stroke, and there are possibly important parallels in terms of pathogenesis.

9.7.3 Hypertensive Retinal Disease

Definition

Hypertensive retinal disease now largely exists as a retinal vasculopathy that is similar to early diabetic retinopathy. It may be classified as mild (mainly arteriolar vascular changes), moderate (microaneurysms, retinal hemorrhages, cotton wool spots, and hard exudates), or severe (moderate findings combined with optic nerve head swelling).

Epidemiology

Hypertension remains a common problem in industrial societies although most patients are

now treated. Recent estimates with contemporary approaches to assessing retinal photographs suggest a prevalence of hypertensive retinopathy of 2–15 % [42].

Etiology

The etiology of hypertension is complex, and for a detailed discussion, please see [43].

Clinical Features

Patients seldom present with visual symptoms as the first manifestation of hypertension. Clinical studies show that outer arteriolar cross-sectional area remains more or less constant as luminal diameter drops and wall thickness increases. The latter is associated with increased vessel opacity and arteriovenous nicking. Other features include cotton wool spots, microaneurysms, hard exudates, hemorrhages, and optic disk swelling.

Histopathology

The arteriolar changes are of thickening of the vessel wall, sometimes with hyalinization. Otherwise, the changes of moderate hypertensive retinopathy are very similar to those of pre-proliferative diabetic retinopathy. In severe hypertensive retinopathy, optic nerve head swelling (papilledema) is identified by the pushing of the peripapillary retina towards the periphery (Fig. 9.61a).

Differential Diagnosis

Similar vascular appearances may be seen with aging in the absence of hypertension. The main differential diagnosis of moderate hypertensive retinopathy is of pre-proliferative diabetic retinopathy, and the two conditions may coexist. Hemorrhages and optic nerve head swelling may be seen in a wide range of conditions including those associated with increased intracranial pressure.

9.7.4 Radiation Retinopathy

Definition

Radiation retinopathy may be acute or chronic and represents the changes seen in the retina following irradiation, usually for tumors of the eye, orbit, or adjacent tissues [44]. It may, however, arise following treatment of nonmalignant conditions such as age-related macular degeneration.

Macroscopy

The macroscopic examination of the eye may be dominated by the primary pathology, for instance, a uveal melanoma, or by other manifestation of ocular irradiation, for instance, rubeosis and glaucoma. Otherwise, the findings are similar to those of diabetic retinopathy although it is said that microaneurysms are less frequent in radiation retinopathy. There may be retinal scarring, and if there is choroidal involvement, choroidal neovascularization.

Histopathology

Acute radiation damage to the retina is rarely seen clinically, but retinal edema and outer retinal damage would be expected. In chronic disease, there is microvascular degeneration with endothelial cell damage dominating. There is resulting capillary closure and retinal ischemia with potential fibrosis and/or neovascularization. Complications such as choriocapillaris loss and choroidal neovascularization will appear similar to other conditions. There are also likely to be findings relating to radiation damage elsewhere in the eye including optic nerve head damage. Secondary vascular glaucoma may arise because of the hypoxic drive and VEGF secretion from hypoxic retina.

Differential Diagnosis

The clinical context is usually unambiguous, but other vaso-obliterative processes such as diabetic retinopathy should be considered. What may present a challenge is where there is diabetes that may have exacerbated the development of radiation retinopathy. If there is an intraocular tumor, there may be changes due the tumor itself to consider. The retina remote to the tumor may be affected by subretinal exudate that can shift and not be apparent at the time of enucleation.

9.7.5 Eales' Disease

Definition

Eales' disease as an entity is debated by some but as generally described relates to a syndrome

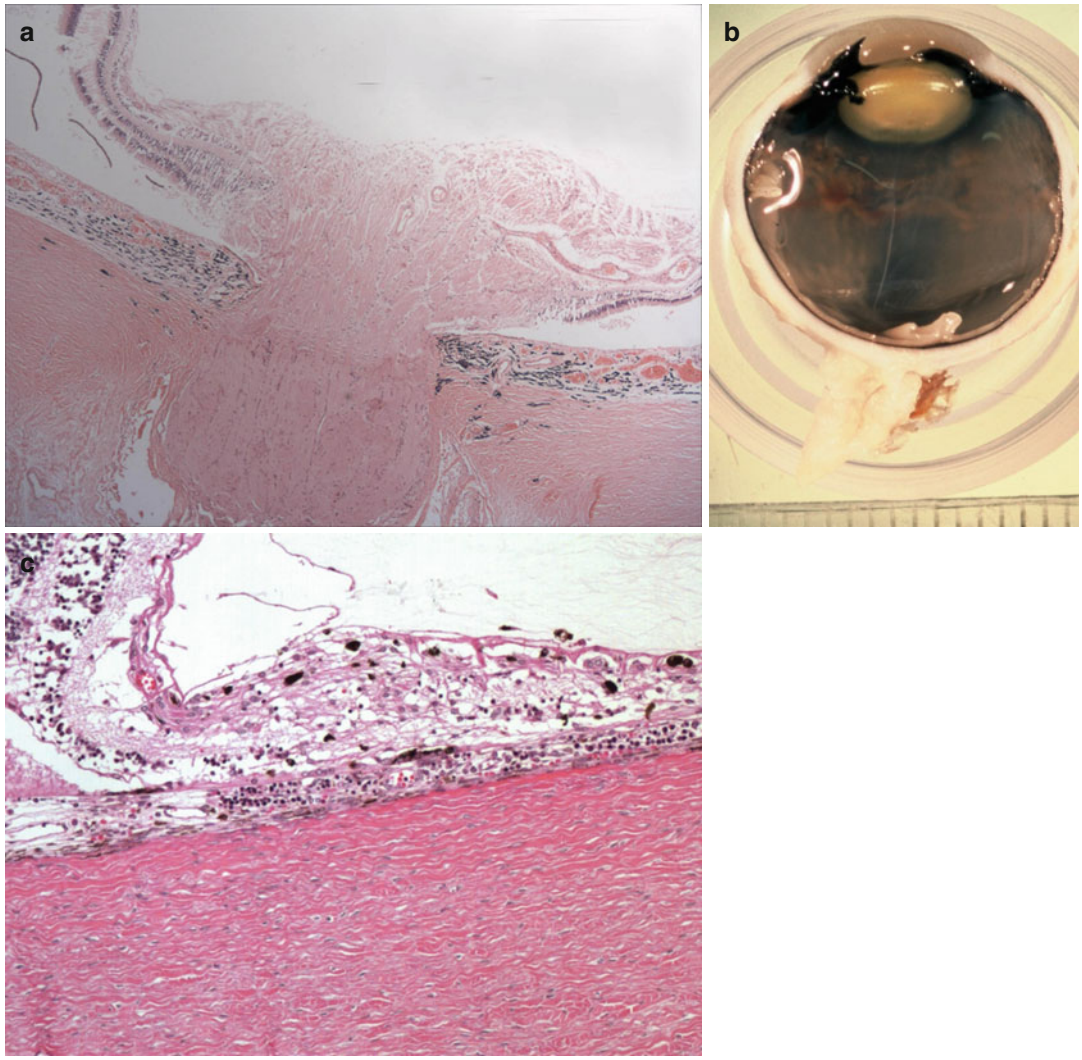

Fig. 9.61 (**a**) Papilledema. Note the displacement of retinal tissue away from the edge of the optic nerve head. (**b**) Macroscopic image of the eye of a patient with retinopathy of prematurity. Note the elevation and hemorrhage at the level of the equator (S Heegaard, Copenhagen, Denmark). (**c**) Microscopy from above case showing vascularized retina on the left and the transition to ischemic disorganized tissue on the right (S Heegaard, Copenhagen, Denmark)

classically, but not exclusively affecting young males. The characteristic features include periphlebitis and peripheral capillary closure.

Epidemiology

The condition is mainly reported from Asia, notably India, Pakistan, and Afghanistan.

Etiology

Etiology of Eales' disease is debated. There has for some time been the view that it is a reaction to tuberculosis infection, and certainly, isolation of mycobacteria from eyes with Eales' disease is very rare [45]. However, a recent study using PCR demonstrates a mycobacterial signal in about 50 % of cases [46].

Clinical Features

There may be perivenular cuffing, evidence of peripheral capillary closure associated with posterior progression and vascular irregularity and vitreous hemorrhage.

Histopathology

There are very few reports of the histopathology of Eales' disease, but perivascular lymphocyte cuffing, cellular thickening of the vessel walls, and vessel closure have been reported.

Differential Diagnosis

The differential diagnosis includes other causes of retinal perivascular inflammation including other infectious diseases and sarcoid. In an enucleation specimen from a patient with tuberculosis, it is important to examine the entire eye for other manifestations of mycobacterial infection.

9.7.6 Collagen Vascular Diseases

Definition

The collagen vascular diseases are a group of systemic autoimmune disorders that include systemic lupus erythematosus (SLE), polyarteritis nodosa, and rheumatoid arthritis.

Histopathology

The findings in the eyes of patients with SLE are variable, but signs of ischemia including cotton wool spots, retinal hemorrhage, and retinal edema with or without frank retinal vasculitis are described [47]. Immune complex deposition in uveal tissues is also reported, and as with other collagen vascular diseases, there may be a serous retinal detachment. In one case with identified anti-retinal antibodies [48], there were punched out lesions of the retina especially peripherally with pigment migration and bone spicule formation. On histology the retinal immune cell population comprised a few T cells, no B cells, and macrophages.

Ocular involvement in polyarteritis is rare but can lead to central retinal artery occlusion and choroidal infarction as well as anterior ischemic optic neuropathy. Patients may also develop retinal vasculitis, iritis, and vitritis. Changes may also develop secondary to renal hypertension.

Rheumatoid disease may cause a retinal vasculitis, but more reports describe the potential impact of hydroxychloroquine on the retina. This antimalarial drug, which can also be used in the treatment of other connective tissue disorders, appears to cause inner retinal damage, but there is little if any description of the pathology.

Differential Diagnosis

The differential diagnosis will depend on the specific findings but in general will include other causes of vasculitis and microvascular disease.

9.7.7 Retinopathy of Prematurity

Definition

Retinopathy of prematurity (ROP) is a disorder of the development of the retinal vascular seen in premature low birth weight babies characterized by impaired development of the peripheral circulation that can lead to hypoxia and neovascularization [49]. In the first phase of the disease, the normal extension of new vessels towards the ora serrate halts with the formation of a ridge of abnormal vessels and proliferating endothelium and relatively undifferentiated mesenchymal cells. In the second phase, neovascularization may develop potentially with hemorrhage, retinal detachment, and blindness.

Synonyms

The older term for this condition is retrolental fibroplasia.

Epidemiology

This condition is more common in whites than black and males than females. Despite the improvements in neonatal care, ROP remains a major health problem.

Etiology

The first critical etiological factor is prematurity. The nasal retinal circulation reaches the ora serrate at around 32 weeks and the temporal by 40. There are probably many risk factors for ROP in addition to the classical mediator of disease, increased inspired oxygen, and these may include hypercapnia, acidosis, and infection.

Clinical Features

The changes are classified according to a well-defined international classification system that is based on the appreciation of three retinal zones. Zone 1 is a circle centered on the optic nerve and is double the diameter of the macula. Zone 2 is a circle that extends from the periphery of zone 1 to the nasal ora serrata. Zone 3 extends from the peripheral of zone 2 to the remainder of the ora serrata. A central clinical feature of ROP is an elevated ridge marking the boundary between normally vascularized and avascular retina. In many cases this is peripheral, and the disease resolves spontaneously. In others, neovascularization and then retinal detachment develop with potentially profound consequences for vision. At any stage of ROP, "plus" disease is defined by the presence of distorted engorged retinal vessels. Laser ablation of the hypoxic retina is the most common therapy. Even in cases that resolve spontaneously, there is evidence that some abnormalities of retinal vasculature and neural organization remain.

Macroscopy

The macroscopic findings will correspond largely to the clinical stage of the disease (Fig. 9.61b), which is likely to be end stage in any eye that is not enucleated for another reason.

Histopathology

The histopathology of the ridge is of elevated retina with a proliferation of endothelial and spindle-shaped cells and, peripherally, avascular retina (Fig. 9.61c). Thereafter, the findings are those of preretinal neovascularization, vitreous hemorrhage, and retinal detachment, possibly with complicating proliferative vitreoretinopathy, equivalent to those seen in other conditions.

Differential Diagnosis

Other causes of retinal hemorrhage and detachment must be considered including persistent hyperplastic primary vitreous and Coats' disease. Occasionally ROP is found in eyes from children dying in unexplained circumstances, and it is important to distinguish ROP from the kinds of retinal hemorrhage and potentially detachment seen in infants with inflicted head injury.

9.7.8 Sickle Retinopathy

Definition

Proliferative sickle retinopathy arises as a result of abnormal peripheral retinal vasculature in patients with sickle cell disease or more commonly those with sickle cell trait.

Clinical Features

Loss of peripheral retinal vasculature is a central feature of sickle retinopathy. The posteriorly displaced peripheral circulation may appear to have an architecture similar to that of normal retina with the density of vessels dropping towards the edge or may appear abnormal with a dense peripheral capillary network with stump and bifurcations [50]. This latter pattern is more common in sickle cell trait, explaining the otherwise paradoxical higher risk of proliferative disease in SC patients. If proliferative disease develops hemorrhage, retinal detachment and proliferative vitreoretinopathy are similar to other conditions where these complications of retinal hypoxia occur.

Histopathology

The abnormalities of retinal circulation are best appreciated in retinal whole mounts, not a methodology in routine use. The microvessels can be visualized with lectin, antibody, or enzyme histochemistry for ADPase [51]. In such preparations, characteristic sea-fan patterns of preretinal neovascularization can be seen [52].

Genetics

A point mutation in the β-globin gene renders erythrocytes less able to traverse capillary beds and particularly in conditions in which low pH vascular occlusions occur.

Predictive and Prognostic Factors

As discussed above, the presence of sickle cell trait (SC) as opposed to sickle cell disease (SS) carries a higher risk of proliferative disease.

9.7.9 Demyelination

Epidemiology

It is well recognized that multiple sclerosis is more prevalent in temperate climates, and it has an estimated mean annual incidence rate of 4.3 cases/100,000 in Europe [53].

Etiology

The detailed etiology of multiple sclerosis remains unclear although autoimmune mechanisms are central to the disease.

Histopathology

One abnormality reported in histopathological studies is the presence in some cases of perivascular lymphocytic cuffs [54]. These may most readily be appreciated in retinal digests [55]. There is retinal ganglion cell loss, thinning of the nerve fiber layer, and retinal gliosis. If retrolaminar, optic nerve is sampled, plaques indistinguishable from those seen in the brain may be found.

9.8 Neoplasms of the Retina

Neoplasms of the retina can be classified as congenital anomalies such as hamartomas, reactive hyperplasias, and true neoplasms that can be either benign or malignant. The cells of origin can be the underlying retinal pigment epithelium (RPE), the retinocytes or retinoblasts, the vascular components of the retina or the retinal glial cells. Retinal metastases are exceptionally rare.

9.8.1 Astrocytoma and Astrocytic (Glial) Hamartoma

Retinal and optic disk astrocytomas and astrocytic hamartomas arise in the inner retinal layers usually within the nerve fiber layer before

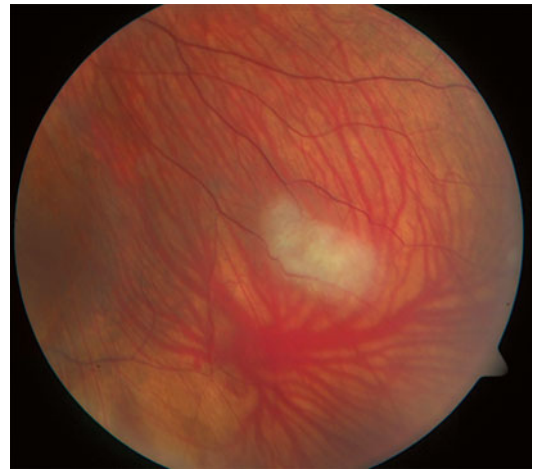

Fig. 9.62 Small peripheral astrocytoma in a patient with tuberous sclerosis complex (TSC)

the nonmyelinated nerve fibers penetrate through the lamina cribrosa and become myelinated (Fig. 9.62). The cells of origin are believed to be in the vast majority of cases retinal astrocytes (Fig. 9.63). Most isolated cases are believed to be congenital and may be considered hamartomas. True astrocytic neoplasms (astrocytomas) in otherwise normal retinal are rare phenomena. They are usually associated with either tuberous sclerosis complex (TSC) or neurofibromatosis type I, but they have also been described independently of these syndromes. They are benign lesions usually with minimal growth potential. During their evolution, both astrocytic hamartomas and true astrocytomas show signs of calcification that can be detected by ultrasound examination and can thus be included in the differential diagnosis of retinoblastoma (Fig. 9.64). In smaller lesions inner retinal thickening can be detected clinically by optical coherence tomography (OCT) (Fig. 9.65). Patients with TSC are more likely to have multiple astrocytomas compared to those with neurofibromatosis and no apparent syndrome [56–60]. Besides retinal astrocytes, also Müller cells and oligodendrocytes can give rise to astrocytomas and astrocytic hamartomas [61–64]. Most astroglial lesions show clear glial differentiation and express glial fibrillary acidic protein (GFAP). Neuron-specific enolase (NSE)

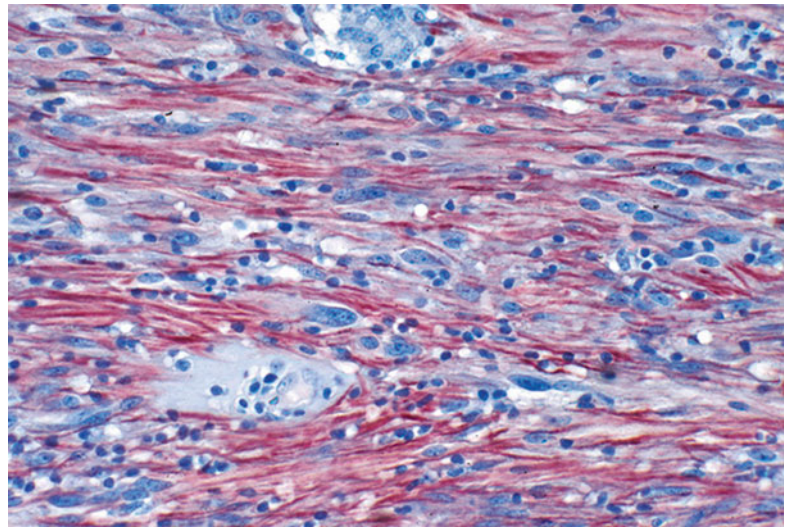

Fig. 9.63 Astrocytoma composed of slender astrocytes stained positive with GFAP (S. Heegaard, Copenhagen, Denmark)

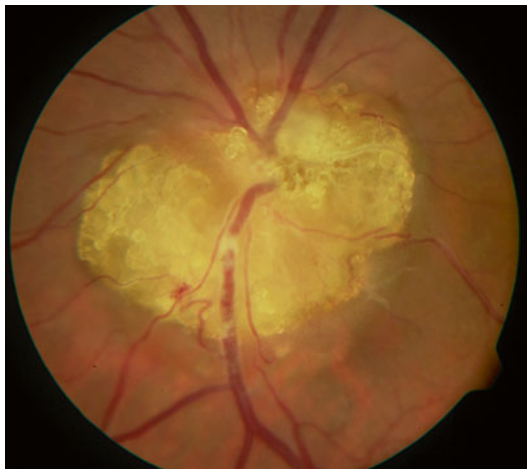

Fig. 9.64 Calcified astrocytoma of the optic disk

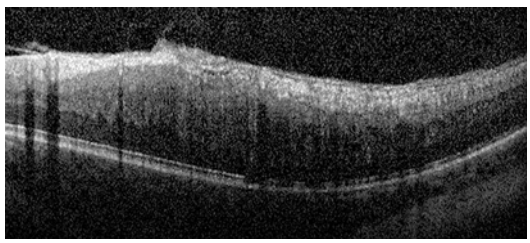

Fig. 9.65 Optical coherence tomography (OCT) shows mainly inner retinal thickening

and S100 expression may also be seen. On rare occasions, aggressive growing variants have been described (Fig. 9.66) [65–70]. Retinal astrocytomas should not be confused with myelinated retinal nerve fibers, which are a congenital anomaly that occurs when optic nerve fiber myelination by oligodendrocytes fails to stop at the lamina cribrosa. This anomaly can occur at the edge of the optic disk but also in more remote retinal areas (Fig. 9.67) [71].

9.8.1.1 Genetics of Syndromes Associated with Retinal Astrocytomas

Tuberous sclerosis complex (TSC) (Bourneville–Pringle disease) is a systemic disorder with an incidence of 1:10.000 and characterized by hamartomas in multiple organ systems. The disease is inherited in approximately 40 % of cases in an autosomal dominant fashion and is caused by mutations at 9q34 or at 16p13.3, leading to inactivation of tumor suppressor genes TSC1 or TSC2, respectively.

Neurofibromatosis type I (NF I) (von Recklinghausen disease) is a systemic disorder caused by a mutation of the neurofibromin gene (NF I-gene) which encodes the neurofibromin protein. Neurofibromin is involved in cell signaling. Patients with NF I may develop multiple plexiform neurofibromas, café au lait spots on their skin, gliomas of the optic nerve, retinal astrocytomas, choroidal nevi, and Lisch nodules on the iris.

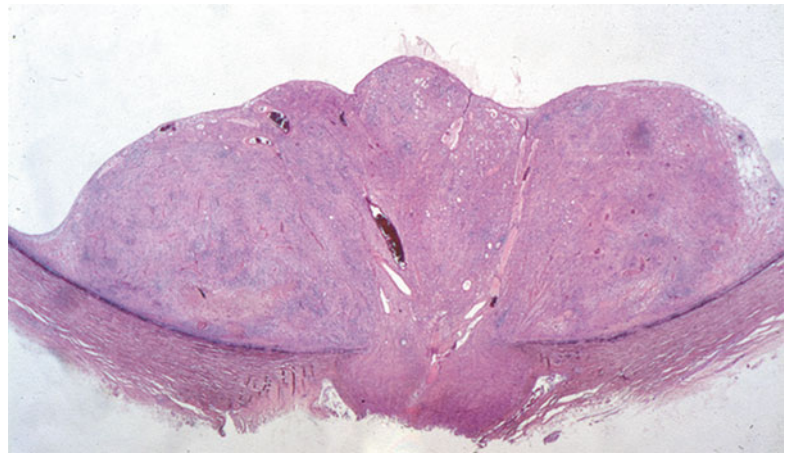

Fig. 9.66 Astrocytomas can exhibit considerable size and in rare instances aggressive behavior (H.E., S. Heegaard, Copenhagen, Denmark)

Fig. 9.67 Parapapillary myelinated nerve fibers can have a somewhat similar appearance to astrocytoma

9.9 Retinal Vascular Tumors

Retinal vascular tumors can be classified in congenital, developmental, and acquired lesions, some of them having a known genetic etiology. Retinal capillary hemangioblastoma or hemangioma can be isolated/sporadic but also be syndromic and associated with von Hippel–Lindau disease. Retinal cavernous hemangioma has also been described as a solitary, sporadic lesion, and as bilateral disease associated with oculoneurocutaneous phacomatoses. Retinal arteriovenous communications are congenital nonneoplastic vascular malformations without known genetic risk factors or causative mutations. Vasoproliferative tumors of the retina are acquired vascular lesions that can be primary or reactive in nature [72, 73].

9.9.1 Retinal Hemangioblastomas (Hemangiomas)

Retinal hemangioblastomas are benign highly vascularized tumors of the retina, which can occur isolated as a solitary tumor in one eye or in approximately 25 % of patients be associated with the von Hippel–Lindau disease, in which case they usually are multifocal and bilateral [74].

Von Hippel–Lindau (VHL) disease is an autosomal dominant multi-tumor syndrome characterized by the development of mostly benign but also malignant neoplasms in different organs throughout life. The estimated prevalence is 1 in 40,000 individuals. The ophthalmic manifestation of VHL disease is the development of retinal hemangioblastomas (retinal angiomatosis). Patients with VHL disease may also develop hemangioblastomas of the central nervous system; cysts of multiple abdominal organs such as kidney, pancreas, and liver; pheochromocytoma; pancreatic islet tumors; endolymphatic sac tumors; and renal cell carcinoma. In the central nervous system, the most common manifestation is in the subtentorial cerebellum and less frequently in the medulla, but tumors can occur also in the spinal cord [75]. Retinal hemangioblastomas are usually the first symptom-

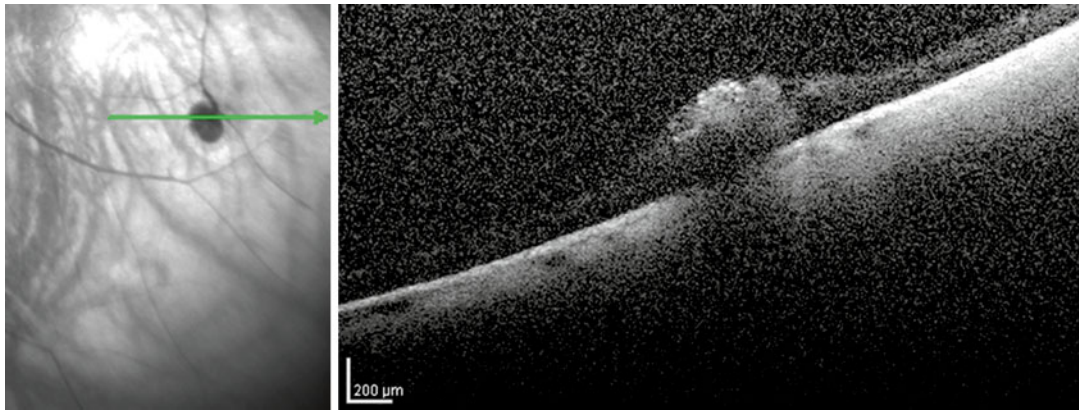

Fig. 9.68 A microangioma is illustrated occupying the inner retina on optical coherence tomography. The *left* insert shows the clinical view of the microangiomas with their feeder vessels. *Arrow* OCT section plane

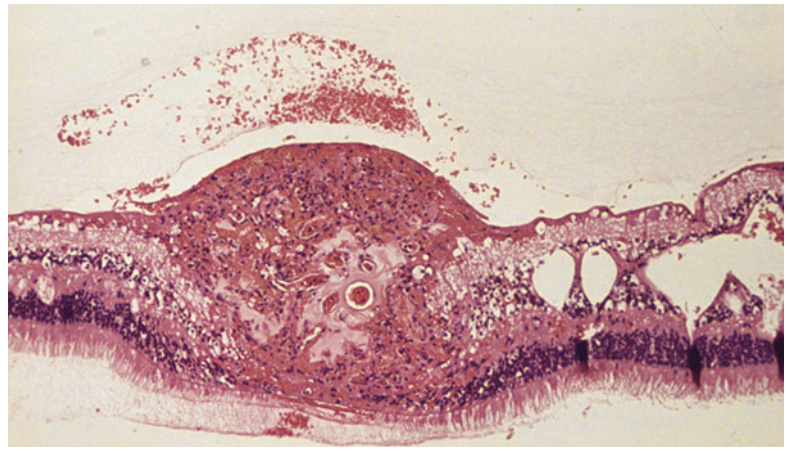

Fig. 9.69 Micrograph showing a small hemangioblastoma mostly occupying the inner retina. There is associated retinal vessel hyalinization, cystoid retinal edema, and a minute vitreous hemorrhage (H.E.)

atic manifestations of VHL disease to become symptomatic, with floaters, metamorphopsia, and occasionally blurred vision usually developing in the third decade of life. Patients may, however, be detected as early as the first decade of life, if because of a family history of VHL disease they are examined and found to have asymptomatic microangiomas representing the earliest stages of the development of hemangioblastomas. Renal clear cell carcinoma occurs in about 70 % of individuals with VHL and is the leading cause of mortality in these patients [75, 76].

Clinical Features

Retinal capillary hemangioblastomas can be classified according to their location, which may be epipapillary, juxtapapillary, or peripheral, and according to their morphology, which may be endophytic, exophytic, or sessile. Location and size of the tumors are of importance regarding ocular morbidity, with epipapillary tumors having the worst prognosis for visual function. Peripheral retinal capillary hemangioblastomas are yellowish-red retinal tumors that have prominent retinal feeder vessels originating from the optic nerve. Small angiomas can be visualized by angiography and by OCT examination (Fig. 9.68). With increasing size, they can have severe remote effects on the retinal function, such as cystoid macular edema and exudative but also tractional retinal detachment (Fig. 9.69) [72, 76].

Histopathology

Depending on the size and age of the hemangioblastomas, either the intrinsic capillary vascular

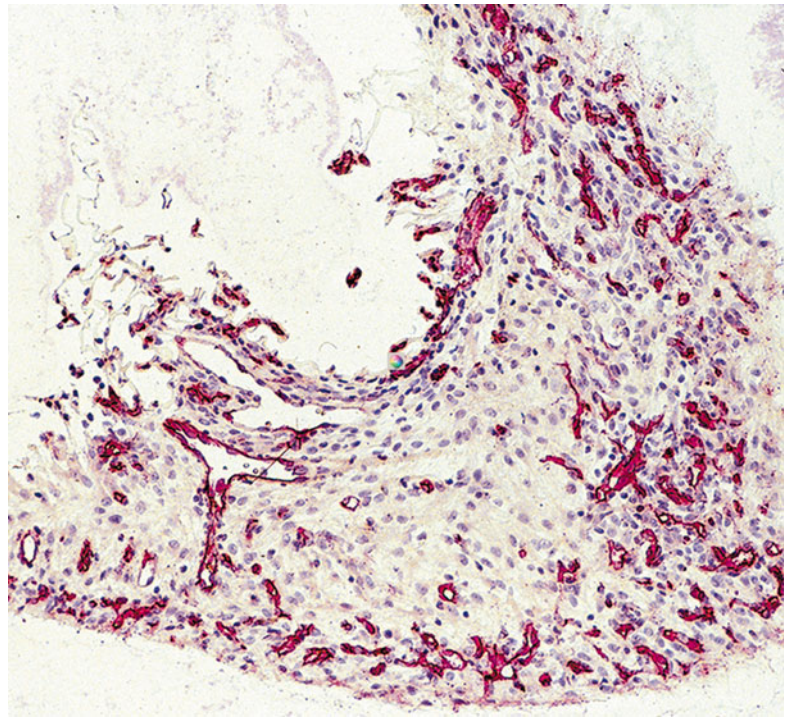

Fig. 9.70 CD31 immunohistochemistry highlights the endothelial cells in the capillaries of the lesion shown in Fig. 9.74

network or the reactive glial elements are more prominent. In the early stages of their development, a minute capillary meshwork is formed which grows with time and attracts a greater circulation (Figs. 9.70 and 9.71). The feeder vessels become more prominent and the collateral effects more pronounced with intraretinal, subretinal, and preretinal hemorrhages, retinal and subretinal lipid exudates, cystoid changes in the adjacent retina, as well as reactive cystoid macular edema (Figs. 9.72 and 9.73). Reactive gliosis develops around the hemangioblastoma, and lipid-laden glial and stromal cells may be present (Figs. 9.69, 9.74, 9.75, and 9.76). More advanced cases can exhibit peripapillary fibrovascular/fibrocellular membrane formation (fibrosis) exhibiting substantial traction on the adjacent retina. In combination with continuous exudation, a combined exudative/tractional retinal detachment can develop causing secondary glaucoma and a blind hemorrhagic painful eye (Figs. 9.73 and 9.75) [77].

Immunohistochemistry

The capillary networks can be visualized with endothelial cell markers (CD31, CD34, etc.), whereas the glial cells stain with GFAP. Some of the stromal cells express VEGF (Figs. 9.70, 9.71, and 9.78).

Genetics

Von Hippel–Lindau disease is an autosomal dominant genetic condition. The VHL gene was cloned in 1993 on the short arm of chromosome 3 in the chromosomal band 3p25.3 and encodes two VHL proteins: a full-length 213 amino acid protein (pVHL30) and a smaller protein (pVHL19) that lacks the first 53 amino acids [78–81]. These are tumor suppressor gene products that regulate cellular homeostasis and angiogenesis through interacting with the intracellular signal transduction pathways associated with the hypoxia-induced transcription factors HIF-1 and HIF-2. Inactivation of the wild-type allele in VHL patients is consistent with a classic Knudson's "two-hit" model of tumor development due to tumor suppressor inactivation, as has been described in retinoblastoma [82]. The VHL proteins suppress upregulation of the HIF, which induce VEGF production and thus angiogenesis. In case of VHL, these proteins are downregulated

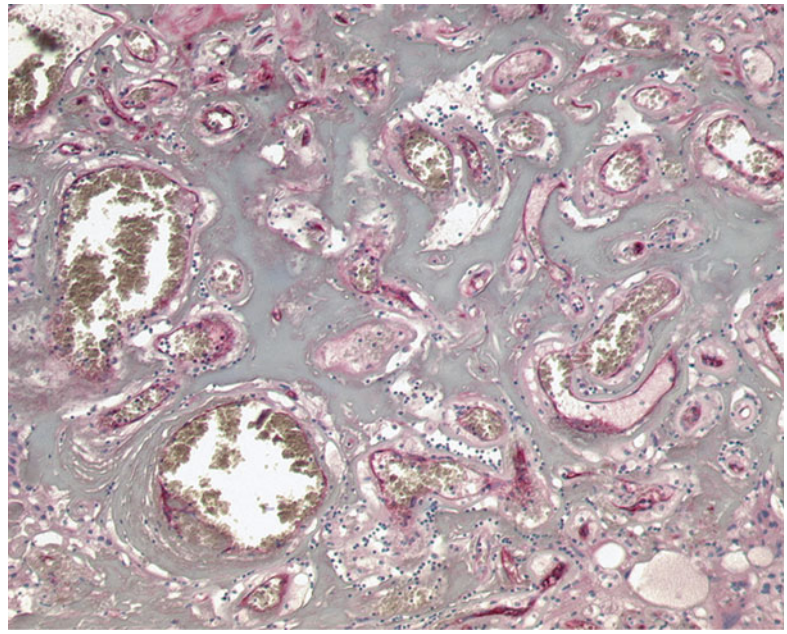

Fig. 9.71 CD31 immunohistochemistry highlights the endothelial cells in the larger hyalinized vessels of the lesion shown in Fig. 9.75. The stroma in this older lesion is much more prominent and fibrotic than in the microangiomas shown in Fig. 9.74

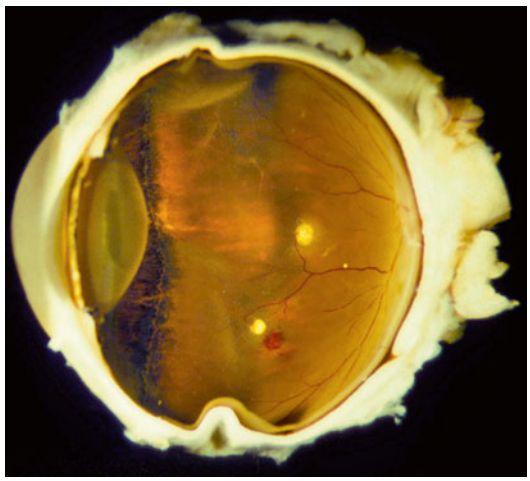

Fig. 9.72 Macroscopic appearance of multifocal hemangioblastomas in a patient with von Hippel–Lindau (vHL) disease. Prominent feeder vessels are visible

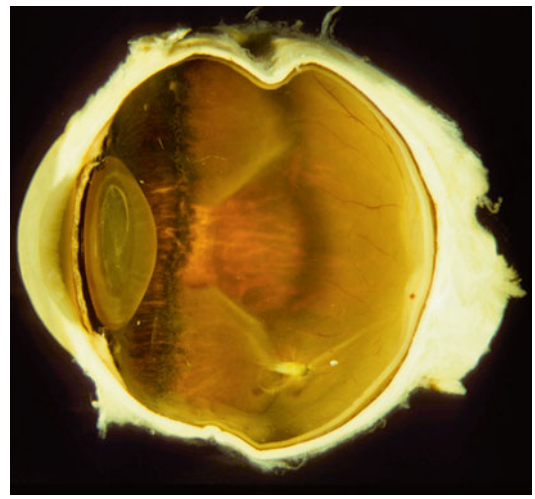

Fig. 9.73 Macroscopic appearance of a regressed unifocal hemangioblastoma showing vitreous traction

due to a VHL gene mutation, and both HIF and VEGF are upregulated, contributing to the typical vascular multi-tumor syndrome VHL. Approximately 20 % of VHL disease patients bear de novo mutations that were not inherited, and therefore there is no family history. It is also important to note that approximately 20 % of unifocal retinal hemangioblastomas are associated with VHL disease [83]. Therefore, all patients with retinal hemangioblastomas have to be worked up for VHL disease.

9.9.2 Retinal Cavernous Hemangioma

Cavernous hemangiomas of the retina are rare vascular lesions, believed to be congenital

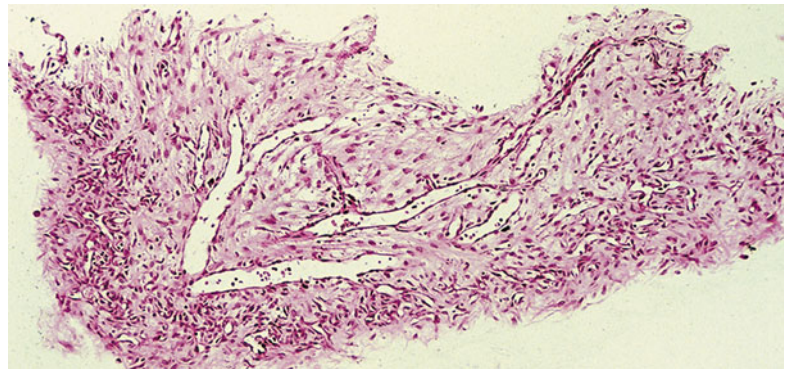

Fig. 9.74 Excised endophytic (epiretinal) hemangioblastoma of a patient with vHL disease. Small capillaries are present at the edge of the lesion. The stroma contains spindle-shaped cells some of which are foamy (lipid laden) (PAS)

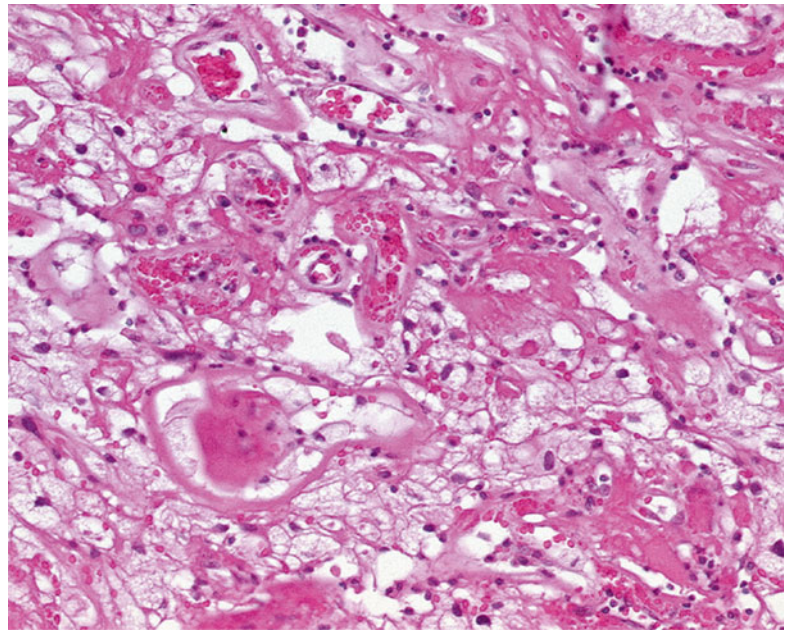

Fig. 9.75 In this larger hemangioblastoma, the vessels are hyalinized and more prominent, as are the surrounding foamy cells (H.E.)

hamartomas that occur mostly isolated but can also be found in association with an oculoneurocutaneous syndrome. In 1928, Hugo Friedrich Kufs described a family affected by cavernous malformations in the brain, retina, and skin and thus defined a novel form of oculoneurocutaneous phacomatosis [84–89]. Retinal cavernous hemangiomas can occur in any retinal location, including in an epipapillary position [90, 91]. They have a violet to red mulberry- or raspberry-like clustered appearance and do not produce intraretinal or subretinal lipid exudation (Figs. 9.79 and 9.80). On fluorescein angiography and optical coherence tomography, the cavernous spaces can easily be detected (Fig. 9.81). There are no feeding vessels present, and they can appear as an intraretinal or preretinal hemorrhage.

Histologically they consist of cavernous thin-walled vascular channels partially filled by a thrombus (Figs. 9.82 and 9.83) and surrounded by a thick basement membrane. There is adjacent reactive gliosis and fibrosis. The cavernous spaces are lined by a vascular endothelium, which can be stained with endothelial cell markers (e.g., CD31) (Fig. 9.84).

Genetics

Cerebral cavernous malformations (CCMs) including retinal cavernous hemangiomas, when associated with an oculoneurocutaneous

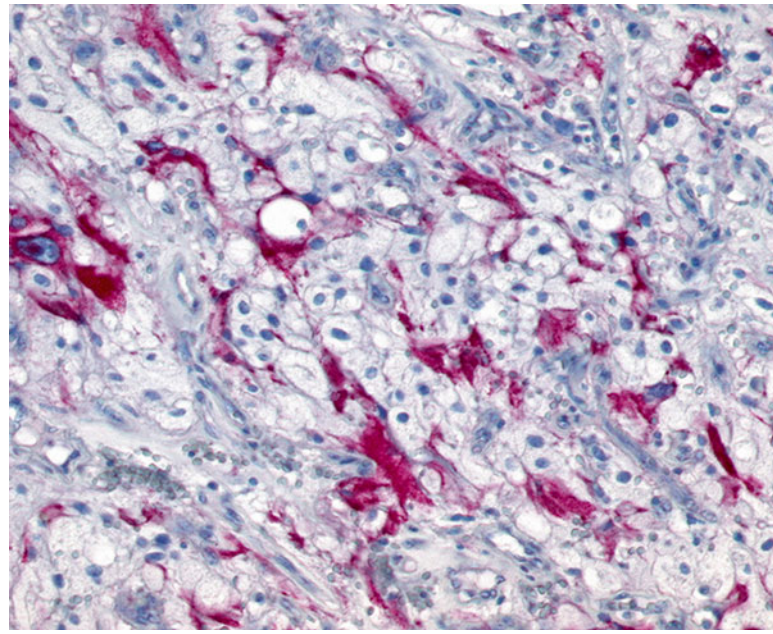

Fig. 9.76 GFAP immunohistochemistry highlights the glial component of the hemangioblastoma

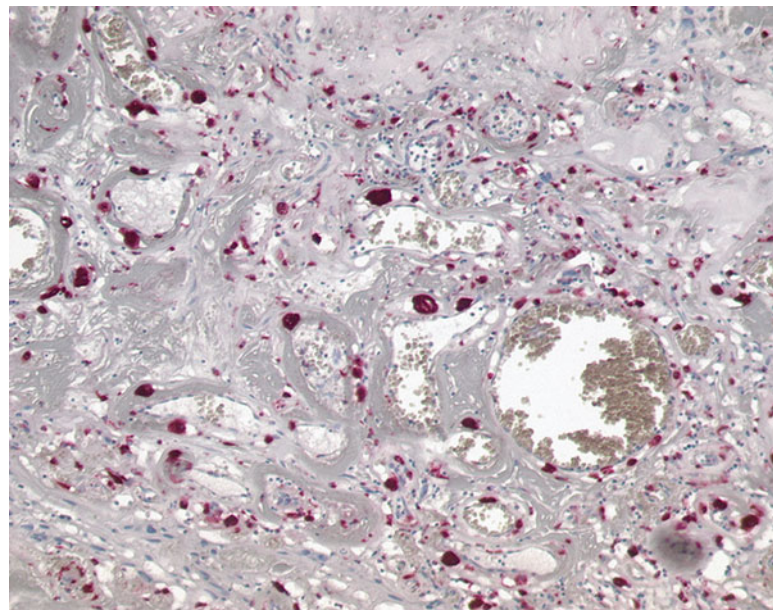

Fig. 9.77 CD68 immunohistochemistry highlights the macrophages in the stroma of the large hemangioblastoma

syndrome, occur predominantly as a consequence of mutations in the genes CCM1 (KRIT1), CCM2, or CCM3 [92–96]. Inherited CCM is characterized by the development of multiple lesions throughout a patient's lifespan that can lead to recurrent cerebral hemorrhages [97–104].

9.9.3 Retinal Arteriovenous (AV) Communication (Retinal Racemose Hemangioma)

Retinal arteriovenous communications although repeatedly referred as retinal racemose hemangiomas are not vascular neoplasms and can occur

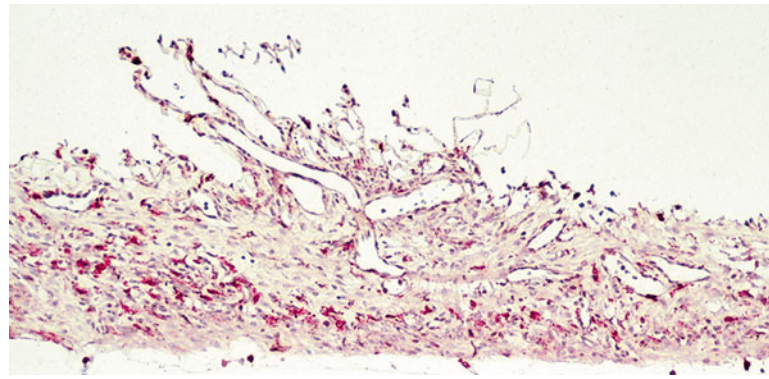

Fig. 9.78 Some of the stromal cells are positively stained with VEGF highlighting the pronounced expression of angiogenic factors in the hemangioblastoma

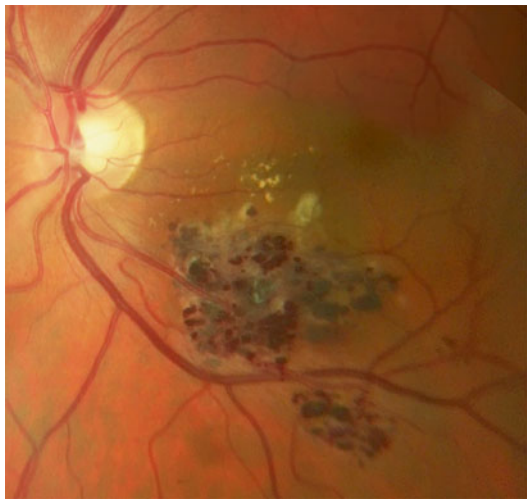

Fig. 9.79 Fundus view of a cavernous retinal hemangioma, with multiple raspberry-like clustered blood-filled caverns

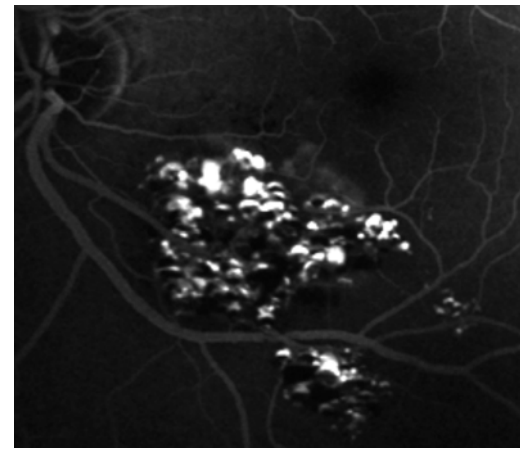

Fig. 9.81 Fluorescein angiography highlights the cavernous spaces. The upper half of the vascular spaces are filled with fluorescein, and the lower contains erythrocyte sedimentation

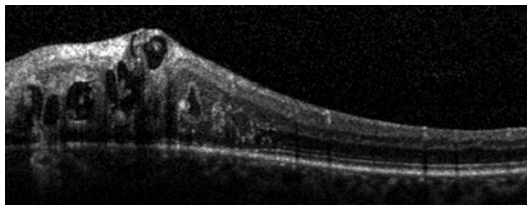

Fig. 9.80 OCT shows that the cavernous spaces occupy all retinal layers

isolated or in association with the Wyburn–Mason syndrome. Since there is no known genetic defect predisposing to these malformations, patients with pathological retinal arteriovenous communications have to be checked for similar AV communications in the central nervous system including the spinal cord, as well as in the orbit and the midface in general (mandible, maxilla, etc.) [105–108]

9.9.4 Vasoproliferative Tumor of the Retina

Vasoproliferative tumors (reactive retinal astrocytic proliferation) of the retina are benign lesions of unknown origin, occurring mostly in otherwise healthy patients between 40 and 60 years of age. They are classified into two types: primary or idiopathic is identified in approximately 75 % of cases and secondary retinal

Fig. 9.82 Epipapillary cavernous hemangioma (H.E.)

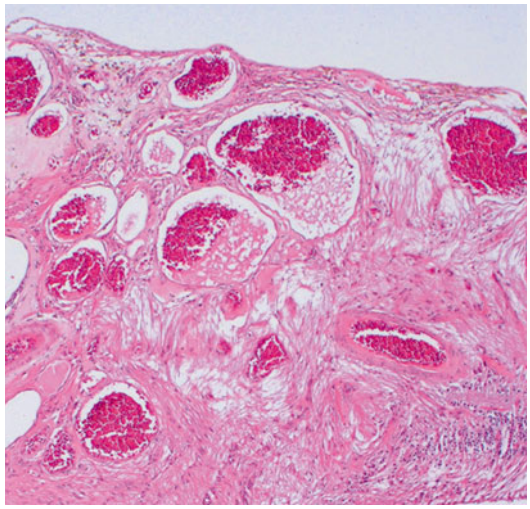

Fig. 9.83 Higher-power image of the epipapillary cavernous hemangioma, showing the erythrocyte sedimentation filling half of the cavernous spaces (H.E.)

vasoproliferative tumors in approximately 25 % of cases [109]. The distinction between the two is based on the presence or absence of other ophthalmic findings such as retinitis pigmentosa, uveitis, Coats' disease, or retinal vasculitis [109–114]. In the presence of these disorders, it is presumed that the vasoproliferative tumors of the retina developed secondary to an inflammatory stimulus associated with the primary condition. A genetic predisposing factor has not been identified yet, although one instance of retinal vasoproliferative tumors occurring in a pair of monozygotic twins has been described [115]. Vasoproliferative tumors of the retina are highly vascularized and usually located at the inferotemporal fundus periphery. On ophthalmoscopy, they have a pink to yellow coloration dependent on the amount of reactive glial tissue present and the amount of lipid and cholesterol deposition in the adjacent retina (Fig. 9.85). They have usually a dome-shaped configuration with a mean largest tumor diameter of 6–7 mm and a tumor thickness of approximately 2–3 mm before they become symptomatic. The presenting symptoms include photopsia, floaters, and visual loss. On ultrasound examination, they are usually highly reflective, and on fluorescein angiography, they display an intense early to late phase hyperfluorescence with late dye leakage (Fig. 9.86). Retinal vasoproliferative tumors can produce visual loss related to cystoid macular edema, tumor exudation and lipid deposition inducing retinal detachment, vitreous hemorrhage, and secondary periretinal membrane formation with retinal distortion. Clinically and histopathologically, primary (idiopathic) vasoproliferative tumors of the retina are indistinguishable from secondary

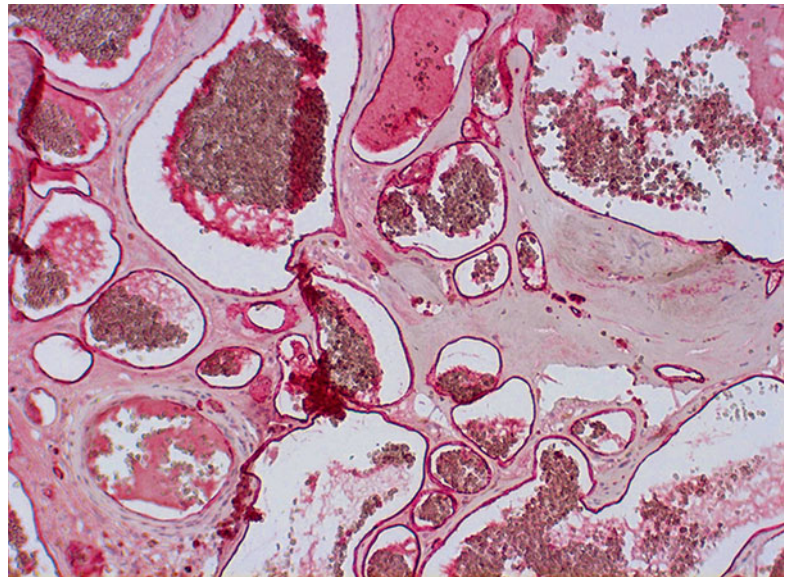

Fig. 9.84 CD31 immunohistochemistry shows the endothelial lining of the cavernous spaces. Moreover the prominent stromal component is highlighted

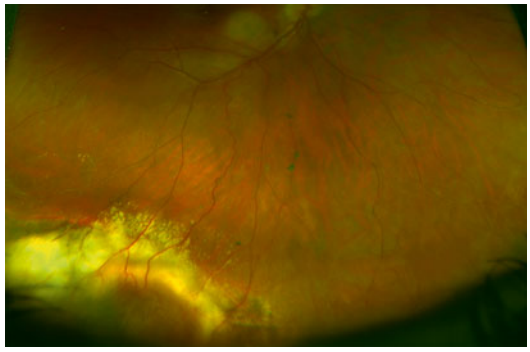

Fig. 9.85 Wide-field fundus view of a peripheral retinal vasoproliferative tumor. The feeding retinal vessels are clearly visible. At the posterior edge of the lesion, typical intra- and subretinal exudation is visible

Fig. 9.86 Fluorescein angiography of the lesion depicted in Fig. 9.85. The feeding and telangiectatic retinal vessels are visible

tumors, although secondary tumors tend to have more often accompanying retinal pigment epithelial alterations.

Histologically retinal vasoproliferative tumors are composed of perfused capillaries surrounded by slender spindle-shaped cells with eosinophilic cytoplasm and small uniform non-pleomorphic nuclei and resemble capillary hemangioblastomas (Fig. 9.87). The spindle-shaped cells are of glial origin and stain positively for GFAP (Fig. 9.88). That is the reason why these tumors have also been classified as reactive retinal astrocytic tumors [116]. The endothelium of the capillary network stains positively for endothelial cell markers such as CD31 and CD34. The small capillaries can be supported by larger dilated blood vessels with hyalinized walls. It is unknown whether the glial proliferation is secondary to a primarily formed vascular network or vice versa. The term "reactionary retinal glioangiosis" has been proposed to describe the prominent gliotic component of these benign tumors. Astroglia of retinal origin can produce a reactive retinal gliosis in various pathological retinal conditions, such as proliferative vitreoretinopathy and both retinal and choroidal inflammatory conditions. Therefore, the glial components of retinal vasoproliferative tumors are probably of retinal origin and most probably reactive in nature [111, 116, 117].

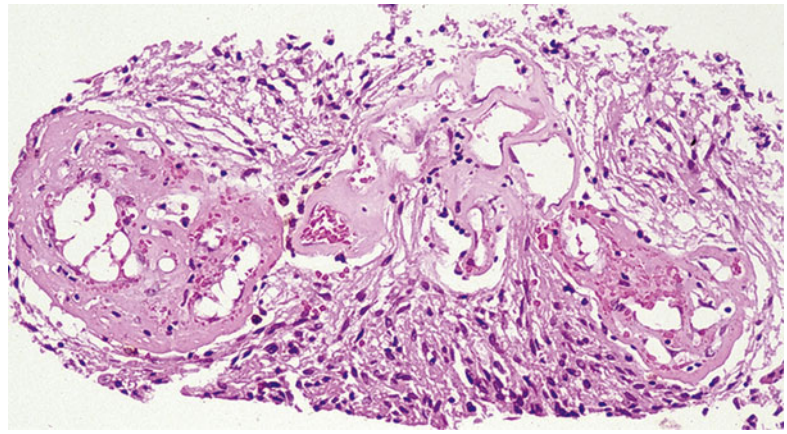

Fig. 9.87 Prominent hyalinized vessels surrounded by reactive gliosis is present (H.E.)

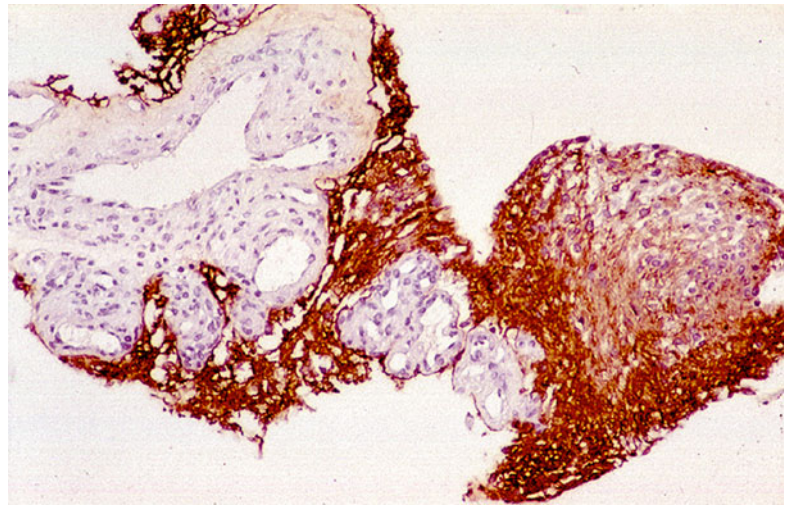

Fig. 9.88 GFAP stain highlights the reactive glial component of the lesion

9.9.5 Retinoblastoma and Retinoma/Retinocytoma

Epidemiology

Retinoblastoma, although a rare tumor, is the most common ocular malignancy in childhood occurring in one in approximately 16,000–20,000 live births. The estimated global annual incidence of retinoblastoma is approximately four per million children under 15 years of age, and it accounts for approximately 3 % of all childhood cancers. It is estimated to be worldwide the most common primary intraocular malignant tumor in all age groups overall, affecting approximately 7,200–8,100 patients on an annual basis, the vast majority being young children [118–120]. There is no sex or race predilection and no significant environmental or socioeconomic predisposing factors have been identified. Most retinoblastomas are diagnosed within the first 3 years of age, and almost all are diagnosed before the age of 5.

Etiology/Genetics

In 1971 Alfred G. Knudson proposed a 2-hit hypothesis in retinoblastoma based on the clinical observations of the biology of the disease (Fig. 9.89) [82]. This hypothesis proved to provide the basis of the genetics of tumor pathogenesis in general, with retinoblastoma serving as the prototypical model. Knudson's hypothesis was confirmed by Friend et al. who cloned the RB1 gene in 1986. Retinoblastoma is caused by

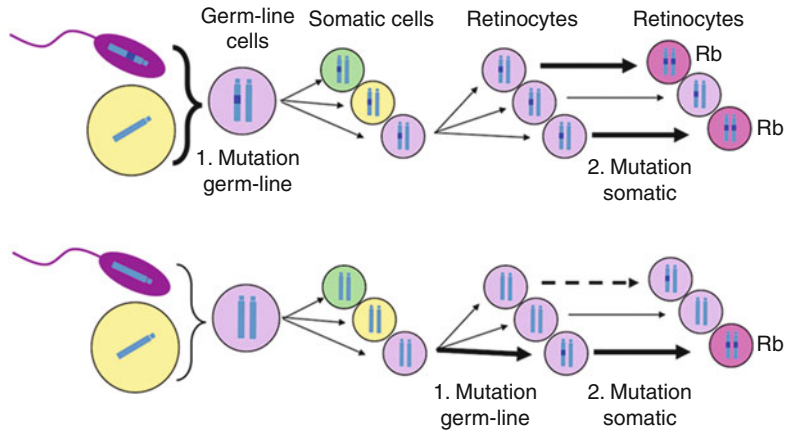

Fig. 9.89 Schematic diagram of Knudson's 2-hit hypothesis. If the first mutation is present in the germ line, all somatic cells already bear one mutant allele. The probability of a second at the somatic stage is high and can occur in several retinoblasts in both eyes but also in other somatic precursor cells. If both mutations occur at the somatic stage, unilateral unifocal retinoblastoma develops

inactivation of both alleles of the RB1 gene, which is located on chromosome 13 within the q14 band region. The RB1 gene encodes for a 110 kDa nuclear phosphoprotein that plays a major role in cell cycle regulation. This protein binds and inhibits transcription factors of the E2F family that are pivotal for the regulation of other genes required for G1/S transition and hence cell cycle progression [121–131].

Localization

Retinoblastoma may occur in any topographic location of the retina, but as a general rule, the younger the individual, the more posterior the location of the tumor. Hence, in older patients the more peripheral and close to the ora serrata are newly developing tumors. Depending on the location of the retinal progenitor cells that carry the mutation, tumors develop in either inner or outer retina.

Classification

Retinoblastoma is classified according to several clinical features and according to the probability of preserving the eye after therapy. In the 1960s Reese and Ellsworth proposed a classification system that could predict the probability of salvaging the eye based on the treatment regimens of that time that included, for a large proportion of patients, primary external beam radiotherapy [132–134]. Today this classification has been revised since primary systemic chemotherapy (chemoreduction) and other consolidating treatment modalities were introduced in the early 1990s. In 2003 the International Retinoblastoma Classification was introduced with a patient staging and an eye grouping, based on a consensus agreement of retinoblastoma experts worldwide taking into account recent treatment developments. The preoperative eye grouping is based on the preoperative assessment of ocular morbidity, whereas tumor staging reflects on the risk the disease poses on the patient's life and well-being (mortality) [135] (Tables 9.5, 9.6, and 9.7).

With regard to the type of tumor growth, several patterns have been described:

Endophytic tumor growth pattern (Fig. 9.90)

When tumors develop in the inner retinal layers, they can give rise to an endophytic tumor. These tumors grow from the retina into the vitreous cavity and can reach a considerable size without causing retinal detachment. With increasing size, endophytic retinoblastomas have a propensity to produce vitreous seeds. These separated tumor nests can fall on neighboring retina producing secondary intraretinal tumors. The vitreous seeds can grow and infiltrate around the vitreous base and zonules as well as extend into the anterior chamber, which can be extremely difficult to detect clinically in early stages of disease. Anterior chamber "inflammation" is an indirect sign for this phenomenon and can be detected as flare, cells, or cellular nodules mimicking granulomatous anterior uveitis on biomicroscopy.

Table 9.5 Differential diagnosis of leukokoria

Diagnosis		Clinical features
Retinoblastoma		Endophytic/exophytic/mixed growth pattern, calcifications, gray-whitish lesions, retinal vascularization penetrates into the tumor, neovascularization
Coat's disease		Retinal detachment, telangiectatic retinal vessels, subretinal cholesterol crystals, yellowish reflex (xanthokoria), affects usually unilateral male patients
Granulomas		Inflammation, retinal detachment, cystic lesion (all features nonspecific)
Congenital cataract		Opacification of the lens
Retrolental fibroplasia	PHPV	Pars plicata villi of ciliary body can be visible, hazy lens, persistent hyaloid artery, persistent tunica vasculosa lentis, retrolental membrane, prominent retinal fold(s)
	ROP	Clinical history of premature birth, retrolental membrane, prominent retinal fold(s)

Table 9.6 Reese–Ellsworth classification

Group	Subgroup	Descriptor	Prognosis
I	Ia	Solitary tumor < 4DD at or behind the equator	Very favorable
	Ib	Multiple tumors, none >4DD, all at or behind the equator	
II	IIa	Solitary tumor 4–10DD at or behind the equator	Favorable
	IIb	Multiple tumors, 4–10DD, behind the equator	
III	IIIa	Any lesion anterior to the equator	Doubtful
	IIIb	Solitary lesion > 10DD behind the equator	
IV	IVa	Multiple tumors, some > 10DD	Unfavorable
	IVb	Any lesion extending anteriorly to the ora serrata	
V	Va	Massive tumors involving over half the retina	Very unfavorable
	Vb	Vitreous seeding	

Table 9.7 International classification of retinoblastoma (ICRB) (grouping of the eye)

Group	Subgroup	Quick reference	Specific features
A	–	Small tumor	Rb size ≤3 mm, located away from the fovea and disk
B	–	Larger tumor	All tumors without tumor dissemination not in group A
		Macula	
		Juxtapapillary	Rb size >3 mm or
		Subretinal fluid	Rb location ≤3 mm from foveola
			≤1,5 mm from the optic disk
			Clear subretinal fluid ≤3 mm from tumor margin
C		Focal seeds	Local tumor dissemination
	C1		Subretinal seeds ≤3 mm from Rb
	C2		Vitreous seeds ≤3 mm from Rb
	C3		Subretinal and vitreous seeds ≤3 mm from Rb
D		Diffuse seeds	Diffuse tumor dissemination
	D1		Subretinal seeds > 3 mm from Rb
	D2		Vitreous seeds >3 mm from Rb
	D3		Subretinal and vitreous seeds > 3 mm from Rb
E	–	Extensive Rb	Unsalvageable eyes
			Tumor occupying >50 % of globe volume or
			neovascular glaucoma
			Opaque media from hemorrhage in anterior chamber, vitreous, or subretinal space
			Invasion of postlaminar optic nerve, choroid >2 mm, sclera, orbit, anterior chamber

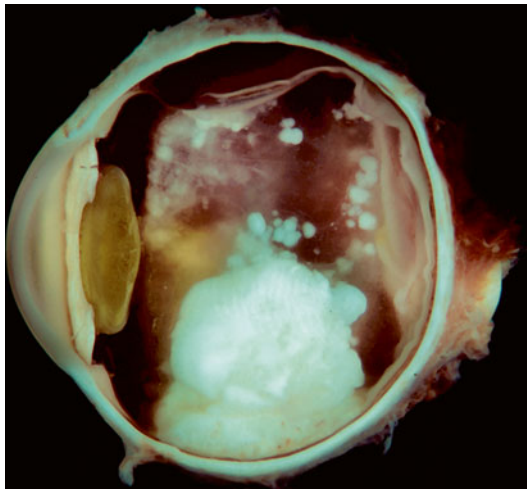

Fig. 9.90 Macroscopic appearance of an endophytic retinoblastoma with vitreous seeds

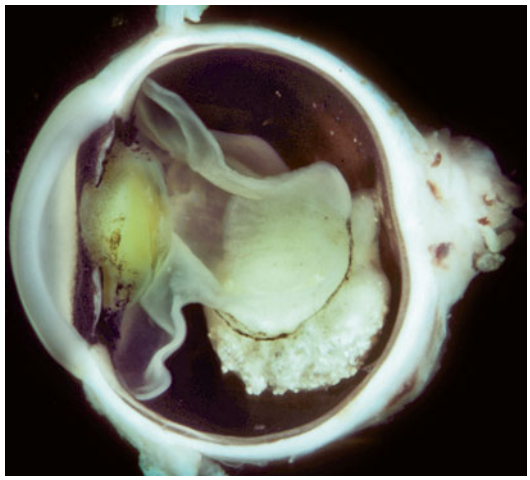

Fig. 9.91 Macroscopic appearance of an exophytic retinoblastoma with retinal detachment

Exophytic tumor growth pattern (Fig. 9.91)

When tumors develop in the outer retina cell layers, they can give rise to an exophytic tumor, i.e., a tumor that grows from the retina towards the choroid. As these tumors grow in size, they produce retinal detachment that surrounds the tumor. With increasing size, subretinal seeds may separate from the primary tumor in the subretinal space and embed on the RPE. These tumor nodules can infiltrate underneath the RPE and are nourished by the oxygen supply of the choriocapillaris. In a later stage, they can infiltrate through Bruch's membrane into the choroid and towards the sclera.

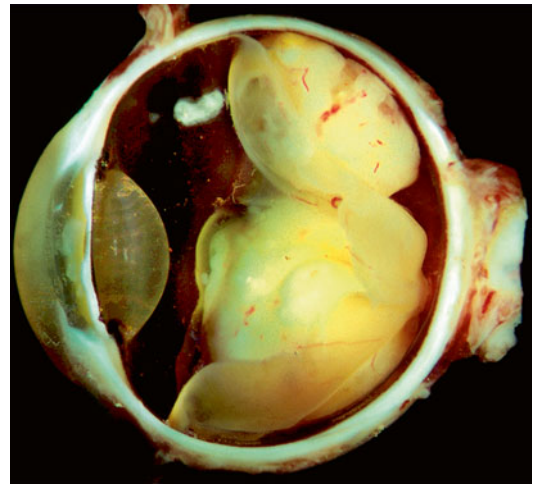

Fig. 9.92 Macroscopic appearance of a combined endophytic/exophytic retinoblastoma

Combined endophytic/exophytic tumor growth pattern (Fig. 9.92)

The majority of advanced retinoblastomas that are enucleated and undergo histopathological examination exhibit a combined endophytic/exophytic growth pattern, where one component may be more pronounced than the other. The presence or extent of additional features such as vitreous, anterior chamber, choroidal, optic nerve, or extrascleral infiltration is clinically more important and requires meticulous histopathological evaluation since these features may have important clinical implications.

Diffuse infiltrative tumor growth pattern

On rare occasions, retinoblastoma can manifest as a diffuse tumor without the apparent evidence of a visible tumor mass. These tumors usually originate from the anterior preequatorial part of the retina close to the vitreous base at the ora serrata and therefore are not easily detectable with conventional ophthalmoscopy. These obscured tumors occur more often in somewhat older children (≥7 years of age) or young adults. Anterior chamber infiltration is common and can be the presenting finding, mimicking an anterior

Fig. 9.93 Cystic vitreous seeds at the vitreous base over the pars plana and pars plicata of the ciliary body. The seeds exhibit an inner necrosis due to oxygen deprivation and become cystic. The cystic seeds can be encountered also in the anterior chamber (H.E.)

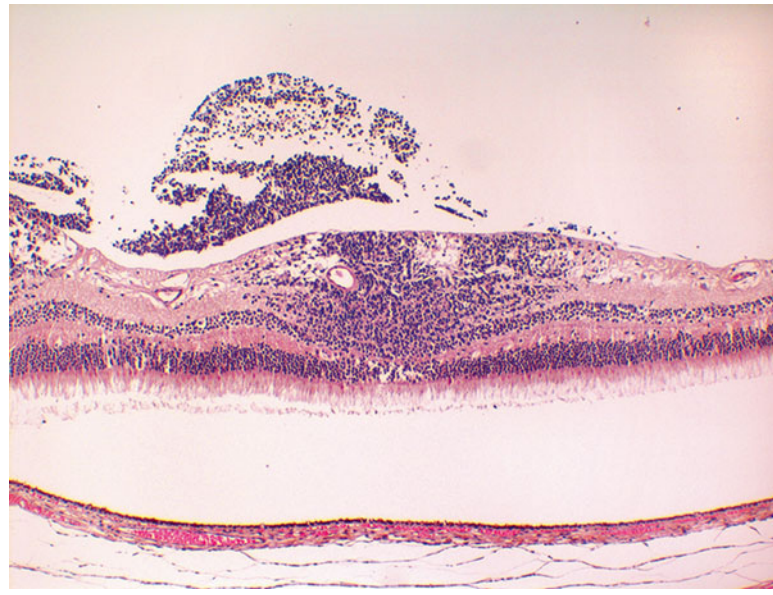

Fig. 9.94 Infiltration of the inner retina, possibly after gravitational embedding of a cystic vitreous seed. Its remaining inner third can be detected just above the retina (H.E.)

(infectious or autoimmune granulomatous) inflammatory process.

Vitreous infiltration (Figs. 9.93 and 9.94)

Especially in case of endophytic retinoblastoma, the probability of vitreous infiltration by nests of retinoblastoma cells ("vitreous seeds") is increased. This finding is of special relevance in the clinical management of these tumors, since it can be very subtle in early stages and yet require more aggressive treatment strategies to achieve sustainable tumor control. Vitreous seeds can undergo gravitational embedding in neighboring retinal areas and produce secondary retinal infiltrates but also infiltrate into the anterior parts of the eye. The extent of vitreous seeds is of importance in the retinoblastoma classifications systems (see Table 9.7).

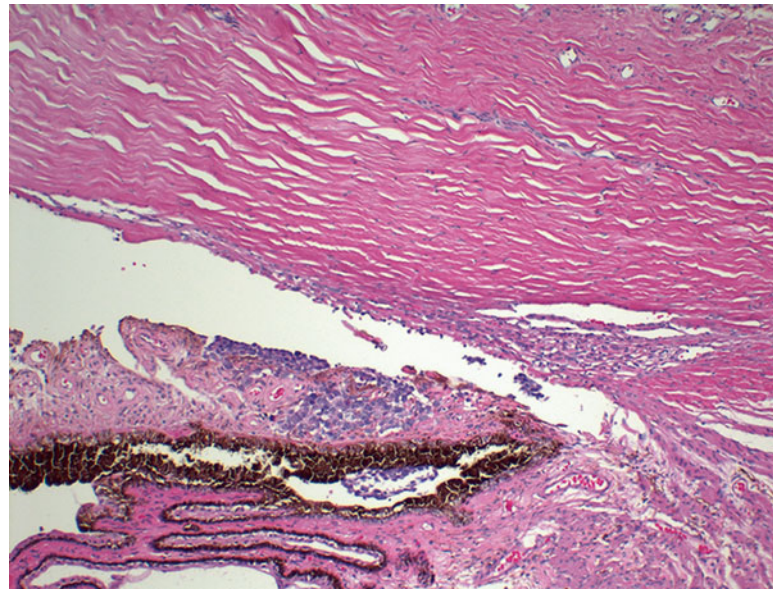

Fig. 9.95 Retinoblastoma cells can seed into the anterior chamber and infiltrate into the iris and the trabecular meshwork, causing secondary glaucoma (H.E.)

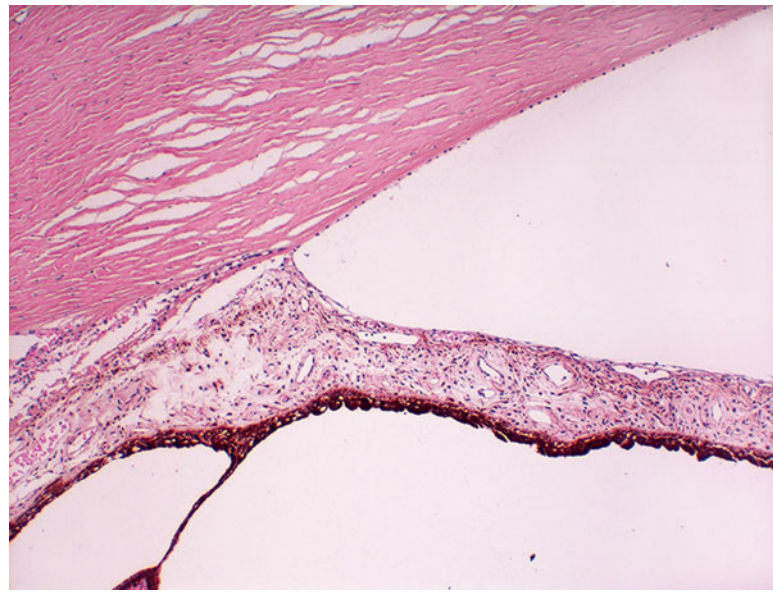

Fig. 9.96 Secondary glaucoma can be caused also by chamber angle occlusion, endothelial downgrowth, and iris and chamber angle neovascularization (H.E.)

Anterior chamber infiltration (Figs. 9.95 and 9.96)

Especially in retinoblastoma originating from more anterior parts of the retina (more often in older children), the tumor can infiltrate into the anterior chamber of the eye. The tumor usually causes secondary glaucoma with or without iris and chamber angle neovascularization and can manifest as an anterior granulomatous uveitis or an aseptic endophthalmitis with a pseudohypopyon. Alternatively retinoblastoma nests and cysts can float in the anterior chamber simulating parasitic infections or an anterior chamber manifestation of medulloepithelioma of the ciliary body epithelium.

Choroidal infiltration

Especially exophytic retinoblastomas have a propensity to infiltrate the choroid. The initiating step is dispersion of subretinal seeds on the surface of the RPE with subsequent infiltration

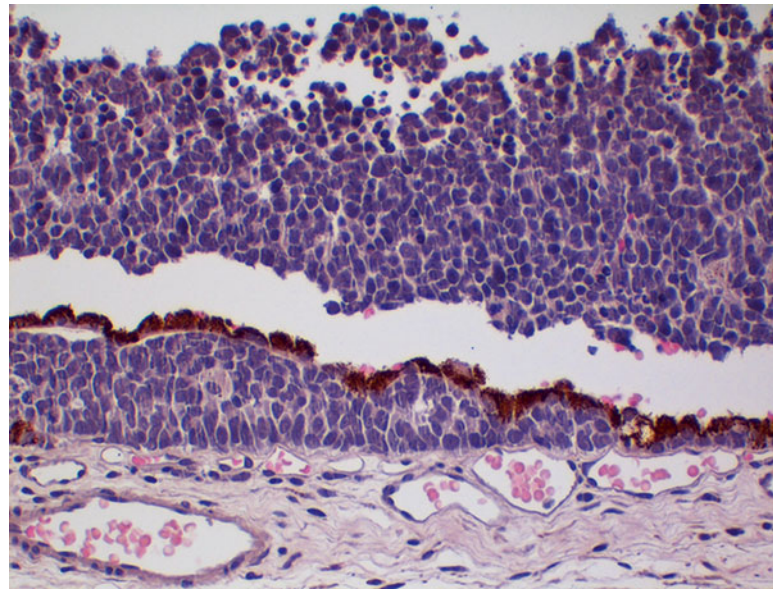

Fig. 9.97 When vitreous seeds fall onto the RPE layer, the first step of choroidal infiltration is sub-RPE infiltration. Bruch's membrane is a strong barrier for further infiltration. Note that the choriocapillaris is free of infiltration (H.E.)

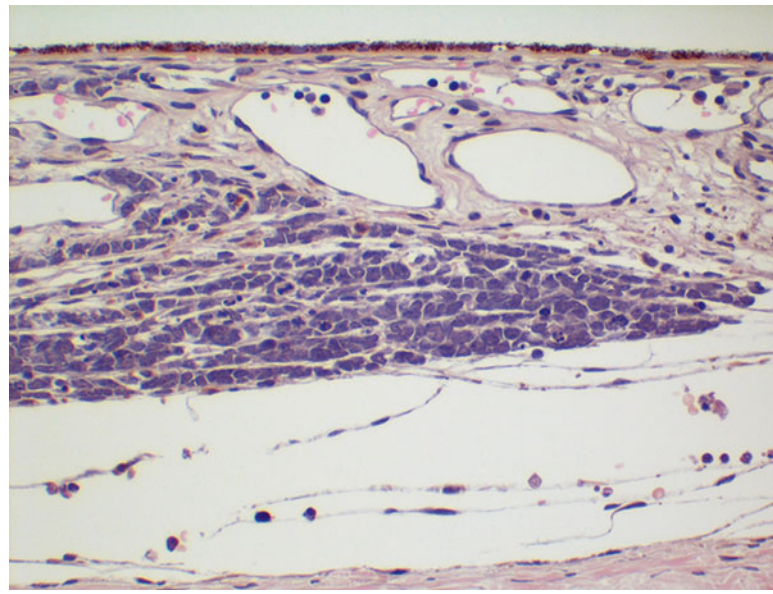

Fig. 9.98 Early choroidal infiltration. The tumor does not reach the sclera, and the infiltration is less that 3 mm in thickness (H.E.)

under the RPE (Fig. 9.97). When these tumor nodules enlarge, they can invade Bruch's membrane and infiltrate into the choriocapillaris. Early choroidal involvement is followed by deeper choroidal infiltration throughout all layers up to the innermost scleral lamellae (Fig. 9.98). Retinoblastoma infiltrating deeper layers of the choroid and the innermost scleral lamellae cells can be compressed resembling reactive lymphocytes (Fig. 9.99). The extent of choroidal infiltration is of importance in the retinoblastoma classifications systems. Most authors agree that with increasing choroidal infiltration, the probability of tumor metastasis increased. However, until recently there was considerable uncertainty as to what amounted to significant or massive choroidal infiltration. During a consensus meeting

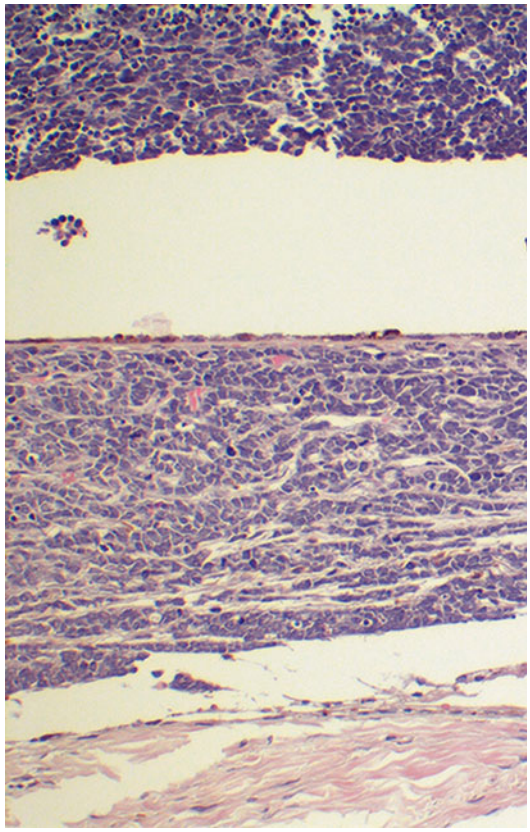

Fig. 9.99 Advanced choroidal infiltration. The tumor has infiltrated the entire choroid and has reached the innermost scleral lamellae (H.E.)

of the International Retinoblastoma Staging Working Group in 2009, it was agreed that massive or significant choroidal infiltration occurs when choroidal infiltration is ≥3 mm in either horizontal or vertical dimension and is reaching the inner scleral fibers. Any choroidal infiltration <3 mm in any dimension is considered to be focal or minimal.

Extrascleral extension

Extrascleral infiltration is a prognostically dismal factor in the assessment of retinoblastoma and is seen in advanced stages of the disease rarely encountered in Europe or North America. The presence of extrascleral extension defines stage pT4 in the TNM and stage E in the ICRB classification systems (see Table 9.7) (Fig. 9.100).

Optic nerve infiltration

Retinoblastomas located at the posterior pole close to the optic disk have a propensity to invade the optic nerve. Early/prelaminar infiltration is present when tumor infiltration stops at the lamina cribrosa of the optic nerve (Fig. 9.101). When the lamina cribrosa is infiltrated, it is defined as laminar infiltration (Fig. 9.102). Infiltration in deeper layers of the optic nerve beyond the "barrier" of lamina cribrosa is defined as postlaminar infiltration

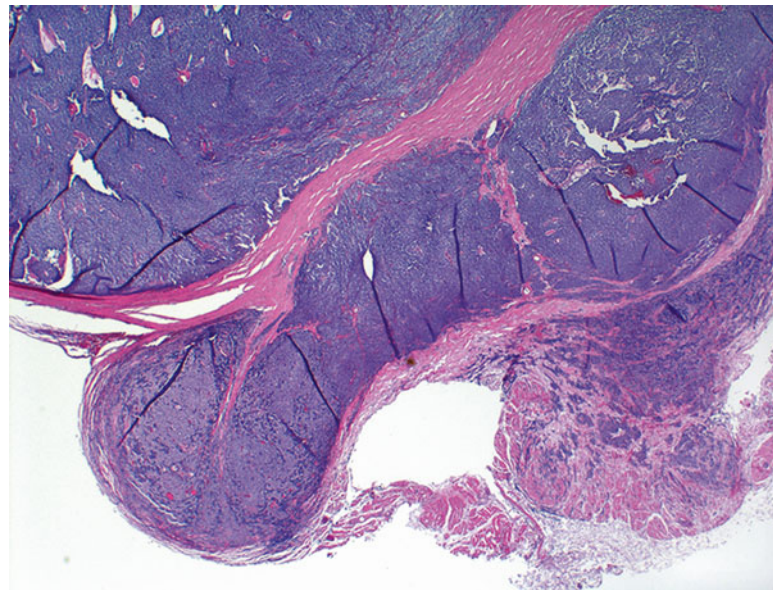

Fig. 9.100 Extrascleral growth of retinoblastoma. The tumor has penetrated the sclera and is infiltrating the orbit and the inferior oblique muscle that can be seen at the *lower right* (H.E., G. Willerding, Berlin, Germany)

(Fig. 9.103). The extent of postlaminar infiltration should be recorded as it defines the stage of the tumor (Table 9.7) and may have clinical implications in the postoperative course and treatment of the patient. In the case of deep optic nerve infiltration, it is of paramount importance to ascertain whether the tumor has been completely or incompletely excised at the transected end of the optic nerve. Reactive astrocyte proliferation within the optic nerve can be misleading and give the false impression of tumor invasion.

Fig. 9.101 Prelaminar optic nerve infiltration. The tumor does not penetrate into the lamina cribrosa that is depicted in this micrograph with an artifactual cleft within the optic nerve (H.E.)

Clinical Features

Approximately 60 % of all retinoblastoma cases are unilateral (sporadic nonheritable), and 40 % of cases are bilateral. Unilateral (sporadic nonheritable) cases are usually diagnosed after the first year of life (in the average between 18 and 24 months of age) and are caused by two somatic mutations. In contrast, bilateral and multifocal retinoblastomas are usually diagnosed half a year earlier, before or around the first birthday (in the average between 3 and 18 months of age), and are always caused by an early germ line mutation with an additional somatic mutation occurring later on during development. The germ line mutation can be either inherited (familial) by one or both parents or can be a new mutation (sporadic heritable). Retinoblastoma secondary to a germ line mutation regardless being familial or spo-

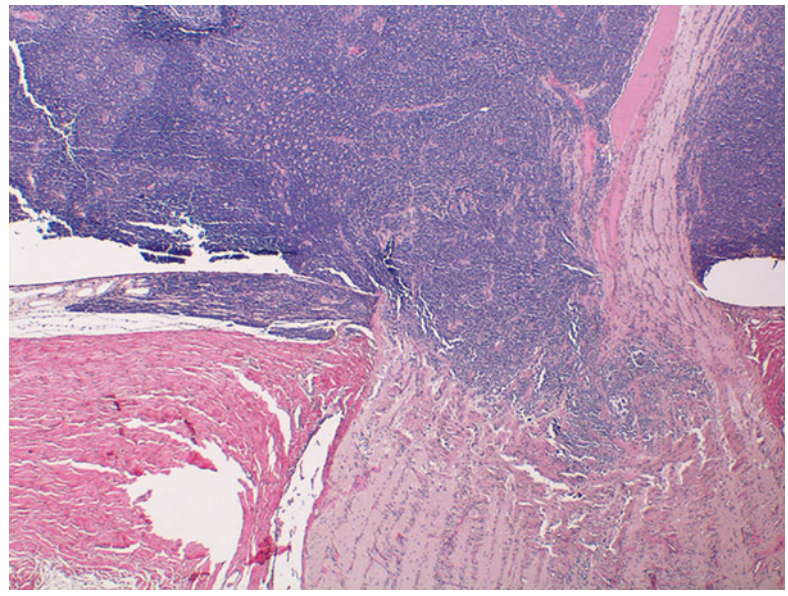

Fig. 9.102 Intralaminar and subtle postlaminar infiltration of the optic nerve (H.E.)

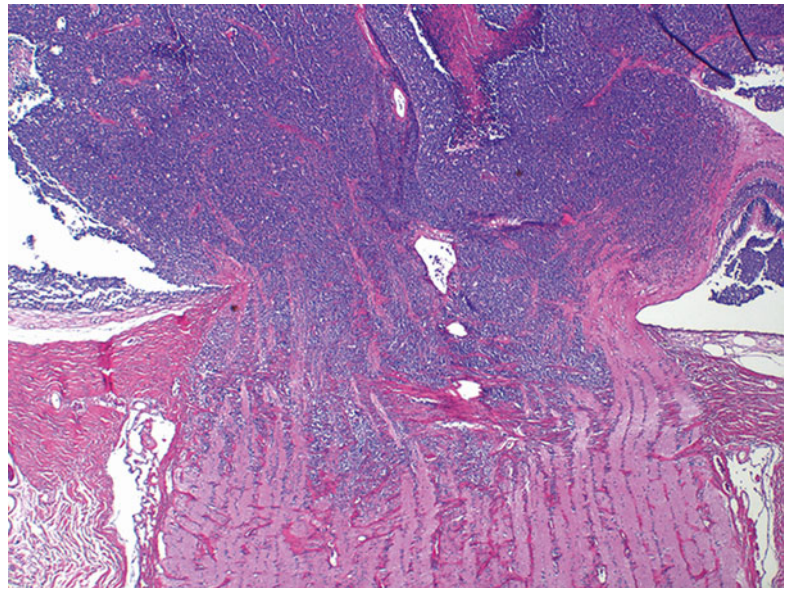

Fig. 9.103 Postlaminar infiltration of the optic nerve (H.E.)

radic can be passed on to the offspring of patients in approximately 50 % of cases [136].

Patients with a germ line mutation have a mutant allele in all somatic cells throughout the body and hence are at a significant risk for developing other non-ocular tumors, either secondary to the treatment of the primary retinoblastoma or independently. This risk increases throughout the lifespan and is associated with the exposure to further mutagenic instances such as radiation or chemotherapy [137, 138].

In rare occasions patients with a germ line mutation can develop "trilateral" retinoblastoma. The majority of these midline intracranial tumors are primitive neuroectodermal pineoblastomas, which resemble histopathologically retinoblastomas, having however more frequently Homer–Wright rosettes [139].

Presenting signs for retinoblastoma can be leukokoria, strabismus, and unspecific "inflammatory" signs of children's eyes. Leukokoria, which is present initially in approximately 60 % of retinoblastoma cases, is a late presenting sign associated with a poorer prognosis for eye preservation, since the tumor needs to acquire considerable size to produce an easily detectable white pupillary reflex. Strabismus is the second most common presenting sign in retinoblastoma being present in approximately 20 % of patients. In the remainder of cases, retinoblastoma presents with atypical and nonspecific signs such as redness and inflammation of the eye, "watering" and/or enlarged eye mimicking congenital tear duct obstruction, or even congenital glaucoma with buphthalmos [140]. Leukokoria (λευκοκορία: Greek for white pupil/pupillary reflex) is the most common presenting sign in patients with retinoblastoma. Leukokoria is an ophthalmological sign where the pupil has a whitish rather than black appearance. It is caused by an abnormal light reflex originating from behind the pupil that can be either caused by a whitish cataract, retropupillary or retrolental membranes, a prominent retinal detachment, and neoplastic or nonneoplastic whitish reflecting tumors of the fundus of the eye. The differential diagnosis of leukokoria includes congenital cataract, persistent hyperplastic primary vitreous (PHPV), Coat's disease (which however presents most commonly with a "xanthokoria" – yellowish reflex – rather than a white reflex), retrolental fibroplasia most commonly secondary to retinopathy of prematurity (ROP), nonneoplastic granulomas (most commonly of parasitic nature, i.e., cysticercosis), neoplastic retinal disease (benign: astrocytoma, malignant: retinoblastoma), or even myelinated nerve fibers of the retina [141–143] (Table 9.5).

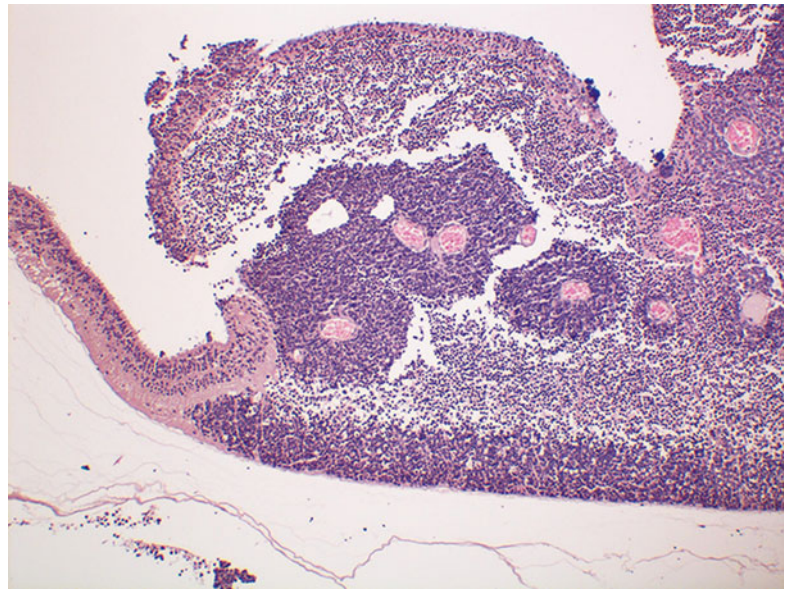

Fig. 9.104 Cuff-like arrangement of viable tumor cells around blood vessels. The tumor cuffs have a radius of approximately 100 μm, which represents the distance to the most remote tumor cell that can still be nourished by oxygenation provided by the central core vessel. Widespread ischemic necrosis with amorphous eosinophilic and basophilic material around these cuff-like clusters is a common feature (H.E.)

Survival is largely depending on the presenting stage of the patient. In some less developed areas of the world (Latin America/Africa/Asia), survival rates of less than 50 % have been reported. On the contrary in unilateral cases treated in Europe and the USA, the prognosis for survival is >95 % after enucleation of the affected eye. The last century has taught us that early diagnosis and adequate treatment are paramount for the survival of the patient [135, 136, 144–148].

Macroscopy

The macroscopic features of retinoblastomas are dependent on the clinical features of the tumor, i.e., endophytic, exophytic, mixed tumor growth pattern, infiltration into adjacent structures, etc. The tumor itself has a heterogeneous whitish-pink to gray coloration, depending on the extent of calcification and necrosis. Calcification is a common feature of retinoblastoma and appears in small clumps that have a bright whitish well-defined appearance. If calcification is very prominent, immersion of the globe in a decalcification solution for 24 hours is advisable. In larger tumors prominent necrosis and hemorrhages can be present, resulting in a darker grayish appearance. Before processing the globe, the optic nerve stump should be measured and the proximal part of it cut off and processed separately, for evaluation of tumor clearance at the surgical resection line.

Histopathology

Microscopy

Retinoblastomas are highly cellular and composed of small cells with hyperchromatic nuclei. These are rapidly growing tumors that can outgrow their blood supply. Cytologically retinoblastoma cells have round to oval nuclei with fine granular chromatin and usually no obvious nucleolus (Fig. 9.108). The cytoplasm and the cellular borders are poorly defined. They have only scarce supporting stroma, and necrosis is a common feature. On low magnification, a circular arrangement of clusters of tumor cells around a central supporting arteriole is a common feature. These ring or cuff-like arrangement of viable tumor cells around blood vessels has been described as “pseudorosettes” (Fig. 9.104). The tumor cuffs around the blood vessels have a radius of approximately 100 μm, which represents the distance to the most remote tumor cell that can still be nourished by oxygenation provided by the central core vessel. Widespread ischemic necrosis around these cuff-like clusters is a common feature; these areas contain amorphous eosinophilic and basophilic material. The

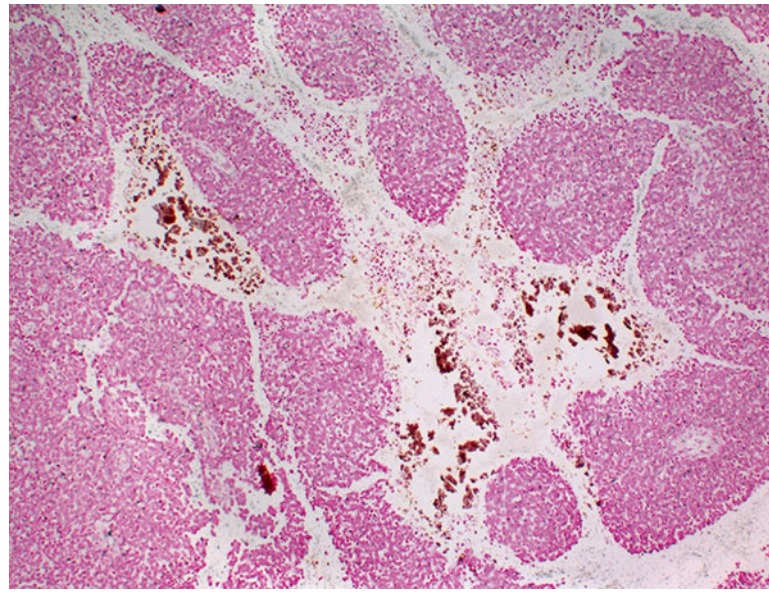

Fig. 9.105 Von Kossa stain highlights the dystrophic calcification in areas of hypoxic tumor cell necrosis

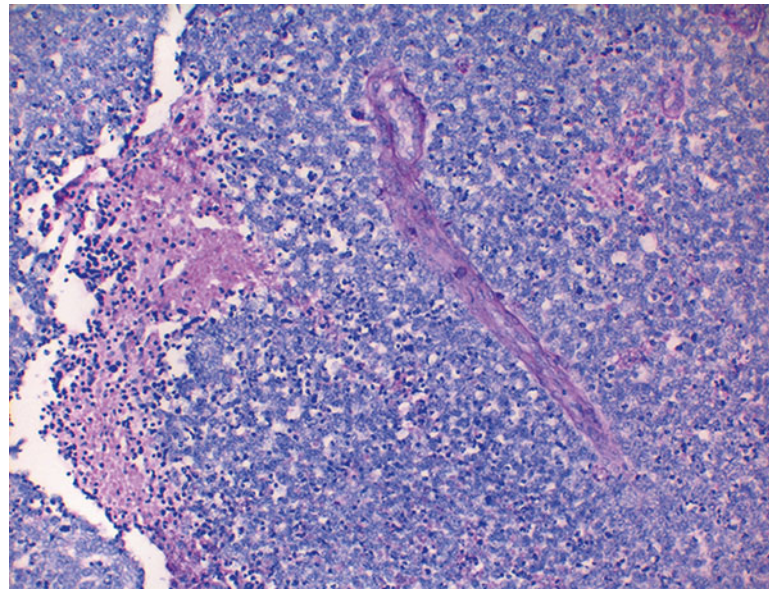

Fig. 9.106 PAS stain highlights the basophilic precipitation of DNA in the walls of tumor supporting blood vessels

basophilic deposits represent calcium salts (dystrophic calcification), secondary to the massive amounts of karyolysis (Fig. 9.105). These calcium deposits initially occur within the mitochondrial membrane, and with progressive necrotic liquefaction of tumor cells, larger calcified structures develop and deposition of basophilic DNA in the walls of tumor supporting blood vessels, the inner limiting membrane of intact retina, and anterior segment (Figs. 9.106 and 9.107). These deposits can be found lining the lens capsule, the iris vessels, and the trabecular meshwork, possibly accounting for some secondary glaucoma which in retinoblastoma patients is not necessarily associated with neovascularization [149].

Retinoblastomas originate from retinoblasts and can show varying degrees of cellular differentiation. Tumor cells can be arranged in such a way to resemble photoreceptor differentiation:

- "Fleurettes" are tumor cell clusters with the presence of the myoid and ellipsoid of the inner and outer photoreceptor segments arranged in semicircular to oval groups resembling a flower bouquet (or a heraldic fleur-de-lys). These more seldom encountered arrangements are more benign appearing and exhibit a higher degree of photoreceptor differentiation (Fig. 9.108).

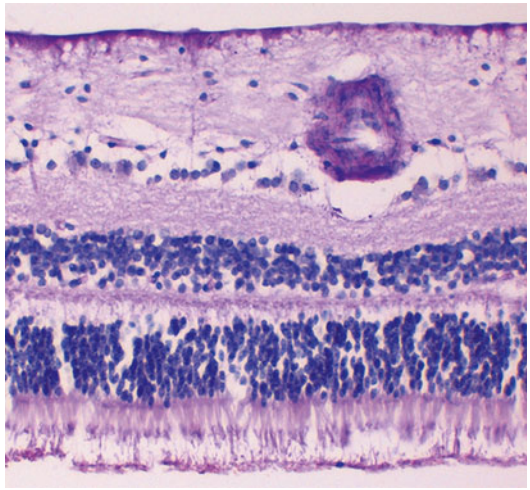

Fig. 9.107 PAS stain highlights the basophilic precipitation of DNA in the walls of normal retinal blood vessels and the internal limiting membrane towards the vitreous cavity

- "Flexner–Wintersteiner rosettes" are circular cellular arrangements of usually one cell row, apparently lined internally by a continuous circular "membrane," analogous to the outer limiting membrane of the retina. The rosette lumen has a diameter of approximately 1–2 retinoblastoma cell nuclei (10–60 μm) and never contains a blood vessel. The lumen is usually optically empty or contains loose eosinophilic fibrillar material that can stain positively for acid mucopolysaccharides (Fig. 9.109).
- "Homer–Wright rosettes" are circular multilayered arrangements surrounding eosinophilic fibrillar material. The cells send out neurofibrillary processes that fill the center of the rosette. A central lumen of the rosette as seen in Flexner–Wintersteiner rosettes is absent. Since Homer–Wright rosettes are also commonly found in a variety of neuroblastic tumors, they are less specific for retinoblastomas (Fig. 9.110).

All these fleurette- and rosette-like arrangements of tumor cells represent the aberrant attempt of the tumor to form photoreceptor cells and to arrange them in a fashion analogous to that seen in the developing retina. The more of these arrangements present within a tumor, the more cytologically differentiated the tumor.

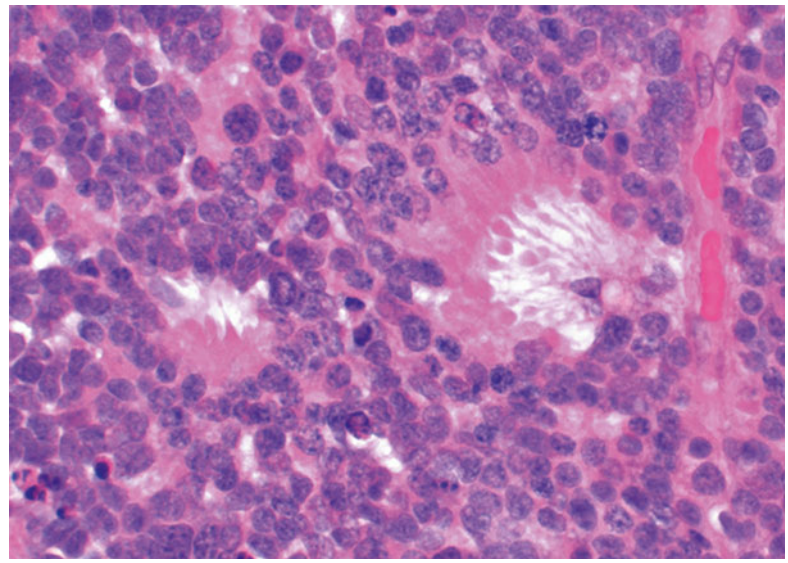

Fig. 9.108 Two "fleurettes" are present resembling a flower bouquet (or a heraldic fleur-de-lys). They are tumor cell clusters with the presence of the myoid and ellipsoid of the inner and outer photoreceptor segments arranged in semicircular to oval groups (H.E.)

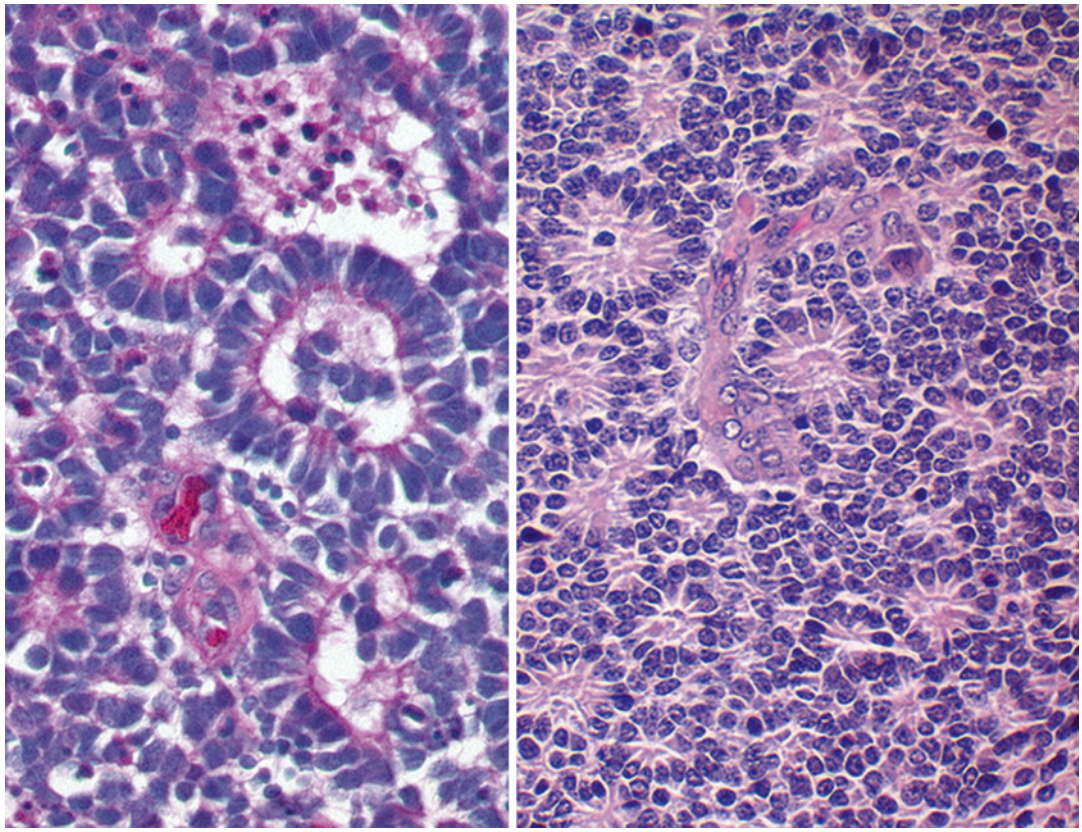

Fig. 9.109 "Flexner–Wintersteiner rosettes" that have circular cellular arrangements of usually one cell row (*right insert*) but can also be multilayered (*left insert*). They are lined internally by a continuous circular membrane, analogous to the outer limiting membrane of the retina and contain a central lumen (H.E.)

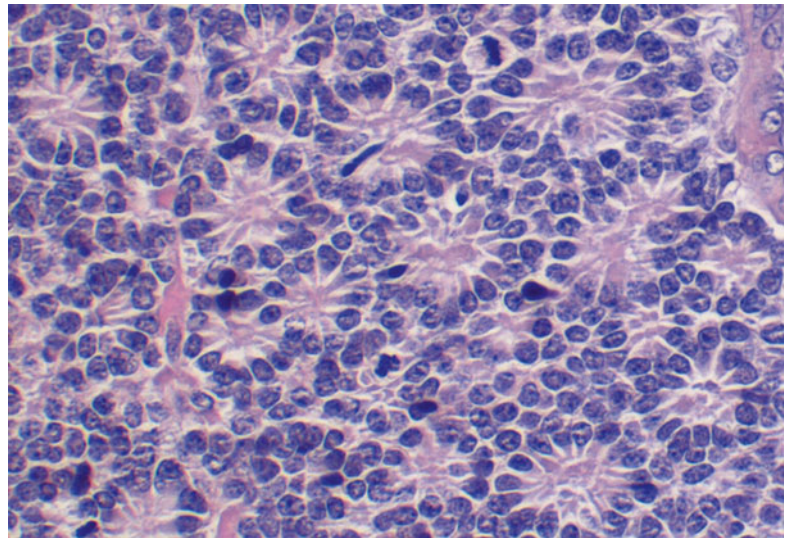

Fig. 9.110 "Homer–Wright rosettes" are circular multilayered arrangements surrounding eosinophilic fibrillar material, without a clear central lumen (H.E.)

Retinoblastomas can also be poorly differentiated, being composed of randomly arranged cells. Usually poorly differentiated parts of the tumor are located more distant to unaffected retina, suggesting a later developmental stage of the tumor. Most retinoblastomas exhibit a mixed differentiation pattern, containing parts of rosetted growth located closer to the tumor base and usually undifferentiated areas located predominantly on the tumor apex. The grade of histological differentiation can be reported as well, moderately, poorly, and undifferentiated (G1–G4).

Mitoses are a common feature in both differentiated and undifferentiated retinoblastoma and can be found also in the rosette formations.

Immunohistochemistry

Immunohistochemically retinoblastomas show positive staining for neuron-specific enolase (NSE), bcl-2, and synaptophysin. Anti-GFAP labeling is generally limited to the reactive glial cells including perivascular glial cells, if present.

Tumor reactions after treatment

Clinically four types of tumor regression have been described after retinoblastoma treatment [149]. These descriptions are primarily based on the clinically observed regression after external beam radiotherapy but are also relevant to the changes seen after chemotherapy and other treatment modalities:

Type I regression (cottage cheese type)

Clinically there is a rapid regression, and the tumor has the typical appearance of cottage cheese, i.e., sharp demarcated white clumps of calcified tissue that can be easily detected due to their ultrahigh reflectivity on ultrasound examination. Histologically this regression type represents complete necrosis with calcification. A loose framework of glial tissue can surround the calcium deposits.

Type II regression (fish flesh type)

The tumor loses its pinkish coloration and vascularity and takes a "fluffy" gray-whitish appearance. A clear distinction between viable and necrotic tissue is challenging both clinically and histologically. Mitoses can still be present, and the proliferation markers (Ki67/PCNA) can show a significant number of positive cells.

Type III regression (mixed cottage cheese type and fish flesh type):

This regression type is characterized clinically and histologically by a mixture of both type I and type II regressions. Calcification and necrosis are present along with "viable"-looking tumor tissue.

Type IV regression (compete tumor regression):

Clinically and histologically, this regression type is characterized by a flat chorioretinal scar and the presence of gliosis.

Tumor Sampling/Artifactual Seeding

Fresh tumor as well as whole blood should be sampled before fixation in all cases for genetic analysis and future counseling of patients and parents. Unfixed retinoblastoma has a milky/viscous consistency and will cause artifactual tumor contamination to the cut surface of adjacent structures of the eye as well as the instruments used for preparation, even when the unfixed globe is trephined at a distant site of the tumor and sampled through the trephination site. Alternatively the unfixed globe can be opened with a very sharp blade conventionally to such an extent that an adequate tumor sample can be harvested. Another way proposed but not advocated by the author is the aspiration of tumor by using a 22-gauge needle through the sclera posteriorly to the lens according to a slightly oblique anteroposterior course under visual control. If these preparations are performed in the operating theater by the surgeon, meticulous care has to be taken not to contaminate the surgical field. The pathologist has to take into account the possibility of contamination artifacts when reporting the histopathology (artifactual seeding). Artifactual seeding is typically composed of small tumor clusters that have irregular borders and that are detached from any naturally expanding or infiltrating tumor borders and are often located within loose cavities of the ocular anatomy, such as the loose choroidal stroma, the detached suprachoroidal space, anterior chamber, subarachnoid space, or even on the outside surface of the eye. Due to the very loose consistency of retinoblastoma, it is generally contraindicated to perform a surgical biopsy in these eyes, due to the high risk

Table 9.8 International classification of retinoblastoma (ICRB) (staging of the patient)

Stage		Substage	Descriptor	Comments
0			Intraocular tumor only	No evidence of regional or metastatic disease; patient may not have had an enucleation
I			Tumor completely removed by enucleation	Retinoblastoma may be present in the non-enucleated eye. High-risk pathology may be present in the enucleated specimen
II			Residual orbital tumor	Microscopic tumor present in the optic nerve at the site of surgical resection (cut end of nerve)
III		(a) Overt orbital extension (b) Preauricular or cervical lymph node extension	Overt regional disease	Orbital or node involvement diagnosed by clinically by neuroimaging
IV	(a) Hematogenous metastasis without CNS disease	1. Single lesion 2. Multiple lesions	Metastatic disease	
	(b) CNS disease	1. Prechiasmatic lesion 2. CNS mass 3. Leptomeningeal disease		

of contaminating the surgical field with viable tumor cells and postoperative uncontrolled tumor recurrence.

Prognostic Factors

High-risk features for metastatic disease include tumor invasion into the anterior chamber, significant (massive) invasion into the choroid of at least 3 mm in any diameter reaching the sclera, postlaminar optic nerve invasion, or a combination of any minimal (focal) choroidal invasion into the choroid of less than 3 mm with any degree of prelaminar or laminar optic nerve invasion. Adjunctive post-enucleation chemotherapy has been proven to be beneficial in preventing metastasis in a significant proportion of patients having the abovementioned high-risk features [150–157].

Standardization of Histopathological Examination

The International Retinoblastoma Staging Working Group has established, during a consensus meeting, pathology guidelines for the examination of enucleated eyes and evaluation of prognostic parameters in retinoblastoma [154]. These guidelines provide guidance on adequate tissue processing, definitions of histological risk factors, and reporting of enucleated eyes with retinoblastoma to serve as the basis for clinical trials (see tumor sampling). The enucleated eyes should be examined by submitting a total of four blocks. The main block contains the central pupil–optic nerve plane, also including the bulk of the tumor (PO block). The PO block should be sectioned in a way to include the optic nerve head, lamina cribrosa, and postlaminar optic nerve in a single plane of section, facilitating adequate evaluation of the extent of optic nerve infiltration. Two additional blocks should contain the remainder of the ocular tissue after having sectioned the PO block (calottes). The fourth block should contain the cross section of the surgical margin of the optic nerve, obtained before opening the eye (Tables 9.6, 9.7, 9.8 and 9.9).

9.9.6 Retinoma (Retinocytoma)

Retinoma or retinocytoma is the benign variant of retinoblastoma and may be encountered as a "forme fruste" of retinoblastoma in relatives of retinoblastoma patients. Clinically, retinomas share characteristics of type 2/3 regression of retinoblastomas after treatment. There may be partial calcification, and vascularization is not a prominent feature [158–162]. Histopathologically,

Table 9.9 Pathologic TNM classification

Primary tumor (pT)	
pTX	Primary tumor cannot be assessed
pT0	No evidence of primary tumor
pT1	Tumor confined to the eye without choroidal or optic nerve invasion
pT2	Tumor with minimal choroidal[a] and/or optic nerve invasion
pT2a	Focal choroidal invasion[a] or prelaminar optic nerve invasion
pT2b	Focal choroidal invasion[a] and prelaminar optic nerve invasion
pT3	Tumor with significant choroidal and/or optic nerve invasion[b]
pT3a	Tumor with massive choroidal[b] or postlaminar but surgically cleared optic nerve invasion
pT3b	Tumor with massive choroidal[b] and postlaminar but surgically cleared optic nerve invasion
pT4	Tumor invades optic nerve to resection line or has extraocular extension elsewhere
pT4a	Tumor invades optic nerve to resection line, but without extraocular extension elsewhere
pT4b	Tumor invades optic nerve to resection line and has extraocular extension elsewhere
Regional lymph nodes (pN)	
pNX	Regional lymph nodes cannot be assessed
pN0	No regional lymph nodes involvement
pN1	Regional lymph nodes involvement (preauricular, cervical)
pN2	Distant lymph nodes involvement
Metastasis (pM)	
cM0	No metastasis
pM1	Metastasis to sites other than CNS
pM1a	Single lesion
pM1b	Multiple lesions
pM1c	CNS metastasis
pM1d	Discrete mass(es) without leptomeningeal and/or CSF involvement
pM1e	Leptomeningeal and/or CSF involvement

[a]Minimal/focal choroidal invasion: choroidal invasion less than 3 mm in any diameter and not reaching the sclera
[b]Significant/massive choroidal invasion: choroidal invasion measures 3 mm or more in any diameter reaching the inner scleral fibers

they are highly differentiated and do not have cytological features of malignancy [163].

9.9.7 Tumors of the Retinal Pigment Epithelium

The retinal pigment epithelium (RPE) is a hexagonal, cuboidal-shaped epithelial monolayer, lying in the interface between the retina and the choroid. Its basement membrane on its outer side forms the inner layer of Bruch's membrane. The rod and cone outer segments are embedded on its inner apical side and are continuously shed into the RPE cytoplasm before undergoing metabolic degradation. RPE cells have a high metabolic rate and a remarkably high reactive/metaplastic capacity, whereas their malignant neoplastic potential is extremely low. The RPE is generally considered in humans an essentially postmitotic cell, without the capability of "restitutio ad integrum," i.e., the ability to healing without scar formation. On the contrary, healing processes in RPE cells generally result in a scar between the outer retina and the underlying tissues that compromises outer retinal function. These reactive processes include atrophy, hypertrophy, hyperplasia, migration, and metaplasia of RPE cells, either alone or in combination. The pigment content of the RPE is mainly responsible for the coloration and the ophthalmoscopic appearance of the fundus of the eye; thus, RPE changes can be detected clinically quite early. More subtle changes have been recently detected clinically by means of fundus autofluorescence and optic coherence tomography (OCT).

9.9.7.1 Simple Hamartoma of the Retinal Pigment Epithelium

Simple hamartoma of the retinal pigment epithelium is a congenital lesion of misplaced RPE within the retina during embryogenesis, which can even protrude through the internal limiting membrane on the retinal surface (Fig. 9.111). Since optical coherence tomography (OCT) is available, their intramacular and epimacular location can be demonstrated morphologically (Fig. 9.112). The lesions are small (<1 mm in diameter and thickness), sharply demarcated, and mostly located in the macular region, usually causing amblyopia, since they are congenital (dependent on their exact location). Throughout life, they can produce a pigmented macular distortion (pigmented macular pucker) [164–167].

9.9.7.2 Combined Hamartoma of the Retina and Retinal Pigment Epithelium

Combined hamartoma of the retina and the retinal pigment epithelium is a congenital lesion, which comprises a combined malformation of the retina and the RPE with a prominent vascular component [168–174]. The lesions are usually located in close proximity to the optic nerve or at the posterior pole but can be also located more anteriorly. Clinically they appear as poorly demarcated gray to brown lesions that can be confused with a uveal lesion such as a melanoma, although on close examination they do not affect the choroid (Fig. 9.113).

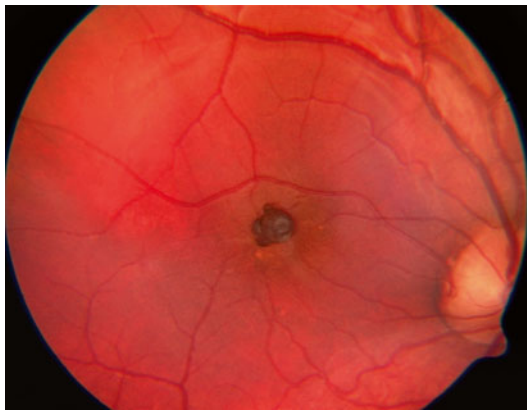

Fig. 9.111 Fundus view of a simple RPE hamartoma located in the foveola, causing severe amblyopia. There is a small mushroom-shaped avascular deeply pigmented lesion protruding through the retina and over the level of the internal limiting membrane. Note the pinpoint RPE atrophy in the foveal region close to the hamartoma nasally and inferiorly

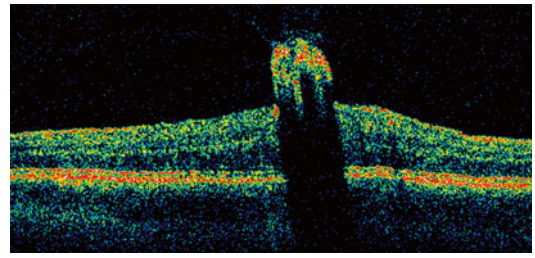

Fig. 9.112 OCT image of the lesion of Fig. 9.111 showing the mushroom-shaped deeply pigmented lesion causing complete signal reflectivity. The vitreous is attached to the apex of the lesion

Fig. 9.113 Fundus view of a combined hamartoma of the retina and the RPE. The lesion is overgrowing the retinal vessels and the optic disk and has a diffuse yellow-gray to brown color and causes retinal surface distortion

Although the lesions contain abnormal telangiectatic vessels, unlike Coats' disease they do not produce exudation, nor do they cause exudative retinal detachment. This is particularly intriguing since on fluorescein angiography, pronounced telangiectasia and late leakage are a constant clinical finding (Figs. 9.114 and 9.115). Macular distortion with epiretinal membrane formation is however a feature, and membrane peeling via vitrectomy has been proposed in such cases by some investigators. Severe amblyopia may be, however, the main limiting factor in

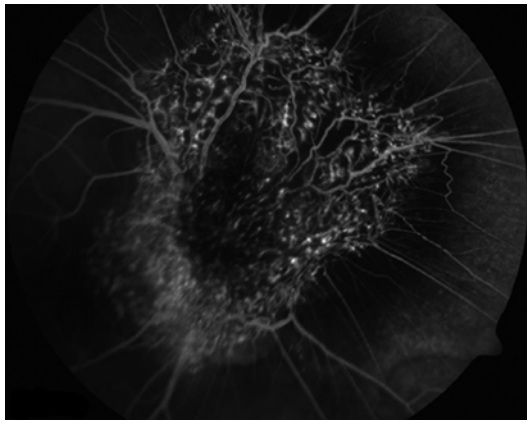

Fig. 9.114 Early arterial phase fluorescein angiography shows abundant telangiectatic vessels within the lesion

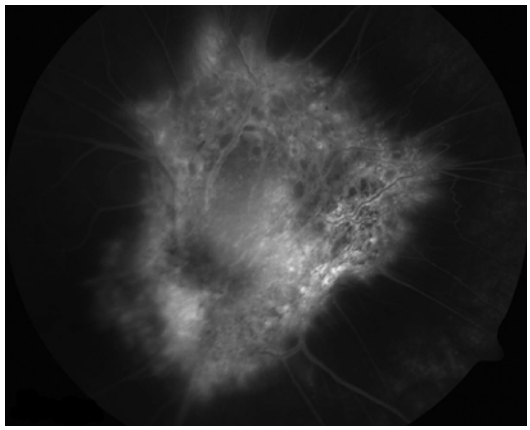

Fig. 9.115 Late venous phase fluorescein angiography shows intense tumor late hyperfluorescence and leakage

achieving a good visual outcome [175–177]. Combined hamartomas of the retina and the retinal pigment epithelium have been associated with neurofibromatosis type II, in contradistinction to neurofibromatosis type I that is associated with retinal astrocytomas, choroidal nevi, and optic nerve gliomas.

Neurofibromatosis type II (NF II) is caused by a mutation in the NF2 gene on chromosome 22, which encodes for Merlin (also called neurofibromin 2 or schwannomin). This protein links actin filaments to cell membranes and is thus important in cell movement. Individuals with NF II develop symmetric, benign tumors. Acoustic neuromas and combined hamartomas of the retina and the retinal pigment epithelium are a feature of this disease.

9.9.7.3 Congenital Hypertrophy of the Retinal Pigment Epithelium (CHRPE)

Congenital hypertrophy of the RPE (CHRPE) can be found as a solitary lesion or as grouped pigmentary abnormalities (bear tracks). Solitary CHRPE has quite typical characteristics. In the early stages the lesions have a jet-black appearance due to their densely packed, large, round melanin granules within the hypertrophic RPE cells and they are completely flat, being composed of a cellular monolayer (Fig. 9.116). Typically they are surrounded by a thin clearly visible depigmented line, which by itself is commonly surrounded by a slightly hyperpigmented band that diffusely blends into the normal fundus coloration (Fig. 9.117). During their evolution, CHRPE lesions become gradually depigmented when atrophic RPE lacunae appear within the black lesion. The lacunae become large and eventually coalesce to produce a completely depigmented lesion. Histopathologically there is RPE hypertrophy with large melanin granules in areas of hyperpigmentation and RPE atrophy in areas of depigmentation. The retina overlying CHRPE lesions shows partial atrophy. In rare instances CHRPE lesions can become thickened due to cellular hyperplasia. These hyperplastic parts of the CHRPE lesions can be due to migration of RPE cells from areas of lacunar atrophy (Fig. 9.118). In cases with three or more CHRPE lesions with hyperplastic features, Gardner syndrome and familial adenomatous polyposis (FAP) have to be considered. They are both caused by an APC gene mutation, and in the case of patients with grouped CHRPE lesions, precancerous colonic polyps may be present, and these can be treated during colonoscopic screening, before colorectal carcinoma develops [178–182].

9.9.7.4 Reactive Hyperplasia of the Retinal Pigment Epithelium

In most instances RPE reactive hyperplasia is due to direct or indirect trauma to the RPE, by means

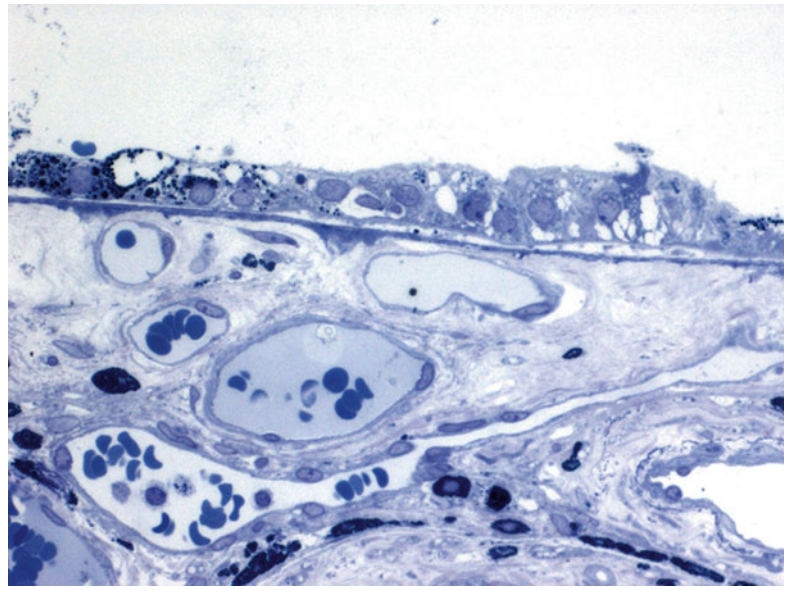

Fig. 9.116 Cellular monolayer of hypertrophic RPE cells. On the left side, there is hyperpigmentation, whereas in the center and on the right side there is depigmentation (semithin section, toloidine blue, A. Parsons, Sheffield, G. Britain)

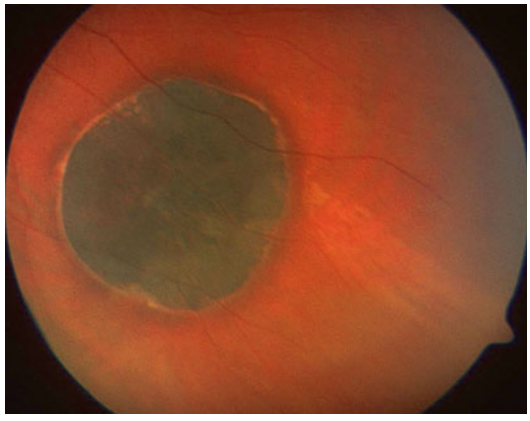

Fig. 9.117 Fundus view of a typical CHRPE lesion. Note the lesion is surrounded by a thin clearly visible depigmented line, which by itself is surrounded by a slightly hyperpigmented band that diffusely goes over to the normal fundus coloration. The overlying retinal vessels appear unremarkable, and there is a discrete segmental RPE atrophy peripheral to the lesion (*lower right*)

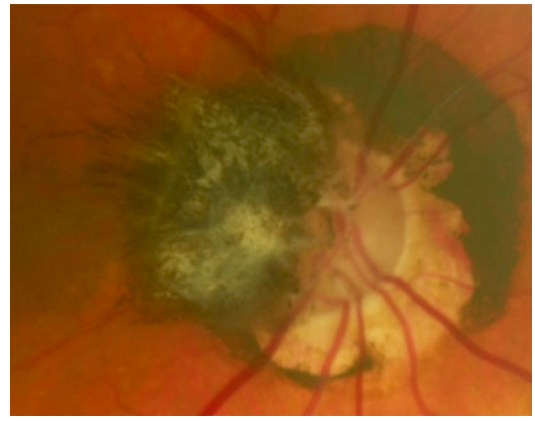

Fig. 9.118 Fundus view of a peripapillary CHRPE lesion with RPE hyperplasia at the temporal margin of the CHRPE. Note the deep glaucomatous excavation and the depigmented RPE lacunae

of either accidental or surgical injury or other infectious, inflammatory, or degenerative eye diseases (laser scar, toxoplasmosis scar, retinitis pigmentosa, etc.). RPE hyperplasia can also be encountered within CHRPE lesions, especially at their margins with adjacent atrophic lacunae within the CHRPE lesions (Figs. 9.118 and 9.119).

9.9.8 RPE Adenoma

RPE adenomas are very rare benign tumors that can have divergent and heterogeneous pigmentation. They are composed of oval, hexagonal to round cells with small nuclei, without prominent nucleoli, and with abundant granularly pigmented cytoplasm. Cells can be vacuolated, and the tumors can display an adenoid-glandular morphological organization (Figs. 9.120 and 9.121) [183–186].

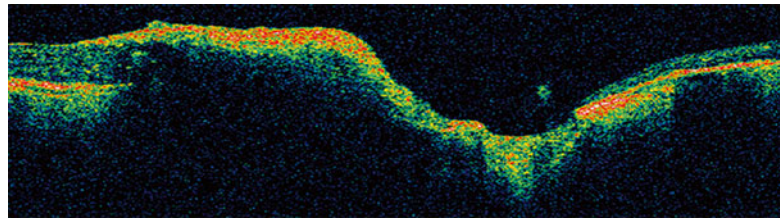

Fig. 9.119 OCT image of lesion Fig. 9.118. Note the high reflectivity on the left (temporally) of the lesion depicting the epiretinal RPE hyperplasia

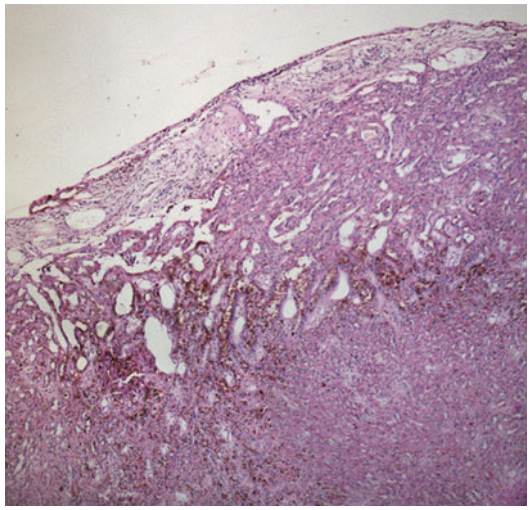

Fig. 9.120 RPE adenoma exhibiting heterogeneous pigmentation and adenoid-glandular morphological structure (H.E., D. Wilson, Portland, USA)

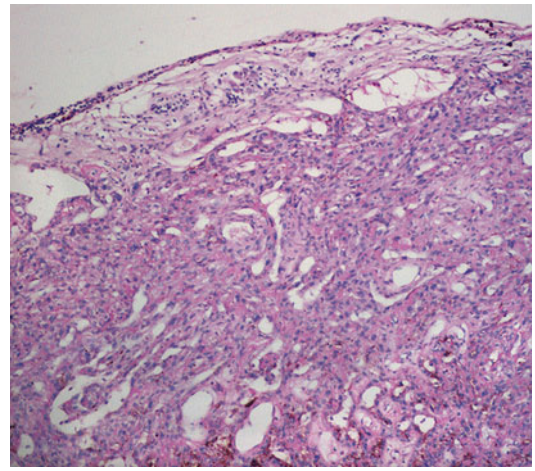

Fig. 9.121 Higher-power view of Fig. 9.120 showing that the tumor is composed of oval cells with small nuclei, without prominent nucleoli. The tumor is moderately vacuolated with a glandular structure (H.E., D. Wilson, Portland, USA)

9.9.9 Adenocarcinoma of the Retinal Pigment Epithelium

The distinction between RPE adenoma and RPE adenocarcinoma is dependent on the typical cytological characteristics implying malignancy, such as pleomorphism, increased mitoses, and proliferation rate, as detected by immunohistochemistry. From the diagnostic point of view, it is important to clearly differentiate between an extremely rare RPE adenocarcinoma, which is a primary tumor of the RPE, and a metastatic adenocarcinoma that is located in the choroid and may or may not have invaded into the RPE. The later metastatic tumors are much more common and can arise from any adenocarcinoma of the body. From the clinical point of view, most RPE adenocarcinomas arise from the edge of a CHRPE lesion that contains some hyperplastic components, thus making these patients eligible for occasional follow-up (Fig. 9.122). Most of RPE adenocarcinomas have prominent retinal feeder vessels, which is an important clinical diagnostic feature (Fig. 9.123, 9.124 and 9.125) [186–192].

9.9.10 Metastatic Tumors to the Retina

Retinal metastasis from systemic malignancies is an especially rare phenomenon.

Leukemia as well as anemia can present with intraretinal dot and blot hemorrhages with or without a central fibrin clot (hemorrhagic infarction). These typical white-centered retinal hemorrhages are named Roth spots (Fig. 9.126). The white-centered retinal hemorrhages are identified as a nonspecific sign caused by the rupture of retinal capillaries, probably followed by the

Fig. 9.122 RPE adenocarcinomas arising from the marginal zone of a CHRPE lesion that contains some depigmented lacunae. The RPE adenocarcinoma has prominent retinal feeder vessels

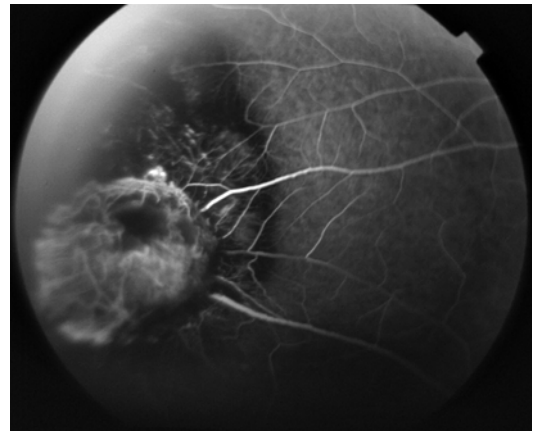

Fig. 9.123 Fluorescein angiography of the lesion Fig. 9.122. The feeder vessels are clearly visible, as well as the intrinsic vascularization of the RPE adenocarcinoma. The base of the tumor within the CHRPE lesion is also partially vascularized, implying the underlying presence of an RPE hyperplasia

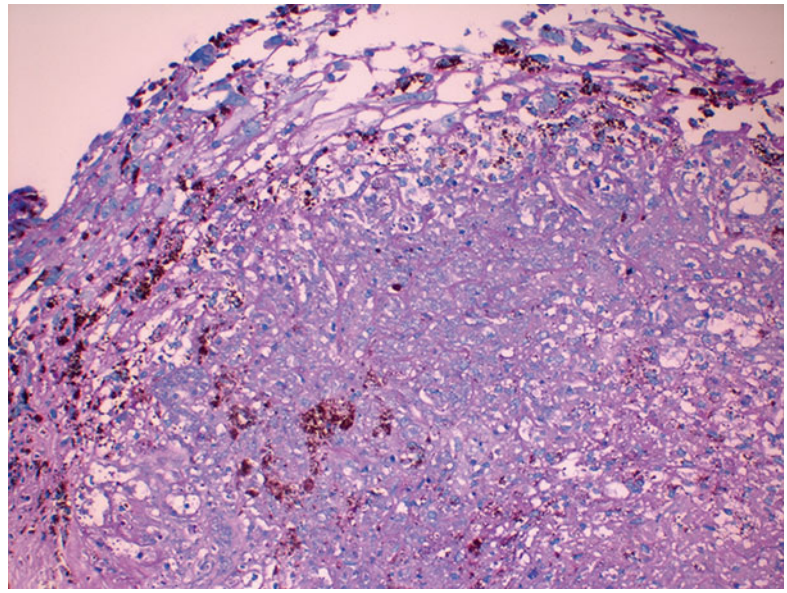

Fig. 9.124 Adenocarcinoma of the RPE. The tumor is composed of sheets of cells separated by reticular connective tissue. Heterogeneous sheetlike pigmentation and partial vacuolization are present in some areas of the tumor (PAS, A. Moulin, Lausanne, Switzerland)

aggregation of fibrin and platelets. Nevertheless, the pathophysiologic explanation for these capillary occlusions and hemorrhages is poorly understood and may be related to endothelial ischemia. This can be secondary to anemia, direct occlusion by leukemic cells, endothelial damage by circulating microorganisms such as bacteria or fungi, and other factors. The white-centered hemorrhages are found especially in the inner retinal layers, as can be demonstrated by optic coherence tomography (Fig. 9.127) [193–197].

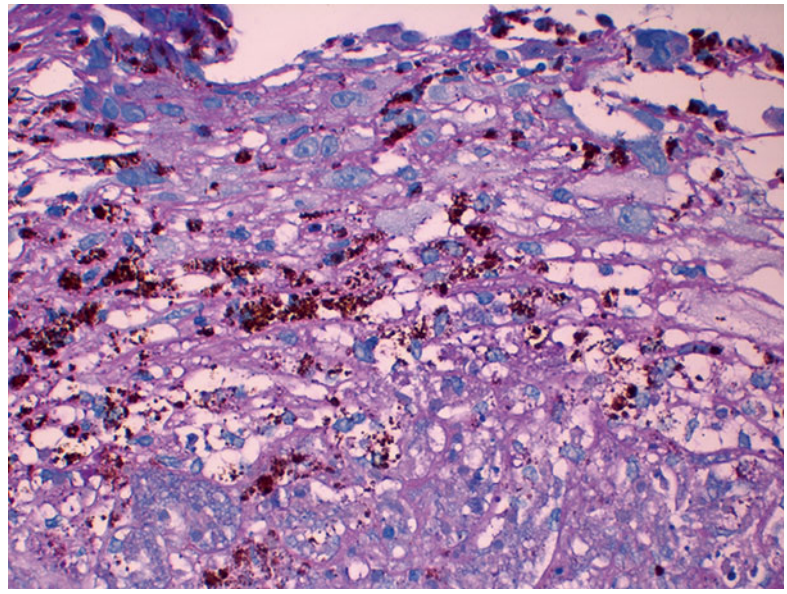

Fig. 9.125 Adenocarcinoma of the RPE: on higher magnification of Fig. 9.124, a fine reticular network of basement membrane-like material surrounding cells with moderate nuclear pleomorphism and prominent nucleoli is present. Some cells contain heavy granular pigmentation (PAS, A. Moulin, Lausanne, Switzerland)

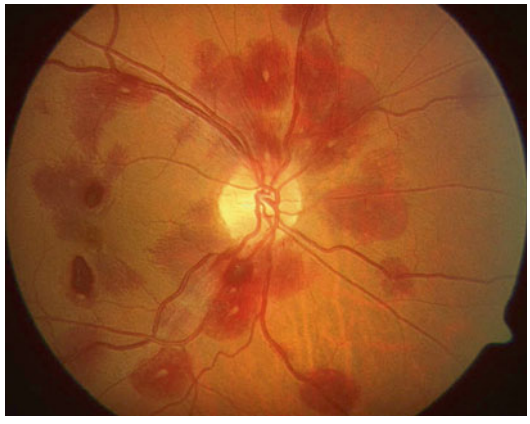

Fig. 9.126 Fundus view of white-centered retinal hemorrhages (Roth spots). These hemorrhages occur in septicemia but also in severe anemia and neoplastic hematological conditions such as leukemia

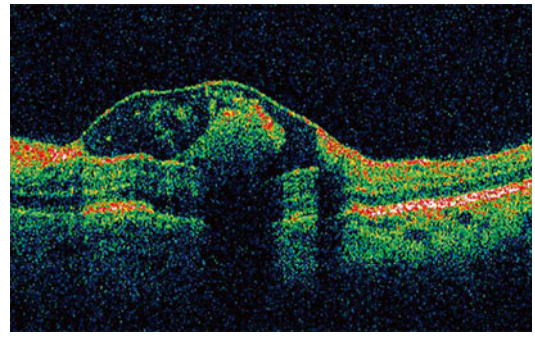

Fig. 9.127 OCT image of a white-centered retinal hemorrhage (Roth spot). The hemorrhage is lying within the inner retinal layers under the internal limiting membrane. It is thought to be due to a rupture of retinal capillaries either by septic emboli or neoplastic cells, probably followed by the aggregation of fibrin and platelets

Cutaneous melanoma can present as a metastatic lesion to the retina and vitreous (Figs. 9.128 and 9.129). In rare occasions even uveal melanoma can have a retinoinvasive component. When a tumor acquires a propensity to invade neural tissues, a retinoinvasive phenotype can be observed that may also manifest as infiltration into the optic nerve. Both these features are extremely unusual for uveal melanomas (Fig. 9.130) [198–203].

Retinal metastasis of an adenocarcinoma has been described in case of a Muir–Torre syndrome (secondary to MLH1/MSH2 mutations) which is associated with cutaneous sebaceous adenomas, adenocarcinoma of the breast, and colonic adenocarcinoma [204].

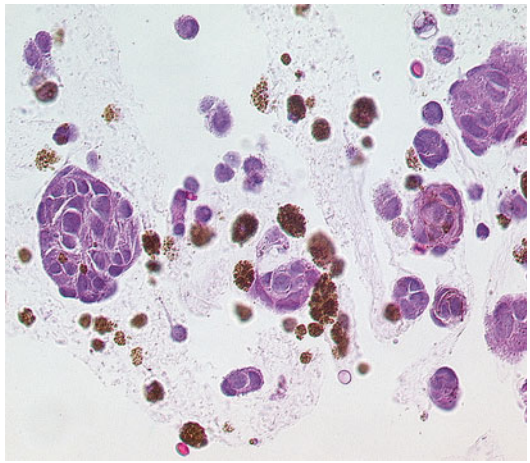

Fig. 9.128 Clusters of melanoma cells in a vitreous biopsy in a patient with metastatic cutaneous melanoma to the retina and the vitreous. The deeply pigmented cells are melanophages (H.E.)

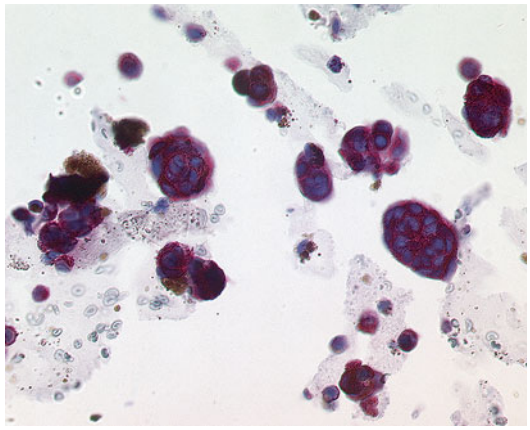

Fig. 9.129 Melan-A immunohistochemistry shows intense immunoreactivity in the melanoma cell clusters within the vitreous cavity

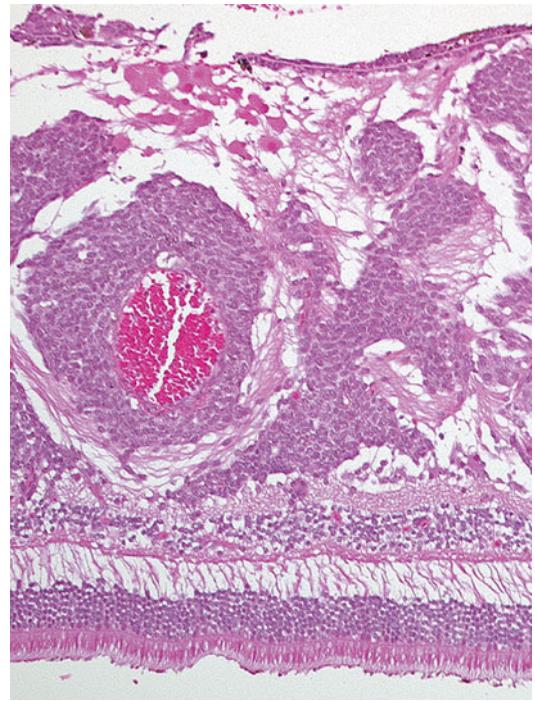

Fig. 9.130 Intraretinal infiltration of a retinoinvasive melanoma that has infiltrated the inner retinal layers and around a retinal arteriole (H.E.)

References

1. Østerberg GA. Topography of the layer of rods and cones in the human retina. Acta Ophthalmol. 1935;13(Supplement 6):1–97.
2. Hirsch J, Curcio CA. The spatial resolution capacity of human foveal retina. Vision Res. 1989;29(9): 1095–101.
3. Curcio CA, Sloan KR, Kalina RE, Hendrickson AE. Human photoreceptor topography. J Comp Neurol. 1990;292(4):497–523.
4. Curcio CA, Allen KA, Sloan KR, Lerea CL, Hurley JB, Klock IB, et al. Distribution and morphology of human cone photoreceptors stained with anti-blue opsin. J Comp Neurol. 1991;312(4):610–24.
5. Goldberg MF. Persistent fetal vasculature (PFV): an integrated interpretation of signs and symptoms associated with persistent hyperplastic primary vitreous (PHPV). LIV Edward Jackson Memorial Lecture. Am J Ophthalmol. 1997;124:587–626.
6. Milam AH, Li ZY, Fariss RN. Histopathology of the human retina in retinitis pigmentosa. Prog Retin Eye Res. 1998;17:175–205.
7. Wilson DJ, Weleber RG, Green WR. Ocular clinicopathologic study of gyrate atrophy. Am J Ophthalmol. 1991;111:24–33.
8. Chong NH, Alexander RA, Gin T, Bird AC, Luthert PJ. TIMP-3, collagen, and elastin immunohistochemistry and histopathology of Sorsby's fundus dystrophy. Invest Ophthalmol Vis Sci. 2000;41: 898–902.
9. Bohigan G. A study of the incidence of culture-positive endophthalmitis after cataract surgery in an ambulatory care center. Ophthalmic Surg Lasers. 1999;30:295–8.
10. Sandvig K, Dannevig L. Postoperative endophthalmitis: establishment and results of a national registry. J Cataract Refract Surg. 2003;29:1273–80.
11. Okada AA, Johnson RP, Liles WC, et al. Endogenous bacterial endophthalmitis: report of a ten-year retrospective study. Ophthalmology. 1994;101:832–8.

12. Wang Y, Abu-Asab MS, Li W, Aronow ME, et al. Autoantibody against transient receptor potential M1 cation channels of retinal ON bipolar cells in paraneoplastic vitelliform retinopathy. BMC Ophthalmol. 2012;12:56.
13. Endophthalmitis Vitrectomy Study Group. Results of the Endophthalmitis Vitrectomy Study: a randomized trial of immediate vitrectomy and of intravenous antibiotics for the treatment of postoperative bacterial endophthalmitis. Arch Ophthalmol. 1995;113:1479–96.
14. Jackson TL, Eykyn SJ, Graham EM, Stanford MR. Endogenous bacterial endophthalmitis: a 17-year prospective series and review of 267 reported cases. Surv Ophthalmol. 2003;48(4):403–23.
15. Schiedler V, Scott IU, Flynn Jr HW, Davis JL, Benz MS, Miller D. Culture-proven endogenous endophthalmitis: clinical features and visual acuity outcomes. Am J Ophthalmol. 2004;137(4):725–31.
16. McGwin Jr G, Xie A, Owsley C. Rate of eye injury in the United States. Arch Ophthalmol. 2005;123:970–6.
17. Sipperley JO, Quigley HA, Gass JDM. Traumatic retinopathy in primates: the explanation of commotio retinae. Arch Ophthalmol. 1978;96:2267–73.
18. Emerson MV, Jakobs E, Green WR. Ocular autopsy and histopathologic features of child abuse. Ophthalmology. 2007;114:1384–94.
19. Topping TM, Abrams GW, Machemer R. Experimental double-perforating injury of the posterior segment in rabbit eyes: the natural history of intraocular proliferation. Arch Ophthalmol. 1979;97:735–42.
20. Wickham L, Sethi CS, Lewis GP, Fisher SK, McLeod DC, Charteris DG. Glial and neural response in short-term human retinal detachment. Arch Ophthalmol. 2006;124:1779–82.
21. Wilson DJ, Green WR. Retinal detachment: a postmortem study of 49 eyes. Am J Ophthalmol. 1987;103:167–79.
22. Klein R, Chou CF, Klein BE, Zhang X, Meuer SM, Saaddine JB. Prevalence of age-related macular degeneration in the US population. Arch Ophthalmol. 2011;129(1):75–80. Epub 2011/01/12.
23. Imamura Y, Engelbert M, Iida T, Freund KB, Yannuzzi LA. Polypoidal choroidal vasculopathy: a review. Surv Ophthalmol. 2010;55(6):501–15. Epub 2010/09/21.
24. Swaroop A, Chew EY, Rickman CB, Abecasis GR. Unraveling a multifactorial late-onset disease: from genetic susceptibility to disease mechanisms for age-related macular degeneration. Annu Rev Genomics Hum Genet. 2009;10:19–43. Epub 2009/05/02.
25. Jackson GR, Owsley C, Curcio CA. Photoreceptor degeneration and dysfunction in aging and age-related maculopathy. Ageing Res Rev. 2002;1(3):381–96. Epub 2002/06/18.
26. Ferris 3rd FL, Wilkinson CP, Bird A, Chakravarthy U, Chew E, Csaky K, et al. Clinical classification of age-related macular degeneration. Ophthalmology. 2013;120(4):844–51. Epub 2013/01/22.
27. Fleckenstein M, Schmitz-Valckenberg S, Martens C, Kosanetzky S, Brinkmann CK, Hageman GS, et al. Fundus autofluorescence and spectral-domain optical coherence tomography characteristics in a rapidly progressing form of geographic atrophy. Invest Ophthalmol Vis Sci. 2011;52(6):3761–6. Epub 2011/02/12.
28. Okubo A, Rosa Jr RH, Bunce CV, Alexander RA, Fan JT, Bird AC, et al. The relationships of age changes in retinal pigment epithelium and Bruch's membrane. Invest Ophthalmol Vis Sci. 1999;40(2):443–9. Epub 1999/02/09.
29. Ramrattan RS, van der Schaft TL, Mooy CM, de Bruijn WC, Mulder PG, de Jong PT. Morphometric analysis of Bruch's membrane, the choriocapillaris, and the choroid in aging. Invest Ophthalmol Vis Sci. 1994;35(6):2857–64. Epub 1994/05/01.
30. Sarks S, Cherepanoff S, Killingsworth M, Sarks J. Relationship of Basal laminar deposit and membranous debris to the clinical presentation of early age-related macular degeneration. Invest Ophthalmol Vis Sci. 2007;48(3):968–77. Epub 2007/02/28.
31. Mullins RF, Russell SR, Anderson DH, Hageman GS. Drusen associated with aging and age-related macular degeneration contain proteins common to extracellular deposits associated with atherosclerosis, elastosis, amyloidosis, and dense deposit disease. FASEB J: Off Publ Fed Am Soc Exp Biol. 2000;14(7):835–46. Epub 2000/04/27.
32. Green WR, Enger C. Age-related macular degeneration histopathologic studies: the 1992 Lorenz E. Zimmerman Lecture. 1992. Retina. 2005;25(5 Suppl):1519–35.
33. Mitry D, Charteris DG, Fleck BW, Campbell H, Singh J. The epidemiology of rhegmatogenous retinal detachment: geographical variation and clinical associations. Br J Ophthalmol. 2010;94(6):678–84. Epub 2009/06/12.
34. Mitry D, Fleck BW, Wright AF, Campbell H, Charteris DG. Pathogenesis of rhegmatogenous retinal detachment: predisposing anatomy and cell biology. Retina. 2010;30(10):1561–72. Epub 2010/11/10.
35. Kirin M, Chandra A, Charteris DG, Hayward C, Campbell S, Celap I, et al. Genome-wide association study identifies genetic risk underlying primary rhegmatogenous retinal detachment. Hum Mol Genet. 2013;22(15):3174–85. Epub 2013/04/16.
36. Morgan IG, Ohno-Matsui K, Saw SM. Myopia. Lancet. 2012;379(9827):1739–48. Epub 2012/05/09.
37. Grossniklaus HE, Green WR. Pathologic findings in pathologic myopia. Retina. 1992;12(2):127–33. Epub 1992/01/01.
38. Cooke Bailey JN, Sobrin L, Pericak-Vance MA, Haines JL, Hammond CJ, Wiggs JL. Advances in the genomics of common eye diseases. Hum Mol Genet. 2013;22:R59–65. Epub 2013/08/22.
39. Tarr JM, Kaul K, Wolanska K, Kohner EM, Chibber R. Retinopathy in diabetes. Adv Exp Med Biol. 2012;771:88–106. Epub 2013/02/09.
40. Roy S, Ha J, Trudeau K, Beglova E. Vascular basement membrane thickening in diabetic retinopathy. Curr Eye Res. 2010;35(12):1045–56. Epub 2010/10/12.

41. Murea M, Ma L, Freedman BI. Genetic and environmental factors associated with type 2 diabetes and diabetic vascular complications. Rev Diabet Stud RDS. 2012;9(1):6–22. Epub 2012/09/14.
42. Grosso A, Cheung N, Veglio F, Wong TY. Similarities and differences in early retinal phenotypes in hypertension and diabetes. J Hypertens. 2011;29(9):1667–75. Epub 2011/08/16.
43. Coffman TM. Under pressure: the search for the essential mechanisms of hypertension. Nat Med. 2011;17(11):1402–9. Epub 2011/11/09.
44. Zamber RW, Kinyoun JL. Radiation retinopathy. West J Med. 1992;157(5):530–3. Epub 1992/11/01.
45. Helm CJ, Holland GN. Ocular tuberculosis. Surv Ophthalmol. 1993;38(3):229–56. Epub 1993/11/01.
46. Singh R, Toor P, Parchand S, Sharma K, Gupta V, Gupta A. Quantitative polymerase chain reaction for Mycobacterium tuberculosis in so-called Eales' disease. Ocul Immunol Inflamm. 2012;20(3):153–7. Epub 2012/04/11.
47. Nag TC, Wadhwa S. Vascular changes of the retina and choroid in systemic lupus erythematosus: pathology and pathogenesis. Curr Neurovasc Res. 2006;3(2):159–68. Epub 2006/05/25.
48. Cao X, Bishop RJ, Forooghian F, Cho Y, Fariss RN, Chan CC. Autoimmune retinopathy in systemic lupus erythematosus: histopathologic features. Open Ophthalmol J. 2009;3:20–5. Epub 2009/06/26.
49. Hartnett ME, Penn JS. Mechanisms and management of retinopathy of prematurity. N Engl J Med. 2012;367(26):2515–26. Epub 2012/12/28.
50. Penman AD, Talbot JF, Chuang EL, Thomas P, Serjeant GR, Bird AC. New classification of peripheral retinal vascular changes in sickle cell disease. Br J Ophthalmol. 1994;78(9):681–9. Epub 1994/09/01.
51. Lutty GA, McLeod DS. Phosphatase enzyme histochemistry for studying vascular hierarchy, pathology, and endothelial cell dysfunction in retina and choroid. Vision Res. 2005;45(28):3504–11. Epub 2005/10/11.
52. McLeod DS, Merges C, Fukushima A, Goldberg MF, Lutty GA. Histopathologic features of neovascularization in sickle cell retinopathy. Am J Ophthalmol. 1997;124(4):455–72. Epub 1997/11/05.
53. Koutsouraki E, Costa V, Baloyannis S. Epidemiology of multiple sclerosis in Europe: a review. Int Rev Psychiatry (Abingdon, England). 2010;22(1):2–13. Epub 2010/03/18.
54. Green AJ, McQuaid S, Hauser SL, Allen IV, Lyness R. Ocular pathology in multiple sclerosis: retinal atrophy and inflammation irrespective of disease duration. Brain J Neurol. 2010;133(Pt 6):1591–601. Epub 2010/04/23.
55. Kerrison JB, Flynn T, Green WR. Retinal pathologic changes in multiple sclerosis. Retina. 1994;14(5):445–51. Epub 1994/01/01.
56. Toteberg-Harms M, Sturm V, Sel S, Sasse A, Landau K. Retinal astrocytomas: long-term follow-up. Klin Monbl Augenheilkd. 2011;228(4):337–9.
57. Drummond SR, Kemp EG. Retinal astrocytoma managed by brachytherapy. Ophthalmology. 2009; 116(3):597.e1.
58. Pathak S, Chatterjee PK, Das S, Majumder N, Ghosh RK. Solitary retinal astrocytoma. J Indian Med Assoc. 2008;106(12):809.
59. Redinova M, Barakova D, Sach J, Kuchynka P. Intraocular astrocytoma without phacomatosis. Eur J Ophthalmol. 2004;14(4):350–4.
60. Arnold AC, Hepler RS, Yee RW, Maggiano J, Eng LF, Foos RY. Solitary retinal astrocytoma. Surv Ophthalmol. 1985;30(3):173–81.
61. Aronow ME, Nakagawa JA, Gupta A, Traboulsi EI, Singh AD. Tuberous sclerosis complex: genotype/phenotype correlation of retinal findings. Ophthalmology. 2012;119(9):1917–23.
62. Bornfeld N, Messmer EP, Theodossiadis G, Meyer-Schwickerath G, Wessing A. Giant cell astrocytoma of the retina. Clinicopathologic report of a case not associated with Bourneville's disease. Retina. 1987;7(3):183–9.
63. Jakobiec FA, Brodie SE, Haik B, Iwamoto T. Giant cell astrocytoma of the retina. A tumor of possible Mueller cell origin. Ophthalmology. 1983;90(12):1565–76.
64. Jarvi O, Oksala A. A retinal astrocytoma (Müller cell glioma). Ophthalmol J Int d'ophtalmologie Int J Ophthalmol Zeitschrift fur Augenheilkunde. 1951; 121(1):30–7.
65. Gunduz K, Eagle Jr RC, Shields CL, Shields JA, Augsburger JJ. Invasive giant cell astrocytoma of the retina in a patient with tuberous sclerosis. Ophthalmology. 1984;106(3):639–42.66.
66. de Juan Jr E, Green WR, Gupta PK, Baranano EC. Vitreous seeding by retinal astrocytic hamartoma in a patient with tuberous sclerosis. Retina. 1984;4(2): 100–2. Epub 1984/01/01.
67. Khawly JA, Matthews JD, Machemer R. Appearance and rapid growth of retinal tumor (reactive astrocytic hyperplasia?). Graefe's Arch Clin Exp Ophthalmol = Albrecht von Graefes Archiv fur klinische und experimentelle Ophthalmologie. 1999;237(1):78–81.
68. Shields CL, Shields JA, Eagle Jr RC, Cangemi F. Progressive enlargement of acquired retinal astrocytoma in 2 cases. Ophthalmology. 2004;111(2):363–8.
69. Shields JA, Eagle Jr RC, Shields CL, Marr BP. Aggressive retinal astrocytomas in 4 patients with tuberous sclerosis complex. Arch Ophthalmol. 2005;123(6):856–63.
70. Tomida M, Mitamura Y, Katome T, Eguchi H, Naito T, Harada T. Aggressive retinal astrocytoma associated with tuberous sclerosis. Clin Ophthalmol. 2012;6:715–20.
71. Shah M, Park HJ, Gohari AR, Bhatti MT. Loss of myelinated retinal nerve fibers from chronic papilledema. J Neuro-Ophthalmol: Off J North Am Neuro-Ophthalmol Soc. 2008;28(3):219–21.
72. Heimann H, Jmor F, Damato B. Imaging of retinal and choroidal vascular tumours. Eye (Lond). 2013; 27(2):208–16. Epub 2012/12/01.
73. Heimann H, Damato B. Congenital vascular malformations of the retina and choroid. Eye. 2010; 24(3):459–67.
74. Kreusel KM, Bechrakis NE, Krause L, Neumann HP, Foerster MH. Retinal angiomatosis in von

Hippel-Lindau disease: a longitudinal ophthalmologic study. Ophthalmology. 2006;113(8):1418–24.
75. Maher ER, Yates JR, Harries R, Benjamin C, Harris R, Moore AT, et al. Clinical features and natural history of von Hippel-Lindau disease. Q J Med. 1990;77(283):1151–63.
76. Kreusel KM, Bornfeld N, Bender BU, Neumann L, Foerster MH, Neumann HP. Retinal capillary angioma. Clinical and molecular genetic studies. Der Ophthalmol Zeitschrift der Deutschen Ophthalmologischen Gesellschaft. 1999;96(2):71–6. Kapillares retinales Angiom. Klinische und molekulargenetische Untersuchungen.
77. Nicholson DH, Green WR, Kenyon KR. Light and electron microscopic study of early lesions in angiomatosis retinae. Am J Ophthalmol. 1976;82(2):193–204.
78. Arjumand W, Sultana S. Role of VHL gene mutation in human renal cell carcinoma. Tumour Biol: J Int Soc Oncodevelopmental Biol Med. 2012;33(1):9–16.
79. Glasker S, Bender BU, Apel TW, Natt E, van Velthoven V, Scheremet R, et al. The impact of molecular genetic analysis of the VHL gene in patients with haemangioblastomas of the central nervous system. J Neurol Neurosurg Psychiatry. 1999;67(6):758–62.
80. Hemberger M, Himmelbauer H, Neumann HP, Plate KH, Schwarzkopf G, Fundele R. Expression of the von Hippel-Lindau-binding protein-1 (Vbp1) in fetal and adult mouse tissues. Hum Mol Genet. 1999;8(2):229–36.
81. Maddock IR, Moran A, Maher ER, Teare MD, Norman A, Payne SJ, et al. A genetic register for von Hippel-Lindau disease. J Med Genet. 1996;33(2):120–7.
82. Knudson Jr AG. Mutation and cancer: statistical study of retinoblastoma. Proc Natl Acad Sci U S A. 1971;68(4):820–3.
83. Kreusel KM, Bechrakis NE, Neumann HP, Schmidt D, Foerster MH. Solitary juxtapapillary capillary retinal angioma and von Hippel-Lindau disease. Can J Ophthalmol J Can d'ophtalmologie. 2007;42(2):251–5.
84. Backhouse O, O'Neill D. Cavernous haemangioma of retina and skin. Eye. 1998;12(Pt 6):1027–8.
85. Chen L, Huang L, Zhang G, Gordon L. Cavernous hemangioma of the retina. Can J Ophthalmol J Can d'ophtalmologie. 2008;43(6):718–20.
86. Colvard DM, Robertson DM, Trautmann JC. Cavernous hemangioma of the retina. Arch Ophthalmol. 1978;96(11):2042–4.
87. Gislason I, Stenkula S, Alm A, Wold E, Walinder PE. Cavernous haemangioma of the retina. Acta Ophthalmol (Copenh). 1979;57(4):709–17.
88. Klein M, Goldberg MF, Cotlier E. Cavernous hemangioma of the retina: report of four cases. Ann Ophthalmol. 1975;7(9):1213–21.
89. Krause U. A case of cavernous haemangioma of the retina. Acta Ophthalmol (Copenh). 1971;49(2):221–31.
90. Davies WS, Thumim M. Cavernous hemangioma of the optic disc and retina. Trans Am Acad Ophthalmol Otolaryngol. 1956;60(2):217–8.
91. Drummond JW, Hall DL, Steen Jr WH, Lusk JE. Cavernous hemangioma of the optic disc. Ann Ophthalmol. 1980;12(9):1017–8.
92. D'Angelo R, Scimone C, Calabro M, Schettino C, Fratta M, Sidoti A. Identification of a novel CCM2 gene mutation in an Italian family with multiple cerebral cavernous malformations and epilepsy: a causative mutation? Gene. 2013;519(1):202–7.
93. Denier C, Gasc JM, Chapon F, Domenga V, Lescoat C, Joutel A, et al. Krit1/cerebral cavernous malformation 1 mRNA is preferentially expressed in neurons and epithelial cells in embryo and adult. Mech Dev. 2002;117(1–2):363–7.
94. Ji BH, Qin W, Sun T, Feng GY, He L, Wang YJ. A novel deletion mutation in CCM1 gene (krit1) is detected in a Chinese family with cerebral cavernous malformations. Yi chuan xue bao = Acta Genetica Sinica. 2006;33(2):105–10.
95. Pilarski RT, Brothman AR, Benn P, Shulman Rosengren S. Attenuated familial adenomatous polyposis in a man with an interstitial deletion of chromosome arm 5q. Am J Med Genet. 1999;86(4):321–4.
96. Toldo I, Drigo P, Mammi I, Marini V, Carollo C. Vertebral and spinal cavernous angiomas associated with familial cerebral cavernous malformation. Surg Neurol. 2009;71(2):167–71.
97. Dellemijn PL, Vanneste JA. Cavernous angiomatosis of the central nervous system: usefulness of screening the family. Acta Neurol Scand. 1993;88(4):259–63.
98. Dobyns WB, Michels VV, Groover RV, Mokri B, Trautmann JC, Forbes GS, et al. Familial cavernous malformations of the central nervous system and retina. Ann Neurol. 1987;21(6):578–83.
99. Drigo P, Mammi I, Battistella PA, Ricchieri G, Carollo C. Familial cerebral, hepatic, and retinal cavernous angiomas: a new syndrome. Child's Nerv Syst:ChNS: Off J Int Soc Pediatr Neurosurg. 1994;10(4):205–9.
100. Marchuk DA, Gallione CJ, Morrison LA, Clericuzio CL, Hart BL, Kosofsky BE, et al. A locus for cerebral cavernous malformations maps to chromosome 7q in two families. Genomics. 1995;28(2):311–4.
101. Mizuno Y, Kurokawa T, Numaguchi Y, Goya N. Facial hemangioma with cerebrovascular anomalies and cerebellar hypoplasia. Brain Dev. 1982;4(5):375–8.
102. Pancurak J, Goldberg MF, Frenkel M, Crowell RM. Cavernous hemangioma of the retina. Genet Central Nerv Syst Involvement Retin. 1985;5(4):215–20.
103. Schwartz AC, Weaver Jr RG, Bloomfield R, Tyler ME. Cavernous hemangioma of the retina, cutaneous angiomas, and intracranial vascular lesion by computed tomography and nuclear magnetic resonance imaging. Am J Ophthalmol. 1984;98(4):483–7.
104. Vanaman MJ, Hervey-Jumper SL, Maher CO. Pediatric and inherited neurovascular diseases. Neurosurg Clin N Am. 2010;21(3):427–41.
105. Tlucek PS, Moreau A, Siatkowski RM, Repka MX. A twisted mess. Surv Ophthalmol. 2012;57(1):77–82.
106. Schmidt D, Pache M, Schumacher M. The congenital unilateral retinocephalic vascular malformation syndrome (bonnet-dechaume-blanc syndrome or

wyburn-mason syndrome): review of the literature. Surv Ophthalmol. 2008;53(3):227–49.
107. Chan WM, Yip NK, Lam DS. Wyburn-Mason syndrome. Neurology. 2004;62(1):99.
108. Hopen G, Smith JL, Hoff JT, Quencer R. The Wyburn-Mason syndrome. Concomitant chiasmal and fundus vascular malformations. J Clin Neuroophthalmol. 1983;3(1):53–62.
109. Rennie IG. Retinal vasoproliferative tumours. Eye. 2010;24(3):468–71.
110. Heimann H, Bornfeld N, Vij O, Coupland SE, Bechrakis NE, Kellner U, et al. Vasoproliferative tumours of the retina. Br J Ophthalmol. 2000;84(10):1162–9.
111. Hiscott P, Mudhar H. Is vasoproliferative tumour (reactive retinal glioangiosis) part of the spectrum of proliferative vitreoretinopathy? Eye. 2009;23(9): 1851–8.
112. Jain K, Berger AR, Yucil YH, McGowan HD. Vasoproliferative tumours of the retina. Eye. 2003;17(3):364–8.
113. Mori K, Ohta K, Murata T. Vasoproliferative tumors of the retina secondary to ocular toxocariasis. Can J Ophthalmol J Can d'ophtalmologie. 2007;42(5):758–9.
114. Murthy R, Honavar SG. Secondary vasoproliferative retinal tumor associated with Usher syndrome type 1. J AAPOS: Off Publ Am Assoc Pediatr Ophthalmol Strabismus / Am Assoc for Pediatr Ophthalmol Strabismus. 2009;13(1):97–8.
115. Wachtlin J, Heimann H, Jandeck C, Kreusel KM, Bechrakis NE, Kellner U, et al. Bilateral vasoproliferative retinal tumors with identical localization in a pair of monozygotic twins. Arch Ophthalmol. 2002;120(6):860–2.
116. Poole Perry LJ, Jakobiec FA, Zakka FR, Reichel E, Herwig MC, Perry A, et al. Reactive retinal astrocytic tumors (so-called vasoproliferative tumors): histopathologic, immunohistochemical, and genetic studies of four cases. Am J Ophthalmol. 2013; 155(3):593–608.e1.
117. Irvine F, O'Donnell N, Kemp E, Lee WR. Retinal vasoproliferative tumors: surgical management and histological findings. Arch Ophthalmol. 2000;118(4):563–9.
118. Seregard S, Lundell G, Svedberg H, Kivela T. Incidence of retinoblastoma from 1958 to 1998 in Northern Europe: advantages of birth cohort analysis. Ophthalmology. 2004;111(6):1228–32.
119. Kivela T. 200 years of success initiated by James Wardrop's 1809 monograph on retinoblastoma. Acta Ophthalmol. 2009;87(8):810–2.
120. Kivela T. The epidemiological challenge of the most frequent eye cancer: retinoblastoma, an issue of birth and death. Br J Ophthalmol. 2009;93(9):1129–31.
121. Genovese C, Trani D, Caputi M, Claudio PP. Cell cycle control and beyond: emerging roles for the retinoblastoma gene family. Oncogene. 2006;25(38): 5201–9.
122. Giacinti C, Giordano A. RB and cell cycle progression. Oncogene. 2006;25(38):5220–7.
123. Hilgendorf KI, Leshchiner ES, Nedelcu S, Maynard MA, Calo E, Ianari A, et al. The retinoblastoma protein induces apoptosis directly at the mitochondria. Genes Dev. 2013;27(9):1003–15.
124. Howard CM, Claudio PP, Gallia GL, Gordon J, Giordano GG, Hauck WW, et al. Retinoblastoma-related protein pRb2/p130 and suppression of tumor growth in vivo. J Natl Cancer Inst. 1998;90(19): 1451–60.
125. Howe JA, Mymryk JS, Egan C, Branton PE, Bayley ST. Retinoblastoma growth suppressor and a 300-kDa protein appear to regulate cellular DNA synthesis. Proc Natl Acad Sci U S A. 1990;87(15):5883–7.
126. Kapatai G, Brundler MA, Jenkinson H, Kearns P, Parulekar M, Peet AC, et al. Gene expression profiling identifies different sub-types of retinoblastoma. Br J Cancer. 2013;109:512–25.
127. Martin J, Bryar P, Mets M, Weinstein J, Jones A, Martin A, et al. Differentially expressed miRNAs in retinoblastoma. Gene. 2013;512(2):294–9.
128. McCarthy N. Retinoblastoma: epigenetic outcome. Nat Rev Cancer. 2012;12(2):80.
129. Murphree AL, Triche TJ. An epigenomic mechanism in retinoblastoma: the end of the story? Genome Med. 2012;4(2):15.
130. Orjuela MA, Cabrera-Munoz L, Paul L, Ramirez-Ortiz MA, Liu X, Chen J, et al. Risk of retinoblastoma is associated with a maternal polymorphism in dihydrofolatereductase (DHFR) and prenatal folic acid intake. Cancer. 2012;118(23):5912–9.
131. Sabelli PA, Liu Y, Dante RA, Lizarraga LE, Nguyen HN, Brown SW, et al. Control of cell proliferation, endoreduplication, cell size, and cell death by the retinoblastoma-related pathway in maize endosperm. Proc Natl Acad Sci U S A. 2013;110(19): E1827–36.
132. Rubin CM, Robison LL, Cameron JD, Woods WG, Nesbit Jr ME, Krivit W, et al. Intraocular retinoblastoma group V: an analysis of prognostic factors. J Clin Oncol: Off J Am Soc Clin Oncol. 1985;3(5):680–5.
133. Abramson DH, Notterman RB, Ellsworth RM, Kitchin FD. Retinoblastoma treated in infants in the first six months of life. Arch Ophthalmol. 1983;101(9): 1362–6.
134. Abramson DH, Schefler AC. Update on retinoblastoma. Retina. 2004;24(6):828–48.
135. Kivela T, Kujala E. Prognostication in eye cancer: the latest tumor, node, metastasis classification and beyond. Eye. 2013;27(2):243–52.
136. Dimaras H, Kimani K, Dimba EA, Gronsdahl P, White A, Chan HS, et al. Retinoblastoma. Lancet. 2012;379(9824):1436–46.
137. Moll AC, Dommering CJ, Bosscha MI, de Graaf P, Kors WA, van Leeuwen FE. Risk factors for the incidence of second cancers in survivors of retinoblastoma with a family history. J Clin Oncol: Off J Am Soc Clin Oncol. 2012;30(24):3028, author reply –9.
138. Kleinerman RA, Schonfeld SJ, Tucker MA. Sarcomas in hereditary retinoblastoma. Clin Sarcoma Res. 2012;2(1):15.
139. Kivela T. Trilateral retinoblastoma: a meta-analysis of hereditary retinoblastoma associated with primary

ectopic intracranial retinoblastoma. J Clin Oncol: Off J Am Soc Clin Oncol. 1999;17(6):1829–37.
140. Balmer A, Gailloud C, Munier F, Uffer S, Guex-Crosier Y. Retinoblastoma. Unusual warning and clinical signs. Ophthalmic Paediatr Genet. 1993; 14(1):33–8.
141. Smirniotopoulos JG, Bargallo N, Mafee MF. Differential diagnosis of leukokoria: radiologic-pathologic correlation. Radiographics Rev Publ Radiol Soc North Am Inc. 1994;14(5):1059–79; quiz 81–2.
142. Melamud A, Palekar R, Singh A. Retinoblastoma. Am Fam Physician. 2006;73(6):1039–44.
143. Kazadi Lukusa A, Aloni MN, Kadima-Tshimanga B, Mvitu-Muaka M, Gini Ehungu JL, Ngiyulu R, et al. Retinoblastoma in the democratic republic of congo: 20-year review from a tertiary hospital in kinshasa. J Cancer Epidemiol. 2012;2012:920468.
144. Margo CE, HL E, Mulla ZD. Retinoblastoma. Cancer Control: J Moffitt Cancer Cent. 1998;5(4): 310–6.
145. Palma J, Sasso DF, Dufort G, Koop K, Sampor C, Diez B, et al. Successful treatment of metastatic retinoblastoma with high-dose chemotherapy and autologous stem cell rescue in South America. Bone Marrow Transplant. 2012;47(4):522–7.
146. Luna-Fineman S, Barnoya M, Bonilla M, Fu L, Baez F, Rodriguez-Galindo C. Retinoblastoma in Central America: report from the Central American association of pediatric hematology oncology (AHOPCA). Pediatr Blood Cancer. 2012;58(4):545–50.
147. MacCarthy A, Birch JM, Draper GJ, Hungerford JL, Kingston JE, Kroll ME, et al. Retinoblastoma in Great Britain 1963–2002. Br J Ophthalmol. 2009; 93(1):33–7.
148. Ramprasad VL, Madhavan J, Murugan S, Sujatha J, Suresh S, Sharma T, et al. Retinoblastoma in India: microsatellite analysis and its application in genetic counseling. Mol Diagn Ther. 2007;11(1):63–70.
149. Bechrakis NE, Bornfeld N, Schueler A, Coupland SE, Henze G, Foerster MH. Clinicopathologic features of retinoblastoma after primary chemoreduction. Arch Ophthalmol. 1998;116(7):887–93.
150. Shields CL, Honavar SG, Meadows AT, Shields JA, Demirci H, Naduvilath TJ. Chemoreduction for unilateral retinoblastoma. Arch Ophthalmol. 2002; 120(12):1653–8.
151. Redler LD, Ellsworth RM. Prognostic importance of choroidal invasion in retinoblastoma. Arch Ophthalmol. 1973;90(4):294–6.
152. Stannard C, Lipper S, Sealy R, Sevel D. Retinoblastoma: correlation of invasion of the optic nerve and choroid with prognosis and metastases. Br J Ophthalmol. 1979;63(8):560–70.
153. Chevez-Barrios P, Hurwitz MY, Louie K, Marcus KT, Holcombe VN, Schafer P, et al. Metastatic and nonmetastatic models of retinoblastoma. Am J Pathol. 2000;157(4):1405–12.
154. Sastre X, Chantada GL, Doz F, Wilson MW, de Davila MT, Rodriguez-Galindo C, et al. Proceedings of the consensus meetings from the International Retinoblastoma Staging Working Group on the pathology guidelines for the examination of enucleated eyes and evaluation of prognostic risk factors in retinoblastoma. Arch Pathol Lab Med. 2009; 133(8):1199–202.
155. Bosaleh A, Sampor C, Solernou V, Fandino A, Dominguez J, de Davila MT, et al. Outcome of children with retinoblastoma and isolated choroidal invasion. Arch Ophthalmol. 2012;130(6):724–9.
156. Kashyap S, Meel R, Pushker N, Sen S, Bakhshi S, Sreenivas V, et al. Clinical predictors of high risk histopathology in retinoblastoma. Pediatr Blood Cancer. 2012;58(3):356–61.
157. Honavar SG, Singh AD, Shields CL, Meadows AT, Demirci H, Cater J, et al. Postenucleation adjuvant therapy in high-risk retinoblastoma. Arch Ophthalmol. 2002;120(7):923–31.
158. Abramson DH. Retinoma, retinocytoma, and the retinoblastoma gene. Arch Ophthalmol. 1983;101(10): 1517–8.
159. Balmer A, Munier F, Gailloud C. Retinoma. Case studies. Ophthalmic Paediatr Genet. 1991;12(3):131–7.
160. Hadjistilianou T, De Francesco S, Martone G, Malandrini A. Retinocytoma associated with calcified vitreous deposits. Eur J Ophthalmol. 2006;16(2): 349–51.
161. Margo C, Hidayat A, Kopelman J, Zimmerman LE. Retinocytoma. A benign variant of retinoblastoma. Arch Ophthalmol. 1983;101(10):1519–31.
162. Wong IB, Farzavandi S. What's your diagnosis? Retinocytoma. J Pediatr Ophthalmol Strabismus. 2010;47(5):268–87.
163. Dimaras H, Khetan V, Halliday W, Orlic M, Prigoda NL, Piovesan B, et al. Loss of RB1 induces non-proliferative retinoma: increasing genomic instability correlates with progression to retinoblastoma. Hum Mol Genet. 2008;17(10):1363–72.
164. Shields CL, Shields JA, Marr BP, Sperber DE, Gass JD. Congenital simple hamartoma of the retinal pigment epithelium: a study of five cases. Ophthalmology. 2003;110(5):1005–11.
165. Shields CL, Materin MA, Karatza EC, Shields JA. Optical coherence tomography of congenital simple hamartoma of the retinal pigment epithelium. Retina. 2004;24(2):327–8.
166. Shukla D, Ambatkar S, Jethani J, Kim R. Optical coherence tomography in presumed congenital simple hamartoma of retinal pigment epithelium. Am J Ophthalmol. 2005;139(5):945–7.
167. Lopez JM, Guerrero P. Congenital simple hamartoma of the retinal pigment epithelium: optical coherence tomography and angiography features. Retina. 2006;26(6):704–6.
168. Schachat AP, Shields JA, Fine SL, Sanborn GE, Weingeist TA, Valenzuela RE, et al. Combined hamartomas of the retina and retinal pigment epithelium. Ophthalmology. 1984;91(12):1609–15.
169. Kaye LD, Rothner AD, Beauchamp GR, Meyers SM, Estes ML. Ocular findings associated with

neurofibromatosis type II. Ophthalmology. 1992; 99(9): 1424–9.
170. Meyer JH, Witschel H. Bilateral combined hamartoma of the retina and the retinal pigment epithelium. Br J Ophthalmol. 1996;80(6):577–8.
171. Fonseca RA, Dantas MA, Kaga T, Spaide RF. Combined hamartoma of the retina and retinal pigment epithelium associated with juvenile nasopharyngeal angiofibroma. Am J Ophthalmol. 2001;132(1):131–2.
172. Ting TD, McCuen 2nd BW, Fekrat S. Combined hamartoma of the retina and retinal pigment epithelium: optical coherence tomography. Retina. 2002;22(1):98–101.
173. Grant EA, Trzupek KM, Reiss J, Crow K, Messiaen L, Weleber RG. Combined retinal hamartomas leading to the diagnosis of neurofibromatosis type 2. Ophthalmic Genet. 2008;29(3):133–8.
174. Shields CL, Thangappan A, Hartzell K, Valente P, Pirondini C, Shields JA. Combined hamartoma of the retina and retinal pigment epithelium in 77 consecutive patients visual outcome based on macular versus extramacular tumor location. Ophthalmology. 2008;115(12):2246–52.e3.
175. Benhamou N, Massin P, Spolaore R, Paques M, Gaudric A. Surgical management of epiretinal membrane in young patients. Am J Ophthalmol. 2002;133(3):358–64. Epub 2002/02/28.
176. Brue C, Saitta A, Nicolai M, Mariotti C, Giovannini A. Epiretinal membrane surgery for combined hamartoma of the retina and retinal pigment epithelium: role of multimodal analysis. Clin Ophthalmol. 2013;7:179–84. Epub 2013/02/05.
177. Cohn AD, Quiram PA, Drenser KA, Trese MT, Capone Jr A. Surgical outcomes of epiretinal membranes associated with combined hamartoma of the retina and retinal pigment epithelium. Retina. 2009;29(6):825–30.
178. Shields CL, Mashayekhi A, Ho T, Cater J, Shields JA. Solitary congenital hypertrophy of the retinal pigment epithelium: clinical features and frequency of enlargement in 330 patients. Ophthalmology. 2003;110(10):1968–76.
179. Meyer CH, Becker R, Schmidt JC, Kroll P. When is congenital hypertrophy of the retinal pigment epithelium (CHRPE) associated with the Gardner's syndrome? An overview with clinical examples. Klin Monbl Augenheilkd. 2002;219(9):644–8. Wann sind kongenitale Hypertrophien des retinalen Pigmentepithels (CHRPE) mit dem Gardner-Syndrom assoziiert? – Eine Ubersicht mit klinischen Beispielen.
180. Shields JA, Shields CL, Singh AD. Acquired tumors arising from congenital hypertrophy of the retinal pigment epithelium. Arch Ophthalmol. 2000;118(5):637–41.
181. Meyer CH, Rodrigues EB, Mennel S, Schmidt JC, Kroll P. Grouped congenital hypertrophy of the retinal pigment epithelium follows developmental patterns of pigmentary mosaicism. Ophthalmology. 2005;112(5):841–7.
182. Kasner L, Traboulsi EI, Delacruz Z, Green WR. A histopathologic study of the pigmented fundus lesions in familial adenomatous polyposis. Retina. 1992;12(1):35–42.
183. Nakamura S, Hikita N, Yamakawa R, Moriya F, Yano H, Furusato E, et al. A clinically challenging diagnosis of adenoma of the retinal pigment epithelium presenting with clinical features of choroidal hemangioma. Clin Ophthalmol. 2012;6:497–502.
184. Wei W, Mo J, Jie Y, Li B. Adenoma of the retinal pigment epithelium: a report of 3 cases. Can J Ophthalmol J Can d'ophtalmologie. 2010;45(2): 166–70.
185. Heegaard S, Larsen JN, Fledelius HC, Prause JU. Neoplasia versus hyperplasia of the retinal pigment epithelium. A comparison of two cases. Acta Ophthalmol Scand. 2001;79(6):626–33.
186. Shields JA, Shields CL, Gunduz K, Eagle Jr RC. Neoplasms of the retinal pigment epithelium: the 1998 Albert Ruedemann, Sr, memorial lecture, Part 2. Arch Ophthalmol. 1999;117(5):601–8.
187. Shields JA, Shields CL, Eagle Jr RC, Singh AD. Adenocarcinoma arising from congenital hypertrophy of retinal pigment epithelium. Arch Ophthalmol. 2001;119(4):597–602.
188. Finger PT, McCormick SA, Davidian M, Walsh JB. Adenocarcinoma of the retinal pigment epithelium: a diagnostic and therapeutic challenge. Graefe's Arch Clin Exp Ophthalmol = Albrecht von Graefes Archiv fur klinische und experimentelle Ophthalmologie. 1996;234 Suppl 1:S22–7.
189. Shields JA, Eagle Jr RC, Shields CL, Brown GC, Lally SE. Malignant transformation of congenital hypertrophy of the retinal pigment epithelium. Ophthalmology. 2009;116(11):2213–6.
190. Trichopoulos N, Augsburger JJ, Schneider S. Adenocarcinoma arising from congenital hypertrophy of the retinal pigment epithelium. Graefe's Arch Clin Exp Ophthalmol = Albrecht von Graefes Archiv fur klinische und experimentelle Ophthalmologie. 2006;244(1):125–8.
191. Edelstein C, Shields CL, Shields JA, Eagle Jr RC. Presumed adenocarcinoma of the retinal pigment epithelium in a blind eye with a staphyloma. Arch Ophthalmol. 1998;116(4):525–8.
192. Minckler D, Allen Jr AW. Adenocarcinoma of the retinal pigment epithelium. Arch Ophthalmol. 1978;96(12):2252–4.
193. Zehetner C, Bechrakis NE. White centered retinal hemorrhages in vitamin b(12) deficiency anemia. Case Rep Ophthalmol. 2011;2(2):140–4.
194. Falcone PM, Larrison WI. Roth spots seen on ophthalmoscopy: diseases with which they may be associated. Conn Med. 1995;59(5):271–3.
195. Rodriguez-Adrian LJ, King RT, Tamayo-Derat LG, Miller JW, Garcia CA, Rex JH. Retinal lesions as clues to disseminated bacterial and candidal infections: frequency, natural history, and etiology. Medicine. 2003;82(3):187–202.

196. Mandic BD, Potocnjak V, Bencic G, Mandic Z, Pentz A, Hajnzic TF. Visual loss as initial presentation of chronic myelogenous leukemia. Coll Antropol. 2005;29 Suppl 1:141–3.
197. Kapadia RK, Steeves JH. Roth spots in chronic myelogenous leukemia. CMAJ Can Med Assoc J = J de l'Assoc medicale canadienne. 2011;183(18):E1352.
198. Zografos L, Mirimanoff RO, Angeletti CA, Frosini R, Beati D, Schalenbourg A, et al. Systemic melanoma metastatic to the retina and vitreous. Ophthalmol J Int d'ophtalmologie Int J Ophthalmol Zeitschrift fur Augenheilkunde. 2004;218(6):424–33.
199. Mack HG, Jakobiec FA. Isolated metastases to the retina or optic nerve. Int Ophthalmol Clin. 1997;37(4):251–60.
200. Leys AM, Van Eyck LM, Nuttin BJ, Pauwels PA, Delabie JM, Libert JA. Metastatic carcinoma to the retina. Clinicopathologic findings in two cases. Arch Ophthalmol. 1990;108(10):1448–52.
201. Eide N, Syrdalen P. Intraocular metastasis from cutaneous malignant melanoma. Acta Ophthalmol (Copenh). 1990;68(1):102–6.
202. Cangiarella JF, Suhrland MJ, Cajigas A, Chess J, Koss LG, Berkowitz D, et al. Esophageal carcinoma metastatic to the retina. Diagnosis of a case by cytologic examination of intraocular vitreous washings. Acta Cytol. 1996;40(5):995–8.
203. Best SJ, Taylor W, Allen JP. Metastatic cutaneous malignant melanoma of the vitreous and retina. Aust N Z J Ophthalmol. 1990;18(4):397–400.
204. Spraul CW, Lang GE, Grossniklaus HE, Lang GK. Metastatic adenocarcinoma to the retina in a patient with Muir-Torre syndrome. Am J Ophthalmol. 1995;120(2):248–50.

The Uvea

10

Sarah E. Coupland and Alexander Moulin

10.1 General Description

The uveal tract (also termed *tunica vasculosa*) consists of the iris, ciliary body and the choroid and is the 'middle' layer of the eye (Fig. 10.1). It is a highly vascularised and pigmented tissue and provides several essential functions to the eye, including nutritive supply to almost all intraocular structures, production of aqueous, secretion of hyaluronic acid into the vitreous and control of accommodation. Although scattered lymphocytes are present between the normal choroidal melanocytes, the uveal tract does not contain lymphatic vessels.

10.2 Embryology, Anatomy and Development

The *iris* is the anterior visible part of the uveal tract. The structure is named after the Greek goddess of the rainbow. The iris has two components: the posterior iris pigmented epithelium derived from neuroectoderm and the iris stroma derived from the neural crest (Fig. 10.2). Its major component, the iris stroma, is a loosely arranged tissue that contains pigmented and non-pigmented cells set in an abundant extracellular matrix containing bundles of type I collagen fibrils and hyaluronidase-sensitive glycosaminoglycans. The cells include melanocytes and fibroblasts. The greatest concentration of iris melanocytes is located in the avascular anterior border layer (Fig. 10.2). The iris vessels have a radial orientation and are ensheathed by a thick mantle of collagen fibres, giving a thick-walled appearance. The anterior surface of the iris has an irregular contour. This is because the papillary portion of the iris is thinner. Embryologically, this thinning results from atrophy of the anterior stroma caused by resorption of the papillary membrane. The anterior surface of the more peripheral iris is characterised by contraction furrows. Defects in the anterior stroma (crypts of Fuchs) are evident clinically. Heavily pigmented rounded clump cells of Koganei (either melanophages or neuroepithelial cells) are often found in the stroma near the sphincter muscle.

The *ciliary body* is the middle part of the uveal tract, interposed between the iris and the choroid. It has two major components: the pars plicata (also known as the 'corona ciliaris') and the pars plana. The anterior pars plicata is composed of a ring of 70–80 ciliary processes, which project into the posterior chamber. Their inner non-pigmented epithelial cells secrete the watery

S.E. Coupland, MBBS, PhD, FRCPath (✉)
Molecular and Clinical Cancer Medicine,
Royal Liverpool and Broadgreen University Hospital NHS Trust, University of Liverpool,
6th Floor Duncan Building, Daulby Street,
Liverpool L69 3GA, UK
e-mail: s.e.coupland@liverpool.ac.uk

A. Moulin, MD, MER, FEBO
Department of Ophthalmology,
Eye Pathology Laboratory,
Jules-Gonin Eye Hospital, University of Lausanne,
Av de France 15, Case postale 133,
Lausanne 1000, Switzerland
e-mail: moulin.alexandre@fa2.ch

S. Heegaard, H. Grossniklaus (eds.), *Eye Pathology: An Illustrated Guide*,
DOI 10.1007/978-3-662-43382-9_10,

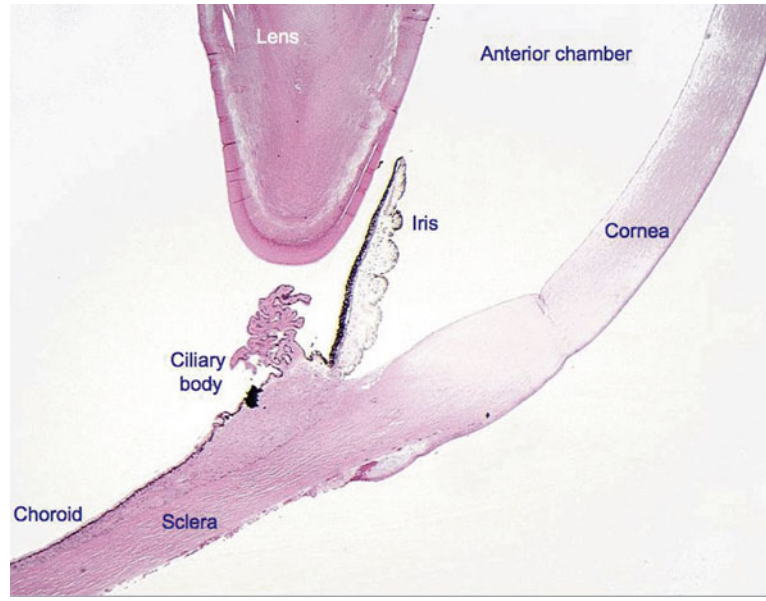

Fig. 10.1 Low-power histological section of the anterior part of the eye demonstrating the anatomical arrangements of the cornea, lens and anterior uvea (iris, ciliary process, ciliary body, pars plana and anterior choroid (×2 objective; HE) (Courtesy of Hardeep Mudhar, Sheffield, UK)

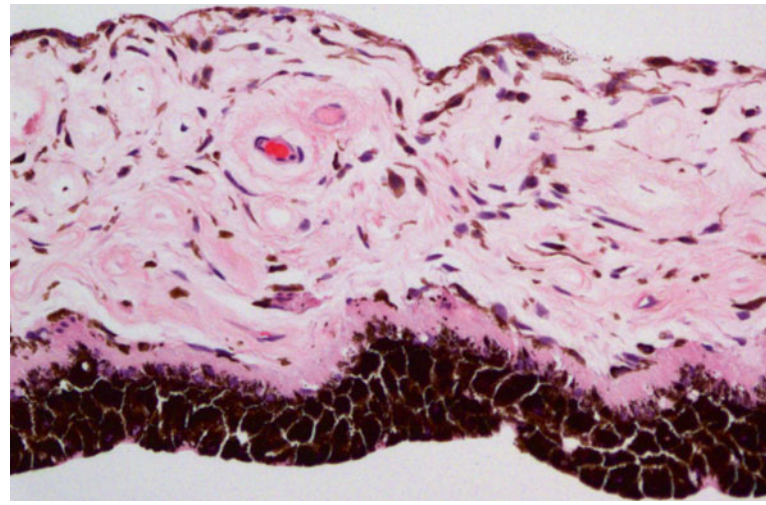

Fig. 10.2 Histological section of a normal iris, demonstrating the posteriorly located iris pigment epithelium, the adjacent dilator muscle, the loose iris stroma with thick-walled capillaries and the anterior accumulation of the normal melanocytes (×20 objective; HE)

aqueous humour that fills the anterior chamber. The aqueous leaves the eye by passing through the trabecular meshwork and its associated drainage channels located between the iris and the peripheral cornea. The ciliary processes of infants are smooth and pigmented. With age, the processes become more hyalinised as collagenous connective tissue accumulates around the vessels in their cores (Fig. 10.3a).

The pars plana (or flat part) of the ciliary body (Fig. 10.3b) is located posterior to the pars plicata and forms a circular band that extends to the ora serrata. The term ora serrata, meaning 'toothed mouth', is derived from the serrated appearance of this junction, caused by alternating dentate projections and oral bays of the peripheral retina (Fig. 10.3c). The dentate processes and oral bays are prominent in the nasal ora serrata. Posterior to the ora, the peripheral retina has a moth-eaten appearance due to the presence of peripheral microcystoid degeneration (Fig. 10.3d).

The outer layer of the ciliary epithelium is pigmented. At the ora serrata, it continues posteriorly as the retinal pigment epithelium (RPE),

whilst the inner non-pigmented ciliary epithelium abruptly thickens to form the neurosensory retina. The stroma of the ciliary body is composed largely of smooth muscle. The ciliary muscle has circular, longitudinal and radial parts, and its primary function is focusing or accommodation (Fig. 10.3e). The longitudinal ciliary muscle of Bruecke attaches to the scleral spur, a ridge of connective tissue located directly behind the trabecular meshwork and the canal of Schlemm. The scleral spur is the only location where the ciliary body is firmly attached to the sclera.

The *choroid* is the posterior part of the uvea and is responsible for supplying oxygen to the outer layers of the retina. It is located between the RPE and the sclera, with Bruch's membrane limiting it internally and the pigmented lamellae of the *lamina fusca* externally (Fig. 10.4). The anterior limit of the choroid is the ora serrata where the ciliary stroma merges irregularly into the

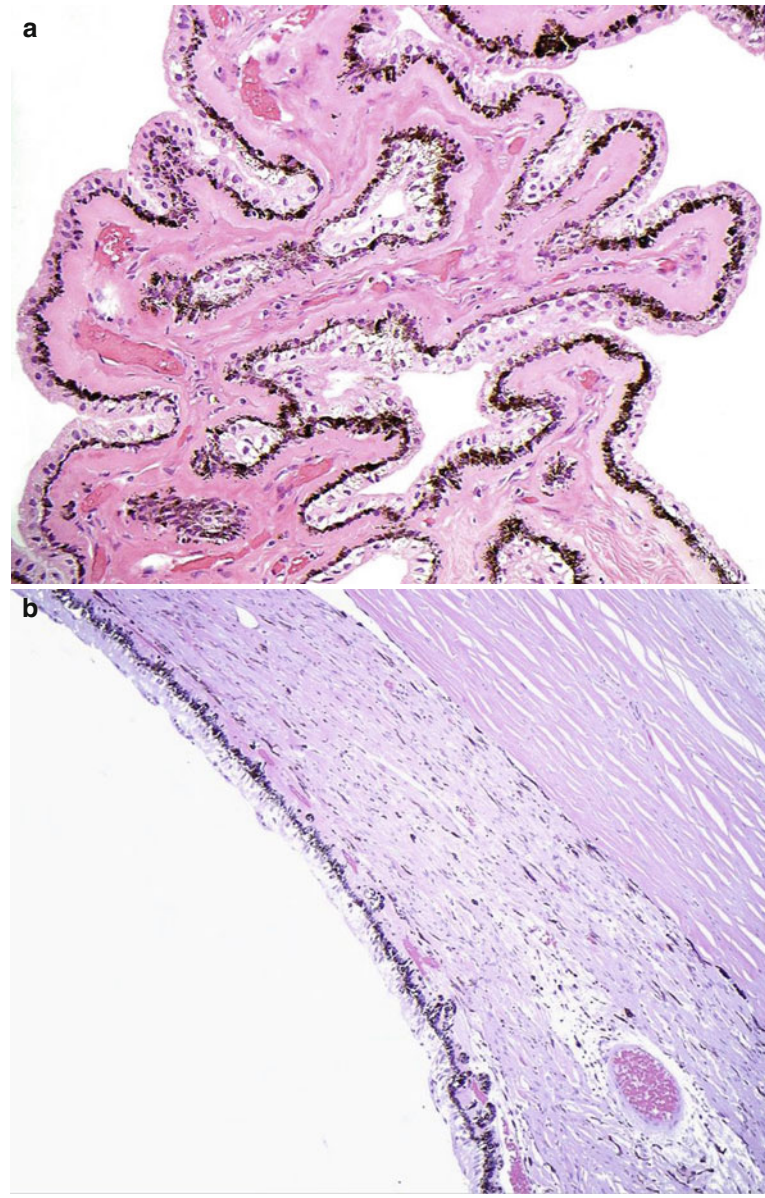

Fig. 10.3 (**a**) High-power magnification of ciliary body processes with the outer non-pigmented epithelium, the inner pigmented layer and the hyalinised stroma with the centrally placed blood vessels (×60 objective; HE) (Courtesy of Hardeep Mudhar, Sheffield, UK). (**b**) The pars plana is the flat part of the ciliary body and forms a circular band that extends to the ora serrata (×20 objective; HE). (**c**) Histological section of the ora serrata: the term ora serrata, meaning 'toothed mouth', is derived from the serrated appearance of this junction, caused by alternating dentate projections and oral bays of the peripheral retina (×60 objective; HE). (**d**) Peripheral microcystoid changes of the peripheral retina, giving it a 'moth-eaten' appearance (×60 objective; HE). (**e**) Histological section of the ciliary muscle, which has circular, longitudinal and radial parts, and its primary function is focusing or accommodation (×100 objective; HE) (Courtesy of Hardeep Mudhar, Sheffield, UK)

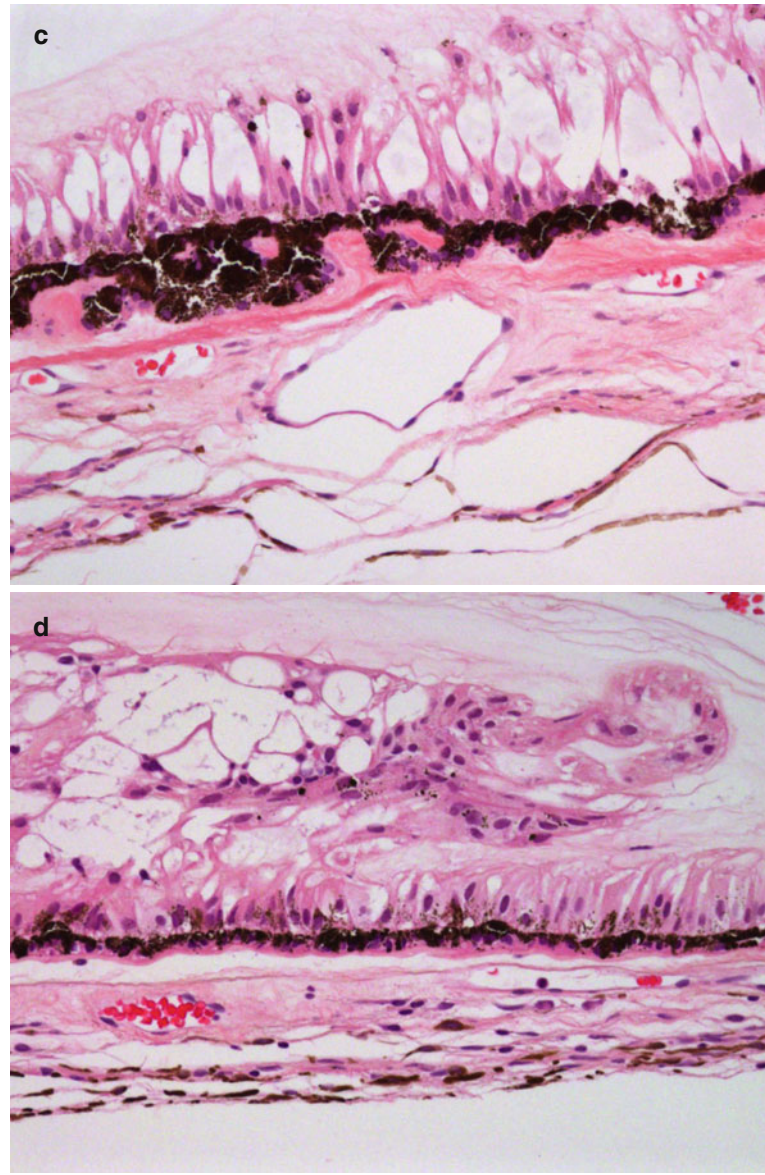

Fig. 10.3 (continued)

Fig. 10.3 (continued)

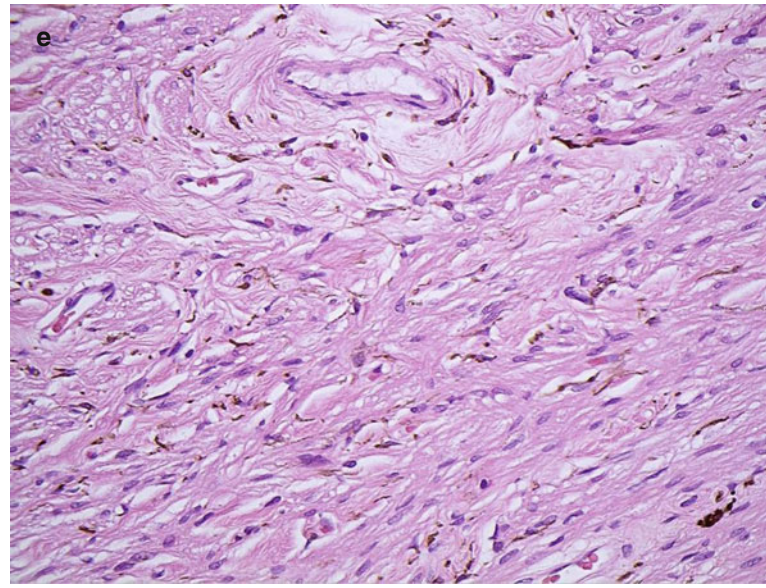

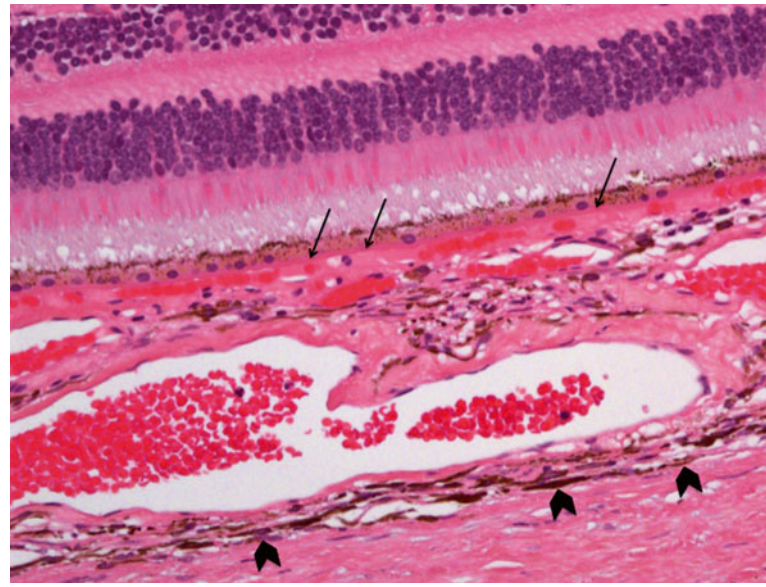

Fig. 10.4 Histological cross section of the choroid and adjacent retina, demonstrating its inner border, Bruch's membrane (*arrows*) and the outer pigmented *lamina fusca* (*arrow heads* chevrons). It can be seen that the inner choriocapillaris contains the smaller capillaries of the lobules with the larger vessels being located externally. The sclera is the outermost coat of the eye (H&E section, ×40 objective)

choroidal stroma. Bruch's membrane arises from a thin basal membrane of the pars plana pigment epithelium. The posterior part of the choroid wraps around the optic nerve and merges with its glial tissue and axons (*Elschnig-Scheide or rim*). Both Bruch's membrane and the RPE also end close to the optic nerve edge. The thickness of the choroid varies with it being the thickest at the posterior pole, measuring 0.22 mm, and decreasing considerably to 0.10 mm at the ora serrata.

The structure of the choroid is generally divided into four layers:

(a) Haller's layer – the outermost layer of the choroid consisting of larger diameter blood vessels
(b) Sattler's layer – the next inner layer comprising mainly medium diameter blood vessels
(c) Choriocapillaris – the layer of capillaries
(d) Bruch's membrane (also termed lamina basalis, complexus basalis, lamina vitra) – the innermost layer of the choroid.

The choroid also consists of the choroidal stroma in which scattered lymphocytes and melanocytes are seen. It is thought that the melanin within the melanocytes aids the choroid limit uncontrolled reflection within the eye that would potentially result in the perception of confusing images.

The blood supply of the choriocapillaris arises from the posterior ciliary arteries, branches of which form the numerous end arterioles within the segments of the choriocapillaris. Each of the segments or lobules, which measure 620–830 nm, forms a miniature capillary system leading from a central blood vessel to the venules at the edge, which in turn drain into the vortex veins, numbering between 3 and 5 behind the equator of the eye. The endothelium of the choriocapillaris is fenestrated allowing for the permeability of substances, such as fluorescein. The choroid is loosely joined to the sclera, and hence there is a potential suprachoroidal space, which blends into the supraciliary space. Together both the supraciliary and suprachoroidal spaces extend from the scleral spur to Elschnig's rim of the optic nerve. They are transected posteriorly only by the numerous posterior ciliary arteries and nerves.

10.3 Congenital Abnormalities

Congenital abnormalities of the uvea can be divided into those affecting the 'uvea as a whole', and those that affect one of the three structures within the uveal tract, particularly the iris.

10.3.1 Uvea (as a Whole)

(a) *Extramedullary haemopoiesis*: In premature infants and less commonly in full-term infants, focal or diffuse extramedullary haemopoiesis may be observed. It is important to differentiate these from leukaemic infiltrates.

(b) *Congenital ocular melanosis*: This is a unilateral condition caused by an increased number of atypical benign uveal melanocytes. The iris is darker and thicker than on the contralateral side, causing *heterochromia iridum*. The increased episcleral pigmentation renders the sclera a pale grey colour. This occurs in the pure ocular form of congenital melanosis and in the oculodermal melanocytosis of the naevus of Ota. White patients with congenital ocular melanosis also have an increased incidence of melanoma.

(c) *Albinism*: The associated disturbance of melanin synthesis affects not only the uveal melanocytes but also the pigment epithelium [1, 2]. Histopathologically, there is an absence or a decrease of melanin pigment within the uveal melanocytes. The pigment deficiency is often complete within the melanocytes whereas pigmentation is decreased but still present within the melanin containing cells of the RPE. Many cases of albinism are associated with foveal aplasia, in which the foveal reflex is absent and no foveal depression can be demonstrated after serial sectioning.

(d) *Colobomas*: These are caused by defects in closure of the embryonic ocular fissure, characteristically occurring inferonasally in the region of the fissure [3, 4]. Colobomas are defined as 'conditions where a portion of the structure of the eye is lacking'. Because the primary defect in a typical coloboma is in the neuroectoderm, absence of the mesectodermal stroma is a secondary phenomenon. An absolute scotoma is present in the region of the coloboma because the overlying retina is absent or dysplastic. Although most colobomas are sporadic, they are occasionally inherited as isolated ocular defects, usually in an autosomal dominant fashion with incomplete penetrance.

10.3.2 Iris (Alone)

(a) *Aniridia*: This is almost always a bilateral malformation that is inherited as an autosomal dominant trait (85 % of cases) or occurs sporadically [5, 6]. An association of the sporadic form of aniridia has been demonstrated

to be associated with Wilm's tumour of the kidney (Miller syndrome) and occurs in 13 % of cases. Most cases of aniridia are caused by mutations in the *PAX6* gene on the short arm of chromosome 11. Miller syndrome is caused by deletions in 11p that include both the *PAX6* gene and the tumour suppressor gene *WT1* [7].

Both variations of aniridia can be associated with congenital or juvenile glaucoma. The designation 'aniridia' is actually a misnomer: these cases actually represent extreme hypoplasia of the iris, which are hidden clinically by opaque limbal tissues. Associated lens opacities and lens colobomas may occur, and foveal aplasia similar to that seen in albinism has been described.

(b) *Corectopia*: There are several causes of corectopia (an eccentric location of the pupil), one of them being an anomalous closure of the embryonic fissure. Corectopia as well as polycoria (the presence of multiple papillary openings) can also be caused by primary dystrophic processes and by mechanical traction caused by the persistence of the anterior tunica vasculosa lentis and pupillary membrane.

A large spectrum of iris anomalies is associated with peripheral congenital corneal opacities (termed *leukomas*) [8, 9]. An example of this is 'Peter's syndrome', which probably represents a delayed separation of the lens vesicle from the overlying surface ectoderm during embryogenesis.

(c) *Von Recklinghausen neurofibromatosis* (*NF-1*): This is one of the most common hereditary diseases, as the *NF-1* gene, which is located on chromosome 17, is quite large and is subject to mutation [10]. Neurofibromin is the protein product of the *NF-1* gene and normally interacts with the *ras* oncogene to decrease growth stimulatory signals. The syndrome *NF-1* is characterised by tumours of Schwann cells, which typically occur in the skin as multiple fibroma molluscum. Ocular findings in NF-1 are numerous, but include Lisch nodules (*melanocytic hamartomas*) on the iris and hamartomatous infiltration of the uvea with tactile corpuscle-like ovoid bodies [11].

(d) *Congenital iris stromal cysts*: These are diagnosed in early childhood with most being recognised before the age of 10 years [12]. They have a thin wall and the lumen contains clear or slightly turbid fluid. Histopathologically, an iris stromal cyst is lined by thin non-keratinising stratified epithelium that sometimes contains goblet cells. It is thought that these develop secondary to developmental displacement of conjunctival epithelium into the iris during embryogenesis. Treatment options include aspiration, laser to the cyst wall, iridectomy or iridocyclectomy, mitomycin C as well as injection of alcohol into the cyst with irrigation.

(e) *Intraocular lacrimal gland choristoma*: This is ectopic placement of lacrimal gland tissue within the eye, with most lesions affecting the eye, but some affecting both the iris and the ciliary body [13]. It appears in early infancy as a fleshy reddish pink mass with a slightly lobulated surface. Clear cysts can appear as a result of the ectopic lacrimal gland secretion and may progressively enlarge to cause iris atrophy, secondary glaucoma and cataract. Histopathological examination reveals normal lacrimal gland tissue. Whilst observation is recommended initially, local resection of the tumour is the treatment of choice.

10.4 Inflammation

Definition

'Uveitis' is the term given to inflammation of the uveal tract [14].

Aetiology

Uveitis is often idiopathic, but it may be associated with systemic disorders including juvenile rheumatoid arthritis, ankylosing spondylitis, Reiter's syndrome, ulcerative colitis, regional enteritis or Behcet's disease. The reader is referred to specific reviews and textbooks, as the details are outwith the scope of the current chapter [14].

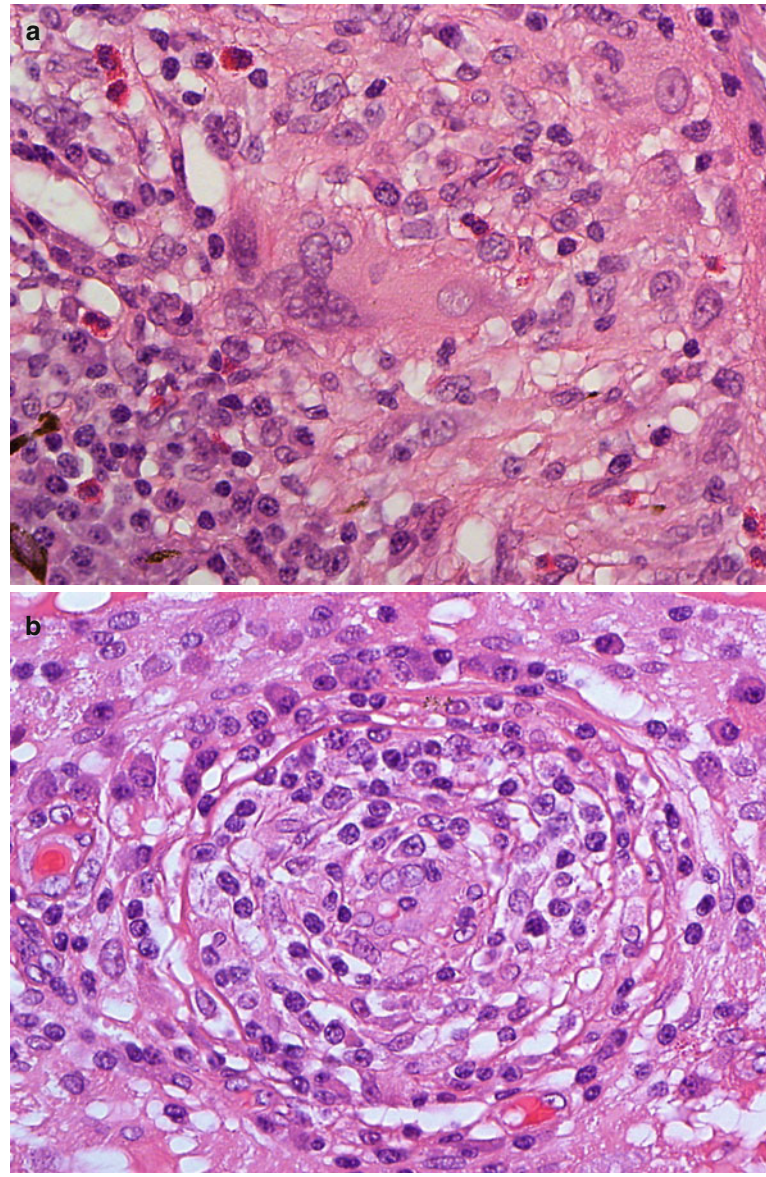

Fig. 10.5 (**a**) Histological section of a non-caseating granulomatous inflammation of the choroid with large multinucleate cells and scattered eosinophilic granulocytes in a patient with Wegener's granulomatosis (×60 objective; HE). (**b**) Obliterative vasculitis of the choroid in Wegener's granulomatosis (×60 objective; HE). Included in the differential diagnosis of such a case is Behcet's disease, although granulomata are unusual in the latter

Histology

Broadly, uveitis can be divided into *granulomatous* and *non-granulomatous* disease. In the latter, microscopy reveals an infiltrate of plasma cells and lymphocytes in the uveal stroma. *Sarcoidosis* is the most common cause of granulomatous uveitis; close to 40 % of all patients with systemic sarcoidosis will have ocular disease at some stage of their disease [15]. The main differential diagnosis to granulomatous uveitis includes other autoimmune diseases (e.g. Wegener's granulomatosis; Fig. 10.5a, b) as well as diseases of infectious origin (e.g. intraocular tuberculosis, leprosy, syphilis, parasites and fungal infections, including candidiasis and Lyme disease). It is important to note, however, that granulomatous inflammation is also found in sympathetic uveitis (see below) and Vogt–Koyanagi–Harada disease.

Special Inflammatory Subtypes

Vogt–Koyanagi–Harada disease (or uveomeningoencephalitic syndrome) is characterised by moderate to severe uveitis (anterior and posterior),

secondary retinal separation, poliosis (whitening of hair), vitiligo (loss of cutaneous melanin), dysacousia and meningitis [16]. Not all patients have all symptoms and the degree of symptomatology differs from patient to patient.

Behcet's disease is a systemic immune complex disease characterised by genital and oral aphthous ulcers and recurrent non-granulomatous iridocyclitis with hypopyon [17, 18]. Uveitis associated with obliterative vasculitis should raise the possibility of this disease.

Histiocytic inflammatory disorders can sometimes involve the uveal tract and include *juvenile xanthogranuloma* (JXG) and *Langerhans' cell histiocytosis*.

JXG is an idiopathic benign inflammatory disorder of young children and occasionally adults [19]. It is characterised by multiple cutaneous yellow-pink papules that develop rapidly and resolve spontaneously without treatment. Most cases are confined to the skin, but involvement of ocular tissue, including the uvea, has been described [20]. On the other hand, many patients with intraocular JXG have no history of cutaneous lesions. Histopathologically, iris JXG presents as a variably sized mass with numerous small capillaries with an infiltration of histiocytes, lymphocytes, eosinophils as well as multinucleate giant cells of Touton type. The stain is negative for S-100P, excluding other histiocytoses such as LCH. JXG is usually responsive to steroids; other methods of treatment include iridectomy or iridocyclectomy.

LCH is a neoplastic proliferation of Langerhans' cells with expression of CD1a, S100 protein and the presence of Birbeck granule on ultrastructural examination. It can be subdivided into (a) eosinophilic granuloma, (b) Hand-Schüller-Christian and (c) Letterer–Siwe disease. Ophthalmic involvement occurs in 10 % of cases, with the choroid being the most commonly involved ocular site (Fig. 10.6a–d). The differential diagnosis includes Rosai–Dorfman disease and necrobiotic xanthogranuloma [19, 21–23].

Treatment and Prognosis

This is dependent on the underlying cause of the inflammation and may require a battery of medications, ranging from glucocorticoid steroids to antimetabolite medications, such as methotrexate, depending on the degree of chronicity and aggressiveness of the inflammation [14]. The type of uveitis and its severity, duration and responsiveness to treatment or any associated illnesses all factor into the ultimate outcome of the disease.

The sequelae of ocular inflammation include corneal scarring and vascularisation, band keratopathy, cataract as well as secondary glaucoma. Intraocular fibrosis, gliosis and membrane (synechiae) formation are caused by attempts at 'organisation' of the inflammation. The end-stage findings can include, however, chronic retinal detachment, ocular shrinkage and hypotony, ultimately resulting in phthisis bulbi (atrophia bulbi with shrinkage and disorganisation). Osseous metaplasia of the RPE is often in the posterior parts of these phthisical eyes.

10.5 Injuries and Trauma

Introduction

The ophthalmic laboratory frequently processes eyes that have been subject to either surgical or nonsurgical trauma. Most cases show intraocular haemorrhage and loss or incarceration of intraocular structures. Injuries and trauma also predisposes to infection, which could be due to organisms introduced into the eye through penetrating injuries or contaminated intraocular foreign bodies, resulting in secondary exogenous endophthalmitis.

Severe contusions to the eye can cause separation of the iris, or iris and ciliary body, from the sclera (*traumatic cyclodialysis*). Trauma severe enough to do this also may cause retinal separation. This often leads to hypotony or phthisis bulbi. It also may be called recession of the chamber angle. It is not treatable.

The main condition to be discussed in this chapter is *sympathetic uveitis* (*sympathetic ophthalmia*).

Definition

Sympathetic uveitis (*ophthalmia*) is a severe bilateral granulomatous inflammation of the uveal tract that follows unilateral trauma or

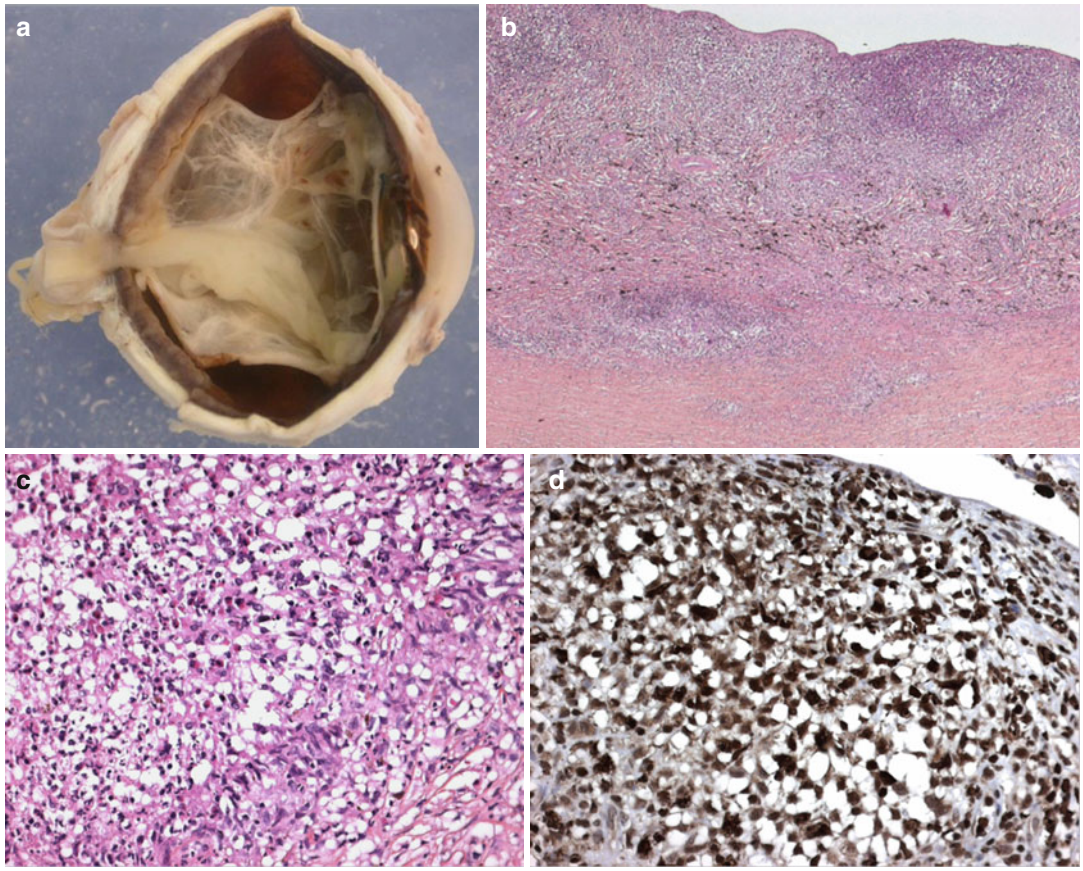

Fig. 10.6 (**a**) Macroscopic picture of an enucleated eye of a child with extensive uveal involvement by Langerhans cell histiocytosis. Thickening of almost the entire uveal tract is seen with an associated complete retinal detachment (×1.5 objective). (**b**) Low-power section of the choroidal thickening caused by a dense cellular infiltration confined to the choroid with some infiltration into the sclera (×10 objective; HE). (**c**) Higher power demonstrates that the infiltrating cells comprise a mixture of spindle cells with admixed eosinophils and occasional scattered multinucleate cells (×40 objective; HE). (**d**) The vast majority of the infiltrating cells demonstrated positivity for CD1a, S100 protein and CD68PG (picture) (×40 objective; PAP immunostaining) (Pictures courtesy of Dr Frederic Charlotte, Paris, France)

surgery, which is usually complicated by incarceration of uveal tissue in the wound [24, 25].

Clinical Features

The patients present with blurred vision, photophobia and signs of inflammation in the uninjured fellow eye accompanied by signs of inflammation in the injured eye. Sympathetic uveitis occurs between 2 weeks and 1 year post-injury in about 90 % of cases, with most occurring in the 3-week to 3-month interval. It will not, however, develop if the injured eye is enucleated within 1 week of the injury. Delayed enucleation of the injured eye places the fellow at risk. Rare cases of sympathetic ophthalmia have been reported following ocular evisceration [26] and following proton beam in uveal melanoma [27].

Aetiology

It is thought to be a T-cell-mediated autoimmune response to uveal or retinal antigens released during or as a result of the injury. It has been proposed that uveal pigment, retinal S antigen and interphotoreceptor retinoid-binding protein could be the possible antigens [24, 25].

Histology

Four characteristic features are found on histopathological examination of enucleated eyes with sympathetic uveitis. These include (1) diffuse thickening of the uvea by a granulomatous infiltrate composed of epithelioid histiocytes, inflammatory giant cells and CD8+ lymphocytes. Plasma cells are rarely seen in the infiltrate, and eosinophils can be found within the infiltrate in deeply pigmented patients. (2) The choriocapillaris is not destroyed by the inflammation, and the retina is spared. (3) The histiocytes usually contain granules of phagocytosed uveal pigment. (4) Nodular aggregates of epithelioid cells, which focally detached the RPE, are found on the inner surface of Bruch's membrane [25]. These nodules, called Dalen–Fuchs nodules, are not pathognomonic for sympathetic uveitis, since they also occur in sarcoidosis and Vogt–Koyanagi–Harada disease.

10.6 Degenerative Conditions of the Uvea

Introduction

Degenerative conditions of the uvea are usually related to increasing age or as a complication of inflammation. Examples include:

(a) *Iris atrophy*: This frequently occurs in previously normal irises as patients get older (senile iris atrophy). The effects on the pupillary border are most visible: the border will appear ragged and the sphincter muscle may be severely affected causing a loss of the pupillary response to light. This is important to remember when evaluating pupillary responses in an elderly patient. Histological examination demonstrates thinning of the sphincter muscle and of the iris stroma. Severe anterior uveitis or chronic glaucoma may result in destruction of the anterior uvea, particularly of the ciliary body. This eventually leads to phthisis bulbi or an enlarged, hypotonic globe, for which there is no treatment apart from enucleation.

(b) *Iris rubeosis*: This is characterised by the formation of new fragile blood vessels on the surface of the iris, extending often into the chamber angle. This neovascularisation is usually associated with disease processes occurring in the retina, e.g. diabetes mellitus with advanced proliferative diabetic retinopathy, which results in the retina becoming ischaemic and releasing a number of angiogenic factors, most importantly vascular endothelial growth factor (VEGF). Other causes of retinal disease causing rubeosis iridis include central retinal vein occlusion, ocular ischaemic syndrome and chronic retinal detachment. It can also be seen following treatment of large choroidal melanomas that undergo the so-called toxic tumour syndrome (a term coined by Prof. Bertil Damato), following either proton beam or plaque therapy, releasing VEGF into the eye. This can be treated by removing the residual necrotic tumour tissue, e.g. by endoresection [28]. The blood vessels in iris rubeosis eventually undergo fibrosis, which may result in the formation of synechiae with the posterior surface of the cornea and in angle closure leading to 'neovascular glaucoma'. Similarly, the iris leaf may be distorted and its papillary margin may be pulled posteriorly (rubeosis entropion uveae) or anteriorly (rubeosis ectropion uveae) (Fig. 10.7a).

(c) *Lacey vacuolation of iris pigment epithelium*: This is due to the accumulation of glycogen and is present in 40 % of enucleated eyes from diabetics. It is termed 'diabetic iridopathy' (Fig. 10.7b).

(d) *Thickening of the ciliary body processes*: This is particularly seen in patients with diabetes mellitus and can be highlighted in the periodic acid-Schiff (PAS) stain (Fig. 10.3a). The cause for this is unclear at present.

(e) *Cystic degeneration of the ciliary body associated with coloboma* [29] and with degenerative retinoschisis [30].

(f) *Choroidal neovascularisation membrane formation* with breakdown of Bruch's membrane is associated with a number of retinal diseases, including wet age-related macular degeneration

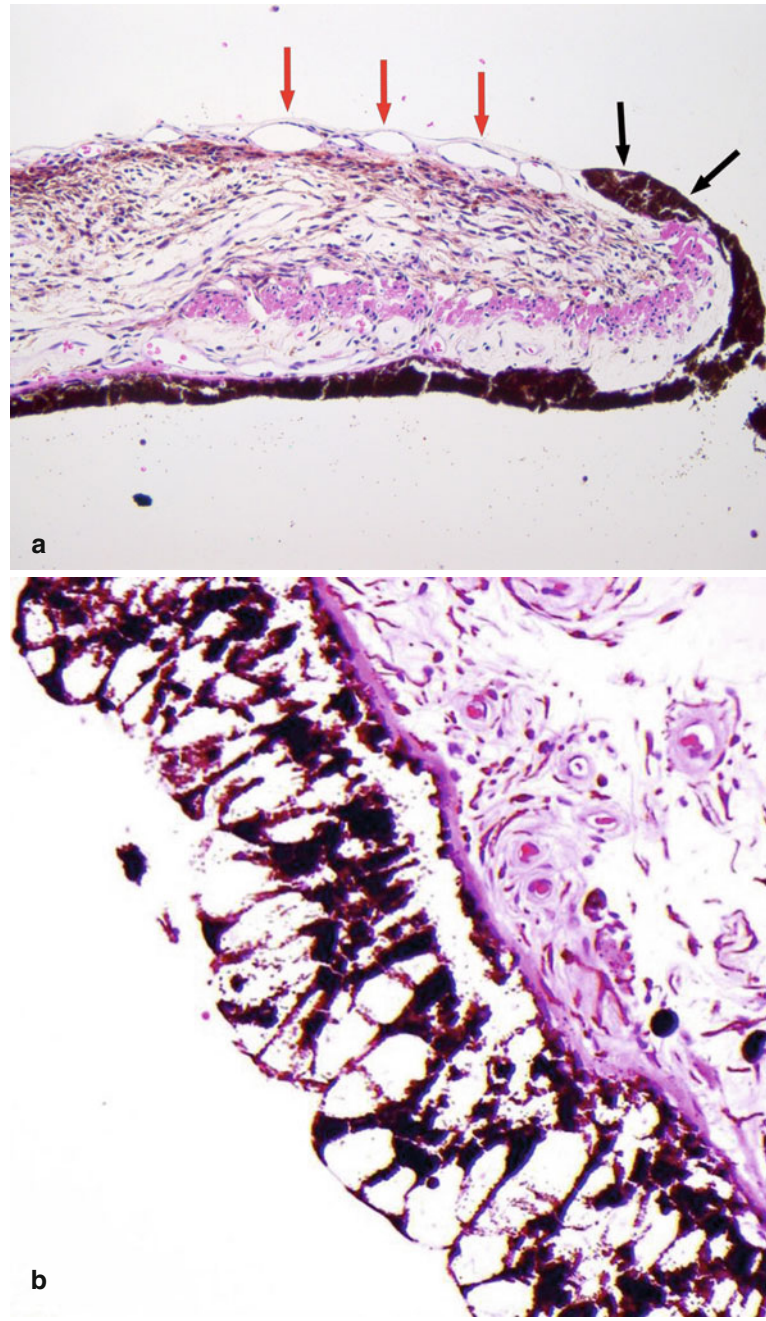

Fig. 10.7 (**a**) High-power histological section of an iris demonstrating ectropia (i.e. outward retraction of the iris pigment layer and adjacent sphincter muscle) (*black arrows*) caused by fibrosis of the fine layer of new blood vessels located on the anterior surface of the iris (*red arrows*). Such iris rubeosis leads to secondary neovascular glaucoma when extending into the anterior chamber angle (×60 objective; HE). (**b**) Lacey vacuolation of the iris pigment epithelium caused by the accumulation of glycogen within the cells, seen in 40 % of diabetic patients (Courtesy of Hardeep Mudhar, Sheffield, UK)

(AMD). AMD is a very common cause of visual loss in older patients. It often produces haemorrhage that can sometimes simulate clinically a pigmented choroidal melanoma. The reader is referred to the numerous major reviews on AMD, as this disease is outwith the scope of this chapter [31–34].

10.7 Neoplasms

10.7.1 Uveal Naevi

Definition

Uveal naevi are benign melanocytic neoplasms that do not demonstrate any cytological atypia and do

not metastasise. They occur in 5 % of adults and are thereby the most common intraocular tumour.

Iris naevi present as pigmented macular lesions, are very slowly progressive and are often completely static over years. When the clinical presentation is not suspicious, in most cases the lesion will not be excised. Should the lesion be removed by, e.g., iridocyclectomy, histology shows a symmetrical well-defined lesion, located in the anterior part of the iris stroma, and usually composed of small spindle cells with small, uniform nuclei. Rounded naevus cells can be observed; epithelioid cells are exceptionally rarely seen and should be considered in the context of the surrounding tissue to differentiate the lesion from a melanoma.

Ciliary body naevi are very rare; the histology is comparable with iris naevi: spindle-shaped cells without atypia and without mitotic figures.

Most *choroidal naevi* typically appear as flat or minimally elevated patches of increased choroidal pigmentation that measure between 1 and 2 mm in diameter and <2 mm in height [28, 35]. Although they may be congenital, choroidal naevi are rarely observed in young children. They may be pigmented or amelanotic, and they can often have an irregular or feathery border. Choroidal naevi can cause the following secondary changes in the tissues surrounding them: (a) narrowing of the choriocapillaris, (b) RPE degeneration and proliferation with only tiny amounts of lipofuscin formation, (c) small serous retinal detachment with photoreceptor damage and (d) choroidal neovascularisation. Histologically, choroidal naevi are bland spindle cell tumours with the naevus cells having small oval- or cigar-shaped nuclei that lack nucleoli or nuclear folds (Fig. 10.8a, b). There is a variable degree of cytoplasmic pigmentation. Mitoses are absent. It is estimated that only 1/10,000–15,000 per year undergo malignant transformation to a melanoma [36, 37].

10.7.2 Melanocytoma

Introduction

Melanocytoma (*syn. magnocellular naevus or hyperpigmented magnocellular naevus*) is a characteristic type of uveal naevus, which merits a separate subsection [38, 39]. Melanocytomas classically involve the optic disc but can also occur in the iris, ciliary body and choroid. They are intensely pigmented and often occur in young patients, with a slightly higher incidence in females.

Clinical Features

Unlike uveal melanoma, it is rare in Caucasians and relatively common in dark-skinned people. For example, 37–50 % of optic disc melanocytomas have been described in African Americans. They may be quite large and difficult to distinguish from a melanoma on clinical findings. This is particularly the case if they extend into the anterior chamber and extraocularly, mimicking malignant invasion.

Histological Evaluation

Histological evaluation of melanocytomas usually requires bleached sections. These reveal a tumour composed of plump polyhedral naevus cells filled with large amounts of strongly pigmented cytoplasm and small discrete nuclei (Fig. 10.9a, b). Nucleoli are usually (but not always) inconspicuous. No mitoses are seen. Melanocytomas are known to undergo spontaneous necrosis, resulting in an infiltration of macrophages, which phagocytose the melanin. There may be associated pigment dispersion, which may reach the anterior chamber and cause obstruction to the drainage angles (*melanocytomalytic glaucoma*) [40].

Genetics

Recent genetic examinations of two ocular melanocytoma have revealed *GNAQ* mutations in these two tumours [41].

Prognosis

Prognosis of melanocytoma for survival is excellent unless there is a very rare malignant transformation to melanoma [42]. This occurs rarely, with a frequency of <1 %. Visual loss may occur in optic disc melanocytomas, however, due to optic nerve damage (e.g. central retinal artery obstruction) and is usually permanent.

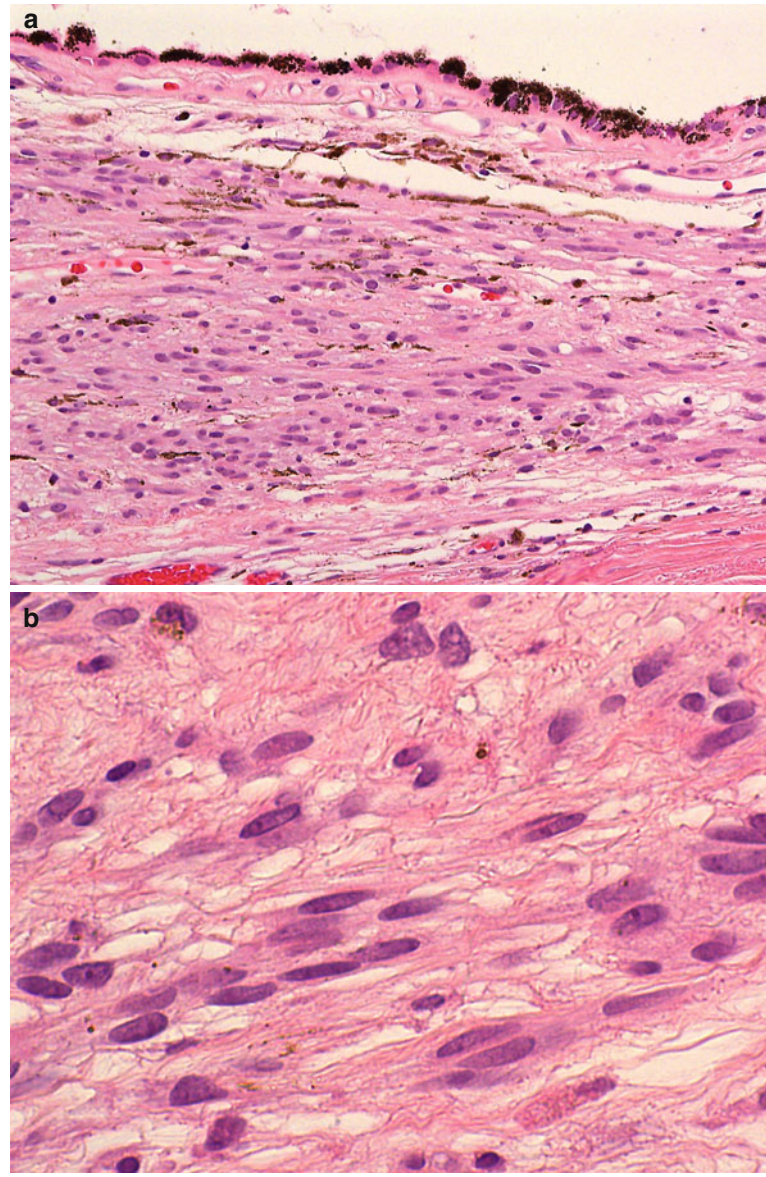

Fig. 10.8 (**a**) Histological section of a choroidal naevus (×40 objective; HE). (**b**) Higher power demonstrates that the naevus consists of loose stroma within which are spindle cells with elongated nuclei and very discrete nucleoli. Mitoses are absent (×60 objective; HE)

10.7.3 Bilateral Diffuse Uveal Proliferation (BDUMP)

Definition

Bilateral diffuse uveal melanocytic proliferation (BDUMP) is a rare paraneoplastic syndrome characterised by an extensive benign proliferation of melanocytes within the uvea, causing bilateral visual loss in patients with an underlying extraocular malignancy [43–45].

Clinical Features

The most common malignant tumours associated with BDUMP are carcinomas, with ovarian and endometrial carcinomas being the most prevalent in women and lung and pancreatic cancer in men [46]. The patients present with gradual loss of vision and increasing intraocular pressure. On ophthalmoscopy, multiple red patches at the level of the retinal pigment epithelium, exudative retinal detachment and rapidly progressing cataracts are typically seen (Fig. 10.10a).

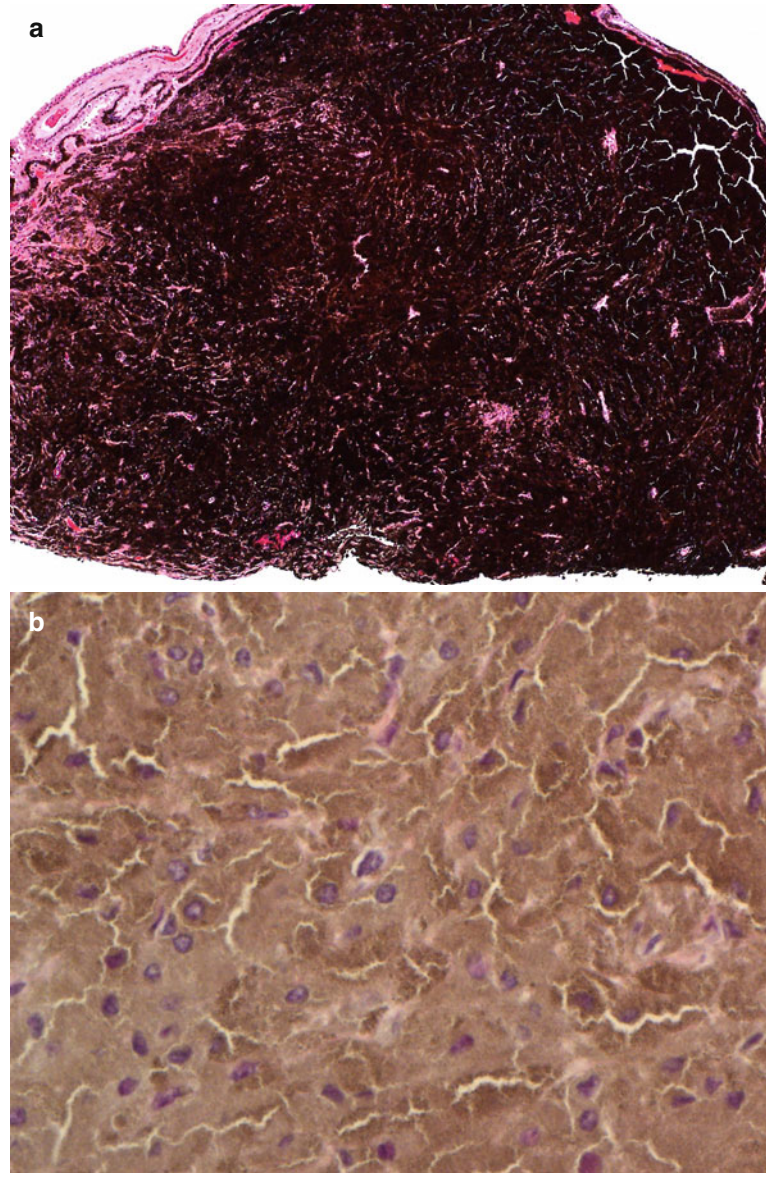

Fig. 10.9 (**a**) Iridocyclectomy specimen of a ciliary body melanocytoma, consisting of strongly pigmented naevus cells (×10 objective; HE). (**b**) The bleached HE sections demonstrate that the melanocytoma is composed of polyhedral naevus cells rich in cytoplasm and with small ovoid nuclei (×60 objective; bleached HE)

Aetiology and Genetics

The exact pathogenesis of BDUMP is unknown; however, many authors speculate that a humoral factor produced by the primary extraocular malignancy induces the melanocytes of the eye to proliferate. Recent genetic analyses demonstrate that the BDUMP cells do not show any changes in copy number for chromosomes 3 and 8 were found (by array comparative genomic hybridisation (CGH)), or *GNAQ*^{Q209} or Ditto^{V600E} mutations [47]. These findings are consistent with unpublished analyses of another case of BDUMP by Coupland et al. using multiplex ligation-dependent probe amplification (MLPA), examining copy number variation of chromosomes 1p, 3, 6 and 8 (unpublished; Fig. 10).

Histology

Histopathological examination of the specimens, usually enucleated eyes, shows diffuse infiltration of melanocytic cells in the choroid, ciliary body and iris root (Fig. 10.5b–d). These comprised a mixture of naevoid and spindle-shaped

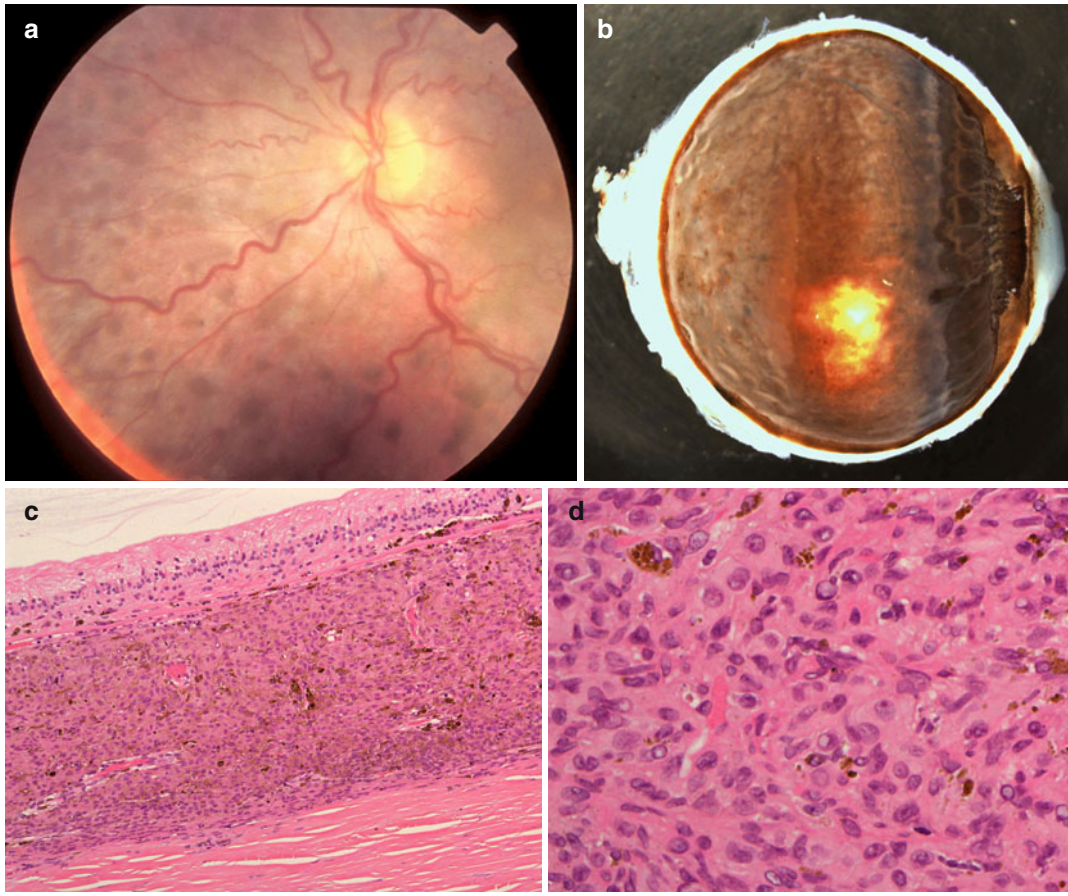

Fig. 10.10 (**a**) Fundoscopy of a 67-year-old woman with loss of vision in her right eye and with a history of a recently diagnosed clear-cell endometrial carcinoma. Multiple small nodular pigmentations within the choroid are seen (Courtesy of Prof. Damato, Liverpool Ocular Oncology Centre). (**b**) Enucleated right eye with a diffuse proliferation of pigmented cells within the uvea, also involving the iris (×1.5 objective). (**c**) Histological section demonstrating the diffuse cellular infiltration of partially pigmented cells limited to the choroid. Bruch's membrane is intact. The overlying retina demonstrates atrophy (×40 objective; HE). (**d**) Higher-power magnification shows that the cellular infiltrate is composed of plump spindle cells with round oval nuclei and small nucleoli. No mitoses are seen. In the background are scattered melanophages (×60 objective; HE)

cells with very occasional cells displaying cellular atypia. No mitotic figures are observed. The cells stain positively with Melan A and HMB45.

Treatment and Prognosis

The management of BDUMP usually consists of treatment of the primary tumour, which should result in regression of the melanocytic proliferation within the uvea of the eye. Should, however, there be no initial response, low-dose external beam radiotherapy and anti-glaucomatous treatment ate considered. The prognosis of the ocular disease is dependent on the response of the primary tumour to therapy.

10.7.4 Uveal Melanoma

Definition

Uveal melanoma is by far the commonest primary intraocular malignancy in adults and is therefore discussed more fully than other tumours. It is a malignant tumour occurring predominantly in the choroid (90 %) with the remainder being confined to the ciliary body and the iris [28].

Epidemiology

The overall incidence of uveal melanoma is six to seven per million per year. It increases with age

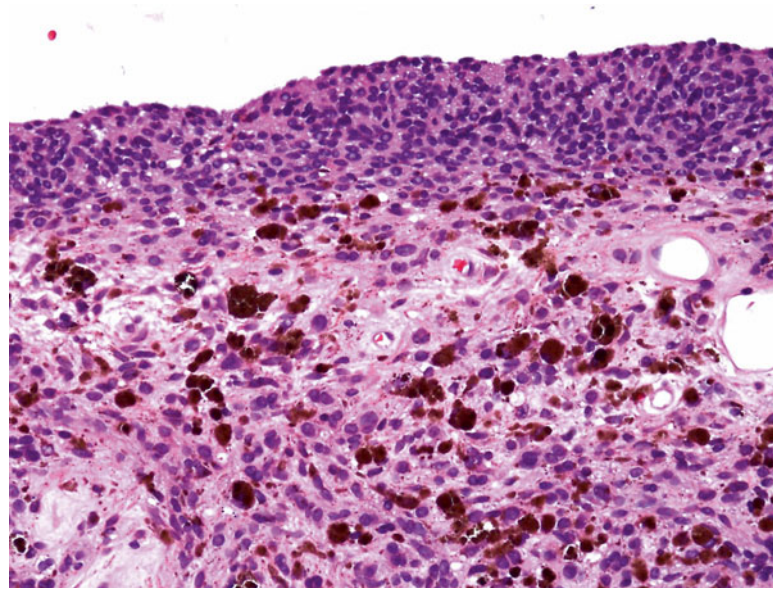

Fig. 10.11 Histological section of an iris melanoma of mixed cell type originating from the stroma but with diffuse spreading on the anterior surface (×40 objective; HE)

from about 2.5 per million between the ages of 15 and 44 years to 25 per million after the age of 65 years. The tumour is extremely rare in children. There is no significant sex difference. Uveal melanoma is much more common in Caucasians than in Africans or Asians. Epidemiological studies suggest that uveal melanoma is two to three times more common in blue/grey than in brown eyes. The importance of sunlight is uncertain but the evidence would suggest that it is unlikely to have a major role in uveal melanoma pathogenesis [28].

Aetiology

The aetiology of uveal melanoma is unknown; however, there are known associations with uveal melanoma. These include ocular melanocytosis (increased population of melanocytes within the uvea and episclera), oculodermal melanocytosis (naevus of Ota, which also involves the periocular skin and meninges), simple and dysplastic cutaneous naevi and cutaneous melanomas and neurofibromatosis type 1. Rare reports of families with an excess of uveal melanoma cases have been published. Recent evidence suggests that patients with a cancer susceptibility may have higher frequencies of uveal melanoma compared with the normal population [48, 49].

Localisation

Uveal melanomas arise in the choroid (80 %), ciliary body (12 %) and iris (8 %). Those occurring in the iris can be single nodular lesions, consist of multiple small nodules (*tapioca iris melanoma*) or extend as a 'carpet-like' growth across its anterior surface (Fig. 10.11) [28].

Clinical Features

Most frequently affected are white individuals in the sixth and seventh decades of life. Most choroidal melanomas are single and confined to one eye. The symptoms of patients with choroidal melanoma include:

(a) Blurred vision caused by retinal detachment, posterior tumour location or vitreous haemorrhage
(b) Visual field loss caused by retinal detachment
(c) Floaters from vitreous haemorrhage
(d) Photopsia described as a ball of light moving across the visual field over several seconds, more noticeably in subdued lighting
(e) Pain secondary to neovascular glaucoma or uveitis

There is a wide range of therapeutic options for the treatment of primary uveal melanoma [28]. These include various forms of radiotherapy, surgical resection and phototherapy. The 5-year local tumour control rates in most specialised treatment centres exceed 90 %. Despite this, almost 50 % of patients with uveal melanoma will develop disseminated disease, predominantly in the liver, but also in the lungs (24 % of patients) and bone (16 %) [28].

Macroscopy

When performing the macroscopy of an enucleated eye with uveal melanoma, care should be taken to observe whether any extraocular melanoma is present. This can occur anteriorly (e.g. at the limbus) (Fig. 10.12a) or posteriorly via the emissary blood vessels or along the optic nerve. Transillumination in a darkened room usually will allow for localisation of the tumour. Sectioning should allow for a PO (pupil optic nerve) block that also includes the tumour. In early cases of choroidal melanoma, the sectioned

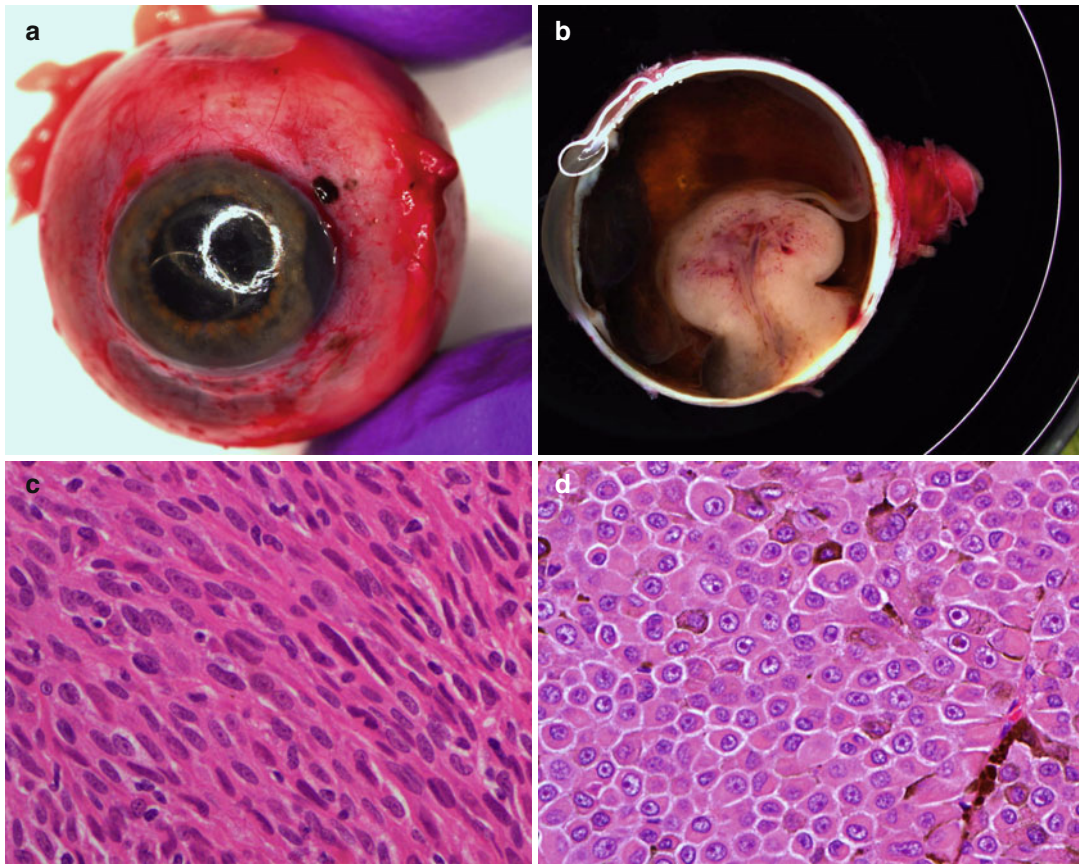

Fig. 10.12 (**a**) Gross examination of a fresh enucleated left eye shows a ciliary body melanoma on the lateral side of the eye with extension into the anterior chamber and with extraocular extension adjacent to the limbus at approx. the 1 o'clock position. (**b**) Sectioning of another fresh enucleated eye following transillumination demonstrates a non-pigmented choroidal melanoma with the classical 'mushroom' shape and central vascular congestion, as a result of Bruch's membrane perforation. The overlying retina is detached. The lens is still in place. Reflection artefacts are present at the upper limbus and sclera. (**c**) Histological section of a spindle B-cell choroidal melanoma (×60 objective; HE). (**d**) Classical epithelioid cell choroidal melanoma with well-demarcated cell membranes almost with the suggestion of intercellular bridging across the artefactual cell gaps, and with voluminous eosinophilic cytoplasm with scattered melanosomes. Nuclei are large with prominent nucleoli. (**e**) Closed connective tissue loops in an epithelioid-celled ciliary body melanoma as demonstrated on HE (×40 objective). (**f**) PAS stain without haematoxylin counterstain highlights the closed connective tissue loops in another uveal melanoma (×20 objective). (**g**) Posterior extraocular extension in a comparatively small choroidal melanoma at the optic disc, with clear trans-scleral extension into the soft tissues adjacent to the optic nerve (×10 objective; HE stain). (**h**) Patchy HSP-27 staining in a choroidal melanoma of epithelioid cell type: loss of HSP-27 protein expression is associated with a loss of chromosome 3 [54]. (**i**) A cytospin of an intraocular biopsy of a choroidal melanoma of spindle cell type surrounded by a mantle of erythrocytes (×60 objective; MGG stain). (**j**) Positivity of the tumour cells in (**i**) for melanocytic marker, Melan A (×60 objective, PAP stain)

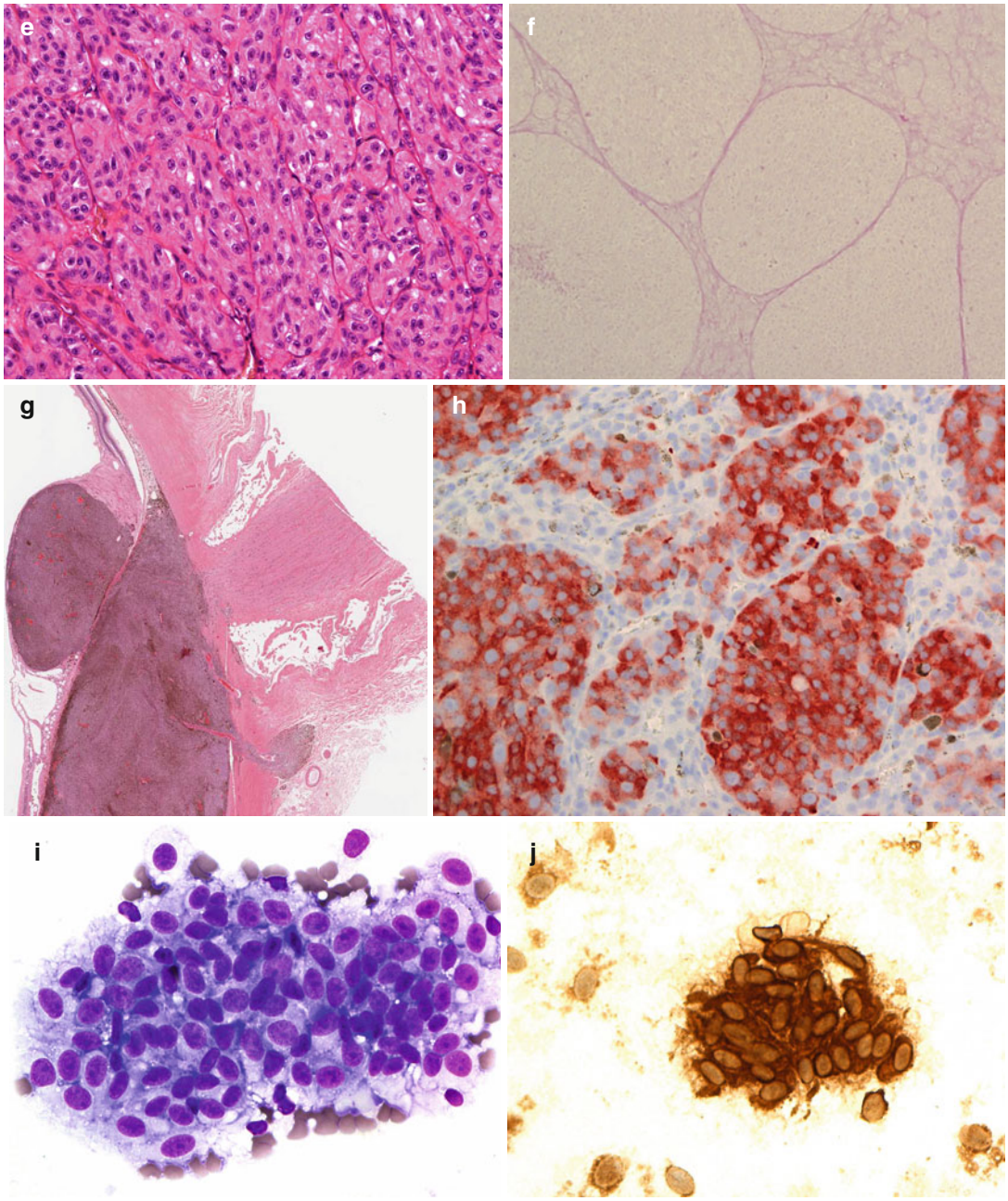

Fig. 10.12 (continued)

tumour profile is oval- or almond-shaped. Although some melanomas diffusely infiltrate the uvea, most choroidal melanomas are well-circumscribed tumours with distinct margins. In many cases, the growing choroidal melanoma perforates Bruch's membrane and pushes into the subretinal space where its apex typically assumes a collar stud or mushroom shape (Fig. 10.12b). Whilst a mushroom-shaped choroidal tumour is usually a choroidal melanoma, exceptionally rarely some metastases of systemic tumours can take on this configuration. The ruptured ends of

Bruch's membrane exert a compressive effect on the 'waist' of the choroidal melanoma causing vascular congestion and dilatation of blood vessels at the apex.

Choroidal melanomas typically cause an exudative serous retinal detachment of the overlying and adjacent retina. The overlying retina is often infiltrated by melanoma cells at the tumour apex, and dark vitreous seeding may be observed macroscopically.

Ciliary body melanomas are less common and tend to be more circular in shape, possibly with a 'diffuse tail' tapering posteriorly into the peripheral choroid. They may deform the crystalline lens and cause unilateral cataract. Occasionally, they may extend into the anterior chamber and seed along the iris surface or the trabecular meshwork, which may involve 360° of the anterior chamber ('ring melanoma').

Histopathology

Uveal melanomas consist predominantly of tumour cells with some admixed reactive cells usually representing a smaller proportion of the tumour's cellular content. According to the modified Callender classification, uveal melanomas consist of spindle B-cells and/or of epithelioid cells (Fig. 10.12c, d) [50]. The former are long and fusiform with a small oval nucleus and a prominent nucleolus (Fig. 10.12c). Epithelioid, which means 'epithelial-like', cells are large and round with abundant eosinophilic cytoplasm, usually distinct cell margins and prominent nucleoli (Fig. 10.12d). Variants of epithelioid cells include wildly anaplastic tumour giant cells and relatively uniform small epithelioid cells. Spindle A cells are now regarded as benign and most commonly seen in uveal naevi (see above).

Notable histological features include:

(a) Pigmentation of the melanoma cells – this can vary considerably between tumours and within tumours.
(b) Lymphocytic and macrophage infiltration, which can be prominent and has been associated with a poorer prognosis.
(c) Connective tissue or extracellular matrix patterns – nine different types have been identified, of which the 'closed (or back-to-back) loops' are associated with a poor prognosis (Fig. 10.12e, f) [51].
(d) Necrosis – varying degrees of necrosis may be found in uveal melanomas. It tends to be more prominent in rapidly growing choroidal melanomas or in tumours that have undergone brachytherapy. Aggregates of melanophages are typically in the necrotic areas. Total infarction of the tumour may results in destruction of adjacent tissues, including the sclera, possibly resulting in extraocular spread. The necrosis may lead to a 'cystic'-like appearance to the tumour on ultrasound biomicroscopy.
(e) Extraocular melanoma extension (Fig. 10.12g) [52].

Special stains of use include:

(a) Masson-Fontana to label melanosomes in amelanotic melanomas
(b) Permanganate or hydrogen peroxide bleach to allow cellular detail to be studied in deeply pigmented tumours
(c) PAS stain without haematoxylin counterstain to analyse microvascular patterns or connective tissue loops (Fig. 10.12f)

Immunoprofile

Positive immunohistochemistry with S-100P, Melan A or HMB45 confirms the diagnosis in most cases. Proliferation markers such as Ki-67 and PC-10 provide an indication of cell turnover. Mitotic figures can be highlighted using PHH3 (also called Ser10) [53]. Recent work using proteomics and immunohistochemistry would suggest that decreased protein expression of HSP-27 is associated with genetic alterations of the uveal melanoma cells, correlating well with chromosome 3 status (Fig. 10.12h) [54].

Differential Diagnosis

The differential diagnosis of posterior uveal melanoma includes other benign and malignant neoplasms, including melanocytic naevi, choroidal haemangioma (see below) and metastasis from distant non-ocular primary neoplasms. The list includes other rare primary intraocular neoplasms that arise in the choroid such as schwannoma, leiomyoma, haemangiopericytoma and

adenomas and adenocarcinomas of the RPE and the ciliary epithelium.

Non-neoplastic conditions that can simulate posterior uveal melanoma include vascular and haemorrhagic lesions (e.g. age-related maculopathy and peripheral exudative haemorrhagic chorioretinopathy), inflammatory and infectious conditions (e.g. nodular posterior scleritis, uveal effusion syndrome and granulomas) and a variety of miscellaneous disorders.

Histogenesis

Uveal melanoma is considered to be a cancer arising from uveal melanocytes. The precursors of melanocytes are non-pigmented melanoblasts derived from the neural crest, which bypass natural tissue barriers and basement membranes of the eye when migrating during embryogenesis. As with processes occurring in the skin, the melanoblasts mature into melanocytes within the uvea and/or give rise to melanocytic stem cells, which maintain the ocular melanocytic 'system'. Although it is known that melanocytic stem cells reside in the hair bulge in the skin, the location of uveal melanocytic stem cells is still unknown [55]. It is hypothesised that various genetic and epigenetic alterations occur along the 'melanoblast–melanocyte–naevus–uveal melanoma' pathway, resulting in their malignant transformation and propensity to spread. It is unclear whether the 'melanoma-initiating' or 'cancer stem-like' cells, recently shown to be present in uveal melanoma cell lines, are derived directly from ocular melanocyte progenitors or from more mature melanocytes that have dedifferentiated.

Recent analysis of gene expression data of uveal melanoma would suggest that dedifferentiation indeed does occur during uveal melanoma development, but this requires further investigation. It is also unclear whether the naevus stage is a prerequisite in uveal melanoma development: it has been estimated that 1 in 8,000 naevi undergo malignant transformation to form uveal melanoma. Histologically, it is exceptionally rare for a residual naevus to be evident adjacent to or within a choroidal melanoma, supporting this observation.

Genetics

GNAQ and *GNA11* mutations are also found in uveal naevi and in most uveal melanoma regardless of their tumour stage, chromosomal constellation or other outcome predictors (see below) [56, 57]. These mutations appear to be necessary but not sufficient for complete malignant transformation to melanoma. These data suggest that *GNAQ* and *GNA11* mutations are early events in the molecular pathogenesis of uveal melanoma.

It has been known for almost 20 years that uveal melanomas show specific chromosomal alterations, which are quite distinct from melanomas at other sites, particularly those of the skin. The most striking abnormality in uveal melanoma is the complete or partial loss of chromosome 3. Other common genetic abnormalities of uveal melanoma include loss on 1p, 6q, 8 and 9p as well as gain on 1q, 6p and 8q [55]. These alterations were initially identified by standard karyotypic analyses. They have subsequently been confirmed by several groups using differing technologies, including fluorescence in situ hybridisation (FISH), CGH, spectral karyotyping, microsatellite analysis (MSA), MLPA and single nucleotide polymorphisms (SNPs) (see also review:[55]).

Prognosis and Predictive Factors

The above-mentioned chromosomal alterations in primary uveal melanoma are clinically relevant because of their correlation with the risk of metastatic death. Chromosome 3 loss is associated with a reduction of the 5-year survival probability from approximately 100 % to 50 %. Similarly, chromosome 8 gain and loss of chromosome 1 significantly correlate with reduced survival. Both chromosome 3 loss and polysomy 8q are also associated with other poor prognostic factors, including increasing tumour basal diameter, ciliary body involvement, presence of epithelioid cells, high mitotic count and closed connective tissue loops. Conversely, gains in chromosome 6p correlate with a good prognosis, suggesting that this aberration has a functionally protective effect [58, 59].

A PCR-based 12-gene assay based on gene expression profiling. The latter technique divides

uveal melanoma into two 'classes' on the basis of an mRNA expression signature: class 1 and class 2. Class 1 uveal melanoma often show 6p and 8q gain. Class 2 uveal melanoma tends to show more aneuploidy with 1p loss, 3 loss, 8p loss and 8q gain [60, 61]. Class 2 uveal melanoma is also strongly associated with inactivating mutations of 'BRCA1-associated protein-1' (BAP1) located at 3p21 [62] (see also review [55]). Increasingly prognostic genetics testing is being performed on small intraocular biopsies (Fig. 10.12i, j). Essential for these analyses is a cytomorphological analysis of the cells being examined, as a 'disomy 3' or Class I result can potentially also be obtained when examining macrophages or indeed metastatic carcinoma.

10.7.5 Choroidal Haemangioma

Definition

Choroidal haemangiomas are relatively rare benign vascular hamartomas composed of relatively large thin-walled vascular channels lined by endothelial cells. They can be subdivided into cavernous, capillary or mixed [63].

Epidemiology

Choroidal haemangiomas occur sporadically or in association with Sturge–Weber syndrome (*syn. encephalotrigeminal angiomatosis*).

Clinical Features

Sporadic cases appear as discrete well-circumscribed orange-red tumours, whilst those in association with Sturge–Weber syndrome are typically more diffuse lesions that give a red 'tomato-ketchup' appearance to the fundus. Both types of haemangiomas are associated with serous retinal detachment. The diffuse choroidal haemangiomas tend to cause symptoms in childhood; in contrast, the circumscribed tumours usually present in adulthood as a unilateral tumour. Symptoms include:

(a) Blurred vision, metamorphopsia and micropsia due to serous retinal detachment affecting the fovea
(b) Hypermetropia if the retina is elevated by the haemangioma or associated fluid

Many patients, however, are asymptomatic, and the tumour is diagnosed incidentally on ophthalmological examination. Treatment options include (a) observation, (b) external beam radiotherapy, (c) plaque radiotherapy (brachytherapy), (d) proton beam therapy, (e) photodynamic therapy and (f) enucleation, if there is intractable pain due to long-standing retinal detachment and the associated neovascular glaucoma [64, 65].

Histopathology

Histology of choroidal haemangiomas is rarely seen, since the condition is usually diagnosed clinically. However, histological sections of enucleated eyes demonstrate a vascular tumour within the choroid composed of large thin-walled blood vessels. The endothelia lining these may be plump; however, they do not show any cytological atypia, and mitoses are not seen (Fig. 10.13). Haemangiomas can induce hyperplasia and fibrous metaplasia of the overlying RPE, which may cause diagnostic difficulties.

10.7.6 Choroidal Osteoma

Definition

Choroidal osteoma (*syn. choroidal osseous choristoma*) is a very rare primary uveal tumour, which is bilateral in about 25 % of cases [66].

Epidemiology and Clinical Features

This tumour is usually detected in early adulthood but can occur in children. Most patients are female. Familial cases have been reported. This condition is usually asymptomatic unless the fovea is involved by the tumour, or there is associated neovascularisation or exudative retinal detachment. It appears as a yellow-orange placoid tumour with sharply defined scalloped margins with pseudopodia-like projections. The differential diagnoses include (a) osseous metaplasia, (b) sclerochoroidal calcification and (c) metastases.

Histology

The mature bone in osseous choristoma is located within the choroid deep to Bruch's membrane,

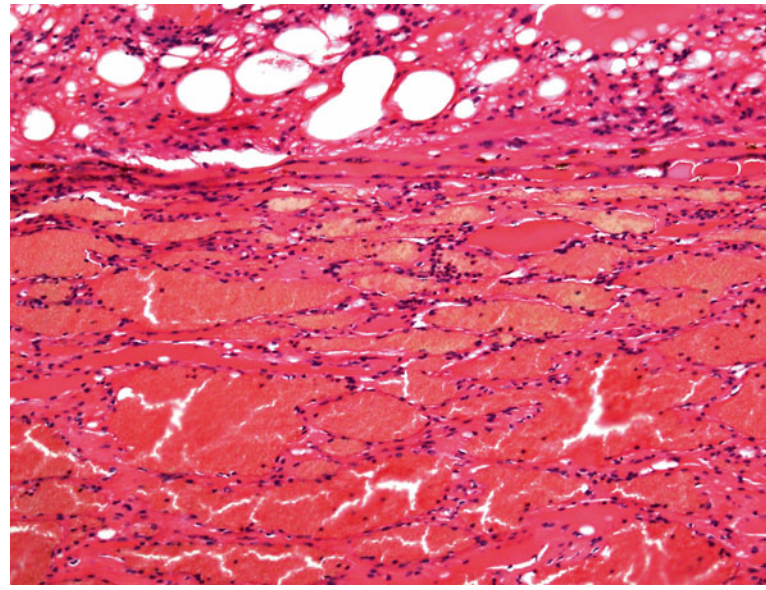

Fig. 10.13 Histological section of an enucleated eye for a diffuse choroidal haemangioma (×40 objective; HE stain). The choroid is replaced by a tumour composed of thin-walled congested capillaries lined by unremarkable endothelium. The overlying retina shows degenerative changes including microcystic degeneration and focal gliosis (×40 objective; HE stain)

not on its inner surface like the osseous metaplasia of the RPE, seen in blind phthisical eyes. They are composed of irregular spicules of bone that are surrounded by an areolar stroma containing large vascular channels. Rarely, haemopoietic cells may be seen within the stroma.

Prognosis

Disciform macular degeneration develops in about 50 % of patients. Visual loss occurs in about 60 % of patients.

10.7.7 Uveal Schwannoma

Definition

According to the WHO classification, a schwannoma (syn. *neurilemmoma*) is a tumour composed of differentiated neoplastic Schwann cells. These benign tumours are usually encapsulated.

Epidemiology

Uveal schwannoma are rare and less than 60 cases have been documented to date. Outside the uveal tract, schwannomas can be found at any age, although a peak in the incidence can be identified between 40 and 60 years old. Within the uvea, the age at presentation ranges from 9 [67] to 74 years old [68], with a mean around 37 years old. Although outside the uvea no sex predilection has been reported, within the uvea schwannomas appear to be more common in women than in men (3/1) [69, 70]. Systemic disease association include neurofibromatosis [71, 72] and *PTEN* hamartoma tumour syndrome [69].

Localisation

Probably reflecting the higher number of ciliary nerves in the choroid, schwannomas have been more commonly reported in the choroid (approximately 50 % of the cases) than in the ciliary body [73–77] (17 %) and the iris (9 %) [78, 79]. In several cases, they can simultaneously arise in the choroid and in the ciliary body [80, 81].

Clinical Features

Decreased visual acuity, ranging from 1 month [69] to 4 years [70], represented the most commonly reported presenting signs. In rare instances, visual field loss [77], eye irritation [82], increased intraocular pressure [83] and leukocoria [69] have been documented. Extraocular extension was observed in few cases [67, 68, 70]. Fundus examination revealed a usually non-pigmented nodular mass [68, 69, 74] [82, 84, 85], which can be accompanied by a serous retinal detachment (Fig. 10.14a, b) [70, 86–89]. In rare cases, a pigmented mass was found [86, 90–92]. The tumour

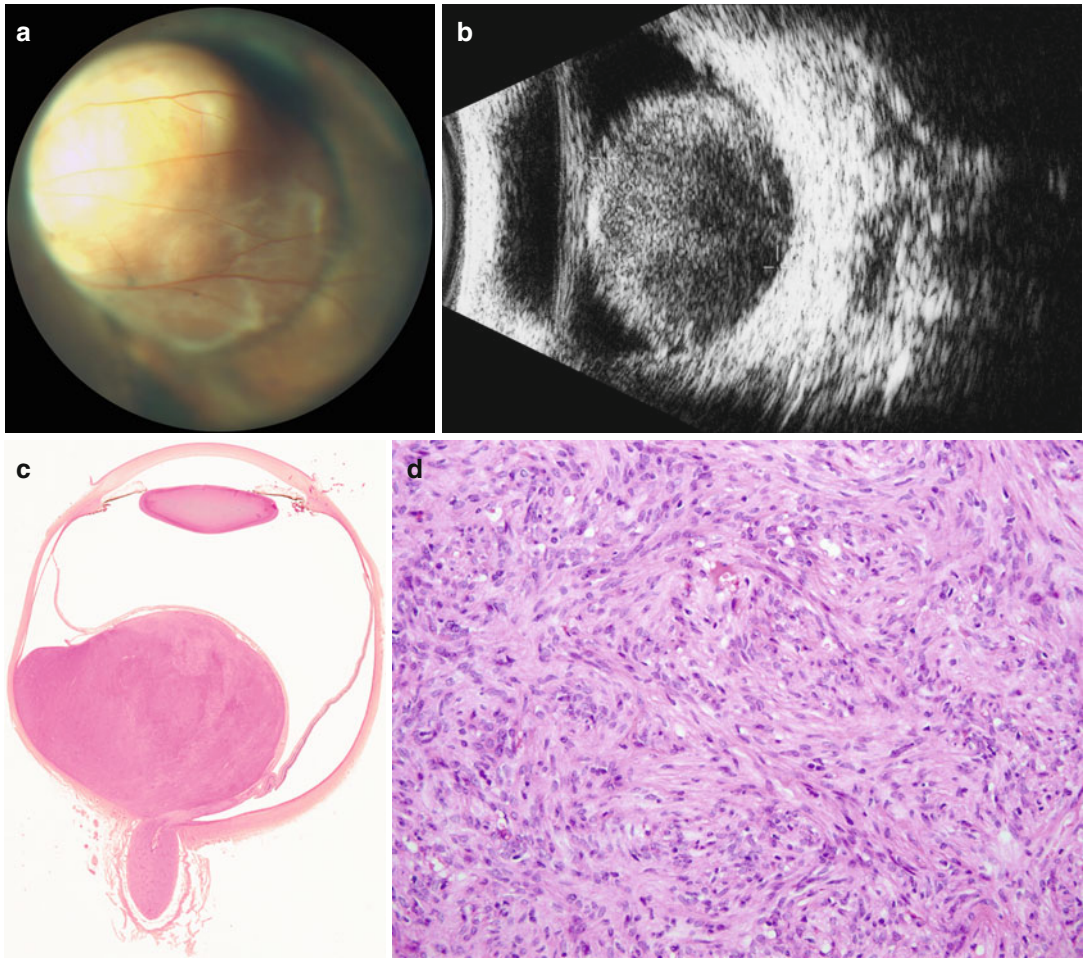

Fig. 10.14 (**a**) Fundoscopy of a patient with a choroidal schwannoma with detachment but not infiltration of the overlying retina with 'stretched' blood vessels. (**b**) Ultrasonography demonstrates a choroidal tumour with a detached retina, with some hypodense areas suggestive of cystic change. (**c**) Enucleation specimen showing a dome-shaped tumour in the posterior choroid adjacent to the optic nerve with associated retinal detachment (×2 objective; HE stain). (**d**) Higher power demonstrates the tumour to be composed of spindle cells with slightly eosinophilic cytoplasm with ill-defined borders, arranged in an organised compact 'Antoni A' pattern. No mitoses are seen (126×; HE stain)

was also exceptionally found to be partially cystic [84, 91, 93] (*personal observation L. Zografos, A. Moulin*). In many cases, the documentation of local growth and the difficulty to rule out an amelanotic melanoma led to enucleation [68, 72, 73, 85, 87] or surgical excision [91, 94].

Either fluorescein angiography or ultrasonography provides little help in the differential diagnosis with uveal melanoma [69, 87, 94]. A recent study [81] evaluating the MRI findings in six schwannomas suggested that the isointense T1 and T2 signals in reference to the brain might help in the distinction with uveal melanoma, which features hyperintense T1 and hypointense T2 signals in reference to the brain.

Microscopy

The tumours are populated by spindle cells with slightly eosinophilic cytoplasm with ill-defined borders (Fig. 10.14c, d). These elongated neoplastic cells contain oval regular nuclei. The cells are organised in compact, cellular areas (Antoni

A pattern) or in less cellular areas with a loose connective tissue matrix (Antoni B). In certain areas, the nuclei form palisades (Verocay bodies). Some cells may also contain lipid. The PAS stain usually demonstrates a thin basement membrane material surrounding the cells. The vessels within the tumour usually display thick, hyalinised walls. A fine capsule has rarely been mentioned or identified only in limited reports [73, 77, 90, 91, 95]. If serial sections are performed, it is sometimes possible to identify the ciliary nerve from which the mass has originated [72].

Only one case has showed a diffuse multinodular involvement of the uvea reminiscent of a plexiform schwannoma [67]. Heavily pigmented cells have been reported in only two cases [67, 86]. In these two pigmented cases, there were no psammoma bodies and adipose-like cells found in pigmented schwannomas associated with *Carney complex* (melanotic schwannoma, myxoma, endocrine tumours and spotty skin pigmentation). Only one cellular schwannoma without Antoni B areas and Verocay bodies has also been reported in the choroid. In cellular schwannomas, mitotic activity is usually limited to 1–4 mitoses/10 HPF, and no areas of necrosis can be found. Although some reports have mentioned schwannoma with an extrascleral spread [67, 68, 70], these tumours displayed histologically benign features, and no malignant peripheral nerve sheath tumour (MPSNT) have been reported in the uvea.

Immunohistochemistry

The tumour cells usually express diffusely S100 protein [68–70, 72, 74, 76, 86, 88, 90, 93] and CD57 (Leu-7). GFAP may also be partially expressed [70, 93]. Neurofilament is not expressed in the tumour [70, 76]. Basal membrane material surrounding the cells has been demonstrated with the expression of collagen IV in two cases [69, 82]. In non-pigmented schwannomas, melanocytic markers (Melan A, HMB45) were usually negative [68, 70, 76, 82, 88, 90, 93], whereas positive in a pigmented schwannoma [86]. Melan A expression was, however, found in a clinically and microscopically non-pigmented schwannoma [69], a finding that was further confirmed by the demonstration of melanosomes on electron microscopy. This ability of melanin synthesis in Schwann cells and in melanoma cells likely underscores their common neural crest origin [86].

Electron Microscopy

Electron microscopy demonstrates interdigitating cellular processes partially surrounded by basement membrane material [67, 68, 70, 72, 76, 82, 86, 94] and long-spacing collagen with a periodicity of 100–120 nm (Luse body) [67, 70, 76, 87, 94]. In pigmented schwannomas, melanosomes could be demonstrated [67, 86].

Differential Diagnosis

The main histological differential diagnosis includes leiomyoma, uveal melanoma and MPNST. Leiomyoma may display nuclear palisading, but Antoni A and Antoni B areas are not found. Furthermore, the immunohistochemical profile of leiomyoma with expression of smooth muscle actin, desmin, caldesmon and calponin differs from the one of schwannoma with an expression of S100 protein. Uveal melanoma are more densely cellular than schwannoma and do not display Verocay bodies, Antoni A and Antoni B areas, nor PAS basement membrane partially surrounding the cells. MPNST demonstrates higher nuclear atypia, necrosis and only partial S100 protein expression.

Genetics

Although a large ciliochoroidal schwannoma has been reported in a 31-year-old man with presumed neurofibromatosis type 2 [72], most uveal schwannomas are sporadic. A choroidal schwannoma developed in a 10-year-old girl with a *PTEN* hamartoma tumour syndrome led to the search for a 'second hit' implicating *PTEN* within the tumour [69]. Although molecular analysis did not identify a loss of heterozygosity for *PTEN* or *PTEN* promoter methylation within the tumour, PTEN mRNA and protein was reduced within the tumour in accordance with animal models evidence suggesting that subtle variation of *PTEN* expression favours the development of various tumour type and modulates tumour progression

[96]. Mutational analysis of *NF2* within that tumour did not reveal any pathological variation, but *NF2* expression was lost at the mRNA and protein level.

10.7.8 Uveal Leiomyomas

Definition

These are rare non-pigmented benign smooth muscle tumours usually arising in either the ciliary body or iris [97].

Clinical Features

Typically, uveal leiomyomas affect young women. Most are situated in the supraciliary space, and they characteristically transmit a yellow light during transillumination.

Histology

Leiomyomas are paucicellular tumours, which are composed of spindle-shaped smooth muscle cells with cigar-shaped nuclei. Immunohistochemistry shows staining with antibodies, such as SMA, caldesmon and calponin. The Ki-67 growth fraction of the tumour cells is very low [98].

Treatment

Circumscribed tumours can be treated with surgical resection, or 'shelling out' of the lesion, if it is located in the suprachoroidal or supraciliary space.

10.7.9 Uveal Lymphoma

Definition

Lymphoma occurring in the uvea can develop primarily at this site or, alternatively, the uvea can be secondarily invaded by a systemic lymphoma. The evidence of monoclonal rearrangement of the heavy immunoglobulin chain (IgH) in the infiltrating lymphoid cells in the uvea demonstrated that entities previously called 'reactive lymphoid hyperplasia' or 'uveal pseudotumours' represent low-grade B-cell lymphoma [99, 100].

Localisation

Uveal lymphomas most commonly arise in the choroid [99, 101–106] and are also often associated with an extraocular extension [100, 101, 107–111]. Ciliary body lymphoma are very rare and limited cases have been reported [101, 112]. Lymphomatous infiltration of the iris is also rare and frequently results from a secondary involvement of a systemic lymphoma [108, 113–115] (see also page 296. Primary intracocular lymphoma).

Clinical Features

The symptoms vary upon the extent of uveal involvement by the lymphoma ranging from generally slowly decreased visual acuity that can be accompanied by metamorphopsia and eventually to pain in advanced cases with glaucoma.

Choroidal lymphoma induce multiple sub-RPE yellow, sometimes creamy [116] to pink nodular elevations more or less associated with areas of RPE hypertrophy and or atrophy. The confluence of these nodules creates eventually a diffuse choroidal thickening. The extent of the infiltration likely triggers RPE dysfunction that leads in many cases to serous retinal detachment. In some instances, a uveal effusion syndrome can be observed [102, 111, 117]. Contrary to primary intraocular retinal lymphoma, the vitreous is usually clear. The differential diagnosis includes Vogt–Koyanagi–Harada disease [118], multifocal choroiditis, birdshot chorioretinopathy, acute multifocal posterior placoid pigment epitheliopathy and metastasis [116]. Sometimes involvement of the conjunctiva with 'salmon patches' can be found [103, 111]. Ultrasonography demonstrates a low internal reflectivity and a diffuse choroidal thickening and is very useful in the assessment of the exteriorisation and extension of the lymphoma. Fluorescein angiography reveals multiple early pinpoint hyperfluorescence [111, 118] with late hyperfluorescence [119]. Indocyanine green angiography shows localised or diffuse early hypofluorescent areas associated with late hypofluorescence and dilated tortuous choroidal vessels [111].

Iris lymphoma can manifest as anterior uveitis with pseudohypopyon [108, 114, 120, 121] accompanied by blurred vision, eye redness and pain [113]. Keratic precipitates that can be mutton-fat [107] and

hyphaema [122] were frequently found in a series of 13 cases [113]. Iris nodules or mass has also been mentioned in several reports [107, 112, 114, 120, 123]. Secondary involvement by a B-cell Non Hodgkin lymphoma [120, 121, 124, 125] or T- or natural killer cell systemic lymphoma [122, 123, 126, 127] is common, and primary iris lymphomas are rare [112, 113, 115, 128]. Conjunctival 'salmon patches' as well as abnormal iris vessels and hyphaema have been suggested to be useful clinical signs in the differential diagnosis with anterior uveitis [113]. Contrary to choroidal lymphomas that usually manifest an indolent clinical course, iris lymphomas, reflecting the aggressive nature of the lymphoma, are associated with an adverse outcome.

10.7.10 Uveal Extranodal Marginal Zone B-Cell Lymphoma

Definition

Uveal extranodal marginal zone lymphoma represents an extranodal lymphoma populated by small B-cells including marginal zone (centrocyte-like) cells, cells resembling monocytoid cells, small lymphocytes and some immunoblasts and centroblast-like cells according to the WHO classification. The infiltrate is located in the marginal zone of reactive B-cell follicles with an extension into the interfollicular region.

Epidemiology

Uveal marginal zone lymphomas tend to occur most commonly between 50 and 70 years old. In reviewing several published cases [99–103, 109, 110, 129] (and three personal unpublished cases), the mean age is 60.5 years old (±2.7). Men seem to be more commonly involved than women, in 69 % and 31 % of the cases, respectively.

Aetiology

Marginal zone lymphomas are assumed to result from a persistent antigenic stimulation resulting in the expansion of post germinal centre B-cells. In the ocular adnexa, an association has been suggested between Chlamydia psittaci and marginal B-cell lymphoma [130–132] with variable geographical distribution [133]. Such an association has not been demonstrated in the uvea.

Macroscopy

In enucleated cases, a diffuse, white, creamy, 'fish flesh' thickening of the uvea can be observed (Fig. 10.15a, b). Theses whitish zones can be continuous with other creamy areas covering the sclera and representing extraocular extension. In some cases, nodular choroidoretinal elevations with areas of RPE atrophy surrounded by circular areas of RPE hypertrophy can be observed.

Histopathology

The expansion of the lymphoma cells surrounds the follicle mantle to build confluent areas that can sometimes lead to complete effacement of the residual follicular architecture. The marginal zone lymphoma cells are of medium size, harbour slightly irregular nuclei with small nucleoli and have a pale cytoplasm (centrocyte-like) (Fig. 10.15c, d). If the cells display more cytoplasm, they can show a monocytoid appearance. The lymphoma can also demonstrate a plasmacytoid differentiation; alternatively, the cells can resemble to small lymphocytes. Few blastic cells (centroblast with one to three nucleoli or immunoblasts with one central prominent nucleolus) can also be found. As observed in uveal melanoma, the lymphoma can extrude itself in the episcleral area through the scleral channels. An infiltration of the choriocapillaris can be observed, as well as a rupture of Bruch's membrane with extension in the RPE (similar to lymphoepithelial lesion observed in marginal zone lymphoma elsewhere) [101]. Areas of RPE fibrous metaplasia alternating with areas of RPE atrophy or hypertrophy can be observed over the tumour (Fig. 10.15e). These modifications are responsible of the angiographic aspect of the tumour with an alternation of hypo- and hyperfluorescent areas.

Immunohistochemistry

The tumours cells express B-cell markers CD20, CD79a and PAX5 (Fig. 10.15f). IgM is also commonly expressed and there is a light chain restriction. There is often an aberrant

expression of the T-cell marker CD43. In the differential diagnosis with small lymphocytic lymphoma, there is usually no expression of CD5 and CD23 in marginal zone lymphoma. Cyclin D1 is not expressed (thereby excluding mantle cell lymphoma). In the distinction with follicular lymphoma that is believed to arise from the follicular centre, there is no expression of CD10 and BCL6. CD21 and CD35 allow the demonstration of the residual follicular dendritic cell network and the extent of the follicular colonisation.

Differential Diagnosis

The main differential diagnoses include small lymphocytic lymphoma (CD5+, CD23+), mantle cell lymphoma (CD5+, cyclin D1+) and eventually follicular lymphoma (CD10+). In diffuse large B-cell lymphoma, there are sheets of transformed blasts (centroblastic or immunoblastic) that exceed by twice the size of a normal lymphocyte. In this lymphoma, the proliferation index (Ki67) is high (>50 %) contrary to marginal zone lymphoma where it is low (Ki-67 growth fraction: 5–15 %).

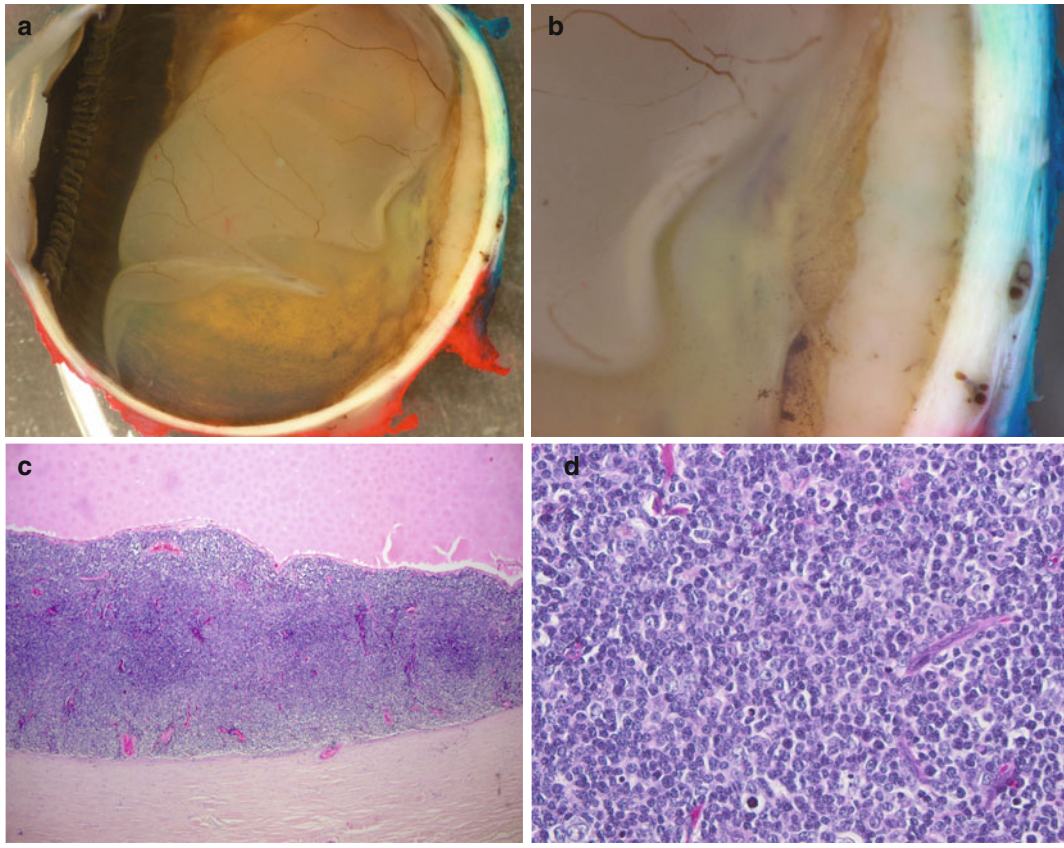

Fig. 10.15 (**a**) Gross examination of a fixed eye removed due to a posterior choroidal thickening. This is 'fish flesh' coloured and moderately firm in consistency. There is an associated subretinal exudate as well as a clear retinal detachment. (**b**) Higher-power magnification shows clearly the 'fish-flesh'-like thickening of the choroid. (**c**) Histological sections reveal a dense cellular infiltration limited to the choroid without penetration of Bruch's membrane. The retina is not present in this field due to the subretinal exudate. (×20 objective; HE section). (**d**) Higher-power magnification shows that the cellular infiltrate is composed of a mixture of centrocyte-like B-cells with varying degree of plasmacellular differentiation, occasional centroblasts and very rare mitoses are present (252×; HE stain). (**e**) In some choroidal EMZL, there is a reaction in the overlying RPE within this case a nodular hyperplasia resulting in focal subretinal changes (40× objective; HE stain). (**f**) Dominant positivity of the lymphocytes within the choroid for the B-cell antigen, CD79a (×10 objective; PAP stain)

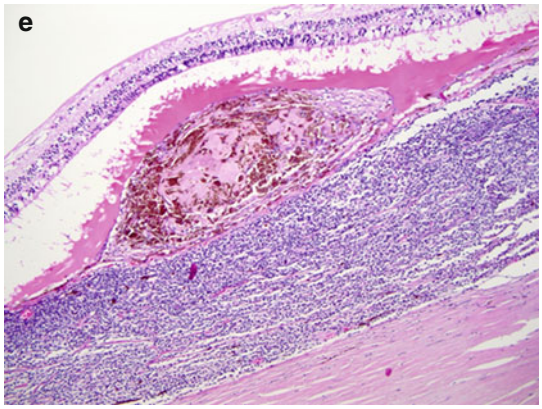

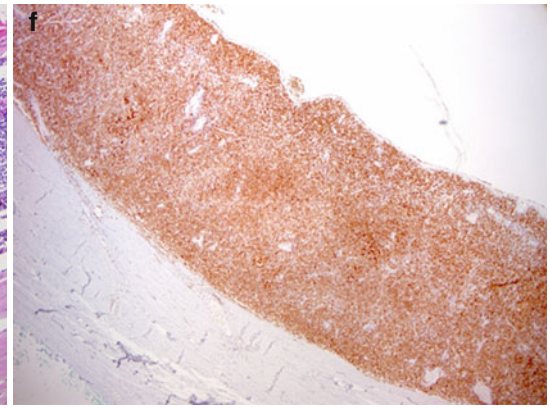

Fig. 10.15 (continued)

Histogenesis

The antigenic drive leading to the expansion of the marginal zone B-cell in the uvea is not known.

Genetics

The t(11;18) (q21;q21) translocation creating the AP1-2-MALT1 protein has been reported in marginal zone lymphomas of the choroid (Coupland S.E., 2005).

Prognosis and Predictive Factors

Marginal zone lymphoma is a radiosensitive tumour that progresses slowly and manifests an indolent behaviour.

10.7.11 Secondary Uveal Lymphoma

High-grade large B-cell lymphoma represents the most common Non-Hodgkin lymphoma and is also the most common lymphoma that can secondarily invade the uvea [120, 121, 134–136]. Multiple myeloma [137, 138] and extramedullary plasmacytoma [139] have also been described in the uvea as well as several reports of lymphoplasmacytic lymphoma [138, 140]. Mantle cell lymphoma has been described in the iris [125] or in the choroid [141] associated with proptosis and diplopia.

10.7.12 Uveal Leukaemia

Introduction

The spectrum of myeloid and lymphoid tumours is vast and it is beyond the scope of this book to analyse in details each entity well described in the fourth edition of World Health Organisation (WHO) classification on haematopoietic and lymphoid tumours. This chapter rather focuses on the clinical and pathological description of leukaemic involvement in the uvea.

Epidemiology

Leukaemic patients can present ocular manifestations in 31–80 % of the cases [142]. In reviewing several studies, it has been found that acute leukaemia slightly more commonly invades the eye (65 %) than chronic leukaemia (59 %) [142]. The nature of the underlying leukaemia affects the age at presentation with acute lymphocytic leukaemia being more common in children (80 %) and chronic lymphocytic leukaemia followed by acute myeloid leukaemia being more common in adults [143]. In a recent prospective clinical study, chronic lymphocytic leukaemia rarely manifested ocular complications, and no complications were directly induced by the leukaemia [144].

Localisation

In an autopsy analysis of 135 patients with leukaemia, the choroid was most commonly

infiltrated in 93 % of the cases, followed by the sclera and episclera in 29 % and retina in 17 % of the cases [142]. Other studies have also demonstrated that the choroid was the most commonly invaded site in leukaemia, in, respectively, 43 % [145] and 65 % [146] of the cases, likely reflecting the rich and dense vascularisation of the choroid. Ciliary body involvement has been found in 13 % of the cases and iris in 2 % [142].

Clinical Features

The range of ocular signs in leukaemia includes intraretinal haemorrhages (flame-shaped or dot haemorrhages, white-centred haemorrhages), cotton wool spots, vascular sheathing, venous tortuosity as well as round retinal infiltrates. In an analysis of 120 patients with leukaemia, retinal leukaemic infiltrates could be found in 3 % of the patients [147]. Although the choroid is commonly infiltrated by leukaemia, fundus manifestations are not always identifiable [145, 148]. In some instances, choroidal leukaemic infiltration can result in central serous retinal detachment [51–59, 149–157]. In these cases, fluorescein angiography reveals multiple mid-phase and late-phase dot-like hyperfluorescence accompanied by accumulation of fluid in the area of neurosensory detachment in the late phase [154–156]. Indocyanine green angiography demonstrates the same mid-phase and late-phase dot-like hyperfluorescence without choroidal leakage contrary to acute central serous chorioretinopathy where such a leakage is typically present [156].

Iris involvement, nodular or diffuse, is rare and accompanied by hypopyon [158–160] that can be tainted with blood [148]. Iris infiltration is more common in acute lymphoblastic leukaemia [158, 161–163]. Iris invasion can also be the first sign of relapse [148, 159].

Microscopy

In acute leukaemia, sheets of blasts diffusely infiltrating the choroid have been reported [157, 164]. In the area macular detachment, pigment granules, macrophages and blasts in the serous detachment, small areas of RPE hyperplasia or RPE degenerative changes such as atrophy or destruction have been described [157, 165]. The alternation of RPE hyperplasia that can form large subretinal aggregates with areas of RPE destruction explain the ‘leopard fundus’ clinically visible in some advanced cases [166].

In chronic myeloproliferative neoplasms, blasts can be found with more or less mature cells of erythroid, myeloblastic, monoblastic or thrombocytic lineage.

Immunohistochemistry

In acute lymphoblastic leukaemia, terminal deoxynucleotidyl transferase (TdT) is expressed in immature lymphoid cells. In B-cell lymphoblastic leukaemia, which represents 85 % of acute lymphoblastic leukaemia, the lymphoblasts express CD19, CD79a, PAX5 and CD10. In T-cell lymphoblastic leukaemia, the lymphoblasts express T-cell markers such as CD3, CD7, CD4, CD8 and CD99.

Chronic lymphocytic leukaemias express CD5 and CD23 as well as CD20 and CD43. In acute myeloid leukaemia, early blasts express CD34, HLA-DR and CD38, whilst cells with more advanced maturation express myeloid antigens CD13, CD15, CD33 and CD65 or monocytoid antigen CD14 and CD64.

Genetics

In chronic myelogenous leukaemia and myeloproliferative neoplasms, translocations or mutations result in constitutive activation of tyrosine kinases. In 90–95 % of chronic myelogenous leukaemia, the t(9;22) (q34;q11.2) translocation creates the BCR-ABL fusion gene with a constitutively active tyrosine kinase domain [167] that triggers reduced adherence to the bone marrow stroma and proliferation as well as resistance to apoptosis.

In acute myelogenous leukaemia, translocations result in fusion genes with loss of function of transcription factors important for haematopoietic development. Multiple translocations have been described and can be associated with a good prognosis t(8;21) (q22;q22) inv(16) (p13.1q22) or bad prognosis t(6;9) (p23;q34),t(3;3) (q21;q26.2). However, the loss of function of transcription factors involved in haematopoietic differentiation is not sufficient

to induce acute myelogenous leukaemia, and activating mutations in tyrosine kinase or downstream effectors (*N-RAS*, *K-RAS*; *FLT3*; *KIT*) are required to confer a proliferative advantage [167].

In B-cell acute lymphoblastic leukaemia, the BCR-ABL fusion gene is associated with a poor prognosis [168]. The *TEL-RUNX1* t(12; 21) (p13,q22) translocation, found in 25 % of B-cell leukaemia, occurs in utero and creates a fusion protein that potentially negatively interferes with genes regulated by the RUNX1 transcription factor [168]. This translocation is associated with a favourable outcome. In other cases, somatic mutations of *PAX5* may be able to block B-cell differentiation [168].

10.7.13 Metastatic Uveal Tumours

Introduction

Although ocular oncologists see more patients with uveal melanoma, metastatic tumours to the eye probably are the most common intraocular malignancies in adults. It is estimated that 4 % of all patients with disseminated carcinoma have intraocular metastases. The metastases have a predilection for the highly vascular choroid. The metastases can be discovered in a patient known to have a malignancy, but they can also be the first presentation of the malignant systemic disease [169, 170].

Clinical Features

Choroidal metastases typically appear as yellow or creamy-yellow dome-shaped or rounded masses. They may be associated with haemorrhage and necrosis. They may be single or multiple and can involve both eyes. Visual loss is caused by the associated exudative retinal detachment. Rarely, metastatic carcinomas can take on a mushroom-shaped form, mimicking a choroidal melanoma (Fig. 10.16a, b).

Histology

Breast and lung carcinomas account for more than two-thirds of uveal metastases (Fig. 10.16c–e). Consequently, histology most often shows an adenocarcinoma. Immunohistochemistry can be used to help to determine the site of the primary tumour, if this is unknown. It is also particularly helpful in small intraocular biopsies when the major clinical differential diagnosis includes melanoma and a metastasis. Her-2 staining and EGF-receptor status can be determined from the biopsy material, enabling treatment management decisions to be made regarding chemotherapy. More rare are the metastases to the choroid from thyroid carcinoma, carcinoid tumours, endometrial carcinoma, haemangiosarcoma and adenocarcinoma of the intestinal tract. Sarcomas rarely metastasise to the eye [171]. Cutaneous melanoma often seeds the vitreous with pigmented cells (Fig. 10.16f).

Treatment

The prognosis of patients with uveal metastasis is generally quite poor, with the mean survival prediction being 9–10 months. Palliative radiotherapy is usually administered to relieve any pain and to prevent continued loss of vision [169, 170].

10.7.14 Other Intraocular Tumours

Introduction

Hyperplasia and neoplasia of the pigment epithelium of the iris, ciliary body or retina and of the non-pigmented ciliary epithelium can result in intraocular tumours of varying sizes and colour. Patients may have an asymptomatic tumour detected on routine examination or may present with deterioration of vision by lens changes or retinal abnormality.

(a) *Ciliary epithelial tumours* can be predominantly non-pigmented or pigmented [172].

The most important congenital neoplasm of the non-pigmented ciliary epithelium is *medulloepithelioma* – a nonhereditary, embryonal neoplasm generally diagnosed in the first decade of life [23]. It arises from the medullary epithelium, or the inner layer of the optic cup, prior to its differentiation into its adult derivatives (Fig. 10.17a). An early clinical feature is a notch in the lens due

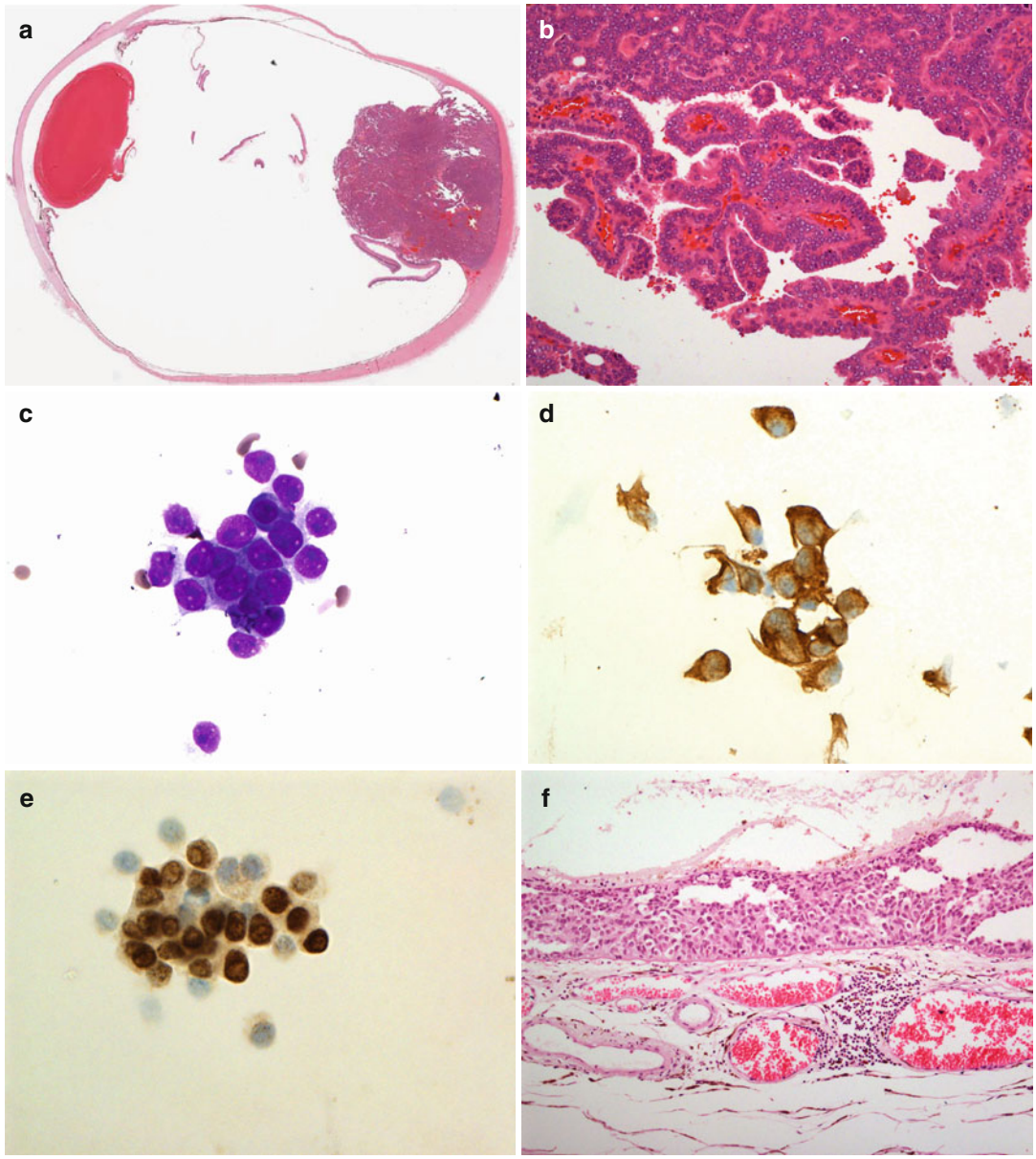

Fig. 10.16 (**a**) Low-power view of an enucleated eye in a patient with an unclear mushroom-shaped choroidal melanoma (×2 objective; HE stain). (**b**) High-power magnification demonstrates that the choroidal tumour is composed of papillae and cords of cells with glass-like nuclei, consistent with a prostate carcinoma. Immunostaining confirmed this diagnosis. (**c**) Cytospin of an intraocular biopsy from a patient with no known primary tumour: the cytospin shows an aggregate of atypical cells with minimal cytoplasm containing tiny vacuoles and with large prominent dense nuclei (×60 objective; MGG stain). (**d**) Immunostaining for the cells reveals clear positivity for the pancytokeratin marker MNF-116 (×60 objective; PAP immunostaining). (**e**) Strong nuclear positivity of the tumour cells for TTF1, indicating that the tumour is likely to be a pulmonary adenocarcinoma (×60 objective; PAP immunostaining). (**f**) Intraretinal infiltration of a cutaneous melanoma: the tumour cells respect Bruch's membrane and do not infiltrate the choroid (×20 objective; HE stain)

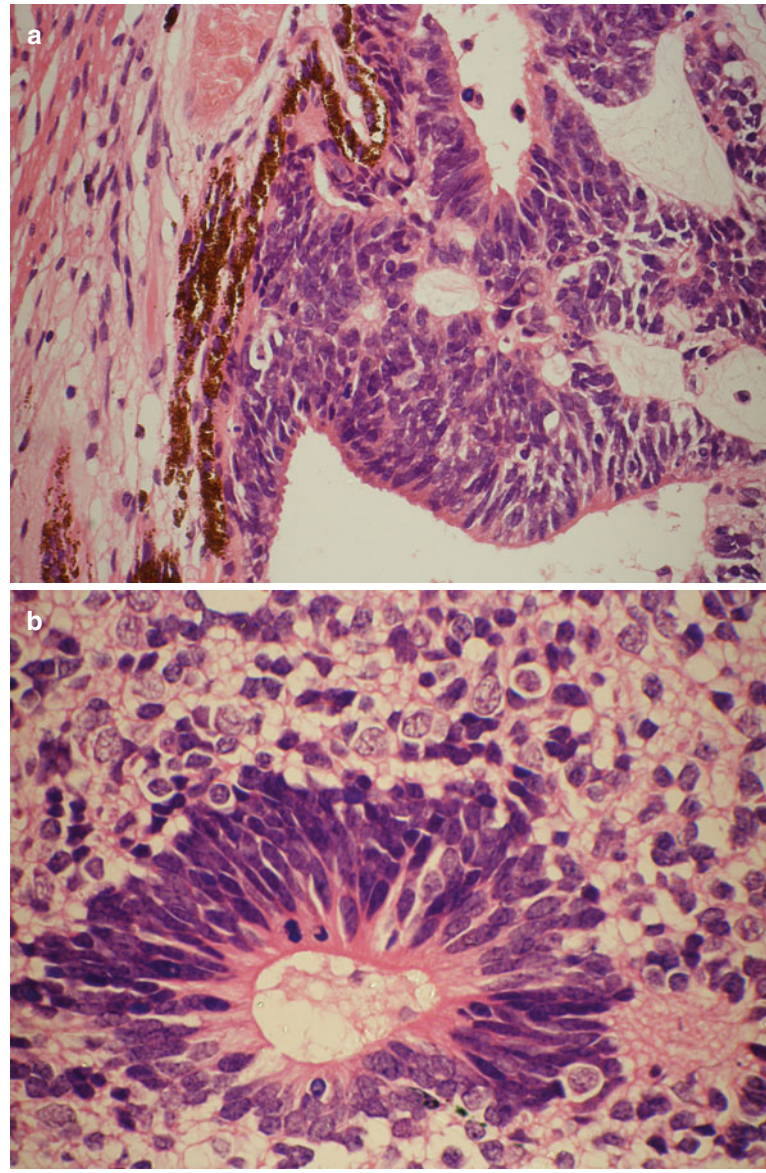

Fig. 10.17 (**a**) A nonteratoid medulloblastoma arising from the non-pigmented ciliary body epithelium in a 2-year-old girl (×40 objective; HE stain). (**b**) A Flexner - WIntersteiner rosette-like structure within a well-differentiated part of the medulloblastoma (×60 objective; HE stain)

to the congenital absence of zonule in the quadrant of the tumour. The tumours themselves are typically fleshy with a pink to tan colour. Clear cysts are often present within the mass and may become a prominent feature of the tumour. Histopathologically, they can be divided into nonteratoid and teratoid types, and both can be cytologically benign or malignant. The nonteratoid type consists purely of cells that resemble ciliary epithelium and is sometimes called diktyoma, derived from the Greek word meaning 'fish net'. Flexner - WIntersteiner rosettes and fleurettes may be seen in well-differentiated tumours (Fig. 10.17b). The teratoid type demonstrates heteroplastic elements such as cartilage, rhabdomyoblasts and brain. Melanin granules are occasionally present within the cytoplasm giving these tumours a pigmented appearance clinically. Eyes with medulloepithelioma are often found to have varying degrees of persistence of the hyaloid

system (see above). Treatment in most cases is enucleation, with some small tumours being treated with iridocyclectomy.

Small pseudoadenomatous proliferations of the non-pigmented ciliary epithelium called *Fuchs' adenomas or coronal adenomas* are a common incidental finding in elderly eyes. These are usually white or yellowish-white in colour and have a diameter of less than 5 mm and a thickness of <1 mm. They are characteristically composed of hyperplastic non-pigmented ciliary epithelium surrounding acellular stroma of amorphous eosinophilic extracellular matrix material.

Tumours can also arise from the pigmented iris, ciliary body and retinal pigment epithelium (IPE, CPE and RPE, respectively) [172]. They are termed either adenoma (*syn. epithelioma*) or adenocarcinoma of the pigment epithelium. Histopathological examination reveals a deeply pigmented tumour that appears to arise from adjacent normal pigment epithelium. It is characterised by cords and tubules of well-differentiated pigment epithelial cells separated by connective tissue septae. Mitoses are not seen. In the ciliary body, the tumour cells may contain large number of vacuoles, which contain a hyaluronidase-resistant acid mucopolysaccharide. The treatment varies with the size and extent of the tumour but does include observation and surgical excision.

Primary neoplasms arising from the RPE are exceedingly rare. Most RPE tumours are jet black in colour and have abruptly elevated margins. They are located on the inner surface of the choroid and frequently perforate the overlying retina, which often shows intraretinal lipid, exudation and dilated vessels.

Histologically, RPE tumours arising from the anterior part of the RPE often demonstrate a vacuolated pattern similar to adenomas of the ciliary epithelium. Tumours arising from the posterior RPE consist of cells arranged in linear strands and may form glands or pseudoglands. Between the cell nests are prominently positive PAS + connective tissue. The degree of cellular atypia, mitotic activity and invasive growth helps to differentiate between an adenoma and a carcinoma of the RPE. Whilst RPE-adenocarcinoma infiltrate locally, they exceptionally rarely metastasise.

(b) *Congenital Hypertrophy of the RPE (CHRPE)* appears on posterior fundus examination as a flat, round or oval pigmented spot. These lesions are surrounded by a depigmented halo and usually develop depigmented lacunae with time. A variant of CHRPE is congenital grouped pigmentation ('bear tracks') [173].

Histological examination reveals patches of tall RPE cells packed with large rounded melanosomes. Within the lacunae, the atrophic outer retina adheres to the denuded inner surface of Bruch's membrane. CHRPE may rarely undergo transformation, for example, to a low-grade adenocarcinoma [174]. When occurring bilaterally, there may be an association of CHPRE with Gardner syndrome (i.e. familial adenomatous polyposis with extracolonic manifestations).

References

1. Russell-Eggitt I. Albinism. Ophthalmol Clin North Am. 2001;14(3):533–46.
2. King RA, Pietsch J, Fryer JP, et al. Tyrosinase gene mutations in oculocutaneous albinism 1 (OCA1): definition of the phenotype. Hum Genet. 2003;113(6):502–13.
3. Ragge NK, Subak-Sharpe ID, Collin JR. A practical guide to the management of anophthalmia and microphthalmia. Eye (Lond). 2007;21(10):1290–300.
4. Shah SP, Taylor AE, Sowden JC, et al. Anophthalmos, microphthalmos, and Coloboma in the United Kingdom: clinical features, results of investigations, and early management. Ophthalmology. 2012;119(2):362–8.
5. Glaser T, Walton DS, Maas RL. Genomic structure, evolutionary conservation and aniridia mutations in the human PAX6 gene. Nat Genet. 1992;2(3):232–9.
6. Davis A, Cowell JK. Mutations in the PAX6 gene in patients with hereditary aniridia. Hum Mol Genet. 1993;2(12):2093–7.
7. Warburg M, Mikkelsen M, Andersen SR, et al. Aniridia and interstitial deletion of the short arm of chromosome 11. Metab Pediatr Ophthalmol. 1980;4(2):97–102.
8. Mataftsi A, Islam L, Kelberman D, Sowden JC, Nischal KK. Chromosome abnormalities and the genetics of congenital corneal opacification. Mol Vis. 2011;17:1624–40.

9. Nischal KK. A new approach to the classification of neonatal corneal opacities. Curr Opin Ophthalmol. 2012;23(5):344–54.
10. Kreusel KM. Ophthalmological manifestations in VHL and NF 1: pathological and diagnostic implications. Fam Cancer. 2005;4(1):43–7.
11. Lewis RA, Riccardi VM. Von Recklinghausen neurofibromatosis. Incidence of iris hamartomata. Ophthalmology. 1981;88(4):348–54.
12. Capo H, Palmer E, Nicholson DH. Congenital cysts of the iris stroma. Am J Ophthalmol. 1993;116(2):228–32.
13. Kim BH, Henderson BA. Intraocular choristoma. Semin Ophthalmol. 2005;20(4):223–9.
14. de Smet MD, Taylor SR, Bodaghi B, et al. Understanding uveitis: the impact of research on visual outcomes. Prog Retin Eye Res. 2011;30(6):452–70.
15. Herbort CP, Rao NA, Mochizuki M. International criteria for the diagnosis of ocular sarcoidosis: results of the first International Workshop on Ocular Sarcoidosis (IWOS). Ocul Immunol Inflamm. 2009;17(3):160–9.
16. Damico FM, Kiss S, Young LH. Vogt-Koyanagi-Harada disease. Semin Ophthalmol. 2005;20(3):183–90.
17. Kacmaz RO, Kempen JH, Newcomb C, et al. Ocular inflammation in Behcet disease: incidence of ocular complications and of loss of visual acuity. Am J Ophthalmol. 2008;146(6):828–36.
18. Mesquida M, Molins B, Llorenc V, et al. Current and future treatments for Behcet's uveitis: road to remission. Int Ophthalmol. 2014;34(2):365–81.
19. Schuler A, Coupland SE, Krause L, Bornfeld N. Malignant and non-malignant uveitis-masquerade syndromes in childhood. Klin Monbl Augenheilkd. 2007;224(6):477–82.
20. DeBarge LR, Chan CC, Greenberg SC, McLean IW, Yannuzzi LA, Nussenblatt RB. Chorioretinal, iris, and ciliary body infiltration by juvenile xanthogranuloma masquerading as uveitis. Surv Ophthalmol. 1994;39(1):65–71.
21. Thanos A, Vavvas D, Young LH, Foster CS. Choroidal neovascular membrane formation and retinochoroidopathy in a patient with systemic langerhans cell histiocytosis: a case report and review of the literature. Case Rep Ophthalmol. 2012;3(1):128–35.
22. Tsai JH, Galaydh F, Ching SS. Anterior uveitis and iris nodules that are associated with Langerhans cell histiocytosis. Am J Ophthalmol. 2005;140(6):1143–5.
23. Rao AA, Naheedy JH, Chen JY, Robbins SL, Ramkumar HL. A clinical update and radiologic review of pediatric orbital and ocular tumors. J Oncol. 2013;2013:975908.
24. Damico FM, Kiss S, Young LH. Sympathetic ophthalmia. Semin Ophthalmol. 2005;20(3):191–7.
25. Chu XK, Chan CC. Sympathetic ophthalmia: to the twenty-first century and beyond. J Ophthal Inflamm Infect. 2013;3(1):49.
26. Griepentrog GJ, Lucarelli MJ, Albert DM, Nork TM. Sympathetic ophthalmia following evisceration: a rare case. Ophthal Plast Reconstr Surg. 2005;21(4):316–8.
27. Brour J, Desjardins L, Lehoang P, et al. Sympathetic ophthalmia after proton beam irradiation for choroidal melanoma. Ocul Immunol Inflamm. 2012;20(4):273–6.
28. Damato B. Progress in the management of patients with uveal melanoma. The 2012 Ashton Lecture. Eye (Lond). 2012;26(9):1157–72.
29. Bonaccolto G. Congenital coloboma associated with cystic degeneration of the ciliary body. AMA Arch Ophthalmol. 1957;57(1):18.
30. Mannino G, Malagola R, Abdolrahimzadeh S, Villani GM, Recupero SM. Ultrasound biomicroscopy of the peripheral retina and the ciliary body in degenerative retinoschisis associated with pars plana cysts. Br J Ophthalmol. 2001;85(8):976–82.
31. Ambati J. Age-related macular degeneration and the other double helix. The Cogan Lecture. Invest Ophthalmol Vis Sci. 2011;52(5):2165–9.
32. Liu MM, Chan CC, Tuo J. Genetic mechanisms and age-related macular degeneration: common variants, rare variants, copy number variations, epigenetics, and mitochondrial genetics. Hum Genomics. 2012;6:13.
33. Ambati J, Atkinson JP, Gelfand BD. Immunology of age-related macular degeneration. Nat Rev Immunol. 2013;13(6):438–51.
34. Ferris 3rd FL, Wilkinson CP, Bird A, et al. Clinical classification of age-related macular degeneration. Ophthalmology. 2013;120(4):844–51.
35. Singh AD, Damato B, Howard P, Harbour JW. Uveal melanoma: genetic aspects. Ophthalmol Clin North Am. 2005;18(1):85–97, viii.
36. Singh AD, Kalyani P, Topham A. Estimating the risk of malignant transformation of a choroidal nevus. Ophthalmology. 2005;112(10):1784–9.
37. Kivela T, Eskelin S. Transformation of nevus to melanoma. Ophthalmology. 2006;113(5):887–8.e881.
38. Reidy JJ, Apple DJ, Steinmetz RL, et al. Melanocytoma: nomenclature, pathogenesis, natural history and treatment. Surv Ophthalmol. 1985;29(5):319–27.
39. Esmaili DD, Mukai S, Jakobiec FA, Kim IK, Gragoudas ES. Ocular melanocytoma. Int Ophthalmol Clin. 2009;49(1):165–75.
40. Fineman MS, Eagle Jr RC, Shields JA, Shields CL, De Potter P. Melanocytomalytic glaucoma in eyes with necrotic iris melanocytoma. Ophthalmology. 1998;105(3):492–6.
41. Mudhar HS, Doherty R, Salawu A, Sisley K, Rennie IG. Immunohistochemical and molecular pathology of ocular uveal melanocytoma: evidence for somatic GNAQ mutations. Br J Ophthalmol. 2013;97(7):924–8.
42. Apple DJ, Craythorn JM, Reidy JJ, Steinmetz RL, Brady SE, Bohart WA. Malignant transformation of an optic nerve melanocytoma. Can J Ophthalmol. 1984;19(7):320–5.

43. Barr CC, Zimmerman LE, Curtin VT, Font RL. Bilateral diffuse melanocytic uveal tumors associated with systemic malignant neoplasms. A recently recognized syndrome. Arch Ophthalmol. 1982;100(2):249–55.
44. Pulido JS, Flotte TJ, Raja H, et al. Dermal and conjunctival melanocytic proliferations in diffuse uveal melanocytic proliferation. Eye (Lond). 2013;27:1058–62.
45. Bechrakis NE, Haas G, Blatsios G. Intraocular manifestations of systemic neoplasms. Klin Monbl Augenheilkd. 2011;228(7):586–592.
46. Chahud F, Young RH, Remulla JF, Khadem JJ, Dryja TP. Bilateral diffuse uveal melanocytic proliferation associated with extraocular cancers: review of a process particularly associated with gynecologic cancers. Am J Surg Pathol. 2001;25(2):212–8.
47. Mudhar HS, Scott I, Ul-Hassan A, et al. Bilateral diffuse uveal melanocytic hyperplasia: molecular characterization and novel association with bilateral renal papillary carcinoma. Histopathology. 2012;61(4):751–4.
48. Carbone M, Ferris LK, Baumann F, et al. BAP1 cancer syndrome: malignant mesothelioma, uveal and cutaneous melanoma, and MBAITs. J Transl Med. 2012;10:179.
49. Carbone M, Yang H, Pass HI, Krausz T, Testa JR, Gaudino G. BAP1 and cancer. Nat Rev Cancer. 2013;13(3):153–9.
50. McLean IW, Zimmerman LE, Evans RM. Reappraisal of Callender's spindle a type of malignant melanoma of choroid and ciliary body. Am J Ophthalmol. 1978;86(4):557–64.
51. Damato B, Duke C, Coupland SE, et al. Cytogenetics of uveal melanoma: a 7-year clinical experience. Ophthalmology. 2007;114(10):1925–31.
52. Coupland SE, Campbell I, Damato B. Routes of extraocular extension of uveal melanoma: risk factors and influence on survival probability. Ophthalmology. 2008;115(10):1778–85.
53. Angi M, Damato B, Kalirai H, Dodson A, Taktak A, Coupland SE. Immunohistochemical assessment of mitotic count in uveal melanoma. Acta Ophthalmol. 2011;89(2):e155–60.
54. Coupland SE, Vorum H, Mandal N, et al. Proteomics of uveal melanomas suggests HSP-27 as a possible surrogate marker of chromosome 3 loss. Invest Ophthalmol Vis Sci. 2009;51(1):12–20.
55. Coupland SE, Lake SL, Zeschnigk M, Damato B. Molecular pathology of uveal melanoma. Eye (Lond). 2013;27(2):230–42.
56. Van Raamsdonk CD, Bezrookove V, Green G, et al. Frequent somatic mutations of GNAQ in uveal melanoma and blue naevi. Nature. 2009;457(7229):599–602.
57. Van Raamsdonk CD, Griewank KG, Crosby MB, et al. Mutations in GNA11 in uveal melanoma. N Engl J Med. 2010;363(23):2191–9.
58. Damato B, Dopierala JA, Coupland SE. Genotypic profiling of 452 choroidal melanomas with multiplex ligation-dependent probe amplification. Clin Cancer Res. 2010;16(24):6083–92.
59. Damato B, Eleuteri A, Taktak AF, Coupland SE. Estimating prognosis for survival after treatment of choroidal melanoma. Prog Retin Eye Res. 2011;30(5):285–95.
60. Onken MD, Worley LA, Ehlers JP, Harbour JW. Gene expression profiling in uveal melanoma reveals two molecular classes and predicts metastatic death. Cancer Res. 2004;64(20):7205–9.
61. Onken MD, Worley LA, Char DH, et al. Collaborative Ocular Oncology Group report number 1: prospective validation of a multi-gene prognostic assay in uveal melanoma. Ophthalmology. 2012;119(8):1596–603.
62. Harbour JW, Onken MD, Roberson ED, et al. Frequent mutation of BAP1 in metastasizing uveal melanomas. Science. 2010;330(6009):1410–3.
63. Singh AD, Kaiser PK, Sears JE. Choroidal hemangioma. Ophthalmol Clin North Am. 2005;18(1):151–61, ix.
64. Heimann H, Damato B. Congenital vascular malformations of the retina and choroid. Eye (Lond). 2010;24(3):459–67.
65. Heimann H, Jmor F, Damato B. Imaging of retinal and choroidal vascular tumours. Eye (Lond). 2013;27(2):208–16.
66. Shields CL, Shields JA, Augsburger JJ. Choroidal osteoma. Surv Ophthalmol. 1988;33(1):17–27.
67. Saavedra E, Singh AD, Sears JE, Ratliff NB. Plexiform pigmented schwannoma of the uvea. Surv Ophthalmol. 2006;51(2):162–8.
68. Lee SH, Hong JS, Choi JH, Chung WS. Choroidal schwannoma. Acta Ophthalmol Scand. 2005;83(6):754–6.
69. Venturini G, Moulin AP, Deprez M, et al. Clinicopathologic and molecular analysis of a choroidal pigmented schwannoma in the context of a PTEN hamartoma tumor syndrome. Ophthalmology. 2012;119(4):857–64.
70. You JY, Finger PT, Iacob C, McCormick SA, Milman T. Intraocular schwannoma. Surv Ophthalmol. 2013;58(1):77–85.
71. Vannas S, Raitta C, Tarkkanen A. Neurilemmoma of the choroid in Recklinghausen's disease. Acta Ophthalmol Suppl. 1974;123:126–33.
72. Freedman SF, Elner VM, Donev I, Gunta R, Albert DM. Intraocular neurilemmoma arising from the posterior ciliary nerve in neurofibromatosis. Pathologic findings. Ophthalmology. 1988;95(11):1559–64.
73. Donovan BF. Neurilemoma of the ciliary body. AMA Arch Ophthalmol. 1956;55(5):672–5.
74. Kuchle M, Holbach L, Schlotzer-Schrehardt U, Naumann GO. Schwannoma of the ciliary body treated by block excision. Br J Ophthalmol. 1994;78(5):397–400.
75. Thaller VT, Perinti A, Perinti A. Benign schwannoma simulating a ciliary body melanoma. Eye (Lond). 1998;12(Pt 1):158–9.
76. Kim IT, Chang SD. Ciliary body schwannoma. Acta Ophthalmol Scand. 1999;77(4):462–6.
77. Hufnagel TJ, Sears ML, Shapiro M, Kim JH. Ciliary body neurilemoma recurring after 15 years. Graefes Arch Clin Exp Ophthalmol. 1988;226(5):443–6.

78. Laverone F. On a case of solitary neurinoma of the iris. Ann Ottalmol Clin Ocul. 1967;93(11):1210–8.
79. Racz M, Szabo J. Two cases of neurilemmoma of the anterior uvea (author's transl). Klin Monbl Augenheilkd. 1973;163(5):605–9.
80. Brewitt H, Huerkamp B, Richter K. Choroid neurilemmoma. Considerations for clinical differential diagnostics. Klin Monbl Augenheilkd. 1976;169(6):750–4.
81. Xian J, Xu X, Wang Z, et al. MR imaging findings of the uveal schwannoma. AJNR Am J Neuroradiol. 2009;30(4):769–73.
82. Matsuo T, Notohara K. Choroidal schwannoma: immunohistochemical and electron-microscopic study. Ophthalmologica. 2000;214(2):156–60.
83. Turell ME, Hayden BC, McMahon JT, Schoenfield LR, Singh AD. Uveal schwannoma surgery. Ophthalmology. 2009;116(1):163, e166.
84. Cho YJ, Won JB, Byeon SH, et al. A choroidal schwannoma confirmed by surgical excision. Korean J Ophthalmol. 2009;23(1):49–52.
85. Packard RB, Harry J. Choroidal neurilemmoma–an unusual clinical misdiagnosis. Br J Ophthalmol. 1981;65(3):189–91.
86. Shields JA, Font RL, Eagle Jr RC, Shields CL, Gass JD. Melanotic schwannoma of the choroid. Immunohistochemistry and electron microscopic observations. Ophthalmology. 1994;101(5):843–9.
87. Shields JA, Sanborn GE, Kurz GH, Augsburger JJ. Benign peripheral nerve tumor of the choroid: a clinicopathologic correlation and review of the literature. Ophthalmology. 1981;88(12):1322–9.
88. Huang Y, Wei W. Choroidal schwannoma presenting as nonpigmented intraocular mass. J Clin Oncol. 2012;30(31):e315–7.
89. Vautrin R, Mertens P, Streichenberger N, Ceruse P, Truy E. Oto-neuro-surgical approach and accessibility to the cochlear nuclei. Significance in auditory brain stem implant. Rev Laryngol Otol Rhinol (Bord). 1998;119(3):171–6.
90. Shields JA, Hamada A, Shields CL, De Potter P, Eagle Jr RC. Ciliochoroidal nerve sheath tumor simulating a malignant melanoma. Retina. 1997;17(5):459–60.
91. Goto H, Mori H, Shirato S, Usui M. Ciliary body schwannoma successfully treated by local resection. Jpn J Ophthalmol. 2006;50(6):543–6.
92. Smith PA, Damato BE, Ko MK, Lyness RW. Anterior uveal neurilemmoma–a rare neoplasm simulating malignant melanoma. Br J Ophthalmol. 1987;71(1):34–40.
93. Kiratli H, Ustunel S, Balci S, Soylemezoglu F. Ipsilateral ciliary body schwannoma and ciliary body melanoma in a child. J AAPOS. 2010;14(2):175–7.
94. Pineda 2nd R, Urban Jr RC, Bellows AR, Jakobiec FA. Ciliary body neurilemoma. Unusual clinical findings intimating the diagnosis. Ophthalmology. 1995;102(6):918–23.
95. Rosso R, Colombo R, Ricevuti G. Neurilemmoma of the ciliary body: report of a case. Br J Ophthalmol. 1983;67(9):585–7.
96. Carracedo A, Alimonti A, Pandolfi PP. PTEN level in tumor suppression: how much is too little? Cancer Res. 2011;71(3):629–33.
97. Shields JA, Shields CL, Eagle Jr RC, De Potter P. Observations on seven cases of intraocular leiomyoma. The 1993 Byron Demorest Lecture. Arch Ophthalmol. 1994;112(4):521–8.
98. Koletsa T, Karayannopoulou G, Dereklis D, Vasileiadis I, Papadimitriou CS, Hytiroglou P. Mesectodermal leiomyoma of the ciliary body: report of a case and review of the literature. Pathol Res Pract. 2009;205(2):125–30.
99. Cockerham GC, Hidayat AA, Bijwaard KE, Sheng ZM. Re-evaluation of "reactive lymphoid hyperplasia of the uvea": an immunohistochemical and molecular analysis of 10 cases. Ophthalmology. 2000;107(1):151–8.
100. Coupland SE, Foss HD, Hidayat AA, Cockerham GC, Hummel M, Stein H. Extranodal marginal zone B cell lymphomas of the uvea: an analysis of 13 cases. J Pathol. 2002;197(3):333–40.
101. Coupland SE, Damato B. Understanding intraocular lymphomas. Clin Experiment Ophthalmol. 2008;36(6):564–78.
102. Coupland SE, Joussen A, Anastassiou G, Stein H. Diagnosis of a primary uveal extranodal marginal zone B-cell lymphoma by chorioretinal biopsy: case report. Graefes Arch Clin Exp Ophthalmol. 2005;243(5):482–6.
103. Fuller ML, Sweetenham J, Schoenfield L, Singh AD. Uveal lymphoma: a variant of ocular adnexal lymphoma. Leuk Lymphoma. 2008;49(12):2393–7.
104. Mudhar HS, Sethuraman C, Khan MD, Jan SU. Intracular, pan-uveal intravascular large B-cell lymphoma associated with choroidal infarction and choroidal tri-lineage extramedullary haemtopoiesis. Histopathology. 2007;51(2):275–9.
105. Coutinho AB, Muccioli C, Martins MC, Belfort Jr R, Sant'Anna AE, Burnier Jr MN. Extranodal B-cell lymphoma of the uvea: a case report. Can J Ophthalmol. 2005;40(5):623–6.
106. Coupland SE, Heimann H, Bechrakis NE. Primary intraocular lymphoma: a review of the clinical, histopathological and molecular biological features. Graefes Arch Clin Exp Ophthalmol. 2004;242(11):901–13.
107. Jensen OA, Johansen S, Kiss K. Intraocular T-cell lymphoma mimicking a ring melanoma. First manifestation of systemic disease. Report of a case and survey of the literature. Graefes Arch Clin Exp Ophthalmol. 1994;232(3):148–52.
108. Lobo A, Larkin G, Clark BJ, Towler HM, Lightman S. Pseudo-hypopyon as the presenting feature in B-cell and T-cell intraocular lymphoma. Clin Experiment Ophthalmol. 2003;31(2):155–8.
109. Sarraf D, Jain A, Dubovy S, Kreiger A, Fong D, Paschal J. Mucosa-associated lymphoid tissue lymphoma with intraocular involvement. Retina. 2005;25(1):94–8.
110. Garcia-Alvarez C, Saornil MA, Blanco G, Mendez MC, Lopez-Lara F. Extranodal B-cell uveal

lymphoma with extraocular involvement. Can J Ophthalmol. 2009;44(2):213–4.
111. Gaucher D, Bodaghi B, Charlotte F, et al. MALT-type B-cell lymphoma masquerading as scleritis or posterior uveitis. J Fr Ophtalmol. 2005;28(1):31–8.
112. Ahmed M, Androudi S, Brazitikos P, Paredes I, Foster CS. 360 degrees iris-ciliary body B-cell lymphoma masquerading as post-cataract uveitis. Semin Ophthalmol. 2004;19(3–4):127–9.
113. Mashayekhi A, Shields CL, Shields JA. Iris involvement by lymphoma: a review of 13 cases. Clin Experiment Ophthalmol. 2013;41(1):19–26.
114. Yahalom C, Cohen Y, Averbukh E, Anteby I, Amir G, Pe'er J. Bilateral iridociliary T-cell lymphoma. Arch Ophthalmol. 2002;120(2):204–7.
115. Yamada K, Hirata A, Kimura A, Tanihara H. A case of primary B-cell type non-Hodgkin lymphoma originating in the iris. Am J Ophthalmol. 2003;136(2):380–2.
116. Jakobiec FA, Sacks E, Kronish JW, Weiss T, Smith M. Multifocal static creamy choroidal infiltrates. An early sign of lymphoid neoplasia. Ophthalmology. 1987;94(4):397–406.
117. Kase S, Saito W, Saito A, Ohno S. Uveal effusion syndrome caused by choroidal invasion of malignant lymphoma. Jpn J Ophthalmol. 2010;54(1):109–10.
118. Mathai A, Lall A, Jain R, Pathengay A. Systemic non-Hodgkin's lymphoma masquerading as Vogt-Koyanagi-Harada disease in an HIV-positive patient. Clin Experiment Ophthalmol. 2006;34(3):280–2.
119. Grossniklaus HE, Martin DF, Avery R, et al. Uveal lymphoid infiltration. Report of four cases and clinicopathologic review. Ophthalmology. 1998;105(7):1265–73.
120. Verity DH, Graham EM, Carr R, van der Walt JD, Stanford MR. Hypopyon uveitis and iris nodules in non-Hodgkin's lymphoma: ocular relapse during systemic remission. Clin Oncol (R Coll Radiol). 2000;12(5):292–4.
121. Berthold S, Kottler UB, Frisch L, Radner H, Pfeiffer N. Secondary glaucoma in hyphema, hypopyon, iris prominence and iris hyperemia. Ophthalmologe. 2005;102(3):290–2.
122. Saga T, Ohno S, Matsuda H, Ogasawara M, Kikuchi K. Ocular involvement by a peripheral T-cell lymphoma. Arch Ophthalmol. 1984;102(3):399–402.
123. Yoo JH, Kim SY, Jung KB, Lee JJ, Lee SJ. Intraocular involvement of a nasal natural killer T-cell lymphoma: a case report. Korean J Ophthalmol. 2012;26(1):54–7.
124. Milman T, Petousis V, McCormick SA, Finger PT. Anterior segment tumor aspiration cutter-assisted biopsy: experience with pathology. Am J Ophthalmol. 2011;152(5):776–83, e771.
125. Economou MA, Kopp ED, All-Ericsson C, Seregard S. Mantle cell lymphoma of the iris. Acta Ophthalmol Scand. 2007;85(3):341–3.
126. Ralli M, Goldman JW, Lee E, Pinter-Brown LC, Glasgow BJ, Sarraf D. Intraocular involvement of mycosis fungoides. Arch Ophthalmol. 2009;127(3):343–5.
127. Shimonagano Y, Nakao K, Sakamoto T, Uozumi K, Haraguchi K. Iris involvement in natural killer/T-cell lymphoma. Jpn J Ophthalmol. 2006;50(6):557–8.
128. Goldey SH, Stern GA, Oblon DJ, Mendenhall NP, Smith LJ, Duque RE. Immunophenotypic characterization of an unusual T-cell lymphoma presenting as anterior uveitis. A clinicopathologic case report. Arch Ophthalmol. 1989;107(9):1349–53.
129. Tavallali A, Shields CL, Bianciotto C, Shields JA. Choroidal lymphoma masquerading as anterior ischemic optic neuropathy. Eur J Ophthalmol. 2010;20(5):959–62.
130. Ponzoni M, Ferreri AJ, Guidoboni M, et al. Chlamydia infection and lymphomas: association beyond ocular adnexal lymphomas highlighted by multiple detection methods. Clin Cancer Res. 2008;14(18):5794–800.
131. Ferreri AJ, Guidoboni M, Ponzoni M, et al. Evidence for an association between Chlamydia psittaci and ocular adnexal lymphomas. J Natl Cancer Inst. 2004;96(8):586–94.
132. Ferreri AJ, Dolcetti R, Magnino S, Doglioni C, Ponzoni M. Chlamydial infection: the link with ocular adnexal lymphomas. Nat Rev Clin Oncol. 2009;6(11):658–69.
133. Chanudet E, Zhou Y, Bacon CM, et al. Chlamydia psittaci is variably associated with ocular adnexal MALT lymphoma in different geographical regions. J Pathol. 2006;209(3):344–51.
134. Duker JS, Shields JA, Ross M. Intraocular large cell lymphoma presenting as massive thickening of the uveal tract. Retina. 1987;7(1):41–5.
135. Fredrick DR, Char DH, Ljung BM, Brinton DA. Solitary intraocular lymphoma as an initial presentation of widespread disease. Arch Ophthalmol. 1989;107(3):395–7.
136. Parikh AH, Khan SH, Wright Jr JD, Oh KT. Systemic non-Hodgkin's lymphoma simulating primary intraocular lymphoma. Am J Ophthalmol. 2005;139(3):573–4.
137. Knapp AJ, Gartner S, Henkind P. Multiple myeloma and its ocular manifestations. Surv Ophthalmol. 1987;31(5):343–51.
138. Orellana J, Friedman AH. Ocular manifestations of multiple myeloma, Waldenstrom's macroglobulinemia and benign monoclonal gammopathy. Surv Ophthalmol. 1981;26(3):157–69.
139. Honavar SG, Shields JA, Shields CL, Demirci H, Ehya H. Extramedullary plasmacytoma confined to the choroid. Am J Ophthalmol. 2001;131(2):277–8.
140. Pilon AF, Rhee PS, Messner LV. Bilateral, persistent serous macular detachments with Waldenstrom's macroglobulinemia. Optom Vis Sci. 2005;82(7):573–8.
141. Ahn ES, Singh AD, Smith SD. Mantle cell lymphoma with uveal metastasis. Leuk Lymphoma. 2010;51(7):1354–5.

142. Leonardy NJ, Rupani M, Dent G, Klintworth GK. Analysis of 135 autopsy eyes for ocular involvement in leukemia. Am J Ophthalmol. 1990;109(4): 436–44.
143. Yamamoto JF, Goodman MT. Patterns of leukemia incidence in the United States by subtype and demographic characteristics, 1997–2002. Cancer Causes Control. 2008;19(4):379–90.
144. Buchan J, McKibbin M, Burton T. The prevalence of ocular disease in chronic lymphocytic leukaemia. Eye (Lond). 2003;17(1):27–30.
145. Robb RM, Ervin LD, Sallan SE. A pathological study of eye involvement in acute leukemia of childhood. Trans Am Ophthalmol Soc. 1978;76:90–101.
146. Kincaid MC, Green WR. Ocular and orbital involvement in leukemia. Surv Ophthalmol. 1983;27(4):211–32.
147. Schachat AP, Markowitz JA, Guyer DR, Burke PJ, Karp JE, Graham ML. Ophthalmic manifestations of leukemia. Arch Ophthalmol. 1989;107(5):697–700.
148. Rosenthal AR. Ocular manifestations of leukemia. A review. Ophthalmology. 1983;90(8):899–905.
149. Riss JM, Kaplanski G, Righini-Chossegros M, Harle JR, Escoffier P, Saracco JB. Bilateral serous detachment of neuroepithelium of the posterior pole disclosing acute leukemia. J Fr Ophtalmol. 1990; 13(11–12):563–8.
150. Stewart MW, Gitter KA, Cohen G. Acute leukemia presenting as a unilateral exudative retinal detachment. Retina. 1989;9(2):110–4.
151. Tang RA, Vila-Coro AA, Wall S, Frankel LS. Case report. Acute leukemia presenting as a retinal pigment epithelium detachment. Arch Ophthalmol. 1988;106(1):21–2.
152. Abdallah E, Hajji Z, Mellal Z, Belmekki M, Bencherifa F, Berraho A. Macular serous detachment revealing acute lymphoblastic leukemia. J Fr Ophtalmol. 2005;28(1):39–44.
153. Thill M, Schwartz R, Fiedler W, Linke S. Bilateral retinal pigment epithelial detachment as the presenting symptom of acute myeloid leukaemia. Eye (Lond). 2006;20(7):851–2.
154. Malik R, Shah A, Greaney MJ, Dick AD. Bilateral serous macular detachment as a presenting feature of acute lymphoblastic leukemia. Eur J Ophthalmol. 2005;15(2):284–6.
155. Fackler TK, Bearelly S, Odom T, Fekrat S, Cooney MJ. Acute lymphoblastic leukemia presenting as bilateral serous macular detachments. Retina. 2006;26(6):710–2.
156. Moulin AP, Bucher M, Pournaras JA, Nguyen C, Ambresin A. Fluorescein and indocyanine green angiography findings in B cell lymphoblastic leukemia mimicking acute central serous chorioretinopathy. Klin Monbl Augenheilkd. 2010;227(4):342–4.
157. Zimmerman LE, Thoreson HT. Sudden Loss of Vision in Acute Leukemia. A clinicopathologic report of two unusual cases. Surv Ophthalmol. 1964;9:467–73.
158. Johnston SS, Ware CF. Iris involvement in leukaemia. Br J Ophthalmol. 1973;57(5):320–4.
159. Arbuthnot CD, Bradbury M, Darbyshire PJ. Relapsing acute myeloid leukaemia manifesting as uveitis with hypopyon. Br J Haematol. 2007; 136(4):520.
160. Abramson DH, Wachtel A, Watson CW, Jereb B, Wollner N. Leukemic hypopyon. J Pediatr Ophthalmol Strabismus. 1981;18(3):42–4.
161. Buggage RR, Myers-Powell B, McManaway 3rd J, Shen D, Robinson MR, Chan CC. Detection of the Philadelphia chromosome in the iris of a child with acute lymphoblastic leukaemia. Histopathology. 2005;46(3):350–2.
162. Schachat AP, Jabs DA, Graham ML, Ambinder RF, Green WR, Saral R. Leukemic iris infiltration. J Pediatr Ophthalmol Strabismus. 1988;25(3):135–8.
163. Martin B. Infiltration of the iris in chronic lymphatic leukaemia. Br J Ophthalmol. 1968;52(10):781–5.
164. Blodi FC. The difficult diagnosis of choroidal melanoma. Arch Ophthalmol. 1963;69:253–6.
165. Brightbill F. An unusual case of central serous retinopathy. Invest Ophthalmol Vis Sci. 1971;10(60):467.
166. Clayman HM, Flynn JT, Koch K, Israel C. Retinal pigment epithelial abnormalities in leukemic disease. Am J Ophthalmol. 1972;74(3):416–9.
167. Kelly LM, Gilliland DG. Genetics of myeloid leukemias. Annu Rev Genomics Hum Genet. 2002;3: 179–98.
168. Teitell MA, Pandolfi PP. Molecular genetics of acute lymphoblastic leukemia. Annu Rev Pathol. 2009;4: 175–98.
169. Shields CL, Shields JA, Gross NE, Schwartz GP, Lally SE. Survey of 520 eyes with uveal metastases. Ophthalmology. 1997;104(8):1265–76.
170. Kreusel KM, Bechrakis N, Wiegel T, Emmerlich T, Foerster MH. Clinical characteristics of choroidal metastasis. Ophthalmologe. 2003;100(8):618–22.
171. Anderson MF, Coupland SE, Bissett D, Atta H, Damato BE. Choroidal metastasis from primary pulmonary leiomyosarcoma. Clin Experiment Ophthalmol. 2011;39(7):705–7.
172. Shields JA, Eagle Jr RC, Shields CL, De Potter P. Acquired neoplasms of the nonpigmented ciliary epithelium (adenoma and adenocarcinoma). Ophthalmology. 1996;103(12):2007–16.
173. Buettner H. Congenital hypertrophy of the retinal pigment epithelium. Am J Ophthalmol. 1975;79(2): 177–89.
174. Trichopoulos N, Augsburger JJ, Schneider S. Adenocarcinoma arising from congenital hypertrophy of the retinal pigment epithelium. Graefes Arch Clin Exp Ophthalmol. 2006;244(1):125–8.

Eyelid Pathology

11

Diva Salomão, Jeannette Tóth, and Susan Kennedy

Abbreviations

AIDS	Acquired immunodeficiency syndrome
AJCC	American Joint Committee on Cancer
AK	Actinic keratosis
ALCL	Anaplastic large cell lymphoma
ANCA	Antineutrophil cytoplasmic autoantibody
BCC	Basal cell carcinoma
BD	Bowen disease
c-ANCA	Cytoplasmic antineutrophil cytoplasmic antibody
CEA	Carcinoembryonic antigen
CNS	Central nervous system
CTNNB1	β-Catenin gene
DNA	Deoxyribonucleic acid
ECG	Electrocardiogram
ELISA	Enzyme-linked immunosorbent assay
EMA	Epithelial membrane antigen
EORTC	European Organisation for Research and Treatment of Cancer
FGFR3	Fibroblast growth factor receptor 3
GLUT1	Glucose transporter 1
GPA	Granulomatosis with polyangiitis
H&E	Hematoxylin and eosin
HHV8	Human herpesvirus 8
HIV	Human immunodeficiency virus
HPV	Human papillomavirus strains
HSV	Herpes simplex virus
JXG	Juvenile xanthogranuloma
KLK5	Kallikrein 5
KPTR	Kiel Pediatric Tumor Registry
KS	Kaposi sarcoma
KSHV	Kaposi sarcoma herpesvirus
LM	Lentigo maligna
LMM	Lentigo maligna melanoma
LOH	Loss of heterozygosity
LYVE1	Lymphatic vessel endothelial receptor 1
MAC	Microcystic adnexal carcinoma
MCC	Merkel cell carcinoma
MF	Mycosis fungoides
mm	Millimeters
MPO	Myeloperoxidase
MTS	Muir–Torre syndrome
NBCCS	Nevoid basal cell carcinoma syndrome
NER	Nucleotide excision repair
NF1	Neurofibromatosis type 1
NSE	Neuron-specific enolase
NXG	Necrobiotic xanthogranuloma
PAR	Protease-activated receptor
PCMC	Primary cutaneous mucinous carcinoma

D. Salomão (✉)
Department of Pathology and Laboratory Medicine, Mayo Clinic, 200 First Street, SW, Rochester, MN 55905, USA
e-mail: salomao.diva@mayo.edu

J. Tóth
2nd Department of Pathology, Faculty of General Medicine, Semmelweis University, 1091 Budapest, Ulloi ut 93, Hungary
e-mail: tjeannette@gmail.com

S. Kennedy
The Royal Victoria Eye and Ear Hospital, Dublin, Republic of Ireland
e-mail: susan.kennedy@rveeh.ie

S. Heegaard, H. Grossniklaus (eds.), *Eye Pathology: An Illustrated Guide*,
DOI 10.1007/978-3-662-43382-9_11,

PCR	Polymerase chain reaction
PEH	Pseudoepitheliomatous hyperplasia
PG	Pyogenic granuloma
PM	Pilomatrixoma
PNET	Primitive neuroectodermal tumor
PR3	Protein 3
SCC	Squamous cell carcinoma
SK	Seborrheic keratosis
SMA	Smooth muscle actin
SP	Squamous papilloma
SSMM	Superficial spreading malignant melanoma
TE	Trichoepithelioma
TL	Trichilemmoma
TLR2	Toll-like receptor 2
UV	Ultraviolet
VEGFR3	Vascular endothelial growth factor receptor 3
WG	Wegener's granulomatosis
WHO	World Health Organization
XP	Xeroderma pigmentosum

11.1 Normal Anatomy

Each human eyelid is composed of six layers. The epidermal surface of the skin of the eyelids forms the outermost layer, and the epithelium covering the palpebral conjunctiva is the innermost layer. Between these lie the dermis, the loose subcutaneous layer, the orbicularis muscle, and the tarsal plate, composed of dense fibrous tissue. The mucocutaneous junction of the lid is located at the eyelid margin just posterior to the openings of the meibomian gland ducts and the lashes. In this location lies the gray zone, a sulcus extending over most of the length of the lid margin. The lid can be split surgically along this line, dividing it into two layers: an anterior one comprising the epidermis and dermis, subcutaneous tissue, and orbicularis muscle and a posterior one composed of the tarsus and palpebral conjunctiva (Fig. 11.1) [1].

11.2 Normal Histology

The outermost layer is thin skin, and the epidermis consists of a stratified squamous epithelium with some papillae. The epidermis is composed of two cell types: the keratinocytes and the dendritic cells. The keratinocytes are arranged in four layers; the deepest is the basal cell layer. The squamous cell layer (stratum spinosum) and granular layer are intermediate, and the nonnucleated keratinized layer is the most superficial. The term "stratum malpighii" is most often used to describe the lower three nucleated layers.

The basal keratinocytes form a single row of cells resting on a basement membrane, which is intimately attached to the dermis. The cells are columnar with their long axes arranged perpendicular to the skin surface. They are connected to each other by intercellular bridges and may

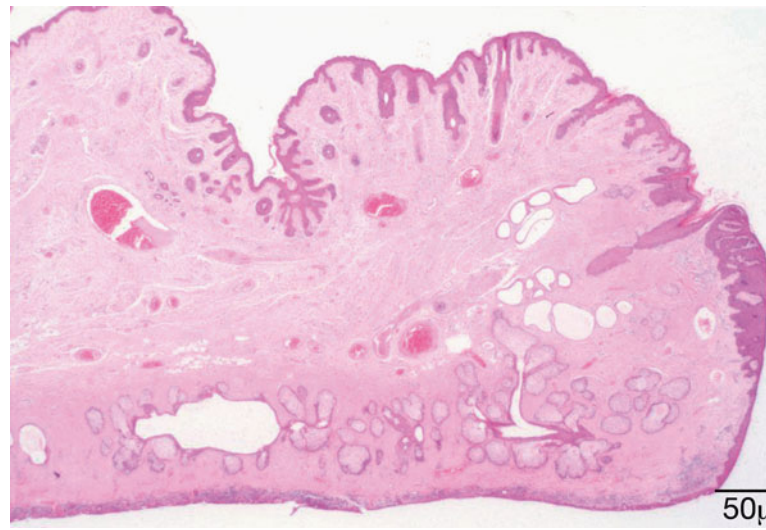

Fig. 11.1 Eyelid – Low-power view of the eyelid showing normal skin appendage structures and tarsal plate containing Meibomian glands (hematoxylin and eosin stain; original magnification 20×)

normally contain variable amounts of melanin pigment derived, in part, from adjacent dendritic melanocytes. The squamous cell layer is composed of a mosaic of polygonal keratinocytes that flatten superficially where they run parallel to the surface. The granular layer forms a row of elongated flat cells containing coarse basophilic keratohyalin granules. The external horny layer consists of flat keratinized cells devoid of nuclei.

There are three types of dendritic cells present in the epidermis: (1) clear cell melanocytes, (2) Langerhans cells, and (3) undetermined dendritic cells.

The dermis is loose and delicate. It contains hair follicles as well as sebaceous and sweat glands. The dermis is composed of a papillary layer and a reticular layer. The papillary dermis forms numerous cone-shaped dermal papillae, which extend upward into the epidermis. The ridges of epidermis separating the papillae are called rete ridges. The reticular dermis contains thick bundles of collagen and variable amounts of elastic and reticulin fibers as well as ground substance containing mucopolysaccharides. Small nerve fibers, blood vessels, and lymphatics are also found in the reticular dermis.

The subcutaneous layer of the eyelids contains a small amount of adipose tissue. It is loosely adhered to the underlying orbicularis muscle. For this reason, swelling of the lids (commonly caused by edema, hemorrhage, or acute inflammation in this layer) is easily visible clinically.

The inner layer is a mucous membrane, the palpebral conjunctiva. The lining epithelium is a low stratified columnar type with goblet cells scattered among the epithelial cells. The stratified squamous epithelium of the skin continues over the margin of the eyelid and is transformed into the stratified columnar type. The thin lamina propria of the palpebral conjunctiva contains connective tissue with elastic and collagenous fibers. Beneath the lamina propria is a plate of dense, collagenous connective tissue, the tarsal, which contains large, specialized sebaceous glands, the tarsal (meibomian) glands. They secrete sebum, which is extruded into the meibomian ducts, the orifices of which open on the lid margin just behind the gray line. This sebaceous material contributes to the lipid component of the tear film.

The free end of the eyelid contains eyelashes, which arise from large, long hair follicles. Associated with the eyelashes are small sebaceous glands (Zeis glands). The apocrine glands of Moll, which empty their secretions into the follicles of the lashes, are located between the hair follicles and large sweat glands. The cells lining these glands show secretory apical granules and areas of decapitation.

Three sets of muscles are present in the eyelid: the extensive palpebral portion of the skeletal muscle, the orbicularis oculi, the skeletal ciliary muscle (of Riolan) in the region of the hair follicles of the eyelashes and tarsal glands, and the smooth, superior tarsal muscle (of Müller). The orbicularis oculi muscle forms an elliptic sheet of concentrically arranged, striated muscle fibers within the eyelids. In the upper lid, the tendons of the levator palpebrae superioris pass through it to insert into the skin and tarsus. A portion of the orbicularis muscle known as the muscle of Riolan consists of striated muscle fibers that lie adjacent to the tarsal plate near the lid margin. Portions of this muscle are located superficial to the meibomian glands, and the remainder (subtarsal portion) lies deep to them. The glands of Moll separate the Riolan muscle from the palpebral portion of the orbicularis. The smooth muscle of Müller in the upper lid lies adjacent to the orbital septum under the levator palpebrae superioris. It originates among the fibers of the levator in the upper lid and the inferior rectus in the lower. The fibers of the superior and inferior Müller's muscle insert, in part, into the margins of the tarsal plates and also insert into collagenous tissue attached to the deep fibers of the orbicularis muscle. Alterations of these muscular structures may lead to ptosis, ectropion, or entropion.

A variety of epidermal appendages (glands and cilia) are present in the lids. The sebaceous glands are holocrine. Their acini possess no lumina and extrude their secretory products by decomposition of their cells. The meibomian glands are situated within the tarsal plates where they are arranged vertically and parallel to each other and are larger in the upper tarsus. The eccrine sweat glands are composed of three segments: a secretory portion, an intradermal

duct, and an intraepidermal duct. The apocrine glands of Moll lie near the lid margin and empty their secretions into the follicles of the lashes. Accessory lacrimal glands with histological features identical to those seen in the main lacrimal gland are often found in the substantia propria of the conjunctiva. The glands of Krause are deeply located in the subconjunctival tissues at the fornices. All of these glands vary in number and are not seen in every section of the eyelid. The hair of the skin of the lid is scanty and fine.

11.3 Congenital and Developmental Abnormalities

Abnormal development and maturation of the ectoderm and mesoderm in the embryonic lid fold may result in several deformities of the eyelid and the palpebral aperture. These may be limited to the eyelid or associated to abnormalities in the globe, orbit, face, skull, and extremities. The severity of the anomaly can vary greatly, and usually the minor defects tend to be isolated to the eyelid region and are, in general, more common than the severe defects [2, 3].

11.3.1 Cryptophthalmia

Rare condition, unilateral or bilateral, it is the result of failure of the eyelid formation. It is characterized by a continuous layer of epidermis extending between the forehead and the cheek, covering a malformed eye in most cases. This condition most often occurs in the setting of multiple malformations involving the skull, midface, extremities, and urogenital tract [4].

11.3.2 Microblepharon

Congenital anomaly characterized by vertical shortage of the upper and/or lower eyelid skin causing nocturnal lagophthalmos, corneal exposure, and cosmetic deformity. This abnormality can be unilateral or bilateral [5].

11.3.3 Coloboma

Coloboma, from the Greek word koloboma, meaning defect, represents a focal disruption in the normal development of the eyelid. The severity of the defect can vary from a small notch in the eyelid margin to a near-total absence of the eyelid (Fig. 11.2). Eyelid colobomas may involve a single or all four lids. The maldevelopment might be related to an amniotic band impingement or faulty lid fusion [6]. As observed in other ocular colobomas, patients with eyelid coloboma have a mutation in the PAX2 gene [7]. Band-like adhesions may join the coloboma to the epibulbar conjunctiva. A continuous bridge of skin and conjunctival mucosa bridges the two unaffected edges of the eyelid. An abrupt loss of lashes, tarsus, and adnexal structures demarcates the borders of the coloboma.

Eyelid colobomas are reported in patients with Goldenhar syndrome [8] and other inherited mandibulofacial dysostosis [9, 10].

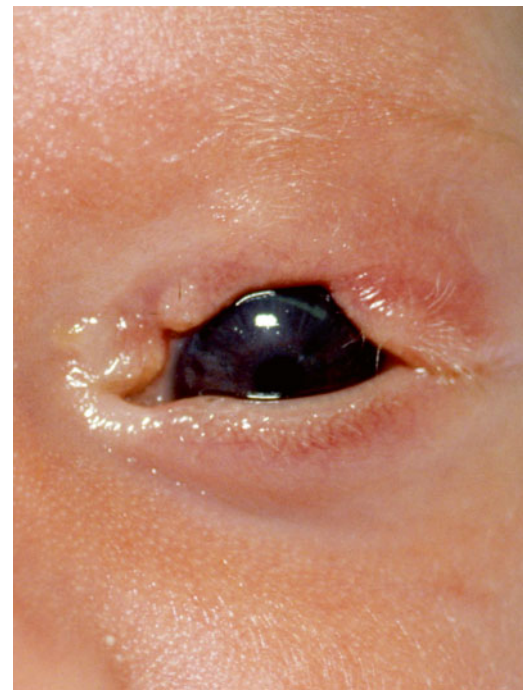

Fig. 11.2 Coloboma – eyelid coloboma in a small infant. The upper eyelid shows an area of absence of lashes and tarsus demarcating the edge of the defect (Clinical picture courtesy of Dr. George Bartley, Mayo Clinic)

11.3.4 Distichiasis

Rare disorder characterized by the presence of an extra row of eyelashes originating from the orifices of abnormally formed meibomian glands. This is the result of an anomalous development of the epithelial germ cells failing to differentiate completely to meibomian glands and instead becoming pilosebaceous units and associated with a mutation in FOXC2 gene [11, 12]. The Moll's glands are usually hypertrophic and the tarsus plate absent or rudimentary. This abnormality is often associated with other malformations [3].

11.3.5 Phakomatous Choristoma

It represents an accessory rest of the surface ectoderm. It forms when cells from the lens placode do not accompany the normal migration into the optic cup and become entrapped into the connective tissue of the eyelid. It is also known as Zimmerman tumor, in honor of the author that first described this entity in 1971 [13]. Clinically, it presents consistently at birth as a palpable nodule in the inferonasal region of the lower eyelid [14, 15], adjacent to the lacrimal sac, occasionally causing nasolacrimal duct obstruction [16]. Histologically, it is characterized by cuboidal, lenslike epithelium surrounded by basal membrane material. These cells might proliferate within a collagenous stroma and also undergo cataractous changes. Ultrastructural studies and immunohistochemical profile show a strong positivity with vimentin and S-100 protein and have confirmed a lenticular origin [14, 16–18].

11.3.6 Xeroderma Pigmentosum

Xeroderma pigmentosum (XP) is a rare, autosomal recessive inherited disorder characterized by defective DNA repair to the damage caused by ultraviolet light, which manifests clinically as photosensitivity, actinic damage to the skin, propensity to early development of cutaneous and ocular neoplasms, and, in some patients, neurological degeneration [19]. Abnormalities affecting the eyelids, conjunctiva, and cornea (areas exposed to ultraviolet radiation) have been reported in 40 % of published cases [20, 21]. The disease affects both sexes equally. It is rare in North America and Europe but is more common in areas with increased consanguinity such as Japan, the Middle East, and India [22, 23].

A defective gene locus has been identified in all seven complementation groups (A–G) and the one variant form of XP [20, 24]. In the complementation group A (MIM +276700), the classical form of XP [mutations located on both chromosome 1 and chromosome 9 (9q22)] have been identified.

The genetic defect causes mutation of nucleotide excision repair (NER) enzymes, leading to a reduction in or elimination of NER [25]. Damage to an epidermal cell's DNA occurs during exposure to ultraviolet (UV) light. If a tumor suppressor gene such as p53 or proto-oncogene is affected, a neoplasm might develop. Patients with XP are at a high risk for developing a variety of cutaneous cancers, such as basal cell carcinoma, squamous cell carcinoma, as well as malignant melanoma [26, 27]. The eyelids are frequently affected. Most patients die before the age of 21 years from metastatic squamous cell carcinoma or melanoma [28, 29].

Eyelid cutaneous changes reflect the local actinic damage (Fig. 11.3), including erythema, hyperpigmentation, atrophy, scarring, and development of neoplasms such as basal cell carcinoma, squamous cell carcinoma, and melanoma in a very young age [20]. These neoplasms have been reported to be multiple and bilateral when affecting a same patient [21].

11.4 Degeneration

11.4.1 Atrophy and Solar Elastosis

The aging skin (chronological) is characterized by atrophy of the epidermis with loss of elasticity [30]. The exposure to ultraviolet radiation (photodamage) in addition to the aging process, at least initially, results in a hypertrophic repair

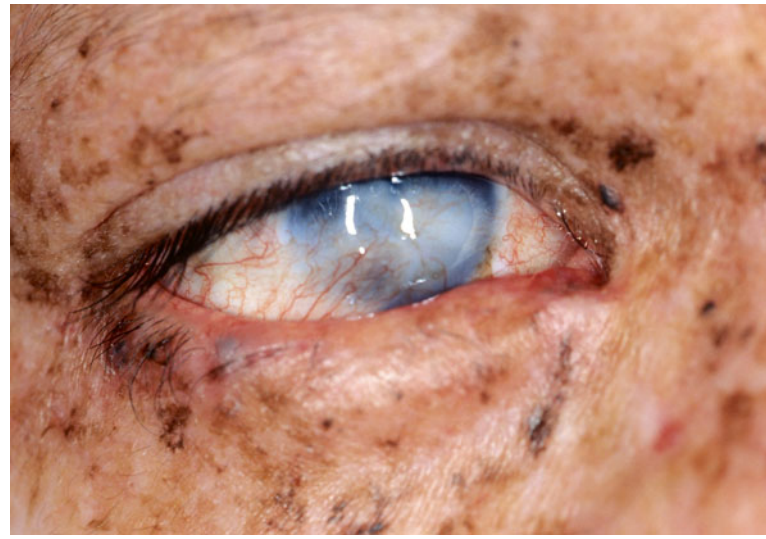

Fig. 11.3 XP – patient with xeroderma pigmentosum showing extensive cutaneous pigmentation and irregularities (Clinical picture courtesy of Dr George Bartley, Mayo Clinic)

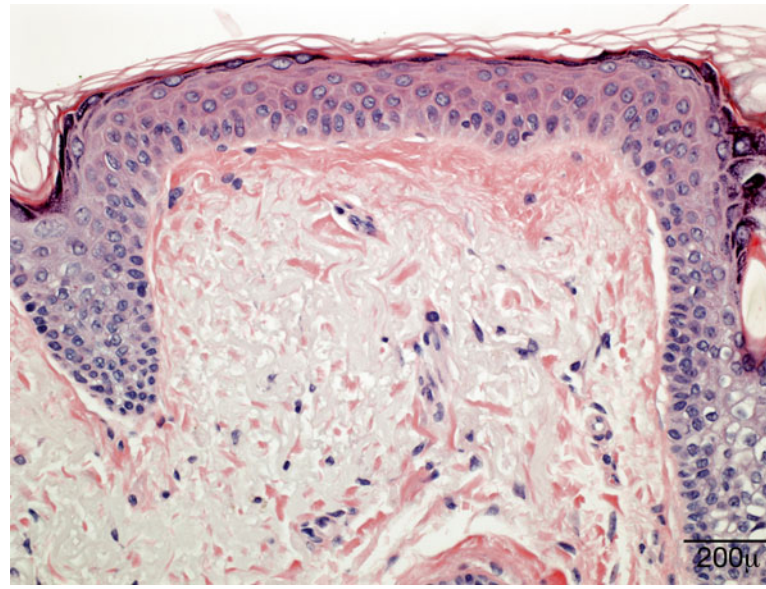

Fig. 11.4 Elastotic degeneration – eyelid biopsy shows in the superficial dermis fragmentation of the collagen and basophilic elastotic degeneration (hematoxylin and eosin stain; original magnification 400×)

response with a thickened epidermis and increased melanogenesis. In the dermis, the actinic damage causes massive elastosis (deposition of abnormal elastic fibers), collagen degeneration, and twisted, dilated microvasculature. These latter changes are recognized as "solar elastosis" [31, 32].

Microscopically, the collagen in the dermis is altered with increased basophilia due to degeneration of both collagen and elastic fibers [33, 34] (Fig. 11.4). The overlying epidermis is usually atrophic with decreased number and size of rete pegs. Patches of increased melanocytes are seen in the basal layer of the epithelium [32, 35].

In certain aging-associated conditions such as senile ectropion (turning out) and entropion (turning in), in addition to the changes described above, one might also find chronic inflammation and dermal scarring. In dermatochalasis (an aging change characterized by redundant upper eyelid skin, hanging in folds over the eye), histologically, the skin appears atrophic; and in the dermis, there is loss of collagen with basophilic degeneration, chronic inflammation, and increased numbers of capillary vessels [36].

11.5 Inflammation

11.5.1 Blepharitis

Definition

There is no stringent definition for blepharitis. In broader terms, blepharitis means inflammation of the eyelids as a whole. Marginal blepharitis refers to inflammation of the eyelid borders, although, in practice, "marginal" is usually omitted so that blepharitis is understood as inflammation of the eyelid border.

Epidemiology

Blepharitis is a common problem in ophthalmology practice, but the true incidence is unknown. It can affect any age group.

Etiology

Multiple pathomechanisms are involved in blepharitis [37]. Anterior blepharitis is often caused by overgrowth of coagulase-negative staphylococci in a patient with seborrheic dermatitis. An imbalance among various ocular bacterial species is also a possibility [38]. Posterior blepharitis is a consequence of meibomian gland dysfunction, conjunctival inflammation, or general conditions such as acne rosacea [39]. The role of Demodex mites (Fig. 11.5) in the etiology of blepharitis is controversial as they are present in healthy subjects as well as in patients with blepharitis, although, in the latter, their number is greatly increased [40].

Clinical Features

Blepharitis is a chronic process. Anterior blepharitis affects the lid margin anterior to the gray line with squamous debris or collarettes around the base of lashes. Posterior blepharitis mostly manifests with problems related to meibomian gland dysfunction leading to tear film instability with irritation and discomfort. Telangiectasia of the eyelid border is a prominent feature of rosacea.

Macroscopy

The eyelids are red and swollen with flakes and collarettes around the base of the lashes (Fig. 11.6).

Histopathology/Immunoprofile

Biopsy is seldom performed for blepharitis unless the condition is unilateral and nonreacting to therapy, hence, suspicious for an underlying malignant condition diffusely infiltrating the lid.

Differential Diagnosis

Pagetoid infiltration of the eyelid epithelium by sebaceous gland carcinoma can mimic chronic blepharitis. The condition is unilateral.

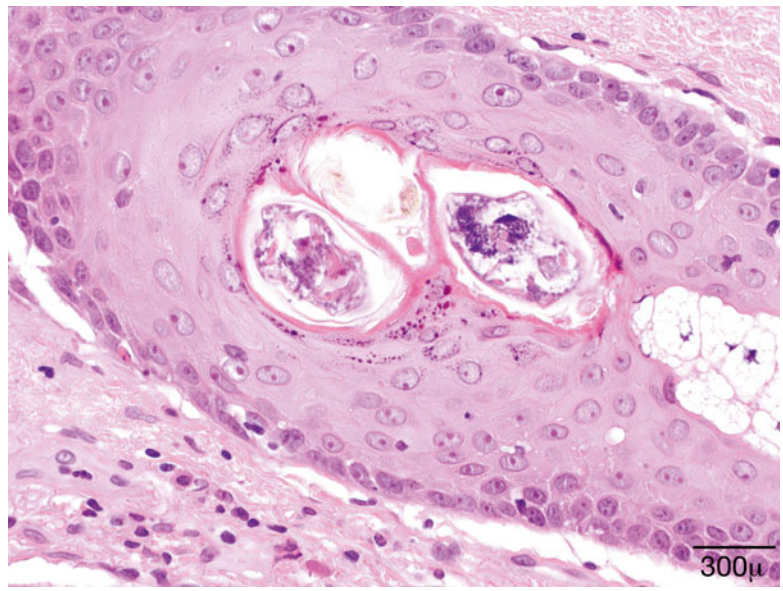

Fig. 11.5 *Demodex folliculorum* – Demodex mites in lash follicle. No evidence of inflammation (hematoxylin and eosin stain; original magnification 600×)

Fig. 11.6 Seborrheic blepharitis – hyperemic swollen eyelids, with telangiectasias and greasy scales on the lashes in young man

Genetics

There is no known genetic predisposition to blepharitis.

Prognosis and Predictive Factors

Chronic blepharitis predisposes to the development of styes and chalazia and can lead to atrophy of the meibomian glands, loss of lashes, and trichiasis (misdirected growth of lashes). The latter is further complicated by ocular surface disease and corneal lesions.

11.5.2 Hordeolum (Stye)

Definition

An acute, clinically painful, purulent infection of the eyelid glands of Zeis (external hordeolum) or Meibom (internal hordeolum), mainly caused by staphylococcal bacteria

Epidemiology

The lesion is fairly common in both children and adults.

Clinical Features

Initially the eyelid is swollen, edematous, and erythematous; then a purulent papule becomes visible. Spontaneous or surgical drainage regularly solves the problem. Histopathological material is usually not submitted.

11.5.3 Chalazion

Definition

A granulomatous reaction to the sebaceous material of the meibomian glands (lipogranuloma)

Epidemiology

This is a very common lesion in young females (10–29 years) and older men (>60 years) [41]. Patients with posterior blepharitis or rosacea are prone to the development of chalazia.

Etiology

Stricture or obstruction of the duct of the meibomian gland leads to disruption of the gland, and lipid material/sebum is spilled into the surroundings and followed by a granulomatous reaction.

Clinical Features

Chalazion presents clinically as a bump in the tarsal plate protruding under the overlying, normal-looking skin. The conjunctival surface may harbor a pyogenic granuloma.

Macroscopy

The material from a curettaged chalazion is jellylike, yellowish gray, and friable. Lesions that extend anteriorly or posteriorly may clinically mimic a malignant tumor and may be excised.

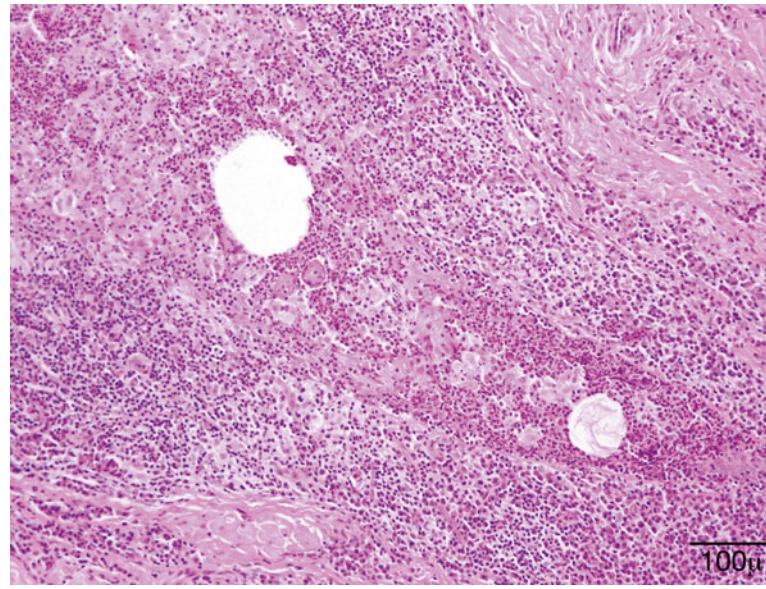

Fig. 11.7 Chalazion-granulomatous reaction with epithelioid macrophages and mixed inflammatory cells centered around dissolved lipid droplets (hematoxylin and eosin stain; original magnification 200×)

Histopathology

Microscopy shows a classic granulomatous reaction composed of epithelioid macrophages, multinucleated giant cells, plasma cells, lymphocytes, and leukocytes, centered around empty spaces corresponding to dissolved lipid (Fig. 11.7).

Differential Diagnosis

Other granulomatous reactions, tuberculous granuloma, sarcoidosis, cat scratch disease [42], insect bite

Prognosis

Very good, may resolve spontaneously, but has a tendency to recur in patients with blepharitis

11.5.4 Acne Rosacea

Definition

Rosacea (acne rosacea) is a common chronic inflammatory skin disease characterized by persistent erythema, telangiectasia, papules, and pustules. It affects mainly the midfacial zone and eyes.

Epidemiology

Rosacea is very common in fair-skinned people of northern ancestry; one-third have a family history of the disease. It mostly affects adults over 30 years of age [43] and shows a female predominance, although ocular rosacea affects both genders equally. It is probably one of the most underdiagnosed skin and ocular conditions.

Etiology

Rosacea reflects an abnormal sensitivity to the environment that is exacerbated by external triggers including UV light, heat, and a variety of microbes. There is an excessive activation of innate immune effector molecules, such as cathelicidin, an antimicrobial peptide, and kallikrein 5 (KLK5), the serine protease responsible for processing cathelicidin [44, 45]. Disturbed cathelicidin processing results in peptide fragments causing inflammation, erythema, and telangiectasia [46]. Infectious agents such as *Demodex* and *Demodex*-associated *Bacillus oleronius* [47–49] may act as triggers by stimulating overexpression of TLR2, which, in turn, enhances KLK5 production in keratinocytes [50].

Clinical Features

Ocular rosacea is characterized by blepharitis, telangiectasia of the eyelid border, recurrent chalazia, and conjunctival hyperemia.

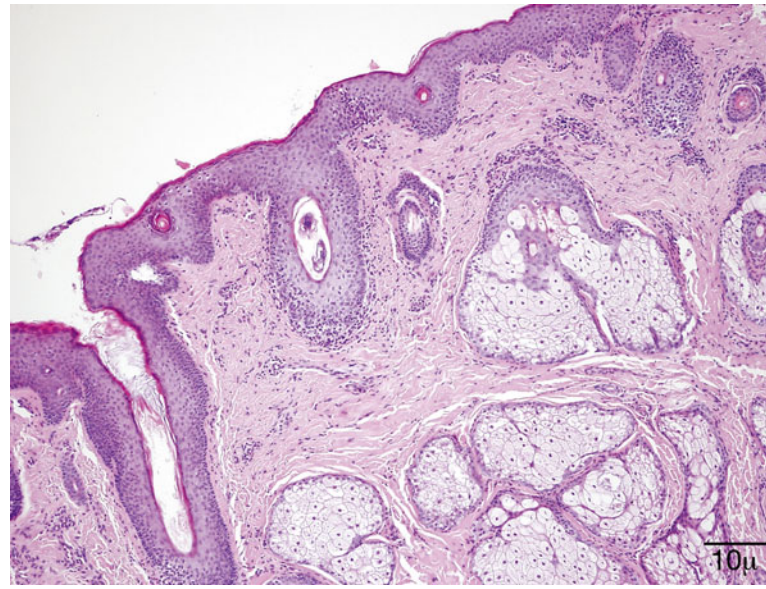

Fig. 11.8 Papular rosacea – perifolliculits with *Demodex folliculorum* and vascular dilation in early rosacea (hematoxylin and eosin stain; original magnification 100×)

Histopathology

Early lesions may show a mild perivascular and perifollicular lymphocytic infiltrate with telangiectasia (Fig. 11.8). In granulomatous rosacea, epithelioid histiocytes and giant cells are organized into tuberculoid granuloma [51].

Differential Diagnosis

Perioral dermatitis follows the use of topical steroids. Clinical correlation is needed to distinguish between the two entities. Granulomatous rosacea must be distinguished from sarcoid, granulomatous infection, and foreign body granuloma. Perifollicular granuloma speaks in favor of granulomatous rosacea [52].

Prognosis

Rosacea is a progressive condition; progression can be delayed by avoiding the triggers that provoke flare-ups (heat, UV radiation, alcohol).

11.5.5 Pyogenic Granuloma

Definition

Pyogenic granuloma (PG) is defined as an inflammatory and hyperplastic lesion by some authors [53] and a vascular tumor (lobular capillary hemangioma) by others; the terms are used interchangeably.

Epidemiology

PG is a very common lesion of the skin and mucous membranes and occurs most frequently in children and young adults.

Etiology

The etiology of PG is uncertain; it has been related to trauma, but a study of 178 cases disclosed a previous trauma in only 7 % [54]. Hormonal influence and/or drugs (retinoid, antiretroviral therapy, antineoplastic agents) have all been implicated in the pathogenesis.

Clinical Features

Clinically, the lesion presents as a rapidly growing, bright red polypoid papule or nodule that bleeds easily (Fig. 11.9).

Histopathology/Immunoprofile

Initially, PG is similar to granulation tissue, with capillaries and venules arranged in a radial pattern. The stroma is markedly edematous and infiltrated by a mixture of inflammatory cells (Fig. 11.10). Fully developed PG shows bland blood vessels proliferating in a lobular pattern, lined by plump endothelial cells. Inflammatory cells are few.

Endothelial cells in PG express WT1 [55, 56], CD34, and CD105 (endoglin) but are GLUT1 negative.

Differential Diagnosis

Bacillary angiomatosis occurs mostly in HIV-infected patients and is usually multiple; the causative *Bartonella* species may be evidenced by Warthin–Starry modified silver stain or a monoclonal antibody [57].

Infantile hemangiomas express GLUT1 [58], which is negative in PG.

Prognosis

The prognosis is usually good. The best treatment option with the lowest recurrence rates is complete surgical excision. Laser therapy and intralesional corticosteroids also give good results.

Fig. 11.9 Pyogenic granuloma – lobulated circumscribed purple tumor at the medial canthus in a young girl

11.5.6 Viral Diseases

11.5.6.1 Molluscum Contagiosum

Definition/Etiology

Molluscum contagiosum is a benign contagious lesion caused by a DNA poxvirus.

Epidemiology

Molluscum contagiosum is most common in children and young adults. It is spread by skin-to-skin contact or autoinoculation; sexual transmission occurs as well. Immunocompromised individuals are at increased risk.

Localization

This occurs mostly on the face and trunk. When located at or close to the eyelid border, follicular conjunctivitis is a complication.

Clinical Features

Molluscum contagiosum presents clinically as small, skin-colored, either solitary or multiple

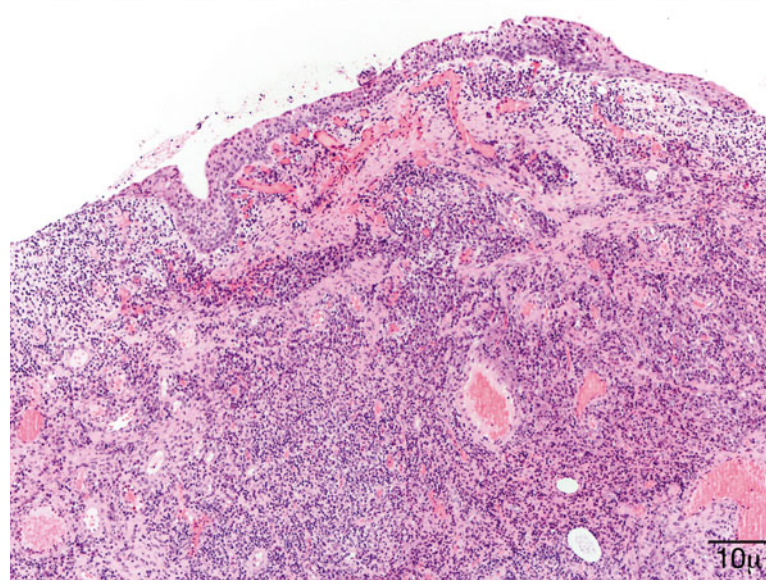

Fig. 11.10 Pyogenic granuloma – proliferating bland vessels, fibrosis, and intense inflammatory infiltrate are observed (hematoxylin and eosin stain; original magnification 100×)

umbilicated papules (Fig. 11.11). The lesions may be more numerous, confluent, and larger in immunocompromised patients.

Histology

Molluscum contagiosum is composed of endophytic lobules of proliferating squamous epithelium, which expands into the dermis. The suprabasal epithelial cells contain large, faintly granular, eosinophilic cytoplasmic inclusions (Henderson–Patterson or molluscum bodies) that displace the nucleus. The molluscum bodies increase in size, become more basophilic, and are finally extruded through a central ostium onto the surface of the skin (Fig. 11.12).

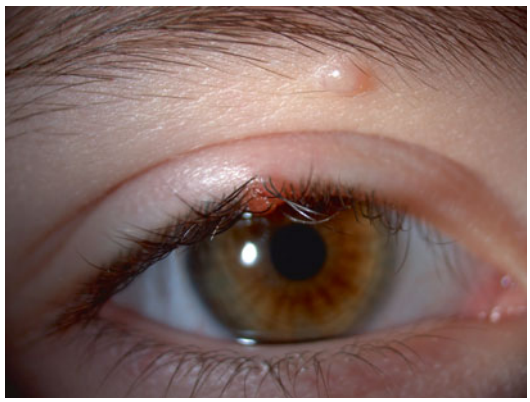

Fig. 11.11 Molluscum – a typical small umbilicated papule is present under the brow and another at the eyelid border in a young child

Differential Diagnosis

The intracytoplasmic eosinophilic inclusions are pathognomonic.

Prognosis

In immunocompetent patients, the lesion may spontaneously involute within 6–12 months. Recurrence is rare whether treated or not.

11.5.6.2 Verruca Vulgaris

Definition

Verruca vulgaris is a benign, rough-surfaced growth caused by certain human papillomavirus strains (HPVs 1, 2, 4).

Epidemiology

Verruca vulgaris is very common; it affects mostly children and adolescents. An increased frequency is noted in immunocompromised patients. Warts are relatively rare on the eyelids.

Clinical Features

The lesion presents as a papillomatous, exophytic papule with hyperkeratosis (Fig. 11.13).

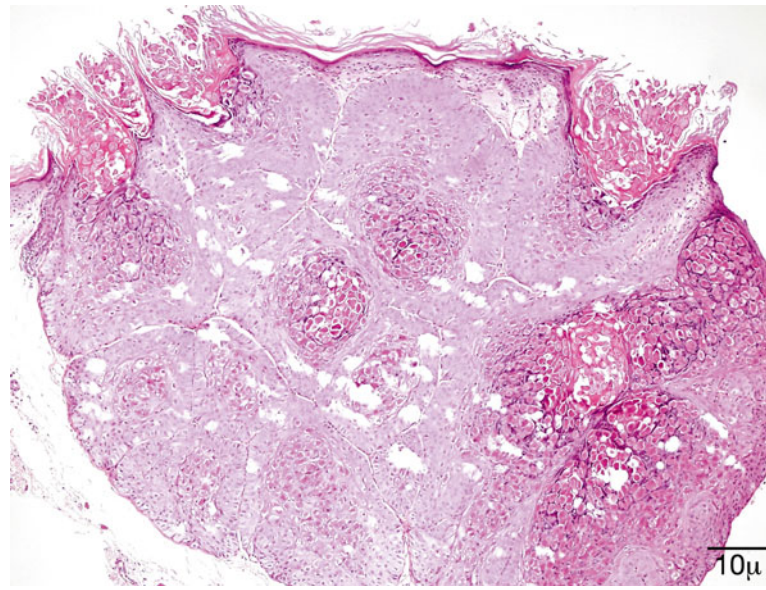

Fig. 11.12 Molluscum – endophytic epithelial lobules and characteristic intracytoplasmic eosinophilic inclusion bodies are conspicuous. Molluscum bodies are also extruded onto the surface (hematoxylin and eosin stain; original magnification 100×)

Histopathology

The surface is hyperkeratotic. The epidermis is papillomatous and acanthotic. The granular cell layer is prominent with coarse keratohyalin granules. Koilocytes are present in the upper layers of the epidermis. The rete ridges are elongated and tend to bend inward (Fig. 11.14).

Differential Diagnosis

The most important differential is from squamous cell carcinoma. Full-thickness atypia and loss of cellular polarity are not seen in verrucae. Actinic keratosis and seborrheic keratosis may have a verruca-like appearance.

Prognosis

Warts may regress spontaneously; however, despite the great variety of treatment options, recurrences are frequent. In immunocompromised patients, the lesions may be widespread and even more resistant to treatment.

Fig. 11.13 Verruca vulgaris – small skin-colored wart on the upper eyelid of a teenager

11.5.6.3 Herpesvirus Infection

Definition

Infection, primary or recurrent, caused by the herpes simplex DNA virus (HSV).

Synonyms

Cold sores

Epidemiology

The distribution of HSV infections is worldwide; 65–90 % of the population shows seropositivity for HSV1 or HSV2. The infection is generally acquired during childhood from an infected

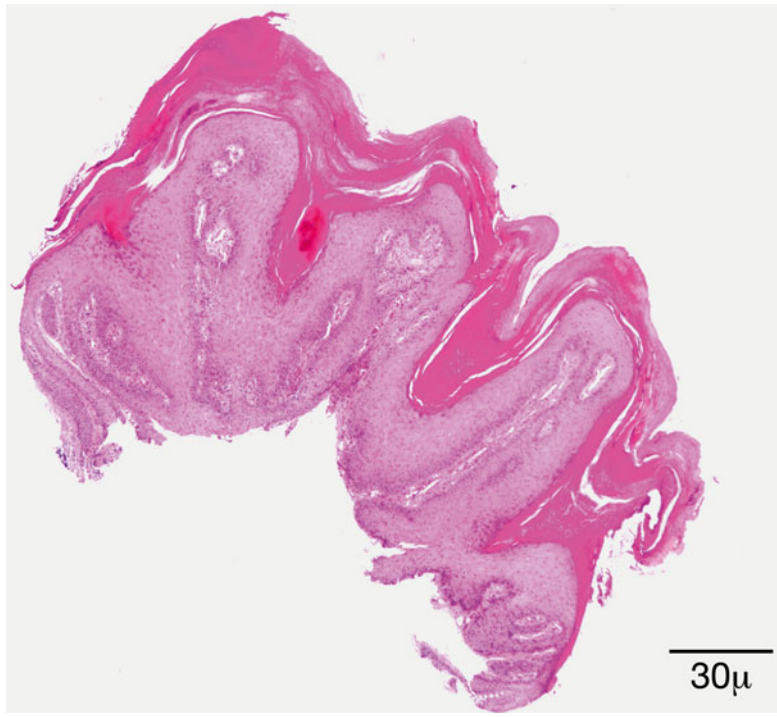

Fig. 11.14 Verruca vulgaris – the lesion is papillomatous; epidermal hyperplasia and hyperkeratosis are present. The rete ridges are elongated and point towards the center (hematoxylin and eosin stain; original magnification 40×)

person who sheds the virus. The virus enters through the skin or mucosa.

Localization

The primary infection mainly affects the oral mucosa, rarely the conjunctiva; however, recurrences are more common in the eye. The actively replicating virus follows the course of the sensory nerves and reaches a sensory ganglion (trigeminal, superior cervical, or ciliary), where it establishes latency.

Clinical Features

Primary infection of the eye may appear as a blepharitis with vesicles/blisters on the eyelid margin, accompanied by conjunctivitis. In about two-thirds of cases, corneal lesions also develop [59]. Recurrent lesions may also take the form of blepharitis or blepharoconjunctivitis, followed several days later by corneal manifestations. In immunosuppressed or HIV-positive patients, the eyelid lesion may become ulcerated [60] or may even mimic a tumor [61, 62].

Histopathology

Early changes are noticed in the epidermal cell nuclei. The nucleus swells and takes on a ground-glass appearance, and the chromatin forms peripheral clumps. There is vacuolization of the cytoplasm first in the basal cell layer; but soon, the entire epidermis is involved, followed by acantholysis and intraepidermal vesicle formation. The cytoplasm of these cells becomes eosinophilic and homogeneous. Some of the cells are multinucleated (Tzanck cells). Eosinophilic intranuclear inclusions may be seen in the multinucleated cells. In the dermis, there is a perivascular lymphohistiocytic inflammation.

Differential Diagnosis

Typical blistering lesions caused by HSV1 or HSV2 are diagnosed clinically. However, lesions mimicking tumors in HIV-positive patients may be biopsied to reach a diagnosis. The inflammatory reaction is granulomatous; nuclear inclusions consistent with HSV may be seen. Culture or PCR may eventually confirm the diagnosis.

Prognosis and Predictive Factors

Although the clinical manifestation is recurrent in a proportion of cases, with time the interval between attacks becomes progressively longer. Corneal complications may lead to severe visual impairment.

11.5.7 Bacterial Infections

Infections with *Streptococcus pyogenes* (group A *Streptococcus*) range from superficial impetigo to deeply invasive disease such as necrotizing fasciitis. *Staphylococcus aureus* may participate in a combined infection [63], especially in cases of necrotizing fasciitis [64]. It seems that the predominant infectious agent varies with geographic regions and socioeconomic level.

Synonyms

Pyoderma, school sores

Epidemiology

Impetigo occurs most commonly in economically disadvantaged, preschool-aged children.

Localization

Mostly seen in the perioral area and on the nose, sometimes affects the eyelids as well

Clinical Features

Minor trauma, bites, or burns of systemic disease may be elicited from the clinical history. Impetigo starts as a papule, quickly evolving into a vesicle with perivesicular erythema. The vesicle turns into pustules that gradually enlarge and break down, forming thick scabs [65]. Bullous impetigo occurs in nontraumatized skin and is characterized by blisters or moist erosions. Necrotizing fasciitis affects the skin and deep soft tissues.

Histopathology

Impetigo is characterized by the development of a subcorneal pustule beneath the granular layer. Gram-positive cocci may be found within the pustule or in neutrophil granulocytes. The dermis shows perivascular infiltration by neutrophil granulocytes and lymphocytes. Thrombosis of

the microcirculatory vessels in necrotizing fasciitis is the pathogenic background for gangrene.

Differential Diagnosis

The diagnosis is usually clinical. Secondarily infected pemphigus and pustular psoriasis seldom affect the eyelids.

Prognosis and Predictive Factors

Impetigo can resolve spontaneously or with local/oral antibiotic treatment. Post-streptococcal glomerulonephritis is a rare complication. Necrotizing fasciitis may be fatal in 10 % of cases; intensive treatment with surgical debridement of affected tissues is mandatory.

11.5.8 Fungal and Parasitic Infections

Definition

Fungal infection of the eyelid can be primary, the consequence of overgrowth of the commensal flora of the eyelid skin, in case of local or systemic immune depression, or direct inoculation into the skin. Another possibility is that the eyelid infection is the manifestation of hematogenous spread of a fungal infection. Parasitic infections are mostly the result of transmission by a vector, e.g., a fly, mosquito, or tick.

Epidemiology

Some fungi and parasites have a worldwide distribution; others are endemic to certain areas. Hence, the geographic location is a significant determining factor in the development of fungal or parasitic infections [66].

11.5.9 Fungal Infections

11.5.9.1 Histoplasmosis

Histoplasma capsulatum is endemic in North America. Cutaneous manifestation is usually only seen in immunocompromised individuals. The histopathological features vary. There is a dermal infiltrate with foamy histiocytes, granulomatous infiltration, and a variable amount of inflammatory cells. The organism appears intra- or extracellularly such as small yeastlike structures within a clear halo.

11.5.9.2 Cryptococcosis

Cryptococcus neoformans has a worldwide distribution. The eyelid cutaneous manifestations are usually part of a systemic disease in immunocompromised patients [67] but can also occur as a primary skin disease. There is a dense dermal infiltrate of foamy histiocytes with or without a granulomatous inflammation. Mucin stains, PAS, and Grocott highlight the thick capsule of the pathogen.

11.5.9.3 Sporotrichosis

Sporotrichosis is caused by the dimorphic fungus *Sporothrix schenckii*. It can present with a disseminated, lymphocutaneous, or cutaneous form. Transmission usually occurs via direct implantation in the skin. The solitary cutaneous form presents as a verrucous or ulcerated nodule. Histology shows a suppurative granuloma; PAS or Grocott stains of multiple serial sections are usually needed to demonstrate the 4–6 μm spores.

11.5.9.4 Blastomycosis

Blastomycosis is endemic in North America. *Blastomyces dermatitidis* is a dimorphic fungus. The inhaled spores transform into yeast and spread hematogenously. The most common extrapulmonary involvement is the skin [68]; eyelid involvement is uncommon [69]. Rarely direct inoculation is followed by a primary cutaneous lesion, which is verrucous or ulcerated. Histologically, the picture closely resembles sporotrichosis. The skin surface shows pseudoepitheliomatous hyperplasia. Fungal spores are thick walled and exhibit a broad-based budding, which helps in its identification.

11.5.10 Parasitic Infections

Leishmaniasis (oriental sore) is a parasitic infection caused by protozoa of the genus *Leishmania*, transmitted by sand fly. Leishmaniasis is endemic in tropical and subtropical areas and the Mediterranean countries. Recently a significant number of leishmaniasis cases have been

reported in travelers [70] to endemic countries; thereupon, this led to an increased awareness of the condition. Leishmaniasis in travelers is characteristically the cutan type [71]. The mucocutaneous type is generally associated with infection acquired in Latin America [72].

In immunocompetent patients, the infection is usually self-limited. It is rare in the eyelid; the clinical presentation can simulate a cutaneous appendage tumor [73], a basal cell carcinoma (BCC) [74], or, more commonly, a chalazion [75]. The typical periocular location is the lateral canthus [76]. The histopathological picture depends on the time of biopsy and on the host response. In the early stages, the presentation mimics a xanthogranulomatous inflammation; macrophages aggregate in the dermis. Later, epidermal hyperplasia develops with ulceration. A dense dermal infiltrate of histiocytes, plasma cells, and lymphocytes is seen. The inflammatory infiltrate later becomes granulomatous. The *Leishmania* amastigotes are recognized in the cytoplasm of histiocytes (Leishman–Donovan bodies) as round organisms seen with hematoxylin and eosin (H&E) or Giemsa stain, as a rule, in the non-granulomatous areas. Recently, polymerase chain reaction (PCR) is also available for diagnostic purposes.

11.5.11 Filarial Infections

Dirofilaria repens is endemic in the Mediterranean area; the reservoirs are dogs or cats, and the larvae are accidentally transmitted to humans by bite of mosquito vectors. It has been reported with increasing frequency from areas outside the endemic territories [77]. The larva cannot survive in humans but is able to wander under the conjunctiva to the orbit, through the bridge of the nose from one eye to the other (personal observations), or to the lacrimal gland [78]. In the eyelid, the infection presents as an anterior cellulitis not responding to conventional therapy and is generally biopsied (Fig. 11.15). The filaria provokes a granulomatous inflammatory reaction with foreign body giant cells and a markedly eosinophilic infiltrate (Fig. 11.16). The worm is recognized by its thick ridged cuticle and well-developed musculature (Fig. 11.17). As there is no blood filariasis, no systemic therapy is necessary.

Fig. 11.15 *Dirofilaria repens* – the elderly male patient had an anterior cellulitis that did not react to conventional therapy. Biopsy disclosed a granulomatous inflammation caused by *D. repens* (Clinical picture courtesy of Dr. Olga Lukáts, Semmelweis University, Dept. of Ophthalmology)

Loa loa is a nematode endemic in the rain forest region of West and Central Africa. The nematodes are transmitted by *Chrysops* flies. Many patients remain asymptomatic for years after the infection. Loa loa has a predilection for the conjunctiva and periocular tissues [79, 80]. In an extensive review of the literature on loaiasis in Europe and the United States from 101 cases reported, 48 experienced eye worm migration [81]. The clinical history provides important clues to the diagnosis (travel to or immigration from endemic countries). The filaria can be demonstrated in blood smears or by PCR.

11.6 Eyelid Lesions with Association to Systemic Diseases

A few lesions occurring in the eyelid region might be associated with systemic disorders. In fact, on occasion, the eyelid lesion might be the first manifestation of disease, hence the importance for both ophthalmologists and ophthalmic pathologists to be aware of these.

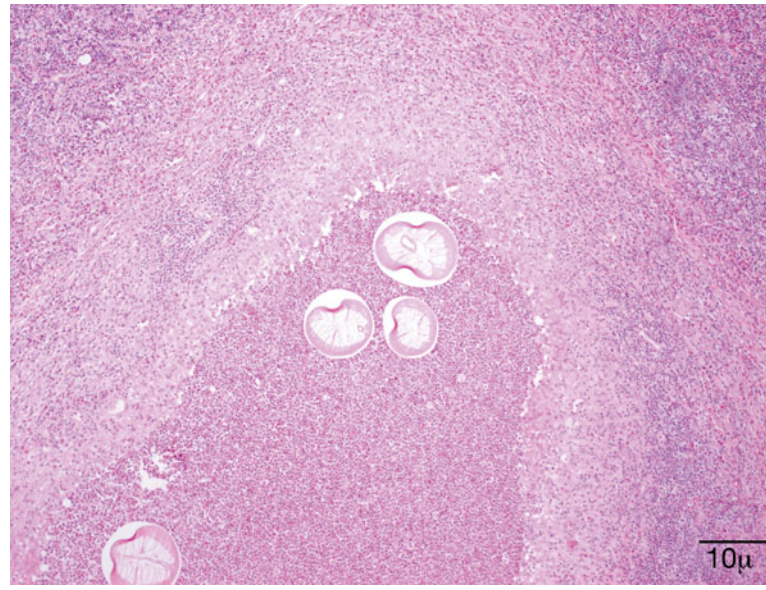

Fig. 11.16 *Dirofilaria repens* – an intense granulomatous reaction with foreign body giant cells and numerous eosinophils is present around cross sections of a worm (hematoxylin and eosin stain; original magnification 100×)

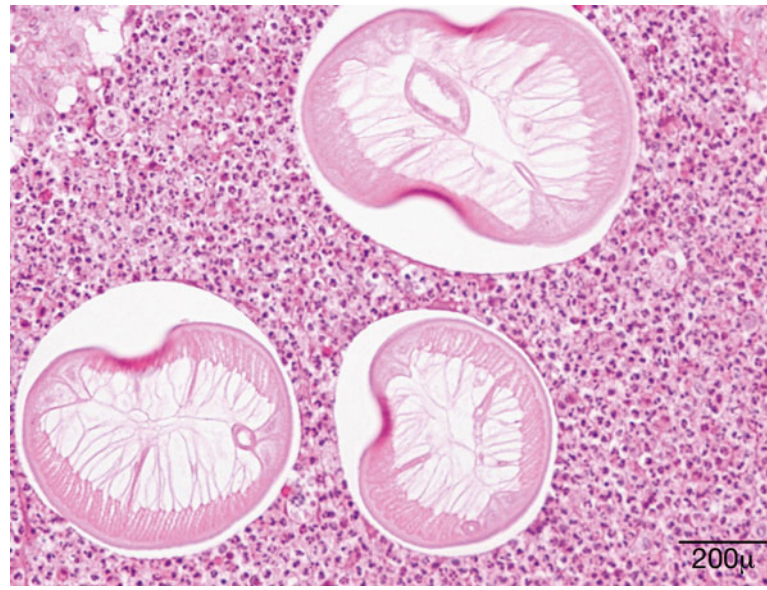

Fig. 11.17 *Dirofilaria repens* – the multilayered ridged cuticle, thick musculature, and the presence of uterus help recognition of a female worm (hematoxylin and eosin stain; original magnification 400×)

11.6.1 Xanthelasma

Definition

It is a form of cutaneous xanthoma, a group of lesions characterized by the accumulation of lipid-rich macrophages also known as foamy cells [82]. These lesions are usually associated with disorders of lipoprotein metabolism, although only a minority of individuals with such disorders develop xanthomas [82, 83]. Therefore, an increased vascular permeability has been implicated in the pathogenesis of these lesions [84].

Clinical Features

The eyelid and periocular skin are the most affected sites. Clinically, xanthelasma presents as yellowish, noninflamed flat or slightly elevated plaques originating in the medial eyelid and

Fig. 11.18 Xanthelasma – It presents clinically as yellowish, non-inflamed flat plaques originating in the medial eyelid and spreading laterally (Clinical picture courtesy of Dr James Garrity, Mayo Clinic)

spreading laterally in a symmetric fashion (Fig. 11.18). These are not painful and do not ulcerate the skin. Xanthelasma is more commonly seen in the Asian and Mediterranean populations.

In approximately 50 % of the patients, these lesions are associated with elevated plasma lipid levels. These might be due to a hereditary genetic abnormality such as dyslipoproteinemia, familial hypertriglyceridemia, familial lipoprotein lipase deficiency, or hyperlipidemias, secondary to diabetes mellitus type II [84–87].

Histological Features

Microscopically, the dermis is infiltrated diffusely by numerous foamy histiocytes, forming perivascular aggregates (Fig. 11.19). The overlying epidermis is not affected. Areas of necrobiosis, vasculitis, or a prominent associated lymphoid infiltrate should not be seen, and the presence of these findings should evoke other diagnoses such as necrobiotic xanthogranuloma.

On immunohistochemistry, the foamy cells are positive for macrophage markers such as CD68 and CD163 and negative for S-100 and CD1a. Because the differential diagnosis also includes lesions with clear cell morphology such as balloon cell melanoma and balloon cell nevus, melanocytic markers might be helpful.

Treatment

Xanthelasma in most patients requires no treatment. Lesions might be treated for cosmetic reasons. Various treatments have been studied, including surgical excision, treatment with chemicals, and ablative laser therapy; but these methods have disadvantages. Recently, nonablative laser therapy has been proposed as a treatment for xanthelasma palpebrarum [88].

11.6.2 Calcinosis Cutis

Definition

The term calcinosis cutis is used to describe a group of diseases characterized by calcium deposits in the skin. Historically, these have been divided into dystrophic type when calcium deposits occur in previously damaged tissue and the less common metastatic form, which is associated with elevated serum calcium and/or phosphate levels [89]. In many cases, the pathogenic mechanism is not identified, and these cases have been assigned as idiopathic. Herein, we will discuss the most common form occurring in the eyelid region, the subepidermal calcified nodule.

Pathogenesis

The pathogenesis is not completely understood. Insoluble compounds of calcium are deposited within the skin, primarily composed of hydroxyapatite crystals or amorphous calcium phosphate, with no known predisposing factors. Although systemic associations, such as hyperparathyroidism, renal insufficiency, and other disorders of calcium/phosphate, have been described in metastatic calcinosis and an underlying tissue abnormality described with dystrophic calcification [90], an underlying systemic or local cause has not been confirmed in association with subepidermal calcified nodules [91].

Clinical Presentation

Subepidermal calcified nodule usually occurs as a small, <5 mm, solitary, white-yellowish nodule on the eyelid of young children in their first or early second decade of life [91, 92]

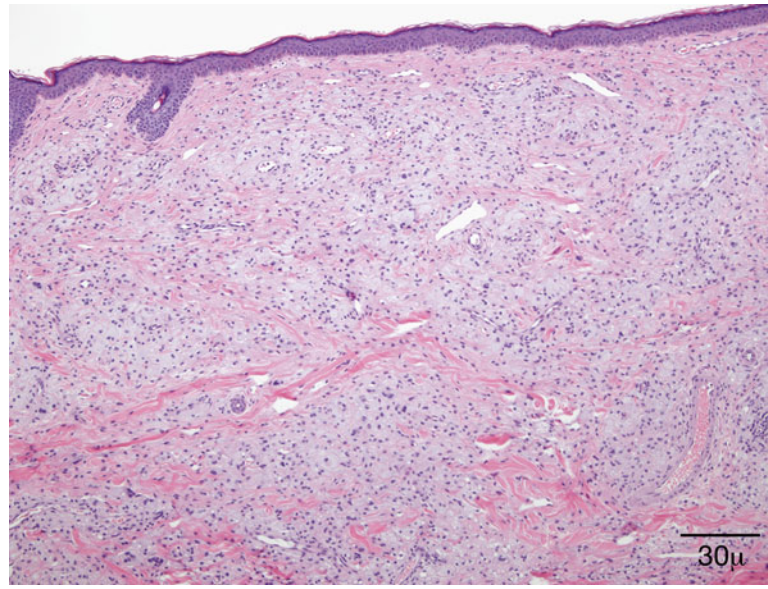

Fig. 11.19 Xanthelasma – Microscopically, it is characterized by a diffuse dermal infiltration of foamy histiocytes (hematoxylin and eosin stain; original magnification 40×)

Fig. 11.20 Calcinosis cutis – solitary white-yellowish nodule in the upper eyelid of a young child (Clinical picture courtesy of Dr. George Bartley, Mayo Clinic)

(Fig. 11.20). Multiple lesions can be seen but are less frequent [93].

Clinically, these might be mistaken for eyelid cyst, molluscum contagiosum, cutaneous horn, or a neoplasm in an older patient [91].

Histopathology

The characteristic finding is the presence of subepithelial, sharply demarcated basophilic amorphous deposits surrounded by variable amounts of histiocytic foreign body giant cell reaction. The overlying epidermis is usually acanthotic and papillomatous with occasional hyperkeratosis (Fig. 11.21). The deposits stain positive with von Kossa stain for calcium, and the histiocytes are positive for CD68 immunostain [91, 92, 94].

Prognosis and Treatment

Surgical excision is usually curative with rare cases of recurrence [91].

11.6.3 Sarcoidosis

Definition

Sarcoidosis is a multisystem disease of unknown etiology characterized by noncaseating granulomas in various organs. Granulomas most often appear in the lungs (85 %) and lymph nodes (34 %), but virtually any organ may be involved including the eye (27 %) and, less commonly, the central nervous system (1 %).

Epidemiology

It affects most commonly young adults of both sexes. Incidence is highest for individuals younger than 40 years and peaks in the age group from 20 to 29 years; a second peak is observed for women over age 50 years. The disease is most prevalent in Northern European countries. In the United States, sarcoidosis is more common in African descendant than Caucasians, with an

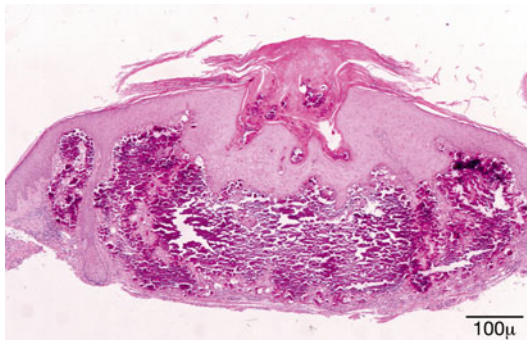

Fig. 11.21 Calcinosis cutis – dermal deposit of amorphous basophilic granular material surrounded by histiocytic foreign body reaction. The overlying epidermis shows acanthosis and hyperkeratosis (hematoxylin and eosin stain; original magnification 200×)

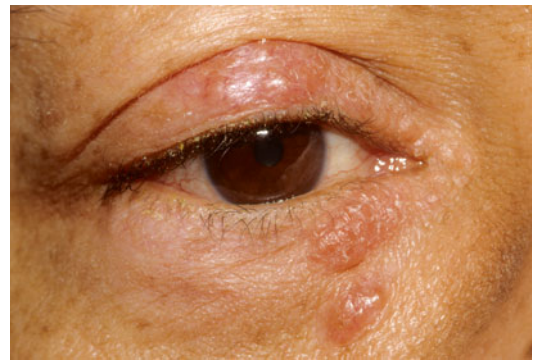

Fig. 11.22 Sarcoidosis – multiple eyelid elevated confluent nodules, grayish white with mild umbilication in areas (Clinical picture courtesy of Dr George Bartley, Mayo Clinic)

annual incidence reported of 35.5 and 10.9/100,000, respectively [95–97].

Pathogenesis

The pathogenesis of this disease is not yet known. The most accepted hypothesis is that in genetically susceptible individuals, sarcoidosis is caused through alteration in immune response after exposure to an environmental, occupational, or infectious agent. Studies have shown an increase in B-cell activity with hypergammaglobulinemia in about 50 % of the patients. Reduced delayed hypersensitivity is also found in many patients. Immune dysregulation due to persistent low virulence antigen that is poorly cleared by the immune system, leading to a chronic T cell of the Th1 subtype response with granulomatous response, has been hypothesized. Medications that increase Th1 response, such as interferon, have been reported to trigger or exacerbate sarcoidosis. GLI1 oncogene has been found to be highly expressed in patients with sarcoidosis [98].

Clinical Features

The eye may be affected by sarcoidosis in a variety of ways, with the most frequent site being the uveal tract [99–101]. Optic nerve and optic nerve head involvement has been reported in about 5 % of patients with sarcoidosis. Sarcoid may involve the lacrimal gland and rarely extends into the adjacent orbital soft tissue, which was observed in only 2 of 202 cases (1 %) studied by Obenauf et al. [101].

Eyelid involvement is extremely rare, with only a few case reports in the literature [102–105]. Clinically, the lesions appear as slightly elevated, grayish-white, mildly umbilicated papules and nodules, some of which might become confluent (Fig. 11.22). Eyelid sarcoidosis may be an isolated manifestation of sarcoidosis or associated with systemic more often than ocular disease [102, 104, 105].

The diagnosis of sarcoidosis is often a matter of exclusion of other diseases including neoplasm. It is made on the basis of signs and symptoms, patient's age, race, and laboratory findings. A definitive diagnosis requires a biopsy to be performed.

Histopathology

The typical lesion in the biopsy is characterized by circumscribed epithelioid granulomas with little or no necrosis and few Langhans giant cells (Fig. 11.23). Giant cells may contain asteroid or Schaumann bodies. A sparse lymphocytic infiltrate may be seen in the periphery of these granulomas, which is the reason these are referred to as "naked granulomas."

Differential Diagnosis

This includes mainly granulomatous infectious processes such as tuberculosis and fungal infection.

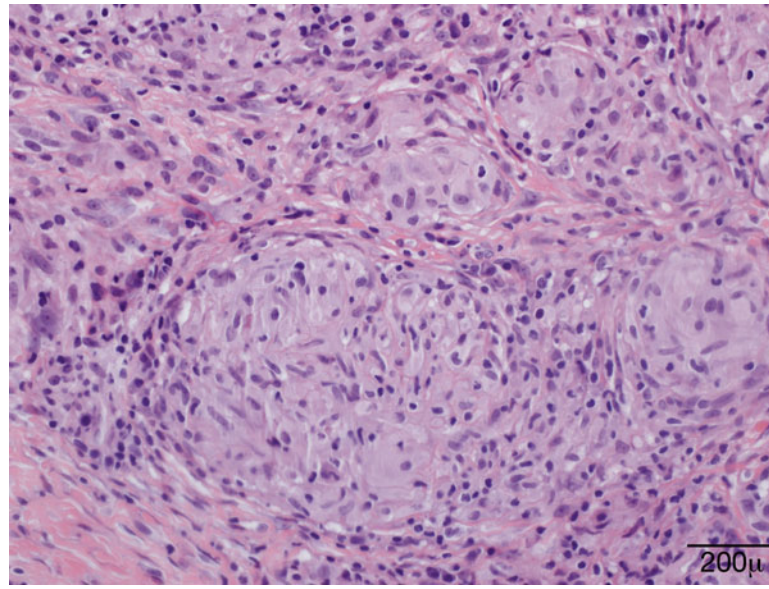

Fig. 11.23 Sarcoidosis – the typical sarcoid lesion is characterized by circumscribed epithelioid granulomas with little or no necrosis and few Langhans giant cells (hematoxylin and eosin stain; original magnification 400×)

Therefore, special stains and tissue cultures for microorganisms must be obtained on a routine basis.

Prognosis

The course of the disease is variable, ranging from self-limited acute disease to a chronic debilitating disease that could result in death. Spontaneous remissions occur in two-thirds of the patients, but 10–30 % of patients have a more chronic or progressive course [106]. The mortality rate is 1–6 %. Death can be due to pulmonary fibrosis leading to respiratory failure, myocardial involvement leading to cardiac arrhythmias and cardiac failure, central nervous system (CNS) involvement, renal insufficiency, and liver disease [107].

11.6.4 Amyloidosis

Definition

Amyloidosis refers to a group of diseases characterized by the extracellular deposition of amorphous, eosinophilic hyaline material, constituted by insoluble fibrous protein aggregates of autologous origin in the connective tissue and perivascular spaces of various organs [108]. Clinically, amyloidosis is divided in five groups: primary systemic, primary localized, secondary to a chronic illness, secondary to multiple myeloma, and familial type. The involvement of the eyelids occurs in the first two forms.

Epidemiology

Primary systemic amyloidosis occurs in approximately 8 per million people per year, with approximately 3,000 new patients annually in the United States [109]. Median age at diagnosis is 64 years, but patients can present at any age. The male-to-female ratio is nearly 2:1. The prevalence of amyloidosis seems to be higher in the black and lower in the Asian populations, and it mirrors the prevalence of multiple myeloma and monoclonal gammopathies in the same populations. The incidence of secondary amyloidosis in the United States has been falling over the decades and accounts for only 3 % of systemic amyloidosis.

Etiology

The etiology of amyloidosis depends on its form. The causes for primary amyloidosis are still not well known, but it seems related to the presence of immunoglobulin free light chain circulating in the blood [110, 111]. The pathogenesis of amyloidosis associated to multiple myeloma and monoclonal gammopathies is better understood and has been the subject of extensive research [112–114].

Fig. 11.24 Amyloid – some patients present clinically with hemorrhagic papules. These lesions have been considered highly indicative of systemic amyloidosis (Clinical picture courtesy of Dr. James Garrity, Mayo Clinic)

Clinical Features

The skin of the eyelids is involved in either primary systemic or localized amyloidosis. Typically, the lesions are symmetrical, bilateral, single, or multiple, confluent yellowish or waxy papules [115]. Purpura is a common manifestation caused by vascular wall fragility, the result of amyloid deposits within the vessel walls (Fig. 11.24). Hemorrhagic papules that affect the eyelids have been considered diagnostic of systemic amyloidosis [116, 117]. Some patients might present with nonspecific chronic eyelid swelling, which might cause delay in the correct diagnosis [118, 119].

Histopathology

Papular lesions are the result of amyloid deposits in the superficial dermis. Clefting is often seen around large deposits. The amyloid also accumulates around and within vascular walls in the dermis and subcutaneous tissue (Fig. 11.25). This finding is observed in hemorrhagic lesions. Amyloid deposits may also be seen around cutaneous adnexa. No or scanty inflammation is observed in association with the amyloid deposits.

Amyloid stains pink with hematoxylin and eosin and metachromatically with crystal violet and methyl violet [120]. With Congo red stain, amyloid is orange in color and displays an apple-green birefringence under polarized light (dichroism) (Fig. 11.26). Amyloid has a bright yellow-green color with Thioflavin T stain.

A number of immunostains were developed to identify the protein components of amyloid and had been used to further classify amyloidosis. Currently, this has been largely replaced by subtyping, using tandem mass spectrometry analysis on formalin-fixed, paraffin-embedded specimens, due to the superior sensitivity and specificity of this latter technique [121].

Prognosis

The prognosis of amyloidosis involving the eyelids depends on the associated underlying disease. If the lesion is localized, surgical resection is the proposed treatment [122].

11.6.5 Juvenile Xanthogranuloma

Definition

It is a form of non-Langerhans cell histiocytosis, classified as World Health Organization (WHO) type II among a group of diseases known as histiocytosis. It is a benign, self-limited condition, rarely associated with systemic manifestations and typically occurring in the early childhood.

Epidemiology

Juvenile xanthogranuloma (JXG) is the most common of the non-Langerhans cell histiocytosis [123], although it is relatively rare. It had a reported incidence of 0.52 % among all pediatric lesions of the Kiel Pediatric Tumor Registry (KPTR) between 1965 and 2001 [124]. JXG may be present at birth; however, most lesions are diagnosed in the first year of life [124, 125]. There is a slight male predominance [124].

Etiology

The cause of JXG is unknown. JXG is a type of non-Langerhans cell histiocytosis, which derives from CD34+ stem cells that differentiate into CD14+ dermal/interstitial dendrocytes, considered to be the precursor cells for JXG [123].

Clinical Presentation

Clinically, it presents as single or multiple lesions, firm and slightly raised papulonodules measuring a few millimeters (Fig. 11.27). These may vary in color from reddish or yellowish to brown. The lesions can occur in any location and are most common on the head/neck and upper

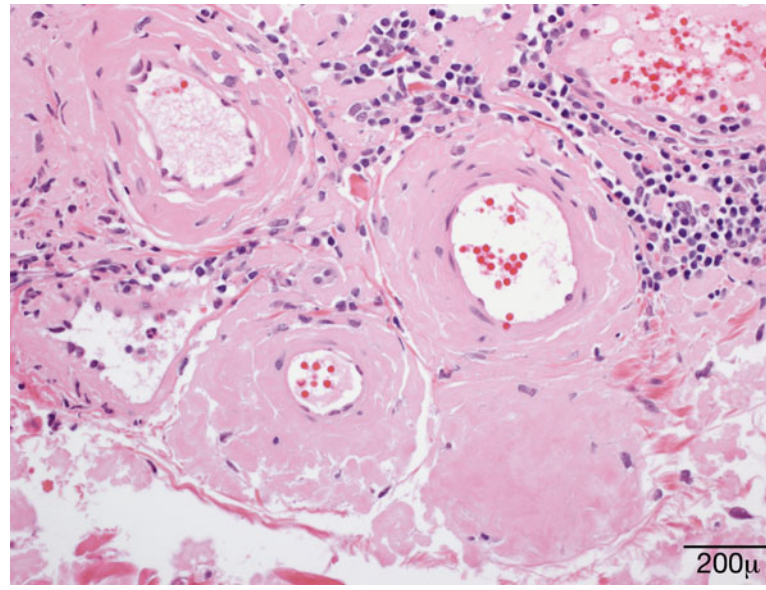

Fig. 11.25 Amyloid – eyelid biopsy shows dermal, predominantly perivascular deposits of amorphous eosinophilic hyaline material (hematoxylin and eosin stain; original magnification 400×)

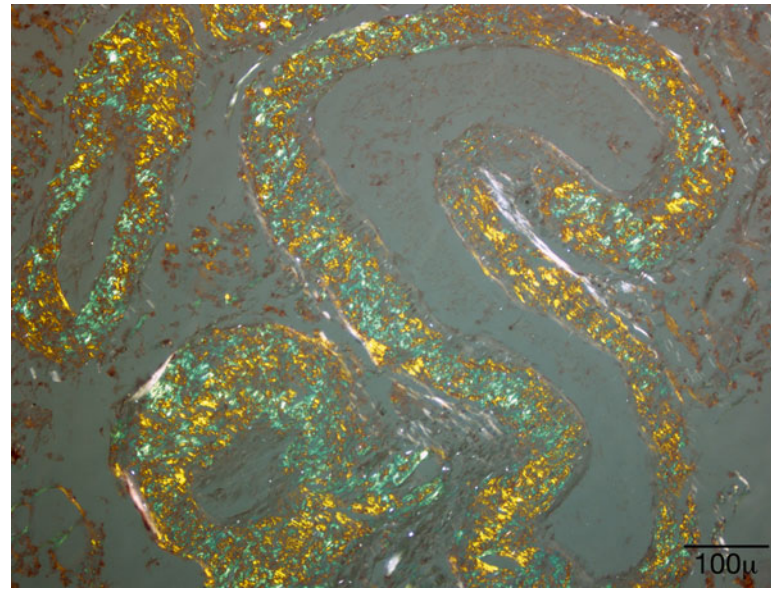

Fig. 11.26 Amyloid – orange in color with Congo red stain, under polarized light, however, amyloid shows an apple-green birefringence, also known as dichroism (hematoxylin and eosin stain; original magnification 200×)

trunk. The lesions are usually solitary, but multiple lesions and extracutaneous systemic involvement may occur, such as the liver, lung, spleen, lymph nodes, bones, and gastrointestinal tract [125, 126].

JXG may involve the skin of the eyelid and less commonly intraocular tissues, such as the iris, ciliary body, cornea, and episclera. Juvenile xanthogranuloma is known to cause spontaneous hyphema if the lesion involves the iris. Other ocular clinical presentations may include uveitis, heterochromia iridis, or an iris mass.

Histopathology

Microscopically, JXG is characterized by a dense dermal and subcutaneous tissue histiocytic infiltrate predominantly containing variable number of Touton giant cells (Fig. 11.28). The latter are

multinucleated giant cells with a ring or wreath of nuclei surrounded by foamy cytoplasm and considered pathognomonic of JXG. Spindle cells can also be seen in the background. Other inflammatory cells such as lymphocytes, eosinophils, neutrophils, and mast cells are rarely present. The infiltrate surrounds the preexisting cutaneous adnexa, and the overlying epidermis is usually normal or thinned. Mature lesions tend to be more lipidized, and regressing lesions may show a prominent fibrous background [127].

Immunostaining is important in establishing the diagnosis. JXG stains positive for factor XIIIa, CD68, CD163, CD14, and fascin. S-100 and CD1a, specific for Langerhans cells, are usually negative [124, 125].

The differential diagnosis includes Langerhans cell histiocytosis, which is positive for CD1a and S-100 immunostains, xanthoma, and less commonly dermatofibroma. These latter two lesions are discussed below.

Fig. 11.27 JXG – small yellowish nodule in the eyelid of a young child. The overlying skin is smooth. No signs of inflammation (Clinical picture courtesy of Dr. Elizabeth Bradley, Mayo Clinic)

Treatment and Prognosis

Cutaneous JXG usually regresses spontaneously and requires no treatment. Ocular JXG should be managed by an ophthalmologist, and the required treatment will depend on type of ocular involvement and complications.

Symptomatic systemic lesions, often due to a mass effect, may require treatment if they do not regress spontaneously [126]. Treatment may involve excision, radiation, or chemotherapy [128].

In general, the prognosis is excellent and disease-related deaths are uncommon but can typically occur in younger children with central nervous system or massive hepatic involvement [129].

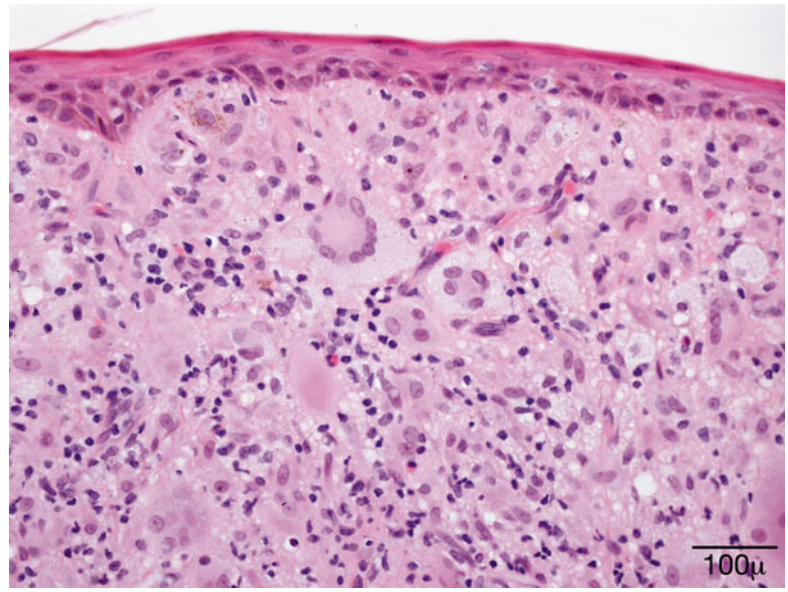

Fig. 11.28 JXG – dense dermal histiocytic infiltrate containing numerous Touton-type giant cells. These are characterized by a ring of nuclei surrounded by foamy histiocytes. A few eosinophils are seen intermixed (hematoxylin and eosin stain; original magnification 200×)

11.6.6 Necrobiotic Xanthogranuloma

Definition

Necrobiotic xanthogranuloma (NXG), a distinctive dermal and subcutaneous xanthogranulomatous reaction, is a rare form of paraneoplastic syndrome often associated with monoclonal paraproteinemia [130] or other hematologic diseases. It is potentially a disfiguring disease that can involve the face, trunk, or extremities with a particular predilection for the periorbital region.

Epidemiology

The prevalence of disease is slightly higher in women than men, and onset is usually in the sixth decade of life (mean age 59.76 years).

Pathogenesis

The pathogenesis of NXG remains unknown. Because of the strong association with paraproteinemia, the causative role of this abnormal immunoglobulin has been speculated. It was thought that perhaps the increased serum immunoglobulins would combine with lipids and be deposited in the skin, leading to a foreign body giant cell reaction and the characteristic histopathological features of necrobiotic xanthogranuloma [131]. Others have thought that the activation of monocytes in vivo may contribute to the intracellular accumulation of lipoprotein-derived lipids, leading to non-inherited xanthomatosis [132, 133].

Clinical Features

Clinically, NXG is characterized by large, often yellow, indurated plaques sometimes associated with telangiectasia (Fig. 11.29). The lesions often become inflamed, leading to superficial ulceration. The most common locations are the periorbital region and thorax. Extensive lesions involving the eyelids may extend into the orbital soft tissues.

The clinical differential diagnosis includes mainly xanthelasma and xanthoma, lesions that are not usually indurated. The association of NXG with monoclonal gammopathy is very characteristic. Although IgG monoclonal gammopathy represents the most common association [134–137], a rare form of IgA gammopathy has also been reported [138], as well as the association with other hematologic disorders such as multiple myeloma, chronic lymphocytic-leukemia, lymphoma, and other less common diseases such as cryoglobulinemia.

Fig. 11.29 NXG – clinical picture shows yellow, indurated plaques in both eyelids (Clinical picture courtesy of Dr. James Garrity, Mayo Clinic)

Histopathology

The histopathology is characterized by infiltrates containing mostly macrophages, foamy cells associated with extensive necrobiosis (degeneration of collagen) surrounded by palisading granulomatous reaction (Fig. 11.30). Numerous giant cells, Touton and foreign-body types, are usually seen. Cholesterol clefts, which have been reported previously, do not appear to be as common as initially thought [134]. Other findings include lymphoid follicles and a mixture of other inflammatory cells.

The differential diagnosis includes other necrobiotic disorders, especially necrobiosis lipoidica, subcutaneous granuloma annulare, and rheumatoid nodule. In NXG, the necrobiosis is more extensive than in other diseases and often occurs in broad bands. More important,

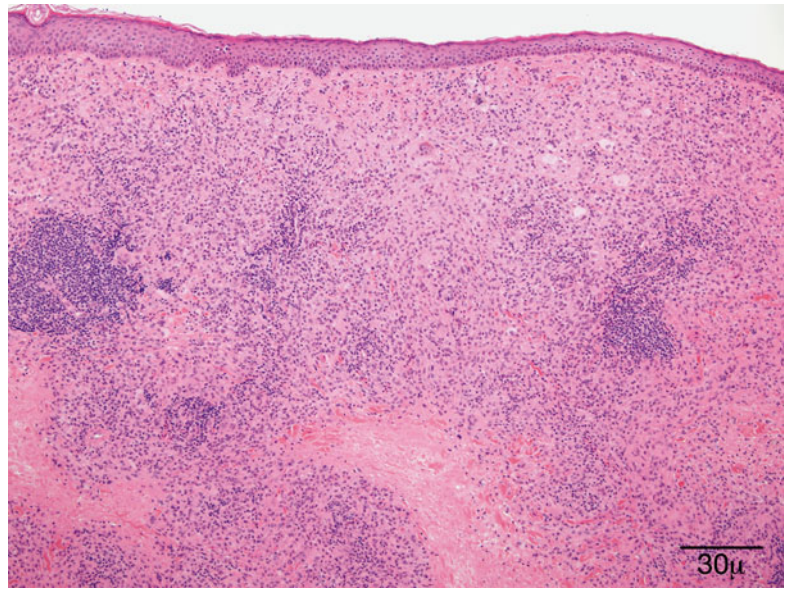

Fig. 11.30 NXG – eyelid biopsy shows dense dermal infiltrate containing mostly macrophages, Touton-type giant cells, and extensive areas of necrobiosis, surrounded by histiocytic granulomatous reaction (hematoxylin and eosin stain; original magnification 40×)

the clinical presentation differs in each of these lesions. Necrobiosis lipoidica tends to affect mainly pretibial areas in diabetic patients. Granuloma annulare is characterized by papules often in young adults, and rheumatoid nodules are seen in patients with clinically apparent rheumatoid arthritis. Other lesions considered in the differential because of the presence of foamy histiocytes and Touton-type giant cells are xanthogranuloma and Erdheim–Chester disease. These entities do not show the necrobiosis that characterizes NXG.

Prognosis

Necrobiotic xanthogranuloma can cause impairing sequela. The cutaneous lesions tend to progress, and the course is unpredictable with periods of stabilization and reduction and more aggressive periods with extensive ulceration [135, 139]. The treatment is difficult and should include management of the underlying systemic disease and control of the skin lesions. Surgical removal of the lesions is generally not recommended because of the risk of recurrence, which was around 42 % in a large series [135]. However, surgery might be necessary to correct scarring and eyelid malfunction. Systemic prednisone and steroid injections have been proposed as alternative forms of treatment as well as low-dose radiation therapy and alkylating regimens.

11.6.7 Granulomatosis with Polyangiitis (Wegener's Granulomatosis)

Definition

Wegener's granulomatosis (WG), recently proposed to be renamed granulomatosis with polyangiitis (GPA) [140], is an uncommon disease defined by vasculitis involving small vessels, extensive "geographic" necrosis, and granulomatous inflammation classically involving the kidneys (glomerulonephritis) and the upper and lower respiratory tract (sinuses, nose, trachea, and lungs). The spectrum and severity of disease is variable, ranging from an indolent course involving one site to extensive multiorgan vasculitis leading to death [141, 142].

Epidemiology

GPA most commonly affects individuals in the fourth or fifth decades of life [141, 143]. The disease can, however, affect people at any age (age range, 5–91 years), with approximately 15 % of cases beginning before 20 years of age [144, 145]. There is no gender predilection; it is most common in Caucasians (97 %) and is quite rare in African Americans (2 %) [141, 146].

Pathogenesis

GPA is considered part of a group of autoimmune disorders known as antineutrophil cytoplasmic

autoantibody (ANCA)-associated vasculitis, which also includes microscopic polyangiitis, Churg–Strauss syndrome, and renal-limited vasculitis [142, 147]. These disorders are characterized by the presence of necrotizing small vessel vasculitis with the presence of serum autoantibodies directed against neutrophil cytoplasmic constituents, in particular, proteinase 3 (PR3) and myeloperoxidase (MPO). ANCA tests can be performed by both indirect immunofluorescence assay and antigen-specific enzyme-linked immunosorbent assay (ELISA) [148, 149]. ANCA are believed to play a role in the pathogenesis of vasculitis via activation of neutrophils, but most importantly, they are useful in the diagnosis and management of these disorders. The specificity of cytoplasmic antineutrophil cytoplasmic antibodies (c-ANCA) in biopsy-proven disease has been shown to be 90 %. The sensitivity depends on the extent and the activity of the disease. c-ANCA is not detected in most patients at complete remission; rising levels may be indicative of relapse [150].

The most commonly postulated scenario for ANCA-mediated vasculitis is the interaction of neutrophils and the endothelial cells via cell adhesion molecules, which results in releasing cytokines with damage to the vascular walls [151, 152]. Although many advances have occurred in the understanding of the pathogenesis of GPA, so far, it is still unknown how tolerance to the autoantigen PR3 is broken and how the immune response is sustained. PR3 induces dendritic cell maturation via the protease-activated receptor (PAR)-2 and evokes a strong Th1-type T-cell response in GPA [153]. Clusters of PR3-positive cells (neutrophils and monocytes) surrounded by antigen-presenting cells (Th1-type, CD4+CD28 effector memory T cells) and maturing B and plasma cells are found in the granulomatous responses of GPA lesions [154]. Several important studies have characterized the role of PR3 and PAR-2 in the initiation of this process. These might provide evidences for a more target-specific anti-inflammatory therapy for these patients.

Clinical Presentation

Ocular symptoms may be the first manifestation of GPA in 16 % of patients [155]. Orbital involvement is the most common manifestation, and it has been reported in 45–70 % of patients. The orbital inflammation can cause pain, diplopia, proptosis, and bone erosion and can lead to vision loss. Other ocular manifestations of GPA are peripheral ulcerative keratitis, scleritis, and, less commonly, uveitis, retinal vasculitis, and optic neuropathy [156, 157].

The eyelid is only rarely involved, and clinical presentations are usually nonspecific, such as lid edema and infiltration [158–160] or inflammation mimicking chalazion [161].

Histopathology

The histological diagnosis is based on the presence of necrobiotic coagulative necrosis, a large number of neutrophils and eosinophils forming small clusters and intermixed with the necrosis; it is associated with histiocytic granulomatous reaction around the large areas of necrosis and small vessel vasculitis. The full picture of necrotizing vasculitis with granulomatosis is seen in the skin in a minority of cases (Fig. 11.31). Sometimes, the findings are quite nonspecific with only chronic inflammation present in the dermis.

Prognosis

The majority of the patients respond well to treatment, although 25–40 % of patients will experience flare-ups. Anatomical problems are common, such as tracheal stenosis, and may require surgery. Long-term complications are common.

11.7 Benign Lesions

11.7.1 Epidermal Inclusion Cyst

Definition

A cystic invagination of the surface squamous epithelium, which has lost continuity with the surface epithelium

Synonym

Epidermoid inclusion cyst

Epidemiology

It can be congenital or secondary to trauma or surgery. Milium is a small retention cyst caused

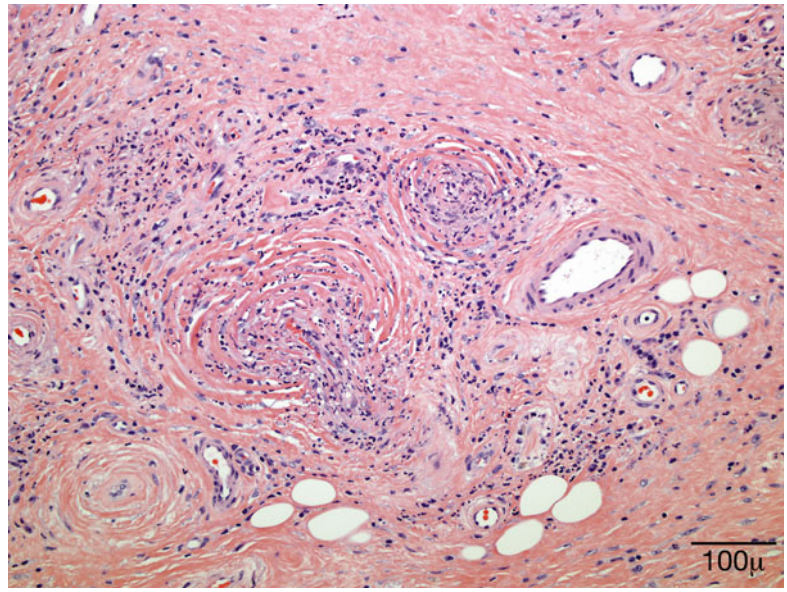

Fig. 11.31 Granulomatosis with polyangiitis. This high power shows the presence of small-vessel vasculitis (hematoxylin-eosin stain; original magnification 200×)

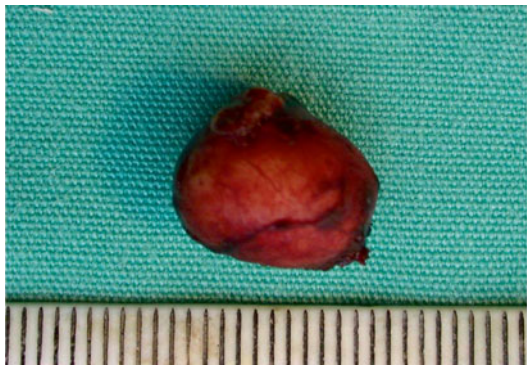

Fig. 11.32 Epidermoid cyst – macroscopic photograph of an intact cyst

by obstruction of the orifices of the pilosebaceous units and rarely has clinical significance. The larger lesions are more clinically evident and can occur in the ocular region.

Clinical Features

Epidermal inclusion cyst is a slowly enlarging, firm, globular lesion involving the dermis or subcutaneous tissue (Fig. 11.32). It is a mobile, painless lesion covered by intact epidermis. It can occur as a very small lesion (milium) or as a large lesion.

A milium appears as one or more small, gray-white, sometimes umbilicated lesions ranging from 1 to 3 mm in diameter. It often has a small keratin plug (blackhead) near the center.

Macroscopy

Thin-walled cyst containing soft material

Histopathology

Epidermal inclusion cysts are lined by keratinizing epithelium and contain keratin (Fig. 11.33). Unlike a dermoid cyst, the lining does not contain dermal appendages. A ruptured epidermoid cyst can incite a severe granulomatous reaction (keratin granuloma) and reactive hyperplasia of the overlying epithelium (Fig. 11.34).

Prognosis

Epidermal inclusion cysts are best managed by local complete excision. An eyelid crease incision provides good results, and the prognosis is excellent. Malignant transformation into basal cell carcinoma or squamous cell carcinoma is a very rare event [162].

11.7.2 Hidrocystoma

Definition

Hidrocystoma is a cystic form of sweat gland adenoma resulting from proliferation of the apocrine or eccrine secretory glands.

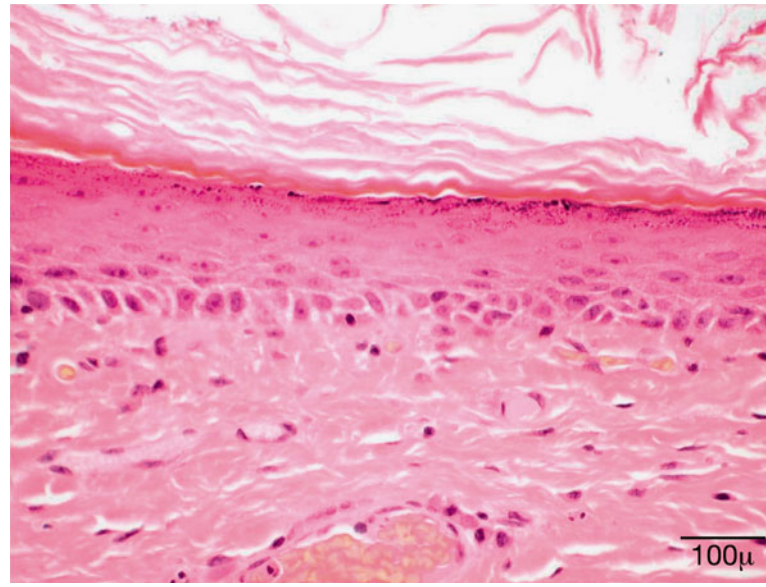

Fig. 11.33 Epidermoid cyst – Cyst lined by organized keratinized squamous epithelium filled with keratin in lumen (hematoxylin and eosin stain; original magnification 200×)

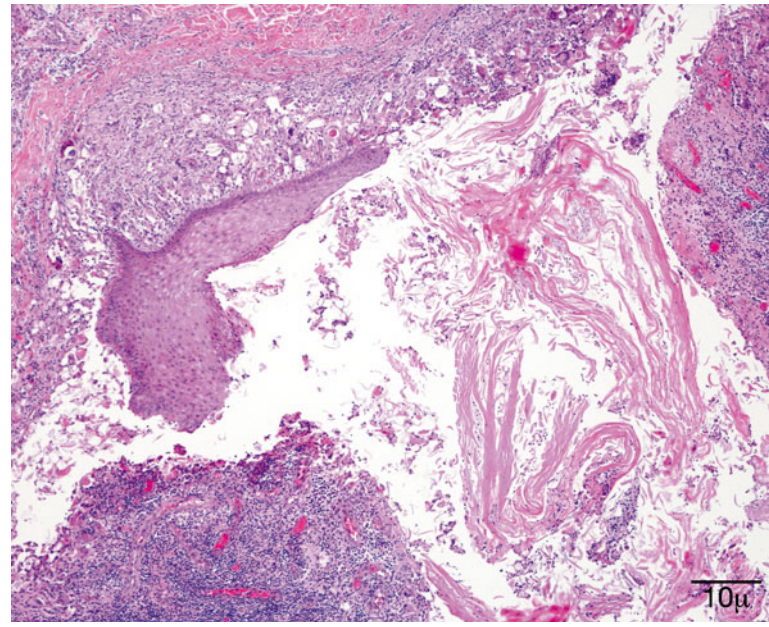

Fig. 11.34 Epidermoid cyst – Ruptured cyst with organizing inflammation in cyst wall and adjacent tissue (hematoxylin and eosin stain; original magnification 100×)

Etiology

An obstruction of the sweat gland ducts immediately above the glandular coil within the deep dermal layer following an inflammatory process or trauma [163]. Hidrocystomas are benign lesions of the eyelid that are differentiated into two histological types: apocrine and eccrine.

The apocrine hidrocystoma or cyst of Moll affects the eyelid border and generally appears following an obstruction of the apocrine secretory duct of the gland of Moll.

The eccrine hidrocystoma or cyst of the eccrine sweat gland originates from the eccrine sweat gland, also known as the gland of Moll. These lesions are regarded as ductal retention cysts and have a similar clinical appearance to that of apocrine hidrocystoma [1]. Eccrine hidrocystomas develop from retention of sweat. Heat,

humidity, and perspiration seem to cause these lesions to become larger, more numerous, and symptomatic. Hence, these tend to increase in number and size in summer and decrease in the winter months [162].

Clinical Features

The most common site for apocrine cysts of Moll is close to the eyelashes, the route of lacrimal drainage. Apocrine hidrocystoma is almost always a solitary lesion. It consists of small, painless, round, translucent, fluid-filled vesicles (Fig. 11.35) [163]

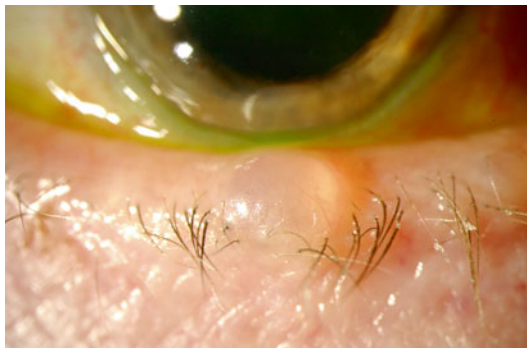

Fig. 11.35 Cyst of Moll (apocrine cyst) – Clinical photograph of well-circumscribed, thin-walled cyst on lower lid

and frequently has a bluish color and may resemble a blue nevus or melanoma [163]. It can range from 1 mm to more than 1 cm in diameter and is filled with clear or milky fluid [163].

Eccrine hidrocystomas generally present as multiple cutaneous vesicles on the lower eyelid [163], in contrast to apocrine hidrocystoma. Eccrine hidrocystomas develop from retention of sweat.

Histopathology

The apocrine hidrocystoma is a cystic lesion with a clear lumen lined by a double layer of cells (Fig. 11.36). The innermost cells are columnar and display an eosinophilic cytoplasm with atypical bulbous expansions typical of cells undergoing decapitation secretion (Fig. 11.37). The outermost layer consists of flattened myoepithelial cells [162]. The apocrine hidrocystoma may be regarded as a form of papillary cystadenoma rather than as a retention cyst [1].

The eccrine hidrocystoma contains only one cystic cavity, which is usually partially collapsed and contains no papillary infoldings. The cyst is usually lined by two layers of small cuboidal epithelial cells; occasionally, only one layer is present. No myoepithelial cells are observed [162].

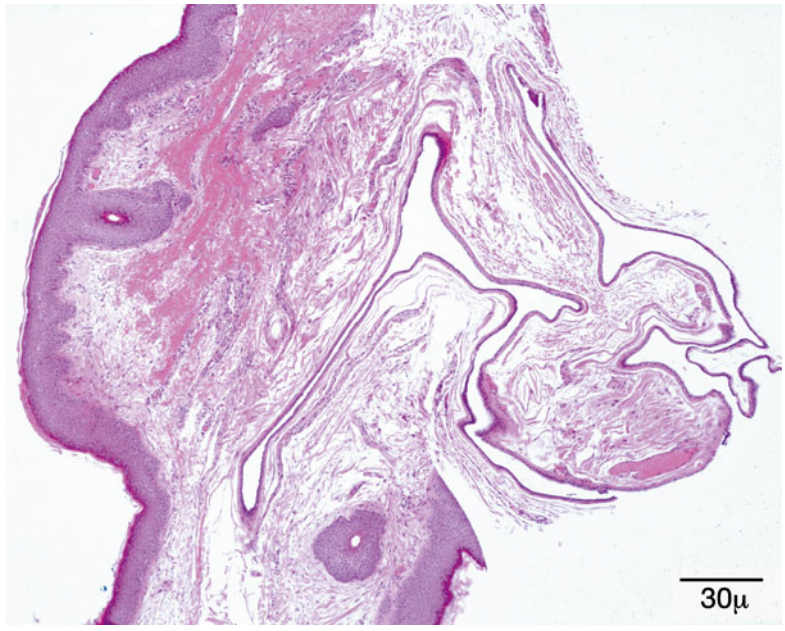

Fig. 11.36 Cyst of Moll (apocrine cyst) – Multiloculated cyst lined by low cuboidal epithelium (hematoxylin and eosin stain; original magnification 40×)

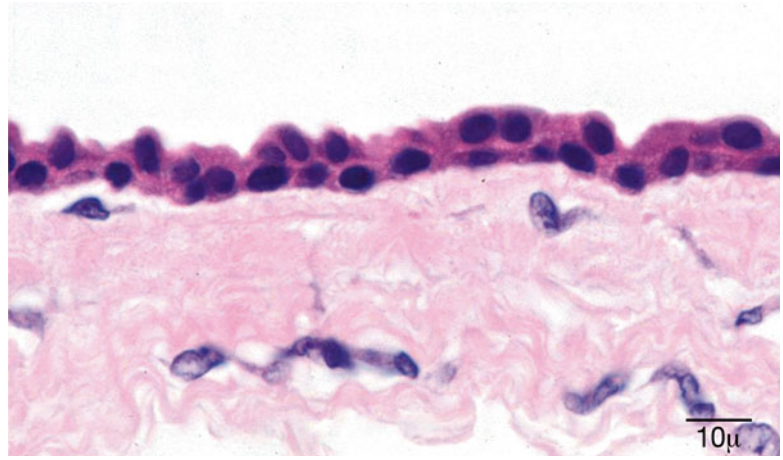

Fig. 11.37 Cyst of Moll (apocrine cyst) – Shows cuboidal epithelium with abundant eosinophilic cytoplasm, which has a granular appearance (hematoxylin and eosin stain; original magnification 100×)

Prognosis

Prognosis of both forms of hidrocystoma is excellent.

11.7.3 Pilar Cyst

Synonym

Sebaceous cyst

Definition

A pilar cyst is usually secondary to occlusion of the duct of a sebaceous gland and can occur on the eyelid and adjacent tissue.

Etiology

It most commonly develops in the meibomian glands of the upper tarsus from retention of meibomian gland material. Less often, it arises from the Zeis glands near the eyelid margin.

Localization

Larger pilar cysts tend to arise in areas where there are numerous large hair follicles. It commonly develops on the scalp (90 %), occasionally in the eyebrow area, and less often in the medial canthus and eyelid [164].

Clinical Features

Pilar cysts of the meibomian gland are a subcutaneous nodule. The extra-meibomian sebaceous cyst is a slow-growing, freely mobile, smooth, subcutaneous lesion, most often in the region of the eyebrow. It often contains a waxy comedo in the center. It is usually solitary but can be multiple [162].

Histopathology

Pilar cysts are characterized by an epithelial lining that does not possess intracellular bridges. The epithelial cells are not stratified as is seen in normal epithelium. The cells on the inner aspect are enucleate (Fig. 11.38). The lumen of the cyst usually contains homogeneous, eosinophilic material. Calcification occurs in about 25 % of cases. The cyst can also rupture and incite a foreign body giant cell reaction [162].

Prognosis

A small, asymptomatic pilar cyst can be managed by observation or compress. It eventually resolves in most cases. A larger or symptomatic lesion can be managed by surgical excision.

11.7.4 Dermoid Cyst

Synonyms

Benign cystic teratoma

Definition

Dermoid cyst is a congenital cystic lesion that can affect the eyelid and/or the orbit.

Etiology

Entrapped ectoderm at a site of embryologic bony fusion

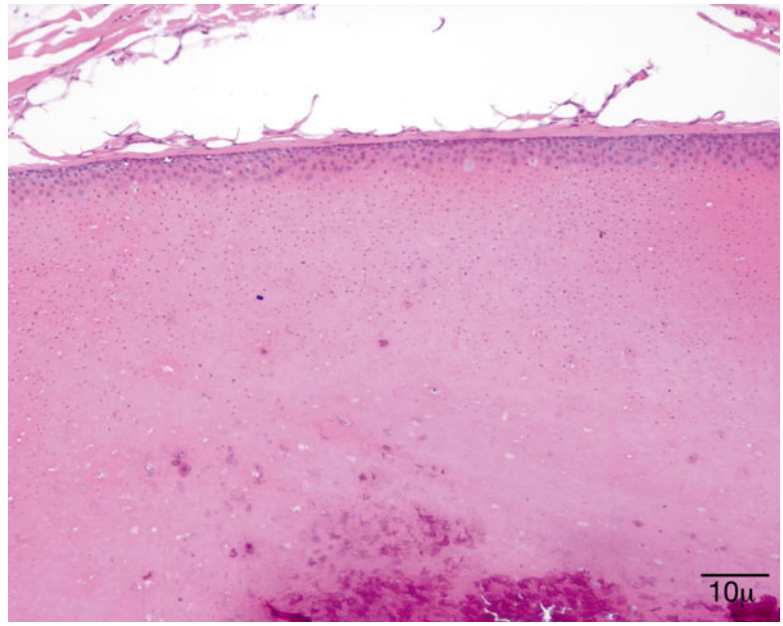

Fig. 11.38 Pilar cyst – Cyst wall showing that the epithelial cells "drift" into the lumen (hematoxylin and eosin stain; original magnification 100×)

Localization

Most dermoid cysts in the ocular region occur at the bony orbital rim superotemporally at the site of the zygomaticofrontal suture as a swelling beneath the lateral aspect of the upper eyelid and eyebrow [162].

Clinical Features

A dermoid cyst is usually slow growing and appears as a smooth, oval-shaped, subcutaneous mass that is not movable because of its attachment to the underlying periosteum (Fig. 11.39) [165]. It usually is located deep in the eyelid skin superotemporally and can occasionally be associated with a fistula that opens through the skin into the eyelid [162]. It can measure from 1 to several centimeters in diameter.

Macroscopy

Thin-walled cyst containing soft, flocculent yellow-white material

Histopathology

Dermoid cysts are lined by stratified epithelium that usually produces keratin, which accumulates in the lumen. The walls of the cyst typically possess adnexal structures, particularly hair follicles,

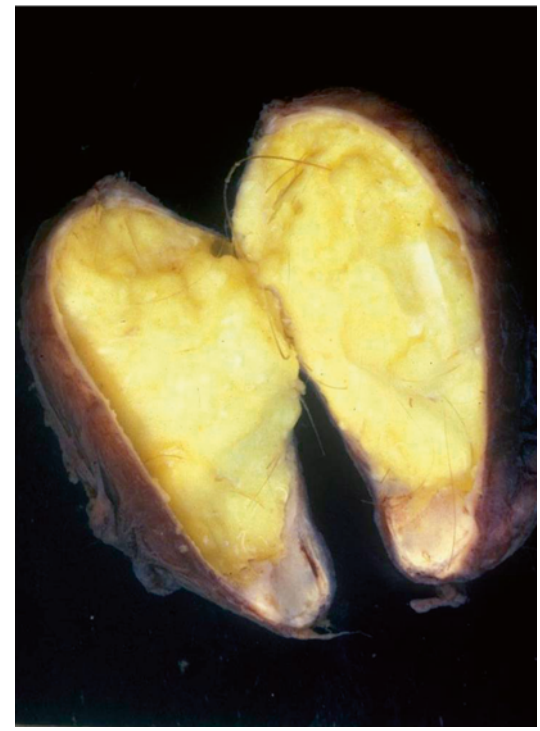

Fig. 11.39 Dermoid cyst – Macroscopic photograph of opened cyst showing cheesy material and hair in wall of cyst

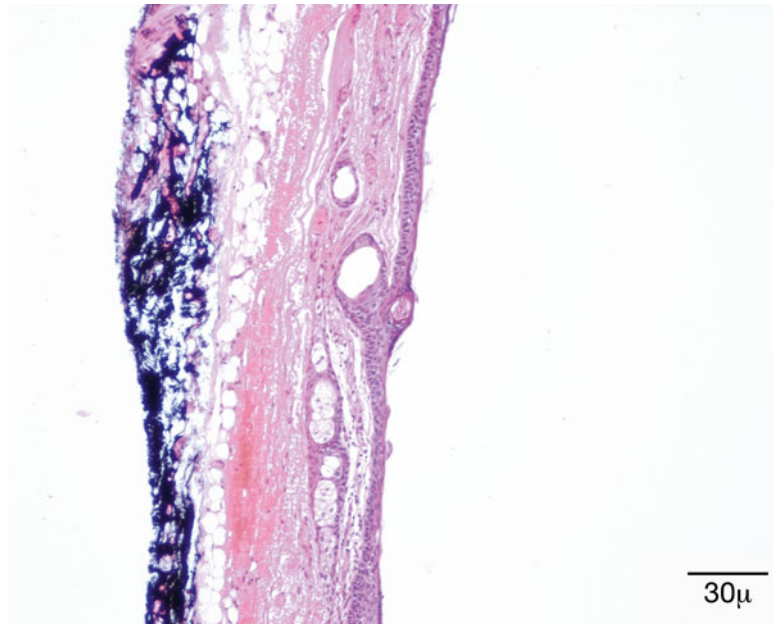

Fig. 11.40 Dermoid cyst – Cyst wall showing skin appendage structures in wall of cyst. This distinguishes a dermoid cyst from epidermoid cyst

sebaceous glands, and eccrine sweat glands (Fig. 11.40).

Differential Diagnosis

Epidermoid or pilar cyst

Prognosis

The treatment consists of complete extirpation. It is important to maintain the integrity of the cyst during surgery since a loss of internal cyst material or remains will usually provoke an intense foreign body granulomatous reaction in the orbit or eyelid [165].

11.7.5 Seborrheic Keratosis

Definition

Seborrheic keratosis (SK) is a common benign tumor of the epidermis that appears in early adulthood and increases in frequency with age.

Synonyms

Senile wart, seborrheic verruca

Epidemiology

SK is more common in whites than in dark-skinned people. There is no sex predilection.

Etiology

The etiology of seborrheic keratosis is unclear. Aging, cumulative UV radiation-induced mutations, and HPVs are proposed as etiologic factors. However, the role of HPVs is contestable, as the prevalence of HPV positivity differs on top of different skin lesions from the prevalence inside the same tumor; 79 % of SKs were HPV positive on the surface but only 19 % inside the tumor tissue [166].

Localization

SK occurs anywhere on the skin surface, with the exception of the palms and soles. They are quite common in the periorbital area.

Clinical Features

SKs present clinically as sharply demarcated pink, tan, or brown papules or plaques with a verrucous surface. Multiple SKs may appear over a short time as a paraneoplastic phenomenon (Leser–Trélat sign). Irritated SKs are surrounded by an erythematous halo and may mimic BCC or squamous cell carcinoma (SCC).

Macroscopy

The size of the lesions varies from a few millimeters to centimeters. The transition between SK

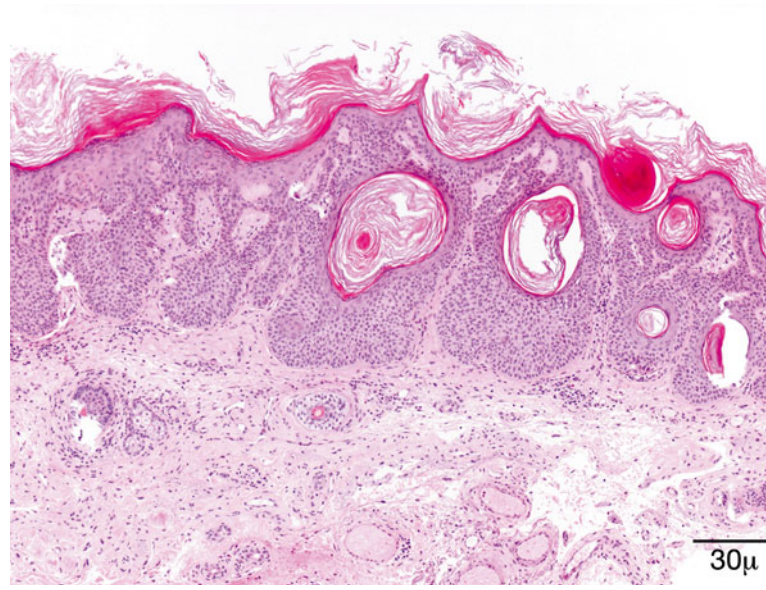

Fig. 11.41 Seborrheic keratosis – Papillomatous projections of digitated SK may mimic a verruca. Broad anastomosing rete ridges and lack of viral cytopathic changes help the differential diagnosis (hematoxylin-eosin stain; original magnification 40×)

and the surrounding normal skin is usually sharply defined.

Histopathology/Immunoprofile

Multiple variants of SK exist. The lesion may be flat, endophytic, or exophytic. The surface is papillomatous; the epidermis is hyperkeratotic and parakeratotic (Fig. 11.41).

The acanthotic type shows a thickened epidermis that extends upward and is composed of cytologically uniform, small basaloid, cuboidal keratinocytes. Horny invaginations and pseudohorn cysts are apparent.

In the reticulated (adenoid) type, a delicate network of interweaving epithelial strands extends into the dermis. Hyperpigmentation of the basaloid cells may be prominent (Fig. 11.42). The features are reminiscent of lentigo senilis.

Irritated SKs display a more pronounced inflammation and numerous squamous eddies. The proliferating keratinocytes may be spindled and proliferate downward; thus, the horizontal demarcation usually seen in non-irritated SKs is broken.

In the clonal type of SK, well-defined nests of cells with slightly enlarged nuclei are located within the epidermis.

Further variants are the hyperkeratotic, digitated, stucco, and inverted follicular keratosis. The latter demonstrates a marked endophytic growth, but the pattern is lobular and noninfiltrative. Squamous eddies are a prominent feature.

Differential Diagnosis

Epidermal nevus, actinic keratosis, SCC in situ, verruca vulgaris, keratotic melanocytic lesion, squamous papilloma, and acanthosis nigricans

Histogenesis

Proliferating keratinocytes are considered the cells of origin.

Genetics

SK is clonal in nature [167]; but no chromosomal imbalance (a common finding in both benign and malignant tumors) was demonstrated by comparative genomic hybridization in a limited number of SKs [168]. Recently, activating mutations in the fibroblast growth factor receptor 3 (FGFR3) gene have been reported to cause benign skin tumors [169]. UV light-induced somatic mutations of FGFR3 occur in a significant proportion of adenoid-type SKs [170]. In another study of multiple SK samples from four

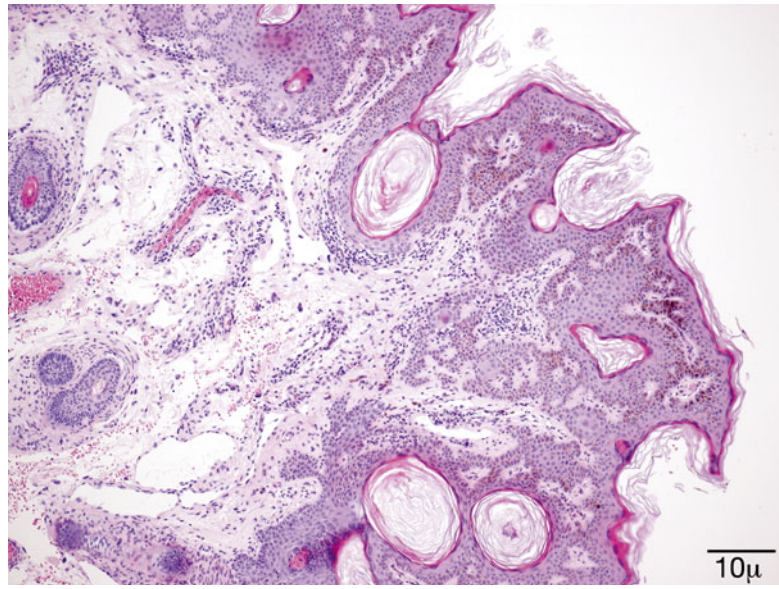

Fig. 11.42 Seborrheic keratosis – This SK exhibits a papillomatous and tentatively reticulate growth pattern with basilar pigmentation. The latter is also a common feature (hematoxylin-eosin stain; original magnification 100×)

patients, 59 % of the tumors harbored FGFR3 mutations, at least, in four loci in each individual patient [171].

Prognosis and Predictive Factors

SKs are benign lesions, although they are a cosmetic concern. However, they may be associated with Bowen disease or rarely BCC. Since they also may mimic malignant tumors, they are biopsied to provide a histopathological diagnosis.

11.7.6 Inverted Follicular Keratosis

Definition

A benign, warty tumor of the epidermis that increases in frequency with age

Epidemiology

Occurs mainly in middle-aged to older adult men, more commonly in Caucasians

Etiology

It may develop rather rapidly over a few months and is believed to have a viral etiology. It was once believed to be of a hair follicle origin. However, there has been no convincing histopathological evidence to support that concept and is now believed to be an inverted irritated seborrheic keratosis [162].

Localization

It is often located on or very near the eyelid margin.

Clinical Features

It has a wartlike appearance that may be pigmented, stimulating a melanocytic lesion.

Histopathology

The epithelium exhibits downward lobular hyperplasia with proliferation of both squamous and basal cells with an endophytic pattern and smooth interface with underlying dermis (Fig. 11.43). Squamous eddies are frequently observed.

Differential Diagnosis

Any pigmented or nonpigmented keratotic lesion, including seborrheic keratosis, actinic keratosis, pigmented melanocytic lesions, and basal cell carcinoma

Prognosis

Benign course; shave excision is usually sufficient.

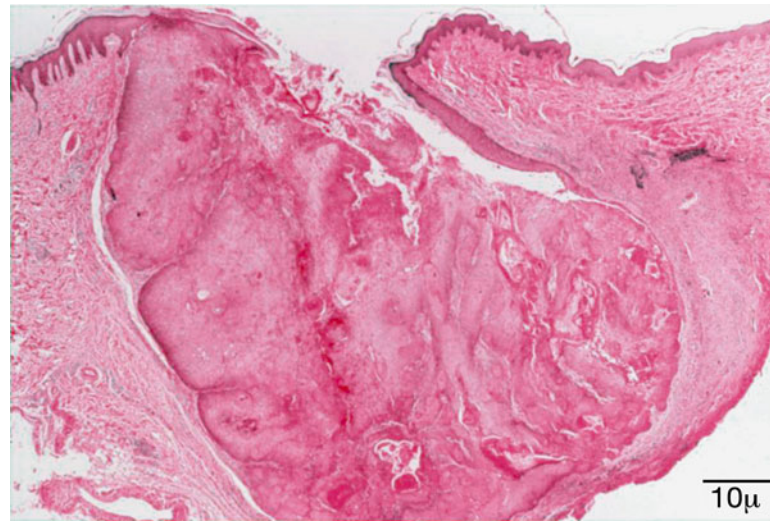

Fig. 11.43 Inverted follicular keratosis – Downward hyperplasia of epithelium with smooth interface between epithelial basement membrane and dermis (hematoxylin-eosin stain; original magnification 100×)

11.8 Premalignant Conditions

11.8.1 Actinic Keratosis

Definition

Actinic keratosis (AK) is a biologically benign, noninvasive epidermal dysplasia developing in sun- or other radiation-damaged skin.

Synonyms

Solar keratosis

Epidemiology

AK affects mostly fair-skinned, elderly patients with a history of chronic UV exposure from sunlight. AKs are more frequent in men with skin types I and II; 73 % of patients with SCC have AKs as well, according to a case-control study in the Netherlands [172]. Furthermore, the same study disclosed that painful sunburns before the third decade of life were also associated with SK.

Etiology

Both environmental and genetic risk factors play a role in the development of AK. UVB-induced mutations of the p53 gene, mutations in ras genes, c-Myc proto-oncogenes, and mutations in tumor suppressor genes, such as p16INK4a, have all been implicated in the pathogenesis of AKs.

Localization

Sun-exposed areas (face, scalp, ears, dorsum of the hands), common in the periorbital region, but rare on the eyelids

Clinical Features

Presents as small, scaly, irregular-shaped, erythematous plaques or papules

Histopathology/Immunoprofile

Although several variants of AK are recognized, all lesions are characterized by atypia of the basal cell layer of the epidermis with elongated hyperchromatic nuclei; eventually, focal suprabasilar atypia is also present (Fig. 11.44). The epidermis is parakeratotic, and the dermis exhibits solar elastosis and dilated vessels. The epidermis is usually thickened but may be atrophic. The histological variants include hypertrophic, acantholytic, proliferative, pigmented, and lichenoid [173].

Differential Diagnosis

Differential diagnosis includes squamous cell carcinoma and seborrheic keratosis. Pigmented AK should be differentiated from solar lentigo and lentiginous melanoma in situ. It is worth mentioning here that melanoma is extremely rare on the eyelids.

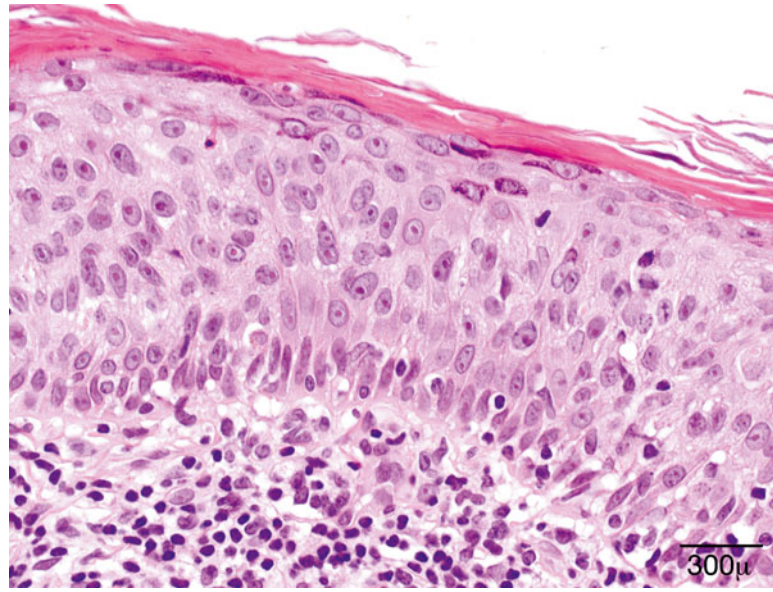

Fig. 11.44 Actinic keratosis – The epidermis is thickened, suprabasilar keratinocytes show cytoplasmic pallor (hematoxylin-eosin stain; original magnification 600×)

Histogenesis

Basal keratinocytes [174] or epidermal stem cells are presumed the cells of origin.

Genetics

Chromosomal alterations and genomic instability [175] are present in AK, leading to increased signals that facilitate proliferation (Ras, Bcl-2) and decreased signaling of p53 as well as molecules regulating keratinocyte proliferation and differentiation [176]. Microarray analysis of AKs, SCCs, and the normal skin from 16 patients revealed 89 genes similarly affected in AK and SCC [177]. Genes that were upregulated in AK and SCC were downregulated in the normal skin and vice versa.

Prognosis and Predictive Factors

AK can regress spontaneously. There is disagreement about the rate of progression from AK to invasive SCC, but 60–97 % of SCCs supposedly originate from AKs [178].

11.8.2 Bowen Disease (Squamous Cell Carcinoma In Situ)

Definition

Bowen disease (BD) is a form of carcinoma in situ of the epidermis.

Epidemiology

It affects mostly individuals in their sixth to eighth decade; men and women are equally affected. There is no valid estimate of the frequency in the eyelids.

Etiology

UV radiation, radiation therapy, and various types of HPV also may have a role, namely, HPVs 16, 18, 2, 31, and 33. Arsenic exposure [179] that causes the production of ROS [132] from medications, contaminated well water, and pesticides have also been associated with BD. Immunosuppressed patients are increasingly at risk [180].

Localization

BD has a predilection for the sun-exposed areas of the body. In males, it affects mostly the head and neck region, while in females, it localizes predominantly to the lower limbs and cheeks.

Clinical Features

It presents as a well-defined, scaly erythematous plaque. Nodular, verrucous, eroded, and pigmented variants are observed.

Histopathology/Immunoprofile

The epidermis is hyperkeratotic and acanthotic. Atypical keratinocytes involving the full thick-

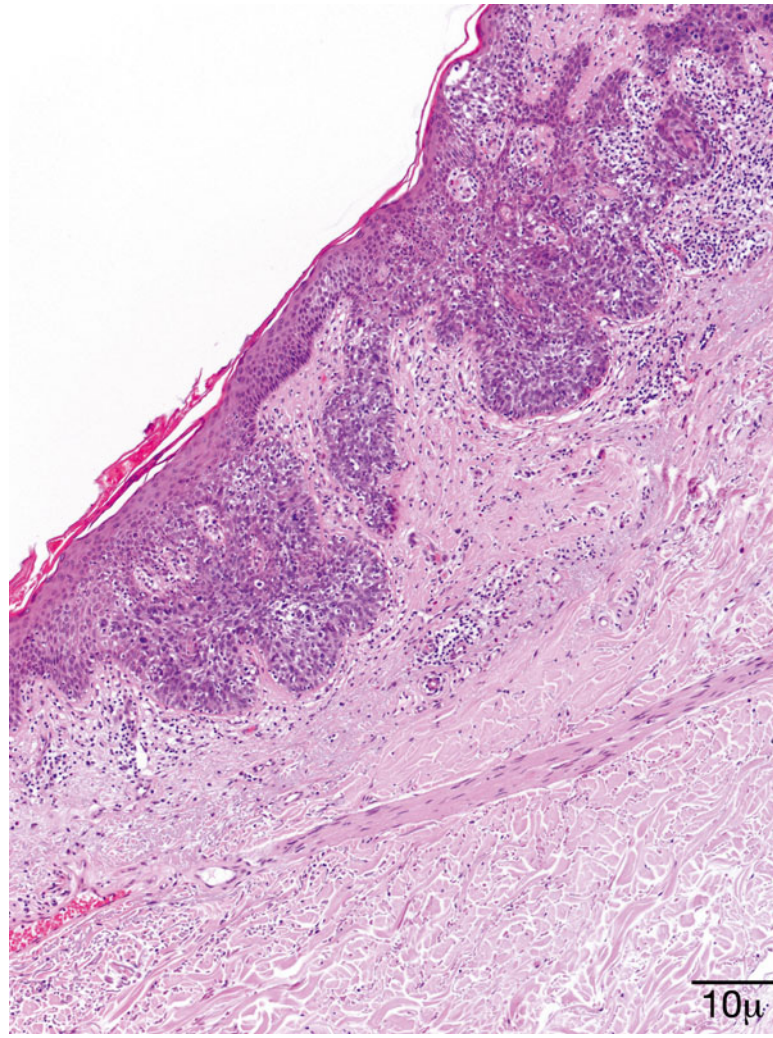

Fig. 11.45 Bowen disease – Loss of polarity and cellular atypia mostly localized to spinous cell layer is characteristic of BD. Cytopathic changes related to HPV are also present in this case (hematoxylin-eosin stain; original magnification 100×)

ness of the epidermis are associated with loss of maturation in the stratum spinosum as well as loss of the granular layer (Fig. 11.45). However, the presence of an intact layer of basal cells [181] is frequently observed, at least, in early lesions [174]. Pagetoid spread of large, pale tumor cells with ground-glass cytoplasm is common. Adnexal structures are frequently involved (Fig. 11.46). Several histological variants exist, and more than one pattern may be present in different areas of the same lesion. Chronic, moderate inflammation in the underlying dermis is common. The different variants include atrophic, verrucous-hyperkeratotic, irregular, and pigmented. BD is positive for AE1–AE3 and CK 10 and does not stain for CAM5.2 (CK18). Clear cell BD express CK13, CK16, and CK15, which are cytokeratins found in the outer root sheath. MIB-1 antibody marks the suprabasal layers more extensively than the basal layer of columnar cells [174].

Differential Diagnosis

Actinic keratosis, squamous cell carcinoma, Paget disease, superficial BCC

Genetics

Loss of the normal tumor suppressor function of p53 has been demonstrated by IHC in 50 % of biopsies from Bowen disease [182]. Direct

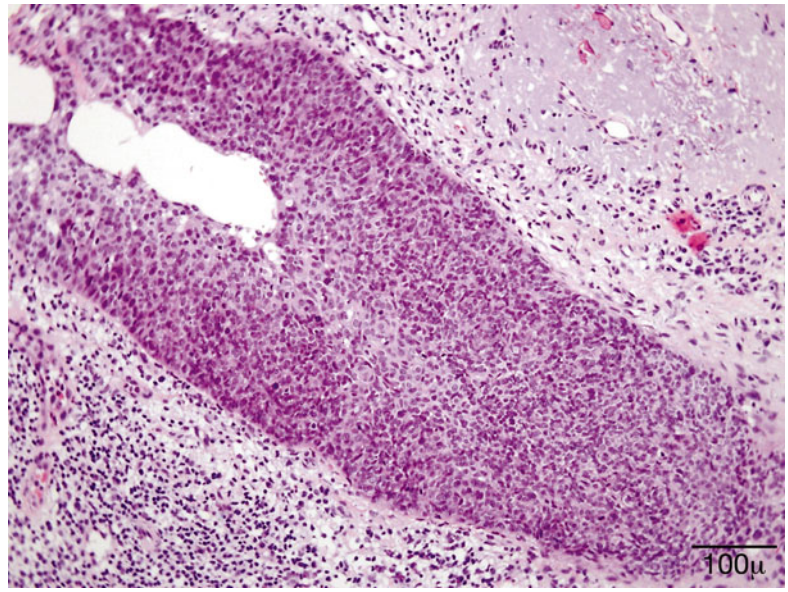

Fig. 11.46 Bowen disease – Intraepithelial extension of BD into adnexal structure should not be misinterpreted as stromal invasion (hematoxylin-eosin stain; original magnification 200×)

sequencing of the p53 gene also revealed mutations in 8 of 20 cases of BD [183].

Prognosis and Predictive Factors

The prognosis is fair; only about 3–5 % of cases progress to invasive squamous cell carcinoma.

11.9 Neoplasms

11.9.1 Epithelial Neoplasms

11.9.1.1 Squamous Papilloma

Definition

Squamous papilloma (SP) is a benign tumor of epithelial origin.

Synonyms

Fibroepithelial polyp, skin tag, acrochordon

Epidemiology

Squamous papilloma is the most common benign tumor of the eyelid. Most occur between the age of 30 and 50 years.

Etiology

Various types of low-risk HPVs are implicated in the development of squamous papilloma.

Localization

Squamous papilloma has a predilection for the eyelid border; multiple lesions may be present.

Clinical Features

Squamous papillomas are slow-growing, sessile or pedunculated pointy outgrowths. The color depends on the amount of surface keratin. Heavily keratinized lesions are whitish, while lesions with less keratin are skin colored.

Histopathology

Squamous papilloma exhibits fingerlike projections of fibrovascular core covered by hyperplastic epidermis with elongated rete ridges and acanthosis. Focal parakeratosis is present (Fig. 11.47).

Differential Diagnosis

At scanning, magnification of the silhouette of verruca vulgaris and seborrheic keratosis may be similar. Verruca may be distinguished by koilocytosis, while seborrheic keratosis may have horn pseudocysts absent in squamous papilloma.

Histogenesis

Squamous papilloma may originate from the surface epithelium and from mucous membranes.

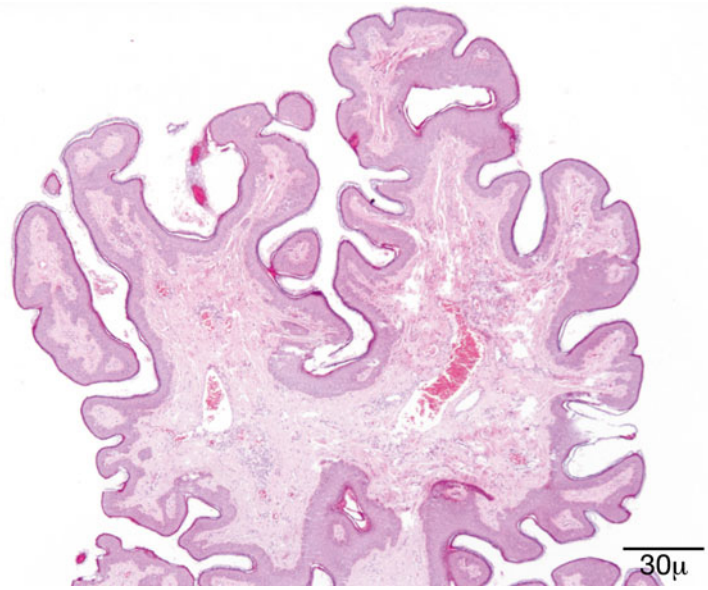

Fig. 11.47 Squamous papilloma – Branching fibrovascular core covered by a variably hyperplastic, hyperkeratosic squamous epithelium (hematoxylin-eosin stain; original magnification 40×)

Prognosis and Predictive Factors

The prognosis of eyelid papillomas is excellent. Malignant transformation does not occur. However, treatment may be needed for cosmetically disturbing lesions. A shave excision is usually sufficient.

11.9.1.2 Basal Cell Carcinoma and Variants

Definition

Basal cell carcinoma (BCC) is the most common skin cancer among Caucasians. It occurs mainly on the sun-exposed areas of the body (face, scalp, periocular area, upper extremities).

Synonyms

Basalioma, basal cell epithelioma

Epidemiology

BCC is the most common malignant tumor of the eyelid skin [184] and accounts for 90 % of all malignant tumors of the eyelids. It affects mainly fair-skinned people over 40 years of age. The male-to-female ratio is between 2:1 and 1.6:1.

Etiology

UV light is considered the principal etiologic factor in both sporadic BCC and BCC associated with a genetic defect (Gorlin syndrome, albinism, Bazex–Dupré–Christol syndrome, xeroderma pigmentosum). Other factors are ionizing radiation and arsenic exposure. Indoor tanning is a culprit recently recognized [185]. Patients affected by BCC are at an increased risk of developing new skin cancers [186, 187].

Localization

BCC is unevenly distributed around the eye. The localization of BCC in order of frequency is the lower eyelid, medial canthus region, upper eyelid, and lateral canthus region. Interestingly, the distribution of periocular BCCs is unrelated to the amount of solar UV radiation to the periocular area [188], the former being evenly scattered over the lids and canthi. BCC tends to involve the eyelid margin with loss of lashes (madarosis).

Clinical Features

BCCs are slowly growing, locally invasive tumors that rarely metastasize but can cause extensive tissue destruction. The most common clinical presentation is a painless pearly nodule with rolled borders and surface telangiectasia (Fig. 11.48). The tumor may exulcerate and bleed, with central crusting (Fig. 11.49). Cystic tumors are translucent with a bluish tinge. The infiltrating type has ill-defined borders and pres-

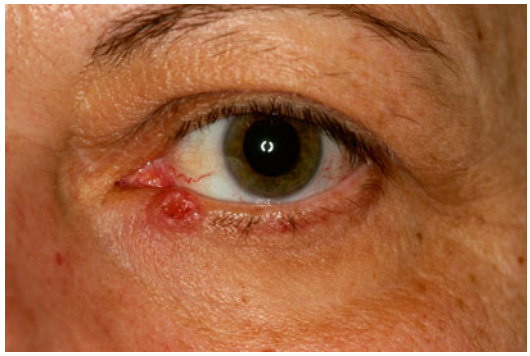

Fig. 11.48 BCC – Small nodular tumor of the lower eyelid. Pearly ulcerated nodule with rolled up edges.

Fig. 11.49 BCC – Ulcerated tumor of the lower lid of a middle-aged woman. The tumor's border is ill-defined, notice the loss of lashes (madarosis)

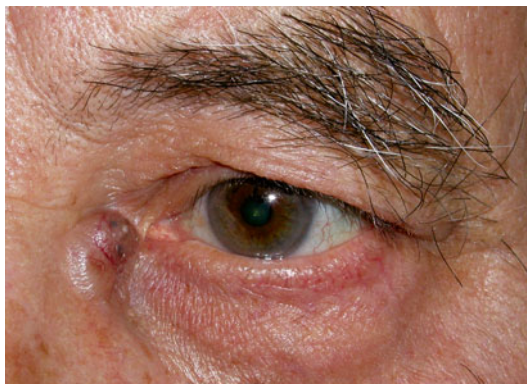

Fig. 11.50 BCC – Irregularly pigmented BCC at the nasal canthus of an elderly man

ents as a pink-to-tan plaque. The surface may be depressed (Fig. 11.50). The lesion is firm to touch. Pigmented BCC may be mistaken for malignant melanoma.

Macroscopy

The most common specimen is an oval or pentagonal (when the tumor is close to or involves the eyelid margin) excision with a well-circumscribed, sometimes cystic, nodular tumor that is either ulcerated or not ulcerated. The sclerosing variant diffusely infiltrates the surgical specimen with whitish strands of tumor tissue blending into the surroundings. An exenteration specimen may eventually be received for a BCC with extensive orbital spread.

Histopathology/Immunoprofile

BCCs are frequently of mixed growth pattern. One pattern may predominate or be present in a pure form.

Nodular BCC is the most common type. It is composed of lobules of basaloid cells with a pushing border (Fig. 11.51). Peripheral palisading and peritumoral clefting with presence of a myxoid stroma are usually present. The tumor cells have a high nuclear-to-cytoplasmic ratio; condensed, finely granular chromatin; inconspicuous nucleoli; and a variable mitotic activity. Apoptotic cells are numerous. An inflammatory reaction in the stroma is composed of a variable population of lymphocytes, plasma cells, and histiocytes.

Superficial BCC is characterized by multifocal aggregates of basaloid tumor cells with multiple connections to the epidermis, separated from each other by areas of the normal skin. Extensive regression may occur and accentuate the seemingly multifocal pattern.

Infiltrative and morpheaform BCC exhibits narrow cords and strands of cells, often accompanied by a prominent stromal reaction and increased collagen deposition. Small, irregularly shaped nodules with only focal or absent peripheral palisading are observed. Stromal mucin and retraction artifact are also missing (Fig. 11.52).

Adenoid BCC usually has a nodular growth pattern with increased stromal mucin filling cribriform or pseudoglandular spaces (Fig. 11.53).

Pigmented BCC is most often of the nodular type. Only about 1 % of BCCs are pigmented. Melanin pigment is found in melanophages, tumor cells, or both [189]. BCC may collide with a melanocytic proliferation.

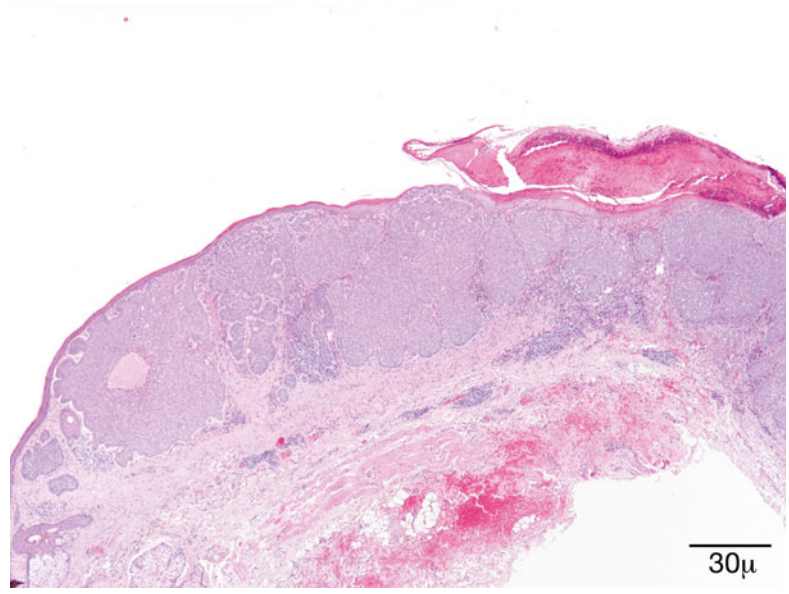

Fig. 11.51 BCC – Nodular aggregates of basaloid cells infiltrate the dermis. Peripheral palisading and clefts between tumor cells and surrounding stroma are conspicuous (hematoxylin-eosin stain; original magnification 40×)

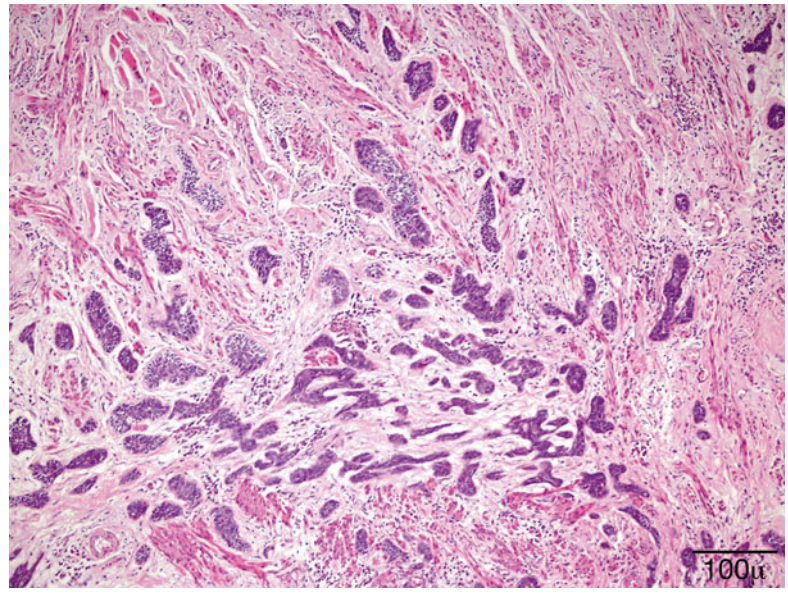

Fig. 11.52 BCC – Infiltrative pattern is characterized by small, irregularly shaped groups or narrow pointed strands of tumor cells. Recurrence rate is high (hematoxylin-eosin stain; original magnification 200×)

BCC with pseudoepitheliomatous hyperplasia is probably due to ulceration or irritation by scratching. Immunohistochemical studies may be necessary to differentiate these cases from SCC. Strong Ber-EP4 positivity and weak focal EMA favor BCC [190, 191].

BCC with squamous differentiation in the deeper infiltrative part of the tumor is seen in 1–3 % of BCCs, mostly in recurrent tumors (Fig. 11.54).

Metatypical and basosquamous BCC can be defined as a BCC differentiating to SCC with intermediate transition zone linking the two [190, 191].

Pleomorphic BCC has marked cellular pleomorphism with huge nuclei but also displays the usual features of conventional BCC.

All variants of BCC are strongly Ber-EP4 positive. The basal layer is CD10 positive [192].

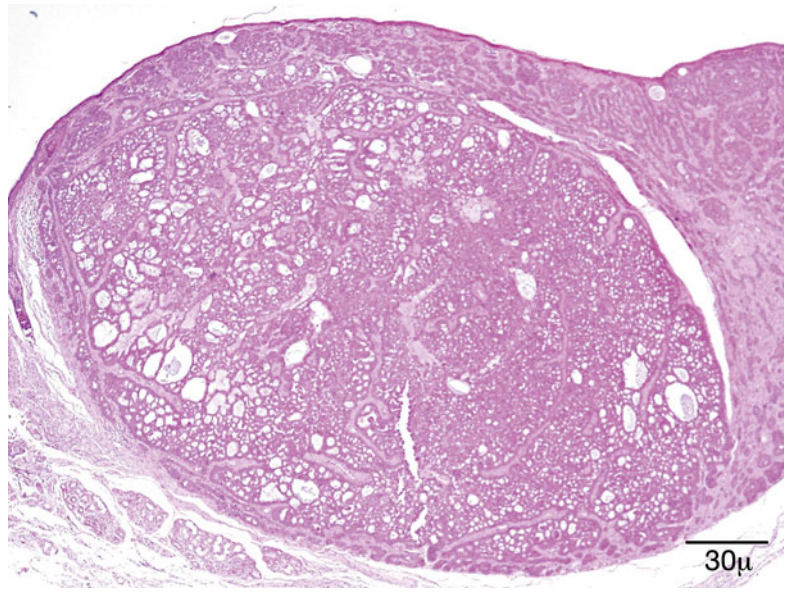

Fig. 11.53 BCC – Tumor with adenoidal features. The nodular tumor shows a cribriform pattern (hematoxylin-eosin stain; original magnification 40×)

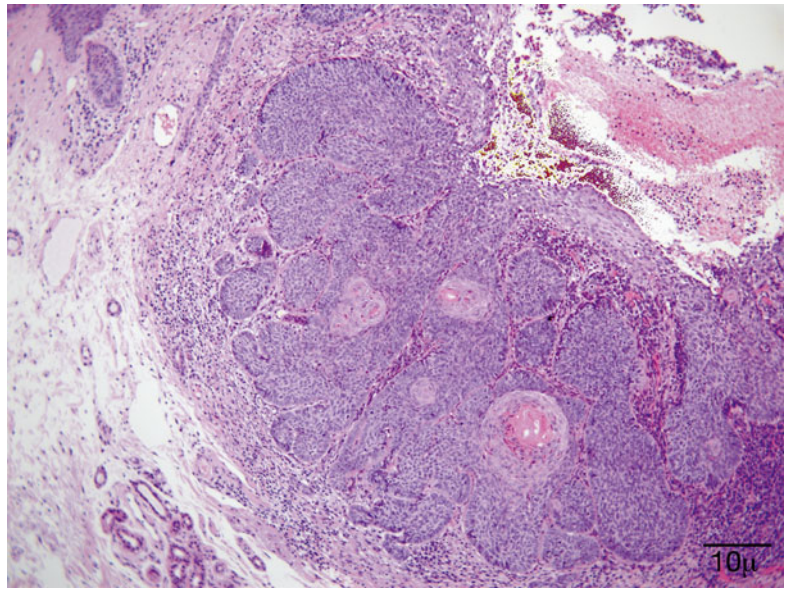

Fig. 11.54 BCC – Squamous differentiation occurs most frequently in ulcerated BCCs, as seen in this otherwise nodular tumor. Dyskeratotic cells are located within the nodules (hematoxylin-eosin stain; original magnification 100×)

They are negative with CK7, AE1–AE3, CAM5.2, and CK20.

Differential Diagnosis

A number of basaloid tumors may mimic BCC. Desmoplastic trichoepithelioma is difficult to differentiate from infiltrative/morpheaform BCC. The presence of Merkel cells in trichoepithelioma can be highlighted by CK20. Merkel cells are not seen in morpheaform BCC [192]. Mitotic activity and severe solar elastosis favor BCC.

Basal cell carcinoma with squamous metaplasia may be difficult to distinguish from squamous cell carcinoma. If areas typical of BCC are absent, Ber-EP4-positive and EMA-negative staining is helpful.

Morpheaform BCC may be confused with the basaloid proliferation of microcystic adnexal

carcinoma. Cytological atypia is more pronounced in BCC; keratocysts are absent.

Merkel cell carcinoma (MCC) may clinically and histologically mimic BCC. The distinction is extremely important, owing to the aggressive behavior of MCC, its propensity to metastasize early in the process of the disease. The nuclei in MCC have a finely granular chromatin and brisk mitotic activity, and apoptotic bodies are conspicuous. CK20 shows a dot-like perinuclear pattern in MCC.

Histogenesis

It is generally accepted that BCC arises from epidermal stem cells located in the bulge of the hair follicles. It is unassociated with a precursor lesion [193].

Genetics

The hedgehog signaling pathway is deregulated in BCC. The gene most often altered in sporadic BCCs is the PTCH gene. Loss-of-function mutations in patched 1 (PTCH1) happen in one-third of sporadic BCCs [194]. Under normal conditions, PTCH inhibits Smoothened (Smo), which functions as a signaling molecule for the expression of downstream target genes involved in transcription and proliferation [195, 196]. UV-specific nucleotide changes (C→T; CC→TT) are detected in both the TP53 and PTCH tumor suppressor genes [197, 198]. Some sporadic BCCs harbor mutations in both alleles of the PTCH gene; however, the mutations are not always characteristic of UV-induced mutagenesis, even in tumors of the sun-exposed skin [199]. Point mutations in the p53 tumor suppressor gene and mutations in the oncogene CDKN2A, a cell cycle regulator, also have a high frequency in BCC.

Prognosis and Predictive Factors

Basal carcinoma of the eyelids is traditionally treated by surgery with margin control. The prognosis for primary nodular tumors is excellent if the excision is complete. In a study involving 270 patients with periocular BCC who underwent 413 procedures, none of the patients with primary nodular BCC suffered recurrence during a 5-year follow-up period [186].

Incomplete primary excision is recognized as the main risk factor for further recurrences [41, 200]. Incomplete excision is more common with morpheaform tumors and medial canthus location. The medial canthus is associated with a high risk of recurrence and invasion into the orbit and paranasal sinuses. Indeed, infiltrative BCC located at the medial canthus represents the main risk factor for exenteration [200]. Positive margins in exenteration specimens may predict intracranial invasion. These data underscore the necessity of reliable margin evaluation and report by the histopathologist.

11.9.1.3 Nevoid Basal Cell Carcinoma Syndrome

Definition

Nevoid basal cell carcinoma syndrome (NBCCS) is a rare autosomal dominant condition characterized by increased susceptibility to BCC, as well as the development of other tumors such as medulloblastoma, fibroma, and rhabdomyosarcoma [201]. Patients also have developmental defects: palmoplantar pits, odontogenic keratocyst of the jaw, macrocephaly, and rib and spine malformations.

Synonyms

Gorlin syndrome, Gorlin–Goltz syndrome

Epidemiology

Nevoid basal cell carcinoma syndrome represents 1/30,827–1/164,000 population [202]. It is almost equally distributed among men and women.

Etiology

Nevoid basal cell carcinoma syndrome is caused by mutations in a tumor suppressor gene located on chromosome 9q [203]. Mutations in the PTCH1 gene (locus 9q22.32) are the cause of NBCCS [202].

Clinical Features

The diagnosis is made in the presence of either two major and one minor criteria or one major and three minor criteria. Affected individuals have coarse facial features, macrocephaly, and boss-

ing of the forehead. Medulloblastoma – primitive neuroectodermal tumor (PNET) – appears earlier than the sporadic form. Odontogenic keratocysts develop during the first decade and may be symptomless. Multiple BCCs appear between puberty and the age of 30 years. Milia-like lesions occur on the palpebral conjunctiva.

Histopathology

The BCCs in NBCCS are indistinguishable from sporadic BCCs.

Prognosis

The prognostic criteria are the same for sporadic BCC. Patients with Gorlin syndrome have a normal life expectancy.

11.9.1.4 Squamous Cell Carcinoma and Variants

Definition

Squamous cell carcinoma (SCC) is an invasive tumor of epidermal origin that propagates to the dermis. SCC is able to produce locoregional and disseminated metastases and is potentially lethal.

Epidemiology

SCC is the second most common malignancy of the eyelid skin after BCC. It represents 5–10 % of malignant eyelid tumors. In different case series, there is a slight [41] or pronounced [204] male predominance. Most patients are in their sixth or seventh decade. The highest incidence is reported from Australia. Solid organ transplant recipients and patients with malignant lymphoma or immunosuppression are at increased risk of developing aggressive SCCs [205–207].

Etiology

Chronic UV exposure is the most important etiologic factor; radiation damage, immunosuppression, chemical carcinogens, HPV infection, and DNA repair defects are also increased risk factors for developing SCC.

Localization

SCC of the skin is localized to sun-exposed areas. Its distribution in the periorbital area is similar to that of BCC, the lower eyelid and nasal canthal area being most frequently affected [204]. It has a strong tendency to involve the eyelid margin.

Clinical Features

SCC may manifest as an erythematous, scaly papule or plaque-like lesion, with either well- or ill-defined borders. Larger nodular tumors have a tendency to ulcerate and exhibit irregular rolled edges. Patients with SCC typically have clinical signs of actinic damage, Bowen disease, or actinic keratosis.

Macroscopy

Superficial SCC is indistinguishable from any type of carcinoma, either in situ or actinic keratosis. Invasive SCC is ill-defined, invades the dermis, and may be plaque-like, wedge shaped, or craterlike.

Histopathology/Immunoprofile

In invasive SCC, irregular masses of epidermal cells proliferate downward into the dermis. As the eyelid dermis is sparse, the tumor can easily reach the orbicular muscle fibers. The contour of the proliferating tumor is often jagged. Discohesive growth manifests by small aggregates or even single tumor cells. The cells exhibit various degrees of atypia, nuclear hyperchromatism and pleomorphism, and mitotic figures (Fig. 11.55). Based on the degree of differentiation and keratinization, SCC is graded as well, moderately, or poorly differentiated. However, there is no direct correlation between the degree of differentiation of a given SCC and its biological behavior [208]. Keratinization is well developed in differentiated tumors. With the formation of squamous pearls, the cells are mildly atypical and have abundant pink cytoplasm. In less well-differentiated SCC, keratinization is less evident and cells have more atypia. In poorly differentiated tumors, the tumor cell nuclei are markedly atypical or anaplastic; keratinization is minimal or nonexistent (Fig. 11.56). The dermis may show a focal or diffuse inflammatory infiltrate that is lymphoplasmacellular or neutrophilic.

SCCs show nuclear positivity for p63. High molecular weight cytokeratin (CK1, CK5, CK10, and CK14) expression is cytoplasmic. Many

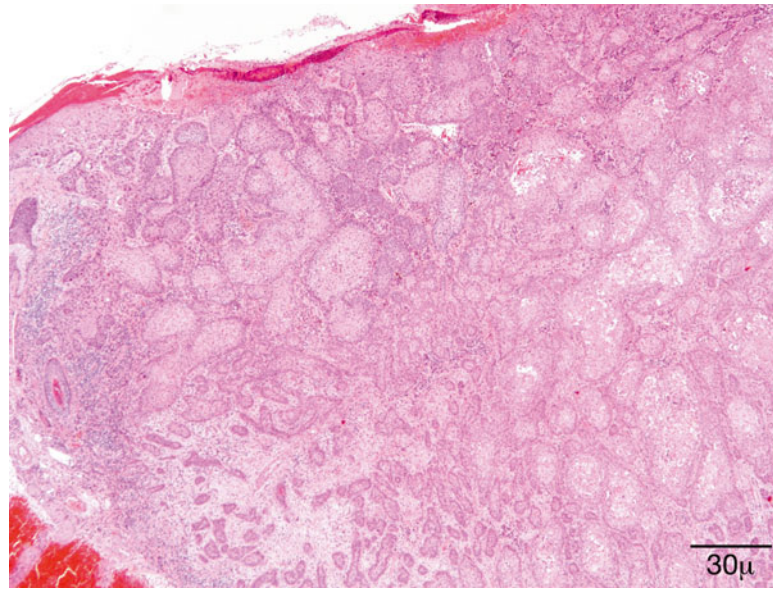

Fig. 11.55 SCC – Well-differentiated invasive SCC from the eyelid of an elderly man. Keratinization is predominant; (hematoxylin-eosin stain; original magnification 40×)

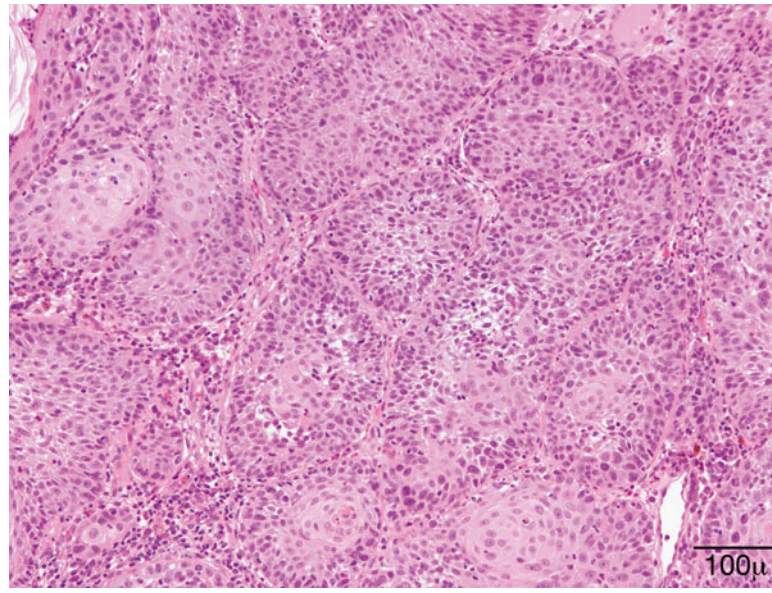

Fig. 11.56 SCC – Poorly differentiated SCC; keratinization is sparse; markedly atypical nuclei are prominent (hematoxylin-eosin stain; original magnification 200×)

SCCs are positive for AE1–AE3; however, negativity does not exclude SCC.

Variants

Acantholytic SCC: There is loss of cohesion between the tumor cells; a typical SCC pattern is mixed with pseudoglandular formations.

Clear cell SCC: The cytoplasm of tumor cells is pale due to the presence of glycogen. They should be differentiated from other clear cell tumors such as clear cell carcinoma; sweat gland carcinoma; sebaceous carcinoma (EMA+, AR+, CAM5.2+), the third most common malignant tumor of the eyelids and periocular region; and trichilemmal carcinoma.

Spindle cell SCC: Predominantly composed of spindle cells, if keratinization is absent, confusion with sarcoma, atypical fibroxanthoma, or spindle cell melanoma is possible. Immunohistochemistry is needed to make the differential diagnosis.

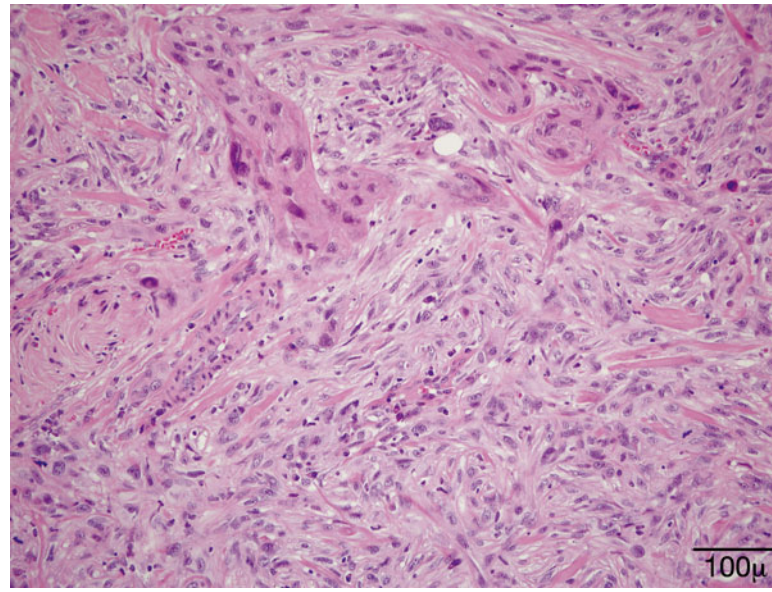

Fig. 11.57 Desmoplastic SCC – At higher magnification, chords of epithelioid tumor cells are recognized (hematoxylin-eosin stain; original magnification 200×)

Desmoplastic SCC: A prominent desmoplastic reaction in certain tumors with thin cords of epithelial cells (Fig. 11.57) and small keratin cysts may imitate a squamatized morpheaform BCC or a microcystic adnexal carcinoma.

Differential Diagnosis

Pseudoepitheliomatous hyperplasia (PEH) may resemble SCC. Knowledge of the clinical background (prior surgery, radiation therapy) is important. In PEH, there is no loss of keratinocyte polarity, and the stroma is reactive. Undifferentiated SCCs can mimic melanoma or sarcoma; immunostains for cytokeratins are needed for the correct diagnosis.

Porocarcinoma has the propensity to invade the lymphatics and is lethal in one-third of patients; it has a dismal prognosis compared to SCC [209]. CK15 and carcinoembryonic antigen (CEA) are useful markers in the differential. Porocarcinoma is CK15+ and CEA stains the ducts, while SCC is CK15-, and CEA is positive in tumor cells [210].

Histogenesis

SCC is a tumor of epidermal keratinocytes. It may occur de novo or following the malignant transformation of a precursor lesion, such as actinic keratosis or Bowen disease.

Genetics

The p53 tumor suppressor gene is mutated in 46–72 % of patients with SCC [211]. These mutations are due to direct absorption of UV light by DNA and produce characteristic C→T or CC→TT tandem mutations at dipyrimidine sites [211, 212]. Patients with xeroderma pigmentosum (XP), a rare autosomal recessive disorder, have a defect in UV-induced DNA damage repair due to an inappropriate nucleotide excision repair system. XP patients are predisposed to malignant skin neoplasms in sun-exposed areas. SCC may develop in early childhood. Some patients may have hundreds of skin tumors over time [21].

Loss of heterozygosity (LOH) on chromosome 9q22 has been observed in the tumor tissue in 60.8 % of SCCs, with the highest loss occurring in and around the PTCH gene [213].

Prognosis and Predictive Factors

Excision with clear margins usually cures most SCCs. However, the periorbital region and eyelids are high-risk anatomical sites, and a number of tumors recur even after apparent complete surgical excision. The main risk factor for local recurrence is incomplete primary excision [41]. Perineural invasion and orbital infiltration frequently coexist [204, 214] and seem more

common than regional lymph node metastasis, which is relatively low [215]. Even if exenteration is necessary, the prognosis is favorable.

11.9.2 Melanocytic Lesions and Neoplasms

Definition
Melanocytic cells, which by definition contain melanosomes and melanin pigment, normally occur as solitary cells in the dermis and vary in size and number, depending on racial origin. Melanocytes are derived from the neural crest and migrate to the skin during embryogenesis. A neoplastic proliferation of melanocytes may be acquired or congenital.

Benign lesions include ephelis (freckle), benign lentigo, a variety of nevi, and lentigo maligna, which is premalignant, and the malignant melanoma.

The benign melanocytic lesions vary considerably in their clinical appearance. They frequently occur on the surface of the eyelid or on the lid margin.

11.9.2.1 Ephelis

Synonym
Freckle

Definition
A localized increase in melanocytic pigmentation in the basal epidermal cells without a proliferation of melanocytes

Etiology
The histogenesis is hyperactivity of melanocytes, which release melanin into the basal epidermal cells.

Clinical Features
This pigmented lesion appears as a small, brown macule scattered over the sun-exposed areas of the skin, including the eyelids. In contrast to lentigo simplex, sunlight exposure deepens the pigmentation of freckles.

Histopathology
There is hyperpigmentation of the basal cell layer but no elongation of the rete ridges. The basal layer of the epidermis contains large, DOPA-positive melanocytes, but their number is not increased.

Prognosis
Prognosis is excellent. Removal is not warranted unless for cosmesis.

11.9.2.2 Lentigo Simplex

Definition
Lentigo simplex is a benign skin lesion usually observed in younger people. It may occur at any age and is not affected by exposure to sunlight.

Etiology
This includes a localized increase in melanocytes, which are functionally active and secrete melanin. It has been proposed that lentigo simplex may evolve into a lentiginous/junctional melanocytic nevus when melanocytes proliferate and aggregate to form small nests in the junctional zone, whereas solar lentigo may be a precursor lesion of seborrheic keratosis [171].

Clinical Features
The lesions measure approximately 1–2 mm in diameter, are flat and brown to black, and are clinically indistinguishable from a melanocytic nevus and junctional nevi.

Histopathology
Lentigo simplex shows a moderate elongation of the epidermal rete ridges and basal hyperpigmentation (Fig. 11.58). The number of melanocytes in the basal epidermal layer may be slightly increased (Fig. 11.59). In contrast to lentigo simplex, solar lentigo displays markedly elongated rete ridges and profound actinic elastosis in the dermis.

Prognosis
The prognosis is excellent. There is no premalignant potential. Multiple lentigines can be found in multiple lentigines syndrome (LEOPARD syndrome), which is associated with electrocardiogram (ECG) conduction defects,

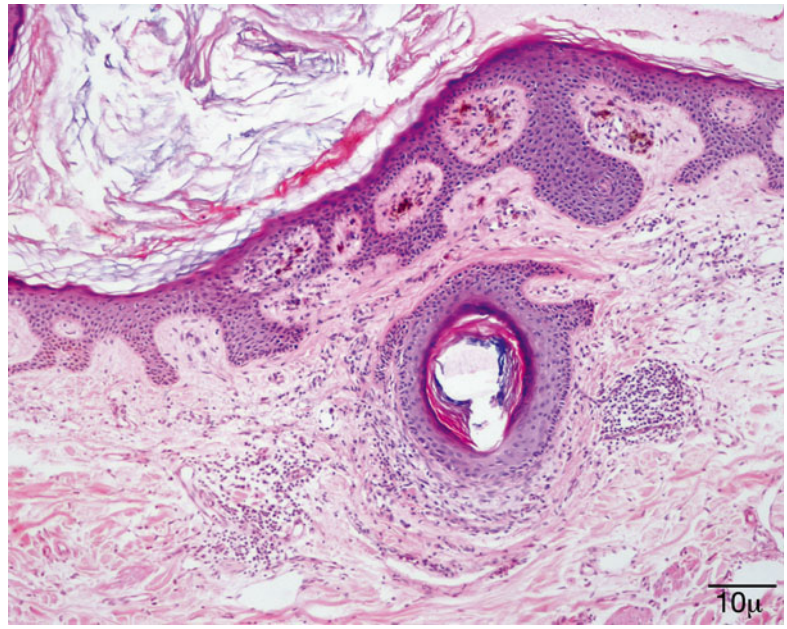

Fig. 11.58 Lentigo simplex – Elongation of rete pegs of epithelium; there is no junctional melanocytic proliferation (hematoxylin-eosin stain; original magnification 100×)

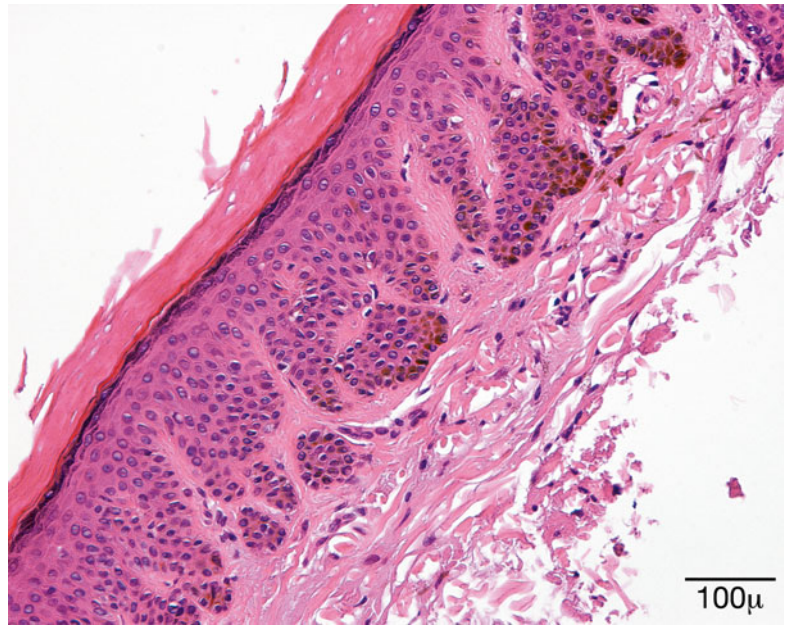

Fig. 11.59 Lentigo simplex – Highlights pigmentation of the basal layer of the epithelium (hematoxylin-eosin stain; original magnification 200×)

ocular hypertelorism and other eye defects, pulmonary stenosis, growth retardation, abnormal genitalia, and sensorineural deafness, and in Carney's syndrome, which has an autosomal dominant inheritance pattern and is associated with bilateral primary pigmented nodular adrenocortical hyperplasia, cutaneous myxomata, breast lesions, pituitary tumors, and melanotic schwannomas.

11.9.2.3 Solar Lentigo

Solar lentigo is characterized clinically by flat epidermis with microscopic acanthosis and circumscribed pigmentation affecting the sun-exposed skin.

Synonyms
Lentigo senilis, actinic lentigo

Epidemiology
This lesion is mainly seen in middle-aged to elderly Caucasians.

Etiology
Related to chronic sun exposure [216, 217]

Localization
Solar lentigo is most common in the skin of the face, including the eyelid. This lesion predominantly affects the sun-exposed skin.

Clinical Features
It is characterized by a well-circumscribed macule, flat lesion, with variably brown pigmentation.

Histopathology/Immunoprofile
The epidermal surface is hyperkeratotic. The epidermis shows atrophy of upper layers with elongation of the rete ridges. Rete ridge hyperplasia is less prominent in lesions involving the face. Increased melanin pigmentation is present, especially in the rete pegs. Intraepithelial melanocytes may be of normal number or increased with mild cellular pleomorphism present. Pigment incontinence may be seen in the dermis or in associated macrophages (melanophages). The dermis shows solar elastosis and mild lymphohistiocytic infiltrate.

Differential Diagnosis
It includes pigmented seborrheic keratosis and lentigo maligna.

Prognosis
It is excellent. Uncommonly, lentigo maligna may arise in long-standing solar lentigo.

11.9.2.4 Junctional Nevus
It arises from the deeper layers of the epidermis ("junctional region") and does not involve the underlying dermis.

Clinical Features
They appear as flat, pigmented lesions.

Histopathology
These appear as nests of melanocytic cells at the dermal–epidermal junction. There is little cellular pleomorphism and no mitotic activity.

Although connected to the epidermis, nevus cells have the capacity of "dropping off" into the dermis, and many nevi that appear to be purely junctional in one area are found to be compound in other areas.

Prognosis
A benign junctional nevus has an excellent prognosis and can be removed locally. This type of nevus, like the compound nevus, has the capacity to evolve into a malignant melanoma. The development of a frank malignant melanoma is associated with increased nuclear pleomorphism, hyperchromatism, increased mitotic activity, and an inflammatory reaction in the underlying dermis.

11.9.2.5 Compound Nevus
This lesion possesses features of both junctional and intradermal nevi (Fig. 11.60). In an appreciable portion of these lesions, nests of intradermal nevus cells show maturation at the dermal base of the lesion. The cells are small and uniform and have little cellular pleomorphism. The amount of intracellular pigment is variable. This type of nevus is more common than the purely junctional nevus and may also undergo malignant changes.

11.9.2.6 Dermal Nevus (Intradermal Nevus)
This is the most common of the three types of nevocellular nevi. Malignant change in a purely intradermal nevus is extremely rare.

Clinical Features
It is a pigmented, raised lesion with a well-circumscribed border (Fig. 11.61). The surface of an intradermal nevus may have a papillomatous domed or pedunculated configuration. Clinically,

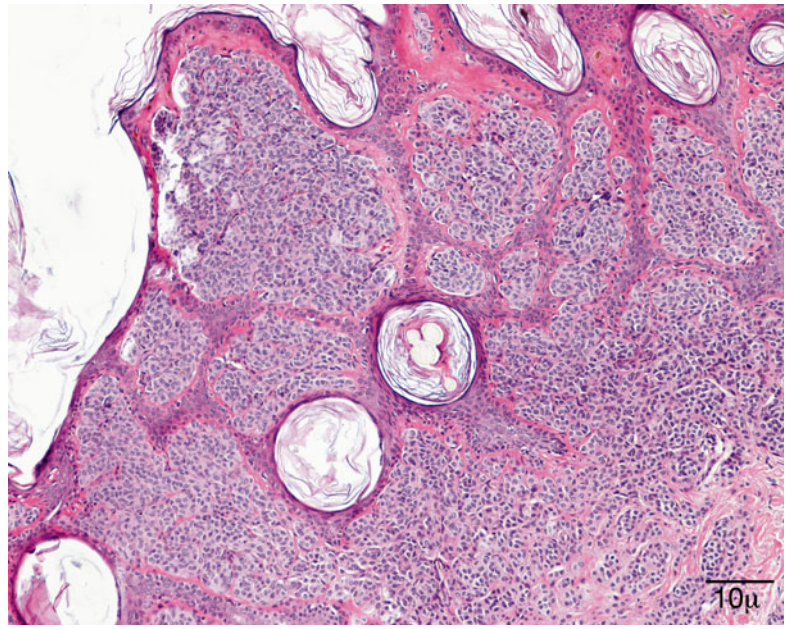

Fig. 11.60 Compound nevus – Proliferation of bland-appearing uniform melanocytic cells in the basal epidermis and dermis. There is no cellular pleomorphism or mitotic activity. Epidermal inclusions are seen. The latter is a benign feature (hematoxylin-eosin stain; original magnification 100×)

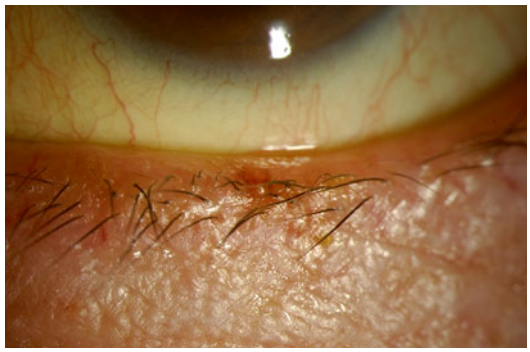

Fig. 11.61 Nevus – Clinical photograph showing a flat pigmented lesion on the lower eyelid

the presence of hairs in an elevated pigmented nodule usually indicates that the lesion is intradermal.

Histopathology

The nests of nevus cells in the dermis are separated from the overlying epidermis by an uninvolved layer of upper dermis (Fig. 11.62). In the eyelid, nevus cells may extend into the deeper dermis and reach the fibers of the orbicularis muscle, giving the false impression of a neoplastic infiltrate. This should not be considered an ominous finding. The presence of nests of large, multinucleated nevus cells may only be found in mature intradermal nevi and are considered to indicate the benign nature of the lesion.

11.9.2.7 Spitz Nevus

Synonym

Epithelioid cell nevus

Definition

Spitz nevus is a form of compound nevus that mainly affects children and young adults. It is exceptionally rare in the elderly.

Clinical Features

The lesion usually presents as a solitary, rounded, or oval dome-shaped papule with a smooth surface. It may also be verrucous, with mild scaling, crusting, or erosion. Ulceration is rare. Its color can vary from pink to reddish brown or purple red, and its growth may be slow or fast. The lesion is often asymptomatic; bleeding and itching rarely occur.

Histopathology

The lesion is a variant of junctional or compound nevus, containing fascicles of spindle-shaped

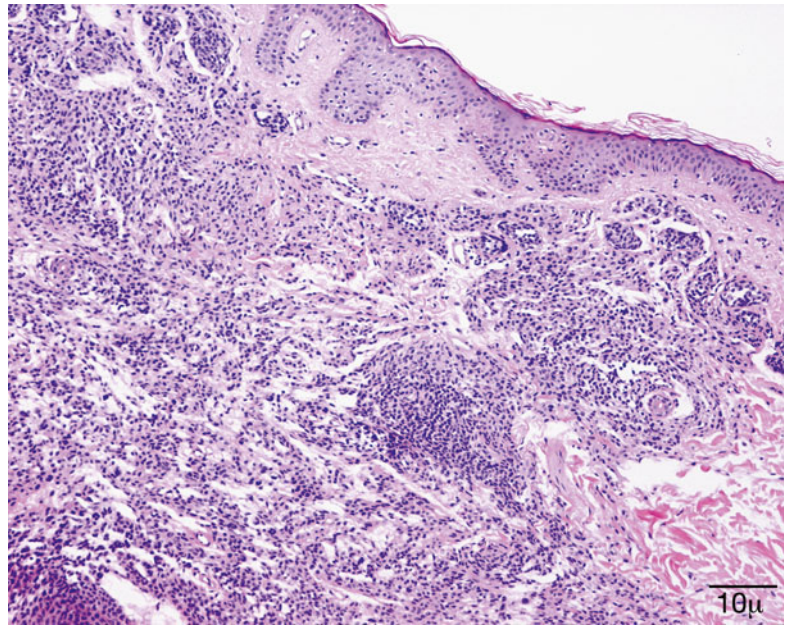

Fig. 11.62 Intradermal nevus – Proliferation of bland-appearing uniform nevus cells in the dermis; there are no junctional cells nests (hematoxylin-eosin stain; original magnification 100×)

cells showing a "windblown" or "raining down" appearance intermixed with larger epithelioid cells with polyhedral outlines. An "active" junctional zone, scattered mitotic figures, and the presence of secondary inflammation may be seen. There may be marked atypia and nuclear pleomorphism. The presence of cell maturation at the base of the tumor is a feature in the histological differentiation of Spitz nevi from melanoma. It differs from melanoma in clinical appearance and age group of occurrence as well as in having a well-circumscribed appearance on low-power microscopy.

Differential Diagnosis

Other nevi and spitzoid variant of malignant melanoma

Prognosis

The lesion usually pursues a benign clinical course, and complete excision is curative.

11.9.2.8 Blue Nevi

Definition

This is an intradermal melanocytic nevus occurring in the deep dermis. The depth of the melanin in the dermis gives the blue appearance, thus the name blue nevi.

Epidemiology

Blue nevus most commonly arises in children and young adults, commonly females, but can occur at any age or as a congenital lesion [218].

Etiology

These lesions arise from deeply located melanocytes that have been arrested in the dermis before reaching the epidermis.

Clinical Features

The blue nevus presents as a dome-shaped, single small lesion of which the dark blue or blue-black color results from the scattering of light by melanin particles within deeply located dermal melanocytes (Fig. 11.63). Satellite nodules of benign blue nevus mimicking metastatic melanoma can also be seen [218].

Histopathology

At low magnification, the lesion is usually a more or less symmetric middermal and/or upper dermal proliferation wedge-shaped configuration, with the base of the lesion parallel to the surface of the epidermis and the apex pointing to deep reticular dermis or subcutaneous tissue (Fig. 11.64) [218]. Blue nevi have a tendency to extend deep into reticular dermis along adnexal structures and/or neurovascular bundles. The overlying epidermis

Fig. 11.63 Blue nevus – Clinical photograph showing a deeply pigmented nodular lesion with smooth surface and circumscribed edge

lacks a junctional component except when the lesion is part of a combined nevus. The diagnostic cell of a blue nevus is a variably pigmented, spindle-shaped dendritic melanocytic, which has a slender, branching network of dendritic processes whose nuclei are small, elongated, and hyperchromatic (Fig. 11.65) [218].

Differential Diagnosis

Hemangioma on clinical appearance, other melanocytic intradermal nevi on histopathology

Prognosis

Benign course; local resection is curative.

11.9.2.9 Combined Nevi

Combined nevi are nevi comprised of both nevocellular cells and blue nevus cells.

Clinical Features

The former may be pigmented or nonpigmented.

Histopathology

They may have a junctional, compound, or subepithelial distribution; the latter are spindle-shaped or multipolar dendritic cells, usually laden with fine melanin granules [219].

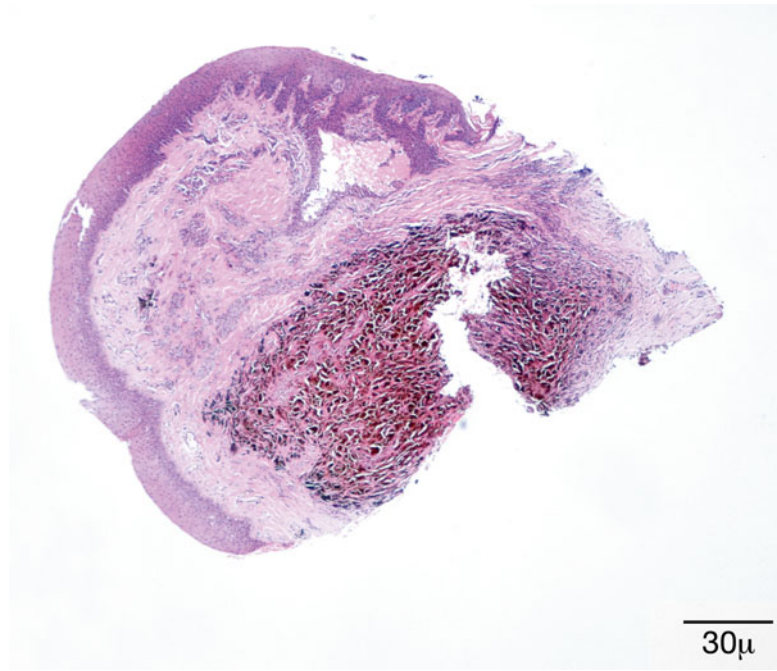

Fig. 11.64 Blue nevus – This shows a proliferation of spindle-shaped pigmented cells in deep dermis. There is no involvement of the superficial dermis (hematoxylin-eosin stain; original magnification 40×)

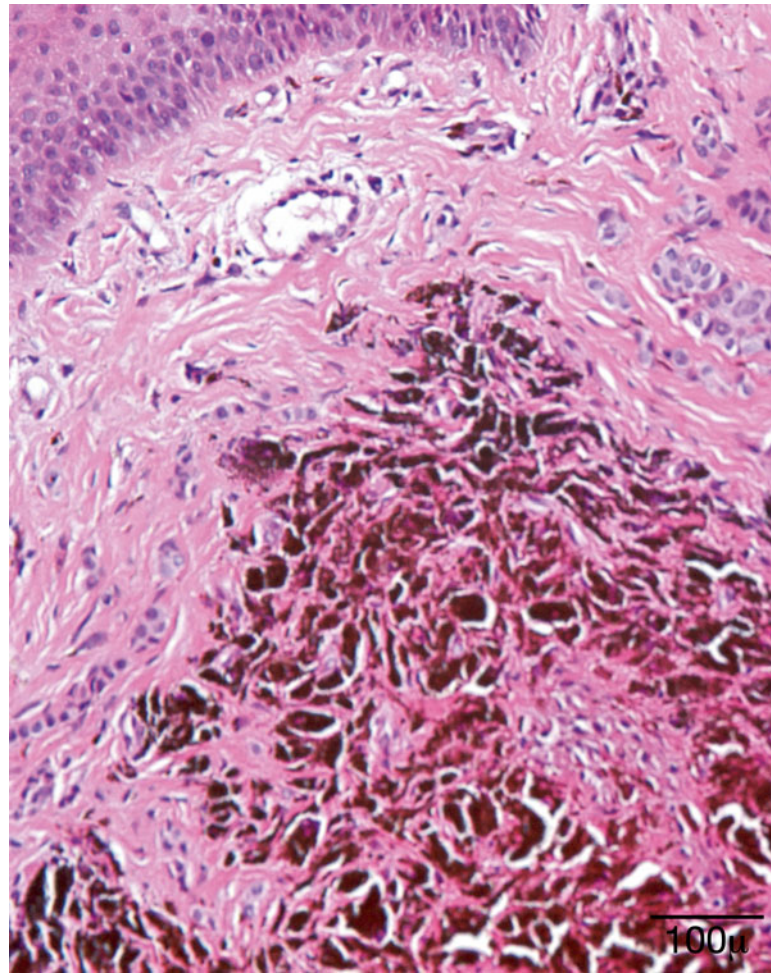

Fig. 11.65 Blue nevus 3 – Highlights heavy melanin pigment in dermal spindle cells (hematoxylin-eosin stain; original magnification 200×)

Prognosis
Benign course

11.9.2.10 Ocular Melanocytosis

Synonyms
Nevus of Ota

Definition
Oculodermal melanocytosis is a congenital pigmentation of the periocular skin, uveal tract, and sometimes the orbit, ipsilateral meninges, and ipsilateral hard palate. The condition is usually unilateral, although bilateral cases have been described [220].

Etiology
It is a sporadic, congenital disease. The skin pigmentation is apparent at or shortly after birth in approximately 50 % of the cases, and development as late as 20 years of age has been reported [162, 220]. Malignant transformation of the eyelid component into cutaneous melanoma is rare.

Clinical Features
The cutaneous lesion is a flat, tan to gray pigmentation that may be somewhat irregular as it tends to follow the distribution of the first and second divisions of the trigeminal nerves. It is bilateral in about 10 % of cases. It is more common in Caucasians but occurs in all racial groups.

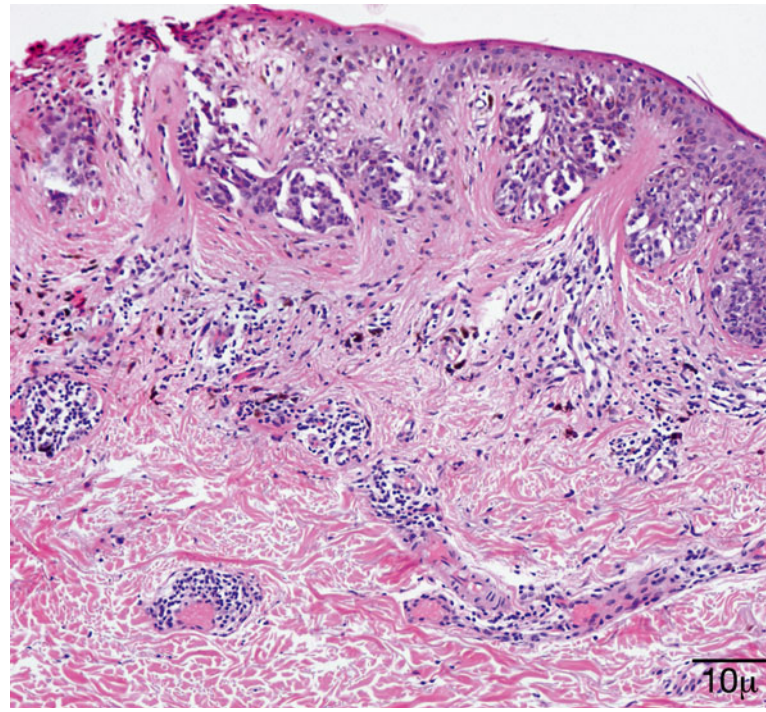

Fig.11.66 Dysplastic nevus–Untidy proliferation of intra-epithelial melanocytic cells showing mild cytological atypia. Bridging of rete pegs by irregular melanocytic nests is a feature of architectural atypia (hematoxylin-eosin stain; original magnification 100×)

Histopathology

It is characterized by excess scattered dendritic melanocytes in the dermis and is not as cellular as a true blue nevus.

Prognosis

Ocular melanocytosis is a benign condition and does not require treatment, except for cosmesis, when laser removal may improve the appearance. It is associated with an increased incidence of uveal malignant melanoma, especially in non-Caucasians [1], and periodic ocular examination is advised.

11.9.2.11 Dysplastic Nevus

Definition

It is a junctional or compound nevus showing atypical features on clinical or histological examination. It may be a precursor of malignant melanoma, and patients with dysplastic nevi are at increased risk for the development of malignant melanoma. It may be sporadic of familial. The reported incidence of sporadic dysplastic nevi in the general population varies from 1.8 to 17 %.

Etiology

The condition is inherited as an autosomal dominant trait [1]. The nevi can progress into radial and subsequently vertical growth phase melanomas [221].

Clinical Features

Dysplastic nevi are characterized by multiple, large, atypical, cutaneous nevi, 5–10 mm in size with irregular outlines and a haphazard mixture of tan, brown, black, and pink coloration. The nevi are usually noticeable in children and adolescents and continue to grow throughout adult life. Numbers vary from a few to hundreds on the skin surface on the body.

Histopathology

Dysplastic nevi show characteristic morphological alterations, including proliferation and variable atypia of epidermal melanocytes, formation of irregular cell nests in the epidermis and basement membrane zone, and the interconnection of these nests and layers (Fig. 11.66) [221]. The dysplastic nevi show areas of atypical melanocytic hyperplasia, patchy lymphocytic dermal infiltrates,

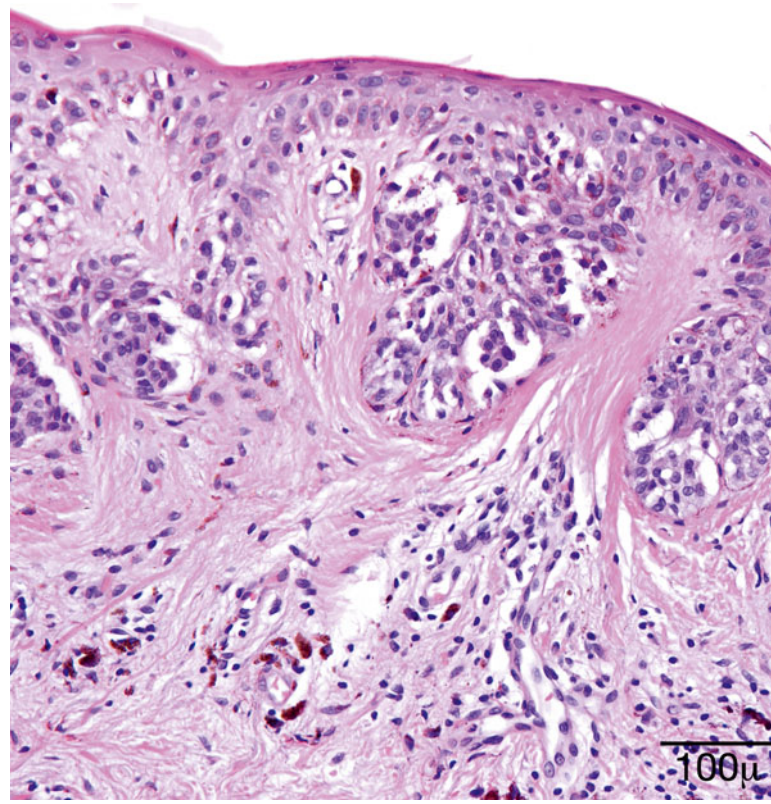

Fig. 11.67 Dysplastic nevus – Eosinophilic fibroplasia between adjacent rete pegs; cellular pleomorphism is observed (hematoxylin-eosin stain; original magnification 200×)

delicate fibroplasias, and neovascularization of the papillary dermis (Fig. 11.67) [1].

Differential Diagnosis

Other melanocytic nevi or malignant melanoma

Prognosis

A dysplastic nevus should be excised fully with margin of uninvolved skin. Persons with the clinical phenotype of dysplastic nevus syndrome as well as having two blood relatives with melanoma have a 100 % lifetime risk of developing one or more melanomas. These individuals should have all moles documented and photographed with periodic clinical follow-up. It is not certain whether there is an increased risk of melanoma developing in sporadic dysplastic nevus.

11.9.2.12 Melanoma In Situ

Melanoma in situ is an atypical intraepithelial melanocytic proliferation confined by the basement membrane of the epithelium [222]. It is also known as the radial or horizontal growth phase. Tumors which have infiltrated the basement membrane are no longer in situ. Two patterns of melanoma in situ are recognized: lentigo maligna melanoma (see corresponding text) and superficial spreading melanoma (see corresponding text).

Prognosis

Melanoma in situ may progress to invasive malignant melanoma. It is cured by complete excision [223].

11.9.2.13 Lentigo Maligna

Synonym

Hutchinson's melanotic freckle

Definition

Lentigo maligna (LM) is an indolent subtype of melanoma in situ with a prolonged radial growth phase.

Etiology

Acquired pigmented lesion due to a proliferation of melanocytes in the basal layer of the epidermis of the sun-exposed skin

Clinical Features

It presents as a flat, slowly enlarging macular lesion with poorly defined irregular borders, prominent asymmetry, and pigment variation, persisting for years on the chronically sun-exposed skin of elderly predominantly white individuals (Fig. 11.68) [224, 225].

Histopathology

Lentigo maligna is a proliferation of melanocytic cells in a linear continuous fashion, initially in the basal layers and then spreading throughout all layers of the epidermis. This is known as a lentiginous proliferation. There is variable cytological atypia and increased mitotic activity (Fig. 11.69). Proliferation markers such as ki-67 show overall low proliferation and an apparently low apoptotic tendency [225].

Fig. 11.68 Lentigo maligna – Clinical photograph showing flat pigmented tumor on the lower eyelid and face

Differential Diagnosis

The differential diagnosis is a benign melanocytic lesion, such as actinic melanocytic hyperplasia, which can occur in association with LM, or nevus with or without dysplasia, or an early intraepithelial phase of superficial spreading malignant melanoma (see below).

Prognosis

If left untreated, it may evolve into the invasive form of lentigo maligna melanoma in approximately 30 % of cases.

11.9.2.14 Invasive Malignant Melanoma

Malignant melanoma accounts for less than 1 % of all malignant neoplasms of the eyelid [226]. Involvement of the eyelid is more common as a complication of conjunctival melanoma [227].

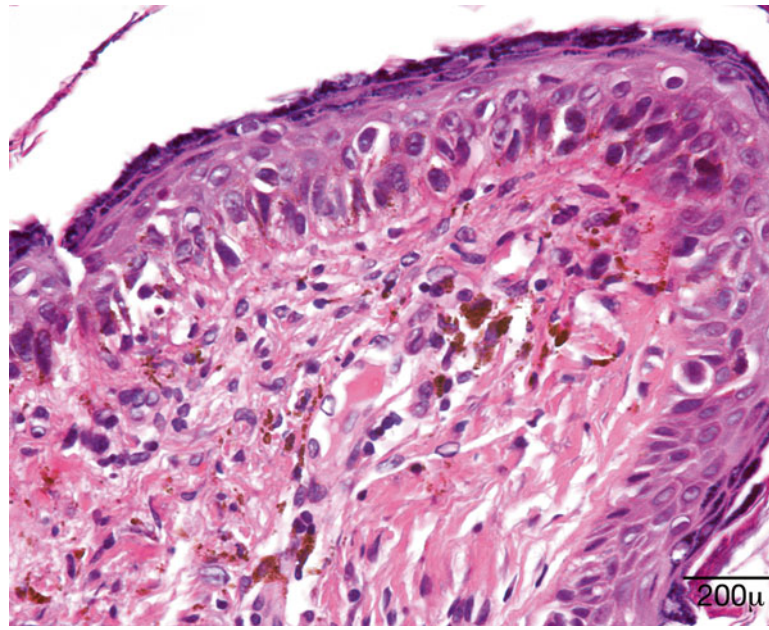

Fig. 11.69 Lentigo maligna – Linear junctional proliferation of atypical melanocytes, dermal melanocytic cell groups, and perivascular inflammatory infiltrate (hematoxylin-eosin stain; original magnification 400×)

Etiology

Cutaneous melanoma generally develops on sun-exposed areas of adult Caucasians who have had excess exposure to ultraviolet light. Those at greater risk include persons with a high number of moles, family members with dysplastic nevi, immunosuppressed, and those with melanoma at another site. It can occur on the eyelid as a primary lesion, metastasis from a distant primary melanoma, or extension of a conjunctival melanoma [162, 228].

Fig. 11.70 Malignant melanoma – Clinical photograph showing a swollen and erythematous upper lid with variegated pigmented areas)

Fig. 11.71 Malignant melanoma – Clinical photograph ulcerated tumor involving lower lid and adjacent periocular skin

Clinical Features

Eyelid melanoma appears as a variably pigmented mass with irregular borders (Fig. 11.70) that can bleed or ulcerate (Fig. 11.71). The primary tumor involves the lower lid in 67 % of cases.

There are three types of primary cutaneous melanoma that can occur in the eyelids: lentigo maligna melanoma, superficial spreading melanoma, and nodular melanoma [1, 162].

Grossniklaus and McLean reported that when cases of melanoma are excluded, 59 % of eyelid melanomas are nodular, 22 % are superficial spreading, and 19 % are lentigo maligna melanoma. Others have found that lentigo maligna melanoma accounts for 90 % of head and neck melanomas [229].

Lentigo maligna melanoma (LMM) occurs when there is progression of the slow-growing lesion more often seen in elderly patients. Superficial spreading malignant melanoma (SSMM) has a pigmented nodular or plaque-like appearance, often with hyperkeratotic cap, surrounded by a flat pigmented zone, and has a pre-existing intraepithelial or radial growth phase.

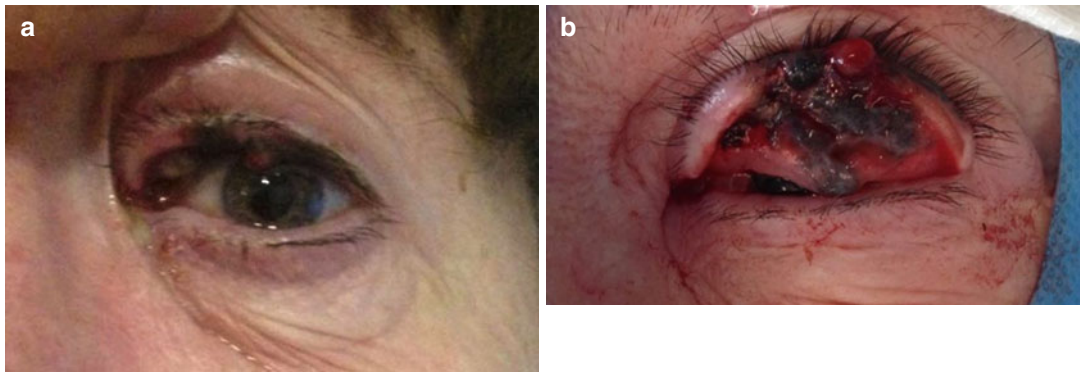

Fig. 11.72 (**a**) Malignant melanoma – Clinical photograph depicts an upper lid nodular melanoma. (**b**) Malignant melanoma – Clinical photograph of same patient with lid everted, demonstrating large pigmented tumor.

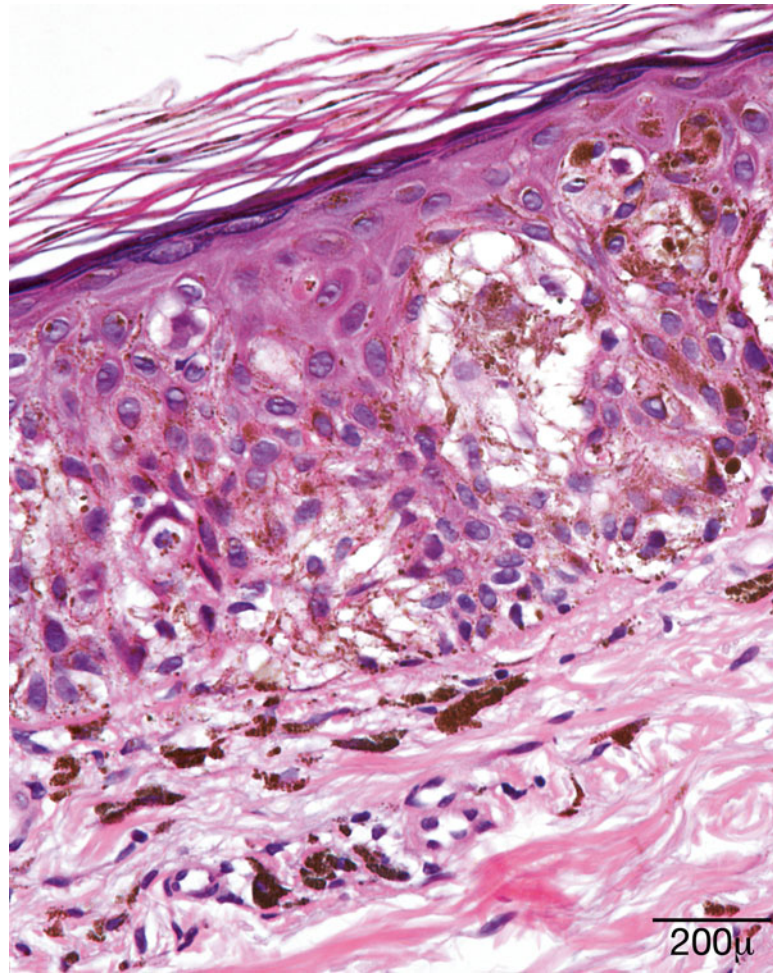

Fig. 11.73 Superficial spreading melanoma in situ – High-power view of intra-epithelial tumor cells (hematoxylin-eosin stain; original magnification 400×)

Nodular melanoma occurs without a preexisting intraepithelial radial growth phase. It is characterized by rapid downward or vertical growth in the dermis (Fig. 11.72a, b).

Histopathology

Unlike the lentiginous continuous basal melanocytic proliferation seen in LM, SSMM has scattered single or grouped atypical melanocytic cells (Fig. 11.73) throughout all layers of the epithelium (Fig. 11.74) in a shotgun pattern (Fig. 11.75), similar to the pattern seen in Paget disease (often called pagetoid spread). The tumor may ulcerate the skin surface.

The dermal tumor cells of invasive malignant melanoma may have a nevoid or spindle cell morphology. More aggressive tumors resemble epithelial cells. Areas of tumor cell loss with replacement by fibrous tissue and pigmented macrophages are known as areas of regression. Histological prognostic factors include Clark level [230], Breslow thickness [231], prominent lymphoid infiltrate, lymphovascular invasion, and mitotic rate/mm^2.

Clark and colleagues measured the depth of tumor based on five levels (epidermal only, penetrating papillary dermis, filling papillary dermis, involving reticular dermis, and subcutaneous involvement) [230].

The tumor depth measured in millimeters is known as Breslow thickness [231]. This measurement has prognostic significance. Tumors whose depth of invasion is <0.75 mm in thickness have an excellent prognosis with a

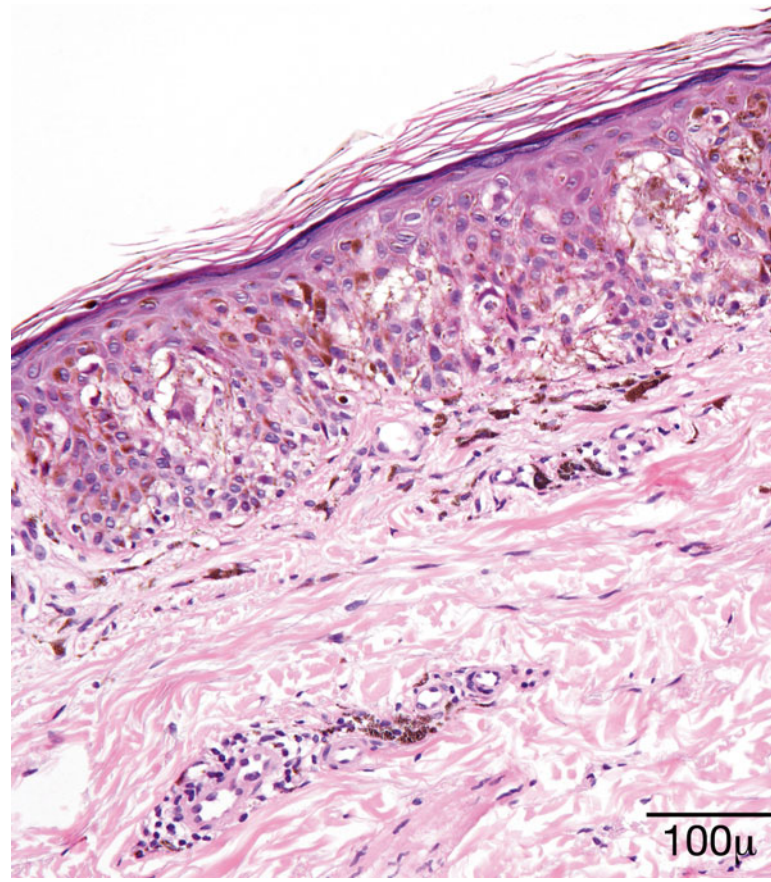

Fig. 11.74 Superficial spreading melanoma in situ – Clusters of large tumor cells and single tumor cells are seen at all levels of epidermis. Melanin-containing macrophages are present in the dermis (hematoxylin-eosin stain; original magnification 400×)

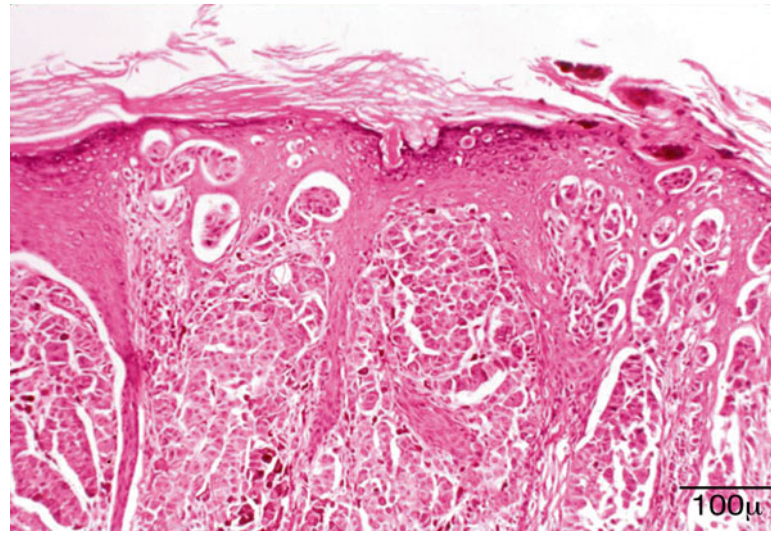

Fig. 11.75 Malignant melanoma, superficial spreading subtype – Large atypical melanocytic cells are scattered in the epidermis in a "shotgun" or pagetoid pattern and infiltrate the dermis as cohesive tumor (hematoxylin-eosin stain; original magnification 200×)

5-year survival of 100 %. Tumors with a thickness of 0.75–1.5 mm have an intermediate prognosis, and those tumors with a depth of >1.5 mm have a poor prognosis and a 5-year survival of 50–60 %.

Tumor cells express melanocytic markers such as Melan-A, tyrosinase, S-100, and HMB-45 on immunohistochemical studies.

Differential Diagnosis

If the tumor is depigmented, it may clinically resemble a primary epithelial malignancy, lymphoma, or metastatic tumor. An SSMM may resemble sebaceous carcinoma, which also has a pagetoid intraepithelial growth pattern.

Prognosis

Two-thirds of eyelid melanomas are invasive at the moment of diagnosis. Thus, early diagnosis remains essential for better prognosis [228]. Melanoma of the eyelid skin has a slightly better prognosis than conjunctival melanoma. Involvement of the lid margin and conjunctiva is associated with a worse prognosis.

The treatment of melanoma is complete excision and eyelid reconstruction [232]. The American Joint Committee on Cancer (AJCC) recommends that, for skin melanoma, an in situ melanoma should have a 0.5 cm margin; a melanoma <2 mm depth should have a 1 cm margin; and a melanoma with >2 mm should have a 2.2 cm margin. These recommendations must be modified in the eyelid skin, where narrow clear margins are acceptable.

Progression of disease occurs via local spread to regional lymph nodes as well as distant metastasis. Once the tumor has spread, the lymph node status is the most important piece of prognostic information [233].

Sentinel lymph node biopsy is not routinely performed in the periocular region at present. Its use for eyelid and conjunctival malignancy has been described in large cancer centers [234, 235]. The positive sentinel node has been variously found in periauricular, parotid, submandibular, and cervical nodes. If the sentinel node is positive, surgical resection of all of the nodes in that basin is considered.

There is no effective targeted systemic chemotherapeutic option for disseminated malignant melanoma. The molecular genetic profile of eyelid melanoma is that of primary skin melanoma at other sites [236]. Molecular targets for treatment of advanced melanoma have focused on the RAS/RAF/MEK/ERK and p13k/AKT pathways, which are centrally involved in the pathogenesis of melanoma [237].

11.9.3 Sebaceous Lesions and Neoplasms

The periorbital region and eyelids contain the most concentration of sebaceous glands in the human body. There are the ordinary sebaceous glands within the pilosebaceous units, Zeis glands, sebaceous glands associated to the eyelashes, and the Meibomian glands, which are the sebaceous glands deeply situated within the tarsus plate. An association between Muir–Torre syndrome (MTS) and sebaceous neoplasms has been described [238].

Muir–Torre syndrome is a rare, hereditary, and autosomal dominant genetic disorder thought to be part of the Lynch syndrome or hereditary nonpolyposis colorectal cancer. Individuals affected are prone to develop neoplasms of the colon, breast, genitourinary, and skin, including sebaceous neoplasms [239]. The genes affected are MLH1 and MSH2 and are involved in DNA mismatch repair [240]. It seems that there is a second group of patients in which the disease is nonfamilial and unassociated with any known mutations [241].

11.9.3.1 Sebaceous Hyperplasia

Sebaceous hyperplasia is common in middle-aged and older individuals and apparently is unrelated to MTS [242]. It presents clinically as single yellow papule or a diffuse eyelid thickening.

Histologically, sebaceous hyperplasia is characterized by well-demarcated enlarged lobules of

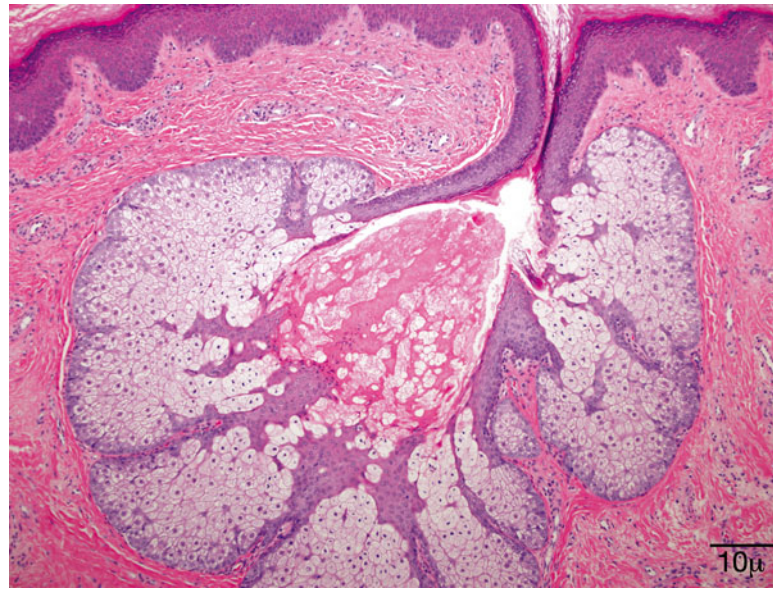

Fig. 11.76 Sebaceous hyperplasia – Sebaceous hyperplasia is characterized by well-demarcated enlarged lobules of normal-appearing sebaceous glands around a dilated gland duct (hematoxylin-eosin stain; original magnification 100×)

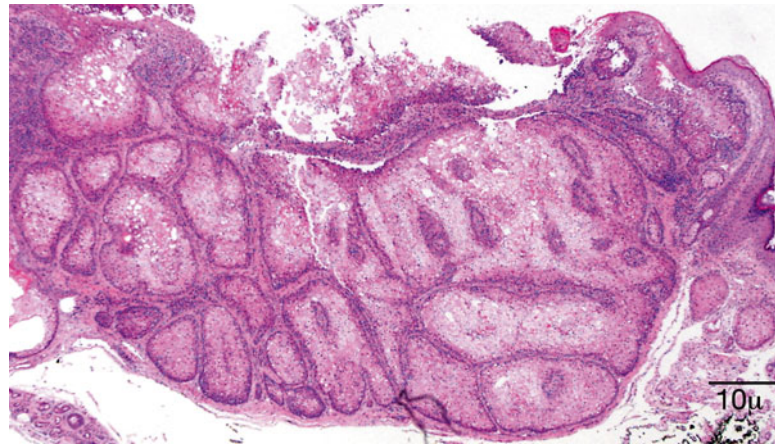

Fig. 11.77 Sebaceous adenoma – Sebaceous adenomas are characterized by a proliferation of irregular lobules of mature appearing sebaceous cells. The lobules are surrounded by a layer of germinative epithelium (hematoxylin-eosin stain; original magnification 100×)

normal-appearing sebaceous glands, usually around a dilated gland duct that leads to a plugged follicular ostium (Fig. 11.76).

11.9.3.2 Sebaceous Adenoma

This is a benign neoplasm that presents most often as a small solitary yellow papule or nodule, smaller than 1 cm in size, in the face or trunk of middle-aged patients. The importance of this neoplasm is its occasional association with internal organ malignancy in patients with MTS [243, 244].

Histologically, these are characterized by multiple irregular lobules of proliferated sebaceous cells. Inside each lobule, the mature sebaceous cells predominate, occupying two-thirds of the lesion (Fig. 11.77). Basaloid-appearing germinative cells line the periphery of the lobules, giving a biphasic appearance to this neoplasm.

11.9.3.3 Sebaceous Carcinoma

Definition

Sebaceous carcinomas are malignant epithelial neoplasms with sebaceous differentiation that arise from meibomian glands, Zeis glands, or other pilosebaceous units in the eyelid.

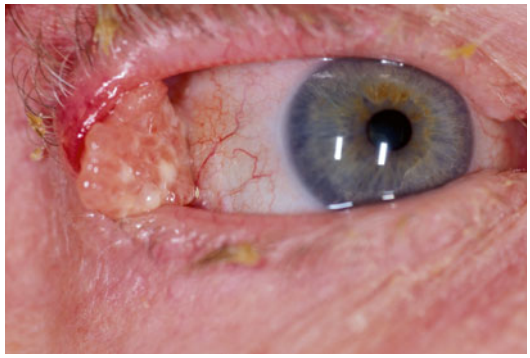

Fig. 11.78 Sebaceous carcinoma – Exophytic mass involving the upper eyelid and extending to the palpebral conjunctiva

Fig. 11.79 Sebaceous carcinoma – Sebaceous carcinoma presenting clinically as eyelid thickening

Epidemiology

This is a disorder of middle-aged and elderly patients (mean age 57–72 years), with a slight female predominance in some studies [245–248]. The incidence of sebaceous carcinoma varies from 1 to 5.5 % of all malignant neoplasms of the eyelid [248]. Sebaceous carcinoma of the eyelid may be prevalent in Asian countries but not in the Asian population living in the United States [245, 248].

It would appear that prior irradiation is an important risk factor, as patients who have been treated previously with radiation for tumors in the head and neck region have a higher incidence of sebaceous carcinoma [249–251].

Clinical Features

The upper eyelid is the most frequently involved site of sebaceous carcinoma [252, 253]. Occasionally, both eyelids are simultaneously involved, and the tumor may appear to be multicentric, which is the result of intraepithelial pagetoid invasion [254]. In such cases, the tumor may masquerade as blepharoconjunctivitis, delaying the correct diagnosis.

Clinically, sebaceous carcinoma usually presents as a circumscribed yellow nodule involving the tarsal plate when viewed from the tarsal conjunctival surface (Fig. 11.78). However, sebaceous carcinoma may also occur as a fungating mass or plaque, causing eyelid thickening (Fig. 11.79). When the origin is from the glands of Zeis, the margin of the eyelid is involved, with thickening and loss of cilia. Intraepithelial spread of tumor cells (pagetoid invasion) may extend as far as the cornea without causing significant thickening of either the conjunctival or corneal epithelium. Occasionally, however, papillary forms develop and cause confusion with squamous cell carcinoma.

Histopathology

Histologically, sebaceous carcinomas are divided into low, medium, and high grade according to the degree of differentiation. In low-grade tumors, a common pattern consists of lobules of various sizes composed of cells resembling benign sebaceous cells (Fig. 11.80). The individual polyhedral cells are characterized by vesicular nuclei with prominent nucleoli and foamy vacuolated cytoplasm as a result of the high lipid content, which is readily demonstrated in frozen sections by the oil red O stain. Higher-grade tumors show scant cytoplasmic vacuolation with more prominent nucleoli, atypical mitoses, and abundant necrosis (Fig. 11.81). The higher-grade lesions are more likely to show pagetoid spread in the overlying epidermis, conjunctival epithelium, or corneal epithelium. The intraepithelial cells show similar morphological features than the ones observed in the invasive component. Pagetoid spread is associated with a poorer prognosis because of the widespread nature of the neoplasm [254].

Immunohistochemical studies have proved very helpful in distinguishing sebaceous carcinoma from other epithelial neoplasms, in particular, clear cell squamous cell carcinoma and clear cell basal cell carcinoma [248, 255, 256]. Sebaceous carcinomas are reactive with antibodies against

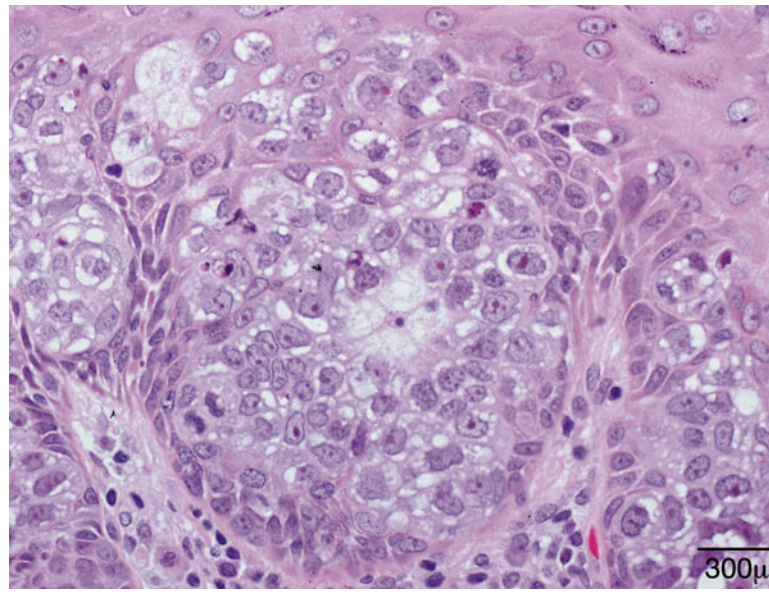

Fig. 11.80 Sebaceous carcinoma – Well-differentiated sebaceous carcinoma. The neoplastic cells show enlarged nuclei and prominent nucleoli but still resemble sebaceous cells (hematoxylin-eosin stain; original magnification 600×)

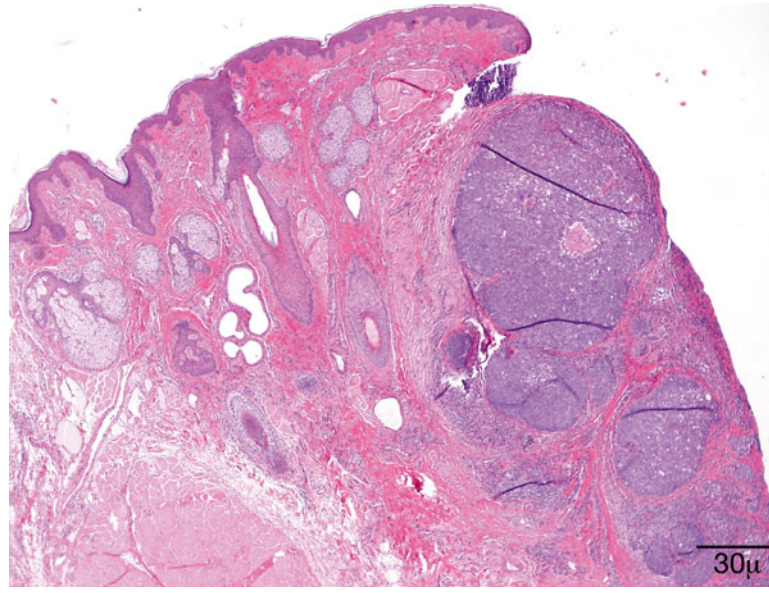

Fig. 11.81 Sebaceous carcinoma 4 – Full-thickness eyelid resection showing invasive poorly differentiated sebaceous carcinoma. The tumor cells have high nuclear cytoplasmic ratio and scant cytoplasm. The tumor nodules show central necrosis (hematoxylin-eosin stain; original magnification 40×)

epithelial membrane antigen (EMA), low molecular weight cytokeratins (CAM5.2 and CA15-3), androgen receptors, and anti-adipophilin [257].

Prognosis

Due to the rarity of sebaceous carcinoma and the variety of clinical presentations, there is usually a delay in the diagnosis. Early case series reported a high mortality rate of 30 % after a 5-year follow-up [258]. The presence of pagetoid spread is associated with a poorer prognosis [254]. Recent reports suggest an improved survival [247]. Metastases usually occur in regional lymph nodes, and death is related to widespread disease.

11.9.4 Adnexal Tumors with Sweat Gland Differentiation

11.9.4.1 Syringoma

Definition

A benign adnexal tumor derived from eccrine ducts

Synonyms
Eccrine syringoma

Epidemiology
It affects mostly young women, and the incidence is unknown. A high prevalence has been reported in female Down syndrome patients [259].

Etiology
The etiology is unknown. One case report demonstrated multiple HPVs in a single tumor, but the significance of this finding is unknown since HPVs are demonstrated in the normal skin as well.

Fig. 11.82 Syringoma clinical – Multiple skin-colored papules and nodules on the lower eyelid in a young woman

Localization
They appear most frequently on the eyelids but can affect other regions (axilla, vulva, and penis) (Fig. 11.82).

Clinical Features
Small skin-colored or slightly yellow papules appear in crops and involve mostly the upper eyelid.

Histopathology/Immunoprofile
There is a circumscribed proliferation of small ducts, solid nests, and cords in the dermis. The ducts are lined by two or more layers of cuboidal or flattened, eosinophilic, or clear cells. Some ducts assume a tadpole configuration (Fig. 11.83).

Differential Diagnosis
Microcystic adnexal carcinoma (MAC) is the most important differential to make and can be challenging in a superficial biopsy or isolated syringoma. The tendency of MAC for in-depth invasion compared to the lateral superficial spreading of syringoma is an indication for the differential diagnosis.

Histogenesis
This is most likely related to eccrine ducts or pluripotent stem cells.

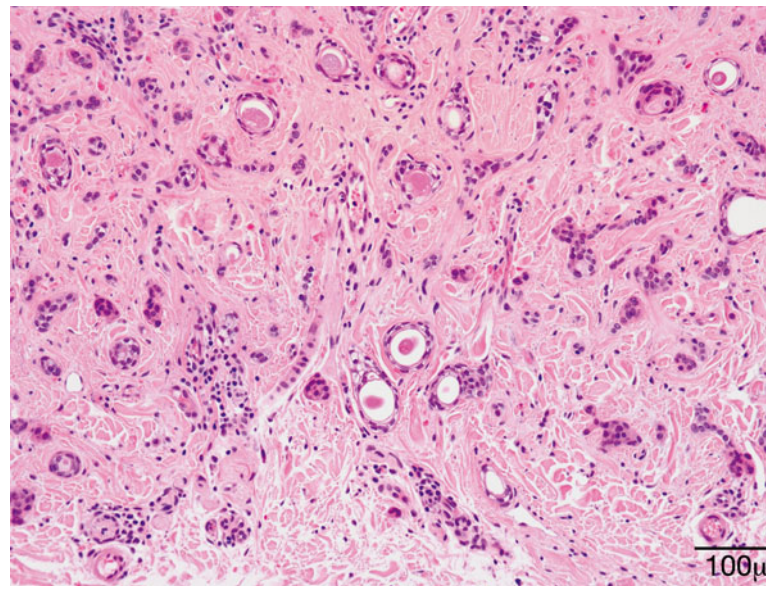

Fig. 11.83 Syringoma – Microscopically, syringoma is characterized by a proliferation of narrow epithelial strands and small ducts dispersed in a fibrous stroma

Fig. 11.84 Chondroid syringoma – Small, firm nodule underneath the eyelid skin. The lesion has been growing over years

Prognosis and Predictive Factors

Cosmetic problems can be an issue; otherwise, the prognosis is excellent.

11.9.4.2 Pleomorphic Adenoma

Definition

Pleomorphic adenoma is a biphasic benign tumor composed of epithelial and connective tissue elements. Histologically, the lesion is analogous to pleomorphic adenoma of the salivary glands.

Synonyms

Mixed tumor of the skin, chondroid syringoma, benign mixed tumor of the sweat glands

Epidemiology

Pleomorphic adenoma occurs in middle-aged or elderly individuals and is more common in men.

Localization

Pleomorphic adenoma generally affects the head and neck region. In the periocular region, it is more common in the upper eyelid and brow area. In the eyelid, it often occurs close to the eyelid margin [260, 261].

Clinical Features

Presents as a firm, symptomless nodule, growing over years, fixed to the overlying skin or attached to the tarsus (Fig. 11.84) [262]. There are no records of specific clinical features.

Macroscopy

Pleomorphic adenoma is usually a well-circumscribed, solitary tumor with a lobulated contour.

Histopathology/Immunoprofile

Pleomorphic adenoma is composed of a mixture of epithelial and stromal components. The epithelial cells form ducts, tubuloglandular structures, cords, or solid nests; single epithelial cells may be present. The ducts show decapitation (apocrine) secretion. The epithelial elements are embedded within a myxoid, alcian blue-positive, chondroid, or fibrous stroma (Fig. 11.85). Clear cell, squamous, sebaceous differentiation is reported. Occasionally, the myoepithelial component is predominant [263]. Immunohistochemistry gives somewhat conflicting results: epithelial cells are CK7+ [261, 264]; myoepithelial cells are variably reported as smooth muscle actin (SMA) positive as well as negative; the same applies to calponin. EMA may be positive in luminal cells; however, in a series of 60 cases of eccrine pleomorphic adenoma, none were EMA positive [264]. S-100 seems to be universally positive in myoepithelial cells. Gross cystic disease fluid protein-15 (GCDFP-15, BRST-2) is variably expressed in the glandular units or luminal secretion.

Differential Diagnosis

The malignant variant has an infiltrative silhouette, cellular atypia, and mitotic figures. Ki-67 proliferative index expression is between 20 and 54 % in pleomorphic carcinoma, compared to 1.6 % in adenoma. It is unclear whether or not tumors with small satellite nodules but no otherwise malignant features should be considered atypical. It is also unclear if this feature has any prognostic significance [265].

Histogenesis

It is thought that pleomorphic adenoma originates from both apocrine and eccrine glands of the skin. Another possibility is that appendageal tumors are neoplasms differentiating toward one or more of the adnexal structures of the skin rather than originating from them [264].

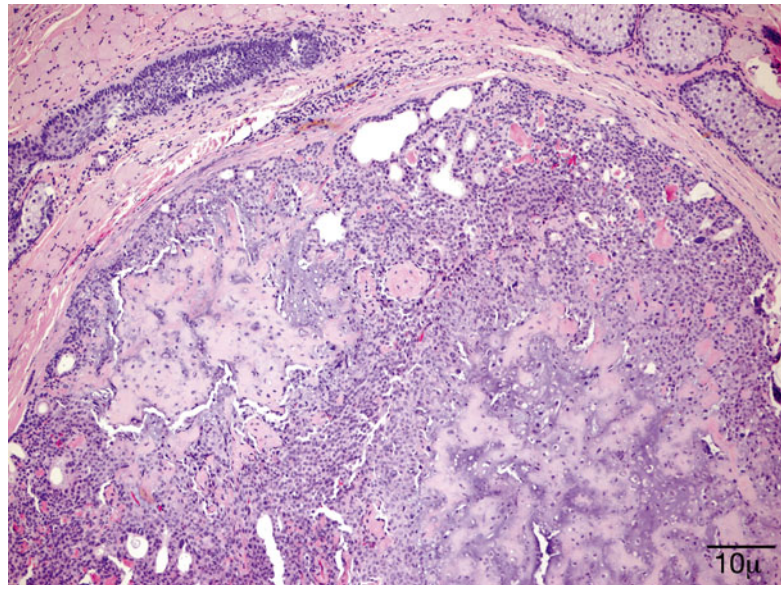

Fig. 11.85 Chondroid syringoma – Large areas of chondroid stroma intermingle with epithelial areas and tubule-glandular structures. Some ducts show decapitation secretion (hematoxylin-eosin stain; original magnification 100×)

Prognosis and Predictive Factors

Pleomorphic adenoma is a benign tumor. Complete surgical excision is usually curative. Multiple recurrences may develop without malignant changes.

11.9.4.3 Low-Grade Mucinous Carcinoma

Definition

Primary cutaneous mucinous carcinoma (PCMC) is a slow-growing adnexal neoplasm.

Epidemiology

Typically, it affects middle-aged or elderly patients. The male-to-female ratio varies between 3:2 and 1:1. It represents 0.2 % of eyelid biopsies [266].

Localization

The tumor localizes mainly to the head and neck region and has a predilection for the eyelids and scalp.

Clinical Features

Low-grade mucinous carcinoma presents clinically as a solitary, partly cystic papule or nodule on the eyelid/eyelid margin. The surface may be slightly lobulated with focal dilated vessels. Madarosis may be a feature. It is virtually by no means suspected clinically and is frequently mistaken for BCC or other more innocuous lesions [267].

Macroscopy

It is a well-circumscribed but nonencapsulated subcutaneous nodule with a gelatinous cut surface [268] and grayish tan in color and may have hemorrhagic areas.

Histopathology/Immunoprofile

PCMC is located in the dermis. It is generally well differentiated and composed of nests and ribbons of rounded or cuboidal cells in which the cytoplasm may be vacuolated (Fig. 11.86). The neoplastic epithelial cells sometimes exhibit a focal cribriform or papillary pattern. The cells are suspended in pools of PAS-positive, diastase-resistant mucin separated by delicate fibrous septa (Fig. 11.87). The mitotic activity is scant. PCMC is immunoreactive for low molecular weight cytokeratins, EMA (Fig. 11.88), CEA, nuclear ER, PR, and BRST-2. Ki-67 is positive in 5–10 % of neoplastic cells. Neuroendocrine markers are focally present. Myoepithelial cells are stained with smooth muscle actin (SMA), calponin, and p63.

Differential Diagnosis

This includes metastatic adenocarcinoma from the breast, gastrointestinal tract, lung, ovary, or

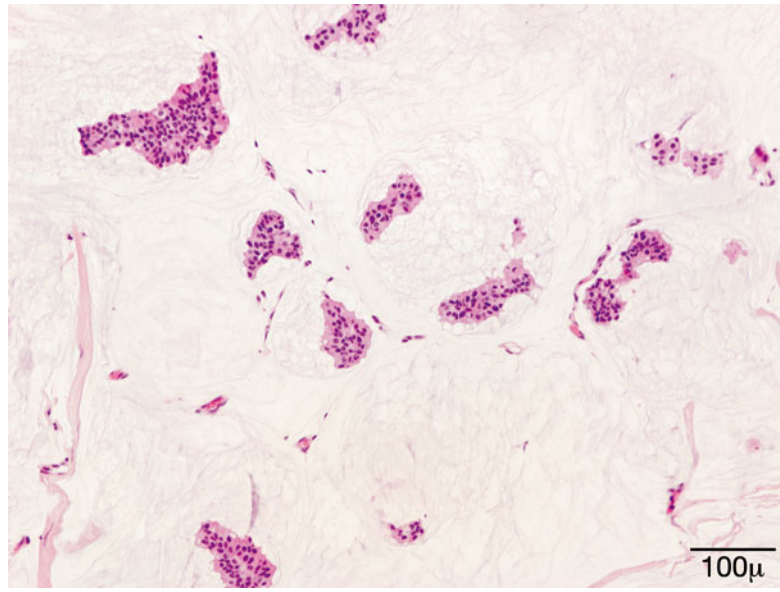

Fig. 11.86 Mucinous adenocarcinoma – Bland epithelial islands and ribbons floating in pools of mucin (hematoxylin-eosin stain; original magnification 200×)

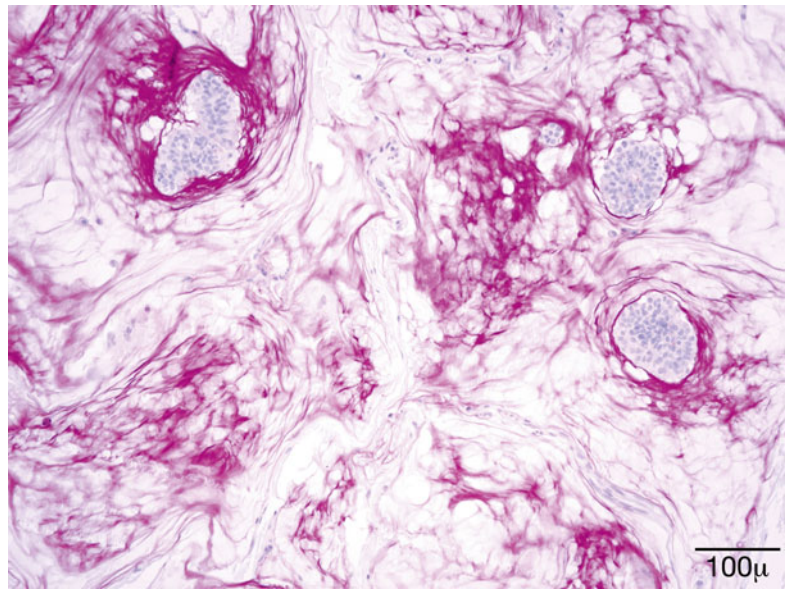

Fig. 11.87 Mucinous adenocarcinoma – PAS-positive pools of mucin in the previous tumor (PAS stain; original magnification 200×)

prostate. An in situ component [269], highlighted by the presence of myoepithelial cells surrounding the epithelial islands, may help to establish the diagnosis [270]. If an in situ component is absent, a primary tumor should be ruled out.

Histogenesis

There is controversy about the origin of PCMC [267]. According to several authors, PCMC of the eyelids originates from the secretory cells of the eccrine coil [271–273]. Others favor an apocrine origin [173].

Prognosis and Predictive Factors

PCMC is a low-grade malignancy. The tumor is locally aggressive with a high rate of recurrence [274]; approximately 10 % metastasize to locoregional lymph nodes. However, death from metastasis is rare.

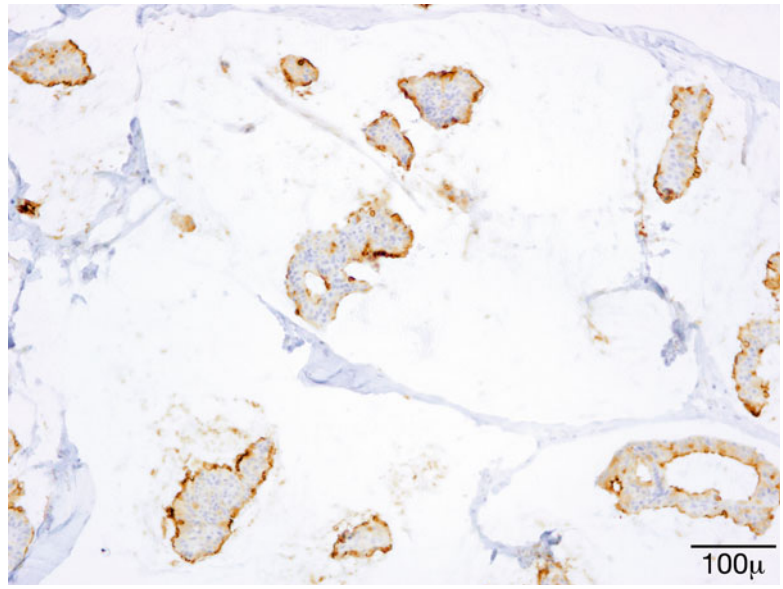

Fig. 11.88 Mucinous adenocarcinoma – Tumor cells in mucinous adenocarcinoma are positive for EMA (EMA immunostain; original magnification 200×)

11.9.5 Adnexal Tumors with Follicular Differentiation

11.9.5.1 Trichoepithelioma

Definition

Trichoepithelioma (TE) is a benign tumor that shows follicular differentiation.

Synonyms

TE is considered by many authorities to be a superficial form of trichoblastoma.

Epidemiology

Sporadic TE typically affects young and older adults. The male-to-female ratio was 2:1 in a series of 18 TE cases involving the eyelids gathered over 30 years [275]. The lesions in the familial type of TE present in childhood or adolescence.

Etiology

Sporadic TE is associated with deletions or LOH at 9q22.3 [276], while familial cases map to 9p21 [277] or the tumor suppressor gene CYLD on chromosome 16q12-q13 [278]. Multiple TEs are found in Brooke–Spiegler syndrome also caused by mutations in CYLD [279].

Localization

TE is rare on the eyelids. The upper eyelid was involved twice as frequently as the lower in the case series previously mentioned [275].

Clinical Features

Sporadic TE typically presents on the face as a slow-growing, small, flesh-colored papule measuring 2–5 mm, although larger nodules have been reported. In familial TE, multiple lesions involve the forehead, nasolabial folds, nose, and eyelids. The lesions grow and multiply over time and may cause serious disfiguration.

Histopathology/Immunoprofile

TE is a symmetric nodular lesion located in the dermis, which is composed of clusters of basaloid cells surrounded by a mantle of markedly cellular stroma (Fig. 11.89). The latter differs from the surrounding stroma. Separation artifact is absent. Small keratin cysts and calcification occur. Papillary mesenchymal bodies are characteristic and signify follicular differentiation. CD34 is expressed in the peritumoral stromal cells [173]. CD10 highlights the papillary mesenchymal cells and peritumoral stroma [190].

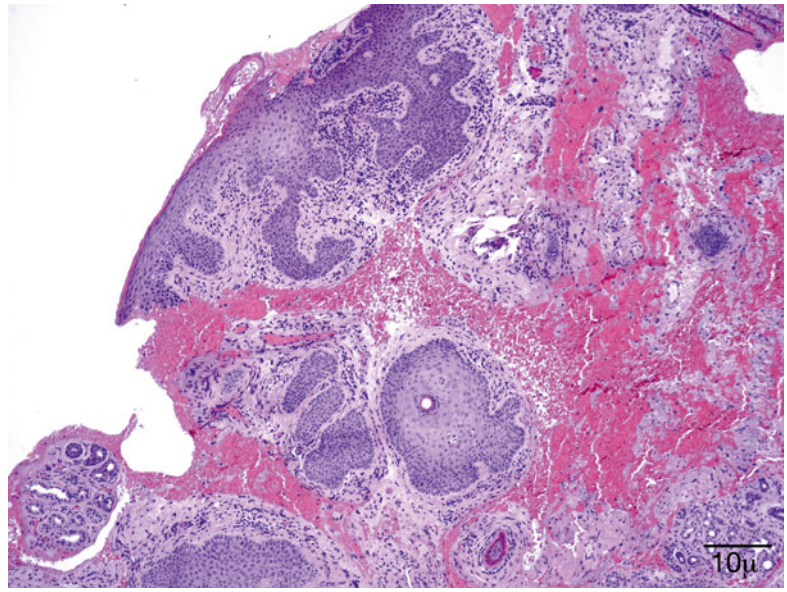

Fig.11.89 Trichoepithelioma–The tumor is composed of basaloid epithelial cells embedded in a cellular fibrous stroma distinct from the surrounding normal dermis (hematoxylin-eosin stain; original magnification 100×)

Differential Diagnosis

It may occasionally be difficult to differentiate between TE and BCC, although mitoses and apoptotic bodies are rare in TE. The clefts between palisading cells and stroma in BCC are not seen in TE, and papillary mesenchymal bodies are usually absent in BCC. Ber-EP4 is diffusely positive in BCC, but the staining is variable in TE [190]. Bcl-2 stains BCC diffusely but typically only the basal cell layer in TE. CK20-positive Merkel cells may be abundant in TE but are usually absent in BCC.

Histogenesis

An origin from the stem cells of the follicular bulge is the current view.

Genetics

Both sporadic and familial TEs have genetic defects as background. Familial TE shows an autosomal dominant hereditary pattern.

Prognosis and Predictive Factors

TEs are benign tumors that mainly cause cosmetic problems, although exulceration may occur. Malignant transformation is exceedingly rare.

11.9.5.2 Trichilemmoma

Definition

Trichilemmoma (TL) is defined as a benign tumor differentiating toward the outer root sheath epithelium of the hair follicle [280].

Epidemiology

The true incidence of solitary (sporadic) TL is not known. In a series of 31 cases involving the periocular region, the mean age of the patients was 56 years (22–88 years) with male predominance [281]. Of 228 benign ocular adnexal tumors, only 11 (4.8 %) were diagnosed as trichilemmomas [282]. Multiple TLs are even more rare and characteristic of Cowden syndrome.

Etiology

The etiology of TL is unclear. Some authors consider TLs as old viral warts [283]; however, others firmly reject that possibility [284]. Different types of HPV DNA were demonstrated by PCR and cloning in paraffin-embedded samples of TLs [285]. However, in situ hybridization with HPV1 and HPV2 and low- and high-risk mixed genital-type probes failed to confirm the presence of HPV in TL [286].

Clinical Features

TL is a small, wartlike, circumscribed lesion, typically presenting on the face. The eyelid is the second most common site for TL after the nose [281].

Histopathology/Immunoprofile

TL is a sharply circumscribed tumor composed of one or more lobules of squamoid cells extending into the upper dermis. The cells have round nuclei and pale pink or clear cytoplasm due to the accumulation of glycogen. Peripheral palisading and a prominent basement membrane are present. Columnar cells close to the basement membrane may have reversed polarity [190].

Desmoplastic TL is a variant that displays a hyalinized or desmoplastic stroma. The tumor cells have a seemingly infiltrative, irregular pattern. It has been rarely reported in the eyelid [287].

CD34 expression seems variable in TLs; both positive [190, 288] and negative results [289] are reported. Nestin, a marker of follicular stem cells, is strongly expressed in TLs, while the cells are weakly positive for K15 and negative for Ber-EP4.

Histogenesis

The immunoprofile of TL (nestin +/K15+/CD34–) suggests an origin in the outer root sheath cells below sebaceous glands.

Differential Diagnosis

Distinction from BCC with trichilemmal differentiation may be difficult; CD34 staining and absent Ber-EP4 speak in favor of TL. The noninvasive contour, lack of cellular atypia, and mitotic activity help distinguish TL from trichilemmal carcinoma.

Prognosis

The prognosis is very good; excision is curative. If multiple lesions are present on the face, Cowden syndrome should be investigated, including imaging studies.

11.9.5.3 Trichofolliculoma

Definition

Trichofolliculoma is a benign, usually solitary, follicular neoplasm.

Epidemiology

Usually occurs in adult but has been reported in childhood [290]

Localization

Trichofolliculoma usually affects the skin of the head and neck. Few cases have been reported on the eyelids [275, 290–292].

Clinical Features

The lesion is a small subcutaneous papule. Occasionally, a small pore-like opening is seen on the surface with a woollike tuft of immature white hair protruding from it. The latter is a highly diagnostic clinical feature [293, 294].

Histopathology/Immunoprofile

Trichofolliculoma consists of a cystically dilated hair follicle filled with keratin. The cystic space is lined by squamous epithelium surrounded by numerous secondary follicles of variable maturity. The stroma is fibroblast rich and encapsulates the epithelial proliferations [294].

Differential Diagnosis

Because of its rarity, it may be confused with the much more common eyelid tumor, basal cell carcinoma [275].

Histogenesis

The lesion is considered a hamartoma.

Prognosis and Predictive Factors

The tumor is benign, although one case that recurred twice has been reported [295]. Complete excision is curative.

11.9.5.4 Pilomatrixoma

Definition

Pilomatrixoma (PM) is a benign nodular cutaneous adnexal tumor with pilar differentiation.

Synonyms

Pilomatricoma, calcifying epithelioma of Malherbe

Fig. 11.90 Pilomatrixoma subcutaneous – Subcutaneous yellowish nodule under the brow of a young child. No sign of inflammation. The first peak of occurrence of pilomatrixoma is during childhood

Epidemiology

PM is the most common hair follicle tumor. There are two time peaks of presentation: 45 % of cases occur before the age of 5 years, but another peak happens in the fifth decade of life [296]. In a series of 16 cases involving the eyelids, 75 % of patients were younger than 13 [297]. There is a marked female predominance in childhood but apparently none in adults [296]. Prevalence is high in Turner syndrome [298].

Etiology

Mutations in the β-catenin gene (CTNNB1) and deregulation of apoptosis play a role in the development of PM.

Localization

PM involves the skin of the head, upper limb, neck, trunk, and lower limbs in decreasing order of frequency. The eyelids, especially the upper lid, and brow are involved in a substantial proportion of cases.

Clinical Features

PM grows slowly and produces a hard, well-defined subcutaneous mass (Fig. 11.90). Although typically solitary, multiple PMs in Kabuki syndrome [299] and familial occurrence have been recorded with myotonic dystrophy [300]. The skin over the tumor is normal but may be hyperemic and give the false impression that the lesion is inflammatory.

Macroscopy

The tumor is small (1–10 mm in diameter), spherical or ovoid, and hard to touch, and the overlying skin is stretched.

Histopathology/Immunoprofile

PM is a well-circumscribed, often encapsulated nodule located in the dermis. It is composed of an admixture of basaloid (matrix) cells usually located at the periphery of the lesion and eosinophilic shadow cells (Fig. 11.91). The latter have a central clear area that corresponds to the vanished nucleus (Fig. 11.92). Calcification and foreign body reaction are common. Morphologically, four stages are distinguished: early, fully developed, early regressive, and later regressive [301]. Basaloid cells predominate in the fully developed stage when mitoses are conspicuous. The development of shadow cells is considered a peculiar form of programmed cell death that does not involve caspase-3 activation or nuclear fragmentation [302]. The basophilic cells are Bcl-2 positive [303].

Differential Diagnosis

Proliferating pilomatrixoma, pilomatrix carcinoma, and BCC with matrical differentiation should be considered in the differential diagnosis. Proliferating PM may histologically suggest malignancy; however, this tumor is circumscribed and symmetric with pushing rather than infiltrating borders (Fig. 11.93) [304]. The silhouette of pilomatrix carcinoma is infiltrating with perineural and vascular invasion.

Histogenesis

PM is thought to develop from hair matrix cells.

Genetics

Marked Bcl-2 expression in PMs is thought to reflect a role for defective apoptosis in promoting the development of PM [303]. Mutations in the β-catenin gene (CTNNB1 gene) stabilize the β-catenin protein in keratinocytes [305]; the protein is translocated to the nucleus where it acti-

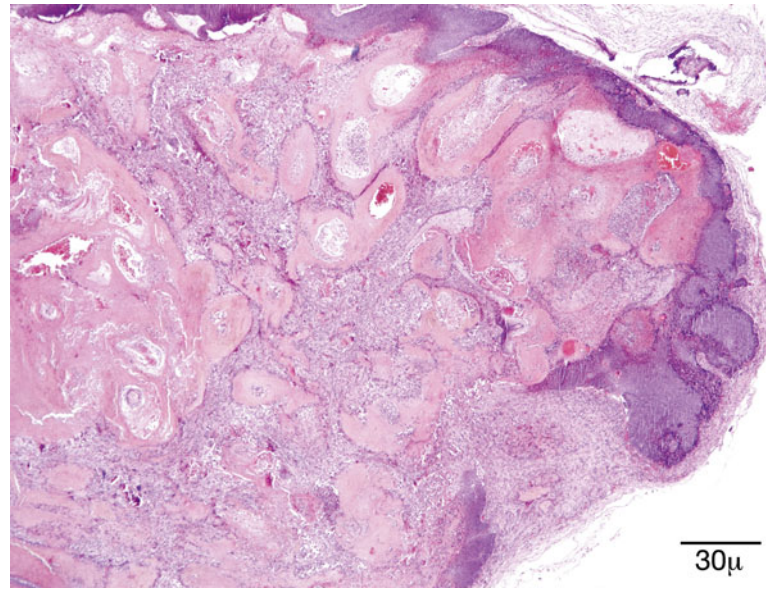

Fig. 11.91 Pilomatrixoma – Two different cell populations are evident in the lesion. Basaloid matrical cells are located at the periphery and deeply eosinophilic ghost cells toward the center (hematoxylin-eosin stain; original magnification 40×)

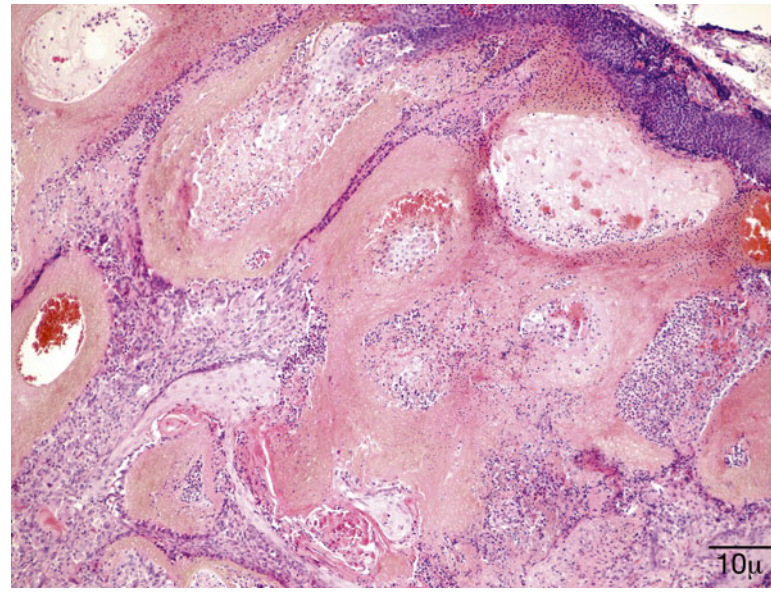

Fig. 11.92 Pilomatrixoma – At higher magnification, a central pale area corresponding to the absent nucleus becomes evident (hematoxylin-eosin stain; original magnification 100×)

vates gene transcription through Wnt [306], resulting in abnormal matrical cell proliferation and the development of pilomatrixoma.

Prognosis and Predictive Factors

Surgical excision of PM is curative; however, proliferating pilomatrixoma has a tendency to recur but does not metastasize.

11.9.6 Merkel Cell Carcinoma

Definition

Merkel cell carcinoma (MCC) is a rare primary malignant cutaneous neoplasm with epithelial and neuroendocrine differentiation. It was first described in 1972 by Cyril Toker as trabecular carcinoma [307].

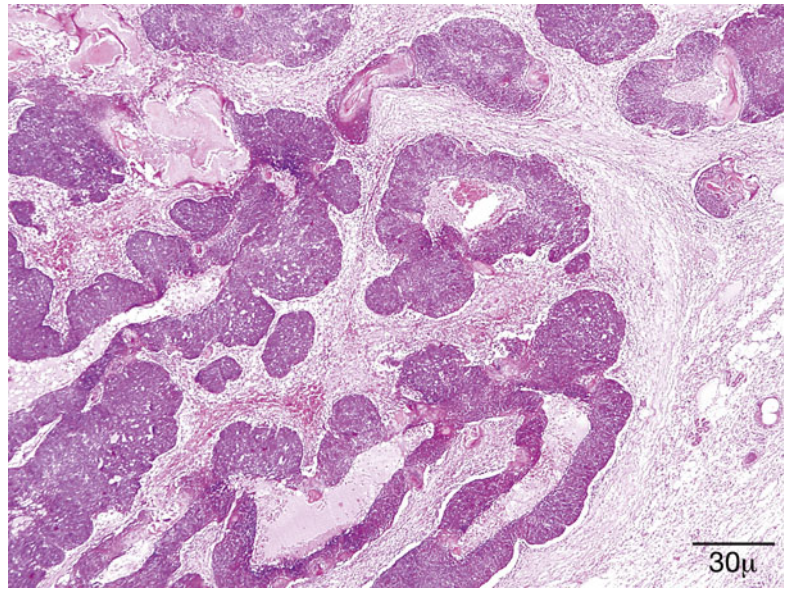

Fig. 11.93 Proliferating pilomatrixoma – This is from an encapsulated lesion several centimeters in diameter. There are numerous islands and nests of matrical cells and only small ghost cell areas, but the silhouette of the tumor is pushing rather than infiltrating (hematoxylin-eosin stain; original magnification 40×)

Synonyms

Other names include neuroendocrine carcinoma of the skin, primary small cell carcinoma of the skin, and cutaneous apudoma.

Etiology

MCC was first thought to be originated from Merkel cells of the skin based on ultrastructural features [308, 309]. However, the current hypothesis is that MCC develops from pluripotent stem cells, which have similar appearance to Merkel cells [310]. Sun exposure or ultraviolet B radiation has been reported as an important risk factor [311]. Recently, a new polyomavirus, named Merkel cell polyomavirus, has been proposed as an etiologic factor in some cases of MCC [312–314].

Epidemiology

The tumor most commonly affects the sun-exposed skin of elderly white adults [315]. There is a relatively higher incidence of this neoplasm in solid organ transplant recipients and in patients with HIV infection, pointing toward an etiologic role of chronic immunosuppression including older age.

The head and neck and extremities are the most frequently affected areas [310, 316, 317]. In the head and neck, the cheek and eyelids are the most common primary sites [318–320]. Females are affected approximately twice as often as men.

Clinical Features

Most tumors present as a rapid-growing painless dome-shaped nodule or red indurated area with occasional ulceration (Fig. 11.94) [321, 322].

Histopathology Features

Histologically, MCC is a small blue cell neoplasm, composed of cells of uniform size with a round to oval nucleus and scant cytoplasm. Nuclear membranes are distinct. The chromatin is finely dispersed, and nucleoli are inconspicuous. Mitotic figures are usually numerous. The neoplasm forms diffuse sheets centered in the dermis and, at times, extends to the subcutaneous tissue (Fig. 11.95). There is a trabecular growth pattern, and ribbons or festoons can be seen mostly in the periphery of the mass [323]; pseudorosettes are rare. The epidermis may be involved in a pagetoid fashion; and, in rare cases, the tumor is entirely limited to the epidermis [324]. Larger lesions may show ulceration, zonal necrosis, and angiolymphatic invasion. Areas of divergent differentiation such as squamoid, glandular, melanocytic, or eccrine have been described [325]. More recently, rhabdomyosarcomatous differentiation, as observed in this

Fig. 11.94 Merkel cell carcinoma – Lower eyelid indurated mass with irregular but not ulcerated surface (clinical picture courtesy of Dr. Elizabeth Bradley, Mayo Clinic)

case, has been reported also [326, 327]. The presence of a biphasic pattern may pose a diagnostic challenge, especially in small biopsies. Prominent islands of rhabdomyosarcomatous differentiation, supported by the immunoprofile of diffuse desmin and myogenin positivity, may lead to an incorrect diagnosis of rhabdomyosarcoma. As Lau and collaborators pointed out, the MCC round cell area might be dismissed as part of the rhabdomyosarcoma [327].

On immunohistochemistry, MCC shows epithelial and neuroendocrine differentiation. The tumor cells express low molecular weight keratins, EMA, and Ber-EP4 [328]. Cytokeratin 20 is a sensitive and quite specific marker [329]. The typical staining pattern for the cytokeratin is a cap-like or paranuclear dot (Fig. 11.96) [330]. Neuroendocrine markers include chromogranin, synaptophysin, neuron-specific enolase (NSE), and CD56. MCC also expresses CD117 [331]; and in a third of the cases, it is positive for CD99 [332].

Differential Diagnosis

The differential diagnosis includes mostly other round cell and poorly differentiated tumors such as melanoma, poorly differentiated squamous cell carcinoma, lymphoma/leukemia, and metastatic

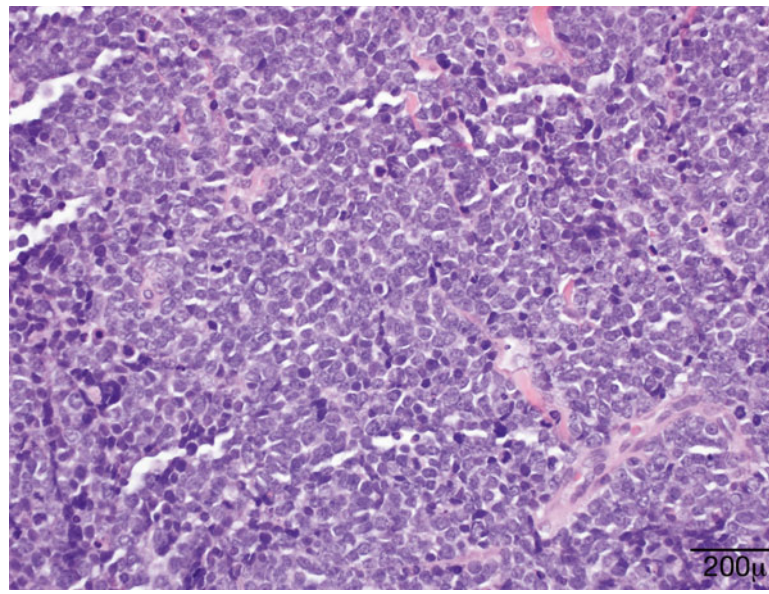

Fig. 11.95 Merkel cell carcinoma – Diffuse dermal infiltrate by small "blue" undifferentiated cells. These are characterized by uniform size, round nucleus with finely dispersed chromatin, inconspicuous nucleoli, and scant cytoplasm. There are numerous mitotic figures (hematoxylin-eosin stain; original magnification 400×)

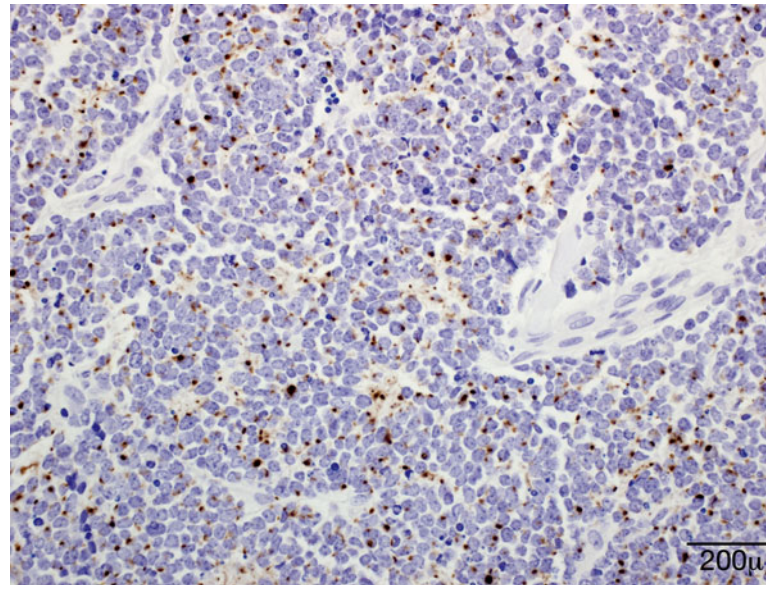

Fig. 11.96 Merkel cell carcinoma – The typical staining pattern of MCC for the cytokeratin is a cap-like or paranuclear dot as observed in this field (low-molecular weight keratin immunostain; original magnification 400×)

neuroendocrine carcinoma. A panel of immunostains including cytokeratins 7 and 20, neuroendocrine markers, and melanoma markers such as HMB45, S-100, Melan-A, and CD45 usually are enough to establish a correct diagnosis. Immunoreactivity with Merkel cell polyomavirus also helps to support the diagnosis [312–314].

Genetics

A number of chromosomal abnormalities have been described in association with Merkel cell carcinoma; deletion of the short arm of chromosome 1 (1p36) and trisomy 6 are among the most frequently observed [333].

Prognosis and Treatment

MMC is an aggressive tumor with frequent involvement of preauricular and cervical lymph nodes. Up to 60 % of patients have positive lymph nodes at presentation [316, 317, 334]. Locoregional (ipsilateral) lymph node involvement increases to 55–79 % during the course of the disease. Distant metastases appear in 70 % of the patients, usually within 2 years [334], mainly to the skin, bone, brain, liver, and lungs. Complete spontaneous regression has been reported in a few patients [317]. In a study by Allen and colleagues, patients with tumors <2 cm in size and without lymphatic spread appear to have a good survival rate of 97 % at 5 years, whereas patients with lymph node metastasis had a survival of 52 % at 5 years [335].

Currently, there are no universally accepted protocols for the treatment of MCC. Surgical excision with negative margins is recommended for local control [321, 334, 336]. The role of sentinel lymph node biopsy is still controversial [320]. Palliative surgery, including lymph node dissection, may still be considered for patients with metastatic disease [337]. Although MCC is a radiosensitive tumor, it has been proposed that radiotherapy for primary eyelid and periocular tumors should be reserved for tumor recurrences, cases with regional lymph node metastases, or positive margins at resection [338]. The role of chemotherapy in the treatment of MCC has not been well studied, and the available data are limited [336].

11.9.7 Mesenchymal (Soft Tissue) Neoplasms

Mesenchymal tumors occurring in the skin are classified according to their lineage of differentiation or immunophenotype in vascular neoplasms, neoplasms with muscle, adipose tissue or neural differentiation, and fibrous or fibrohistiocytic neoplasms.

Herein, we will describe the mesenchymal neoplasms most commonly observed in the eyelid skin.

11.9.7.1 Fibrous and Fibrohistiocytic Neoplasms

Fibrous Histiocytoma

Definition

Benign mesenchymal neoplasm frequently observed in the extremities and only rarely in the face and eyelid [339, 340]

Synonym

Dermatofibroma, histiocytoma, sclerosing hemangioma

Epidemiology

Fibrous histiocytomas are rarely seen in the eyelid [341]. They may occur at any age group, with a predilection to patients in their third and fourth decades of life [342].

Clinical Features

Most lesions are solitary, round, or oval well-circumscribed papules. The early lesions may be reddish, while the older ones are brown to tan colored. They are usually asymptomatic, long-standing lesions.

Histopathology

Fibrous histiocytomas are vascularized lesions, characterized by a proliferation of spindle-shaped and/or round cells, centered in the reticular dermis and admixed with variable amounts of macrophages. Bundles of collagen may become entrapped between the proliferating spindle cells. Overlying epidermal hyperplasia is often associated with superficial dermal nodules.

These lesions display a variable immunoprofile. The early lesions show stronger immunoreactivity with histiocytic markers such as CD68, PGM1, and CD163. Aging lesions show a mixture of histiocytic and fibroblasts markers.

The most important differential diagnosis is with dermatofibrosarcoma protuberans and Kaposi sarcoma.

Prognosis and Predictive Factors

The vast majority of the lesions are benign, but incomplete excision may result in recurrence.

11.9.7.2 Neural Tumors

Peripheral nerve tumors only rarely arise in the skin. Most often, the eyelid abnormality is a sign of a deeper located orbital mass. The greater significance of cutaneous neural tumors is their affiliation with neurocutaneous syndromes (phakomatoses). In this section, we will describe the features of the two most common periorbital cutaneous peripheral nerve sheath tumors.

Neurofibroma

Definition

It is a benign peripheral nerve sheath tumor comprised of a mixture of intraneural fibroblasts, Schwann cells, perineurial-like cells, and interspersed residual myelinated and unmyelinated nerve fibers.

Epidemiology

Neurofibromas are the most common of the peripheral nerve sheath tumors, the majority occurring sporadically as solitary lesions. Less commonly, they occur as multiple tumors in patients with neurofibromatosis type 1 (NF1). All races, ages, and sexes are affected.

Clinical Features

Neurofibromas occurring in the skin of the eyelid are usually asymptomatic. They present as a mobile, soft, and pedunculated mass or less commonly as a plaque-like lesion. Patients with NF1 have multiple tumors and other associated findings such as pigmented cutaneous macules, Lisch nodules in the iris, axillary or inguinal freckling, optic nerve glioma, and bone dysplasia [343]. Plexiform tumors involving small cutaneous nerves will give a clinical impression of "bag of worms."

A few cases in the eyelid have been mistaken by chalazion [344, 345].

Histopathology

Neurofibromas are, in general, paucicellular lesions. The cells are loosely arranged and

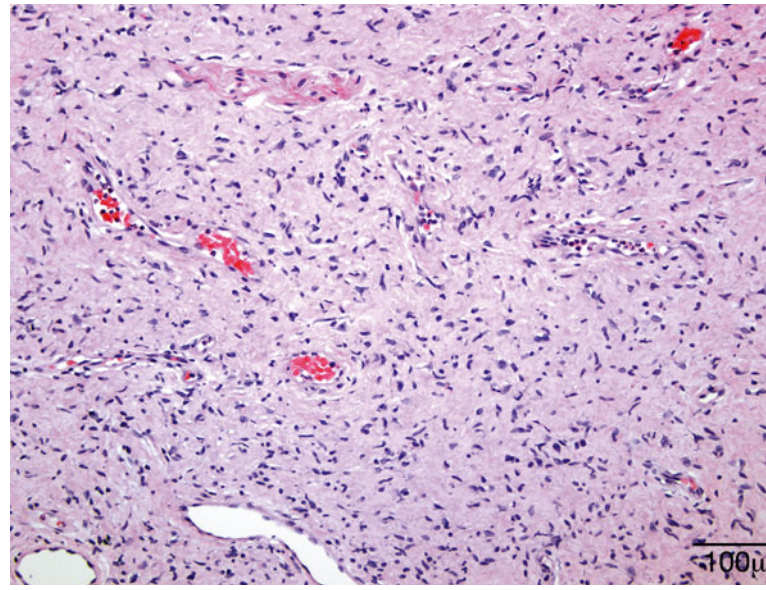

Fig. 11.97 Neurofibroma – The cells in this neoplasm are loosely arranged and diffusely infiltrate the dermis. The neoplastic cells are spindle with wavy, comma-shaped nuclei and very scanty cytoplasm (hematoxylin-eosin stain; original magnification 200×)

diffusely infiltrate the involved nerve. These lesions are composed of spindle cells with wavy, comma-shaped nuclei and very scanty cytoplasm. These cells are separated and intermixed with wavy collagen fibers, myxoid stroma, and mast cells (Fig. 11.97). In the center of the lesion, residual neurites are identified. Nerve fascicles of plexiform neurofibroma are expanded by dispersed tumor cells enmeshed in myxoid stroma. Mitoses are rarely present.

The tumor cells are immunoreactive for S-100 protein, but the percentage of positive cells is lower than in schwannomas. Staining for collagen VI is common. CD34 stains the admixed fibroblasts. Residual axons can be demonstrated using immunostains for neurofilament.

Genetics

Neurofibromas are monoclonal neoplasms that develop sporadically or in association with NF1, most likely due to inactivation of both copies of the NF1 gene on chromosome 17.

Prognosis and Predictive Factors

Localized neurofibromas are consistently benign and have a very low recurrence rate if completely excised. A small percentage, <10 %, of plexiform neurofibromas may undergo malignant transformation in patients with NF1 [346].

Schwannoma

Definition

It is a benign, usually encapsulated tumor composed of a proliferation of Schwann cells.

Synonyms

Neurilemmoma, neurilemma, benign peripheral nerve sheath tumor

Epidemiology

Schwannomas are extremely rare in the eyelids with only a few cases reported in the literature [347, 348]. Most patients are middle-aged adults [349], but rare pediatric cases have also been reported [350].

Clinical Features

These are usually solitary lesions in the eyelid, asymptomatic, slow-growing, presenting as a small firm nodule with smooth surface, and have been clinically mistaken as chalazion or inclusion cyst [351].

Macroscopy

On gross examination, these are encapsulated, spherical nodules with a firm fibrous tan-colored cut surface. Eyelid schwannomas reported in the literature have only been a few millimeters in size.

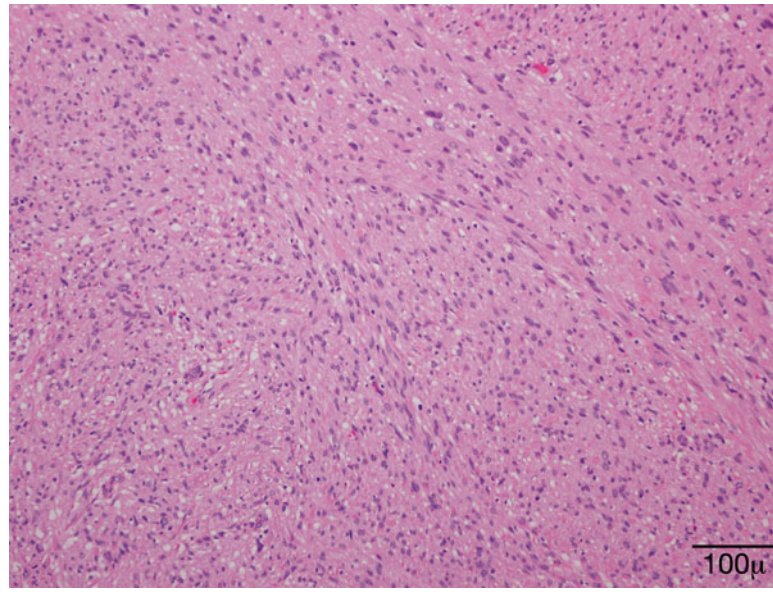

Fig. 11.98 Schwannoma – Cellular areas of schwannomas are composed of spindle cells with elongated nuclei arranged in compact fascicles (hematoxylin-eosin stain; original magnification 200×)

Histopathology

Schwannoma has a biphasic pattern with highly cellular areas composed of spindle cells showing elongated nuclei and arranged in compact fascicles (Antoni A pattern) admixed with less cellular areas, with cells showing an oval to rounded nuclei and are loosely entwined within a clear myxoid matrix (Antoni B pattern). Each tumor shows a variation in the proportion of these two patterns with some tumors revealing a predominance of cellular areas (Fig. 11.98). Verocay bodies, nuclear palisading around fibrillary cellular processes, are characteristic of this neoplasm. Small- to medium-sized vessels with thrombosis and perivascular hyalinization can be observed. Scattered large pleomorphic or bizarre nuclei can be present in some cases and correspond to degenerative changes. Mitosis and necrosis are not features of this neoplasm.

On immunohistochemistry, the neoplastic Schwann cells show strong immunoreactivity with S-100 protein (Fig. 11.99). These cells are negative for HMB-45 and other melanocytic markers as well as smooth muscle actin and CD34. Neurofilament is absent.

The differential diagnosis includes leiomyoma and less likely a nevus, which can be ruled out by the immunoprofile described above.

Genetics

The presentation of multiple schwannomas may be a manifestation of neurofibromatosis type 2, an autosomal dominant disorder caused by inactivation of a tumor suppressor encoded in chromosome 22.

Prognosis and Predictive Factors

Schwannoma is a benign tumor with a very low recurrence potential. Most eyelid cases reported have not recurred after complete excisions [349, 350, 352].

11.9.7.3 Vascular Neoplasms

Capillary Hemangioma

Definition

It is the most common vascular lesion affecting the eyelids. Most lesions are observed at birth or within a few weeks of life and, for this reason, are considered congenital or hamartomatous growths.

Synonyms

Strawberry hemangioma, infantile hemangioma, strawberry nevus

Epidemiology

It is the most common tumor of infancy, affecting approximately 10 % of children, mainly

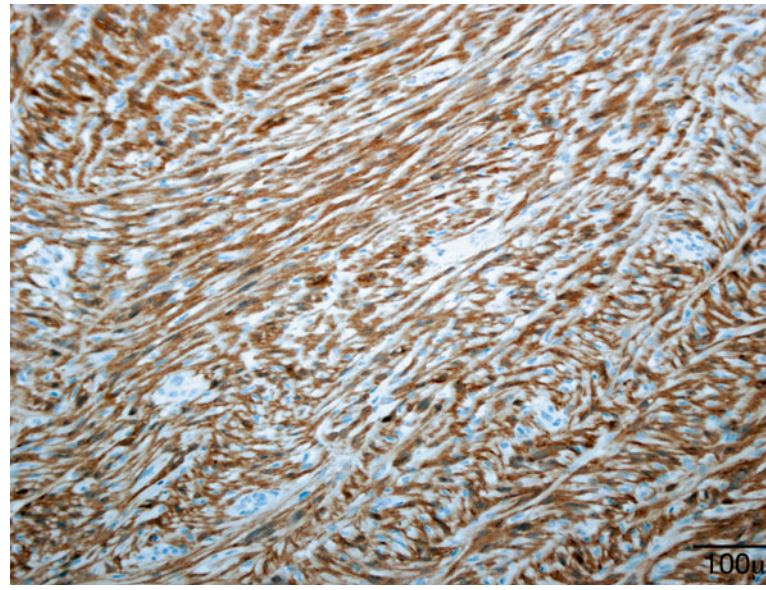

Fig. 11.99 Schwannoma – The neoplastic cells in schwannomas show strong and uniform immunoreactivity with S-100 protein immunostain (hematoxylin-eosin stain; original magnification 200×)

occurring in female and Caucasian patients. It frequently presents in small children at birth or shortly thereafter. On occasion, it can be seen in adult patients [353, 354].

Etiology

Recent studies have demonstrated endothelial cell clonality, suggesting a role for a somatic mutation [355, 356].

Clinical Features

Most lesions are solitary, red, or purplish raised nodules in the eyelid. These are soft to touch and have an irregular pebbly surface. The size of capillary hemangiomas can vary from a few millimeters to sizeable elevated masses covering a large surface of the face. Substantial facial hemangiomas may be associated with multiple congenital anomalies, including ocular, arterial, and cardiac abnormalities [357].

The natural course of capillary hemangiomas is to exhibit a rapid growth phase lasting from a few months to 2 years, followed by slow regression or shrinkage of the lesion, taking anywhere from a few years to approximately 6 years of age.

Histopathology

It is characterized by a nonencapsulated proliferation of capillary vessels and perivascular pericytes. Proliferative phase lesions are cellular and show lobular conglomerates of endothelial cells and pericytes with an enlarged nucleus and tiny small vascular lumina (Fig. 11.100). Brisk mitotic activity can be present. During regression phases, the endothelial cells and pericytes flatten, lumina enlarge, and mitotic activity decreases. The lobular appearance is more evident (Fig. 11.101). Capillary vessels are progressively replaced by connective tissue.

Immunohistochemically, these neoplasms express strong endothelial positivity for several antigens including factor VIII, CD31, CD34, and GLUT1 [356].

The differential diagnosis includes other vascular neoplasms and spindle cell proliferations in very cellular lesions.

Genetics

No cytogenetic abnormalities have been reported.

Prognosis and Predictive Factors

Large eyelid hemangiomas may lead to visual impairment, causing astigmatism and consequent amblyopia. Therapeutic measurements with intralesional corticosteroid injections, cryotherapy, and laser ablation may help to reduce tumor size, alleviate symptoms, and prevent future complications.

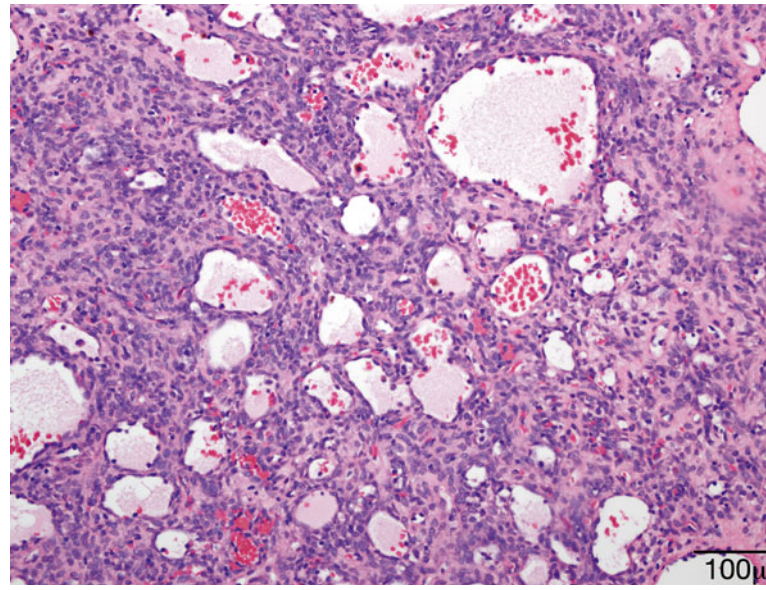

Fig. 11.100 Capillary hemangioma – Proliferation of small capillary vessels and pericytes (hematoxylin-eosin stain; original magnification 200×)

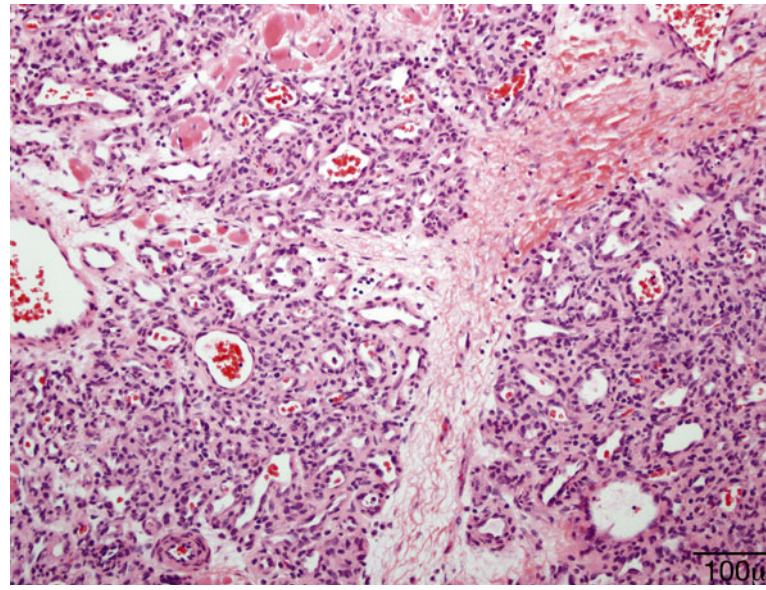

Fig. 11.101 Hemangioma – Note lobulated appearance of the neoplasm. Lobules are composed of small capillary-size vessels (hematoxylin-eosin stain; original magnification 200×)

Cavernous Hemangioma

Unlike capillary hemangiomas, cavernous hemangiomas are most often diagnosed in adults. These present as slow-growing, indolent masses that do not regress spontaneously. Cavernous hemangiomas are rarely de novo lesions in the eyelid, and their presence involving the lids in most cases signals the presence of a large orbital mass. Histologically, they are characterized by large, dilated, endothelial-lined vascular spaces filled with blood. Therefore, the detailed description of these lesions can be found in the orbital chapter of this book.

Lymphangioma

It refers to a vascular malformation involving the lymphatic vessels of the superficial dermis.

Synonyms

Lymphangioma circumscriptum

Epidemiology
It usually is present at birth or appears early in life, rarely affecting younger adults [358].

Clinical Features
Clinically, these lesions are localized and consist of multiple small vesicle-like cysts, often covered with a verrucous surface and clustered in a nodule or plaque. Purplish areas may be present, a result of hemorrhage or thrombosis of a nearby blood vessel.

Rarely, superficial lymphatic cutaneous malformations are also associated with visceral lesions [359, 360].

Macroscopy
The excised lesions show dilated vascular spaces involving the superficial dermis.

Histopathology
It is characterized by the presence of irregular-shaped, dilated lymphatic vessels located in the superficial dermis and covered by hyperplastic and hyperkeratotic epidermis. Blood or more often serous fluid may be present within the vascular spaces. If intralesional hemorrhage has occurred, erythrocytes and hemosiderin-laden macrophages may be seen.

On immunohistochemistry, the usual endothelial markers, such as CD31 and factor VIII, do not differentiate lymphatics. New markers such as D2-40 and PROX1 may be helpful, since these are expressed specifically in lymphatic endothelium [361, 362].

Histogenesis
Lymphangioma circumscriptum most likely represents sequestrated dermal lymphatic vessels that have failed to link with the rest of the lymphatic system, resulting in lymphatic stasis [363].

Prognosis and Predictive Factors
These are usually localized and superficial lesions that only cause cosmetic problems and do not require treatment. The presence of a deeper component may explain cases of recurrence after superficial excisions.

Angiosarcoma

Definition
It is an uncommon, highly malignant neoplasm of endothelial cell origin.

Synonyms
Lymphangiosarcoma, hemangiosarcoma

Epidemiology
This neoplasm most commonly involves elderly white male patients [364, 365]. True isolated eyelid angiosarcomas are extremely rare [366–368].

Clinical Features
Angiosarcoma begins as an ill-defined red plaque that resembles a bruise or a stye [368]. Lesions can become quite large before metastasis, which is usually hematogenous. The borders of the lesion may extend for centimeters beyond the visible lesion.

Histopathology
On low power, small, irregular thin-walled blood vessels infiltrate between the collagen fibers of the dermis. On closer examination, well-differentiated tumors show mild cytological atypia, while in poorly differentiated angiosarcomas, the endothelial cells are protuberant with an enlarged and hyperchromatic nucleus (Fig. 11.102). The edges of the neoplasm are poorly circumscribed, resulting in difficulty obtaining a complete resection with clear margins. Mitotic figures are not uncommon. In the epithelioid variant, the cells lining the blood vessels resemble epithelial cells with abundant eosinophilic cytoplasm and prominent nucleoli.

On immunohistochemistry, the cells are usually positive for a number of vascular markers, including CD31, CD34, factor VIII or VWF, and most recently FLI-1. Angiosarcomas are consistently negative for human herpesvirus 8 (HHV8), a marker for Kaposi sarcoma.

Differential Diagnosis
The differential diagnosis includes other vascular proliferations, Kaposi sarcoma, and pseudovascular squamous cell carcinoma.

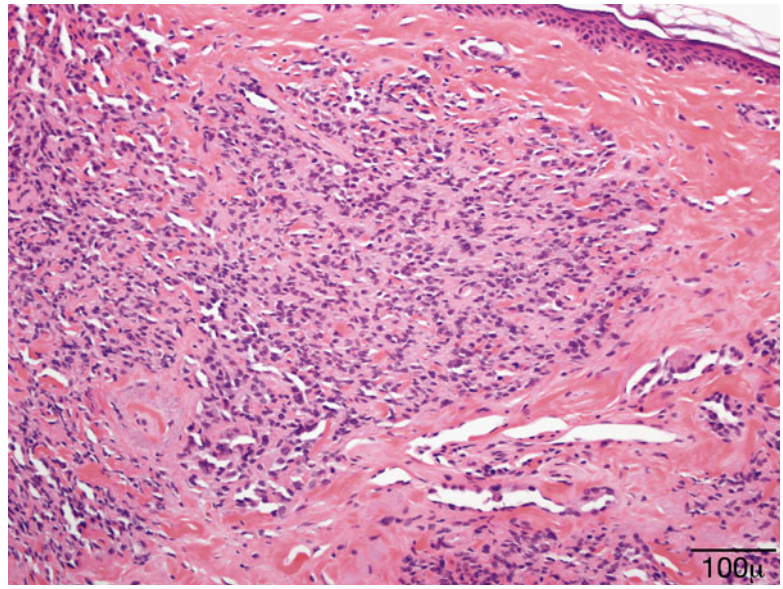

Fig. 11.102 Angiosarcoma – Microscopically, well-differentiated angiosarcomas are characterized by small, irregular thin-walled blood vessels infiltrating between the collagen fibers and mild cytological atypia (hematoxylin-eosin stain; original magnification 200×)

Genetics

Cytogenetic studies have detected a number of chromosomal abnormalities, the most frequent involving chromosomes 5, 7, 8, 13, 20, and 22 and Y chromosome [369]. However, a consistent abnormality as described in post-radiation angiosarcoma has not been observed in a large number of sporadic angiosarcomas [370].

Prognosis and Predictive Factors

The prognosis is poor and associated with multiple local recurrences, metastases, and limited survival despite various treatment modalities [368].

Kaposi Sarcoma

It is a low-grade vascular malignancy associated with Kaposi sarcoma herpesvirus/human herpesvirus 8 (KSHV/HHV8) infection. Recognized clinical forms of KS include the classical (elderly patients), endemic (African), iatrogenic (associated to immunosuppression), and the epidemic or acquired immunodeficiency syndrome (AIDS)-related form.

Epidemiology

The epidemic form, or AIDS-related form, is the most common subtype encountered in the clinical practice. Ocular involvement occurs in approximately 20 % of patients with AIDS-related Kaposi sarcoma (KS) [371, 372]. However, cases of eyelid involvement in patients without HIV or any risk factor for immunosuppression have also been reported [373, 374].

Clinical Features

Periocular KS may present as a patch, a plaque, or a nodule [375]. The typical appearance is a solid, red-violet, slightly elevated tumor involving the eyelid skin or the lid margin and extending to the conjunctiva. The lesion tends to be multifocal, with one or more lesions involving the eyelids. Patients may also present with recurrent eyelid hemorrhage or chronic lid edema from lymphatic obstruction [371]. Clinically, the differential diagnosis includes pyogenic granuloma, chalazion, hemangioma, bacillary angiomatosis, or Merkel cell tumor [376].

Histopathology

The characteristic histology of KS is a proliferation of spindle-shaped cells, slit-like vascular channels, fibroblasts, inflammatory cells, and extravasated red blood cells (Fig. 11.103). The latter is an expected finding. Typical KS lesions are devoid of marked cellular pleomorphism, necrosis, or significant number of mitotic figures. Lesions biopsied in different stages of

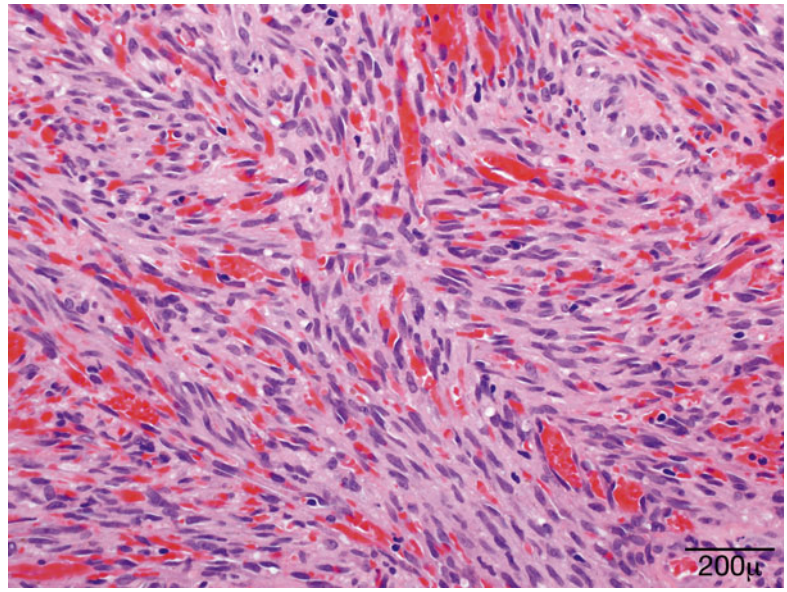

Fig. 11.103 Kaposi sarcoma – Microscopically, Kaposi sarcoma is characterized by a proliferation of spindle-shaped cells, slit-like vascular channels, and extravasated red blood cells. The neoplastic cells do not usually display marked pleomorphism (hematoxylin-eosin stain; original magnification 400×)

disease can reveal various morphological features [377].

Immunohistochemistry reveals positivity with endothelial vascular markers, such as CD31, CD34, and factor VIII, as well as a strong positivity with HHV8, the latency-associated nuclear antigen, a very specific marker for KS [377].

Differential Diagnosis

The differential diagnosis includes other vascular and spindle cell lesions.

Histogenesis

Ultrastructural analysis supports the theory that the pathognomonic spindle cell of KS originates from vascular endothelial cells [371, 373].

Infection with HHV8 reprograms the host endothelial cells so that they resemble lymphatic endothelium. Like other herpesviruses, HHV8 remains latent within cells and has developed a variety of mechanisms to evade the host immune system. DNA fragments of HHV8 have been found in 90 % of confirmed KS cases [378]. HHV8 is thought to sensitize vascular endothelial cells to the increased levels of cytokines present within tissues of HIV-infected patients, with subsequent proliferation of these cells and upregulation of several lymphatic-associated genes, such as lymphatic vessel endothelial receptor 1 (LYVE1), podoplanin, and vascular endothelial growth factor receptor 3 (VEGFR3) (with additional mutational events) leading to the formation of KS [377].

Prognosis and Predictive Factors

At present, there is no cure for KS. Treatment goals include symptom palliation, prevention of progression, and improving cosmesis.

11.10 Hematopoietic/Lymphoid Neoplasms

11.10.1 Lymphoid Hyperplasia

Cutaneous lymphoid hyperplasia is the most common mimicker of cutaneous lymphoma. Clinically, it may present as a nodule, plaque, or papule; the etiology is not always known but may be related to drugs, tattoos, insect bites, or others [379].

Histologically, cutaneous lymphoid hyperplasia shows a lymphocytic predominance with a mixture of B and T cells in nodular or diffuse configuration within the dermis. Other inflammatory cells such as histiocytes, eosinophils, and

plasma cells are also present. Additional features favoring benignity include the presence of a grenz zone separating the uninvolved epidermis, sharply demarcated lymphoid follicles with tingible body macrophages, and a "pushing" border of the infiltrate [380, 381].

Immunohistochemical studies reveal a predominance of CD3+ T lymphocytes with a population of CD20+ B lymphocytes in the follicular areas. Well-formed germinal centers retain positive staining for Bcl-6 and CD10, and the cells in the germinal centers are negative for Bcl-2. CD68 highlights the presence of tingible body macrophages [381].

The prognosis is excellent, and the lesions resolve as soon as the inciting cause for this cutaneous reaction is removed.

11.10.2 Primary Cutaneous Lymphomas

The skin is the second most common site of involvement by extranodal lymphoma [382]. Cutaneous lymphomas are a heterogeneous group of T- and B-cell neoplasms that present in the skin without evidence of extracutaneous disease at the time of the diagnosis.

The classification of cutaneous lymphomas is very challenging. The most current classification is a modification of the WHO and the European Organization for Research and Treatment of Cancer (EORTC) Cutaneous Lymphoma Group classifications and incorporates morphological, immunophenotypic, and clinical features [383].

Eyelid involvement by primary cutaneous lymphoma is rare. Herein, we have selected to discuss a few entities that have been reported to involve primarily the eyelid. Many lymphomas involve the eyelid by extension from tumors originating in the conjunctiva or in the orbit [384, 385]. These entities are discussed in the conjunctiva and orbital chapters.

Comprehensive descriptions of cutaneous lymphoma subtypes can be found in major textbooks of dermatopathology, WHO books, and published articles on this subject [51, 386, 387].

11.10.3 Mycosis Fungoides

Definition

It is the most common form of cutaneous T-cell lymphoma, considered a low-grade peripheral epidermotropic T-cell lymphoma with very distinct histological and phenotypic features.

Synonyms

None

Epidemiology

Most frequently affects adults over the age of 50 years with a slight male predominance.

Etiology

The etiology of mycosis fungoides is unknown.

Clinical Features

Clinically, mycosis fungoides (MF) is characterized by a progression from patches to plaques and eventually cutaneous tumors that have a tendency to ulcerate. In the advanced stages of the disease, it spreads into the peripheral blood to involve the bone marrow, lymph nodes, and viscera.

The eyelids are involved in less than a third of patients with MF and present often with ulceration and ectropion [388–390].

Histopathology

MF is characterized by marked epidermotropism. The histopathological findings vary in the several stages of disease. In the early stages, the diagnosis is difficult as the disease closely resembles chronic dermatitis and it is patchy in nature. The most specific finding is the presence of Pautrier microabscesses, characterized by the presence of intraepithelial, medium to large, hyperconvoluted, cerebriform lymphocytes but only observed in 10 % of the cases. Most often, one sees a band-like infiltrate in the superficial dermis involving rete ridges and single, isolated, or small clusters of atypical cells infiltrating the epidermis. With the progression of the disease, the dermal infiltrates become diffuse, and the proportion of tumor cells increase in numbers and size. Reactive T cells, plasma cells, and eosinophils

that could have been present earlier tend to disappear at this tumoral stage.

The classical immunophenotype for MF is CD2+, CD3+, CD4+, CD5+, CD45RO+, CD8−, TCRbeta+, and CD30−. Monoclonal rearrangement of T-cell receptor gamma genes is a common finding later in the disease.

Genetics

There are only a few studies on chromosomal aberrations in cutaneous T-cell lymphomas. The most frequent losses occur in chromosomes 1p, 17p, 10q, and 19; and the most frequent gains involve chromosomes 4, 18, and 17 [391].

Prognosis and Predictive Factors

The majority of MF patients have an indolent clinical course over several years. Advanced stages of disease and older age indicate a poor prognosis.

11.10.4 Primary Cutaneous Anaplastic Large Cell Lymphoma

This represents a form of CD30+ T-cell lymphoma that also includes lymphomatoid papulosis and borderline CD30+ T-cell proliferations. The expression of CD30 is the hallmark of the neoplastic cells. CD30 is a cytokine receptor that belongs to the tumor necrosis factor receptor family.

Synonyms

Regressing atypical histiocytosis, primary cutaneous large T-cell lymphoma, CD30+

Epidemiology

Primary cutaneous anaplastic large cell lymphoma (CALCL) is the second most common cutaneous T-cell lymphoma. It affects patients in their sixth decade of life with a slight predominance in men [392]. CALCL is a common form of T-cell lymphoma in HIV-infected patients [393].

Histogenesis

Activated skin-homing T cells

Fig. 11.104 Cutaneous lymphoma- Fast-growing nodule in the eyelid that rapidly ulcerated (clinical picture courtesy of Dr. Jeannette Tóth)

Clinical Features

Clinically, cutaneous ALCL presents as a single or multi-grouped nodules or masses. In the eyelid, a few cases described fast-growing lesions that are occasionally ulcerated (Fig. 11.104) or have been mistaken initially for inflammatory processes [392, 394, 395]. Simultaneous orbital involvement has also been reported [396].

Histopathology

This lesion is characterized by dense, nodular infiltration of atypical lymphoid cells involving the entire dermis and subcutaneous tissue. The neoplastic cells demonstrate pleomorphic, anaplastic, or immunoblastic morphology (Fig. 11.105). The hallmark feature includes the presence of large, bizarre cells with irregularly shaped nuclei and one or more prominent nucleoli. Multinucleated tumor cells can be seen. Epidermotropism is not always present, but mitoses are easily observed. Small reactive lymphocytes may be found within and around the tumor nodule. Because of the cohesive appearance of the tumor infiltrate, the differential diagnosis includes malignant melanoma and undifferentiated carcinoma.

ALCL is defined by CD30 positivity in at least 75 % of the neoplastic cells (Fig. 11.106). Primary cutaneous CD30+ ALCL has an activated T-cell phenotype with expression of CD2, CD3, CD4, CD45RO, CD25, CD71, and HLA-DR. In contrast to nodal ALCL, cutaneous ALCL does not express EMA. Primary cutane-

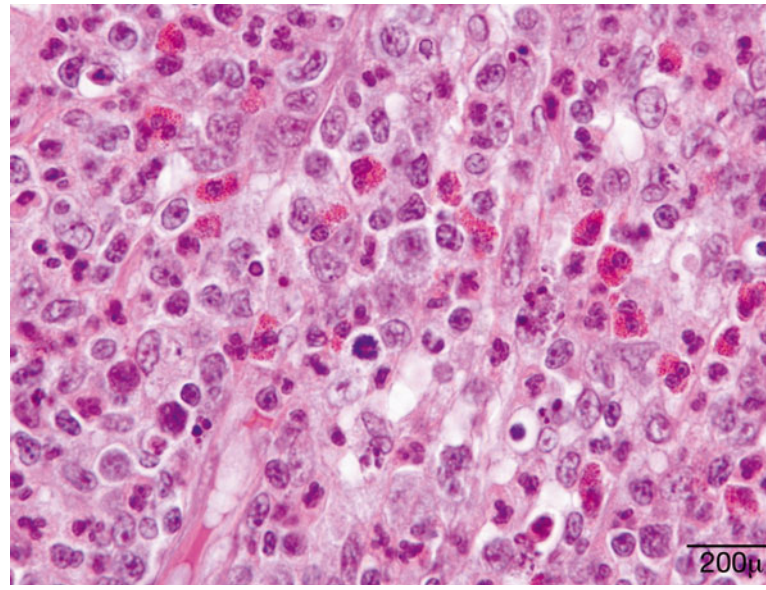

Fig. 11.105 Cutaneous lymphoma – The neoplastic cells show pleomorphic, anaplastic nuclei with one or multiple prominent nucleoli. Mitoses are easily observed. Numerous intermixed eosinophils (hematoxylin-eosin stain; original magnification 400×)

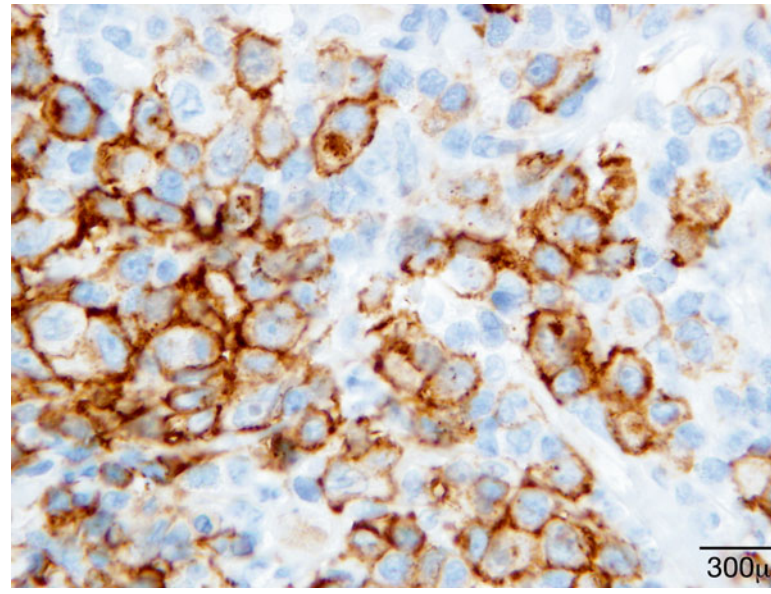

Fig. 11.106 Cutaneous lymphoma – ALCL is characterized by CD30 positivity in at least 75% of the neoplastic cells (CD30 immunostain; original magnification 600×)

ous ALCL is, in general, negative for the anaplastic lymphoma-related tyrosine kinase (ALK).

Genetics

Clonal rearrangements of T-cell receptor genes are detected in the majority of cases [397]. The translocation t(2;5) (p23;q35), which results in the expression of a fusion protein characteristic of nodal ALCL, is not observed in primary cutaneous ALCL.

Prognosis and Predictive Factors

Cutaneous ALCL, in general, has a good prognosis with a 5-year reported survival of 90 % [387].

11.10.5 Cutaneous Follicular Lymphoma

It is one of the most common types of primary cutaneous B-cell lymphomas.

Synonyms

Cutaneous follicle center lymphoma, reticulohistiocytoma, and Crosti lymphoma [386]

Epidemiology

It manifests predominantly in middle-aged adults with no gender predominance. It represents approximately 10 % of all cutaneous lymphomas [383, 398].

Follicular lymphomas are the third most common type of ocular adnexa lymphoma [399]; in the eyelid, it is usually an extension from orbital or conjunctival lymphomas.

Etiology

The etiology is unknown.

Clinical Features

It presents with firm, erythematous to purplish plaques or nodules. The overlying skin is usually smooth. The lesions are indolent and persist for months or years.

Histopathology

It is characterized by a monomorphic proliferation of follicle center cells (centrocytes and centroblasts) in a follicular, follicular and diffuse, or diffuse growth pattern. The neoplastic proliferation in the dermis displays few mitoses and no tingible body macrophages or immunoblasts. These latter features are important in the differential diagnosis with reactive lymphoid hyperplasia. Grading of cutaneous follicular lymphomas, based on the proportion of centroblasts, has not proven to be prognostically pertinent.

On immunohistochemistry, the neoplastic cells express CD19+, CD20+, CD22+, CD79a+, and Bcl-6 and have a variable of CD10. These cells are negative for Bcl-2, MUM1, CD5, and CD43.

Genetics

Clonal rearrangement of immunoglobulin genes is detected in most cases. However, Bcl-2 gene rearrangement and t(14, 18) chromosomal translocation characterizing the nodal disease are absent in the primary cutaneous form.

Prognosis and Predictive Factors

Primary cutaneous follicular lymphomas have an excellent prognosis with a 5-year survival of more than 95 % [383].

11.10.6 Cutaneous Diffuse Large B-Cell Lymphoma

Neoplastic proliferation of large transformed B cells

Synonyms

Diffuse large B-cell lymphoma

Epidemiology

It represents 5–10 % of cutaneous B-cell lymphomas. The median age of presentation is around 70 years. This neoplasm is more common in women.

Histogenesis

Transformed peripheral B cell of likely post-germinal center origin [400]

Clinical Features

The cases of cutaneous diffuse large B-cell lymphoma occurring in the eyelids have presented in various forms including purplish mass, eyelid swelling, eyelid discoloration, or with focal ulceration [401–404].

Histopathology

This neoplasm is characterized histologically by a diffuse dermal, monomorphous infiltrate, by medium to large B cells, morphologically resembling centroblasts, large noncleaved cells with eccentric nucleoli, or resembling immunoblasts, with prominent centrally placed nucleoli.

The neoplastic B cells express CD19+, CD20+, CD22+, Bcl-2+, MUM1+, and CD79a+. These cells are negative for CD10, CD5, CD138, and cyclinD1 and show variable expression of Bcl-6.

Genetics

The immunoglobulin genes are clonally rearranged, but the translocation (14;18) observed in

secondary cutaneous B-cell lymphomas is not detected in this lymphoma subtype.

Prognosis and Predictive Factors

The prognosis in primary cutaneous eyelid large B-cell lymphoma is not well known.

11.11 Eyelid Involvement by Other Hematopoietic Disorders

The eyelid may be involved in a number of other hematopoietic disorders such as leukemia [405– 408] and plasmacytoma [409, 410].

11.12 Metastatic Tumors

Metastatic tumors to the eyelids are uncommon as are cutaneous metastases in general. The incidence of cutaneous metastases varies in different studies from 1.2 to 4.4 % [411–413]. A study from Denmark [414] found 8 cases of metastatic malignancy to the eyelid, from a total of 81 cases of metastases to the eye and periocular tissues, in the period from 1969 to 1998. The eyelid was the third most common location (10 %), following the uvea (64 %) and the orbit (26 %) [414].

As for cutaneous metastases, metastatic tumors to the eyelid usually occur at late stages of disease. The most common primary sites are the breast [415], lung, and cutaneous melanoma [414]. Other less frequent sites of origin are the stomach, colon, and thyroid gland [416]. In only a minority of cases, the site of origin remains unknown [414].

A history of widespread disease is helpful in determining if a unilateral lesion represents metastatic disease. Histological comparison with the original tumor proves to be very useful; however, site-specific immunostains, such as TTF-1 and mammaglobin, might also be helpful to confirm a certain site of origin.

References

1. Spencer WH. Ophthalmic pathology: an atlas and textbook. 3rd ed. Philadelphia: W.B. Saunders; 1985.
2. Crawford JS. Congenital eyelid anomalies in children. J Pediatr Ophthalmol Strabismus. 1984;21(4):140–9.
3. Katowitz WR, Katowitz JA. Congenital and developmental eyelid abnormalities. Plast Reconstr Surg. 2009;124(1 Suppl):93e–105.
4. Slavotinek AM, Tifft CJ. Fraser syndrome and cryptophthalmos: review of the diagnostic criteria and evidence for phenotypic modules in complex malformation syndromes. J Med Genet. 2002; 39(9):623–33 [Review].
5. Bernardini FP, Kersten RC, de Conciliis C, Devoto MH. Unilateral microblepharon. Ophthal Plast Reconstr Surg. 2004;20(6):467–9 [Case Reports].
6. Johnson CC. Developmental abnormalities of the eyelids. The 1985 Wendell Hughes lecture. Ophthal Plast Reconstr Surg. 1986;2(4):219–32 [Review].
7. Cunliffe HE, McNoe LA, Ward TA, Devriendt K, Brunner HG, Eccles MR. The prevalence of PAX2 mutations in patients with isolated colobomas or colobomas associated with urogenital anomalies. J Med Genet. 1998;35(10):806–12 [Research Support, Non-U.S. Gov't].
8. Feingold M, Baum J. Goldenhar's syndrome. Am J Dis Child. 1978;132(2):136–8.
9. Yeung A, Amor D, Savarirayan R. Familial upper eyelid coloboma with ipsilateral anterior hairline abnormality: two new reports of MOTA syndrome. Am J Med Genet A. 2009;149A(4):767–9 [Case Reports].
10. Zechi-Ceide RM, Guion-Almeida ML, Jehee FS, Rocha K, Passos-Bueno MR. Mandibulofacial dysostosis, severe lower eyelid coloboma, cleft palate, and alopecia: a new distinct form of mandibulofacial dysostosis or a severe form of Johnson-McMillin syndrome? Am J Med Genet A. 2010;152A(7):1838–40 [Case Reports].
11. Brice G, Mansour S, Bell R, Collin JR, Child AH, Brady AF, et al. Analysis of the phenotypic abnormalities in lymphoedema-distichiasis syndrome in 74 patients with FOXC2 mutations or linkage to 16q24. J Med Genet. 2002;39(7):478–83 [Research Support, Non-U.S. Gov't].
12. Fang J, Dagenais SL, Erickson RP, Arlt MF, Glynn MW, Gorski JL, et al. Mutations in FOXC2 (MFH-1), a forkhead family transcription factor, are responsible for the hereditary lymphedema-distichiasis syndrome. Am J Hum Genet. 2000;67(6):1382–8 [Research Support, Non-U.S. Gov't Research Support, U.S. Gov't, P.H.S.].
13. Zimmerman LE. Phakomatous choristoma of the eyelid. A tumor of lenticular anlage. Am J Ophthalmol. 1971;71(1 Pt 2):169–77.
14. Dithmar S, Schmack I, Volcker HE, Grossniklaus HE. Phakomatous choristoma of the eyelid. Graefes Arch Clin Exp Ophthalmol. 2004;242(1):40–3 [Case Reports Review].
15. Szyfelbein K, Kozakewicz HP, Syed NA, Zembowicz A. Phakomatous choristoma of the eyelid: a report of a case. J Cutan Pathol. 2004;31(7):506–8 [Case Reports].

16. Verb SP, Roarty JD, Black EH, Poulik J, Grynspan D. Phakomatous choristoma: a rare orbital tumor presenting as an eyelid mass with obstruction of the nasolacrimal duct. J AAPOS. 2009;13(1):85–7 [Case Reports].
17. Kamada Y, Sakata A, Nakadomari S, Takehana M. Phakomatous choristoma of the eyelid: immunohistochemical observation. Jpn J Ophthalmol. 1998;42(1):41–5 [Case Reports Review].
18. Mansour AM, Barber JC, Reinecke RD, Wang FM. Ocular choristomas. Surv Ophthalmol. 1989;33(5):339–58 [Research Support, Non-U.S. Gov't Review].
19. DiGiovanna JJ, Kraemer KH. Shining a light on xeroderma pigmentosum. J Invest Dermatol. 2012;132(3 Pt 2):785–96 [Research Support, N.I.H., Intramural Review].
20. Kraemer KH, Lee MM, Scotto J. Xeroderma pigmentosum. Cutaneous, ocular, and neurologic abnormalities in 830 published cases. Arch Dermatol. 1987;123(2):241–50 [Historical Article].
21. Ramkumar HL, Brooks BP, Cao X, Tamura D, Digiovanna JJ, Kraemer KH, et al. Ophthalmic manifestations and histopathology of xeroderma pigmentosum: two clinicopathological cases and a review of the literature. Surv Ophthalmol. 2011;56(4):348–61 [Case Reports Research Support, N.I.H., Intramural Research Support, Non-U.S. Gov't Research Support, U.S. Gov't, Non-P.H.S. Review].
22. Hirai Y, Kodama Y, Moriwaki S, Noda A, Cullings HM, Macphee DG, et al. Heterozygous individuals bearing a founder mutation in the XPA DNA repair gene comprise nearly 1% of the Japanese population. Mutat Res. 2006;601(1-2):171–8 [Research Support, N.I.H., Extramural Research Support, N.I.H., Intramural Research Support, Non-U.S. Gov't Research Support, U.S. Gov't, Non-P.H.S.].
23. Kleijer WJ, Laugel V, Berneburg M, Nardo T, Fawcett H, Gratchev A, et al. Incidence of DNA repair deficiency disorders in western Europe: xeroderma pigmentosum, Cockayne syndrome and trichothiodystrophy. DNA Repair (Amst). 2008;7(5):744–50 [Research Support, Non-U.S. Gov't].
24. Broughton BC, Cordonnier A, Kleijer WJ, Jaspers NG, Fawcett H, Raams A, et al. Molecular analysis of mutations in DNA polymerase eta in xeroderma pigmentosum-variant patients. Proc Natl Acad Sci U S A. 2002;99(2):815–20 [Research Support, Non-U.S. Gov't].
25. Boyle J, Ueda T, Oh KS, Imoto K, Tamura D, Jagdeo J, et al. Persistence of repair proteins at unrepaired DNA damage distinguishes diseases with ERCC2 (XPD) mutations: cancer-prone xeroderma pigmentosum vs. non-cancer-prone trichothiodystrophy. Hum Mutat. 2008;29(10):1194–208.
26. Bradford PT, Goldstein AM, Tamura D, Khan SG, Ueda T, Boyle J, et al. Cancer and neurologic degeneration in xeroderma pigmentosum: long term follow-up characterises the role of DNA repair. J Med Genet. 2011;48(3):168–76 [Research Support, N.I.H., Intramural].
27. Kraemer KH, Lee MM, Andrews AD, Lambert WC. The role of sunlight and DNA repair in melanoma and nonmelanoma skin cancer. The xeroderma pigmentosum paradigm. Arch Dermatol. 1994;130(8):1018–21.
28. English JS, Swerdlow AJ. The risk of malignant melanoma, internal malignancy and mortality in xeroderma pigmentosum patients. Br J Dermatol. 1987;117(4):457–61.
29. Li L. Nucleotide excision repair. In: Wei Q, Li L, Chen DJ, editors. DNA repair, genetic instability, and cancer. 1st ed. Hackensack: World Scientific Publishing Co. Pte. Ltd.; 2007. p. 75–6.
30. Gilchrest BA. A review of skin ageing and its medical therapy. Br J Dermatol. 1996;135(6):867–75 [Review].
31. Bhawan J, Andersen W, Lee J, Labadie R, Solares G. Photoaging versus intrinsic aging: a morphologic assessment of facial skin. J Cutan Pathol. 1995;22(2):154–9 [Comparative Study Multicenter Study Research Support, Non-U.S. Gov't].
32. Castanet J, Ortonne JP. Pigmentary changes in aged and photoaged skin. Arch Dermatol. 1997;133(10):1296–9 [Review].
33. Chen VL, Fleischmajer R, Schwartz E, Palaia M, Timpl R. Immunochemistry of elastotic material in sun-damaged skin. J Invest Dermatol. 1986;87(3):334–7 [Research Support, Non-U.S. Gov't Research Support, U.S. Gov't, P.H.S.].
34. Stevanovic DV. Elastotic degeneration. A light and electron microscopic study. Br J Dermatol. 1976;94(1):23–9.
35. Warren R, Gartstein V, Kligman AM, Montagna W, Allendorf RA, Ridder GM. Age, sunlight, and facial skin: a histologic and quantitative study. J Am Acad Dermatol. 1991;25(5 Pt 1):751–60 [Research Support, Non-U.S. Gov't].
36. Yanoff M, Sassani JW. Ocular pathology. 6th ed. Philadelphia: Mosby Elsevier; 2009.
37. Lemp MA, Nichols KK. Blepharitis in the United States 2009: a survey-based perspective on prevalence and treatment. Ocul Surf. 2009;7(2 Suppl):S1–14 [Research Support, N.I.H., Extramural Research Support, Non-U.S. Gov't].
38. Lee SH, Oh DH, Jung JY, Kim JC, Jeon CO. Comparative ocular microbial communities in humans with and without blepharitis. Invest Ophthalmol Vis Sci. 2012;53(9):5585–93 [Comparative Study Research Support, Non-U.S. Gov't].
39. Nelson JD, Shimazaki J, Benitez-del-Castillo JM, Craig JP, McCulley JP, Den S, et al. The international workshop on meibomian gland dysfunction: report of the definition and classification subcommittee. Invest Ophthalmol Vis Sci. 2011;52(4):1930–7 [Research Support, N.I.H., Extramural Research Support, Non-U.S. Gov't Review].
40. Liu J, Sheha H, Tseng SC. Pathogenic role of Demodex mites in blepharitis. Curr Opin Allergy Clin

Immunol. 2010;10(5):505–10 [Research Support, N.I.H., Extramural Review].
41. Nemet AY, Deckel Y, Martin PA, Kourt G, Chilov M, Sharma V, et al. Management of periocular basal and squamous cell carcinoma: a series of 485 cases. Am J Ophthalmol. 2006;142(2):293–7.
42. Ozdal PC, Codere F, Callejo S, Caissie AL, Burnier MN. Accuracy of the clinical diagnosis of chalazion. Eye (Lond). 2004;18(2):135–8.
43. Spoendlin J, Voegel JJ, Jick SS, Meier CR. A study on the epidemiology of rosacea in the U.K. Br J Dermatol. 2012;167(3):598–605 [Research Support, Non-U.S. Gov't].
44. Yamasaki K, Di Nardo A, Bardan A, Murakami M, Ohtake T, Coda A, et al. Increased serine protease activity and cathelicidin promotes skin inflammation in rosacea. Nat Med. 2007;13(8):975–80 [Research Support, N.I.H., Extramural Research Support, Non-U.S. Gov't Research Support, U.S. Gov't, Non-P.H.S.].
45. Yamasaki K, Gallo RL. The molecular pathology of rosacea. J Dermatol Sci. 2009;55(2):77–81 [Review].
46. Reinholz M, Ruzicka T, Schauber J. Cathelicidin LL-37: an antimicrobial peptide with a role in inflammatory skin disease. Ann Dermatol. 2012;24(2):126–35.
47. Lacey N, Delaney S, Kavanagh K, Powell FC. Mite-related bacterial antigens stimulate inflammatory cells in rosacea. Br J Dermatol. 2007;157(3):474–81 [Research Support, Non-U.S. Gov't].
48. Li J, O'Reilly N, Sheha H, Katz R, Raju VK, Kavanagh K, et al. Correlation between ocular Demodex infestation and serum immunoreactivity to Bacillus proteins in patients with Facial rosacea. Ophthalmology. 2010;117(5):870–7.e1 [Case Reports].
49. O'Reilly N, Menezes N, Kavanagh K. Positive correlation between serum immunoreactivity to Demodex-associated Bacillus proteins and erythematotelangiectatic rosacea. Br J Dermatol. 2012;167(5):1032–6 [Research Support, Non-U.S. Gov't].
50. Yamasaki K, Kanada K, Macleod DT, Borkowski AW, Morizane S, Nakatsuji T, et al. TLR2 expression is increased in rosacea and stimulates enhanced serine protease production by keratinocytes. J Invest Dermatol. 2011;131(3):688–97 [Research Support, N.I.H., Extramural Research Support, Non-U.S. Gov't Research Support, U.S. Gov't, Non-P.H.S.].
51. Weedon D. Skin pathology. 2nd ed. Edinburgh: Churchill Livingstone; 2002.
52. Fung MA. Inflammatory diseases of the dermis and epidermis. In: Busam KJ, editor. Dermatopathology – Foundations in diagnostic pathology. Philadelphia: Saunders Elsevier; 2010.
53. Requena L, Sangueza OP. Cutaneous vascular proliferation. Part II. Hyperplasias and benign neoplasms. J Am Acad Dermatol. 1997;37(6):887–919. [Review]; quiz 20-2.
54. Patrice SJ, Wiss K, Mulliken JB. Pyogenic granuloma (lobular capillary hemangioma): a clinicopathologic study of 178 cases. Pediatr Dermatol. 1991;8(4):267–76.
55. Al Dhaybi R, Powell J, McCuaig C, Kokta V. Differentiation of vascular tumors from vascular malformations by expression of Wilms tumor 1 gene: evaluation of 126 cases. J Am Acad Dermatol. 2010;63(6):1052–7.
56. Trindade F, Tellechea O, Torrelo A, Requena L, Colmenero I. Wilms tumor 1 expression in vascular neoplasms and vascular malformations. Am J Dermatopathol. 2011;33(6):569–72.
57. Caponetti GC, Pantanowitz L, Marconi S, Havens JM, Lamps LW, Otis CN. Evaluation of immunohistochemistry in identifying Bartonella henselae in cat-scratch disease. Am J Clin Pathol. 2009;131(2):250–6 [Evaluation Studies].
58. North PE, Waner M, Mizeracki A, Mihm Jr MC. GLUT1: a newly discovered immunohistochemical marker for juvenile hemangiomas. Hum Pathol. 2000;31(1):11–22.
59. Dawson CR, Togni B. Herpes simplex eye infections: clinical manifestations, pathogenesis and management. Surv Ophthalmol. 1976;21(2):121–35 [Case Reports Research Support, U.S. Gov't, P.H.S.].
60. Brandao ML, Fernandes NC, Batista DP, Santos N. Refractory pemphigus vulgaris associated with herpes infection: case report and review. Rev Inst Med Trop Sao Paulo. 2011;53(2):113–7 [Case Reports Review].
61. Blieden LS, Chevez-Barrios P, Yen MT. Herpes simplex vegetans presenting as an eyelid mass. Ophthal Plast Reconstr Surg. 2011;27(3):e58–9 [Case Reports Research Support, Non-U.S. Gov't].
62. Sturm JM, Levine MR, Singh A, Lash RH. Herpetic lesion mimicking lower eyelid malignancy. Ophthal Plast Reconstr Surg. 2006;22(2):147–8 [Case Reports].
63. Empinotti JC, Uyeda H, Ruaro RT, Galhardo AP, Bonatto DC. Pyodermitis. An Bras Dermatol. 2012;87(2):277–84 [Review].
64. Tambe K, Tripathi A, Burns J, Sampath R. Multidisciplinary management of periocular necrotising fasciitis: a series of 11 patients. Eye (Lond). 2012;26(3):463–7 [Case Reports].
65. Stevens DL, Bisno AL, Chambers HF, Everett ED, Dellinger P, Goldstein EJ, et al. Practice guidelines for the diagnosis and management of skin and soft-tissue infections. Clin Infect Dis. 2005;41(10):1373–406 [Practice Guideline].
66. Klotz SA, Penn CC, Negvesky GJ, Butrus SI. Fungal and parasitic infections of the eye. Clin Microbiol Rev. 2000;13(4):662–85 [Review].
67. Coccia L, Calista D, Boschini A. Eyelid nodule: a sentinel lesion of disseminated cryptococcosis in a patient with acquired immunodeficiency syndrome. Arch Ophthalmol. 1999;117(2):271–2 [Case Reports].
68. Altman JS, Tonelli DG, Bukhalo M. Red, scaly lesion on the upper eyelid. Am Fam Physician. 2007;76(10):1533–4 [Case Reports].
69. Bartley GB. Blastomycosis of the eyelid. Ophthalmology. 1995;102(12):2020–3 [Case Reports

Research Support, Non-U.S. Gov't Research Support, U.S. Gov't, P.H.S.].
70. Poeppl W, Oeser C, Grabmeier-Pfistershammer K, Walochnik J, Burgmann H. Clinical findings and management of imported cutaneous leishmaniasis: report of 14 cases from Austria. Travel Med Infect Dis. 2013;11:90–4.
71. Pavli A, Maltezou HC. Leishmaniasis, an emerging infection in travelers. Int J Infect Dis. 2010; 14(12):e1032–9 [Review].
72. Schwartz E, Hatz C, Blum J. New world cutaneous leishmaniasis in travellers. Lancet Infect Dis. 2006;6(6):342–9 [Review].
73. Veraldi S, Bottini S, Curro N, Gianotti R. Leishmaniasis of the eyelid mimicking an infundibular cyst and review of the literature on ocular leishmaniasis. Int J Infect Dis. 2010;14 Suppl 3:e230–2 [Case Reports Review].
74. Jaouni T, Deckel Y, Frenkel S, Ilsar M, Pe'er J. Cutaneous leishmaniasis of the eyelid masquerading as basal cell carcinoma. Can J Ophthalmol. 2009;44(5):e47 [Case Reports Letter].
75. Rahimi M, Moinfar N, Ashrafi A. Eyelid leishmaniasis masquerading as chalazia. Eye (Lond). 2009;23(3):737 [Case Reports Letter].
76. Yaghoobi R, Maraghi S, Bagherani N, Rafiei A. Cutaneous leishmaniasis of the lid: a report of nine cases. Korean J Ophthalmol. 2010;24(1):40–3.
77. Fodor E, Fok E, Maka E, Lukats O, Toth J. Recently recognized cases of ophthalmofilariasis in Hungary. Eur J Ophthalmol. 2009;19(4):675–8 [Case Reports].
78. Yuen KS, Tse MW, Choi PC, Chan WM, Lam DS. Unusual presentation of dirofilariasis as a lacrimal mass. Eye (Lond). 2004;18(9):959–60. [Case Reports Letter Research Support, Non-U.S. Gov't.
79. Bowler GS, Shah AN, Bye LA, Saldana M. Ocular loiasis in London 2008–2009: a case series. Eye (Lond). 2011;25(3):389–91 [Case Reports Review].
80. De Silva DJ, Strouthidis NG, Tariq S, Davies N. An unusual cause of acute lid swelling. Eye (Lond). 2006;20(2):271–2 [Case Reports Letter].
81. Antinori S, Schifanella L, Million M, Galimberti L, Ferraris L, Mandia L, et al. Imported Loa loa filariasis: three cases and a review of cases reported in non-endemic countries in the past 25 years. Int J Infect Dis. 2012;16(9):e649–62 [Case Reports Review].
82. Parker F. Xanthomas and hyperlipidemias. J Am Acad Dermatol. 1985;13(1):1–30 [Research Support, Non-U.S. Gov't].
83. Cruz Jr PD, East C, Bergstresser PR. Dermal, subcutaneous, and tendon xanthomas: diagnostic markers for specific lipoprotein disorders. J Am Acad Dermatol. 1988;19(1 Pt 1):95–111 [Research Support, Non-U.S. Gov't Review].
84. Wilkinson SM, Atkinson A, Neary RH, Smith AG. Normolipaemic plane xanthomas: an association with increased vascular permeability and serum lipoprotein(a) concentration. Clin Exp Dermatol. 1992;17(3):211–3 [Case Reports].
85. Bergman R. The pathogenesis and clinical significance of xanthelasma palpebrarum. J Am Acad Dermatol. 1994;30(2 Pt 1):236–42 [Review].
86. Bergman R. Xanthelasma palpebrarum and risk of atherosclerosis. Int J Dermatol. 1998;37(5):343–5 [Review].
87. Gomez JA, Gonzalez MJ, de Moragas JM, Serrat J, Gonzalez-Sastre F, Perez M. Apolipoprotein E phenotypes, lipoprotein composition, and xanthelasmas. Arch Dermatol. 1988;124(8):1230–4.
88. Park EJ, Youn SH, Cho EB, Lee GS, Hann SK, Kim KH, et al. Xanthelasma palpebrarum treatment with a 1,450-nm-diode laser. Dermatol Surg. 2011;37(6): 791–6.
89. Touart DM, Sau P. Cutaneous deposition diseases. Part II. J Am Acad Dermatol. 1998;39(4 Pt 1):527–44. [Review]; quiz 45-6.
90. Elder DE, Elenitsas R, Johnson BL, Murphy GF. Lever's histopathology of the skin. 9th ed. Philadelphia: Lippincott Williams & Wilkins; 2004.
91. Kim HJ, Johnson PB, Kropinak M, Brazzo B, Sims L, Lauer S, et al. Subepidermal calcified nodules of the eyelid. Ophthal Plast Reconstr Surg. 2009;25(6): 489–90 [Research Support, Non-U.S. Gov't].
92. Nguyen J, Jakobiec FA, Hanna E, Fay A. Subepidermal calcified nodule of the eyelid. Ophthal Plast Reconstr Surg. 2008;24(6):494–5 [Case Reports].
93. Nico MM, Bergonse FN. Subepidermal calcified nodule: report of two cases and review of the literature. Pediatr Dermatol. 2001;18(3):227–9 [Case Reports Review].
94. Cursiefen C, Junemann A. Subepidermal calcified nodule. Arch Ophthalmol. 1998;116(9):1254–5 [Case Reports].
95. Rybicki BA, Iannuzzi MC. Epidemiology of sarcoidosis: recent advances and future prospects. Semin Respir Crit Care Med. 2007;22(1):22–35 [Review].
96. Rybicki BA, Major M, Popovich Jr J, Maliarik MJ, Iannuzzi MC. Racial differences in sarcoidosis incidence: a 5-year study in a health maintenance organization. Am J Epidemiol. 1997;145(3):234–41 [Comparative Study Research Support, Non-U.S. Gov't Research Support, U.S. Gov't, P.H.S. Review].
97. Rybicki BA, Maliarik MJ, Major M, Popovich Jr J, Iannuzzi MC. Epidemiology, demographics, and genetics of sarcoidosis. Semin Respir Infect. 1998;13(3):166–73 [Review].
98. Macaron NC, Cohen C, Chen SC, Arbiser JL. gli-1 Oncogene is highly expressed in granulomatous skin disorders, including sarcoidosis, granuloma annulare, and necrobiosis lipoidica diabeticorum. Arch Dermatol. 2005;141(2):259–62 [Comparative Study Research Support, U.S. Gov't, P.H.S.].
99. Bonfioli AA, Orefice F. Sarcoidosis. Semin Ophthalmol. 2005;20(3):177–82 [Review].
100. Heiligenhaus A, Wefelmeyer D, Wefelmeyer E, Rosel M, Schrenk M. The eye as a common site for

the early clinical manifestation of sarcoidosis. Ophthalmic Res. 2011;46(1):9–12.
101. Obenauf CD, Shaw HE, Sydnor CF, Klintworth GK. Sarcoidosis and its ophthalmic manifestations. Am J Ophthalmol. 1978;86(5):648–55 [Research Support, U.S. Gov't, P.H.S.].
102. Brownstein S, Liszauer AD, Carey WD, Nicolle DA. Sarcoidosis of the eyelid skin. Can J Ophthalmol. 1990;25(5):256–9 [Case Reports].
103. Hall JG, Cohen KL. Sarcoidosis of the eyelid skin. Am J Ophthalmol. 1995;119(1):100–1 [Case Reports Research Support, Non-U.S. Gov't].
104. Kim YJ, Kim YD. A case of scar sarcoidosis of the eyelid. Korean J Ophthalmol. 2006;20(4):238–40 [Case Reports].
105. Pessoa de Souza Filho J, Martins MC, Sant'Anna AE, Coutinho AB, Burnier Jr MN, Rigueiro MP. Eyelid swelling as the only manifestation of ocular sarcoidosis. Ocul Immunol Inflamm. 2005;13(5):399–402 [Case Reports].
106. Judson MA, Baughman RP, Thompson BW, Teirstein AS, Terrin ML, Rossman MD, et al. Two year prognosis of sarcoidosis: the ACCESS experience. Sarcoidosis Vasc Diffuse Lung Dis. 2003;20(3):204–11 [Comparative Study Research Support, U.S. Gov't, P.H.S.].
107. Swigris JJ, Olson AL, Huie TJ, Fernandez-Perez ER, Solomon J, Sprunger D, et al. Sarcoidosis-related mortality in the United States from 1988 to 2007. Am J Respir Crit Care Med. 2011;183(11):1524–30 [Research Support, N.I.H., Extramural].
108. Falk RH, Comenzo RL, Skinner M. The systemic amyloidoses. N Engl J Med. 1997;337(13):898–909 [Research Support, Non-U.S. Gov't Research Support, U.S. Gov't, P.H.S. Review].
109. Kyle RA, Linos A, Beard CM, Linke RP, Gertz MA, O'Fallon WM, et al. Incidence and natural history of primary systemic amyloidosis in Olmsted County, Minnesota, 1950 through 1989. Blood. 1992;79(7):1817–22 [Research Support, Non-U.S. Gov't Research Support, U.S. Gov't, P.H.S.].
110. Abraham RS, Katzmann JA, Clark RJ, Bradwell AR, Kyle RA, Gertz MA. Quantitative analysis of serum free light chains. A new marker for the diagnostic evaluation of primary systemic amyloidosis. Am J Clin Pathol. 2003;119(2):274–8 [Comparative Study Research Support, Non-U.S. Gov't Research Support, U.S. Gov't, P.H.S.].
111. Kumar S, Dispenzieri A, Katzmann JA, Larson DR, Colby CL, Lacy MQ, et al. Serum immunoglobulin free light-chain measurement in primary amyloidosis: prognostic value and correlations with clinical features. Blood. 2010;116(24):5126–9 [Research Support, N.I.H., Extramural Research Support, U.S. Gov't, P.H.S.].
112. Cenci S. The proteasome in terminal plasma cell differentiation. Semin Hematol. 2012;49(3):215–22 [Research Support, Non-U.S. Gov't Review].
113. Kumar SK, Dispenzieri A, Lacy MQ, Hayman SR, Buadi FK, Zeldenrust SR, et al. Changes in serum-free light chain rather than intact monoclonal immunoglobulin levels predicts outcome following therapy in primary amyloidosis. Am J Hematol. 2011;86(3):251–5 [Comparative Study Research Support, N.I.H., Extramural Research Support, U.S. Gov't, Non-P.H.S.].
114. Rajkumar SV, Dispenzieri A, Kyle RA. Monoclonal gammopathy of undetermined significance, Waldenstrom macroglobulinemia, AL amyloidosis, and related plasma cell disorders: diagnosis and treatment. Mayo Clin Proc. 2006;81(5):693–703 [Research Support, N.I.H., Extramural Review].
115. Kumar S, Sengupta RS, Kakkar N, Sharma A, Singh S, Varma S. Skin involvement in primary systemic amyloidosis. Mediterr J Hematol Infect Dis. 2013; 5(1):e2013005.
116. Brownstein MH, Elliott R, Helwig EB. Ophthalmologic aspects of amyloidosis. Am J Ophthalmol. 1970;69(3):423–30.
117. Landa G, Aloni E, Milshtein A, Marcovich A, Mozes M, Pollack A. Eyelid bleeding and atypical amyloidosis. Am J Ophthalmol. 2004;138(3):495–6 [Case Reports].
118. Caggiati A, Campanella A, Tenna S, Cogliandro A, Potenza C, Persichetti P. Primary amyloidosis of the eyelid: a case report. In Vivo. 2010;24(4):575–8 [Case Reports].
119. Chee E, Kim YD, Lee JH, Woo KI. Chronic eyelid swelling as an initial manifestation of myeloma-associated amyloidosis. Ophthal Plast Reconstr Surg. 2013;29(1):e12–4.
120. Buxbaum JN, Linke RP. A molecular history of the amyloidoses. J Mol Biol. 2012;421(2-3):142–59 [Research Support, N.I.H., Extramural Review].
121. Vrana JA, Gamez JD, Madden BJ, Theis JD, Bergen 3rd HR, Dogan A. Classification of amyloidosis by laser microdissection and mass spectrometry-based proteomic analysis in clinical biopsy specimens. Blood. 2009;114(24):4957–9.
122. Tyradellis C, Peponis V, Kulwin DR. Surgical management of recurrent localized eyelid amyloidosis. Ophthal Plast Reconstr Surg. 2006;22(4):308–9 [Case Reports].
123. Weitzman S, Jaffe R. Uncommon histiocytic disorders: the non-Langerhans cell histiocytoses. Pediatr Blood Cancer. 2005;45(3):256–64 [Review].
124. Janssen D, Harms D. Juvenile xanthogranuloma in childhood and adolescence: a clinicopathologic study of 129 patients from the kiel pediatric tumor registry. Am J Surg Pathol. 2005;29(1):21–8.
125. Dehner LP. Juvenile xanthogranulomas in the first two decades of life: a clinicopathologic study of 174 cases with cutaneous and extracutaneous manifestations. Am J Surg Pathol. 2003;27(5):579–93.
126. Freyer DR, Kennedy R, Bostrom BC, Kohut G, Dehner LP. Juvenile xanthogranuloma: forms of

systemic disease and their clinical implications. J Pediatr. 1996;129(2):227–37 [Case Reports Research Support, Non-U.S. Gov't Review].
127. Hernandez-Martin A, Baselga E, Drolet BA, Esterly NB. Juvenile xanthogranuloma. J Am Acad Dermatol. 1997;36(3 Pt 1):355–67. [Research Support, U.S. Gov't, P.H.S. Review]; quiz 68-9.
128. Stover DG, Alapati S, Regueira O, Turner C, Whitlock JA. Treatment of juvenile xanthogranuloma. Pediatr Blood Cancer. 2008;51(1):130–3 [Case Reports Review].
129. Hu WK, Gilliam AC, Wiersma SR, Dahms BB. Fatal congenital systemic juvenile xanthogranuloma with liver failure. Pediatr Dev Pathol. 2004;7(1):71–6 [Case Reports].
130. Kossard S, Winkelmann RK. Necrobiotic xanthogranuloma with paraproteinemia. J Am Acad Dermatol. 1980;3(3):257–70 [Case Reports].
131. Bullock JD, Bartley GB, Campbell RJ, Yanes B, Connelly PJ, Funkhouser JW. Necrobiotic xanthogranuloma with paraproteinemia: case report and a pathogenetic theory. Trans Am Ophthalmol Soc. 1986;84:342–54 [Case Reports].
132. Matsui M, Nishigori C, Toyokuni S, Takada J, Akaboshi M, Ishikawa M, et al. The role of oxidative DNA damage in human arsenic carcinogenesis: detection of 8-hydroxy-2′-deoxyguanosine in arsenic-related Bowen's disease. J Invest Dermatol. 1999;113(1):26–31.
133. Spicknall KE, Mehregan DA. Necrobiotic xanthogranuloma. Int J Dermatol. 2009;48(1):1–10 [Review].
134. Finan MC, Winkelmann RK. Histopathology of necrobiotic xanthogranuloma with paraproteinemia. J Cutan Pathol. 1987;14(2):92–9.
135. Ugurlu S, Bartley GB, Gibson LE. Necrobiotic xanthogranuloma: long-term outcome of ocular and systemic involvement. Am J Ophthalmol. 2000;129(5):651–7 [Research Support, Non-U.S. Gov't].
136. Wood AJ, Wagner MV, Abbott JJ, Gibson LE. Necrobiotic xanthogranuloma: a review of 17 cases with emphasis on clinical and pathologic correlation. Arch Dermatol. 2009;145(3):279–84.
137. Valentine EA, Friedman HD, Zamkoff KW, Streeten BW. Necrobiotic xanthogranuloma with IgA multiple myeloma: a case report and literature review. Am J Hematol. 1990;35(4):283–5 [Case Reports Review].
138. Fortson JS, Schroeter AL. Necrobiotic xanthogranuloma with IgA paraproteinemia and extracutaneous involvement. Am J Dermatopathol. 1990;12(6):579–84 [Case Reports].
139. Mehregan DA, Winkelmann RK. Necrobiotic xanthogranuloma. Arch Dermatol. 1992;128(1):94–100 [Review].
140. Falk RJ, Gross WL, Guillevin L, Hoffman G, Jayne DR, Jennette JC, et al. Granulomatosis with polyangiitis (Wegener's): an alternative name for Wegener's granulomatosis. Ann Rheum Dis. 2011;70(4):704 [Letter].
141. Abdou NI, Kullman GJ, Hoffman GS, Sharp GC, Specks U, McDonald T, et al. Wegener's granulomatosis: survey of 701 patients in North America. Changes in outcome in the 1990s. J Rheumatol. 2002;29(2):309–16 [Research Support, Non-U.S. Gov't].
142. Jennette JC, Falk RJ. Small-vessel vasculitis. N Engl J Med. 1997;337(21):1512–23 [Historical Article Review].
143. Hoffman GS, Kerr GS, Leavitt RY, Hallahan CW, Lebovics RS, Travis WD, et al. Wegener granulomatosis: an analysis of 158 patients. Ann Intern Med. 1992;116(6):488–98.
144. Mohammad AJ, Jacobsson LT, Mahr AD, Sturfelt G, Segelmark M. Prevalence of Wegener's granulomatosis, microscopic polyangiitis, polyarteritis nodosa and Churg-Strauss syndrome within a defined population in southern Sweden. Rheumatology (Oxford). 2007;46(8):1329–37.
145. Stegmayr BG, Gothefors L, Malmer B, Muller Wiefel DE, Nilsson K, Sundelin B. Wegener granulomatosis in children and young adults. A case study of ten patients. Pediatr Nephrol. 2000;14(3):208–13.
146. Watts RA, Al-Taiar A, Scott DG, Macgregor AJ. Prevalence and incidence of Wegener's granulomatosis in the UK general practice research database. Arthritis Rheum. 2009;61(10):1412–6 [Research Support, Non-U.S. Gov't].
147. Chen M, Yu F, Zhang Y, Zhao MH. Antineutrophil cytoplasmic autoantibody-associated vasculitis in older patients. Medicine (Baltimore). 2008;87(4):203–9 [Comparative Study].
148. Cross CE, Lillington GA. Serodiagnosis of Wegener's granulomatosis: pathobiologic and clinical implications. Mayo Clin Proc. 1989;64(1):119–22.
149. Rao JK, Weinberger M, Oddone EZ, Allen NB, Landsman P, Feussner JR. The role of antineutrophil cytoplasmic antibody (c-ANCA) testing in the diagnosis of Wegener granulomatosis. A literature review and meta-analysis. Ann Intern Med. 1995;123(12):925–32 [Meta-Analysis Research Support, U.S. Gov't, Non-P.H.S.].
150. Kyndt X, Reumaux D, Bridoux F, Tribout B, Bataille P, Hachulla E, et al. Serial measurements of antineutrophil cytoplasmic autoantibodies in patients with systemic vasculitis. Am J Med. 1999;106(5):527–33.
151. Brouwer E, Stegeman CA, Huitema MG, Limburg PC, Kallenberg CG. T cell reactivity to proteinase 3 and myeloperoxidase in patients with Wegener's granulomatosis (WG). Clin Exp Immunol. 1994;98(3):448–53 [Comparative Study Research Support, Non-U.S. Gov't].
152. Holland M, Hewins P, Goodall M, Adu D, Jefferis R, Savage CO. Anti-neutrophil cytoplasm antibody IgG subclasses in Wegener's granulomatosis: a possible pathogenic role for the IgG4 subclass. Clin Exp Immunol. 2004;138(1):183–92 [Research Support, Non-U.S. Gov't].

153. Csernok E, Ai M, Gross WL, Wicklein D, Petersen A, Lindner B, et al. Wegener autoantigen induces maturation of dendritic cells and licenses them for Th1 priming via the protease-activated receptor-2 pathway. Blood. 2006;107(11):4440–8 [Research Support, Non-U.S. Gov't].
154. Lamprecht P, Gross WL. Current knowledge on cellular interactions in the WG-granuloma. Clin Exp Rheumatol. 2007;25(1 Suppl 44):S49–51 [Research Support, Non-U.S. Gov't Review].
155. Haynes BF, Fishman ML, Fauci AS, Wolff SM. The ocular manifestations of Wegener's granulomatosis. Fifteen years experience and review of the literature. Am J Med. 1977;63(1):131 [Case Reports Review].
156. Bullen CL, Liesegang TJ, McDonald TJ, DeRemee RA. Ocular complications of Wegener's granulomatosis. Ophthalmology. 1983;90(3):279–90.
157. Spalton DJ, Graham EM, Page NG, Sanders MD. Ocular changes in limited forms of Wegener's granulomatosis. Br J Ophthalmol. 1981;65(8):553–63 [Case Reports].
158. Gajic-Veljic M, Nikolic M, Peco-Antic A, Bogdanovic R, Andrejevic S, Bonaci-Nikolic B. Granulomatosis with Polyangiitis (Wegener's Granulomatosis) in Children: report of three cases with cutaneous manifestations and literature review. Pediatr Dermatol. 2013;30:e37–42.
159. Jordan DR, Addison DJ. Wegener's granulomatosis. Eyelid and conjunctival manifestations as the presenting feature in two individuals. Ophthalmology. 1994;101(3):602–7 [Case Reports].
160. Ricketti AJ, Cleri DJ, Moser RL, Bilyk JR, Vernaleo JR, Unkle DW. A 44-year-old man with bilateral eyelid swelling. Allergy Asthma Proc. 2012;33(2):205–11 [Case Reports].
161. Ismail AR, Theaker JM, Manners RM. Wegener's granulomatosis masquerading as upper lid chalazion. Eye (Lond). 2007;21(6):883–4 [Case Reports Letter].
162. Shields JA, Shields CL. Eyelid, conjunctival and orbital tumours: an atlas and textbook. 2nd ed. Philadelphia: Lippincott Williams & Wilkins; 2007.
163. Couto Junior Ade S, Batista GM, Calafiori IG, Radael VC, Mendes WB. Hidrocystoma: surgical management of cystic lesions of the eyelid. An Bras Dermatol. 2010;85(3):368–71 [Case Reports].
164. Laumann AE, Rommel JA, Mirzabeigi M, James WD. Pilar cyst (Trichilemmal Cyst). http://emedicine.medscape.com/article/1058907-overview#a0101.2011: Available from: http://emedicine.medscape.com/article/1058907-overview#a0101.
165. Correa Perez ME, Sanchez-Tocino H, Mateos GB. Dermoid cyst in childhood, diagnosed as ptosis. Arch Soc Esp Oftalmol. 2010;85(6):215–7 [Case Reports].
166. Forslund O, Lindelof B, Hradil E, Nordin P, Stenquist B, Kirnbauer R, et al. High prevalence of cutaneous human papillomavirus DNA on the top of skin tumors but not in "Stripped" biopsies from the same tumors. J Invest Dermatol. 2004;123(2):388–94 [Research Support, Non-U.S. Gov't].
167. Nakamura H, Hirota S, Adachi S, Ozaki K, Asada H, Kitamura Y. Clonal nature of seborrheic keratosis demonstrated by using the polymorphism of the human androgen receptor locus as a marker. J Invest Dermatol. 2001;116(4):506–10.
168. Hallermann C, Gunawan B, Bertsch HP. No chromosomal imbalances in seborrheic keratoses detectable by comparative genomic hybridization. J Invest Dermatol. 2004;123(6):1204–5 [Letter].
169. Logie A, Dunois-Larde C, Rosty C, Levrel O, Blanche M, Ribeiro A, et al. Activating mutations of the tyrosine kinase receptor FGFR3 are associated with benign skin tumors in mice and humans. Hum Mol Genet. 2005;14(9):1153 [Comparative Study Research Support, Non-U.S. Gov't].
170. Hafner C, van Oers JM, Hartmann A, Landthaler M, Stoehr R, Blaszyk H, et al. High frequency of FGFR3 mutations in adenoid seborrheic keratoses. J Invest Dermatol. 2006;126(11):2404–7.
171. Hafner C, Hartmann A, Real FX, Hofstaedter F, Landthaler M, Vogt T. Spectrum of FGFR3 mutations in multiple intraindividual seborrheic keratoses. J Invest Dermatol. 2007;127(8):1883–5.
172. Kennedy C, Bajdik CD, Willemze R, De Gruijl FR, Bouwes Bavinck JN. The influence of painful sunburns and lifetime sun exposure on the risk of actinic keratoses, seborrheic warts, melanocytic nevi, atypical nevi, and skin cancer. J Invest Dermatol. 2003;120(6):1087–93.
173. Prieto VG, Shea CR, Celebi JT, Busam KJ. Adnexal tumors. In: Busam KJ, editor. Dermatopathology. Philadelphia: Saunders Elsevier; 2010. p. 381–436.
174. Saglam O, Salama M, Meier F, Chaffins M, Ma C, Ormsby A, et al. Immunohistochemical staining of palisading basal cells in Bowen's disease and basal involvement in actinic keratosis: contrasting staining patterns suggest different cells of origin. Am J Dermatopathol. 2008;30(2):123–6.
175. Kanellou P, Zaravinos A, Zioga M, Stratigos A, Baritaki S, Soufla G, et al. Genomic instability, mutations and expression analysis of the tumour suppressor genes p14(ARF), p15(INK4b), p16(INK4a) and p53 in actinic keratosis. Cancer Lett. 2008;264(1):145–61.
176. Ratushny V, Gober MD, Hick R, Ridky TW, Seykora JT. From keratinocyte to cancer: the pathogenesis and modeling of cutaneous squamous cell carcinoma. J Clin Invest. 2012;122(2):464–72 [Research Support, N.I.H., Extramural Research Support, Non--U.S. Gov't Review].
177. Padilla RS, Sebastian S, Jiang Z, Nindl I, Larson R. Gene expression patterns of normal human skin, actinic keratosis, and squamous cell carcinoma: a spectrum of disease progression. Arch Dermatol. 2010;146(3):288–93 [Comparative Study].
178. Ceilley RI, Jorizzo JL. Current issues in the management of actinic keratosis. J Am Acad Dermatol. 2013;68(1 Suppl 1):S28–38.

179. Graham JH, Mazzanti GR, Helwig EB. Chemistry of Bowen's disease: relationship to arsenic. J Invest Dermatol. 1961;37:317–32.
180. Sobha S, Reck AC, Pathmanathan T, Butler RE. Bowen's disease of the eyelid in a renal transplant recipient on immunosuppressants. Aust N Z J Ophthalmol. 1999;27(6):447 [Case Reports Letter].
181. Ishida H, Kumakiri M, Ueda K, Lao LM, Yanagihara M, Asamoto K, et al. Comparative histochemical study of Bowen's disease and actinic keratosis: preserved normal basal cells in Bowen's disease. Eur J Histochem. 2001;45(2):177–90 [Comparative Study].
182. Hughes JH, Robinson RA. p53 expression in Bowen's disease and in microinvasive squamous cell carcinoma of the skin. Mod Pathol. 1995;8(5):526–9.
183. Campbell C, Quinn AG, Ro YS, Angus B, Rees JL. p53 mutations are common and early events that precede tumor invasion in squamous cell neoplasia of the skin. J Invest Dermatol. 1993;100(6):746–8 [Research Support, Non-U.S. Gov't].
184. Deprez M, Uffer S. Clinicopathological features of eyelid skin tumors. A retrospective study of 5504 cases and review of literature. Am J Dermatopathol. 2009;31(3):256–62 [Review].
185. Wehner MR, Shive ML, Chren MM, Han J, Qureshi AA, Linos E. Indoor tanning and non-melanoma skin cancer: systematic review and meta-analysis. BMJ. 2012;345:e5909 [Comparative Study Meta-Analysis Research Support, N.I.H., Extramural Review].
186. Ho SF, Brown L, Bamford M, Sampath R, Burns J. 5 years review of periocular basal cell carcinoma and proposed follow-up protocol. Eye (Lond). 2013;27(1):78–83.
187. Kiiski V, de Vries E, Flohil SC, Bijl MJ, Hofman A, Stricker BH, et al. Risk factors for single and multiple basal cell carcinomas. Arch Dermatol. 2010;146(8):848–55.
188. Lindgren G, Diffey BL, Larko O. Basal cell carcinoma of the eyelids and solar ultraviolet radiation exposure. Br J Ophthalmol. 1998;82(12):1412–5.
189. Kirzhner M, Jakobiec FA. Clinicopathologic and immunohistochemical features of pigmented basal cell carcinomas of the eyelids. Am J Ophthalmol. 2012;153(2):242–52 e2.
190. Carr RA, Sanders DSA. Basaloid skin tumours: mimics of basal cell carcinoma. Curr Diagn Pathol. 2007;13(4):273–300.
191. Carr RA, Taibjee SM, Sanders DSA. Basaloid skin tumours: basal cell carcinoma. Curr Diagn Pathol. 2007;13(4):252–72.
192. Sanders DSA, Carr RA. The use of immunohistochemistry in the differential diagnosis of common epithelial tumours of the skin. Curr Diagn Pathol. 2007;13(4):237–51.
193. Marks R, Rennie G, Selwood T. The relationship of basal cell carcinomas and squamous cell carcinomas to solar keratoses. Arch Dermatol. 1988;124(7):1039–42 [Research Support, Non-U.S. Gov't].
194. Gailani MR, Stahle-Backdahl M, Leffell DJ, Glynn M, Zaphiropoulos PG, Pressman C, et al. The role of the human homologue of Drosophila patched in sporadic basal cell carcinomas. Nat Genet. 1996;14(1):78–81 [Research Support, Non-U.S. Gov't Research Support, U.S. Gov't, P.H.S.].
195. Bonifas JM, Pennypacker S, Chuang PT, McMahon AP, Williams M, Rosenthal A, et al. Activation of expression of hedgehog target genes in basal cell carcinomas. J Invest Dermatol. 2001;116(5):739–42 [Research Support, Non-U.S. Gov't Research Support, U.S. Gov't, P.H.S.].
196. Hutchin ME, Kariapper MS, Grachtchouk M, Wang A, Wei L, Cummings D, et al. Sustained Hedgehog signaling is required for basal cell carcinoma proliferation and survival: conditional skin tumorigenesis recapitulates the hair growth cycle. Genes Dev. 2005;19(2):214–23 [Research Support, U.S. Gov't, P.H.S.].
197. Heitzer E, Lassacher A, Quehenberger F, Kerl H, Wolf P. UV fingerprints predominate in the PTCH mutation spectra of basal cell carcinomas independent of clinical phenotype. J Invest Dermatol. 2007;127(12):2872–81 [Research Support, Non-U.S. Gov't].
198. Zhang H, Ping XL, Lee PK, Wu XL, Yao YJ, Zhang MJ, et al. Role of PTCH and p53 genes in early-onset basal cell carcinoma. Am J Pathol. 2001;158(2):381–5 [Research Support, U.S. Gov't, P.H.S.].
199. Aszterbaum M, Rothman A, Johnson RL, Fisher M, Xie J, Bonifas JM, et al. Identification of mutations in the human PATCHED gene in sporadic basal cell carcinomas and in patients with the basal cell nevus syndrome. J Invest Dermatol. 1998;110(6):885–8 [Research Support, Non-U.S. Gov't Research Support, U.S. Gov't, P.H.S.].
200. Iuliano A, Strianese D, Uccello G, Diplomatico A, Tebaldi S, Bonavolonta G. Risk factors for orbital exenteration in periocular basal cell carcinoma. Am J Ophthalmol. 2012;153(2):238–41 e1 [Comparative Study].
201. Lo Muzio L. Nevoid basal cell carcinoma syndrome (Gorlin syndrome). Orphanet J Rare Dis. 2008;3:32 [Review].
202. Evans DG, Farndon PA. Nevoid basal cell carcinoma syndrome. In: Pagon RA, Bird TD, Dolan CR, Stephens K, Adam MP, editors. GeneReviews. University of Seattle; 2013.
203. Bale AE, Gailani MR, Leffell DJ. Nevoid basal cell carcinoma syndrome. J Invest Dermatol. 1994;103(5 Suppl):126S–30 [Research Support, Non-U.S. Gov't Review].
204. Donaldson MJ, Sullivan TJ, Whitehead KJ, Williamson RM. Squamous cell carcinoma of the eyelids. Br J Ophthalmol. 2002;86(10):1161–5.
205. Espana A, Redondo P, Fernandez AL, Zabala M, Herreros J, Llorens R, et al. Skin cancer in heart

transplant recipients. J Am Acad Dermatol. 1995;32(3):458–65 [Comparative Study Review].
206. Ong CS, Keogh AM, Kossard S, Macdonald PS, Spratt PM. Skin cancer in Australian heart transplant recipients. J Am Acad Dermatol. 1999;40(1):27–34.
207. Shome D, Bell D, Esmaeli B. Eyelid carcinoma in patients with systemic lymphoma. J Ophthalmic Vis Res. 2010;5(1):38–43.
208. Smoller BR. Squamous cell carcinoma: from precursor lesions to high-risk variants. Mod Pathol. 2006;19 Suppl 2:S88–92.
209. Shiohara J, Koga H, Uhara H, Takata M, Saida T. Eccrine porocarcinoma: clinical and pathological studies of 12 cases. J Dermatol. 2007;34(8):516–22.
210. Hoang MP. Role of immunohistochemistry in diagnosing tumors of cutaneous appendages. Am J Dermatopathol. 2011;33(8):765–71. [Review]; quiz 72-4.
211. Brash DE, Rudolph JA, Simon JA, Lin A, McKenna GJ, Baden HP, et al. A role for sunlight in skin cancer: UV-induced p53 mutations in squamous cell carcinoma. Proc Natl Acad Sci U S A. 1991;88(22):10124–8 [Research Support, Non--U.S. Gov't Research Support, U.S. Gov't, P.H.S.].
212. Giglia-Mari G, Sarasin A. TP53 mutations in human skin cancers. Hum Mutat. 2003;21(3):217–28 [Research Support, Non-U.S. Gov't Review].
213. Danaee H, Karagas MR, Kelsey KT, Perry AE, Nelson HH. Allelic loss at Drosophila patched gene is highly prevalent in basal and squamous cell carcinomas of the skin. J Invest Dermatol. 2006;126(5):1152–8 [Research Support, N.I.H., Extramural].
214. Soysal HG, Markoc F. Invasive squamous cell carcinoma of the eyelids and periorbital region. Br J Ophthalmol. 2007;91(3):325–9.
215. Reifler DM, Hornblass A. Squamous cell carcinoma of the eyelid. Surv Ophthalmol. 1986;30(6):349–65 [Historical Article Review].
216. Bastiaens M, Hoefnagel J, Westendorp R, Vermeer BJ, Bouwes Bavinck JN. Solar lentigines are strongly related to sun exposure in contrast to ephelides. Pigment Cell Res. 2004;17(3):225–9.
217. Monestier S, Gaudy C, Gouvernet J, Richard MA, Grob JJ. Multiple senile lentigos of the face, a skin ageing pattern resulting from a life excess of intermittent sun exposure in dark-skinned caucasians: a case-control study. Br J Dermatol. 2006;154(3):438–44 [Multicenter Study].
218. Zembowicz A, Phadke PA. Blue nevi and variants: an update. Arch Pathol Lab Med. 2011;135(3):327–36 [Review].
219. Crawford JB, Howes Jr EL, Char DH. Combined nevi of the conjunctiva. Arch Ophthalmol. 1999;117(9):1121–7 [Case Reports].
220. Swann PG, Kwong E. The naevus of Ota. Clin Exp Optom. 2010;93(4):264–7 [Case Reports].
221. Gao L, van Nieuwpoort FA, Out-Luiting JJ, Hensbergen PJ, de Snoo FA, Bergman W, et al. Genome-wide analysis of gene and protein expression of dysplastic naevus cells. J Skin Cancer. 2012;2012:981308.
222. Weyers W, Bonczkowitz M, Weyers I, Bittinger A, Schill WB. Melanoma in situ versus melanocytic hyperplasia in sun-damaged skin. Assessment of the significance of histopathologic criteria for differential diagnosis. Am J Dermatopathol. 1996;18(6):560–6.
223. McKenna JK, Florell SR, Goldman GD, Bowen GM. Lentigo maligna/lentigo maligna melanoma: current state of diagnosis and treatment. Dermatol Surg. 2006;32(4):493–504 [Review].
224. Costa MC, Abraham LS, Barcaui C. Lentigo maligna treated with topical imiquimod: dermatoscopy usefulness in clinical monitoring. An Bras Dermatol. 2011;86(4):792–4 [Case Reports].
225. Tsatsou F, Trakatelli M, Patsatsi A, Kalokasidis K, Sotiriadis D. Extrinsic aging: UV-mediated skin carcinogenesis. Dermatoendocrinology. 2012;4(3):285–97.
226. Garner A, Koornneef L, Levene A, Collin JR. Malignant melanoma of the eyelid skin: histopathology and behaviour. Br J Ophthalmol. 1985;69(3):180–6.
227. Vaziri M, Buffam FV, Martinka M, Oryschak A, Dhaliwal H, White VA. Clinicopathologic features and behavior of cutaneous eyelid melanoma. Ophthalmology. 2002;109(5):901–8.
228. Borgognoni L, Sestini S, Gerlini G, Brandani P, Giannotti V, Gelli R, et al. "Saddle" tailored upper eyelid island myocutaneous flap to repair full-thickness lower eyelid defects after melanoma excision. Ophthal Plast Reconstr Surg. 2011;27(1):55–9 [Case Reports].
229. Grossniklaus HE, McLean IW. Cutaneous melanoma of the eyelid. Clinicopathologic features. Ophthalmology. 1991;98(12):1867–73 [Research Support, Non-U.S. Gov't].
230. Clark Jr WH, From L, Bernardino EA, Mihm MC. The histogenesis and biologic behavior of primary human malignant melanomas of the skin. Cancer Res. 1969;29(3):705–27.
231. Breslow A. Thickness, cross-sectional areas and depth of invasion in the prognosis of cutaneous melanoma. Ann Surg. 1970;172(5):902–8.
232. Cook Jr BE, Bartley GB. Treatment options and future prospects for the management of eyelid malignancies: an evidence-based update. Ophthalmology. 2001;108(11):2088–98. [Research Support, Non-U.S. Gov't Review]; quiz 99–100, 121.
233. Morton DL, Thompson JF, Cochran AJ, Mozzillo N, Elashoff R, Essner R, et al. Sentinel-node biopsy or nodal observation in melanoma. N Engl J Med. 2006;355(13):1307–17 [Multicenter Study Randomized Controlled Trial Research Support, N.I.H., Extramural].
234. Pfeiffer ML, Savar A, Esmaeli B. Sentinel lymph node biopsy for eyelid and conjunctival tumors:

what have we learned in the past decade? Ophthal Plast Reconstr Surg. 2013;29(1):57–62.
235. Savar A, Ross MI, Prieto VG, Ivan D, Kim S, Esmaeli B. Sentinel lymph node biopsy for ocular adnexal melanoma: experience in 30 patients. Ophthalmology. 2009;116(11):2217–23 [Clinical Trial].
236. Tsao H, Goel V, Wu H, Yang G, Haluska FG. Genetic interaction between NRAS and BRAF mutations and PTEN/MMAC1 inactivation in melanoma. J Invest Dermatol. 2004;122(2):337–41 [Research Support, Non-U.S. Gov't Research Support, U.S. Gov't, P.H.S.].
237. Meier F, Schittek B, Busch S, Garbe C, Smalley K, Satyamoorthy K, et al. The RAS/RAF/MEK/ERK and PI3K/AKT signaling pathways present molecular targets for the effective treatment of advanced melanoma. Front Biosci. 2005;10:2986–3001 [Research Support, Non-U.S. Gov't Review].
238. Schwartz RA, Torre DP. The Muir-Torre syndrome: a 25-year retrospect. J Am Acad Dermatol. 1995;33(1):90–104 [Historical Article Review].
239. Abbas O, Mahalingam M. Cutaneous sebaceous neoplasms as markers of Muir-Torre syndrome: a diagnostic algorithm. J Cutan Pathol. 2009;36(6):613–9 [Review].
240. Ponti G, Losi L, Pedroni M, Lucci-Cordisco E, Di Gregorio C, Pellacani G, et al. Value of MLH1 and MSH2 mutations in the appearance of Muir-Torre syndrome phenotype in HNPCC patients presenting sebaceous gland tumors or keratoacanthomas. J Invest Dermatol. 2006;126(10):2302–7 [Research Support, Non-U.S. Gov't].
241. Ponti G, Ponz de Leon M. Muir-Torre syndrome. Lancet Oncol. 2005;6(12):980–7 [Research Support, Non-U.S. Gov't Review].
242. Cesinaro AM, Ubiali A, Sighinolfi P, Trentini GP, Gentili F, Facchetti F. Mismatch repair proteins expression and microsatellite instability in skin lesions with sebaceous differentiation: a study in different clinical subgroups with and without extracutaneous cancer. Am J Dermatopathol. 2007;29(4):351–8.
243. Agiannidis C, Pana ZD, Molyva D, Kalokasidis K, Mixiou M. Metachronous occurrence of colorectal cancer in a muir-torre syndrome patient presenting with recurrent sebaceous adenoma of the eyelid: case report and updated review of the literature. J Cutan Med Surg. 2012;16(6):394–9.
244. Rishi K, Font RL. Sebaceous gland tumors of the eyelids and conjunctiva in the Muir-Torre syndrome: a clinicopathologic study of five cases and literature review. Ophthal Plast Reconstr Surg. 2004;20(1):31–6 [Duplicate Publication Research Support, Non-U.S. Gov't Review].
245. Dasgupta T, Wilson LD, Yu JB. A retrospective review of 1349 cases of sebaceous carcinoma. Cancer. 2009;115(1):158–65.
246. Rao NA, Hidayat AA, McLean IW, Zimmerman LE. Sebaceous carcinomas of the ocular adnexa: a clinicopathologic study of 104 cases, with five-year follow-up data. Hum Pathol. 1982;13(2):113–22 [Research Support, U.S. Gov't, P.H.S.].
247. Shields JA, Demirci H, Marr BP, Eagle Jr RC, Shields CL. Sebaceous carcinoma of the eyelids: personal experience with 60 cases. Ophthalmology. 2004;111(12):2151–7 [Research Support, Non--U.S. Gov't Review].
248. Shields JA, Demirci H, Marr BP, Eagle Jr RC, Shields CL. Sebaceous carcinoma of the ocular region: a review. Surv Ophthalmol. 2005;50(2):103–22 [Research Support, Non-U.S. Gov't Review].
249. Howrey RP, Lipham WJ, Schultz WH, Buckley EG, Dutton JJ, Klintworth GK, et al. Sebaceous gland carcinoma: a subtle second malignancy following radiation therapy in patients with bilateral retinoblastoma. Cancer. 1998;83(4):767–71 [Case Reports Review].
250. Kivela T, Asko-Seljavaara S, Pihkala U, Hovi L, Heikkonen J. Sebaceous carcinoma of the eyelid associated with retinoblastoma. Ophthalmology. 2001;108(6):1124–8 [Case Reports Research Support, Non-U.S. Gov't Review].
251. Rundle P, Shields JA, Shields CL, Eagle Jr RC, Singh AD. Sebaceous gland carcinoma of the eyelid seventeen years after irradiation for bilateral retinoblastoma. Eye (Lond). 1999;13(Pt 1):109–10 [Case Reports Letter Research Support, Non-U.S. Gov't].
252. Ho M, Liu DT, Chong KK, Ng HK, Lam DS. Eyelid tumours and pseudotumours in Hong Kong: a ten-year experience. Hong Kong Med J. 2013;19(2):150–5.
253. Xu XL, Li B, Sun XL, Li LQ, Ren RJ, Gao F, et al. Eyelid neoplasms in the Beijing Tongren Eye Centre between 1997 and 2006. Ophthalmic Surg Lasers Imaging. 2008;39(5):367–72.
254. Chao AN, Shields CL, Krema H, Shields JA. Outcome of patients with periocular sebaceous gland carcinoma with and without conjunctival intraepithelial invasion. Ophthalmology. 2001;108(10):1877–83 [Comparative Study Research Support, Non-U.S. Gov't].
255. Ansai S, Mitsuhashi Y, Kondo S, Manabe M. Immunohistochemical differentiation of extraocular sebaceous carcinoma from other skin cancers. J Dermatol. 2004;31(12):998–1008 [Evaluation Studies].
256. Sinard JH. Immunohistochemical distinction of ocular sebaceous carcinoma from basal cell and squamous cell carcinoma. Arch Ophthalmol. 1999;117(6):776–83.
257. Ansai S, Takeichi H, Arase S, Kawana S, Kimura T. Sebaceous carcinoma: an immunohistochemical reappraisal. Am J Dermatopathol. 2011;33(6):579–87 [Comparative Study].
258. Boniuk M, Zimmerman LE. Sebaceous carcinoma of the eyelid, eyebrow, caruncle, and orbit. Trans Am Acad Ophthalmol Otolaryngol. 1968;72(4):619–42 [Case Reports].
259. Schepis C, Siragusa M, Palazzo R, Ragusa RM, Massi G, Fabrizi G. Palpebral syringomas and Down's syndrome. Dermatology. 1994;189(3):248–50.

260. Ogawa R, Mitsuhashi K, Oki K, Hyakusoku H. A rare case of chondroid syringoma arising from the lower eyelid with ectropion. Plast Reconstr Surg. 2006;118(6):137e–40 [Case Reports].
261. Palioura S, Jakobiec FA, Zakka FR, Iwamoto M. Pleomorphic adenoma (formerly chondroid syringoma) of the eyelid margin with a pseudocystic appearance. Surv Ophthalmol. 2013;58:486–91.
262. Mandeville JT, Roh JH, Woog JJ, Gonnering RS, Levin PS, Mazzoli RA, et al. Cutaneous benign mixed tumor (chondroid syringoma) of the eyelid: clinical presentation and management. Ophthal Plast Reconstr Surg. 2004;20(2):110–6.
263. Huerva V, Sanchez MC, Egido RM, Matias-Guiu X. Pleomorphic adenoma with extensive myoepithelial component (myoepithelioma) of the lower eyelid. Ophthal Plast Reconstr Surg. 2008;24(3):223–5 [Case Reports].
264. Kazakov DV, Kacerovska D, Hantschke M, Zelger B, Kutzner H, Requena L, et al. Cutaneous mixed tumor, eccrine variant: a clinicopathologic and immunohistochemical study of 50 cases, with emphasis on unusual histopathologic features. Am J Dermatopathol. 2011;33(6):557–68 [Case Reports Review].
265. Gündüz K, Demirel S, Heper AO, Günalp İ. A rare case of atypical chondroid syringoma of the lower eyelid and review of the literature. Surv Ophthalmol. 2006;51(3):280–5.
266. Hoguet A, Warrow D, Milite J, McCormick SA, Maher E, Della Rocca R, et al. Mucin-producing sweat gland carcinoma of the eyelid: diagnostic and prognostic considerations. Am J Ophthalmol. 2013;155(3):585–92.e2.
267. Zhang Q, Wojno TH, Fitch SD, Grossniklaus HE. Mucinous eccrine adenocarcinoma of the eyelid: report of 6 cases. Can J Ophthalmol. 2010;45(1):76–8 [Research Support, Non-U.S. Gov't].
268. Breiting L, Dahlstrom K, Christensen L, Winther JF, Breiting V. Primary mucinous carcinoma of the skin. Am J Dermatopathol. 2007;29(6):595–6 [Case Reports Letter].
269. Kazakov DV, Suster S, LeBoit PE, Calonje E, Bisceglia M, Kutzner H, et al. Mucinous carcinoma of the skin, primary, and secondary: a clinicopathologic study of 63 cases with emphasis on the morphologic spectrum of primary cutaneous forms: homologies with mucinous lesions in the breast. Am J Surg Pathol. 2005;29(6):764–82 [Case Reports Comparative Study].
270. Qureshi HS, Salama ME, Chitale D, Bansal I, Ma CK, Raju U, et al. Primary cutaneous mucinous carcinoma: presence of myoepithelial cells as a clue to the cutaneous origin. Am J Dermatopathol. 2004;26(5):353–8 [Case Reports].
271. Liszauer AD, Brownstein S, Codere F. Mucinous eccrine sweat gland adenocarcinoma of the eyelid. Can J Ophthalmol. 1988;23(1):17–21 [Case Reports].
272. Snow SN, Reizner GT. Mucinous eccrine carcinoma of the eyelid. Cancer. 1992;70(8):2099–104 [Case Reports Review].
273. Wright JD, Font RL. Mucinous sweat gland adenocarcinoma of eyelid: a clinicopathologic study of 21 cases with histochemical and electron microscopic observations. Cancer. 1979;44(5):1757–68 [Research Support, U.S. Gov't, P.H.S. Review].
274. Chauhan A, Ganguly M, Takkar P, Dutta V. Primary mucinous carcinoma of eyelid: a rare clinical entity. Indian J Ophthalmol. 2009;57(2):150–2 [Case Reports].
275. Simpson W, Garner A, Collin JR. Benign hair-follicle derived tumours in the differential diagnosis of basal-cell carcinoma of the eyelids: a clinicopathological comparison. Br J Ophthalmol. 1989;73(5):347–53 [Case Reports].
276. Matt D, Xin H, Vortmeyer AO, Zhuang Z, Burg G, Boni R. Sporadic trichoepithelioma demonstrates deletions at 9q22.3. Arch Dermatol. 2000;136(5):657–60 [Research Support, Non-U.S. Gov't].
277. Harada H, Hashimoto K, Ko MS. The gene for multiple familial trichoepithelioma maps to chromosome 9p21. J Invest Dermatol. 1996;107(1):41–3.
278. Salhi A, Bornholdt D, Oeffner F, Malik S, Heid E, Happle R, et al. Multiple familial trichoepithelioma caused by mutations in the cylindromatosis tumor suppressor gene. Cancer Res. 2004;64(15):5113–7.
279. Young AL, Kellermayer R, Szigeti R, Teszas A, Azmi S, Celebi JT. CYLD mutations underlie Brooke-Spiegler, familial cylindromatosis, and multiple familial trichoepithelioma syndromes. Clin Genet. 2006;70(3):246–9 [Case Reports Research Support, N.I.H., Extramural Research Support, Non-U.S. Gov't].
280. Headington JT, French AJ. Primary neoplasms of the hair follicle. Histogenesis and classification. Arch Dermatol. 1962;86:430–41.
281. Hidayat AA, Font RL. Trichilemmoma of eyelid and eyebrow. A clinicopathologic study of 31 cases. Arch Ophthalmol. 1980;98(5):844–7 [Research Support, U.S. Gov't, P.H.S.].
282. Ozdal PC, Callejo SA, Codere F, Burnier Jr MN. Benign ocular adnexal tumours of apocrine, eccrine or hair follicle origin. Can J Ophthalmol. 2003;38(5):357–63.
283. Ackerman AB. Trichilemmoma. Arch Dermatol. 1978;114(2):286 [Letter].
284. Brownstein MH. Trichilemmoma. Benign follicular tumor or viral wart? Am J Dermatopathol. 1980;2(3):229–31.
285. Rohwedder A, Keminer O, Hendricks C, Schaller J. Detection of HPV DNA in trichilemmomas by polymerase chain reaction. J Med Virol. 1997;51(2):119–25.
286. Stierman S, Chen S, Nuovo G, Thomas J. Detection of human papillomavirus infection in trichilemmomas and verrucae using in situ hybridization. J Cutan Pathol. 2010;37(1):75–80.
287. Keskinbora KH, Buyukbabani N, Terzi N. Desmoplastic trichilemmoma: a rare tumor of the eyelid. Eur J Ophthalmol. 2004;14(6):562–4 [Case Reports].

288. Illueca C, Monteagudo C, Revert A, Llombart-Bosch A. Diagnostic value of CD34 immunostaining in desmoplastic trichilemmoma. J Cutan Pathol. 1998;25(8):435–9.
289. Kanoh M, Amoh Y, Sato Y, Katsuoka K. Expression of the hair stem cell-specific marker nestin in epidermal and follicular tumors. Eur J Dermatol. 2008;18(5):518–23 [Research Support, Non-U.S. Gov't].
290. Carreras Jr B, Lopez-Marin Jr I, Mellado VG, Gutierrez MT. Trichofolliculoma of the eyelid. Br J Ophthalmol. 1981;65(3):214–5 [Case Reports].
291. Steffen C, Leaming DV. Trichofolliculoma of the upper eyelid. Cutis. 1982;30(3):343–5 [Case Reports].
292. Taniguchi S, Hamada T. Trichofolliculoma of the eyelid. Eye (Lond). 1996;10(Pt 6):751–2 [Case Reports Letter].
293. Shields JA, Shields CL. Eyelid, conjunctival and orbital tumours: an atlas and textbook. 2nd ed. Philadelphia: Lippincott Williams & Wilkins; 2007. p. 82.
294. Kligman AM, Pinkus H. The histogenesis of nevoid tumors of the skin. The folliculoma–a hair-follicle tumor. Arch Dermatol. 1960;81:922–30.
295. Morton AD, Nelson CC, Headington JT, Elner VM. Recurrent trichofolliculoma of the upper eyelid margin. Ophthal Plast Reconstr Surg. 1997;13(4):287–8 [Case Reports].
296. O'Connor N, Patel M, Umar T, Macpherson DW, Ethunandan M. Head and neck pilomatricoma: an analysis of 201 cases. Br J Oral Maxillofac Surg. 2011;49(5):354–8.
297. Levy J, Ilsar M, Deckel Y, Maly A, Anteby I, Pe'er J. Eyelid pilomatrixoma: a description of 16 cases and a review of the literature. Surv Ophthalmol. 2008;53(5):526–35.
298. Handler MZ, Derrick KM, Lutz RE, Morrell DS, Davenport ML, Armstrong AW. Prevalence of pilomatricoma in Turner syndrome: findings from a multicenter study. JAMA Dermatol. 2013;20: 1–6.
299. Hamahata A, Kamei W, Ishikawa M, Konoeda H, Yamaki T, Sakurai H. Multiple pilomatricomas in kabuki syndrome. Pediatr Dermatol. 2013;30(2): 253–5.
300. Graells J, Servitje O, Badell A, Notario J, Peyri J. Multiple familial pilomatricomas associated with myotonic dystrophy. Int J Dermatol. 1996; 35(10):732–3 [Case Reports].
301. Kaddu S, Soyer HP, Hodl S, Kerl H. Morphological stages of pilomatricoma. Am J Dermatopathol. 1996;18(4):333–8.
302. Nakamura T. Comparative immunohistochemical analyses on the modes of cell death/keratinization in epidermal cyst, trichilemmal cyst, and pilomatricoma. Am J Dermatopathol. 2011;33(1):78–83 [Comparative Study].
303. Farrier S, Morgan M. bcl-2 expression in pilomatricoma. Am J Dermatopathol. 1997;19(3):254–7.
304. Kaddu S, Soyer HP, Wolf IH, Kerl H. Proliferating pilomatricoma. A histopathologic simulator of matrical carcinoma. J Cutan Pathol. 1997;24(4): 228–34.
305. Chan EF, Gat U, McNiff JM, Fuchs E. A common human skin tumour is caused by activating mutations in beta-catenin. Nat Genet. 1999;21(4):410–3 [Research Support, Non-U.S. Gov't Research Support, U.S. Gov't, P.H.S.].
306. Xia J, Urabe K, Moroi Y, Koga T, Duan H, Li Y, et al. beta-Catenin mutation and its nuclear localization are confirmed to be frequent causes of Wnt signaling pathway activation in pilomatricomas. J Dermatol Sci. 2006;41(1):67–75.
307. Toker C. Trabecular carcinoma of the skin. Arch Dermatol. 1972;105(1):107–10.
308. Tang CK, Toker C. Trabecular carcinoma of the skin: an ultrastructural study. Cancer. 1978;42(5):2311–21 [Case Reports].
309. Warner TF, Uno H, Hafez GR, Burgess J, Bolles C, Lloyd RV, et al. Merkel cells and Merkel cell tumors. Ultrastructure, immunocytochemistry and review of the literature. Cancer. 1983;52(2):238–45.
310. Suarez C, Rodrigo JP, Ferlito A, Devaney KO, Rinaldo A. Merkel cell carcinoma of the head and neck. Oral Oncol. 2004;40(8):773–9 [Review].
311. Miller RW, Rabkin CS. Merkel cell carcinoma and melanoma: etiological similarities and differences. Cancer Epidemiol Biomarkers Prev. 1999;8(2):153–8 [Comparative Study].
312. Buck CB, Lowy DR. Getting stronger: the relationship between a newly identified virus and Merkel cell carcinoma. J Invest Dermatol. 2009;129((1):9–11 [Comment].
313. Feng H, Shuda M, Chang Y, Moore PS. Clonal integration of a polyomavirus in human Merkel cell carcinoma. Science. 2008;319(5866):1096–100 [Research Support, N.I.H., Extramural Research Support, Non-U.S. Gov't].
314. Kreuter A. A new polyomavirus linked to Merkel cell carcinoma. Arch Dermatol. 2008;144(10):1393 [News].
315. Heath M, Jaimes N, Lemos B, Mostaghimi A, Wang LC, Penas PF, et al. Clinical characteristics of Merkel cell carcinoma at diagnosis in 195 patients: the AEIOU features. J Am Acad Dermatol. 2008;58(3):375–81 [Research Support, N.I.H., Extramural Research Support, Non-U.S. Gov't].
316. Barrett RV, Meyer DR. Eyelid and periocular cutaneous Merkel cell carcinoma (aka. neuroendocrine or trabecular carcinoma). Int Ophthalmol Clin. 2009;49(4):63–75 [Review].
317. Missotten GS, de Wolff-Rouendaal D, de Keizer RJ. Merkel cell carcinoma of the eyelid review of the literature and report of patients with Merkel cell carcinoma showing spontaneous regression. Ophthalmology. 2008;115(1):195–201 [Case Reports Research Support, Non-U.S. Gov't].
318. Brissett AE, Olsen KD, Kasperbauer JL, Lewis JE, Goellner JR, Spotts BE, et al. Merkel cell carcinoma

of the head and neck: a retrospective case series. Head Neck. 2002;24(11):982–8.
319. Chen L, Zhu L, Wu J, Lin T, Sun B, He Y. Giant Merkel cell carcinoma of the eyelid: a case report and review of the literature. World J Surg Oncol. 2011;9:58 [Case Reports Research Support, Non--U.S. Gov't Review].
320. Esmaeli B, Naderi A, Hidaji L, Blumenschein G, Prieto VG. Merkel cell carcinoma of the eyelid with a positive sentinel node. Arch Ophthalmol. 2002;120(5):646–8 [Case Reports].
321. Liao PB. Merkel cell carcinoma. Dermatol Ther. 2008;21(6):447–51.
322. Soltau JB, Smith ME, Custer PL. Merkel cell carcinoma of the eyelid. Am J Ophthalmol. 1996;121(3):331–2 [Case Reports].
323. Leong AS, Phillips GE, Pieterse AS, Milios J. Criteria for the diagnosis of primary endocrine carcinoma of the skin (Merkel cell carcinoma). A histological, immunohistochemical and ultrastructural study of 13 cases. Pathology. 1986;18(4): 393–9.
324. LeBoit PE, Crutcher WA, Shapiro PE. Pagetoid intraepidermal spread in Merkel cell (primary neuroendocrine) carcinoma of the skin. Am J Surg Pathol. 1992;16(6):584–92 [Comparative Study].
325. Gould E, Albores-Saavedra J, Dubner B, Smith W, Payne CM. Eccrine and squamous differentiation in Merkel cell carcinoma. An immunohistochemical study. Am J Surg Pathol. 1988;12(10):768–72.
326. Fernandez-Figueras MT, Puig L, Gilaberte M, Gomez-Plaza Mdel C, Rex J, Ferrandiz C, et al. Merkel cell (primary neuroendocrine) carcinoma of the skin with nodal metastasis showing rhabdomyosarcomatous differentiation. J Cutan Pathol. 2002;29(10):619–22 [Case Reports].
327. Lau PP, Ting SH, Ip YT, Tsang WY, Chan JK. Merkel cell carcinosarcoma: Merkel cell carcinoma with embryonal rhabdomyosarcoma-like component. Ann Diagn Pathol. 2012;16(5):388–91 [Case Reports].
328. Sibley RK, Dahl D. Primary neuroendocrine (Merkel cell?) carcinoma of the skin. II. An immunocytochemical study of 21 cases. Am J Surg Pathol. 1985;9(2):109–16.
329. Miettinen M. Keratin 20: immunohistochemical marker for gastrointestinal, urothelial, and Merkel cell carcinomas. Mod Pathol. 1995;8(4):384–8 [Case Reports].
330. Jensen K, Kohler S, Rouse RV. Cytokeratin staining in Merkel cell carcinoma: an immunohistochemical study of cytokeratins 5/6, 7, 17, and 20. Appl Immunohistochem Mol Morphol. 2000;8(4): 310–5.
331. Su LD, Fullen DR, Lowe L, Uherova P, Schnitzer B, Valdez R. CD117 (KIT receptor) expression in Merkel cell carcinoma. Am J Dermatopathol. 2002;24(4):289–93.
332. Nicholson SA, McDermott MB, Swanson PE, Wick MR. CD99 and cytokeratin-20 in small-cell and basaloid tumors of the skin. Appl Immunohistochem Mol Morphol. 2000;8(1):37–41 [Comparative Study].
333. Gancberg D, Feoli F, Hamels J, de Saint-Aubain N, Andre J, Rouas G, et al. Trisomy 6 in Merkel cell carcinoma: a recurrent chromosomal aberration. Histopathology. 2000;37(5):445–51 [Research Support, Non-U.S. Gov't].
334. Peters 3rd GB, Meyer DR, Shields JA, Custer PL, Rubin PA, Wojno TH, et al. Management and prognosis of Merkel cell carcinoma of the eyelid. Ophthalmology. 2001;108(9):1575–9.
335. Allen PJ, Bowne WB, Jaques DP, Brennan MF, Busam K, Coit DG. Merkel cell carcinoma: prognosis and treatment of patients from a single institution. J Clin Oncol. 2005;23(10):2300–9 [Research Support, Non-U.S. Gov't].
336. Bichakjian CK, Lowe L, Lao CD, Sandler HM, Bradford CR, Johnson TM, et al. Merkel cell carcinoma: critical review with guidelines for multidisciplinary management. Cancer. 2007;110(1):1–12 [Review].
337. Veness MJ, Palme CE, Morgan GJ. Merkel cell carcinoma: a review of management. Curr Opin Otolaryngol Head Neck Surg. 2008;16(2):170–4 [Review].
338. Nicoletti AG, Matayoshi S, Santo RM, Ferreira VR. Eyelid merkel cell carcinoma: report of three cases. Ophthal Plast Reconstr Surg. 2004;20(2): 117–21 [Case Reports].
339. Betharia SM, Ramakrishna K, Sen S, Kashyap S, Thanikachalam S. Dermatofibroma of the eyelid: a case report. Orbit. 2000;19(3):161–4.
340. Mentzel T, Kutzner H, Rutten A, Hugel H. Benign fibrous histiocytoma (dermatofibroma) of the face: clinicopathologic and immunohistochemical study of 34 cases associated with an aggressive clinical course. Am J Dermatopathol. 2001;23(5): 419–26.
341. Jordan DR, Addison DJ, Anderson RL. Fibrous histiocytoma. An uncommon eyelid lesion. Arch Ophthalmol. 1989;107(10):1530–1 [Case Reports Research Support, Non-U.S. Gov't].
342. Kargi E, Kargi S, Gun B, Hosnuter M, Altinyazar C, Aktunc E. Benign fibrous histiocytoma of the eyelid with an unusual clinical presentation. J Dermatol. 2004;31(1):27–31 [Case Reports].
343. Sippel KC. Ocular findings in neurofibromatosis type 1. Int Ophthalmol Clin. 2001;41(1):25–40. [Review]. Winter.
344. Shibata N, Kitagawa K, Noda M, Sasaki H. Solitary neurofibroma without neurofibromatosis in the superior tarsal plate simulating a chalazion. Graefes Arch Clin Exp Ophthalmol. 2012;250(2):309–10 [Case Reports Letter].
345. Tey A, Kearns PP, Barr AD. Plexiform neurofibroma masquerading as a persistent chalazion-a case report. Eye (Lond). 2006;20(8):946–8 [Case Reports Letter].
346. Evans DG, Baser ME, McGaughran J, Sharif S, Howard E, Moran A. Malignant peripheral nerve

sheath tumours in neurofibromatosis 1. J Med Genet. 2002;39(5):311–4 [Case Reports].
347. Shields JA, Guibor P. Neurilemoma of the eyelid resembling a recurrent chalazion. Arch Ophthalmol. 1984;102(11):1650 [Case Reports].
348. Siddiqui MA, Leslie T, Scott C, Mackenzie J. Eyelid schwannoma in a male adult. Clin Experiment Ophthalmol. 2005;33(4):412–3 [Case Reports].
349. Lopez-Tizon E, Mencia-Gutierrez E, Gutierrez-Diaz E, Ricoy JR. Schwannoma of the eyelid: report of two cases. Dermatol Online J. 2007;13(2):12 [Case Reports].
350. Shields JA, Kiratli H, Shields CL, Eagle Jr RC, Luo S. Schwannoma of the eyelid in a child. J Pediatr Ophthalmol Strabismus. 1994;31(5):332–3 [Case Reports Research Support, Non-U.S. Gov't].
351. Touzri RA, Errais K, Zermani R, Benjilani S, Ouertani A. Schwannoma of the eyelid: apropos of two cases. Indian J Ophthalmol. 2009;57(4):318–20 [Case Reports].
352. Cheng KH, Karres J, Kros JM, Kijlstra A, van Dekken H. Cyst-like schwannoma on the eyelid margin. J Craniofac Surg. 2012;23(4):1215–6 [Case Reports].
353. Murphy BA, Dawood GS, Margo CE. Acquired capillary hemangioma of the eyelid in an adult. Am J Ophthalmol. 1997;124(3):403–4 [Case Reports].
354. Peralta RJ, Warner TF, Potter HA, Albert DM. Adult capillary hemangioma. Arch Ophthalmol. 2012;130(8):999 [Case Reports].
355. Boye E, Yu Y, Paranya G, Mulliken JB, Olsen BR, Bischoff J. Clonality and altered behavior of endothelial cells from hemangiomas. J Clin Invest. 2001;107(6):745–52 [In Vitro Research Support, Non-U.S. Gov't Research Support, U.S. Gov't, P.H.S.].
356. Walter JW, North PE, Waner M, Mizeracki A, Blei F, Walker JW, et al. Somatic mutation of vascular endothelial growth factor receptors in juvenile hemangioma. Genes Chromosomes Cancer. 2002;33(3):295–303.
357. Metry DW, Dowd CF, Barkovich AJ, Frieden IJ. The many faces of PHACE syndrome. J Pediatr. 2001;139(1):117–23 [Research Support, Non--U.S. Gov't Review].
358. Goble RR, Frangoulis MA. Lymphangioma circumscriptum of the eyelids and conjunctiva. Br J Ophthalmol. 1990;74(9):574–5 [Case Reports].
359. Irvine AD, Sweeney L, Corbett JR. Lymphangioma circumscriptum associated with paravesical cystic retroperitoneal lymphangioma. Br J Dermatol. 1996;134(6):1135–7 [Case Reports].
360. Mordehai J, Kurzbart E, Shinhar D, Sagi A, Finaly R, Mares AJ. Lymphangioma circumscriptum. Pediatr Surg Int. 1998;13(2-3):208–10 [Case Reports].
361. Fukunaga M. Expression of D2-40 in lymphatic endothelium of normal tissues and in vascular tumours. Histopathology. 2005;46(4):396–402 [Comparative Study].
362. Kahn HJ, Bailey D, Marks A. Monoclonal antibody D2-40, a new marker of lymphatic endothelium, reacts with Kaposi's sarcoma and a subset of angiosarcomas. Mod Pathol. 2002;15(4):434–40 [Research Support, Non-U.S. Gov't].
363. Whimster IW. The pathology of lymphangioma circumscriptum. Br J Dermatol. 1976;94(5):473–86.
364. Burroughs JR, Hsueh JB, Sayre R. Re: "Two cases of periocular cutaneous angiosarcoma". Ophthal Plast Reconstr Surg. 2012;28(5):386–7. [Comment Letter]; author reply 7.
365. Wiwatwongwana D, White VA, Dolman PJ. Two cases of periocular cutaneous angiosarcoma. Ophthal Plast Reconstr Surg. 2010;26(5):365–6 [Case Reports].
366. Bray LC, Sullivan TJ, Whitehead K. Angiosarcoma of the eyelid. Aust N Z J Ophthalmol. 1995;23(1):69–72 [Case Reports].
367. Conway RM, Hammer T, Viestenz A, Holbach LM. Cutaneous angiosarcoma of the eyelids. Br J Ophthalmol. 2003;87(4):514–5 [Case Reports Research Support, Non-U.S. Gov't].
368. Papalas JA, Manavi CK, Woodward JA, Sangueza OP, Cummings TJ. Angiosarcoma of the eyelid: a clinicopathologic comparison between isolated unilateral tumors and tumors demonstrating extrapalpebral involvement. Am J Dermatopathol. 2010;32(7):694–9 [Case Reports Comparative Study].
369. Schuborg C, Mertens F, Rydholm A, Brosjo O, Dictor M, Mitelman F, et al. Cytogenetic analysis of four angiosarcomas from deep and superficial soft tissue. Cancer Genet Cytogenet. 1998;100(1):52–6 [Research Support, Non-U.S. Gov't].
370. Cheah AL, Goldblum JR, Billings SD. Molecular diagnostics complementing morphology in superficial mesenchymal tumors. Semin Diagn Pathol. 2013;30(1):95–109 [Review].
371. Brun SC, Jakobiec FA. Kaposi's sarcoma of the ocular adnexa. Int Ophthalmol Clin. 1997;37(4):25–38 [Review].
372. Shuler JD, Holland GN, Miles SA, Miller BJ, Grossman I. Kaposi sarcoma of the conjunctiva and eyelids associated with the acquired immunodeficiency syndrome. Arch Ophthalmol. 1989;107(6):858–62 [Research Support, Non-U.S. Gov't].
373. Kalinske M, Leone Jr CR. Kaposi's sarcoma involving eyelid and conjunctiva. Ann Ophthalmol. 1982;14(5):497–9 [Case Reports].
374. Reiser BJ, Mok A, Kukes G, Kim JW. Non-AIDS-related Kaposi sarcoma involving the tarsal conjunctiva and eyelid margin. Arch Ophthalmol. 2007;125(6):838–40 [Case Reports].
375. Dugel PU, Gill PS, Frangieh GT, Rao NA. Treatment of ocular adnexal Kaposi's sarcoma in acquired immune deficiency syndrome. Ophthalmology. 1992;99(7):1127–32 [Research Support, Non-U.S. Gov't Research Support, U.S. Gov't, P.H.S.].

376. Kim JW, Lee DK. Unusual eyelid, periocular, and periorbital cutaneous malignancies. Int Ophthalmol Clin. 2009;49(4):77–96 [Review].
377. Radu O, Pantanowitz L. Kaposi sarcoma. Arch Pathol Lab Med. 2013;137(2):289–94 [Review].
378. Chang Y, Cesarman E, Pessin MS, Lee F, Culpepper J, Knowles DM, et al. Identification of herpesvirus-like DNA sequences in AIDS-associated Kaposi's sarcoma. Science. 1994;266(5192):1865–9.
379. Sarantopoulos GP, Palla B, Said J, Kinney MC, Swerdlow SM, Willemze R, et al. Mimics of cutaneous lymphoma: report of the 2011 society for hematopathology/european association for haematopathology workshop. Am J Clin Pathol. 2013;139(4):536–51.
380. Baldassano MF, Bailey EM, Ferry JA, Harris NL, Duncan LM. Cutaneous lymphoid hyperplasia and cutaneous marginal zone lymphoma: comparison of morphologic and immunophenotypic features. Am J Surg Pathol. 1999;23(1):88–96 [Comparative Study].
381. Bergman R, Khamaysi K, Khamaysi Z, Ben Arie Y. A study of histologic and immunophenotypical staining patterns in cutaneous lymphoid hyperplasia. J Am Acad Dermatol. 2011;65(1):112–24.
382. Burg G, Kempf W. Cutaneous lymphomas. Basic and clinical dermatology. New York: Marcel Dekker; 2005.
383. Willemze R, Jaffe ES, Burg G, Cerroni L, Berti E, Swerdlow SH, et al. WHO-EORTC classification for cutaneous lymphomas. Blood. 2005;105(10):3768–85 [Review].
384. Coupland SE, Krause L, Delecluse HJ, Anagnostopoulos I, Foss HD, Hummel M, et al. Lymphoproliferative lesions of the ocular adnexa. Analysis of 112 cases. Ophthalmology. 1998;105(8):1430–41.
385. Smith LB, Pynnonen MA, Flint A, Adams JL, Elner VM. Progressive eyelid and facial swelling due to follicular lymphoma. Arch Ophthalmol. 2009;127(8):1068–70 [Case Reports Letter Research Support, N.I.H., Extramural Research Support, Non-U.S. Gov't].
386. Burg G, Kempf W, Cozzio A, Feit J, Willemze R, SJ E, et al. WHO/EORTC classification of cutaneous lymphomas 2005: histological and molecular aspects. J Cutan Pathol. 2005;32(10):647–74 [Review].
387. LeBoit PE. In: LeBoit PE, Burg G, Weedon D, Sarasin A, editors. Pathology and genetics of skin tumours (IARC WHO Classification of Tumours). Lyon: IARC Press; 2006.
388. Game JA, Davies R. Mycosis fungoides causing severe lower eyelid ulceration. Clin Experiment Ophthalmol. 2002;30(5):369–71 [Case Reports].
389. Mitra A, Bandyopadhyay C, Aluwihare N, Sandramouli S. A rare case of bilateral eyelid ulceration with mycosis fungoides. Ann Ophthalmol. 2009;41(2):112. [Case Reports]. Summer.
390. Stenson S, Ramsay DL. Ocular findings in mycosis fungoides. Arch Ophthalmol. 1981;99(2):272–7 [Research Support, Non-U.S. Gov't].
391. Mao X, Lillington D, Scarisbrick JJ, Mitchell T, Czepulkowski B, Russell-Jones R, et al. Molecular cytogenetic analysis of cutaneous T-cell lymphomas: identification of common genetic alterations in Sezary syndrome and mycosis fungoides. Br J Dermatol. 2002;147(3):464–75 [Research Support, Non-U.S. Gov't].
392. Sanka RK, Eagle Jr RC, Wojno TH, Neufeld KR, Grossniklaus HE. Spectrum of CD30+ lymphoid proliferations in the eyelid lymphomatoid papulosis, cutaneous anaplastic large cell lymphoma, and anaplastic large cell lymphoma. Ophthalmology. 2010;117(2):343–51 [Case Reports Research Support, N.I.H., Extramural Research Support, Non-U.S. Gov't].
393. Saggini A, Anemona L, Chimenti S, Sarmati L, Torti C, Di Stefani A, et al. HIV-associated primary cutaneous anaplastic large cell lymphoma: a clinicopathological subset with more aggressive behavior? Case report and review of the literature. J Cutan Pathol. 2012;39(12):1100–9.
394. Koestinger A, McKelvie P, McNab A. Primary cutaneous anaplastic large-cell lymphoma of the eyelid. Ophthal Plast Reconstr Surg. 2012;28(1):e19–21 [Case Reports].
395. Mencia-Gutierrez E, Gutierrez-Diaz E, Salamanca J, Martinez-Gonzalez MA. Cutaneous presentation on the eyelid of primary, systemic, CD30+, anaplastic lymphoma kinase (ALK)-negative, anaplastic large-cell lymphoma (ALCL). Int J Dermatol. 2006;45(6):766–9 [Case Reports].
396. Koreen IV, Cho RI, Frueh BR, Elner VM. Primary cutaneous anaplastic large cell lymphoma of the medial canthus and orbit. Ophthal Plast Reconstr Surg. 2009;25(1):63–5 [Case Reports].
397. Greisser J, Palmedo G, Sander C, Kutzner H, Kazakov DV, Roos M, et al. Detection of clonal rearrangement of T-cell receptor genes in the diagnosis of primary cutaneous CD30 lymphoproliferative disorders. J Cutan Pathol. 2006;33(11):711–5 [Research Support, Non-U.S. Gov't].
398. Bradford PT, Devesa SS, Anderson WF, Toro JR. Cutaneous lymphoma incidence patterns in the United States: a population-based study of 3884 cases. Blood. 2009;113(21):5064–73 [Research Support, N.I.H., Intramural].
399. Coupland SE, Hummel M, Stein H. Ocular adnexal lymphomas: five case presentations and a review of the literature. Surv Ophthalmol. 2002;47(5):470–90 [Case Reports Review].
400. Gellrich S, Rutz S, Golembowski S, Jacobs C, von Zimmermann M, Lorenz P, et al. Primary cutaneous follicle center cell lymphomas and large B cell lymphomas of the leg descend from germinal center cells. A single cell polymerase chain reaction analysis. J Invest Dermatol. 2001;117(6):1512–20 [Research Support, Non-U.S. Gov't].

401. Fernandez E, Rey A, Sabater N, Alos L, Burnier Jr MN. An unusual presentation of primary diffuse large B-cell lymphoma of the eyelid. Can J Ophthalmol. 2012;47(6):e55–6 [Letter].
402. Huerva V, Canto LM, Marti M. Primary diffuse large B-cell lymphoma of the lower eyelid. Ophthal Plast Reconstr Surg. 2003;19(2):160–1 [Case Reports].
403. Hwang CK, Melson MR, Grossniklaus HE. Diffuse large B cell lymphoma of the eyelid in a patient with AIDS. Br J Ophthalmol. 2011;95(5):739–40. [Case Reports Research Support, N.I.H., Extramural Research Support, Non-U.S. Gov't]; quiz 40, 54.
404. Pandya VB, Conway RM, Taylor SF. Primary cutaneous B cell lymphoma presenting as recurrent eyelid swelling. Clin Experiment Ophthalmol. 2008;36(7):672–4 [Case Reports].
405. Ford JG, Yeatts RP, Hartz JW, Chauvenet A. Granulocytic sarcoma of the eyelid as a presenting sign of leukemia. J Pediatr Ophthalmol Strabismus. 1993;30(6):386–7 [Case Reports].
406. Hattori T, Amano H, Nagai Y, Ishikawa O. Leukemia cutis in a patient with acute monocytic leukemia presenting as unique facial erythema. J Dermatol. 2008;35(10):671–4 [Case Reports].
407. Sandoval C, Davis A, Jayabose S. Eyelid mass as the presenting finding in a child with Down syndrome and acute megakaryoblastic leukemia. Pediatrics. 2005;115(3):810 [Case Reports].
408. Thomas SA, Durairaj VD. Isolated myeloid sarcoma presenting in all four eyelids. Ophthal Plast Reconstr Surg. 2007;23(4):336–8 [Case Reports].
409. Lim CC, Soong TK, Chuah KC, Subrayan V. Extramedullary plasmacytoma of the eyelid: a case report and review of literature. Clin Exp Optom. 2013;96:349–51.
410. Maheshwari R, Maheshwari S. Extramedullary pasmacytoma masquerading as chalazion. Orbit. 2009;28(2-3):191–3 [Case Reports].
411. Krumerman MS, Garret R. Carcinomas metastatic to skin. N Y State J Med. 1977;77(12):1900–3.
412. Rosen T. Cutaneous metastases. Med Clin N Am. 1980;64(5):885–900.
413. Su WPD, Powell FC, Goellner JR, Wick MR. Malignant tumors metastatic to the skin. Unusual illustrative cases. Pathology of unusual malignant cutaneous tumors. New York: Marcel Dekker; 1985. p. 357–97.
414. Fahmy P, Heegaard S, Jensen OA, Prause JU. Metastases in the ophthalmic region in Denmark 1969–98. A histopathological study. Acta Ophthalmol Scand. 2003;81(1):47 [Research Support, Non-U.S. Gov't].
415. Shinohara MM, Tozbikian G, Wolfe JT, Shin SJ, Mies C, Elenitsas R. Cutaneous metastatic breast carcinoma with clear cell features. J Cutan Pathol. 2013;40:753–7.
416. Lee JH, Jung KE, Kim HS, Lee JY, Kim HO, Park YM. Cutaneous metastasis of papillary thyroid carcinoma to the thyroidectomy scar. Int J Dermatol. 2014;53:e223–4.

12 The Orbit, Including the Lacrimal Gland and Lacrimal Drainage System

Robert M. Verdijk, Irene Pecorella, and Cornelia M. Mooy

12.1 General Description

The orbit is the smallest unit of the body to contain all conceivable tissue types. The orbit can be narrowly defined as an enclosure bordered by bony structures, called the bony orbit (Fig. 12.1). Functionally the orbit may be defined as a space that contains all tissues and organs that contribute to the function of the eye, called the orbital cavity (Fig. 12.2). Tumors of the orbit arise primarily from soft tissues and bones. Around 30 % of cases in orbital referral practice are an orbital manifestation of systemic disease. Thyroid-related orbitopathy (Graves' disease), the most common cause of proptosis in adults, is the prime example of such an association between orbital and systemic disease. The proximity of the paranasal sinuses may lead to the secondary spread of sinus neoplasia and infections or inflammation into the confines of the orbit. Tumors may invade the orbit secondarily from ocular adnexa and other periorbital structures. Metastases to the orbit originate from various organs. The intimate relationship to the facial skeleton, coupled with the relatively thin bone of the orbital floor and medial wall, provides a locus minoris resistentiae for orbital soft tissue and bony injury.

12.1.1 Classification and Frequency

The nucleus of this chapter is a consecutive series of 1,077 orbital biopsies and resections retrieved from the files of the Department of Pathology of the Erasmus MC University (the Netherlands) for the 25-year period, 1987–2012. This series proved a logical source for illustrations to aid the ophthalmic pathologist in daily diagnostic practice. Other illustrations were obtained from the Department of Experimental Medicine, University of Rome "Sapienza," Rome, Italy, and cases presented at the European Ophthalmic Pathology Society and Verhoeff-Zimmerman Society or other ophthalmic pathology meetings as referenced. The most frequent lesions of the orbit in our series are of an inflammatory nature (29 %), closely followed by cysts (13 %), epithelial lesions (14 % primary and secondary), and lymphomas (10 %) (Table 12.1). Lesions of the soft tissue and bone lead to the most diverse number of diagnoses, of which vascular, meningeal, and neurogenic tumors are the most frequent. Metastasis represents 3 % of all orbital tumors. We have considered all orbital lesions including those of the lacrimal gland ($N=216$, Table 12.2). The lesions of the lacrimal sac were evaluated separately ($N=238$, Table 12.3).

R.M. Verdijk, MD, PhD (✉)
Department of Ophthalmic Pathology,
Erasmus MC University, Rotterdam, The Netherlands
e-mail: r.verdijk@erasmusmc.nl

I. Pecorella, MD, PhD
Department of Experimental Medicine,
University of Rome "Sapienza", Rome, Italy
e-mail: irene.pecorella@uniroma1.it

C.M. Mooy, MD, PhD
Laboratory for Pathology,
Dordrecht, The Netherlands
e-mail: nmooy@paldordrecht.nl

S. Heegaard, H. Grossniklaus (eds.), *Eye Pathology: An Illustrated Guide*,
DOI 10.1007/978-3-662-43382-9_12,

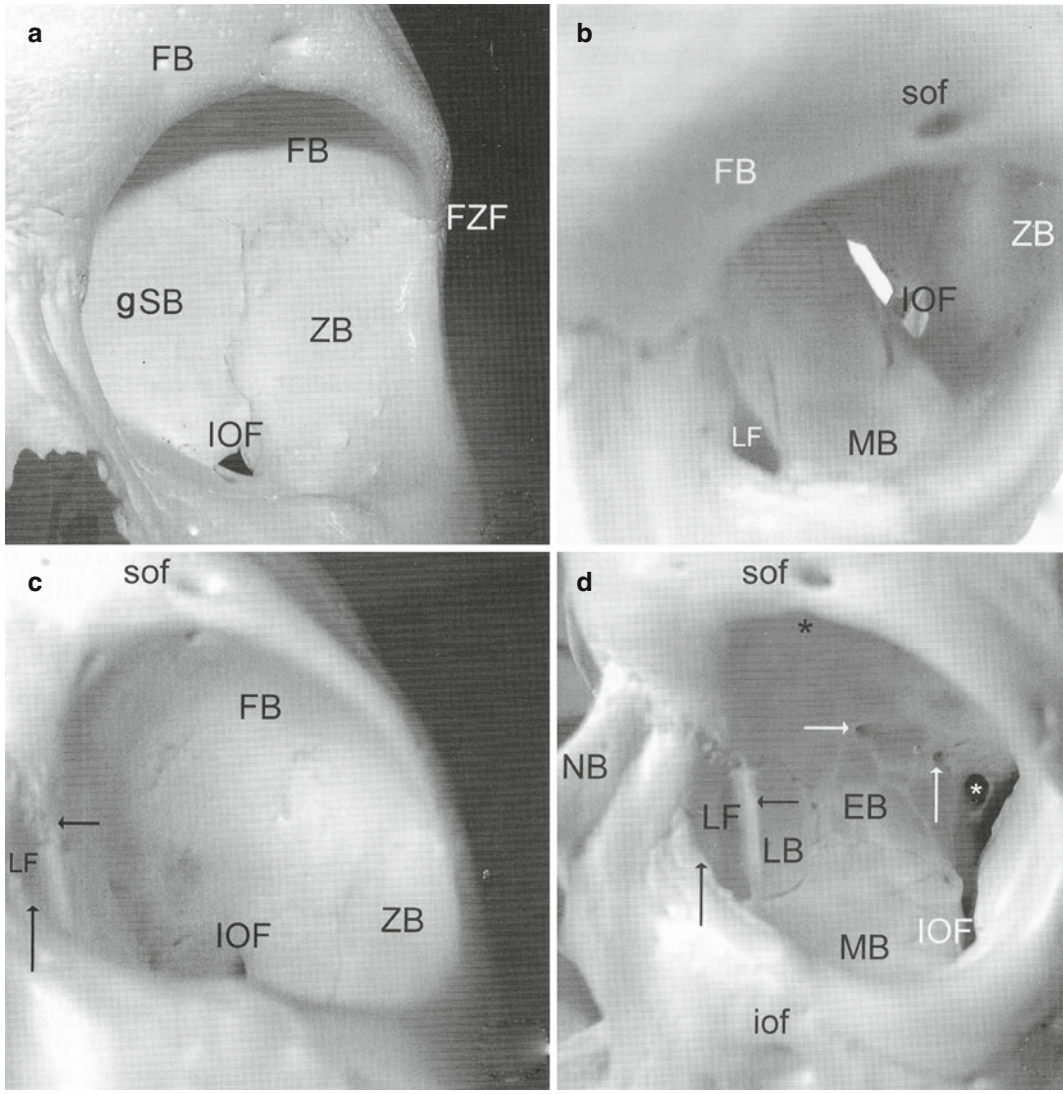

Fig. 12.1 Anatomy of the bony orbit: (**a**) lateral wall, (**b**) floor, (**c**) roof, and (**d**) medial wall. *FB* frontal bone, *FZF* frontozygomatic fissure, *gSB* greater sphenoid bone, *ZB* zygomatic bone, *IOF* inferior orbital fissure, *LF* lacrimal fossa, *MB* maxillary bone, *sof* superior orbital foramen, *NB* nasal bone, *EB* ethmoidal bone, *LB* lacrimal bone, *iof* inferior orbital foramen; *horizontal black arrow*: posterior lacrimal crest; *vertical black arrow*, anterior lacrimal crest; *horizontal white arrow*, anterior ethmoidal foramen; *vertical white arrow*, posterior ethmoidal foramen; *black asterisk*, superior orbital notch; white asterisk, optic canal (Reproduced from: Karcioglu [460])

12.2 Embryology, Anatomy, and Development

12.2.1 Embryology

A recent complete review of ocular and periocular embryogenesis has been provided in the second edition of the monograph by Barishak [1]. The organization of the orbit and its bony walls is governed by the optic cup and optic vesicle, which determine the morphogenesis of the orbital soft tissue contents and the bony orbital walls [2]. The embryonic and early fetal phase, during which one may speak of a "regio orbitalis," is followed by a period of a primordial orbit which extends until after birth [3]. Unlike the trunk and extremities,

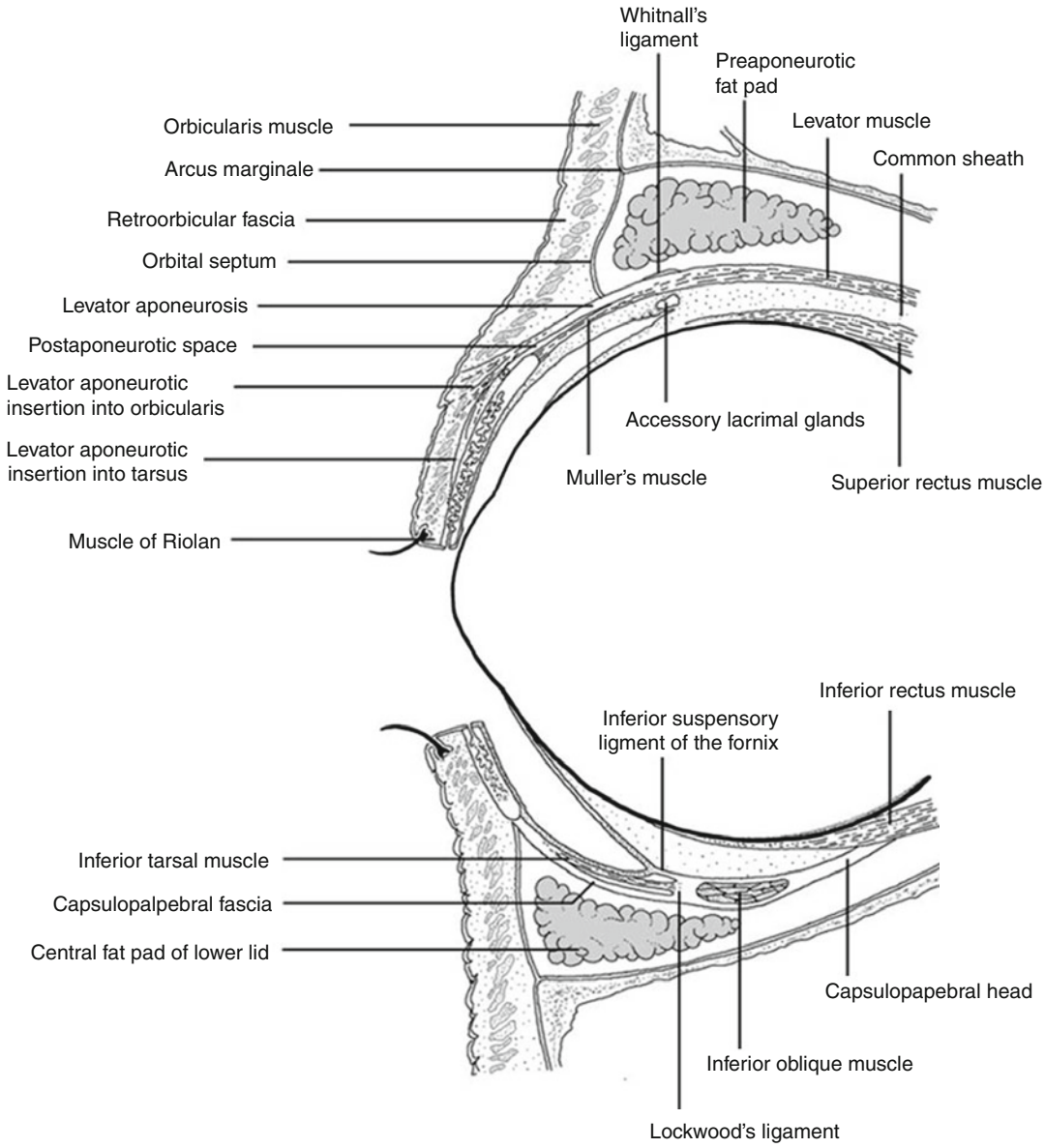

Fig. 12.2 Anatomy of the orbital cavity: central sagittal drawing of the orbital cavity including the orbital septum and the eyelids (Reproduced from Naumann et al. [461])

the orbital bone and ocular connective tissue are derived from neural crest cells, not mesoderm. The connective tissue contributions of the neural crest are collectively referred to as mesectoderm. In the region of the brain rostral to the developing inner ear, the mesodermal segments are called somitomeres. The somitomeres give rise to the myoblasts of the extraocular muscles and vascular endothelium in and around the eye. It is important to point out that the mesenchyme is a broad term for any embryonic connective tissue, whereas mesoderm specifically relates to the middle embryonic layer. In the orbit, the mesenchyme consisting of fibrous and fibroadipose tissue, meninges of the optic nerve, sclera and episclera, vascular pericytes and striated extraocular muscle, satellite cells, peripheral nerve cellular elements, osteocytes, and cartilaginous elements are distinctive in being progeny

Table 12.1 Histopathologic diagnoses of orbital lesions (total $N = 1{,}077$)

Diagnosis (category)	*N*	Relative %	Absolute %
Cysts	**139**	**100**	**13**
Dermoid	92	66	8.5
Epidermoid	9	6.5	<1
Inclusion	2	16	2
Eccrine	1	<1	<1
Respiratory	1	<1	<1
Pseudocyst	1	<1	<1
Lacrimal gland	24	17	1.6
Dacryops	3	2	<1
Nasolacrimal duct	2	1	<1
Mucocele	4	3	<1
Degenerations	**69**	**100**	**6.5**
Fat prolapse	16	23	1.4
Lacrimal gland prolapse	8	12	<1
Scar/fibrosis	19	28	1.7
Cholesterol granuloma	10	14	1
Hematic cyst	4	6	<1
Necrosis	4	6	<1
Radiation change	2	3	<1
Amyloid	2	3	<1
Xanthoma	1	1	<1
Oncocytic metaplasia	1	1	<1
Thromboembolism	1	1	<1
Dacryolith	1	1	<1
Inflammation	**310**	**100**	**29**
Infection	10	3	<1
Abscess	5	1.5	<1
Cellulitis	1	<1	<1
Osteomyelitis	1	<1	<1
Chronic inflammation ECI	40	13	1
IOI	92	29.5	8.5
Florid lymphoid hyperplasia	23	7	2
Sarcoidosis	29	9	2.5
Xanthogranuloma	17	5	1.5
Wegener's granulomatosis	12	4	1
Sjögren syndrome	4	1	<1
Churg–Strauss	1	<1	<1
Giant cell vasculitis	1	<1	<1
Pyogenic granuloma	4	1	<1
Granulation tissue	12	4	1
Granuloma NOS	1	<1	<1
Foreign body granuloma	13	4	1
Rheumatoid arthritis granuloma	1	<1	<1
Graves' orbitopathy	5	1.5	<1
Paraffinoma	8	2.5	<1
Florid subperiosteal reaction	1	<1	<1
Dacryoadenitis	19	6	2
Dacryocystitis	10	3	<1

Table 12.1 (continued)

Diagnosis (category)	*N*	Relative %	Absolute %
Muscle	**5**	**100**	**1.5**
CPEO	3	60	<1
Hypertrophy	1	20	<1
Atrophy	1	20	<1
No diagnosis/normal	**37**	–	**3**
Vascular	**66**	**100**	**6**
Cavernous hemangioma	37	56	3
Capillary hemangioma	7	11	<1
AVM	6	10	<1
Varix	6	10	<1
Lymphangioma	5	7.5	<1
Angiofibroma	2	3	<1
Epithelioid hemangioma	1	1.5	<1
Angiomyxomas	1	1.5	<1
Masson tumor	1	1.5	<1
Meningioma	**58**	**100**	**5**
Meningothelial	26	45	2
Transitional	19	33	2
Psammomatous	4	7	<1
Fibrous	2	3.5	<1
Microcystic	2	3.5	<1
Chordoid	3	5	<1
Anaplastic	2	3.5	<1
Neurogenic	**27**	**100**	**2.5**
Neurofibroma	12	44	1
Traumatic neuroma	5	19	<1
Schwannoma	3	11	<1
Granular cell tumor	1	1.5	<1
MPNST	1	1.5	<1
Ganglioneuroma	1	1.5	<1
Optic glioma	1	1.5	<1
Olfactory neuroblastoma	1	1.5	<1
Retinoblastoma	1	1.5	<1
Glioblastoma	1	1.5	<1
Bone and soft tissue	**58**	**100**	**5**
Chondroma	1	1.5	<1
Chondrosarcoma	7	12	<1
Osteoma	6	10	<1
Osteoid osteoma	1	1.5	<1
Osteosarcoma	1	1.5	<1
Osteopetrosis	1	1.5	<1
Ossifying fibroma	1	1.5	<1
Fibrous dysplasia	7	12	1
Nodular fasciitis	1	1.5	<1
Fibromatosis	2	3	<1
IMT	1	1.5	<1
Haemangiopericytoma	3	5	<1

(continued)

Table 12.1 (continued)

Diagnosis (category)	*N*	Relative %	Absolute %
Fibrous histiocytoma	3	5	<1
Malignant fibrous histiocytoma	1	1.5	<1
Dermolipoma	4	7	<1
Spindle cell lipoma	1	1.5	<1
Liposarcoma	2	3	<1
Leiomyoma	1	1.5	<1
Leiomyosarcoma	1	1.5	<1
Embryonal rhabdomyosarcoma	7	12	<1
Alveolar rhabdomyosarcoma	1	1.5	<1
Glomus tumor	2	3	<1
Sarcoma NOS	1	1.5	<1
Ewing sarcoma	1	1.5	<1
Myositis ossificans	1	1.5	<1
Melanoma	**16**	**100**	**1.5**
Conjunctival	5	31	<1
Skin	4	25	<1
Uveal	6	38	<1
Nose	1	1	<1
Hematopoietic	**105**	**100**	**10**
Malt/marginal zone	43	41	4
Follicular	22	21	2
DLBCL	13	12	1
Mantle cell	9	8.5	1
Lymphoplasmacytic	4	4	<1
B-CLL	3	3	<1
Plasmacytoma	3	3	<1
Burkitt	1	1	<1
T cell	1	1	<1
LCH	4	4	<1
Chloroma/AML	2	2	<1
Epithelial (**primary/secondary**)	**149**	**100**	**14**
Apocrine hidradenoma	1	0.5	<1
Oncocytoma	1	0.5	<1
Inverted papilloma	10	7	1
Undifferentiated carcinoma	32	21.5	3
Adenocarcinoma NOS	5	3	<1
Basal cell carcinoma	11	7	<1
Squamous cell carcinoma	37	25	3.5
Basosquamous carcinoma	1	1	<1
Adenosquamous	1	1	<1
Verrucous	1	1	<1
Sebaceous	10	7	1
Pleomorphic adenoma	23	15	2
AdenoCa ex PA	2	1	<1
Squamous Ca ex P.A.	1	0.5	<1
Adenoid cystic carcinoma	1	0.5	<1
Acinic cell carcinoma	1	0.5	<1
Polymorphous low-grade adenocarcinoma	1	0.5	<1

Table 12.1 (continued)

Diagnosis (category)	*N*	Relative %	Absolute %
Sinonasal adenocarcinoma	5	3	<1
Sweat gland carcinoma	2	1	<1
Merkel cell carcinoma	1	0.5	<1
Small cell carcinoma	1	0.5	<1
Transitional cell carcinoma	1	0.5	<1
Metastasis	**36**	**100**	**3**
Mammacarcinoma	13	36	1
Neuroendocrine carcinoma	5	14	<1
Undifferentiated carcinoma	3	8	<1
Adenocarcinoma NOS	3	8	<1
Thyroid carcinoma	3	8	<1
Melanoma skin	3	8	<1
Prostate carcinoma	2	6	<1
Salivary gland adenocarcinoma	1	3	<1
Pituitary carcinoma	1	3	<1
Lung carcinoma	1	3	<1
Nasal cavity carcinoma	1	3	<1
Miscellaneous	**2**	–	**<1**
Teratoma	2	–	<1

of the mesectoderm [4, 5]. The migration of the neural crest cells proceeds over the face along two routes, which meet in the area of the orbit [6]. The maxillary wave of neural crest cells curves around the developing eye from below, while a frontonasal anlage migrates over the prosencephalon and the optic stalk from above [7]. Thus the floor and lateral wall of the orbit are contributed by the maxillary process, whereas the lacrimal and ethmoidal bones are contributed by the frontonasal process. Within the first 2 months of embryogenesis, the rudiments of the orbital bones are laid down. A unique mechanism of bone formation may be present in the maxillary and frontal bones of the orbit by way of ossification of the orbital muscle of Müller that forms the lateral and caudal walls of the embryonic orbit. In view of the developmental histology, the orbital muscle is a very unique smooth muscle mass in the human body: it connects between bones and is replaced by collagenous fibers even in fetuses. Moreover, the orbital muscle is likely to play a critical role as a septum to maintain a mechanical condition within the orbital space for the normal development of extraocular structures [8]. The lesser wing of the sphenoid bone is initially cartilaginous, but the greater wing and the rest of the orbital bones are membranous and ossify and fuse between the sixth and seventh months of gestation. The significance of this migratory pattern is important for understanding the location of congenital orbital, eyelid, and lacrimal anomalies. A failure of fusion between the neural crest waves results in clefting syndromes that involve the orbit. The typical location of the dermoid cysts at the frontozygomatic and frontomaxillary suture lines is the result of a sequestration of surface ectoderm in the areas of neural crest cell fusion. The superficial spread and deep invasion of basal cell carcinoma on the midface may be partially due to the location of the embryonic fusion planes. The orbital axes rotate from the early stages of optic cup development to adulthood. As the orbital bones develop, the eyes converge from an initial 180° position between the lateral orbital wall and the skull axis to 115° at birth, 68° in infancy, and their final position 45° in adulthood [9].

12.2.2 Anatomy and Histology

The orbits are pyramid-like or pear-shaped structures mainly limited by bony walls that protect and contain the eyeball and its adnexa.

Table 12.2 Histopathologic diagnoses of lacrimal gland lesions ($N=216$)

Diagnosis (category)	*N*	Relative %	Absolute %
Cysts	**31**	**100**	**14**
Lacrimal gland cyst	24	77	
Dacryops	3	10	
Dermoid cyst	2	6.5	
Epidermoid cyst	1	3	
Squamous cell carcinoma	1	3	
Degenerations	**5**	**100**	**2**
Fibrosis	2	40	
Dacryolith	1	20	
Oncocytic metaplasia	1	20	
Thromboemboli	1	20	
Inflammation	**106**	**100**	**49**
Dacryoadenitis	44	42	
IOI, sclerosing dacryoadenitis	29	27	
Sarcoidosis	16	15	
Lymphoid hyperplasia	9	8.5	
Wegener's granulomatosis	3	3	
Sjögren syndrome	2	2	
Xanthogranuloma	1	1	
Rheumatoid granuloma	1	1	
Giant cell vasculitis	1	1	
No diagnosis	**17**	–	**8**
Lymphoma	**26**	**100**	**12**
Malt	12	46	
Follicular	5	20	
Mantle cell	5	20	
DLBCL	3	12	
Lymphoplasmacytic	1	4	
Epithelial	**30**	**100**	**14**
Pleomorphic adenoma	16	53	
AdenoCa ex PA	2	7	
Squamous Ca ex PA	1	3.5	
Adenocarcinoma NOS	3	10	
Adenoid cystic carcinoma	3	10	
Sebaceous carcinoma	2	7	
Acinic cell carcinoma	1	<1	
Oncocytoma	1	<1	
Apocrine hidradenoma	1	<1	
Metastasis	**1**	–	**0.5**
Melanoma skin	1	–	

The stalks are the optic canals. The distance from the apex posteriorly to the orbital rim anteriorly varies from 40 to 50 mm, and the volume is 30 cm^3. Seven bones comprise the orbital walls: frontal, greater and lesser wings of the sphenoid, ethmoid, palatine, maxilla, zygomatic, and lacrimal (Fig. 12.1). They separate the intraorbital tissues from the paranasal sinuses. Several apertures in the orbital bones allow the passage of blood vessels and nerves (Fig. 12.1). The orbital septum is a membranous sheet that acts as the anterior boundary of

Table 12.3 Histopathologic diagnoses of lacrimal sac lesions ($N = 138$)

Diagnosis (category)	*N*	Relative %	Absolute %
Cysts	**1**	–	**<1**
Nasolacrimal duct	1	–	<1
Degenerations	**4**		**3**
Dacryolith	2		1.5
Fibrosis	2		1.5
Inflammation	**104**	**100**	**75**
Dacryocystitis	88	85	65
Infection	3	3	2
Foreign body granuloma	3	3	2
Lipogranuloma	2	2	1.5
Granuloma	2	2	1.5
Granulation tissue	2	2	1.5
Lymphoid hyperplasia	1	1	<1
Sarcoidosis	3	3	2
No diagnosis	**11**		**8**
Lymphoma	**2**	–	**1.5**
DLBCL	1	–	
B-CLL	1	–	
Soft tissue	**6**	–	**4**
Fibrous histiocytoma	3	–	2
Hemangioma	3	–	2
Epithelial	**10**	**100**	**7**
Inverted papilloma	2	20	1.5
Squamous cell carcinoma	2	20	1.5
Transitional cell carcinoma	2	20	<1
Adenoid cystic carcinoma	1	10	<1
Adenocarcinoma NOS	1	10	<1
Adenocarcinoma nasal sinus	1	10	<1
Melanoma (primary)	1	10	<1

the orbit. It extends from the periosteum and periorbita at the orbital rim superiorly. It passes inferiorly into the eyelids to separate them from the orbit (preseptal and postseptal space) and fuses with the upper or lower eyelid retractors 2–4 mm from the tarsus (Fig. 12.2).

The contents of the orbit include the globe, optic nerve and meningeal sheaths, the extraocular striated muscles, levator palpebrae superior muscle and tendons, connective tissue fascia, and fat. Fibrocartilaginous tissue of the orbit is present in the trochlea of the tendon of the superior oblique muscle. Smooth muscle tissue is present in the remnants of the embryonal muscle of Müller. Connective tissue septa (the orbital reticulum) divide and connect orbital fat lobules and compartments [10–14]. A funnel-shaped muscle cone divides the orbit into an intraconal and extraconal space. The former is limited anteriorly by the posterior portion of the eye and includes the optic nerve, blood vessels, and nerves that supply the eye. A third "peripheral" or extraperiosteal space is defined as the potential space between the periosteum and the bony walls. Several central and peripheral nerves traverse the orbit. The ciliary ganglion, which transmits parasympathetic and sympathetic nerve fibers, is a 1.1-mm flat, oval structure that lies between the optic nerve and the lateral rectus muscle. The blood supply of the orbit mainly comes from the branches of the external and internal carotid arteries. The lateral orbit and forehead are supplied by the superficial temporal artery, a branch of the external carotid artery. The supraorbital and lacrimal arteries arise from the internal carotid arteries. The venous system of the orbit drains to the superior ophthalmic vein, which is joined by other veins coming from the eye and by the inferior ophthalmic vein at the orbital apex. The veins drain posteriorly into the cavernous sinus and inferiorly into the pterygoid plexus. There are no identifiable lymphatic vessels or lymph nodes in the bony orbit. The tissues from the most anterior part of the orbit drain into the lymphatics of the conjunctiva and eyelid.

12.3 Congenital Abnormalities

The spectrum of congenital abnormalities of the orbit includes choristomas, progonomas, hamartomas, and congenital malformations. Only choristomas and congenital malformations will be discussed in this section. For reasons of clarity, hamartomatous (most vascular) lesions will be discussed later in the section on vascular neoplasms. Progonoma is now considered a type of PNET and will be duly discussed in the neoplasm section.

12.3.1 Choristomas

12.3.1.1 Epithelial Cystic Choristoma

Definition

Dermoid, epidermoid, conjunctival, and respiratory cysts of the orbit are choristomas, i.e., cysts lined with mature epithelium that is not normally present in the orbit.

Epidemiology

Epithelial cystic choristomas represent 30–50 % of the excised orbital tumors in children [15–17]. According to our series they constitute only 10 % of orbital tumors in patients from all ages.

Etiology

Epithelial cystic choristomas arise from a congenital rest of differentiated embryonic ectodermal tissue at the site of closure of a fetal cleft as described in the section on embryology.

Localization

Dermoid cysts are the most common cystic lesions and have a propensity for the superotemporal or supranasal anterior quadrants of the orbit.

Clinical Features

Typical is a superotemporal swelling of the orbit. CT scan demonstrates the bony relationship to the cystic lesion in 87 % of the cases, particularly at the frontal zygomatic suture. Rarely, these lesions may extend into the intracranial cavity through the bone. Deep-seated dermoids with bony involvement produce a characteristic punched-out appearance with hyperostotic margins, when the bone is viewed by x-ray and show a classical dumbbell sign on CT or MRI (Fig. 12.3).

Macroscopy

Dermoid cysts have a thin capsule and the lumen contains keratinous debris, hairs, and yellow lipid deposits. Dermoid cysts are usually spherical or oval in shape and range in size from 0.5 to 1.0 cm; an occasional lesion may reach 3 cm in size.

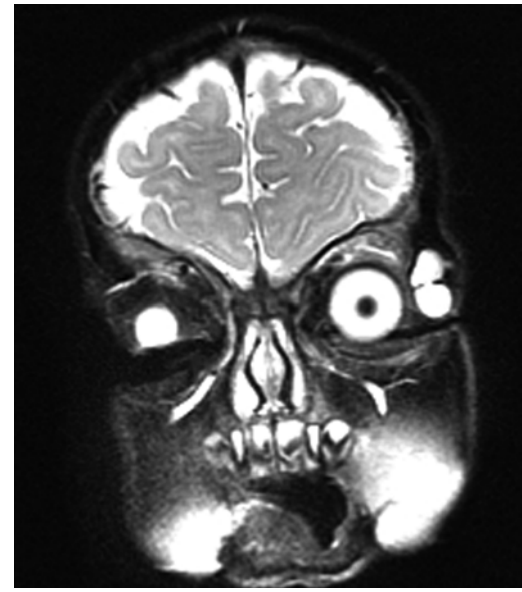

Fig. 12.3 MRI dermoid cyst: T2-weighted MR image showing a dumbbell-shaped lesion at the frontozygomatic fissure (Dr. Robert M. Verdijk)

Histopathology

The lining of the dermoid cyst is composed of stratified squamous epithelium. Pilosebaceous units are observed in the cyst walls composed of dermal connective tissue (Fig. 12.4). When cysts rupture, the lining is partly replaced by a lipogranulomatous inflammatory response that extends into the adjacent orbital tissues. Rarely, the cyst wall does not contain adnexal structures (epidermoid cyst). Other rare cysts are lined by a double layer of cuboidal epithelium resembling conjunctiva (conjunctival cyst) or by ciliated cells (respiratory cyst). A combination of these is possible (Fig. 12.5).

Differential Diagnosis

Traumatic conjunctival cysts may also show keratinization, but will not contain adnexal structures. Cholesterol granuloma does not show an epithelial lining. Mucocele of the paranasal sinus may also be lined with respiratory or squamous metaplastic epithelium. These lesions generally develop in older patients.

Histogenesis

The typical location of dermoid cysts at the frontozygomatic and frontomaxillary suture lines is

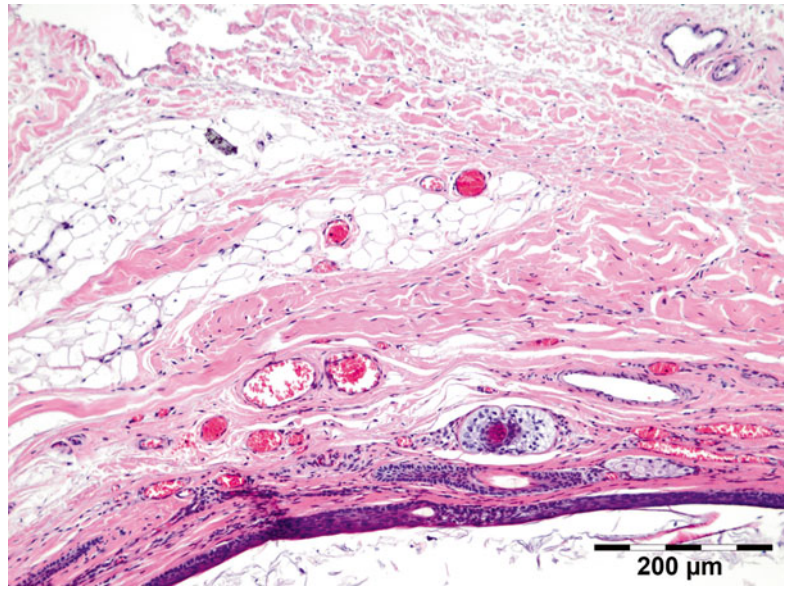

Fig. 12.4 Dermoid cyst: cyst wall lined by keratinizing epithelium with hair follicles and associated sebaceous glands in a dermis-like collagen and subcutaneous-like fat (HE 100×) (Dr. Robert M. Verdijk)

Fig. 12.5 Epithelial cystic choristoma: cyst wall partly lined by stratified squamous epithelium with goblet cells, partly lined by pseudostratified columnar epithelium with ciliated cells and goblet cells. Sebaceous glands indicating epidermal differentiation. Ciliated dermoid cyst (HE 200×) (Dr. Laura Bredow, Freiburg University; this case was presented at the 40th "Jahrestagung der Deutschsprachigen Ophthalmopatologen," Erlangen, 2012)

the result of a sequestration of surface ectoderm in areas of neural crest cell fusion.

Genetics

Not applicable.

Prognosis and Predictive Factors

Some degree of rupture of the dermoid with granulomatous inflammation replacing the epithelium occurs in about 25 % of our cases of orbital dermoids. Rupture with accompanying inflammation and scarring may lead to larger, flat, or multilobulated lesions. The abrupt onset of manifestations may suggest the development of a malignant tumor. Complete resection of the intraosseous parts of the lesion is essential to prevent recurrence. Epithelial cystic choristomas have a very low capacity for malignant transformation to carcinoma.

12.3.1.2 Dermolipoma

These are not true orbital choristomas and will be described in the chapter on conjunctiva. Dermolipomas, however, frequently extend into the orbit and can be diagnosed as lipoma when prior presence of dermolipoma was not mentioned in the provided clinical information. We have diagnosed 4 cases in our series (<1 %).

12.3.1.3 Ectopic Lacrimal Gland (Cyst)

Definition

Lacrimal gland tissue in the deep orbital area outside and not in continuity with the lacrimal gland situated at the superotemporal quadrant.

Epidemiology

Rare.

Etiology

Sequestration of parts of the lacrimal anlagen.

Localization

Deep in the orbit or in the anterior quadrants other than the superior temporal quadrant.

Clinical Features

Although ectopic lacrimal glands of the orbit can be symptomatic at any age, they mostly present during the first three decades of life. Since the lesions are congenital, the reasons for their delayed manifestation are unclear [18].

Macroscopy

The specimen is composed of relatively normal-looking lacrimal gland tissue that may undergo cystic change to form a tense, thin-walled, clear fluid-filled cyst.

Histopathology

Microscopic examination shows normal-appearing lacrimal gland tissue, often with a moderate nonspecific inflammatory cell infiltration. Cystic cases show a cyst lined with cuboidal cells and occasional acini in the cyst wall (Fig. 12.6).

Differential Diagnosis

Clinical correlation is required to make this diagnosis since the normal lacrimal gland may extend as far as to the posterior part of the globe on the temporal side. The cuboidal lining ectopic lacrimal gland cyst may show resemblance to the lining of conjunctival cysts or dacryops.

Histogenesis

Not applicable.

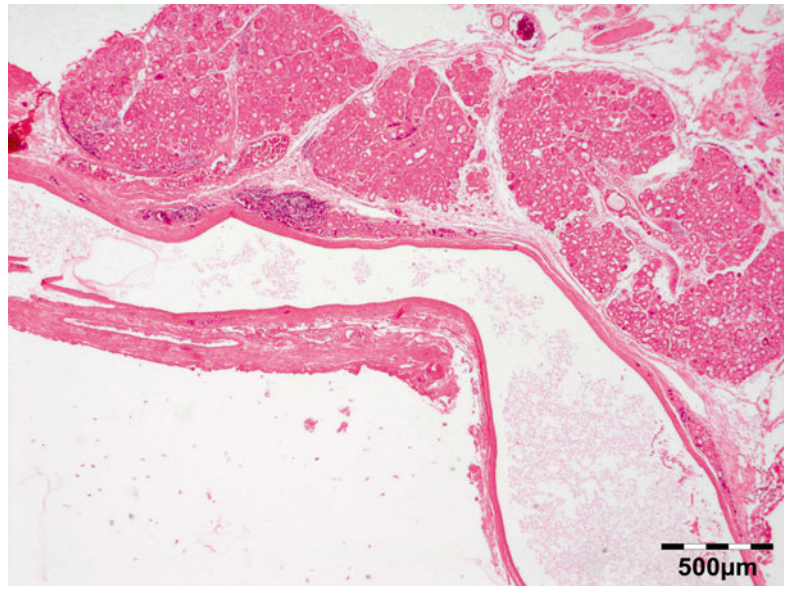

Fig. 12.6 Lacrimal gland cyst: cyst lined by cuboidal epithelium. Lacrimal gland tissue is present in the cyst wall (HE 25×) (Dr. Robert M. Verdijk)

Genetics
Not applicable.

Prognosis and Predictive Factors
Mostly the complications are inflammatory. Vascular lesions, pleomorphic adenoma, and very rare cases of carcinoma have developed in ectopic lacrimal gland tissue.

12.3.1.4 Osseous Choristoma
One case of an osseous choristoma to replace extraocular muscle has been reported [19]. Three cases of osseous choristoma which involved the lids, bulbar conjunctiva, and orbital tissue temporally have been reported [20, 21].

12.3.1.5 Ectopic Lymph Node
One case of an ectopic lymph node located in the lacrimal gland region has been reported [22].

12.3.1.6 Ectopic Pituitary Adenoma
One case of an ectopic pituitary adenoma in the orbit has been reported [23].

12.3.2 Teratoma

It has long been considered a choristoma but is now known to be a well-differentiated nonseminomatous germ cell tumor (NSGCT) and will be discussed in the section on neoplasms.

12.3.3 Hamartoma

Hamartomas are proliferations of disorganized tissues that are encountered in their normal location. Most vascular lesions will be discussed in the section on vascular neoplasms

12.3.3.1 Varix

Definition
A type of vascular aneurysm in the orbit. Orbital varices are a vascular hamartoma typified by a plexus of low-pressure, low-flow, thin-walled, and distensible vessels that intermingle with the normal orbital vessels [24].

Epidemiology
Orbital varix is a rare entity, accounting for less than 1 % of all orbital lesions in our series. Orbital varix represented 10 % of all vascular orbital lesions. Although it is believed to be congenital, and thus present at birth, patients typically do not become symptomatic until later childhood or early adulthood (10–30 years of age). Cases have however been reported at essentially any age [25].

Etiology
Orbital venous varices are divided into primary and secondary. Primary orbital varices are idiopathic and most likely congenital. They are confined to the orbit. Secondary orbital venous varices are those that are acquired due to increased blood flow as a result of intracranial arteriovenous malformations, caroticocavernous fistula, and dural arteriovenous fistula, which drain via the orbit [25, 26].

Localization
Mostly a massively enlarged ophthalmic vein is located in the superior orbit. Most of the lesions are unilateral, but rarely may they be bilateral.

Clinical Features
Evanescent unilateral proptosis is the principal sign of orbital varix. In 20 % of the cases, Phleboliths may form in association with varix and may aid in radiological diagnosis [24].

Macroscopy
The varix has features of a thin-walled vessel with a large lumen that may show phleboliths.

Histopathology
Smooth muscle cells of the media are often decreased in numbers. In the lumen a phlebolith may be present.

Differential Diagnosis
Hemangioma, lymphangioma, idiopathic orbital inflammation (IOI), carotid cavernous fistula, and dural shunt.

Histogenesis
The ophthalmic vein is of mesodermal origin.

Genetics
No genetic abnormalities have been reported.

Prognosis and Predictive Factors
Most orbital varices may be managed conservatively and only warrant surgery in the presence of recurrent thrombosis, disfiguring proptosis, or acute visual loss. Alternatively endovascular coiling has been reported in selected cases.

12.3.4 Congenital Malformations

12.3.4.1 Microphthalmos with Cyst
Isolated microphthalmia associated with colobomatous cyst results from a defect in the closure of the embryonic fissure at the 7- to 20-mm stage of development. Microphthalmia can be associated with either a small, clinically undetectable cyst or a large, typically inferior cyst that deforms the eye and its surroundings. It is usually unilateral, although bilateral cases have been described [27] (see also page 20).

12.3.4.2 Meningoencephalocele and Ectopic Brain Tissue

Definition
Saclike herniations of the brain that protrude into the orbit.

Synonyms
Not true synonyms, but depending on contents, these lesions are designated meningocele, encephalocele, or meningoencephalocele (see below).

Epidemiology
Rare.

Etiology
The cephalocele probably is a cleavage disorder where some portion is separated from the neurectoderm by subsequent bone development. A true cephalocele should have some communication with the brain cavity; otherwise, one should classify the lesion as ectopic brain tissue. Only very rare cases of ectopic brain tissue without connection to the brain have been reported. These probably represent a completely sequestrated herniation [28]. Other theories on ectopic brain tissue include neuroectodermal rests with a potential for differentiation, preferential development of one germ layer of a teratoma into the neural cell lines, and a true astrocytoma.

Localization
These herniations may be classified according to position or contents. The latter classification can only be determined by histologic examination as meningocele, encephalocele, or meningoencephalocele [15]. The former classification distinguishes anterior (frontoethmoidal) or posterior encephaloceles.

Clinical Features
Broad nasal bridge. Orbital swelling. Associations are with microphthalmia, orbital varices, colobomas, and morning glory syndrome [29].

Macroscopy
Meningoencephaloceles consist of jumbled often highly vascularized fragments of glossy white brain tissue and arachnoid.

Histopathology
Microscopic examination may show a dense fibrous wall with neural- and arachnoid-like tissue (Fig. 12.7).

Differential Diagnosis
Microphthalmos with cyst.

Histogenesis
Not applicable.

Genetics
Neurofibromatosis is often associated with posterior encephaloceles.

Prognosis and Predictive Factors
Pre- or postoperative liquor leakage may occur and should be addressed since this may offer a potential route for infectious agents into the brain cavity.

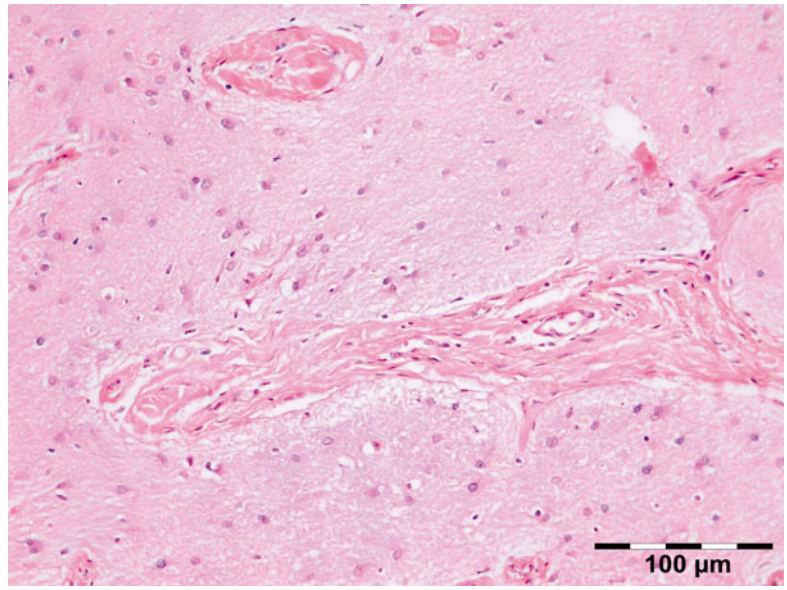

Fig. 12.7 Encephalocele: glial tissue with astrocytes, oligodendroglial cells, and microglia with interspersed fibrous collagen-rich strands (HE 200×) (Dr. Jose G. Cunha Vaz; this case was presented at the EOPS meeting, Munich, 1977, case 77–41)

12.4 Inflammatory Diseases

Orbital inflammatory diseases are mass-forming lesions occurring in patients of various ages. The spectrum ranges from disease caused by infection, surgical procedures, trauma, and foreign bodies to nonspecific inflammation caused by immune reactions and local disease or secondary to an underlying systemic inflammatory disease and myofibroblastic neoplasms [30].

12.4.1 Infectious

Microorganisms: Acute/chronic/granulomatous inflammation may be caused by a host of microorganisms such as bacteria (e.g., *S. pneumoniae*, *S. aureus*, *S. pyogenes*, *H. influenzae*, *Actinomyces*, *Mycobacterium tuberculosis* (Fig. 12.8)), fungi (*Aspergillus fumigatus* (Fig. 12.9), mucormycosis (Fig. 12.10)), maggots (myiasis), and parasites (helminths; see below). In many cases infectious disease is related to extension of infection from adjacent areas such as preseptal fat, nasal cavities, or the cranial cavity. Orbital cellulitis may develop after a penetrating trauma. Osteomyelitis may present as an orbital infection (Fig. 12.11). Infections represented 10 % of all inflammatory lesions in our series. Some cases may be related to immune-compromised state due to either diabetes mellitus, HIV/AIDS, or immunosuppressive therapies for autoimmune disease, chemotherapy for malignancy, stem cell transplantation, or solid organ transplantation. When infectious disease is suspected, a combination of histochemical stains like Gram, Giemsa, Grocott, PAS, alcian blue, and Ziehl–Neelsen should be performed in order to increase the chances of identification of the microorganisms. Immunohistochemistry may aid the identification of *Toxoplasma*, *Treponema pallidum,* HSV, VZV, or EBV when indicated.

Helminths: Man may become infected by three types of larval cysts of tapeworms: (1) the hydatid of *Echinococcus granulosus*, a larval cyst of variable size in which daughter cysts develop; (2) coenurus, a larger single bladder worm of *Taenia multiceps*, 5 cm or more in diameter, containing several hundreds of scoleces; and (3) *Cysticercus cellulosae*, a small bladder worm of *Taenia solium*, containing one single scolex [31]. The adult worms of Onchocerca on the other hand may cause a tumor known as onchocercoma.

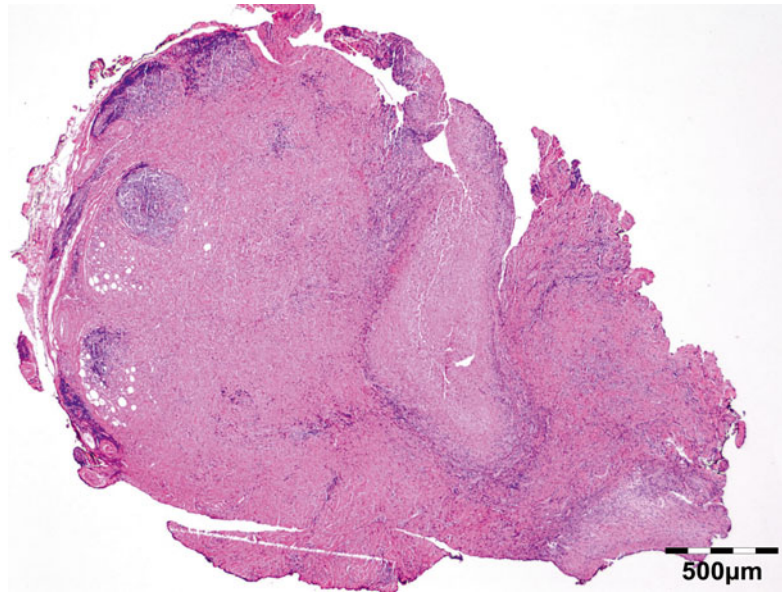

Fig. 12.8 Tuberculosis: necrotizing granuloma. *Mycobacterium tuberculosis* could only be demonstrated by PCR. The patient showed a good response to tuberculostatic therapy (HE 25×) (Dr. Robert M. Verdijk)

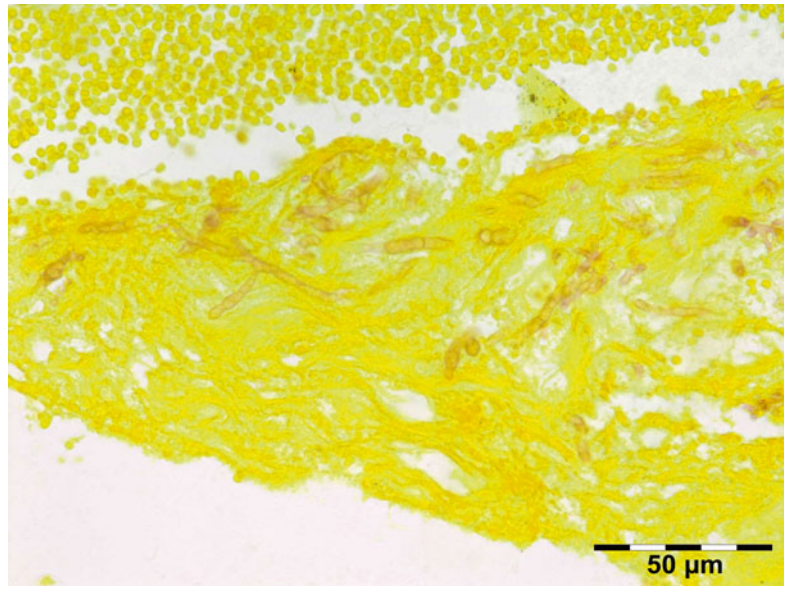

Fig. 12.9 *Aspergillus*: septated hyphae showing branching at acute angles, often 45° fit the diagnosis of *Aspergillus* (Grocott 400×) (Dr. Pierre Danis; this case was presented at the EOPS meeting, Toulouse, 1974, case 74–31)

12.4.1.1 Hydatid Cyst

Definition

Infestation with the larval cyst of *Echinococcus granulosus*.

Epidemiology

Echinococcus granulosus has a worldwide distribution, mainly in sheep- and cattle-raising countries. The definitive hosts are dogs or other canids.

Etiology

Humans become infected by ingesting eggs on fomites or in food and water contaminated with dog feces.

Localization

Oncospheres are released in the intestine and the cysts develop most commonly in the liver (60–70 %) and lungs (20 %). Hydatid disease involving the orbit represents <1 % of all cases [15, 32].

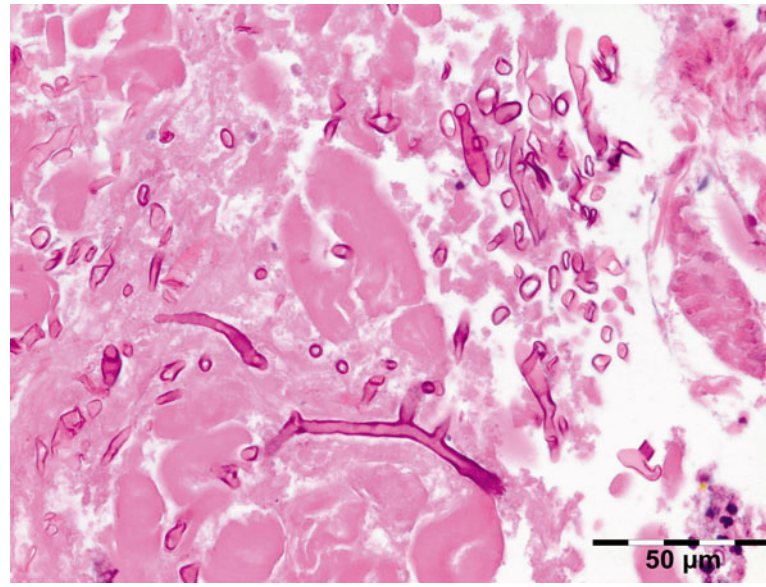

Fig. 12.10 Mucormycosis: broad nonseptated hyphae showing branching at 90° angle fit the diagnosis of Mucormycosis. The cell walls are typically well delineated in HE sections (HE 400×) (Dr. Robert M. Verdijk)

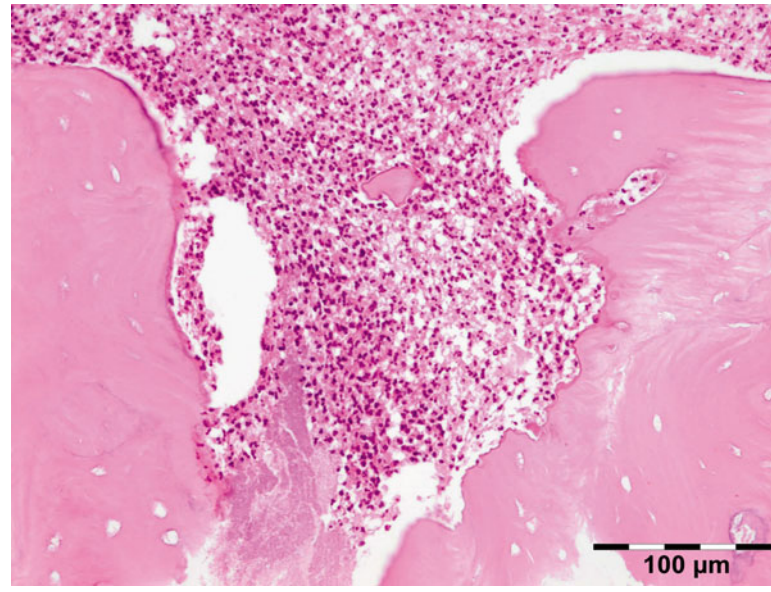

Fig. 12.11 Osteomyelitis: nonvital bony sequesters are seen in an acute inflammatory background with neutrophils. Note the loss of chromatin staining in the osteocytes of the lamellar bone (HE 200×) (Dr. Robert M. Verdijk)

Clinical Features

The patient may present with a variety of symptoms and signs, including painless proptosis, oculomotor palsies, and eyelid edema. On MRI orbital hydatid cysts usually appear as a well-defined, thin-walled, oval-shaped lesions with fine peripheral rim enhancement of their fibrous capsule after contrast medium administration.

Macroscopy

The cysts are typically white, subspherical in shape, and fluid filled.

Histopathology

The cyst wall consists of an inner nucleated germinal layer of epithelium and an opaque, elastic acellular laminated layer of varying thickness that is surrounded externally by a host-derived

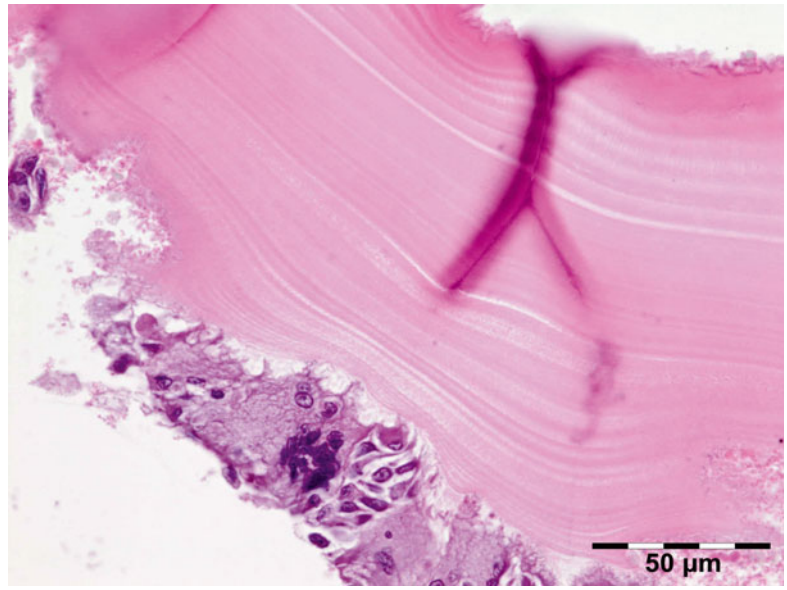

Fig. 12.12 Hydatid cyst: typical lamellated outer cyst wall surrounded by inflammatory cells including multinucleated giant cells (PAS 400×) (Dr. Martine Brihaye-van Geertruyden; this case was presented at the EOPS meeting, Rotterdam, 1967, case 67–25)

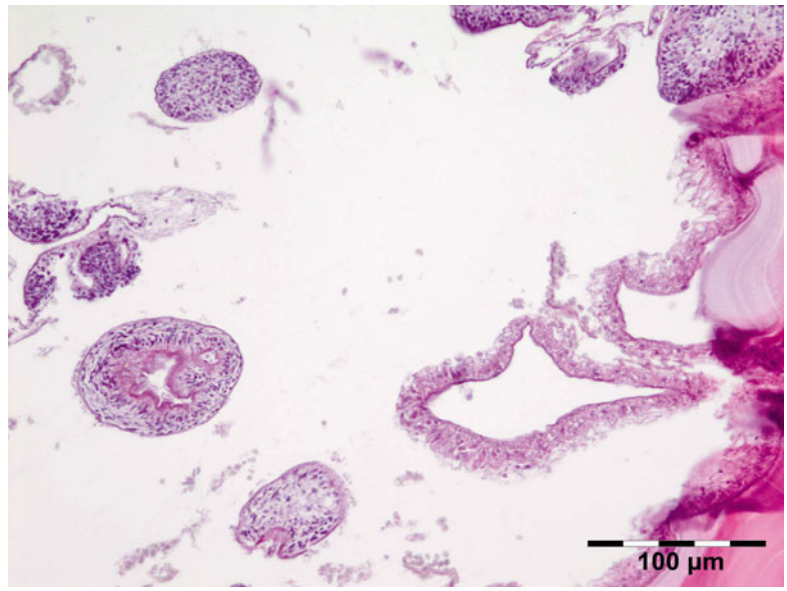

Fig. 12.13 Hydatid cyst: inner cyst wall with a nucleated germinal layer of epithelium. Brood capsules attached to the germinal layer and free floating daughter cysts can be seen (PAS 200×) (Dr. Martine Brihaye-van Geertruyden)

fibrous layer of tissue (Fig. 12.12). Brood capsules develop from the germinal layer and mature to form protoscoleces (Fig. 12.13). Each scolex is about 100 µm across and contains suckers, a double crown of hooklets (Fig. 12.14), and calcareous bodies. Daughter cysts are usually produced within the mother cavity. Death and degeneration of free brood capsules results in protoscoleces in the fluid contents, referred to as hydatid sand.

Differential Diagnosis

Coenurus and cysticercosis.

Histogenesis

Not applicable.

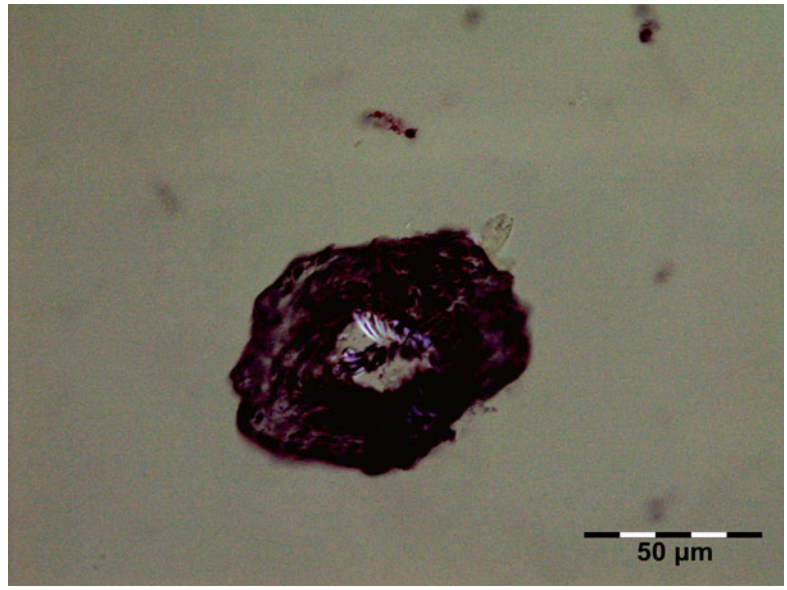

Fig. 12.14 Hydatid cyst: birefringence easily identifies protoscoleces (polarized light 200×) (Dr. Martine Brihaye-van Geertruyden)

Genetics
Not applicable.

Prognosis and Predictive Factors
Most patients with orbital parasitic cysts have recovered reasonably good vision following surgical extirpation of the mass or antihelminthic medication.

12.4.1.2 Coenurus

Definition
Infestation with coenuri of *Taenia multiceps*.

Epidemiology
Taenia multiceps distribution is worldwide.

Etiology
Its most common definite host is the domestic dog, or other canids. Humans become infected in the same way as described for *Echinococcus*.

Localization
After about 3 months, coenuri of *T. multiceps* develop in the central nervous system preferably, especially in the cerebrospinal fluid pathways, and in the eye and orbit [31].

Clinical Features
Redness of the eye and cystic tumor.

Macroscopy
A coenurus is a white or gray spherical or ovoid unilocular cyst which varies from a few millimeters to 2 cm in diameter.

Histopathology
The cyst wall is surrounded by a thin layer of host-derived fibrous tissue that often shows minimal inflammatory reaction. However, the degenerating coenurus may be heavily infiltrated by mononuclear and polymorphonuclear inflammatory cells with a great number of eosinophils (Fig. 12.15). Inside the fibrous wall, the wall of a cystic larva consists of a thin outer cuticular layer (the tegument) 5 µm thick, covered with microvilli. The inner cellular layer contains smooth muscle fibers lined by a row of tegumental cells and parenchyma (Fig. 12.16). The circular cavity is filled with fluid. The inner wall has a linearly arranged large number of inverted scoleces. Each scolex contains a rostellum with a double row of small hooks of two sizes. Everted scoleces may be present.

Differential Diagnosis
Hydatid cyst and cysticercosis.

Histogenesis
Not applicable.

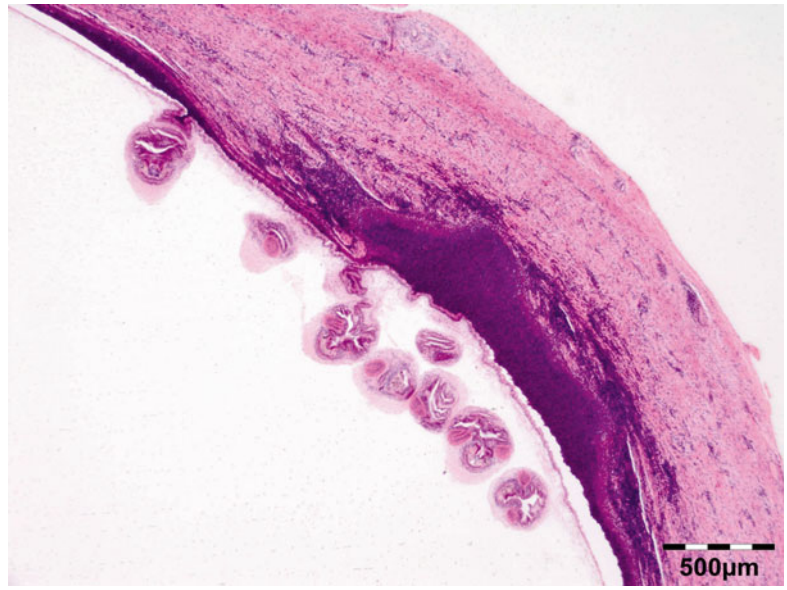

Fig. 12.15 Coenurus: the cyst wall is surrounded by a heavy mononuclear and polymorphonuclear infiltrate. The circular cavity is filled by fluid. The inner wall has a linearly arranged large number of inverted and everted scoleces (HE 25×) (Dr. Robert M. Verdijk)

Fig. 12.16 Coenurus: the inner cellular layer with smooth muscle fibers is lined by a row of tegumental cells and parenchyma. Each scolex contains a rostellum with a double row of small hooks of two sizes (HE 200×) (Dr. Robert M. Verdijk)

Genetics

Not applicable.

Prognosis and Predictive Factors

Most patients with orbital parasitic cysts have recovered reasonably good vision following surgical extirpation of the mass or antihelminthic medication.

12.4.1.3 Cysticercosis

Definition

Infestation with the cystic larval form of the swine tapeworm *Taenia solium*.

Epidemiology

T. solium is cosmopolitan in spread. Orbital and adnexal cysticercosis is now considered a common disease in endemic regions such as Mexico, Africa, India, China, Indonesia, Eastern Europe, and South and Central America [33].

Etiology

Cysticercosis is caused by hematogenous spread and encystment of the larval form of the swine tapeworm *Taenia solium*. The worm passes its life cycle in two hosts. Humans are the definitive hosts and the adult parasites live in the small

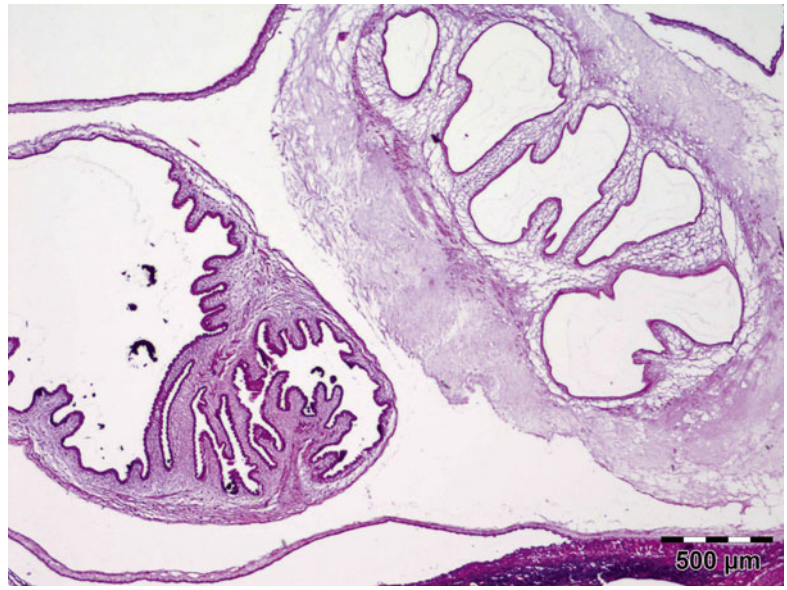

Fig. 12.17 Cysticercoma: a cyst containing fluid. The single invaginated scolex often cannot be found in histology sections. The cyst wall is raised into projections. The cysticercus is surrounded by fibrous tissue and caused virtually no inflammatory response (HE 25×) (Dr. Robert M. Verdijk)

intestine for several years. The pig is the intermediate host and the main host of the larva. Man acquires infection through the ingestion of infective cysts present in contaminated food such as undercooked pork.

Localization

The parasites reach the bloodstream via the intestine and then undergo passive hematogenous spread to other tissues and organs, tending to embed themselves in areas with a high metabolic turnover and good glycogen supply such as the central nervous system, eye, and striated muscles [34]. As a definitive host, man harbors the adult tapeworm, and as an intermediate host, man harbors the bladder worm or cysticercus.

Clinical Features

The various clinical presentations of cysticercosis are redness of the eye, proptosis, restriction of ocular motility, and cystic tumor.

Macroscopy

Cysticerci are spherical to oval milky white cysts about 1 cm in diameter when fully developed.

Histology

The cyst contains fluid and a single invaginated scolex (Fig. 12.17). The scolex has four large suckers and a rostellum with a double row of large and small hooklets. The cyst wall is 100–200 µm thick and often is raised into projections that are 10–25 µm in diameter. The tegument is usually less than 5 µm and its outer surface is covered with microvilli. Numerous smooth muscle fibers lie immediately beneath the tegument and extend into the parenchyma. A row of tegumental cell lies beneath the muscle fibers. The cysticercus is surrounded by fibrous tissue and often causes virtually no inflammatory response. However, when cysticerci degenerate, there is an infiltration of neutrophils, histiocytes, and eosinophils. Eventually a granulomatous reaction may occur characterized by histiocytes, epithelioid cells, and foreign body giant cells, leading to fibrosis and calcification.

Differential Diagnosis

Cysticercosis can masquerade as any of the subacute, acute, or chronic inflammatory or cystic lesions of the orbit. Hydatid cyst, coenurus.

Histogenesis

Not applicable.

Genetics

Not applicable.

Prognosis and Predictive Factors

Surgical removal of extraocular muscle cysts is usually contraindicated. Treatment with antihelminthic drugs under steroid cover has a high success rate in cyst elimination.

12.4.1.4 Onchocercoma

Definition
Infestation with the adult worm of *Onchocerca volvulus*.

Epidemiology
Onchocerca volvulus is commonly found in West, Central, and East Africa, in South America, and less commonly in the Middle East.

Etiology
Humans are the only definitive host for *O. volvulus*. The intermediate host or vector is the black fly (*Simulium*). The parasite is acquired through the bite of an infected fly.

Localization
The adult worm of *Onchocerca* is most often seen in the subcutaneous tissues and conjunctiva but may extend into the anterior orbit.

Clinical Features
It is the cause of river blindness in man; the orbit may be affected by onchocercomas which are palpable nodi that may occur adherent to the periosteum of the orbital bones [35].

Macroscopy
Nodular fibrous tissue, sometimes the outline of the worms can be observed on cut surface.

Histopathology
Histologically the nodule consists of three zones (Fig. 12.18): an external poorly vascularized, fibrous capsule, an intermediate fibrocellular layer consisting mainly of granulation tissue, and a central zone which, depending on the age of the nodule, may contain adult worms (Fig. 12.19) and microfilariae, or the caseous remnants of dead worms.

Differential Diagnosis
Other infectious diseases of the orbit.

Histogenesis
Not applicable.

Genetics
Not applicable.

Prognosis and Predictive Factors
Antihelminthic drugs as ivermectin are effective in eradicating the worms.

12.4.2 Reactive Inflammation

12.4.2.1 Cholesterol Granuloma

Definition
Foreign body reaction against cholesterol crystals.

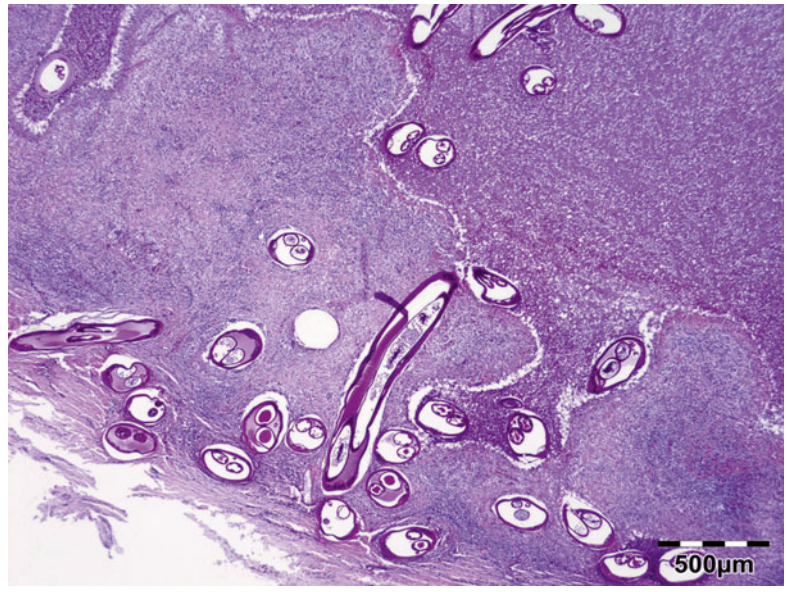

Fig. 12.18 Onchocercoma: a fibrous capsule surrounds granulation tissue with granuloma formation and adult worms (PAS 25×) (Dr. Robert M. Verdijk)

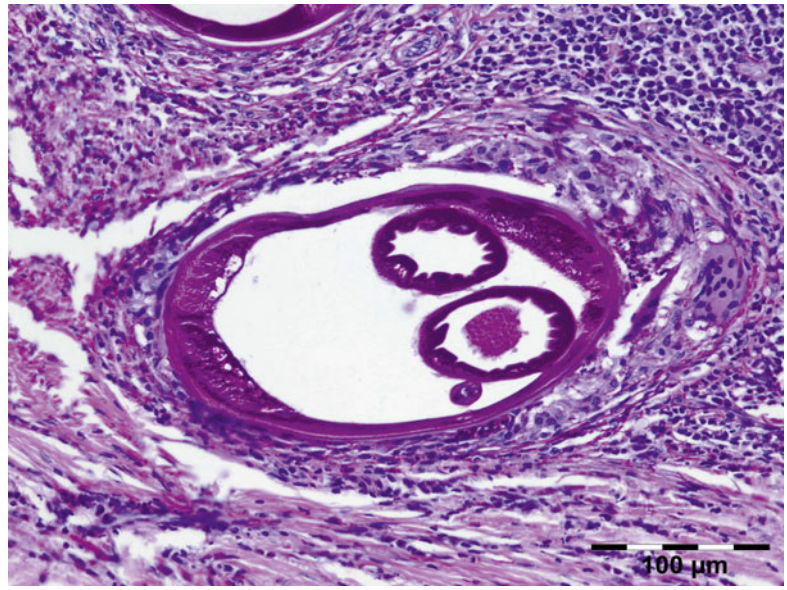

Fig. 12.19 Onchocercoma: adult female worm surrounded by a dense inflammatory infiltrate containing multinucleated giant cells. The cuticle shows ridges. Inside the worm muscle cells, gut, and uterus can be seen (PAS 200×) (Dr. Robert M. Verdijk)

Synonyms

The term "cholesteatoma" has incorrectly been used for any lesion containing cholesterol crystals and should be avoided.

Epidemiology

A rare entity.

Etiology

Cholesterol granuloma of the orbit has been associated with a previous trauma. They are relatively rare and represented only 1 % of all orbital lesions in our series. Approximately 50 % of the cases of orbital cholesterol granulomas, however, are not associated with previous trauma. Thus, pathogenesis of cholesterol granuloma still remains unclear. It has been suggested that cholesterol is produced as a result of the breakdown of blood components, and this is followed by foreign body granuloma formation. The adjacent bony resorption is believed to be initiated by the prostaglandins produced by the platelets within the hematoma.

Localization

CT usually shows an isodense to hypodense osteolytic lesion in the superolateral bony orbit with an extraconal soft tissue mass, leading to inferior and anterior displacement of the globe.

Clinical Features

Typically, orbital cholesterol granulomas have a male predilection and occur between the ages of 30 and 60 years [36]. Orbital cholesterol granulomas have characteristic radiologic imaging findings.

Macroscopy

Reddish-brown granular material may be accompanied by thick, reddish-brown fluid.

Histopathology

Shows numerous slit-like spaces that represent cholesterol crystals surrounded by multinucleated foreign body-type giant cells, lipid-laden histiocytes, and clusters of hemosiderin deposits or hematoidin crystals (Fig. 12.20). Focal areas of calcified bone trabeculae may be noted. Scarce fibrous, amorphous, and necrotic areas may also be present.

Differential Diagnosis

Although the histopathological features of epidermoid cysts (cholesteatoma) and cholesterol granuloma can be very similar, the differentiating histopathological feature is the presence of epithelial elements in epidermoid or cholesteatoma and their absence in cholesterol granulomas [37]. Giant cell reparative granuloma of bone.

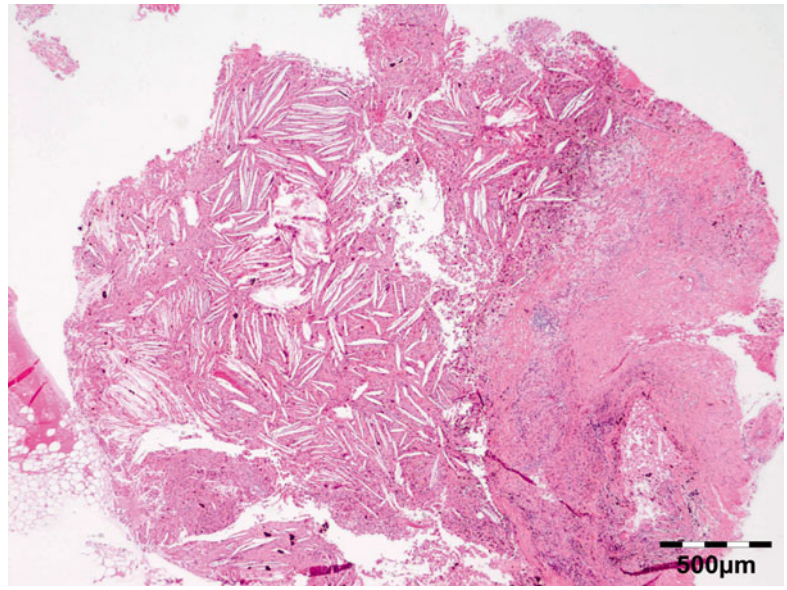

Fig. 12.20 Cholesterol granuloma: slit-like spaces that represent cholesterol crystals are surrounded by multinucleated foreign body-type giant cells, lipid-laden histiocytes, and clusters of hemosiderin deposits or hematoidin crystals. Focal areas of dystrophic calcification are present within amorphous and necrotic areas (HE 25×) (Dr. Robert M. Verdijk)

Histogenesis
Not applicable.

Genetics
Not applicable.

Prognosis and Predictive Factors
May recur after surgery.

12.4.2.2 Paraffinoma/Sclerosing Lipogranuloma

Definition
Lipogranulomatous inflammation reactive to exogenous paraffin (Fig. 12.21), silicone oil (used in retinal detachment) [38], Vaseline ointment containing antibiotics/ointment plug (after endonasal surgery) [39], or hydrogel (Fig. 12.22).

Epidemiology
Rare; paraffinoma represented only 1 % of all orbital lesions in our series and only 2.5 % of all inflammatory lesions.

Etiology
May be the result of surgical procedures or medical treatment but may also be observed as self-inflicted lesions such as unprofessional corrective introduction of exogenous materials into the tissues.

Localization
Extraconal.

Clinical Features
The symptoms are of a space-occupying inflammatory lesion.

Macroscopy
Normal pink to yellowish tissue may be observed.

Histopathology
The xanthogranulomatous inflammation exists as interstitial vacuolar clear rounded spaces with varying diameter surrounded by foamy macrophages giving the appearance of a "Swiss cheese pattern." In the case of ointment plugs, pigment of iodine may be observed. In older lesions the single granulomas consisting of tightly packed epithelioid cells may be separated by small strands of collagenous tissue containing vessels and lymph follicles, sometimes with germinal centers. The longer the granulomas exist, the more the vacuoles decrease in number while strands of dense connective tissue predominate, surrounding small islands of epithelioid histiocytes. Larger vacuoles are replaced by concentric layers of hyaline tissue.

Differential Diagnosis
Xanthoma, xanthogranuloma.

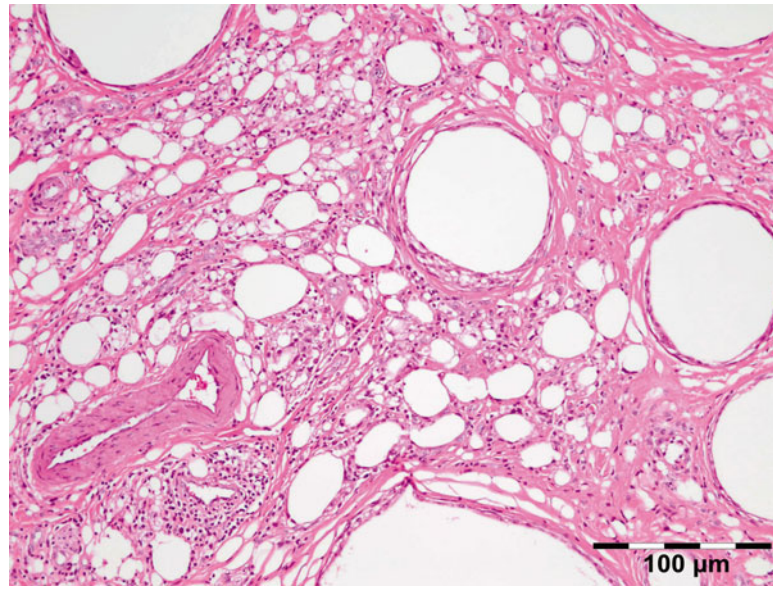

Fig. 12.21 Paraffinoma: a xanthogranulomatous inflammation with interstitial vacuolar clear rounded spaces with varying diameter surrounded by foamy macrophages, a "Swiss cheese pattern" (HE 200×) (Dr. Robert M. Verdijk)

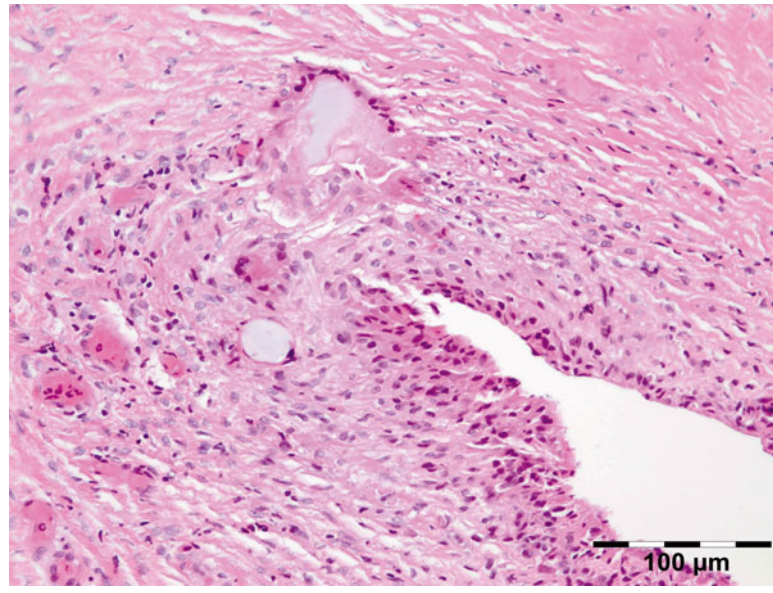

Fig. 12.22 Hydrogel granuloma: granulomatous inflammation with slit-like spaces and multinucleated macrophages filled with basophilic amorphous material (HE 200×) (Dr. Robert M. Verdijk)

Histogenesis

Not applicable.

Genetics

Not applicable.

Prognosis and Predictive Factors

Though not a common event, postoperative paraffin granuloma is a severe complication leading to chronic and recurrent disease with considerable functional impairment. The use of paraffin-containing ointment in sinus surgery should be abandoned, especially if peri- or postoperative bleeding occurs.

12.4.3 Immune Reactive Diseases

12.4.3.1 Thyroid Eye Disease

Definition

Graves' disease is an autoimmune inflammatory disorder, caused by thyroid autoantibodies resulting in hyperthyroidism.

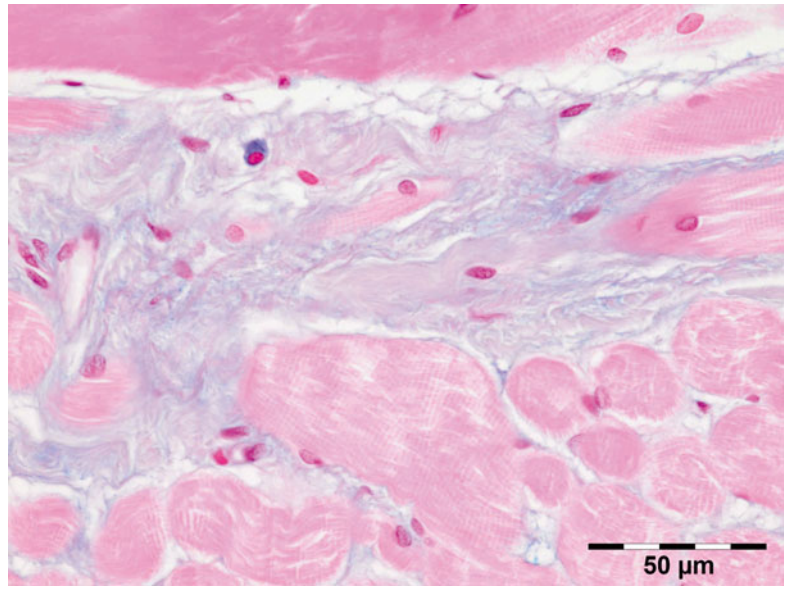

Fig. 12.23 Graves' orbitopathy: striated muscle fibers are separated by a widened interstitium with increased glycosaminoglycans that stain positive for alcian blue. An occasional mucin-stained macrophage is present (alcian blue 400×) (Dr. Robert M. Verdijk)

Epidemiology

About 30–50 % of patients with thyroid dysfunction will also suffer from Graves' orbitopathy. Thyroid eye disease usually presents during midlife but may occur in children, adolescents, and the elderly. These samples are rarely submitted for histopathological examination and represented only 1.5 % of all inflammatory lesions in our series.

Etiology

Inflammatory cells in the orbit produce factors activating orbital fibroblasts that probably play a key role in the pathogenesis of thyroid eye disease [40].

Localization

Involves the interstitial tissues of the extraocular muscles, most commonly the inferior rectus and medial rectus muscles. Also the orbital and preseptal fat may be involved.

Clinical Features

Swelling of the eye muscles, resulting in upper eyelid retraction, redness, conjunctivitis, and proptosis [41].

Macroscopy

Firm white edematous tissue fragments.

Histopathology

Histologic evaluation shows an increase of glycosaminoglycans (largely hyaluronic acid) that stain positive for alcian blue and collagen staining positive for Sirius red. A cellular infiltration may show admixed lymphocytes, plasma cells, macrophages, and mast cells (Fig. 12.23).

Differential Diagnosis

Infection, IOI.

Histogenesis

Fibroblasts and inflammatory cells are mesodermal-derived tissue. Tentatively, it might be that because the extraocular muscles are of mesectodermal rather than of mesodermal origin, they may be immunologically distinct from skeletal muscles.

Genetics

No genetic abnormalities have been reported.

Prognosis and Predictive Factors

Patients who fail to improve on medical or radiotherapeutic treatment may improve on decompressive surgery.

12.4.3.2 Inflammatory Pseudotumors

Idiopathic Orbital Inflammatory (IOI) Disease

Definition

A space-occupying inflammatory disorder that simulates a neoplasm but has no recognizable cause.

Synonyms

Idiopathic inflammatory pseudotumor (IIP), orbital pseudotumor. When restricted to the extraocular muscles, this condition may be called orbital myositis; when restricted to the lacrimal gland, it is frequently called (sclerosing) dacryoadenitis.

Epidemiology

IOI is one of the most common acute, painful orbital masses in the adult population. IOI is the second most common cause of exophthalmos following Grave's orbitopathy [42] and the third most common orbital disorder following thyroid orbitopathy and lymphoproliferative disease, accounting for 5–17.6 % of orbital disorders [43, 44]. IOI represented 8.5 % of all orbital lesions in our series and 29.5 % of all inflammatory lesions. There is no age, sex, or race predilection, but it is most frequently seen in middle-aged individuals. Pediatric cases account for 17 % of all cases of IOI [45].

Etiology

The exact etiology of IOI is unknown, but infectious and immune-mediated mechanisms have been postulated. IOI has also been observed in association with Crohn's disease, systemic lupus erythematosus, rheumatoid arthritis, diabetes mellitus, myasthenia gravis, and ankylosing spondylitis, all of which strengthen the basis of IOI being an immune-mediated disease. Response to corticosteroid treatment and immunosuppressive agents also supports this idea [43].

Localization

IOI can range from a diffuse inflammatory process to a more localized inflammation of the extraocular muscles (myositis), the adjacent adipose tissue, or the lacrimal gland (sclerosing dacryoadenitis).

Clinical Features

The symptoms are those of a space-occupying mass, associated with proptosis, and cranial nerve palsy (Tolosa–Hunt syndrome). The diagnosis is most commonly made on a clinical basis; however, in atypical cases orbital biopsy is required to exclude other orbitopathies [46]. IOI is a diagnosis of exclusion, both clinically and histopathologically.

Macroscopy

Gray-white solid mass with a variable aspect of fibrosis.

Histopathology

IOI is a nongranulomatous inflammation of lymphocytes, plasma cells, eosinophilic granulocytes, and often lymphoid follicles. The stroma may vary from edematous to fibrotic/sclerotic. It has been shown that the sclerosing subtype has a poorer response to steroid treatment (Fig. 12.24) [47].

Differential Diagnosis

Specific inflammatory reaction patterns such as multinucleated giant cells, granuloma, xanthogranuloma, vasculitis, necrosis, or necrobiosis should not be present.

Genetics

Oligoclonal or pseudomonoclonal B- or T-cell populations may be demonstrable, which however by itself does not provide proof of a lymphoma.

Prognosis and Predictive Factors

Response to corticosteroid treatment supports the postulate of immune-mediated disease [43]. Therapeutic modalities included observation alone, antibiotics, oral corticosteroids, intravenous corticosteroids, adjunctive radiation therapy, and systemic immunosuppressive drugs.

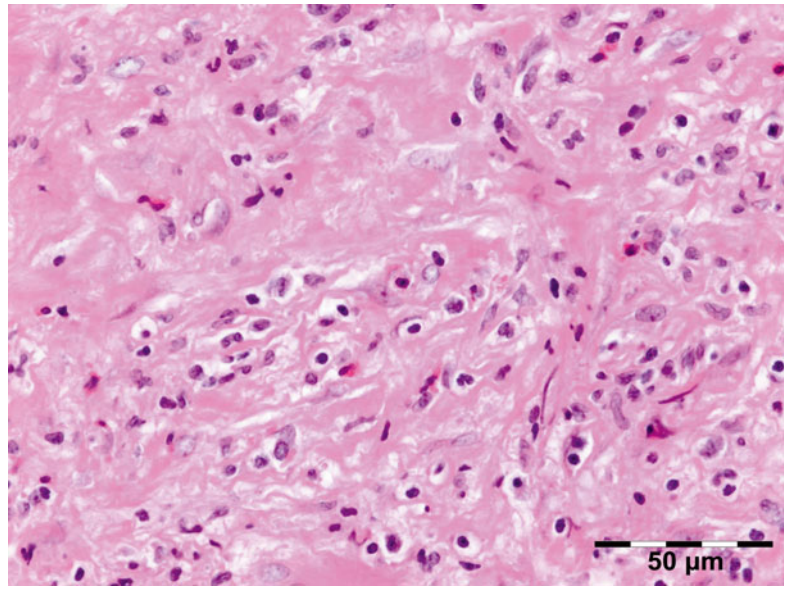

Fig. 12.24 Idiopathic orbital inflammation (IOI): inflammation of lymphocytes, plasma cells, eosinophilic granulocytes, and histiocytes. The stroma is severely fibrotic/sclerotic with an increase in collagen fibers (HE 400×) (Dr. Robert M. Verdijk)

IG4-Related Orbital Disease (IGRD)

Definition

IGRD is a recently defined inflammatory process characterized by tissue infiltration by IgG4-bearing plasma cells.

Epidemiology

IGRD affects males and females equally which is in contrast to IGRD pancreatitis [48]; the mean age of onset is 55 years.

Etiology

The pathogenesis of IgG4-related disease (IGRD) is poorly understood; findings consistent with both an autoimmune disorder and an allergic disorder are present [49].

Localization

Classical sites of involvement include the pancreas, hepatobiliary tract, salivary gland, lymph nodes, and retroperitoneum. IgG4-associated disease is now recognized as a systemic process. IGRD may also affect the lacrimal glands and periocular tissues [50]. IGRD also appears to account for 25–50 % of orbital pseudotumors and is additionally recognized now as a cause of orbital myositis (IgG4-related orbital myositis) [51]. The eyelid, lacrimal gland, extraocular muscle, orbital soft tissue, and nasolacrimal duct may all be affected. The conjunctiva has not been reported; the lacrimal gland is most common [49, 52–54]. Simultaneous involvement of two pairs of lacrimal glands, submandibular glands, or parotid glands is known as Mikulicz's disease.

Clinical Features

Presenting symptoms are painless eyelid swelling, proptosis with or without diplopia, and elevated levels of serum IgG4. IGRD is commonly associated with asthma and allergic rhinitis [52]. IgG4 may be a common marker for a heterogeneous group of diseases rather than a separate entity [55].

Macroscopy

Gray-white solid mass with a variable aspect of fibrosis.

Histopathology

IGRD is characterized by varying degrees of focal or diffuse fibrosis and IgG4-positive-rich lymphoplasmacytic infiltration, with subsets of pseudolymphomatous, mixed, or xanthogranulomatous pattern (Figs. 12.25 and 12.26) [56, 57]. For the histologic diagnosis of IGRD, the areas of maximum IgG4-positive

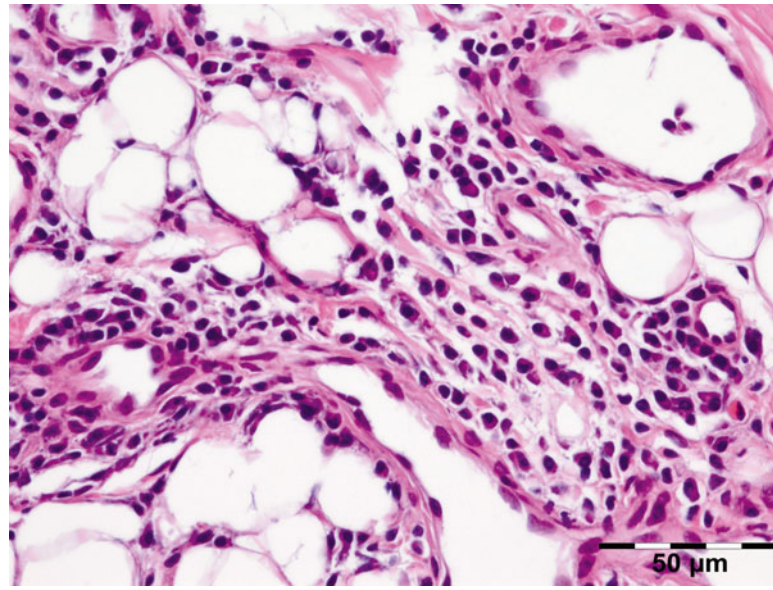

Fig. 12.25 IgG4-related orbital disease: the early phase of the disease shows a rich lymphoplasmacytic infiltration with perivascular involvement and a slight increase in collagen fibers (HE 400×) (Dr. Robert M. Verdijk)

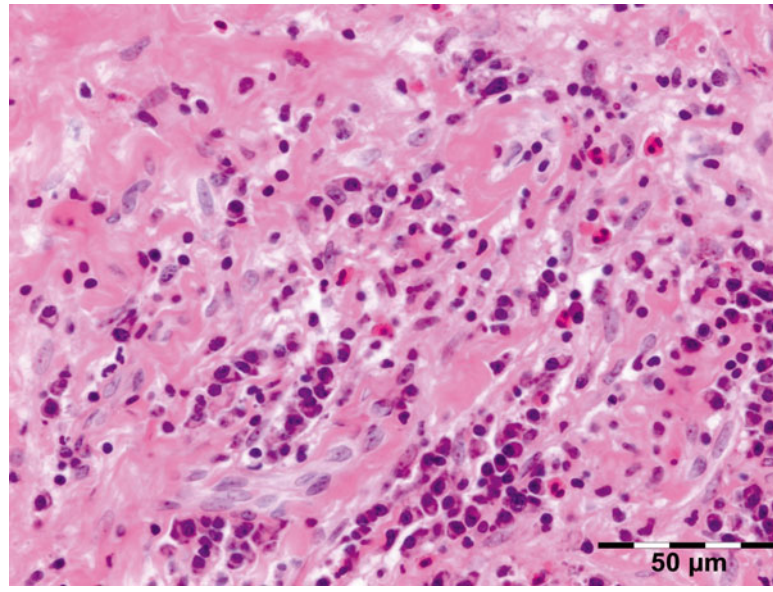

Fig. 12.26 IgG4-related orbital disease: the biopsy of a late recurrence (same patient as Fig. 12.25) after 20 years shows a severely sclerotic lesion with a rich lymphoplasmacytic infiltration with admixed eosinophils. Phlebitis or vasculitis is not always present in orbital disease (HE 400×) (Dr. Robert M. Verdijk)

staining should be selected [48]. The number of IgG4-positive plasma cells per high-power field (HPF) regarded as sufficient varies somewhat from tissue to tissue. Generally, the minimum for making the diagnosis for most tissues is from 30 to 50 IgG4-positive cells/HPF. The ratio of IgG4+/IgG+ should excess 0.4 (Figs. 12.27 and 12.28) [48]. Obliterative phlebitis is not a common feature in orbital IGRD [49].

Differential Diagnosis

IOI, Wegener's granulomatosis.

Genetics

No genetic abnormalities have been reported.

Prognosis and Predictive Factors

A good initial therapeutic response to glucocorticoids is characteristic. Patients may improve spontaneously without treatment, but

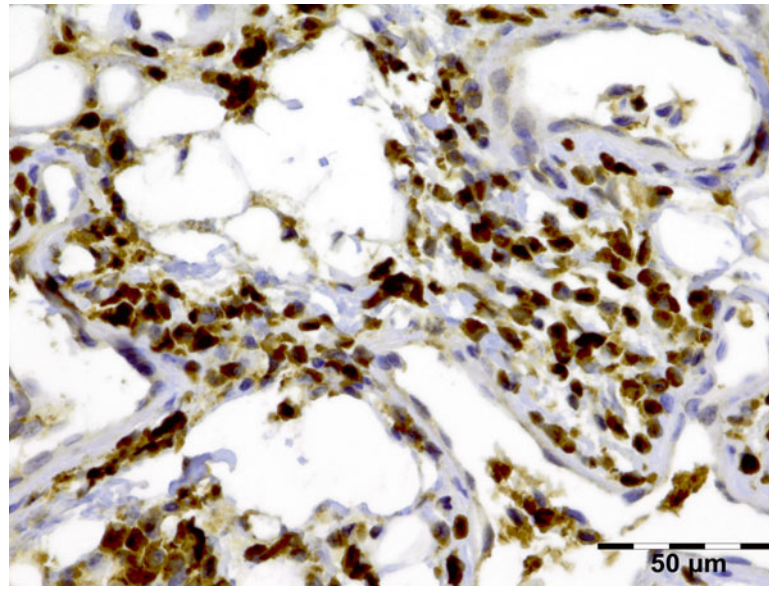

Fig. 12.27 IgG4-related orbital disease: immunohistochemical staining for IgG shows an increased amount of IgG-positive plasma cells of over 50/HPF (IgG IH 400×) (Dr. Robert M. Verdijk)

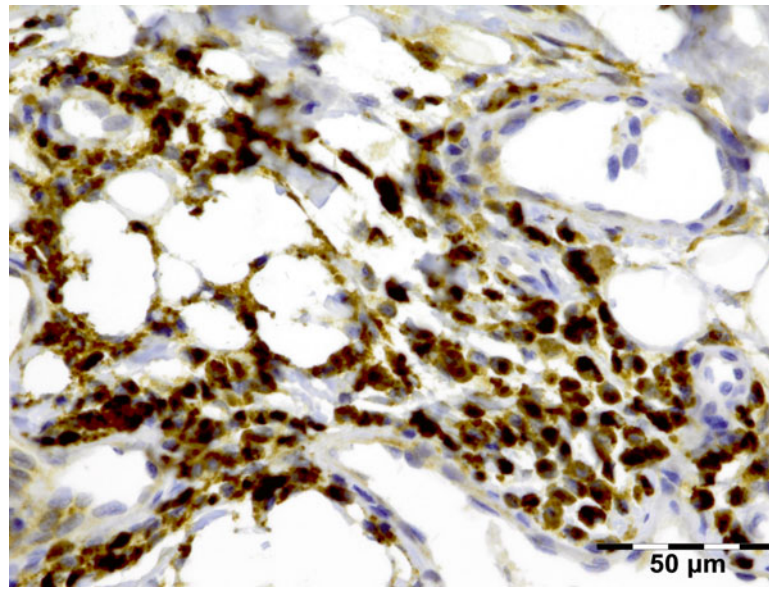

Fig. 12.28 IgG4-related orbital disease: immunohistochemical staining for IgG4 shows a clearly increased amount of IgG-positive plasma cells of over 50/HPF in a high ratio when compared to IgG (IgG4 IH 400×) (Dr. Robert M. Verdijk)

many relapse in time. Sustained benefit may be observed in treated patients, but relapses are common after discontinuation of therapy. Additional organs and tissues may become involved over time, sometimes despite apparently effective treatment. Extranodal marginal zone B-cell lymphoma of the mucosa-associated lymphoid tissue may be associated with IGRD [58].

Xanthogranulomatous Inflammatory Diseases

Definition

A disease characterized by histiocytes, Touton giant cells, and lymphocytic inflammation.

Orbital xanthogranulomatous disease constitutes a group of entities with varying manifestations that are poorly understood. The clinical

presentation in adults consists of uni- or bilateral orbital mass lesions or periocular yellow-brown infiltrates that may mimic xanthelasmata. These abnormalities tend to progress, causing eyelid disfigurement, eyeball displacement, eyeball motility disturbances, and – rarely – optic neuropathy. Orbital xanthogranulomatous disease is now considered to constitute a spectrum of four entities: adult-onset xanthogranuloma (AOX) (solitary lesion without systemic findings), adult-onset asthma and periocular xanthogranuloma (AAPOX), necrobiotic xanthogranuloma (NBX), and Erdheim–Chester disease (ECD). The association between orbital xanthogranuloma and other autoimmune diseases may be present. In a patient series, the co-occurrence of asthma, psoriasis, granuloma annulare, and idiopathic thrombocytopenic purpura was noted [59].

Epidemiology

Xanthogranulomatous disease of the orbit is rare, representing 5 % of all inflammatory orbital lesions and only 1.5 % of all orbital diseases in our series, making prospective evaluation or meta-analysis impossible. Usually, the onset is in middle age.

Etiology

According to the 2008 WHO classification [60], the disease should be classified as a dendritic cell disorder. Dendritic cells are derived from myeloid stem cells and the circulating peripheral blood monocyte pool. Dendritic cell disorders include Langerhans cell histiocytosis (LCH) (CD1a, S-100 positive) and non-LCH (CD1a -, CD68+, FXIIIa+), including juvenile xanthogranuloma, solitary reticulohistiocytoma, and ECD. In a retrospective case series, we have identified IgG4-positive plasma cells in 50 % of all orbital xanthogranulomas indicating an immunomodulatory mechanism that involves IgG4 production in many cases [61].

Localization

Patients classified as AOX, AAPOX, and NBX typically have preseptal and anterior orbital involvement. ECD tends to be diffuse and intraconal. Yellow skin lesions are found in all the syndromes [59].

Genetics

No genetic abnormalities have been reported except for ECD.

Erdheim–Chester Disease (ECD)

Erdheim–Chester disease (synonyms: Erdheim–Chester syndrome, polyostotic sclerosing histiocytosis). The disease involves an infiltration of lipid-laden macrophages, multinucleated giant cells, an inflammatory infiltrate of lymphocytes and histiocytes, and varying fibrosclerosis. It is the most devastating of the adult xanthogranulomas and is characterized by dense, progressive, recalcitrant fibrosclerosis of the orbit and internal organs, including the mediastinum; pericardium; pleural, perinephric, and retroperitoneal spaces; the bone marrow; and a generalized sclerosis of the long bones. A more complete description is given below in Sect. 12.7.11.2.

Adult-Onset Xanthogranuloma (AOX)

AOX is an isolated xanthogranulomatous lesion without systemic involvement and is associated with immune dysfunction: lymphoproliferative disease (benign/malignant) [59]. The extraocular muscles, adnexal tissue, and lacrimal gland may be affected by an infiltration of foamy histiocytes, Touton giant cells, lymphocytes, and varying degrees of fibrosis (Fig. 12.29). Adult-onset xanthogranuloma is the least aggressive of the xanthogranulomatous syndromes. It is strictly limited to the anterior orbital tissue, without any systemic findings, internal organ involvement, or immune dysfunction such as monoclonal gammopathy or lymphoproliferative disease.

Adult-Onset Asthma with Periocular Xanthogranuloma (AAPOX)

AAPOX is a syndrome that was described by Jakobiec et al. [62]. It is rare (approximately 25 cases reported in the literature) and affects adults aged between 22 and 74 years, with a male to female ratio of 2:1. The association with lymphadenopathy suggests an underlying stimulation and proliferation of B-cell populations [59]. It

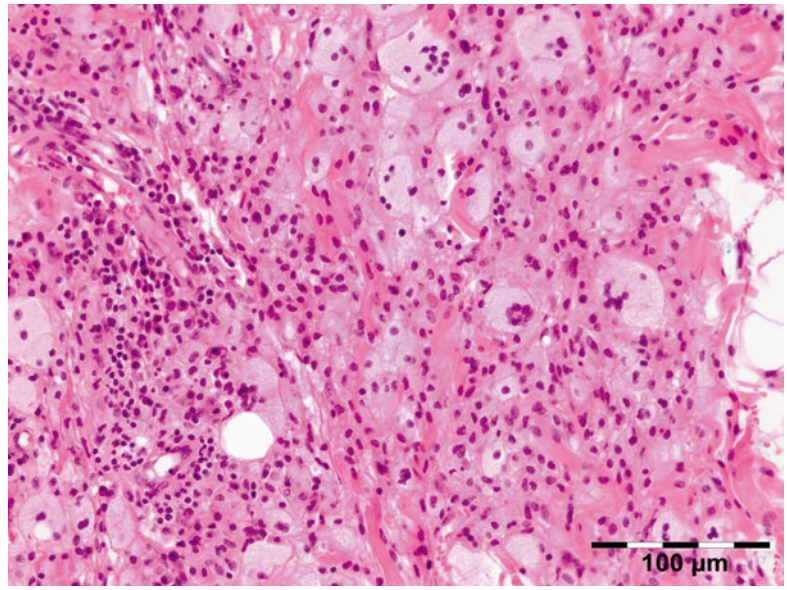

Fig. 12.29 Adult-onset xanthogranuloma (AOX): the tissue is infiltrated by foamy histiocytes, Touton giant cells, and lymphocytes with a low degree of fibrosis (HE 200×) (Dr. Robert M. Verdijk)

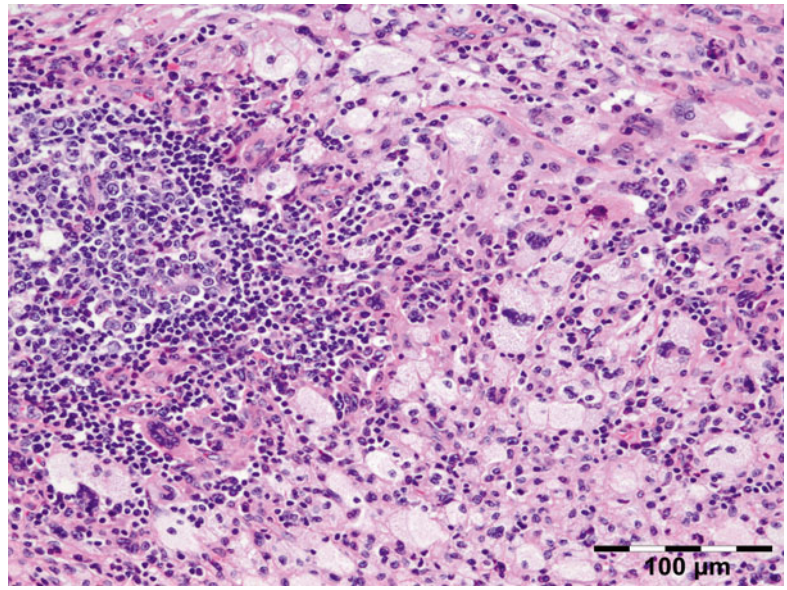

Fig. 12.30 Adult-onset asthma with periocular xanthogranuloma (AAPOX): like in all xanthogranulomas, there are foamy histiocytes and Touton giant cells. Note the large lymphoid aggregates with classic germinal centers (HE 200×) (Dr. Robert M. Verdijk)

affects the eyelids and orbit. Orbital involvement affects the anterior and preseptal compartments. Intraconal involvement has only been reported in one patient. AAPOX always presents with bilateral yellow or orange, indurated, and non-ulcerated xanthomatous periocular masses. In addition to asthma, cases of AAPOX often have increased polyclonal IgG levels and lymphadenopathy. Histopathologic examination typically finds foamy histiocytes, Touton giant cells, and large lymphoid aggregates with classic germinal centers and no necrosis or fibrosis (Fig. 12.30). AAPOX is not a sight-threatening disease, but visual function can be impaired in the long term by eyelid occlusion or extraocular muscle infiltration.

Necrobiotic Xanthogranuloma

NBX is associated with immune dysfunction with monoclonal paraproteinemia (80 %),

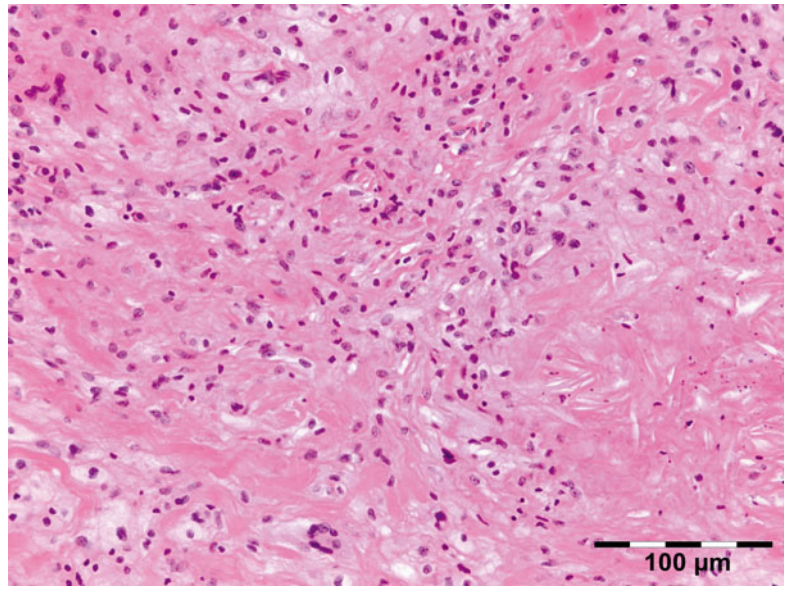

Fig. 12.31 Necrobiotic xanthogranuloma (NBX): in addition to a xanthogranulomatous inflammation with foamy histiocytes and Touton giant cells, there is necrosis surrounded by palisading epithelioid histiocytes. Fibrosis is another feature shown (HE 200×) (Dr. Robert M. Verdijk)

hypocomplementemia, cryoglobulinemia, multiple myeloma, and non-Hodgkin lymphoma (NHL) [62]. It is localized in the subcutaneous skin of the eyelids and anterior orbit but also occurs throughout the body. NBX affects adults (mean age 60 years). Although skin lesions are seen in all the syndromes, those in NBX have a strong propensity to ulcerate and fibrose. Internal organ involvement occurs in NBX but is often found only at autopsy. On histology there is a xanthogranulomatous inflammation with foamy histiocytes, Touton giant cells, and varying degrees of fibrosis. The presence of necrobiosis is required. Necrosis with palisading epithelioid histiocytes differentiates it from the other adult orbital xanthogranulomatous diseases (Fig. 12.31).

Prognosis

Time to development of associated malignancy ranges from 8 years before the skin lesions to 11 years after the skin lesions. Overall survival is 100 % at 10 years and 90 % at 15 years [63].

Juvenile Orbital Xanthogranuloma (JOX)

JOX, occurs only in children, patients are under 20 years of age (80–90 % under 2 years). It is localized in the orbit [64], and eyelids, conjunctiva, and iris may be involved. Patients usually present with yellow-red skin nodules that regress spontaneously. Iris infiltration can cause hyphema and glaucoma. Histopathology reveals an infiltrate of histiocytes with a finely vacuolated or xanthomatous cytoplasm, lymphocytes, and eosinophils. JOX pathology is notable for Touton giant cells. Immunohistochemistry shows positive staining for factor XIIIa, CD68, CD163, fascin, and CD14 and negative staining for CD1A, GFAP, desmin, keratin, CD99, and S-100. The differential diagnosis consists of xanthoma, other non-LCH, granulocytic sarcoma, or solitary fibrous histiocytoma. JOX has been described in patients suffering from NF1 or NF2. One case with a chromosomal aberration 46,XY,inv(13)(q21q33)c has been described [65]. Lesions usually regress or stabilize with time and have an excellent prognosis. Surgical excision is the mainstay treatment of choice in solitary lesions.

Wegener's Granulomatosis (WG)

Definition

Small vessel vasculitis with autoimmune attack by ANCAs (antineutrophil cytoplasmic antibodies).

Synonyms

Granulomatosis with polyangiitis, ANCA-associated granulomatous vasculitis (professional

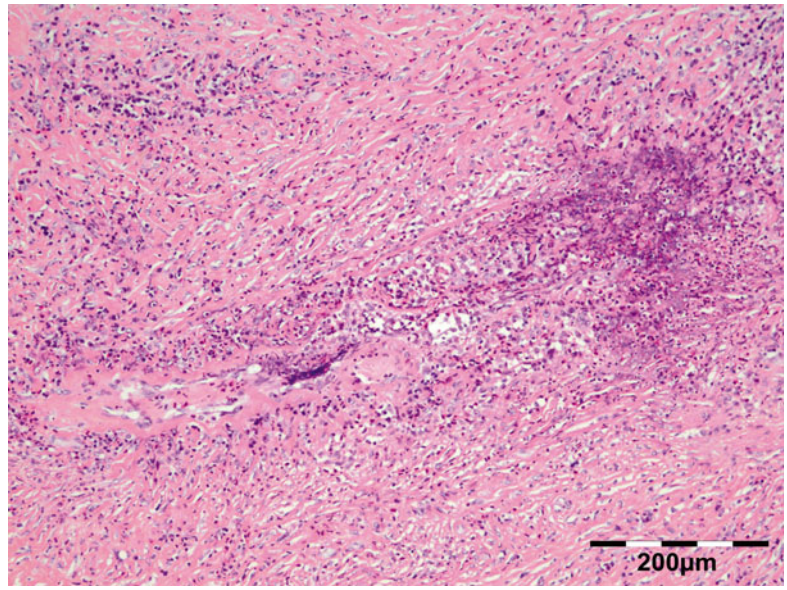

Fig. 12.32 Wegener's granulomatosis: there is a mixed inflammatory cell population containing lymphocytes, histiocytes, eosinophilic, and notably neutrophilic polymorphonuclear cells in an angiocentric orientation and necrotic vasculitis. There is a severe sclerosis and areas of necrosis (HE 100×) (Dr. Robert M. Verdijk)

bodies have advocated a more descriptive name since 2000 [66]; however this has not been generally adopted).

Epidemiology

WG represented 4 % of inflammatory lesions in our series. The incidence is ten cases per million per year. Ninety percent of the patients are white. While it mainly occurs in the middle-aged, it has been reported in much younger and older patients.

Etiology

It is presumed that the ANCAs are responsible for the inflammation in WG.

Localization

WG may present as an orbital mass without obvious upper respiratory or systemic features, but often is associated with ear nose and throat features and/or scleritis.

Clinical Features

C-ANCA testing is initially often negative but may become positive during late reactivation [67].

Macroscopy

Fibrotic, often hemorrhagic tissue fragments.

Histopathology

Orbital biopsies typically have features of mixed sclerosing, often angiocentric, inflammation, with fat disruption and small areas of necrosis, and focal microabscesses (Fig. 12.32). The findings of smudgy necrosis must not be regarded as a nonspecific finding (Fig. 12.33) [67]. Often there is no presence of fibrinoid necrosis of the vessels.

Differential Diagnosis

Infectious granulomatous vasculitis, temporal arteritis, polyarteritis nodosa.

Histogenesis

Not applicable.

Genetics

HLA-DPB1 association with WG has been described; it is still the strongest and best replicated risk locus for this condition. Numerous other associations, including CTLA4, CD226, and copy number polymorphisms of FCGR3B, still need further investigation, before reliable conclusions can be drawn.

Prognosis and Predictive Factors

Twenty-five to forty percent of patients suffer from flare-ups, but a majority respond well to

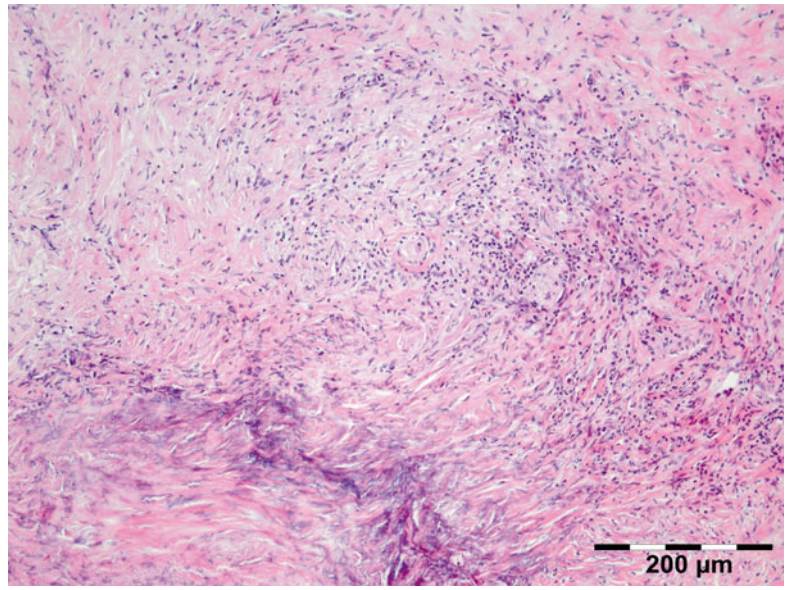

Fig. 12.33 Wegener's granulomatosis: smudgy necrosis as depicted in the lower left of the photograph is not an aspecific finding in orbital inflammatory pseudotumors (HE 100×) (Dr. Robert M. Verdijk)

treatment. Relapses can be long and troublesome. Long-term complications are very common (86 %): mainly chronic renal failure, hearing loss, and deafness. Patients with the limited form of WG have a better prognosis because of the absence of kidney disease.

Vasculitis

Noninfectious vasculitides, apart from WG, comprise a large number of diseases. Many of these diseases can affect the orbit and lead to a clinical presentation, which mimics numerous other orbital processes. Orbital disease can be the initial presentation of a systemic vasculitis and early diagnosis can help prevent long-term, potentially fatal, consequences [68]. Panniculitis, also known as lupus erythematosus profundus involving orbital structures as the primary presenting symptom of SLE, has been described [69]. Churg–Strauss syndrome has been described in patients presenting with ocular manifestations and concurrent ear, nose, and throat symptoms and arthralgia or with positive ANCA and eosinophilia (Fig. 12.34) [70]. In rare cases orbital infarction may be associated with giant cell arteritis (Fig. 12.35) [71].

Sarcoidosis

Sarcoidosis is a multisystem disorder characterized histopathologically by noncaseating granulomas. It affects both sexes equally, and although it can present at any age, it usually develops before 50 years of age. In the United States, the annual incidence of sarcoidosis is estimated to be 36 in 100,000 for black persons and 11 in 100,000 for white persons, with 3.8-fold greater risk of developing sarcoidosis in black persons. Sarcoidosis most commonly involves the lungs and the mediastinal lymph nodes (86–92 %), the eye and ocular adnexa (10–50 %), the peripheral lymph nodes (33 %), the skin (10–40 %), the central nervous system (10 %), and the heart (5 %). Sarcoidosis can affect any part of the eye, orbit, and adnexal structures. Orbital and adnexal involvement includes the lacrimal gland in 63 % (19/30), the eyelid in 17 % (5/30), the orbit in 13 % (4/30), and the lacrimal sac in 7 % (2/30) [72]. Sarcoidosis represented 9 % of inflammatory lesions in our series and 2.5 % of all orbital lesions. Orbital and adnexal sarcoidosis usually presents as enlargement of the lacrimal gland(s) but also can present as a diffuse, solid mass with irregular infiltration of orbital structures, extraocular muscles, or lacrimal sac. The most common signs are those of inflammation: erythema (70 %) and edema of the eyelids (36 %). Thirty-seven percent of patients with periorbital sarcoidosis (11/30) have known

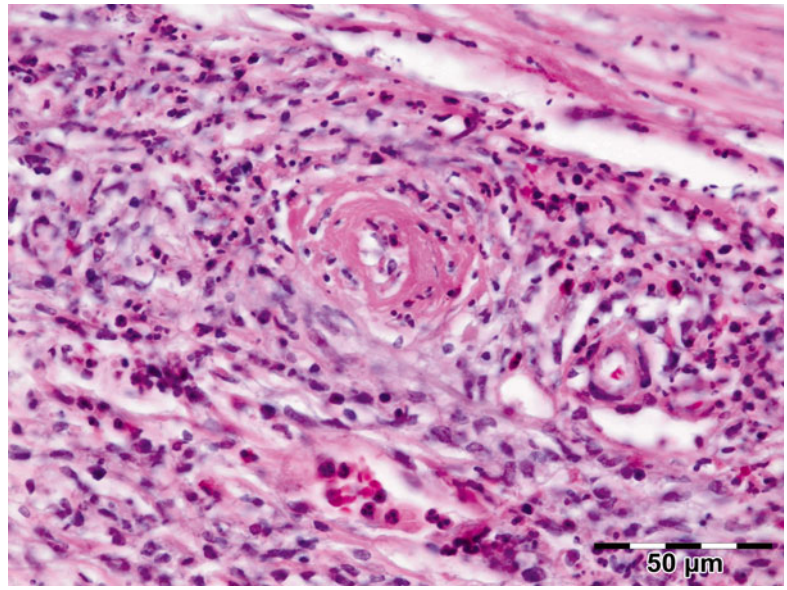

Fig. 12.34 Churg–Strauss syndrome: depicted is a necrotic vasculitis with a notable eosinophilic infiltrate and fibrosis. The histology is comparable to Wegener's granulomatosis. This patient had peripheral blood eosinophilia in addition to positive ANCA (HE 400×) (Dr. Robert M. Verdijk)

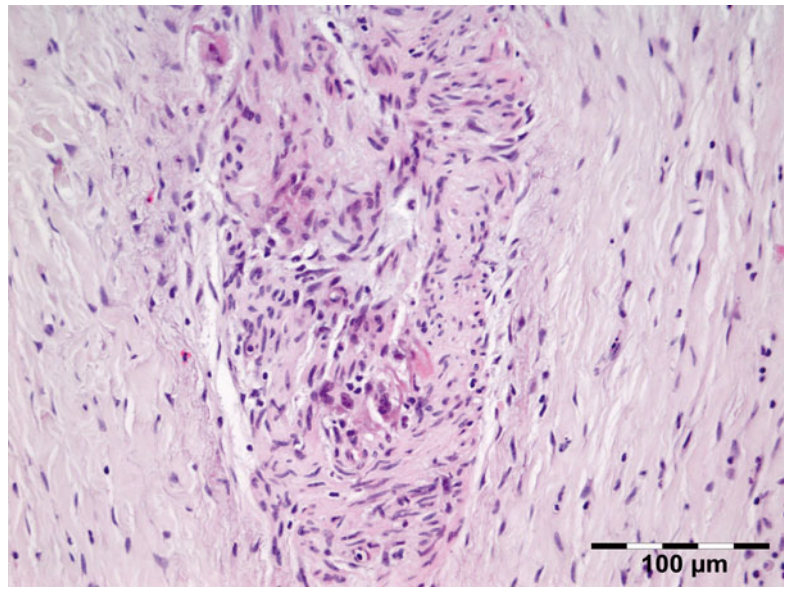

Fig. 12.35 Giant cell arteritis: thick-walled muscular artery infiltrated by lymphocytes, histiocytes, and multinucleated giant cells. In the fibrotic surrounding stroma admixed eosinophils are present (HE 400×) (Dr. Robert M. Verdijk)

systemic disease [72]. Of 63 % (19/30) of cases with only orbital disease, systemic disease initially was found in 27 % (8/30), subsequently in 7 % (2/30), and never in 30 % (9/30) [72]. On computed tomography scans, the lesions were well circumscribed in 85 % (25/30) and diffuse in 15 % (5/30) [72]. The lesion consists of generally non-necrotizing granulomas (Fig. 12.36). Management includes systemic steroids, excision, and observation. Periocular steroid injections have been used for localized orbital disease with good results.

12.5 Injuries

12.5.1 Traumatic Neuroma

Definition

A proliferation of Schwann cells and connective tissue on the proximal end of a severed nerve.

Epidemiology

Unknown; may occur more often postsurgery without clinical symptoms. Traumatic neuroma

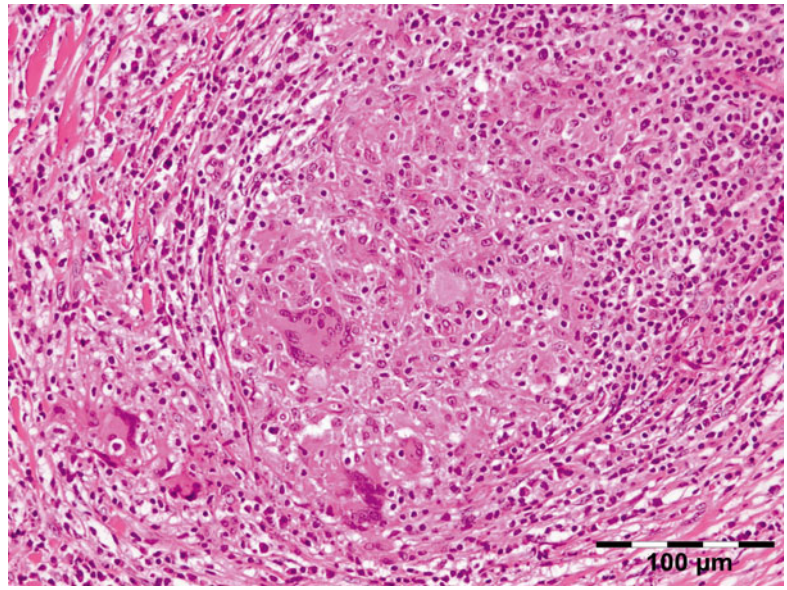

Fig. 12.36 Sarcoidosis: a central non-necrotizing granuloma consisting of histiocytes and multinucleated giant cells is surrounded by lymphocytes and plasma cells. There is a severe fibrosis of the stroma (HE 200×) (Dr. Robert M. Verdijk)

represented less than 1 % of all orbital lesions in our series and 19 % of all neurogenic tumors.

Etiology
New axons emerge and tend to follow the Schwann cells.

Localization
At the site of previous trauma or surgical procedure.

Clinical Features
The mass may assume tumorlike proportions. Simple resection is the proper treatment option [73].

Macroscopy
Fibrotic nerve tissue.

Histopathology
The erratically ensheathed axons are embedded in scar tissue and course in all directions (Fig. 12.37).

Differential Diagnosis
Neurofibroma, perineurioma.

Histogenesis
The orbital nerves are derived from the cranial nerves.

Genetics
Not applicable.

Prognosis and Predictive Factors
Recurrence of traumatic neuroma may occur after resection.

12.6 Degenerations

12.6.1 Fat/Lacrimal Gland Prolapse

Definition
Fat/lacrimal gland prolapse is an acquired lesion, characterized by a herniation of intraconal fat due to weakness of the Tenon capsule by the aging process, trauma, or surgery.

Epidemiology
In adults it is associated with elderly adipose patients. Fat and lacrimal gland prolapse represented 2 % of all lesions in our series and 35 % of all degenerative lesions.

Etiology
Orbital fat prolapse may be congenital when the fibrous tissues of the orbital septum are absent or underdeveloped [20] or may be the result of trauma or degeneration [74].

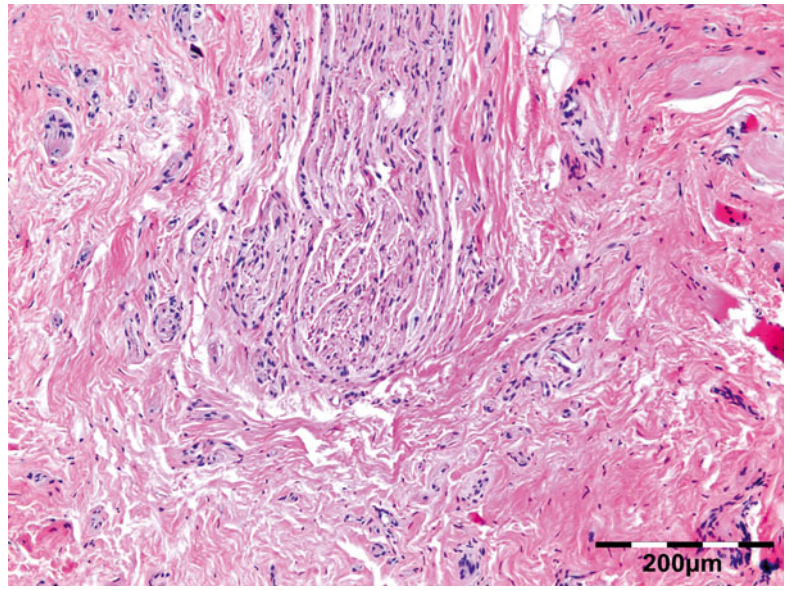

Fig. 12.37 Traumatic neuroma: centrally a nerve fiber is shown in a fibrotic stroma surrounded by erratically ensheathed axons that course in all directions (HE 100×) (Dr. Robert M. Verdijk)

Localization
Fat prolapse usually occurs in the lateral canthal area beneath the temporal or superotemporal bulbar conjunctiva.

Clinical Features
Patients with subconjunctival fat prolapse present with a fatty mass in the lateral canthal area either unilaterally or bilaterally.

Macroscopy
Normal fatty tissue is observed.

Histopathology
Normal fatty tissue is observed.

Differential Diagnosis
Fat prolapse and dermolipoma are two distinct entities of the orbit that are often confused clinically. The distinction with extremely rare lipoma of the orbit cannot be made on a histopathologic basis.

Histogenesis
Orbital fat is of mesenchymal origin as is the orbital septum.

Genetics
No genetic defects have been described.

Prognosis and Predictive Factors
Surgical removal through a perilimbal conjunctival incision can easily be done if the lesion is cosmetically unacceptable or causes discomfort.

12.6.2 Amyloidosis

Definition
Amyloidosis is a disorder of protein metabolism characterized by the extracellular deposition of abnormal protein fibrils.

Epidemiology
Orbital amyloidosis is extremely rare regardless of the etiology and represented only two cases (far less than 1 %) in our series.

Etiology
A classification system divides amyloidoses into three categories: (1) local amyloidosis, (2) hereditary systemic amyloidosis, and (3) acquired systemic amyloidosis [75]. Acquired systemic amyloidoses can be further subdivided into systemic AL amyloidosis (previously known as primary amyloidosis), reactive systemic AA amyloidosis (previously known as secondary amyloidosis), Aβ2M amyloidosis (dialysis-

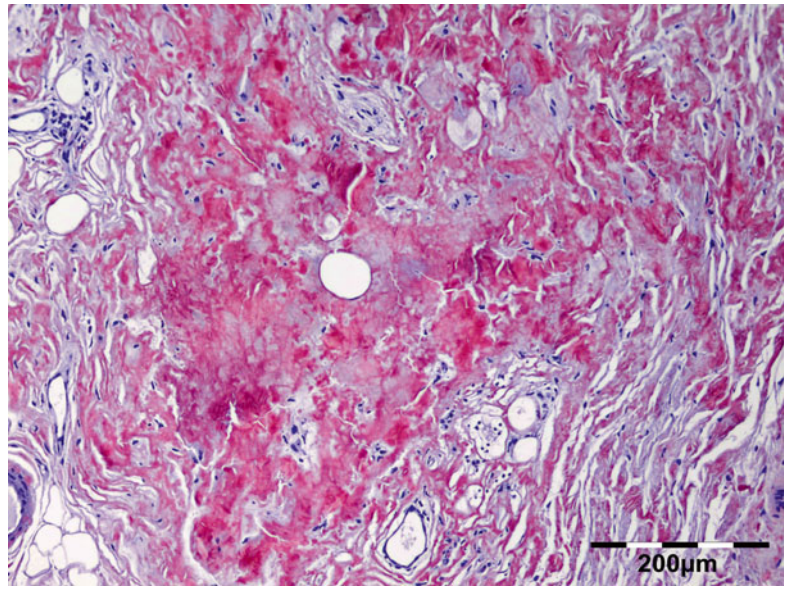

Fig. 12.38 Amyloidosis: the fat tissue shows interstitial deposits of eosinophilic amorphous hyaline material (Congo red 100×) (Dr. Robert M. Verdijk)

associated), and ATTR amyloidosis (senile amyloidosis). Systemic AL amyloidosis is almost always associated with a plasma cell dyscrasia, with multiple myeloma accounting for 20 % of these cases. Controversy exists in the literature as to whether orbital amyloidosis is more frequently due to primary localized disease or secondary to systemic amyloidosis.

Localization

It may be localized [76] or distributed throughout the body, causing organ damage and serious morbidity.

Clinical Features

The implication of missing a potentially life-threatening disease necessitates that a systemic investigation be completed before the diagnosis of primary localized orbital amyloidosis is made [77].

Macroscopy

The biopsy consists of fibroadipose tissue with a flesh-colored to yellow waxy appearance.

Histopathology

The tissues show interstitial deposits of eosinophilic amorphous hyaline material. Complete diagnosis of amyloid may be carried out in two steps on tissue sections. Congo red stain reveals the hyaline stromal deposits (Fig. 12.38) to demonstrate apple-green birefringence under polarized light (Fig. 12.39). The second diagnostic step is the identification of the amyloid protein. Immunohistochemistry using a panel of antibodies directed against kappa or lambda light chain, AA protein, ATTR protein, and Abeta2M may be used.

Genetics

ATTR amyloid is associated with hereditary syndromes including familial amyloid polyneuropathies and familial amyloid cardiomyopathies and can be diagnosed by molecular genetic analysis [78].

Prognosis and Predictive Factors

Each of the chemical amyloid types has a different prognosis and requires a different therapy.

12.7 Neoplasms

Neoplasms may vary from benign to high-grade malignant. In soft tissue sarcomas the modified three-tiered FNCLCC system is based on a score obtained by evaluating three parameters: tumor differentiation, mitotic rate, and amount of tumor

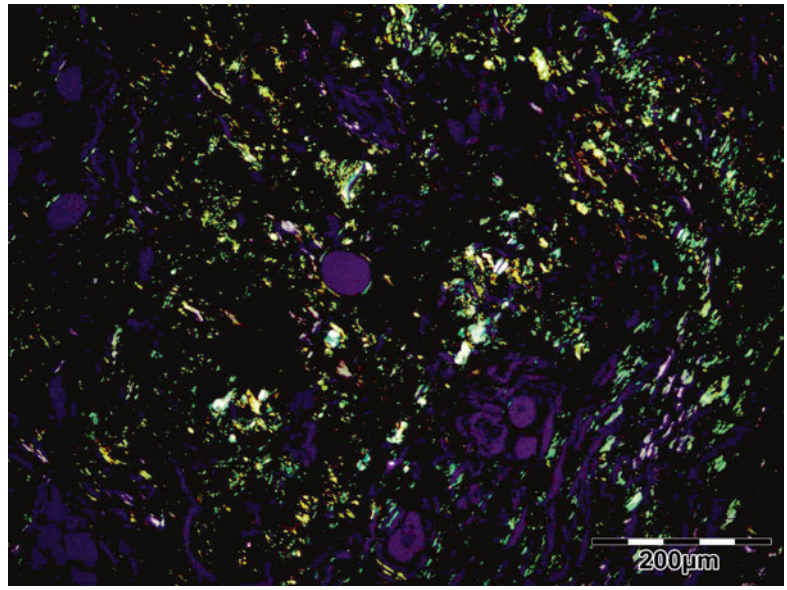

Fig. 12.39 Amyloidosis: apple-green birefringence can be demonstrated under polarized light (Congo red, polarized light 100×) (Dr. Robert M. Verdijk)

necrosis. A score is attributed independently to each parameter and the grade is obtained by adding the three attributed scores. Tumor differentiation: Score 1: sarcomas closely resembling normal adult mesenchymal tissue (e.g., low-grade leiomyosarcoma). Score 2: sarcomas for which histologic typing is certain (e.g., myxoid liposarcoma). Score 3: embryonal and undifferentiated sarcomas, sarcomas of doubtful type, synovial sarcomas, osteosarcomas, and PNET. Mitotic count: Score 1: 0–9 mitoses per 10 HPF. Score 2: 10–19 mitoses per 10 HPF. Score 3: >20 mitoses per 10 HPF. Tumor necrosis: Score 0: no necrosis. Score 1: <50 % tumor necrosis. Score 2: >50 % tumor necrosis. Histologic grade: Grade 1: total score 2, 3. Grade 2: total score 4, 5. Grade 3: total score 6, 7, 8.

12.7.1 Fibroblastic/Myofibroblastic/Fibrohistiocytic Tumors

12.7.1.1 Nodular Fasciitis

Definition

Nodular fasciitis is a benign, reactive, self-limiting, fibroblastic lesion [79].

Synonyms

The original designation of subcutaneous pseudosarcomatous fibromatosis should be avoided.

Epidemiology

Nodular fasciitis occurs in all age groups but more often in young adults. There is no sex predilection for nodular fasciitis or intravascular fasciitis, but cranial fasciitis is more frequent in boys. We only encountered one case in our series.

Etiology

Unknown.

Localization

Nodular fasciitis is typically located anteriorly in the periorbital area and is well circumscribed. Nodules most commonly develop in the subcutaneous or superficial fascia of the extremities. Nodular fasciitis is rarely observed in the head and neck region of adults; however, these locations are more common in infants and children [80]. In children it tends to occur in the anterior periorbital tissues, but it has also been reported to occur in the orbit where it can simulate a dermoid cyst [81]. Other cases involved the Tenon capsule [82, 83].

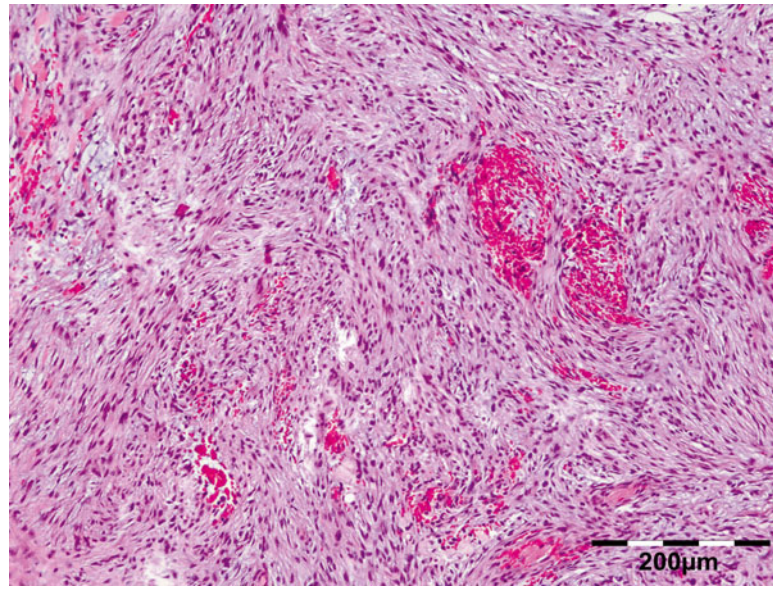

Fig. 12.40 Nodular fasciitis: spindle cell fibroblasts are arranged in parallel bundles extending in all directions resembling cells in tissue culture loose appearing and myxoid. There are extravasated red cells and few chronic inflammatory cells (HE 100×) (Dr. Robert M. Verdijk)

Clinical Features

Mostly these are solitary masses that grow rapidly in a course of several weeks. In about 50 % of the cases the swelling is painful.

Macroscopy

Nodular fasciitis may appear circumscribed or infiltrative but has no capsule or pseudocapsule. The cut surface varies from myxoid to fibrous, and occasionally there is central cystic change.

Histopathology

Classically there is the proliferation of spindle cell fibroblasts which are frequently arranged in parallel bundles extending in all directions resembling cells in tissue culture (Fig. 12.40). Mitoses may be numerous, but the spindle cell nuclei are never hyperchromatic and atypical mitoses are virtually never seen [84, 85]. The lesion may be highly cellular, but typically it is at least partly loose appearing and myxoid. There is normally little collagen. Extravasated red cells, chronic inflammatory cells, and multinucleated osteoclast-like giant cells are frequently identified. The lesional border is typically, at least focally, infiltrative. A vascular component may consist of capillary spaces or endothelial cells lined up in columns. Stains for SMA and MSA are usually positive, consistent with myofibroblastic differentiation but this does not distinguish nodular fasciitis from many other mesenchymal proliferations. CD68 staining is present in the osteoclast-like giant cells and occasionally in spindle cells. Keratin and S-100 protein are typically negative.

Differential Diagnosis

Myxoma, fibrous histiocytoma, fibromatosis, inflammatory myofibroblastic tumor (IMT), sarcoma (fibrosarcoma, myxofibrosarcoma). The lesion is myofibroblastic in nature.

Genetics

Normal diploid DNA.

Prognosis and Predictive Factors

There is no evidence of aggressive clinical behavior, recurrence, or metastasis.

12.7.1.2 Myofibroma/ Myofibromatosis

Definition

Myofibroma and myofibromatosis are terms used to denote the solitary (myofibroma) or multicentric (myofibromatosis) occurrence of benign neoplasms composed of myoid cells arranged around thin-walled blood vessels [79].

Synonyms

Congenital fibrosarcoma, congenital generalized fibromatosis, infantile myofibromatosis.

Epidemiology

Although rare, with only two cases in our series, myofibroma is the most common fibrous tumor of childhood. Solitary cases are more common in males.

Etiology

Infantile myofibromatosis was first described by Stout in 1954 as "congenital generalized fibromatosis" and was renamed as infantile myofibromatosis by Chung and Enzinger in 1981 after recognition of the myofibroblastic nature of the lesion (referenced in [86]). Myofibroma(tosis) forms a morphological continuum with myopericytoma and so-called infantile hemangiopericytoma and infantile myofibromatosis.

Localization

Approximately half of solitary myofibromas occur in the cutaneous/subcutaneous tissues of the head and neck region. Solitary tumors may be located intraosseous in the craniofacial bones [87–89].

Clinical Features

Solitary myofibroma is characterized by the presence of one nodule in the skin, muscle, bone, or subcutaneous tissue. The multicentric type can be divided into two subtypes: multicentric lesions with or without visceral involvement. The tumors are benign, nonencapsulated, and locally infiltrating and generally follow a benign course. Isolated orbital infantile myofibromas are rare tumors in the head and neck. The mass-like clinical presentation and variable histologic features result in frequent misdiagnosis and potentially inappropriate clinical management. Twenty-four patients with orbital infantile myofibroma or myofibromatosis were reviewed [87] aged newborn to 10 years (mean, 34.8 months), who presented with a painless mass in the infra- or supraorbital regions, usually increasing in size and associated with exophthalmos. The tumors were twice as frequent on the left as on the right. Patients experienced symptoms for an average of 2.7 months before clinical presentation. The tumors involved the bone or the soft tissues of the orbit, some with extension into the nasal or oral cavity.

Macroscopy

The mean tumor size is 3.0 cm. Grossly, tumors are well circumscribed, firm to rubbery, homogeneous, and white gray. Myofibromas have a firm, fibrous cut surface and are grayish white, light tan to brown, or purplish in color. They often have central yellow/necrotic areas and/or cystic spaces filled with caseous-like material or hemorrhage.

Histopathology

Histologically characterized by a (multi)nodular mitotic active proliferation of spindly shaped myofibroblasts without significant atypia [90]. Myofibroblasts are spindle shaped with pale pink cytoplasm and have elongated, tapering nuclei with a vesicular chromatin pattern and one or two small nucleoli (Fig. 12.41). Myoid whorls or nodules often hyalinize, with a pseudochondroid appearance. Within the center of the nodules, there are less well-differentiated, rounded, polygonal, or spindle-shaped cells, with slightly larger, hyperchromatic nuclei. These cells have relatively scant cytoplasm and are arranged around thin-walled, irregularly branching, hemangiopericytoma-like blood vessels. Both the myofibroblastic and more primitive components are positive for vimentin and smooth muscle actin, while the myofibroblastic component is more strongly positive for panactin HHF-35. Both components are negative for S-100 protein, epithelial membrane antigen, and keratin.

Differential Diagnosis

Nodular fasciitis, neurofibroma, infantile fibromatosis, fibrous histiocytoma, juvenile hyaline fibromatosis, fibrous hamartoma of infancy, fibromatosis colli, leiomyoma, infantile hemangiopericytoma, infantile fibrosarcoma, Ewing sarcoma/primitive neuroectodermal tumor, and lymphoma.

Histogenesis

The lesion is myofibroblastic in nature.

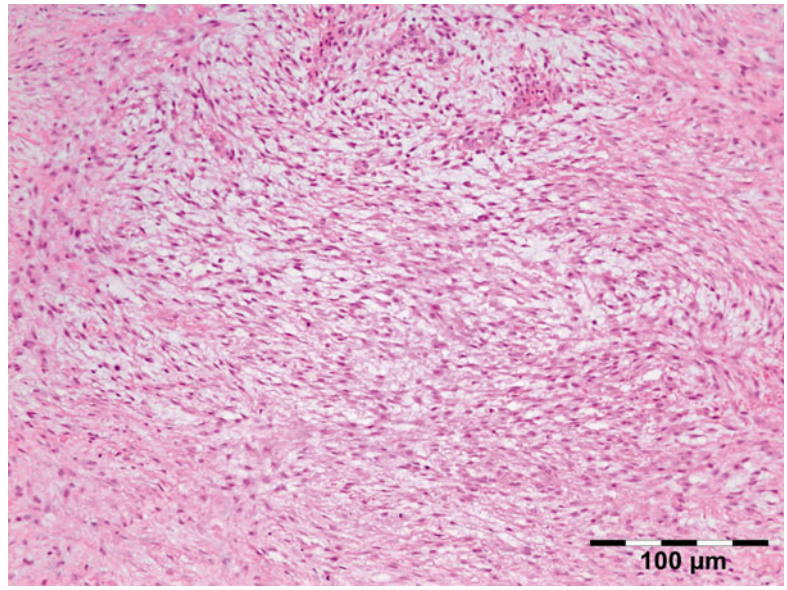

Fig. 12.41 Myofibromatosis: spindle-shaped myofibroblasts with pale pink cytoplasm and elongated, tapering nuclei with a vesicular chromatin pattern can be seen in a fascicular pattern and formation of myoid whorls (HE 200×) (Dr. Robert M. Verdijk)

Genetics

Sporadic cases with del(6)(q12;q15), monosomy 9q, and trisomy 16q have been reported.

Prognosis and Predictive Factors

The extent of the disease is the most important prognostic factor. Solitary lesions often resolve after (incomplete) resection. Recurrences, however may develop. Complete excision with close follow-up is the preferred treatment [91].

12.7.1.3 Juvenile Hyaline Fibromatosis

Juvenile hyaline fibromatosis has rarely been described as an eyelid tumor scalloping the superior orbital osseous rim [92]. Fibrous hamartoma of infancy and fibromatosis colli have not been described in the orbit.

12.7.1.4 Infantile Hemangiopericytoma

Infantile hemangiopericytoma occurs rarely in the orbit [93]. It is currently considered that a broad spectrum of benign infantile myofibroblastic lesions exists containing an immature-appearing cellular component with a distinctive, hemangiopericytoma-like vascular pattern. Infantile myofibromatosis and so-called infantile hemangiopericytoma almost certainly represent different stages of maturation of the same (single) entity [94].

12.7.1.5 Inflammatory Myofibroblastic Tumor (IMT)

Definition

Inflammatory myofibroblastic tumor (IMT) is a lesion composed of myofibroblastic spindle cells accompanied by an inflammatory infiltrate of plasma cells, lymphocytes, and eosinophils [79].

Epidemiology

Rare; we only encountered one case in our series.

Etiology

Inflammatory myofibroblastic tumor (IMT) is considered to be a neoplastic counterpart of idiopathic inflammatory pseudotumor (IIP).

Localization

IMT mainly occurs in the lung and abdomen of children and young adults. IMT of the orbit has rarely been described [95–98].

Clinical Features

Painful exophthalmos of the eye.

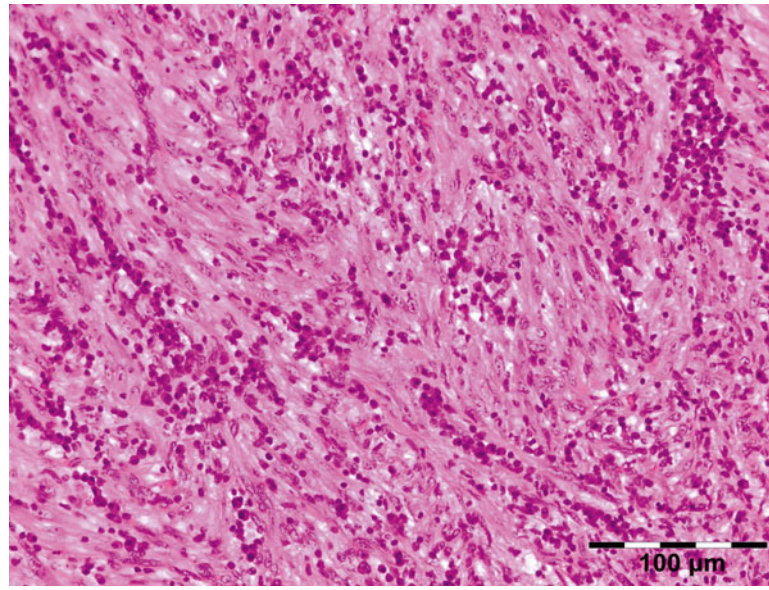

Fig. 12.42 Inflammatory myofibroblastic tumor (IMT): the lesion is composed of a compact fascicular pattern of plump myofibroblasts with an infiltrate of mainly plasma cells and admixed lymphocytes (HE 200×) (Dr. Robert M. Verdijk)

Macroscopy

Lobular, multinodular, or bosselated with a hard rubbery white, gray, yellow, or red cut surface.

Histopathology

Histopathology is characterized by a predominantly myofibroblastic lesion. Plump or spindled myofibroblasts may be in an edematous myxoid background with abundant blood vessels and an infiltrate of plasma cells, lymphocytes, and eosinophils (Fig. 12.42) to resemble granulation tissue, nodular fasciitis, or other reactive processes. Another pattern is characterized by a compact fascicular spindle cell proliferation with variable myxoid and collagenized regions and a distinctive inflammatory infiltrate with diffuse inflammation, small aggregates of plasma cells, or lymphoid nodules resembling fibromatosis, fibrous histiocytoma, or a smooth muscle neoplasm. Ganglion cell-like myofibroblasts with vesicular nuclei, eosinophilic nucleoli, and abundant amphophilic cytoplasm can be seen. Certain lesions resemble a scar or desmoid-type fibromatosis, with platelike collagen, lower cellularity, and relatively sparse inflammation with plasma cells and eosinophils. Highly atypical polygonal cells with oval vesicular nuclei, prominent nucleoli, and variable mitoses, including atypical forms, are seen in rare IMTs which undergo histologic malignant transformation. Subsets of IMT show aberrant expression of anaplastic lymphoma kinase (ALK), and immunohistochemical expression of ALK is noted in 68 % of the cases (Fig. 12.43) [99]. However, ALK positivity is not specific for IMT. Strong diffuse cytoplasmic reactivity for vimentin is present in virtually all IMT. Reactivity for smooth muscle actin and muscle-specific actin varies from a focal to a diffuse pattern in the spindle cell cytoplasm, and desmin is identified in many cases. Focal cytokeratin immunoreactivity is seen in about one-third of cases. Myogenin, myoglobin, and S-100 protein are negative. TP53 immunoreactivity is rare and has been reported in association with recurrence and malignant transformation.

Differential Diagnosis

Inflammatory malignant fibrous histiocytoma, Hodgkin lymphoma, xanthogranulomatous inflammation secondary to Erdheim–Chester disease, pseudotumor resulting from (atypical) mycobacterial infection, inflammatory fibrosarcoma.

Histogenesis

The lesion is myofibroblastic in nature.

Genetics

IMTs are heterogeneous genetically. ALK rearrangements occur mainly in children and young adults and are detectable by fluorescence in situ

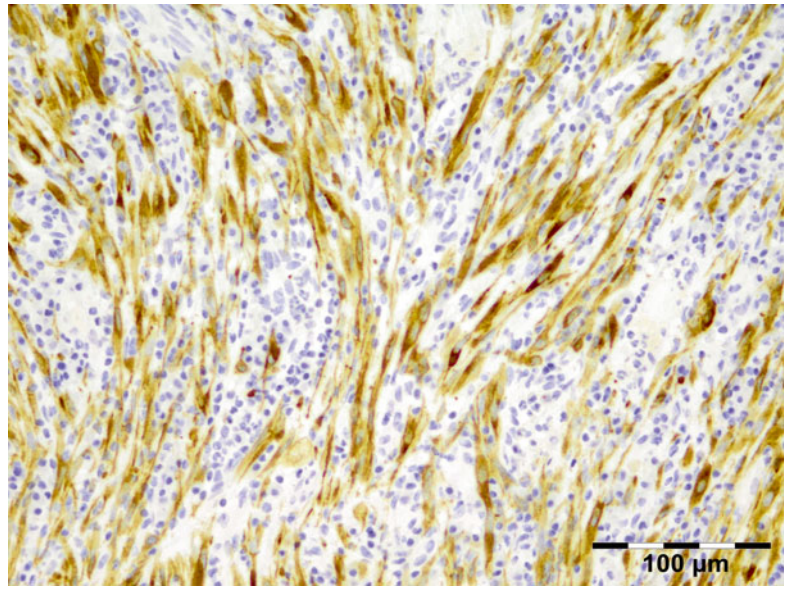

Fig. 12.43 IMT: the myofibroblasts stain positive for ALK1 (ALK1 IH 200×) (Dr. Robert M. Verdijk)

hybridization. The cytogenetic rearrangements activate the ALK receptor tyrosine kinase gene in chromosome band 2p23. IMT is therefore considered to be a clonal neoplastic lesion. By contrast, such rearrangements are uncommon in IMT diagnosed in adults beyond 40 years old.

Prognosis and Predictive Factors

Cellularity or mitotic counts are not prognostic markers. Cytological atypia, ganglion cell-like cells, and p53 expression may identify tumors that are more likely to pursue an aggressive course.

12.7.1.6 Solitary Fibrous Tumor/ Hemangiopericytoma/Giant Cell Angiofibroma

Definition

Tumors of benign to uncertain behavior, CD34-positive, collagen-rich, specialized fibroblastic lesions, which have overlapping or histologically identical features [79].

Epidemiology

Rare; we only encountered one case of hemangiopericytoma in our series. These are tumors of adults with an equal sex distribution.

Etiology

Recently, a large series of these collagen-rich fibroblastic tumors of the orbit has been explored. Forty-one fibroblastic orbital tumors, originally diagnosed as hemangiopericytoma ($n=16$), fibrous histiocytomas ($n=9$), mixed tumors (hemangiopericytoma/fibrous histiocytoma) ($n=14$), and giant cell angiofibromas of orbit ($n=2$), were evaluated. Upon histologic review with the addition of CD34 immunostaining, all cases were reclassified as solitary fibrous tumor [100].

Localization

Hemangiopericytoma and solitary fibrous tumors with the addition of giant cell angiofibromas are uncommon neoplasms found in deep soft tissue on many locations, including the orbit.

Clinical Features

Patients may present with an usually painless orbital mass and proptosis. Duration of symptoms may range from 3 to 96 months [100]. Many (41 %) patients present with an orbital mass, 20 % with proptosis, 5 % with painful mass, and 5 % with painless mass.

Macroscopy

Most SFTs present as well-circumscribed, often partially encapsulated, masses, measuring from 0.4 to 5.0 cm [100]. On section, they frequently have a multinodular, whitish, and firm appearance; myxoid and hemorrhagic changes are occasionally observed. Tumor necrosis and

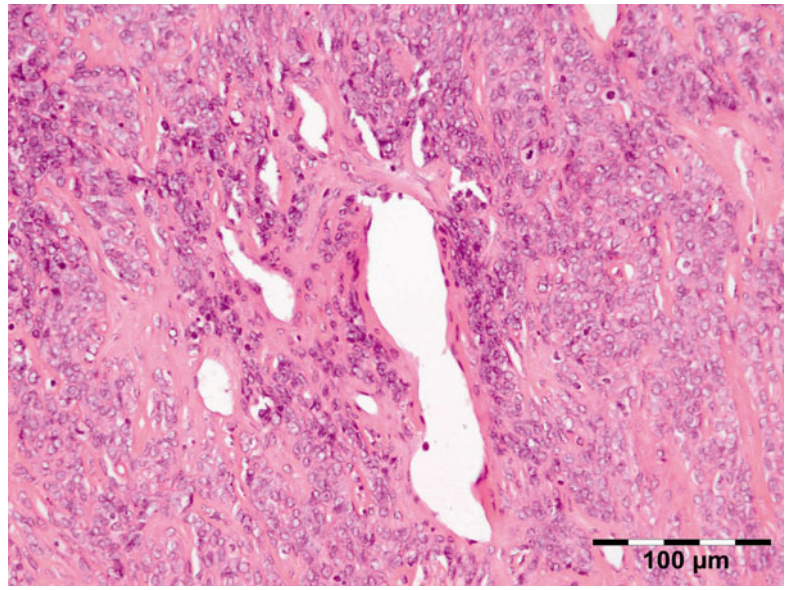

Fig. 12.44 SFT/Hemangiopericytoma: a hypercellular area is shown with round to spindle-shaped tumor cells that have little cytoplasm with indistinct borders and dispersed chromatin within vesicular nuclei. There is a collagenous background with branching vessels. Mitoses can be observed and should not exceed 3 mitoses per 10 high-power fields (HE 200×) (Dr. Robert M. Verdijk)

infiltrative margins (about 10 % of cases) are mostly observed in locally aggressive or malignant tumors.

Histopathology

Typical SFTs show a patternless architecture characterized by a combination of alternating hypocellular and hypercellular areas separated from each other by thick bands of hyalinized, somewhat keloidal, collagen and branching staghorn-like vessels (Fig. 12.44). The nonatypical, round to spindle-shaped tumor cells have little cytoplasm with indistinct borders and dispersed chromatin within vesicular nuclei. Myxoid change, areas of fibrosis, and interstitial mast cells are commonly observed. Mitoses are generally scarce, rarely exceeding 3 mitoses per 10 high-power fields. SFTs may contain mature adipocytes and/or giant multinucleated stromal cells which used to be restricted to so-called lipomatous hemangiopericytoma and giant cell angiofibroma. Malignant SFTs are usually hypercellular lesions, showing at least focally moderate to marked cytological atypia, tumor necrosis, numerous mitoses (>4 mitoses per 10 high-power fields), and/or infiltrative margins. Rare cases show abrupt transition from conventional benign-appearing SFT to high-grade sarcoma, likely representing a form of dedifferentiation. However, overall outcome for malignant solitary fibrous tumors of the eye should be further explored [100]. Tumor cells in SFT are characteristically immunoreactive for CD34. Twenty to thirty-five percent of them are also variably positive for epithelial membrane antigen, BCL-2, and smooth muscle actin. Focal and limited reactivity for S-100 protein, cytokeratins, and/or desmin has also occasionally been reported.

Differential Diagnosis

Fibrous histiocytoma, mesenchymal chondrosarcoma, glomangioma.

Histogenesis

The lesion is fibroblastic in nature.

Genetics

SFTs are cytogenetically heterogeneous, the most common finding being rearrangements of the long arm of chromosome 12.

Prognosis and Predictive Factors

Local recurrences of SFT are possible and usually follow an incomplete initial excision. Recurrent tumors in the orbit have shown the tendency to infiltrate the surrounding tissues

and the bone, rendering complete secondary excision more difficult [101].

12.7.1.7 Fibrous Histiocytoma

Definition

A diverse group of mesenchymal tumors that show fibroblastic differentiation [79].

Epidemiology

Fibrous histiocytoma was in the past considered to be the most common primary mesenchymal orbital tumor of adults. In our series they represented only 6.5 % of all bone and soft tissue tumors and less than 1 % of all orbital lesions.

Etiology

Unknown.

Localization

The upper and nasal portions of the orbit are the most common sites of involvement.

Clinical Features

The tumors occur at a median age of 43 years. The most common signs and symptoms are proptosis (60 %), mass (46 %), and decreased vision (25 %).

Macroscopy

Usually the tumor consists of a lobulated circumscribed pseudo-encapsulated mass of variable size made up of rubbery-to-firm grayish-white, sometimes yellowish-tan, tissue. Occasionally, cystic or hemorrhagic reddish-brown areas may be noted, and in a few tumors, areas with a mucoid appearance are present. The size of the tumors range from 1 to 15 cm in greatest diameter. In contrast, malignant fibrous histiocytomas (MFH) usually display infiltrating margins and generally are larger than the benign lesions.

Histopathology

Deep fibrous histiocytomas usually show a prominent storiform pattern, sometimes combined with hemangiopericytoma-like areas. Contrary to conventional cutaneous lesions, most lesions show monomorphism and usually lack secondary elements such as foamy cells and giant cells but usually show scattered lymphocytes. Thus, they more closely resemble the cellular variant of cutaneous fibrous histiocytoma. The tumor cells are cytologically bland and generally spindle shaped with elongated or plump vesicular nuclei and eosinophilic, ill-defined cytoplasm. In the benign lesions, there is no nuclear pleomorphism or hyperchromasia, and mitoses, although commonly present, are usually less than 5 per 10 high-power fields. The stroma may show myxoid change or hyalinization and rarely osteoclast-like giant cells or metaplastic ossification. Small foci of necrosis may be present. Recurrent fibrous histiocytomas display infiltrating margins and areas of hypercellularity, but no significant nuclear pleomorphism or cellular atypia should be observed [102]. Malignant fibrous histiocytoma (MFH) show infiltrating edges as well as one or more histologic criteria of malignancy, including nuclear pleomorphism, bizarre multinucleated tumor giant cells, and areas of necrosis (Fig. 12.45) [102]. Immunohistochemistry shows similar results as in cutaneous lesions with negativity for epithelial markers, desmin, and S-100 protein. Alpha-smooth muscle actin may be positive in some parts of the lesion. CD34 is negative, and if positive, solitary fibrous tumor should be considered.

Differential Diagnosis

In a recent study, cases previously designated as fibrous histiocytoma showed overlapping morphologic and immunohistochemical features with giant cell angiofibroma, orbital hemangiopericytoma, and SFT and have been reclassified as SFT [100].

Histogenesis

The origin of the neoplasm is probably a primitive mesenchymal cell.

Genetics

The genetic aspects of benign fibrous histiocytomas and MFH are difficult to evaluate because of the shifting diagnostic criteria used throughout the years.

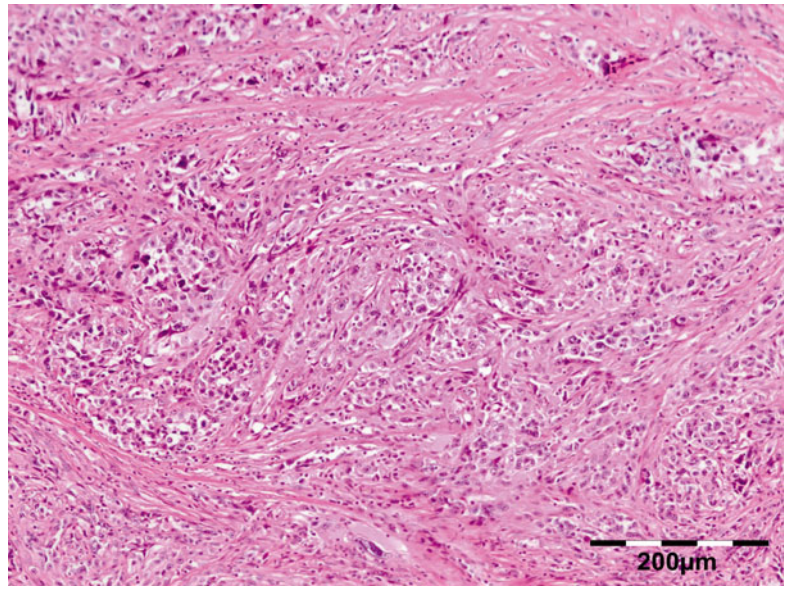

Fig. 12.45 Malignant fibrous histiocytoma (MFH): spindle to epithelioid cells with nuclear pleomorphism, bizarre multinucleated tumor giant cells, and atypical mitosis can be seen in a fibrotic stroma (HE 100×) (Dr. Robert M. Verdijk)

Prognosis and Predictive Factors

Based on the histopathologic features, the tumors have been classified in three groups: benign, locally aggressive, and malignant [102].

12.7.1.8 Myxoma and Angiomyxoma

Myxomas are rare, benign neoplasms of mesenchymal origin that usually develop in soft tissues. Myxomas of the orbit are rare. Median age at presentation is 56 years (range, 4–69). Two angiomyxomas occurred in children ages 4 and 7 years whose tumors were locally aggressive and recurred. Pathologically, the tumors are poorly circumscribed. Histopathology showes them to be hypocellular, containing stellate and spindled cells in an abundant, loose, myxoid stroma rich in hyaluronic acid. Small blood vessels are rare in myxomas but abundant in angiomyxomas (Fig. 12.46). Tumor cells are frequently immunoreactive for vimentin, CD34, and factor XIIIa. Vascularity and bone involvement appear to be important prognostic features for recurrence. Complete resection with a margin of healthy tissue appears to be the treatment of choice [103]. The differential diagnosis is with other neoplasms that may contain myxomatous areas. Multiple myxomas and angiomyxomas may be associated with Carney's complex of multiple myxomas, blotchy skin pigmentation, schwannomas, and endocrine disturbances.

12.7.1.9 Myxofibrosarcoma

Definition

Myxofibrosarcoma (MFS), formerly known as myxoid variant of malignant fibrous histiocytoma (MFH), is a malignant mesenchymal tumor that comprises a spectrum of malignant fibroblastic lesions with variably myxoid stroma and pleomorphism and with a distinctively curvilinear vascular pattern.

Epidemiology

Rare.

Etiology

Unknown.

Localization

The most common locations of MFS are the limb and limb girdle followed by the head and neck, retroperitoneum, and mediastinum. There have been two cases described of MFS occurring in the orbit [104].

Clinical Features

MFS occurs in older adults.

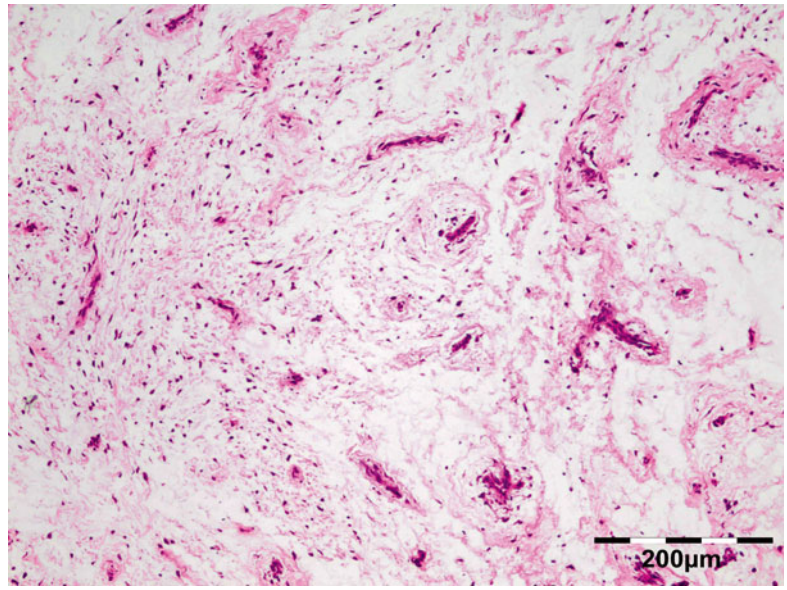

Fig. 12.46 Angiomyxoma: a hypocellular lesion composed of stellate and spindled cells in an abundant, loose, myxoid stroma rich in hyaluronic acid is observed. Abundant blood vessels are typical of angiomyxoma (HE 100×) (Dr. Ian W. McLean; this case was presented at the combined Verhoeff-EOPS meeting, Houston, 1996, case 96–14)

Macroscopy

Superficial tumors typically consist of multiple, variably gelatinous or firmer nodules, whereas deep-seated neoplasms often form a single mass with an infiltrative margin. In high-grade lesions, areas of tumor necrosis are often found.

Histopathology

The histopathology is characterized by a hypocellular neoplasm composed of only few, non-cohesive, plump spindle or stellate tumor cells with ill-defined, slightly eosinophilic cytoplasm and atypical, enlarged, hyperchromatic nuclei in a myxoid stroma composed of hyaluronic acid. A characteristic finding is the presence of prominent elongated, curvilinear, thin-walled blood vessels with a perivascular condensation of tumor cells and/or inflammatory cells (mainly lymphocytes and plasma cells). Frequently, so-called pseudolipoblasts (vacuolated neoplastic fibroblastic cells with cytoplasmic acid mucin) are noted. Myxofibrosarcoma shows a broad spectrum of cellularity, pleomorphism, and proliferative activity. High-grade neoplasms are composed in large part of solid sheets and cellular fascicles of spindled and pleomorphic tumor cells with numerous, often atypical, mitoses, areas of hemorrhage, and necrosis. Bizarre, multinucleated giant cells with abundant eosinophilic cytoplasm (resembling myoid cells) and irregular-shaped nuclei are noted. Tumor cells stain positively for vimentin, and in a minority of cases, some spindled or larger eosinophilic tumor cells express muscle-specific actin and/or alpha-smooth muscle actin, suggestive of focal myofibroblastic differentiation; desmin, CD68, Mac 387, and FXIIIa are negative.

Differential Diagnosis

Myxoma, fibrosarcoma.

Histogenesis

The lesion is (myo)fibroblastic in nature.

Genetics

In general, the karyotypes tend to be highly complex, with extensive intratumoral heterogeneity.

Prognosis and Predictive Factors

The clinical behavior appears to be closely related to tumor grade with increased risk for local recurrence according to higher grades.

12.7.1.10 Infantile Fibrosarcoma (IF)

Infantile fibrosarcoma (IF) is a rare soft tissue sarcoma that presents either at birth or in the first year of life. IF has been once described as metastasis in the orbit [105].

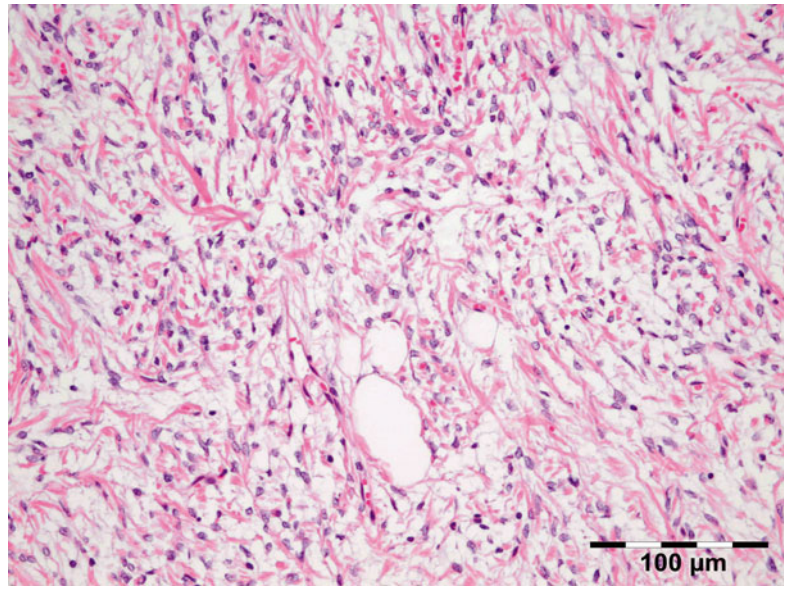

Fig. 12.47 Spindle cell lipoma: the lesion is composed of bland spindled cells arranged in parallel bands with occasional adipocytes. The thick ropelike collagen bundles are typical of the lesion. The molecular studies showed a typical polysomy signal with the MDM2 FISH probe (HE 200×) (Dr. Robert M. Verdijk)

12.7.2 Adipocytic Tumors

12.7.2.1 Lipoma

Definition

Lipoma is a benign tumor composed of mature adipocytes [79].

Epidemiology

Lipoma is the most common soft tissue neoplasm in adults but is extremely rare to occur in the orbit. We have no example in our series. A few spindle cell lipomas of the orbit have been reported [106, 107]. Our series also contained one spindle cell lipoma. Pleomorphic lipoma has been described in the orbit [108]. Intramuscular lipoma was only once described in the orbit [109].

Etiology and Localization

Diagnosed orbital lipomas in fact are often orbital fat prolapse.

Clinical Features

Are of an orbital mass.

Macroscopy

Lipomas should be well circumscribed and have a slightly less yellow tan, when compared to normal orbital fat. Different types are basically similar in appearance.

Histopathology

Conventional lipoma is composed of lobules of mature adipocytes. The cells are identical to the surrounding adipose tissue except for slight variation in the size and shape of the cells in lipomas. Lipomas can occasionally have areas of abundant fibrous tissue (fibrolipoma) [110]. Spindle cell lipoma is composed of bland mitotically inactive spindled cells arranged in parallel bands between the fat cells and associated with thick ropelike collagen bundles (Fig. 12.47). Pleomorphic lipoma is characterized by small spindled and rounded hyperchromatic cells and multinucleated giant cells with radially arranged nuclei. Immunohistochemistry may aid in the diagnosis of spindle cell and pleomorphic lipomas. Mature adipocytes stain positive for S-100 protein, vimentin, and CD34 (Fig. 12.48). The spindle cells in both spindle cell and pleomorphic lipomas on the other hand are strongly positive for CD34 and may rarely be positive for S-100 protein. Few cases of lipomatous hemangiopericytoma (adipocytic variant of solitary fibrous tumor) of the orbit have been described [111].

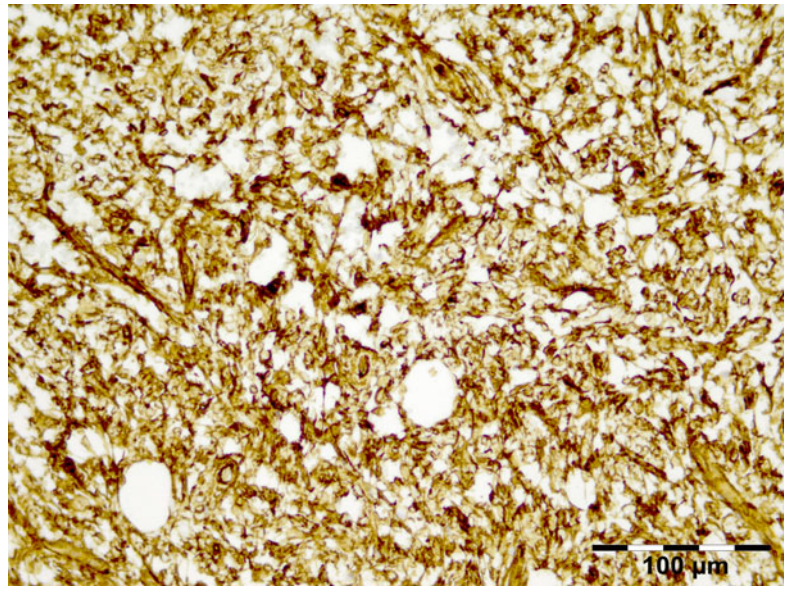

Fig. 12.48 Spindle cell lipoma: the lesional cells stain positive for CD34 (CD34 IH 200×) (Dr. Robert M. Verdijk)

Differential Diagnosis

Many reported cases have been simple orbital fat or fat prolapse.

Histogenesis

The adipocytes are of mesodermal origin.

Genetics

Chromosome aberrations have been found in 55–75 % of lipomas. The pattern of cytogenetic aberrations is heterogeneous. Chromosome 12 polysomy was noted in 89 % of spindle cell and pleomorphic lipomas, while all angiolipomas and lipomas were nonamplified and eusomic. Thus fluorescence in situ hybridization is a sensitive, although not specific, tool for identification of spindle cell and pleomorphic lipomas.

Prognosis and Predictive Factors

Lipoma has an excellent prognosis.

12.7.2.2 Liposarcoma

Definition

Malignant mesenchymal neoplasm composed either entirely or in part of a mature adipocytic proliferation [79].

Epidemiology

Liposarcoma, the most common soft tissue sarcoma in adults, will rarely involve the orbit, either primarily [112–114] or as a metastasis [115].

Etiology

None.

Localization

Only 1 % of liposarcomas occur in the face. Our series contained only one liposarcoma.

Clinical Features

The patients present with painless or painful proptosis. The histologic subtypes (well differentiated (WDL), myxoid, dedifferentiated (DDL), and pleomorphic) are entirely separate diseases with different morphology, genetics, and natural history [116].

Macroscopy

Liposarcoma usually consists of large multinodular yellow masses that may contain solid, often tan-gray dedifferentiated areas. Dedifferentiated areas often show necrosis.

Histopathology

In contrast to benign lipoma, significant variation in cell size is appreciable. Focal adipocytic

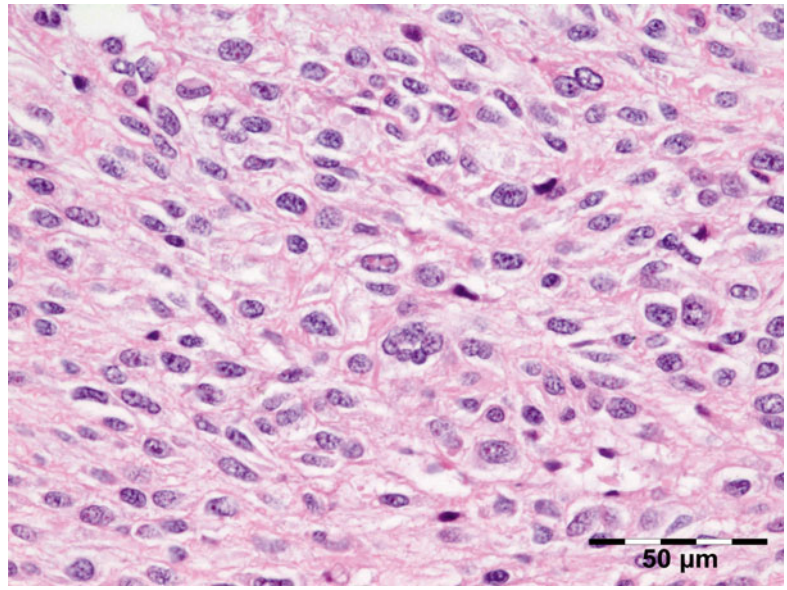

Fig. 12.49 Liposarcoma: this lesion is composed of plump to spindled cells; as is often the case no lipoblasts are present. Centrally a multinucleated floret cell is depicted (HE 400×) (Dr. Robert M. Verdijk)

nuclear atypia and hyperchromasia is present. Hyperchromatic stromal cells tend to be more numerous within fibrous septa. A varying number (from many to none) of monovacuolated or multivacuolated lipoblasts and multinucleated cells (floret cells) may be found (Fig. 12.49). Floretlike cells, however, may be observed in in situ and prolapsed orbital fat [117]. Dedifferentiation is represented by the transition from liposarcoma to non-lipogenic sarcoma which, in most cases, is high grade.

Differential Diagnosis

Many types of sarcoma.

Histogenesis

Mesenchymal stem cell with adipocytic potential.

Genetics

Both well-differentiated (WDL) and dedifferentiated liposarcomas (DDL) show amplification of MDM2. MDM2/chromosome 12 fluorescence in situ hybridization is a sensitive and specific tool in evaluating low-grade lipomatous neoplasms. However, p16 (Fig. 12.50) is the most sensitive and specific marker for detecting WDL/DDL, and the combination of immunohistochemical staining with CDK4 and p16 is of more discriminatory value than the combination of either with MDM2 (Fig. 12.51), the least sensitive and specific of the three markers [118].

Prognosis and Predictive Factors

Prognosis is related to the site and size and pathologic type and grade. Despite the difficulty in obtaining wide surgical margins, the small tumor size at presentation and the apparent predominance of the well-differentiated type mean that the prognosis for orbital liposarcoma is generally good [116].

12.7.3 Myogenic Tumors

12.7.3.1 Smooth Muscle Tumors

Leiomyoma

Definition

A benign smooth muscle tumor [79].

Epidemiology

Orbital leiomyoma is a curiosity affecting males twice as frequently as females [119, 120]. We encountered only one case in our series.

Etiology

Posterior tumors are believed to originate from smooth muscle cells of vessel walls; anterior

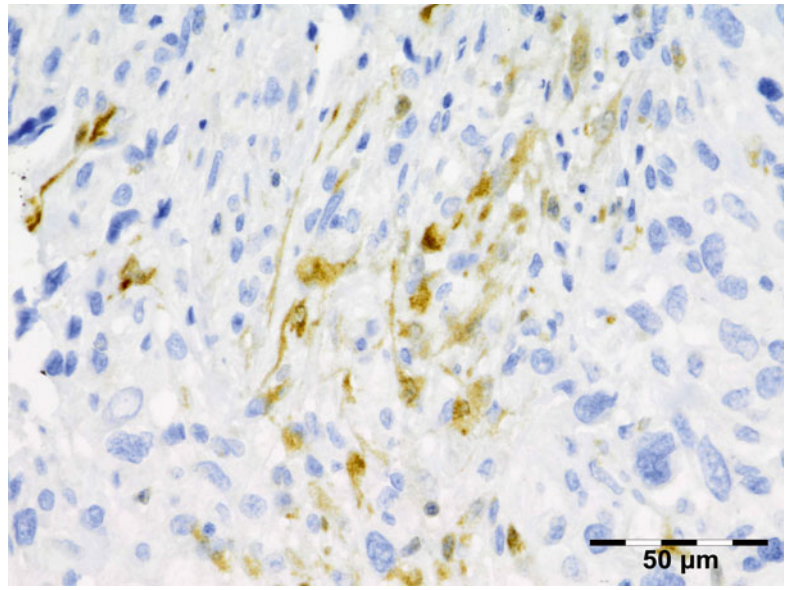

Fig. 12.50 Liposarcoma: positive cytoplasmic staining of the spindle cells for p16 is strongly suggestive for liposarcoma (p16 IH 400×) (Dr. Robert M. Verdijk)

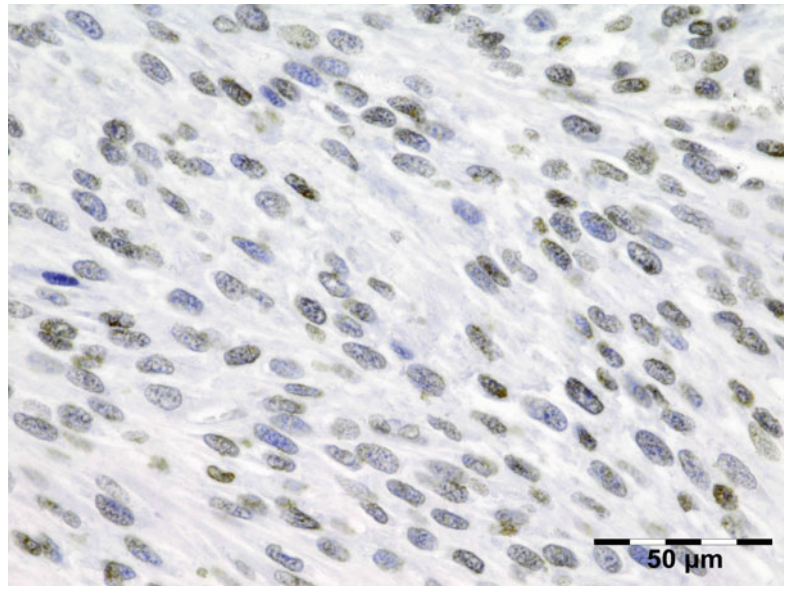

Fig. 12.51 Liposarcoma: positive nuclear staining of the spindle cells for MDM2 supports the diagnosis of liposarcoma (MDM2 IH 400×) (Dr. Robert M. Verdijk)

lesions may arise from the capsulopalpebral or Müller muscle.

Localization

Can be located anywhere in the orbit.

Clinical Features

They are well-encapsulated, slowly progressive solitary tumors that occur in the third and fourth decades.

Macroscopy

Leiomyomas are well-circumscribed, gray-white tumors (Fig. 12.52).

Histopathology

Tumors are composed of cells that closely resemble normal smooth muscle cells because they have eosinophilic cytoplasm with hematoxylin and eosin; fuchsinophilic, red-staining cytoplasm with Masson trichrome technique;

and bland, uniform blunt-ended, cigar-shaped nuclei. They are arranged in orderly intersecting fascicles in a fibrous stroma rich in dilated sinusoidal capillaries (Fig. 12.53). They are highly differentiated and possess little or no atypia and, at most, an extremely low level of mitotic activity. Necrosis should not been present. Tumor cells are always positive for actin (Fig. 12.54) and desmin at least focally. S-100 protein is negative.

Fig. 12.52 Leiomyoma: gross examination shows a well-circumscribed, yellowish to gray-white tumor with a diameter of less than 2 cm (Dr. Robert M. Verdijk)

Differential Diagnosis

Nerve sheath tumors or fibrous histiocytoma.

Histogenesis

Smooth muscle cells.

Genetics

No genetic aberrations have been reported

Prognosis and Predictive Factors

Recurrence after incomplete excision may occur. Malignant transformation in the absence of external beam radiation has not been described [119, 121].

12.7.3.2 Leiomyosarcoma

Definition

Malignant tumor composed of cells showing distinct smooth muscle features [79].

Epidemiology

Leiomyosarcoma is a rare orbital tumor; we encountered only one case in our series.

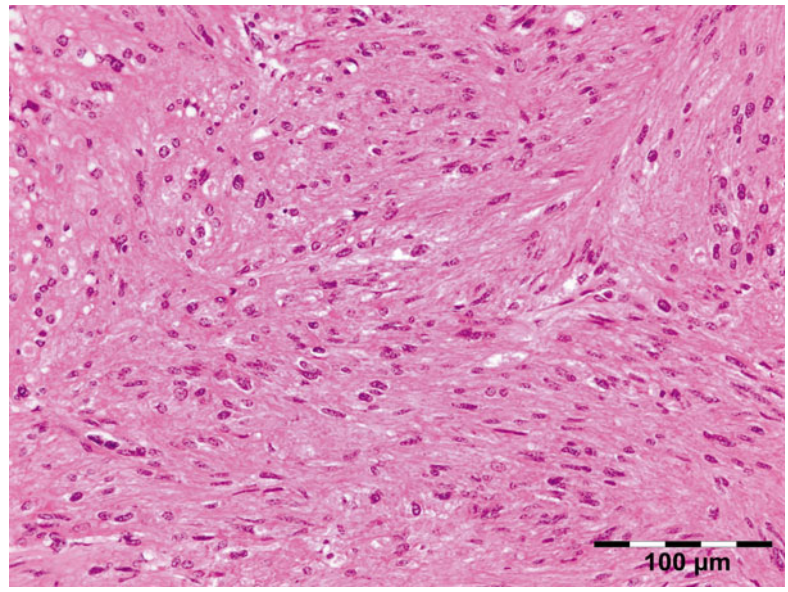

Fig. 12.53 Leiomyoma: the lesion is composed of a fascicular pattern of smooth muscle spindle cells with eosinophilic cytoplasm and bland, uniform blunt-ended, cigar-shaped nuclei (HE 200×) (Dr. Robert M. Verdijk)

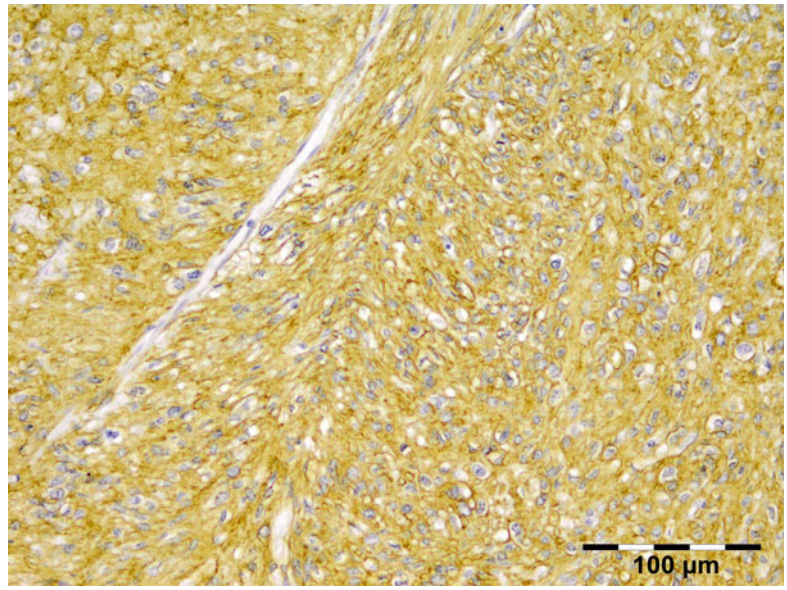

Fig. 12.54 Leiomyoma: the lesional cells show a cytoplasmic staining for smooth muscle actin (smooth muscle antigen IH 200×) (Dr. Robert M. Verdijk)

Etiology

Leiomyosarcomas of the orbit often are metastases [122]; it either occurs de novo in elderly patients [123] or may develop as a radiation-induced sarcoma in children and young adults [124].

Localization

May occur anywhere in the orbit.

Clinical Features

They are usually rapidly developing infiltrating masses.

Macroscopy

A fleshy mass, with colors varying from gray to white to tan. A whorled character may be evident. Larger examples may display hemorrhage, necrosis, or cystic change.

Histopathology

Histologic diagnosis rests upon demonstration of smooth muscle differentiation. The typical histologic pattern of leiomyosarcoma is that of intersecting, sharply marginated groups of spindle cells. This pattern may be less well defined in areas of some tumors, and occasionally there is a focal storiform, palisaded, or hemangiopericytoma-like arrangement. Fibrosis or myxoid change may be present. Hyalinized, hypocellular zones and coagulative tumor necrosis are frequent in larger leiomyosarcomas. The tumor cell nuclei are characteristically elongated and blunt ended and may be indented or lobulated. Nuclear hyperchromatism and pleomorphism are generally notable, although they may be focal, mild, or occasionally absent. Mitotic figures can usually be found readily, although they may be few or patchy, and atypical mitoses are often seen (Fig. 12.55). The cytoplasm varies from typically eosinophilic to pale and, in the former instance, is often distinctly fibrillar. Cytoplasmic vacuolation is frequently apparent, particularly in cells cut transversely. Epithelioid cytomorphology, multinucleated osteoclast-like giant cells, very prominent chronic inflammatory cells, and granular cytoplasmic change are unusual findings. Occasional soft tissue leiomyosarcomas contain areas with a nonspecific, poorly differentiated, pleomorphic appearance in addition to typical areas. Rarely, an osteosarcoma-like or rhabdomyosarcomatous component is associated with leiomyosarcoma. The use of immunohistochemistry with positive staining for desmin (Fig. 12.56), actin, and smooth muscle actin is of aid. S-100 protein is negative. Ultrastructural studies may be of help but have become largely superfluous with the advent of immunohistochemistry.

Differential Diagnosis

Sarcoma with leiomyomatous features.

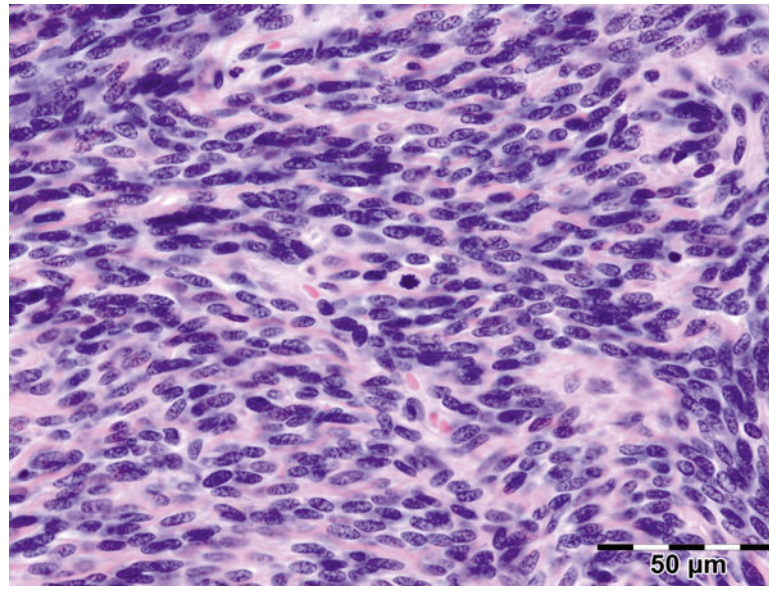

Fig. 12.55 Leiomyosarcoma: the lesion is composed of intersecting, sharply marginated groups of spindle cells. The tumor cell nuclei are elongated and blunt. Nuclear hyperchromatism and pleomorphism are mild. Mitotic figures can be readily observed (HE 400×) (Dr. Robert M. Verdijk)

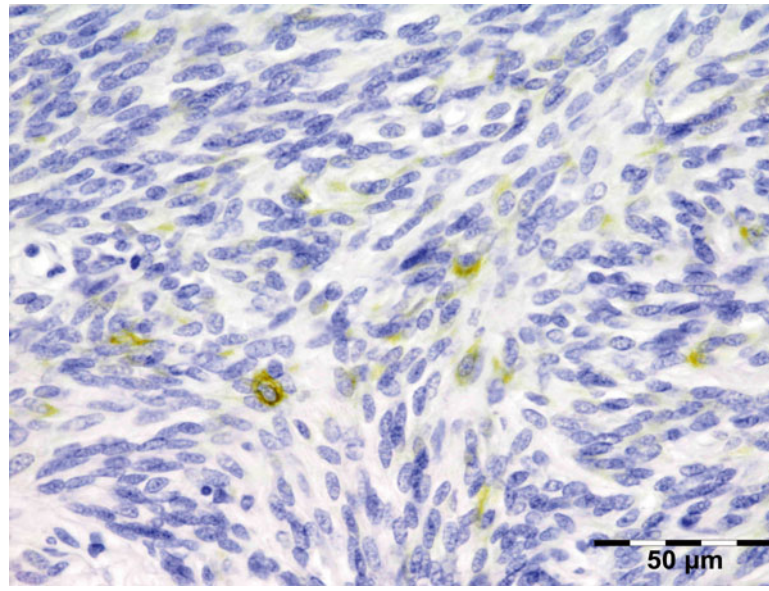

Fig. 12.56 Leiomyosarcoma: sparse but distinct positivity for desmin can be observed in the tumor cells (desmin IH 400×) (Dr. Robert M. Verdijk)

Histogenesis

Smooth muscle cells.

Genetics

Most karyotypes are complex and no consistent aberrations have been noted.

Prognosis and Predictive Factors

May be treated with surgical excision combined with postoperative radiation.

12.7.4 Rhabdomyomatous Tumors

12.7.4.1 Rhabdomyoma

Definition

Extracardiac rhabdomyoma (RM) is a rare benign neoplasm of skeletal muscle differentiation that is classified into cardiac and extracardiac types. Extracardiac RM is further classified into adult (A-RM) and fetal (F-RM) types, depending on the degree of differentiation[79].

Epidemiology
In A-RM the median age is 60 years (range 33–80 years) with a 3:1 male predominance. In F-RM median age is 4 years (range, 3 days to 58 years) with a 2.4:1 male predominance.

Etiology
Unlike cardiac RM, there is no association with tuberous sclerosis.

Localization
RM occurs most often in the head and neck. Only five cases with occurrence in the orbit have been reported in the literature [125]. A-RM is often solitary (70 %) but may be multinodular (26 %) with discrete nodules in the same anatomic area. F-RM presents as a well-defined solitary mass involving soft tissue or mucosa.

Clinical Features
Progressive proptosis.

Macroscopy
The gross specimen consists of grayish-white tissue with hard fleshy consistency and some reddish components.

Histopathology
Reveals fetal or mature non-atypical rhabdoid differentiation.

Differential Diagnosis
Rhabdomyosarcoma.

Histogenesis
From rhabdomyoblastic cells.

Genetics
Some cases of F-RM are associated with nevoid basal cell syndrome.

Prognosis and Predictive Factors
Complete excision is the recommended treatment to prevent local recurrence.

12.7.4.2 Rhabdomyosarcoma (RMS)

Definition
Malignant soft tissue sarcoma that recapitulates the phenotypic and biological features of skeletal muscle [79].

Epidemiology
RMS is the most common soft tissue sarcoma in children [126, 127]. We have diagnosed eight rhabdomyosarcomas in our series, of which seven were primary and of the embryonal type and one is alveolar rhabdomyosarcoma as a metastasis.

Etiology
The cause of most rhabdomyosarcomas is unknown.

Localization
The greatest proportion of tumors occur within the head and neck (about 47 %) and orbit (7 %) [128].

Clinical Features
About 42 % of patients with orbital rhabdomyosarcoma are aged 5–9 years; they present with proptosis or dysconjugate gaze [129]. Embryonal rhabdomyosarcomas constitute the most common subtype of rhabdomyosarcoma of the orbit by far. A special subtype of embryonal rhabdomyosarcoma is botryoid rhabdomyosarcoma (involving the conjunctiva) [130]. Alveolar rhabdomyosarcoma infrequently occurs in the orbit and may represent metastatic disease. Pleomorphic rhabdomyosarcoma is a high-grade sarcoma occurring almost exclusively in adults.

Macroscopy
Embryonal rhabdomyosarcomas form poorly circumscribed, fleshy, pale tan masses that directly impinge upon neighboring structures. Spindle cell rhabdomyosarcomas, like other spindle cell lesions, form firm, fibrous tumors with tan-yellow, whorled cut surfaces. Botryoid tumors, as the name implies, have a characteristic polypoid appearance with clusters of small, sessile, or pedunculated nodules that abut the epithelial surface of the conjunctiva. Alveolar rhabdomyosarcoma is so named because of the macroscopic impression of thin crisscrossing fibrous bands that appear as spaces between cellular regions of the tumor (reminiscent of lung alveoli).

Histopathology
RMS are composed of primitive mesenchymal cells in various stages of myogenesis, i.e., rhabdomyoblasts. Stellate cells with lightly

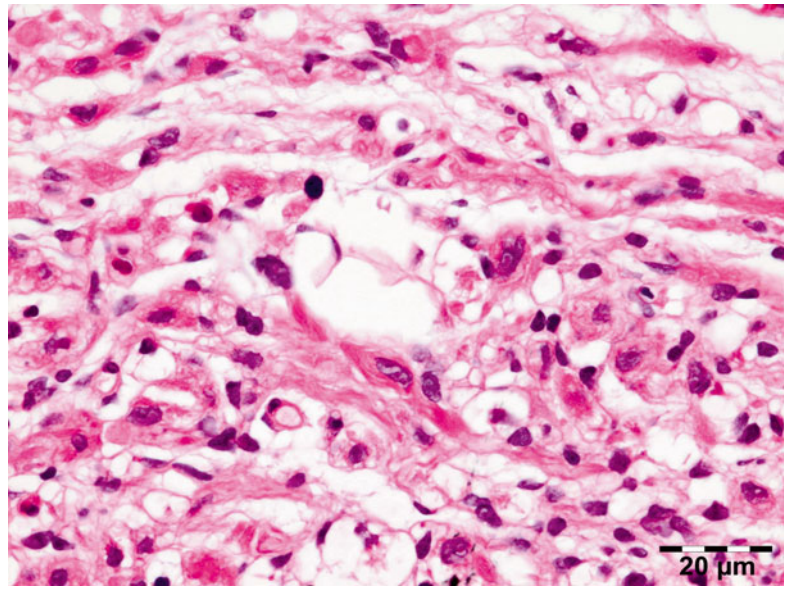

Fig. 12.57 Embryonal rhabdomyosarcoma: the lesion is composed of primitive mesenchymal cells with lightly amphophilic cytoplasm and central, oval nuclei, cells with more cytoplasmic eosinophilia and elongated shapes, "tadpole," "strap," or "spider" cell. Cells with bright eosinophilia, cytoplasmic cross striations, and multinucleation prove rhabdoid differentiation (HE 630×) (Dr. Robert M. Verdijk)

amphophilic cytoplasm and central, oval nuclei represent the most primitive end of this spectrum. As these cells differentiate, they progressively acquire more cytoplasmic eosinophilia and elongate shapes, manifested in descriptive terms such as "tadpole," "strap," and "spider" cell. Bright eosinophilia, cytoplasmic cross striations, and multinucleation indicate terminal differentiation, and myotube forms may be evident (Fig. 12.57). Differentiation tends to be more evident following chemotherapy. The histologic architecture of embryonal rhabdomyosarcoma is typically composed of alternating areas of dense, compact cellularity and loose, myxoid tissues. The botryoid variant of embryonal rhabdomyosarcoma contains linear aggregates of tumor cells that tightly abut the conjunctival surface. This feature, known as a "cambium layer," typifies these tumors which are extremely rare but may extend into the orbit. Densely arrayed whorls or fascicles of spindle cells constitute the spindle cell variant of embryonal rhabdomyosarcoma. These spindle cells often resemble smooth muscle cells, but cytoplasmic cross striations, if present, and/or bright eosinophilia indicates striated muscle differentiation. The presence of enlarged, atypical cells with hyperchromatic nuclei defines the anaplastic variant of rhabdomyosarcoma. This feature may be seen in both embryonal and alveolar tumors but is more prevalent in the former. Bizarre, multipolar mitoses are also often present. Anaplastic features can be focal or diffuse. Focal anaplasia indicates the presence of only single, dispersed anaplastic cells, whereas diffuse anaplasia indicates the presence of clone-like clusters of anaplastic cells.

All alveolar rhabdomyosarcomas exhibit round cell cytological features reminiscent of lymphomas but with primitive myoblastic differentiation. Typical alveolar rhabdomyosarcomas produce fibrovascular septa that separate the tumor cells into discrete nests (Fig. 12.58). These nests contain central clusters of cells with loss of cohesion around the periphery. Tumor cells align the septa in a picket fence pattern. Giant cells with rhabdomyoblastic differentiation are common. Solid variant alveolar rhabdomyosarcomas lack the fibrovascular stroma and form sheets of round cells with variable rhabdomyoblastic differentiation (often little).

Mixed embryonal/alveolar rhabdomyosarcomas contain foci with embryonal histology, i.e., myxoid stroma and spindle cell myoblasts as well as areas with alveolar histology. The alveolar foci usually contain nests with fibrous stroma, although highly cellular solid foci resembling lymphoma may occur.

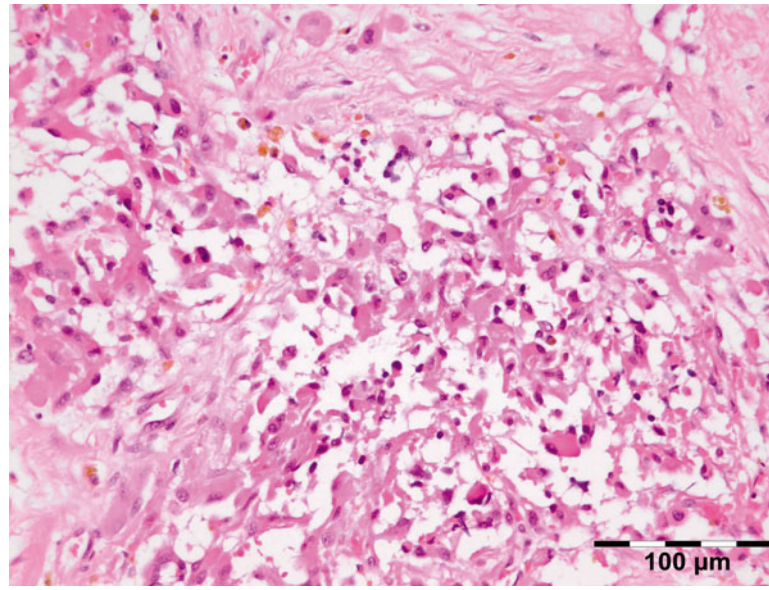

Fig. 12.58 Alveolar rhabdomyosarcoma: this metastatic lesion post chemotherapy shows fibrovascular septa that separate the tumor cells into discrete nests. The nests contain central clusters of cells with loss of cohesion around the periphery. Giant cells with rhabdomyoblastic differentiation are typically present (HE 200×) (Dr. Robert M. Verdijk)

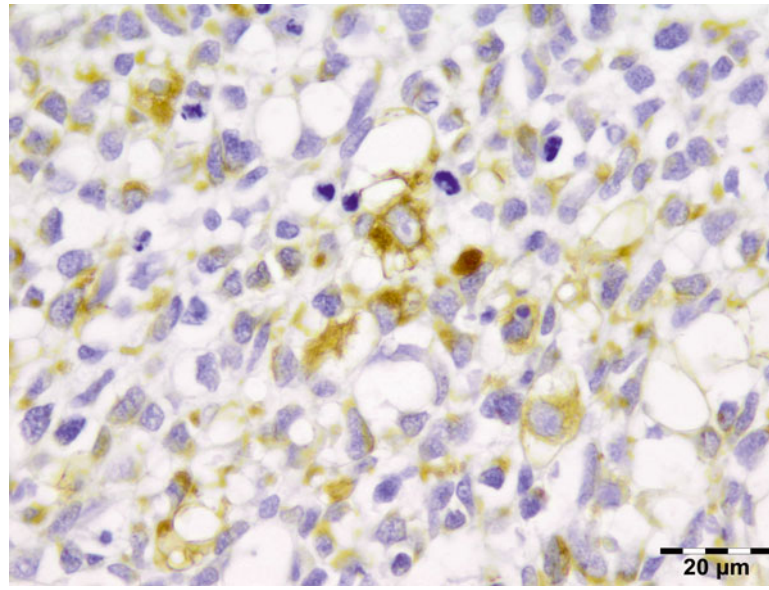

Fig. 12.59 Embryonal rhabdomyosarcoma: the rhabdomyoblasts, especially the more differentiated cells, stain positive for desmin (desmin IH 630×) (Dr. Robert M. Verdijk)

Pleomorphic rhabdomyosarcomas are composed of bizarre polygonal, round, and spindle cells which display evidence of skeletal muscle differentiation [131]. No embryonal or alveolar component should be identified [132–134]. Cross striations are vanishingly rare.

Immunohistochemical evidence of at least one skeletal muscle-specific marker is required for the diagnosis of rhabdomyosarcoma. The presence of these markers correlates with the degree of tumor cell differentiation. Thus, only vimentin is present in the cytoplasm of the most primitive cells. Antibodies against MyoD1 and myogenin are highly specific and sensitive for rhabdomyosarcoma and are currently used as standard antibodies for diagnosis. Muscle markers such as desmin (Fig. 12.59) and muscle-specific actin (HHF-35) are shared by other cells with a myogenic phenotype. Occasional aberrantly expressed markers include cytokeratin, S-100

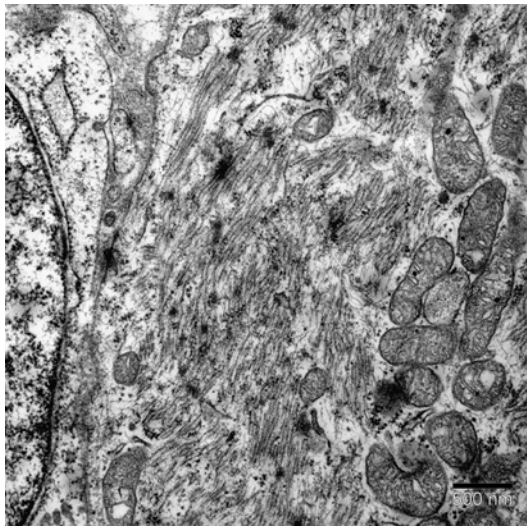

Fig. 12.60 Embryonal rhabdomyosarcoma: ultrastructural characteristics consist of bundles of five and 15-nm thick and thin filaments punctuated by abortive Z-bands that can be observed as irregular dense *black dotted* areas (EM) (Dr. Robert M. Verdijk)

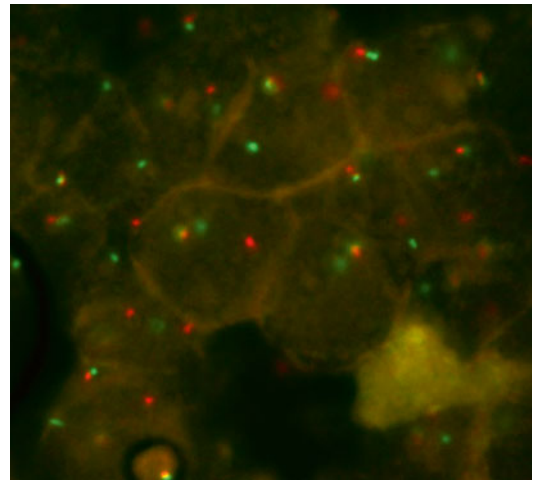

Fig. 12.61 Alveolar rhabdomyosarcoma: fluorescence in situ hybridization (FISH) is an easy tool to determine the presence of fusion signals of the translocation t(1;13) (FISH 400×) (Dr. Robert M. Verdijk)

protein, neurofilaments, and B-cell proteins such as CD20 and immunoglobulin. The Pax5 protein can be present in alveolar RMS as a nuclear staining [135]. Smooth muscle actin and neuron-specific enolase staining occur rather frequently (in 10 and 30 % of rhabdomyosarcomas, respectively). With the use of immunohistochemical markers, the need for ultrastructural studies has become obsolete in many cases; however for the more challenging diagnoses, rhabdomyosarcomas exhibit a range of ultrastructural characteristics corresponding to those of developing striated muscle, primarily bundles of 5- and 15-nm thick and thin filaments punctuated by abortive Z-bands (Fig. 12.60).

Differential Diagnosis

Rhabdomyoma, other small blue round cell tumors.

Histogenesis

Rhabdomyoblasts.

Genetics

Embryonal rhabdomyosarcomas may result from sporadic or inherited mutations. Genetic syndromes that may be associated with rhabdomyosarcoma are neurofibromatosis (4–5 % risk of any one of numerous malignancies), Li–Fraumeni syndrome, Rubinstein–Taybi syndrome, Gorlin basal cell nevus syndrome, Beckwith–Wiedemann syndrome, and Costello syndrome. Cytogenetic studies of embryonal rhabdomyosarcoma have found complex structural and numerical chromosomal changes. Cytogenetic analyses can be used to demonstrate translocations that are consistently and specifically associated with alveolar rhabdomyosarcoma [136, 137]. Fluorescence in situ hybridization (FISH) is an easy tool to determine if translocations t(1;13) or t(2;13), associated with the alveolar subtype, are present (Fig. 12.61). In many centers, the use of RT-PCR to screen for a panel of translocations associated with soft tissue sarcomas is becoming a routine adjunct to morphologic analysis to help ascertain the diagnosis.

Prognosis and Predictive Factors

Treatment responses and prognoses vary widely depending on location and histology. In patients with localized orbital disease, overall 5-year survival rates have improved to more than 80 % with the combined use of surgery, radiation therapy, and chemotherapy [129, 138]. Alveolar

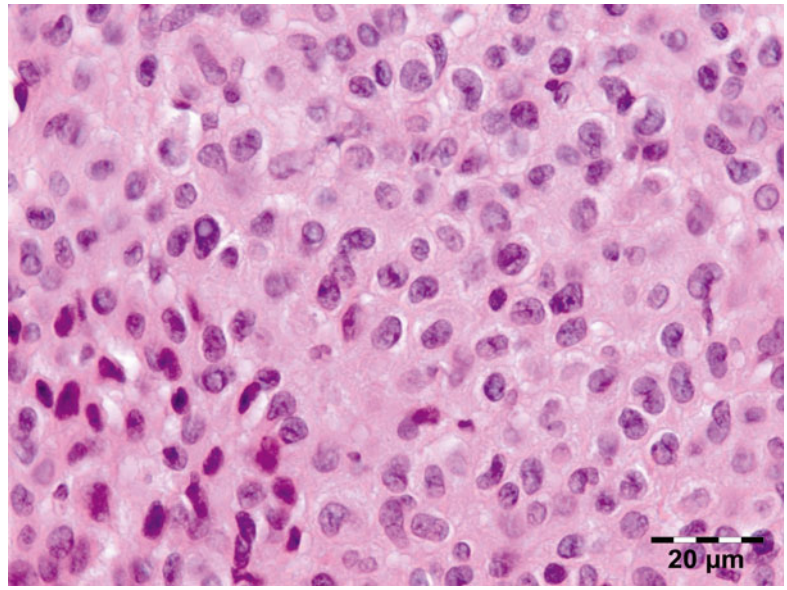

Fig. 12.62 Glomangioma: the lesion is composed of small, uniform, rounded cells with a centrally placed, round nucleus and lightly eosinophilic cytoplasm. Each cell is surrounded by a basal lamina (HE 630×) (Dr. Robert M. Verdijk)

RMS has a worse prognosis when compared to alveolar RMS.

12.7.5 Pericytic (Perivascular) Tumors

Perivascular neoplasms comprise traditionally glomus tumor and hemangiopericytoma (HPC).

12.7.5.1 Glomus Tumor

Definition

Glomus tumors are mesenchymal neoplasms composed of cells that closely resemble the modified smooth muscle cells of the normal glomus body [79].

Synonyms

Typical glomus tumors are subcategorized as "solid glomus tumor," "glomangioma," and "glomangiomyoma" depending on the relative prominence of glomus cells, vascular structures, and smooth muscle.

Epidemiology

Glomus tumors are very rarely reported in the head region. Our series contained two glomus tumors; we are aware of three other reported cases of glomus tumors confined to the orbit [139].

Etiology

None.

Localization

This tumor is commonly found in the hand, where it often occurs as a small painful lesion beneath the fingernails. Although it may be present in many other locations, it is rare in the orbit [139].

Clinical Features

The patient may present with acute proptosis and ocular pain.

Macroscopy

Highly vascularized tissue.

Histopathology

Glomus cells are small, uniform, rounded cells with a centrally placed, round nucleus and amphophilic to lightly eosinophilic cytoplasm. Each cell is surrounded by basal lamina, seen best on PAS or toluidine blue histochemical stains (Fig. 12.62). Nests of glomus cells surround capillary-sized vessels. Glomangiomas, comprising approximately 20 % of glomus tumors, are characterized by dilated veins

surrounded by small clusters of glomus cells. Glomus tumors of all types typically express smooth muscle actin and have abundant pericellular type IV collagen production. H-caldesmon is also positive. Other markers, including desmin, CD34, cytokeratin, and S-100 protein, are usually negative.

Differential Diagnosis
Hemangioma, smooth muscle tumors.

Histogenesis
Perivascular precursor cell.

Genetics
The genetic events underlying sporadic glomus tumors are not known. A gene for multiple inherited glomus tumors has been linked to chromosome 1p21-22.

Prognosis and Predictive Factors
The vast majority of the glomus tumors are benign, so they are treated by a simple surgical excision. A 10 % risk of local recurrence is related to an incomplete removal of the tumor. The malignant form of glomus tumor is exceptional.

12.7.5.2 Myopericytoma
The existence of HPC as a separate entity has been questioned because a number of neoplasms of different lines of differentiation are characterized by a HPC-like vascular growth pattern. Myopericytoma represents a recently delineated entity showing an HPC-like vascular pattern. Myopericytoma represents a distinct perivascular, myoid neoplasm of the skin and soft tissues, characterized by a broad morphologic spectrum of concentrically perivascular growing myoid tumor cells that stain positively for Alpha-SMA and often for h-caldesmon, whereas desmin is usually negative. Most cases of myopericytoma behave in a benign fashion, but local recurrences and rarely metastases may occur in atypical and malignant neoplasms [138]. All myopericytomas are located in subcutaneous and superficial soft tissue of distal extremities [140]. Myopericytoma in the orbit has so far not been described.

12.7.6 Vascular Tumors

12.7.6.1 Juvenile Hemangioma

Definition
An immature form of capillary hemangioma that develops in the perinatal period [79].

Epidemiology
Our series contained seven capillary hemangiomas (11 % of all vascular lesions) confirming the fact that this tumor is common in the head and neck region [141].

Etiology
Used to be considered a hamartoma, that is, a congenital lesion composed of tissue normally present at the involved site. Now more likely considered to be neoplastic.

Localization
Often involves the periocular structures.

Clinical Features
The tumor usually presents in the first few weeks of life as an elevated cherry-red lesion involving the skin. The tumors initially are characterized by rapid diffuse growth for a period of 6–12 months, followed by a slow phase of natural resolution. Seventy percent of lesions resolve by the age of 7 years.

Macroscopy
The tumors are multinodular purple-red in color.

Histopathology
The histology is of capillary blood vessels that may vary from highly cellular areas with solid sheets of plump endothelial cells (Fig. 12.63) to clearly recognizable capillary vessels that may be accompanied by a progressive diffuse interstitial fibrosis (Fig. 12.64). Some mitotic activity usually is visible, but other features of malignant alteration are absent. The lesional cells stain positive for endothelial cell markers CD31 and CD34 and, in contrast to other hemangiomas, stain positive for GLUT-1, a marker normally present in retinal and CNS vasculature.

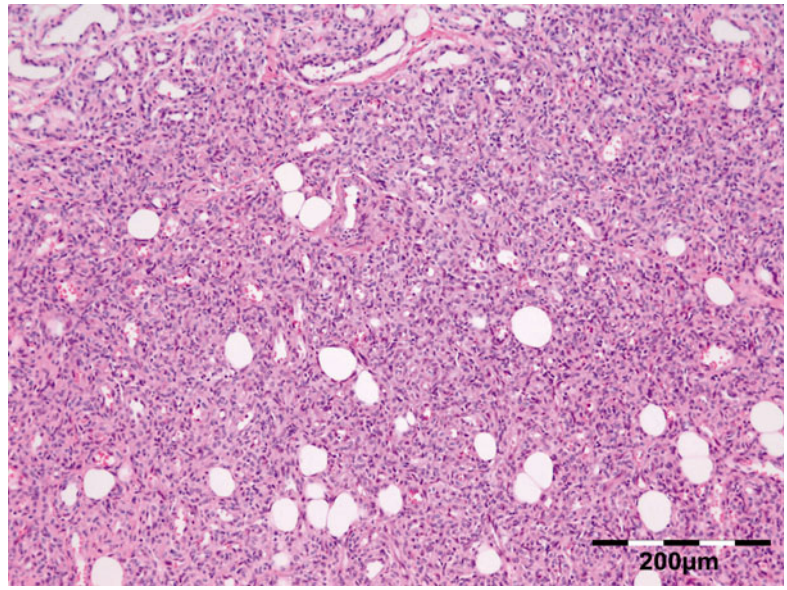

Fig. 12.63 Capillary hemangioma: this solid variant is composed of highly cellular areas with solid sheets of plump endothelial cells (HE 100×) (Dr. Robert M. Verdijk)

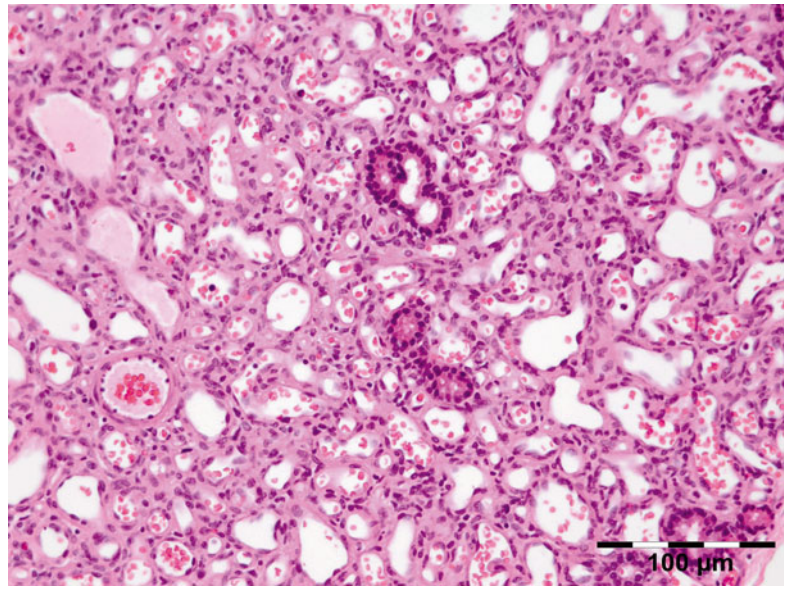

Fig. 12.64 Capillary hemangioma: this vascular type shows clearly recognizable capillary vessels and interstitial fibrosis. Some remaining ducts of the lacrimal gland can be seen (HE 200×) (Dr. Robert M. Verdijk)

Differential Diagnosis

Clinical differential diagnosis is most challenging with rhabdomyosarcoma, lymphangioma, chloroma, and neuroblastoma. Histologic differential diagnosis is not very difficult.

Histogenesis

Vascular endothelial cell origin.

Genetics

Juvenile hemangiomas are monoclonal proliferations based on nonrandom X-inactivation. Some cases harbor somatic mutations of VEGFR2 or VEGFR3 indicating a neoplastic origin and not hamartomatous.

Prognosis and Predictive Factors

Operative treatment now is rarely performed with the advent of laser treatment and steroid

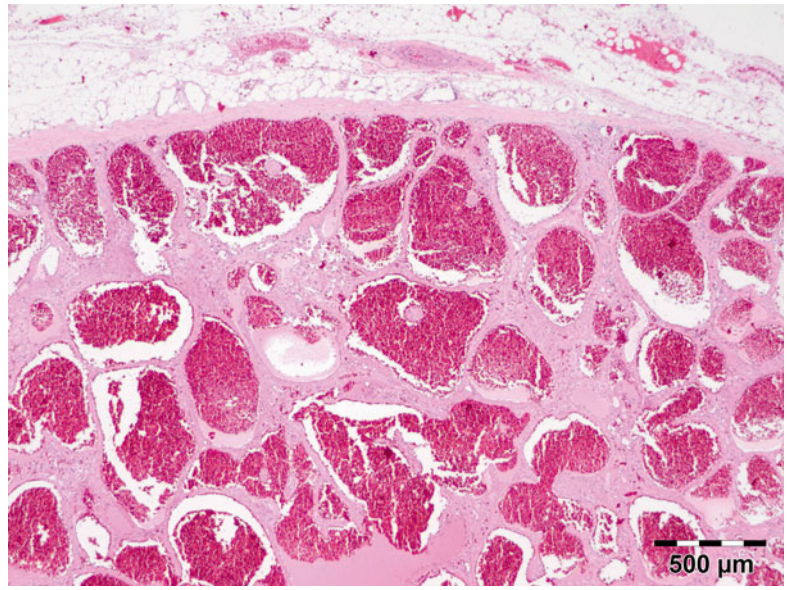

Fig. 12.65 Cavernous hemangioma: the lesion is well demarcated and composed of large dilated blood-filled vessels lined by flattened non-atypical endothelium. The vascular walls are thickened by adventitial fibrosis (HE 25×) (Dr. Robert M. Verdijk)

injections, most recently combined by systemic beta-blockers. The tumor often has a diffuse growth and is difficult to remove.

12.7.6.2 Cavernous Hemangioma

Definition
Well-circumscribed low-flow vascular tumor composed of regular- and large-sized vascular spaces [79].

Epidemiology
Cavernomas ($n=37$) are the most common type of vascular malformation of the orbit encountered in 56 % of vascular lesions and 3 % of all lesions in our series.

Etiology
Unknown.

Localization
Most lesions are located in the retrobulbar region, but they may occur anywhere in the orbit.

Clinical Features
Usually occurs in adults, with a female preponderance. Patients often present with proptosis. Symptomatic lesions require surgical resection [74, 141].

Macroscopy
The tumor is usually well encapsulated and is often completely removed. The cut surface shows cavernous blood-filled channels with a sponge-like appearance.

Histopathology
Shows large dilated blood-filled vessels lined by flattened non-atypical endothelium. The walls are often thickened by an adventitial fibrosis (Fig. 12.65). Mature bone is occasionally present.

Differential Diagnosis
Vascular malformations, lymphangioma.

Histogenesis
Hamartomatous vascular lesion.

Genetics
No genetic abnormalities have been reported with orbital cavernous hemangiomas.

Prognosis and Predictive Factors
Tumors causing symptoms are easily removed and no recurrences are observed.

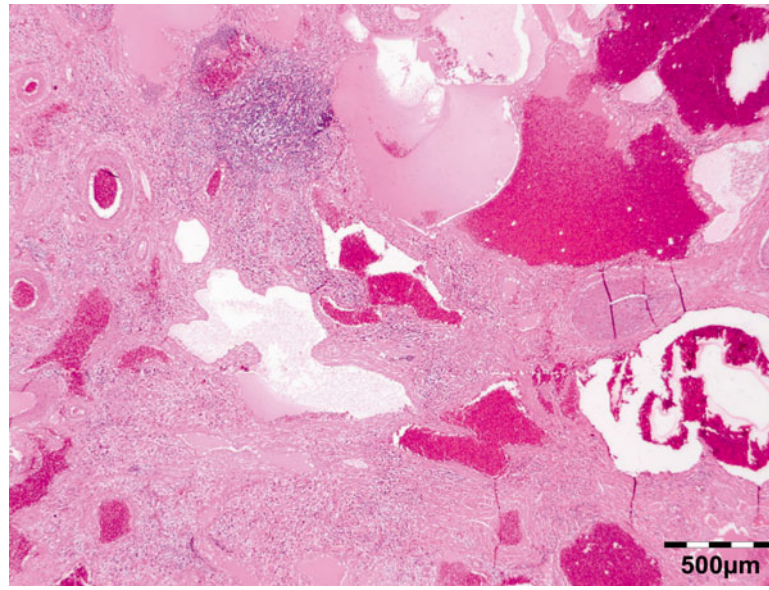

Fig. 12.66 Arteriovenous-lymphatic malformation: the lesion is characterized by vessels of different size, which include veins and arteries. Note that the veins outnumber the arteries. In this case a combination with lymphatic vessels can be observed (HE 25×) (Dr. Robert M. Verdijk)

12.7.6.3 Arteriovenous Hemangioma/ Malformation (AVH/ AVM)

Definition
Nonneoplastic vascular lesion characterized by the presence of arteriovenous shunts [79].

Epidemiology
Deep-seated AVH is uncommon; our series contained 5 AVM out of 66 vascular lesions (8 %).

Etiology
Unknown.

Localization
Angiography demonstrates a high-flow angioma with feeders usually from the ophthalmic artery and external feeders from the maxillary artery.

Clinical Features
Deep-seated AVH affects children and young adults [74]. They are characterized by pulsating exophthalmos with evidence of bruit, occasional hemorrhage, thrombosis, or a caput medusae.

Macroscopy
Tumors are ill defined and contain variable numbers of small and large blood vessels, many of which are dilated.

Histopathology
AVH is characterized by large numbers of vessels of different size, which include veins and arteries with the former largely outnumbering the latter. Areas resembling a cavernous or capillary hemangioma are frequent, as are thrombosis and calcification. Combinations with lymphatic vessels can be observed (Fig. 12.66). Elastic stains are helpful in distinguishing between arteries and veins.

Differential Diagnosis
This diagnosis always requires clinicopathological and radiological correlation.

Histogenesis
Hamartomatous vascular lesion.

Genetics
No genetic abnormalities have been described.

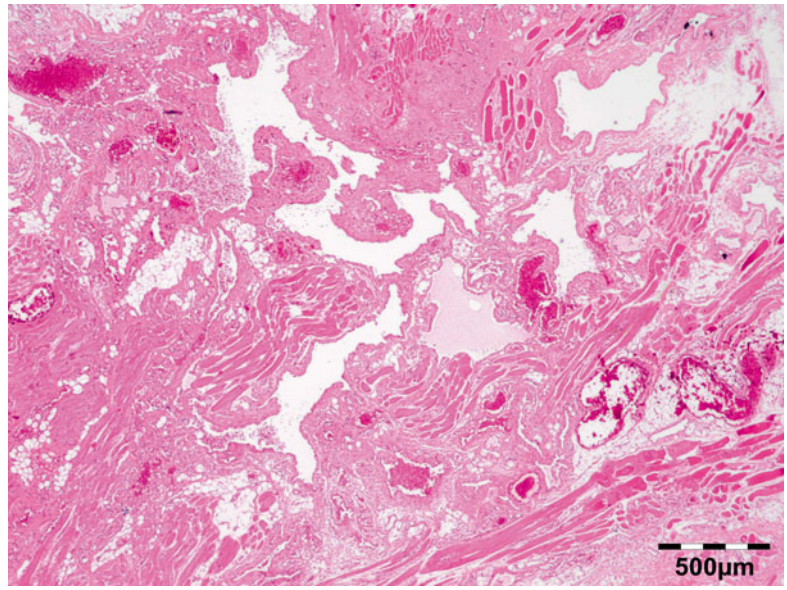

Fig. 12.67 Lymphangioma: the lesion is characterized by thin-walled, dilated lymphatic vessels of different sizes, which are lined by a flattened endothelium. The lumina contain proteinaceous fluid, lymphocytes, and sometimes erythrocytes (HE 25×) (Dr. Robert M. Verdijk)

Prognosis and Predictive Factors

Treatment is difficult because of the degree of involvement, which has to be determined by angiographic examination. Local recurrence is common because of the difficulties in achieving complete excision [74].

12.7.6.4 Lymphangioma

Definition

A benign, cavernous/cystic vascular lesion composed of dilated lymphatic channels [79].

Epidemiology

Lymphangiomas are common pediatric lesions. Lymphangiomas account for less than 10 % of vascular lesions and less than 1 % of all orbital lesions, depending on the case series. In our series, out of a total of 1,077 orbital lesions, 66 were vascular malformations (6 %), and of these, 5 (7.5 %) were lymphangiomas.

Etiology

Venous lymphatic malformations or lymphangiomas originate from the venous system and differentiate to lymphatic vessels.

Localization

Lymphangiomas may occur as intraconal as well as extraconal tumors.

Clinical Features

Lymphangiomas most often present at birth or during the first years of life. There is a tendency for the tumor to fluctuate in size with changes in posture, exertion and straining, and displacement of the eye. Secondary hemorrhage can lead to a sudden onset of painful proptosis [74].

Macroscopy

Multicystic or spongy mass, the cavities of which contain watery to milky fluid.

Histopathology

Lymphangiomas are characterized by thin-walled, dilated lymphatic vessels of different size, which are lined by a flattened endothelium and frequently surrounded by lymphocytic aggregates. The lumina may either be empty or contain proteinaceous fluid, lymphocytes, and sometimes erythrocytes (Fig. 12.67). Larger vessels can be invested by a smooth muscle layer, and long-standing lesions reveal interstitial fibrosis and stromal inflammation. Qualifying histopathological designations such as capillary, cavernous, or cystic are not currently used in the nomenclature of lymphangiomas since they are of no clinical relevance. Stromal mast cells are common and hemosiderin deposition is frequently seen. Positive staining for podoplanin (D2-40) is seen in lymphangiomas in contrast to

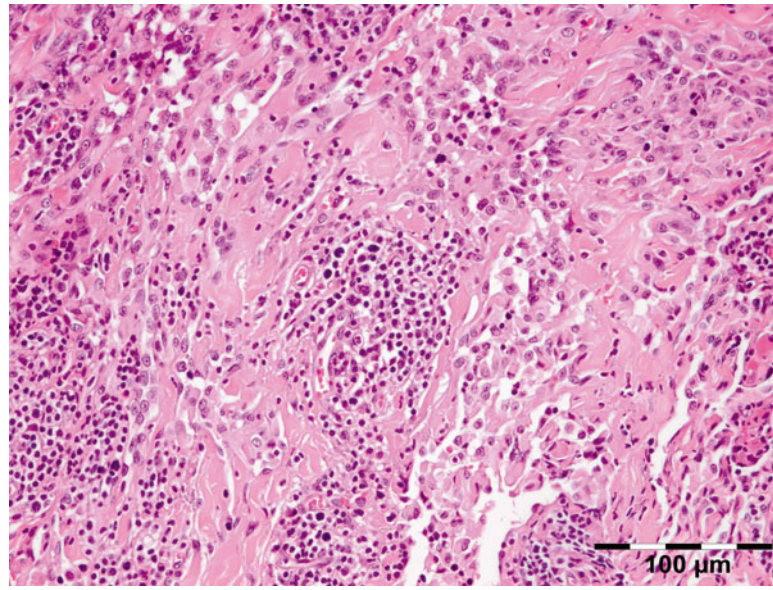

Fig. 12.68 Epithelioid hemangioma: the lesion is composed of vascular structures lined by plump endothelial cells that protrude into the lumen. Surrounding the vessels, there is a prominent inflammatory infiltrate with (in this case) occasional eosinophils (HE 200×) (Dr. Robert M. Verdijk)

hemangiomas. The endothelium demonstrates variable expression of FVIII-rAg and CD31 but usually not for CD34.

Differential Diagnosis

Hemangioma, vascular malformations.

Histogenesis

Hamartomatous vascular lesion containing lymphatic vessels.

Genetics

Cystic lymphangiomas ("cystic hygroma") of the neck are often associated with Turner syndrome.

Prognosis and Predictive Factors

Treatment options for orbital lymphangiomas include conservative management; partial surgical resection of the major cyst; needle aspiration; intralesional injection of steroids, interferon, or sclerosing agents; and local radiotherapy. It is, in general, difficult to remove the orbital lymphangioma completely. They are not encapsulated, do not remain within anatomic boundaries, tend to penetrate into normal orbital structures, and can bleed profusely during surgery. New hemorrhagic cysts may form after incomplete resection. About half of the patients develop recurrences [74].

12.7.6.5 Epithelioid Hemangioma (Angiolymphoid Hyperplasia with Eosinophilia)

Epithelioid hemangioma is a benign vascular tumor with well-formed but often immature vessels, the majority of which are lined by plump, epithelioid (histiocytoid) endothelial cells. It is rare and represented only 1.5 % of all vascular lesions in our series. It presents as nodules or erythematous subcutaneous papules, usually in the head and neck region of young women [142]. It can occur in all races. Histologically, most lesions are well circumscribed and composed of vessels lined by plump endothelial cells that protrude into the lumen in a "tombstone fashion." Surrounding the vessels, there is usually a prominent inflammatory infiltrate (Fig. 12.68). The endothelial cells stain positive for CD31 (Fig. 12.69). A large proportion of eosinophils can often be seen. Kimura's disease is now known to represent separate entity [143] probably representing an allergic or autoimmune response that typically presents as subcutaneous nodules in the head and neck region of young Asian males [142]. There remains considerable controversy as to whether epithelioid hemangioma (angiolymphoid hyperplasia with eosinophilia) is a reactive lesion or a true neoplasm. Systemic associations include blood eosinophilia, nephrotic syndrome due to IgE deposition

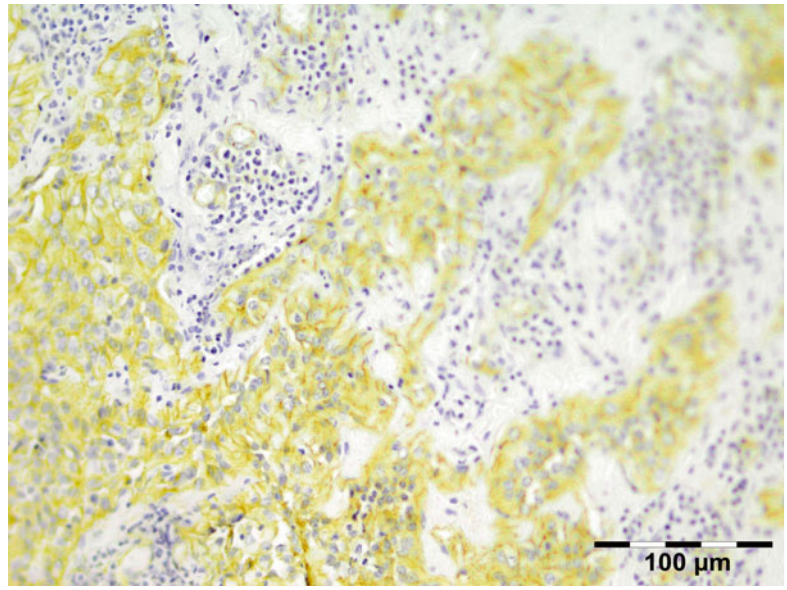

Fig. 12.69 Epithelioid hemangioma: the epithelioid endothelial cells stain positive for CD31 (CD31 IH 200×) (Dr. Robert M. Verdijk)

in the renal glomeruli, lymphadenopathy, and, less common, asthma, tuberculosis, and Loeffler syndrome. Complete local excision and follow-up are optimal management for epithelioid hemangioma. Local recurrence is reported to occur in up to one-third of patients.

12.7.6.6 Angiosarcoma/Epithelioid Hemangioendothelioma

Angiosarcoma accounts for less than 1 % of soft tissue sarcomas and has a predilection for the skin and superficial soft tissues [86]. Localization of angiosarcoma in the orbit is rare (only one case in our series), accounting for less than 3 % [144] of angiosarcomas (Fig. 12.70). Angiosarcoma may develop postirradiation. Epithelioid hemangioendothelioma is a vascular malignancy of endothelial cell origin, very rarely involving the orbit [145].

12.7.7 Germ Cell Tumors

12.7.7.1 Teratoma

Definition

Teratomas contain tissue or tissues derived from all three primary germ layers: ectoderm, mesoderm, and endoderm.

Epidemiology

Rare orbital teratomas, embryonal carcinomas, endodermal sinus tumors (yolk sac carcinomas), and germinomas of the orbit have been reported [146]. We encountered two teratomas out of 1,077 lesions in our series.

Etiology

Teratomas belong to a class of tumors known as nonseminomatous germ cell tumor (NSGCT) [147]. Thus they are neoplasms as opposed to the historic designation as choristomas. In the orbit, teratomas arise from misdirected or ectopic germ cells [147], or they may secondarily involve the orbit originating from the intracranial or nasopharyngeal region [146].

Localization

No specific localization.

Clinical Features

Teratomas comprise approximately 1 % of orbital tumors in childhood. The congenital orbital tumor may be large at the time of birth. The preferred treatment is local excision.

Macroscopy

Pathologic examination discloses a circumscribed but not encapsulated, often multicystic, lesion.

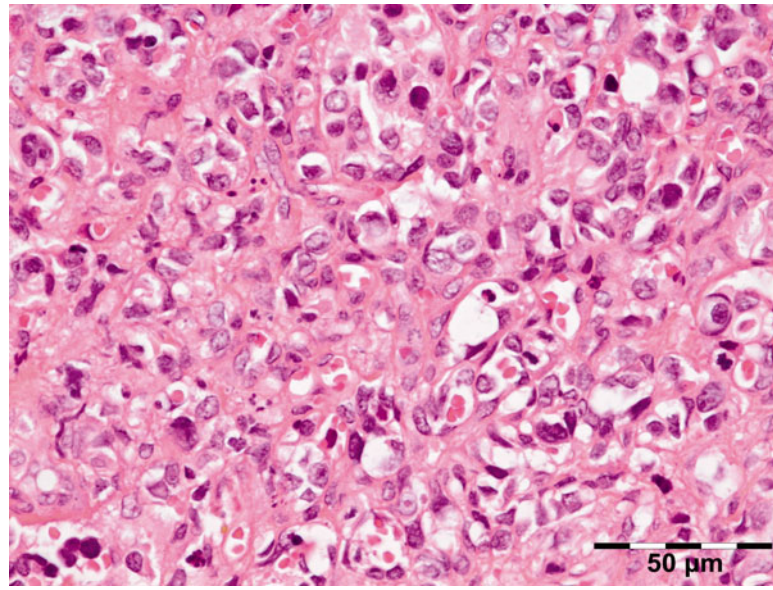

Fig. 12.70 Angiosarcoma: the lesion is composed of atypical epithelioid to spindle-like cells that form slit-like spaces filled with erythrocytes. Regularly cells show intracytoplasmic lumina with erythrocytes. The nuclei are polymorphic and polychromatic with mitoses (HE 400×) (Dr. Robert M. Verdijk)

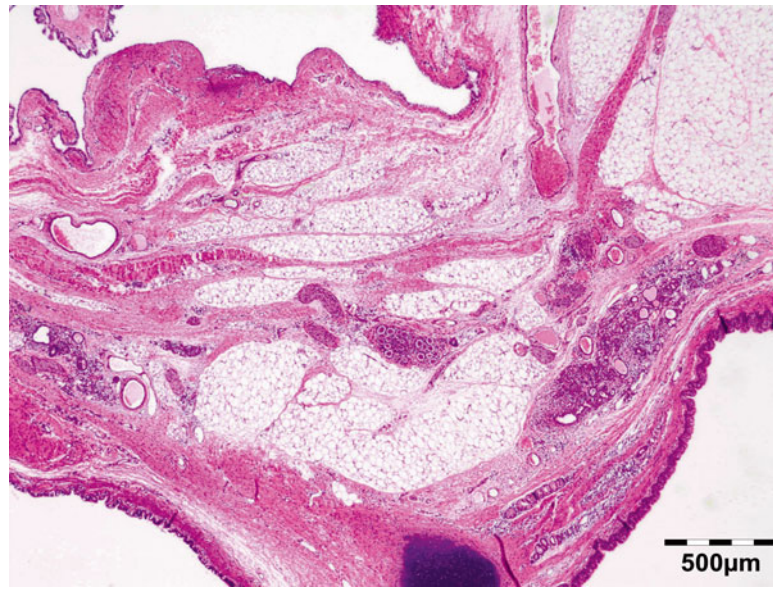

Fig. 12.71 Teratoma: mature stromal elements may be composed of fat, cartilage bone, dermal elements, or glial tissue (HE 25×) (Dr. Robert M. Verdijk)

Histopathology

Mature stromal elements may be composed of fat, cartilage bone, dermal elements, or glial tissue (Fig. 12.71). Mature epithelium can resemble epidermis and respiratory, gastrointestinal, or urothelial tissues (Fig. 12.72). Choroid plexus (Fig. 12.73) or retinal pigment epithelium may be present. Immaturity, usually manifest as immature neuroepithelium but sometimes additionally or rarely solely as cellular, mitotically active glia, is important to assess. Immature teratomas may be graded according to a system developed by Norris et al. [148] and modified by Gonzalez-Crussi [149]: grade 1 neoplasms contain immature neuroepithelium that involves no more than a single low-power (40×) field on the slide with the greatest amount of such tissue; grade 2 neoplasms contain immature tissue that involves more than one but not exceeding three low-power fields on any slide; and grade 3 neoplasms contain immature tissues

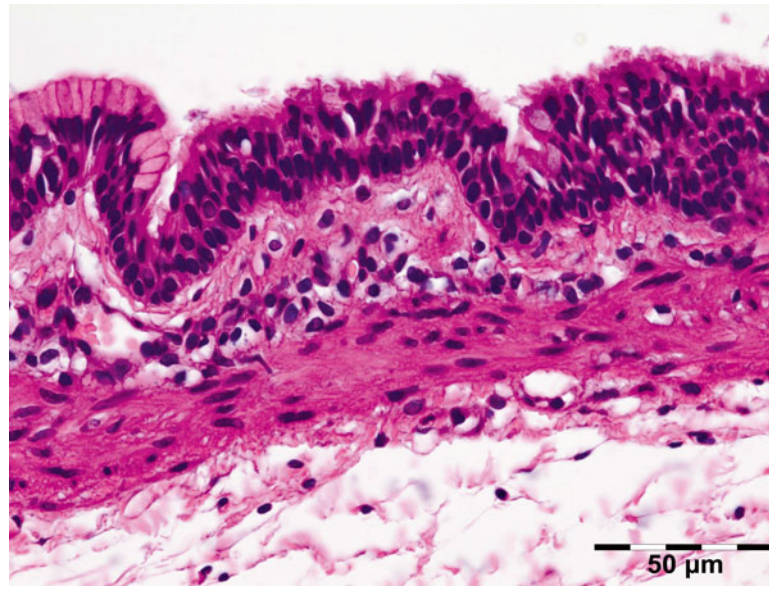

Fig. 12.72 Teratoma: mature epithelium may resemble gastric/respiratory epithelium (HE 400×) (Dr. Robert M. Verdijk)

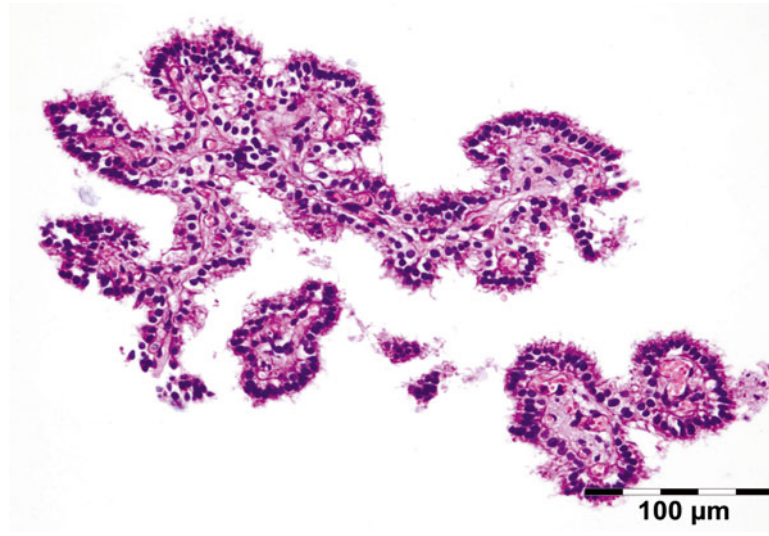

Fig. 12.73 Teratoma: choroid plexus (HE 200×) (Dr. Robert M. Verdijk)

that involve four or more low-power fields on any slide. Malignant transformation may occur after the development of the teratoma ("post-teratomatous" malignant transformation) [147]. This applies to those teratomas that develop malignant somatic neoplasms, such as sarcoma, a phenomenon reported thrice within the orbit [150–152], but also potential squamous cell carcinoma, adenocarcinoma, and malignant melanoma may develop. The prognostically most important malignant component to be identified in teratomas is yolk sac tumor which can lead to metastatic disease after complete surgical resection [153]. Immunohistochemistry shows staining patterns that are specific for the different tissue types that are reproduced. Minor yolk sac tumor components can be identified using a combination of α-fetoprotein and glypican-3.

Differential Diagnosis

Cystic lesions of the orbit.

Histogenesis

Non seminomatous pluripotent germ cell origin, gonocyte or primordial gonadal stem cell.

Genetics

These tumors are diploid with partially erased biparental imprinting. Gain of 12p is often present.

Prognosis and Predictive Factors

Teratomas of the orbit almost always are mature teratomas, but they may contain immature components [154]. Teratomas may be classified using the grading system adapted from Gonzalez-Crussi [149] by Norris [155]: 0 or mature (benign); 1 or immature, probably benign; 2 or immature, possibly malignant (cancerous); and 3 or frankly malignant. If frankly malignant, the tumor is a cancer for which additional cancer staging applies.

12.7.7.2 Yolk Sac Tumor/Endodermal Sinus Tumor

Definition

NSGCT with yolk sac differentiation.

Epidemiology

Rare.

Etiology

Like orbital teratoma, YST are NSGCT thought to arise from the yolk sac.

Localization

These tumors usually occur in the gonads but have been described rarely in the orbit [146, 156, 157].

Clinical Features

They have a clinical presentation similar to embryonal rhabdomyosarcoma as aggressive tumors of early childhood.

Macroscopy

Hemorrhagic loose tissue fragments.

Histopathology

The tumor is composed of cords of cells that form a pseudopapillary pattern with a fine intervening stroma (Schiller–Duval bodies). The epithelial cells have anaplastic features and there may be myxomatous and necrotic areas. The tumor cells stain positive for alpha fetoprotein. Nuclear positive staining for OKT-3/4 is present.

Differential Diagnosis

Metastatic YST, metastatic carcinoma.

Histogenesis

Non seminomatous pluripotent germ cell origin, gonocyte or primordial gonadal stem cell.

Genetics

Not applicable.

Prognosis and Predictive Factors

Orbital lesions may have a relatively good prognosis due to early presentation.

12.7.7.3 Primary Germinoma of the Orbit

Germinoma of the orbit has been reported only rarely [146, 158]. Germinomas are extragonadal seminomatous germ cell tumors. Orbital metastatic seminoma from the testes has been reported and primary seminoma of the testes should therefore be excluded for this diagnosis. Germinomas usually present in the typical midline pineal and third ventricular intracranial locations. Excision is not beneficial for intracranial germinoma, which is typically cured by radiotherapy. The patient may present with a history of visual loss and exophthalmos. The lesion consists of large, round cells with hyperchromatic nuclei, prominent eosinophilic nucleoli, and clear, vacuolated, periodic acid–Schiff-positive cytoplasm. Neoplastic cells often are surrounded by lymphocytes, macrophages, and plasma cells. Immunohistochemical staining reveals the cytoplasm of the tumor cells to be immunoreactive for placental alkaline phosphatase. Nuclear positive staining for OKT-3/4 is present. Focal cytoplasmic staining for AE1/AE3 cytokeratins may be observed. Tumor cells are negative for leukocyte common antigen, CD68, S-100 protein, vimentin, alpha fetoprotein, CD30, and beta human chorionic gonadotropin.

12.7.8 Neural Tumors

12.7.8.1 Neurofibroma

Definition

Hamartomatous benign peripheral nerve sheath tumors.

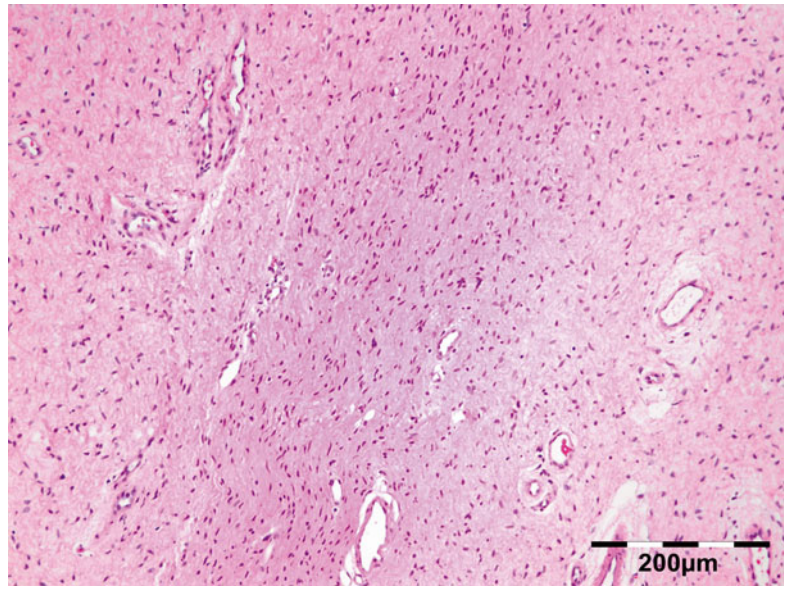

Fig. 12.74 Neurofibroma: neurofibroma shows a diffuse proliferation of Schwann cells, nerve sheath fibroblasts, and less markedly axons permeating the lesion in a haphazard fashion (HE 100×) (Dr. Robert M. Verdijk)

Epidemiology

We have observed 12 neurofibromas in our series accounting for 44 % of all neurogenic lesions and 1 % of all orbital lesions.

Etiology

None.

Localization

The preferred localization is to the superior orbit.

Clinical Features

Orbital symptoms usually show an onset in the first decade as proptosis or displacement of the eye. Changes of the bony orbit are frequent manifestations of the disease and usually consist of bone destruction or, less frequently, bone hypertrophy. In about 10 % of neurofibromatosis type 1 patients, malignant peripheral nerve sheath tumors may develop from neurofibroma as will be discussed below. The solitary diffuse orbital neurofibroma not associated with neurofibromatosis type 1 seems to affect an older age group and often has an uncomplicated course [159, 160].

Macroscopy

Well-defined yellow to white tumor.

Histopathology

Neurofibromas show a diffuse proliferation of Schwann cells, nerve sheath fibroblasts, and less markedly axons permeating the lesion in a haphazard fashion (Fig. 12.74). Neurofibromas can either occur inside or outside the perineurium. Other structures may be present such as melanin-containing cells, ganglion cells, or striated muscle cells (benign Triton tumor). Degenerative changes may result in gelatinous or myxomatous tissue. Increased cellularity may be seen in cellular neurofibromas. Mitotic figures are not usually present and may denote atypical neurofibroma. Malignant change requires a triad of increased cellularity, nuclear pleomorphism, and increased mitotic figures. Neurofibroma show a disperse positive staining of only a portion of the tumor cells for S-100 in contrast to schwannoma which stains diffusely positive.

Differential Diagnosis

Traumatic neuroma, Schwannoma, low-grade MPNST.

Histogenesis

Hamartomatous mixture of endoneurial-derived fibroblastic cells, Schwann cells, and axons.

Genetics

Plexiform neurofibromas mainly occur in the context of neurofibromatosis type 1.

Prognosis and Predictive Factors

Radical surgical resection often proves difficult and frequent recurrences may lead to severe visual impairment [159, 160].

12.7.8.2 Schwannoma

Definition

Schwannomas are benign peripheral nerve sheath tumors derived from Schwann cells.

Synonyms

Older terminology such as neurinoma, perineural fibroma, or neurilemmoma should be avoided as these designate tumors containing connective tissue elements other than Schwann cells.

Epidemiology

It accounts for 0.7–2.3 % of all histopathologically proven orbital tumors; we have diagnosed three cases in our series accounting for 11 % of all neurogenic lesions. Mostly they are solitary sporadic tumors, but they may occur in 10 % of patients suffering from neurofibromatosis type 1.

Etiology

None.

Localization

Schwannoma of the orbit arise from the nerve sheaths of the third, fourth, fifth, and sixth cranial nerves, ciliary ganglion, or supraorbital nerves.

Clinical Features

Schwannomas present as slowly progressing, well-defined, unilateral orbital masses [161].

Macroscopy

A solid encapsulated white or yellowish gray round to oval mass, sometimes causing bony indentation. The tumor grows by simple fusiform expansion. The axons of the affected nerve may be stretched over the surface of the tumor.

Histopathology

The tumor is composed mainly of Schwann cells that may show two types of growth, referred to as Antoni type A and type B. The Schwann cells are long and fusiform with tapering poles. The nucleus is also spindle shaped. The more common Antoni type A areas show cells arranged in wavy, flowing, interlacing, or whorled bundles (Fig. 12.75). The elongated nuclei tend to be arranged in rows with intervening spaces devoid of nuclei, palisades resembling grotesque tactile corpuscles (Verocay bodies), which may be considered the most typical feature of these tumors. In the Antoni type B areas, there are fewer cells in a loose arrangement with a myxoid appearance with microcysts which coalesce to form cystic spaces. The nuclei do not assume a palisade arrangement. Blood vessels show thick collagen sheaths. Phagocytes loaded with lipoid material may at times be a striking feature. Nuclear atypia with hyperchromatic pleomorphic nuclei can be observed in ancient Schwannoma (Fig. 12.76) [162]. Mitotic figures with counts of 6 mitoses per 10 HPF can be observed. True malignant change of Schwannoma is very rare and may often be misdiagnosed schwannomatous neurofibroma. Schwannoma are strongly and uniformly positive for S-100 (Fig. 12.77), are negative to focally positive for CD34, and are usually surrounded by an EMA-positive staining capsule.

Differential Diagnosis

Schwannomatous neurofibroma, SFT, leiomyoma.

Histogenesis

Schwannomas are derived from Schwann cells.

Genetics

Multiple schwannomas may be seen with neurofibromatosis type 2 which can be associated with optic nerve meningioma as well. Schwannomatosis is a separate disease entity associated with multiple schwannomas related

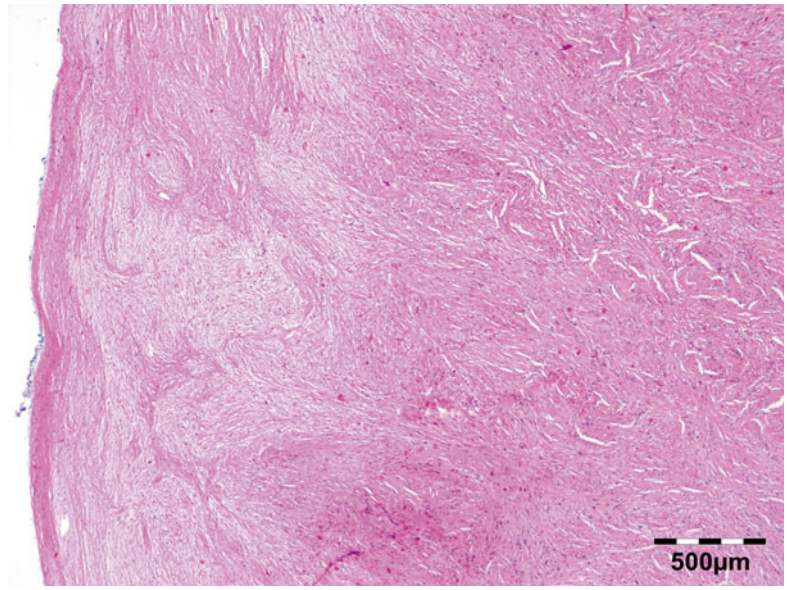

Fig. 12.75 Schwannoma: the more common Antoni type A areas show cells arranged in wavy, flowing, interlacing, or whorled bundles (HE 25×) (Dr. Robert M. Verdijk)

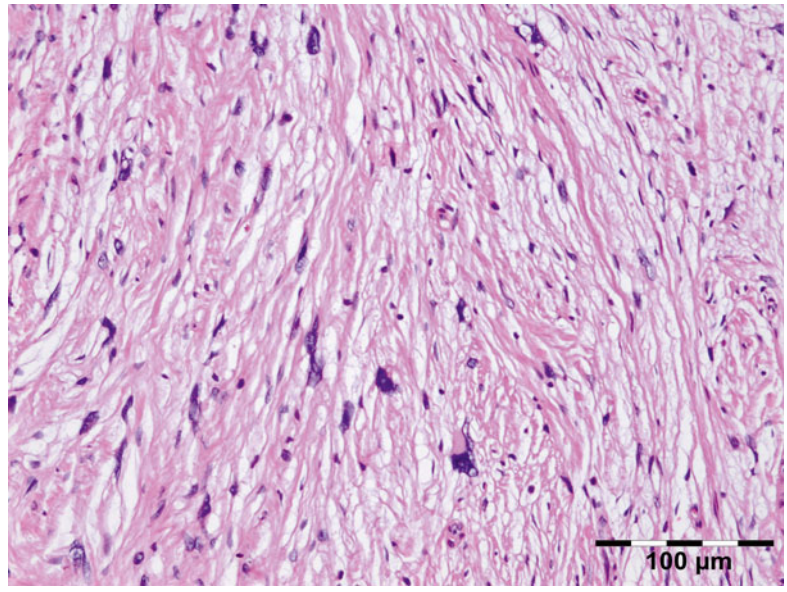

Fig. 12.76 Schwannoma ancient: nuclear atypia with hyperchromatic pleomorphic nuclei can be observed in ancient schwannoma (HE 200×) (Dr. Robert M. Verdijk)

to a separate gene locus on chromosome 22 close to *NF2*. Schwannoma in patients suffering from neurofibromatosis type 2 or schwannomatosis tends to have a plexiform appearance (Fig. 12.78).

Prognosis and Predictive Factors

Radical surgical resection can often be easily obtained and recurrences are rare even after incomplete resection.

12.7.8.3 Granular Cell Tumor

Granular cell tumor is a lesion of neural origin and may arise in any part of the body, most notably in the tongue, chest wall, and upper extremities [163]. It is characterized by rounded, polygonal, or slightly spindled cells with acidophilic granular cytoplasm (Fig. 12.79) that stains PAS and S-100 (Fig. 12.80) positive. Older lesions may exhibit a marked desmoplastic stroma. Sporadic cases

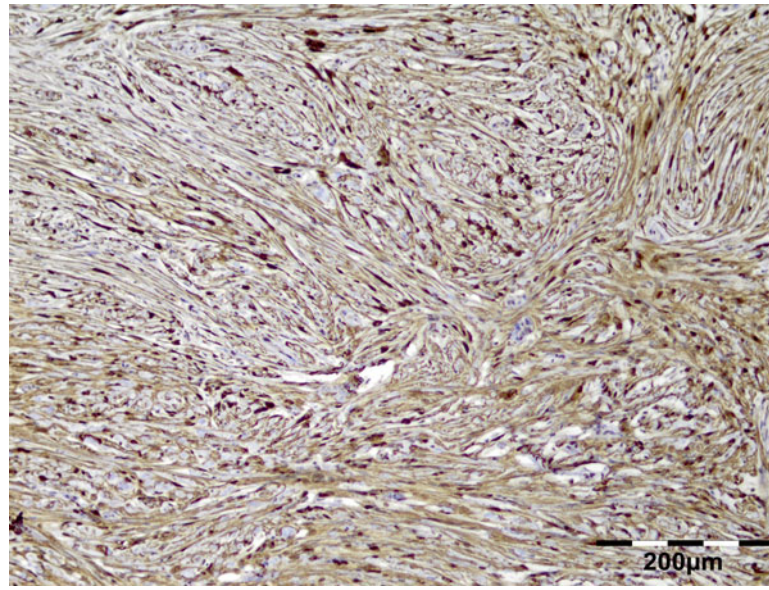

Fig. 12.77 Schwannoma: schwannomas are strongly and uniformly positive (nuclear and cytoplasmic) for S-100 (S-100 IH 100×) (Dr. Robert M. Verdijk)

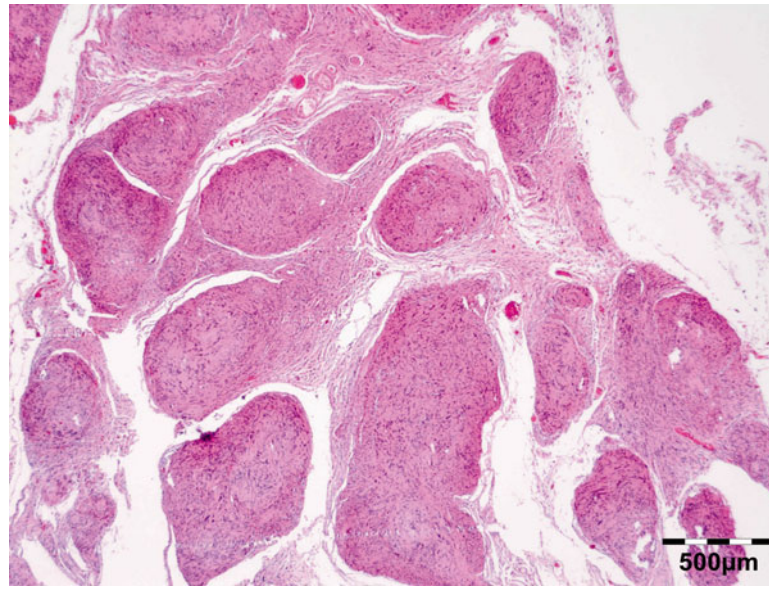

Fig. 12.78 Plexiform schwannoma: schwannomas in patients suffering from neurofibromatosis type 2 or schwannomatosis tend to have a plexiform appearance (HE 25×) (Dr. Robert M. Verdijk)

were recognized in the orbicularis muscle, lacrimal sac, eyelids, caruncle, conjunctiva, and the ciliary body. We have diagnosed one case of orbital granular cell tumor in our series. While most of the granular cell tumors are discrete and well delineated from the surrounding tissues, some may be infiltrative and molded to the globe, invade the sclera, or surround the optic nerve sheath. A striking feature of the tumor is the involvement of extraocular muscles in 43 % of cases [164].

12.7.8.4 Malignant Peripheral Nerve Sheath Tumor (MPNST)

Definition

Any malignant tumor arising from or differentiating toward cells intrinsic to the nerve sheath.

Synonyms

Older designations such as malignant schwannoma, neurofibrosarcoma, or mesenchymoma should be avoided.

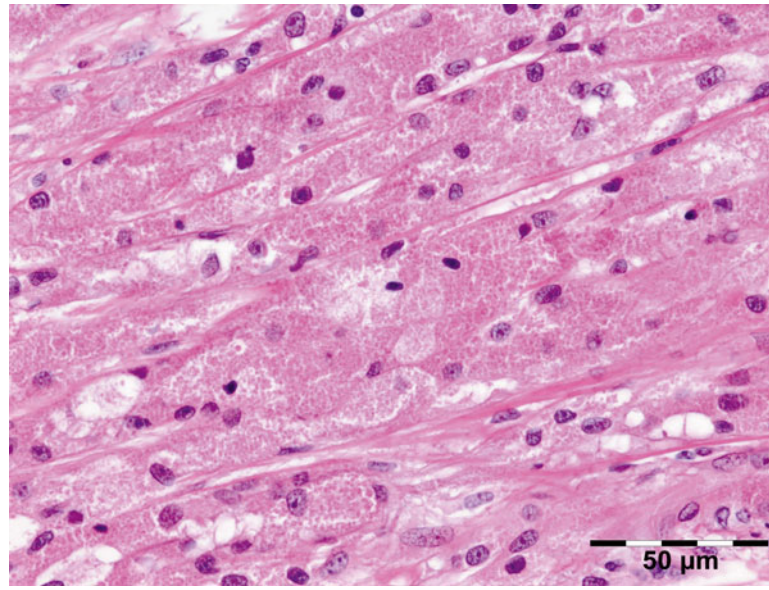

Fig. 12.79 Granular cell tumor: characterized by rounded, polygonal, or slightly spindled cells with acidophilic granular cytoplasm (HE 400×) (Dr. Robert M. Verdijk)

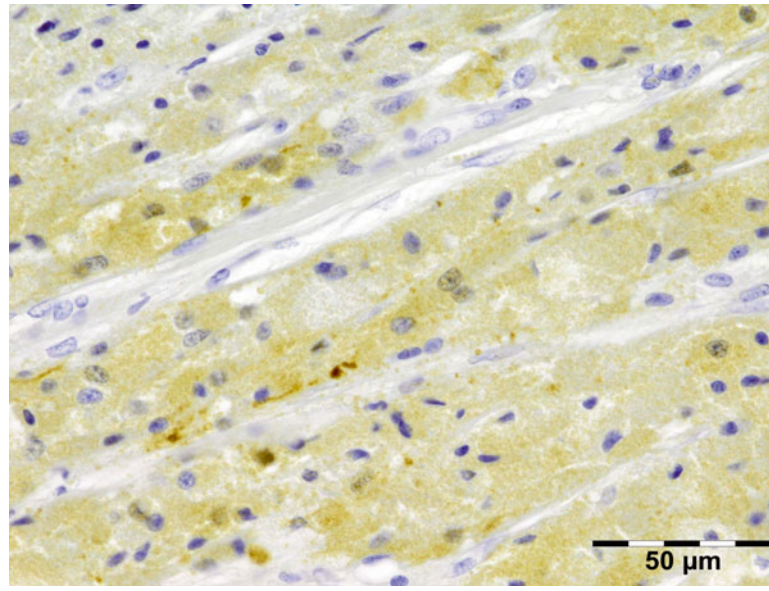

Fig. 12.80 Granular cell tumor: stains cytoplasmic positive with S-100 (S-100 IH 400×) (Dr. Robert M. Verdijk)

Epidemiology

MPNST in the orbit is uncommon but has been described in a child with NF1 [165]. We have described a sporadic case in an adult [166].

Etiology

Most MPNSTs arise de novo. In a series of MPNST diagnosed in our laboratory, a plexiform neurofibroma was documented as a precursor lesion in 11 % of the cases, most of which had NF1 [166]. Extremely rare examples arise in schwannoma, ganglioneuroma/ganglioneuroblastoma, or pheochromocytoma.

Localization

Often there is a relation to a peripheral nerve.

Clinical Features

Individuals with the common autosomal dominant hereditary disorder neurofibromatosis type

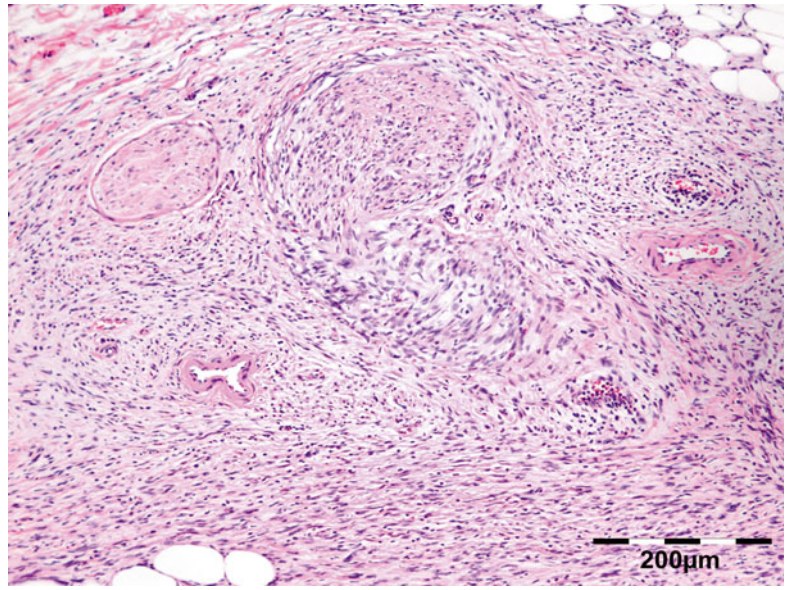

Fig. 12.81 MPNST: spindle cells with indistinct cytoplasmic margins and wavy or S-shaped nuclei that are arranged in fascicles with alternating cellular and myxoid areas (HE 100×) (Dr. Robert M. Verdijk)

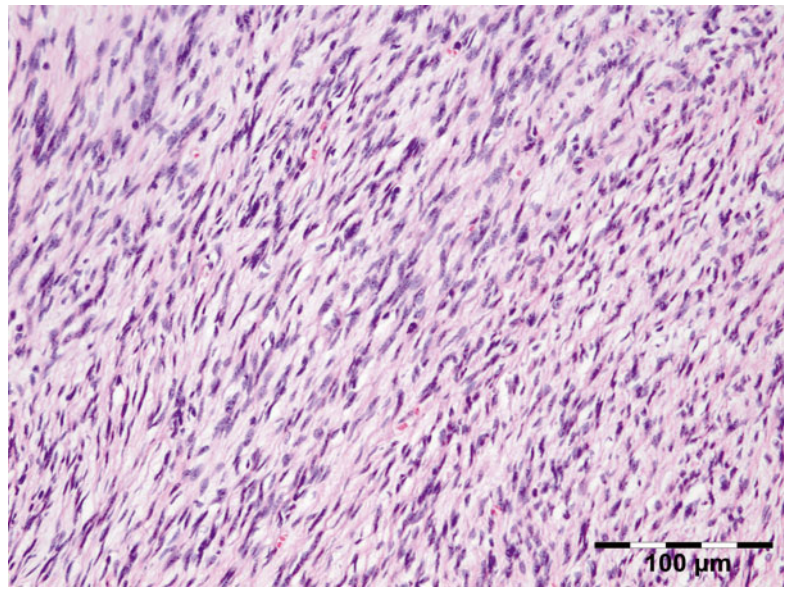

Fig. 12.82 MPNST: brisk mitotic activity is present (HE 200×) (Dr. Robert M. Verdijk)

1 (NF1) are predisposed to develop MPNSTs at an incidence of 2 % [167, 168].

Macroscopy

MPNST may be fusiform or globular and may be associated with a nerve or plexiform neurofibroma. Most MPNSTs are surrounded by a fibrous pseudocapsule.

Histopathology

Morphologic criterion for the diagnosis of MPNST is the presence of spindle cells with indistinct cytoplasmic margins and wavy or S-shaped nuclei that are arranged in fascicles with alternating cellular and myxoid areas (Fig. 12.81). Brisk mitotic activity is present (Fig. 12.82). In our experience of 95 consecutive cases of MPNST at different locations

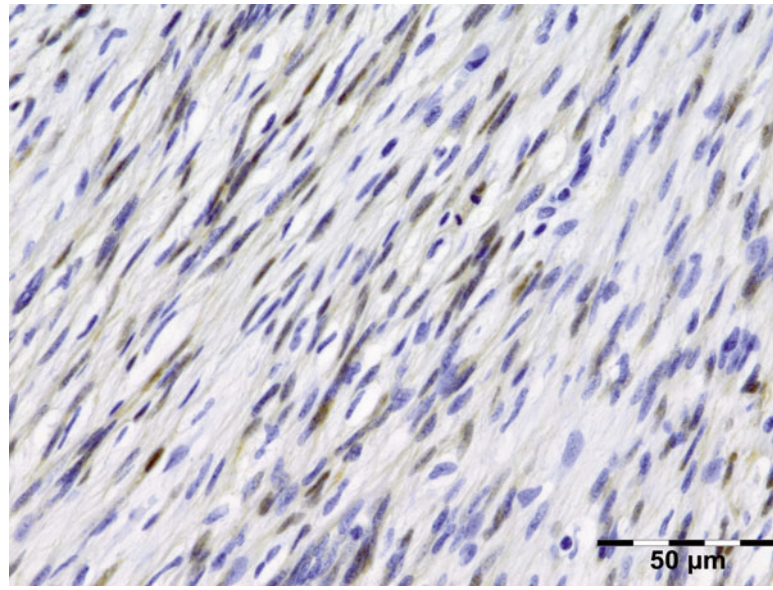

Fig. 12.83 MPNST: S-100 staining is often in dispersed, single-tumor cells (S-100 IH 400×) (Dr. Robert M. Verdijk)

[166], the main histologic growth pattern was fascicular (97 %), followed by myxoid (72 %), epithelioid (59 %), and storiform (27 %). Divergent differentiation with the rhabdoid (13 %) or chondroid (11 %) growth pattern was rare. Only very rarely was one of these growth patterns exclusively present. Nuclear pleomorphism and/or the presence of giant cells was noted in approximately a third of cases (36 %). Pleomorphism and giant cells were more often observed in the tumors in the extremities versus the other locations. Attenuated collagen fiber formation was seen in 75 %. Necrosis was more often present in NF1-related tumors (85 % vs. 53 %). S-100 staining was positive in 65 % of tumors (Fig. 12.83); the staining was often in dispersed, single-tumor cells. S-100 staining was not significantly associated with tumors that showed an epithelioid growth pattern or any other growth pattern.

Differential Diagnosis

Synovial sarcoma, spindle cell melanoma, IMT, SFT.

Histogenesis

The tumor is derived from endoneurial fibroblastic cells and Schwann cells.

Genetics

MPNST may develop sporadically or be related to NF1. In 23 % of tumors, p53 mutations are observed [166].

Prognosis and Predictive Factors

Radical resection is the preferred treatment, since the tumor is not very sensitive to chemotherapy or irradiation.

12.7.8.5 Small Blue Round Cell Tumors (SBRCT)

SBRCT is any one of a group of malignant neoplasms consisting of small round cells that stain blue on routine H&E-stained sections. These tumors are more frequently seen in children than adults. They typically represent undifferentiated cells. The predominance of blue staining is due to the fact that the cells consist predominantly of nucleus; thus they have scant cytoplasm. Only the SBRCT that occur in the orbit will be discussed.

Rhabdomyosarcoma (See Sect. 12.7.4.2)
XXX

Neuroblastoma/Ganglioneuroma

Definition

Malignant tumor derived from variable amounts of neuroblastic cells, ganglion cells, and schwannian stroma.

Epidemiology

Neuroblastomas are the most common type of extracranial solid tumors presenting in

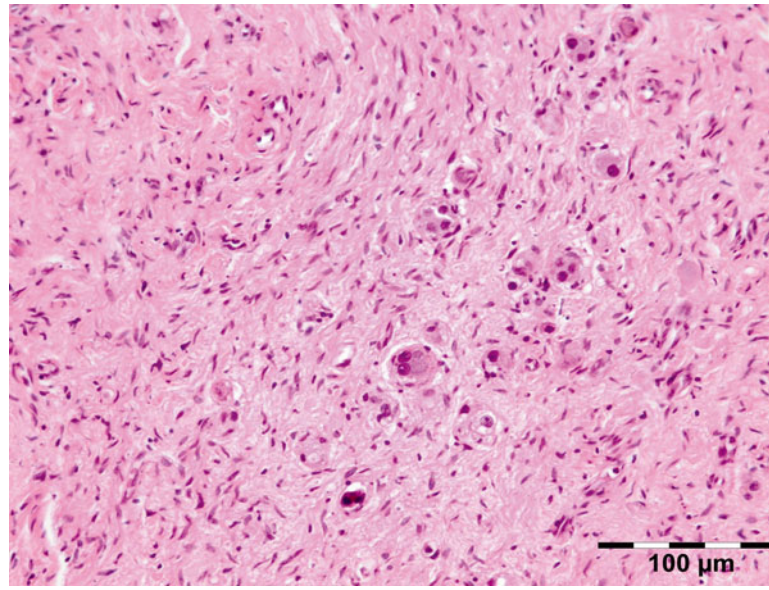

Fig. 12.84 Ganglioneuroma: (schwannian stroma-dominant) maturing type (HE 200×) (Dr. Robert M. Verdijk)

childhood. It is second only to rhabdomyosarcoma as the most frequent orbital malignancy in children (>90 % of pediatric orbital malignancies) [24].

Etiology

Unknown.

Localization

Ophthalmic manifestations occur in 20–50 % of patients with neuroblastoma. Neuroblastoma often metastasizes to the bone and has a propensity to metastasize to the orbit. This was first identified in 1907 by Hutchison and the presentation of neuroblastoma with periorbital involvement is known as "Hutchison's syndrome" [169].

Clinical Features

It is unclear why the orbital bones are frequent targets of metastases, but as a result, these children often present with periorbital ecchymoses and proptosis at presentation or the so-called "raccoon eyes." Accompanying visual loss and blindness also occur in a subset of these patients and prompt initiation of therapy for children with orbital involvement may prevent further loss of vision. Most patients with neuroblastoma are less than 2 years old; they are rarely over 8 years of age. There is no definite gender bias. Most patients with orbital metastatic neuroblastoma have abdominal primary tumors. In three-quarters of patients, excessive amounts of catecholamine metabolites are found in the urine.

Macroscopy

Neuroblastomas are lobulated masses that have soft fleshy gray hemorrhagic aspect.

Histopathology

It is recommended that the International Neuroblastoma Classification should be used when describing tumor samples. There are four categories in this group of tumors: neuroblastoma (schwannian stroma-poor), ganglioneuroblastoma intermixed (schwannian stroma-rich), ganglioneuroma (schwannian stroma-dominant) maturing or mature (Fig. 12.84), and ganglioneuroblastoma nodular (composite, schwannian stroma-rich/stroma-dominant and stroma-poor). Within each category, one or more subtypes are recognized. Microscopically, tumors in the neuroblastoma category are composed of neuroblastic cells with scant cytoplasm and round to ovoid, hyperchromatic, or densely speckled nuclei that form groups or nests separated by delicate, often incomplete, stromal septa without or with

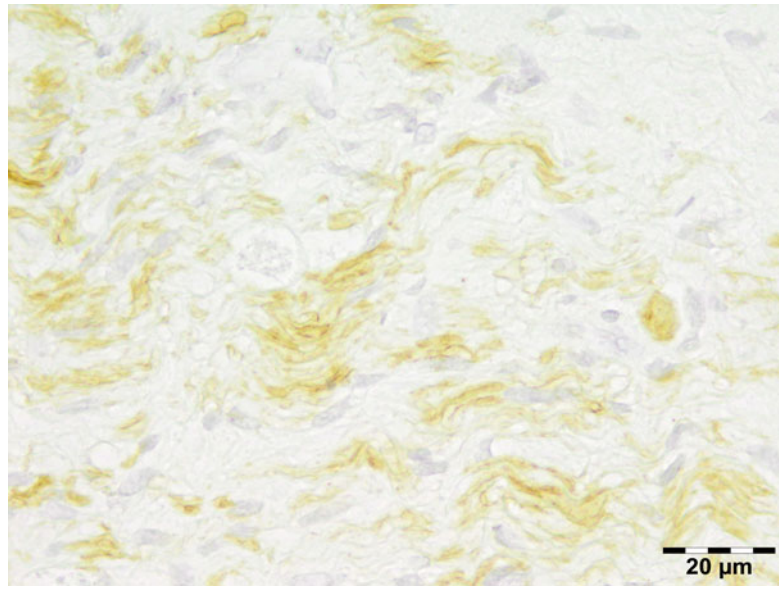

Fig. 12.85 Ganglioneuroma: neurofilament (*NF*) staining identifies ganglion cells in ganglioneuroma (NF IH 630×) (Dr. Robert M. Verdijk)

limited schwannian proliferation. Neural fibrils can be identified and the characteristic arrangements of cell clusters are termed "Homer Wright rosettes"; they consist of round or ovoid clusters of cells surrounding a central core of light pink neuropil. Tumors in the ganglioneuroblastoma intermixed category and the ganglioneuroma category are characterized by a presence of ganglioneuromatous tissue, where mature and/or maturing ganglion cells are individually scattered in a background of highly developed schwannian stroma. For exact criteria we refer to the papers by Shimada [128, 170].

Immunohistochemistry can be used to differentiate these tumors from other small round blue tumors (Ewing sarcoma, non-Hodgkin lymphoma, rhabdomyosarcoma, and the blastemal subtype of Wilms tumor). Neuroblastomas do not stain for CD99 (which is characteristic for Ewing sarcoma), WT-1 (which is characteristic for Wilms tumor), or CD45 (which is positive in lymphomas); neuronal markers (NSE [neuron-specific enolase], synaptophysin, and chromogranin A) are not specific for NBL, and neurofilament staining identifies ganglion cells in ganglioneuroma (Fig. 12.85).

Differential Diagnosis

Other primary tumors of childhood, including Ewing sarcoma and Wilms tumor, only rarely metastasize to the orbit.

Histogenesis

These tumors are derived from neuroblastic progenitor cells.

Genetics

Several genetic loci have been identified; germline mutations in only two specific genes, ALK (anaplastic lymphoma kinase) and Phox2B, have been reported to date. In contrast to ALK, which is mutated in both hereditary and sporadic NBL, Phox2b mutations have been detected only in a rare subset of sporadic tumors. NBL has been divided into two broad genetic categories: (1) those with an abnormal gain of whole chromosomes and (2) those with segmental changes. Segmental changes in 1p and 17q are usually also associated with amplification (extra copies) of MYCN oncogene (MNA). MNA is most commonly detected by FISH (fluorescence in situ hybridization) and defined by the INRG as greater than or equal to ten copies.

Prognosis and Predictive Factors

More young children die from NBL than from any other types of cancer. In clinical practice approximately half of all neuroblastomas are metastatic at diagnosis and require intensive combination therapy with chemotherapy, surgery, and radiation. The prognosis and treatment for NBL are highly dependent on molecular, genetic, and pathologic tests. Furthermore, screening, diagnosis, and surveillance studies rely on the measurement of urine catecholamines, which are elevated in more than 90 % of NBL patients.

12.7.8.6 Ewing Sarcoma/Primary Peripheral Primitive Neuroectodermal Tumor (ES/pPNET)

Definition

ES/pPNET are defined as round cell sarcomas that show varying degrees of neuroectodermal differentiation.

Epidemiology

It is the second most common sarcoma in the bone and soft tissue in children. ES/pPNET shows a slight predilection for males with the ratio of 1.4:1. Primary orbital ES/pPNET is extremely rare and limited cases have been reported [171].

Etiology

The term Ewing sarcoma has been used for those tumors that lack evidence of neuroectodermal differentiation as assessed by light microscopy, immunohistochemistry, and electron microscopy, whereas the term pPNET has been employed for tumors that demonstrate neuroectodermal features as evaluated by one or more of these modalities.

Localization

Rarely metastasize to the orbit.

Clinical Features

Nearly 80 % of patients are younger than 20 years, and the peak age incidence is during the second decade of life [172].

Macroscopy

The tumor in the bone and soft tissue is tan-gray and often necrotic and hemorrhagic. Some soft tissue tumors may be associated with a large peripheral nerve.

Histopathology

The microscopic morphology of the tumor is variable. Most cases are composed of uniform small round cells with round nuclei containing fine chromatin, scanty clear or eosinophilic cytoplasm, and indistinct cytoplasmic membranes (Fig. 12.86). The cytoplasm of the tumor cells frequently contains PAS-positive glycogen. In some cases Homer Wright rosettes are present. Necrosis is common with viable cells frequently perivascular in distribution. CD99 is expressed in almost all cases in a characteristic membranous fashion, though it is not specific (Fig. 12.87). Vimentin stains most tumor cells, and neural markers such as neuron-specific enolase (NSE), S-100, and synaptophysin are frequently expressed [173]. ES/pPNET has also been shown to stain with keratins in some cases.

Differential Diagnosis

A differential diagnosis should be made with other small round cell tumors.

Histogenesis

Although the histogenetic origin has been debated over the years, increasing evidence from immunohistochemical, cytogenetic, and molecular genetic studies supports a mesenchymal progenitor cell origin for all ES/pPNET [174]. The ES/pPNET group includes small round cell tumors of the bone, soft tissue, and nerve with morphological attributes of the germinal neuroepithelium. Peripheral ES/pPNET also occur within the craniospinal vault, the meninges, and the cranial and spinal nerve roots.

Genetics

Gene rearrangements between the EWS gene on chromosome 22q12 and members of the

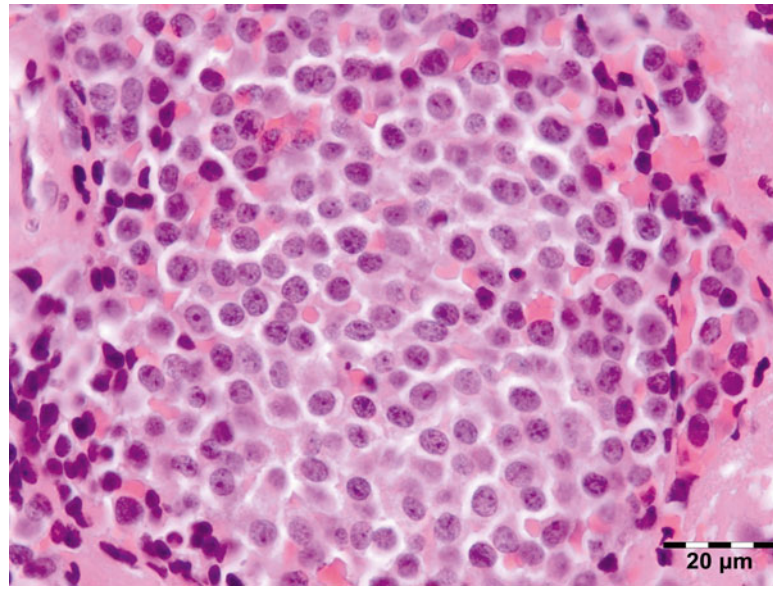

Fig. 12.86 Ewing sarcoma: composed of uniform small round cells with round nuclei containing fine chromatin, scanty clear or eosinophilic cytoplasm, and indistinct cytoplasmic membranes (HE 630×) (Dr. Robert M. Verdijk)

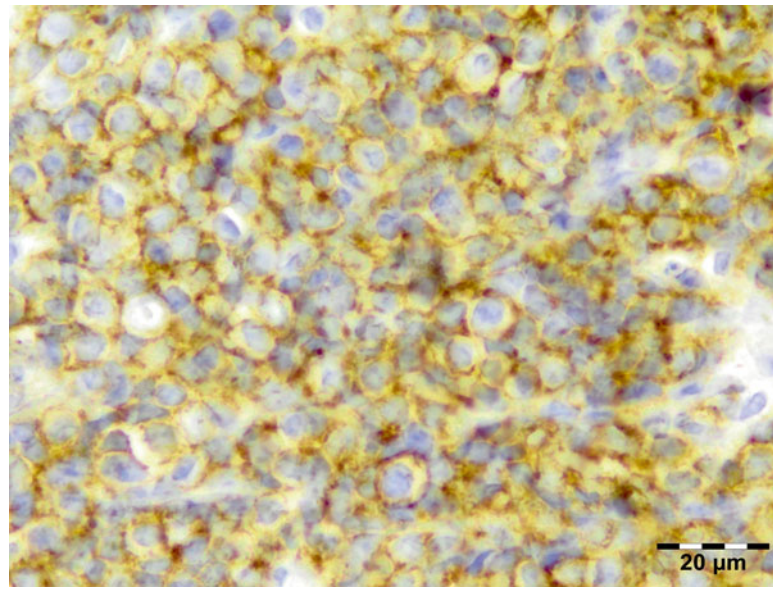

Fig. 12.87 Ewing sarcoma: CD99 is expressed in almost all cases in a characteristic membranous fashion (CD99 IH 630×) (Dr. Robert M. Verdijk)

ETS gene family are common (translocation t(11;22)(q24q12)) specific to ES/pPNET. The fusion gene is designated EWS/FLI-1. Another 10–15 % of cases have a variant translocation fusing EWS to a closely related ETS gene. Most cases can be identified using genetic diagnostic testing with interphase fluorescence in situ hybridization approaches.

Prognosis and Predictive Factors

Although bone invasion and extraorbital extension are possible, systemic metastases are uncommon in the cases of orbital ES/pPNETs. Surgery has been the initial treatment in most cases; chemotherapy with or without radiotherapy is considered the best additional treatment. The orbital ES/pPNET could be less aggressive than other

forms of ES/pPNETs, since most of the patients reported were alive after the follow-up period (at least 6 months) [171].

12.7.8.7 Retinoblastoma

Extension of retinoblastoma into the orbit is a well-known complication and is represented once in our series. The tumor will be discussed in the chapter on the retina.

Wilms Tumor (Nephroblastoma)

Metastasis to the orbit is extremely rare [175].

Small Cell Lymphoma (See Also Lymphomas, Sect. 12.7.10.2)

Precursor B lymphoblastic lymphoma (pre-BLL) of the orbit in a child occurs rarely as an unusual presentation of a non-Hodgkin lymphoma [176]. Precursor B-cell lymphoblastic leukemia is a form of lymphoid leukemia, sometimes additionally classified as a lymphoma, as designated leukemia/lymphoma. On histology it consists of small- to medium-sized blast cells with scanty cytoplasm. Nucleoli are inconspicuous. Eighty to ninety percent are of the B-cell phenotype (CD 79a positive) with cytoplasmic μ heavy chain and nuclear positivity with TdT. Most cases are immunoreactive with CD10 and CD19. There is variable staining with CD45, CD20, CD22, and CD13. It consists of the following subtypes: t(9;22)-BCR/ABL, t(v;11q23)-MLL rearrangement, t(1;19)-E2A/PBX1, t(12;21)-ETV/CBFα, and t(17;19)-E2A-HLF [177].

Burkitt's lymphoma (BL) is a highly aggressive tumor of medium-sized proliferating B cells, typically with translocations resulting in deregulation of the c-myc oncogene. Clinical subtypes include endemic, sporadic, and immunodeficiency-associated BL. Endemic BL occurs in equatorial Africa, representing the most common malignancy of childhood with an incidence peak at 4–7 years. Sporadic BL is seen throughout the world, mainly in children and young adults. BL accounts for approximately 30–50 % of all childhood lymphomas. Immunodeficiency-associated BL is seen primarily in association with HIV infection, occurring after an initial manifestation of AIDS. Epstein–Barr virus (EBV) is found in 25–40 % of all the cases. On histology Burkitt's lymphoma of the orbit is composed of closely packed B lymphocytes. Foci of histiocytes impart a starry sky appearance to the tumor. It is very important to differentiate this tumor from diffuse large cell lymphoma that requires a different treatment. If there is doubt, gene expression analysis can be helpful. The orbital lesions in Burkitt's lymphoma appear as well-circumscribed masses on CT and MRI scans [178].

Medulloblastoma

Medulloblastoma is a neoplasm of the cerebellum and should not be confused with medulloepithelioma of the eye (Fig. 12.88). Metastasis from a medulloblastoma to the intraorbital portion of the optic nerve is extremely rare.

12.7.8.8 Optic Nerve Glioma

It will be discussed in the chapter on the optic nerve.

12.7.8.9 Glioblastoma

It may present as a primary malignant tumor of the optic nerve [179] or may involve the orbit through the extension from primary intracranial lesions as in our series (Fig. 12.89). Positive staining for glial fibrillary acid protein (GFAP) aids in the diagnosis (Fig. 12.90).

12.7.9 Chondro-osseous Tumors

12.7.9.1 Paget's Disease

Definition

Paget's disease is a localized disorder of bone remodeling that can result in enlarged and misshapen bones.

Synonyms

Osteitis deformans.

Epidemiology

Paget's disease of the bone is a fairly common disorder; it was however not represented in our series of 1,077 orbital lesions.

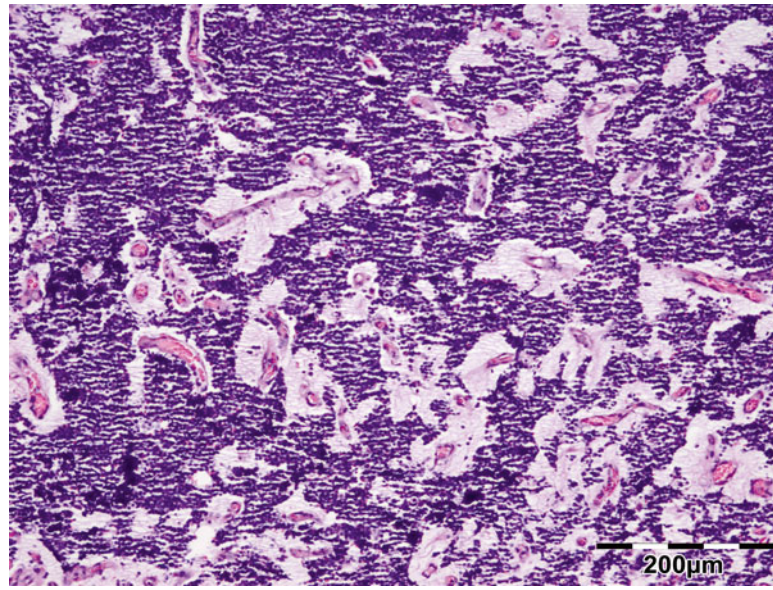

Fig. 12.88 Medulloepithelioma: medulloepithelioma of the eye may infiltrate the orbit (HE 100×) (Dr. Robert M. Verdijk)

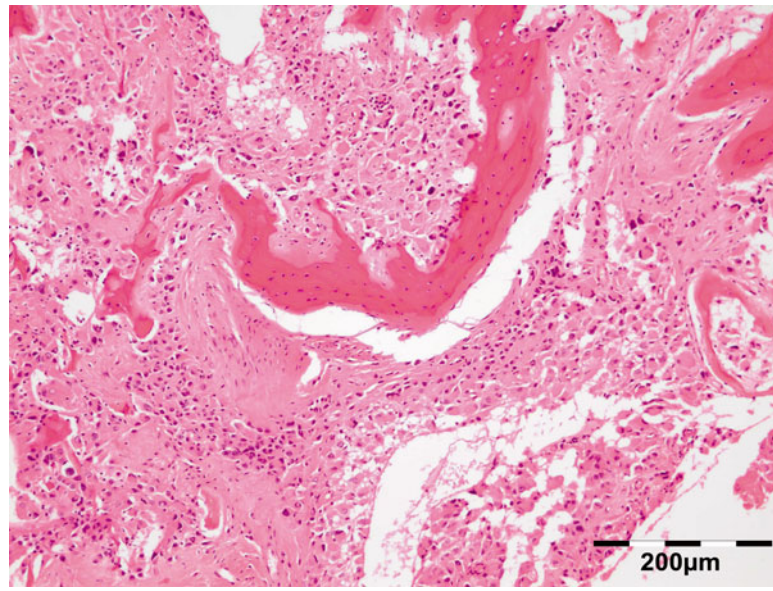

Fig. 12.89 Glioblastoma: may involve the orbit through extension from primary intracranial lesions (HE 100×) (Dr. Robert M. Verdijk)

Etiology

Paget's disease of the bone is of obscure origin.

Localization

The disease affects the skeleton more or less focally. Solitary lesions of the orbital bones have been described [180].

Clinical Features

It usually appears in those over 40, is more common in men, and occasionally occurs in several members of one family.

Macroscopy

The bone grossly appears thickened and coarsened with a compacted pumice-like architecture.

Histopathology

The osseous tissue in fully evolved Paget's disease shows an architecture with innumerable osseous fragments of irregular size faceted together and bounded by correspondingly irregular cement lines. The chaotic jigsaw pattern is the histologic hallmark for Paget's disease. In an active lesion, lively cyclic osteoclastic resorption and new bone

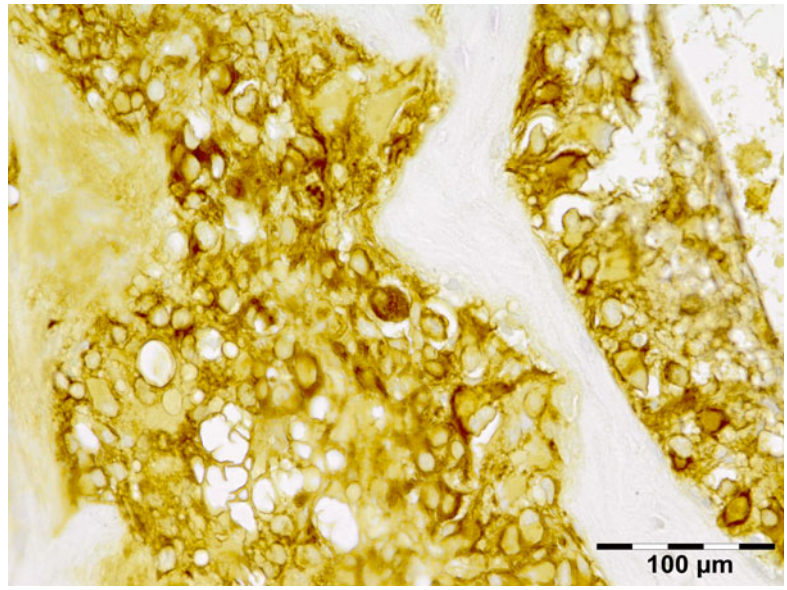

Fig. 12.90 Glioblastoma: positive staining for glial fibrillary acid protein (GFAP) aids in the diagnosis (GFAP IH 200×) (Dr. Robert M. Verdijk)

deposition may be seen with concomitant chronic inflammatory, fibrous scarring of the marrow. In the cooling-off phase, osteoclastic activity and fibrous scarring are less prominent.

Differential Diagnosis

Renal osteodystrophy, osteomalacia, osteosarcoma.

Histogenesis

Unknown.

Genetics

Predisposition to Paget's disease may have a genetic component linked to a region of chromosome arm 18q.

Prognosis and Predictive Factors

Incidence of sarcomatous changes in Paget's disease is estimated to be 0.7–0.95 %, and osteosarcomas represent 50–60 % of Paget's sarcomas [181].

12.7.9.2 Giant Cell Tumor of Bone

Giant cell tumors represent 5 % of all primary bone tumors. It is more common in females and appears in the third to fourth decade at the epiphysis of long bones. Rarely giant cell tumors occur in the cranial bones [182]. One case involving the orbit was presented at the EOPS and Verhoeff Society Meeting in 2006 by Dr Howes. The diagnosis is made on basis of the finding of multinucleated osteoclasts evenly distributed in the lesion. The mesenchymal cells in the background are precursor cells that produce RANKL, necessary for osteoclast differentiation. Curettage or local resection mostly cures the affliction.

12.7.9.3 Fibrous Dysplasia

Definition

Fibrous dysplasia (FD) is a benign medullary fibro-osseous lesion which may involve one or more bones.

Epidemiology

Fibrous dysplasia occurs in children and adults and affects all racial groups with an equal sex distribution. Our series contained seven cases of fibrous dysplasia of the orbital bones representing 12 % of all bone and soft tissue lesions [183, 184].

Etiology

Activating mutations of the G proteins have been identified in both the monostotic and polyostotic forms and may be etiologically important.

Localization

The gnathic bones are the most common site of involvement in surgical series (because they are often symptomatic). In women, long bones are more often involved, whereas the ribs and the

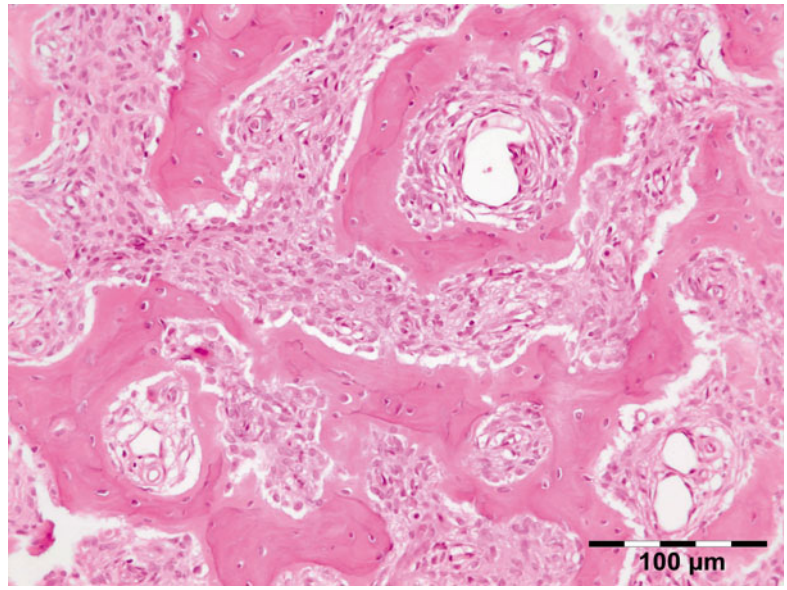

Fig. 12.91 Fibrous dysplasia: the fibrous component is composed of cytological bland spindle cells with a low mitotic rate. The osseous component is comprised of irregular curvilinear trabeculae of woven (or rarely lamellar) bone that lacks osteoblastic rims (HE 200×) (Dr. Robert M. Verdijk)

skull are favored sites in men. In the monostotic form, about 35 % of cases involve the head, a second 1/3 occur in the femur and tibia, and an additional 20 % in the ribs. In the polyostotic form, the femur, pelvis, and tibia are involved in the majority of cases.

Clinical Features

Long-standing facial asymmetry, proptosis, and globe displacement are common presentations. The majority of cases with orbital involvement have monostotic fibrous dysplasia, with the frontal bone followed by the sphenoid and ethmoid most commonly affected.

Macroscopy

The bone is often expanded and the lesional tissue has a tan-gray color with a firm-to-gritty consistency. There may be cysts, which may contain some yellow-tinged fluid.

Histopathology

The lesion is generally well circumscribed and composed of fibrous and osseous components, which are present in varying proportions within the same lesion. The fibrous component is composed of cytological bland spindle cells with a low mitotic rate. The osseous component is comprised of irregular curvilinear trabeculae of woven (or rarely lamellar) bone (Fig. 12.91) that lack osteoblastic rims as seen in osteofibrous dysplasia or callus formation. Occasionally, the osseous component may take the form of rounded psammomatous or cementum-like bone. Secondary changes such as foam cells, multinucleate giant cells, a secondary aneurysmal bone cyst, or myxoid change may occur.

Differential Diagnosis

Osteofibrous dysplasia, callus, osteosarcoma, ossifying fibroma, Paget's disease of bone.

Histogenesis

Mesenchymal precursor cell.

Genetics

Activating mutations in the GNAS1 gene, encoding the alpha subunit of stimulatory G protein, have been demonstrated in fibrous dysplasia.

Prognosis and Predictive Factors

Malignant transformation to osteosarcoma, fibrosarcoma, chondrosarcoma, and giant cell sarcoma rarely occurs, often heralded by rapid progression and increasing pain. Prior radiotherapy increases this risk from 0.4–0.5 % to 15.0 %.

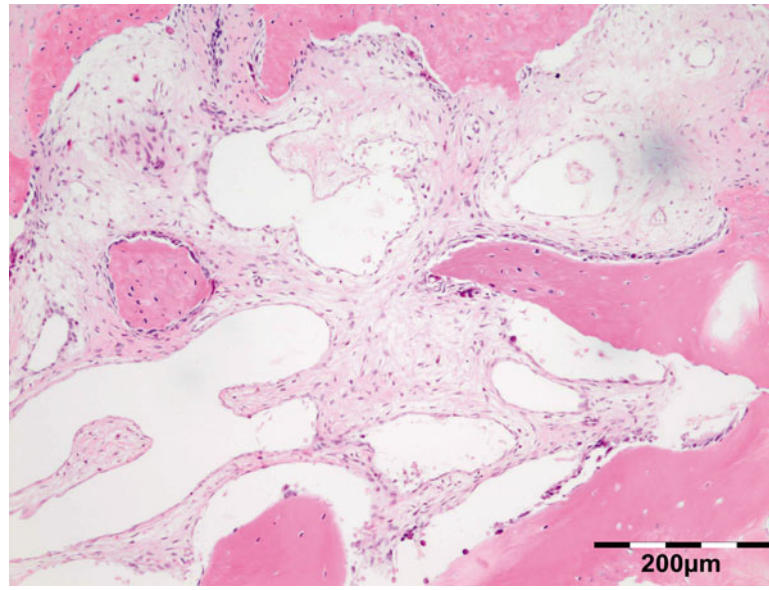

Fig. 12.92 Osteofibrous dysplasia. Prominent osteoblastic rims differentiate this lesion from fibrous dysplasia (HE 200×) (Dr. Robert M. Verdijk)

12.7.9.4 Osteofibrous Dysplasia

Osteofibrous dysplasia (OFD) is a selflimited benign fibro-osseous lesion of bone characteristically involving the tibia during infancy and childhood. Multifocal lesions oriented longitudinally along the cortical axis are not unusual. The histopathologic findings differentiate osteofibrous dysplasia from fibrous dysplasia since the irregular fragments of woven bone are often rimmed by lamellar layers of bone laid down by well defined osteoblasts. See Fig. 12.92.

12.7.9.5 Osteopetrosis

Definition

Excessive formation of dense trabecular bone leading to pathological fractures.

Synonyms

The terms Marble bone disease and Albers-Schonberg disease should be avoided.

Epidemiology

Rare, we have diagnosed one case of osteopetrosis in our series.

Etiology

Osteopetrosis means a low function of osteoclasts, which induces bone resorption with a decrease in bone density. It is believed to arise due to the failure of osteoclasts to resorb immature bone. This leads to abnormal bone marrow cavity formation.

Localization

Symptomatic orbital osteopetrosis is localized near the cranial nerve foramina.

Clinical Features

Signs and symptoms of bone marrow failure may be present. Impaired bone remodeling associated with dysregulated activity of osteoclasts for this condition may typically result in bony narrowing of the cranial nerve foramina, which typically results in cranial nerve (especially optic nerve) compression [185].

Macroscopy

When cut open, the bone contains a large amount of densified spongiosa that has crowded out the myeloid marrow to result in a grayish impression. Abnormal remodeling of primary woven bone to lamellar bone results in "brittle" bone that is prone to fracture.

Histopathology

Histology shows primitive "woven" bone to persist into adulthood. Two main forms can be distinguished on the basis of the presence or absence of osteoclasts. In the osteoclast-rich form (Fig. 12.93), which comprises the large majority of cases, a normal to high number of

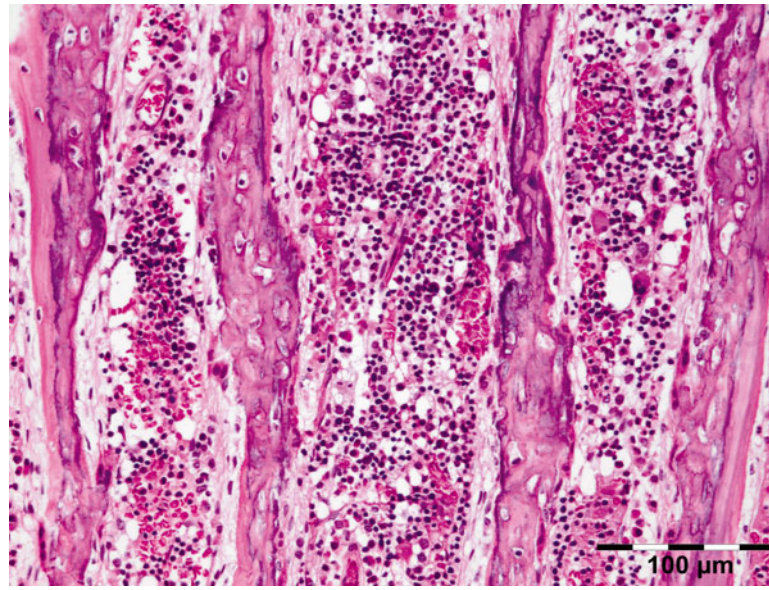

Fig. 12.93 Osteopetrosis: primitive "woven" bone in the osteoclast-rich form (HE 200×) (Dr. Robert M. Verdijk)

mature, nonfunctional osteoclasts is present, whereas in the osteoclast-poor form these specialized cells are absent because of a defect in osteoclast differentiation.

Differential Diagnosis
None.

Histogenesis
Osteoclast dysfunction mediates the pathogenesis of this disease.

Genetics
Osteopetrosis has several genetic forms: a benign late form with autosomal dominant inheritance, an early form with X-linked inheritance, and a malignant early form with autosomal recessive inheritance [186].

Prognosis and Predictive Factors
Compression of the optic nerve is the most important complication of osteopetrosis.

12.7.9.6 Osteoid Osteoma

Definition
Osteoid osteoma is a benign bone-forming tumor characterized by small size, limited growth potential, and disproportionate pain.

Epidemiology
Osteoid osteoma usually affects children and adolescents, although it is occasionally seen in older individuals. It is more common in males. Our series had only one case of osteoid osteoma.

Etiology
Unknown.

Localization
Osteiod osteoma has been reported in virtually every bone except for the sternum, but it is most common in the long bones, particularly in the proximal femur. Orbital involvement has been reported [187–189].

Clinical Features
The usual presenting symptom is pain. The pain, at first intermittent and mild with nocturnal exacerbation, eventually becomes relentless to the point of interfering with sleep. On the other hand, it is characteristic for salicylates and nonsteroidal anti-inflammatory drugs to completely relieve the pain for hours at a time; 80 % of patients report this characteristic feature. On plain x-ray, the lesion is characterized by dense cortical sclerosis surrounding a radiolucent nidus.

Macroscopy
Osteoid osteoma is a small cortically based, red, gritty, or granular round lesion surrounded by ivory white sclerotic bone.

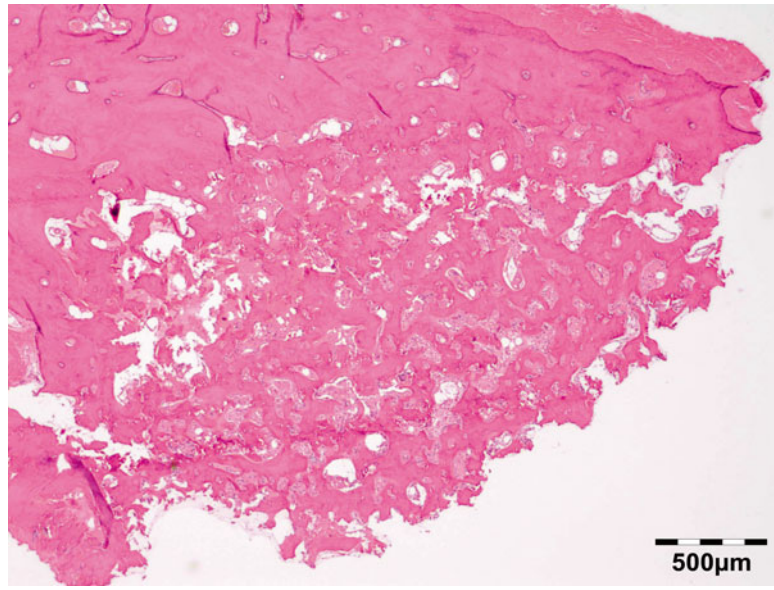

Fig. 12.94 Osteoid osteoma: a sheetlike configuration, the nidus is very often organized into microtrabecular arrays that are lined by plump appositional osteoblasts (HE 25×) (Dr. Robert M. Verdijk)

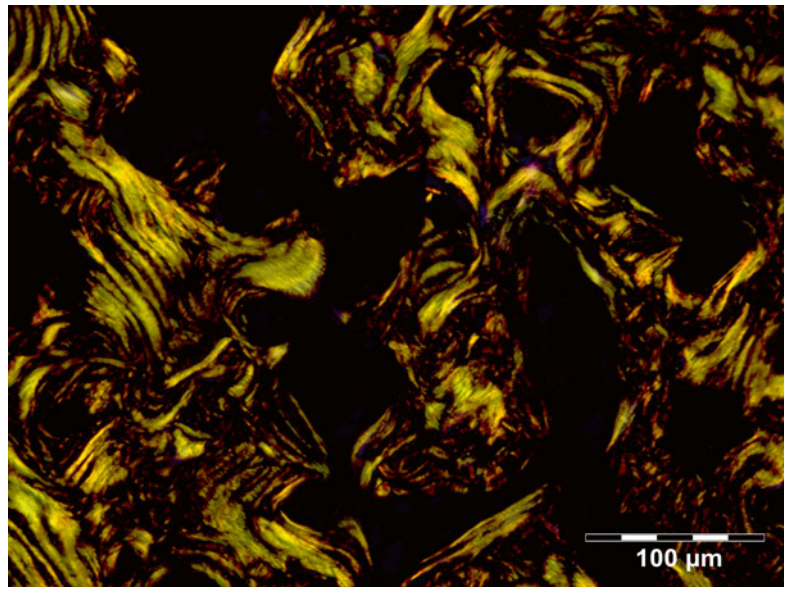

Fig. 12.95 Osteoid osteomas: the interface between osteoid osteoma and the surrounding reactive woven bone is very abrupt and well circumscribed (polarized light 200×) (Dr. Robert M. Verdijk)

Histopathology

The tumor consists of a central area of vascularized connective tissue within which are differentiating osteoblasts producing osteoid and sometimes bone, called the nidus. The osteoid may be microscopically disposed in a sheetlike configuration, but very often it is organized into microtrabecular arrays that are lined by plump appositional osteoblasts (Fig. 12.94). The interface between osteoid osteoma and the surrounding reactive bone is very abrupt and well circumscribed (Fig. 12.95).

Prognosis and Predictive Factors

The prognosis of osteoid osteoma is excellent. Recurrences are rare. Some lesions have been reported to have disappeared despite the lack of surgical therapy.

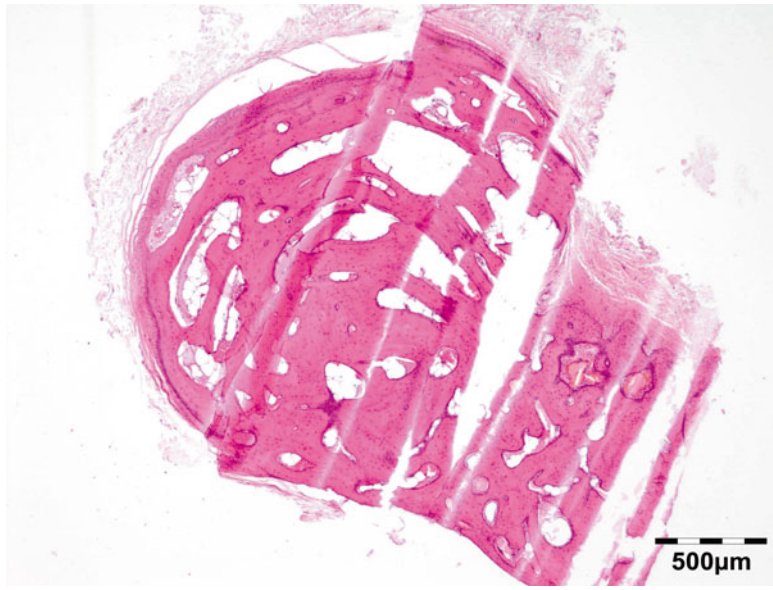

Fig. 12.96 Osteoma: mature type is defined by large trabeculae of mature lamellar bone with or without osteoblastic rimming and separated by paucicellular fibrous stoma (HE 25×) (Dr. Robert M. Verdijk)

12.7.9.7 Osteoma

Definition

Osteomas are benign, generally slow-growing, bone-forming tumors limited almost exclusively to craniofacial and jaw bones.

Epidemiology

Orbital involvement is usually a result of invasion from adjacent sinuses and occurs most frequently in the ethmoidal, frontoethmoidal, and frontal regions [190]. We encountered six osteomas representing 10 % of all lesions of the soft tissue and bone.

Etiology

Traumatic, infectious, and developmental theories have been proposed, but its origins remain unknown.

Localization

Osteomas can be subdivided into bone surface tumors (or exostoses) that primarily involve the cranial vault, mandible, and external auditory canal and the more common sino-orbital osteomas that arise from bones that define the paranasal sinuses, nasal cavity, and orbit.

Clinical Features

The most common signs and symptoms are headache (51 %), visual changes (36 %), sinusitis (29 %), pain (24 %), and proptosis/globe displacement (24 %) [190].

Macroscopy

Osteomas have a glistening, white-to-pink, smooth, or bosselated surface and are composed predominantly of dense mature lamellar bone with little medullary stroma.

Histopathology

Mature type is defined by large trabeculae of mature lamellar bone with or without osteoblastic rimming and separated by paucicellular fibrous stoma (Fig. 12.96). Mixed ivory/mature type is defined as a tumor with at least one low-power field (40x magnification) each of ivory and mature patterns.

Differential Diagnosis

The presence of osteoblastoma-like areas and Paget-like bone may be observed [190].

Histogenesis

Unknown.

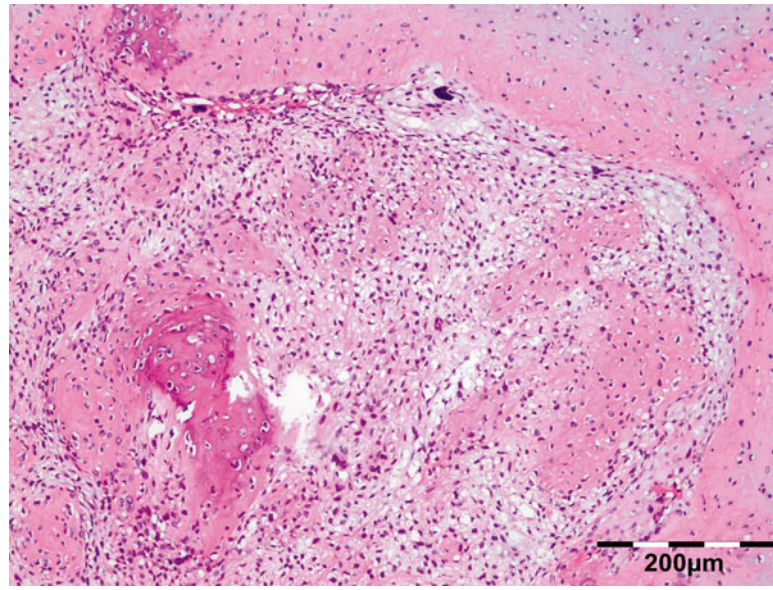

Fig. 12.97 Chondroblastic osteosarcoma: sarcomatous stroma with foci of osteoid production, which may display a characteristic lacelike or filigreed pattern. The anaplastic cells can be osteoblastic and chondroblastic (HE 100×) (Dr. Robert M. Verdijk)

Genetics

Gardner's syndrome is uncommon but should always be considered when dealing with osteomas.

Prognosis and Predictive Factors

If asymptomatic, osteomas should be treated conservatively. Recurrence after excision is rare.

12.7.9.8 Osteosarcoma

Definition

High-grade malignant tumor in which the neoplastic cells produce osteoid.

Epidemiology

Primary malignant bone tumors arising in or near the orbit are rare, but the most common of these is osteosarcoma. We have observed one case in our series.

Etiology

Most osteosarcomas arise de novo but some are secondary to Paget's disease, fibrous dysplasia, or radiotherapy. Patients with familial retinoblastoma are also prone to developing osteosarcoma as a second tumor.

Localization

About 10 % of orbital osteosarcomas arise in the craniofacial region, most frequently from the gnathic bones.

Clinical Features

Orbital osteosarcomas are most frequent in the fourth to fifth decades and present over several months with a progressive mass effect.

Macroscopy

This is an infiltrating, white-to-tan tumor with a texture varying from soft to gritty.

Histopathology

There is a sarcomatous stroma with foci of osteoid production, which may display a characteristic lacelike or filigreed pattern. The anaplastic cells can be osteoblastic, chondroblastic (Fig. 12.97), or fibroblastic, though they may appear less malignant with incorporation into the osteoid (the so-called normalization of malignant osteoid).

Differential Diagnosis

Paget's disease of the bone.

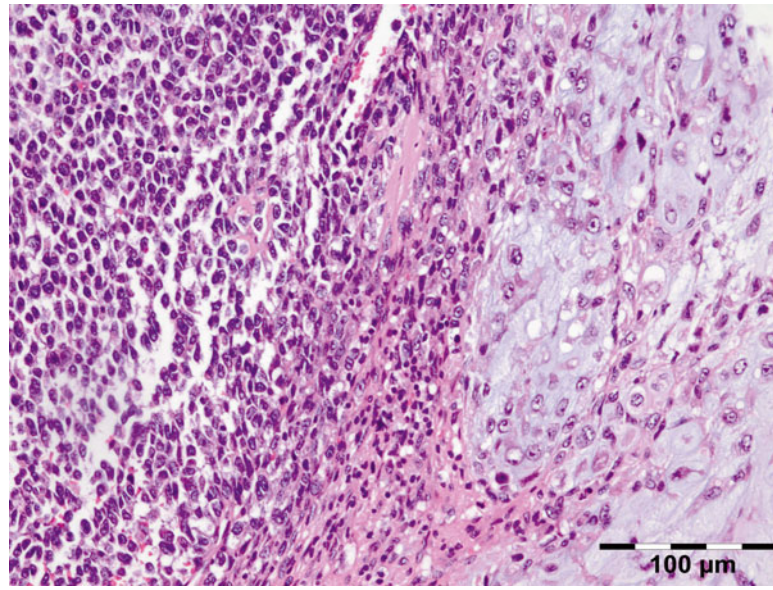

Fig. 12.98 Extraskeletal chondrosarcoma: the tumor is characterized by undifferentiated mesenchymal cells with islands of mature hyaline cartilage (HE 200×) (Dr. Robert M. Verdijk)

Histogenesis
Mesenchymal precursor cell.

Genetics
Osteosarcomas are chromosomally complex with both numerical and structural genetic alterations, although no single mutation or chromosomal translocation has proven to be pathognomonic for these lesions.

Prognosis and Predictive Factors
Low-grade central osteosarcoma is a rare type of osteosarcoma, representing fewer than 2 % of all osteosarcomas. Approximately 80 % of these tumors are located in the long bones, and they are particularly common in the distal and proximal tibia. However, they are rare in the craniofacial bones, and this tumor type has once reported to occur in the orbit [191]. Treatment regimens include preoperative chemotherapy, resection, and postoperative chemotherapy with postoperative radiotherapy being used for residual tumor. Though 5-year survival rates approach 70 % for peripheral sites, the prognosis remains poorer with craniofacial tumors due to delay of diagnosis and difficulties in obtaining complete resection.

12.7.9.9 Extraskeletal Osteosarcoma
Extraskeletal osteosarcoma is a malignant tumor that produces osteoid. It develops in soft tissue without continuity to the bone or periosteum. It is rare and comprises fewer than 5 % of all osteosarcomas. Extraskeletal osteosarcoma primarily affects patients above 50 years of age and has a poor prognosis and has once been reported to occur in the orbit [192].

12.7.9.10 Extraskeletal Mesenchymal Chondrosarcoma
Extraskeletal mesenchymal chondrosarcoma is relatively uncommon; we observed only one case in our series. Orbital location is extremely rare: only 16 cases have been reported until now. The tumor is characterized by undifferentiated mesenchymal cells with islands of mature hyaline cartilage (Fig. 12.98) [193].

12.7.9.11 Chordoma

Definition
Chordoma is a low to intermediate-grade malignant tumor that recapitulates notochord.

Epidemiology
Chordoma most commonly presents after age 30.

Etiology
Unknown.

Localization
Sites of involvement are the axial spine (sacral 60 %, sphenooccipital/nasal 25 %, cervical 10 %, and thoracolumbar 5 %). Orbital involvement of

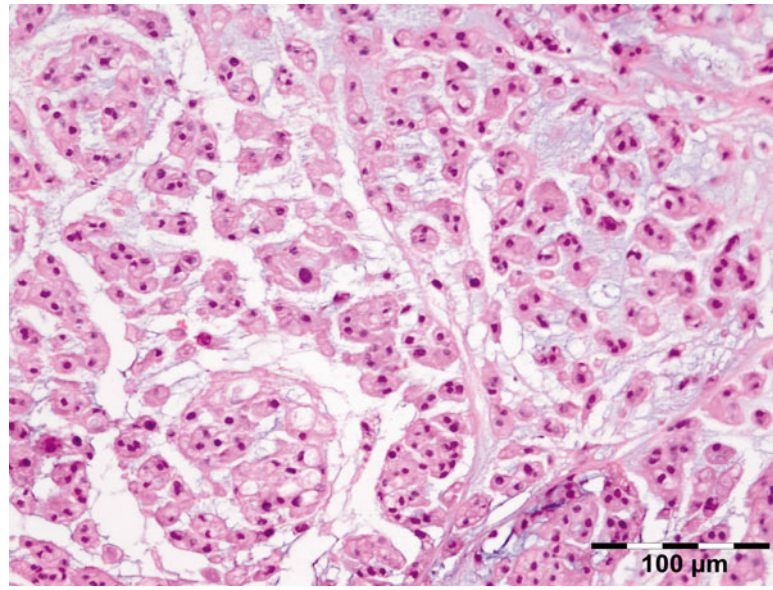

Fig. 12.99 Chordoma: the tumor cells are arranged in sheets or cords or float singly within an abundant myxoid stroma. They typically have an abundant pale vacuolated cytoplasm (the classic "physaliphorous cells") and show mild to moderate nuclear atypia (HE 200×) (Dr. Andrew P. Ferry; this case was presented at the combined Verhoeff-EOPS meeting, London, 1971, case 71–02)

chordoma usually is the result of extension of intracranial chordoma of the sella or skull base [194, 195] but may in rare cases originate from the bones of the orbital wall [196].

Clinical Features

Being a slow-growing mass, chordoma usually produces nonspecific symptoms for months to years before the diagnosis is made. In most cases it is associated with extension beyond the contours of the bone into the surrounding soft tissues.

Macroscopy

Chordoma is a lobulated, glistening, grayish tan to bluish white, muco-gelatinous to friable, dark-red hemorrhagic tumor.

Histopathology

The tumor cells are arranged in sheets, cords, or float singly within an abundant myxoid stroma (Fig. 12.99). They typically have an abundant pale vacuolated cytoplasm (the classic "physaliphorous cells"). They show mild to moderate nuclear atypia. Mitoses are infrequent. In the chondroid variants, there are areas that may mimic hyaline or myxoid cartilage. The immunophenotype of chordomas shows reactivity with antibodies against S-100 protein, pan-keratin, low molecular cytokeratins, and epithelial membrane antigen (EMA).

Differential Diagnosis

Chordoid chondrosarcoma, chordoid meningioma.

Histogenesis

Chordoma is supposedly derived from derivatives of the notochord.

Genetics

Due to chordoma's relatively rare occurrence, knowledge of molecular changes specific to chordoma is limited.

Prognosis and Predictive Factors

Incomplete resection will result in local recurrence that may lead to extensive destructive growth.

12.7.10 Meningeal Tumors

12.7.10.1 Meningioma WHO Grade I (e.g., Meningothelial, Fibrous, Psammomatous)

Definition

Benign neoplasm of meningothelial cells.

Epidemiology

Meningiomas comprised 58 cases (5 %) of all orbital tumors in our series. Most meningiomas are WHO grade I tumors [197]. The meningothelial subtype was most frequently observed (45 %,

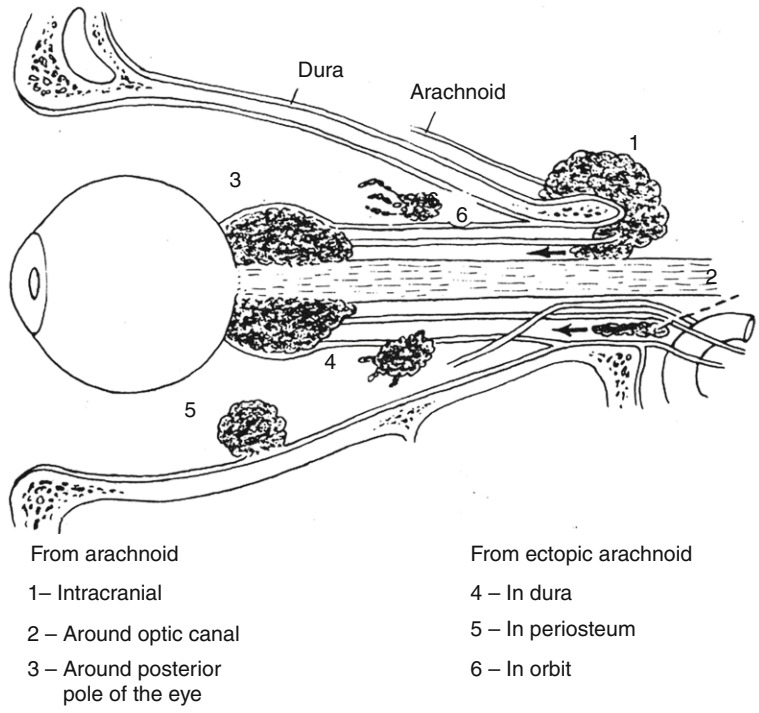

Fig. 12.100 Drawing meningiomas (Walsh): primary intraorbital meningiomas mostly arise from the arachnoid around the optic canal or the posterior pole of the eyeball. Less frequently meningiomas arise from ectopic arachnoid in the dura, the periosteum, or the orbit (Adapted after Walsh [197])

N=26), followed by the transitional (33 %, *N*=19), the psammomatous (7 %, *N*=4), fibrous (3.5 %, *N*=2), and microcystic (3.5 %, *N*=2) subtype. WHO grade II meningiomas were all of the chordoid subtype (5 %, *N*=3); two tumors were WHO grade III meningiomas based on mitotic activity (3.5 %).

Etiology

Most meningiomas in the orbit originate intracranially, often at the sphenoidal ridge, and extend into the orbit at the apex. Primary intraorbital meningiomas mostly arise from the arachnoid around the optic canal or the posterior pole of the eyeball. Less frequently meningiomas arise from ectopic arachnoid in the dura, the periosteum, or the orbit (Fig. 12.100 adapted after Walsh [198]).

Localization

Ectopic or extracranial meningioma may also develop in the region of the glabella and lung. Often the tumor is located between the orbit and cranium and the primary site of origin cannot be determined with certainty (see also page 250).

Clinical Features

The tumors frequently show a growth en plaque encroaching the optic nerve or have a globular shape inducing proptosis. The symptomatology may be so diverse that clinical diagnosis is difficult or impossible. The tumor cells often express estrogen receptors and may show an increased growth rate in puberty and pregnancy. Radiological signs of an extra-axial tumor of the cranial cavity or a tumor of the optic nerve sheath showing a dural tail aid the diagnosis. Often hyperostosis of the adjacent bone is observed.

Macroscopy

Gray-white fibrous tumor.

Histopathology

The tumor is composed of spindle to polygonal or epithelioid cells, with uniform round to oval nuclei containing delicate chromatin and occasional central clearing. Some nuclei contain either clear holes or eosinophilic pseudo inclusions formed by intranuclear invagina-

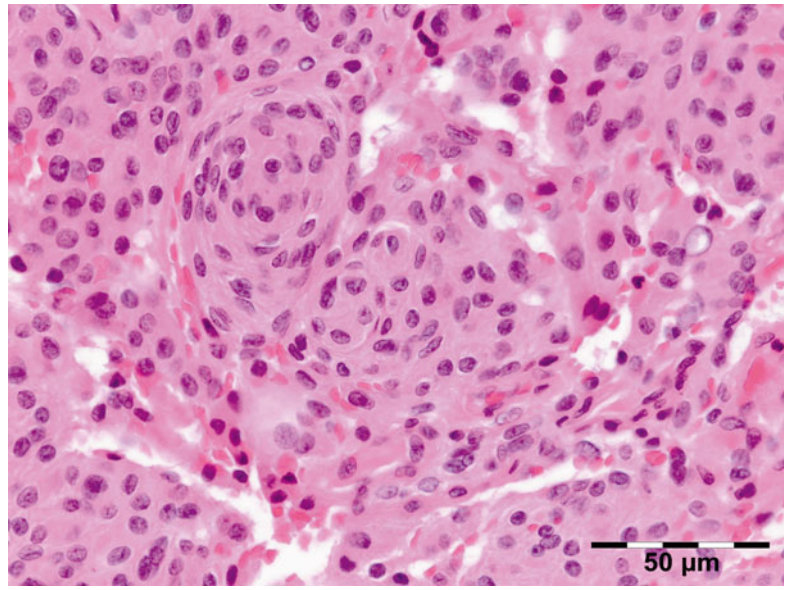

Fig 12.101 Meningotheliomatous meningioma: the cells are arranged in lobules and whorls of different sizes (HE 400×) (Dr. Robert M. Verdijk)

tions of cytoplasm. Nuclear atypia may occur, most often reflecting degenerative changes rather than aggressive biology. Mitoses may be accepted to a maximum of 4/10 HPF as a feature of WHO grade I tumors [197]. MIB-1 (Ki-67) nuclear staining may aid to identify foci of increased mitotic activity and is usually below 5 % [199]. It is of critical importance to be acquainted with the highly diverse growth patterns of grade I meningioma in order to avoid misdiagnosis with carcinoma or soft tissue tumors. The most frequent and classical growth pattern is the meningotheliomatous pattern where the cells are arranged in lobules of different size (Fig. 12.101) with whorls. Varying amounts of stroma are interspersed throughout the sheets of cells. Some areas may be exceedingly vascular and others may be partially hyalinized. The transitional growth pattern has mixed meningothelial and fibrous features. The psammomatous growth pattern is composed mainly of whorls. These whorls consist of concentric layers of cells and may show a central vascular channel. The central core of the whorls can show varying degrees of hyalinization and deposition of calcium salts which results in the formation of psammoma bodies (Fig. 12.102). The fibrous growth pattern contains a large proportion of connective tissue. Spindle-shaped tumor cells with elongated nuclei form parallel or storiform bundles. Microcystic meningiomas are characterized by tumor cells with thin elongate processes and a variable mucinous matrix; these cells more closely resemble arachnoidal trabecular cells rather than cap cells. Secretory meningioma is a separate subtype with the presence of numerous PAS (periodic acid–Schiff)-positive eosinophilic intracellular inclusions within gland-like spaces. These inclusions, known as pseudopsammoma bodies, are immunoreactive for CEA and other epithelial and secretory markers. The angiomatous subtype has been defined as having more than 50 % tumor volume occupied by blood vessels. Mast cells and histiocytic cells can be found in all meningioma subtypes. The rare lymphoplasmacyte-rich subtype features extensive inflammatory infiltrates. Metaplastic meningiomas are rare, being characterized by focal or widespread mesenchymal differentiation with formation of bone, cartilage, fat, and xanthomatous tissue elements.

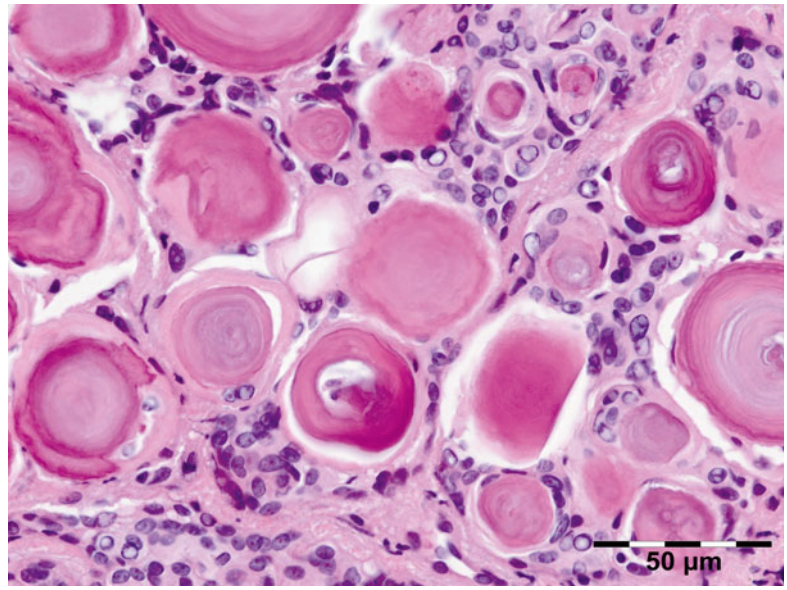

Fig. 12.102 Psammomatous meningioma: with whorls consisting of concentric layers of cells. The central core of the whorls can show varying degrees of hyalinization and deposition of calcium salts which results in the formation of psammoma bodies (HE 400×) (Dr. Robert M. Verdijk)

Differential Diagnosis

Metastatic carcinoma, schwannoma.

Histogenesis

The tumors arise from the meningocytes or "cap cells" found in the arachnoid of the brain and optic nerve.

Genetics

Meningioma may be a feature of neurofibromatosis type 1 or type 2 [200].

Prognosis and Predictive Factors

Meningioma with otherwise completely benign features may show bone destruction and extension into the soft tissues causing considerable morbidity and hamper complete surgical resection. The current WHO classification lists 16 different variants or subtypes, falling into three grade designations [197]. Four subtypes are higher grade by definition and include chordoid (WHO grade II), clear cell (WHO grade II), rhabdoid (WHO grade III), and papillary (WHO grade III) meningiomas. However, the required fraction of such variant histology in mixed tumor types to warrant the higher-grade designation remains unresolved. A comment can be made in the pathology report that the significance of a focally higher-grade morphology is unclear at this time but that close follow-up is recommended due to the potential for more aggressive behavior. Prior irradiation is a known risk factor for meningiomas [200].

12.7.10.2 Atypical Meningioma WHO Grade II (Includes Chordoid and Clear Cell Meningioma)

Definition

Atypical meningiomas (WHO grade II [197]) are tumors with increased mitotic activity and/or three or more of the following characteristics: sheetlike growth, spontaneous necrosis, increased cellularity, prominent nucleoli, and small cells with high nuclear-to-cytoplasmic ratio.

Epidemiology

In our series atypical meningiomas comprised 5 % (3/58) of all meningiomas that involved the orbit.

Etiology

See 12.7.9.1.

Localization

Chordoid meningiomas are typically large supratentorial tumors; it is therefore not surprising that

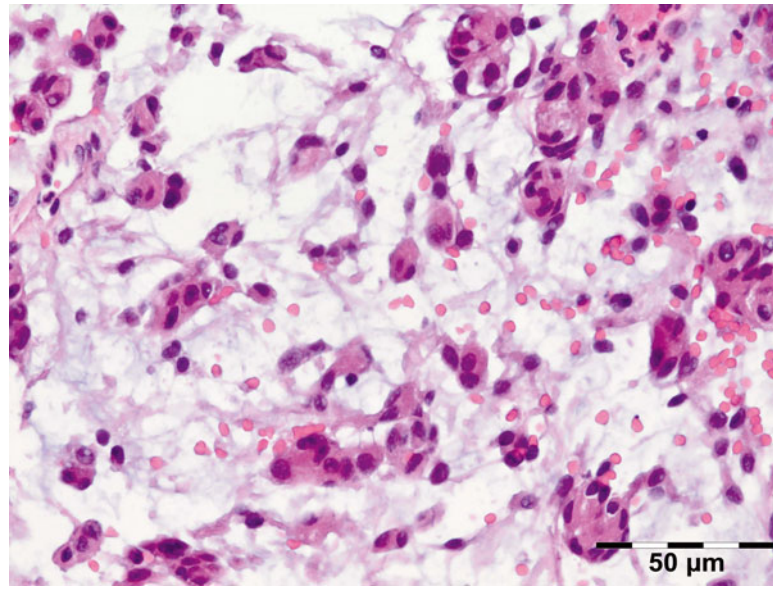

Fig. 12.103 Chordoid meningioma: resembles chordoma with cords or trabeculae of eosinophilic epithelioid cells, a mucin-rich stroma, and clear vacuoles resembling physaliphorous cells (HE 400×) (Dr. Robert M. Verdijk)

all the atypical meningiomas in our series were chordoid meningiomas. The majority of clear cell meningiomas occur in the spinal region and posterior fossa.

Clinical Features

Chordoid and clear cell meningiomas have high recurrence rates. Clear cell meningiomas occur in younger patients, including children.

Macroscopy

The macroscopic appearance may be fibrous or soft (chordoid meningiomas often are myxoid) with variable necrosis.

Histopathology

Meningothelial differentiation as described above with increased mitotic activity, defined as four or more mitoses within any ten consecutive high-power fields (40× objective magnification). The term "atypical" is misleading, since cytological atypia is not common in atypical meningiomas. Necrosis must be spontaneous, prior to embolization or radiation. Chordoid meningioma resembles chordoma with cords or trabeculae of eosinophilic epithelioid cells, a mucin-rich stroma, and clear vacuoles resembling physaliphorous cells (Fig. 12.103). Usually, the chordoid pattern is intermingled with meningothelial or transitional tumor areas, although a pure chordoid pattern may be encountered. Psammoma bodies are uncommon. Clear cell meningioma is composed of polygonal PAS-positive staining cells that often show regional meningothelial differentiation.

Differential Diagnosis

Chordoma, clear cell neoplasms.

Histogenesis

See 12.7.9.1.

Genetics

See 12.7.9.1.

Prognosis and Predictive Factors

Atypical meningiomas show an increased recurrence rate after resection when compared to grade I meningiomas.

12.7.10.3 Anaplastic (Malignant) Meningioma, WHO Grade III (and Includes Rhabdoid Papillary Meningioma)

Definition

Anaplastic (malignant, WHO grade III [197]) meningiomas show distinct features of malignancy that include either the presence of 20 or

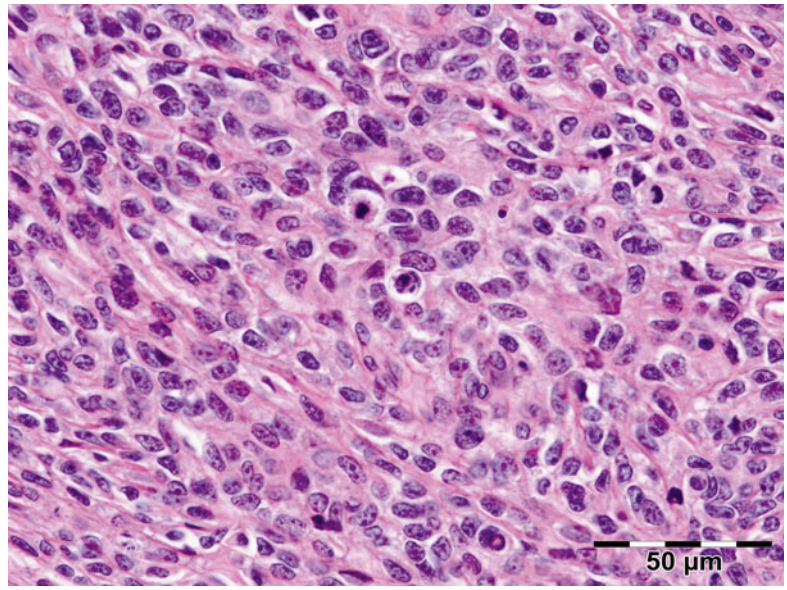

Fig. 12.104 Anaplastic meningioma: features of malignancy such as high mitotic counts or the presence of frank anaplasia can be observed (HE 400×) (Dr. Robert M. Verdijk)

more mitoses per 10 high-power fields or the presence of frank anaplasia.

Epidemiology
Rare; in our series 3.5 % (2/58) of the meningiomas of the orbit were of anaplastic (WHO grade III) nature.

Etiology
See 12.7.9.1.

Localization
Often extension from intracranial tumors.

Clinical Features
Of a space-occupying mass.

Macroscopy
Tan-gray fibrous tissue with areas of necrosis.

Histopathology
A firm diagnosis requires the presence of either classic meningothelial histology in portions of the tumor, a clinical history of lower grade meningioma in the same location previously, and/or supportive immunohistochemical or ultrastructural data. Features of malignancy such as high mitotic counts with 20 or more mitoses per 10 high-power fields or the presence of frank anaplasia, defined as carcinoma-, melanoma-, or sarcoma-like histology, and necrosis are present (Fig. 12.104). Classical meningothelial features are usually preserved in portions of the tumor. Brain invasion is frequently found in the intracranial parts. Rhabdoid meningiomas are characterized by sheets of rhabdoid cells with eccentric nuclei and prominent nucleoli. The eosinophilic cytoplasm often contains a paranuclear globular inclusion that consists of whorled bundles of intermediate filaments ultrastructurally. Papillary meningioma is a rare variant, characterized by a perivascular papillary or pseudopapillary growth pattern, partial loss of cellular cohesion, and structures resembling ependymoma-like perivascular pseudorosettes.

Differential Diagnosis
Sarcomas and carcinomas of different types.

Histogenesis
See 12.7.9.1.

Genetics
See 12.7.9.1.

Prognosis and Predictive Factors
A substantial proportion of patients will develop distant metastasis. MIB-1 helps to assess the proliferation potential of a meningioma, while PR expression is roughly inversely correlated to tumor grade. However, none of these markers are

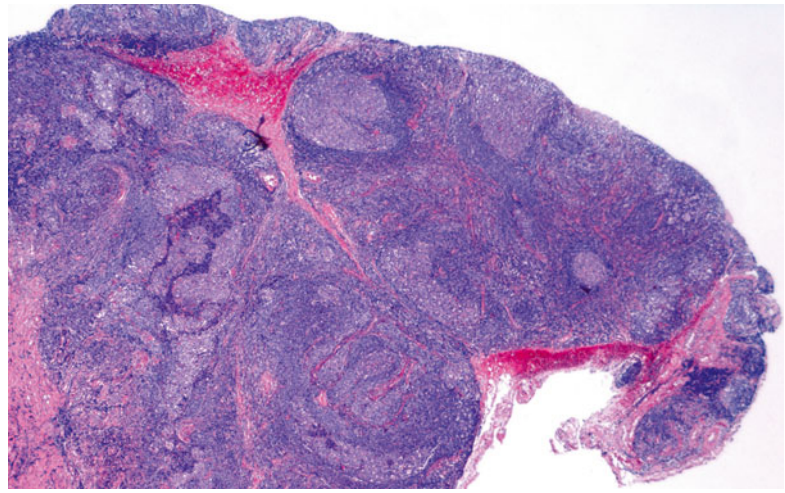

Fig. 12.105 Lymphoid hyperplasia: a dense infiltration of small bland lymphocytes with the formation of primary and secondary follicles reminiscent of normal lymph node architecture (HE 12,5×) (Dr. Robert M. Verdijk)

included in the 2007 WHO grading scheme [197], which is partly attributed to the lack of standardization for the assessment of MIB-1 proliferation values, given high interlaboratory variability.

12.7.11 Lymphoid Tumors

12.7.11.1 Lymphoid Hyperplasia

Definition

Some lymphoid proliferations have historically been termed (reactive) lymphoid hyperplasia (RLH) or atypical lymphoid hyperplasia or collectively pseudolymphoma [201]. It is widely recognized that the generally hypocellular lymphoid cell-poor orbital pseudotumors and the usually hypercellular, lymphoid cell-rich lymphoid hyperplasia represent distinct entities [202].

Epidemiology

The incidence of reactive lymphoid hyperplasia in the ocular adnexa varies considerably in the literature, ranging from 6 to 40 % (average, 23 %) in studies investigating lymphoproliferative lesions in these locations [203]. We observed lymphoid hyperplasia in 2 % of all lesions of the orbit representing 7 % of inflammatory lesions.

Etiology

There has been a shift in diagnostic patterns, with previously thought benign ocular adnexal lymphoproliferative lesions being reclassified as extranodal marginal zone lymphomas ENMZL [204]. In the conjunctiva there is still a role for designating lesions as RLH if they exhibit nonconfluent, well-defined hyperplastic follicles.

Localization

LH preferentially involves the conjunctiva, but reactive lymphoid hyperplasia may occur in almost all locations of the ocular adnexa. The posterior orbital area is rarely involved.

Clinical Features

A heretofore undescribed "multifocal RLH" syndrome must be distinguished from follicular lymphoma. Conjunctival RLH can usually be managed surgically without radiotherapy, but "multifocal RLH" required systemic treatment in 2 of 3 patients [205].

Macroscopy

Elastic salmon coloured tissue.

Histopathology

A dense infiltration of small bland lymphocytes with the formation of primary and secondary follicles reminiscent of normal lymph node architecture (Fig. 12.105). Reactive germinal follicles are common and often contain tangible bodies in macrophages and significant mitotic activity (Fig. 12.106). The lymphocyte population is mixed with polyclonal B cells and polyclonal T

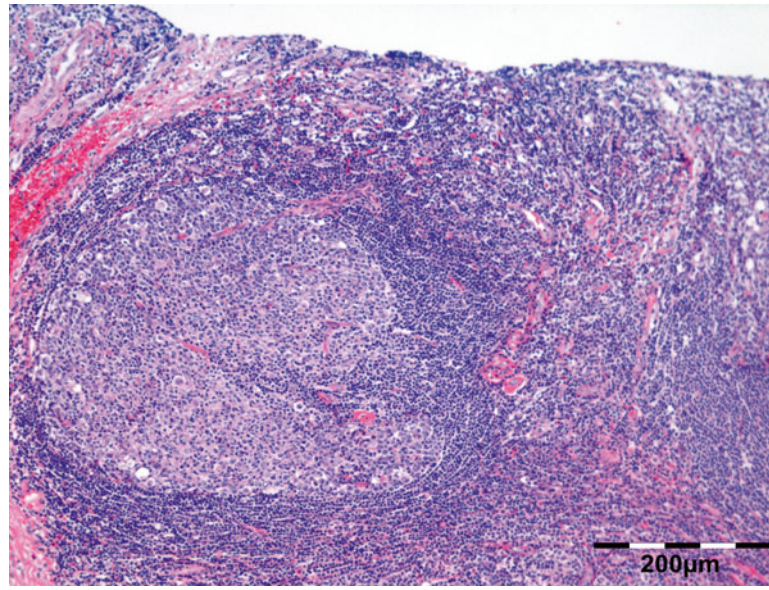

Fig. 12.106 Lymphoid hyperplasia: reactive germinal follicles are common and often contain tangible bodies in macrophages and significant mitotic activity (HE 100×) (Dr. Robert M. Verdijk)

cells with a predominance of T cells, scattered macrophages and plasma cells. A correct diagnosis of RLH versus follicular lymphoma can be reliably established employing immunohistochemical methods. BCL-2 is negative in RLH. CD10 identifies follicular center cells and Ki67 quantifies cells in S-phase. CD21 and CD23 detect dendritic cell scaffoldings of indistinct germinal centers. Although the reactive lymphoid hyperplasia infiltrates can be extensive with parting of skeletal muscle fibers or acini of the lacrimal gland, destruction of adjacent tissue is not usually apparent; fibrosis or sclerosis is unusual for reactive lymphoid hyperplasia. Further, lymphoepithelial lesions are not present.

Differential Diagnosis

Follicular lymphoma (FL): BCL-2 is positive in follicular centers of follicular lymphoma. Cave: one cell population that normally expresses BCL-2 is the B cells that are present within primary (or "resting") follicles, and it is only the germinal center area of a secondary ("activated") follicle that normally lacks BCL-2. In RLH, CD10 and BCL-6 are expressed almost exclusively by the follicular center cells. In contrast in FL, the expression of CD10 and BCL-6 is seen in both follicular and interfollicular neoplastic B cells [206].

Histogenesis

The pathogenesis of reactive lymphoid hyperplasia remains unclear: according to current knowledge it appears to be a result of antigen hyperstimulation. In some cases, there is an association with Sjögren syndrome or Wegener's granulomatosis; in the majority, the cause of the antigen hyperstimulation is unknown.

Genetics

None.

Prognosis and Predictive Factors

Historically, management options for orbital RLH have included observation, surgical debulking, systemic corticosteroids, and local radiotherapy. Recently, intraorbital injection of triamcinolone acetonide has been advocated [207]. Recurrent orbital masses responded well to treatment with intravenous rituximab [208].

12.7.11.2 Lymphoma

Definition

The ocular adnexal lymphoma (OAL) represents malignant lymphoid neoplasms, which can develop as primary or secondary tumor manifestations.

Epidemiology

Lymphoma localized in the ocular region (eyelid, conjunctiva, lacrimal drainage system, orbit, and intraocular) is one of the most common orbital malignancies [209, 210].

Primary OAL lymphomas constitute a heterogeneous group and represent less than 1 % of all non-Hodgkin lymphoma (NHL) but 8 % of all extranodal NHL. 78 % of lymphomas involving the ocular adnexa are primary, whereas 22 % are secondary [211]. OAL is primarily a disease of older adults (peak age 65 years) with a slight female preponderance. The incidence is increasing [212]; we encountered 105 hematopoietic lesions in our series, representing 10 % of all orbital lesions. Most lymphomas are low-grade B-cell lymphoma, with extranodal marginal zone lymphoma (ENMZL) as the most common type (41 %). Follicular lymphoma constitutes 21 %, DLBCL 10 %, mantle cell lymphoma 8.5 %, small cell lymphocytic lymphoma/chronic lymphocytic leukemia 7 %, plasmacytoma 3 %, and only one case each of Burkitt's lymphoma and T-cell lymphoma. Almost all (92 %) ENMZL are primary ocular adnexal lymphoma [211].

The most common secondary lymphoma subtype is follicular lymphoma: 31 % follicular lymphoma patients had a prior history of lymphoma. Patients with mantle cell lymphoma, chronic lymphocytic leukemia, lymphoplasmacytic lymphoma, and splenic marginal zone lymphoma almost always had a prior history of lymphoma [211]. T or T/NK lymphomas are rare and represent approximately 1–3 % of all lymphoproliferative lesions in these sites, mostly an extension of the tumor stage of mycosis fungoides or systemic T-cell lymphoma [213].

Etiology

Chronic antigen stimulation is implicated as a causative agent in the development of some mature B-cell proliferations: there are associations involving *Helicobacter pylori* with gastric or conjunctival MALT lymphoma and *Chlamydia psittaci* with ocular adnexal lymphoma. Recently, *H. pylori* or *C. pneumoniae* genomic fingerprints were detected in two of seven primary orbital MALT lymphomas [214].

Fig. 12.107 CT scan of an extranodal marginal zone (ENMZL) lymphoma: the deep orbital tissue is considered as true extranodal/nonfunctional mucosa-associated tissue (Dr. Robert M. Verdijk)

Localization

OAL can be solitary or multicentric, unilateral, or bilateral. Dissemination can occur to ipsilateral and/or contralateral regional lymph nodes as well as to more distant nodes. The deep orbital tissue is considered as true extranodal/nonfunctional mucosa-associated tissue (ENMZL) (Fig. 12.107), whereas the lacrimal gland, the conjunctiva, and the lacrimal sac are considered as functional mucosa-associated tissues [215]. Mucosa-associated lymphoid tissue lymphoma (MALT) is therefore not synonymous with ENMZL and is characterized by mucosal location and lymphoepithelial lesions. Furthermore, lymphoma arising in the lacrimal sac was surprisingly predominantly DLBCL [216].

Clinical Features

Are of a space-occupying mass.

Macroscopy

White to salmon pink fleshy tissue.

Histopathology

Lymphomas show different histologic patterns according to subclassification. In general there are monomorphous sheets of lymphocytes that infiltrate the orbital tissues.

MALT/ENMZ lymphomas are composed of small- to medium-sized cells with round or indented nuclei, clumped chromatin, and

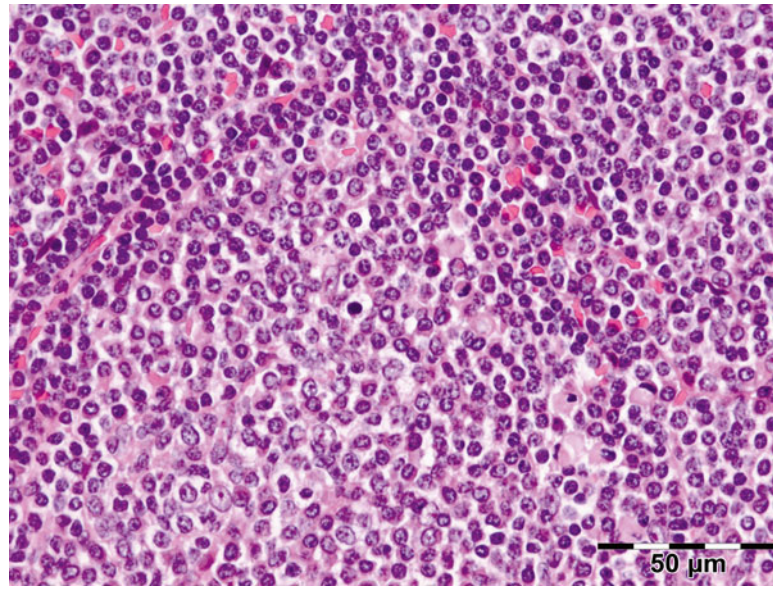

Fig. 12.108 Extranodal marginal zone (ENMZ)/MALT lymphoma: composed of a small- to medium-sized cells with round or indented nuclei, clumped chromatin, and inconspicuous to moderately abundant, often pale (monocytoid) cytoplasm (HE 400×) (Dr. Robert M. Verdijk)

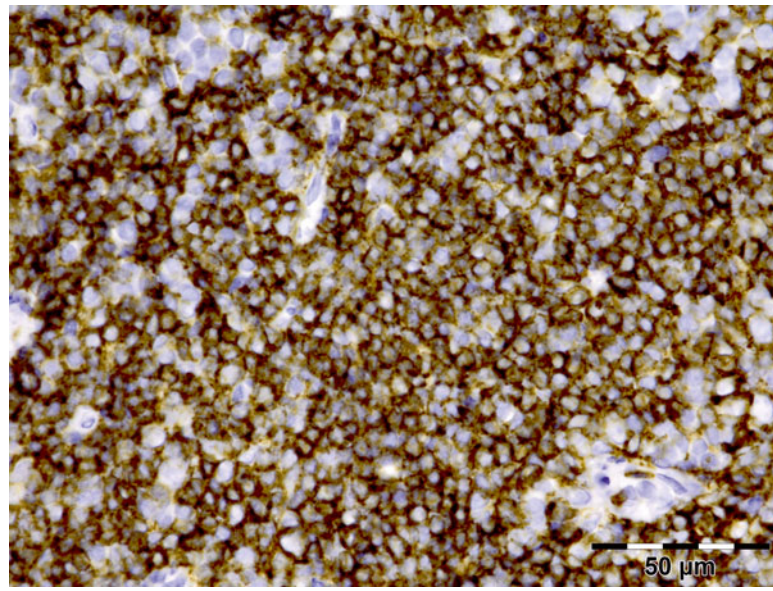

Fig. 12.109 Extranodal marginal zone (ENMZ)/MALT lymphoma: positive for B-cell lineage markers (CD20 IH 630×) (Dr. Robert M. Verdijk)

inconspicuous to moderately abundant, often pale (monocytoid) cytoplasm (Fig. 12.108). Other than monocytoid cells, lymphoepithelial lesions (in MALT), marginal zone involvement, and follicular colonization, most of the findings are rather nonspecific for distinction from other small B lymphomas. Plasmacytoid differentiation is frequent. They lack specific markers of other small cell lymphomas and are positive for B lineage markers (Fig. 12.109) and BCL-2 (Fig. 12.110). There is no specific positive immunologic marker: they are negative for CD23, bcl1, CD5, and CD10.

Follicular lymphomas (FL) are composed of uniform, densely packed follicles, which may coalesce, simulating diffuse areas, with compression of interfollicular stroma and vessels, which can be highlighted by reticulin stain. The follicular

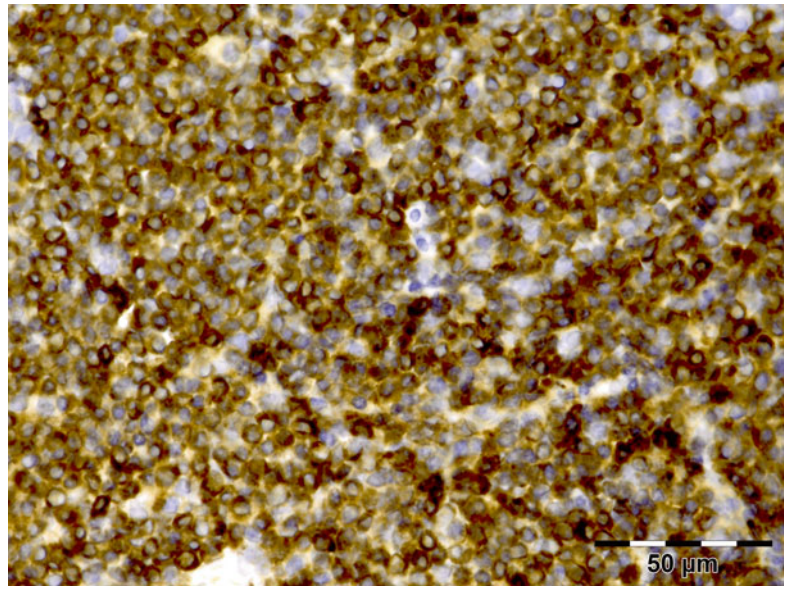

Fig. 12.110 Extranodal marginal zone (ENMZ)/ MALT lymphoma: positive for BCL-2 and shows expansion of follicular dendritic cell networks staining positive for CD21, CD23, and CD35 (BCL-2 IH 630×) (Dr. Robert M. Verdijk)

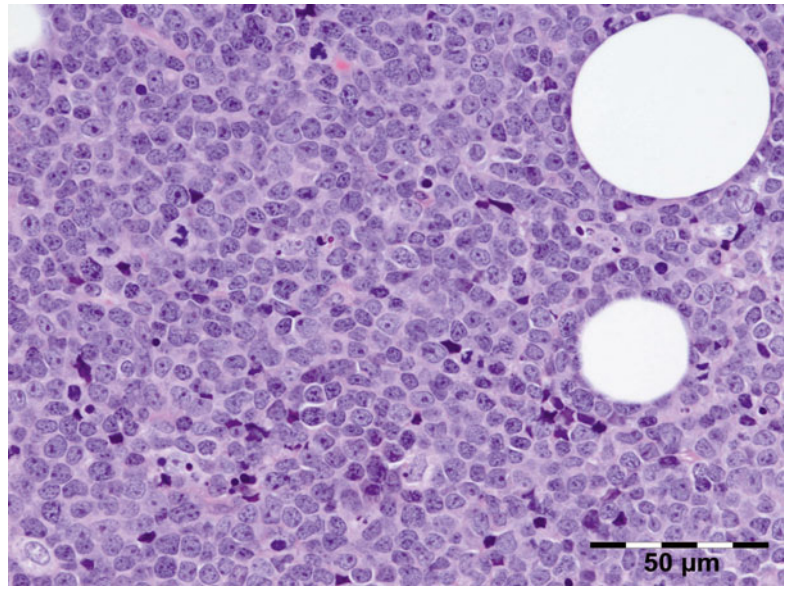

Fig. 12.111 Follicular lymphoma: the B-cell population is uniformly atypical. Small cells have cleaved, indented, angulated nuclei; large cells may be cleaved or non-cleaved (HE 400×) (Dr. Robert M. Verdijk)

population is uniformly atypical. Small cells have cleaved, indented, angulated nuclei; large cells may be cleaved or non-cleaved. Mitotic figures are less frequent in follicular lymphoma than reactive hyperplasia; however, grade 3 lymphoma may have high mitotic rate. Interfollicular zone is typically composed of small reactive cells. FL are BCL-2 and CD10 positive in 85 % of cases: BCL-2 is quite specific versus germinal centers. CD10 is quite specific versus other small B lymphomas. They also stain positive for BCL-6 and show expansion of follicular dendritic cell networks staining positive for CD21, CD23, and CD35 (Figs. 12.111 and 12.112).

Mantle cell lymphomas display a vague follicular pattern or diffuse pattern, with frequent

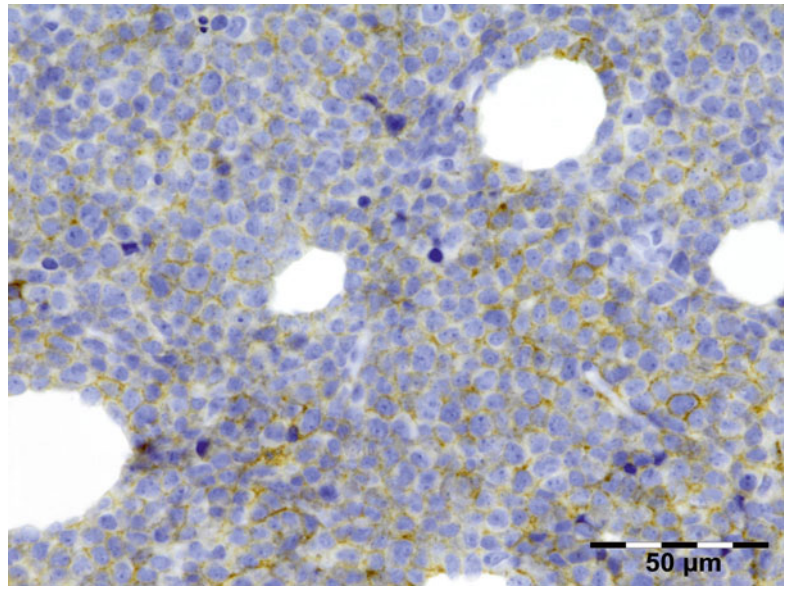

Fig. 12.112 Follicular lymphoma: follicular lymphoma B cells are positive for CD10 (CD10 IH 400×) (Dr. Robert M. Verdijk)

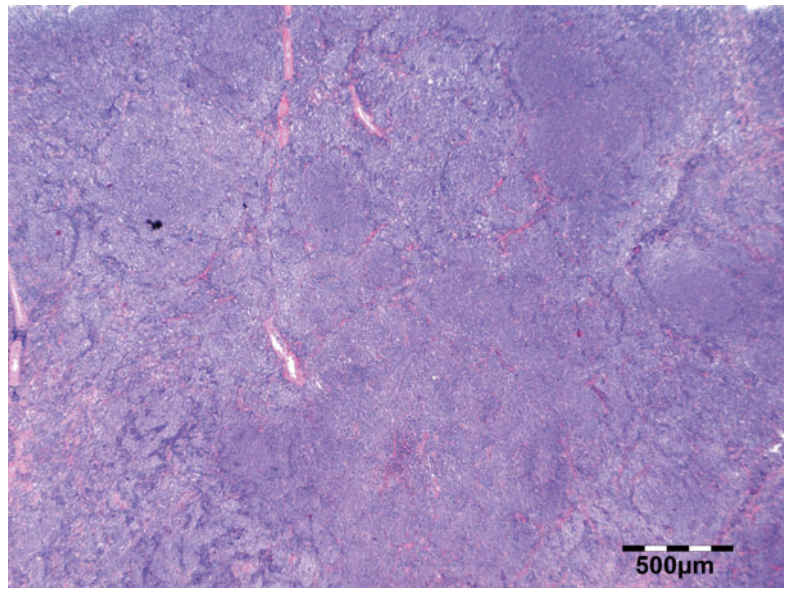

Fig. 12.113 Mantle cell lymphoma: mantle cell lymphoma displays a vague follicular pattern or diffuse pattern, with frequent pericapillary hyaline deposits (HE 25×) (Dr. Robert M. Verdijk)

pericapillary hyaline deposits (Fig. 12.113), and are composed of a uniform population of small- to medium-sized cells with mild to moderate nuclear irregularities. Scattered histiocytes are frequent, but no tingible bodies. The lymphocytes stain positive for CD79a and CD20, weak positive for CD5 (Fig. 12.114), and positive with cyclin D1 (Fig. 12.115). Bcl1 expression is seen in 85 %; BCL1-negative cases may have cyclinD2 (CCND2) or cyclin D3 (CCND3) expression.

Small cell lymphocytic lymphoma (SLL)/chronic lymphocytic leukemia (CLL) is histologically indistinguishable, CLL defined as having circulating B lymphocytes >4,000/mm^3. The architecture effaced by sheets of small

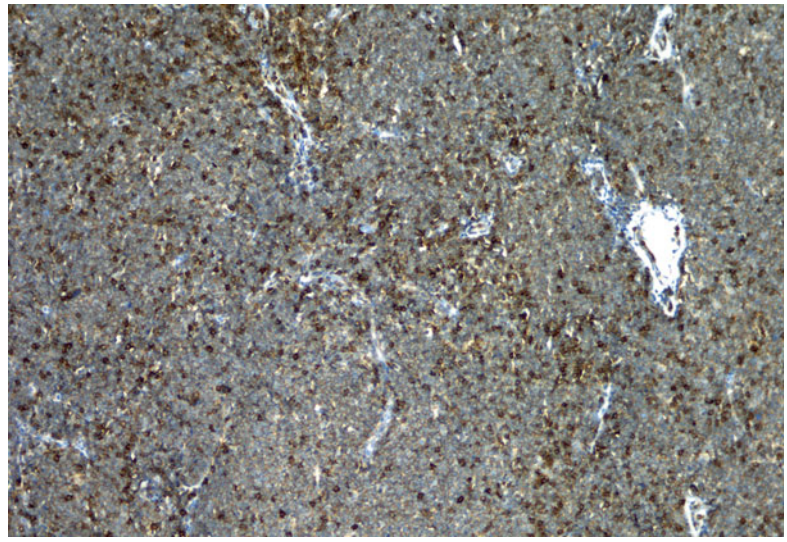

Fig. 12.114 Mantle cell lymphoma: mantle cell lymphoma stains positive for CD79a, CD20, and cyclin D1 and weak positive staining for CD5 (CD5 IH 100×) (Dr. Robert M. Verdijk)

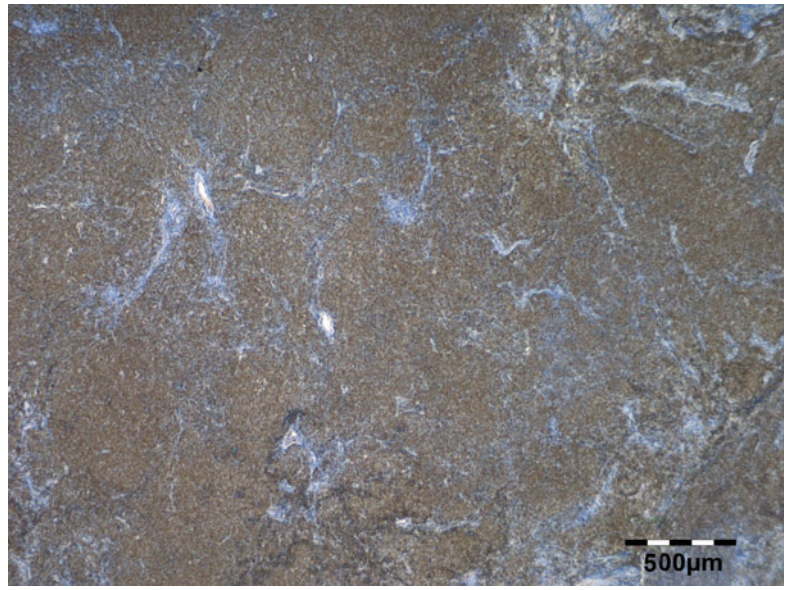

Fig. 12.115 Mantle cell lymphoma, positive for cyclin D1 (cyclinD1 IH 25×) (Dr. Robert M. Verdijk)

B lymphocytes with clumped chromatin and small or inconspicuous nucleoli (Fig. 12.116). Plasmacytoid differentiation may be prominent. Pseudofollicular proliferation centers are frequent with pale, vague nodules containing larger prolymphocytes and paraimmunoblasts. SLL/CLL are positive for CD79a, CD20, and CD23 (Fig. 12.117) and weakly positive for CD5.

Diffuse large B-cell lymphomas (DLBCL) show diffuse effacement of normal architecture and are composed of large non-cohesive cells which make up over 50 % of the population or are present in confluent foci. The usual appearance is large vesicular nuclei with multiple irregular eosinophilic nucleoli (Fig. 12.118).

Differential Diagnosis

Small blue round cell malignancies.

Histogenesis

Orbital lymphomas mostly are of B-cell origin and rarely T-cel or NK-cel origin.

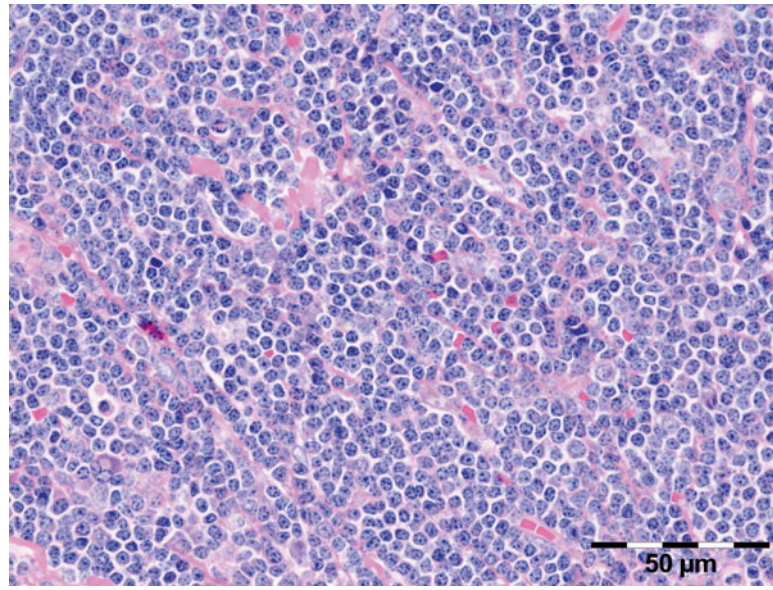

Fig. 12.116 CLL: sheets of small B lymphocytes with clumped chromatin and small or inconspicuous nucleoli (Giemsa 400×) (Dr. Robert M. Verdijk)

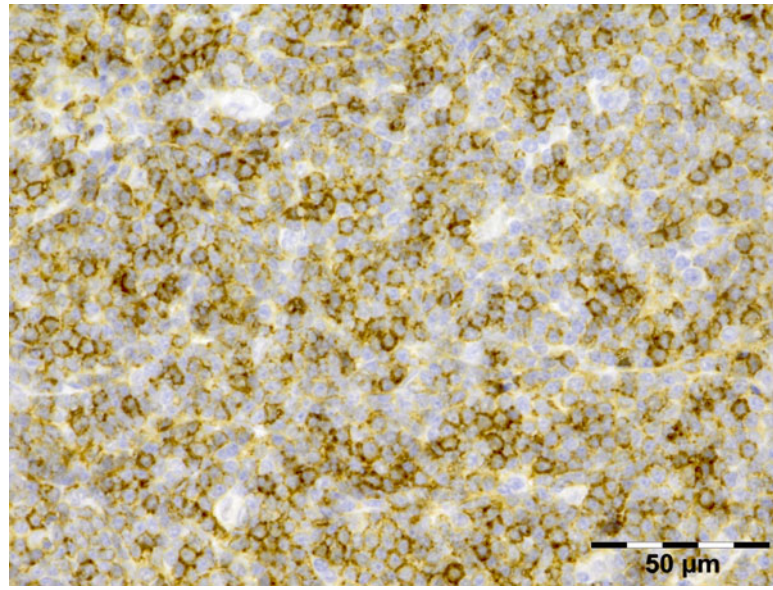

Fig. 12.117 CLL: SLL/CLL are positive for CD79a, CD20, and CD23 and weakly positive for CD5 (CD23 IH 400×) (Dr. Robert M. Verdijk)

Genetics

At molecular level there is clonal rearrangement of immunoglobulin heavy chain (Ig-H) and light chain (Ig-L). Translocations include t(11;18)(q21;q21) in 15–40 %, t(14;18)(q32;q21) in 10 %, and t(1;14)(p22;q32) in 5 % of MALT lymphoma's [217]. The different incidence of the translocations in MALT-type lymphomas from distinct anatomical sites is probably linked to specific prelymphomatous conditions (geographical, environmental, or other unknown conditions) that lead to the neoplastic transformation [218].

Prognosis and Predictive Factors

Major prognostic criteria for the ocular adnexal lymphomas include anatomic location of the tumor, stage of disease at first presentation,

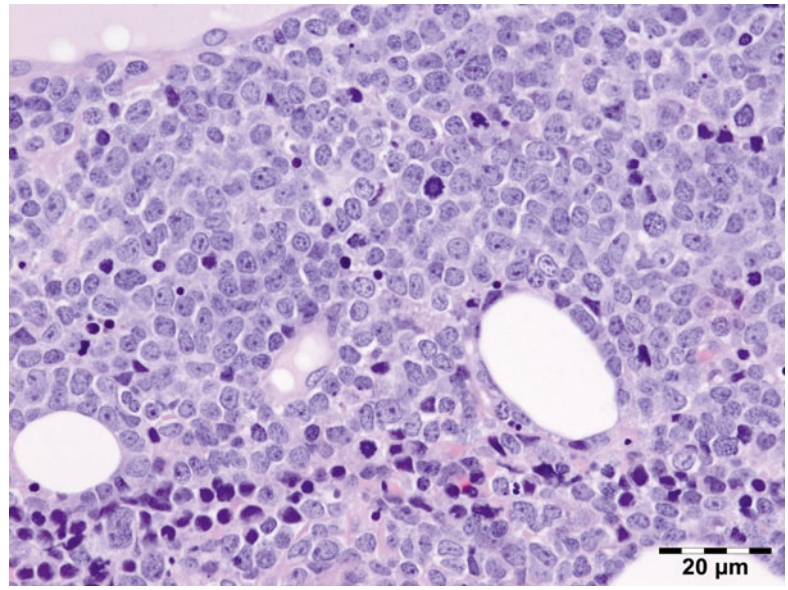

Fig. 12.118 Diffuse large B-cell lymphoma (DLBCL): have large atypical lymphoid cells with irregular large nuclei and multiple irregular eosinophilic nucleoli (HE 630×) (Dr. Robert M. Verdijk)

lymphoma subtype as determined using the REAL classification, immunohistochemical markers determining factors such as tumor growth rate, and the serum lactate dehydrogenase level [219]. Primary OAL should be staged according to the TNM classification devised for OAL. Briefly primary OAL are TNM-staged as follows: "I" if confined to the conjunctiva, "II" with orbital involvement, "III" with cutaneous (preseptal eyelid) involvement, and "IV" if there is direct extraorbital spread [220]. Prefix "b" indicates bilateral lymphoma involving ocular adnexal structures; "m" prefix indicates the presence of multiple primary tumors in 1 ocular adnexal structure. The "r" prefix indicates a recurrent tumor when staged after a documented disease-free interval. The "y" prefix indicates those cases in which classification is performed during or following initial multimodality therapy (College of American Pathologists, based on AJCC/UICC TNM, 7th edition). Most ocular adnexal lymphomas are localized (stage I) at presentation, and radiation therapy provides excellent local control [221]. Radiotherapy with or without systemic chemotherapy and/or immunotherapy is applied according to clinical staging and histologic subtyping. The 10-year, disease-specific mortality, which varies according to lymphoma subtype, is approximately 5–10 % [204].

Precursor B lymphoblastic lymphoma (pre-BLL) of the orbit in a child occurs rarely as an unusual presentation of a non-Hodgkin lymphoma [222].

Hodgkin disease of the orbit is extremely rare [223].

12.7.11.3 Multiple Myeloma/ Waldenström Macroglobulinemia

Orbital and intracranial structures are very rarely involved by multiple myeloma. It frequently involves the head and neck with a predilection for the nasopharynx, tonsils, nasal cavity, and paranasal sinuses in cases with extramedullary involvement. Orbital involvement is a very rare finding representing only 3 % of hematopoietic lesions in our series [224]. Only 37 cases in literature showed such involvement [225]. Morphologic characteristics are interstitial clusters or sheets of cells with plasma cell characteristics, with variable morphology: large cells with prominent nucleoli to small cells with "lymphocytoid" appearance, monoclonal for light chains (Figs. 12.119, 12.120, and 12.121).

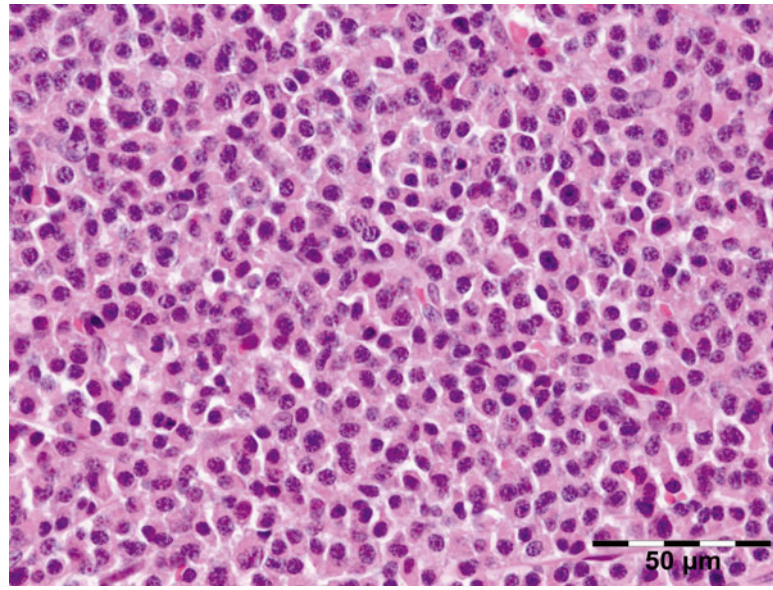

Fig. 12.119 Multiple myeloma: clusters or sheets of cells with plasma cell characteristics, with variable morphology (HE 400×) (Dr. Robert M. Verdijk)

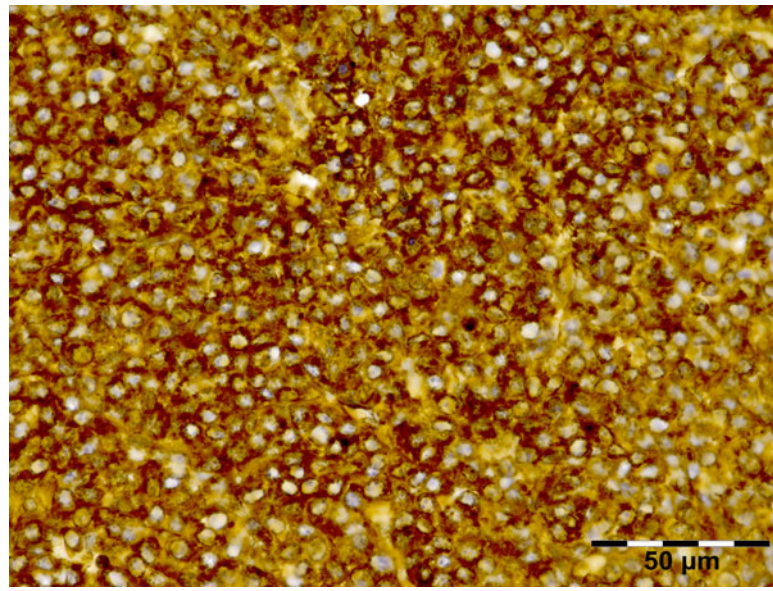

Fig. 12.120 Multiple myeloma: monoclonal for light chain (kappa IH 400×) (Dr. Robert M. Verdijk)

Rarely, multiple myeloma and secondary amyloidosis may present with bilateral orbital masses [77]. Waldenström macroglobulinemia (WM) is a low-grade B-cell lymphoplasmacytic lymphoma characterized by monoclonal IgM paraproteinemia. Waldenström macroglobulinemia has been rarely described in the orbit [226]. Histologically, WM is indistinguishable from other lymphoplasmacytic lymphoma or extranodal mucosa-associated lymphoid tumor. The World Health Organization recognized this overlap with the combined term lymphoplasmacytic lymphoma/WM. About ten cases of orbital masses in patients with WM were found in a recent review of the literature [226].

12.7.11.4 Granulocytic Sarcoma

Primary granulocytic sarcoma (synonyms: extramedullary myeloblastoma, chloroma) of the orbit is rare [227]. Secondary orbital or ocular

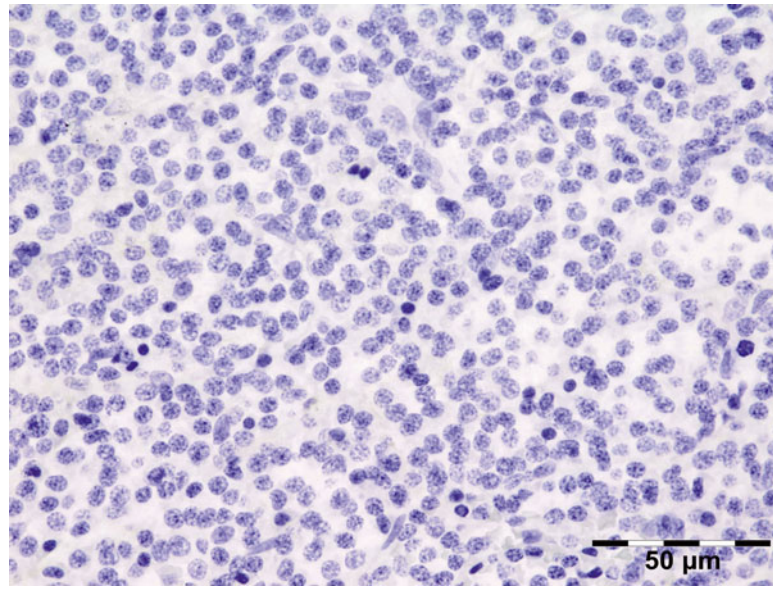

Fig. 12.121 Multiple myeloma: negative for light chain (lambda IH 400×) (Dr. Robert M. Verdijk)

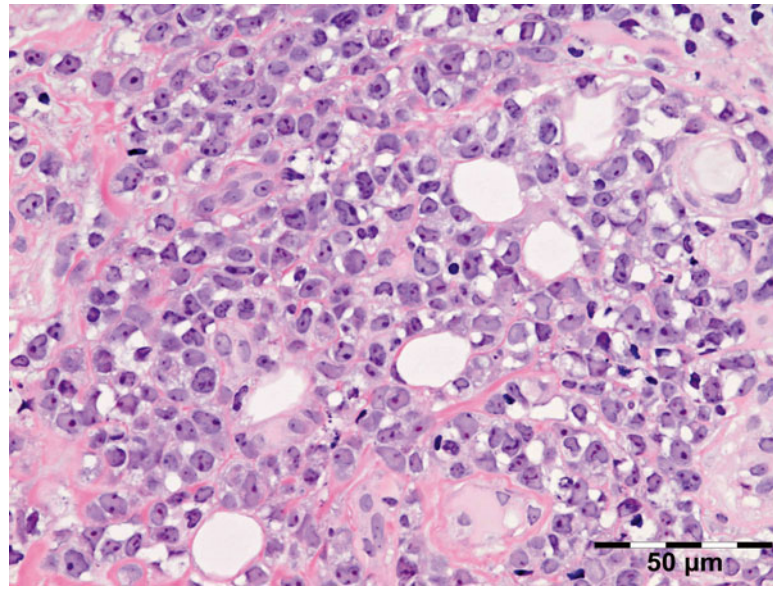

Fig. 12.122 Acute myelogenous leukemia (AML) in the orbit: large atypical myeloid cells with irregular cytoplasmic borders are scattered through the fat and fibrous tissue (HE 400× plastic) (Dr. Robert M. Verdijk)

lesions were noted more commonly in children with acute myeloid leukemia (AML) (66.6 %) compared to acute lymphocytic leukemia (ALL) (15.1 %) [228]. Orbital myeloid sarcoma is a rare entity in adults and highly associated with myelodysplastic syndromes, especially acute myelogenous leukemia (AML) which we observed two times in our series (Fig. 12.122) [229].

12.7.12 Dendritic Cell Disorders

12.7.12.1 Langerhans Cell Histiocytosis (LCH)

Definition

LCH is a neoplastic proliferation of Langerhans cells.

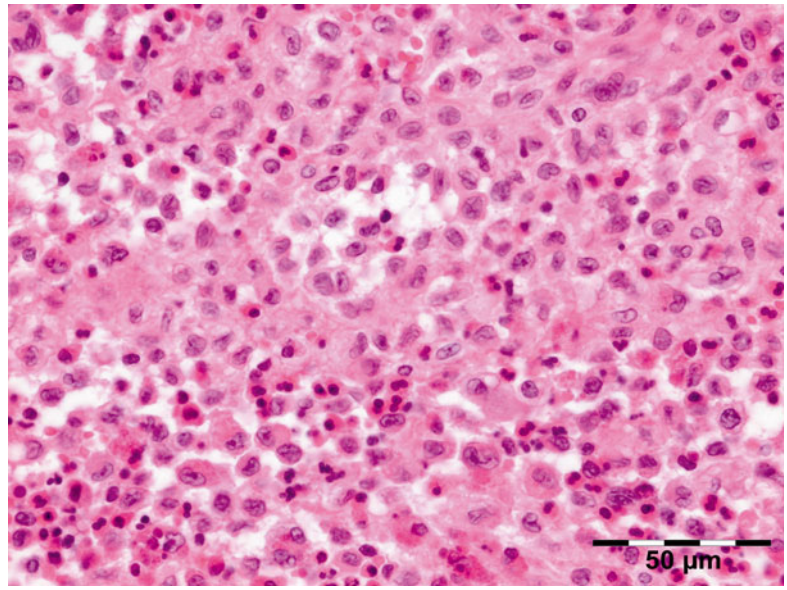

Fig. 12.123 Langerhans cell histiocytosis (LCH): Langerhans cells, which are of intermediate size with indistinct cytoplasmic borders and eosinophilic to clear cytoplasm with oval nuclei which frequently are indented, irregular in outline, and typically possess nuclear grooves. Chromatin is either diffusely dispersed or condensed along the nuclear membrane admixed eosinophils are typical (HE 400×) (Dr. Robert M. Verdijk)

Synonyms

Terminology such as eosinophilic granuloma, Langerhans cell granulomatosis, histiocytosis X, or Hand–Schüller–Christian disease and Letterer–Siwe disease should be avoided in pathology reports since these are clinical phenotypes of disease.

Epidemiology

LCH is a relatively rare disorder, accounting for less than 1 % of all osseous lesions. LCH represented 4 % of hematopoietic lesions in our series and under 1 % of all orbital lesions.

Etiology

Unknown.

Localization

Although any bone may be involved, there is a predilection for LCH to involve the bones of the skull, notably the calvarium, and rarely the orbit [230].

Clinical Features

LCH involving the bone has been reported in a wide age distribution ranging from the first months to the eighth decade of life with 80–85 % of cases seen in patients under the age of 30 and 60 % under the age of 10. Males are affected twice as often as females.

Macroscopy

The involved tissue is soft and is red in color.

Histopathology

The diagnosis depends on the recognition of Langerhans cells, which are of intermediate size with indistinct cytoplasmic borders, with eosinophilic to clear cytoplasm with oval nuclei which frequently are indented, are irregular in outline, and typically possess nuclear grooves. Chromatin is either diffusely dispersed or condensed along the nuclear membrane (Fig. 12.123). In osseous LCH, the Langerhans cells are found in nests or clusters. The Langerhans cells are frequently admixed with inflammatory cells including large numbers of eosinophils as well as lymphocytes, neutrophils, and plasma cells. Necrosis is common and does not portend an aggressive clinical course. Multinucleated osteoclast-like giant cells and occasionally lipid-laden histiocytes may be present. The cells of LCH can exhibit a relatively brisk mitotic rate, with up to five to six mitoses per 10 high-power fields. Langerhans cells

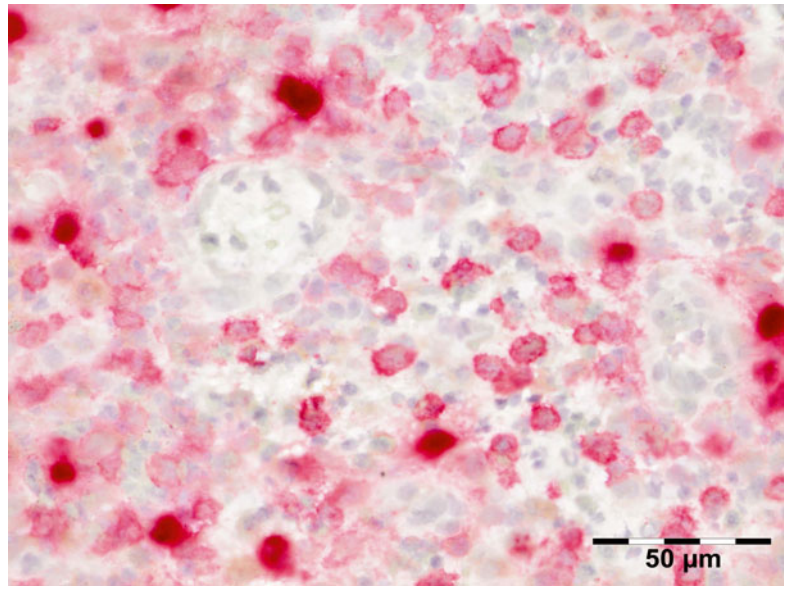

Fig. 12.124 Langerhans cell histiocytosis (LCH). Langerhans cells stain positive for CD1a (CD1a IH 400×) (Dr. Robert M. Verdijk)

have a characteristic immunophenotype which includes expression of membrane-based CD1a (Fig. 12.124) and S-100 protein in both a nuclear and cytoplasmic pattern. Langerhans cells contain unique ultrastructural intracytoplasmic "tennis racket"-shaped inclusions known as Birbeck granules which are thought to arise from the cell membrane.

Differential Diagnosis

Other histiocytoses, dendritic cell sarcoma.

Histogenesis

Langerhans cells.

Genetics

BRAF(V600E) gain-of-function mutations have been observed in 57 % of cases of Langerhans cell histiocytosis (LCH) and 54 % of cases of Erdheim–Chester disease (ECD), but not in other types of histiocytoses, indicating that these are clonal diseases [231].

Prognosis and Predictive Factors

Orbital involvement typically manifests as a solitary lesion that carries a favorable prognosis.

12.7.12.2 Erdheim–Chester Disease

(See Also Sect. 12.4.3.2.3)

Definition

Erdheim–Chester disease (ECD) is a rare histiocytosis characterized by infiltration of skeleton and viscera by lipid-laden histiocytes leading to fibrosis and osteosclerosis.

Synonyms

Lipogranulomatosis, lipoid granulomatosis, lipid (cholesterol) granulomatosis, polyostotic sclerosing histiocytosis.

Epidemiology

We encountered only two cases of ECD in our series.

Etiology

None.

Localization

While the orbit/adnexal xanthogranuloma tends to be anterior in AOX, AAPOX, and NBX, it is often diffuse in ECD and leads to visual loss [59].

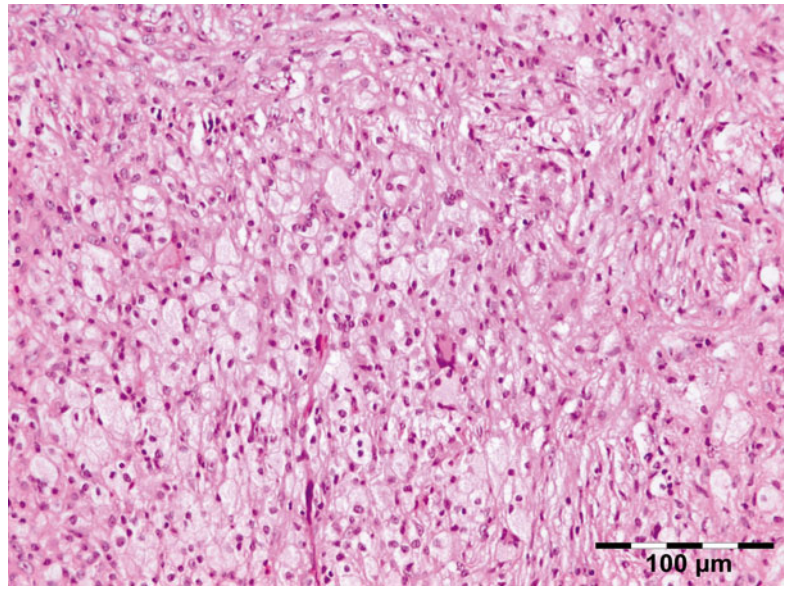

Fig. 12.125 Erdheim–Chester disease (ECD): foamy histiocytes and Touton giant cells (HE 200×) (Dr. Robert M. Verdijk)

Clinical Features

ECD is the most devastating of the adult xanthogranulomas. In Erdheim–Chester disease, xanthoma cells infiltrate the bone, heart, lungs, retroperitoneum, and perinephric and other tissues [231]. The disease demonstrates a slight male predominance with a peak incidence in the fifth through the seventh decades.

Macroscopy

The lesions appear as sulfur yellow and variably firm.

Histopathology

ECD is diagnosed histopathologically by the presence of foamy histiocytes and Touton giant cells (Fig. 12.125). ECD is characterized by dense, progressive, recalcitrant fibrosclerosis. No necrobiosis may be present. Immunohistochemistry confirms the monocyte/macrophage lineage of the lipid-laden foamy histiocytes and giant cells by their expression for lysozyme, Mac387, CD68 (Kp-1), CD4, alpha-1-antichymotrypsin, alpha-1-antitrypsin, and S-100 protein (variable). They are negative for CD1a.

Differential Diagnosis

Other xanthogranulomas, AOX, AAPOX, NBX, xanthoma.

Histogenesis

None.

Genetics

BRAF(V600E) gain-of-function mutations have been observed in 54 % of cases of ECD and 57 % of cases of LCH but not in other types of histiocytoses [231].

Prognosis and Predictive Factors

Bone involvement is common and death frequent, despite aggressive therapies; however the use of vemurafenib may offer new therapeutic opportunities in BRAF(V600E)-positive cases [232].

12.7.12.3 Rosai–Dorfman Disease

Definition

A rare disorder characterized by nonmalignant proliferation of distinctive S-100-positive histiocytes within lymph node sinuses and other extranodal sites, exhibiting lymphophagocytosis or emperipolesis.

Synonyms

Also known as sinus histiocytosis with massive lymphadenopathy.

Epidemiology
Rosai–Dorfman disease of the orbit is very rare.

Etiology
Unknown.

Localization
The reported ophthalmic manifestations include eyelid and orbital mass and rarely uveitis [233]. Orbital involvement could be an isolated extranodal manifestation or associated with concurrent systemic disease.

Clinical Features
It is a self-limiting disorder of unknown etiology that occurs worldwide in children and young adults presenting with a firm rubbery mass causing proptosis and bilateral in 57 % of cases. The median age at presentation was 13 years (range 5–65); median duration of symptoms was 6 years (range 3–15). Lymphadenopathy was noted in 57 % and extranodal involvement in 43 % [233].

Macroscopy
Salmon colored soft rubbery tissue.

Histopathology
The lesion is composed of lymphocytes and histiocytes. Individual histiocytes may contain lymphocytes and other inflammatory cells in the cytoplasm called emperipolesis.

Differential Diagnosis
Other inflammatory conditions of the orbit, lymphoma.

Histogenesis
Unknown.

Genetics
SLC29A3 mutations have been described in familial cases of Rosai-Dorfman disease.

Prognosis and Predictive Factors
The disease is usually indolent but may follow a relapsing and remitting course. Anecdotal responses to chemotherapy or radiation have been reported.

12.7.12.4 Castleman Disease

Definition
Castleman disease (CD) is a heterogeneous group of lymphoproliferative disorders of uncertain cause.

Synonyms
Angiofollicular lymphoid hyperplasia.

Epidemiology
Rarely, CD may involve various extranodal sites, including tissues depleted of lymphatics, such as the brain and the orbit. Less than ten cases of orbital CD have been reported so far [234, 235].

Etiology
Unknown.

Localization
Localized and multicentric CD may be different clinical disorders with overlapping histologic features.

Clinical Features
Orbital localized (mostly) hyaline-vascular CD cases presented with symptoms according to the site of involvement (orbit), were not associated with systemic symptoms nor increased mortality, and were asymptomatic with no evidence of recurrence or systemic manifestation according to postoperative follow-up of at least 1 year. Whereas multicentric disease is a systemic lymphoproliferative disorder characterized by lymphadenopathy, hepatosplenomegaly, constitutional symptoms, anemia, hypoalbuminemia, and hypergammaglobulinemia. Multicentric CD may be HHV-8-associated.

Histopathology
Three histologic variants (hyaline vascular, plasma cell, and mixed) of CD have been described. There is a dense infiltration of lymphocytes and plasma cells. The lymphoid cells form reactive germinal centers. In the hyaline-vascular type, the follicular center contain prominent hyaline vasculature (Fig. 12.126). In the plasma cell type, the interfollicular zone contains a prominent plasma cell population often associated with a proliferation of thin-walled capillaries. Immunohistochemical demonstration of HHV-8 may aid the diagnosis

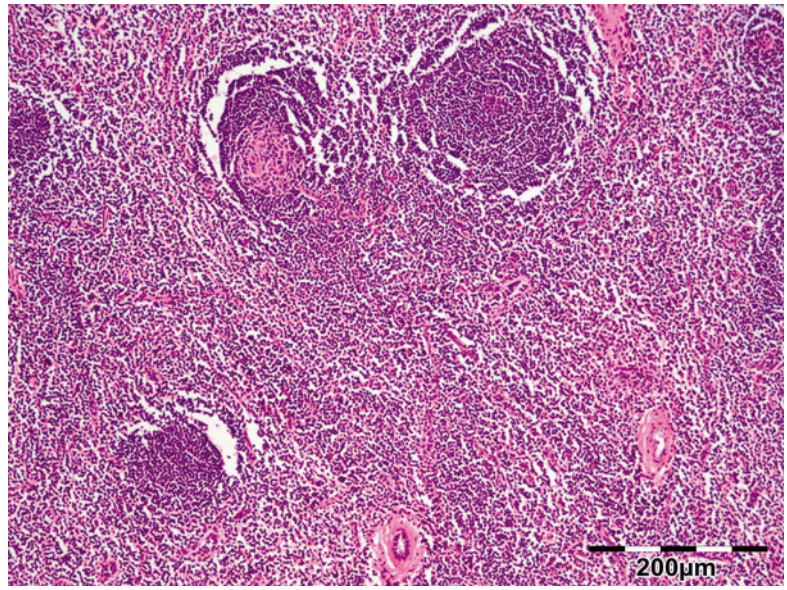

Fig. 12.126 Castleman disease: in the hyaline-vascular type the follicular center contains prominent hyaline vasculature (HE 200×) (Dr. Brian Clark; this case was presented at the EOPS meeting, Beograd, 2004, case 04–10)

of HHV-8-associated multicentric CD and may prompt testing for HIV.

Differential Diagnosis

IOIP, IGRD, lymphoma.

Prognosis and Predictive Factors

Although surgery has been almost always curative for unicentric CD of either hyaline-vascular type or plasma cell type, there is no gold standard therapy for multicentric CD. In particular, various therapeutic approaches, encompassing surgical resection, cytoreductive chemotherapy, radiation therapy, immune modulators (corticosteroids, interferon-a, all-trans retinoic acid, thalidomide), antiviral therapy, and monoclonal antibodies (anti-IL-6 monoclonal antibody and anti-CD20 monoclonal antibody [rituximab]) have been tried in MCD with variable results.

12.7.13 Tumors of Uncertain Differentiation

12.7.13.1 Primary Synovial Sarcoma

Definition

Synovial sarcoma is a mesenchymal spindle cell tumor which displays variable epithelial differentiation, including glandular formation, and has a specific chromosomal translocation t(X;18)(p11;q11).

Epidemiology

Synovial sarcoma is one of the most common soft tissue malignancies of adolescents and young adults. Synovial sarcomas of the head and neck are rare, making up only 10 % of all synovial sarcomas and typically localizing to the hypopharynx or parapharyngeal space [236, 237].

Etiology

There are no specific predisposing factors. The specific chromosomal translocation t(X;18)(p11;q11) is most likely of importance.

Localization

Primary synovial sarcoma of the orbit is extremely rare [238]. Metastatic synovial sarcoma should always be considered [239].

Clinical Features

Are of a space-occupying mass.

Macroscopy

The tumor is tan or gray and soft when lacking fibrous stroma.

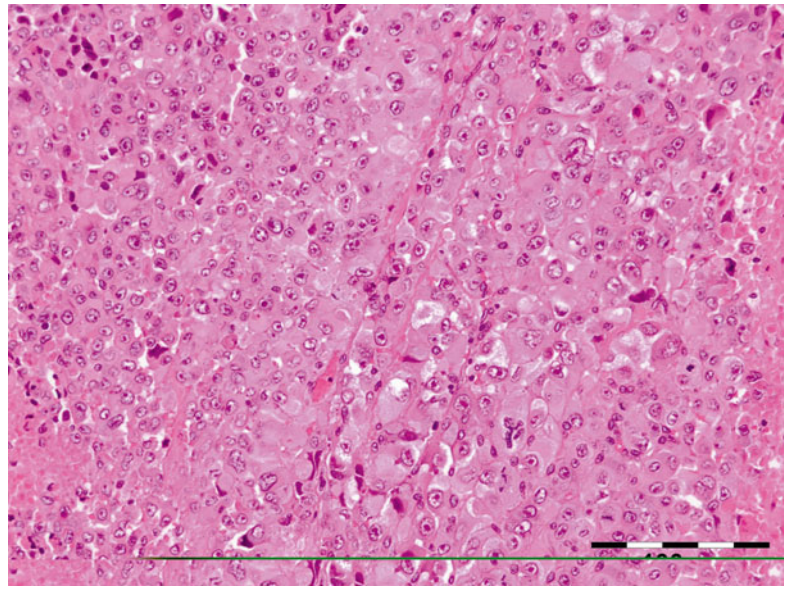

Fig. 12.127 Rhabdoid tumor: neoplastic cells with large nuclei, prominent nucleoli, and abundant, eccentric cytoplasm with variably prominent eosinophilic, cytoplasmic "inclusions" (HE 200×) (Dr. Ralph C. Eagle Jr.; this case was presented at the joint Verhoeff-EOPS meeting, Houston, 1996, case 96-06)

Histopathology

It may be biphasic (consisting of epithelioid cells admixed with spindle cells) or monophasic (spindle cells with little or no evidence of epithelioid differentiation). About 90 % of all synovial sarcoma express cytokeratins in the epithelial component and in rare cells in the spindle cell component.

Differential Diagnosis

Many types of sarcoma, including liposarcoma and MPNST.

Histogenesis

Synovial sarcoma is thought to be derived from as yet unknown multipotent stem cells capable of differentiating into mesenchymal and/or epithelial structures.

Genetics

Synovial sarcoma is associated with the chromosome translocation t[x;18][p11.2;q11.2] causing a transcribed fusion product of two genes, SYT and SSX1, or SSX2. Diagnosis may be confirmed by fluorescence in situ hybridization (FISH) or reverse transcription polymerase chain reaction (RT-PCR).

Prognosis and Predictive Factors

Adequate local excision with postoperative radiotherapy can control local recurrence. Up to 50 % of SS recur, usually within 2 years. Some 40 % metastasize, commonly to the lungs and bones and also regional lymph nodes.

12.7.13.2 Extrarenal Rhabdoid Tumor

Soft tissue rhabdoid tumor is a malignant tumor of infants and children, characterized by neoplastic cells with large nuclei, prominent nucleoli, and abundant, eccentric cytoplasm with variably prominent eosinophilic, cytoplasmic "inclusions" (Figs. 12.127 and 12.128). Occurrence of the tumor in the orbit has been presented at the EOPS and Verhoeff Ophthalmic Pathology Society thrice, in 1991 by Drs Jakobiec and Hidayat and in 1996 by Dr Eagle. The cytoplasmic inclusions are ultrastructurally composed of whorls of intermediate filaments. Since a rhabdoid phenotype may be present in a wide spectrum of tumors, particularly those occurring in adults, the diagnosis of rhabdoid tumor requires exclusion of an underlying alternative line of differentiation such as carcinomas, sarcomas, meningiomas, melanomas, lymphomas, and mesotheliomas [240, 241]. Rhabdoid tumors have been described as primarily unencapsulated masses, generally less than 5 cm in greatest dimension. The cut surface is soft and gray to tan in color. Foci of both hemorrhage and necrosis are frequently observed. The majority of rhabdoid tumors co-express vimentin

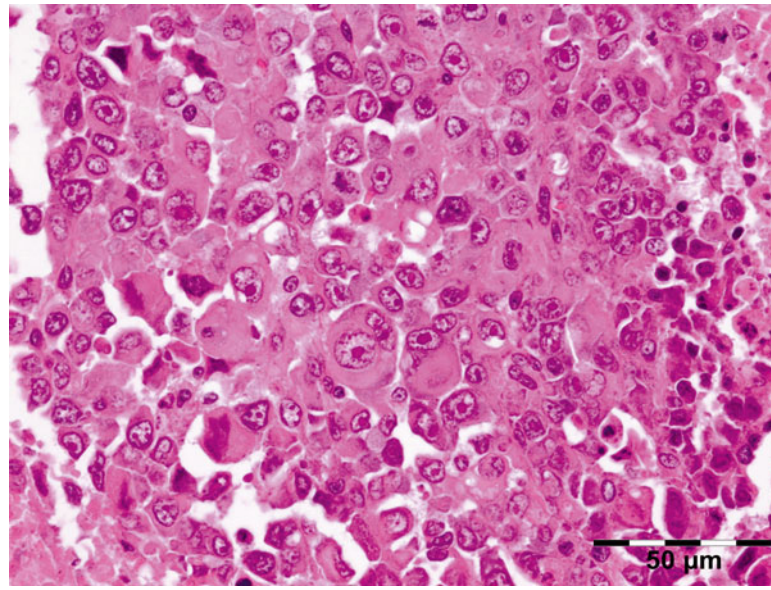

Fig. 12.128 Rhabdoid tumor: neoplastic cells with large nuclei, prominent nucleoli, and abundant, eccentric cytoplasm with variably prominent eosinophilic, cytoplasmic "inclusions" (HE 400×) (Dr. Ralph C. Eagle Jr.)

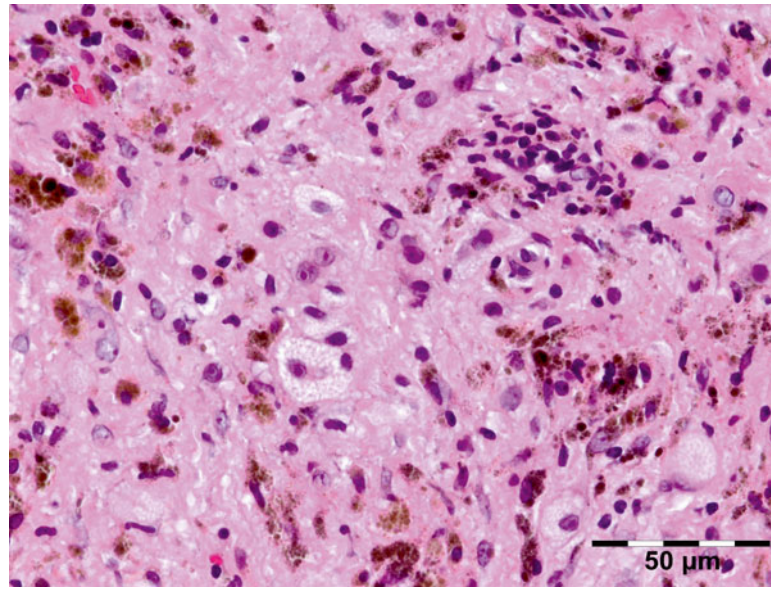

Fig. 12.129 Melanoma arising from oculodermal melanocytosis (nevus of Ota): heavily pigmented spindle cells of the preexisting blue nevus of the orbit are mixed with large epithelioid melanoma cells with foamy cytoplasm and polymorphic nuclei featuring large irregular nucleoli (HE 400×) (Dr. Robert M. Verdijk)

and an epithelial antigen, such as keratin, epithelial membrane antigen, and/or CAM5.2. In addition, a significant percentage of tumors frequently express neuroectodermal antigens such as CD99, synaptophysin, and/or NSE. Expression of muscle-specific actin and focal S-100 positivity are also not uncommon. However, despite the frequent polyphenotypic appearance, desmin, myoglobin, and CD34 are not expressed. Rhabdoid tumors are characterized by either a homozygous deletion or partial/complete isodisomy of chromosome 22. Homozygous deletions seem to be present in the majority of cases in which a translocation is documented.

12.7.14 Miscellaneous Tumors

12.7.14.1 Orbital Melanoma

Primary orbital melanomas are rare and arise from congenital melanocytic lesions including

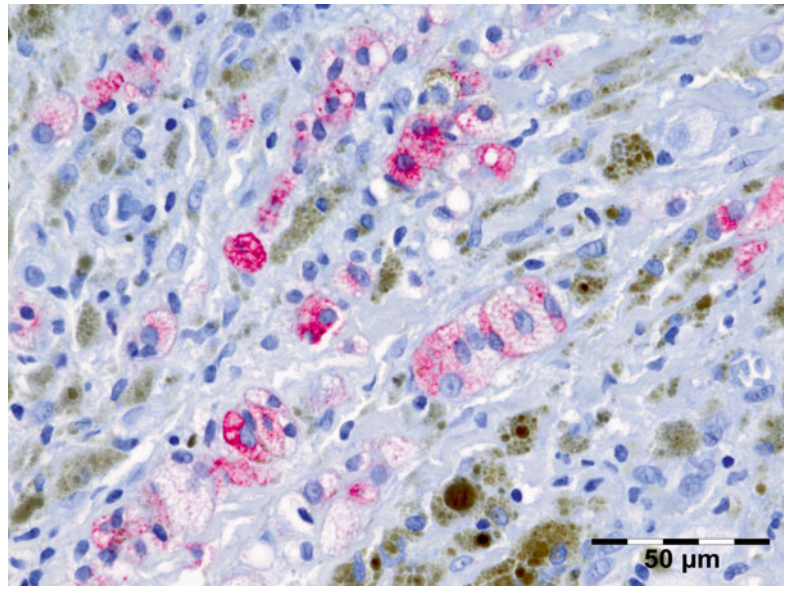

Fig. 12.130 Melanoma in nevus of Ota (HMB45 IH 400×) (Dr. Robert M. Verdijk)

oculodermal melanocytosis (nevus of Ota) (Figs. 12.129 and 12.130) as was also demonstrated at the EOPS and Verhoeff Society by Dr van Ginderdeuren in 2006, blue nevus, and cellular blue nevus. Orbital melanomas metastasize hematogenously, primarily to the liver [242].

12.7.14.2 Melanotic Neuroectodermal Tumor of Infancy (MNTI)

MNTI is an uncommon rapidly growing neoplasm of neural crest origin that primarily develops in the maxilla of infants in their first year of life. The bones of the orbital wall may therefore be involved, and extension into the orbit may occur [243]. The tumor has a fibrous appearance and may show black pigmentation. Microscopically there is a biphasic cell population of large epithelioid cells with cytoplasmic melanin granules and a small blue round cell population (Fig. 12.131). The stroma is fibrous and variably vascularized. The epithelioid cells stain positive for keratins (Fig. 12.132) and HMB45 (Fig. 12.133). The small neuroblasts stain positive for CD56 and synaptophysin (Fig. 12.134) [244]. Radical surgical excision is usually curative, but patients should be followed up closely because recurrence may occur in 10–20 % of cases [243].

12.7.14.3 Primary Orbital Carcinoid and Paraganglioma

They are unique neuroendocrine neoplasms arising in specialized neural crest cells and may be adrenal or extra-adrenal. These are usually benign, slow-growing vascular tumors found in the abdomen, thorax, head, and neck region. Head and neck paraganglioma is primarily located in the temporal bone and carotid body. Orbital paraganglioma is very rare and peculiar in histogenesis; the tumors may originate from the ciliary ganglion [245]. Carcinoid tumors arise from the enterochromaffin system. Primary carcinoid (neuroendocrine tumor) tumor of the orbit is extremely rare [246]. Tumors may be partly encapsulated grayish brown and soft. The cut surface often is hemorrhagic and friable. Microscopic appearance is of a highly cellular tumor of round to polygonal cells with finely granular eosinophilic cytoplasm. A typical "Zellballen" pattern may be highlighted by reticulin staining and immunohistochemistry for S-100, which highlights the sustentacular cells around the "Zellballen." The tumor cells are positive for chromogranin and synaptophysin. Positive staining for keratins favors the diagnosis of carcinoid, which is not expected to have sustentacular cells. A panel of keratins and additional staining should be used

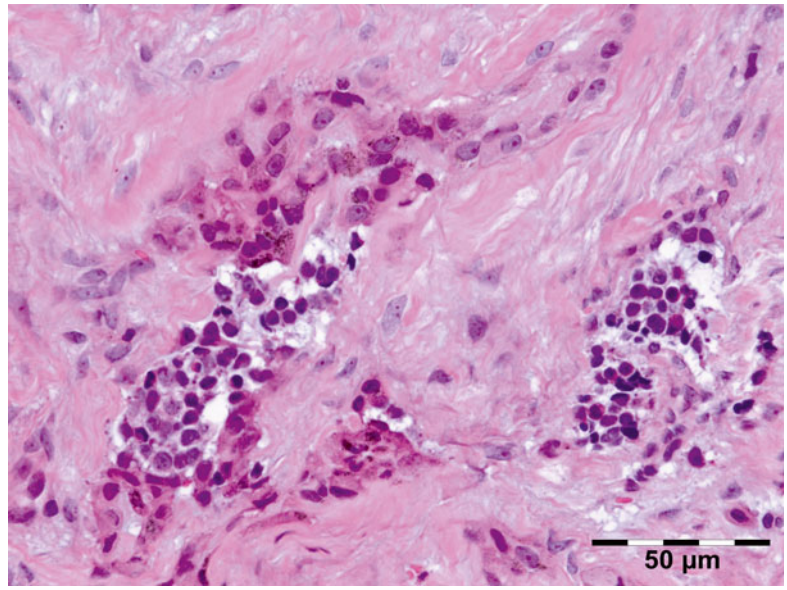

Fig. 12.131 Melanotic neuroectodermal tumor of infancy (MNETI): biphasic cell population of large epithelioid cells with cytoplasmic melanin granules and a small blue round cell population. The stroma is fibrous and variably vascularized (HE 400×) (Dr. Robert M. Verdijk)

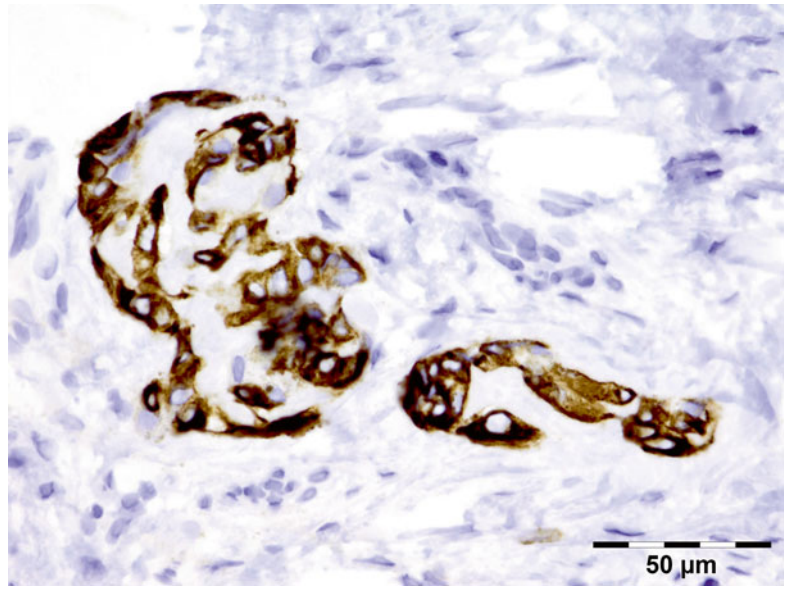

Fig. 12.132 Melanotic neuroectodermal tumor of infancy (MNETI): pan-keratin antibody (AE1/AE3) stains the epithelioid RPE-like cells (pan-keratin IH 400×) (Dr. Robert M. Verdijk)

in order to exclude metastatic carcinoid from the lung or intestine.

12.7.14.4 Alveolar Soft Part Sarcoma

Alveolar soft part sarcoma (ASPS) is a rare soft tissue tumor of uncertain cellular origin. It accounts for only 1 % of all sarcomas, which themselves represent only a small proportion of human tumors. ASPS can arise in any soft tissue of the body, but there is an unexplained predilection for the right side. The most common site for pediatric ASPS is in the head and neck region, although involvement of the orbit is rare, with fewer than 30 reported cases [247].

Epidemiology

Accounting for less than 1 % of STS, it presents at almost every part of the body with a predominance of the trunk and the proximal extremities and usually affects patients younger than 40 years.

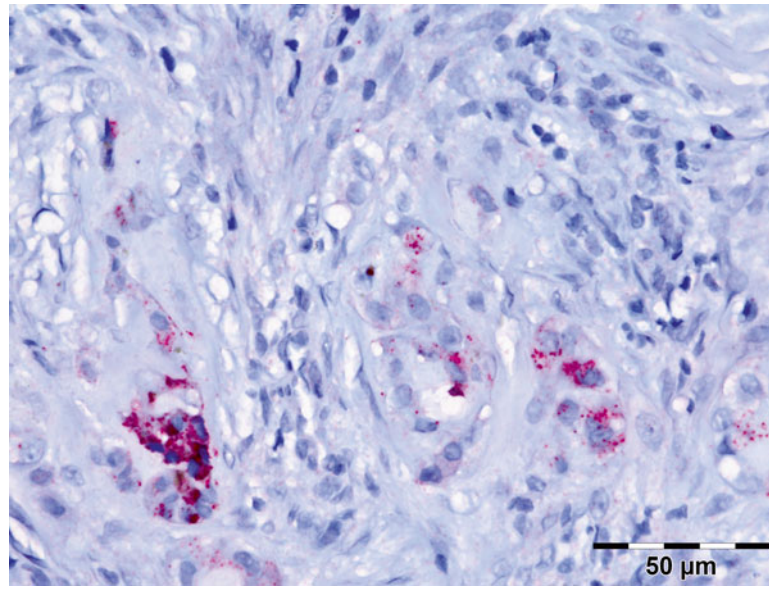

Fig. 12.133 Melanotic neuroectodermal tumor of infancy (MNETI): HMB45 antibody stains the epithelioid RPE-like cells (HMB45 IH 400×) (Dr. Robert M. Verdijk)

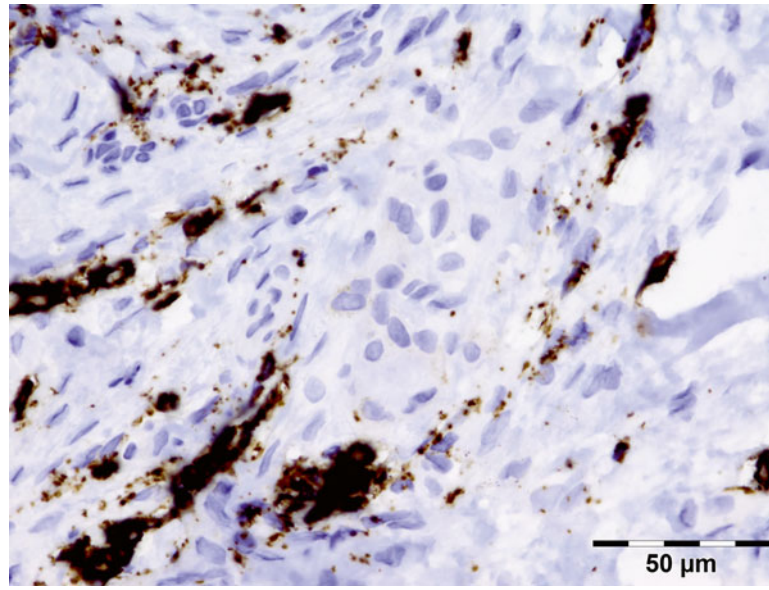

Fig. 12.134 Melanotic neuroectodermal tumor of infancy (MNETI): synaptophysin antibody stains the small neurocytic cells (synaptophysin IH 400×) (Dr. Robert M. Verdijk)

Etiology

The predominant theory has been that ASPS is a muscle-derived tumor, this being based on cellular morphology and molecular markers. Recent cytogenetic studies revealed chromosome rearrangements at t(X;17)(p11;q25) resulting in the ASPL-TFE3 fusion gene, but the origin of ASPS still remains unclear [248].

Macroscopy

Solid tumor mass located within the soft tissues. Necrosis is not a striking macroscopic appearance of this sarcoma.

Histopathology

Tumor growth characterized by a central loss of cohesion in cell lobules, depicting

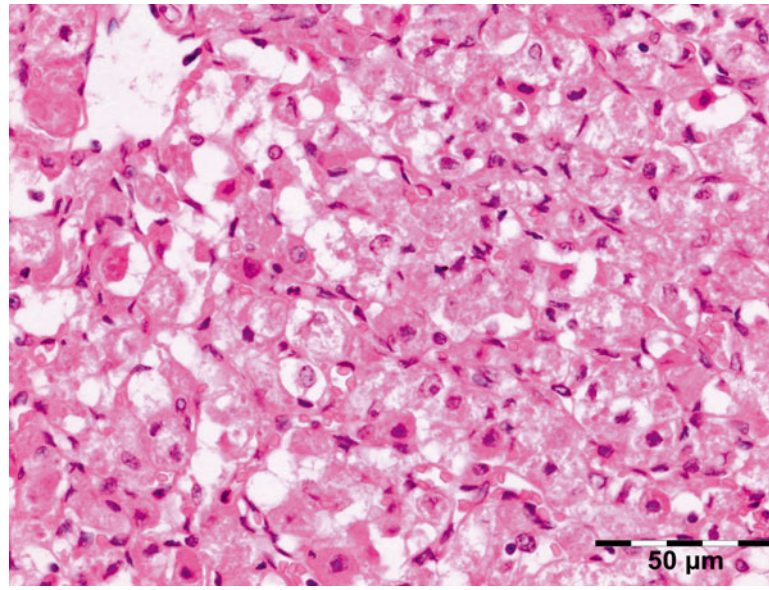

Fig. 12.135 Alveolar soft part sarcoma (ASPS): the tumor is characterized by a central loss of cohesion in cell lobules, depicting a pseudoalveolar architecture. Round tumor cell lobules, delineated by fibrovascular septa, containing round to polygonal-shaped tumor cells with eosinophilic cytoplasm, vesicular nuclei, and prominent nucleoli (HE 400×) (Dr. Stefan Seregard; this case was presented at the EOPS meeting, Beograd, 2004, case 04-12)

a pseudoalveolar architecture. Tumor cell lobules, delineated by fibrovascular septa, containing round to polygonal-shaped tumor cells with eosinophilic cytoplasm, vesicular nuclei, and prominent nucleoli (Fig. 12.135). Crystalline inclusions could be detected in 5 of 11 alveolar soft part sarcomas. Using immunohistochemistry, variable immunohistochemical reactions could be observed with reactivity for S-100 in 2 of 5 examined tumors, focal reactivity for desmin in 4 of 6 tumors, reactivity for actin in 1 of 7 tumors, and weak reactivity for NSE in 1 examined ASPS specimen. No reactivity could be obtained in any tumor for cytokeratins, HMB 45, myogenin, CD31, CD34, factor VIII, and synaptophysin [249].

12.7.15 Secondary Orbital tumors

12.7.15.1 Direct Extension

In a series of orbital biopsies, secondary tumors constituted 48.0 %. Of these were 35.5 % cases with eyelid tumors, 27.9 % cases with intraocular tumors, 26.1 % cases with conjunctival tumors, 5.0 % cases with nasopharyngeal tumors, 4.2 % cases with sinus carcinomas, 0.6 % cases with intracranial meningiomas, 0.6 % cases with esthesioneuroblastomas (Fig. 12.136), and 0.2 % cases with chordoma. We have seen a case of sebaceous carcinoma of the lacrimal sac extending into the orbit (Fig. 12.137) as well as Merkel cell carcinoma (Fig. 12.138). The three most frequent tumors making secondary orbital invasion were basal cell eyelid carcinoma (24.6 %), squamous cell conjunctival carcinoma (23.8 %), and retinoblastoma (23.5 %). Squamous cell carcinoma, from various sites of origin, was the most frequent histopathologic tumor variant, accounting for 41.0 % cases [250].

12.7.15.2 Metastatic

Metastasis is an important cause of orbital disease in the adult, representing approximately 3 % of all orbital tumors in our series. Breast carcinoma is the most common metastatic tumor found in women followed by lung carcinoma. In men the most common are lung and prostate. We observed mainly metastatic breast carcinoma, 36 %, followed by neuroendocrine carcinoma, 14 %; undifferentiated carcinoma, 8 %; adenocarcinoma NOS, 8 %; thyroid carcinoma, 8 %; melanoma of the skin, 8 %; prostate carcinoma, 6 %; and lung carcinoma, carcinoma from the nasal cavity, salivary gland adenocarcinoma, and pituitary carcinoma (3 % each). The common presenting symptoms are proptosis, diplopia, pain, and vision loss. The average age at presentation is in the seventh decade, most being female. On

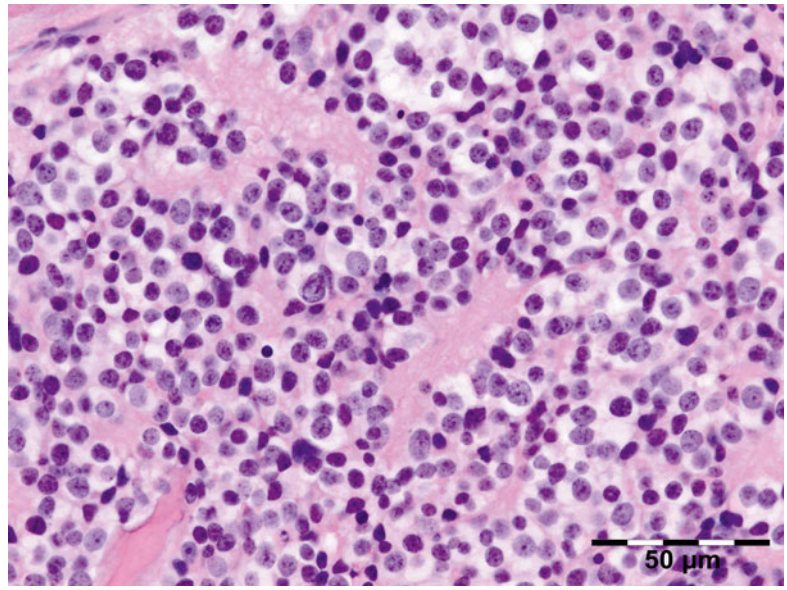

Fig. 12.136 Olfactory neuroblastoma (esthesioneuroblastoma): direct extension in the orbit of small blue round cells with nuclei that show a fine speckled chromatin pattern and small nucleoli (HE plastic 400×) (Dr. Robert M. Verdijk)

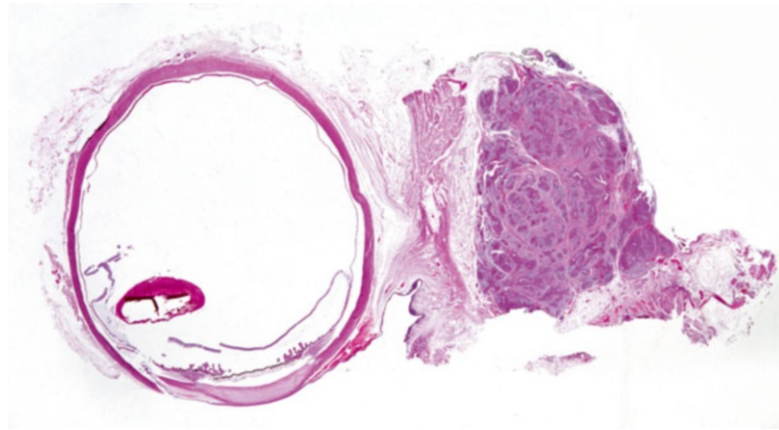

Fig. 12.137 Sebaceous carcinoma of the lacrimal sac extending into the orbit: a tumor with a lobular architecture can be observed in the orbital fat (HE no magnification) (Dr. Robert M. Verdijk)

CT, the most common finding is a well-defined, contrast-enhancing, intraconal mass. The orbital bony walls are also a common site for metastasis, especially with prostate cancers. Biopsy may be necessary for diagnosis and the prognosis with orbital metastasis of systemic cancer is very poor (average survival – 10 months). Fibrous or sometimes mucinous appearance may be observed in resection specimens. The microscopic growth pattern is related to the primary tumor (Fig. 12.139). Determination of primary origin of carcinomas is often possible and necessary for adequate clinical management of patients. After a metastasis is determined to be a carcinoma on the basis of screening immunostains, a panel of tissue- or organ-specific markers can be used in an attempt to determine or suggest the origin. Most "tumor- or organ-specific" markers may variably react with other tumor types also; hence, for metastatic tumors of unknown origin, the use of a panel of markers is strongly encouraged (Figs. 12.140, 12.141, and 12.142) [251].

12.8 Lacrimal Gland

12.8.1 General Description

The lacrimal glands are paired almond-shaped glands that secrete the aqueous layer of the tear

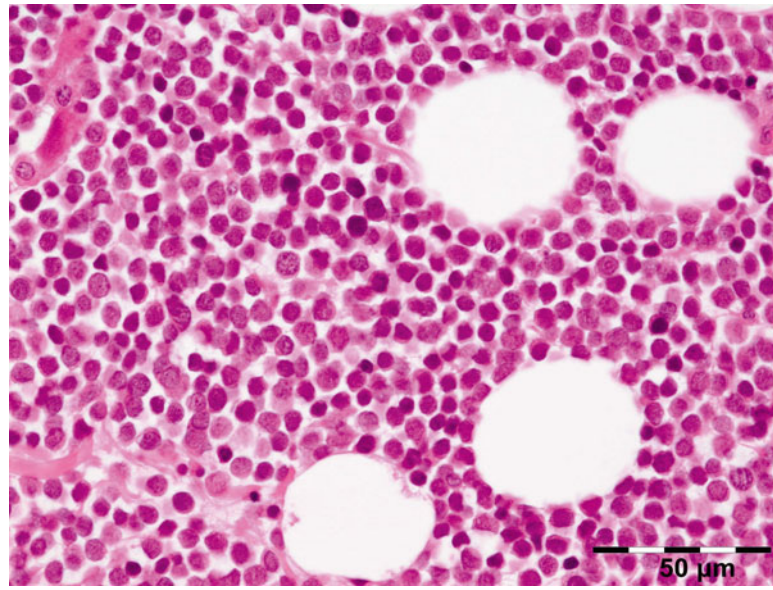

Fig. 12.138 Merkel cell carcinoma extending into the orbit: small blue round cells with nuclei that show a fine speckled chromatin and small or absent nucleoli (HE 400×) (Dr. Robert M. Verdijk)

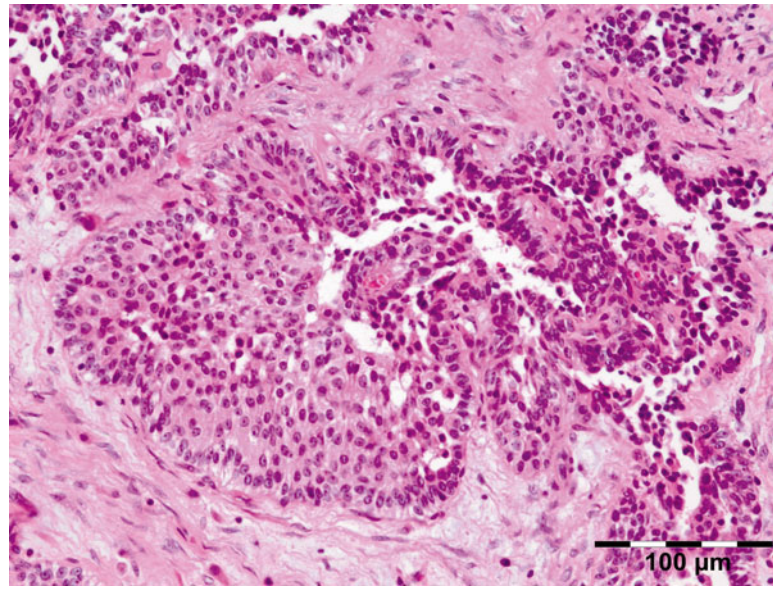

Fig. 12.139 Metastatic urothelial cell carcinoma in the orbit: transitional cell features of the tumor cells can be observed (HE 200×) (Dr. Robert M. Verdijk)

film. They are situated in the upper, outer portion of each orbit. A wide variety of diseases can affect the lacrimal gland requiring different treatment strategies. Correct handling is essential as removal of the lacrimal gland may cause dry eye, and vision and life may be threatened if malignant tumors are not treated properly. In general, lesions affecting the palpebral portion of the lacrimal gland are diagnosed earlier when compared to lesions mainly affecting the orbital lobe. The history of a long-standing (>1–2 years), noninfiltrating lacrimal gland lesion suggests a benign tumor, such as a pleomorphic adenoma; a shorter history suggests either an inflammatory or a malignant process. Pain most commonly is seen with inflammatory lesions of the lacrimal gland, but adenoid cystic carcinomas and other malignancies also can present with pain secondary to perineural or bony involvement.

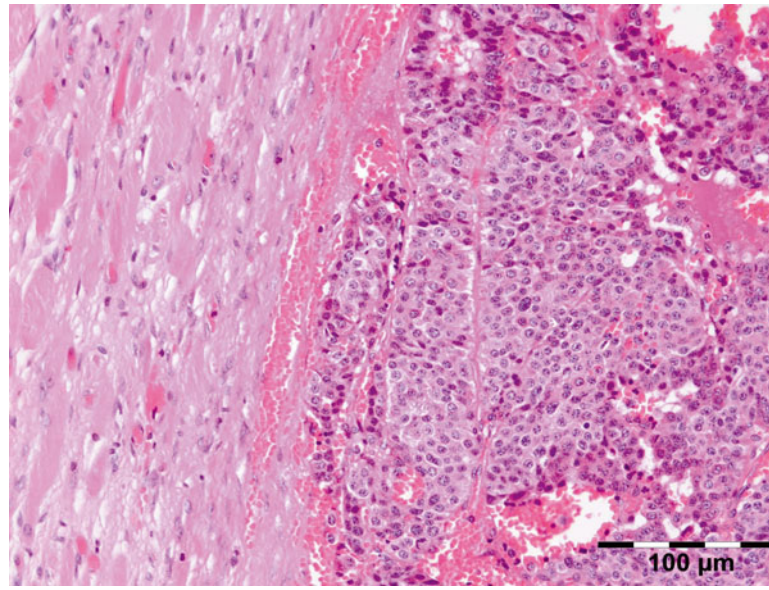

Fig. 12.140 Metastatic carcinoid in the orbit, originating from the gut: nested and trabecular arrangement of small cells with nuclei that show a fine speckled chromatin and small or absent nucleoli (HE 200×) (Dr. Robert M. Verdijk)

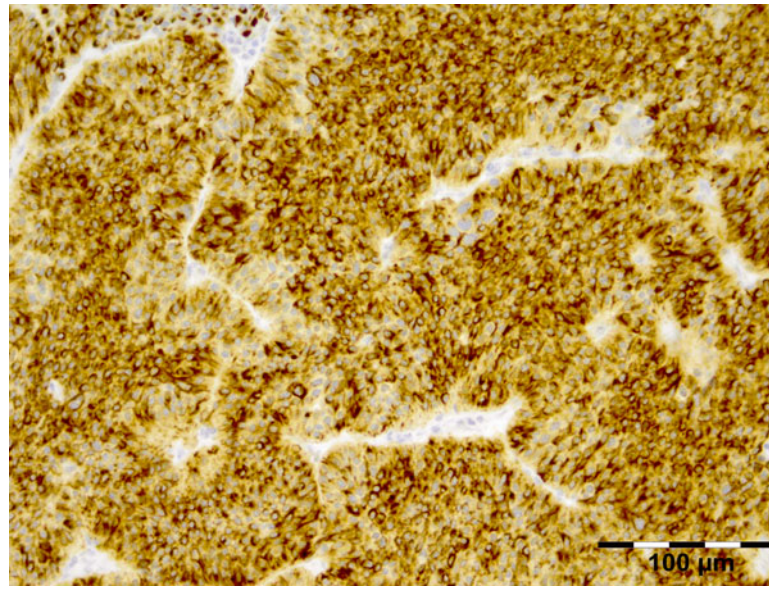

Fig. 12.141 Metastatic carcinoid in the orbit, originating from the gut: pan-keratin (keratin 8–18) stains the cytoplasm of the tumor cells (pan-keratin IH 200×) (Dr. Robert M. Verdijk)

12.8.1.1 Classification and Frequency

From a Danish series of 232 lacrimal gland lesions, the incidence rate of lacrimal gland lesions was 1.3/1,000,000/year. The overall annual age- and gender-adjusted incidence rate more than doubled during the study period, owing to an increase in nonmalignant lesions. Approximately half of the lesions were neoplasms and 55 % of these were malignant. Classification of epithelial lacrimal gland lesions has changed over the last decade, and it is now generally accepted that these tumors should be classified in the same way as corresponding lesions in the salivary glands. Dacryops constituted 10 %, inflammatory lesions 27 %, normal tissue 12 %, benign tumors 23 %, and malignant tumors 29 %. Patients with malignant neoplasms were significantly older than patients with benign neoplasms (63 vs. 48 years). The indication for surgical intervention was suspicion of a tumor in

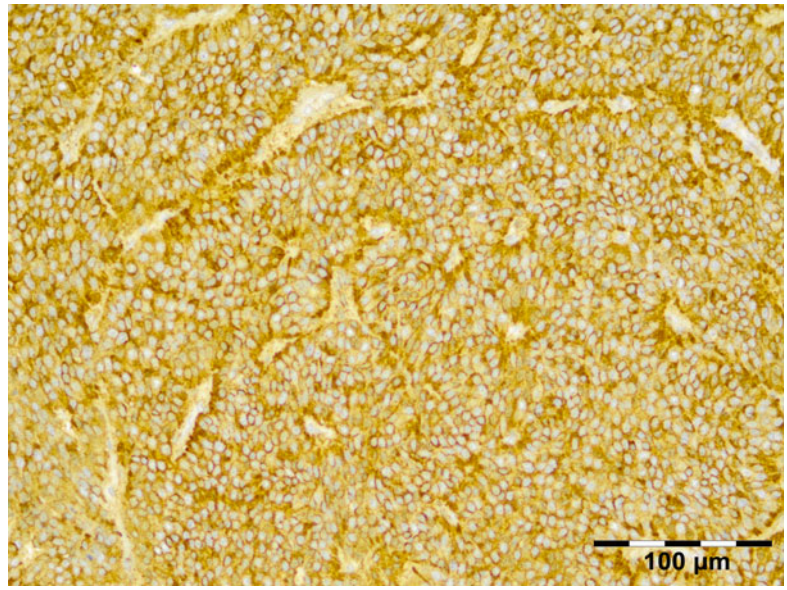

Fig. 12.142 Metastatic carcinoid in the orbit, originating from the gut: chromogranin A stains the cytoplasm of the tumor cells (chromogranin A IH 200×) (Dr. Robert M. Verdijk)

more than 90 % of the neoplastic lesions and in 30 % of the nonneoplastic lesions [252].

Our own series of 216 histologically confirmed lacrimal gland lesions was retrieved from the files of the Department of Pathology of the Erasmus MC University for the 25-year period of 1987–2012 (Table 12.2). The most frequent diagnoses constituted inflammatory conditions (49 %), followed by neoplasms (27 %) and cysts (14 %). Approximately one-quarter (27 %, $n=58$) of the lesions were neoplastic and 72 % of these were malignant. Lymphomas constituted 12 % of all lacrimal gland lesions and pleomorphic adenoma 10 % (Table 12.2). The proportional differences in diagnoses may be explained by selection bias since our series is based on a single institution, whereas the Danish numbers are based on a national registry.

12.8.2 Embryology, Anatomy, and Development

12.8.2.1 Embryology

The lacrimal gland arises from a thickening of the ectoderm of the superior conjunctival fornix at about the 22- to 25-mm crown–rump length embryo stage (46–48 days). The initial cells proliferate in the form of five or six rounded epithelial buds. The mesenchymal cells that surround the point of epithelial budding are of neural crest origin [4]. Appearance of a central lumen in the interior of the epithelial buds is initially seen in 28.5-mm CR embryos. In 47- to 67-mm embryos (10–12 weeks), the expansion of the superior levator palpebrae muscle divides the lacrimal gland into the orbital and palpebral lobes. Epithelial buds continue to invaginate from the fornix epithelium until the 15th week of development. The tubular invagination of the lacrimal gland extends and branches multiple times to give the lobular structure of the mature gland. The formation of the acini and glandular stroma, together with the full development of vascularization and glandular innervation, is completed between the 13th and the 16th weeks [253]. Epithelial–mesenchymal interaction appears to play an important role in the development of the lacrimal gland. Recent studies have shown that normal lacrimal gland development requires the expression of both the soluble mediator fibroblast growth factor (FGF) 10 in mesenchyme adjacent to the lacrimal gland primordium and a wild-type level of the transcription factor Pax6 in the conjunctival epithelium [254].

12.8.2.2 Anatomy and Histology

The main lacrimal gland is located in a depression of the zygomatic process of the frontal bone,

above the lateral end of the eye. The gland is bilobed, consisting of two contiguous lobes: an orbital portion, measuring 20×12×5 mm and weighing 0.78 g, and a smaller inferior, palpebral portion, representing one-third or one-half of the orbital lobe. The superior portion is separated from the inferior by the fibrous expansion of the superior levator palpebrae muscle and lies within the back part of the upper eyelid, above the superior fornix. The inferior part is located anteriorly. A thin pseudocapsule covers the gland. The lacrimal gland is an eccrine secretory gland. It is divided into numerous lobules with short-branched gland tubules and acinar portions of cylindrical cells that secrete lysozyme, tear lipocalin, lactoferrin, and IgA. A basal layer of myoepithelial cells surrounds the acinar cells. The secreted fluid exits the gland through the excretory duct. Eight to 12 major lacrimal ducts from the orbital lobe pass through and join with ducts from the palpebral lobe. From the inferior margin of the palpebral lobe, the lacrimal ducts run obliquely beneath the conjunctiva for a short distance and empty into the external part of the upper conjunctival fornix, approximately 5 mm above the lateral tarsal border. The tears flow across the ocular surface and drain through the lacrimal passages.

Minor or accessory lacrimal glands are present in the ocular adnexa. The glands of Krause are more numerous in the upper temporal fornix (42 glands vs. 6–8 in the lower fornix). Their ducts unite into a rather long duct or sinus which opens into the fornix. The glands of Wolfring (or Ciaccio) reside in the upper border of the tarsus. Other accessory lacrimal glands are present in the caruncle.

The main lacrimal gland is vascularized by the lacrimal artery, a branch of the ophthalmic artery, arising lateral to the optic nerve and running forward along the upper border of the lateral rectus muscle in company with the lacrimal nerve, a branch of the first division of the trigeminal nerve, which provides sensory innervation. Tear secretion is mediated by parasympathetic output and vasoactive intestinal polypeptide (VIP) mediated fibers. The venous drainage is through the lacrimal vein, which opens into the ophthalmic vein.

12.9 Congenital Abnormalities

An aberrant lacrimal gland is an unusual congenital and developmental abnormality and differs from an ectopic gland. Several cases of aberrant lacrimal gland associated with other congenital abnormalities have been described [255]. Congenital fistulae of the lacrimal gland are rarely reported. Since their original description by Beer, 17 cases have been recorded in the literature, only one of which was bilateral [256].

12.10 Inflammation

The lacrimal gland belongs to the mucosa-associated lymphoid system. Plasma cells account for approximately 50 % of all mononuclear cells present and the vast majority of them produce IgA. T cells, representing the second most common cell type, are located predominantly in lymphocytic foci and singly in the interstitium. CD8 antigen-positive (suppressor/cytotoxic) T cells predominate over CD4 antigen-positive (helper) T cells [257]. A regular presence of a lymphoid tissue has been demonstrated also in the lacrimal drainage mucosa. The lacrimal drainage-associated lymphoid tissue is more extensive in the lacrimal sac, in the nasolacrimal duct, and in the common canaliculus, where a low flow rate can be assumed because of the widening of the lumen and the limited amount of tear fluid [258].

12.10.1 Dacryoadenitis

Definition

Inflammatory condition of the lacrimal gland.

Etiology

Includes infectious processes resulting from bacterial, viral, or fungal systemic diseases and noninfectious diseases associated with systemic inflammatory disorders.

In infectious dacryoadenitis, the causative organism may be blood borne (acute dacryoadenitis secondary to systemic infection) or ascends

through the ductules to infect the lacrimal gland, particularly in association with obstruction of the nasolacrimal duct. Infection may also spread to the lacrimal gland transneuronally or via traumatic injury [259]. Mumps, Epstein–Barr, measles, influenza, and herpes viruses and cytomegalovirus, staphylococcus, and gonococcus are usually implied. Fungal pathogens rarely cause dacryoadenitis.

Noninfectious dacryoadenitis usually is lacrimal gland involvement of systemic diseases and has been discussed in the section on inflammatory conditions of the orbit.

Epidemiology

Acute dacryoadenitis is uncommon (only 1 in 10,000 ophthalmic cases) [260]; therefore, data about its prevalence are sparse. The infrequency of cases of acute dacryoadenitis may reflect the fact that the gland is hidden in a bony cavity. In developed countries dacryoadenitis associated with systemic inflammatory disorders is more common than infectious processes.

Clinical Features

May be acute, subacute, or chronic. Acute dacryoadenitis is typically infectious in nature. It develops over a few days to a week and may occur at any age [261]. Both infectious and noninfectious acute severe cases may be characterized by an abrupt onset of tenderness, warmth, redness, and painful swelling, with a characteristic S shape, of the lateral third of the upper eyelid. Other symptoms may include fever; ipsilateral preauricular lymphadenopathy, particularly with viral infections; eye redness; and photosensitivity. Infectious dacryoadenitis is usually associated with leukocytosis. Lacrimal gland abscess, orbital abscess, or cellulitis with restriction of the extraocular muscle movement may follow when the infection is not treated appropriately. Pain with eye movement suggests an orbital cellulitis. Resolution of symptoms may take as long as 1 month [262]. Chronic dacryoadenitis is more common than acute dacryoadenitis and is usually associated with systemic diseases. Some infectious diseases such as tuberculosis or syphilis cause slow onset of symptoms and they may remain for a long time. Chronic dacryoadenitis is often present in an indolent manner, with progressive enlargement of the outer portion of the upper eyelid over several months or years. Lacrimal gland enlargement is usually bilateral with systemic conditions. The gland is mobile and mild ptosis secondary to enlargement of the gland is possible.

Histopathology

Lacrimal gland biopsy is usually not necessary in acute infectious dacryoadenitis and will show in mild cases only foci of polymorphonuclear cell infiltrate. Subacute and chronic dacryoadenitis associated with systemic diseases show different microscopical features related to the underlying pathological condition as described in the section on orbital inflammatory disease.

12.10.1.1 Dacryoadenitis Secondary to Sjögren Syndrome (SS)

Etiology

Chronic immune system stimulation, characterized by exocrine gland dysfunction and a variable systemic course, which may be primary or occur in connection with autoimmune rheumatic diseases. Cytokines and autoantibodies may be involved in decreasing neurosecretory circuits and inducing glandular dysfunction.

Epidemiology

Primary SS is frequently seen in middle-aged, perimenopausal women.

Clinical Features

Enlargement of the lacrimal glands is rare. Loss of glandular parenchyma leads to diminished lacrimal gland function. Symptoms of dry eye (keratoconjunctivitis sicca) affect 67.5 % of SS patients [263] and may include burning, itching, foreign body, or soreness sensations in mild cases, even though the eyes' appearance is normal. Other ocular complaints may include photophobia, eye fatigue, lid irritation and swelling, decreased visual acuity, mucoid discharge in the eyes, and the sensation of a film across the visual field. In severe cases, slit-lamp examination may reveal filamentary keratitis, i.e., the presence of

mucus filaments within the preocular tear film adhering to the corneal surface or small superficial erosions of the corneal epithelium. Ocular complications may include corneal ulceration, corneal scarring, and even perforation.

Histopathology

Lesions are characterized initially by mononuclear cell infiltration into periductular regions, followed by the progressive destruction of lacrimal ductules and the acinar glands, associated with autoimmune mechanisms. The infiltrate contains T cells, B cells, and plasma cells, with a predominance of activated CD4+ helper T cells.

Differential Diagnosis

Xerophthalmia, xerostomia, and enlargement of the lacrimal and parotid glands can result from other diseases, particularly granulomatous inflammations, and the adverse effects of drugs (e.g., antidepressants, anticholinergics, beta-blockers, diuretics, antihistamines, some antiarrhythmic and antiepileptic drugs). The presence of serum autoantibodies, including antinuclear antibody (ANA), rheumatoid factor (RF), or Sjögren syndrome-specific antibodies (i.e., anti-Ro [SS-A], anti-La [SS-B]), and the constellation of characteristic systemic symptoms may help in establishing the correct diagnosis. Biopsy of accessory salivary glands may prove necessary for the significant proportion of patients with negative serology.

12.10.2 IgG4-Related Chronic Sclerosing Dacryoadenitis

IgG4-related chronic sclerosing dacryoadenitis is formerly known as Mikulicz's disease (see description earlier in the chapter). For the lacrimal gland the required number of IgG4 positive plasma cells is 100/40x HPF.

12.10.3 Dacryoadenitis Secondary to Thyroid Disease

Sclerosing inflammation of the lacrimal gland can be associated with Riedel struma (invasive fibrous thyroiditis that preferentially affects young women), both of which can also be components of multifocal fibrosclerosis [264].

12.10.4 Dacryoadenitis Secondary to Connective Tissue Diseases

Instances of dacryoadenitis associated with systemic lupus erythematosus have been described [265]. Wegener's granulomatosis of the lacrimal gland is generally a manifestation of orbital involvement of the disease [266]. Sarcoidosis may involve the lacrimal gland.

12.11 Injuries

The lacrimal gland is well protected from injuries by virtue of its anatomical location in the lacrimal fossa of the frontal bone. It is further shielded by the orbital margin which is well developed in adults. The occurrence of prolapse of the lacrimal gland due to injury was first noticed by von Graefe. Since then a few cases have been reported [267].

12.12 Degenerations

Lacrimal gland stones represent a very rare but relevant differential diagnosis when a patient presents with unilateral persistent conjunctivitis or with a tumor in the lateral canthus. Treatment is excision under local anesthesia [268]. Degenerative fat and lacrimal gland prolapse is discussed under Sect. 12.6.1. Degenerative cystic lesions include dacryocele (dacryops) which is a retention cyst of a gland ductule. It generally presents in young adults with signs and symptoms of inflammation in the superotemporal conjunctival fornix. Primary localized amyloidosis of the lacrimal gland is a rare occurrence [269]. Senile atrophy occurs as a result of senescent involution of the lacrimal gland [270].

Table 12.4 Classification of the primary epithelial tumors of the lacrimal gland

Benign tumors
Pleomorphic adenoma
Warthin's tumor
Basal cell adenoma
Myoepithelioma
Oncocytoma
Cystadenoma
Low-grade tumors
Carcinoma ex pleomorphic adenoma
Polymorphous low-grade carcinoma
Mucoepidermoid carcinoma, grades 1 and 2
Epithelial–myoepithelial carcinoma
Cystadenocarcinoma and papillary cystadenocarcinoma
Acinic cell carcinoma
Basal cell adenocarcinoma
Mucinous adenocarcinoma
High-grade tumors
Carcinoma ex pleomorphic adenoma (malignant mixed tumor) that includes adenocarcinoma and adenoid cystic carcinoma arising in a pleomorphic adenoma
Adenoid cystic carcinoma, not otherwise specified
Adenocarcinoma, not otherwise specified
Mucoepidermoid carcinoma, grade 3
Ductal adenocarcinoma
Squamous cell carcinoma
Sebaceous adenocarcinoma
Myoepithelial carcinoma
Lymphoepithelial carcinoma
Other rare and unclassifiable carcinomas

Adapted from the Seventh Edition of the *AJCC Cancer Staging Manual* (2009) published by Springer Science and Business Media LLC

12.13 Neoplasms

Lacrimal gland lesions represent 5–25 % of orbital tumors, and the proportion in the literature that are epithelial range from 23 to 70 % of biopsied cases [261, 271–273]. In a survey of 1,264 cases of orbital space-occupying lesions at a referral ocular oncology service over a period of 30 years, Shields et al. observed that lacrimal gland tumors represent almost 9 % of the space-occupying orbital lesions. Among the epithelial lesions, approximately 55 % were classified as benign and 50 % as malignant, with increasing incidence of malignancy in the elderly population. This is in accordance with our findings given in Table 12.2. Among malignant lacrimal gland tumors, adenoid cystic carcinoma (ACC) was the most common (66 %), followed by carcinoma ex pleomorphic adenoma (18 %), primary adenocarcinoma (9 %), and mucoepidermoid carcinoma (3 %) [210, 274].

The classification of lacrimal gland tumors has been recently modified on the basis of the World Health Organization classification of salivary gland tumors [275], which comprises adenomas, carcinomas, nonepithelial tumors, malignant lymphomas, secondary tumors, unclassified tumors, and tumorlike lesions. Weis et al. proposed in 2009 an updated classification scheme based on a retrospective multicenter study of 118 cases of lacrimal epithelial neoplasias [276]. Tumors were divided into "benign," "malignant low grade," and "malignant high grade." The histologically diverse classification of salivary gland tumors was applied to the epithelial lacrimal gland neoplasms in their series, and new entities such as ductal carcinoma, acinic cell carcinoma, primary squamous cell carcinoma, mucoepidermoid carcinoma, oncocytic carcinoma, polymorphous low-grade adenocarcinoma, myoepithelial carcinoma, lymphoepithelial carcinoma, etc. were included (Table 12.4). Adequate microscopical study of multiple neoplastic areas is mandatory in view of the possible variety of cell components in a single tumor. Currently molecular studies have no established role in routine diagnosis.

12.13.1 Benign Mesenchymal Tumors

12.13.1.1 Granular Cell Tumor

Granular cell tumor of the lacrimal gland is rare [277]; the features are described under Sect. 12.7.7.3.

12.13.1.2 Hemangioma

Vascular lesions such as cavernous hemangioma, epithelioid hemangioma, and hemangioendothelioma can grow within the lacrimal gland; the features are described under Sect. 12.7.5.

12.13.1.3 Solitary Fibrous Tumor

This rare spindle cell neoplasm frequently arises in the pleura. The clinical behavior (slow progressive and painless mass with unilateral proptosis) and tomographic findings (mild bony remodeling without calcifications) are similar to that of pleomorphic adenoma. Treatment is with en bloc excision. Recurrences are common and malignant transformation even several years after surgery has been documented. The features are described under Sect. 12.7.1.6.

12.13.2 Benign Epithelial Lacrimal Gland Tumors

Benign lacrimal gland tumors present clinically as a noninfiltrating, painless, and slow-growing lacrimal gland mass. They can occur in the orbital lobe or the palpebral lobe of the lacrimal gland. Proptosis and inferomedial displacement of the globe are common. There may be restricted eye motility and diplopia. The mean age at presentation is 39 years, but tumors can occur at any age.

12.13.2.1 Pleomorphic Adenoma (PA)

Definition

A benign lacrimal gland tumor with pleomorphic microscopical appearance.

Synonyms

Benign mixed tumor.

Epidemiology and Etiology

PA is the most common epithelial tumor of the lacrimal gland [278] (Table 12.2). Nevertheless, it remains an uncommon tumor overall, accounting for only 0.6 [279]–2 % (Table 12.1) of all orbital cases. The maximum incidence is around the third to fifth decades of life and is unusual in teenagers [280].

Clinical Features

The clinical features associated with PA of the lacrimal gland include painless fullness of the superotemporal lid and orbit, nonaxial proptosis, diplopia, and impairment of vision. There may also be restricted eye motility. Atypical presentations include abrupt orbital inflammation mimicking orbital cellulitis, a painful subcutaneous nodule, and calcification with bony erosion on orbital imaging [281]. The tumor grows over a period of years (>1–2 years). Computed tomography (CT) scan reveals a well-circumscribed, pseudo-encapsulated mass in the superotemporal fossa causing frequent expansion and remodeling of the bone of the lacrimal gland fossa, with no evidence of any bone invasion or destruction. The mass may flatten the globe. The palpebral lobe of the lacrimal gland is less often involved than the orbital lobe (10 % vs. 90 % of the cases), mainly in younger patients [282, 283]. In such cases PA could be misdiagnosed as a chalazion [284]. The presence of calcification and bone erosion radiologically in a lacrimal gland tumor does not necessarily indicate malignancy [285]. Suspicion of a pleomorphic adenoma based on clinical history and radiological signs is key to avoid an incisional biopsy. Because recurrent pleomorphic adenomas can undergo malignant changes, adequate management requires a complete excision of the lesion through a lateral orbitotomy to avoid a rupture or breach of the pseudocapsule. The 5-year recurrence rate is 3 % for completely excised lesions and 32 % for incompletely excised tumors. Previous studies reported a 10 % incidence of malignant transformation of recurrent adenomas by 20 years after treatment and 20 % by 30 years. Some advocate the use of fine-needle aspiration biopsy. Recurrent lacrimal gland pleomorphic adenoma tends to develop multifocally and may be widespread in the operative field. Computed tomography shows recurrent tumor nodules that are often associated with irregular bony erosion and remodeling despite these recurrences being usually benign. Repeated recurrence requiring further surgery with potential significant morbidity remains a lifelong risk, and malignant transformation in recurrent lacrimal gland pleomorphic adenoma may also occur [286]. Anecdotal instances of PA arising from accessory lacrimal glands have been reported in the literature [287–289].

Macroscopy

Gross examination of the PA reveals a rounded or oval soft mass with circumscribed, often

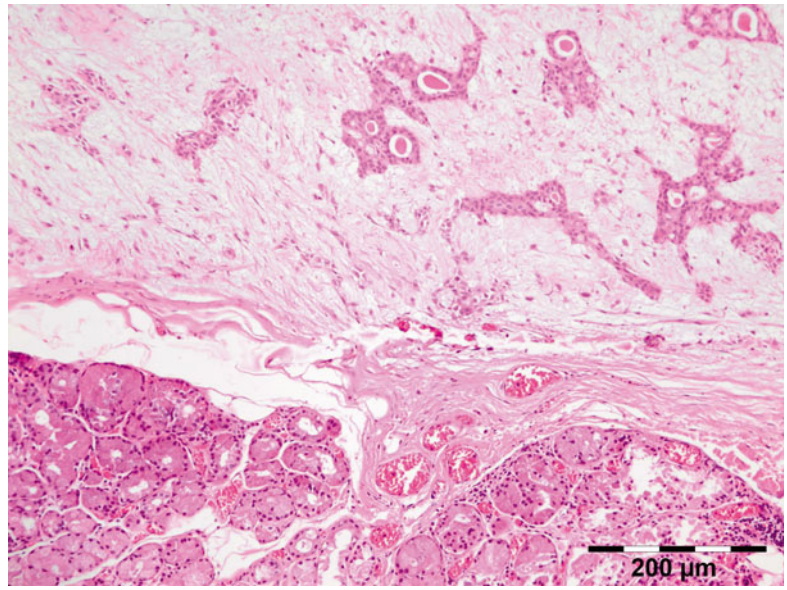

Fig. 12.143 Pleomorphic adenoma of the lacrimal gland: tubular structures enveloped by myoepithelial mantles are submerged in a chondromyxoid stroma (HE 100×) (Dr. Robert M. Verdijk)

markedly bosselated margins. The tumor appears partially pseudo-encapsulated and may show a clear plane of cleavage with the adjoining lacrimal gland. The cut surface is mostly solid and white, with occasional cystic structures. Tumors of long duration may contain foci of calcification. The mean diameter is 24.5 mm, ranging from 10 to 40 mm [276].

Histopathology–Immunoprofile

The tumor is formed by a mixture of epithelial, myoepithelial, and stromal components and shows a marked histologic diversity. The prototypic histologic appearance consists of tubular structures enveloped by myoepithelial mantles submerging in a chondromyxoid stroma (Fig. 12.143). The epithelial cells are cuboidal in shape and occasionally show a clear cytoplasm. They are cytologically bland and typically have vacuolated nuclei, without prominent nucleoli. They are arranged in nests, sheets, ducts, tubules, or trabeculae, with an outer sheath of proliferated myoepithelial cells. These may be small and dark or have plasmacytoid, epithelioid, spindle, oncocytic, or clear cell morphology. The stroma is myxoid or fibrous with focal chondroid, chondromyxoid, hyaline (Fig. 12.144), and, very rarely, osseous and adipose differentiation. Cartilage formation is specific for PA and is initiated by the myoepithelial cells. Necrosis, calcifications, and mitosis are rare. Crystalloids composed of tyrosine or oxalate are uncommonly seen (Fig. 12.145). Small tumor pseudopods extending outside the pseudocapsule are believed to be responsible for the frequent local tumor recurrences [276]. Three histologic types have been described: myxoid, or stroma-rich PA, is the most common subtype. It is hypocellular and has the highest rate of recurrence. In the cellular subtype, the myoepithelial cells and the epithelial cells form solid areas with only occasional tubular lumina. In the classic subtype, the two components are present in equal proportion. This distinction has no prognostic or therapeutic significance. PA should be thoroughly sampled in order to detect areas of malignant dedifferentiation. These are hallmarked by the presence of cellular anaplasia, necrosis, and increased mitotic activity. The immunohistochemical profile of PA is consistent with both epithelial and mesenchymal differentiation: the ductal epithelial areas stain with carcinoembryonic antigen (CEA) (Fig. 12.146), S-100, actin, and epithelial membrane antigen (EMA), whereas the proliferated myoepithelial cells co-express vimentin and pancytokeratin and are immunoreactive for p63, calponin, S-100 protein (Fig. 12.147), alpha-smooth muscle actin, GFAP, CD10, and muscle-specific

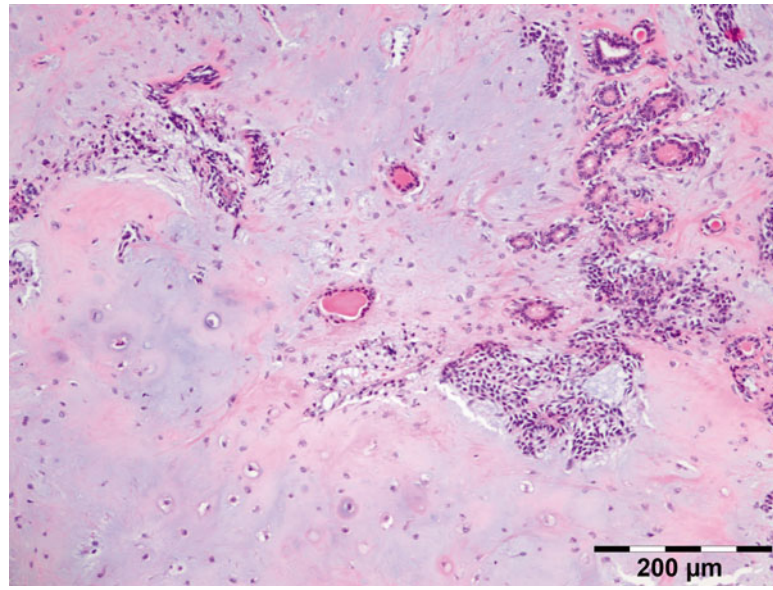

Fig. 12.144 Pleomorphic adenoma of the lacrimal gland: tubular and solid epithelial elements in a fibrous-chondroid stroma (HE 100×) (Dr. Robert M. Verdijk)

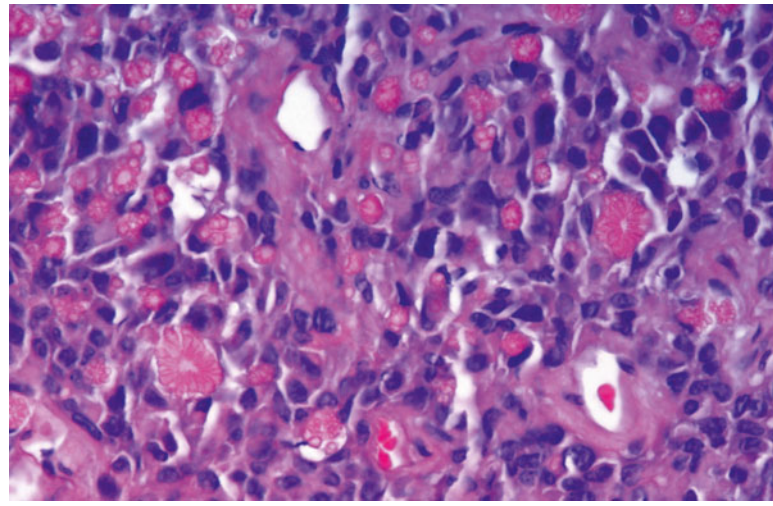

Fig. 12.145 Pleomorphic adenoma of the lacrimal gland: crystalloids composed of tyrosine or oxalate are uncommonly seen (HE 400×) (Dr. Irene Pecorella)

actin [290]. In the chondroid areas the myoepithelial cells are positive only for vimentin. Tumor capsules vary from a few micrometers to a few hundred micrometers in thickness and are incomplete in some [276].

Differential Diagnosis

Due to great microscopical variability of PA, misdiagnoses can occur when examining a small bioptic sample, where the characteristic biphasic pattern of differentiation may not be appreciated. When the hyaline stromal component creates a cylindromatous aspect, a differential diagnosis with the tubular variant of adenoid cystic carcinoma is required. Squamous or mucous metaplasia and conspicuous clear cell change can be confused with mucoepidermoid carcinoma. Occasionally the entire tumor is affected by oncocytic change and may be misdiagnosed as an oncocytoma. A positive GFAP immunoreaction of the neoplastic myoepithelial cells helps in the differential diagnosis with the low-grade polymorphous adenocarcinoma, where this reaction is absent. Finally, the expression of bone morphogenetic protein-2 (BMP-2) is specific to epithelial and myoepithelial cells of pleomorphic

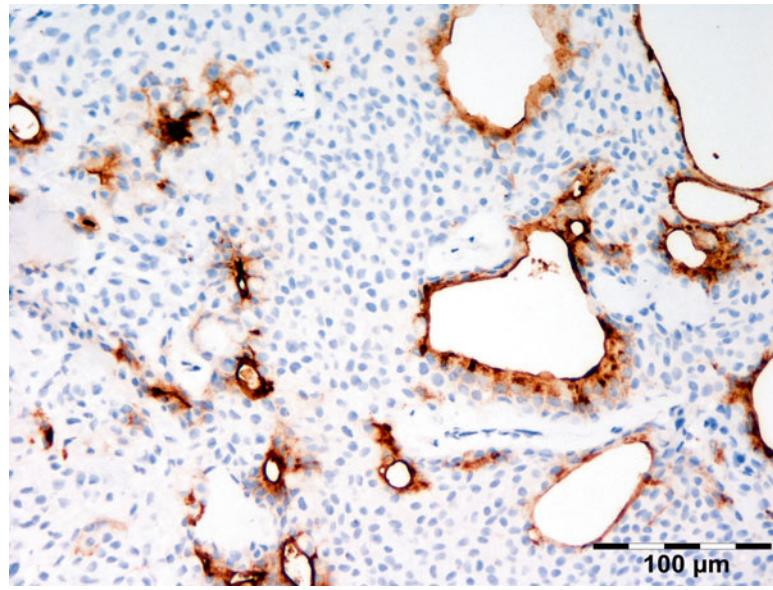

Fig. 12.146 Pleomorphic adenoma of the lacrimal gland: the ductal epithelium stains positive with carcino-embryonic antigen (CEA IH 200×) (Dr. Irene Pecorella)

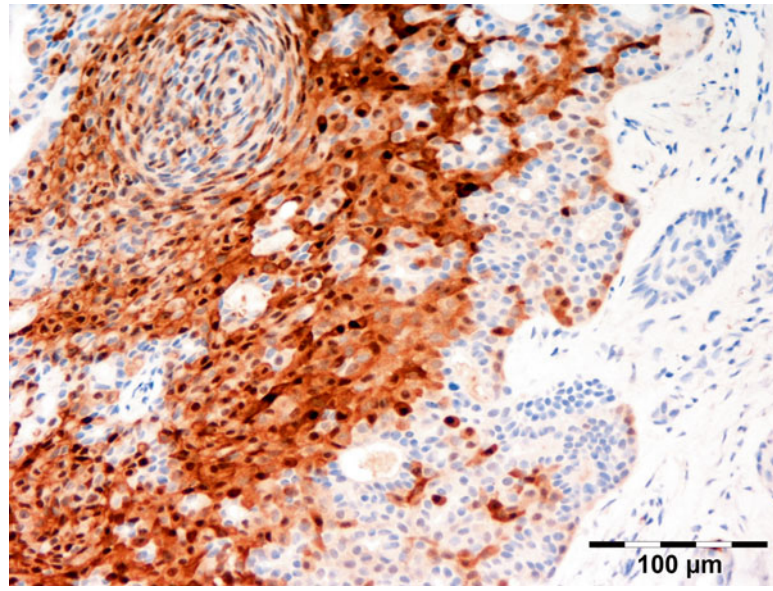

Fig. 12.147 Pleomorphic adenoma of the lacrimal gland: myoepithelial cells co-express S-100 protein (S-100 IH 200×) (Dr. Irene Pecorella)

adenoma and may possibly be applied as a useful marker in differentiating pleomorphic adenomas from other lacrimal gland tumors [291].

Histogenesis

Cell cultures of PA are monoclonal, probably deriving from a common precursor of myoepithelial and ductal cells. There is increasing evidence that the epithelial and myoepithelial cell populations share phenotypical and genotypical characteristics supporting the "modified myoepithelial cell model" for PA histogenesis [292]. Myoepithelial cells express a dual epithelial and smooth muscle phenotype and are likely of ectodermal origin. The neoplastic myoepithelial cells differentiate to stellate cells, which produce myxoid matrix, generating stromal myxoid areas and further differentiate to chondroplastic cells, which through mucopolysaccharide synthesis develop the cartilaginous areas [293].

Genetics

Most of the molecular information about PA comes from the study of salivary gland neoplasms. Cytogenetic studies in salivary gland PA have revealed that most of these tumors have highly specific chromosome abnormalities, namely, 3p21, 8q12, and 12q13–15 rearrangements and trisomy 8 [294]. However, the only lacrimal gland PA that was studied by molecular cytogenetics failed to show clonal translocations or numerical abnormalities involving chromosome 8 or 12 [295]. Future studies on larger numbers of cases will help to clarify the genetics of lacrimal gland PA.

Prognosis and Predictive Factors

The prognosis of PA of the lacrimal gland is good when the lesion is completely excised with an intact capsule or along with the orbital lobe of the lacrimal gland and the overlying periorbita. This usually requires a lateral orbitotomy as the lesion most commonly arises within the orbital lobe of the lacrimal gland. Local recurrence after surgery has been attributed to different factors: the type of surgery, lesions of the pseudocapsule due to intraoperative maneuvers, and insufficient preoperative diagnostics leading to an underestimation of tumor extension, in particular in cases with multifocal origin of the tumor [296]. Recurrences following primary surgery are difficult to treat, and a course of several recurrences has to be expected during a long-term follow-up. An increased incidence of malignant transformation (10 % after 20 years and 20 % after 30 years) is associated with incomplete resection [297], which often leads to repeated recurrences (as high as 30 % over 15 years in some studies). Preoperative biopsy carries an increased risk of recurrence and, therefore, should be followed by careful removal of the tumor with the biopsy track. However, a recurrence rate of 3 % within 5 years has been reported even when the excision was complete [298].

12.13.2.2 Warthin's Tumor (WT)

Definition

A benign tumor composed of papillary oncocytic epithelium and a dense lymphoid stroma.

Synonyms

Papillary cystadenoma lymphomatosum, cystadenolymphoma, or adenolymphoma.

Epidemiology

WT is second in frequency among benign salivary gland tumors but has been infrequently reported in the lacrimal gland [299].

Etiology

A strong link between salivary WT, cigarette smoking, and radiation exposure has been demonstrated, but this finding has not been confirmed so far in the lacrimal gland counterpart, due to low number of lacrimal gland entities.

Clinical Features

A painless, slowly growing swelling.

Macroscopy

Sharply demarcated, thinly encapsulated spherical to ovoid mass with internal cystic areas, containing clear or mucoid fluid. Solid areas are tan to white in color.

Histopathology

Epithelial columnar cells are arranged in solid nests or in glandular and often cystic spaces containing eosinophilic secretions and papillary projections. A double cell layer of epithelial cells, comprising inner columnar eosinophilic or oncocytic cells and an outer small basal cells, lines the cysts and papillae and is surrounded by pronounced lymphoid stromal infiltrate (Fig. 12.148). Mature follicular formations, with germinal centers, are often present. No calcification is observed microscopically. Immunohistochemistry has no role in the diagnosis of WT.

Differential Diagnosis

The combination of cystic spaces and abundant lymphoid tissue is rather unique for WT in the lacrimal gland. In rare instances mucoepidermoid carcinoma may arise from or coexist with WT.

Histogenesis

A plausible theory is that WT is a benign epithelial proliferation that attracts a heavy lymphoid

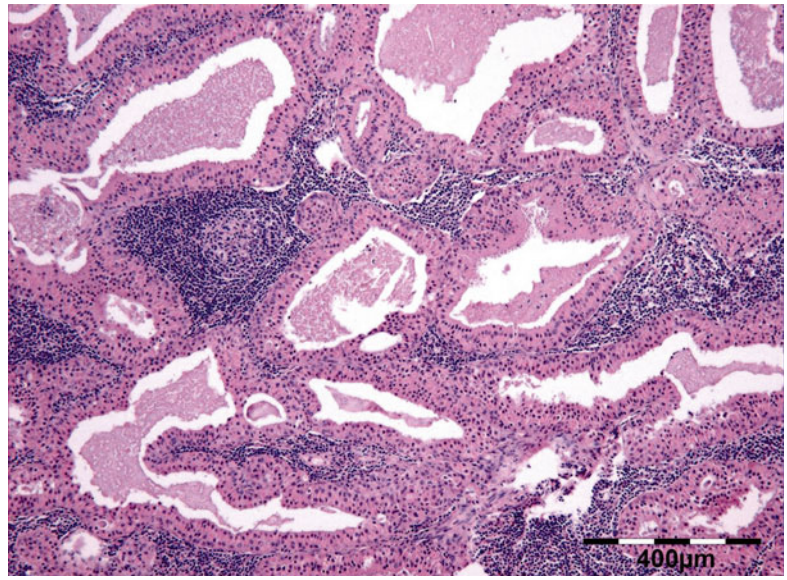

Fig. 12.148 Warthin's tumor of the lacrimal gland: inner columnar oncocytic cells and an outer layer of small basal cells, lines cysts and papillae and is surrounded by pronounced lymphoid stromal infiltrate (HE 50×) (Dr. Irene Pecorella)

reaction, as unlike the findings in the parotid gland, no lymph nodes are usually present in the lacrimal gland [300].

Genetics

Translocations of chromosomes 11q21 and 19p13 have been implied in the development of both WT and mucoepidermoid carcinoma.

Prognosis and Predictive Factors

WT are benign, with extremely low incidence of malignant transformation.

12.13.2.3 Basal Cell Adenoma (BCA)

Definition

First recognized as a specific entity in 1967 by Kleinsasser and Klein [301], BCA is a monomorphic adenoma, characterized by the basaloid appearance of the tumor cells.

Epidemiology and Etiology

BCA represents 2 % of all benign epithelial tumors of the salivary glands and is even rarer in the lacrimal gland. None was present in a series of 118 epithelial lacrimal gland neoplasms from four contributing institutions [276]. It is typically seen in men in their seventh decade.

Clinical Features

A solitary, well-defined, movable nodule. The membranous type occasionally coexists with multiple dermal cylindromas or trichoepitheliomas (Brooke–Spiegler syndrome, autosomal dominant salivary gland–skin adnexal tumor syndrome) or Warthin's tumor.

Macroscopy

Most tumors are encapsulated, often cystic. The membranous type is usually unencapsulated and multifocal in 50 % of the cases.

Histopathology–Immunoprofile

The tumor is characterized by isomorphic basaloid ductal cells with bland cytology and occasional peripheral palisading. These are arranged in a solid, trabecular, tubular, or membranous pattern of growth with a distinct basement membrane-like material and interposed fibrous stroma (Fig. 12.149). Tumor islands and trabeculae are well demarcated from stroma, which by definition should not be chondromyxoid. The myoepithelial component in the BCA is histologically inapparent without the use of immunomarkers (Fig. 12.150) [302]. The solid pattern is the most common. Here and there, an obvious tubule or duct may be seen and it may occasionally contain acinar cells, squamous whorls, or

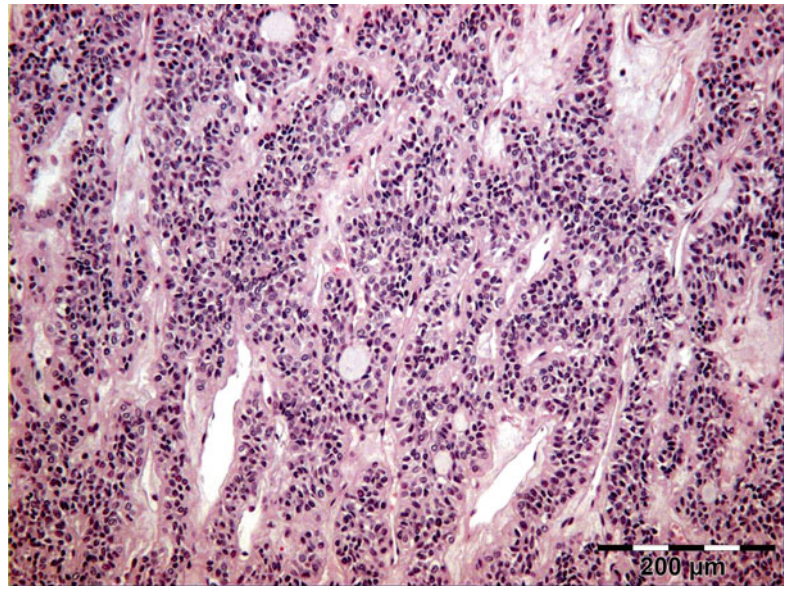

Fig. 12.149 Basal cell adenoma of the lacrimal gland: tumor islands and trabeculae are well demarcated from fibrous stroma (HE 200×) (Dr. Irene Pecorella)

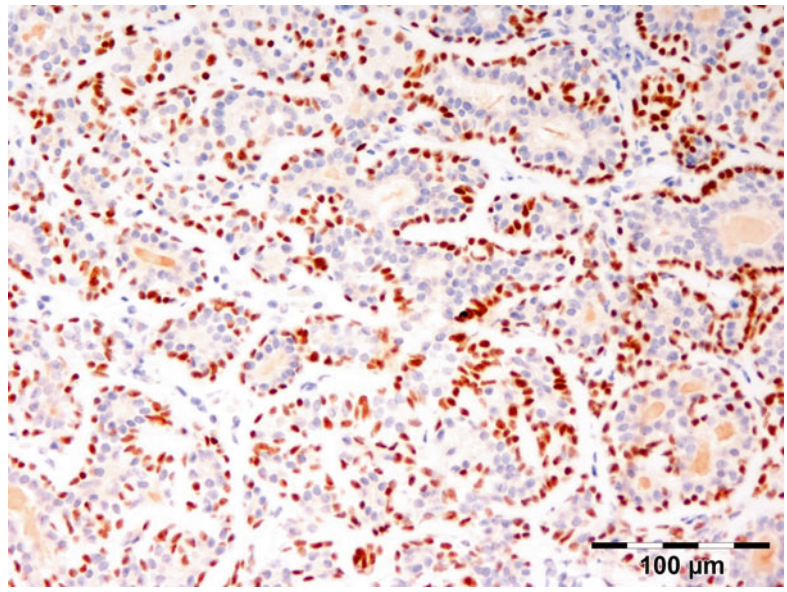

Fig. 12.150 Basal cell adenoma of the lacrimal gland: the myoepithelial nuclei in the BCA stain positive with p63 (p63 IH 200×) (Dr. Irene Pecorella)

keratinization. The membranous pattern (dermal analogue tumor) is the less frequent, with clinical and histologic resemblance to dermal cylindroma. It shows thick bands of hyaline membrane around and inside epithelial islands. Recently, a cystic variant of BCA has been described in the lacrimal gland [303]. In addition to the usual pan-cytokeratin immunoreactivity, cytokeratin 14 is positive in the tubular type of BCA. Myoepithelial markers (p63, calponin, actin, GFAP, S-100) can be variably demonstrated in the peripherally located basaloid cells.

Histogenesis

In the normal lacrimal gland, basal cells are the abluminal cells in the striated ducts, excretory ducts, and salivary ducts. Differently from myoepithelial cells they are immunoreactive for p63 and high molecular weight cytokeratin, but not the myoid markers. The immunoprofile

of BCA indicates ductal and myoepithelial differentiation.

Differential Diagnosis

BCA may overlap morphologically with adenoid cystic carcinoma and is cytologically similar to basal cell carcinoma [304], but it lacks infiltrative areas. It also lacks the myxoid, chondroid, and mesenchymal components of pleomorphic adenoma. Since the 1991 WHO classification, it excludes canalicular adenoma, which was formerly called a basal cell adenoma.

Prognosis

BCA is usually cured by surgical excision; however, the membranous type has a recurrence rate of approximately 25 % and may undergo malignant transformation in up to 28 % of cases.

12.13.2.4 Oncocytoma

Definition

A benign epithelial tumor made of oncocytic cells.

Synonyms

Oxyphilic adenoma or oncocytic adenoma.

Epidemiology and Etiology

A very rare entity in the lacrimal gland [305, 306]. We observed only one case in our series (Table 12.2). Most of the oncocytic lesions of the orbit and eye adnexa have origin outside the lacrimal gland (caruncle, conjunctiva, lacrimal sac, accessory lacrimal gland, semilunar plica, eyelid margin, and peripunctally) [307]. It affects patients with a mean age of 62 years, although there is a single description of this tumor in an 18-month-old African infant [308]. There is no gender predilection. No clear etiological factors have yet been identified, although for the salivary gland counterpart an association with radiation therapy or radiation exposure (20 % of the instances), trisomy 7, or Birt–Hogg–Dubé syndrome is reported.

Clinical Features

The clinical presentation is variable, but all the patients complain discomfort due to a swelling of the lacrimal gland and proptosis. Compression signs involve the upper lid, with dilatation of conjunctival vessels. Usually there are no visual abnormalities. CT or MRI scans reveal a mass in the lacrimal fossa, displacing the eyeball inferomedially and with an homogeneous signal pattern and no invasion of the bone. Rarely it is synchronous with Warthin's tumor or carcinoma ex pleomorphic adenoma.

Macroscopy

Oncocytoma is well circumscribed by a fibrous capsule. The cut surface is solid, red-brown in color, and lobulated and may have cystic spaces. The brown color is due to high cytochrome content of the oncocytes.

Histopathology–Immunoprofile

Oncocytomas have an "organoid" architecture and are composed of cords or sheets of large uniform cells with granular, eosinophilic cytoplasm and a central, round nucleus, containing a small nucleolus. The tumor cells are separated by a thin fibrous stroma and may form tubules or glandular spaces (Fig. 12.151). Occasionally cells may show clearing of nuclei. The granular aspect of the cytoplasm is due to a high content in mitochondria (as much as 60 % of the cytoplasm), as demonstrated by ultrastructural studies. The increased concentration of mitochondria is accompanied by a gradual disappearance from the cytoplasm of other cytoplasmic membrane systems and loss of plasmalemmar specializations [309]. Histochemical stainings, such as PTAH and colloidal iron, are of limited usefulness compared to immunohistochemistry using an antimitochondrial antibody against cytochrome-c oxidase. The immunoprofile of lacrimal gland oncocytoma is based on the very few cases studied with this method: the tumor cells show positive staining for cytokeratin 5/6, cytokeratin 7, cytokeratin 8/18, cytokeratin 10/13, and mitochondria markers; negative staining has been recorded for epithelial membrane antigen (EMA), myoepithelial markers [310], vimentin, estrogen receptors, CK20, HepPar1, AFP, CA19-9, TTF, S-100, chromogranin, and synaptophysin [311]. Basal cells, not identifiable with routine light microscopy, stain with p63.

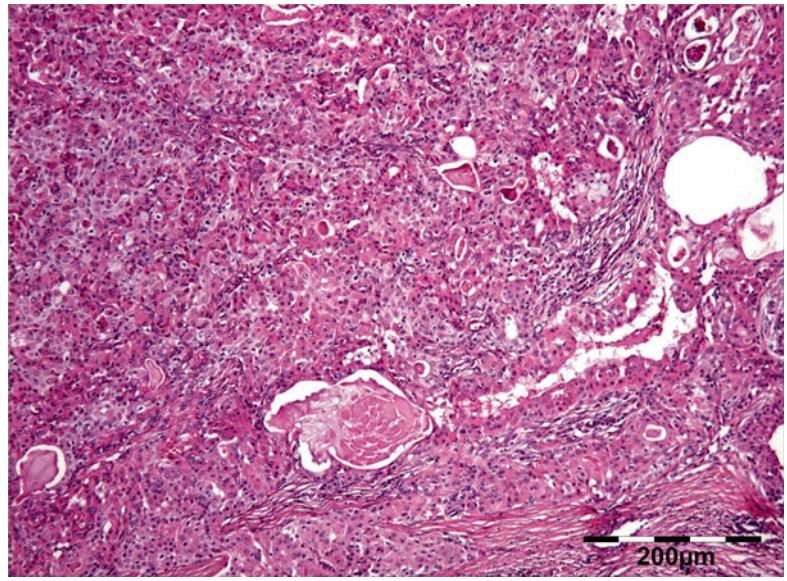

Fig. 12.151 Oncocytoma of the lacrimal gland: cords and sheets of large uniform cells with granular, eosinophilic cytoplasm and a central, round, nucleus, containing a small nucleolus (HE 100×) (Dr. Irene Pecorella)

Histogenesis

Oncocytomas are believed to originate from the ductal cell lining. Since the first description of oncocytes made by Hamperl in 1931 [312], it is widely considered that the oncocytic phenotype is the result of compensation for the functional abnormality at aging.

Differential Diagnosis

Lacrimal gland tumors may show focal areas of oncocytic metaplasia or hyperplasia that may resemble oncocytoma. Oncocytic nonneoplastic metaplasia can be excluded by the absence of a clinically evident, well-circumscribed, and encapsulated mass. Multiple, unencapsulated nodules favor the diagnosis of nodular oncocytosis, a hyperplastic change which may present with generalized enlargement of the lacrimal glands. Warthin's tumor can be recognized by a bilayered cystic oncocytic epithelium with papillary fronds and the presence of extensive and consistent lymphoid tissue with germinal centers (see Sect. 12.14.2.2).

Genetics

There are no genetic studies on lacrimal gland oncocytoma, but the occurrence of respiratory complex I (CI)-truncating mutations has been extensively reported in other benign oncocytic tumors. Such genetic lesions strongly impair cell respiration and contributes to maintaining the tumor in a low-proliferating, benign state [313].

Prognosis and Predictive Factors

True benign oncocytoma of the lacrimal gland is successfully cured with complete surgical resection.

12.13.2.5 Myoepithelioma (MYO)

Definition

A benign monomorphic adenoma composed exclusively, or almost exclusively, of neoplastic myoepithelial cells, formerly considered a variant of pleomorphic adenoma. MYO was recognized as a histologically distinct entity by the World Health Organization (WHO) in 1991.

Synonyms

Myoepithelial adenoma, benign myoepithelial tumor.

Epidemiology

This is an uncommon benign tumor of the lacrimal gland, accounting for only 1 out of 118 cases in Weis and colleagues' series of lacrimal epithelial tumors [276]. Additional anecdotal cases are present in the English literature [314, 315]. The

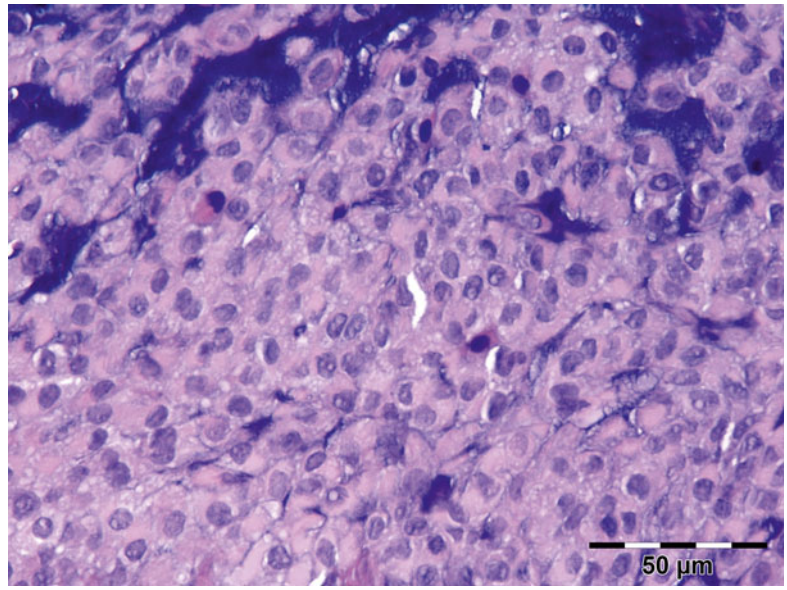

Fig. 12.152 Myoepithelioma of the lacrimal gland: sheets of myoepithelial cells are surrounded by a collagenous or mucoid stroma (HE 400×) (Dr. Irene Pecorella)

age at presentation ranges from 23 to 77 years and there is no significant gender prevalence [316].

Etiology

No clear etiologic factor has been identified for MYO.

Clinical Features

A slow-growing, painless, solid lesion, which may be associated with myasthenia gravis [317].

Macroscopy

A well-circumscribed solid lacrimal gland mass, with a smooth surface and lobulated contour. The lesion is partially circumscribed by a thin fibrous capsule and measures up to 3.5 cm in diameter [316]. The cut surface is glistening and gray-white, tan, or yellow-tan in color.

Histopathology–Immunoprofile

MYO is composed almost exclusively of sheets, islands, or cords of myoepithelial cells with rare ducts (10 % or less). The myoepithelial cells display uniform, central nuclei and eosinophilic granular or fibrillar cytoplasm. A mixture of cells exhibiting spindle, epithelioid, plasmacytoid or hyaline, clear, oncocytic cytoplasmic features may be present in one tumor; otherwise a single cell type, usually spindle cell morphology, may prevail. Spindle cell MYO displays interlacing fascicles of cells with central fusiform nuclei, eosinophilic cytoplasm, and tapered ends. Plasmacytoid MYO contains round to ovoid cells with abundant eosinophilic cytoplasm and eccentrically located nuclei. The cells are separated by abundant mucoid stroma. Epithelioid MYO can form pseudoglandular structures and are surrounded by a collagenous or mucoid stroma (Fig. 12.152). Clear cell MYO, the rarest kind, is composed of polygonal cells containing large amounts of glycogen in the cytoplasm. Chondroid metaplasia has been reported in some cases of myoepithelioma. The immunohistochemical profile of the neoplastic cells is CK7+, CK14+, 5/6+, vimentin+, muscle-specific actin variably positive, calponin+, GFAP+, S-100+, and p63+. Myoepithelial cells are typically negative for CEA, signifying no tubular differentiation. It should be reminded that vimentin and S-100 are negative in normal myoepithelial cells.

Differential Diagnosis

Distinction from a pleomorphic adenoma with myoepithelial prominence is based on the lower proportion of these cells in PA, not reaching the required 90–95 %. Additionally, MYO usually contains only rare ducts and no myxochondroid or chondroid areas. The differential diagno-

sis of clear cell MYO with other salivary gland tumors with clear cells (such as mucoepidermoid carcinoma, acinic cell carcinoma, epithelial–myoepithelial carcinoma, oncocytoma and clear cell carcinoma, or mixed epithelioid and clear cell carcinoma) relies on the characteristic immunoprofile of the myoepithelial cells. In contrast to myoepithelial carcinoma with a very bland cell morphology, myoepitheliomas have a non-infiltrative, well-circumscribed periphery and lack necrotic and hemorrhagic foci. The cells of the plasmacytoid variant of MYO may simulate a plasma cell tumor, skeletal muscle, or "rhabdoid" cells. However, the immunoprofile will be in the former in agreement with a myoepithelial tumor.

Histogenesis

The neoplastic cell population in MYO are myoepithelial-like cells in nature, despite the possible lack of myogenous differentiation in some histologic subtype, which could be due to an inhibitory process mediated by the extracellular matrix [318].

Genetics

Structural alterations of chromosomes 1, 9, 12, and 13: t(1;12)(q25;q12), del(9) (q22.1q22.3), and del(13)(q12q22) were reported in a parotid MYO [319].

Prognosis and Predictive Factors

MYO has a benign behavior and usually does not recur after complete surgical excision. It only rarely undergoes malignant transformation, especially in long-standing epithelial tumors or in tumors with multiple recurrences [320].

12.13.3 Malignant Epithelial Neoplasms of the Lacrimal Gland

Primary malignant neoplasms of the lacrimal gland are mainly epithelial tumors. They are uncommon, accounting for only 17.5 % of lacrimal gland masses collected during a 23-year period in a published series [321] and about 10 % in our series (Table 12.2). Metastatic carcinoma to the lacrimal gland is even rarer, representing 7 % of all lacrimal fossa masses, and can be observed particularly with breast and lung carcinoma [322]. Most of the primary malignant epithelial tumors arise de novo, though in some cases they may derive from a malignant transformation in preexisting pleomorphic adenoma (Table 12.2). The clinical presentation is that of a rapidly growing and palpable mass that causes proptosis, globe displacement, diplopia, ptosis, visual loss, and pain.

Table 12.5 TNM classification of the malignant lacrimal gland tumors

T1	Tumor 2 cm or smaller in greatest dimension, with or without extraglandular extension into the orbital soft tissue
T2	Tumor larger than 2 cm but not larger than 4 cm in greatest dimension
T3	Tumor larger than 4 cm in greatest dimension
T4	Tumor invades periosteum or orbital bone or adjacent structures
T4a	Tumor invades periosteum
T4b	Tumor invades orbital bone
T4c	Tumor invades adjacent structures (brain, sinus, pterygoid fossa, temporal fossa)

From the Seventh Edition of the *AJCC Cancer Staging Manual* (2009) published by Springer Science and Business Media LLC

Because the lacrimal and salivary glands share similar characteristics, the American Joint Committee on Cancer classification (AJCC) has aligned the classification with those of the salivary gland (Table 12.4). Recently, Weis et al. proposed a new expanded classification of the lacrimal gland tumors, as there has been no official update of the lacrimal gland tumor classification since the World Health Organization (WHO) publication of 1980 [276]. They also adjusted the size of the lacrimal gland to the TNM classification of the salivary tumors (Table 12.5).

The most common malignant epithelial tumors of the lacrimal gland are, in order, adenoid cystic carcinoma, mucoepidermoid carcinoma, and carcinoma ex pleomorphic adenoma (malignant mixed tumor). Other rare cases of a wide variety of other histologic types analogous to their salivary gland counterparts have also been described, mostly as individual case reports [276]. A fast-growing lesion with bone

destruction of the lacrimal fossa in association with pain is highly suspicious of a malignant epithelial tumor. CT and MRI are very valuable to assess lacrimal gland lesion. Suspicious bone areas should also be examined pathologically. Unfortunately, there is no standard grading scheme applicable to all types of lacrimal gland malignancies.

12.13.3.1 Adenoid Cystic Carcinoma (ACC)

Definition

A carcinoma formed by sheets of basaloid cells containing round gland-like spaces or cysts, with a typical cribriform or "Swiss cheese" pattern.

Synonyms

ACC was initially termed "cylindroma" by Robin and colleagues in 1854 and got the present name only in 1930 [323].

Epidemiology and Etiology

Most ACCs arise in the minor salivary glands (60 %), usually in the oral cavity (palate). Non-salivary ACC can occur in almost any site with a secretory gland component, including the lacrimal gland, breast, uterine cervix, vulva, esophagus, external ear, tracheobronchial tree, and prostate. ACC is the most common malignant neoplasm of the lacrimal gland (>70 % of all cases) [324], yet it accounts for only 1.9 % of all orbital tumors and 3.8 % of all primary orbital tumors [325]. The incidence of ACC of the lacrimal gland in the Danish registry amounts to 0.1 per year per million [252]. We observed 3 cases in our series of 216 lacrimal gland lesions (Table 12.2). Lacrimal gland ACC generally affects young to middle-aged patients (range 6.5–79 years).

Clinical Features

ACC is clinically characterized by its indolent slow growth, with an initial asymptomatic period. In most cases the tumor goes unnoticed until it has invaded local nerves and structures. Pain usually accompanies varying degrees of "S"-shaped ptosis, proptosis, and inferomedial displacement of the globe as retrograde perineural invasion occurs. Temporal sensory loss in the distribution of the lacrimal nerve may also occur. Less common findings include motility restriction, elevated intraocular pressure, and chorioretinal folds. Imaging studies of the tumor show peri- and intraneural infiltration, bony erosion, irregular margins, focal calcification within the lesion, and intracranial spread in 4–36 % of cases [326]. ACC shows also propensity for early hematogenous and lymphatic dissemination, which favors local recurrence and late distant metastases. Palpation of the preauricular region may reveal neck lymph node involvement. A median latency of 42 months for distant metastases was recorded in a recent study on 125 ACC in China, the most common sites being the lungs, brain, and bone. Liver and skin metastases were also present [327].

Macroscopy

At gross examination, lacrimal gland ACC appears as a firm, poorly encapsulated mass. While seemingly circumscribed, with a globular appearance, there is usually infiltration of the surrounding orbital soft tissues and bone on closer examination. The tumor measures up to 42 mm in diameter [276]. The cut surface is firm, white to gray white in color, with a solid texture. Hemorrhage and necrosis are rare features and should raise the suspicion of high-grade transformation into dedifferentiated ACC [328]. These are not the myxomatous areas seen in pleomorphic adenoma or the cysts seen in Warthin's tumor.

Histopathology and Immunoprofile

The tumor is heterogeneous, consisting of varying amounts of a tubular, cribriform (Fig. 12.153), or solid pattern. A distinct dual cell population of epithelial cells with intercalated duct cell differentiation and myoepithelial relatively uniform basaloid cells, with angulated, hyperchromatic nuclei and scant, indistinct, clear to eosinophilic cytoplasm, is observed. Perineural involvement is the rule (Fig. 12.154) and extension along vascular structures is a characteristic. The most common type of tumor histology is cribriform, with a "Swiss cheese" appearance. Islands of basaloid cells with scanty cytoplasm and round to ovoid

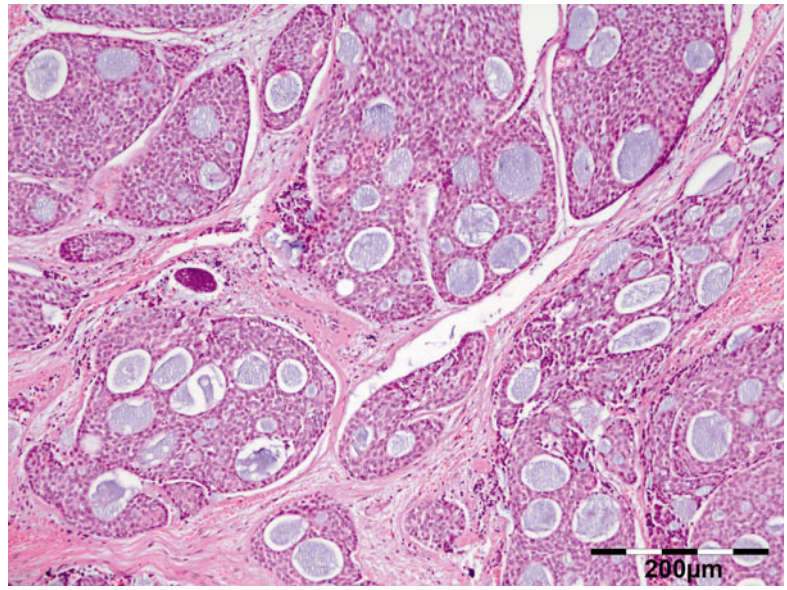

Fig. 12.153 Adenoid cystic carcinoma of the lacrimal gland: the most common histologic pattern is cribriform, with a "Swiss cheese" appearance (HE 100×) (Dr. Robert M. Verdijk)

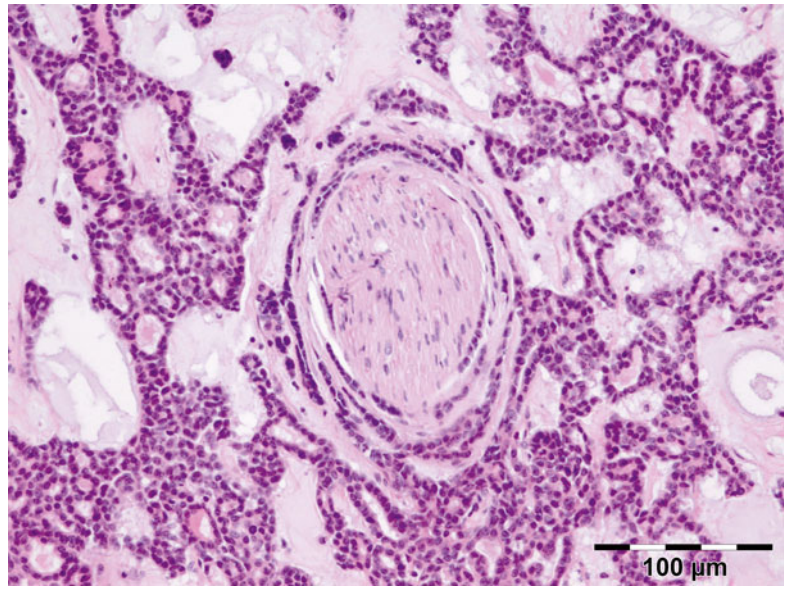

Fig. 12.154 Adenoid cystic carcinoma of the lacrimal gland: perineural growth is a common feature (HE 200×) (Dr. Robert M. Verdijk)

basophilic nuclei of regular form surround variably sized cystlike spaces, referred to as "pseudocysts" (Fig. 12.155). The cystlike spaces contain basophilic mucoid material and/or weakly eosinophilic, periodic acid–Schiff-positive, basement membrane material, accounting for the synonym "cylindroma." Necrosis is distinctly uncommon. In the tubular/ductal pattern, well-formed ducts with small lumina or cystic spaces show an outer myoepithelial layer of basaloid cells and an inner, epithelial layer composed of slightly larger cuboidal cells with more distinct, eosinophilic cytoplasm and round to ovoid nuclei. The ductlike structures contain amorphous, eosinophilic material. The tumor nests are surrounded by variable amounts of eosinophilic, often hyalinized stroma compressing the tumor cells into thin strands or chains, forming a "trabecular" pattern. There may be minimal nuclear pleomorphism and no mitotic activity or cell necrosis. The solid

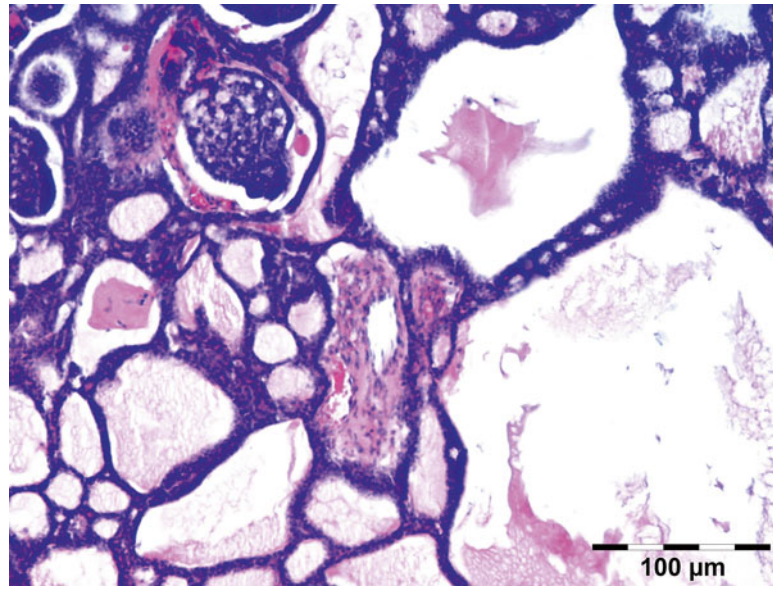

Fig. 12.155 Adenoid cystic carcinoma of the lacrimal gland: variably sized cystlike spaces (pseudocysts) (HE 200×) (Dr. Irene Pecorella)

(basaloid) pattern contains at least 30 % aggregates of basaloid cells with dark, regular small nuclei, without tubular or cystic formation. Nuclear pleomorphism may be more pronounced and mitotic figures (<10/HPF) and individual cell necrosis, or comedonecrosis may also be seen. A complete basal layer surrounds the cell aggregates and p53 expression is rare. The surrounding stroma is generally myxoid.

Tumor is graded according to Szanto et al. [329] as follows: grade I = cribriform or tubular, grade II = cribriform or tubular with <30 % solid areas, and grade III = cribriform or tubular with >30 % solid areas. Often, the overall rather bland microscopic appearance belies the clinical course of this highly malignant neoplasm. Extensive sampling and thorough histologic examination are important in order to detect dedifferentiated areas with aggressive behavior. Transition of ACC to high-grade adenocarcinoma or undifferentiated carcinoma is characterized by solid confluent sheets of malignant cells with nuclear pleomorphism, prominent nucleoli, increased (>10 per high-power field) mitotic activity, and cell necrosis[328]. Loss of ductal–myoepithelial differentiation is apparent. Other findings include large foci of comedonecrosis, micropapillary and squamoid growth patterns, and fibrocellular desmoplasia. Dedifferentiation to high-grade areas has been associated with p53 gene alteration and overexpression of p53 protein and cyclin D1 in >50 % of malignant cells [330] and shows increased expression of the cellular proliferation marker Ki-67. Also the bone of the superior and lateral orbital wall should be examined microscopically, as Esmaeli recently observed that it is involved in 50 % of the ACCs [331]. Immunohistochemical reactivity for S-100, smooth muscle actin, smooth muscle myosin, and p63 is present in the myoepithelial component surrounding the pseudocysts in ACC. The lumina of the pseudocysts and tubules demonstrates intense positivity against AE1/AE3, CK 8/18, EMA, and basement membrane components such as type IV collagen and laminin. Strong immunohistochemical positivity for c-KIT/CD117 has been demonstrated in most ACC, regardless of grade. CD43, a marker of T cells and histiocytes, has been reported to be preferentially expressed in ACC [332].

Differential Diagnosis

The differential diagnosis is largely that of other benign and malignant neoplasms that arise in these locations. A combination of two or even all three ACC histologic subtypes is often observed. This can complicate the diagnosis since the erratic patterns can be misdiagnosed as being a

different type. Polymorphous low-grade adenocarcinoma may also exhibit ductal, tubular, and cribriform structures. Perineural invasion is also common. However, it lacks a dual population of ductal and myoepithelial cells and typically has negative or low (<50 % of cells) expression of c-KIT. Pleomorphic adenoma contains a dual population of ductal and myoepithelial cells but can be identified by the presence of mesenchymal, especially cartilaginous, differentiation in the stroma and by its immunohistochemical expression of glial fibrillary acidic protein (GFAP). Basal cell adenocarcinoma should be differentiated from solid ACC; however, the former shows the presence of a capsule, peripheral palisaded nuclei, and no stromal and perineural invasion.

Histogenesis

ACC arises specifically from the intercalated ducts, and electron microscopy shows that it arises from cells that can differentiate into epithelial and myoepithelial cells.

Genetics

No strong genetic or environmental risk factors have been identified for ACC. Recently von Holstein et al. reported that lacrimal gland ACCs are frequently positive for the MYB–NFIB fusion, resulting from the (6;9)(q22–23;p23–24) translocation; they overexpress MYB and its downstream targets and have genomic profiles characterized by losses involving 6q, 12q, and 17p and gains involving 19q, 8q, and 11q [333]. The gains in q8 are associated with c-myc amplification. MYB–NFIB fusion is a crucial oncogenic step in the development of dedifferentiated ACC [334]. Also deletions in 1p32-26 have been associated with an aggressive course [335]. A comprehensive review of the molecular pathogenesis and phenotype of ACC can be found in the articles published by Le Tourneau et al. [336] and Jaso and Malhotra [337].

Prognosis and Predictive Factors

In general, older age, advanced stage, major nerve involvement, and the presence of perineural invasion or positive resection margin, high histologic grade, and high expression of Ki-67 appear to be significantly poor prognostic factors. Vascular endothelial growth factor (VEGF) is highly expressed in ACC and its expression correlates with stage, tumor size, vascular invasion, recurrence, and metastasis [338]. P53 alteration appears to be an independent prognostic marker [339].

Tumors with a solid pattern are the most infiltrative and are associated with a 5-year survival rate of only 21 % [340]. Deletion of 1p-32–36 is often detected in the solid tumor phenotype and is associated with decreased overall survival [341]. Tumor aneuploidy also correlates with more aggressive disease and a poor prognosis [342]. Currently, lacrimal gland ACC remains an extremely difficult disease to treat. The classic treatment is complete resection or orbital exenteration followed by postsurgical radiotherapy. Completely negative margins may not be attainable, due to the tumor's propensity for invasion into adjacent structures. With unresectable locoregional recurrence after surgery, there is so far no known effective chemotherapy regimen. Patients with the well-differentiated cribriform pattern have a better than average prognosis (70 % at 5-year survival) [343]. Approximately 80 % of patients with ACC survive for 5 years, only to have tumors recur and progress in a substantial number of cases despite definitive treatment. Distant metastases often defeat successful treatment of patients with ACC, despite locoregional control, and are associated with a survival at 5 and 10 years less than 50 and 20 %, respectively [344]. Death commonly is due to intracranial spread and pulmonary metastasis. No formal guidelines exist regarding the most appropriate mode and duration of surveillance. The outcome for patients with ACC in the lacrimal gland is reportedly poorer than that with ACC in the salivary gland [327]. The prognostic impact of ACC origin could derive from different diagnostic and surgical accessibility, bringing about differences of stage and surgical outcome [345]. Thorough histologic examination of ACC in order to detect any solid or dedifferentiated component and evaluation of the margins as well as perineural invasion are important.

12.13.3.2 Carcinoma Ex Pleomorphic Adenoma (Ca ex PA) and Pleomorphic Carcinoma (PC)

Definition

Carcinoma ex pleomorphic adenoma of the lacrimal gland is a malignant lacrimal gland tumor component of any type in the background of a benign pleomorphic adenoma. Pleomorphic carcinoma is a malignant biphasic tumor arising de novo, with no concomitant benign component [346].

Synonyms

Malignant mixed tumor, carcinoma in pleomorphic adenoma, or pleomorphic adenocarcinoma.

Epidemiology

Ca ex PA accounts for 12 % among malignant neoplasms of the lacrimal gland [274]. We observed 3 cases in our series of 216 lacrimal gland lesions (Table 12.2). It occurs in the sixth to the seventh decade of life and is rarely encountered in patients younger than 30 years.

Etiology

The exact etiologic factors associated with malignant transformation are largely ill defined. Malignant change may result from aberrant protein expression and promoter methylation of p16 gene [347].

Clinical Features

Most commonly, a clinical history of a long-standing mass or an excised and/or recurrent pleomorphic adenoma is present. The risk of malignant transformation in an indolent PA increases with time (9.5 % for tumors present for more than 15 years) [297, 348]. The clinical signs of malignant degeneration in a long-standing PA are represented by a rapidly progressive, painful enlargement of the mass one or more decades after the initial presentation. De novo occurrences of a pleomorphic carcinoma are also possible [25]. Destructive bone erosion is very frequent. The mass may extend to periorbital tissue, lateral orbital rim, and temporal muscle. Invasion of intraorbital structures may extend intracranially into the cavernous sinus [349, 350]. The superficial location of those lesions arising from the palpebral lobe of the gland leads to early detection [283].

Macroscopy

Foci of hemorrhage and necrosis and infiltrative margins are characteristic for the outgrowth of a malignancy in a PA [351]. However, some Ca ex PA are well circumscribed.

Histopathology–Immunoprofile

Ca ex PA is the most commonly malignant transformation encountered in PA (99 % of all cases) [352]; it may show predominant or mixed features of an adenocarcinoma NOS [353] or an undifferentiated or poorly differentiated carcinoma. Squamous cell carcinoma, adenoid cystic carcinoma [354], epithelial–myoepithelial carcinoma [355], and ductal carcinoma [356] have also been described to occur. Other histologic varieties deriving from malignant transformation of a PA are carcinosarcoma, which consists of both carcinomatous and sarcomatous components originating from pleomorphic adenoma (so-called true malignant mixed tumor), and the metastasizing mixed tumor, also known as "metastasizing benign pleomorphic adenoma, metastasizing benign mixed tumor, and metastasizing mixed tumor" [357]. The latter is histologically a benign PA showing one or more foci of metastatic, histologically benign deposits. Carcinosarcoma is extremely rare in the lacrimal gland [358]. High-grade tumors frequently contain necrotic or hemorrhagic foci and high mitotic activity. Low-grade carcinoma such as polymorphous low-grade adenocarcinoma, adenoid cystic carcinoma, mucoepidermoid carcinoma, epithelial–myoepithelial carcinoma, and myoepithelial carcinoma can also occur infrequently. Malignant cellular changes should be observed adjacent to typical pleomorphic adenoma. If the benign component does not appear, the diagnosis is of pleomorphic carcinoma only [346]. In situ Ca ex PA is a noninvasive lacrimal gland neoplasm affecting the luminal layer of the PA glands [359]. Intracapsular carcinoma is a tumor that breaks from the confines of the myoepithelial layer to invade the surrounding stroma,

without violation of the fibrous capsule of the PA. Minimally invasive Ca ex PA extend to <1.5 mm from the capsule of the residual benign PA and frankly invasive carcinoma to >1.5 mm from the capsule. In the study of Tortoledo and colleagues, extension greater than 6 mm was predictive of a 70.5 % recurrence rate compared with 16.5 % recurrence for tumors extending less than 6 mm [360]. The histologic grading of the tumor follows the one in use for that individual tumor. p53 protein overexpression is observed in 41–75 % of cases [361].

Differential Diagnosis

Well-differentiated Ca ex PA, exhibiting morphologically limited nuclear atypia, may be confirmed by their immunoreactivity for p53 [362].

Genetics

Overexpression of HER-2/neu has been found preferentially in high-grade areas of Ca ex PA [363]. Also genetic changes associated with the development of chromosome arm 17p alterations have been found to correlate significantly with high disease stage and an increased proliferative rate in these tumors, possibly representing an event preceding malignant transformation and progression [364]. Additionally, PA and the adenoma component of Ca ex PA show a significant incidence (52 %) of loss of heterozygosity (LOH) at chromosome arms 8q and 12q. Therefore, LOH at 12q loci may identify a subset of adenoma with potential progression to carcinoma [364]. Alterations of p53 gene and p53 protein overexpression suggest that the gene may play a role in transformation.

Prognosis and Predictive Factors

Invasive Ca ex PA extending >1.5 mm beyond the capsule is an aggressive tumor with a grim prognosis. The median survival in these cases is of less than 5 years [355]. Up to 60–70 % of patients with aggressive Ca ex PA develop local or distant metastasis in the lymph nodes, the bone (especially vertebral bodies), and the brain. Poor outcome has also been found to be associated with high histologic grade of malignant component. Intracapsular and minimally invasive carcinomas have an excellent prognosis when they are resected with intact capsule. Careful dissection of the neoplasm is mandatory when a Ca ex PA has formed in a cystic structure, due to the elevated risk of rupture in the cystic wall during surgery [354].

12.13.3.3 Primary Adenocarcinoma, NOS (ADC)

Definition and Synonyms

An epithelial neoplasm that lacks the histopathologic features that characterize the other more specific carcinoma types.

Epidemiology and Etiology

ADC comprises approximately 10 % of the primary epithelial tumors of the lacrimal gland [274, 324]. It more commonly affects men with a range of age of 18–80 years (mean 56 years).

Clinical Features

A rapidly asymptomatic growing mass that causes exophthalmos, blepharoptosis, dystopia, eyeball deviation, diplopia, and visual loss. Pain can be secondary to involvement of the bone or nerve. Adenocarcinomas apparently arising from an accessory lacrimal gland are very rarely encountered.

Macroscopy

A well-demarcated white or yellowish mass, partly cystic, sometimes with ill- defined, necrotic or hemorrhagic areas.

Histopathology–Immunoprofile

The diagnosis of ADC is essentially one of exclusion as it lacks morphologic features of the recognized variants of lacrimal gland adenocarcinoma. Microscopic examination may show features of a low grade, intermediate grade or high grade, according to the degree of tumor differentiation. In general, the architectural pattern is heterogeneous, and the cells may form glands or duct-like structures (Fig. 12.156) or are arranged in sheets and cords. Papillary areas are also observed. Often a peripheral "Indian file" pattern is observed. Low-grade ADC features

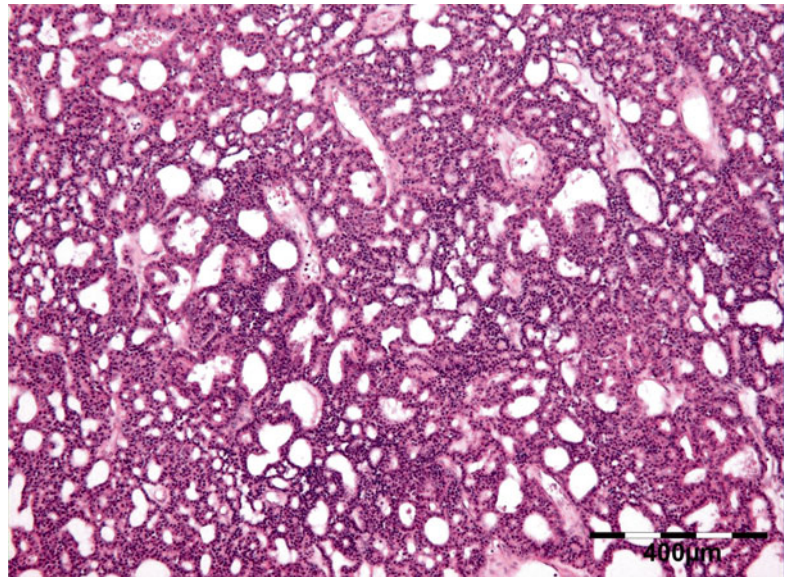

Fig. 12.156 Primary adenocarcinoma, NOS, of the lacrimal gland: in this case the cells form glands and duct-like structures (HE 50×) (Dr. Irene Pecorella)

cytologically bland isomorphic cuboidal or columnar cells with little evidence of the mitotic activity, often forming duct-like structures and cystic spaces (Fig. 12.157). However, multiple sectioning will demonstrate an infiltrative growth into the parenchyma or surrounding tissues. In high-grade ADC, solid, densely cellular sheets of pleomorphic tumor cell prevail, with little duct formation. Mitotic figures are numerous and areas of necrosis are common. ADK exceptionally can show dual cell differentiation. The tumor cells are markedly positive for S-100, EMA, and cytokeratins, including cytokeratin 7 [365]. Less predictable positivity with CEA and muscle-specific actin is observed [310]. Neuroendocrine markers can occasionally be also detected.

Differential Diagnosis

ADC requires exclusion of other specific lacrimal gland carcinomas and metastatic deposits of systemic primaries. The presence of ductal differentiation helps in the distinction from undifferentiated carcinoma.

Prognosis and Predictive Factors

High-grade tumors have an aggressive behavior and an average survival of 1.5 years [325]. Mortality is associated with distant metastases [366].

12.13.3.4 Mucoepidermoid Carcinoma (MEC)

Definition

Mucoepidermoid carcinoma is a malignant epithelial neoplasm characterized by squamous, mucous, and intermediate cells. It may occur as a low-grade or high-grade tumor. Progression from a low grade to a high grade or dedifferentiation of a high grade is also possible.

Synonyms

Mixed epidermoid and mucus-secreting carcinoma.

Epidemiology

MEC is the second most common malignant neoplasms in the lacrimal gland [324], despite being utterly rare in this location, comprising only about 1–2 % of all lacrimal gland neoplasms [367]. The mean age of patients at presentation is 49 years and females are more often affected than men (F:M = 3:2) [368]. It has also been infrequently reported in children [367].

Etiology

Exposure to radiation appears to increase the risk of MEC. A possible association with papillomavirus was recently suggested [369].

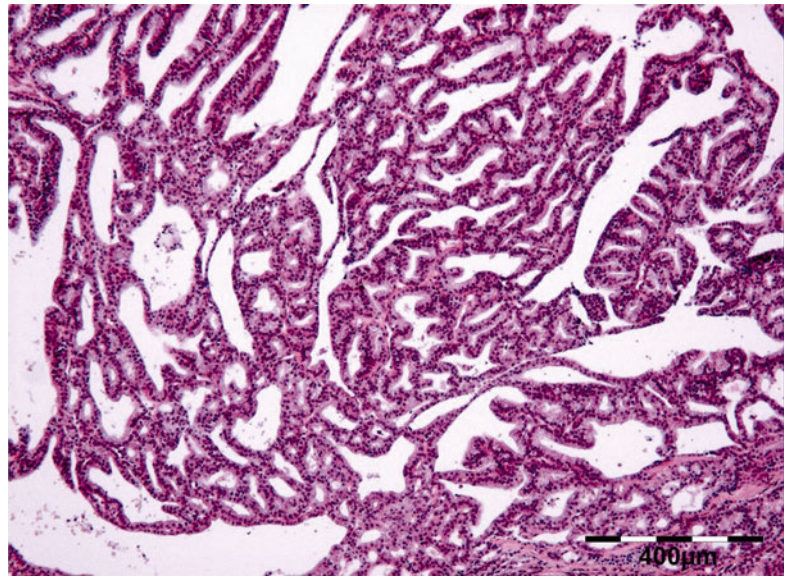

Fig. 12.157 Primary adenocarcinoma, NOS, of the lacrimal gland: in this case the cells form duct-like structures and cystic spaces (HE 50×) (Dr. Irene Pecorella)

Clinical Features

Low-grade MEC is a painless, slowly enlarging firm mass causing proptosis and medial/downward displacement of the eye. High-grade lesions present as rapidly growing, painful lesions with infiltrative edge and sometimes with regional lymph node metastasis. Anecdotal cases of MEC arising from an accessory lacrimal gland have been reported [370].

Macroscopy

A circumscribed soft tumor with grayish-white lobulated, variably solid and cystic, cut surfaces. The cysts contain viscid mucoid material. A pseudocapsule is often present.

Histopathology–Immunoprofile

MEC is basically composed of a mixture of three different cell types: a mucus-secreting cell, an epidermoid cell, and an intermediate or basal cell which seems to be able to differentiate into the other two cell types. These cells are arranged in cystic or glandular structures and solid areas. A lymphoid infiltrate is often also present. Oncocyte-rich variants have been described in the lacrimal gland [371, 372]. Eviatar and Hornblass divided MEC into high- and low-grade tumors, based on histopathologic features [368]. Low-grade MEC is composed of prominent cystic structures lined by mature epidermoid cells, with no signs of keratinization, or by intermediate and mucous-producing bland-looking cells embedded in a mucoid background or sclerotic stroma with chronic inflammatory cell infiltration. Containing cells outnumber the epidermoid cell elements and stain positive with PAS and alcian blue (Fig. 12.158). The mitotic rate is low and there is little cellular atypia. In intermediate-grade MEC, mucous cells and epidermoid cells are equally represented and show increasing pleomorphism and mitotic figures. The cystic structures are fewer and smaller in size compared to low-grade MEC. Of importance, frank squamous features such as intercellular bridges and keratinization are almost never seen in low- to intermediate-grade MEC. High-grade MEC is characterized by the presence of anaplasia of epidermoid tumor cells that grow in solid sheets, with few if any cysts (Fig. 12.159). It shows poorly defined margins, neural invasion, and necrosis and a mitotic rate of 4 or more/10HPF [373]. Cystic, spindle cell and clear cell variants of MEC are described. MEC is cytokeratin positive and expresses, in varying proportions, a variety of membrane-bound mucins, cytokeratin 7, EMA, CEA, and S-100. Neither the tumor cells nor the stromal cells express myoepithelial markers, though intermediate and squamous cells are positive for p63.

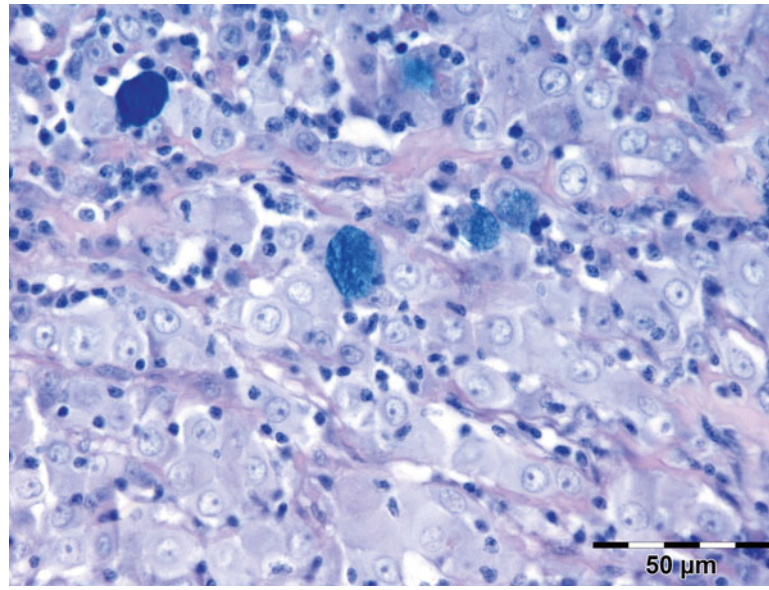

Fig. 12.158 Mucoepidermoid carcinoma of the lacrimal gland: mature epidermoid cells, with no signs of keratinization, and intermediate and mucous-producing bland-looking cells positive for alcian blue (alcian blue 400×) (Dr. Irene Pecorella)

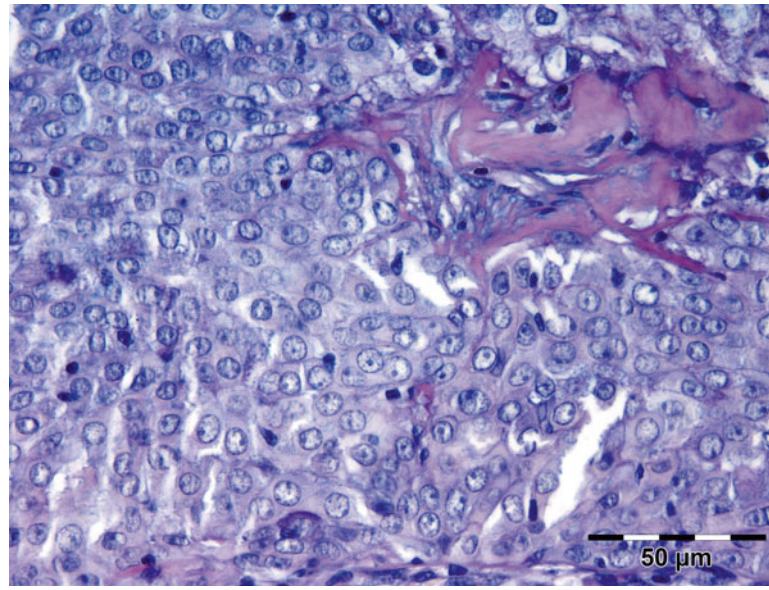

Fig. 12.159 Mucoepidermoid carcinoma of the lacrimal gland: high-grade MEC is characterized by anaplasia of epidermoid tumor cells that grow in solid sheets, with few if any cysts (HE 400×) (Dr. Irene Pecorella)

Differential Diagnosis

High-grade MEC could be mistaken for squamous cell carcinoma due to its prevalent squamous cell component. Positive immunostaining for MUC5AC and cytokeratin 7 may prove helpful in this differential diagnosis. Low-grade MEC can be indistinguishable from pleomorphic adenoma. Predominantly cystic low-grade MEC may be misdiagnosed as benign cystic lesion, and a paucicellular tumor with abundant extravasated mucin could be misdiagnosed as mucocele.

Histogenesis

MEC is believed to arise from the epithelium of the large ducts. One case was shown to have originated from the ductular epithelial cells in a chronic dacryops [372]. Exceptionally, MEC can arise in a dedifferentiated pleomorphic adenoma.

Genetics

Recent cytogenetic studies demonstrated that all different cell types that constitute up to 70 % low-grade MEC show a t(11;19)(q21-22;p13) translocation which results in the expression in these tumor cells of a CRTC1-MAML2 (mastermind-like gene family) fusion [374]. The detection of fusion-positive MECs may represent a clinically useful biomarker of a significantly better prognosis compared to those with fusion-negative tumors [375]. An increased HER-2 gene expression and gene amplification is another recent finding in MEC, duct carcinoma, and adenocarcinomas NOS. HER-2 is an oncogene that encodes for a transmembrane glycoprotein receptor involved in cell growth and differentiation and a member of the EGFR signal transduction family. High-grade tumors have been shown to harbor mutations at codon 12 and/or 13 of the H-ras gene [376].

Prognosis and Predictive Factors

Prognosis is dependent on grade. Low-grade MECs have an excellent prognosis (90–98 % survival) and usually only require surgical excision with clear margins. They may invade locally and recur in 15 % of cases. High-grade tumors recur in about 25 % and have only 50 % 5-year survival, despite exenteration with radiotherapy. Mortality is increased, if bony involvement is present. High MUC1 expression is associated with high histologic grade, high rate of recurrence and metastasis, and short disease-free interval. Conversely, expression of MUC4, a surrogate marker of tumor differentiation, is related to low histologic grade, low recurrence rate, and a long disease-free interval [377].

12.13.3.5 Ductal Adenocarcinoma (DA)

Definition

Firstly described by Katz et al. in 1996 as an adenocarcinoma of the lacrimal gland with close resemblance to high-grade mammary ductal carcinoma [378].

Synonyms

Duct carcinoma or ductal carcinoma.

Epidemiology and Etiology

Only 16 cases have been reported in the lacrimal gland [324, 356, 378, 379]. Among them only two were female. The mean age at presentation was 60 year.

Clinical Features

Those already described for other infiltrative malignant high-grade neoplasms of the lacrimal gland. The duration of symptoms ranged from 1 to 18 months [379]. DA may also arise as the malignant component of a carcinoma ex pleomorphic adenoma [356].

Macroscopy

An infiltrative mass with ill-defined, irregular margins. The cut surface reveals a yellowish-white solid tumor.

Histopathology–Immunoprofile

DA shares the characteristic histologic features of intraductal and infiltrating breast ductal carcinoma and is composed of large pleomorphic epithelioid tumor cells with vesicular nuclei, prominent nucleoli, granular, eosinophilic cytoplasm often with an apocrine quality, and well-defined borders, arranged in duct-type structures with intraluminal papillary projections and cribriform pattern, surrounded by prominent basement membrane. "Roman bridge" formation and intraductal comedonecrosis are often present. An incomplete peripheral cuff of myoepithelial cells is often detectable [310]. The tumor cells display a high proliferation rate. Most have evidence of perineural and intravascular invasion. The stroma surrounding the infiltrative neoplastic component is desmoplastic. Di Palma and colleagues recently devised a molecular subclassification of DA into luminal androgen receptor-positive, HER-2, and basal-like phenotypes, based on the one in use for breast adenocarcinoma [380]. Immunohistochemically, DA are positive for cytokeratins 7,10, 17, 18, and 19, EMA, and CEA and also often react with BRST-2 but are negative for estrogen or progesterone receptor, smooth muscle actin, and S-100 protein. Most DA show positive membrane staining for

HER-2. Androgen receptor expression is rare among lacrimal gland neoplasms and is mainly restricted to DA and adenocarcinoma NOS [379]. DA may undergo dedifferentiation into a sarcomatoid variant, comprising anaplastic spindle or multinucleated giant cells.

Differential Diagnosis

The absence of goblet cells and squamous cells in DA may help in ruling out high-grade mucoepidermoid carcinoma.

Histogenesis

DA arises from the ductal epithelium.

Genetics

Mutations and overexpression of the TP53 gene and protein are frequently reported. Also HER-2/neu protein has been found to be overexpressed in lacrimal gland DA [379].

Prognosis and Predictive Factors

This is a malignant, high-grade, primary epithelial neoplasm which shows an aggressive clinical behavior and poor prognosis. Most of the few reported cases with primary DC had regional or distant lymph node involvement and/or distant metastases. Most frequent sites of distant metastases are the lung, bone, and brain. The 5-year survival rate is approximately 40 %[379]. Inactivation of CDKN2A/p16 gene, located on chromosome 9q21, is associated with progression of DA.

12.13.3.6 Squamous Cell Carcinoma

Definition and Synonyms

An exceedingly rare tumor of the lacrimal gland exhibiting only malignant squamous elements.

Epidemiology

SCC accounts for <2 % of the primary malignancies of the lacrimal gland [274]. In most reported cases, it arose from the malignant transformation of the squamous component of a pleomorphic adenoma [273, 297, 381]. Only few instances of de novo primary SCC of the lacrimal gland are known [275, 381].

Etiology

Cases of SCC arising from an epithelium-lined cyst within the lacrimal gland are also described [382, 383]. The cyst is believed to result from a dacryops or posttraumatic epithelial implantation or to be choristomatous.

Clinical Features

A rapidly progressive firm and smooth non-tender mass causing proptosis with inferonasal globe displacement, lid edema, and chemosis with or without pain. Regional lymph node involvement is common.

Macroscopy

A poorly encapsulated mass.

Histopathology–Immunoprofile

Well-differentiated SCC show infiltrating nests of highly keratinizing tumor cells, while no keratinization is seen in poorly differentiated tumors (Fig. 12.160). Perineural and bone invasion can be observed. SCC immunoreact with antibodies against CK13, CK14, CK19, and vimentin; diffuse positivity for p63 is noticed in the basaloid type. CK7 is variable.

Differential Diagnosis

The main differential diagnosis is with a metastatic spread of SCC in the lacrimal gland. Squamous metaplasia may occur in Warthin's tumor, pleomorphic adenoma, or oncocytoma, particularly after inflammation or infarct. Adenoid cystic carcinoma is p63+ and resembles basaloid squamous cell carcinoma. Mucoepidermoid carcinoma contains intermediate cells and mucus cells and is often cytokeratin 7+.

Histogenesis

SCC is believed to originate from a dysplastic squamous epithelium lining a lacrimal duct [384], a lacrimal duct cyst (dacryops), or, less likely, from a choristomatous epithelium [382, 383]. It may also arise from the malignant transformation of a pleomorphic adenoma [273, 297, 381] (Table 12.2).

Genetics

No genetic studies have been performed on this tumor due to its rarity.

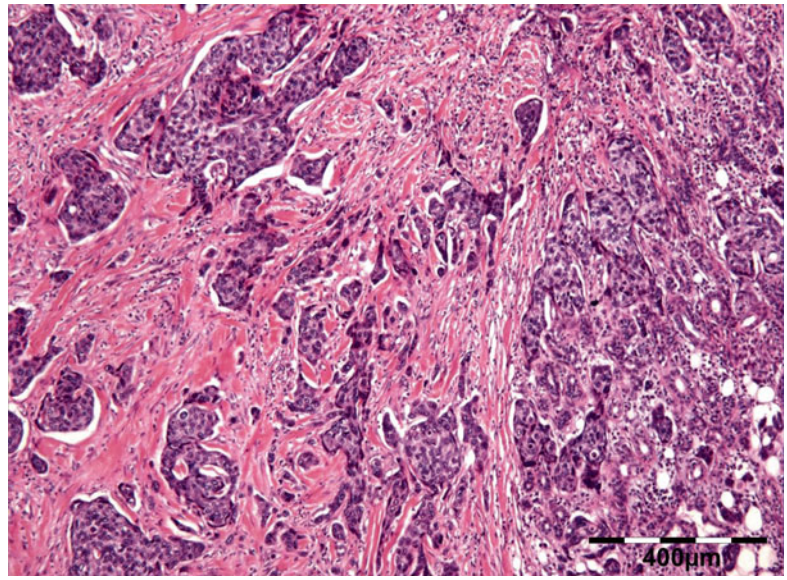

Fig. 12.160 Squamous cell carcinoma of the lacrimal gland: infiltrating nests of highly atypical keratinizing tumor cells (HE 50×) (Dr. Irene Pecorella)

Prognosis and Predictive Factors

No recurrences were noted in the published reports. Incomplete excisions should be treated with postoperative radiation treatment to prevent recurrence.

12.13.3.7 Sebaceous Carcinoma (SC)

Definition and Synonyms

A high-grade malignant epithelial tumor composed of cells showing differentiation toward sebaceous epithelium.

Epidemiology and Etiology

An exceptionally rare tumor of the lacrimal gland [273, 385]. Our series of 216 lacrimal gland lesions contained two cases (Table 12.2). Most cases occurred in middle-aged individuals. However, the youngest reported patient was 35 years old [385].

Clinical Features

SC lacks specific clinical and imaging signs and presents as a rapidly evolving, unilateral, painful massive swelling of the lacrimal gland of hard consistency at palpation. Upper eyelid ptosis, proptosis, and impaired ocular motility have occurred in the instances reported in the literature. Often systemic metastases are already present at diagnosis.

Macroscopy

A rock hard mass, fixed on palpation. The color varies from grayish white to yellow tan. They are partially encapsulated with pushing or locally infiltrating margins.

Histopathology–Immunoprofile

Malignant neoplasm composed predominantly of sebaceous cells of varying maturity arranged in nests and/or sheets of large epithelial cells with different degrees of nuclear atypia; well-differentiated SC show minimally atypical cells with abundant vacuolated cytoplasm (Fig. 12.161). High-grade SC show pleomorphic cells with high nuclear/cytoplasmic ratio, high mitotic index, frequent intratumoral necrosis, and foci of sebaceous differentiation (Fig. 12.162). The fat content in the tumor cells can be confirmed by fat stains on unprocessed, fixed material. Tumor tissue stains diffusely for HMFG 1(human milk fat globule 1), EMA (Fig. 12.163), and p63 (Fig. 12.164), moderately for keratins, and negatively for CEA.

Differential Diagnosis

Orbital extension from an eyelid sebaceous tumor or metastatic spread from other areas of the body should be ruled out before making the

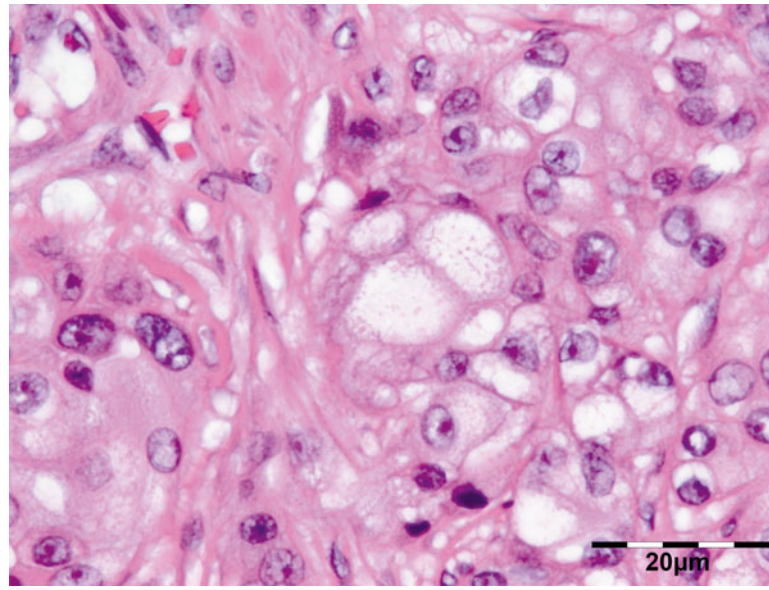

Fig. 12.161 Sebaceous carcinoma (SC) of the lacrimal gland: well-differentiated SC show minimally atypical cells with abundant vacuolated cytoplasm (HE 630×) (Dr. Robert M. Verdijk)

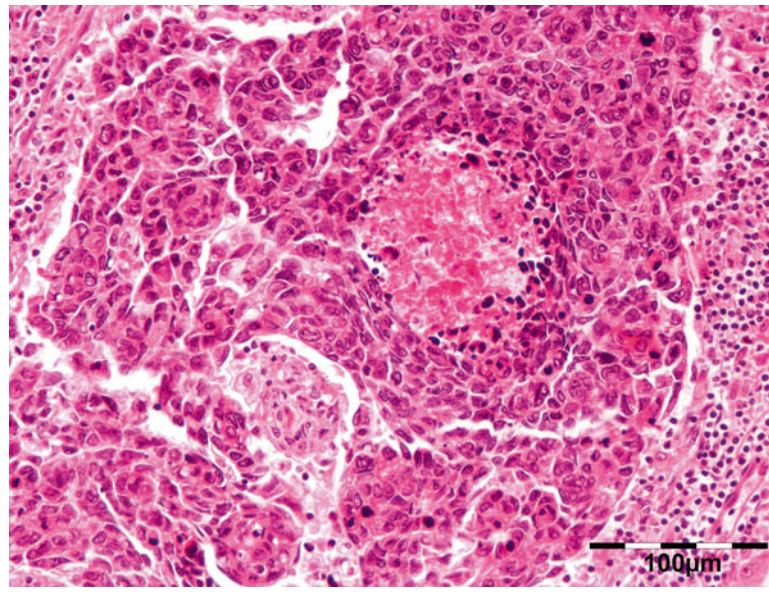

Fig. 12.162 Sebaceous carcinoma (SC) of the lacrimal gland: high-grade SC show pleomorphic cells with high nuclear/cytoplasmic ratio, high mitotic index, frequent intratumoral necrosis, and foci of sebaceous differentiation (HE 200×) (Dr. Irene Pecorella)

diagnosis of a primary lacrimal gland SC [386]. Warthin's tumor, mucoepidermoid carcinoma, and pleomorphic adenoma may contain areas of sebaceous differentiation.

Histogenesis

The origin of sebaceous differentiation in lacrimal glands is unknown. SC is believed to arise either from heterotopic sebaceous cells in the lacrimal gland or from sebaceous metaplasia of the lacrimal gland ducts [385]. Konrad and Thiel reported sebaceous differentiation within a metastasizing carcinoma which originated in a pleomorphic adenoma [387].

Genetics

There are no studies on the genetics of lacrimal SC.

Prognosis and Predictive Factors

A very aggressive tumor which shows early propensity to spread to regional draining lymph nodes. Exenteration, lymph node dissection,

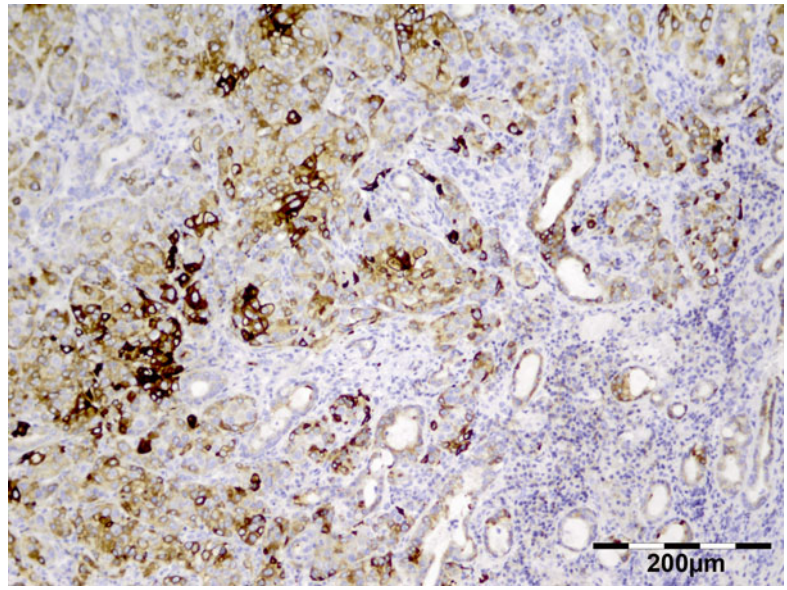

Fig. 12.163 Sebaceous carcinoma (SC) of the lacrimal gland: tumor cells stain diffusely for epithelial membrane antigen (EMA IH 100×) (Dr. Robert M. Verdijk)

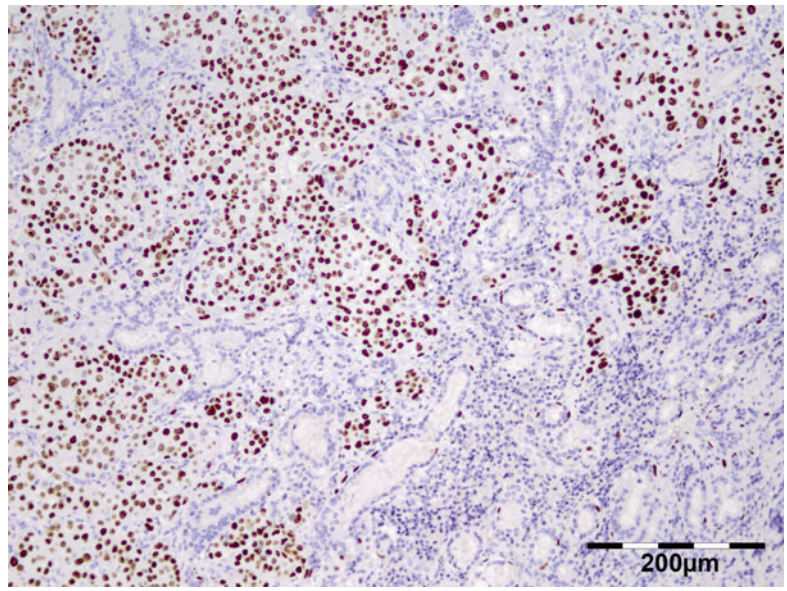

Fig. 12.164 Sebaceous carcinoma (SC) of the lacrimal gland: tumor cells nuclei stain positive for p63 (p63 antibody 100×) (Dr. Robert M. Verdijk)

and postoperative radiotherapy are indicated. Nevertheless, the prognosis remains poor, with local recurrences and metastases leading to death within 2 years postoperatively.

12.13.3.8 Lymphoepithelial Carcinoma (LEC)

Definition

LEC is an undifferentiated tumor that is associated with a dense lymphoid stroma.

Synonyms

Undifferentiated carcinoma with lymphoid stroma, carcinoma ex lymphoepithelial lesion.

Epidemiology and Etiology

LECs in nasopharynx and salivary glands are often associated with Epstein–Barr virus (EBV) infection [388] and, more recently, with the human papilloma virus (HPV) [389]. It was demonstrated that the viral DNA is specifically located in the malignant cells and not in the lymphocytes

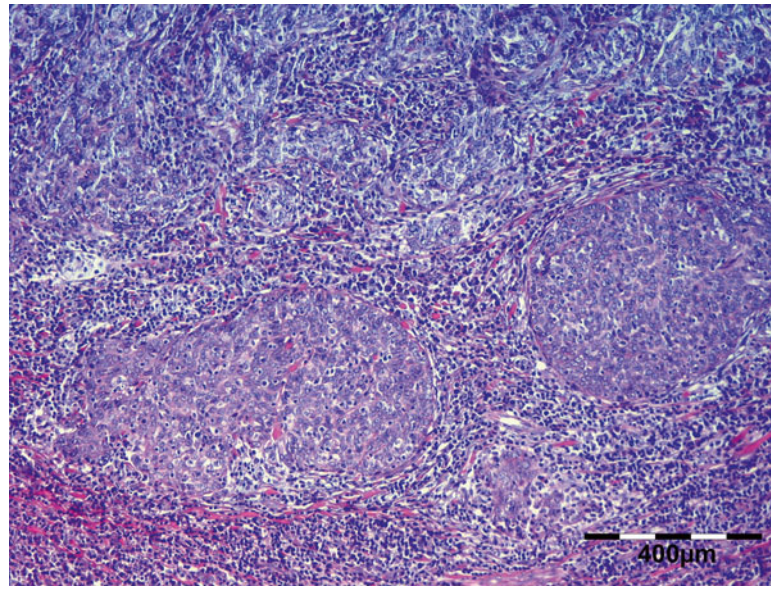

Fig. 12.165 Lymphoepithelial carcinoma of the lacrimal gland: lymphoplasmacytic infiltration associated with an epithelial proliferation of nonkeratinizing, poorly differentiated, squamous cells (HE 50×) (Dr. Irene Pecorella)

or in the benign epithelium. It is more commonly encountered in Eskimo and Chinese rather than Western populations.

Clinical Features

Upper lid fullness, diplopia, and proptosis were noted in one case [390]. CT of the orbit did not show bony involvement.

Macroscopy

A partially encapsulated mass with a tan-white cut surface. Zonal necrosis and hemorrhage are not typical features.

Histopathology–Immunoprofile

LEC is characterized by a nonneoplastic lymphoplasmacytic infiltration associated with an epithelial proliferation of nonkeratinizing, poorly differentiated, squamous cells composing irregular sheets, islands, and strands of carcinoma (Fig. 12.165). The cells are large, with indistinct cell borders resulting in syncytial appearance, eosinophilic cytoplasm, and oval vesicular nuclei with prominent nucleoli. Although epidermoid features are manifest, the overall appearance is that of undifferentiated carcinoma. The epithelial cells are widely separated by fibrous septa (Figs. 12.166 and 12.167). The presence of lymphoid follicles with germinal centers varies from none to many, with sometimes a "starry sky" pattern and variable amounts of collagenous tissue present within the lymphoid component. Immunohistochemically, most of the tumor cells are positive for pan-cytokeratin, cytokeratin 5, and cytokeratin 6. The surrounding cellular infiltrate is a mixture of CD20- and CD3-positive B and T lymphocytes, occasionally forming large lymphoid follicles. Negative immunohistochemical and in situ hybridization results for EBV were obtained in the reported ocular adnexal LEC [390], except one case [391].

Differential Diagnosis

Metastasis of amelanotic melanoma or lacrimal gland localization of large cell lymphoma should be ruled out. Immunohistochemistry with the antibodies to cytokeratins, S-100 protein, HMB45, or lymphocytic markers can help make a distinction.

Genetics

There are no studies on the genetics of LEC.

Prognosis and Predictive Factors

Despite the poor differentiation and high-grade histologic appearance, its clinical course is

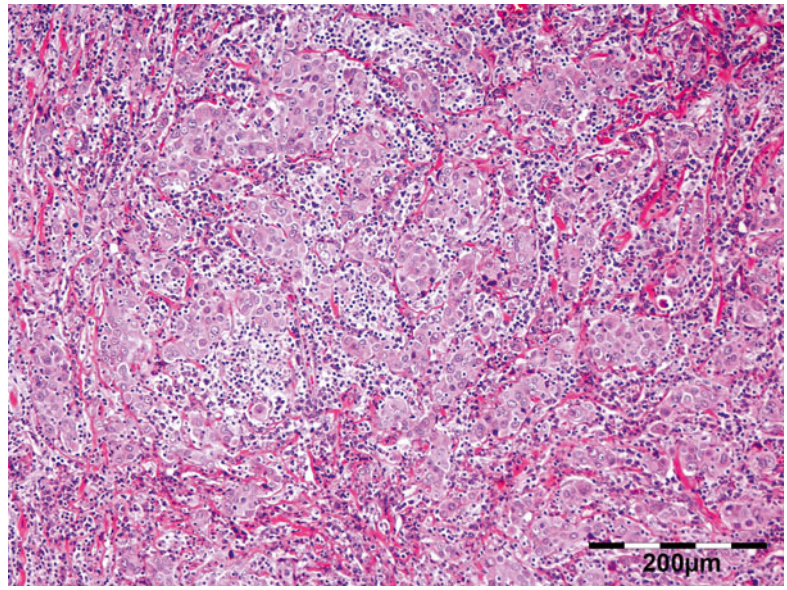

Fig. 12.166 Lymphoepithelial carcinoma of the lacrimal gland: epithelial cells are widely separated by fibrous septa (HE 100×) (Dr. Irene Pecorella)

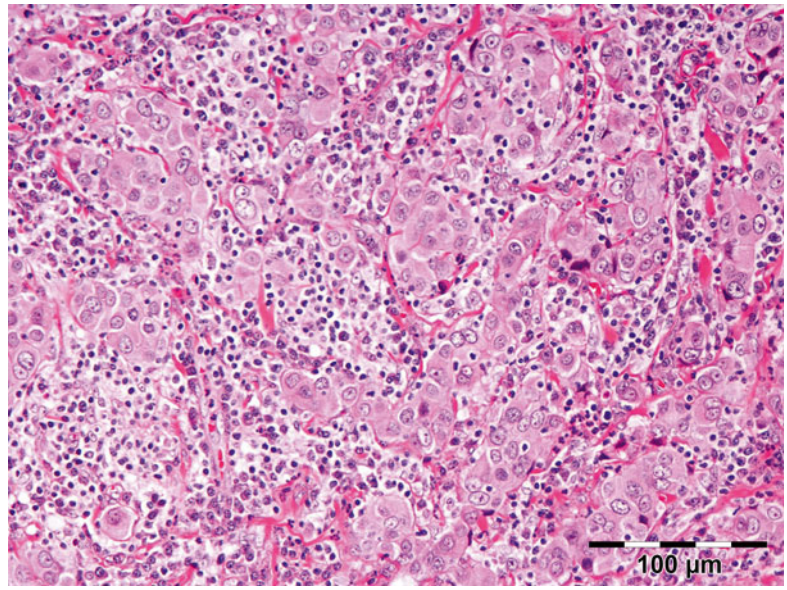

Fig. 12.167 Lymphoepithelial carcinoma of the lacrimal gland: epithelial cells are widely separated by fibrous septa (HE 200×) (Dr. Irene Pecorella)

better than other poorly differentiated tumors [392], possibly due to the presence of the lymphoid stroma that has a role in limiting the aggressiveness of this carcinoma. However, LEC has a strong tendency to metastasize to the regional lymph nodes. Advanced disease, the presence of metastases on diagnosis, and histologic features such as high mitotic rate, anaplasia, and necrosis are predictors of a worse prognosis.

12.13.3.9 Polymorphous Low-Grade Adenocarcinoma (PLGA)

Definition

A malignant tumor of low-grade cytology, histologic diversity, and infiltrative growth pattern.

Synonyms

Lobular carcinoma, low-grade papillary adenocarcinoma, or terminal duct carcinoma.

Epidemiology and Etiology

This lesion was first fully characterized in 1984 [393] and is becoming increasingly recognized. Formerly, this newly described entity was often included within the unclassifiable adenocarcinomas. PLGA occurs most almost exclusively in the minor salivary glands, particularly the palate, and has rarely been described in the lacrimal gland [273, 394]. It shows a peak in the seventh decade and a 2:1 female predilection, while it is rare in teenagers [395].

Clinical Features

Slow growing, tender, not painful lesion. The case described by Selva and colleagues presented as a lacrimal abscess [395].

Macroscopy

A nonencapsulated, firm, yellow-tan mass. Although often well circumscribed, PLGA is an infiltrative neoplasm.

Histopathology–Immunoprofile

PLGA exhibits low cytological grades and low mitotic index, uniform pale "washed-out" appearance, and often evidence of perineural invasion and extensive infiltration of the adjacent tissue. The neoplastic cells are uniform, small to medium in size, cuboidal or columnar, and arranged in a variety of architectural patterns within an individual lesion, including cribriform, papillary, solid, lobular, pseudo adenoid, tubular, and trabecular areas. Clear cytoplasm; oxyphilic, squamous, and mucinous metaplasia; and intratubular calcification are sometimes present. Stromal mucinization and hyalinization are common [395]. Mitotic figures are rare and necrosis is not seen. All histologic patterns share low-grade cytology with uniform, bland vesicular nuclei with stippled chromatin and inconspicuous nucleoli. Tumors exhibit extension into surrounding tissues including the bone. Immunoreactivity with vimentin, cytokeratin, EMA, and S-100 is commonly observed. Rarely the tumor cells of different histologic patterns react with myoepithelial markers or GFAP [310].

Differential Diagnosis

PLGA may share with pleomorphic adenoma a characteristic focal slate gray-blue stroma which may mimic the mucoid/myxoid matrix of pleomorphic adenoma. However, pleomorphic adenoma is immunopositive for markers of myoepithelial differentiation. The differential diagnosis also commonly includes adenoid cystic carcinoma because of common cribriform, tubular, and solid growth patterns and perineural invasion. The differential diagnosis relies on the significant degree of nuclear atypia present in ACC.

Histogenesis

In the major salivary glands, PLGA may be observed arising from a pleomorphic adenoma [360].

Genetics

There are no studies on the genetics of PLGA.

Prognosis and Predictive Factors

Patients with PLGA have the highest survival rate (96 %) among those with salivary gland malignancies [360]. A relatively low incidence (6.5 %) of metastasis to the regional lymph nodes has been reported [396]. The papillary cystic pattern has now been associated with established tendency to aggressive clinical behavior and protracted clinical course [397].

12.13.3.10 Epithelial–Myoepithelial Carcinoma (EMC)

Definition

A rare malignant neoplasm composed of two cell types that typically form duct-like structures. EMC was recognized by WHO in 1991 and is most commonly described in the parotid gland. Recently, although extremely rare, it has also been reported in the lacrimal gland [398, 399].

Synonyms

Adenomyoepithelioma, clear cell adenoma, tubular solid adenoma, epimyoepithelial carcinoma, and clear cell carcinoma.

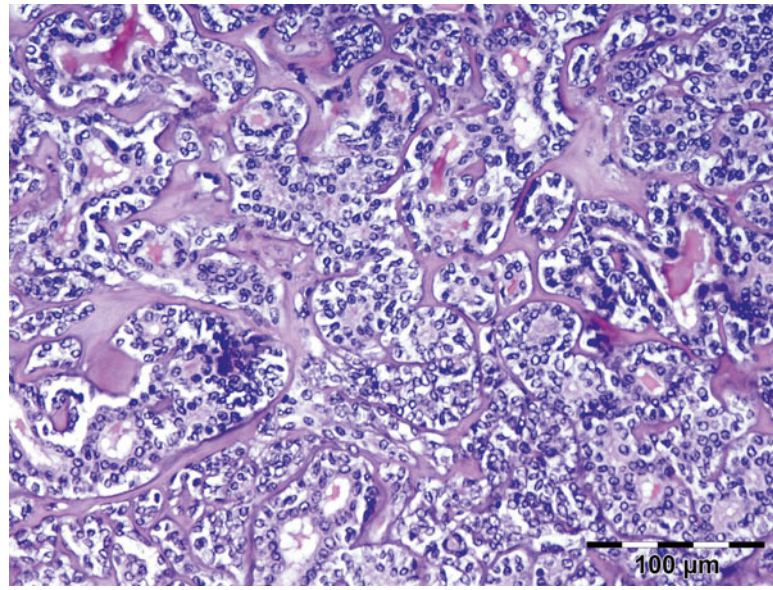

Fig. 12.168 Epithelial–myoepithelial carcinoma of the lacrimal gland: epithelial cells are arranged in branching tubules with one layer of myoepithelial cells. A well-defined, eosinophilic basement membrane surrounds the tubular areas and forms hyalinized thick intervening material. Tubular lumens may contain eosinophilic, PAS-positive proteinaceous material (HE 100×) (Dr. Irene Pecorella)

Epidemiology

Salivary EMC occurs more frequent in elderly women (approximately 60 % of cases), especially in the sixth to the seventh decade. Three of the four reported lacrimal gland EME occurred in aged man (mean age 73 years).

Etiology

There appears to be no association with cigarette smoking or other risk factors.

Clinical Features

EME can appear de novo [398] or from malignant transformation of a benign tumor [399]. The rare reported cases presented a painless mass growing for up to 8 years [399], with sudden increase in size. Although none of these cases showed areas of benign myoepithelioma, the slow growth of EME would suggest either a malignant degeneration or a low-grade malignancy. Bony erosion is not a feature in lacrimal gland EME.

Macroscopy

Grossly, the tumor in the lacrimal gland measures approximately 25 mm and is multinodular and circumscribed, often well-encapsulated mass with glistening white-to-tan and firm-to-feel cut surface. No areas of hemorrhage, necrosis, or calcification are seen.

Histopathology–Immunoprofile

EME shows a biphasic low-grade neoplastic cell population of eosinophilic ductal epithelial cells arranged in branching tubules and one or many layers of oval to spindled, clear, or plasmacytoid myoepithelial cells. A well-defined, PAS-positive basement membrane surrounds the tubular areas and may extend to form an eosinophilic, hyalinized thick intervening material. The tubular lumens may contain eosinophilic, PAS-positive proteinaceous material (Fig. 12.168). Solid areas composed of nests and sheets of myoepithelial cells, often with clear cytoplasmic changes, separated by scant fibrillary stroma, can also be observed. The cytological appearance is usually bland. Mitotic figures are rare and no high-grade nuclear atypia or cell necrosis is present. The tumor exhibits lobulated and pushing rather than infiltrative tissue growth patterns. However, prominent perineural invasion was reported by Singh G and colleagues in lacrimal gland EME [400], and myoepithelial low-grade anaplasia was noted in two of the four reported cases [400]. A high-grade component may develop through dedifferentiation from a low-grade salivary EMC in exceptional cases, though there is no such case reported in the lacrimal gland. The ductal epithelial cells strongly react for pan-cytokeratin AE1/AE3, cytokeratin

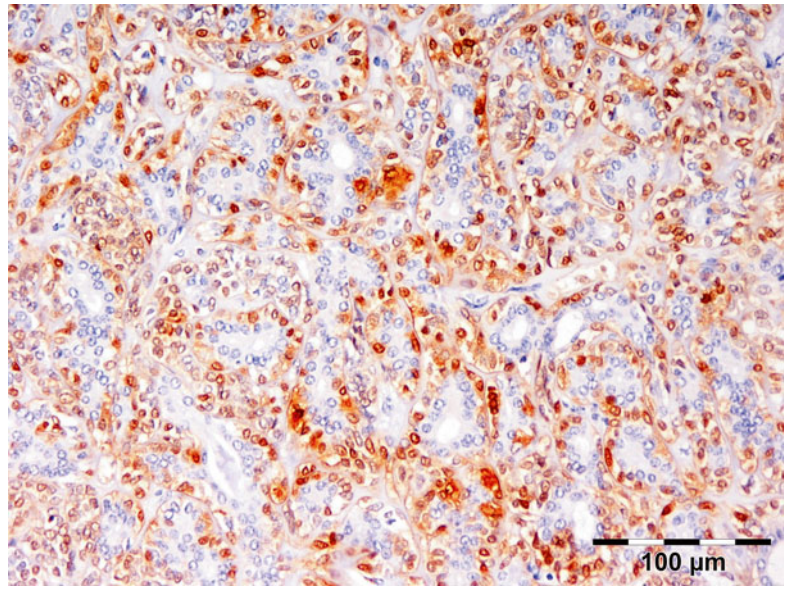

Fig. 12.169 Epithelial–myoepithelial carcinoma of the lacrimal gland: the ductal epithelial cells are negative for S-100. The myoepithelial cell component shows strong nuclear and cytoplasmic reactivity for S-100 (S-100 antibody 200×) (Dr. Irene Pecorella)

14, EMA, and c-KIT/CD117 and are negative for S-100 (Fig. 12.169) and smooth muscle actin. The myoepithelial cell component shows strong nuclear and cytoplasmic reactivity for S-100 (Fig. 12.169); patchy cytoplasmic reactivity for smooth muscle actin, p63, and calponin; and weak cytoplasmic reactivity for pan-cytokeratin. The Ki-67 proliferation index is slightly higher in the myoepithelial areas than in the ductal component.

Differential Diagnosis

The main histologic differential diagnosis is from the tubular variant of ACC, which also can show a double-layered, duct-like structure and biphasic pattern. However, ACC is more heterogeneous, also showing areas with cribriform or solid pattern and contains small basaloid myoepithelial cells with dark, angulated, hyperchromatic nuclei. Compared to ACC, EME shows peritubular sheets of myoepithelial cells, lacks basophilic mucosubstance in the microcystic spaces, and has a relatively lower Ki67 index. Additionally, the inner ductal cell layer in ACC stain positive for the S-100 protein, whereas only the outer ductal cell layer in ECM is positive for the S-100 protein. Differentiation from pleomorphic adenoma and its malignant counterpart is based on the absence of stromal elements, classically the chondromyxoid stroma. In addition, GFAP reactivity is not noted in the myoepithelial component of EMCs.

Histogenesis

EMC has been postulated to arise from the intercalated ducts of the salivary or lacrimal glands, because the tubular growth pattern of this tumor recapitulates this phenotype and intercalated duct hyperplasia is observed in some cases of EMC [401]. However, two different cell populations, already committed to luminal and myoepithelial differentiation, grow in cell cultures of EME carcinoma, in agreement with the biphasic pattern observed morphologically [402]. One case of EME arose in a PA [399].

Genetics

Genetic analysis, including polymerase chain reaction–single-strand conformational polymorphism (PCR-SSCP) and nucleotide sequencing, revealed a mutation in codon 207 (aspartic acid to glycine) of the p53 tumor suppressor gene in a salivary gland EME [403]. Others observed nuclear staining of myoepithelial cells for β-catenin protein in ten cases of ECM, which may explain the slow growth compared with other carcinomas [404].

Prognosis and Predictive Factors

In the salivary gland, EMC is basically a low-grade malignancy with rare mortality, 5-year survival rates of approximately 94 %, and 10-year disease-free survival of 81.8 %[405]. A recurrence rate of 36.3 %, even decades after initial surgery, is reported. EME with a solid growing pattern, nuclear atypia, DNA aneuploidy, and high proliferative activity generally have a more aggressive behavior and a higher frequency of local recurrences and metastases [406]. Also margin status, angiolymphatic invasion, tumor necrosis, and myoepithelial anaplasia are histologic predictors of recurrence in the salivary glands [405]. The behavior of lacrimal gland tumors is yet to be determined owing to its rarity. However, the four cases reported so far showed no recurrence or metastases after a maximum follow-up of 30 months [400].

12.13.3.11 Cystadenocarcinoma (CAC)

Definition

A group of malignant, cytomorphologically diverse, epithelial tumors characterized by an invasive, predominantly cystic pattern of growth. Papillary cystadenocarcinoma was first defined in 1991 by the World Health Organization as a separate entity.

Synonyms

Malignant papillary cystadenoma, papillary cystadenocarcinoma, low-grade papillary adenocarcinoma, or mucus-producing adenopapillary carcinoma.

Epidemiology and Etiology

CAC is an extremely rare malignant neoplasm (2 % of malignant salivary gland tumors), more commonly affecting the parotid gland, the sublingual gland, and minor salivary glands. CAC is a just recently described entity in the lacrimal gland [407, 408].

Clinical Features

CAC causes an S-shaped lid painless ptosis over a long period of time. The patient described by Peng X and colleagues was a 35-year-old man complaining progressive exophthalmos for six months. Following tumor enucleation, there was no recurrence in a 9-year follow-up [408]. The patient reported by Devoto MH and Croxatto JO noticed a progressive painless upper lid ptosis of 5-year duration. The tumor was excised completely with an intact capsule through a lateral orbitotomy. There was no evidence of local recurrences or dissemination after a 1-year follow-up [407]. Other clinical data on CAC derive from the salivary gland counterpart. Foss RD and coll. published in 1996 their series of 57 cases with salivary gland cystadenocarcinoma. The mean patient age in this series was 59 years (ranging from 20 to 86 years); both genders were equally affected [409].

Macroscopy

A circumscribed, not encapsulated multinodular firm, rubberlike reddish mass. On sectioning, cut surface is partly solid and partly cystic. The cysts contain brown exudate and yellowish deposits [410].

Histopathology–Immunoprofile

The neoplasm is characterized by variably sized multicystic spaces lined by papillary endophytic projections. The cysts are lined by cuboidal or low columnar epithelial cells with eosinophilic cytoplasm and small, round, hyperchromatic, nuclei. The cell cytoplasm is abundant and finely vacuolated. Periodic acid–Schiff (PAS) stain reveals abundant PAS-positive material in the cytoplasm of tumor cells. Mucus-secreting cells and clear cells can also be present. Mitotic figures are usually scarce. Less often, the cuboidal cells are larger and have abundant eosinophilic cytoplasm, centrally located irregular nuclei with coarse chromatin, prominent nucleoli, and 1–5 mitotic figures per 10 high-power fields. The cysts contain a proteinaceous exudate with detached viable and necrotic neoplastic cells and, sometimes, foci of calcification. They are surrounded by a limited collagenous matrix. Papillary projections are lined by a double layer of cells. Ruptured cysts with hemorrhage and solid areas (usually limited in extent) may be present. The neoplastic epithelial cells stain positive with cytokeratin and

negative with vimentin and glial fibrillary acidic protein (GFAP).

Differential Diagnosis

These tumors need to be differentiated from cystic variants of several more common lacrimal gland carcinomas: polymorphous low-grade adenocarcinoma, mucoepidermoid carcinoma, and papillary cystic variant of acinic cell carcinoma. Sometimes the distinction with cystadenoma may be difficult because the neoplasms have similar architecture and also because cystadenocarcinoma often shows little atypia. Differentiation of tumor types depends largely on the identification of actual infiltration of lacrimal gland by either cystic or solid epithelium in cystadenocarcinomas. Step sections of a borderline tumor may yield unequivocal evidence of invasion.

Histogenesis

The histogenesis of CAC is still unknown.

Genetics

There are no cytogenetic studies on this tumor.

Prognosis and Predictive Factors

CAC shows a relatively nonaggressive, low-grade behavior when the lesion is completely excised. Complete surgical excision is considered as adequate in these cases, and there is no need for additional radiotherapy.

12.13.3.12 Acinic Cell Carcinoma (AC)

Definition

A malignant epithelial neoplasm partly composed by neoplastic serous acinar cells.

Synonyms

Acinic cell adenocarcinoma or acinous cell carcinoma.

Epidemiology and Etiology

Only a few cases of AC are reported in the lacrimal gland [410, 411]. Our series of 216 lacrimal gland lesions contained only one cas (Table 12.2). The salivary gland counterpart of this tumor is known to have a familial occurrence and to occur quite commonly in children.

Clinical Features

The natural history of AC is characterized by the protracted course of disease progression. This is usually a slow-growing and painless mass but can develop extensive destruction of the bone and intracranial extension [412].

Macroscopy

Often encapsulated, tan-gray, firm to soft, solid/cystic mass. Because of the encapsulation, they may mistakenly be believed to be benign.

Histopathology–Immunoprofile

This tumor shows multidirectional differentiation toward acinar, ductal, as well as myoepithelial elements. The histopathological pattern may be solid, microcystic, papillary cystic, or follicular. Mixed patterns are also possible. The solid and microcystic patterns are observed most commonly. In the microcystic pattern, round or polygonal vacuolated cells with round to ovoid eccentric nuclei and prominent nucleoli surround microcystic spaces containing mucoid material (Fig. 12.170). Alternatively, polyhedral acinar serous cells with small, dark, eccentric nuclei and basophilic granular cytoplasm are observed. Zymogen secretory granules in the cytoplasm stain with PAS and PAS-D, alcian blue, colloidal iron, and mucicarmine. PAS staining is negative in the vacuolated cells. Small intercalated ductal cells are also a component of this neoplasm. The latter cells are round to cuboidal with eosinophilic granular cytoplasm and centrally located nuclei. Few mitotic figures are present. Clear cells are rarely seen and do not stain with PAS. Enlargement of the microcystic spaces produces a fenestrated or follicular pattern. Prominent lymphoid follicles at the periphery may be observed and have been associated with a better outcome of the tumor. The papillary cystic pattern is characterized by marked cystic change with papillary fronds. Positive immunostaining of the neoplastic cells is obtained using cytokeratins, alpha1-antitrypsin, and CEA; however, it is not helpful in differentiating AC from other types of lacrimal gland tumors [310].

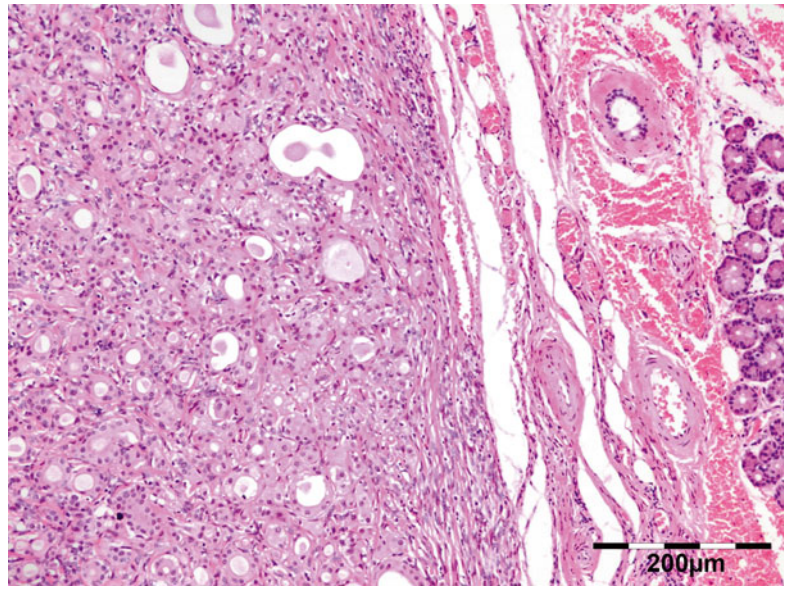

Fig. 12.170 Acinic cell carcinoma of the lacrimal gland: round or polygonal vacuolated cells with round to ovoid eccentric nuclei and prominent nucleoli surround microcystic spaces containing mucoid material (HE 100×) (Dr. Robert M. Verdijk)

Differential Diagnosis

The basophilic staining of the AC cells is rather unique among lacrimal gland tumors and may help in the differential diagnosis.

Histogenesis

AC is believed to be derived either from the intercalated duct cells (terminal duct cells) or from serous acinar cells.

Genetics

There are no cytogenetic analyses of lacrimal gland AC. Changes in the tumor suppressors CDKN2A and PPP1R13B have been highlighted in the salivary gland counterpart [412].

Prognosis and Predictive Factors

AC is considered to be a low-grade neoplasm with high potential for local and multiple recurrences (up to half of the patients), especially after inadequate tumor excision. The median time to first recurrence is 3 years; however, recurrences can occur up to 30 years after presentation [413]. A subset of patients presents with higher-grade histology and/or advanced local, regional, and distant disease that portends a poorer outcome [414]. Dedifferentiation with myoepithelial features after multiple resections has been reported [415].

12.13.3.13 Basal Cell Adenocarcinoma (BCCA)

Definition

A malignant epithelial tumor composed of a basaloid cell population.

Synonyms

Basaloid carcinoma, carcinoma ex monomorphic adenoma, malignant basal cell adenoma, malignant basal cell tumor, and basal cell carcinoma.

Epidemiology and Etiology

Little is known on the lacrimal gland BCCA, where the true incidence of these tumors may have been underestimated as they can be misdiagnosed with a solid basaloid adenoid cystic carcinoma. The salivary gland counterparts affect individuals with a median age at presentation of 60 years, with no gender predilection. However, one of the two lacrimal gland cases reported in the literature was a 36-year-old woman [304].

Clinical Features

A slowly progressive mass in the superotemporal region, increasing in size over a period of years [304].

Macroscopy

A partially encapsulated mass with irregular contours and rubbery in texture. The cut surface is tan white, homogeneous, with no cystic spaces or areas of necrosis [416].

Histopathology–Immunoprofile

BCCA is cytologically similar to basal cell adenoma, but it shows local infiltration and neural and vascular invasion and has a small potential for regional or distant metastasis. The solid pattern is the most common. It is characterized by solid sheets or anastomosing bands of minimally atypical basaloid epithelial cells, with occasional ductal formations, lined with cuboidal cells. The solid sheets tend to be round, oval, or irregular in shape and different in size. Incomplete palisading of dark cells with basophilic, non-angular nuclei can be observed at the periphery of the lobules. Thin septa or thick bands of collagenous stroma enclose the lobules. The mitotic count is low. The trabecular type is composed of interconnecting cords and bands of basaloid cell. The uncommon tubular type is characterized by small lumina or pseudolumina. Periodic acid–Schiff (PAS)-positive hyaline basement membrane material surrounds the tumor nests in the membranous type of BCCA. The tumor cells are cytokeratin-immunopositive, while they do not react with glial fibrillary acidic protein and smooth muscle actin.

Differential Diagnosis

Until recently, basaloid tumors of the salivary glands were largely considered a solid type of adenoid cystic carcinoma (basaloid adenoid cystic carcinoma). However, BCCA carries a better prognosis and appears microscopically less aggressive, with no necrosis, little nuclear and cellular pleomorphism, and a lower mitotic cell count (1–3 mitosis/10 HPF). Other distinctive features of BCCA are the peripheral palisading of small dark and large pale cells and the immunohistochemical lack of positivity for smooth muscle actin. Basaloid type of pleomorphic adenoma may be ruled out by the lack of myxoid or chondromyxoid matrix in BCCA.

Histogenesis

BCCA may arise de novo or from a preexisting basal cell adenoma.

Genetics

There is no information on the genetic defects in lacrimal gland BCCA. The salivary gland counterpart share the same alterations in the CYLD gene as dermal cylindromas.

Prognosis and Predictive Factors

BCCA is considered of low-grade malignancy, despite being infiltrative and locally destructive. The patient reported by Khalil M and colleagues was alive and well 10 years after exenteration of the orbit [304].

12.13.3.14 Mucinous Adenocarcinoma (MA)

Definition and Synonyms

Low-grade adenocarcinoma forming large pools of mucin.

Epidemiology and Etiology

MA is a rarely encountered and poorly understood tumor of the lacrimal gland. It usually arises in patients over 50 years of age. Males are affected more frequently than females [417].

Clinical Features

A slow-growing, painless swelling.

Macroscopy

The tumor is nodular and ill defined. The cut surface is grayish white, with gelatinous contents.

Histopathology–Immunoprofile

Cords, nests or clusters, cribriform masses, and strands of epithelial cells floating in mucus-filled cystic cavities, separated by fine fibrovascular septa, which create a somewhat lobulated architecture. Individual tumor cells are small and monotonous, with a low mitotic index. They usually possess clear cytoplasm and darkly stained, centrically placed nuclei. Tumor cells often form incomplete duct-like structure. Both intracellular and extracellular mucins stain positively with

PAS, PAS-D, and alcian blue at pH 2.5. Positive immunoreaction only to cytokeratins 7, 8, 18, and 19, S-100, CEAm, and EMA is observed.

Differential Diagnosis

Extravasated mucin is also present in mucoepidermoid carcinoma. However, differently from the latter, MA does not contain intermediate and epidermoid cells. Primary MA of the lacrimal gland should be differentiated from a metastatic gastrointestinal carcinoma. Differently from the latter, MA does not stain with cytokeratin 20 antibody. Another possible differential diagnosis is that with the mucin-rich variant of duct carcinoma, a rare type of salivary duct carcinoma, which has not been so far observed in the lacrimal gland. Immunoreactivity for androgen receptor and the presence in this subtype of duct carcinoma of both conventional duct and mucinous adenocarcinoma-like areas should help clarify the diagnosis.

Histogenesis

MA may originate from acinic cell of mucous acinus or multipotential cell of the lacrimal gland.

Genetics

Several DNA copy number aberrations have been detected in MA of minor salivary glands [418].

Prognosis and Predictive Factors

Despite a low metastatic potential, MC has a propensity for local recurrence and regional lymph node metastases. It is also insensitive to radiotherapy.

12.13.3.15 Oncocytic Adenocarcinoma (OCA)

Definition

A proliferation of malignant oncocytes with adenocarcinomatous architectural phenotypes.

Synonyms

Malignant oncocytoma or malignant oxyphilic adenoma.

Epidemiology and Etiology

OCA most commonly involves the caruncle, the conjunctiva, the lacrimal sac, and, more rarely, the lacrimal gland. To date, only few cases of lacrimal gland OCA have been reported [419, 420]. All the case had an intracranial extension at the presentation, with a maximum follow-up of 6 months.

Clinical Features

OCA usually presents as a palpable supratemporal mass causing diplopia and proptosis.

Macroscopy

Grossly, OCA appears as an unencapsulated and irregularly shaped tan to gray mass. The cut surface is pale yellow or light brown, with a solid texture, sometimes containing areas of cystic degeneration, necrosis, or hemorrhage.

Histopathology–Immunoprofile

The neoplastic cells display eosinophilic granular cytoplasm and centrally situated round, vesicular nuclei with prominent nucleoli. The nuclear-to-cytoplasmic ratio is low (Fig. 12.171). The cell cytoplasm is characterized ultrastructurally by numerous mitochondria. The cells are arranged in solid sheets, duct-like structures, and cords. Marked cell pleomorphism is seen in most cases. Classically, PTAH staining depicts small, dark-blue cytoplasmic granules, which represent mitochondria. Perineural and vascular invasion are invariably noted.

Differential Diagnosis

Oncocytomas occasionally share the diagnostic features of OCA. Therefore, the diagnosis of malignancy should be based on a combination of clinical and histopathological features: cellular and nuclear pleomorphism, local infiltration, and presence of metastases. Also, Ki-67-positive cells are more numerous in OCA than in benign oncocytoma. Acinic cell adenocarcinoma can be differentiated from OCA by the basophilic quality of the cytoplasmic granules. Immunohistochemistry for mitochondria may be helpful for the adjuvant diagnosis.

Histogenesis

This tumor arises de novo in the ductal cell lining of the lacrimal gland or may derive from a malignant degeneration of a preexisting oncocytoma.

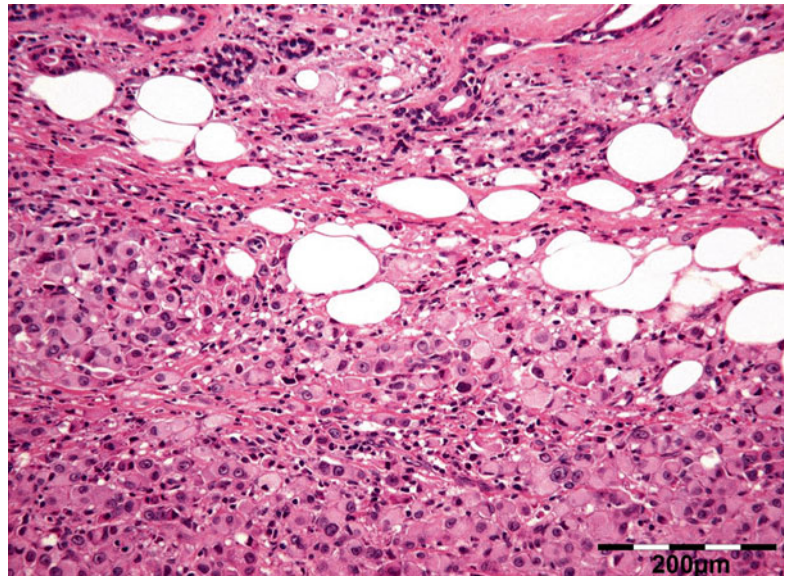

Fig. 12.171 Oncocytic adenocarcinoma of the lacrimal gland: the tumor cells display eosinophilic granular cytoplasm and centrally situated round, vesicular nuclei with prominent nucleoli. The nuclear-to-cytoplasmic ratio is low (HE 100×) (Dr. Irene Pecorella)

Genetics

There are no studies on the genetics of OCA.

Prognosis and Predictive Factors

This is a high-grade neoplasm with infiltrative growth pattern and tendency to recur and metastasize. In those patients with follow-up, the maximum period of survival after initial presentation was 2 years [420].

12.13.3.16 Large Cell Carcinoma (LCCA)

Definition and Synonyms

Together with small cell carcinoma and lymphoepithelial carcinoma, LCCA is a specific subtype of undifferentiated carcinoma recently included in the World Health Organization classification of tumors of the salivary glands. It is characterized by the absence of acinar, ductal, epidermoid, or myoepithelial differentiation under light microscopy.

Epidemiology and Etiology

The first and only example of primary undifferentiated LCCA of the lacrimal gland was reported by Bernardini et al. [421].

Clinical Features

A painful, rapidly progressing, firm mass adherent to adjacent tissues.

Macroscopy

A poorly circumscribed, whitish solid mass, deeply infiltrating the surrounding orbital tissues.

Histopathology–Immunoprofile

LCCA shows large polygonal or round cells >30 µm in diameter, with well-defined eosinophilic cytoplasm and ovoid nuclei containing prominent nucleoli and coarse chromatin. The cells are arranged in cords and trabeculae or irregular sheets of discohesive cells with frequent mitotic figures and apoptotic cells. The proliferation index Ki-67 is >50 %. The tumor cells show positive immunoreactivity for AE1/A3 cytokeratin and cytokeratin 7 antibodies and are negative for cytokeratin 20.

Differential Diagnosis

Metastatic disease, primary epithelial malignancies, and orbital lymphoma should be ruled out. Large cell carcinoma should not be confused with adenocarcinoma NOS, which may show ductular arrangement.

Prognosis and Predictive Factors

The patient described by Bernardini et al. was treated with an extended lid-sparing exenteration and concomitant radical neck lymphadenectomy, which disclosed massive involvement of the regional neck lymph nodes. Adjunctive radiotherapy was administered postoperatively to both

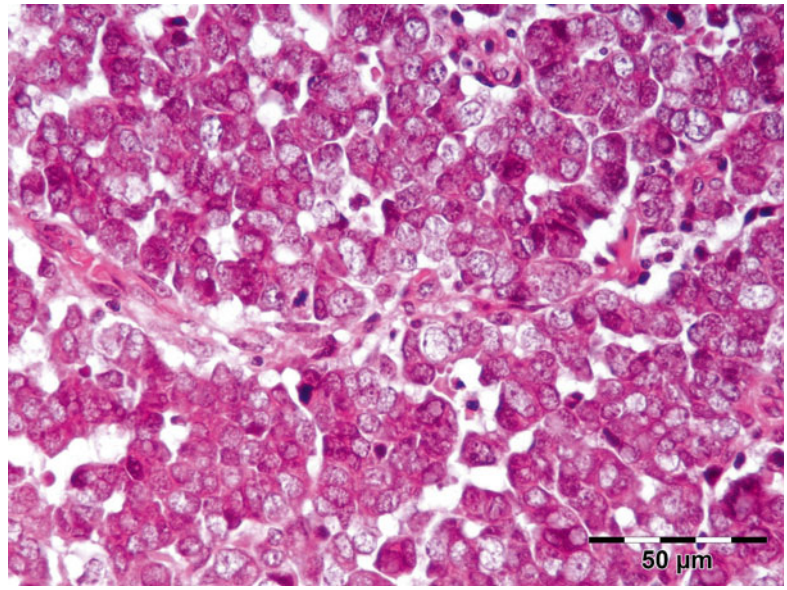

Fig. 12.172 Merkel cell carcinoma of the lacrimal gland: nests of uniformly sized basophilic cells with large round nuclei, finely dispersed chromatin, small nucleoli, and scant cytoplasm can be seen (HE 400×) (Dr. Irene Pecorella)

surgical sites. The patient was alive with no evidence of local recurrences or distant metastases after a follow-up of 15 months.

12.13.3.17 Merkel Cell Carcinoma (MCC)

Definition and Synonyms

Neuroendocrine tumor that occurs most commonly in the dermis of sun-exposed skin in elderly Caucasian patients. In rare instances it has arisen in other primary sites, including the oral mucosa, the parotid gland, and the lacrimal gland [422].

Epidemiology and Etiology

An exceedingly rare malignancy in the lacrimal gland, with only two cases reported in the literature [423, 424]. This tumor appears in the seventh and eighth decade of life and shows almost no gender difference. Incidence is elevated in immunodepressed patients.

Clinical Features

Lacrimal gland MCC manifests as a painless firm, non-tender upper eyelid swelling, characterized by rapid growth.

Histopathology–Immunoprofile

Nests of uniformly sized basophilic cells with large round nuclei, finely dispersed chromatin, small nucleoli, and scant cytoplasm are observed (Fig. 12.172). The presence of areas of focal necrosis, mitotic activity, and lymphocytic infiltration are very common. There are basically three histologic patterns: the first one is the trabecular type, the second one is formed by sheets and clusters of malignant cells, and the third is the intermediate type (the most common one). The tumor cells show dot-like paranuclear immunohistochemical expression for CK20 and variable diffuse expression for CK56, synaptophysin, chromogranin, and CD57 (leu-7).

Differential Diagnosis

The solid variant of adenoid cystic carcinoma may mimic MEC, though immunohistochemical testing reveals a characteristic paranuclear dot-like staining pattern with cytokeratin only in the latter. MEC and small cell carcinoma of the salivary gland have an identical immunohistochemical staining pattern.

Histogenesis

A virus, termed Merkel cell polyomavirus, has recently been implicated in the development of MCC [425].

Prognosis and Predictive Factors

MCC shows an aggressive course. However, no recurrences after surgical excision and

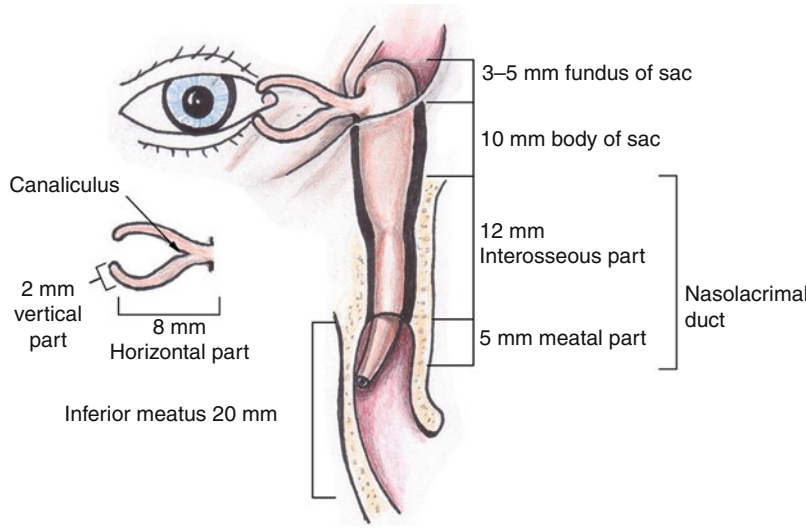

Fig. 12.173 Schematic representation of the lacrimal drainage system (Adapted from http://oralmaxillo-facialsurgery.blogspot.nl/2010/05/nasolacrimal-system-anatomy.html)

subsequent local radiation were observed in two reported cases [423, 424].

12.13.3.18 Other Unusual Malignant Lacrimal Gland Neoplasms

Other unusual lacrimal gland neoplasms include myoepithelial carcinoma [276, 426], adenosquamous carcinoma [427], and carcinosarcoma, a mixed tumor with carcinomatous (ductal or undifferentiated carcinoma) and sarcomatous components (mainly chondrosarcoma) [273, 276].

Malignant lymphoma of the lacrimal gland comprises about 10 % of all lacrimal gland lesions [252] (Table 12.2). Lymphoma is mostly found in elderly women; most lacrimal gland lymphomas are low grade, and the prognosis is relatively good [428]. CT scan of lymphoproliferative lesions usually demonstrate an eccentric-shaped lesion with significant contrast enhancement. Systemic lymphoma develops in 20–30 % of patients with malignant lymphoma of the lacrimal gland. Incidence is much higher if the initial presentation is with bilateral lacrimal gland involvement [429].

12.14 Lacrimal Drainage System

12.14.1 General Description

The nasolacrimal drainage system serves as a conduit for tear flow from the external eye to the nasal cavity. It consists of the puncta, canaliculi, lacrimal sac, and the nasolacrimal duct (Fig. 12.173).

12.14.2 Embryology, Anatomy, and Development

12.14.2.1 Embryology

At 32 days' embryonic gestation, the maxillary and frontonasal prominences appear, and as these processes enlarge, a groove forms between them. The ectoderm from the floor of the groove becomes entrapped between the processes and detaches from the surface ectoderm as a cord of epithelium. At the same time, cords of epithelium invaginate at the upper and lower lid margins, eventually forming the canaliculi. These epithelial cords fuse to form the nasolacrimal drainage system [430]. Canalization of the epithelial cords occurs simultaneously throughout their entire length, beginning at 4 months' gestation. Remnants of epithelium within the cords form inconsistent, valve-like folds. A membranous covering consisting of conjunctival and canalicular epithelium remains over the puncta, and a covering consisting of nasal and nasolacrimal epithelium remains over the nasolacrimal duct outlet. The punctal membranes open at full term. Epithelium at the site of the future lacrimal sac is initially thicker, and canalization in this area is more extensive.

12.14.2.2 Anatomy and Histology

Puncta are openings 0.3 mm in diameter located on the medial aspect of the upper and lower eyelid margins. Each punctum sits on top of an elevated mound known as the papilla lacrimalis. The inferior punctum is approximately 0.5 mm lateral to the superior punctum, with distances to the medial canthus of 6.5 mm and 6.0 mm, respectively. Tears within the medial canthal area enter the puncta to pass into the canaliculi. Canaliculi have an initial vertical segment, measuring 2 mm, followed by an 8-mm horizontal segment. The angle between the vertical and horizontal segments is approximately 90°, and the canaliculi dilate at the junction to form the ampulla. In most individuals, the horizontal portion of the canaliculi converges to form the common canaliculus. Canaliculi pierce the lacrimal fascia before entering the lacrimal sac. At its entrance to the lacrimal sac, the common canaliculus may dilate slightly, forming the sinus of Maier. Canaliculi are lined by nonkeratinized, stratified squamous epithelium and are surrounded by elastic tissue, which permits dilation to two or three times the normal diameter. The oblique entrance of the common canaliculus into the lacrimal sac forms the valve of Rosenmüller, which prevents retrograde reflux of fluid from the sac into the canaliculi [431]. The lacrimal sac sits within the lacrimal fossa, which is bound anteriorly by the frontal process of the maxillary bone (anterior lacrimal crest) and posteriorly by the lacrimal bone (posterior lacrimal crest) (Fig. 12.173). Differing proportions of lacrimal bone and maxillary bone make up the lacrimal fossa; the position of the vertically oriented suture between them is variable. The lacrimal sac is lined by a double-layered epithelium (superficial is columnar, and deep is flatter). It can be divided into a fundus superiorly and a body inferiorly. The fundus extends 3–5 mm above the superior portion of the medial canthal tendon, and the body extends approximately 10 mm below the fundus to the osseous opening of the nasolacrimal canal. At the posterior lacrimal crest, the orbital periosteum splits to envelop the lacrimal sac as a covering known as the lacrimal fascia. This periosteum then continues inferiorly to enclose the nasolacrimal duct. The lacrimal fascia is surrounded by fibers of the orbicularis oculi muscle; the superficial head of the muscle travels around the front of the sac to attach to the anterior lacrimal crest, and the deep head of the muscle travels behind the sac to attach to the posterior lacrimal crest. Between the lacrimal fascia and the lacrimal sac lies a venous plexus. The nasolacrimal duct consists of a 12-mm superior intraosseous portion and a 5-mm inferior membranous portion. The lacrimal sac is a preseptal structure. The double layer of epithelium similar to that observed in the lacrimal sac lines the nasolacrimal duct. The venous plexus surrounding the lacrimal sac continues inferiorly to surround the nasolacrimal duct, eventually connecting to the vascular tissue of the inferior turbinate [432].

12.15 Congenital Abnormalities

12.15.1 Congenital Nasolacrimal Duct Obstruction

Congenital nasolacrimal duct obstruction occurs in approximately 5 % of normal newborn infants. The blockage occurs most commonly at the distal end of the duct. There is no sex predilection and no genetic predisposition. The blockage can be unilateral or bilateral. The rate of spontaneous resolution is estimated to be 90 % within the first year of life [433–435]. General stenosis of the duct is the second most common cause of duct obstruction. Congenital proximal lacrimal outflow dysgenesis involves maldevelopment of the punctum and canaliculus. Proximal outflow dysgenesis can occur concurrently with distal obstruction. Congenital lacrimal sac mucocele or dacryocystocele occurs when there is a membranous cyst extending from the distal end of the duct into the nose. The nasolacrimal duct sac is filled at birth with clear amniotic fluid. The fluid becomes purulent within days of birth and neonatal dacryocystitis occurs. Children with Down syndrome, craniosynostosis, Goldenhar sequence, clefting syndromes, hemifacial microsomia, or any

midline facial anomaly are at an increased risk for congenital nasolacrimal duct obstruction. When nasolacrimal duct obstruction is secondary to a congenital barrier, it is referred to as dacryocystoceles. Dacryocystocele is an umbrella term that refers to any diffuse, centrifugal enlargement of the lacrimal sac that results from combined proximal and distal obstructions in the tear drainage system. In infants, dacryocystoceles are transitory as the result of spontaneously reversible factors [436].

12.15.2 Congenital Lacrimal Fistula

Congenital lacrimal fistulas, also known as lacrimal anlage ducts, are supernumerary lacrimal canaliculi that connect the skin to the common canaliculus or the lacrimal. These rare developmental abnormalities often lead to epiphora [437]. Originally a solid epithelial cord, the canaliculi canalize around day 60 of gestational age and the puncta are patent by the seventh fetal month [437]. It has been postulated that this cord of epithelial cells, also known as the lacrimal anlage, fails to involute in cases of congenital lacrimal fistula. Congenital lacrimal fistulas typically arise from the common canaliculus or the lacrimal sac. Lacrimal fistulas have a histologic structure very similar to that of typically developed canaliculi. Those that have been reported usually have a stratified squamous epithelial lining identical to that of a normal canaliculus [438].

12.16 Inflammation

The lacrimal excretory system is prone to infection and inflammation for various reasons. This mucous membrane-lined tract is contiguous with two surfaces (conjunctival and nasal mucosal) that are normally colonized with bacteria. The functional purpose of the lacrimal excretory system is to drain tears from the eye into the nasal cavity. Stagnation of tears in a pathologically closed lacrimal drainage system can result in dacryocystitis.

12.16.1 Dacryocystitis

Definition

Dacryocystitis is an inflammation of the nasolacrimal sac.

Epidemiology and Etiology

Dacryocystitis is frequently caused by nasolacrimal duct obstruction or infection. Inflammatory lesions comprised the most frequent diagnosis in 75 % of biopsies of the lacrimal sac according in our series (Table 12.3). It is most commonly caused by *Staphylococcus aureus* and *Streptococcus pneumoniae* [439, 440]. Stones (dacryolith) in the lacrimal canal are probably due to low-grade inflammation, including mycoses (*Arachnia propionica* = a bacterial species causing lacrimal canaliculitis and typical actinomycosis (Fig. 12.174); it is the type species of the genus *Arachnia*; synonym(s): *Propionibacterium propionicus*). In a series of lacrimal gland ductulitis, 6.7 % had dacryoliths; 73.3 % with canaliculitis had canalicular concretions. Patients with canalicular concretions were older than those with dacryoliths at DCR: 70.6 years versus 51.1 years. Women made up the majority of both groups: 81.8 % with canalicular concretions and 59.1 % with dacryoliths. *Actinomyces* was isolated in canalicular concretions 90.9 % and only 13,6 % in dacryoliths. In none of the 11 canalicular concretions were fungi identified, compared with 2 of 22 dacryoliths (9.1 %) [441]. Infective lacrimal gland ductulitis, commonly from *Actinomyces* infection, should be considered in patients with unexplained chronic mucopurulent conjunctivitis [442]. A rare report of sarcoid of the lacrimal sac has been described [443]. We have observed 3 cases in our series of 138 lacrimal sac lesions (Table 12.3).

Clinical Features

Dacryocystitis causes pain, redness, and swelling over the inner aspect of the lower eyelid and epiphora. Acquired dacryocystitis can be acute or chronic. Acute dacryocystitis is heralded by the sudden onset of pain and redness in the medial canthal region.

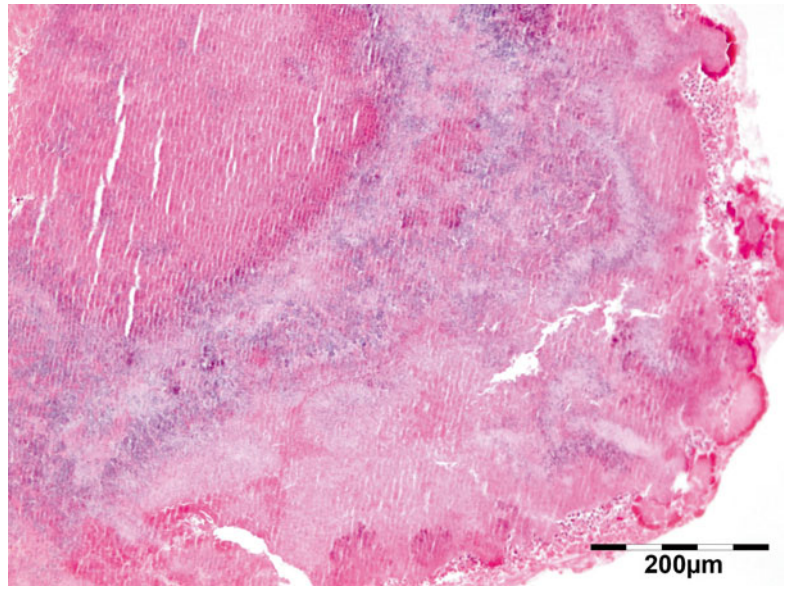

Fig. 12.174 Dacryolith of the lacrimal punctum: calcifications and basophilic microorganisms with a Splendore–Hoeppli phenomenon compatible with *Actinomyces* (HE 100×) (Dr. Robert M. Verdijk)

Histopathology

On microscopy the cyst wall is atrophic with degenerative changes; also hyperplasia and chronic inflammatory infiltrate can be seen.

Differential Diagnosis

The differential diagnosis of medial canthal swellings centered on the lacrimal sac spans malformations, diverticula, dermoid/epidermoid cysts, sac inflammations/infections causing swelling without generalized sac enlargement, encephaloceles, and primary epithelial tumors, as well as extrinsic tumors impinging on the sac [436].

Prognosis and Predictive Factors

Mucocele of the lacrimal sac arises from complication of chronic inflammation of the lacrimal sac, with distention of the sac due to low-grade obstructive lesion or hypersecreting mucosa. Cyst contents may be clear, milky, gelatinous, fibrinous, or flocculent and may be sterile or infected. In adults, the presence of mucus in the content of a dacryocystocele leads to the modified term of dacryocystomucocele. If infection supervenes, which almost always occurs in protracted cases and adds the clinical dimension of a dacryocystitis, then a dacryocystomucopyocele is created. Dacryocystocele and its congeners are much rarer in adults than in children [436]. In adults, secondary proximal irreversible fibrotic strictures or bony changes around the nasolacrimal duct typically arise from chronic inflammation or low-grade infection. Other possible causations of duct obstruction, in addition to florid mucosal edema, include encroachment on the duct by enlarged contiguous ethmoid air cells; a sinus mucocele or sinusitis; idiopathic, posttraumatic, or dysplastic bony remodeling of the wall of the duct; and a neoplasm, all of which require some form of surgical intervention, typically dacryocystorhinostomy.

12.17 Injuries

Acquired nasolacrimal duct or canalicular obstructions can occur following trauma, viral conjunctivitis, acute dacryocystitis, and use of topical antiviral medications. Lacrimal sac fistulae can arise after an episode of dacryocystitis, usually forming below the medial canthus [444].

12.18 Degenerations

Localized orbital amyloidosis involving the lacrimal sac and nasolacrimal duct has been described rarely [445].

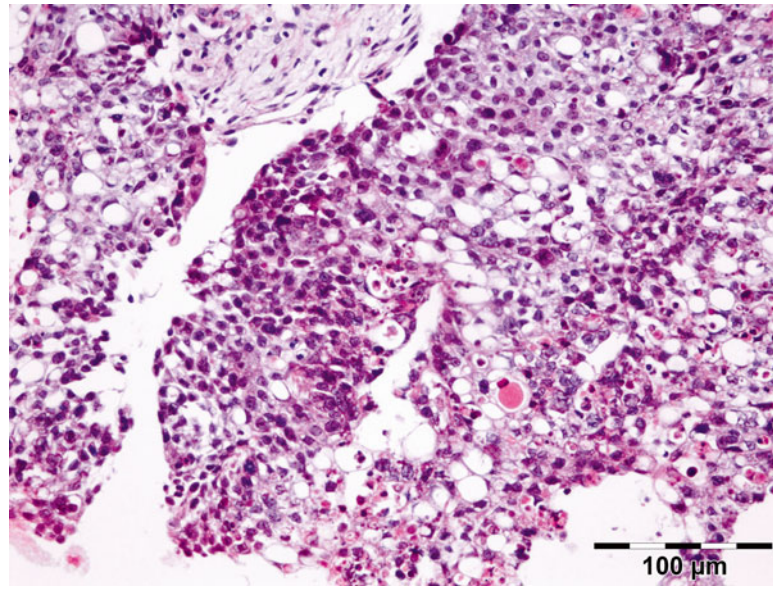

Fig. 12.175 Transitional cell carcinoma of the lacrimal sac: large polygonal cells in a loose syncytial arrangement infiltrating the submucosal stroma (HE 200×) (Dr. Robert M. Verdijk)

12.19 Neoplasms of the Lacrimal Drainage System

Tumors of the lacrimal drainage system are rare. Almost 85 % are located in the upper part of the lacrimal drainage system (lower and upper lacrimal point, lower and upper canaliculus) and merely 15 % are located in the lacrimal sac and nasolacrimal duct. These tumors mostly become apparent by symptoms like epiphora. One should be aware of the fact that this symptom can always be masqueraded by a tumor [446].

Benign tumors include squamous papilloma, transitional cell papilloma, or mixture of squamous and transitional cell papilloma. They can grow exophytic or endophytic. Inverted papilloma show an endophytic growth pattern [447, 448]. HPV (type 6 and 11) has been associated with lacrimal sac papilloma and carcinoma [449].

In a clinicopathological study of 115 lacrimal sac neoplasms in adults, the mean age was 52 years. The most common presenting signs and symptoms were epiphora, recurrent dacryocystitis, and/or lacrimal sac mass. The tumors were divided into epithelial and nonepithelial neoplasms. Benign epithelial tumors included squamous and transitional cell papillomas (32), oncocytomas (4), and benign mixed tumors (2). The malignant epithelial neoplasms included squamous cell carcinoma (22), transitional cell carcinoma (5), adenocarcinoma (4), mucoepidermoid (3), adenoid cystic (3), and poorly differentiated carcinoma (1). The nonepithelial tumors consisted of fibrous histiocytoma (13), lymphoid lesions (10), malignant melanoma (6), hemangiopericytoma (1), lipoma (1), granulocytic sarcoma (1), and neurofibroma (1) [450]. In our series of 238 lacrimal sac biopsies, only 7 % represented epithelial neoplasms (Table 12.3). Oncocytoma develops in the lacrimal sac or caruncle, usually in elderly women. The CK profile is similar to the lacrimal and accessory lacrimal gland duct elements and supports the theory that these lesions originate in the lacrimal and accessory lacrimal glands [307]. Malignant tumors include transitional cell carcinoma (100 % mortality) (Fig. 12.175), malignant melanoma (Fig. 12.176), squamous cell carcinoma (Fig. 12.177) with a recurrence rate of 50 %, lymphoma, mucoepidermoid carcinoma [451], and adenocarcinoma [452, 453] (Fig. 12.178). The most prevalent type is squamous cell carcinoma (SCC). These tumors generally present with aspecific symptoms suggestive of chronic dacryocystitis, with the result that diagnosis and treatment are often delayed [454]. SCC is usually moderately differentiated (Fig. 12.177), similar to nasal or conjunctival squamous cell carcinoma. It often spreads along

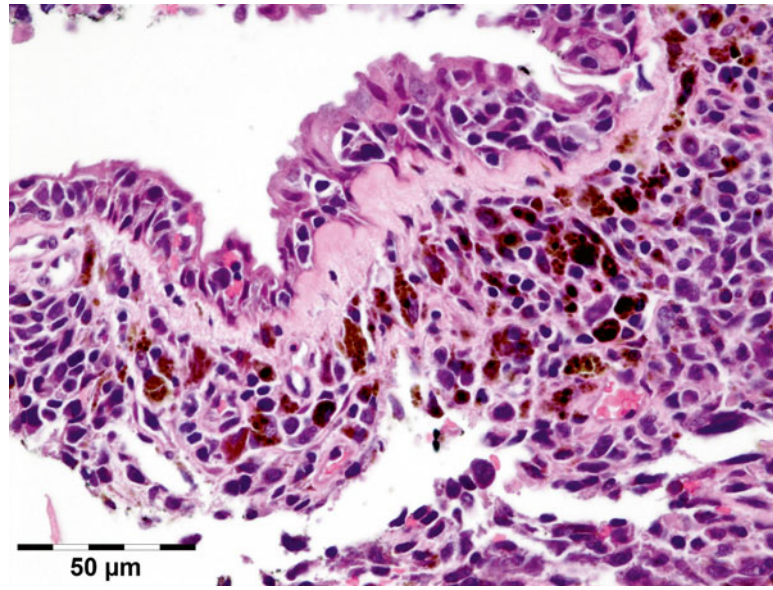

Fig. 12.176 Primary malignant melanoma of the lacrimal sac: intraepithelial nests of severely atypical melanocytes in combination with stromal infiltration (HE 400×) (Dr. Robert M. Verdijk)

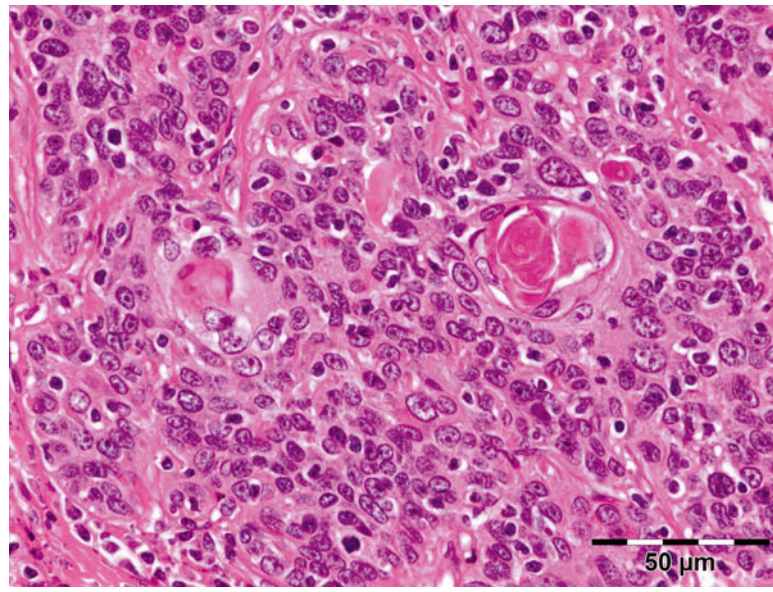

Fig. 12.177 Squamous cell carcinoma of the lacrimal sac: infiltrating islands of atypical polygonal cells displaying dyskeratosis (HE 100×) (Dr. Robert M. Verdijk)

surfaces, as well as showing infiltrating features. The lung is the most common site for metastases and then the bone and remote viscera. HPV (type 6 and 18) has been associated with SCC [449]. Transitional cell carcinoma is the second most common epithelial cancer of the lacrimal sac and may cause death if inadequate or delayed therapy. The mean age of those afflicted with transitional cell carcinoma was 47–50 years, similar to other lacrimal sac tumors which mainly occur in the fourth to fifth decade of life. Benign transitional cell papillomas were found to occur earlier at the age of 40 years [450] (Fig. 12.179). Transitional cell carcinoma is a carcinoma with recognizable stratified columnar epithelium and exophytic and endophytic papillary lesions. Mitotic figures are conspicuous, cellular, and nuclear pleomorphism. Ultimately, evidence of extension into the wall of the sac with penetration of the epithelial basement membrane is needed. (Fig. 12.175). Histologic

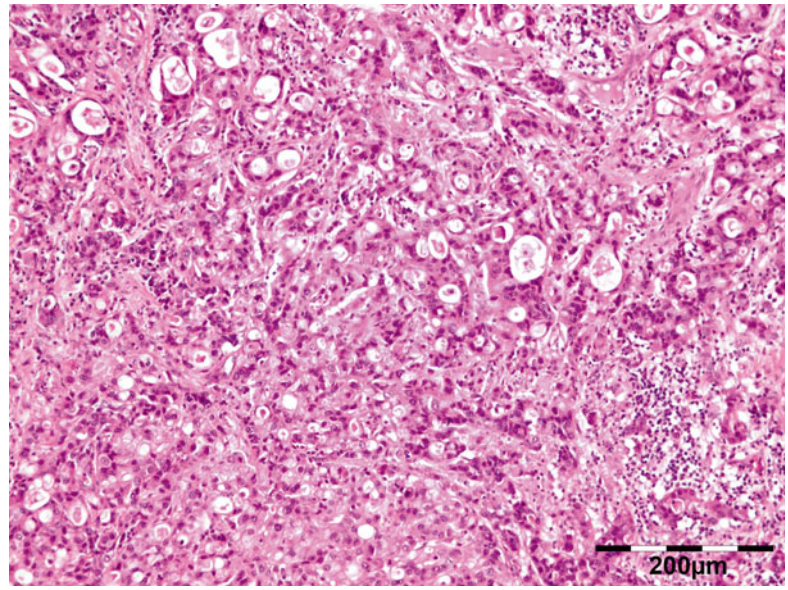

Fig. 12.178 Adenocarcinoma NOS of the lacrimal sac: diffuse infiltrating tubule forming malignant cells (HE 100×) (Dr. Robert M. Verdijk)

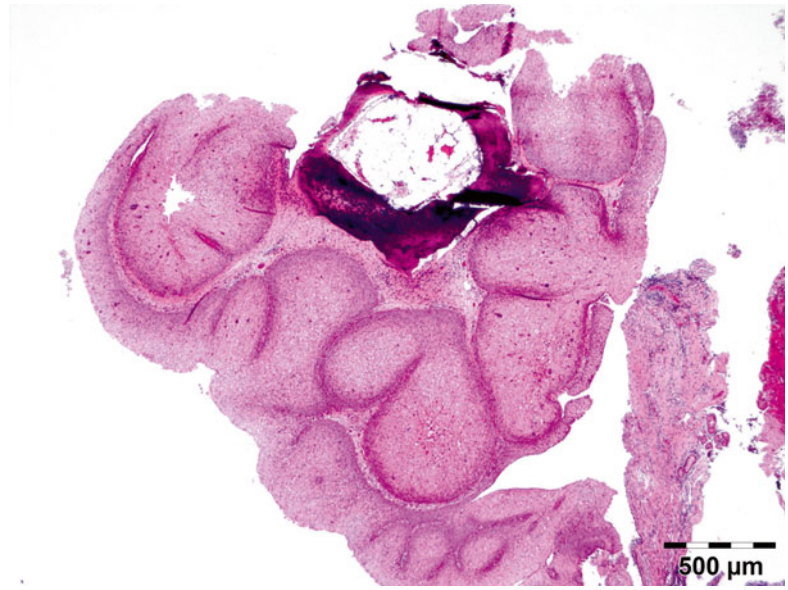

Fig. 12.179 Inverted papilloma of the lacrimal sac: nonkeratinizing acanthotic squamous epithelium showing an inverted papillomatous growth pattern (HE 25×) (Dr. Robert M. Verdijk)

distinction between benign papilloma and a carcinoma can be very difficult and sometimes impossible, in which case the initial surgery should aim for complete excision. A state intermediate between benignity and unequivocal malignancy seems to exist and repeated recurrence correlates with increasing histologic evidence of malignancy. The prognosis for carcinoma of the lacrimal sac is not encouraging. Human papillomavirus has been detected by PCR in many carcinomas of the lacrimal sac. Poor prognostic factors are marked pleomorphism, numerous mitotic figures, and stromal invasion. Treatment requires extensive surgical excision and radiation therapy; 50 % recur, and recurrences may cause death. Primary melanoma of the lacrimal sac is extremely rare [455, 456] (Fig. 12.177). Lymphoma of the lacrimal sac accounts for 50 % of all nonepithelial malignancies of the lacrimal sac. DLBCL and MALT lymphoma are equally common in the lacrimal sac

in contrast with the remaining periorbital and/or orbital region where MALT lymphoma predominates [216]. Mesenchymal tumors account for ±30 % of nonepithelial tumors; fibrous histiocytoma was the most common [457–459] (Fig. 12.178).

All photographs were made by Robert M Verdijk and Irene Pecorella and that the authors wish to acknowledge Frank van der Panne for assistence in editing the figures.

References

1. Barishak YR. Embryology of the eye and its adnexae. 2, revised edth ed. Freiburg: Karger; 2001. p. 132.
2. Jones KL, Higginbottom MC, Smith DW. Determining role of the optic vesicle in orbital and periocular development and placement. Pediatr Res. 1980;14(5):703–8.
3. de Haan AB, et al. The prenatal development of the human orbit. Strabismus. 2006;14(1):51–6.
4. Johnston MC, et al. Origins of avian ocular and periocular tissues. Exp Eye Res. 1979;29(1):27–43.
5. Le Lievre CS, Le Douarin NM. Mesenchymal derivatives of the neural crest: analysis of chimaeric quail and chick embryos. J Embryol Exp Morph. 1975;34(1):125–54.
6. Johnston MC, Bhakdinaronk A, Reid YC. An expanded role of the neural crest in oral and pharyngeal development. Symp Oral Sens Percept. 1973;4:37–52.
7. Johnston MC. A radioautographic study of the migration and fate of cranial neural crest cells in the chick embryo. Anat Rec. 1966;156(2):143–55.
8. Osanai H, et al. Human orbital muscle: a new point of view from the fetal development of extraocular connective tissues. Invest Ophthalmol Vis Sci. 2010;52(3):1501–6.
9. Fries PD, Katowitz JA. Congenital craniofacial anomalies of ophthalmic importance. Surv Ophthalmol. 1990;35(2):87–119.
10. Koornneef L. The development of the connective tissue in the human orbit. Acta Morph Neerl Scand. 1976;14(4):263–90.
11. Koornneef L. Orbital septa: anatomy and function. Ophthalmology. 1979;86(5):876–80.
12. Koornneef L. New insights in the human orbital connective tissue. Result of a new anatomical approach. Arch Ophthalmol. 1977;95(7):1269–73.
13. Koornneef L. Details of the orbital connective tissue system in the adult. Acta Morph Neerlandica Scand. 1977;15(1):1–34.
14. Koornneef L. Eyelid and orbital fascial attachments and their clinical significance. Eye (Lond). 1988;2(Pt 2):130–4.
15. Henderson JW, et al. Orbital cysts. In: Henderson JW, editor. Orbital tumors. Philadelphia: W.B. Saunders; 1973. p. 86–123.
16. Shields JA, Shields CL. Orbital cysts of childhood–classification, clinical features, and management. Surv Ophthalmol. 2004;49(3):281–99.
17. West JA, Drewe RH, McNab AA. Atypical choristomatous cysts of the orbit. Aust N Z J Ophthalmol. 1997;25(2):117–23.
18. von Domarus H. A lacrimal gland cyst in the orbit. J Craniomaxillofac Surg. 1987;15(2):106–9.
19. Suh MH, et al. Osseous choristoma of an extraocular muscle. J AAPOS. 2008;12(1):83–4.
20. Iliff WJ, Green WR. Orbital tumors in children. In: Jakobiec FA, editor. Ocular and adnexal tumors. Birmingham: Aesculapium Publishing Company; 1978. p. 669–84.
21. Moon JH, et al. Bilateral ocular osseous choristomas. Pediatr Radiol. 2005;35(11):1145–6.
22. Wolter JR, Roosenberg RJ. Ectopic lymph node of the orbit simulating a lacrimal gland tumor. Am J Ophthalmol. 1977;83(6):908–14.
23. Wang H, et al. Ectopic pituitary adenoma in the spheno-orbital region. J Neuroophthalmol. 2010;30(2):135–7.
24. Rootman J. Diseases of the orbit: a multidisciplinary approach. 2nd ed. Philadelphia: Lippincott Williams & Wilkins; 2003. p. 579.
25. Karcioğlu ZA. Orbital tumors: diagnosis and treatment. 1st ed. New York: Springer; 2005.
26. Weill A, et al. Embolization of an orbital varix after surgical exposure. AJNR Am J Neuroradiol. 1998;19(5):921–3.
27. Porges Y, et al. Hereditary microphthalmia with colobomatous cyst. Am J Ophthalmol. 1992;114(1):30–4.
28. Mihora LD, et al. Ectopic orbital brain diagnosed 20 years after symptomatic presentation. Orbit. 2009;28(2–3):185–7.
29. Islam N, et al. Orbital varices, cranial defects, and encephaloceles: an unrecognized association. Ophthalmology. 2004;111(6):1244–7.
30. Chan JK. Inflammatory pseudotumor: a family of lesions of diverse nature and aetiologies. Adv Anat Pathol. 1996;3(3):156–71.
31. Manschot WA. Coenurus infestation of eye and orbit. Arch Ophthalmol. 1976;94(6):961–4.
32. Brihaye M, et al. Hydatid cyst of the orbit. Bull Soc Belge Ophtalmol. 1967;146:317–28.
33. Pushker N, et al. Ocular and orbital cysticercosis. Acta Ophthalmol Scand. 2001;79(4):408–13.
34. Manschot WA. Intraocular cysticercus. Arch Ophthalmol. 1968;80(6):772–4.
35. Orihel TC, Eberhard ML. Zoonotic filariasis. Clin Microbiol Rev. 1998;11(2):366–81.
36. McNab AA, Wright JE. Orbitofrontal cholesterol granuloma. Ophthalmology. 1990;97(1):28–32.
37. Fukuta K, Jackson IT. Epidermoid cyst and cholesterol granuloma of the orbit. Br J Plast Surg. 1990;43(5):521–7.

38. Donker DL, et al. Blepharoptosis and upper eyelid swelling due to lipogranulomatous inflammation caused by silicone oil. Am J Ophthalmol. 2005;140(5):934–6.
39. Witschel H, Geiger K. Paraffin induced sclerosing lipogranuloma of eyelids and anterior orbit following endonasal sinus surgery. Br J Ophthalmol. 1994;78(1):61–5.
40. van Steensel L, et al. Orbit-infiltrating mast cells, monocytes, and macrophages produce PDGF isoforms that orchestrate orbital fibroblast activation in Graves' ophthalmopathy. J Clin Endocrinol Metab. 2012;97(3):E400–8.
41. Soeters MR, et al. Optimal management of Graves orbitopathy: a multidisciplinary approach. Neth J Med. 2011;69(7):302–8.
42. LeBedis CA, Sakai O. Nontraumatic orbital conditions: diagnosis with CT and MR imaging in the emergent setting. Radiographics. 2008;28(6):1741–53.
43. Yuen SJ, Rubin PA. Idiopathic orbital inflammation: distribution, clinical features, and treatment outcome. Arch Ophthalmol. 2003;121(4):491–9.
44. Yuen SJ, Rubin PA. Idiopathic orbital inflammation: ocular mechanisms and clinicopathology. Ophthalmol Clin N Am. 2002;15(1):121–6.
45. Belanger C, et al. Inflammatory disorders of the orbit in childhood: a case series. Am J Ophthalmol. 2010;150(4):460–3.
46. Swamy BN, et al. Idiopathic orbital inflammatory syndrome: clinical features and treatment outcomes. Br J Ophthalmol. 2007;91(12):1667–70.
47. Rootman J, et al. Idiopathic sclerosing inflammation of the orbit. A distinct clinicopathologic entity. Ophthalmology. 1994;101(3):570–84.
48. Divatia M, Kim SA, Ro JY. IgG4-related sclerosing disease, an emerging entity: a review of a multisystem disease. Yonsei Med J. 2012;53(1):15–34.
49. Cheuk W, Chan JK. IgG4-related sclerosing disease: a critical appraisal of an evolving clinicopathologic entity. Adv Anat Pathol. 2010;17(5):303–32.
50. Takahira M, et al. IgG4-related chronic sclerosing dacryoadenitis. Arch Ophthalmol. 2007;125(11):1575–8.
51. Wallace ZS, et al. IgG4-related systemic disease as a cause of "idiopathic" orbital inflammation, including orbital myositis, and trigeminal nerve involvement. Surv Ophthalmol. 2012;57(1):26–33.
52. Matsui S, et al. Respiratory involvement in IgG4-related Mikulicz's disease. Mod Rheumatol. 2011;22(1):31–9.
53. Plaza JA, et al. Orbital inflammation with IgG4-positive plasma cells: manifestation of IgG4 systemic disease. Arch Ophthalmol. 2011;129(4):421–8.
54. Go H, et al. Ocular adnexal IgG4-related disease: comparative analysis with mucosa-associated lymphoid tissue lymphoma and other chronic inflammatory conditions. Histopathology. 2012;60(2):296–312.
55. Andrew N, Kearney D, Selva D. IgG4-related orbital disease: a meta-analysis and review. Acta Ophthalmol. 2013;91(8):694–700.
56. Singh K, Rajan KD, Eberhart C. Orbital necrobiotic xanthogranuloma associated with systemic IgG4 disease. Ocul Immunol Inflamm. 2010;18(5):373–8.
57. Mudhar HS, Bhatt R, Sandramouli S. Xanthogranulomatous variant of immunoglobulin G4 sclerosing disease presenting as ptosis, proptosis and eyelid skin plaques. Int Ophthalmol. 2011;31(3):245–8.
58. Kubota T, et al. Ocular adnexal marginal zone B cell lymphoma infiltrated by IgG4-positive plasma cells. J Clin Pathol. 2010;63(12):1059–65.
59. Sivak-Callcott JA, et al. Adult xanthogranulomatous disease of the orbit and ocular adnexa: new immunohistochemical findings and clinical review. Br J Ophthalmol. 2006;90(5):602–8.
60. Jaffe R, et al. Histiocytic and dendritic neoplasms. In: Swerdlow SH, editor. WHO classification of tumours of haematopoietic and lymphoid tissues. Geneva: IARC; 2008. p. 354–5.
61. Verdijk RM, et al. Raised numbers of IgG4-positive plasma cells are a common histopathological finding in orbital xanthogranulomatous disease. Orbit. 2013;33(1):17–22.
62. Jakobiec FA, et al. Periocular xanthogranulomas associated with severe adult-onset asthma. Trans Am Ophthalmol Soc. 1993;91:99–125; discussion 125–9.
63. Ugurlu S, Bartley GB, Gibson LE. Necrobiotic xanthogranuloma: long-term outcome of ocular and systemic involvement. Am J Ophthalmol. 2000;129(5):651–7.
64. Johnson TE, et al. Extensive juvenile xanthogranuloma involving the orbit, sinuses, brain, and subtemporal fossa in a newborn. Ophthal Plast Reconstr Surg. 2010;26(2):133–4.
65. Betts DR, et al. Constitutional balanced chromosomal rearrangements and neoplasm in children. J Pediatr Hematol Oncol. 2001;23(9):582–4.
66. Woywodt A, Matteson EL. Wegener's granulomatosis – probing the untold past of the man behind the eponym. Rheumatology (Oxford). 2006;45(10):1303–6.
67. Perry SR, Rootman J, White VA. The clinical and pathologic constellation of Wegener granulomatosis of the orbit. Ophthalmology. 1997;104(4):683–94.
68. Perumal B, et al. Non-infectious orbital vasculitides. Eye (Lond). 2012;26(5):630–9.
69. Ohsie LH, Murchison AP, Wojno TH. Lupus erythematosus profundus masquerading as idiopathic orbital inflammatory syndrome. Orbit. 2012;31(3):181–3.
70. Jordan N, et al. Dacryoadenitis and diffuse orbital inflammation: unusual first presentations of Churg-Strauss syndrome. Orbit. 2011;30(3):160–1.
71. Borruat FX, et al. Orbital infarction syndrome. Ophthalmology. 1993;100(4):562–8.
72. Demirci H, Christianson MD. Orbital and adnexal involvement in sarcoidosis: analysis of clinical features and systemic disease in 30 cases. Am J Ophthalmol. 2011;151(6):1074–80.e1.
73. Messmer EP, et al. Amputation neuroma of the orbit. Report of two cases and review of the literature. Ophthalmology. 1984;91(11):1420–3.

74. Schick U, Hassler W. Treatment of deep vascular orbital malformations. Clin Neurol Neurosurg. 2009;111(10):801–7.
75. Knowles 2nd DM, et al. Amyloidosis of the orbit and adnexae. Surv Ophthalmol. 1975;19(6):367–84.
76. Murdoch IE, et al. Primary localised amyloidosis of the orbit. Br J Ophthalmol. 1996;80(12):1083–6.
77. Goshe JM, et al. Myeloma-associated orbital amyloidosis. Orbit. 2010;29(5):274–7.
78. Connors LH, et al. Tabulation of human transthyretin (TTR) variants, 2003. Amyloid. 2003;10(3):160–84.
79. Fletcher CD, Unni KK, Mertens F. Pathology and genetics of tumours of soft tissue and bone. In: Kleihues P, Sobin LH, editors. World Health Organization classification of tumours. Lyon: IARCPress; 2002.
80. DiNardo LJ, Wetmore RF, Potsic WP. Nodular fasciitis of the head and neck in children. A deceptive lesion. Arch Otolaryngol Head Neck Surg. 1991;117(9):1001–2.
81. Shields JA, et al. Orbital nodular fasciitis simulating a dermoid cyst in an 8-month-old child. Case report and review of the literature. Ophthal Plast Reconstr Surg. 2001;17(2):144–8.
82. Tolls RE, Mohr S, Spencer WH. Benign nodular fasciitis originating in Tenon's capsule. Arch Ophthalmol. 1966;75(4):482–3.
83. Ferry AP, Sherman SE. Nodular fasciitis of the conjunctiva apparently originating in the fascia bulbi (Tenon's capsule). Am J Ophthalmol. 1974;78(3):514–7.
84. Riffle JE, et al. Nodular fasciitis of the orbit: a case report and brief review of the literature. Case Rep Ophthalmol Med. 2011;2011:235956.
85. Damasceno RW, et al. Nodular fasciitis of the eyelid and anterior orbit in children: case report and review of the literature. Ophthalmologe. 2009;106(9):829–31.
86. Weiss SW, Goldblum JR. Enzinger & Weiss's soft tissue tumors. 5th ed. Philadelphia: Mosby; 2008.
87. Mynatt CJ, Feldman KA, Thompson LD. Orbital infantile myofibroma: a case report and clinicopathologic review of 24 cases from the literature. Head Neck Pathol. 2011;5(3):205–15.
88. Gatibelza ME, et al. Isolated infantile myofibromatosis of the upper eyelid: uncommon localization and long-term results after surgical management. J Pediatr Surg. 2012;47(7):1457–9.
89. Bloom RI, et al. A case of congenital myofibroma of the orbit presenting at birth. Orbit. 2013;32(1):33–5.
90. Duffy MT, Harris M, Hornblass A. Infantile myofibromatosis of orbital bone. A case report with computed tomography, magnetic resonance imaging, and histologic findings. Ophthalmology. 1997;104(9):1471–4.
91. Calsina M, et al. Solitary orbital myofibroma: clinical, radiographic, and histopathologic findings. A report of two cases. Orbit. 2011;30(4):180–2.
92. De Wan J, Evens F, De Mey A. Eyelid tumour and juvenile hyaline fibromatosis. Br J Plast Surg. 2005;58(1):106–11.
93. Pushker N, et al. Infantile hemangiopericytoma of the orbit treated with primary chemotherapy. J Pediatr Ophthalmol Strabismus. 2012;49:e23–5.
94. Mentzel T, et al. Infantile hemangiopericytoma versus infantile myofibromatosis. Study of a series suggesting a continuous spectrum of infantile myofibroblastic lesions. Am J Surg Pathol. 1994;18(9):922–30.
95. Polito E, et al. Inflammatory myofibroblastic tumor of the orbit. Ophthalmologica. 2007;221(5):353–5.
96. Cessna MH, et al. Expression of ALK1 and p80 in inflammatory myofibroblastic tumor and its mesenchymal mimics: a study of 135 cases. Mod Pathol. 2002;15(9):931–8.
97. O'Malley DP, et al. Intraocular inflammatory myofibroblastic tumor with ALK overexpression. Arch Pathol Lab Med. 2004;128(1):e5–7.
98. Sa HS, et al. Inflammatory myofibroblastic tumor of the orbit presenting as a subconjunctival mass. Ophthal Plast Reconstr Surg. 2005;21(3):211–5.
99. Yamamoto H, et al. Inflammatory myofibroblastic tumor versus IgG4-related sclerosing disease and inflammatory pseudotumor: a comparative clinicopathologic study. Am J Surg Pathol. 2009;33(9):1330–40.
100. Furusato E, et al. Orbital solitary fibrous tumor: encompassing terminology for hemangiopericytoma, giant cell angiofibroma, and fibrous histiocytoma of the orbit: reappraisal of 41 cases. Hum Pathol. 2010;42(1):120–8.
101. Bernardini FP, et al. Solitary fibrous tumor of the orbit: is it rare? Report of a case series and review of the literature. Ophthalmology. 2003;110(7):1442–8.
102. Font RL, Hidayat AA. Fibrous histiocytoma of the orbit. A clinicopathologic study of 150 cases. Hum Pathol. 1982;13(3):199–209.
103. Hidayat AA, et al. Myxomas and angiomyxomas of the orbit: a clinicopathologic study of 6 cases. Ophthalmology. 2007;114(5):1012–9.
104. Zhang Q, et al. Myxofibrosarcoma of the orbit: a clinicopathologic case report. Ophthal Plast Reconstr Surg. 2010;26(2):129–31.
105. Russell H, et al. Infantile fibrosarcoma: clinical and histologic responses to cytotoxic chemotherapy. Pediatr Blood Cancer. 2009;53(1):23–7.
106. Bartley GB, et al. Spindle cell lipoma of the orbit. Am J Ophthalmol. 1985;100(4):605–9.
107. Johnson BL, Linn Jr JG. Spindle cell lipoma of the orbit. Arch Ophthalmol. 1979;97(1):133–4.
108. Daniel CS, et al. Pleomorphic lipoma of the orbit: a case series and review of literature. Ophthalmology. 2003;110(1):101–5.
109. Dutton JJ, Wright Jr JD. Intramuscular lipoma of the superior oblique muscle. Orbit. 2006;25(3):227–33.
110. Kim MH, et al. Fibrolipoma of the orbit. Ophthal Plast Reconstr Surg. 2011;27(1):e16–8.
111. Farah-Klibi F, et al. Lipomatous hemangiopericytoma (adipocytic variant of solitary fibrous tumor) of the orbit. A case report with review of the literature. Pathologica. 2006;98(6):645–8.

112. Jakobiec FA, et al. MDM2-positive atypical lipomatous neoplasm/well-differentiated liposarcoma versus spindle cell lipoma of the orbit. Ophthal Plast Reconstr Surg. 2010;26(6):413–5.
113. Madge SN, et al. Primary orbital liposarcoma. Ophthalmology. 2010;117(3):606–14.
114. Shinder R, et al. Primary orbital liposarcoma misdiagnosed as thyroid associated orbitopathy. Orbit. 2012;31(4):264–6.
115. Hannachi Sassi S, et al. Orbital metastasis of liposarcoma. J Fr Ophtalmol. 2007;30(9):e28.
116. Cai YC, et al. Primary liposarcoma of the orbit: a clinicopathologic study of seven cases. Ann Diagn Pathol. 2001;5(5):255–66.
117. Ebrahimi KB, Ren S, Green WR. Floretlike cells in in situ and prolapsed orbital fat. Ophthalmology. 2007;114(12):2345–9.
118. Thway K, et al. Diagnostic utility of p16, CDK4, and MDM2 as an immunohistochemical panel in distinguishing well-differentiated and dedifferentiated liposarcomas from other adipocytic tumors. Am J Surg Pathol. 2012;36(3):462–9.
119. Arat YO, et al. Leiomyoma of the orbit and periocular region: a clinicopathologic study of four cases. Ophthal Plast Reconstr Surg. 2005;21(1):16–22.
120. Fernandes BF, et al. Orbital leiomyoma: histopathologic and immunohistochemical findings of a rare tumor. Ophthal Plast Reconstr Surg. 2009;25(1):59–61.
121. Gunduz K, et al. Orbital leiomyoma: report of a case and review of the literature. Surv Ophthalmol. 2004;49(2):237–42.
122. Chen J, Wei R, Ma X. Orbital metastasis of retroperitoneal leiomyosarcoma. Med Oncol. 2012;29(1):392–5.
123. Hou LC, Murphy MA, Tung GA. Primary orbital leiomyosarcoma: a case report with MRI findings. Am J Ophthalmol. 2003;135(3):408–10.
124. Klippenstein KA, Wesley RE, Glick AD. Orbital leiomyosarcoma after retinoblastoma. Ophthalmic Surg Lasers. 1999;30(7):579–83.
125. Li YP, et al. Rhabdomyoma of the orbit. J Pediatr Ophthalmol Strabismus. 2008;45(2):113–5.
126. Stout AP. Rhabdomyosarcoma of the skeletal muscles. Ann Surg. 1946;123(3):447–72.
127. Arndt CA, Crist WM. Common musculoskeletal tumors of childhood and adolescence. N Engl J Med. 1999;341(5):342–52.
128. Newton Jr WA, et al. Histopathology of childhood sarcomas, Intergroup Rhabdomyosarcoma Studies I and II: clinicopathologic correlation. J Clin Oncol. 1988;6(1):67–75.
129. Kodet R, et al. Orbital rhabdomyosarcomas and related tumors in childhood: relationship of morphology to prognosis–an Intergroup Rhabdomyosarcoma study. Med Pediatr Oncol. 1997;29(1):51–60.
130. Polito E, et al. A case of primary botryoid conjunctival rhabdomyosarcoma. Graefes Arch Clin Exp Ophthalmol. 2006;244(4):517–9.
131. Qualman SJ, et al. Intergroup Rhabdomyosarcoma Study: update for pathologists. Pediatr Dev Pathol. 1998;1(6):550–61.
132. Chaves E. Pleomorphic rhabdomyosarcoma of the orbit. Presentation of a case. Rev Bras Oftalmol. 1967;26(1):73–82.
133. Furlong MA, Fanburg-Smith JC. Pleomorphic rhabdomyosarcoma in children: four cases in the pediatric age group. Ann Diagn Pathol. 2001;5(4):199–206.
134. Furlong MA, Mentzel T, Fanburg-Smith JC. Pleomorphic rhabdomyosarcoma in adults: a clinicopathologic study of 38 cases with emphasis on morphologic variants and recent skeletal muscle-specific markers. Mod Pathol. 2001;14(6):595–603.
135. Sullivan LM, Atkins KA, LeGallo RD. PAX immunoreactivity identifies alveolar rhabdomyosarcoma. Am J Surg Pathol. 2009;33(5):775–80.
136. Barr FG. Molecular genetics and pathogenesis of rhabdomyosarcoma. J Pediatr Hematol Oncol. 1997;19(6):483–91.
137. Sumegi J, et al. Recurrent t(2;2) and t(2;8) translocations in rhabdomyosarcoma without the canonical PAX-FOXO1 fuse PAX3 to members of the nuclear receptor transcriptional coactivator family. Genes Chromosome Cancer. 2010;49(3):224–36.
138. Punyko JA, et al. Long-term survival probabilities for childhood rhabdomyosarcoma. A population-based evaluation. Cancer. 2005;103(7):1475–83.
139. Ulivieri S, et al. Orbital glomangioma. Orbit. 2012;31(4):216–8.
140. Granter SR, Badizadegan K, Fletcher CD. Myofibromatosis in adults, glomangiopericytoma, and myopericytoma: a spectrum of tumors showing perivascular myoid differentiation. Am J Surg Pathol. 1998;22(5):513–25.
141. Rosca TI, et al. Vascular tumors in the orbit–capillary and cavernous hemangiomas. Ann Diagn Pathol. 2006;10(1):13–9.
142. Acocella A, Catelani C, Nardi P. Angiolymphoid hyperplasia with eosinophilia: a case report of orbital involvement. J Oral Maxillofac Surg. 2005;63(1):140–4.
143. Seregard S. Angiolymphoid hyperplasia with eosinophilia should not be confused with Kimura's disease. Acta Ophthalmol Scand. 2001;79(1):91–3.
144. Lopes M, Duffau H, Fleuridas G. Primary sphenoorbital angiosarcoma: case report and review of the literature. Neurosurgery. 1999;44(2):405–7; discussion 407–8.
145. Lyon DB, Tang TT, Kidder TM. Epithelioid hemangioendothelioma of the orbital bones. Ophthalmology. 1992;99(12):1773–8.
146. Kivela T, Tarkkanen A. Orbital germ cell tumors revisited: a clinicopathological approach to classification. Surv Ophthalmol. 1994;38(6):541–54.
147. Oosterhuis JW, et al. Why human extragonadal germ cell tumours occur in the midline of the body: old concepts, new perspectives. Int J Androl. 2007;30(4):256–63; discussion 263–4.
148. Norris HJ, Zirkin HJ, Benson WL. Immature (malignant) teratoma of the ovary: a clinical and pathologic study of 58 cases. Cancer. 1976;37(5):2359–72.
149. Gonzalez-Crussi F. Extragonadal teratomas. In: Hartmann WH, editor. Atlas of tumor pathology.

2nd ed. Washington, DC: Armed Forces Institute of Pathology; 1982.
150. Bernoulli R. On a primary teratoid sarcoma of the orbit. Opt Acta Lond. 1962;143:370–7.
151. Mahesh L, et al. Malignant teratoma of the orbit: a clinicopathological study of a case. Orbit. 2003;22(4):305–9.
152. Soares E, da Silva Lopes K, de Souza Andrade J. Orbital malignant teratoma. A case report. Orbit. 1983;2:235–42.
153. Garden JW, McManis JC. Congenital orbital-intracranial teratoma with subsequent malignancy: case report. Br J Ophthalmol. 1986;70(2):111–3.
154. Ogun OA, et al. Congenital orbital teratoma: a case report and challenges of its management in a resource limited setting. Pan Afr Med J. 2012;12:3.
155. O'Connor DM, Norris HJ. The influence of grade on the outcome of stage I ovarian immature (malignant) teratomas and the reproducibility of grading. Int J Gynecol Pathol. 1994;13(4):283–9.
156. Kiratli H, Erkan Balci K, Guler G. Primary orbital endodermal sinus tumor (yolk sac tumor). J AAPOS. 2008;12(6):623–5.
157. Margo CE, et al. Endodermal sinus tumor (yolk sac tumor) of the orbit. Ophthalmology. 1983;90(12):1426–32.
158. Perrini P, et al. Primary germinoma of the orbit. Neurosurgery. 2005;57(4):E813.
159. Altan-Yaycioglu R, Hintschich C. Clinical features and surgical management of orbitotemporal neurofibromatosis: a retrospective interventional case series. Orbit. 2010;29(5):232–8.
160. Singhal D, et al. Soft tissue management of orbitotemporal neurofibromatosis. J Craniofac Surg. 2013;24(1):269–72.
161. Spencer WH. Ophthalmic Pathology: An Atlas and Textbook, 4th edition. Philadelphia: W.B. Saunders; 1996. p. 125–155.
162. Pecorella I, Toth J, Lukats O. Ancient schwannoma of the orbit. Pathologica. 2012;104(4):182–4.
163. Dolman PJ, Rootman J, Dolman CL. Infiltrating orbital granular cell tumour: a case report and literature review. Br J Ophthalmol. 1987;71(1):47–53.
164. Poyraz CE, Kiratli H, Soylemezoglu F. Granular cell tumor of the inferior rectus muscle. Korean J Ophthalmol. 2009;23(1):43–5.
165. Romero-Rojas AE, Diaz-Perez JA, Lozano-Castillo A. Malignant peripheric nerve sheath tumor of the orbit: first description of orbital location in a patient with NF1. Neurocirugia (Astur). 2010;21(1):37–45.
166. Verdijk RM, et al. TP53 mutation analysis of malignant peripheral nerve sheath tumors. J Neuropathol Exp Neurol. 2010;69(1):16–26.
167. Overweg-Plandsoen WC, et al. Neurofibromatosis type 1: a survey of 195 patients. Ned Tijdschr Geneeskd. 1997;141(13):624–9.
168. Poyhonen M, Niemela S, Herva R. Risk of malignancy and death in neurofibromatosis. Arch Pathol Lab Med. 1997;121(2):139–43.
169. Rothenberg AB, et al. Neuroblastoma-remembering the three physicians who described it a century ago: James Homer Wright, William Pepper, and Robert Hutchison. Pediatr Radiol. 2009;39(2):155–60.
170. Okamatsu C, et al. Clinicopathological characteristics of ganglioneuroma and ganglioneuroblastoma: a report from the CCG and COG. Pediatr Blood Cancer. 2009;53(4):563–9.
171. Romero R, et al. Peripheral primitive neuroectodermal tumour of the orbit. Br J Ophthalmol. 2011;95(7):915–20.
172. Chokthaweesak W, et al. Primitive neuroectodermal tumor of the orbit in adults: a case series. Ophthal Plast Reconstr Surg. 2011;27(3):173–9.
173. Luo W, Xiao EH. CT, MRI and pathologic features of peripheral primitive neuroectodermal tumors: a report of eight cases with literature review. Ai Zheng. 2008;27(6):627–32.
174. Jedlicka P. Ewing Sarcoma, an enigmatic malignancy of likely progenitor cell origin, driven by transcription factor oncogenic fusions. Int J Clin Exp Pathol. 2010;3(4):338–47.
175. Fratkin JD, et al. Wilms' tumor metastatic to the orbit. JAMA. 1977;238(17):1841–2.
176. Kahwash SB, Qualman SJ. Cutaneous lymphoblastic lymphoma in children: report of six cases with precursor B-cell lineage. Pediatr Dev Pathol. 2002;5(1):45–53.
177. Randolph TR. Advances in acute lymphoblastic leukemia. Clin Lab Sci. 2004;17(4):235–45.
178. Gunduz K, Esmaeli B. Diagnosis and Management of Malignant Tumors of the Eyelid, Conjunctiva, and Orbit. Expert Rev Ophthalmol. 2008;3(1):63–75.
179. Hoyt WF, et al. Malignant optic glioma of adulthood. Brain. 1973;96(1):121–32.
180. Tari AS, Fard MA. Solitary orbital paget disease: a case report. Orbit. 2010;29(4):219–21.
181. Goldberg S, et al. Sarcomatous transformation of the orbit in a patient with Paget's disease. Ophthalmology. 2000;107(8):1464–7.
182. Harris AE, et al. Giant cell tumor of the skull: a case report and review of the literature. Surg Neurol. 2004;61(3):274–7.
183. Goisis M, et al. Fibrous dysplasia of the orbital region: current clinical perspectives in ophthalmology and cranio-maxillofacial surgery. Ophthal Plast Reconstr Surg. 2006;22(5):383–7.
184. Selva D, et al. Primary bone tumors of the orbit. Surv Ophthalmol. 2004;49(3):328–42.
185. Chen CJ, et al. Malignant infantile osteopetrosis initially presenting with neonatal hypocalcemia: case report. Ann Hematol. 2003;82(1):64–7.
186. Stark Z, Savarirayan R. Osteopetrosis. Orphanet J Rare Dis. 2009;4:5.
187. Kashkouli MB, et al. Primary endo-orbital osteoid osteoma. Orbit. 2008;27(3):211–3.
188. Dhermy P, Mazabraud A, Offret G. Tumors and pseudo-tumoral dysplasias of orbital bones. Arch Ophtalmol Paris. 1977;37(4):249–72.
189. Blodi FC. Pathology of orbital bones. The XXXII Edward Jackson Memorial lecture. Am J Ophthalmol. 1976;81(1):1–26.

190. McHugh JB, Mukherji SK, Lucas DR. Sino-orbital osteoma: a clinicopathologic study of 45 surgically treated cases with emphasis on tumors with osteoblastoma-like features. Arch Pathol Lab Med. 2009;133(10):1587–93.
191. Morita R, Shimada K, Kawakami S. Low-grade central osteosarcoma of the orbit. J Craniofac Surg. 2012;23(3):e178–80.
192. Fan JC, et al. Primary orbital extraskeletal osteosarcoma. Orbit. 2011;30(6):297–9.
193. Khouja N, et al. Mesenchymal extraskeletal chondrosarcoma of the orbit. Report of a case and review of the literature. Surg Neurol. 1999;52(1):50–3.
194. Daicker BC. Orbital chordoma. Ophthalmologica. 1978;176(4):236–9.
195. Vidor I, et al. Chordoma of the anterior cranial fossa and ethmoids with orbital involvement. Orbit. 2008;27(6):444–50.
196. Moshari A, et al. Ectopic chordoma with orbital invasion. Am J Ophthalmol. 2001;131(3):400–1.
197. Louis DN, et al. WHO classification of tumours of the central nervous system. In: Bosman FT, editor. World Health Organization classification of tumours. 4th ed. Lyon: International Agency for Research on Cancer; 2007.
198. Walsh F. Meningiomas, primary within the orbit and optic canal. In: Neuro-ophthalmology, Symposium of the University of Miami and the Bascom Palmer Eye Institute. Halladale: Huffman Pub Co.; 1969.
199. Mawrin C, Perry A. Pathological classification and molecular genetics of meningiomas. J Neurooncol. 2010;99(3):379–91.
200. Wiemels J, Wrensch M, Claus EB. Epidemiology and etiology of meningioma. J Neurooncol. 2010;99(3):307–14.
201. Jakobiec FA, McLean I, Font RL. Clinicopathologic characteristics of orbital lymphoid hyperplasia. Ophthalmology. 1979;86(5):948–66.
202. Knowles DM. Malignant lymphomas and lymphoid hyperplasias that occur in the ocular adnexa (orbit, conjunctiva and eyelids). In: Knowles DM, editor. Neoplastic hematopathology. Philadelphia: Lippincott Williams & Wilkins; 2001. p. 1304.
203. McKelvie PA, et al. Ocular adnexal lymphoproliferative disease: a series of 73 cases. Clin Exp Ophthalmol. 2001;29(6):387–93.
204. Coupland SE, et al. Prognostic value of cell-cycle markers in ocular adnexal lymphoma: an assessment of 230 cases. Graefes Arch Clin Exp Ophthalmol. 2004;242(2):130–45.
205. Stacy RC, et al. Unifocal and multifocal reactive lymphoid hyperplasia vs follicular lymphoma of the ocular adnexa. Am J Ophthalmol. 2010;150(3):412–26.e1.
206. Dogan A, et al. CD10 and BCL-6 expression in paraffin sections of normal lymphoid tissue and B-cell lymphomas. Am J Surg Pathol. 2000;24(6):846–52.
207. Andrew NH, Kearney D, Selva D. Intraorbital corticosteroid injection for orbital reactive lymphoid hyperplasia. Eye (Lond). 2013;27:561–3.
208. Ho HH, et al. Treatment of benign lymphoid hyperplasia of the orbit with rituximab. Ophthal Plast Reconstr Surg. 2010;26(1):11–3.
209. Johansen S, et al. Orbital space-occupying lesions in Denmark 1974–1997. Acta Ophthalmol Scand. 2000;78(5):547–52.
210. Shields JA, Shields CL, Scartozzi R. Survey of 1264 patients with orbital tumors and simulating lesions: The 2002 Montgomery lecture, part 1. Ophthalmology. 2004;111(5):997–1008.
211. Ferry JA, et al. Lymphoma of the ocular adnexa: a study of 353 cases. Am J Surg Pathol. 2007;31(2):170–84.
212. Sjo LD, et al. Increasing incidence of ophthalmic lymphoma in Denmark from 1980 to 2005. Invest Ophthalmol Vis Sci. 2008;49(8):3283–8.
213. Henderson JW, Banks PM, Yeatts RP. T-cell lymphoma of the orbit. Mayo Clin Proc. 1989;64(8):940–4.
214. Chan CC, et al. Detection of *Helicobacter pylori* and *Chlamydia pneumoniae* genes in primary orbital lymphoma. Trans Am Ophthalmol Soc. 2006;104:62–70.
215. Jakobiec FA. Ocular adnexal lymphoid tumors: progress in need of clarification. Am J Ophthalmol. 2008;145(6):941–50.
216. Sjo LD, et al. Primary lymphoma of the lacrimal sac: an EORTC ophthalmic oncology task force study. Br J Ophthalmol. 2006;90(8):1004–9.
217. Coupland SE, Damato B. Lymphomas involving the eye and the ocular adnexa. Curr Opin Ophthalmol. 2006;17(6):523–31.
218. Sjo LD, et al. Extranodal marginal zone lymphoma in the ocular region: clinical, immunophenotypical, and cytogenetical characteristics. Invest Ophthalmol Vis Sci. 2009;50(2):516–22.
219. Coupland SE, Hummel M, Stein H. Ocular adnexal lymphomas: five case presentations and a review of the literature. Surv Ophthalmol. 2002;47(5):470–90.
220. Coupland SE, et al. A TNM-based clinical staging system of ocular adnexal lymphomas. Arch Pathol Lab Med. 2009;133(8):1262–7.
221. Uno T, et al. Radiotherapy for extranodal, marginal zone, B-cell lymphoma of mucosa-associated lymphoid tissue originating in the ocular adnexa: a multiinstitutional, retrospective review of 50 patients. Cancer. 2003;98(4):865–71.
222. Faridpooya K, et al. Precursor B lymphoblastic lymphoma of the orbit in a child: an unusual presentation of a non-Hodgkin lymphoma. Orbit. 2006;25(2):153–7.
223. Sahjpaul R, Elisevich K, Allen L. Hodgkin's disease of the orbit with intracranial extension. Ophthalmic Surg Lasers. 1996;27(3):239–42.
224. Rodman HI, Font RL. Orbital involvement in multiple myeloma. Review of the literature and report of three cases. Arch Ophthalmol. 1972;87(1):30–5.
225. Howling SJ, et al. Case report: the CT features of orbital multiple myeloma. Clin Radiol. 1998;53(4):304–5.

226. Ranchod TM, et al. Waldenstrom macroglobulinemia of the orbit. Ophthal Plast Reconstr Surg. 2008;24(1):76–7.
227. Ohta K, et al. Primary granulocytic sarcoma in the sphenoidal bone and orbit. Childs Nerv Syst. 2003;19(9):674–9.
228. Russo V, et al. Orbital and ocular manifestations of acute childhood leukemia: clinical and statistical analysis of 180 patients. Eur J Ophthalmol. 2008;18(4):619–23.
229. Mangla D, Dewan M, Meyer DR. Adult orbital myeloid sarcoma (granulocytic sarcoma): two cases and review of the literature. Orbit. 2012;31(6):438–40.
230. Herwig MC, et al. Langerhans cell histiocytosis of the orbit: five clinicopathologic cases and review of the literature. Surv Ophthalmol. 2013;58(4):330–40.
231. Haroche J, Arnaud L, Amoura Z. Erdheim-Chester disease. Curr Opin Rheumatol. 2012;24(1):53–9.
232. Haroche J, et al. Dramatic efficacy of vemurafenib in both multisystemic and refractory Erdheim-Chester disease and Langerhans cell histiocytosis harboring the BRAF V600E mutation. Blood. 2013;121(9):1495–500.
233. Vemuganti GK, Naik MN, Honavar SG. Rosai dorfman disease of the orbit. J Hematol Oncol. 2008;1:7.
234. Alyahya GA, Prause JU, Heegaard S. Castleman's disease in the orbit. A 20-year follow-up. Acta Ophthalmol Scand. 2002;80(5):540–2.
235. Venizelos I, et al. Orbital involvement in Castleman disease. Surv Ophthalmol. 2010;55(3):247–55.
236. Ratnatunga N, et al. Primary biphasic synovial sarcoma of the orbit. J Clin Pathol. 1992;45(3):265–7.
237. Votruba M, et al. Primary monophasic synovial sarcoma of the conjunctiva. Br J Ophthalmol. 2002;86(12):1453–4.
238. Liu K, et al. Primary synovial sarcoma in the orbit. J AAPOS. 2012;16(6):582–4.
239. Wladis EJ, Farber MG, Nepo AG. Metastatic synovial sarcoma to the orbit. Ophthal Plast Reconstr Surg. 2012;28(6):e131–2.
240. Gunduz K, et al. Malignant rhabdoid tumor of the orbit. Arch Ophthalmol. 1998;116(2):243–6.
241. Kook KH, et al. A case of congenital orbital malignant rhabdoid tumor: systemic metastasis following exenteration. Ophthalmologica. 2009;223(4):274–8.
242. Gunduz K, et al. Periorbital cellular blue nevus leading to orbitopalpebral and intracranial melanoma. Ophthalmology. 1998;105(11):2046–50.
243. Nakanishi K, et al. Recurrent melanotic neuroectodermal tumor in the orbit successfully treated with resection followed by pediculated periosteal flaps. Pediatr Blood Cancer. 2008;51(3):430–2.
244. Kapadia SB, et al. Melanotic neuroectodermal tumor of infancy. Clinicopathological, immunohistochemical, and flow cytometric study. Am J Surg Pathol. 1993;17(6):566–73.
245. Makhdoomi R, et al. Orbital paraganglioma – a case report and review of the literature. Clin Neuropathol. 2010;29(2):100–4.
246. Mititelu M, Stanton CA, Yeatts RP. Primary neuroendocrine tumor of the orbit progressing to neoplastic meningitis. Ophthal Plast Reconstr Surg. 2008;24(3):231–3.
247. Rose AM, Kabiru J, Rose GE. Alveolar soft-part sarcoma of the orbit. Afr J Paediatr Surg. 2011;8(1):82–4.
248. Joyama S, et al. Chromosome rearrangement at 17q25 and xp11.2 in alveolar soft-part sarcoma: a case report and review of the literature. Cancer. 1999;86(7):1246–50.
249. Daigeler A, et al. Alveolar soft part sarcoma: clinicopathological findings in a series of 11 cases. World J Surg Oncol. 2008;6:71.
250. Gunalp I, Gunduz K. Secondary orbital tumors. Ophthal Plast Reconstr Surg. 1997;13(1):31–5.
251. Krishna M. Diagnosis of metastatic neoplasms: an immunohistochemical approach. Arch Pathol Lab Med. 2010;134(2):207–15.
252. von Holstein SL, et al. Lacrimal gland lesions in Denmark between 1974 and 2007. Acta Ophthalmol. 2013;91(4):349–54.
253. de la Cuadra-Blanco C, Peces-Pena MD, Merida-Velasco JR. Morphogenesis of the human lacrimal gland. J Anat. 2003;203(5):531–6.
254. Makarenkova HP, et al. FGF10 is an inducer and Pax6 a competence factor for lacrimal gland development. Development. 2000;127(12):2563–72.
255. Kural G, Serifoglu A, Erture S. A case of aberrant lacrimal gland and fistula. Br J Ophthalmol. 1989;73(5):376–7.
256. O'Connor MA, Archer DB, Hart PM. Congenital fistulae of the lacrimal gland. Br J Ophthalmol. 1985;69(9):711–3.
257. Wieczorek R, et al. The immunoarchitecture of the normal human lacrimal gland. Relevancy for understanding pathologic conditions. Ophthalmology. 1988;95(1):100–9.
258. Knop E, Knop N. Lacrimal drainage-associated lymphoid tissue (LDALT): a part of the human mucosal immune system. Invest Ophthalmol Vis Sci. 2001;42(3):566–74.
259. Rai P, Shah SA, Kirshan H. Acute Dacryadenitis-analysis of 23 cases. Med Channel. 2009;15:71–6.
260. Srivastava V. Acute suppurative dacryoadenitis. Med J Armed Forces India. 2000;56:151–2.
261. Shields CL, et al. Clinicopathologic review of 142 cases of lacrimal gland lesions. Ophthalmology. 1989;96(4):431–5.
262. Hurwitz JJ. A practical approach to the management of lacrimal gland lesions. Ophthalmic Surg. 1982;13(10):829–36.
263. Al-Hashimi I, et al. Frequency and predictive value of the clinical manifestations in Sjogren's syndrome. J Oral Pathol Med. 2001;30(1):1–6.
264. Jakobiec FA, Stacy RC, Hatton MP. Clinical characterization and immunopathologic features of sclerosing dacryoadenitis and riedel thyroiditis. Arch Ophthalmol. 2010;128(12):1626–8.

265. Burkhalter E. Unique presentation of systemic lupus erythematosus. Arthritis Rheum. 1973;16(3):428.
266. Pulido JS, et al. Ocular manifestations of patients with circulating antineutrophil cytoplasmic antibodies. Arch Ophthalmol. 1990;108(6):845–50.
267. Nahata MC, Sethi PK. Traumatic prolapse of the lacrimal gland. Indian J Ophthalmol. 1973;21(1):43–4.
268. Halborg J, et al. Stones in the lacrimal gland: a rare condition. Acta Ophthalmol. 2009;87(6):672–5.
269. Prabhakaran VC, et al. Amyloidosis of lacrimal gland. Indian J Ophthalmol. 2009;57(6):461–3.
270. Damato BE, et al. Senile atrophy of the human lacrimal gland: the contribution of chronic inflammatory disease. Br J Ophthalmol. 1984;68(9):674–80.
271. Shields JA, et al. Classification and incidence of space-occupying lesions of the orbit. A survey of 645 biopsies. Arch Ophthalmol. 1984;102(11):1606–11.
272. Kennedy RE. An evaluation of 820 orbital cases. Trans Am Ophthalmol Soc. 1984;82:134–57.
273. Ni C, Kuo PK, Dryja TP. Histopathological classification of 272 primary epithelial tumors of the lacrimal gland. Chin Med J (Engl). 1992;105(6):481–5.
274. Shields JA, et al. Review: primary epithelial malignancies of the lacrimal gland: the 2003 Ramon L. Font lecture. Ophthal Plast Reconstr Surg. 2004;20(1):10–21.
275. Barnes L, et al. Pathology and genetics of head and neck tumours. 3rd ed. World Health Organization Classification of Tumours, vol 9. Lyon: IARC Press; 2005.
276. Weis E, et al. Epithelial lacrimal gland tumors: pathologic classification and current understanding. Arch Ophthalmol. 2009;127(8):1016–28.
277. von Holstein SL, et al. Granular cell tumour of the lacrimal gland. Acta Ophthalmol. 2009;87(8):926–7.
278. Snaathorst J, et al. Primary epithelial tumors of the lacrimal gland; a retrospective analysis of 22 patients. Int J Oral Maxillofac Surg. 2009;38(7):751–7.
279. Prabhakaran VC, et al. Lesions mimicking lacrimal gland pleomorphic adenoma. Br J Ophthalmol. 2010;94(11):1509–12.
280. Gupta A, Khandelwal A. Lacrimal gland pleomorphic adenoma: an inconceivable diagnosis in a child. BMJ Case Rep. 2013;2013:bcr009138.
281. Vagefi MR, et al. Atypical presentations of pleomorphic adenoma of the lacrimal gland. Ophthal Plast Reconstr Surg. 2007;23(4):272–4.
282. Rose GE, Wright JE. Pleomorphic adenoma of the lacrimal gland. Br J Ophthalmol. 1992;76(7):395–400.
283. Vangveeravong S, et al. Tumors arising in the palpebral lobe of the lacrimal gland. Ophthalmology. 1996;103(10):1606–12.
284. Ramlee N, Ramli N, Tajudin LS. Pleomorphic adenoma in the palpebral lobe of the lacrimal gland misdiagnosed as chalazion. Orbit. 2007;26(2):137–9.
285. Sen S, et al. Pleomorphic adenomas of the lacrimal gland: a clinicopathological analysis. Clin Exp Ophthalmol. 2004;32(5):523–5.
286. McNab AA, Satchi K. Recurrent lacrimal gland pleomorphic adenoma: clinical and computed tomography features. Ophthalmology. 2011;118(10):2088–92.
287. Tong JT, et al. Benign mixed tumor arising from an accessory lacrimal gland of Wolfring. Ophthal Plast Reconstr Surg. 1995;11(2):136–8.
288. Saini JS, Mukherjee AK, Naik P. Pleomorphic adenoma of Krause's gland in lower lid. Indian J Ophthalmol. 1985;33(3):181–2.
289. Venkataramayya K. Pleomorphic adenoma of Krause's gland. Indian J Ophthalmol. 1976;23(4):38–9.
290. Grossniklaus HE, Abbuhl MF, McLean IW. Immunohistologic properties of benign and malignant mixed tumor of the lacrimal gland. Am J Ophthalmol. 1990;110(5):540–9.
291. Zhao M, et al. Immunohistochemical demonstration of bone morphogenetic protein-2 and type II collagen in pleomorphic adenoma of salivary glands. J Oral Pathol Med. 1998;27(7):293–6.
292. Dardick I. Mounting evidence against current histogenetic concepts for salivary gland tumorigenesis. Eur J Morphol. 1998;36(Suppl):257–61.
293. Margaritescu C, et al. Tumoral stroma of salivary pleomorphic adenoma – histopathological, histochemical and immunohistochemical study. Rom J Morphol Embryol. 2005;46(3):211–23.
294. Bullerdiek J, et al. Cytogenetic subtyping of 220 salivary gland pleomorphic adenomas: correlation to occurrence, histological subtype, and in vitro cellular behavior. Cancer Genet Cytogenet. 1993;65(1):27–31.
295. Alyahya GA, et al. Pleomorphic adenoma arising in an accessory lacrimal gland of Wolfring. Ophthalmology. 2006;113(5):879–82.
296. Maran AG, Mackenzie IJ, Stanley RE. Recurrent pleomorphic adenomas of the parotid gland. Arch Otolaryngol. 1984;110(3):167–71.
297. Font FR, Gamel JW. Epithelial tumors of the lacrimal gland: analysis of 265 cases. In: Jakobiec FA, editor. Ocular and adnexal tumors. Birmingham: Aesculapius; 1978. p. 787–805.
298. Chandrasekhar J, Farr DR, Whear NM. Pleomorphic adenoma of the lacrimal gland: case report. Br J Oral Maxillofac Surg. 2001;39(5):390–3.
299. Bonavolonta G, et al. Warthin tumor of the lacrimal gland. Am J Ophthalmol. 1997;124(6):857–8.
300. Thompson AS, Bryant Jr HC. Histogenesis of papillary cystadenoma lymphomatosum (Warthin's tumor) of the parotid salivary gland. Am J Pathol. 1950;26(5):807–49.
301. Kleinsasser O, Klein HJ. Basal cell adenoma of the salivary glands. Arch Klin Exp Ohren Nasen Kehlkopfheilkd. 1967;189(3):302–16.
302. Zarbo RJ, et al. Salivary gland basal cell and canalicular adenomas: immunohistochemical demonstration of myoepithelial cell participation and morphogenetic considerations. Arch Pathol Lab Med. 2000;124(3):401–5.
303. Silbert JE, Braich P, Misra RP. Basal cell cystadenoma of the lacrimal gland: diagnostic pitfalls of a basaloid pattern in lacrimal tumours. Int Ophthalmol. 2011;31(1):43–6.

304. Khalil M, Arthurs B. Basal cell adenocarcinoma of the lacrimal gland. Ophthalmology. 2000;107(1):164–8.
305. Hartman LJ, Mourits MP, Canninga-van Dijk MR. An unusual tumour of the lacrimal gland. Br J Ophthalmol. 2003;87(3):363.
306. Economou MA, Seregard S, Sahlin S. Oncocytoma of the lacrimal gland. Acta Ophthalmol Scand. 2007;85(5):576–7.
307. Ostergaard J, Prause JU, Heegaard S. Oncocytic lesions of the ophthalmic region: a clinicopathological study with emphasis on cytokeratin expression. Acta Ophthalmol. 2011;89(3):263–7.
308. Riedel K, Stefani FH, Kampik A. Oncocytoma of the ocular adnexa. Klin Monbl Augenheilkd. 1983;182(6):544–8.
309. Tandler B. Fine structure of oncocytes in human salivary glands. Virchows Arch Pathol Anat Physiol Klin Med. 1966;341(4):317–26.
310. Prasad AR, et al. The myoepithelial immunophenotype in 135 benign and malignant salivary gland tumors other than pleomorphic adenoma. Arch Pathol Lab Med. 1999;123(9):801–6.
311. Calle CA, et al. Oncocytoma of the lacrimal gland: case report and review of the literature. Orbit. 2006;25(3):243–7.
312. Hamperl H. Benign and malignant oncocytoma. Cancer. 1962;15:1019–27.
313. Porcelli AM, et al. The genetic and metabolic signature of oncocytic transformation implicates HIF1alpha destabilization. Hum Mol Genet. 2010;19(6):1019–32.
314. Font RL, Garner A. Myoepithelioma of the lacrimal gland: report of a case with spindle cell morphology. Br J Ophthalmol. 1992;76(10):634–6.
315. Grossniklaus HE, et al. Myoepithelioma of the lacrimal gland. Arch Ophthalmol. 1997;115(12):1588–90.
316. Bolzoni A, et al. Benign myoepithelioma of the lacrimal gland: report of a case. Eur Arch Otorhinolaryngol. 2005;262(3):186–8.
317. Sassano P, et al. Interleukine-6 (IL-6) may be a link between myasthenia gravis and myoepithelioma of the parotid gland. Med Hypotheses. 2007;68(2):314–7.
318. Jaeger RG, et al. Expression of smooth-muscle actin in cultured cells from human plasmacytoid myoepithelioma. Oral Surg Oral Med Oral Pathol Oral Radiol Endod. 1997;84(6):663–7.
319. el-Naggar AK, et al. Cytogenetic analysis of a primary salivary gland myoepithelioma. Cancer Genet Cytogenet. 1999;113(1):49–53.
320. Okudela K, et al. Myoepithelioma of the lacrimal gland: report of a case with potentially malignant transformation. Pathol Int. 2000;50(3):238–43.
321. Font RL, Smith SL, Bryan RG. Malignant epithelial tumors of the lacrimal gland: a clinicopathologic study of 21 cases. Arch Ophthalmol. 1998;116(5):613–6.
322. Ferry AP, Font RL. Carcinoma metastatic to the orbit. Mod Probl Ophthalmol. 1975;14:377–81.
323. Stell PM. Adenoid cystic carcinoma. Clin Otolaryngol Allied Sci. 1986;11(4):267–91.
324. Paulino AF, Huvos AG. Epithelial tumors of the lacrimal glands: a clinicopathologic study. Ann Diagn Pathol. 1999;3(4):199–204.
325. Henderson JW. Intrinsic neoplasms of the lacrimal gland. In: Henderson JW, editor. Orbital tumors. Philadelphia: W.B. Saunders; 1973. p. 409–43.
326. Font RL, Croxatto JO, Rao NA. Tumors of the lacrimal gland. In: Tumors of the eye and ocular adnexa. Washington, DC: American Registry of Pathology/ Armed Forces Institute of Pathology; 2006. p. 223–346.
327. Zhou Q, et al. Increased numbers of P63-positive/ CD117-positive cells in advanced adenoid cystic carcinoma give a poorer prognosis. Diagn Pathol. 2012;7:119.
328. Seethala RR, et al. Adenoid cystic carcinoma with high-grade transformation: a report of 11 cases and a review of the literature. Am J Surg Pathol. 2007;31(11):1683–94.
329. Szanto PA, et al. Histologic grading of adenoid cystic carcinoma of the salivary glands. Cancer. 1984;54(6):1062–9.
330. Chau Y, et al. Dedifferentiation of adenoid cystic carcinoma: report of a case implicating p53 gene mutation. Hum Pathol. 2001;32(12):1403–7.
331. Esmaeli B, et al. Surgical management of locally advanced adenoid cystic carcinoma of the lacrimal gland. Ophthal Plast Reconstr Surg. 2006;22(5):366–70.
332. Woo VL, Bhuiya T, Kelsch R. Assessment of CD43 expression in adenoid cystic carcinomas, polymorphous low-grade adenocarcinomas, and monomorphic adenomas. Oral Surg Oral Med Oral Pathol Oral Radiol Endod. 2006;102(4):495–500.
333. von Holstein SL, et al. Adenoid cystic carcinoma of the lacrimal gland: MYB gene activation, genomic imbalances, and clinical characteristics. Ophthalmology. 2013;120:2130–8.
334. Mitani Y, et al. Comprehensive analysis of the MYB-NFIB gene fusion in salivary adenoid cystic carcinoma: incidence, variability, and clinicopathologic significance. Clin Cancer Res. 2010;16(19):4722–31.
335. Seethala RR. Histologic grading and prognostic biomarkers in salivary gland carcinomas. Adv Anat Pathol. 2011;18(1):29–45.
336. Le Tourneau C, et al. Role of chemotherapy and molecularly targeted agents in the treatment of adenoid cystic carcinoma of the lacrimal gland. Br J Ophthalmol. 2011;95(11):1483–9.
337. Jaso J, Malhotra R. Adenoid cystic carcinoma. Arch Pathol Lab Med. 2011;135(4):511–5.
338. Zhang J, Peng B. In vitro angiogenesis and expression of nuclear factor kappaB and VEGF in high and low metastasis cell lines of salivary gland adenoid cystic carcinoma. BMC Cancer. 2007;7:95.
339. Preisegger KH, et al. Prognostic impact of molecular analyses in adenoid cystic carcinomas of the salivary gland. Onkologie. 2001;24(3):273–7.

340. Gamel JW, Font RL. Adenoid cystic carcinoma of the lacrimal gland: the clinical significance of a basaloid histologic pattern. Hum Pathol. 1982;13(3):219–25.
341. Rao PH, et al. Deletion of 1p32-p36 is the most frequent genetic change and poor prognostic marker in adenoid cystic carcinoma of the salivary glands. Clin Cancer Res. 2008;14(16):5181–7.
342. Luna MA, et al. Flow cytometric DNA content of adenoid cystic carcinoma of submandibular gland. Correlation of histologic features and prognosis. Arch Otolaryngol Head Neck Surg. 1990;116(11):1291–6.
343. Lee DA, et al. A clinicopathologic study of primary adenoid cystic carcinoma of the lacrimal gland. Ophthalmology. 1985;92(1):128–34.
344. Esmaeli B, et al. Outcomes in patients with adenoid cystic carcinoma of the lacrimal gland. Ophthal Plast Reconstr Surg. 2004;20(1):22–6.
345. Lin YC, et al. Clinicopathological features of salivary and non-salivary adenoid cystic carcinomas. Int J Oral Maxillofac Surg. 2012;41(3):354–60.
346. Bernardini FP, Devoto MH, Croxatto JO. Epithelial tumors of the lacrimal gland: an update. Curr Opin Ophthalmol. 2008;19(5):409–13.
347. Hu YH, et al. Aberrant protein expression and promoter methylation of p16 gene are correlated with malignant transformation of salivary pleomorphic adenoma. Arch Pathol Lab Med. 2011;135(7):882–9.
348. Currie ZI, Rose GE. Long-term risk of recurrence after intact excision of pleomorphic adenomas of the lacrimal gland. Arch Ophthalmol. 2007;125(12):1643–6.
349. Ahn JY, et al. Pleomorphic adenocarcinoma of the lacrimal gland with multiple intracranial and spinal metastases. World J Surg Oncol. 2007;5:29.
350. Yamasaki T, et al. Multiple intracranial metastases following malignant evolution in recurrent pleomorphic adenoma of the lacrimal gland – case report. Neurol Med Chir (Tokyo). 1990;30(13):1038–42.
351. Chang CJ, et al. Carcinoma ex pleomorphic adenoma of the lacrimal gland: a case report. Ann Ophthalmol (Skokie). 2006;38(2):141–4.
352. Olsen KD, Lewis JE. Carcinoma ex pleomorphic adenoma: a clinicopathologic review. Head Neck. 2001;23(9):705–12.
353. Galatoire O, et al. Adenocarcinoma in a pleomorphic adenoma of the lacrimal gland: a case study. J Fr Ophtalmol. 2005;28(8):896–901.
354. Takahira M, et al. Cystic carcinoma ex pleomorphic adenoma of the lacrimal gland. Ophthal Plast Reconstr Surg. 2007;23(5):407–9.
355. Perzin KH, et al. Lacrimal gland malignant mixed tumors (carcinomas arising in benign mixed tumors): a clinico-pathologic study. Cancer. 1980;45(10):2593–606.
356. Ishida M, et al. Case of ductal adenocarcinoma ex pleomorphic adenoma of the lacrimal gland. Rinsho Byori. 2009;57(8):746–51.
357. Harada H. Histomorphological investigation regarding to malignant transformation of pleomorphic adenoma (so-called malignant mixed tumor) of the salivary gland origin: special reference to carcinosarcoma. Kurume Med J. 2000;47(4):307–23.
358. Takahira M, et al. Carcinosarcoma of the lacrimal gland arising from a pleomorphic adenoma. Am J Ophthalmol. 2005;140(2):337–40.
359. Mensink HW, Mooy C, Paridaens D. In situ adenocarcinoma ex pleomorphic adenoma of the lacrimal gland. Clin Exp Ophthalmol. 2005;33(6):669–71.
360. Tortoledo ME, Luna MA, Batsakis JG. Carcinomas ex pleomorphic adenoma and malignant mixed tumors. Histomorphologic indexes. Arch Otolaryngol. 1984; 110(3):172–6.
361. Cheuk W, Chan JK. Advances in salivary gland pathology. Histopathology. 2007;51(1):1–20.
362. Ohtake S, et al. Precancerous foci in pleomorphic adenoma of the salivary gland: recognition of focal carcinoma and atypical tumor cells by P53 immunohistochemistry. J Oral Pathol Med. 2002;31(10):590–7.
363. Rosa JC, et al. Immunohistochemical study of c-erbB-2 expression in carcinoma ex-pleomorphic adenoma. Histopathology. 1996;28(3):247–52.
364. El-Naggar AK, et al. Molecular genetic alterations in carcinoma ex-pleomorphic adenoma: a putative progression model? Gene Chromosome Cancer. 2000;27(2):162–8.
365. Baek SO, et al. Primary adenocarcinoma of the lacrimal gland. Arch Plast Surg. 2012;39(5):578–80.
366. Clauser L, et al. Adenocarcinoma of the lacrimal gland: report of a case. J Oral Maxillofac Surg. 2002;60(3):318–21.
367. Sofinski SJ, et al. Mucoepidermoid carcinoma of the lacrimal gland. Case report and review of the literature. Ophthal Plast Reconstr Surg. 1986;2(3):147–51.
368. Eviatar JA, Hornblass A. Mucoepidermoid carcinoma of the lacrimal gland: 25 cases and a review and update of the literature. Ophthal Plast Reconstr Surg. 1993;9(3):170–81.
369. Isayeva T, et al. Salivary mucoepidermoid carcinoma: demonstration of transcriptionally active human papillomavirus 16/18. Head Neck Pathol. 2013;7(2):135–48.
370. Dithmar S, et al. Mucoepidermoid carcinoma of an accessory lacrimal gland with orbital invasion. Ophthal Plast Reconstr Surg. 2000;16(2):162–6.
371. Pulitzer DR, Eckert ER. Mucoepidermoid carcinoma of the lacrimal gland. An oxyphilic variant. Arch Ophthalmol. 1987;105(10):1406–9.
372. Levin LA, et al. Mucoepidermoid carcinoma of the lacrimal gland. Report of a case with oncocytic features arising in a patient with chronic dacryops. Ophthalmology. 1991;98(10):1551–5.
373. Brandwein MS, et al. Mucoepidermoid carcinoma: a clinicopathologic study of 80 patients with special reference to histological grading. Am J Surg Pathol. 2001;25(7):835–45.
374. Von Holstein SL, et al. CRTC1-MAML2 gene fusion in mucoepidermoid carcinoma of the lacrimal gland. Oncol Rep. 2012;27(5):1413–6.

375. Behboudi A, et al. Molecular classification of mucoepidermoid carcinomas-prognostic significance of the MECT1-MAML2 fusion oncogene. Gene Chromosome Cancer. 2006;45(5):470–81.
376. Yoo J, Robinson RA. H-ras gene mutations in salivary gland mucoepidermoid carcinomas. Cancer. 2000;88(3):518–23.
377. Handra-Luca A, et al. MUC1, MUC2, MUC4, and MUC5AC expression in salivary gland mucoepidermoid carcinoma: diagnostic and prognostic implications. Am J Surg Pathol. 2005;29(7):881–9.
378. Katz SE, et al. Primary ductal adenocarcinoma of the lacrimal gland. Ophthalmology. 1996;103(1):157–62.
379. Kubota T, Moritani S, Ichihara S. Clinicopathologic and immunohistochemical features of primary ductal adenocarcinoma of lacrimal gland: five new cases and review of literature. Graefes Arch Clin Exp Ophthalmol. 2013;251(8):2071–6.
380. Di Palma S, et al. Salivary duct carcinomas can be classified into luminal androgen receptor-positive, HER2 and basal-like phenotypes*. Histopathology. 2012;61(4):629–43.
381. Wright JE, Rose GE, Garner A. Primary malignant neoplasms of the lacrimal gland. Br J Ophthalmol. 1992;76(7):401–7.
382. Fenton S, et al. Primary squamous cell carcinoma of the lacrimal gland. Eye (Lond). 2003;17(3):424–5.
383. Su GW, Patipa M, Font RL. Primary squamous cell carcinoma arising from an epithelium-lined cyst of the lacrimal gland. Ophthal Plast Reconstr Surg. 2005;21(5):383–5.
384. Hotta K, et al. Primary squamous cell carcinoma of the lacrimal gland. Clin Exp Ophthalmol. 2005;33(5):534–6.
385. Briscoe D, et al. Primary sebaceous carcinoma of the lacrimal gland. Br J Ophthalmol. 2001;85(5):625–6.
386. Mooy CM. Intraepithelial sebaceous neoplasia invading the lacrimal gland. Br J Ophthalmol. 1997;81(7):612–3.
387. Konrad EA, Thiel HJ. Adenocarcinoma of the lacrimal gland with sebaceous differentiation. A clinical study using light and electron microscopy. Graefes Arch Clin Exp Ophthalmol. 1983;221(2):81–5.
388. Chan JK, et al. Specific association of Epstein-Barr virus with lymphoepithelial carcinoma among tumors and tumorlike lesions of the salivary gland. Arch Pathol Lab Med. 1994;118(10):994–7.
389. Singhi AD, et al. Lymphoepithelial-like carcinoma of the oropharynx: a morphologic variant of HPV-related head and neck carcinoma. Am J Surg Pathol. 2010;34(6):800–5.
390. Rao NA, et al. Lymphoepithelial carcinoma of the lacrimal gland. Arch Ophthalmol. 2002;120(12):1745–8.
391. Liu YT, et al. Lymphoepithelial carcinoma of the lacrimal sac. Eye (Lond). 2009;23(7):1612–5.
392. Bloching M, Hinze R, Berghaus A. Lymphepithelioma-like carcinoma of the lacrimal gland. Eur Arch Otorhinolaryngol. 2000;257(7):399–401.
393. Evans HL, Batsakis JG. Polymorphous low-grade adenocarcinoma of minor salivary glands. A study of 14 cases of a distinctive neoplasm. Cancer. 1984;53(4):935–42.
394. Selva D, et al. Polymorphous low-grade adenocarcinoma of the lacrimal gland. Arch Ophthalmol. 2004;122(6):915–7.
395. Castle JT, et al. Polymorphous low grade adenocarcinoma: a clinicopathologic study of 164 cases. Cancer. 1999;86(2):207–19.
396. Kemp BL, et al. Terminal duct adenocarcinomas of the parotid gland. J Laryngol Otol. 1995;109(5):466–8.
397. Evans HL, Luna MA. Polymorphous low-grade adenocarcinoma: a study of 40 cases with long-term follow up and an evaluation of the importance of papillary areas. Am J Surg Pathol. 2000;24(10):1319–28.
398. Wiwatwongwana D, et al. Unusual carcinomas of the lacrimal gland: epithelial-myoepithelial carcinoma and myoepithelial carcinoma. Arch Ophthalmol. 2009;127(8):1054–6.
399. Ostrowski ML, et al. Clear cell epithelial-myoepithelial carcinoma arising in pleomorphic adenoma of the lacrimal gland. Ophthalmology. 1994;101(5):925–30.
400. Singh G, et al. Epithelial-myoepithelial carcinoma of the lacrimal gland: a rare case. Ann Diagn Pathol. 2012;16(4):292–7.
401. Chetty R. Intercalated duct hyperplasia: possible relationship to epithelial-myoepithelial carcinoma and hybrid tumours of salivary gland. Histopathology. 2000;37(3):260–3.
402. Watt FM, Hogan BL. Out of Eden: stem cells and their niches. Science. 2000;287(5457):1427–30.
403. Daa T, et al. Epithelial-myoepithelial carcinoma harboring p53 mutation. APMIS. 2001;109(4):316–20.
404. Furuse C, et al. Beta-catenin and E-cadherin expression in salivary gland tumors. Int J Surg Pathol. 2006;14(3):212–7.
405. Seethala RR, Barnes EL, Hunt JL. Epithelial-myoepithelial carcinoma: a review of the clinicopathologic spectrum and immunophenotypic characteristics in 61 tumors of the salivary glands and upper aerodigestive tract. Am J Surg Pathol. 2007;31(1):44–57.
406. Tralongo V, Daniele E. Epithelial-myoepithelial carcinoma of the salivary glands: a review of literature. Anticancer Res. 1998;18(1B):603–8.
407. Devoto MH, Croxatto JO. Primary cystadenocarcinoma of the lacrimal gland. Ophthalmology. 2003;110(10):2006–10.
408. Peng X, et al. Papillary cystadenocarcinoma of the lacrimal gland. Ann Ophthalmol (Skokie). 2010;42 Spec No:15–9.
409. Foss RD, Ellis GL, Auclair PL. Salivary gland cystadenocarcinomas. A clinicopathologic study of 57 cases. Am J Surg Pathol. 1996;20(12):1440–7.
410. De Rosa G, et al. Acinic cell carcinoma arising in a lacrimal gland. First case report. Cancer. 1986;57(10):1988–91.

411. Jang J, et al. Acinic cell carcinoma of the lacrimal gland with intracranial extension: a case report. Ophthal Plast Reconstr Surg. 2001;17(6):454–7.
412. Nichols AC, et al. A case report and genetic characterization of a massive acinic cell carcinoma of the parotid with delayed distant metastases. Case Rep Oncol Med. 2013;2013:270362.
413. Lewis JE, Olsen KD, Weiland LH. Acinic cell carcinoma. Clinicopathologic review. Cancer. 1991;67(1):172–9.
414. Hoffman HT, et al. National Cancer Data Base report on cancer of the head and neck: acinic cell carcinoma. Head Neck. 1999;21(4):297–309.
415. Piana S, et al. Dedifferentiated acinic cell carcinoma of the parotid gland with myoepithelial features. Arch Pathol Lab Med. 2002;126(9):1104–5.
416. Muduly DK, et al. Basal cell adenocarcinoma of lacrimal gland. Orbit. 2011;30(6):300–2.
417. Lee GA, Cominos D, Sullivan TJ. Clinicopathological report: mucinous carcinoma of the eyelid. Aust N Z J Ophthalmol. 1999;27(1):71–3.
418. Uchida K, et al. Screening for DNA copy number aberrations in mucinous adenocarcinoma arising from the minor salivary gland: two case reports. Cancer Genet Cytogenet. 2010;203(2):324–7.
419. Kalantzis G, et al. Oncocytic adenocarcinoma of the lacrimal gland: an unusual presentation. Eye (Lond). 2013;27(1):104–5.
420. Dorello U. Carcinoma oncocitario della ghiandola lacrimale. Riv Otoneurooftalmol. 1961;36:452–61.
421. Bernardini FP, Croxatto JO, Bandelloni R. Primary undifferentiated large cell carcinoma of the lacrimal gland. Ophthalmology. 2011;118(6):1189–92.
422. Kivela T, Tarkkanen A. The Merkel cell and associated neoplasms in the eyelids and periocular region. Surv Ophthalmol. 1990;35(3):171–87.
423. Gess AJ, Silkiss RZ. A merkel cell carcinoma of the lacrimal gland. Ophthal Plast Reconstr Surg. 2012;28(1):e11–3.
424. Luaces Rey R, et al. Merkel cell carcinoma of the head and neck: report of seven cases. Med Oral Patol Oral Cir Bucal. 2008;13(6):E390–4.
425. Feng H, et al. Clonal integration of a polyomavirus in human Merkel cell carcinoma. Science. 2008;319(5866):1096–100.
426. Iida K, et al. A case of malignant myoepithelioma in the lacrimal gland. Nihon Ganka Gakkai Zasshi. 2001;105(1):42–6.
427. Cherian I, et al. Adenosquamous carcinoma of the lacrimal gland. BMJ Case Rep. 2010;2010: bcr0720103192.
428. Rasmussen P, et al. Malignant lymphoma of the lacrimal gland: a nation-based study. Arch Ophthalmol. 2011;129(10):1275–80.
429. Farmer JP, et al. Lymphoproliferative lesions of the lacrimal gland: clinicopathological, immunohistochemical and molecular genetic analysis. Can J Ophthalmol. 2005;40(2):151–60.
430. Sevel D. Development and congenital abnormalities of the nasolacrimal apparatus. J Pediatr Ophthalmol Strabismus. 1981;18(5):13–9.
431. Tucker NA, Tucker SM, Linberg JV. The anatomy of the common canaliculus. Arch Ophthalmol. 1996;114(10):1231–4.
432. Ipek E, et al. Morphological and morphometric evaluation of lacrimal groove. Anat Sci Int. 2007;82(4):207–10.
433. Paul TO. Medical management of congenital nasolacrimal duct obstruction. J Pediatr Ophthalmol Strabismus. 1985;22(2):68–70.
434. Nelson LR, Calhoun JH, Menduke H. Medical management of congenital nasolacrimal duct obstruction. Ophthalmology. 1985;92(9):1187–90.
435. Petersen RA, Robb RM. The natural course of congenital obstruction of the nasolacrimal duct. J Pediatr Ophthalmol Strabismus. 1978;15(4):246–50.
436. Perry LJ, et al. Giant dacryocystomucopyocele in an adult: a review of lacrimal sac enlargements with clinical and histopathologic differential diagnoses. Surv Ophthalmol. 2012;57(5):474–85.
437. Welham RA, Bergin DJ. Congenital lacrimal fistulas. Arch Ophthalmol. 1985;103(4):545–8.
438. Masi AV. Congenital fistula of the lacrimal sac. Arch Ophthalmol. 1969;81(5):701–4.
439. Oill PA, et al. Specialty conference. Infectious disease emergencies. Part V: patients presenting with localized infections. West J Med. 1977;126(3):196–208.
440. Marthin JK, et al. Lesions of the lacrimal drainage system: a clinicopathological study of 643 biopsy specimens of the lacrimal drainage system in Denmark 1910–1999. Acta Ophthalmol Scand. 2005;83(1):94–9.
441. Repp DJ, Burkat CN, Lucarelli MJ. Lacrimal excretory system concretions: canalicular and lacrimal sac. Ophthalmology. 2009;116(11):2230–5.
442. Hay-Smith G, Rose GE. Lacrimal gland ductulitis caused by probable Actinomyces infection. Ophthalmology. 2012;119(1):193–6.
443. Murphy CL, Murgatroyd H. Sarcoidosis of the lacrimal sac – an unusual case. Br J Ophthalmol. 2013;97: 1351.
444. Litwin AS, et al. Acquired lacrimal sac fistula mimicking basal cell carcinoma. Br J Dermatol. 2013;168(6):1348–50.
445. Marcet MM, et al. Localized orbital amyloidosis involving the lacrimal sac and nasolacrimal duct. Ophthalmology. 2006;113(1):153–6.
446. Kroll J, Busse H. Tumours of the lacrimal passages. Klin Monbl Augenheilkd. 2008;225(1):91–5.
447. Golub JS, et al. Inverted papilloma of the nasolacrimal system invading the orbit. Ophthal Plast Reconstr Surg. 2007;23(2):151–3.
448. Raemdonck TY, et al. Inverted papilloma arising primarily from the lacrimal sac. Orbit. 2009;28(2–3):181–4.
449. Sjo NC, et al. Human papillomavirus: cause of epithelial lacrimal sac neoplasia? Acta Ophthalmol Scand. 2007;85(5):551–6.
450. Stefanyszyn MA, et al. Lacrimal sac tumors. Ophthal Plast Reconstr Surg. 1994;10(3):169–84.
451. Brar ST, Meyer D. Diagnosis and management of mucoepidermoid carcinoma of the lacrimal duct. Orbit. 2011;30(1):34–6.

452. Brannan PA, et al. A case of primary adenocarcinoma of the lacrimal sac. Orbit. 2005;24(4):291–3.
453. Baredes S, et al. Adenocarcinoma ex-pleomorphic adenoma of the lacrimal sac and nasolacrimal duct: a case report. Laryngoscope. 2003;113(6):940–2.
454. De Stefani A, et al. Squamous cell carcinoma of the lacrimal drainage system: case report and literature review. Tumori. 1998;84(4):506–10.
455. Kuwabara H, Takeda J. Malignant melanoma of the lacrimal sac with surrounding melanosis. Arch Pathol Lab Med. 1997;121(5):517–9.
456. Li YJ, et al. Primary malignant melanoma of the lacrimal sac. BMJ Case Rep. 2012;2012:bcr006349.
457. Woo KI, Suh YL, Kim YD. Solitary fibrous tumor of the lacrimal sac. Ophthal Plast Reconstr Surg. 1999;15(6):450–3.
458. Charles NC, Palu RN, Jagirdar JS. Hemangiopericytoma of the lacrimal sac. Arch Ophthalmol. 1998; 116(12):1677–80.
459. Bajaj MS, et al. Neurofibroma of the lacrimal sac. Orbit. 2002;21(3):205–8.
460. Karcioglu ZA, editor. Orbital tumors diagnosis and treatment. New York: Springer; 2005.
461. Naumann GOH, Holbach LM, Kruse FE, editors. Applied pathology for ophthalmic microsurgeons. Berlin/New York: Springer; 2008.

Index

S. Heegaard, H. Grossniklaus (eds.), *Eye Pathology: An Illustrated Guide*,
DOI 10.1007/978-3-662-43382-9, © Springer-Verlag Berlin Heidelberg 2015